CROP PHYSIOLOGY UNDER LED LIGHTING

EDITED BY: Leo Marcelis, Eiji Goto, Bernard Grodzinski, Sissel Torre, Jason Wargent and Bruce Bugbee

PUBLISHED IN: Frontiers in Plant Science

frontiers Research Topics

Frontiers eBook Copyright Statement

The copyright in the text of individual articles in this eBook is the property of their respective authors or their respective institutions or funders. The copyright in graphics and images within each article may be subject to copyright of other parties. In both cases this is subject to a license granted to Frontiers.

The compilation of articles constituting this eBook is the property of Frontiers.

Each article within this eBook, and the eBook itself, are published under the most recent version of the Creative Commons CC-BY licence. The version current at the date of publication of this eBook is CC-BY 4.0. If the CC-BY licence is updated, the licence granted by Frontiers is automatically updated to the new version.

When exercising any right under the CC-BY licence, Frontiers must be attributed as the original publisher of the article or eBook, as applicable.

Authors have the responsibility of ensuring that any graphics or other materials which are the property of others may be included in the CC-BY licence, but this should be checked before relying on the CC-BY licence to reproduce those materials. Any copyright notices relating to those materials must be complied with.

Copyright and source acknowledgement notices may not be removed and must be displayed in any copy, derivative work or partial copy which includes the elements in question.

All copyright, and all rights therein, are protected by national and international copyright laws. The above represents a summary only. For further information please read Frontiers' Conditions for Website Use and Copyright Statement, and the applicable CC-BY licence.

ISSN 1664-8714
ISBN 978-2-88974-276-9
DOI 10.3389/978-2-88974-276-9

About Frontiers

Frontiers is more than just an open-access publisher of scholarly articles: it is a pioneering approach to the world of academia, radically improving the way scholarly research is managed. The grand vision of Frontiers is a world where all people have an equal opportunity to seek, share and generate knowledge. Frontiers provides immediate and permanent online open access to all its publications, but this alone is not enough to realize our grand goals.

Frontiers Journal Series

The Frontiers Journal Series is a multi-tier and interdisciplinary set of open-access, online journals, promising a paradigm shift from the current review, selection and dissemination processes in academic publishing. All Frontiers journals are driven by researchers for researchers; therefore, they constitute a service to the scholarly community. At the same time, the Frontiers Journal Series operates on a revolutionary invention, the tiered publishing system, initially addressing specific communities of scholars, and gradually climbing up to broader public understanding, thus serving the interests of the lay society, too.

Dedication to Quality

Each Frontiers article is a landmark of the highest quality, thanks to genuinely collaborative interactions between authors and review editors, who include some of the world's best academicians. Research must be certified by peers before entering a stream of knowledge that may eventually reach the public - and shape society; therefore, Frontiers only applies the most rigorous and unbiased reviews.
Frontiers revolutionizes research publishing by freely delivering the most outstanding research, evaluated with no bias from both the academic and social point of view. By applying the most advanced information technologies, Frontiers is catapulting scholarly publishing into a new generation.

What are Frontiers Research Topics?

Frontiers Research Topics are very popular trademarks of the Frontiers Journals Series: they are collections of at least ten articles, all centered on a particular subject. With their unique mix of varied contributions from Original Research to Review Articles, Frontiers Research Topics unify the most influential researchers, the latest key findings and historical advances in a hot research area! Find out more on how to host your own Frontiers Research Topic or contribute to one as an author by contacting the Frontiers Editorial Office: frontiersin.org/about/contact

CROP PHYSIOLOGY UNDER LED LIGHTING

Topic Editors:
Leo Marcelis, Wageningen University and Research, Netherlands
Eiji Goto, Chiba University, Japan
Bernard Grodzinski, University of Guelph, Canada
Sissel Torre, Norwegian University of Life Sciences, Norway
Jason Wargent, Massey University, New Zealand
Bruce Bugbee, Utah State University, United States

Citation: Marcelis, L., Goto, E., Grodzinski, B., Torre, S., Wargent, J., Bugbee, B., eds. (2022). Crop Physiology Under LED Lighting. Lausanne: Frontiers Media SA. doi: 10.3389/978-2-88974-276-9

Table of Contents

05 ***Regulation of Ascorbate Accumulation and Metabolism in Lettuce by the Red:Blue Ratio of Continuous Light Using LEDs***
Lingyan Zha, Wenke Liu, Qichang Yang, Yubin Zhang, Chengbo Zhou and Mingjie Shao

18 ***Substituting Far-Red for Traditionally Defined Photosynthetic Photons Results in Equal Canopy Quantum Yield for CO_2 Fixation and Increased Photon Capture During Long-Term Studies: Implications for Re-Defining PAR***
Shuyang Zhen and Bruce Bugbee

32 ***Growth Responses of Red-Leaf Lettuce to Temporal Spectral Changes***
Qingwu Meng and Erik S. Runkle

46 ***UV-B Induced Flavonoids Contribute to Reduced Biotrophic Disease Susceptibility in Lettuce Seedlings***
Emily R. McLay, Ana Clara Pontaroli and Jason J. Wargent

59 ***Metabolic Profile and Performance Responses of* Ranunculus asiaticus *L. Hybrids as Affected by Light Quality of Photoperiodic Lighting***
Petronia Carillo, Emilia Dell'Aversana, Giuseppe Carlo Modarelli, Giovanna Marta Fusco, Stefania De Pascale and Roberta Paradiso

73 ***Response of Basil Growth and Morphology to Light Intensity and Spectrum in a Vertical Farm***
Dorthe H. Larsen, Ernst J. Woltering, Celine C. S. Nicole and Leo F. M. Marcelis

89 ***Producing Enhanced Yield and Nutritional Pigmentation in Lollo Rosso Through Manipulating the Irradiance, Duration, and Periodicity of LEDs in the Visible Region of Light***
Laura Cammarisano, Iain S. Donnison and Paul R. H. Robson

99 ***Regulation of Early Plant Development by Red and Blue Light: A Comparative Analysis Between* Arabidopsis thaliana and Solanum lycopersicum**
Kiki Spaninks, Jelmer van Lieshout, Wim van Ieperen and Remko Offringa

112 ***Spectral Composition of Light Affects Sensitivity to UV-B and Photoinhibition in Cucumber***
Carolina Falcato Fialho Palma, Victor Castro-Alves, Luis Orlando Morales, Eva Rosenqvist, Carl-Otto Ottosen and Åke Strid

126 ***Dissecting the Genotypic Variation of Growth Responses to Far-Red Radiation in Tomato***
Yongran Ji, Theoharis Ouzounis, Henk J. Schouten, Richard G. F. Visser, Leo F. M. Marcelis and Ep Heuvelink

135 ***LED Lighting Strategies Affect Physiology and Resilience to Pathogens and Pests in Eggplant (*Solanum melongena L.*)***
J. Anja Dieleman, H. Marjolein Kruidhof, Kees Weerheim and Kirsten Leiss

150 ***Adding Far-Red to Red-Blue Light-Emitting Diode Light Promotes Yield of Lettuce at Different Planting Densities***
Wenqing Jin, Jorge Leigh Urbina, Ep Heuvelink and Leo F. M. Marcelis

159 ***Floral Induction in the Short-Day Plant Chrysanthemum Under Blue and Red Extended Long-Days***
Malleshaiah SharathKumar, Ep Heuvelink, Leo F. M. Marcelis and Wim van Ieperen

172 ***High Light Intensity Applied Shortly Before Harvest Improves Lettuce Nutritional Quality and Extends the Shelf Life***
Qianxixi Min, Leo F. M. Marcelis, Celine C. S. Nicole and Ernst J. Woltering

184 ***Only Extreme Fluctuations in Light Levels Reduce Lettuce Growth Under Sole Source Lighting***
Ruqayah Bhuiyan and Marc W. van Iersel

196 ***Plant Factories Are Heating Up: Hunting for the Best Combination of Light Intensity, Air Temperature and Root-Zone Temperature in Lettuce Production***
Laura Carotti, Luuk Graamans, Federico Puksic, Michele Butturini, Esther Meinen, Ep Heuvelink and Cecilia Stanghellini

207 ***The Effect of Red & Blue Rich LEDs vs Fluorescent Light on Lollo Rosso Lettuce Morphology and Physiology***
Laura Cammarisano, Iain S. Donnison and Paul R. H. Robson

217 ***Impact of Different Daily Light Integrals and Carbon Dioxide Concentrations on the Growth, Morphology, and Production Efficiency of Tomato Seedlings***
Brandon M. Huber, Frank J. Louws and Ricardo Hernández

236 ***Photosynthetic Physiology of Blue, Green, and Red Light: Light Intensity Effects and Underlying Mechanisms***
Jun Liu and Marc W. van Iersel

250 ***Seasonal Efficiency of Supplemental LED Lighting on Growth and Photomorphogenesis of Sweet Basil***
Jan Andreas Solbach, Andreas Fricke and Hartmut Stützel

266 ***Supplemental LED Lighting Effectively Enhances the Yield and Quality of Greenhouse Truss Tomato Production: Results of a Meta-Analysis***
Elisa Appolloni, Francesco Orsini, Giuseppina Pennisi, Xavier Gabarrell Durany, Ivan Paucek and Giorgio Gianquinto

280 ***Improving the Predictive Value of Phytochrome Photoequilibrium: Consideration of Spectral Distortion Within a Leaf***
Paul Kusuma and Bruce Bugbee

299 ***LED Intercanopy Lighting in Blackberry During Spring Improves Yield as a Result of Increased Number of Fruiting Laterals and Has a Positive Carryover Effect on Autumn Yield***
Anabel Rivas, Kang Liu and Ep Heuvelink

frontiers in Plant Science

ORIGINAL RESEARCH
published: 29 May 2020
doi: 10.3389/fpls.2020.00704

Regulation of Ascorbate Accumulation and Metabolism in Lettuce by the Red:Blue Ratio of Continuous Light Using LEDs

Lingyan Zha[1,2], Wenke Liu[1,2], Qichang Yang[1,2,3], Yubin Zhang[1,2], Chengbo Zhou[1,2] and Mingjie Shao[1,2]*

[1] Institute of Environment and Sustainable Development in Agriculture, Chinese Academy of Agricultural Sciences, Beijing, China, [2] Key Laboratory of Energy Conservation and Waste Management of Agricultural Structures, Ministry of Agriculture and Rural Affairs, Beijing, China, [3] Institute of Urban Agriculture, Chinese Academy of Agriculture Science, Chengdu, China

Ascorbate (AsA), an antioxidant that cannot be synthesized and stored by the human body, plays an essential role in the proper functioning of both plants and humans. With the goal of increasing the AsA level in lettuce, the effects of different ratios of red (R) to blue (B) light (75R:25B, 50R:50B, and 25R:75B) on AsA pool sizes as well as the transcript levels and activities of key enzymes involved in AsA metabolism were constantly monitored for 12 days under continuous light (200 $\mu mol \cdot m^{-2} \cdot s^{-1}$) from LEDs. The results showed that lettuce biomass was positively correlated with the ratio of red light, while the AsA pool size had a positive correlation with the ratio of blue light during the whole experiment. The 25R:75B treatment increased the expression of genes involved in AsA biosynthesis (*GMP*, *GME*, *GGP*, *GPP*, *GLDH*) and regeneration (*APX*, *MDHAR*, *DHAR*, and *GR*) on day 3 but only significantly elevated the activities of enzymes involved in AsA regeneration (APX, MDHAR, DHAR, and GR) subsequently. AsA regeneration enzymes (MDHAR, DHAR and GR) had greater correlations with the AsA level than the AsA synthesis enzyme (GLDH). Thus, it is concluded that a high ratio of blue light elevated the AsA level mainly by promoting AsA regeneration rather than biosynthesis. Taken together, altering the red:blue ratio of continuous light from high to low before harvest is recommended for lettuce cultivation to achieve both high yield and high quality.

Keywords: ascorbic acid, enzyme activity, expression level, light quality, regulatory mechanism

OPEN ACCESS

Edited by:
Bernard Grodzinski, University of Guelph, Canada

Reviewed by:
Tse-Min Lee, National Sun Yat-sen University, Taiwan
Vijay Pratap Singh, University of Allahabad, India

***Correspondence:**
Wenke Liu
liuwenke@caas.cn

Specialty section:
This article was submitted to Crop and Product Physiology, a section of the journal Frontiers in Plant Science

Received: *08 February 2020*
Accepted: *05 May 2020*
Published: *29 May 2020*

Citation:
Zha L, Liu W, Yang Q, Zhang Y, Zhou C and Shao M (2020) Regulation of Ascorbate Accumulation and Metabolism in Lettuce by the Red:Blue Ratio of Continuous Light Using LEDs. Front. Plant Sci. 11:704. doi: 10.3389/fpls.2020.00704

INTRODUCTION

Ascorbate, the reduced form of vitamin C, is well recognized as one of the most pivotal antioxidants in plants (Gallie, 2013; Ntagkas et al., 2018). It has multiple essential functions in the regulation of many physiological processes in plants (Davey et al., 2000). The metabolic pathway of AsA in plants has been well established since Wheeler et al. (1998) proposed the main AsA biosynthetic pathway: the L-galactose pathway (D-mannose pathway). In this pathway, D-glucose is catalyzed to AsA by a series of enzymes, including several key enzymes:

Abbreviations: APX, ascorbate peroxidase; AsA, ascorbate; DHA, dehydroascorbate; DHAR dehydroascorbate reductase; GGP, GDP-L-galactose phosphorylase; GLDH, L-galactono-1,4-lactone dehydrogenase; GME, GDP-D-mannose 3′,5′-epimerase; GMP, GDP-D-mannose pyrophosphorylase; GPP, L-galactose-1-P phosphatase; GR, glutathione reductase; MDHAR, monodehydroascorbate reductase; T-AsA, total ascorbate.

GDP-d-mannose pyrophosphorylase (GMP), GDP-d-mannose 3′5-epimerase (GME), GDP-L-galactose phosphorylase (GGP), L-galactose-1-phosphate phosphatase (GPP), and L-galactono-1,4-lactone dehydrogenase (GLDH), which catalyzes the final step. After AsA is synthesized, it is oxidized to monodehydroascorbate (MDHA) by ascorbate peroxidase (APX), and MDHA is then spontaneously disproportionated to dehydroascorbate (DHA). Fortunately, MDHA and DHA can be reduced back to AsA by monodehydroascorbate reductase (MDHAR) and dehydroascorbate reductase (DHAR), respectively. The electron donors of these two enzymes are NADPH and glutathione, respectively, and the latter electron donor is recovered from oxidized glutathione by glutathione reductase (GR) (Ntagkas et al., 2018).

Sufficient AsA level is also vital for maintaining the proper physiological function of the human body (Ntagkas et al., 2018). However, unlike in plants, although AsA is indispensable for the human body, it cannot be synthesized and stored by humans. Thus, AsA in the human body can only be provided by the diet, especially by vegetables. Compared with vegetables cultivated in open fields, those cultivated in protected horticulture, which occupy a large part of the vegetable market, often have relatively lower AsA levels. Furthermore, with the improvement of human awareness of food safety and health, low nutritional quality has become a reason for consumers to resist the purchase and consumption of vegetables that cultivated in protected horticulture. This resistance has seriously restricted the development and application of protected horticulture, including greenhouses and plant factories. Increasing effective light is a direct and effectual way to improve the AsA levels, as the relatively weak irradiance in protected horticulture is one of the main reasons for the low AsA level of vegetable cultivated in protected horticulture (Massot et al., 2010). Continuous light is an operative way to increase effective light by maximizing light period in protected horticulture. Although numerous studies have shown that continuous light induced severe leaf damage of some sensitive plant species, such as tomato, there were also some species could tolerance continuous light and showed positive responses (Sysoeva et al., 2010; Velez-Ramirez et al., 2011). Our previous study indicated that continuous light improved both the yield and AsA level of hydroponic lettuce without causing any leaf injury and dysfunction compared with lettuce grown under a normal photoperiod (16 h light /8 h dark) (Zha et al., 2019b). Optimize light parameters of continuous light could further elevate AsA level, as light is the most vital environment factor affecting AsA level (Ntagkas et al., 2018). We have discovered that increasing the light intensity of continuous light can further improve the AsA level, but consumed more electric energy at the same time (Zha et al., 2019a). Improving AsA levels by light quality regulation might be more preferable from the energy perspective.

The effect of different light qualities on AsA content has been studied in many plants, including lettuce (Chen et al., 2016), basil and parsley (Samuolienë et al., 2016), and citrus fruits (Zhang et al., 2015). The majority of studies have shown that the short-wavelength spectrum (e.g. UV-A, blue light) is more conducive to increasing the AsA content compared to long-wavelength spectrum (Zhang et al., 2015; Dutta Gupta, 2017). However, the opposite results have also been reported. For example, Ma et al. (2014) found that red light irradiation after harvest could effectively suppress the reduction of AsA levels in broccoli, while blue light could not. Such inconsistent results indicate that the effect of light quality on AsA level is not certain; it is influenced by many factors, such as plant species, light intensity, or other environmental factors (Dutta Gupta, 2017). To date, most previous studies have focused on the response of the AsA quantity to light quality, but the mechanisms and physiological basis of light quality regulation on AsA metabolism has relatively been less studied. Zhang et al. (2015) found that blue light upregulated the expression of AsA biosynthetic genes and AsA regeneration genes to increase the AsA content compared with that under dark conditions. Similar to Zhang, several researchers explained the mechanism of light quality or other environmental factors regulating AsA accumulation by investigating changes in gene expression (Mastropasqua et al., 2012; Massot et al., 2013; Ma et al., 2014; Zhang et al., 2015). However, gene expression is sometimes not consistent with AsA content (Pignocchi et al., 2003; Bartoli et al., 2006), as translation, posttranscriptional regulation, and other processes occur after transcription. In fact, mRNA level of a particular gene not often has direct correlation with its protein content in plants (Veìlez-Bermuìdez and Schmidt, 2014). Therefore, to understand the process by which light quality regulates AsA metabolism, it is necessary to explore at both the levels of transcription and enzyme activity.

Red and blue lights are recognized as the most important spectrum for plant growth because they are not only the major light source for photosynthesis but they also regulate many morphogenetic responses in plants through photoreceptors (Xu et al., 2012; Lin et al., 2013), but monochromatic red or blue light is not conducive to plant growth. Currently, the main light sources in protected horticulture are red and blue LED lights, thus it is more practical to explore the influence of the red:blue ratio on AsA accumulation and metabolism. Lettuce is the main vegetable species cultivated in plant factories and has abundant ascorbate, which is equivalent to the level in some fruits (e.g. tomato). To elevate the potential of the promoting effect of continuous light on ascorbate accumulation in lettuce, the red:blue ratio of the continuous light needs to be optimized. In the present study, the effects of the red:blue light ratio on ascorbate accumulation and the activities and gene expression of enzymes related to ascorbate metabolism were investigated under continuous light using LEDs. We hypothesize that regulation of red:blue light ratio on AsA involves several regulatory points in its metabolism pathway at both transcriptional and enzymatic level, and correlate with oxidative stress under continuous light. The objective of this study is to provide new lighting strategies to enhance AsA level in lettuce and explore the mechanism of red and blue light regulating on AsA metabolism.

MATERIALS AND METHODS

Plant Materials and Light Treatments

Lettuce plants were hydroponically cultivated in an environment-controlled plant factory with atmospheric carbon dioxide,

TABLE 1 | Light spectrum, light intensity, and photoperiod of each treatment at each growth stage of lettuce. W: white LED light, R: red LED light, B: blue LED light.

Treatments	Germination stage (15 days)	Acclimation stage (10 days)	Treatment stage (12 days)
75R:25B	W: 200 $\mu mol \cdot m^{-2} \cdot s^{-1}$ 16/8 h	R: 150 $\mu mol \cdot m^{-2} \cdot s^{-1}$ B: 50 $\mu mol \cdot m^{-2} \cdot s^{-1}$ 16/8 h	R: 150 $\mu mol \cdot m^{-2} \cdot s^{-1}$ B: 50 $\mu mol \cdot m^{-2} \cdot s^{-1}$ 24/0 h
50R:50B			R: 100 $\mu mol \cdot m^{-2} \cdot s^{-1}$ B: 100 $\mu mol \cdot m^{-2} \cdot s^{-1}$ 24/0 h
25R:75B			R: 50 $\mu mol \cdot m^{-2} \cdot s^{-1}$ B: 150 $\mu mol \cdot m^{-2} \cdot s^{-1}$ 24/0 h

23 ± 3°C air temperature, and 50–60% relative humidity. Lettuce seeds were sown on soaked sponges (2.5 × 2.5 × 2.5 cm) on plastic germination trays and then germinated under white LED (200 $\mu mol \cdot m^{-2} \cdot s^{-1}$, 16/8 h) light after sprouting. Two weeks later, the seedlings were transplanted from the germination trays to a recirculating hydroponic culture system equipped with red and blue LED light panels. To make the lettuce seedlings grow evenly and adapt to the new system, all seedlings were exposed to uniform light conditions (75R:25B, 200 $\mu mol \cdot m^{-2} \cdot s^{-1}$, 16/8 h) for 10 days. Then, seedlings were randomly divided into three groups (39 plants for each group) to receive continuous light (200 $\mu mol \cdot m^{-2} \cdot s^{-1}$) of different light qualities: 75R:25B, 50R:50B, and 25R:75B (**Table 1** and **Figure 1**). Modified Hoagland nutrient solution (pH≈5.8; EC≈1.6 $dS \cdot m^{-1}$) was applied for plant cultivation and was circulated for 60 min every day. The light intensity was measured by a light sensor logger (Li-1500) and a quantum sensor (LI-190R, Lincoln, NE, United States), and the light spectra were confirmed by a spectroradiometer (Avaspec-2048CL, Avates, Apeldoorn, Netherlands).

Sampling and Measurements of Growth Parameters

The samples used for the physiological and gene expression determinations were collected at 21:00 (the end of the light period at the germination and acclimation stages) every 3 days (0, 3, 6, 9, and 12 days) after the start of the treatments. Leaves without petioles from four lettuce plants were sampled from each treatment at each sampling time and were kept as four biological replicates. The collected leaves were immediately frozen in liquid nitrogen and stored in an ultralow temperature freezer (−80°C) until analysis. For the measurement of growth parameters, another five plants were sampled on day 12 after the beginning of the treatment. The shoots and roots of the lettuce plants were separated to determine the fresh weight (FW), respectively. The main petioles of all leaves were then removed to accurately measure the leaf FW and leaf area with an area meter (LI-3100, Li-Cor Biosciences, Lincoln, NE, United States). Specific leaf FW was the ratio of leaf FW to leaf area. After these determinations, all shoots and roots were dried in an oven at 80°C for the determination of shoot and root dry weights (DW), which were used to calculate the root/shoot ratio and shoot DW/FW ratio.

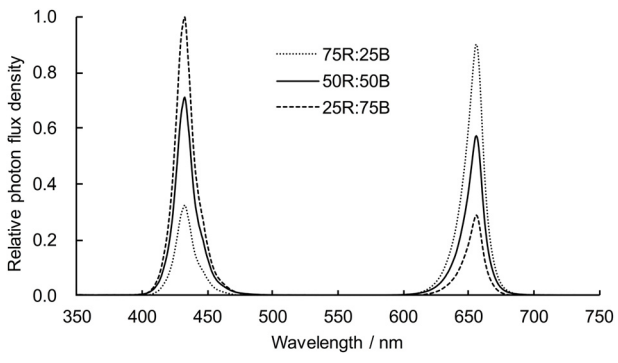

FIGURE 1 | Light spectra of light treatments.

Ascorbate Pool Size Assays

The total ascorbate (T-AsA) and AsA concentrations of the four biological replicates were determined by UPLC according to the methods of Spiìnola et al. (2012) and Campos et al. (2009) with some adaptations. Frozen leaf tissue (0.1 g) was homogenized in 1 mL precooled extractant solution that contained 1.5% (w/v) metaphosphoric acid, 4% (v/v) acetic acid, and 0.5 mM EDTA. After centrifugation (15000 × *g*, 4 °C, 15 min), the supernatant was filtered through PTFE filters (0.22 μm) and collected to assay the concentration of T-AsA and AsA. For the T-AsA content determination, 50 μL supernatant was mixed with filtered (0.22 μm PTFE filters) dithiothreitol (10 μL, 750 mM), Tris (190 μL, 275 mM), and sulfuric acid (50 μL, 0.4 M) and then incubated for 30 min at 25 °C. The reaction mixture was analyzed by an Acquity UPLC system (Waters Corp, United States) with an Acquity UPLC HSS T3 column (2.1 × 100 mm, 1.8 μm, Waters). The column was eluted with 0.1% (v/v) formic acid with a flow rate of 0.25 $mL \cdot min^{-1}$. The absorbance at 245 nm was monitored by a Waters Acquity UPLC photodiode array (PDA) (Waters Corp, United States) detection system. The AsA content was analyzed in a similar manner except that 10 μL deionized H_2O was substituted for the dithiothreitol. The DHA content was calculated as the difference between the T-AsA and AsA contents.

Enzyme Activity Assays

The extraction of GalLDH (EC 1.3.2.3), APX (EC 1.11.1.11), MDHAR (EC 1.6.5.4), DHAR (EC 1.8.5.1), and GR (EC 1.8.1.7), as well as the determination of the activities of these enzymes, have been described in detail previously (Zha et al., 2019a). Four biological replicates were used to perform the enzyme activity assay.

Hydrogen Peroxide and Malondialdehyde Content Assays

The hydrogen peroxide (H_2O_2) and malondialdehyde (MDA) contents of the four biological replicates were assayed by UV-VIS spectrophotometer (Shimadzu UV-1800, Kyoto, Japan) according to the method of Brennan and Frenkel (1977) and Yang et al. (2010), respectively. H_2O_2 was extracted from 0.1 g

fresh frozen leaf tissue by homogenization with 1 mL precooled acetone. After centrifugation (10,000 *g*, 20 min, 4°C), 1 mL supernatant was mixed with 0.1 mL of 10% (v/v) titanium sulfate and 0.2 mL ammonia and centrifuged at 4,000 *g* for 10 min at 25°C. The precipitate was then dissolved in 1 mL 2 M H_2SO_4 to measure the absorbance at 412 nm. The MDA was extracted from 0.1 g fresh-frozen leaf tissue by homogenization with 1 ml cold 10% trichloroacetic acid. After centrifugation (15,000 *g*, 10 min, 4°C), 0.5 mL supernatant and 0.5 mL 0.6% thiobarbituric acid were mixed and boiled at 100 °C for 20 min and then quickly cooled to room temperature. The reaction mixture was centrifuged at 15,000 *g* for 10 min to collect the supernatants, which were used to measure the absorbance at 450, 532, and 600 nm.

Total RNA Extraction and RT-qPCR Analysis

The total RNA of the lettuce leaves was extracted by the RNAprep Pure Plant Plus Kit (DP441, Tiangen Biotech Co., Ltd., Beijing, China) according to the manufacturer's instructions. The quality and concentration of total RNA was determined by an ultra-micromole plate spectrophotometer (TECAN, Infinite M200 Pro, Switzerland). 2 μg total RNA was used for reverse transcription using the FastKing RT kit (KR116, Tiangen Biotech Co., Ltd., Beijing, China) in a 20 μL reaction and the reverse transcription PCR was conducted according to the instructions. Quantitative RT-PCR analysis was performed using a multicolor real-time PCR detection system (Bio-Rad, Hercules, CA, United States). For the qPCR, each reaction included 9 μL 100X diluted cDNA, 1 μL primer (initial concentration was 10 μM) and 10 μL PCR buffer including SYBR green. The optimized program of the PCR protocol included initial denaturation at 95°C for 5 min, followed by 39 cycles of 95°C for 10 s, 60°C for 30 s, and 72°C for 30 s. The primers sequences are presented in **Supplementary Table S1**. 18S rRNA was used as housekeeping gene. To compare the gene expression levels under varying red:blue light ratios and different days of continuous light, the gene expression level of every measured enzyme in the lettuce leaves before the continuous light was quantified as 1. For relative quantification, the $2^{-(\Delta\Delta Ct)}$ method was used according to Livak and Schmittgen (2001). Three independent biological replicates were used for each treatment.

Statistical Analysis

Growth (n = 5) and physiological (n = 4) parameters were subjected to one-way ANOVA and two-way ANOVA, respectively, by SPSS 18.0 (International Business Machines Corporation). For two-way ANOVA, light treatment and days of light treatments were considering as two factors, and the results were list in **Table 3**. After variance analysis, Tukey's test ($p < 0.05$) was used to make post-hoc multiple comparisons among means of different light treatments at each time point. Correlation and significance tests among AsA pool sizes and enzyme activities were calculated using the Pearson correlation coefficient with a two-tailed test. Principal component analysis (PCA) was performed by Canoco 5.0 (Microcomputer Power, Ithaca, NY, United States).

RESULTS

Plant Growth

After 12 days of continuous light with different ratios of red:blue light, the shoot FW of lettuce increased significantly with increasing red:blue light ratio, and the differences in shoot FW between the 25R:75B and 75R:25B treatments reached a significant level (**Table 2**). Although the shoot DW and leaf area also showed a positive correlation with the red:blue light ratio, the differences in them between 50R:50B and 75R:25B treatments were greater than those between 25R:75B and 50R:50B, and there was no significant difference in these parameters among the treatments. The root FW, root DW, and root/shoot ratio of 75R:25B treatments were the highest and significantly greater than those of the other two treatments. Both the shoot DW/FW and specific leaf FW were the lowest under the 50R:50B treatment, but the differences among treatments were not significant.

Ascorbate Pool

In general, under continuous light with different red:blue light ratios, the T-AsA, AsA, and DHA contents in lettuce leaves showed positive correlations with the ratio of blue light (**Figure 2**). Compared to the 75R:25B treatment, the T-AsA content of 25R:75B increased by 14.4∼25.8%. The differences in T-AsA content in lettuce between 25R:75B and 75R:25B treatments reached a significant level during the whole experiment. There was no significant difference in T-AsA content between 50R:50B and 75R:25B as well as 25R:75B and 50R:50B. The differences in T-AsA content between 25R:75B and 50R:50B were greater than those between 50R:50B and 75R:25B. There was no significant difference in the AsA and DHA contents among treatments except on day 3, when the AsA content under the 25R:75B treatment was significantly higher than that under the 75R:25B treatment. In addition, the change tendencies of the AsA levels in lettuce under the 25R:75B and 75R:25B treatments remained relatively stable. However, under the 50R:50B treatment, the AsA and DHA contents continuously decreased and increased from day 3 to day 9, respectively, which resulted in the decline of the AsA/T-AsA ratio at the same time. The AsA/T-AsA ratio of 75R:25B treatment was the highest among treatments on day 6 and 9, but red:blue light ratio had no significant effect on AsA/T-AsA ratio (**Table 3**).

Ascorbate Biosynthesis

Changes in the expression of several critical AsA biosynthetic genes (*GMP*, *GME*, *GGP*, *GPP*, and *GLDH*) and the activity of the last synthetase (GLDH) in response to continuous light at different red:blue light ratios were analyzed in lettuce (**Figure 3**). The expression of the abovementioned genes in lettuce leaves was upregulated by the 25R:75B treatment on day 3, but they nearly increased 2∼3-fold from day 3 to day 9 under the other two treatments, resulting in a greater transcript level than that under

TABLE 2 | The shoot fresh weight (FW), shoot dry weight (DW), shoot DW/FW, root/shoot ratio, leaf area, and specific leaf FW of lettuce plants grown under continuous light (200 $\mu mol \cdot m^{-2} \cdot s^{-1}$) with different red:blue ratios.

Treatments	Shoot FW (g)	Shoot DW (g)	Shoot DW/FW (%)	Root FW	Root DW	Root/shoot ratio	Leaf area (dm^2)	Specific leaf FW (g/dm^2)
25R:75B	88.5 b	2.98 a	3.40 a	8.5b	0.44b	0.149 b	11.10 a	4.13 a
50R:50B	94.2 ab	3.02 a	3.25 a	8.7b	0.46b	0.151 b	11.75 a	4.07 a
75R:25B	99.5 a	3.55 a	3.36 a	11.0a	0.62a	0.187 a	12.70 a	4.23 a

The samples were taken on the 12th day after treatment. Values are the means of five replicates. Different letters indicate significant differences between different treatments at $p < 0.05$ according to the Tukey test.

TABLE 3 | *P*-values of the two-way ANOVA for the effects of light treatments (Light) and days of light treatments (Day) on the physiological parameters.

	T-AsA	AsA	DHA	AsA/T-AsA	GalLDH	APX	MDHAR	DHAR	GR	H_2O_2	MDA
$P_{(Light)}$	**	**	*	ns	ns	**	**	**	**	**	*
$P_{(Day)}$	ns	ns	ns	ns	*	**	**	ns	**	**	**
$P_{(Light \times Day)}$	ns	ns	ns	ns	ns	ns	*	ns	ns	*	ns

*Non-significant (ns) indicates $p > 0.05$, * and ** indicate significant at $p \leq 0.05$ and 0.01, respectively.*

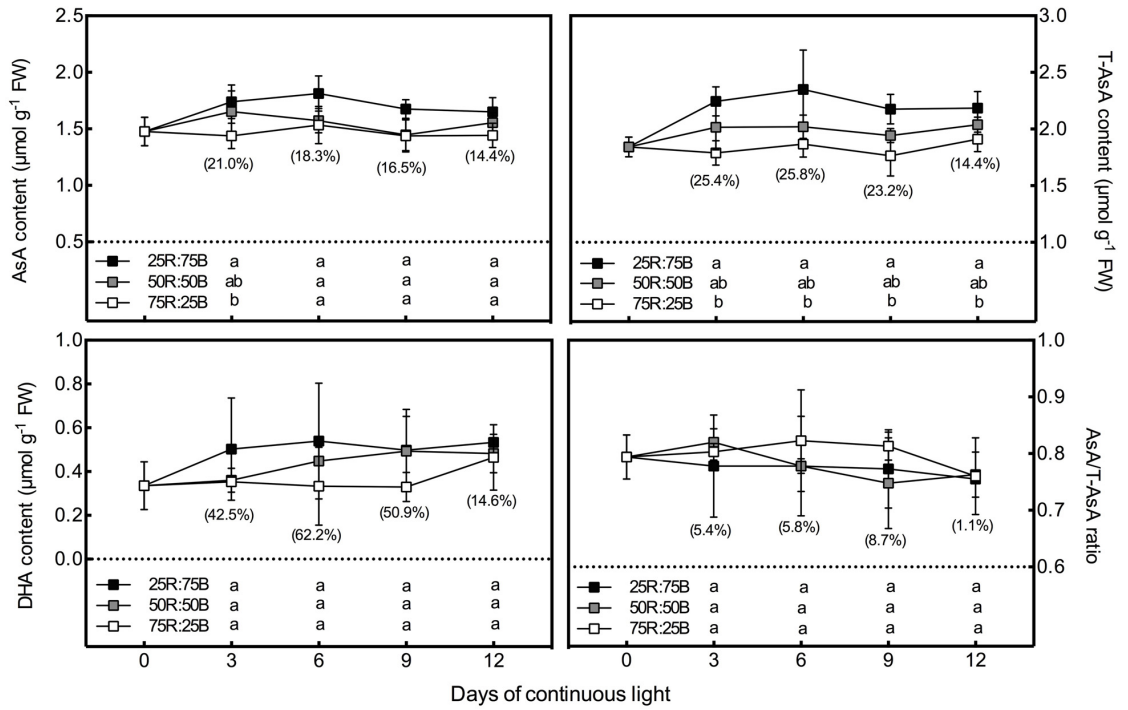

FIGURE 2 | Effects of the red:blue light ratio on the total ascorbate (T-AsA), ascorbate (AsA) and dehydroascorbate (DHA) contents as well as the AsA/T-AsA ratio in lettuce leaves under continuous light (200 $\mu mol \cdot m^{-2} \cdot s^{-1}$). Values and bars represent the means of four replicates ± SD. Different letters in the same column indicate significant differences at the $p < 0.05$ level according to Tukey test. Data in brackets were the increasing rate of the maximum value to the minimum value on the same day.

the 25R:75B treatment on day 9. Unlike gene expression, GLDH activity presented little response to the red:blue light ratio under continuous light. There was no significant difference in GLDH activity among treatments.

Ascorbate Oxidation and Reduction (Ascorbate-Glutathione Cycle)

As shown in **Figure 4**, the changes in the gene expression levels and activities of enzymes involved in AsA oxidation and reduction in response to the red:blue light ratio under continuous light were analyzed. Similar to the biosynthetic genes, all the genes we investigated that involved in AsA oxidation (*APX 1*, *APX 2*) and reduction (*DHAR 1*, *DHAR 2*, *MDHAR 1*, *MDHAR 2*, *MDHAR 3*, *GR 1*, and *GR 2*) were more highly expressed under the 25R:75B treatment on day 3. The transcript levels of *APX 1*, *APX 2*, *DHAR 1*, *MDHAR 2*, *MDHAR 3*, *GR 1*, and *GR 2* under the 50R:50B and 75R:25B treatments showed much greater increases than those under the 25R:75B treatment from day 3 to day 9;

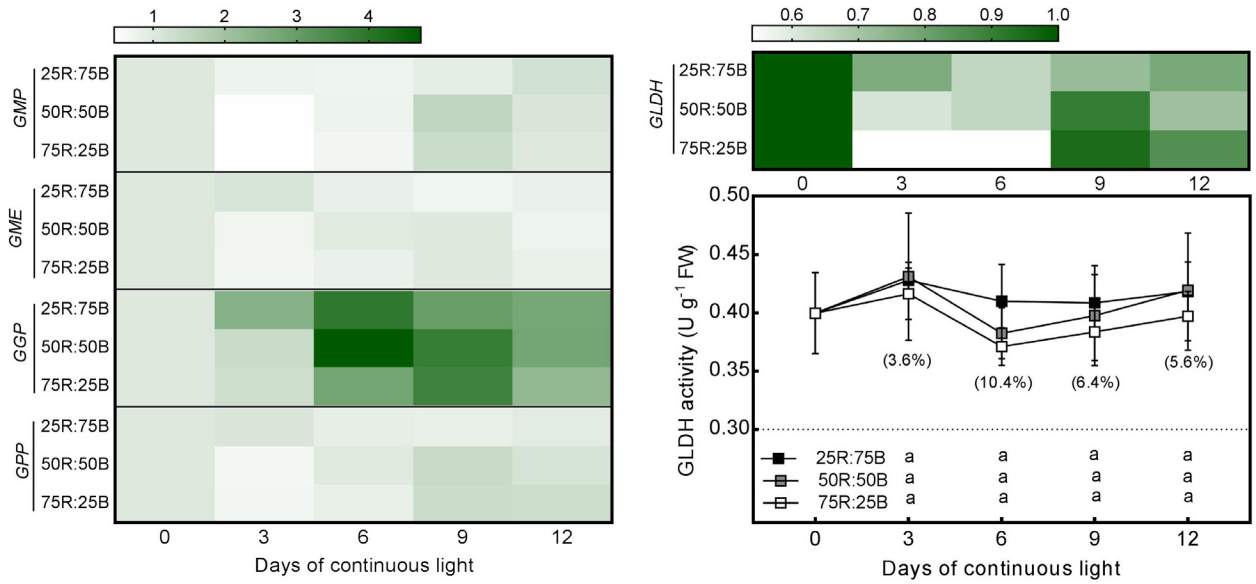

FIGURE 3 | Effects of the red:blue light ratio on the transcript level of enzymes involved in the AsA biosynthesis pathway and activity of L-galactono-1,4-lactone dehydrogenase (GalLDH) in lettuce leaves under continuous light (200 200 μmol·m^{-2}·s^{-1}). Transcript level data are the mean values of three replications. Enzyme activity data are the mean values ± SD of four replications. Different letters indicate significant differences between different red:blue light ratio treatments at $p < 0.05$ according to Tukey test. Data in brackets were the increasing rate of the maximum value to the minimum value on the same day.

thus, the expression levels of these genes were lowest under the 25R:75B treatment on day 9.

The change tendencies of APX and GR activities with time and the differences in their activities among treatments were quite similar (**Figures 4A,B**). Activities of APX and GR in all treatments decreased gradually with time during the first 9 days. They decreased most rapidly under the 75R:25B treatment and slowest under the 25R:75B treatment. Therefore, the APX and GR activities had a positive correlation with the blue light levels on day 6 and day 9, and the differences in their activity between the 75R:25B and 25R:75B treatments reached a significant level. During the whole experimental period, the MDHAR activity of lettuce leaves grown under continuous light remained the lowest and the highest under the 75R:25B and 25R:75B treatments, respectively, and the difference between the LL and HL leaves reached a significant level on day 6 and day 9 (**Figure 4C**). The DHAR activity in the 75R:25B treatment also remained at the lowest level and was significantly lower than that in the 25R:75B treatment, except on day 6 (**Figure 4D**).

H_2O_2 and MDA Content

Figure 5 shows that there was a significant positive correlation between the H_2O_2 content in lettuce leaves and the ratio of blue light. The H_2O_2 content of the 25R:75B treatment was significantly higher than that of the 75R:25B treatment during the whole test period, and the difference in H_2O_2 between the 75R:25B and 50R:50B treatments reached a significant level on days 6 and 9. The content of H_2O_2 in the 25R:75B and 50R:50B treatments increased constantly with time during the first 9 days but decreased obviously from days 9 to 12. However, the H_2O_2 content was maintained at a relatively stable level under the 75R:25B treatment. Compared with H_2O_2, the red:blue light ratio had no significant influence on the MDA content during the first 9 days. As the MDA content under the 75R:25B treatment increased constantly from day 3 to day 12, it was significantly higher than that of the 50R:50B treatment on day 12.

Correlation Analysis and Principal Components Analysis

The correlation coefficients among the indexes of AsA pool levels and enzymes activities, analyzed by Pearson's correlation are listed in **Table 4**. Among the five enzymes involved in AsA metabolism, GLDH activity was not correlated with AsA pool levels, including T-AsA, AsA, and DHA. Activities of MDHAR, DHAR, and GR had significant correlations with both T-AsA and AsA levels, while APX activity only had a significant correlation with AsA level. Meanwhile, APX activity had an extremely strong correlation with GR activity. The biplot (**Figure 6**) of PCA results showed that AsA pool levels and enzymes activities were negatively related to PC1, while the AsA/T-AsA was positively related to PC1. In general, the points of different light treatments were mainly separated along PC1.

DISCUSSION

Continuous Light With a High Red:Blue Ratio Is Conducive to Lettuce Growth

Red light and blue light are the most important light spectra for plants, as their photosynthetic relative quantum efficiencies are much greater than those of other light spectra (McCree, 1972; Stutte, 2009). Many studies have focused on the effects of

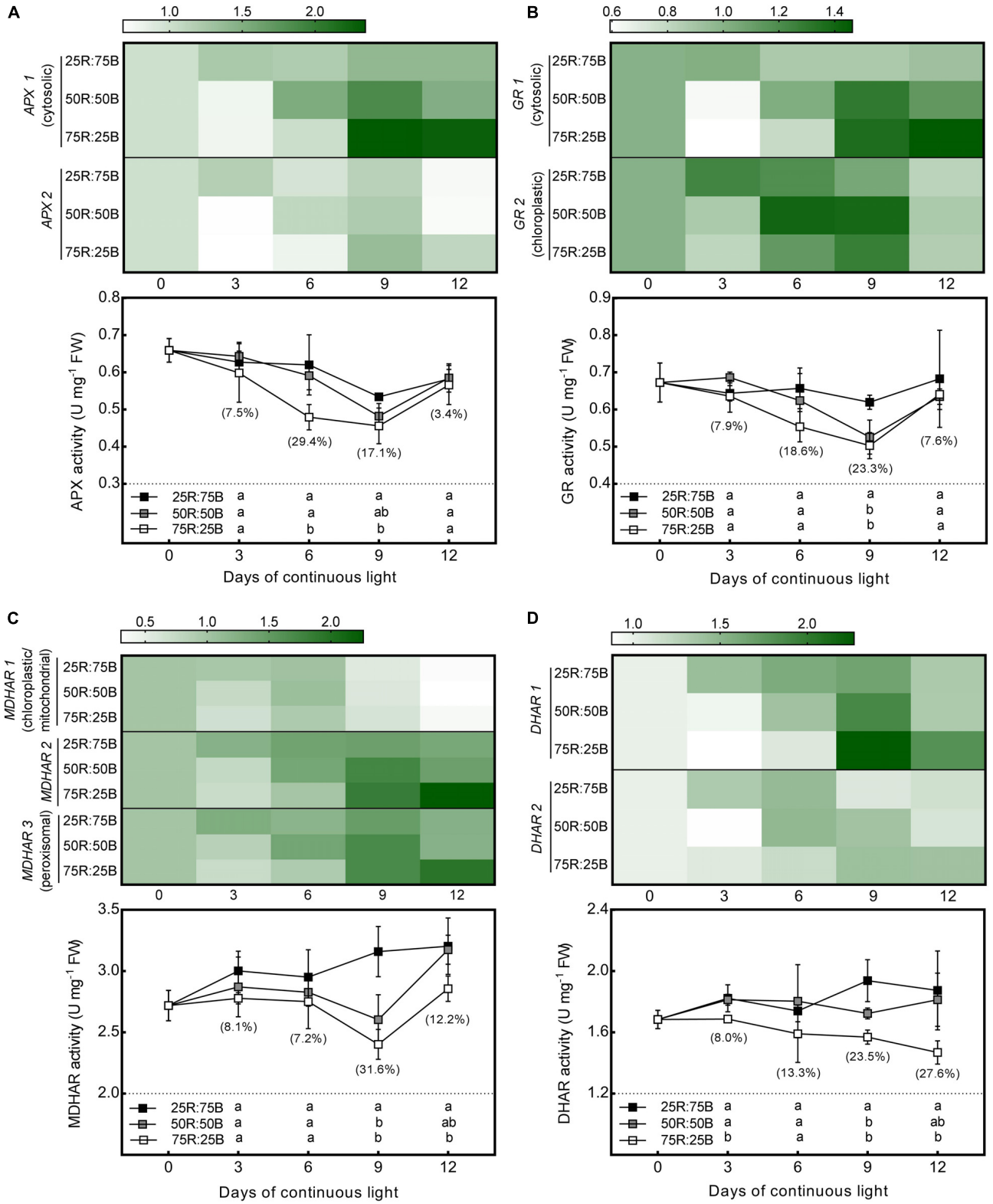

FIGURE 4 | Effects of the red:blue light ratio on the transcript level and activity of APX **(A)**, GR **(B)**, MDHAR **(C)**, DHAR **(D)** in lettuce leaves under continuous light (200 $\mu mol \cdot m^{-2} \cdot s^{-1}$). Transcript level data are the mean values of three replications. Enzyme activity data are the mean values ± SD of four replications. Different letters indicate significant differences between different red:blue light ratio treatments at $p < 0.05$ according to Tukey test. Data in brackets were the increasing rate of the maximum value to the minimum value on the same day.

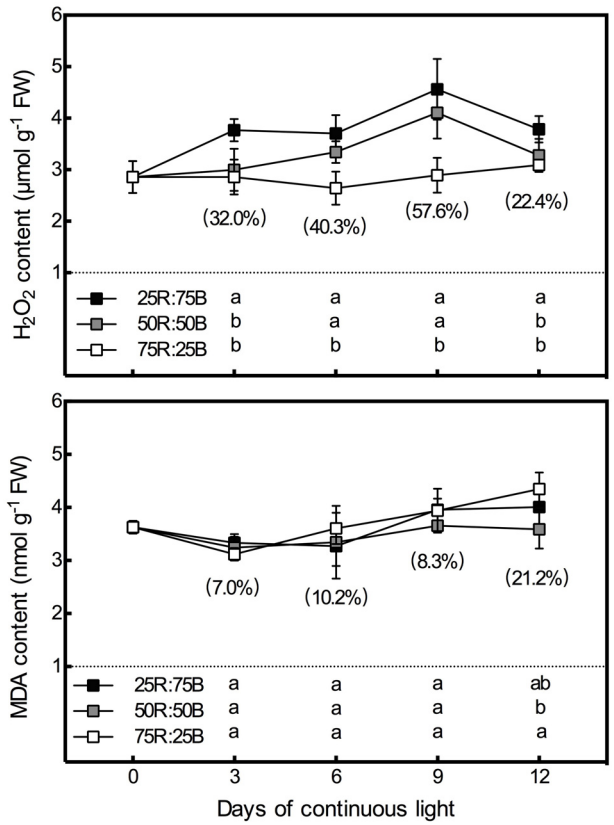

FIGURE 5 | Effects of the red:blue light ratio on the H_2O_2 and MDA contents in lettuce leaves under continuous light (200 μmol·m^{-2}·s^{-1}) (200 μmol·m^{-2}·s^{-1}). Data are the mean values ± SD of four replications. Different letters indicate significant differences between different red:blue light ratio treatments at $p < 0.05$ according to Tukey test. Data in brackets were the increasing rate of the maximum value to the minimum value on the same day.

the red:blue light ratio on the growth of vegetables, including lettuce, which is the main plant species cultivated in plant factories. Although the optimal ratio of red:blue light for lettuce growth was not unified due to various varieties and environment factors, most studies have shown that light spectrum with a predominating portion of red light (e.g. 75∼90%) is more conducive to increasing lettuce biomass under a normal photoperiod (Cope et al., 2014; Wang et al., 2016). Our results indicated that this phenomenon also emerged under continuous light. This is because red light has higher relative quantum efficiency than blue light (McCree, 1972; Stutte, 2009), and photosynthetic capacity will be decreased when the proportion of blue light exceeds 50%, even though moderate blue light (e.g. 7%) is essential for preventing dysfunctional photosynthesis under pure red light (Hogewoning et al., 2010). The positive correlation between biomass and red light ratio partly related to leaf area which also positively correlated with red light ratio, since high level of blue light inhibits leaf area expansion (Bugbee, 2016). Root elongation is also inhibited by excessive blue light (Oyaert et al., 1999; Spalding and Folta, 2005), the root FW, root DW, and root/shoot ratio in the present study were significantly elevated by 75R:25B treatment. It has been reported that red light and blue light regulate root growth by affecting the distribution of phytchormones (Drozdova et al., 2001). Overall, continuous light with high ratio of red light can elevate lettuce photosynthetic efficiency and photosynthetic products synthesis, while promote transportation of photosynthetic products from shoot to root. Vigorous roots in turn supply more water and mineral nutrition for shoot growth.

Continuous Light With a Low Red:Blue Ratio Is Conducive to AsA Accumulation in Lettuce

Previous studies have indicated that long-wavelength light (e.g. red light) is conducive to the growth of plants, while short-wavelength light (e.g. blue light, UV A) is conducive to the promotion of nutritional quality through stimulating the accumulation of secondary metabolites, such as ascorbate, flavonoids, and anthocyanins (Li and Kubota, 2009; Ren et al., 2014). Consistent with previous results, our results indicate that although lettuce gained greater biomass under the higher red:blue light ratio (75R:25B), the ascorbate pool was improved by the higher ratio of blue light (25R:75B) with the same total light intensity. The more effective impact of blue light than red light on enhancing the AsA content in the juice sacs of citrus fruits (Zhang et al., 2015) and oat leaves

TABLE 4 | Pearson's correlation coefficients among the AsA pool sizes and enzyme activities in lettuce exposed to continuous light of different red:blue ratios.

	T-AsA	AsA	DHA	AsA/T-AsA	GLDH	APX	MDHAR	DHAR	GR
T-AsA	1								
AsA	0.93**	1						0.9∼1.0	
DHA	0.82**	0.55	1					0.8∼0.9	
AsA/T-AsA	−0.43	−0.08	−0.87**	1				0.7∼0.8	
GLDH	0.5	0.48	0.37	−0.2	1			0.6∼0.7	
APX	0.56	0.59*	0.33	−0.09	0.75**	1		0.5∼0.6	
MDHAR	0.71**	0.62*	0.65*	−0.44	0.58*	0.58*	1		
DHAR	0.66*	0.64*	0.49	−0.27	0.56	0.44	0.68*	1	
GR	0.58*	0.59*	0.41	−0.18	0.71**	0.92**	0.77**	0.47	1

*Correlation was significant at *$p < 0.05$; **$p < 0.01$. The deeper the color is, the greater the correlation coefficient.*

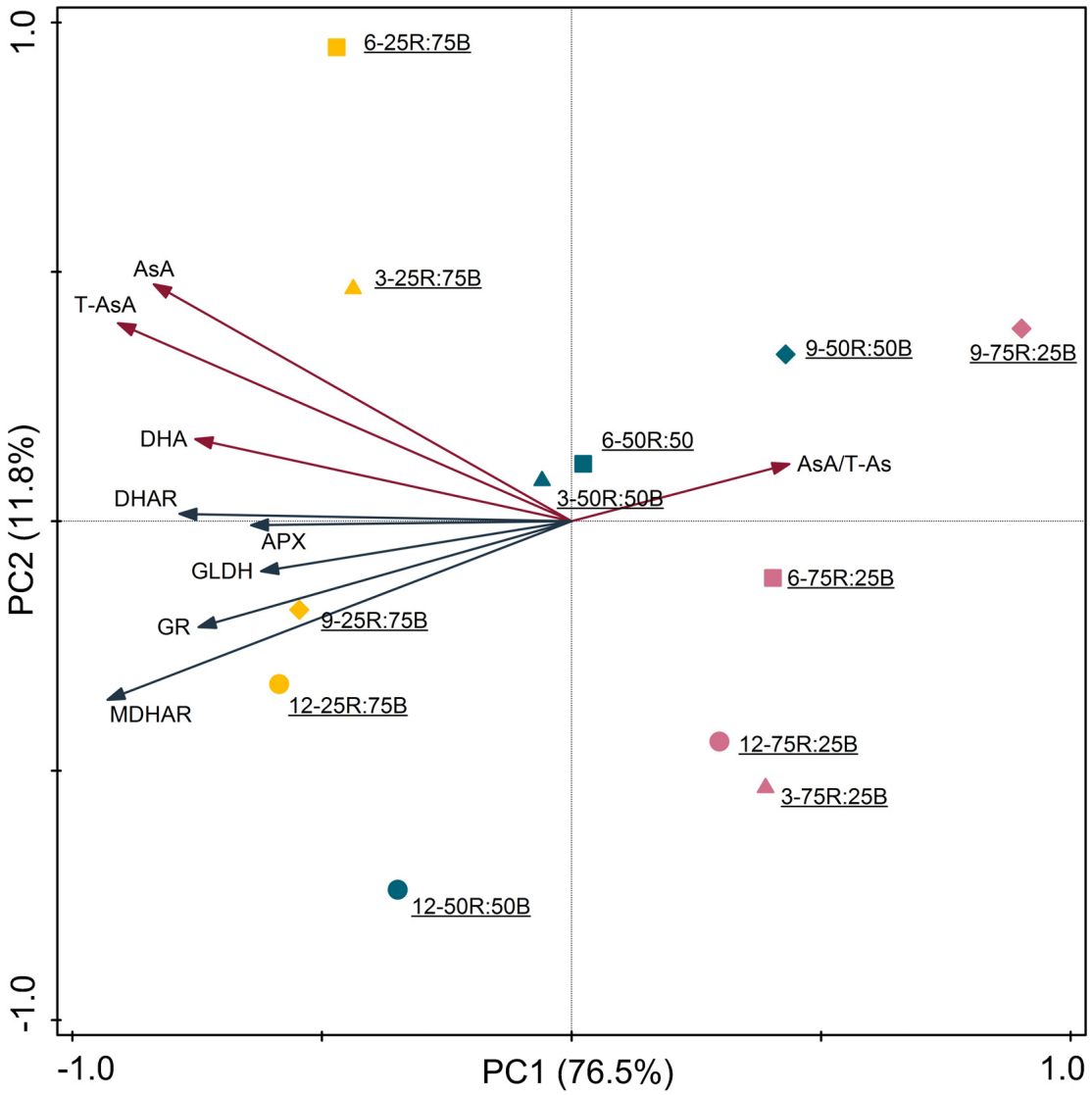

FIGURE 6 | Principal component analysis of AsA pool sizes and enzyme activities in lettuce leaves under continuous light of different red:blue ratios (yellow symbol-25R:75B; blue symbol-50R:50B; red symbol-75R:25B) on different days (△–day 3; □–day 6, ◇–day 9,◯–day 12). Biplot of the first two principal components (PC1,2) of the measured network topological properties.

(Mastropasqua et al., 2012) has also been proposed. Some studies have shown that the opposite result also occurred under some conditions. For instance, Ma et al. (2014) found that red light was more effective than blue light in suppressing AsA reduction in postharvest broccoli. This might be related to the greater APX activity under blue light. Furthermore, some previous studies have suggested that photochromes and blue-light photoreceptors are involved in the regulation of AsA metabolism by red and blue light (Bienger and Schopfer, 1970; Bartoli et al., 2009; Mastropasqua et al., 2012). There is a coaction between phytochrome and blue-light photoreceptors, as the former can absorb blue light and the latter can modulate responsiveness to the active form of phytochrome (Mohr, 1994; Mastropasqua et al., 2012).

Continuous Light With a Low Red:Blue Ratio Improves AsA Accumulation by Promoting AsA Regeneration Rather Than Biosynthesis

To clarify the contribution of AsA biosynthesis and regeneration process to the promoting effect of blue light on AsA content, the gene expression levels and enzyme activities of several enzymes involved in these processes were investigated in the present study. In the AsA biosynthesis pathway, the transcript levels of *GMP*, *GME*, *GGP*, *GPP*, and *GLDH* were all upregulated by the 25R:75B treatment on day 3. Among these genes, *GGP* and *GLDH* presented the greatest and lowest responses to light treatments, respectively, which were 1.94

and 1.43-fold more expressed under 25R:75B compared to 75R:25B treatment. While the red:blue light ratio had no significant effect on GLDH activity (**Figure 3**). These results illustrated that the contribution of biosynthesis to the AsA increase under high ratio of blue light was limited, and they also demonstrated that, compared to *GMP*, *GME*, *GGP*, and *GPP*, GLDH expression and activity were not limiting, as reported by previous research (Alhagdow et al., 2007; Massot et al., 2013). Inconsistent changes of biosynthetic gene expression and GLDH activity had been proposed in several previous studies (Pignocchi et al., 2003; Mastropasqua et al., 2012). The mechanism driving this phenomenon must be complicated. Besides the posttranscriptional regulation, there are other mechanisms that could modulate GLDH activity directly, such as redox regulation (Bartoli et al., 2005; Leferink et al., 2009). Another result about biosynthesis process that needs to be noted was that *GGP* showed the greatest response to not only the red:blue light ratio but also to continuous light. A similar observation has been reported in Arabidopsis grown under continuous light (Yabuta et al., 2007). According to many previous studies, *GGP* was recognized as a key control gene in AsA metabolism, as it exhibited great differences among different environmental conditions, including different light conditions (Yabuta et al., 2007; Li et al., 2013).

For the AsA regeneration process, on the one hand, the increase in MDHAR, DHAR, and GR activities and gene transcription levels can theoretically promote AsA accumulation as they catalyze the reduction of DHA and MDHA. On the other hand, although the increase of APX activity consume more AsA, it also elevates AsA regeneration efficiency with the improvement of MDHAR and DHAR activities. In a previous study, *CitAPX3*, *CitchAPX*, *CitMDHAR1*, *CitMDHAR2*, *CitDHAR2*, *CitGR*, and *CitchGR* genes expression level along with AsA content were greater under blue LED light than dark conditions in citrus juice sacs (Zhang et al., 2015). Similar to the previous study, the expression levels of *APX1*, *APX2*, *MDHAR 1*, *MDHAR 2*, *MDHAR 3*, *DHAR 1*, *DHAR 2*, *GR 1*, and *GR 2* were all upregulated by the 25R:75B treatment on day 3. The significant higher activities of APX, MDHAR, DHAR, and GR under 25R:75B were observed subsequently. According to previous studies, increases in AsA content were often accompanied by increased APX, MDHAR, DHAR, and GR activities and gene expression levels, especially under some stress conditions (Mastropasqua et al., 2012; Gallie, 2013; Zha et al., 2019a). These results indicate that the maintenance of greater AsA levels under continuous light with a low red:blue ratio was attributed to the upregulated activities and gene expressions of enzymes involved in AsA regeneration rather than biosynthesis.

Notably, if we formulate conclusions only based on gene expression, we might mistakenly infer that AsA synthesis also contributes to the greater AsA levels induced by the continuous light with a higher ratio of blue light. In fact, during the process of the expression of a particular gene, the relationships among mRNA, protein content, and enzyme activity are quite complicated, and their correlations are often not obvious and not entirely recognized in plants (Veìlez-Bermuìdez and Schmidt, 2014; Liu et al., 2016; Szymanska et al., 2017).

Regulation of Red:Blue Ratio on AsA Under Continuous Light Correlates With Oxidative Stress

In addition to AsA, the levels of several other antioxidants were also elevated by blue light, such as carotene (Ma et al., 2012), anthocyanins, and flavonoids (Li and Kubota, 2009; Ren et al., 2014). Furthermore, the enzymes involved in AsA regeneration are substantial components of enzymatic antioxidant system. This demonstrates that regulation of red:blue ratio on AsA correlates with oxidative stress under continuous light. Although continuous light (200 $\mu mol \cdot m^{-2} \cdot s^{-1}$, 15 days) didn't induce leaf injury on lettuce in our previous study, it increased photo-oxidative pressure, which was characterized by enhanced ROS content and antioxidant activity (Zha et al., 2019b). Additionally, it had been reported that high ratio of blue light aggravated continuous light induced injury on tomato (Demers and Gosselin, 2002). In the present study, the H_2O_2 content presented a positive correlation with the ratio of blue light during the whole experiment. Thus AsA pool size, as well as the activities and gene expressions of APX, DHAR, MDHAR, and GR activity were activated by the high ratio of blue light to synergistically repress H_2O_2 generation and prevent cell oxidation. Photo-oxidative effect of continuous light with low red:blue ratio might due to the higher energy of blue light than red light at the same photon flux density. It has been reported that the gene expression and activity of AsA regeneration enzymes were activated by various environmental stresses (Haghjou et al., 2009; Gill and Tuteja, 2010), including photo-oxidative stress (Karpinski et al., 1999). Surprisingly, inconsistent with the H_2O_2 content, the MDA content was significantly higher under the 75R:25B treatment on day 12, indicating more severe membrane lipid peroxidation. This might be correlated with the greater amount and size of starch grains under 75R:25B treatment. Excessive starch accumulation under continuous light causes damage to the chloroplast structure (Aro and Valanne, 1979; Gestel et al., 2005). Thus, reactive oxygen species will leak from chloroplasts and cause severe membrane lipid peroxidation. In addition, it has been demonstrated that continuous light-induced leaf chlorosis was correlated with the starch accumulation (Haque et al., 2015).

Regulation of Red:Blue Light Ratio on AsA Regeneration Related Gene Expression Depending on the Cell Compartment

Previous studies have confirmed that AsA recycling process occurs in several subcellular compartments, including mitochondria, chloroplasts, peroxisomes and cytosol (Koshiba, 1993; Yamaguchi et al., 1995; Jimenez et al., 1997), and each enzyme involved in AsA cycling has several isoenzymes (Smirnoff, 2011). In previous cases, different isoforms of APX, DHAR, MDHAR, and GR often showed different gene expression patterns or activities (Nishikawa et al., 2003; Gallie, 2013;

Cocetta et al., 2014). In the present study, the transcription levels of genes encoding for different isoforms of these four enzymes were all up-regulated by 25R:75B on day 3. Different expression pattern of isoenzymes mainly emerged in the later experimental stage. According this, genes encoding different isoenzymes could be divided into two groups: chloroplast and others (cytosol, peroxisomal, and unidentified). Expression level of two chloroplast group genes (*MDHAR 1* and *GR 2*) under all treatments decreased sharply in the later experimental stage. By contrast, the cytosolic isoforms (*APX1* and *GR1*) presented greater responses to red:blue light ratio, meanwhile, the expression patterns of other unidentified isoforms were very similar with cytosolic isoforms. Nishikawa et al. (2003) also found transcription of AsA regeneration enzymes in harvested broccoli florets were inactivated in chloroplasts, but not in the cytosol, which might attribute to the excess generation of ROS in chloroplast under stress (Mano et al., 2001; Nishikawa et al., 2003). Moreover, H_2O_2 leaks from chloroplasts and peroxisomes into the cytosol, leading to the high demand of cytosol for AsA to protect the cells from oxidative damage (Nishikawa et al., 2003), oxidized AsA (MDHA and DHA) is then transported into the cytosol for reduction to AsA (Takahama, 2004). These demonstrated that AsA regeneration in cytosol takes on more and longer responsibility to defense stress than that in chloroplast. In addition, another interesting result in the present study is that expression levels of all genes except chloroplastic isoforms (*MDHAR 1* and *GR 2*) under the 50R:50B and 75R:25B treatments presented remarkable increases after day 3 and reached higher levels than those under the 25R:75B treatment. This demonstrated that the influence of the red:blue light ratio on AsA metabolism has the potential to reverse after 12 days of continuous light.

CONCLUSION

In summary, a high ratio of red light was effective for enhancing the biomass and growth of hydroponic lettuce under continuous light, while the AsA pool size was elevated by a high ratio of blue light. According to the responses of gene expression and the activity of enzymes involved in AsA biosynthesis and regeneration, we concluded that the AsA regeneration process contributed more to AsA accumulation under continuous light with high ratio of blue light than biosynthesis. Since the high ratio of blue light has little influence on the activity of the final AsA synthase (GLDH), though it enhances the transcript level of genes involved in AsA biosynthesis. The response of the AsA metabolism to the blue light level at the gene expression level occurred earlier than the response at the enzymatic level. To have an integrative consideration, applying continuous light with a high ratio of red light for prophase cultivation and continuous light with a high ratio of blue light for preharvest irradiation will be conducive for both yield and quality.

DATA AVAILABILITY STATEMENT

The datasets generated for this study are available on request to the corresponding author.

AUTHOR CONTRIBUTIONS

WL was the recipient of funds. WL and LZ conceived the experiment. LZ, YZ, CZ, and MS prepared the plant materials, collected samples, and undertook experiments. LZ analyzed the data and prepared the manuscript. All authors contributed to the manuscript revision.

FUNDING

This research was financed by the National Natural Science Foundation of China (NSFC) (No. 31672202) and Central Public-interest Scientific Institution Basal Research Fund (No. BSRF201711).

SUPPLEMENTARY MATERIAL

The Supplementary Material for this article can be found online at: https://www.frontiersin.org/articles/10.3389/fpls.2020.00704/full#supplementary-material

REFERENCES

Alhagdow, M., Mounet, F., Gilbert, L., Nunes-Nesi, A., Garcia, V., Just, D., et al. (2007). Silencing of the mitochondrial ascorbate synthesizing enzyme L-galactono-1,4-lactone dehydrogenase affects plant and fruit development in tomato. *Plant Physiol.* 145, 1408–1422. doi: 10.1104/pp.107.106500

Aro, E. M., and Valanne, N. (1979). Effect of continous Light on CO2 fixation and chloroplast structure of the mosses *Pleurozium schreberi* and *Ceratodon purpureus*. *Physiol. Plant* 45, 460–466. doi: 10.1111/j.1399-3054.1979.tb02614.x

Bartoli, C. G., Guiamet, J. J., Kiddle, G., Pastori, G. M., Di Cagno, R., Theodoulou, F. L., et al. (2005). Ascorbate content of wheat leaves is not determined by maximal l-galactono-1,4-lactone dehydrogenase (GalLDH) activity under drought stress. *Plant Cell Environ.* 28, 1073–1081. doi: 10.1111/j.1365-3040.2005.01338.x

Bartoli, C. G., Tambussi, E. A., Diego, F., and Foyer, C. H. (2009). Control of ascorbic acid synthesis and accumulation and glutathione by the incident light red/far red ratio in Phaseolus vulgaris leaves. *FEBS Lett.* 583, 118–122. doi: 10.1016/j.febslet.2008.11.034

Bartoli, C. G., Yu, J., Gómez, F., Fernández, L., McIntosh, L., and Foyer, C. H. (2006). Inter-relationships between light and respiration in the control of ascorbic acid synthesis and accumulation in *Arabidopsis thaliana* leaves. *J. Exp. Bot.* 57, 1621–1631. doi: 10.1093/jxb/erl005

Bienger, I., and Schopfer, P. (1970). Photomodulation by phytochrome of the rate of accumulation of ascorbic acid in mustard seedlings (*Sinapis alba* L.). *Planta* 93, 152–159. doi: 10.1007/BF00387122

Brennan, T., and Frenkel, C. (1977). Involvement of hydrogen peroxide in the regulation of senescence in pear. *Plant Physiol.* 59, 411–416. doi: 10.1104/pp.59.3.411

Bugbee, B. (2016). Towards an optimal spectral quality for plant growth and development: the importance of radiation capture. *Acta Hortic.* 1134, 1–12.

Campos, F. M., Ribeiro, S. M. R., Della Lucia, C. M., Pinheiro-Sant'Ana, H. M., and Stringheta, P. C. (2009). Optimization of methodology to analyze ascorbic

and dehydroascorbic acid in vegetables. *Química Nova* 32, 87–91. doi: 10.1590/S0100-40422009000100017

Chen, X., Xue, X., Guo, W., Wang, L., and Qiao, X. (2016). Growth and nutritional properties of lettuce affected by mixed irradiation of white and supplemental light provided by light-emitting diode. *Sci. Hortic.* 200, 111–118. doi: 10.1016/j.scienta.2016.01.007

Cocetta, G., Baldassarre, V., Spinardi, A., and Ferrante, A. (2014). Effect of cutting on ascorbic acid oxidation and recycling in fresh-cut baby spinach (*Spinacia oleracea* L.) *leaves*. *Postharvest Biol. Technol.* 88, 8–16. doi: 10.1016/j.postharvbio.2013.09.001

Cope, K. R., Snowden, M. C., and Bugbee, B. (2014). Photobiological interactions of blue light and photosynthetic photon flux: effects of monochromatic and broad-spectrum light sources. *Photochem. Photobiol.* 90, 574–584. doi: 10.1111/php.12233

Davey, M. W., Van Montagu, M., Inzed, D., Sanmartin, M., Kanellis, A., Smirnoff, N., et al. (2000). Plant L-ascorbic acid: chemistry, function, metabolism, bioavailability and effects of procession. *J. Sci. Food Agric.* 80, 825–860.

Demers, D. A., and Gosselin, A. (2002). Growing greenhouse tomato and sweet pepper under supplemental lighting: optimal photoperiod, negative effects of long photoperiod and their causes. *Acta Hort.* 580, 83–88.

Drozdova, I. S., Bondar, V. V., Bukhov, N. G., Kotov, A. A., Kotova, L. M., Maevskaya, S. N., et al. (2001). Effects of light spectral quality on morphogenesis and source–sink relations in radish plants. *Russ. J. Plant Physl.* 48, 415–420. doi: 10.1023/a:1016725207990

Dutta Gupta, S. (2017). *Light-Emitting Diodes (LEDs) for Improved Nutritional Quality. Light Emitting Diodes for Agriculture: Smart Lighting*. Cham: Springer, doi: 10.1007/978-981-10-5807-3

Gallie, D. R. (2013). The role of L-ascorbic acid recycling in responding to environmental stress and in promoting plant growth. *J. Exp. Bot.* 64, 433–443. doi: 10.1093/jxb/ers330

Gestel, N. C., Nesbit, A. D., Gordon, E. P., Green, C., Pare, P. W., Thompson, L., et al. (2005). Continuous light may induce photosynthetic downregulation in onion-consequences for growth and biomass partitioning. *Physiol. Plant* 125, 235–246. doi: 10.1111/j.1399-3054.2005.00560.x

Gill, S. S., and Tuteja, N. (2010). Reactive oxygen species and antioxidant machinery in abiotic stress tolerance in crop plants. *Plant Physiol. Biochem.* 48, 909–930. doi: 10.1016/j.plaphy.2010.08.016

Haghjou, M. M., Shariati, M., and Smirno, N. (2009). The effect of acute high light and low temperature stresses on the ascorbate–glutathione cycle and superoxide dismutase activity in two *Dunaliella salina* strains. *Physiol. Plant* 135, 272–280. doi: 10.1111/j.1399-3054.2008.01193.x

Haque, M. S., Kjaer, K. H., Rosenqvist, E., and Ottosen, C.-O. (2015). Continuous light increases growth, daily carbon gain, antioxidants, and alters carbohydrate metabolism in a cultivated and a wild tomato species. *Front. Plant Sci.* 6:522. doi: 10.3389/fpls.2015.00522

Hogewoning, S. W., Trouwborst, G., Maljaars, H., Poorter, H., van Ieperen, W., and Harbinson, J. (2010). Blue light dose-responses of leaf photosynthesis, morphology, and chemical composition of *Cucumis sativus* grown under different combinations of red and blue light. *J. Exp. Bot.* 61, 3107–3117. doi: 10.1093/jxb/erq132

Jimenez, A., Hernandez, J. A., Del Riìo, L. A., and Sevilla, F. (1997). Evidence for the presence of the ascorbate-glutathione cycle in mitochondria and peroxisomes of pea leaves. *Plant Physiol.* 114, 275–284. doi: 10.1104/pp.114.1.275

Karpinski, S., Reynolds, H., Karpinska, B., Wingsle, G., Creissen, G., and Mullineaux, P. (1999). Systemic signaling and acclimation in response to excess excitation energy in *Arabidopsis*. *Science* 284, 654–657. doi: 10.1126/science.284.5414.654

Koshiba, T. (1993). *Cytosolic ascorbate* peroxidase in seedlings and leaves of maize (*Zea mays*). *Plant Cell Physiol.* 34, 713–721. doi: 10.1093/oxfordjournals.pcp.a078474

Leferink, N. G. H., Van Duijn, E., Barendregt, A., Heck, A. J. R., and Van Berkel, W. J. H. (2009). Galactonolactone dehydrogenase requires a redox-sensitive thiol for optimal production of vitamin C. *Plant Physiol.* 150, 596–605. doi: 10.1104/pp.109.136929

Li, J., Liang, D., Li, M., and Ma, F. (2013). Light and abiotic stresses regulate the expression of GDP-L-galactose phosphorylase and levels of ascorbic acid in two kiwifruit genotypes via light-responsive and stress-inducible cis-elements in their promoters. *Planta* 238, 535–547. doi: 10.1007/s00425-013-1915-z

Li, Q., and Kubota, C. (2009). Effects of supplemental light quality on growth and phytochemicals of baby leaf lettuce. *Environ. Exp. Bot.* 67, 59–64. doi: 10.1016/j.envexpbot.2009.06.011

Lin, K. H., Huang, M. Y., Huang, W. D., Hsu, M. H., Yang, Z. W., and Yang, C. M. (2013). The effects of red, blue, and white light-emitting diodes on the growth, development, and edible quality of hydroponically grown lettuce (*Lactuca sativa* L. var. capitata). *Sci. Hortic.* 150, 86–91. doi: 10.1016/j.scienta.2012.10.002

Liu, Y., Beyer, A., and Aebersold, R. (2016). On the dependency of cellular protein levels on mRNA abundance. *Cell* 165, 535–550. doi: 10.1016/j.cell.2016.03.014

Livak, K. J., and Schmittgen, T. D. (2001). Analysis of relative gene expression data using real-time quantitative PCR and the 2-ΔΔCt method. *Methods* 25, 402–408. doi: 10.1006/meth.2001.1262

Ma, G., Zhang, L., Kato, M., Yamawaki, K., Kiriiwa, Y., Yahata, M., et al. (2012). Effect of blue and red led light irradiation on β-cryptoxanthin accumulation in the flavedo of citrus fruits. *J. Agric. Food Chem.* 60, 197–201. doi: 10.1021/jf203364m

Ma, G., Zhang, L., Setiawan, C. K., Yamawaki, K., Asai, T., Nishikawa, F., et al. (2014). Effect of red and blue LED light irradiation on ascorbate content and expression of genes related to ascorbate metabolism in postharvest broccoli. *Postharvest Biol. Technol.* 94, 97–103. doi: 10.1016/j.postharvbio.2014.03.010

Mano, J., Ohno, C., Domae, Y., and Asada, K. (2001). Chloroplastic ascorbate peroxidase is the primary target of methylviologen-induced photooxidative stress in spinach leaves: its relevance to monodehydroascorbate radical detected with in vivo ESR. *Biochim. Biophys. Acta Bioenerg.* 1504, 275–287. doi: 10.1016/s0005-2728(00)00256-5

Massot, C., Bancel, D., Lopez Lauri, F., Truffault, V., Baldet, P., Stevens, R., et al. (2013). High temperature inhibits ascorbate recycling and light stimulation of the ascorbate pool in tomato despite increased expression of biosynthesis genes. *PLoS One* 8:e84474. doi: 10.1371/journal.pone.0084474

Massot, C., Genard, M., Stevens, R., and Gautier, H. (2010). Fluctuations in sugar content are not determinant in explaining variations in vitamin C in tomato fruit. *Plant Physiol. Biochem.* 48, 751–757. doi: 10.1016/j.plaphy.2010.06.001

Mastropasqua, L., Borraccino, G., Bianco, L., and Paciolla, C. (2012). Light qualities and dose influence ascorbate pool size in detached oat leaves. *Plant Sci.* 183, 57–64. doi: 10.1016/j.plantsci.2011.11.009

McCree, K. J. (1972). The action spectrum, absorptance and quantum yield of photosynthesis in crop plants. *Agric. Meteorol.* 9, 191–216. doi: 10.1016/0002-1571(71)90022-7

Mohr, H. (1994). "Co-action between pigment systems," in *Photomorphogenesis in Plants*, eds R. E. Kendrick, and G. H. M. Kronenburg, (Dordrecht: Kluwer Academic), 353–357.

Nishikawa, F., Kato, M., Hyodo, H., Ikoma, Y., Sugiura, M., and Yano, M. (2003). Ascorbate metabolism in harvested broccoli. *J. Exp. Bot.* 54, 2439–2448. doi: 10.1093/jxb/erg283

Ntagkas, N., Woltering, E. J., and Marcelis, L. F. M. (2018). Light regulates ascorbate in plants: an integrated view on physiology and biochemistry. *Environ. Exp. Bot.* 147, 271–280. doi: 10.1016/j.envexpbot.2017.10.009

Oyaert, E., Volckaert, E., and Debergh, P. C. (1999). Growth of chrysanthemum under coloured plastic films with different light qualities and quantities. *Sci. Hortic.* 79, 195–205. doi: 10.1016/s0304-4238(98)00207-6

Pignocchi, C., Fletcher, J. M., Wilkinson, J. E., Barnes, J. D., and Foyer, C. H. (2003). The function of ascorbate oxidase in tobacco. *Plant Physiol.* 132, 1631–1641. doi: 10.1104/pp.103.022798

Ren, J., Guo, S., Xu, C., Yang, C., Ai, W., Tang, Y., et al. (2014). Effects of different carbon dioxide and LED lighting levels on the anti-oxidative capabilities of Gynura bicolor DC. *Adv. Space Res.* 53, 353–361. doi: 10.1016/j.asr.2013.11.019

Samuolienë, G., Brazaitytë, A., Viršilë, A., Jankauskienë, J., Sakalauskienë, S., and Duchovskis, P. (2016). Red light-dose or wavelength-dependent photoresponse of antioxidants in herb microgreens. *PLoS One* 11:e0163405. doi: 10.1002/jsfa.6173

Smirnoff, N. (2011). Vitamin C: biosynthesis of vitamins in plants. *Adv. Bot. Res.* 59, 107–177.

Spalding, E. P., and Folta, K. M. (2005). Illuminating topics in plant photobiology. *Plant Cell Environ.* 28, 39–53. doi: 10.1111/j.1365-3040.2004.01282.x

Spiìnola, V., Mendes, B., Camara, J. S., and Castilho, P. C. (2012). An improved and fast UHPLC-PDA methodology for determination of L-ascorbic and

dehydroascorbic acids in fruits and vegetables. *Anal. Bioanal. Chem.* 403, 1049–1058. doi: 10.1007/s00216-011-5668-x

Stutte, G. W. (2009). Light-emitting diodes for manipulating the phytochrome apparatus. *Hortscience* 44, 231–234. doi: 10.21273/HORTSCI.44.2.231

Sysoeva, M. I., Markovskaya, E. F., and Shibaeva, T. (2010). Plants under continuous light: review. *Plant Stress* 4, 5–17.

Szymanska, R., Ślesak, I., Orzechowska, A., and Kruk, J. (2017). Physiological and biochemical responses to high light and temperature stress in plants. *Environ. Exp. Bot.* 139, 165–177. doi: 10.1016/j.envexpbot.2017.05.002

Takahama, U. (2004). Oxidation of vacuolar and apoplastic phenolic substrates by peroxidase: Physiological significance of the oxidation reactions. *Phytochem. Rev.* 3, 207–219. doi: 10.1023/b:phyt.0000047805

Velez-Ramirez, A. I., van Ieperen, W., Vreugdenhil, D., and Millenaar, F. F. (2011). Plants under continuous light. *Trends Plant Sci.* 16, 310–318.

Veìlez-Bermuìdez, I. C., and Schmidt, W. (2014). The conundrum of discordant protein and mRNA expression. Are plant special? *Front. Plant Sci.* 5:619. doi: 10.3389/fpls.2015.00619

Wang, J., Lu, W., Tong, Y., and Yang, Q. (2016). Leaf morphology, photosynthetic performance, chlorophyll fluorescence, stomatal development of lettuce (*Lactuca sativa* L.) exposed to different ratios of red light to blue light. *Front. Plant Sci.* 7:250. doi: 10.3389/fpls.2016.00250

Wheeler, G. L., Jones, M. A., and Smirnoff, N. (1998). The biosynthetic pathway of vitamin C in higher plants. *Nature* 393, 365–369. doi: 10.1038/30728

Xu, H. L., Xu, Q. C., Li, F. L., Feng, Y. Z., Qin, F. F., and Fang, W. (2012). Applications of xerophytophysiology in plant production-LED blue light as a stimulus improved the tomato crop. *Sci. Hortic.* 148, 190–196. doi: 10.1016/j.scienta.2012.06.044

Yabuta, Y., Mieda, T., Rapolu, M., Nakamura, A., Motoki, T., Maruta, T., et al. (2007). Light regulation of ascorbate biosynthesis is dependent on the photosynthetic electron transport chain but independent of sugars in *Arabidopsis*. *J. Exp. Bot.* 58, 2661–2671. doi: 10.1093/jxb/erm124

Yamaguchi, K., Mori, H., and Nishimura, M. (1995). A novel isoenzyme of ascorbate peroxidase localized on glyoxysomal and leaf peroxisomal membranes in pumpkin. *Plant Cell Physiol.* 36, 1157–1162. doi: 10.1093/oxfordjournals.pcp.a078862

Yang, F., Wang, Y., and Miao, L. F. (2010). Comparative physiological and proteomic responses to drought stress in two poplar species originating from different altitudes. *Physiol. Plant.* 139, 388–400. doi: 10.1111/j.1399-3054.2010.01375.x

Zha, L. Y., Liu, W. K., Zhang, Y. B., Zhou, C. B., and Shao, M. J. (2019a). Morphological and physiological stress responses of lettuce to different intensities of continuous light. *Front. Plant Sci.* 10:1440. doi: 10.3389/fpls.2019.01440

Zha, L. Y., Zhang, Y. B., and Liu, W. K. (2019b). Dynamic responses of ascorbate pool and metabolism in lettuce to long-term continuous light provided by red and blue LEDs. *Environ. Exp. Bot.* 163, 15–23. doi: 10.1016/j.envexpbot.2019.04.003

Zhang, L., Ma, G., Yamawaki, K., Ikoma, Y., Matsumoto, H., Yoshioka, T., et al. (2015). Regulation of ascorbic acid metabolism by blue LED light irradiation in citrus juice sacs. *Plant Sci.* 233, 134–142. doi: 10.1016/j.plantsci.2015.01.010

Conflict of Interest: The authors declare that the research was conducted in the absence of any commercial or financial relationships that could be construed as a potential conflict of interest.

Copyright © 2020 Zha, Liu, Yang, Zhang, Zhou and Shao. This is an open-access article distributed under the terms of the Creative Commons Attribution License (CC BY). The use, distribution or reproduction in other forums is permitted, provided the original author(s) and the copyright owner(s) are credited and that the original publication in this journal is cited, in accordance with accepted academic practice. No use, distribution or reproduction is permitted which does not comply with these terms.

frontiers in Plant Science

ORIGINAL RESEARCH
published: 11 September 2020
doi: 10.3389/fpls.2020.581156

Substituting Far-Red for Traditionally Defined Photosynthetic Photons Results in Equal Canopy Quantum Yield for CO_2 Fixation and Increased Photon Capture During Long-Term Studies: Implications for Re-Defining PAR

Shuyang Zhen *† *and Bruce Bugbee*

Crop Physiology Laboratory, Department of Plants Soils and Climate, Utah State University, Logan, UT, United States

OPEN ACCESS

Edited by:
Carl-Otto Ottosen, Aarhus University, Denmark

Reviewed by:
Erik Harry Murchie, University of Nottingham, United Kingdom
Shardendu Kumar Singh, AeroFarms, United States

***Correspondence:**
Shuyang Zhen
shuyang.zhen@tamu.edu

†Present address:
Shuyang Zhen, Department of Horticultural Sciences, Texas A&M University, College Station, TX, United States

Specialty section:
This article was submitted to Crop and Product Physiology, a section of the journal Frontiers in Plant Science

Received: *08 July 2020*
Accepted: *31 August 2020*
Published: *11 September 2020*

Citation:
Zhen S and Bugbee B (2020) Substituting Far-Red for Traditionally Defined Photosynthetic Photons Results in Equal Canopy Quantum Yield for CO_2 Fixation and Increased Photon Capture During Long-Term Studies: Implications for Re-Defining PAR. Front. Plant Sci. 11:581156. doi: 10.3389/fpls.2020.581156

Far-red photons regulate shade avoidance responses and can have powerful effects on plant morphology and radiation capture. Recent studies have shown that far-red photons (700 to 750 nm) efficiently drive photosynthesis when added to traditionally defined photosynthetic photons (400–700 nm). But the long-term effects of far-red photons on canopy quantum yield have not yet been determined. We grew lettuce in a four-chamber, steady-state canopy gas-exchange system to separately quantify canopy photon capture, quantum yield for CO_2 fixation, and carbon use efficiency. These measurements facilitate a mechanistic understanding of the effect of far-red photons on the components of plant growth. Day-time photosynthesis and night-time respiration of lettuce canopies were continuously monitored from seedling to harvest in five replicate studies. Plants were grown under a background of either red/blue or white light, each background with or without 15% (50 μmol m^{-2} s^{-1}) of far-red photons substituting for photons between 400 and 700 nm. All four treatments contained 31.5% blue photons, and an equal total photon flux from 400 to 750 nm of 350 μmol m^{-2} s^{-1}. Both treatments with far-red photons had higher canopy photon capture, increased daily carbon gain (net photosynthesis minus respiration at night), and 29 to 31% more biomass than control treatments. Canopy quantum yield was similar among treatments (0.057 ± 0.002 mol of CO_2 fixed in gross photosynthesis per mole of absorbed photons integrated over 400 to 750 nm). Carbon use efficiency (daily carbon gain/gross photosynthesis) was also similar for mature plants (0.61 ± 0.02). Photosynthesis increased linearly with increasing photon capture and had a common slope among all four treatments, which demonstrates that the faster growth with far-red photon substitution was caused by enhanced photon capture through increased leaf expansion. The equivalent canopy quantum yield among

treatments indicates that the absorbed far-red photons were equally efficient for photosynthesis when acting synergistically with the 400–700 nm photons.

Keywords: canopy photosynthesis, carbon use efficiency, far-red photons, quantum yield, phytochrome equilibrium, radiation capture

INTRODUCTION

Plants capture light as fuel for photosynthesis and perceive fluctuations in their radiation environments as signals that trigger changes in plant shape, biochemical composition, developmental stages and resource allocation (Kendrick and Kronenberg, 1994). These adaptive responses are mainly directed by three aspects of light: spectral quality, quantity, and duration. Among the photoreceptors, the red/far-red absorbing phytochromes are of crucial importance in sensing vegetation shade and eliciting shade avoidance responses that often maximize plant growth and fitness in crowded stands (Smith, 1982; Schmitt et al., 1995). Green leaves absorb efficiently in the photosynthetically active region of the spectrum (PAR; 400 to 700 nm) but strongly transmit and reflect longer wavelength far-red photons above 700 nm (Woolley, 1971; Kasperbauer, 1987). This selective attenuation causes the red (R) to far-red (FR) ratio to decrease in forest understories or within dense canopies compared to unfiltered sunlight (Federer and Tanner, 1966; Holmes and Smith, 1977; Casal, 2013). Even before plants are directly shaded, small quantities of additional far-red reflected by neighboring plants are perceived *via* phytochromes as an early warning signal of competition and induce rapid stem elongation in shade-avoiding seedlings (Ballaré et al., 1987). Increased stem (and petiole) extension growth is a most prominent shade avoidance response (Smith and Whitelam, 1997; Franklin, 2008).

Additionally, reduced branching and tillering, lower leaf to stem dry mass ratio, smaller proportion of biomass allocation to the roots, hyponastic (upward bending) leaves with reduced chlorophyll (chl) content, and earlier flowering are among the most frequently observed responses to low R:FR ratios in shade-avoiding species adapted to open habitats (Morgan and Smith, 1979; Kasperbauer, 1987; Halliday et al., 1994; Smith and Whitelam, 1997; Casal, 2012). Those shade-avoidance responses are also induced in agronomic crops under high density monocultures and can cause crops to be more prone to drought and lodging and negatively affect yield, thus are often considered undesirable (Morgan et al., 2002).

Unlike the shade-avoiding species, some plants tolerate shade without showing a strong, or any phytochrome-mediated stem extension growth. Instead, those shade-tolerant species maximize radiation capture through leaf expansion, which is accompanied with thinner leaves and increased fractional biomass allocation to leaves (Gommers et al., 2013). Photosynthetic efficiency is also optimized under shade light environments (*i.e.* reduced PAR and relatively enriched FR) *via* adaptive changes in the structure, composition and function of thylakoid membranes, *e.g.* increased PSII:PSI ratio and lower chl a:b ratio (Anderson et al., 1988; Chow et al., 1990a; Valladares and Niinemets, 2008). Both shade-avoiding and -tolerant species perceive shade using the same family of photoreceptors (*i.e.* phytochromes) and share a number of overlapping responses (*e.g.* reductions in leaf thickness). The underlying regulatory pathways that lead to the contrasting phenotypic responses between two strategies remain unclear (see Gommers et al., 2013 for an in-depth discussion of potential regulators of shade tolerance responses).

Because crop productivity exhibits a strong linear correlation with radiation intercepted by canopies (Monteith, 1977; Gifford et al., 1984; Beadle and Long, 1985), increased leaf expansion and accelerated canopy closure are desirable traits, especially in annual crops. Recent advances in light emitting diode (LED) technology enable precise control of spectral quality in controlled environment crop production (Massa et al., 2008; Kusuma et al., 2020). Perhaps the most powerful effect is the simulation of shade through FR supplementation, often without reducing light intensity in the PAR region. This change has been reported to promote leaf expansion in various leafy greens, fruiting vegetables, and ornamental species, which increases growth primarily through increased radiation capture (Casal et al., 1987; Goins et al., 2001; Li and Kubota, 2009; Stutte et al., 2009; Park and Runkle, 2017; Kalaitzoglou et al., 2019).

One important difference between simulated shade and natural vegetation shade is that natural shade significantly reduces total photon flux (Casal, 2012). Leaf expansion induced by far-red photons may interact with photon flux as it is partly dependent on supply of photosynthates (Dale, 1988). Heraut-Bron et al. (1999) observed that lowering R:FR ratio induced leaf expansion of white clover when plants were grown under high photosynthetic photon flux density (PPFD) of 320 $\mu mol\ m^{-2}\ s^{-1}$ but not under low PPFD of 110 $\mu mol\ m^{-2}\ s^{-1}$. Leaf expansion induced by far-red supplementation in most simulated shade studies have been conducted under medium to high light conditions. In order to promote beneficial leaf expansion with a high fraction of FR photons, an adequate photon flux in the PAR region is likely needed.

While the photomorphogenic effects of FR photons are largely well characterized, far-red photons (λ > 700 nm) are generally thought to be ineffective for photosynthesis due to their poor photosynthetic efficiency when applied alone (Emerson and Lewis, 1943; McCree, 1972; Inada, 1976). Far-red photons are thus excluded from the current definition of photosynthetic photons. However, pioneering research by Emerson and co-

Abbreviations: CUE, carbon use efficiency; DCG, daily carbon gain; LAI, leaf area index, LED, light emitting diode; Canopy P_{gross} and P_{net}, canopy gross and net photosynthetic rate; PAR, photosynthetically active radiation from 400 to 700 nm; PPFD, photosynthetic photon flux density integrated over 400 to 700 nm; PFD, photon flux density; R_{dark}, dark respiration.

workers found that photosynthetic rate is enhanced under simultaneous illumination of short- and long-wavelength (λ >685 nm) photons (Emerson et al., 1957; Emerson and Rabinowitch, 1960). This phenomenon, known as the Emerson enhancement effect, indicates that the effect of different wavelength photons on photosynthesis may not be simply additive. This finding contributed to the subsequent identification of two photosystems with different absorption properties (Hill and Bendall, 1960; Duysens and Amesz, 1962). More recent work demonstrates that most of the shorter wavelength photons from 400 to 680 nm over-excite photosystem II (PSII), while longer wavelength far-red photons preferentially excite photosystem I (PSI) (Evans, 1987; Hogewoning et al., 2012; Laisk et al., 2014; Zhen et al., 2018). When combining far-red with shorter wavelength photons, the balance of excitation distribution between PSII and PSI is restored, thus leading to increased leaf photochemical efficiency (Zhen and van Iersel, 2017) and photosynthetic rate (Hogewoning et al., 2012; Murakami et al., 2018). Scaling up from leaf to canopy level, Zhen and Bugbee (2020) found that far-red photons (700–750 nm) are equally efficient at driving canopy photosynthesis when added to 400 to 700 nm photons in 14 diverse crop species. These recent findings warrant re-consideration of the photosynthetic value of far-red photons.

Following canopy photon capture and photosynthetic efficiency, the third determinant of daily carbon gain and productivity is the conversion efficiency of carbon fixed in gross photosynthesis into biomass, *i.e.* carbon use efficiency (Gifford et al., 1984; Bugbee and Monje, 1992). The loss of carbon to respiration at whole-plant/canopy level can be more than 50% of gross photosynthesis (Amthor, 1989). To our knowledge, the effects of far-red photons on canopy quantum yield (moles of CO_2 fixed in gross photosynthesis per mole of absorbed photons; a measure of photosynthetic photon use efficiency) and carbon use efficiency (CUE = ratio of C incorporated into biomass to C fixed in gross photosynthesis) during long-term crop cultivation have not been studied. Most previous studies have added far-red photons as a supplement, which complicates interpretation of the results because total photon flux from 400 to 750 nm is not constant.

Our objective was to quantify the effects of far-red substitution for 400–700 nm photons on radiation capture, canopy quantum yield, carbon use efficiency, and biomass allocation of a model crop lettuce. This quantitative approach can provide a mechanistic understanding of the effect of far-red photons on plant growth. Continuous measurement of canopy quantum yield for CO_2 fixation can provide additional evidence for changing the definition of photosynthetic active radiation to include far-red photons (700–750 nm).

MATERIALS AND METHODS

Plant Materials

Lettuce (*Lactuca sativa* cv. Waldmann's Dark Green) was seeded in 1.7 L containers filled with calcined clay (Greens Grade; Profile, Buffalo Grove, IL) in a glass-covered greenhouse and then moved into a multi-chamber gas exchange system two to four days after emergence. The calcined clay substrate was rinsed with de-ionized water prior to use as described by Adams et al. (2014) and soaked with a hydroponic nutrient solution (Utah hydroponic refill solutions for dicots with $FeCl_3$ and iron-chelating agent EDDHA doubled in concentration; USU Crop Physiology Laboratory, 2018). The pH of the hydroponic solution was adjusted to 5.8 with nitric acid and the electric conductivity of the solution was 1 ± 0.1 mS/cm. This low pH minimized bicarbonate effects on CO_2 fluxes from the root-zone (van Iersel and Bugbee, 2000). Seedlings were selected for uniformity and thinned to one plant per container. Five replicate studies were conducted.

Light Treatments and Growing Conditions

Sixteen uniform seedlings were moved into a steady-state gas exchange system with four acrylic chambers (100 L/chamber with four plants per chamber; 36 cm × 47 cm × 59 cm; w × l × h), similar to the multi-chamber gas exchange system described by van Iersel and Bugbee (2000). Each chamber consisted of one spectral treatment, with cool white, red, blue, and far-red LEDs (Ray 22; Fluence Bioengineering, Austin, TX, USA) placed on top of the chambers. The four light treatments were: white 350, red/blue (RB) 350, white 300 + far-red (FR) 50, and RB 300 + FR 50 (see **Figure 1** for spectral distributions). The numbers following each type of light (*e.g.* RB 300) indicate the average photon flux density in μmol m^{-2} s^{-1} [±1 μmol m^{-2} s^{-1}; measured at 13 locations across the chamber floor area of 0.17 m^2 using a spectroradiometer (SS-110; Apogee Instruments, Logan, UT, USA)]. The blue (400–500 nm): green (501–600 nm): red (601–700 nm) ratio was in 31.5:45.2:23.3 in white 350 and 31.5:0.1:68.4 in RB 350. Phytochrome photoequilibrium [PPE, an indicator of the relative amount of active phytochrome in the far-red-absorbing P_{fr} form] under each light spectrum was calculated using the phytochrome photoconversion coefficients by Sager et al. (1988) (**Table 1**).

Chamber walls were lined with highly reflective Mylar to eliminate side lighting and increase light uniformity. The reflective walls also help to simulate light environment of a canopy because they reflect FR photons similar to neighboring plants. Two of the treatments had FR photons (700–750 nm) substituting for ~15% of the conventionally defined white or RB photosynthetic photons. All four treatments contained 31.5% blue photons and equal total photon flux of 350 μmol m^{-2} s^{-1} from 400 to 750 nm. Photoperiod was 14/10 h light/dark. Daily light integral was 17.64 mol m^{-2} d^{-1}.

Plants were grown under elevated CO_2, with the CO_2 concentration [CO_2] in the pre-chamber air streams enriched to 800 μmol mol^{-1}. CO_2 enrichment is a common practice in controlled environment crop production. Controlling CO_2 to a constant elevated level also reduces noises in the gas exchange measurements caused by un-steady [CO_2] in the ambient air in urban areas. Air flow rate through the chambers was gradually increased from 11 to 37 mmol s^{-1} (15 to 50 standard L min^{-1}) from seedling to mature plant stage. Air inside the chambers was mixed with fans (793 L min^{-1}; Model A36-B10A-15T2-000, Globe Motors). The [CO_2] inside the chambers ranged from

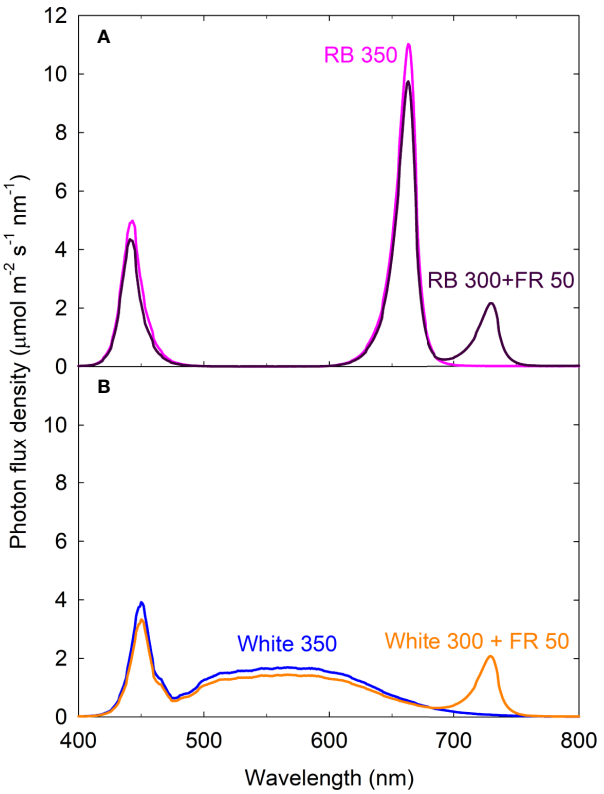

FIGURE 1 | Spectral distributions of four light treatments composed of red/blue (RB; peaks at 443 and 663 nm), white (peak at 450 nm with secondary peak at 567 nm), and far-red (FR; peak at 730 nm) photons. The numbers following each type of light (*e.g.* RB 350) indicate photon flux density in μmol m^{-2} s^{-1}. All four treatments had equal total photon flux of 350 μmol m^{-2} s^{-1} (400 to 750 nm) and 31.5% blue photons.

TABLE 1 | Effect of Spectral Quality on Growth, Morphology, and Chlorophyll Content of Lettuce.

	Spectra and photon flux density			
	RB 350	**RB 300 + FR 50**	**White 350**	**White 300 + FR 50**
(PPE)	**(0.87)**	**(0.82)**	**(0.84)**	**(0.70)**
Shoot fresh mass (g)	130^{b}	179^{a}	129^{b}	167^{a}
Shoot dry mass (g)	8.6^{b}	11.3^{a}	8.5^{b}	11.2^{a}
Shoot dry/fresh mass (%)	6.7^{a}	6.4^{a}	6.6^{a}	6.8^{a}
Root dry mass (g)	1.61^{a}	1.85^{a}	1.61^{a}	1.95^{a}
% root	16.1^{a}	14.7^{a}	16.6^{a}	15.3^{a}
Leaf area (cm^2)	3091^{b}	4423^{a}	3111^{b}	4228^{a}
Leaf mass per area (g m^{-2})	28.2^{a}	25.5^{c}	27.5^{ab}	26.5^{bc}
Chl content (μmol m^{-2})	272^{a}	218^{b}	267^{a}	213^{b}
Leaf photon absorption	0.927	0.798	0.838	0.686

PPE, Phytochrome photoequilibrium; RB, red and blue; FR, far-red. The number following each type of light (e.g. RB 350) indicates photon flux density in μmol m^{-2} s^{-1}. Biomass and leaf area were expressed on a per chamber basis (i.e. the sum of four plants). Data represent means from five replicate studies with different letters indicate significant differences between means ($P \leq 0.05$; $n = 5$). Leaf photon absorption of incident photons under each spectral treatment (mol $_{absorbed}$ $mol^{-1}{}_{incident}$) was integrated from 400 to 750 nm.

740 (with mature plants) to 800 μmol mol^{-1} (seedlings) during the light periods and from 800 (seedlings) to 820 μmol mol^{-1} (mature plants) during the dark respiration periods. Flow rates through the chambers were adjusted depending the size and photosynthetic rate of canopies to maintain the [CO_2] inside each chamber within 5 μmol mol^{-1} of each other. Chamber air temperature was controlled with resistance heaters and maintained constant at 25 ± 0.1°C day/night. Plants were watered daily with the hydroponic nutrient solution described above (Bugbee, 2004).

Canopy Gas Exchange Measurements and Calculations

The pre- and post-chamber air streams were sampled every second using two infra-red gas analyzers (reference and differential IRGA; LI-6252; LI-COR, Lincoln, NE). Each chamber was sampled for 30 s, and then the tubing that connected the chambers to the differential IRGA was purged for 40 s before the next chamber was sampled. Canopy gas exchange rate [net photosynthetic rate during the light period ($P_{net,\ light}$) and dark respiration rate (R_{dark}; negative values) in μmol_{CO2} $m^{-2}{}_{ground\ area}$ s^{-1}] was calculated from the mass flow rate and delta [CO_2] between the pre- and post-chamber air streams and recorded using a datalogger (CR1000; Campbell Scientific, Logan, UT, USA) throughtout the entire course of the study.

To eliminate the mole fraction dilution of CO_2 analysis by water vapor, the air streams sampled by the IRGAs were first passed through nafion dryers (Perma Pure, Lakewood, NJ, USA) and then columns of magnesium perchlorate to completely remove water vapor.

To determine the photosynthetic value of FR photons, far-red LEDs in the two FR substitution treatments were turned off for 30 to 40 min during the days prior to harvest.

$P_{net,\ light}$ and R_{dark} was averaged over the 14 h of light period and 10 h of dark period respectively, on a daily basis. The averaged values (in units of mol_{CO2} $m^{-2}{}_{ground\ area}$ h^{-1}) were used in the subsequent calculations of gas exchange parameters (Eqs 1–3).

Canopy gross photosynthesis (P_{gross}; g d^{-1}) was calculated as:

$$P_{gross} = (P_{net,\ light} + |R_{dark}|) \times 14\,h \times 0.17\,m^2 \times 30\,g\,mol^{-1} \quad (1)$$

Where $|R_{dark}|$ was the absolute value of dark respiration. 14 was the light period in hours, and 0.17 was the chamber ground area in m^2. 30 represents grams dry mass per mole of CO_2 assimilated, assuming a carbon content of 0.4 g g^{-1} in plant tissues. This calculation of P_{gross} also assumes that respiration rate was similar in the light and dark. There is ongoing research and discussion on whether respiration rate in the light is similar, higher, or lower than respiration in the dark (Sharp et al., 1984; Atkin et al., 1998; Frantz et al., 2004 and citations therein). We assumed that respiration rate in light and dark was the same, which is the standard assumption in canopy photosynthesis research (van Iersel, 2003).

Daily carbon gain (DCG; a measure of canopy growth rate in g d^{-1}) was calculated as:

$$DCG = (P_{net,\,light} \times 14\,h - |R_{dark}| \times 10\,h) \times 0.17\ m^2 \times 30\ g\ mol^{-1} \quad (2)$$

Where 14 was the light period in hours, and 10 was the dark period in hours.

Carbon use efficiency (CUE; the ratio of daily net carbon gain to the total amount of carbon fixed in gross photosynthesis) was calculated from Eqs (1) and (2) as:

$$CUE = DCG/P_{gross} \quad (3)$$

Imaging of Canopy Ground Cover

Plants were taken out of the gas exchange chambers for 2 to 3 min daily for top down photos of the canopies, taken with a digital camera placed 130 cm above the plant base. Images were analyzed using a Python program, available as open source at https://github.com/jakobottar/green-pixel-analysis. The fraction of canopy ground cover was calculated as the ratio of green pixels (plant tissues) to the total pixel count of an area equal to the chamber ground area as described by Klassen et al. (2004).

Growth Parameters and Chlorophyll Content

Plants were destructively harvested 17 to 20 days after transferred into the gas exchange chambers, when the largest canopies were near canopy closure. Shoot fresh weight and total leaf number of all four plants in each spectral treatment were recorded. Leaf chlorophyll content (μmol m^{-2}) was measured on five representative leaves per plant and averaged over four plants per treatment (MC-100 chlorophyll meter; Apogee Instruments, Logan, UT). Total leaf area per chamber was measured using a leaf area meter (LI-3000; LI-COR, Lincoln, NE, USA). Shoots and roots were oven-dried to a constant mass (at least 48 h at 80°C). Root percent mass was calculated as root dry mass/(total shoot and root dry mass). Leaf mass per area (g m^{-2}), a measure of leaf thickness, was calculated as leaf dry mass/total leaf area.

Leaf Photon Absorption and Canopy Photon Capture

Leaf light absorptance was determined on the day of harvest using a spectroradiometer (PS300; Apogee Instruments) similar to the method of Nelson and Bugbee (2015). The absorptance spectrum was then multiplied by the spectral output of LEDs to obtain the leaf photon absorption under each spectral treatment (mole of photons absorbed by a single layer of leaf per mole of incident photons).

Canopy photon capture (mole of photons absorbed per mole of incident photons) was estimated by multiplying the fraction of canopy ground cover by the leaf photon absorption under each spectral treatment. This gave a good estimate in small canopies with only one layer of leaves. However, the canopy photon capture would be under-estimated in larger canopies that had over-lapping layers of leaves. To account for this, the number of leaf layers in each canopy at harvest was calculated as total leaf area at harvest (m^2) divided by the projected canopy ground cover (m^2). The projected canopy ground cover (or projected canopy leaf area) was determined from top down photos (*i.e.* percent ground cover multiplied by chamber ground area of 0.17 m^2). Canopies of lettuce had relatively horizontal leaf orientation and typically did not form over-lapping leaves until one week prior to harvest. The projected canopy leaf area was thus used to estimate total canopy leaf area in young canopies. When leaves started to overlap, total canopy leaf area was interpolated from a regression function (exponential growth) fitted to the canopy leaf area estimated for young canopies and the final total canopy leaf area at harvest. The number of layers of leaves during the week prior to harvest was then calculated as the interpolated total canopy leaf area on each day divided by the projected canopy leaf area.

Using lettuce grown under spectral treatment RB 300 + FR 50 as an example, a single layer of leaves absorbed 0.798 moles of photons (integrated over 700 to 750 nm) per mole of incident photons (**Table 1**). Photon absorption with more than one layer of leaves was estimated using the Beer–Lambert equation: canopy photon absorption = $1 - e^{-(k \times LAI)}$; where the extinction coefficient (k = 1.6) was derived by setting the photon absorption to 0.798 and LAI to 1. Thus, with two layers of overlapping leaves photon absorption would approximately equal to $1 - e^{-(1.6 \times 2)} = 0.959$ mol of photons absorbed per mole of incident photons. With an average of 2.6 layers of leaves at harvest, photon absorption in areas covered by leaves was adjusted to $1 - e^{-(1.6 \times 2.6)} = 0.984$ mol of photons absorbed per mole of incident photons.

Canopy Quantum Yield

Canopy quantum yield for CO_2 fixation (moles of CO_2 fixed in gross photosynthesis per mole of photons absorbed from 400 to 750 nm) was calculated as:

$$\text{Canopy quantum yield} = P_{gross}/\text{canopy absorbed photons} \quad (4)$$

Note that P_{gross} here is expressed in units of moles of CO_2 fixed per mole of incident photons for the simplicity of the equation. To convert P_{gross} from g d^{-1} in Eq. (1) to mol_{CO2} $mol^{-1}_{incident\ photon}$, the P_{gross} values in g d^{-1} need to be first divided by 30 g mol^{-1} (grams of dry mass per mole of carbon assimilated), then divided by 0.17 m^2 (chamber ground area), and then divided by17.64 mol $_{incident\ photons}$ m^{-2} d^{-1} (total daily photon flux density at canopy level).

Statistical Analysis

Data were analyzed using regression (linear and sigmoid) in Sigmaplot (Systat Software, San Jose, CA) and ANOVA in Statistical Analysis Systems (SAS Institute, Cary, NC, USA). Mean separation was performed using Fisher's protected least significant difference (LSD, $P = 0.05$). Canopy gas exchange measurements from two representative replicate studies were included in data analysis. Growth parameters and chlorophyll content were obtained from all five replicate studies.

RESULTS

Biomass, Leaf Area, and Chlorophyll Content

Lettuce grown under the two control treatments without far-red (white 350 and RB 350) had nearly identical dry mass and leaf area at harvest. In contrast, both treatments with 15% FR substitution, either with a white or RB background light, had 29 to 31% increase in total biomass (shoot and root) and a 36–43% increase in leaf area (**Table 1**). Leaves of plants grown with far-red were thinner with a 4–10% decrease in leaf mass per area, ~20% lower chlorophyll content, and less efficient absorption of the incident photon on single leaf basis (**Table 1**). Dry mass partitioning to the roots, indicated by % root, did not differ significantly among the four spectral treatments even though it tended to be slightly reduced in the two treatments with FR (**Table 1**).

Canopy Gas Exchange and Carbon Use Efficiency

Canopy $P_{net,\ light}$ and R_{dark} under all four spectral treatments increased exponentially from seedling to young plant stage over the first two weeks, followed by slower increases during the third week as plants quickly approached canopy closure (**Figure 2**; also see **Supplementary Figure S1** for additional dataset). Gas exchange rates were identical among all four treatments when uniformly sized seedlings were first moved into the chambers and remained similar between the white 350 and RB 350 treatments throughout the entire course of the study. Plants grown under the two FR substitution treatments, however, gradually showed higher $P_{net,\ light}$ and R_{dark} (**Figure 2**) and gained more carbon per day than the control treatments (**Figure 3**). These measurements were consistent with the differences in plant dry mass under the four treatments. At harvest, dry mass predicted from the cumulative daily carbon gain obtained from gas exchange measurement was 103.9 ± 3.4% of the measured total dry mass in two representative replicate studies.

A decrease in $P_{net,\ light}$ was detected within 5 min (note that each chamber was sampled every 4 min and 40 s) when the far-red LEDs in the two FR substitution treatments were turned off (**Figure 2**; insets), indicating that far-red photons directly contribute to canopy photosynthesis.

Carbon use efficiency (CUE) was lower for seedlings and gradually increased as plants matured (**Figure 4**). CUE for mature plants was similar under all four treatments, with an average of 0.61 ± 0.02 (SD) over the last six days prior to harvest.

Ground Cover and Canopy Photon Capture

Fractional ground cover and canopy photon capture increased over time in a similar manner as gas exchange rates and daily carbon gain (**Figure 5**; also see **Figures 2**, **3**). The FR substitution treatments consistently had higher fractional ground cover than the control treatments, especially after one week into the study (**Figures 5A, B**).

The higher fractional ground cover translated into higher canopy photon capture in the FR substitution treatments, although to a smaller extent (**Figures 5C, D**). This was because 1) leaves of plants grown with far-red were thinner with lower chlorophyll content and less efficient photon absorption especially in the green and far-red regions, and 2) far-red photons in the 15% FR substitution treatments were less efficiently absorbed than the 400 to 700 nm photons in the control treatments (**Figure 6** and **Table 1**). Leaf photon absorption under each of the four light treatments was shown in **Table 1**.

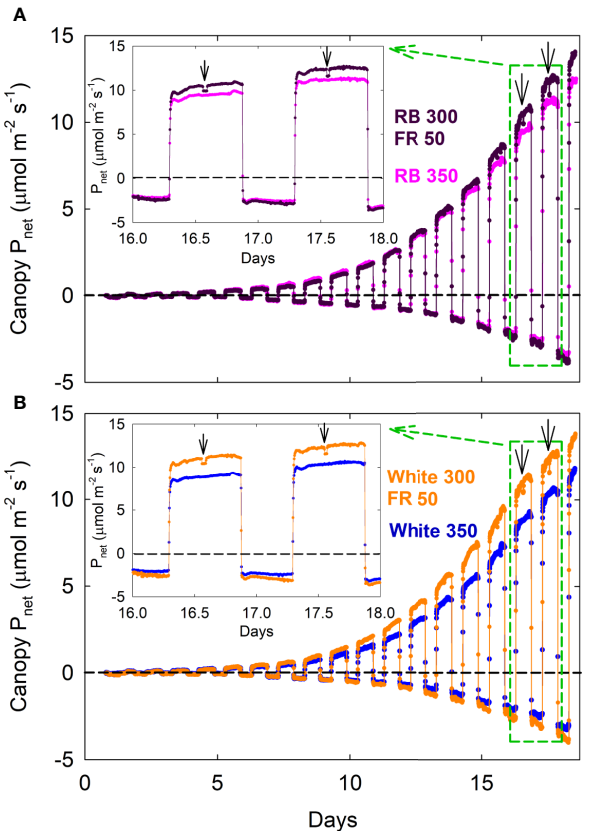

FIGURE 2 | Canopy net photosynthetic rate [P_{net}; net gas exchange rates in light (positive) and dark (negative) expressed as $\mu mol_{CO2}\ m^{-2}{}_{ground\ area}\ s^{-1}$] of lettuce under red/blue (RB) and white, with or without far-red substitution. The numbers following each type of light (*e.g.* RB 350) indicate photon flux density in µmol m^{-2} s^{-1}. Plants were seeded in a greenhouse and moved into a multi-chamber gas exchange system on day zero, four days after seedling emergence. Downward pointing arrows indicate when far-red LEDs were turned off. This representative dataset of P_{net} was used to calculate daily carbon gain shown in Rep 1 of **Figure 3** carbon use efficiency in **Figure 4**, and canopy quantum yield in **Figure 7**.

Canopy Quantum Yield

Canopy quantum yield (moles of CO_2 fixed in gross photosynthesis per mole of absorbed photons integrated over 400 to 750 nm) was similar among all four light treatments, with an average of 0.057 ± 0.002 (SD) (**Figure 7**). This indicates that the absorbed far-red photons were as efficient as red/blue and white photons.

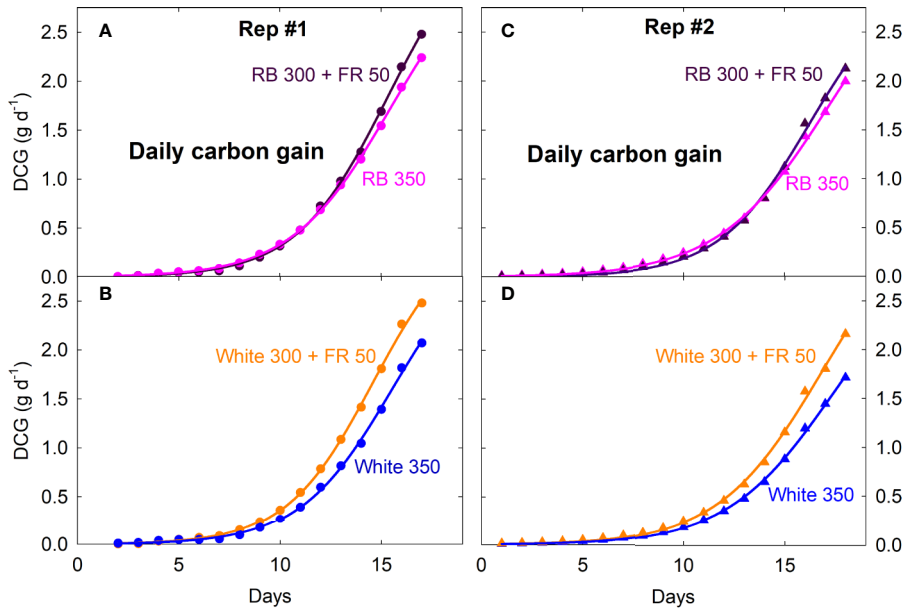

FIGURE 3 | Daily carbon gain (DCG, a measure of canopy growth rate) of lettuce under four spectral treatments from seedling to mature plants. RB, red and blue; FR, far-red. The numbers following each type of light (*e.g.* RB 350) indicate photon flux density in μmol m^{-2} s^{-1}. Plants were moved into the gas exchange system from a greenhouse on day zero (four days after emergence in Rep 1 and two days after emergence in Rep 2).

Correlation Between Canopy Photosynthesis and Photon Capture

Canopy P_{gross} of all four treatments increased linearly with increasing photon capture and had a common slope; daily carbon gain of all four treatments also showed a common linear correlation with canopy photon capture (**Figure 8**).

DISCUSSION

Beneficial leaf expansion elicited by far-red has been increasingly explored as means to improve production efficiency of high-value leafy green vegetables and ornamentals in greenhouses and indoor vertical farms (Goins et al., 2001; Li and Kubota, 2009; Stutte et al., 2009; Park and Runkle, 2017; Meng et al., 2019). Most of the previous studies added far-red photons as a supplement to photosynthetic photons within 400–700 nm, and the enhanced plant growth has been, in general, attributed solely to increased radiation capture through leaf expansion.

Far-red supplementation comes with an energy cost and it remains unclear whether it is cost effective to add far-red photons or to increase the traditionally defined photosynthetic photons (400 to 700 nm) by the same amount. Far-red photons contain lower energy and thus can be generated with higher efficacy (moles of photons per unit of electric energy) than red, blue, and green photons using current LED technology (Kusuma et al., 2020). Recent research on the photosynthetic effect of far-red photons has provided compelling evidence that far-red photons (700–750 nm) significantly increase leaf and canopy photosynthesis when added to photons within 400 to 700 nm (Zhen and Bugbee, 2020 and citations therein). These results indicate that far-red photons should be substituted for 400 to 700 nm photons instead of supplemented. Substitution facilitates the separation of the direct effect of far-red photons on canopy photosynthesis (by comparing the canopy quantum yield in treatments with and without far-red substitution) from their indirect effect on plant growth through altering canopy morphology and radiation capture. This provides a mechanistic understanding of the effect of far-red photons on plant growth during long-term crop cultivation.

Leaf Expansion and Phytochrome Photoequilibrium

The increased leaf expansion in the far-red substitution treatments was presumably caused by a decrease in phytochrome photoequilibria (PPE) compared to the control treatments (white or red/blue light) (**Table 1**). PPE has been widely used to estimate the fraction of phytochromes in the active P_{fr} form relative to the total phytochrome pool (Sager et al., 1988). An inverse linear response between stem elongation rate PPE has been well-established in shade-avoiding species (Morgan and Smith, 1976; Morgan and Smith, 1979) but the relationship between leaf expansion and PPE appears to be species-specific (Smith and Whitelam, 1997; Gommers et al., 2013). The reverse correlation between leaf expansion and PPE in this study is similar to the findings by Park and Runkle (2017). However, the slope of the relationship varied with the background light (**Supplementary Figure S2**). It is noteworthy that the total canopy leaf area was nearly identical in both treatments with far-red substitution,

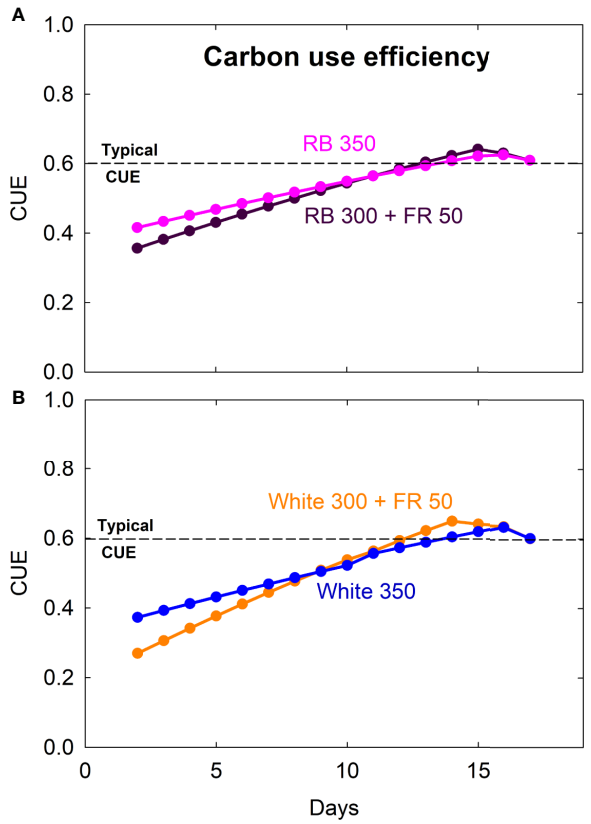

FIGURE 4 | Carbon use efficiency (CUE = daily carbon gain ÷ gross photosynthesis) of lettuce grown under red/blue (RB) and white light, with or without far-red (FR) substitution. The numbers following each type of light (*e.g.* RB 350) indicate photon flux density in μmol m^{-2} s^{-1}. Dashed lines indicate a typical CUE value of 0.6 that has been reported for mature plants.

despite that the estimated PPE differed greatly (0.70 under white *versus* 0.82 under red/blue background light). Similarly, canopy leaf area was nearly identical in the two control treatments in spite of the variation in PPE: 0.84 under white and 0.87 under red/blue light.

Phytochrome photoequilibria cannot be directly determined in green leaves due to the masking effect of chlorophylls (which also fluoresce) (Siegelman and Butler, 1965; Holmes and Fukshansky, 1979). Instead, PPE has been estimated from the spectral distribution of incident light and the photoconversion coefficients of phytochrome P_r and P_{fr} that are purified from etiolated tissue (Sager et al., 1988). It has been recognized that PPE estimated based on this approach may not consistently predict plant responses. Contributing factors for the variability were reviewed by Rajapakse and Kelly (1994). Among which, the incident light that reaches phytochrome is filtered by chlorophylls, thus PPE estimated from incident light spectrum often do not reflect PPE within different layers of cells within a leaf, nor in leaves from different positions within a canopy (Morgan and Smith, 1978; Jose and Schäfer, 1978; Holmes and Fukshansky, 1979). The white LED light in this study contained a large fraction of green photons and a much smaller fraction of red photons compared to the red/blue light (**Figure 1**). The absorption spectrum of phytochrome ranges from 300 to 800 nm (Sager et al., 1988). Because chlorophylls more efficiently absorb red photons than green photons, the extent of chlorophyll masking effect on the phytochrome response most likely differed under the white and red/blue light. This may be responsible for the different relationships between leaf expansion and estimated PPE under white and red/blue light.

Leaf Light Absorptance, Canopy Ground Cover, and Radiation Capture

The increased yield in response to FR supplementation is often attributed to increased photon capture (Goins et al., 2001; Li and Kubota, 2009; Stutte et al., 2009; Park and Runkle, 2017), but canopy photon capture is rarely quantified. Most studies report only leaf area at harvest, which non-linearly correlates with canopy photon capture due to overlapping of leaves. Goins et al. (2001) reported that lettuce grown with 12% added far-red photons consistently had higher canopy ground cover over a two-week growing period than plants that received equal photon flux in the PAR region. As expected, the increased leaf expansion under the far-red substitution treatments led to greater fractional canopy ground cover (**Figures 5A, B**). Fractional ground cover was found to be highly correlated with canopy photon absorption (r^2 = 0.99) of lettuce (Klassen et al., 2004), but the relationship was nonlinear and varied over time. Other factors, including leaf optical properties and the spectral distribution of incident light, can significantly alter spectral effects on canopy photon capture.

Leaf thickness and chlorophyll content affect leaf optical properties (Vogelmann, 1993). Reduced leaf chlorophyll concentration is a nearly universal response to FR irradiation among a wide range of species, regardless of changes in leaf expansion (Morgan and Smith, 1979; Casal et al., 1987; Smith and Whitelam, 1997; Li and Kubota, 2009; Meng et al., 2019). Several causes for this decrease in chlorophyll content have been suggested, including 1) limited photosynthate supply in shade-avoiding species that had reduced leaf expansion, 2) a dilution effect when leaf expansion is promoted, and 3) a direct effect on chlorophyll biosynthesis due to reduced amount of active P_{fr} relative to the total pool of phytochromes (see Casal et al., 1987 and references therein). The stimulatory effect of far-red photons on leaf expansion has likely contributed to the 'dilution' of chlorophyll content per unit leaf area. The reduction in leaf chlorophyll content and thickness (indicated by the lower leaf mass per area in **Table 1**) of lettuce grown with far-red substitution resulted in low leaf light absorptance, especially in the green and far-red regions of the spectrum (**Figure 6**).

In addition, the far-red photons were less efficiently absorbed by the leaves, which reduced canopy photon capture (**Table 1**). As a result, the magnitude of increase in canopy photon capture in the FR substitution treatments was smaller than indicated by the fractional ground cover. Therefore, the use of total leaf area or canopy ground cover would likely lead to over-estimation of canopy photon capture.

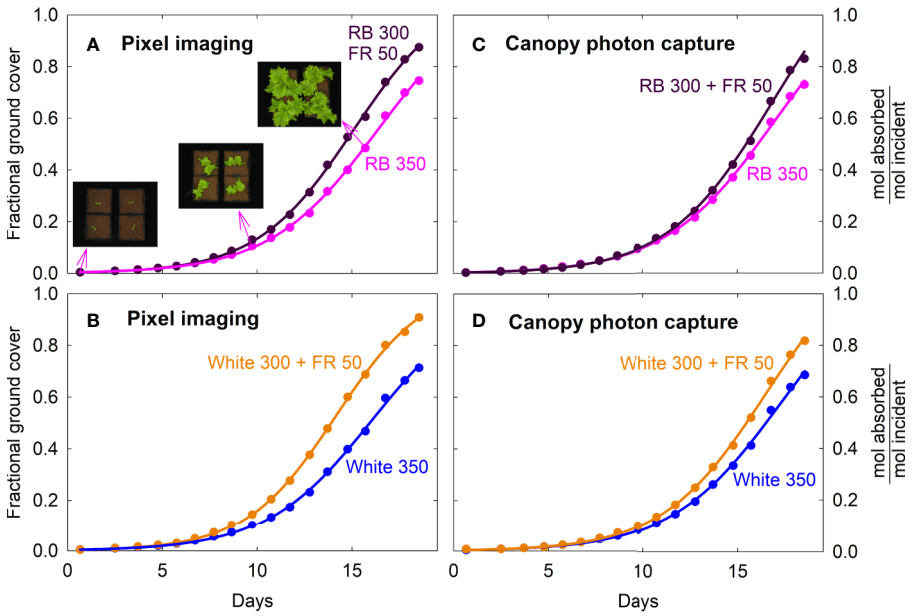

FIGURE 5 | Fraction of ground cover and canopy photon capture of lettuce under four spectral treatments. Fraction of ground cover was obtained from green pixel analysis of top down photos of the canopies. Canopy photon capture (moles of photon absorbed from 400 to 750 nm per mole of incident photons) was estimated from ground cover, leaf photon absorption of the incident spectra and leaf area index. RB, red and blue; FR, far-red. The numbers following each type of light (*e.g.* RB 350) indicate photon flux density in µmol m^{-2} s^{-1}.

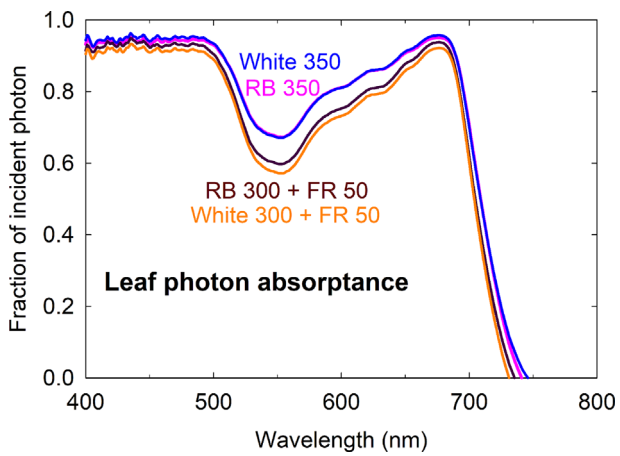

FIGURE 6 | Leaf photon absorptance of lettuce grown under four spectral treatments. RB, red and blue; FR, far-red. The numbers following each type of light (*e.g.* RB 350) indicate photon flux density in µmol m^{-2} s^{-1}.

Predicted Dry Mass From Gas Exchange Measurements

All gas exchange systems measure the carbon assimilation rate in moles of carbon (CO_2) fixed per unit time. To convert P_{gross} and DCG from moles of carbon to grams of biomass, we assumed that the canopy carbon content of lettuce was 0.4 g $_{carbon}$ $g^{-1}_{dry\ mass}$. Carbon fraction in plants has often been assumed to be 43 to 45% (Epstein and Bloom, 2005), but this fraction varies widely with the composition of the biomass (carbohydrates, lignin, proteins, lipids; Amthor, 2010). The carbon fraction thus varies with type of vegetation (leaves, stems and roots) and species (Vertregt and Penning de Vries, 1987; Monje and Bugbee, 1998). It also varies during ontogeny (Ho, 1976; Hadley and Causton, 1984).

Growing conditions also affect carbon fraction. Becker et al. (2015) found that the carbon fraction in leaves of green lettuce decreased from 0.4 to 0.38 g g^{-1} as nitrogen availability increased. Monje and Bugbee (1998) reported that leaf carbon content of wheat increased from 0.38 under ambient CO_2 to 0.4 g g^{-1} under elevated CO_2. These changes were small but reproducible. Lettuce is about 85% leaves (**Table 1**). Roots tend to have a higher carbon content than leaves (0.44 to 0.45 g g^{-1} in roots of wheat; Monje and Bugbee, 1998). The weighted carbon content of the combined leaves and roots of the plants in these studies in thus estimated to be 0.4 g g^{-1}. With this value, the dry mass at harvest predicted from the cumulative DCG averaged 103.9% of the measured total dry mass. This close match validates the accuracy of the gas exchange measurements.

Canopy Quantum Yield: Short-Term *Versus* Long-Term Response to Far-Red Photons

Measurements of canopy gas exchange rate coupled with canopy photon absorption enable the calculation of canopy quantum yield, a measure of photosynthetic efficiency expressed as moles of CO_2 fixed in gross photosynthesis per mole of photons

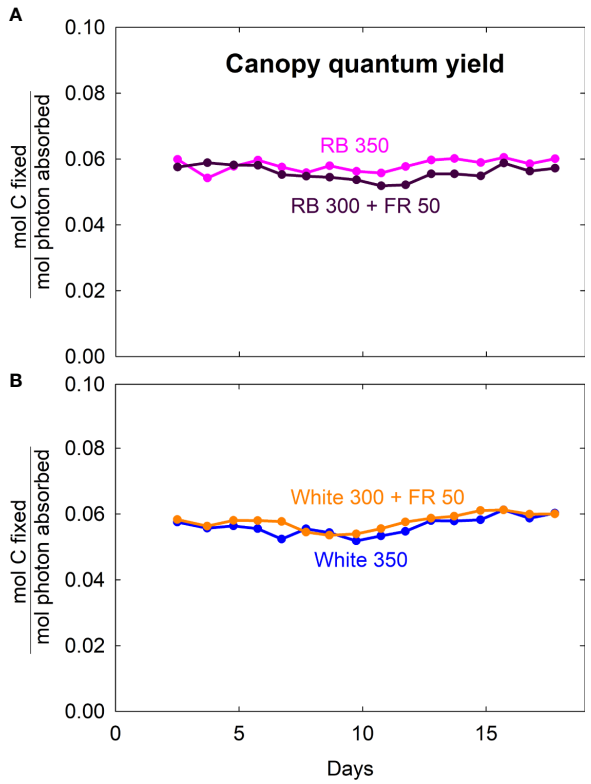

FIGURE 7 | Canopy quantum yield (moles of carbon fixed in gross photosynthesis per mole of photons absorbed from 400 to 750 nm) of lettuce grown under red/blue (RB) and white light, with or without far-red (FR) substitution. The numbers following each type of light (*e.g.* RB 350) indicate photon flux density in µmol m^{-2} s^{-1}.

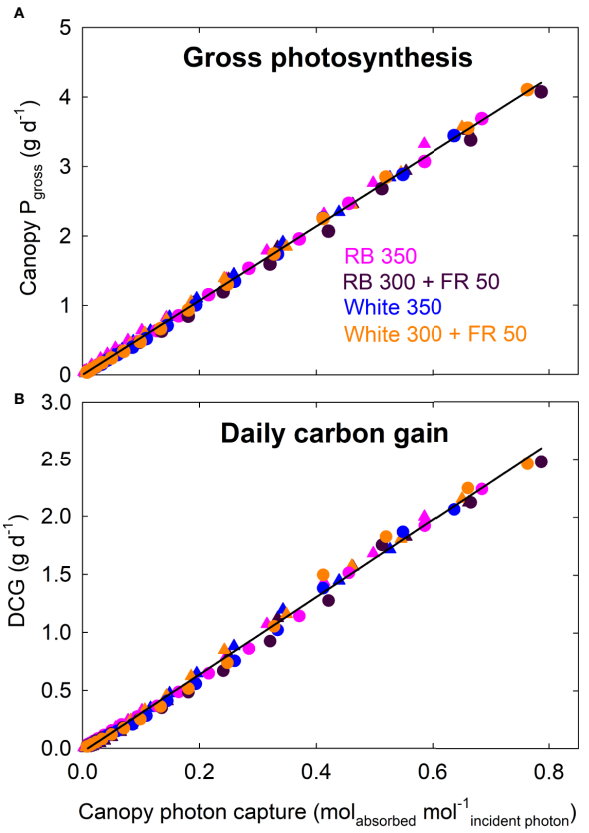

FIGURE 8 | Canopy gross photosynthesis (P_{gross}) and daily carbon gain (DCG) as a function of canopy photon capture of lettuce. Canopy P_{gross} (and DCG) of all four treatments increased linearly with increasing photon capture and had a common slope. RB, red and blue; FR, far-red. The numbers following each type of light (*e.g.* RB 350) indicate photon flux density in µmol m^{-2} s^{-1}. Circles represent data from Rep 1, and triangles represent data from Rep 2 (see DCG in **Figure 3**).

absorbed. We calculated quantum yield using wavelengths from 400 to 750 nm. To our knowledge, this is the first report of the long-term effect of far-red photons on canopy quantum yield. The lack of difference in canopy quantum yield among the four spectral treatments indicates that the absorbed far-red photons were equally efficient as red/blue or white photons (**Figure 7**). This is also indicated by the nearly identical relationship between canopy P_{gross} and photon capture among the treatments (**Figure 8A**).

On an incident photon flux basis, Zhen and Bugbee (2020) showed that the short-term (hours) response of canopy photosynthesis to far-red photons from 700 to 750 nm was equal to 400 to 700 nm photons when applied simultaneously. Because far-red photons are less efficiently absorbed than 400 to 700 nm photons, the far-red photons had a higher canopy quantum yield on an absorbed photon basis. This difference between short-term and long-term responses indicates that the efficiency of light utilization for photosynthesis may have acclimated to far-red radiation during long-term growth. Possible changes include modifications in leaf thickness, chlorophyll content (**Table 1**), chl a:b ratio (Gommers et al., 2013; Kalaitzoglou et al., 2019), PSI:PSII ratio, electron transport and photosynthetic capacity, rubisco content and activity (Chow et al., 1990a; Chow et al., 1990b; Anderson et al., 1995), as well as in the biosynthesis of photoprotective pigments carotenoids and anthocyanins (Li and Kubota, 2009; Stutte et al., 2009; Kalaitzoglou et al., 2019).

Carbon Use Efficiency

Respiration is often assumed to be a fixed fraction of gross photosynthesis in modeling maximum productivity per unit input of solar energy (Zhu et al., 2008; Zhu et al., 2010; Amthor, 2010). A constant CUE of ~0.5 has been widely used in forest growth models (Waring et al., 1998; DeLucia et al., 2007). Gifford (1994) reported that the ratio of respiration to gross photosynthesis of whole plants (which equals to 1—CUE) was constant around 0.4 (a CUE of ~0.6) in diverse annual and perennial species and was minimally affected by plant age and growth temperature (15 to 30°C). Monje and Bugbee (1998) found that CUE of wheat grown under near-optimal conditions (high light and ample water and nutrients) was constant around 0.6 (except during the first week after emergence and final week when plants senesced) despite changes in carbon partitioning to

leaves, stems, and seeds. The response was not affected by [CO_2] even though canopy quantum yield and biomass production increased significantly when [CO_2] was elevated to 1200 mol mol^{-1} (Monje and Bugbee, 1998).

However, reports have conflicted on whether CUE stays constant among species, environmental conditions, and developmental stages (Amthor, 2000; Cannell and Thornley, 2000). A constant CUE means that plants always respire the same fraction of carbohydrates regardless of growth rate. To better understand the link between respiration and growth, respiration is frequently divided into two functional components—*growth respiration* that is determined by the synthesis of new biomass (proportional to growth rate) and *maintenance respiration* that keeps existing biomass functional (proportional to plant size) (McCree, 1970; Amthor, 1989; Amthor, 2000). The respiration required per unit of new growth (*i.e.* growth respiration coefficient) depends on the chemical composition of the biomass being synthesized (Penning de Vries et al., 1974; Amthor, 2010). The respiration required to maintain existing biomass per unit time (*i.e.* maintenance respiration coefficient) is affected by metabolic rate (associated with temperature), but it can also be influenced by the chemical composition, especially tissue nitrogen content (Cannell and Thornley, 2000). van Iersel (2003) showed that CUE can be expressed as function of relative growth rate and growth and maintenance respiration coefficients. Because of the ontogenetic changes in plant tissue composition and relative growth rate, a constant CUE is unlikely unless growth and/or maintenance respiration coefficient change concurrently with relative growth rate. van Iersel (2003) further demonstrated that CUE of lettuce decreased from 0.6 in young plants (24-day old) to 0.2 in old plants (66-day old). This was mainly due to the decrease in relative growth rate and increase in the fraction of maintenance respiration with increasing plant size. The carbon use efficiency of fast-growing and compositionally simple crops like lettuce is expected to be relatively more constant under optimal conditions, where a higher relative growth rate would reduce the importance of maintenance respiration (van Iersel, 2003). Frantz et al. (2004) found that the CUE of rapidly growing lettuce (~15 to 35 day old) under optimal conditions (high light, elevated CO_2, and a constant day/night temperature of 25°C) was stable around 0.62. Decreasing night temperature from 34 to 17°C reduced nighttime respiration rate and allocation to shoot/root, but only slightly altered CUE.

In this study, CUE of young/newly matured lettuce plants (~16–22 days after emergence) was similar under all four treatments, with an average of 0.61 ± 0.02. This is consistent with the values reported for lettuce of similar age by van Iersel (2003) and Frantz et al. (2004). However, CUE of younger seedlings was not determined in the previous studies because of the difficulties in obtaining accurate gas exchange measurements with small plants. With an improved gas-exchange system, we observed that CUE of young lettuce seedlings gradually increased within the first 2 weeks after emergence, similar to the gradual increase in CUE of wheat during the first 8 days after emergence (Monje and Bugbee, 1998). A gradual increase in CUE was also reported in young vinca seedlings as the ratio of respiration to photosynthesis decreased during the first few weeks of plant development (van Iersel and Seymour, 2000). The similarity in CUE of young/newly matured lettuce plants among the spectral treatments indicates that the phenotypical changes caused by FR radiation had little effect on CUE.

CONCLUDING REMARKS

Overall, we found that neither canopy quantum yield nor carbon use efficiency were affected when substituting far-red for traditionally defined photosynthetic photons. This indicates that the absorbed far-red photons (700–750 nm) were equally efficient for photosynthesis when acting synergistically with 400–700 nm photons. Crop yield increased with far-red substitution due to increased leaf expansion and canopy radiation capture mediated by phytochromes during long-term plant cultivation. These data, coupled with previous studies, provide compelling evidence that the current definition of photosynthetically active radiation should be extended to include photons from 700 to 750 nm.

DATA AVAILABILITY STATEMENT

All datasets presented in this study are included in the article/ **Supplementary Material**.

AUTHOR CONTRIBUTIONS

SZ and BB designed the experiment. SZ performed the experiment, analyzed data, and wrote the first draft. SZ and BB discussed the data and revised the manuscript.

FUNDING

This work was supported by the Utah Agricultural Experiment Station, Utah State University; by the NASA-CUBES project award number NNX17AJ31G; and by the USDA-NIFA-SCRI award number 2018-51181-28365 (LAMP Project). Any opinions, findings, and conclusions or recommendations expressed in this material are those of the authors and do not necessarily reflect the views of the National Aeronautics and Space Administration (NASA) or the USDA.

ACKNOWLEDGMENTS

We thank Jakob Johnson for helping with the image analysis of canopy ground cover and Alec Hay for technical support.

SUPPLEMENTARY MATERIAL

The Supplementary Material for this article can be found online at: https://www.frontiersin.org/articles/10.3389/fpls.2020.581156/full#supplementary-material

SUPPLEMENTARY FIGURE 1 | Canopy net photosynthetic rate (P_{net}; μmol_{CO2} $m^{-2}{}_{ground\ area}$ s^{-1}) of lettuce under red/blue (RB) and white, with or without far-red substitution. The numbers following each type of light (*e.g.* RB 350) indicate photon flux density in $\mu mol\ m^{-2}\ s^{-1}$. Plants were seeded in a greenhouse and moved into a multi-chamber gas exchange system two days after seedling emergence (indicated by Day 0 on the x-axis). Downward pointing arrows indicate when far-red LEDs were turned off.

SUPPLEMENTARY FIGURE 2 | Relationships between estimated phytochrome photoequilibria (PPE) and leaf area of lettuce grown with or without far-red photons under two background light spectra—white and red/blue (RB). The decrease in the estimated PPE under each background light was due to a 15% far-red substitution. All four spectral treatments had equal total photon flux of 350 $\mu mol\ m^{-2}\ s^{-1}$ (400 to 750 nm) and 31.5% blue photons.

REFERENCES

Adams, C., Jacobson, A., and Bugbee, B. (2014). Ceramic aggregate sorption and desorption chemistry: implications for use as a component of soilless media. *J. Plant Nutr.* 37, 1345–1357. doi: 10.1080/01904167.2013.837921

Amthor, J. S. (1989). *Respiration and crop productivity* (New York, USA: Springer-Verlag).

Amthor, J. S. (2000). The McCree–de Wit–Penning de Vries–Thornley respiration paradigms: 30 years later. *Ann. Bot.* 86, 1–20. doi: 10.1006/anbo.2000.1175

Amthor, J. S. (2010). From sunlight to phytomass: on the potential efficiency of converting solar radiation to phyto-energy. *New Phytol.* 188, 939–959. doi: 10.1111/j.1469-8137.2010.03505.x

Anderson, J. M., Chow, W. S., and Goodchild, D. J. (1988). Thylakoid membrane organisation in sun/shade acclimation. *Funct. Plant Biol.* 15, 11–26. doi: 10.1071/PP9880011

Anderson, J. M., Chow, W. S., and Park, Y.II (1995). The grand design of photosynthesis: acclimation of the photosynthetic apparatus to environmental cues. *Photosynth. Res.* 46, 129–139. doi: 10.1007/BF00020423

Atkin, O. K., Evans, J. R., and Siebke, K. (1998). Relationship between the inhibition of leaf respiration by light and enhancement of leaf dark respiration following light treatment. *Funct. Plant Biol.* 25, 437–443. doi: 10.1071/PP97159

Ballaré, C. L., Sánchez, R. A., Scopel, A. L., Casal, J. J., and Ghersa, C. M. (1987). Early detection of neighbour plants by phytochrome perception of spectral changes in reflected sunlight. *Plant Cell Environ.* 10, 551–557. doi: 10.1111/1365-3040.ep11604091

Beadle, C. L., and Long, S. P. (1985). Photosynthesis – is it limiting to biomass production? *Biomass* 8, 119–168. doi: 10.1016/0144-4565(85)90022-8

Becker, C., Urlić, B., Jukić Špika, M., Kläring, H. P., Krumbein, A., Baldermann, S., et al. (2015). Nitrogen limited red and green leaf lettuce accumulate flavonoid glycosides, caffeic acid derivatives, and sucrose while losing chlorophylls, β-carotene and xanthophylls. *PLoS One* 10, e0142867. doi: 10.1371/journal.pone.0142867

Bugbee, B., and Monje, O. (1992). The limits of crop productivity. *BioScience* 42, 494–502. doi: 10.2307/1311879

Bugbee, B. (2004). Nutrient Management in Recirculating Hydroponic Culture. *In:* Proceedings of the South Pacific Soilless Culture Conference. M. Nichols (ed.). *Acta Hortic.* 648, 99–112. doi: 10.17660/ActaHortic.2004.648.12

Cannell, M. G. R., and Thornley, J. H. M. (2000). Modelling the components of plant respiration: some guiding principles. *Ann. Bot.* 85, 45–54. doi: 10.1006/anbo.1999.0996

Casal, J. J., Aphalo, P. J., and Sánchez, R. A. (1987). Phytochrome effects on leaf growth and chlorophyll content in Petunia axilaris. *Plant Cell Environ.* 10, 509–514. doi: 10.1111/j.1365-3040.1987.tb01829.x

Casal, J. J. (2012). "Shade avoidance," in *The Arabidopsis book.* 10, e0157. doi: 10.1199/tab.0157

Casal, J. J. (2013). Photoreceptor signaling networks in plant responses to shade. *Annu. Rev. Plant Biol.* 64, 403–427. doi: 10.1146/annurev-arplant-050312-120221

Chow, W. S., Melis, A., and Anderson, J. M. (1990a). Adjustments of photosystem stoichiometry in chloroplasts improve the quantum efficiency of photosynthesis. *Proc. Natl. Acad. Sci.* 87, 7502–7506. doi: 10.1073/pnas.87.19.7502

Chow, W. S., Goodchild, D. J., Miller, C., and Anderson, J. M. (1990b). The influence of high levels of brief or prolonged supplementary far-red illumination during growth on the photosynthetic characteristics, composition and morphology of Pisum sativum chloroplasts. *Plant Cell Environ.* 13, 135–145. doi: 10.1111/j.1365-3040.1990.tb01285.x

Dale, J. E. (1988). The control of leaf expansion. *Annu. Rev. Plant Physiol. Plant Mol. Biol.* 39, 267–295. doi: 10.1146/annurev.pp.39.060188.001411

DeLucia, E. H., Drake, J. E., Thomas, R. B., and Gonzalez-Meler, M. (2007). Forest carbon use efficiency: is respiration a constant fraction of gross primary production? *Global Change Biol.* 13, 1157–1167. doi: 10.1111/j.1365-2486.2007.01365.x

Duysens, L. N. M., and Amesz, J. (1962). Function and identification of two photochemical systems in photosynthesis. *Biochim. Biophys. Acta* 64, 243–260. doi: 10.1016/0006-3002(62)90735-7

Emerson, R., and Lewis, C. M. (1943). The dependence of the quantum yield of chlorella photosynthesis on wavelength of light. *Am. J. Bot.* 30, 165–178. doi: 10.1002/j.1537-2197.1943.tb14744.x

Emerson, R., and Rabinowitch, E. (1960). Red drop and role of auxiliary pigments in photosynthesis. *Plant Physiol.* 35, 477–485. doi: 10.1104/pp.35.4.477

Emerson, R., Chalmers, R., and Cederstrand, C. (1957). Some factors influencing the long-wave limit of photosynthesis. *Proc. Natl. Acad. Sci. U. S. A.* 43, 133–143. doi: 10.1073/pnas.43.1.133

Epstein, E., and Bloom, A. J. (2005). *Mineral nutrition of plants: principles and perspectives. 2nd edition* (Sunderland, Massachusetts: Sinauer Assoc. Inc).

Evans, J. R. (1987). The dependence of quantum yield on wavelength and growth irradiance. *Aust. J. Plant Physiol.* 14, 69–79. doi: 10.1071/PP9870069

Federer, C. A., and Tanner, C. B. (1966). Spectral distribution of light in the forest. *Ecology* 47, 555–560. doi: 10.2307/1933932

Franklin, K. A. (2008). Shade avoidance. *New Phytol.* 179, 930–944. doi: 10.1111/j.1469-8137.2008.02507.x

Frantz, J. M., Cometti, N. N., and Bugbee, B. (2004). Night temperature has a minimal effect on respiration and growth in rapidly growing plants. *Ann. Bot.* 94, 155–166. doi: 10.1093/aob/mch122

Gifford, R. M., Thorne, J. H., Hitz, W. D., and Giaquinta, R. T. (1984). Crop productivity and photoassimilate partitioning. *Science* 225, 801–808. doi: 10.1126/science.225.4664.801

Gifford, R. M. (1994). The global carbon cycle: a viewpoint on the missing sink. *Funct. Plant Biol.* 21, 1–15. doi: 10.1071/pp9940001

Goins, G. D., Ruffe, L. M., Cranston, N. A., Yorio, N. C., Wheeler, R. M., and Sager, J. C. (2001). *Salad crop production under different wavelengths of red light-emitting diodes (LEDs)* (SAE Technical Paper No. 2001-01-2422). doi: 10.4271/2001-01-2422

Gommers, C. M., Visser, E. J., St Onge, K. R., Voesenek, L. A., and Pierik, R. (2013). Shade tolerance: when growing tall is not an option. *Trends Plant Sci.* 18, 65–71. doi: 10.1016/j.tplants.2012.09.008

Hadley, P., and Causton, D. R. (1984). Changes in percentage organic carbon content during ontogeny. *Planta* 160, 97–101. doi: 10.1007/BF00392856

Halliday, K. J., Koornneef, M., and Whitelam, G. C. (1994). Phytochrome B and at least one other phytochrome mediate the accelerated flowering response of Arabidopsis thaliana L. to low red/far-red ratio. *Plant Physiol.* 104, 1311–1315. doi: 10.1104/pp.104.4.1311

Heraut-Bron, V., Robin, C., Varlet-Grancher, C., Afif, D., and Guckert, A. (1999). Light quality (red: far-red ratio): does it affect photosynthetic activity, net CO2 assimilation, and morphology of young white clover leaves? *Can. J. Bot.* 77, 1425–1431. doi: 10.1139/b99-099

Hill, R., and Bendall, F. (1960). Function of the two cytochrome components in chloroplasts: A working hypothesis. *Nature* 186, 136–137. doi: 10.1038/186136a0

Ho, L. C. (1976). Variation in the carbon/dry matter ratio in plant material. *Ann. Bot.* 40, 163–165. doi: 10.1093/oxfordjournals.aob.a085109

Hogewoning, S. W., Wientjes, E., Douwstra, P., Trouwborst, G., van Ieperen, W., Croce, R., et al. (2012). Photosynthetic quantum yield dynamics: From photosystems to leaves. *Plant Cell* 24, 1921–1935. doi: 10.1105/tpc.112.097972

Holmes, M. G., and Fukshansky, L. (1979). Phytochrome photoequilibria in green leaves under polychromatic radiation: a theoretical approach. *Plant Cell Environ.* 2, 59–65. doi: 10.1111/j.1365-3040.1979.tb00774.x

Holmes, M. G., and Smith, H. (1977). The function of phytochrome in the natural environment—II. The influence of vegetation canopies on the spectral energy distribution of natural daylight. *Photochem. Photobiol.* 25, 539–545. doi: 10.1111/j.1751-1097.1977.tb09125.x

Inada, K. (1976). Action spectra for photosynthesis in higher plants. *Plant Cell Physiol.* 17, 355–365. doi: 10.1093/oxfordjournals.pcp.a075288

Jose, A. M., and Schäfer, E. (1978). Distorted phytochrome action spectra in green plants. *Planta* 138, 25–28. doi: 10.1007/BF00392909

Kalaitzoglou, P., van Ieperen, W., Harbinson, J., van der Meer, M., Martinakos, S., Weerheim, K., et al. (2019). Effects of continuous or end-of-day far-red light on tomato plant growth, morphology, light absorption and fruit production. *Front. Plant Sci.* 10, 322. doi: 10.3389/fpls.2019.00322

Kasperbauer, M. J. (1987). Far-red light reflection from green leaves and effects on phytochrome-mediated assimilate partitioning under field conditions. *Plant Physiol.* 85, 350–354. doi: 10.1104/pp.85.2.350

R. E. Kendrick and G. H. Kronenberg (Eds.) (1994). *Photomorphogenesis in plants. 2nd ed* (Dordrecht, The Netherlands: Kluwer Academic Publishers).

Klassen, S. P., Ritchie, G., Frantz, J. M., Pinnock, D., and Bugbee, B. (2004). "Real-time imaging of ground cover: Relationships with radiation capture, canopy photosynthesis, and daily growth rate," in *Digital imaging and spectral techniques: applications to precision agriculture and crop physiology*. (American Society of Agronomy), vol. 66, 1–14.

Kusuma, P., Pattison, P. M., and Bugbee, B. (2020). From physics to fixtures to food: current and potential LED efficacy. *Hortic. Res.* 7, 1–9. doi: 10.1038/s41438-020-0283-7

Laisk, A., Oja, V., Eichelmann, H., and Dall'Osto, L. (2014). Action spectra of photosystems II and I and quantum yield of photosynthesis in leaves in State 1. *Biochim. Biophys. Acta* 1837, 315–325. doi: 10.1016/j.bbabio.2013.12.001

Li, Q., and Kubota, C. (2009). Effects of supplemental light quality on growth and phytochemicals of baby leaf lettuce. *Environ. Exp. Bot.* 67, 59–64. doi: 10.1016/j.envexpbot.2009.06.011

Massa, G. D., Kim, H. H., Wheeler, R. M., and Mitchell, C. A. (2008). Plant productivity in response to LED lighting. *HortScience* 43, 1951–1956. doi: 10.21273/HORTSCI.43.7.1951

McCree, K. J. (1970). "An equation for the rate of respiration of white clover grown under controlled conditions," in *Prediction and measurement of photosynthetic productivity*. Ed. I. Šetlík (Wageningen: Centre for Agricultural Publishing and Documentation), 221–229.

McCree, K. J. (1972). The action spectrum, absorptance and quantum yield of photosynthesis in crop plants. *Agric. Meteorol.* 9, 191–216. doi: 10.1016/0002-1571(71)90022-7

Meng, Q., Kelly, N., and Runkle, E. S. (2019). Substituting green or far-red radiation for blue radiation induces shade avoidance and promotes growth in lettuce and kale. *Environ. Exp. Bot.* 162, 383–391. doi: 10.1016/j.envexpbot.2019.03.016

Monje, O., and Bugbee, B. (1998). Adaptation to high CO_2 concentration in an optimal environment: radiation capture, canopy quantum yield and carbon use efficiency. *Plant Cell Environ.* 21, 315–324. doi: 10.1046/j.1365-3040.1998.00284.x

Monteith, J. L. (1977). Climate and the efficiency of crop production in Britain. *Philos. Trans. R. Soc Lond. B Biol. Sci.* 281, 277–294. doi: 10.1098/rstb.1977.0140

Morgan, D. C., and Smith, H. (1976). Linear relationship between phytochrome photoequilibrium and growth in plants under simulated natural radiation. *Nature* 262, 210–212. doi: 10.1038/262210a0

Morgan, D. C., and Smith, H. (1978). The relationship between phytochrome-photoequilibrium and Development in light grown Chenopodium album L. *Planta* 142, 187–193. doi: 10.1007/BF00388211

Morgan, D. C., and Smith, H. (1979). A systematic relationship between phytochrome-controlled development and species habitat, for plants grown in simulated natural radiation. *Planta* 145, 253–258. doi: 10.1007/BF00454449

Morgan, P. W., Finlayson, S. A., Childs, K. L., Mullet, J. E., and Rooney, W. L. (2002). Opportunities to improve adaptability and yield in grasses. *Crop Sci.* 42, 1791–1799. doi: 10.2135/cropsci2002.1791

Murakami, K., Matsuda, R., and Fujiwara, K. (2018). A mathematical model of photosynthetic electron transport in response to the light spectrum based on excitation energy distributed to photosystems. *Plant Cell Physiol.* 59, 1643–1651. doi: 10.1093/pcp/pcy085

Nelson, J. A., and Bugbee, B. (2015). Analysis of environmental effects on leaf temperature under sunlight, high pressure sodium and light emitting diodes. *PLoS One* 10, e0138930. doi: 10.1371/journal.pone.0138930

Park, Y., and Runkle, E. S. (2017). Far-red radiation promotes growth of seedlings by increasing leaf expansion and whole-plant net assimilation. *Environ. Exp. Bot.* 136, 41–49. doi: 10.1016/j.envexpbot.2016.12.013

Penning de Vries, F., Brunsting, A. H. M., and van Laar, H. H. (1974). Products, requirements and efficiency of biosynthesis a quantitative approach. *J. Theor. Biol.* 45, 339–377. doi: 10.1016/0022-5193(74)90119-2

Rajapakse, N. C., and Kelly, J. W. (1994). Problems of reporting spectral quality and interpreting phytochrome-mediated responses. *HortScience* 29, 1404–1407. doi: 10.21273/HORTSCI.29.12.1404

Sager, J. C., Smith, W. O., Edwards, J. L., and Cyr, K. L. (1988). Photosynthetic efficiency and phytochrome photoequilibria determination using spectral data. *Trans. ASAE* 31, 1882–1889. doi: 10.13031/2013.30952

Schmitt, J., McCormac, A. C., and Smith, H. (1995). A test of the adaptive plasticity hypothesis using transgenic and mutant plants disabled in phytochrome-mediated elongation responses to neighbors. *Am. Nat.* 146, 937–953. doi: 10.1086/285832

Sharp, R. E., Matthews, M. A., and Boyer, J. S. (1984). Kok effect and the quantum yield of photosynthesis: light partially inhibits dark respiration. *Plant Physiol.* 75, 95–101. doi: 10.1104/pp.75.1.95

Siegelman, H. W., and Butler, W. L. (1965). Properties of phytochrome. *Annu. Rev. Plant Physiol.* 16, 383–392. doi: 10.1146/annurev.pp.16.060165.002123

Smith, H., and Whitelam, G. C. (1997). The shade avoidance syndrome: multiple responses mediated by multiple phytochromes. *Plant Cell Environ.* 20, 840–844. doi: 10.1046/j.1365-3040.1997.d01-104.x

Smith, H. (1982). Light quality, photoperception, and plant strategy. *Annu. Rev. Plant Physiol.* 33, 481–518. doi: 10.1146/annurev.pp.33.060182.002405

Stutte, G. W., Edney, S., and Skerritt, T. (2009). Photoregulation of bioprotectant content of red leaf lettuce with light-emitting diodes. *HortScience* 44, 79–82. doi: 10.21273/HORTSCI.44.1.79

USU Crop Physiology Laboratory (2018). *"Utah Monocot/Dicot Solution" Nutrients. Paper 2*. Available at: https://digitalcommons.usu.edu/cgi/viewcontent.cgi?article=1001&context=cpl_nutrients.

Valladares, F., and Niinemets, Ü. (2008). Shade tolerance, a key plant feature of complex nature and consequences. *Annu. Rev. Ecol. Evol. S.* 39, 237–257. doi: 10.1146/annurev.ecolsys.39.110707.173506

van Iersel, M. W., and Bugbee, B. (2000). A multiple chamber, semicontinuous, crop carbon dioxide exchange system: design, calibration, and data interpretation. *J. Am. Soc Hortic. Sci.* 125, 86–92. doi: 10.21273/JASHS.125.1.86

van Iersel, M. W., and Seymour, L. (2000). Growth respiration, maintenance respiration, and carbon fixation of vinca: a time series analysis. *J. Am. Soc Hortic. Sci.* 125, 702–706. doi: 10.21273/JASHS.125.6.702

van Iersel, M. W. (2003). Carbon use efficiency depends on growth respiration, maintenance respiration, and relative growth rate. A case study with lettuce. *Plant Cell Environ.* 26, 1441–1449. doi: 10.1046/j.0016-8025.2003.01067.x

Vertregt, N. F. W. T., and Penning de Vries, F. (1987). A rapid method for determining the efficiency of biosynthesis of plant biomass. *J. Theor. Biol.* 128, 109–119. doi: 10.1016/S0022-5193(87)80034-6

Vogelmann, T. C. (1993). Plant tissue optics. *Annu. Rev. Plant Biol.* 44, 231–251. doi: 10.1146/annurev.pp.44.060193.001311

Waring, R. H., Landsberg, J. J., and Williams, M. (1998). Net primary production of forests: a constant fraction of gross primary production? *Tree Physiol.* 18, 129–134. doi: 10.1093/treephys/18.2.129

Woolley, J. T. (1971). Reflectance and transmittance of light by leaves. *Plant Physiol.* 47, 656–662. doi: 10.1104/pp.47.5.656

Zhen, S., and Bugbee, B. (2020). Far-red photons have equivalent efficiency to traditional photosynthetic photons: Implications for redefining photosynthetically active radiation. *Plant Cell Environ.* 43, 1259–1272. doi: 10.1111/pce.13730

Zhen, S., and van Iersel, M. W. (2017). Far-red light is needed for efficient photochemistry and photosynthesis. *J. Plant Physiol.* 209, 115–122. doi: 10.1016/j.jplph.2016.12.004

Zhen, S., Haidekker, M., and van Iersel, M. W. (2018). Far-red light enhances photochemical efficiency in a wavelength-dependent manner. *Physiol. Plant.* 167, 21–33. doi: 10.1111/ppl.12834

Zhu, X. G., Long, S. P., and Ort, D. R. (2008). What is the maximum efficiency with which photosynthesis can convert solar energy into biomass? *Curr. Opin. Biotech.* 19, 153–159. doi: 10.1016/j.copbio.2008.02.004

Zhu, X. G., Long, S. P., and Ort, D. R. (2010). Improving photosynthetic efficiency for greater yield. *Annu. Rev. Plant Biol.* 61, 235–261. doi: 10.1146/annurev-arplant-042809-112206

Conflict of Interest: The authors declare that the research was conducted in the absence of any commercial or financial relationships that could be construed as a potential conflict of interest.

Copyright © 2020 Zhen and Bugbee. This is an open-access article distributed under the terms of the Creative Commons Attribution License (CC BY). The use, distribution or reproduction in other forums is permitted, provided the original author(s) and the copyright owner(s) are credited and that the original publication in this journal is cited, in accordance with accepted academic practice. No use, distribution or reproduction is permitted which does not comply with these terms.

frontiers in Plant Science

ORIGINAL RESEARCH
published: 22 October 2020
doi: 10.3389/fpls.2020.571788

Growth Responses of Red-Leaf Lettuce to Temporal Spectral Changes

Qingwu Meng† *and Erik S. Runkle**

Controlled-Environment Lighting Laboratory, Department of Horticulture, Michigan State University, East Lansing, MI, United States

OPEN ACCESS

Edited by:
Eiji Goto,
Chiba University, Japan

Reviewed by:
Roberta Paradiso,
University of Naples Federico II, Italy
Elizabeth Van Volkenburgh,
University of Washington, United States

***Correspondence:**
Erik S. Runkle
runkleer@msu.edu

†Present address:
Qingwu Meng,
Department of Plant and Soil Sciences, University of Delaware, Newark, DE, United States

Specialty section:
This article was submitted to Crop and Product Physiology, a section of the journal Frontiers in Plant Science

Received: *11 June 2020*
Accepted: *30 September 2020*
Published: *22 October 2020*

Citation:
Meng Q and Runkle ES (2020) Growth Responses of Red-Leaf Lettuce to Temporal Spectral Changes. Front. Plant Sci. 11:571788. doi: 10.3389/fpls.2020.571788

Lighting is typically static for indoor production of leafy greens. However, temporal spectrum differentiation for distinct growth phases can potentially control age-specific desirable traits. Spectral effects can be persistent yet dynamic as plants mature, necessitating characterization of time-dependent responses. We grew red-leaf lettuce (*Lactuca sativa* L.) "Rouxai" in a growth room at 23°C and under a 20-h photoperiod created by warm-white (WW), blue (B; peak = 449 nm), green (G; peak = 526 nm), red (R; peak = 664 nm), and/or far-red (FR; peak = 733 nm) light-emitting diodes. From day 0 to 11, plants received six static lighting treatments with the same total photon flux density (400–800 nm): WW_{180}, R_{180}, $B_{20}R_{160}$, $B_{20}G_{60}R_{100}$, $B_{20}R_{100}FR_{60}$, or B_{180} (subscripts denote photon flux densities in $\mu mol \cdot m^{-2} \cdot s^{-1}$). On day 11, plants grown under each of the six treatments were transferred to all treatments, which created 36 temporal spectrum alternations. Plant growth, morphology, and coloration were measured on days 11 and 25. Increasing B radiation from 0 to 100% in static treatments decreased shoot fresh and dry weights and increased foliage redness of seedlings and mature plants. Compared to $B_{20}R_{160}$, $B_{20}R_{100}FR_{60}$ increased shoot fresh weight, but not dry weight, on both days. However, other phenotypic responses under static treatments changed over time. For example, leaf length under B_{180} was 35% lower on day 11 but similar on day 25 compared to that under R_{180}. In the B_{20} background, substituting G_{60} for R radiation did not influence shoot weight on day 11 but decreased it by 19% on day 25. When plants were switched from one treatment to another on day 11, the treatments applied before day 11 influenced final shoot weight and, to a lesser extent, leaf length and foliage coloration on day 25. In comparison, effects of the treatments applied after day 11 were more pronounced. We conclude some phenotypic responses to light quality depend on time and sequential light quality treatments had cumulative effects on lettuce growth. The temporal complexity of spectral responses is critical in photobiological research and creates opportunities for time-specific spectrum delivery to optimize crop characteristics.

Keywords: controlled environment, dynamic lighting, LEDs, light quality, morphology, plant growth

INTRODUCTION

The spectral composition of lighting in controlled environments can regulate a wide range of commercially relevant crop traits such as harvestable yield, morphology, coloration, and nutritional quality (Carvalho and Folta, 2014a). Red (R; 600–700 nm) radiation is typically more effective at stimulating extension growth and biomass accumulation of leafy greens than blue (B; 400–500 nm) or B + R radiation (Ohashi-Kaneko et al., 2007; Son and Oh, 2013; Lee et al., 2014). In contrast, B radiation generally suppresses extension growth (Cope et al., 2014; Wollaeger and Runkle, 2014) but stimulates production of bioactive compounds (Son and Oh, 2013; Lee et al., 2014; Kopsell et al., 2015). Green (G; 500–600 nm) radiation penetrates deep in the leaf and crop canopy to promote photosynthesis (Terashima et al., 2009; Brodersen and Vogelmann, 2010). Far-red (FR; 700–800 nm) radiation can induce shade-avoidance symptoms (Cerdán and Chory, 2003; Meng and Runkle, 2019) and regulate anthocyanin production (Carvalho and Folta, 2014b). The combined effects of these wavebands on plant growth and development are often complicated by synergistic or antagonistic interactions. Characterization of these spectral effects on various edible crops has been advanced by research with adjustable arrays of multicolored light-emitting diodes (LEDs) in controlled environments.

Electric lighting is substituted for sunlight to provide photosynthetically active photons for indoor-grown leafy greens. It is generally static throughout the production cycle, whereas field-grown plants undergo fluctuations in light quality, intensity, and duration throughout the day and production cycle. Static lighting feeds constant energy to light-harvesting antennae of photosystem II and maintains steady electron transport and proton generation to produce NADPH and ATP, respectively, which are used in carbon fixation (Armbruster et al., 2014). In contrast, the dynamic nature of sunlight necessitates responsive and efficient photosynthetic acclimation through regulation of energy channeling and dissipation to maintain high photosynthetic efficiency (Demmig-Adams et al., 2012). In arabidopsis [*Arabidopsis thaliana* (L.) Heynh.], K^+ efflux antiporter 3 mediated H^+/K^+ antiport to facilitate rapid restoration of photosystem II quantum efficiency after plants were transferred from high to low light or from darkness to low light (Armbruster et al., 2014). Such mechanisms allow plants to thrive in continuously changing light environments.

Switching from static to dynamic lighting for indoor crop production adds the temporal factor in crop responses to improve crop traits. Temporal spectrum differentiation can occur in large or small segments of the crop life cycle to elicit age-dependent, desirable attributes. For example, anthocyanin accumulation in red-leaf lettuce (*Lactuca sativa* L.) is unnecessary for seedlings but desirable for mature plants at harvest. It can be induced rapidly by ≥4 days of end-of-production supplemental lighting from B and/or R LEDs (Owen and Lopez, 2015; Gómez and Jiménez, 2020). In addition, R radiation induced excessive extension growth of lettuce "Crispa" seedlings but increased dry weight of mature plants compared to B or B + R radiation (Chen et al., 2014). Therefore, it could be potentially beneficial to produce compact seedlings under B or B + R radiation and then switch to R radiation to promote growth of mature plants. After the seedling phase, weekly progressive spectrum alternations of B and/or R radiation influenced shoot growth, morphology, and phytochemical accumulation of lettuce "Sunmang" (Son et al., 2017). A greater dose of B radiation increased secondary metabolite concentrations, whereas a greater dose of R radiation increased shoot weight and projected leaf area (Son et al., 2017). Changing the spectrum in shorter periods of plant development can also modulate final crop phenotypes. For example, 4-day sequential B, R, and/or FR lighting treatments influenced stem elongation, anthocyanin concentration, and antioxidant capacity of kale (*Brassica napus* L. var. *sabellica*) seedlings, showing strong plant plasticity in response to spectral changes (Carvalho and Folta, 2014b). Furthermore, staggering B and R radiation within the day increased shoot weight of romaine lettuce (*Lactuca sativa* L. var. *longifolia*) compared to simultaneous B + R radiation (Jishi et al., 2016).

Under changing light conditions, a light response can be transient or persistent. Examples of a transient light response include stomatal opening and phototropism under B radiation as well as increasing net photosynthesis with incremental increases in photon flux densities. These rapid responses are reversible after the light condition changes. On the other hand, a spectrum applied in an early developmental phase can have persistent and irreversible influence on subsequent phenotypic responses. For example, the addition of FR radiation to B + R radiation during seedling development of snapdragon (*Antirrhinum majus* L.) promoted flowering when plants were finished in a greenhouse environment (Park and Runkle, 2017). In addition, B or R radiation applied for 7 days after emergence influenced leaf area and shoot dry weight of lettuce "Grand Rapids" 16 or 42 days after emergence, irrespective of a switch to the opposite waveband on day 7 (Eskins et al., 1995). However, such sustained spectral effects were not observed in other lettuce studies with a fixed spectrum early in seeding development and varying spectra afterward (Johkan et al., 2010; Son and Oh, 2013). Furthermore, the influence of a spectrum on lettuce growth and morphology can vary with each developmental phase. For example, when applied day 10–17 after seed sow, B radiation decreased leaf area and shoot fresh weight of lettuce "Banchu Red Fire" on day 17 but increased them on day 45 compared to R radiation (Johkan et al., 2010). The discrepancies in these studies likely result from different genetic backgrounds, light intensities, and spectral contexts.

Here, we expanded static spectral combinations to include G, FR, and warm-white (WW) radiation and created a wide array of lighting treatments shifted temporally between the seedling and mature phases of indoor lettuce production. The objectives of this study were (1) to investigate how spectral treatments for lettuce seedlings influence phenotypes of mature plants grown under different spectra; (2) to compare lettuce growth under single wavebands, combinations of two or three wavebands, and WW radiation; and (3) to find temporal spectral combinations

for desirable lettuce growth and morphology. We postulated that (1) the spectral effects during the seedling stage would persist through the mature phase, regardless of the finishing spectral environment; (2) substituting G radiation for R radiation would increase lettuce growth during the seedling stage but have little influence on growth of mature plants; and (3) B radiation alone would inhibit leaf expansion and dry weight during the seedling phase but promote them during the mature phase.

MATERIALS AND METHODS

The Propagation Phase

This experiment was performed in a refrigerated walk-in growth room of the Controlled-Environment Lighting Laboratory (Michigan State University, East Lansing, MI). We chose lettuce to study because it is the most widely grown hydroponic crop in indoor vertical farms for its short stature, fast growth rate, and high value. Our previous studies showed generally similar growth responses of green- and red-leaf lettuce, so we studied red-leaf lettuce because of its unique foliage coloration in response to spectral alternations (Meng and Runkle, 2019; Meng et al., 2019). Seeds of red oakleaf lettuce "Rouxai" were obtained from a commercial seed producer (Johnny's Selected Seeds, Winslow, ME, United States) and sown in a rockwool substrate with 200 2.5-cm-wide cubes per sheet (AO 25/40 Starter Plugs; Grodan, Milton, ON, Canada) on April 28 and 29, 2018 for two blocks. The substrate was presoaked in deionized water supplemented with diluted (1:31) 95–98% sulfuric acid (J.Y. Baker, Inc., Phillipsburg, NJ, United States), a water-soluble fertilizer (12N–$4P_2O_5$–$16K_2O$ RO Hydro FeED; JR Peters, Inc., Allentown, PA, United States), and magnesium sulfate (Epsom salt; Pennington Seed, Inc., Madison, GA, United States) to achieve a pH of 3.9 and an electrical conductivity of 1.6 $mS{\cdot}cm^{-1}$. The nutrient solution contained the following nutrients (in $mg{\cdot}L^{-1}$): 125 N, 42 P, 167 K, 73 Ca, 49 Mg, 39 S, 1.7 Fe, 0.52 Mn, 0.56 Zn, 0.13 B, 0.47 Cu, and 0.13 Mo. Seed trays were covered with transparent humidity domes and placed under six different lighting treatments, each at a total photon flux density (TPFD; 400–800 nm) of 180 $\mu mol{\cdot}m^{-2}{\cdot}s^{-1}$ with a 20-h photoperiod. Air temperature was set at 20°C from April 28 to 30, 2018 and increased to 23°C for the remainder of the experiment. From day 1 to 11, seedlings were subirrigated as needed using the same nutrient solution with a pH of 5.8 adjusted with potassium bicarbonate. The humidity domes were removed on May 3, 2018 for both blocks.

The Production Phase

On day 11, when the second true leaf was expanding, seedlings in rockwool cubes were transplanted into 36-cell rafts (36 2.5-cm-wide holes on each lightweight raft measuring 60.9 cm × 121.9 cm × 2.5 cm; Beaver Plastics, Ltd., Acheson, AB, Canada) floating in flood tables (1.22 m × 0.61 m × 0.18 m; Active Aqua AAHR24W; Hydrofarm, Petaluma, CA, United States) on three-tier racks (Indoor Harvest, Houston, TX, United States). Plants were spaced 20 cm apart horizontally and 15 cm apart diagonally. The recirculating nutrient solution was mixed as described for seedlings to provide the following nutrients (in $mg{\cdot}L^{-1}$): 150 N, 50 P, 200 K, 88 Ca, 58 Mg, 47 S, 2.1 Fe, 0.63 Mn, 0.68 Zn, 0.15 B, 0.56 Cu, and 0.15 Mo. It was oxygenated with a circular air stone (20.3 × 2.5 cm; Active Aqua AS8RD; Hydrofarm) connected to a 60-W air pump (Active Aqua AAPA70L; Hydrofarm). The pH, electrical conductivity, and temperature of the nutrient solution for each lighting canopy were measured daily using a portable pH and electrical conductivity meter (HI9814; Hanna Instruments, Woonsocket, RI, United States) (**Table 1**). Potassium bicarbonate was used to increase pH when it dropped below 5.5.

Environmental Conditions

Temperature in the growth room was regulated with an industrial ventilation and air-conditioning unit (HBH030A3C20CRS; Heat Controller, LLC., Jackson, MI, United States) connected to a wireless thermostat (Honeywell International, Inc., Morris Plains, NJ, United States). The deep-flow hydroponic system was equipped with two light quantum sensors (LI-190R; LI-COR, Inc., Lincoln, NE, United States), two thermocouples (0.13-mm type E; Omega Engineering, Inc., Stamford, CT, United States), two infrared sensors (OS36-01-K-80F; Omega Engineering, Inc.), a CO_2 transmitter (GMD20; Vaisala, Inc., Louisville, CO, United States), and a relative humidity and temperature probe (HMP110; Vaisala, Inc.). All sensors were connected to a datalogger (CR1000; Campbell Scientific, Inc., Logan, UT, United States) with a multiplexer (AM16/32B; Campbell Scientific, Inc.), which recorded environmental parameters every 10 s and logged hourly averages using computer software (LoggerNet; Campbell Scientific, Inc.). The air temperature, canopy temperature, CO_2 concentration, and relatively humidity throughout the experiment (mean ± standard deviation) were 22.5 ± 1.0°C, 24.1 ± 0.9°C, 392 ± 31 ppm, and 44 ± 8%, respectively.

Lighting Treatments

Seedlings were grown under WW_{180}, R_{180}, $B_{20}R_{160}$, $B_{20}G_{60}R_{100}$, $B_{20}R_{100}FR_{60}$, or B_{180} LEDs (PHYTOFY RL; OSRAM, Beverley, MA, United States), where the subscript following each LED type indicates its photon flux density (in $\mu mol{\cdot}m^{-2}{\cdot}s^{-1}$). The peak wavelengths of WW, B, G, R, and FR LEDs were 639, 449, 526, 664, and 733 nm, respectively. The outputs of seven color channels, including five used in this study, in each LED fixture were independently controlled with software (Spartan Control Software; OSRAM). The specifications, layout, and positioning of the LED fixtures were as described by Meng et al. (2019). Spectra were measured at seven locations at plant canopy of each lighting treatment using a portable spectroradiometer (PS200; Apogee Instruments, Inc., Logan, UT, United States) (**Figure 1**). The single-band photon flux densities, photosynthetic photon flux density (PPFD; 400–700 nm), TPFD, yield photon flux density [YPFD, an integrated value based on relative quantum efficiency (McCree, 1972) and spectral data], phytochrome photoequilibrium [PPE, an estimated value based on phytochrome absorption coefficients and spectra data (Sager et al., 1988)], ratio of B to R radiation (B:R), and ratio of R to FR radiation (R:FR) for each lighting treatment were subsequently

TABLE 1 | The pH, electrical conductivity, and water temperature (mean ± standard deviation) of nutrient solutions for six lighting treatment plots in two blocks during the lettuce production phase.

Lighting treatment	pH		Electrical conductivity ($mS \cdot cm^{-1}$)		Water temperature (°C)	
	Block 1	Block 2	Block 1	Block 2	Block 1	Block 2
WW_{180}	6.0 ± 1.0	6.2 ± 0.9	1.8 ± 0.0	1.8 ± 0.1	23.7 ± 0.3	23.3 ± 0.3
R_{180}	6.1 ± 1.0	6.3 ± 0.9	1.9 ± 0.1	1.7 ± 0.1	22.9 ± 0.2	23.9 ± 0.4
$B_{20}R_{160}$	6.1 ± 1.0	6.3 ± 0.9	1.9 ± 0.1	1.7 ± 0.1	22.9 ± 0.2	23.9 ± 0.4
$B_{20}G_{60}R_{100}$	6.1 ± 1.0	6.3 ± 0.9	1.9 ± 0.1	1.7 ± 0.1	22.9 ± 0.2	23.9 ± 0.4
$B_{20}R_{100}FR_{60}$	6.0 ± 1.0	6.2 ± 0.9	1.8 ± 0.0	1.8 ± 0.1	23.7 ± 0.3	23.3 ± 0.3
B_{180}	6.0 ± 1.0	6.2 ± 0.9	1.8 ± 0.0	1.8 ± 0.1	23.7 ± 0.3	23.3 ± 0.3

Plants were grown under warm-white (WW) or mixed blue (B; 400–500 nm), green (G; 500–600 nm), red (R; 600–700 nm), and far-red (FR; 700–800 nm) light-emitting diodes (LEDs). The number following each LED type is its respective photon flux density in $\mu mol \cdot m^{-2} \cdot s^{-1}$.

calculated (**Table 2**). To study the temporal effects of light quality, lighting treatments were switched between the propagation phase (day 0–11) and the production phase (day 11–25). Seedlings grown under each of the six lighting treatments were transferred to all six lighting treatments on day 11. This created a total of 36 unique temporal lighting combinations, six of which were static (without transfers) throughout the experiment (**Table 3**).

Data Collection and Analysis

Shoot fresh and dry weights, leaf morphology, and coloration data were collected on ten young lettuce plants per block grown under each of the six static lighting treatments on day 11 and on eight mature lettuce plants per block grown under each of the 36 temporal lighting combinations on day 25. Shoot fresh weight was measured with an analytical balance (GR-200; A&D Store, Inc., Wood Dale, IL, United States) for young plants and a different one (GX-1000; A&D Store, Inc.) for mature plants based on capacities. Length of the fifth most mature true leaf was measured to quantify extension growth. The International Commission on Illumination Lab color space analysis was conducted on a representative leaf per plant using a colorimeter (Chroma Meter CR-400; Konica Minolta Sensing, Inc.). L^*, a^*, and b^* indicate foliage brightness (ranging from 0 for black to 100 for diffuse white), greenness–redness (corresponding to negative–positive directions), and blueness–yellowness (corresponding to negative–positive directions), respectively. Subsequently, plants were dried in an oven (Blue M, Blue Island, IL) at 60°C for ≥5 days followed by dry weight measurements with the same analytical balances as for shoot fresh weight.

Data on young and mature lettuce plants were analyzed with the PROC MIXED procedure and Tukey's honestly significant difference test ($\alpha = 0.05$) in SAS (version 9.4; SAS Institute, Inc., Cary, NC, United States). Data from static treatments were analyzed as a randomized complete block design with two blocks (using opposite racks of the growth room), six static lighting treatments, and subsampling ($n = 10$), assuming fixed block effects. Data from alternate treatments were analyzed as a strip-split-plot design with two blocks, six whole-plot levels (post-transplant lighting treatments), six subplot levels (pre-transplant lighting treatments), and subsampling ($n = 8$), assuming fixed block effects. The split-plot design included whole plots arranged in a randomized complete block design.

RESULTS

Static Lighting Treatments for Young and Mature Lettuce

On day 11, shoot fresh weight was 40–44% lower, and shoot dry weight was 39–42% lower, under B_{180} than under WW_{180} and R_{180} (**Figure 2A**). Partial substitution of R radiation in $B_{20}R_{160}$ with 60 $\mu mol \cdot m^{-2} \cdot s^{-1}$ of G radiation ($B_{20}G_{60}R_{100}$) or FR radiation ($B_{20}R_{100}FR_{60}$) did not influence shoot dry weight, whereas the substitution with FR radiation increased shoot fresh weight by 18%. Substituting 20 $\mu mol \cdot m^{-2} \cdot s^{-1}$ of B radiation for R radiation ($B_{20}R_{160}$ versus R_{180}) decreased shoot dry weight by 15%, but not shoot fresh weight. On day 25, increasing substitution of R radiation with B radiation decreased shoot fresh and dry weights (**Figure 2B**). Shoot fresh weight was 63–65% lower, and shoot dry weight was 52–57% lower, under B_{180} than under R_{180} or WW_{180}. Substituting 60 $\mu mol \cdot m^{-2} \cdot s^{-1}$ of G radiation for R radiation in $B_{20}R_{160}$ decreased shoot fresh and dry weights by 19%. The same substitution with FR radiation increased shoot fresh weight by 22%, but not shoot dry weight.

On day 11, leaves were the longest under WW_{180}, R_{180}, and $B_{20}R_{100}FR_{60}$ and the shortest under B_{180} (**Figure 2C**). Increasing substitution of R radiation with B radiation decreased leaf length. Substituting 60 $\mu mol \cdot m^{-2} \cdot s^{-1}$ of G or FR radiation for R radiation in $B_{20}R_{160}$ increased leaf length by 11 or 42%, respectively. On day 25, leaves were the longest under $B_{20}R_{100}FR_{60}$ and the shortest under $B_{20}R_{160}$ and $B_{20}G_{60}R_{100}$ (**Figure 2D**). Compared to WW_{180}, leaves were 8% shorter under R_{180} and similar under B_{180}. Although substituting 20 $\mu mol \cdot m^{-2} \cdot s^{-1}$ of B radiation for R radiation decreased leaf length by 11%, leaf length was similar under R_{180} and B_{180}. Substituting 60 $\mu mol \cdot m^{-2} \cdot s^{-1}$ of FR radiation for R radiation in $B_{20}R_{160}$ increased leaf length by 41%, but the same substitution with G radiation did not influence it.

On day 11, foliage brightness (L^*) was the greatest under R_{180}, followed by WW_{180} and $B_{20}R_{100}FR_{60}$ (**Figure 3A**). Adding B

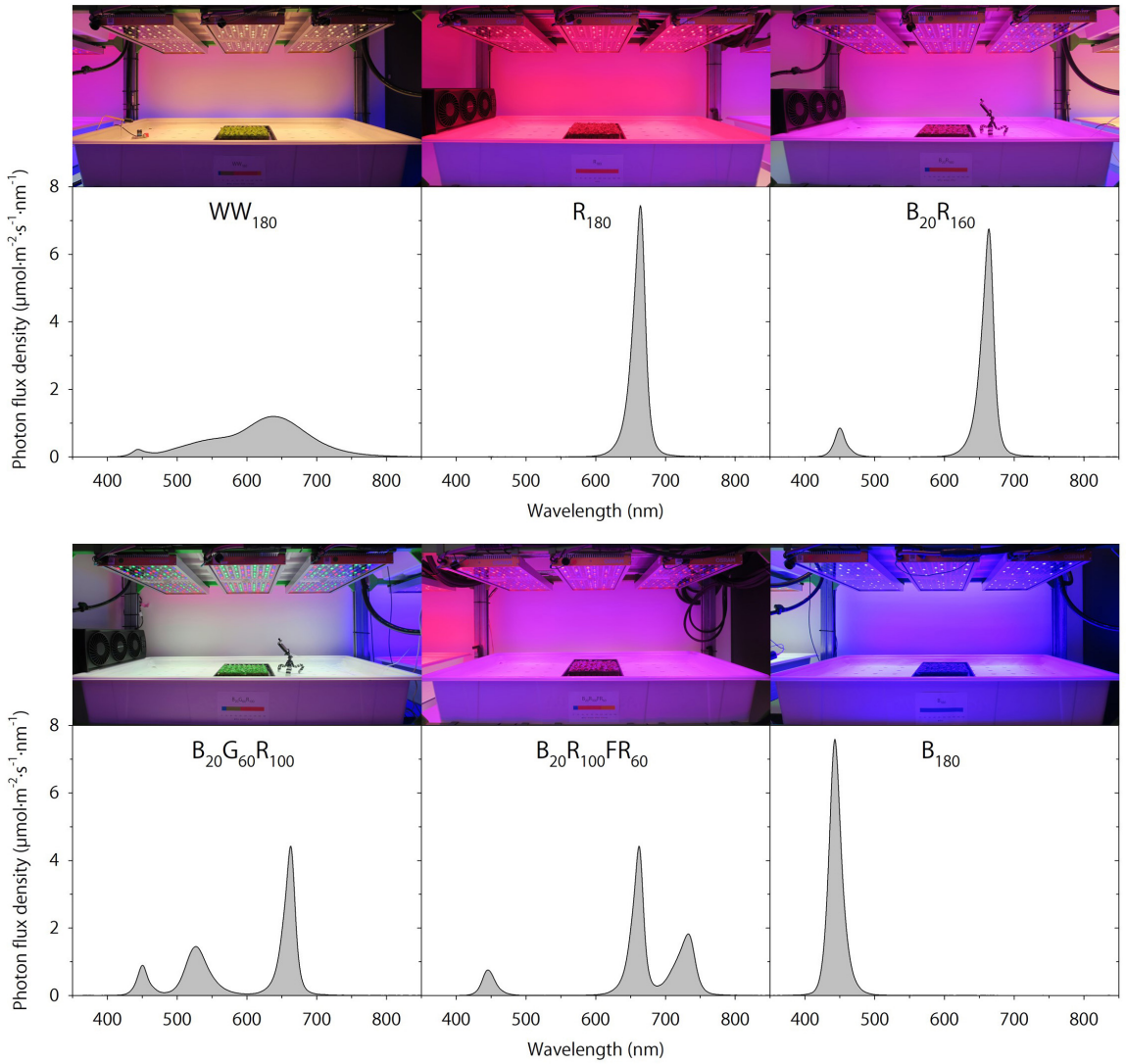

FIGURE 1 | Spectral distributions of six lighting treatments delivered by warm-white (WW) or mixed blue (B; 400–500 nm), green (G; 500–600 nm), red (R; 600–700 nm), and far-red (FR; 700–800 nm) light-emitting diodes (LEDs). The number following each LED type is its respective photon flux density in $\mu mol \cdot m^{-2} \cdot s^{-1}$.

radiation to R_{180} decreased brightness. Substituting R radiation in $B_{20}R_{160}$ with G or FR radiation increased brightness, especially with FR radiation. On day 25, leaves were the brightest under R_{180} and WW_{180} and the darkest under B_{180} (**Figure 3B**). Increasing substitution of R radiation with B radiation decreased brightness. Leaves were brighter when R radiation in $B_{20}R_{160}$ was substituted with FR radiation, but not G radiation.

On day 11, leaves were the least red (lowest a^*) and yellowest (highest b^*) under R_{180}, followed by WW_{180} and $B_{20}R_{100}FR_{60}$, and the reddest and least yellow under B_{180} (**Figures 3C,E**). The inclusion of B radiation in an R background increased redness and decreased yellowness, whereas the inclusion of G or FR radiation decreased redness and increased yellowness. At the same photon flux density, FR radiation reduced redness and increased yellowness more than G radiation. The a^* and b^* trends on day 25 were similar to those on day 11, except that there were no differences between R_{180} and WW_{180} or between $B_{20}G_{60}R_{100}$ and $B_{20}R_{100}FR_{60}$ on day 25 (**Figures 3D,F**).

Temporal Lighting Combinations for Mature Lettuce

Data on day 25 from 36 temporal lighting combinations are shown in **Figure 4**. Within each eventual treatment applied day 11–25, the initial treatments applied day 0–11 significantly influenced final shoot fresh and dry weights and leaf length on day 25, but not foliage red-green coloration. Irrespective of the eventual treatment, final shoot fresh and dry weights were generally the greatest when plants were initially grown under WW_{180}, R_{180}, or $B_{20}R_{100}FR_{60}$ and the lowest when initially grown under B_{180}. Responses of final shoot fresh and dry weights to initial treatments $B_{20}R_{160}$ and $B_{20}G_{60}R_{100}$ were variable within

TABLE 2 | Spectral characteristics of six lighting treatments delivered by warm-white (WW) or mixed blue (B; 400–500 nm), green (G; 500–600 nm), red (R; 600–700 nm), and far-red (FR; 700–800 nm) light-emitting diodes (LEDs).

	LED lighting treatment					
	WW_{180}	R_{180}	$B_{20}R_{160}$	$B_{20}G_{60}R_{100}$	$B_{20}R_{100}FR_{60}$	B_{180}
Single-band photon flux density ($\mu mol \cdot m^{-2} \cdot s^{-1}$)						
B	12.5	0.3	19.2	22.9	18.8	178.4
G	52.8	0.7	0.7	59.7	0.8	0.9
R	98.1	176.9	158.5	99.4	102.2	0.5
FR	18.1	2.1	1.9	1.3	60.7	0.1
Integrated photon flux density ($\mu mol \cdot m^{-2} \cdot s^{-1}$)						
PPFD	163.3	177.9	178.4	181.9	121.8	179.7
TPFD	181.4	180.0	180.3	183.2	182.4	179.9
YPFD	149.5	165.0	162.1	156.5	119.3	134.4
Radiation ratio						
B:R	0.13	0.00	0.12	0.23	0.18	386.80
R:FR	5.42	83.96	82.98	76.19	1.68	3.49
PPE	0.829	0.882	0.880	0.878	0.764	0.480

The number following each LED type is its respective photon flux density in $\mu mol \cdot m^{-2} \cdot s^{-1}$. Integrated parameters include the photosynthetic photon flux density (PPFD; 400–700 nm), the total photon flux density (TPFD; 400–800 nm), and the yield photon flux density [YPFD; the product of relative quantum efficiency (McCree, 1972) and spectral data from 300 to 800 nm]. The estimated phytochrome photoequilibrium (PPE) was calculated as described by Sager et al. (1988).

each eventual treatment. Final leaf length within each eventual treatment was mostly similar under initial treatments except B_{180}, under which final leaf length within each eventual treatment was slightly lower than that under some other initial treatments.

The Effects of Initial and Eventual Lighting Treatments on Mature Lettuce

To dissect the effects of initial (applied day 0–11) and eventual (applied day 11–25) lighting treatments on lettuce harvested on day 25, data of plants grown under the same initial treatments were pooled for initial treatment analysis, whereas data of plants grown under the same eventual treatments were pooled for eventual treatment analysis. The effects of the six lighting treatments on final shoot fresh and weight weights, leaf length, and color parameters were different when applied day 0–11 versus day 11–25 (**Figures 5,6**).

When the lighting treatments were applied day 0–11, final shoot fresh and dry weights (on day 25) were the greatest under WW_{180}, R_{180}, and $B_{20}R_{100}FR_{60}$, followed by $B_{20}R_{160}$ and $B_{20}G_{60}R_{100}$, and the lowest under B_{180} (**Figure 5A**). In addition, final leaf length under WW_{180} and R_{180} was slightly greater than that under $B_{20}R_{100}FR_{60}$ and B_{180} (**Figure 5C**). Leaves were slightly brighter under $B_{20}G_{60}R_{100}$ than under B_{180}, slightly redder under $B_{20}R_{160}$ and B_{180} than under $B_{20}G_{60}R_{100}$, and slightly yellower under $B_{20}G_{60}R_{100}$ than under B_{180} (**Figures 6A,C,E**). Otherwise, leaf color parameters were similar under most treatments.

Treatment effects were more pronounced when applied day 11–25. Final shoot fresh and dry weights were the greatest under R_{180}, followed by WW_{180} and $B_{20}R_{100}FR_{60}$, and the lowest under B_{180} (**Figure 5B**). Partially substituting B radiation for R_{180} decreased shoot weight. Substituting 60 $\mu mol \cdot m^{-2} \cdot s^{-1}$ of G and FR radiation for R radiation in $B_{20}R_{160}$ decreased and increased shoot weight, respectively. Final leaf length was the greatest under $B_{20}R_{100}FR_{60}$, followed by WW_{180} and B_{180}, and lowest under $B_{20}R_{160}$ and $B_{20}G_{60}R_{100}$ (**Figure 5D**). Leaf length under R_{180} was between that under WW_{180} and $B_{20}R_{160}$. Leaf color was the brightest under WW_{180} and R_{180}, followed by $B_{20}R_{100}FR_{60}$, and the least bright under B_{180} (**Figure 6B**). Leaf brightness under $B_{20}R_{160}$ and $B_{20}G_{60}R_{100}$ was between that under $B_{20}R_{100}FR_{60}$ and that under B_{180}. Leaves were the reddest under B_{180}, followed by $B_{20}R_{160}$, and the least red under R_{180}, followed by WW_{180} (**Figure 6D**). Compared to $B_{20}R_{160}$, leaf redness was reduced with substitutional G and FR radiation, especially with the latter. The b^* trend was the opposite of the a^* trend (**Figure 6F**).

DISCUSSION

When lettuce "Rouxai" received static lighting throughout this study, phenotypic responses during the propagation and production phases were generally similar but varied under some treatments. On days 11 and 25, increasing B:R decreased shoot fresh and dry weights, increased leaf redness, and decreased leaf brightness and yellowness. In addition, increasing B:R decreased leaf length on day 11. These results are consistent with the notion that B radiation generally inhibits extension growth and shoot weight while promoting accumulation of chlorophylls, anthocyanins, and other secondary metabolites (Son and Oh, 2013; Kopsell et al., 2015; Wollaeger and Runkle, 2015). However, compared to R_{180}, leaf length on day 25 was lower under $B_{20}R_{160}$ but similar under B_{180}. Aberrant promotion of extension growth and weight gain by B radiation alone was previously observed in cucumber (*Cucumis sativus* L.) and cherry tomato (*Solanum lycopersicum* L. var. *cerasiforme*) seedlings and lettuce "Grand Rapids" (Eskins et al., 1995; Liu et al., 2009; Hernández and Kubota, 2016). We showed a novel

TABLE 3 | Temporal lighting combinations during lettuce propagation and production.

Day 0–11 (propagation)	Day 11–25 (production)
WW_{180}	WW_{180}
	R_{180}
	$B_{20}R_{160}$
	$B_{20}G_{60}R_{100}$
	$B_{20}R_{100}FR_{60}$
	B_{180}
R_{180}	WW_{180}
	R_{180}
	$B_{20}R_{160}$
	$B_{20}G_{60}R_{100}$
	$B_{20}R_{100}FR_{60}$
	B_{180}
$B_{20}R_{160}$	WW_{180}
	R_{180}
	$B_{20}R_{160}$
	$B_{20}G_{60}R_{100}$
	$B_{20}R_{100}FR_{60}$
	B_{180}
$B_{20}G_{60}R_{100}$	WW_{180}
	R_{180}
	$B_{20}R_{160}$
	$B_{20}G_{60}R_{100}$
	$B_{20}R_{100}FR_{60}$
	B_{180}
$B_{20}R_{100}FR_{60}$	WW_{180}
	R_{180}
	$B_{20}R_{160}$
	$B_{20}G_{60}R_{100}$
	$B_{20}R_{100}FR_{60}$
	B_{180}
B_{180}	WW_{180}
	R_{180}
	$B_{20}R_{160}$
	$B_{20}G_{60}R_{100}$
	$B_{20}R_{100}FR_{60}$
	B_{180}

Plants were grown under static or alternate lighting treatments delivered by warm-white (WW) or mixed blue (B; 400–500 nm), green (G; 500–600 nm), red (R; 600–700 nm), and far-red (FR; 700–800 nm) light-emitting diodes (LEDs). The number following each LED type is its respective photon flux density in $\mu mol \cdot m^{-2} \cdot s^{-1}$.

temporal shift of the B radiation function from growth inhibition during the seedling phase to promotion of leaf expansion, but not shoot weight, during the production phase of lettuce. Therefore, temporal specificity should be considered at least in some crops when evaluating spectral influence on plant growth.

Extension growth in arabidopsis seedlings is regulated by the activities of cryptochromes 1 and 2, which depend on the B photon flux density (Pedmale et al., 2016). Cryptochromes 1 and 2 interacted with phytochrome-interacting factors 4 and 5 in low B radiation to promote hypocotyl growth, whereas active repression of phytochrome-interacting factor 4 and degradation of cryptochrome 2 and phytochrome-interacting factor 5 in high B radiation restricted it (Pedmale et al., 2016). In the present study, all leaves of lettuce seedlings grown under high B radiation exhibited typical inhibition of extension growth. However, as lettuce matured, layers of newer leaves emerged from the central meristem and covered older ones. The newer leaves were directly exposed to abundant B radiation, whereas the older ones became shaded and received less B radiation (Franklin, 2016). Therefore, the responses and interactions of cryptochromes and phytochrome-interacting factors likely differed in upper and lower leaves, which mostly received high and low B radiation, respectively. The decrease in the incident B photon flux density with leaf maturity could explain the shift from inhibited extension growth of seedlings to promoted extension growth of mature plants under externally static and strong B radiation.

We also observed dynamic growth responses of lettuce to substitutional G radiation. Substituting 60 $\mu mol \cdot m^{-2} \cdot s^{-1}$ of G radiation for R radiation influenced lettuce shoot weight and leaf length differently on days 11 and 25. It did not affect shoot fresh and dry weights but increased leaf length on day 11. In contrast, it decreased shoot fresh and dry weights but did not affect leaf length on day 25. However, when growing lettuce "Rouxai" under WW radiation for 4 days before varying spectral treatments, plants under $B_{20}G_{60}R_{100}$ had higher shoot fresh weight, but similar shoot dry weight and leaf length, compared to those under $B_{20}R_{160}$ on day 30 or 33 (Meng et al., 2020). In a similar study, substituting 36 $\mu mol \cdot m^{-2} \cdot s^{-1}$ of G radiation for R radiation in static $B_{24}R_{126}$ increased shoot fresh and dry weights and leaf area of lettuce "Waldmann's Green" on day 28, whereas G radiation alone from fluorescent lamps decreased them (Kim et al., 2004). These discrepancies can at least partly be attributed to adaptive responses to G radiation in photosynthetic acclimation and plant architecture, which could change throughout growth phases based on spectral history, sampling time, and other environmental factors.

We consider two phenomena to explain the shifting responses to G radiation in this study. First, the commonly cited McCree curve shows the spectral region near G radiation had the lowest quantum yield when data were expressed on an absorbed photon basis considering the leaf absorption spectrum (McCree, 1972). However, when the same data were expressed on an incident photon basis without considering the leaf absorption spectrum, the photosynthetic efficacy of incident G radiation was comparable to that of incident B radiation and about half that of incident R radiation (McCree, 1972). Therefore, partial substitution of incident R radiation with incident G radiation could reduce overall photosynthetic efficacy and thus weight gain in some species and cultivars. Indeed, at the same B photon flux density of 15, 30, or 45 $\mu mol \cdot m^{-2} \cdot s^{-1}$, substituting 15 $\mu mol \cdot m^{-2} \cdot s^{-1}$ of G radiation for R radiation at a constant PPFD of 150 $\mu mol \cdot m^{-2} \cdot s^{-1}$ reduced the leaf net photosynthetic rate of lettuce "Green Skirt" without affecting leaf morphology (Kang et al., 2016). In addition, the leaf net photosynthetic rate of lettuce was lower under G radiation alone than under R or B

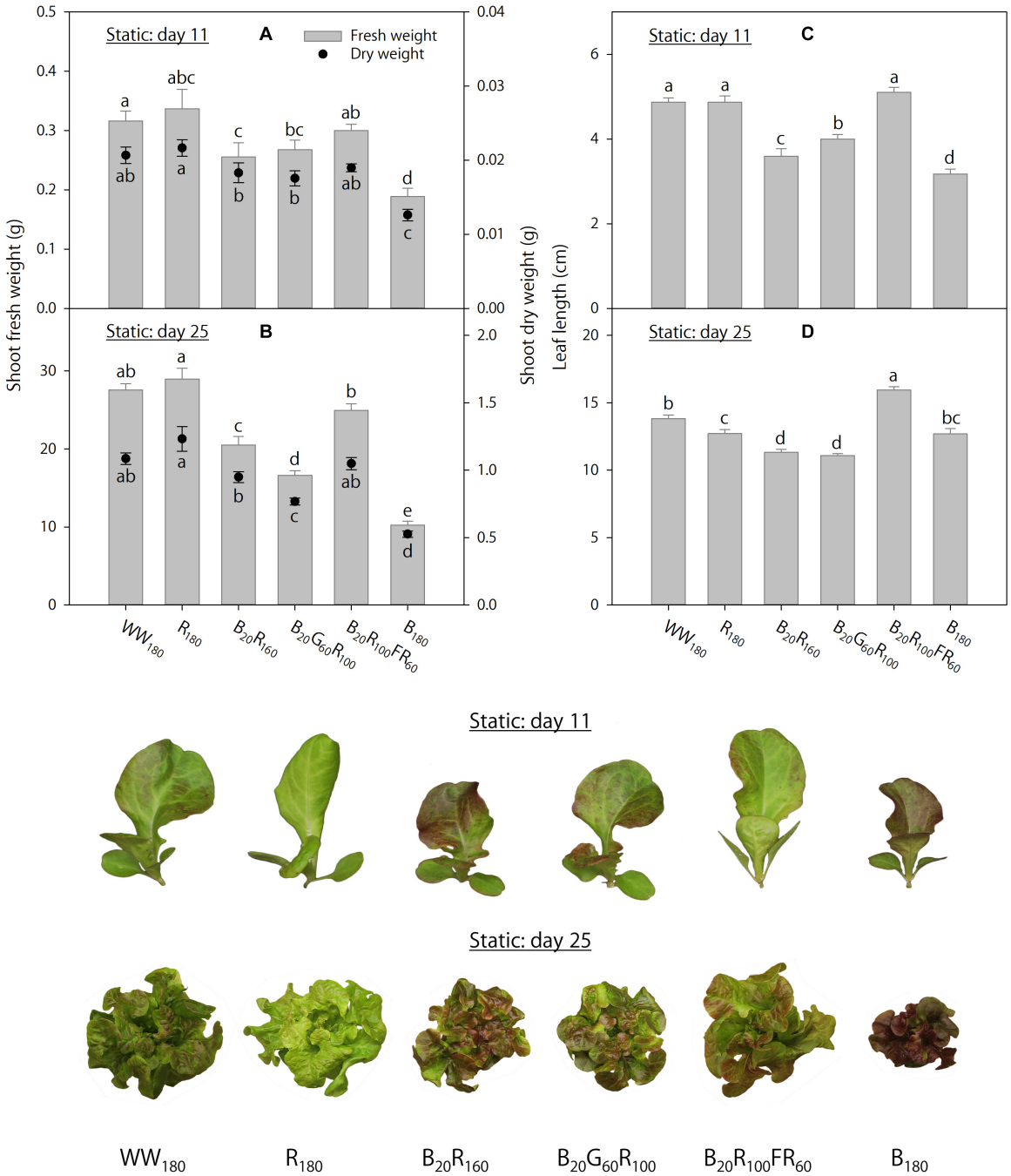

FIGURE 2 | Shoot fresh and dry weights and leaf length on days 11 and 25 of lettuce "Rouxai" grown under six static lighting treatments delivered by warm-white (WW) or mixed blue (B; 400–500 nm), green (G; 500–600 nm), red (R; 600–700 nm), and far-red (FR; 700–800 nm) light-emitting diodes (LEDs). The number for each LED type is its photon flux density in $\mu mol \cdot m^{-2} \cdot s^{-1}$. Means followed by different letters within each parameter are significantly different based on Tukey's honestly significant difference test ($\alpha = 0.05$). Error bars show standard errors.

radiation alone, B + R radiation, or B + G + R radiation (Kim et al., 2004; Kang et al., 2016).

Second, when delivered at a sufficiently high photon flux density, G radiation can reverse B-induced growth inhibition and elicit the shade-avoidance response, such as accelerated hypocotyl and petiole elongation (Folta and Maruhnich, 2007; Zhang et al., 2011; Wang and Folta, 2013). In arabidopsis, G radiation reversed activation of cryptochrome 1 and degradation of cryptochrome 2 by B radiation (Bouly et al., 2007). Accumulation of cryptochrome 2 in substitutional G radiation can promote activity of phytochrome-interacting factors 4 and 5 and thus increase extension growth (Pedmale et al., 2016).

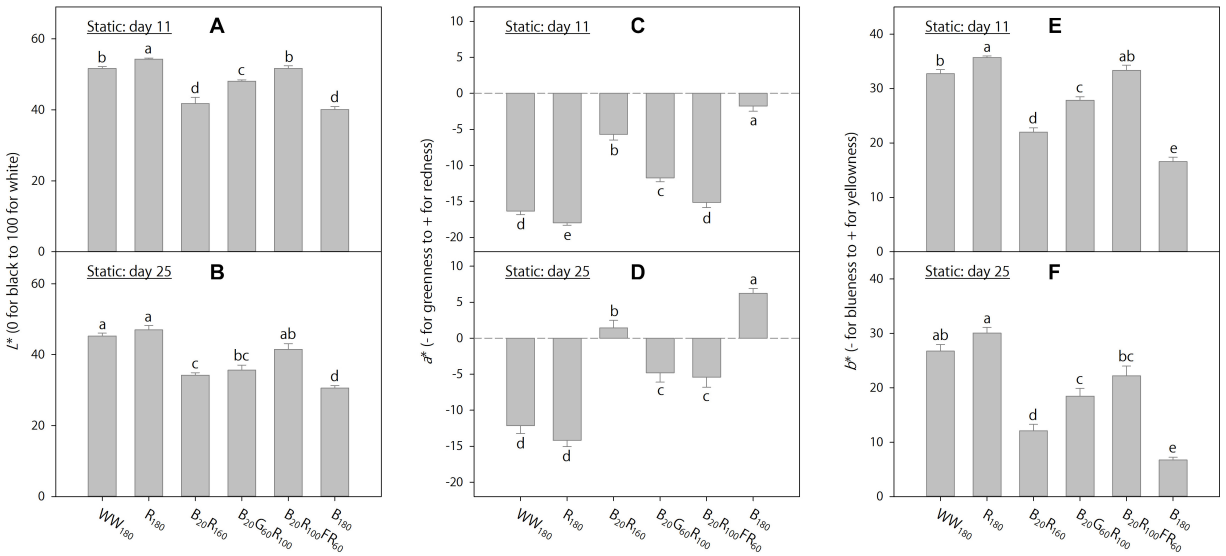

FIGURE 3 | Lab color space parameters on days 11 and 25 of lettuce "Rouxai" grown under six static lighting treatments delivered by warm-white (WW) or mixed blue (B; 400–500 nm), green (G; 500–600 nm), red (R; 600–700 nm), and far-red (FR; 700–800 nm) light-emitting diodes (LEDs). The number for each LED type is its photon flux density in $\mu mol \cdot m^{-2} \cdot s^{-1}$. Means followed by different letters in each graph are significantly different based on Tukey's honestly significant difference test ($\alpha = 0.05$). Error bars show standard errors.

Besides stem growth, partially substituting G radiation for R radiation in constant B radiation promoted leaf expansion of lettuce "Waldmann's Green" (Kim et al., 2004), which likely increased light capture for photosynthesis. In addition, completely substituting G radiation for R radiation in $B_{80}R_{80}$ increased leaf area of tomato (*S. lycopersicum* L.) seedlings but did not influence shoot fresh or dry weight (Wollaeger and Runkle, 2014), which resembles the lettuce seedling response to G radiation on day 11 in the present study. In other studies, the inclusion of G radiation generally did not influence plant growth (Hernández and Kubota, 2016; Snowden et al., 2016), indicating G radiation effects could depend on the genotype, spectral context, and timing of treatments.

Taken together, the varying responses to substitutional G radiation observed on days 11 and 25 in the present study could be attributed to a changing balance between its reduction of instantaneous photosynthesis and its enhancement of whole-plant photosynthesis through increased leaf expansion and light interception. As lettuce grown under B + R radiation received less overall B radiation later in production because of leaf layering, its sensitivity to additional shade signals such as G radiation (when added) subsided. This could explain why leaf length under $B_{20}G_{60}R_{100}$ was initially greater than that under $B_{20}R_{160}$ on day 11 but eventually was similar to it on day 25. Increased leaf expansion likely compensated for reduced net photosynthesis in G radiation on day 11, leading to comparable shoot weight under $B_{20}R_{160}$ and $B_{20}G_{60}R_{100}$. The lack of such compensation on day 25 resulted in lower shoot weight under substitutional G radiation.

In contrast, FR radiation was a stronger shade signal than G radiation at the same photon flux density (Meng et al., 2019) and consistently increased leaf length by 41–42% on days 11 and 25 when added to B + R radiation. Lettuce grown under $B_{20}R_{100}FR_{60}$ had similar shoot dry weight and 17–22% higher shoot fresh weight (partly due to increases in moisture content) compared to that under $B_{20}R_{160}$, although $B_{20}R_{100}FR_{60}$ was 32% lower in the PPFD and 26% lower in the YPFD. The similar TPFDs across all lighting treatments cannot explain differences in shoot dry weight. In addition, **Figure 7** plots shoot dry weight against the relative PPFD, YPFD, leaf length, PPFD × leaf length, or YPFD × leaf length for all lighting treatments. Only YPFD × leaf length was linearly related with shoot dry weight (**Figure 7**). Therefore, the similar dry weight with the FR radiation substitution ($B_{20}R_{100}FR_{60}$ versus $B_{20}R_{160}$) was likely the product of the reduced YPFD (74% of that for $B_{20}R_{160}$) and increased light interception (141–142% of that under $B_{20}R_{160}$). This suggests that changes in shoot dry weight can be predicted by multiplying percentage changes in the YPFD (to account for the changing instantaneous photosynthetic rate and quantum efficiency) and percentage changes in leaf size (to account for changing light interception due to morphological acclimation). The YPFD is a better predictor of plant biomass than the PPFD because it accounts for relative quantum efficiency and the contribution of FR radiation to net photosynthesis, albeit less significant than B, G, or R radiation. Lastly, light interception may be better estimated with leaf area instead of leaf length.

Increasing B:R intensified red coloration of lettuce "Rouxai," whereas substitutional G or FR radiation decreased B-induced anthocyanin accumulation of plants treated with static lighting on days 11 and 25. Similarly, increasing the B photon flux density from 20 to 80 $\mu mol \cdot m^{-2} \cdot s^{-1}$ increased anthocyanin concentration of lettuce "Red Sails" in a dose-dependent manner; however, the inclusion of G radiation reduced anthocyanin accumulation in lettuce "Red Sails" and arabidopsis

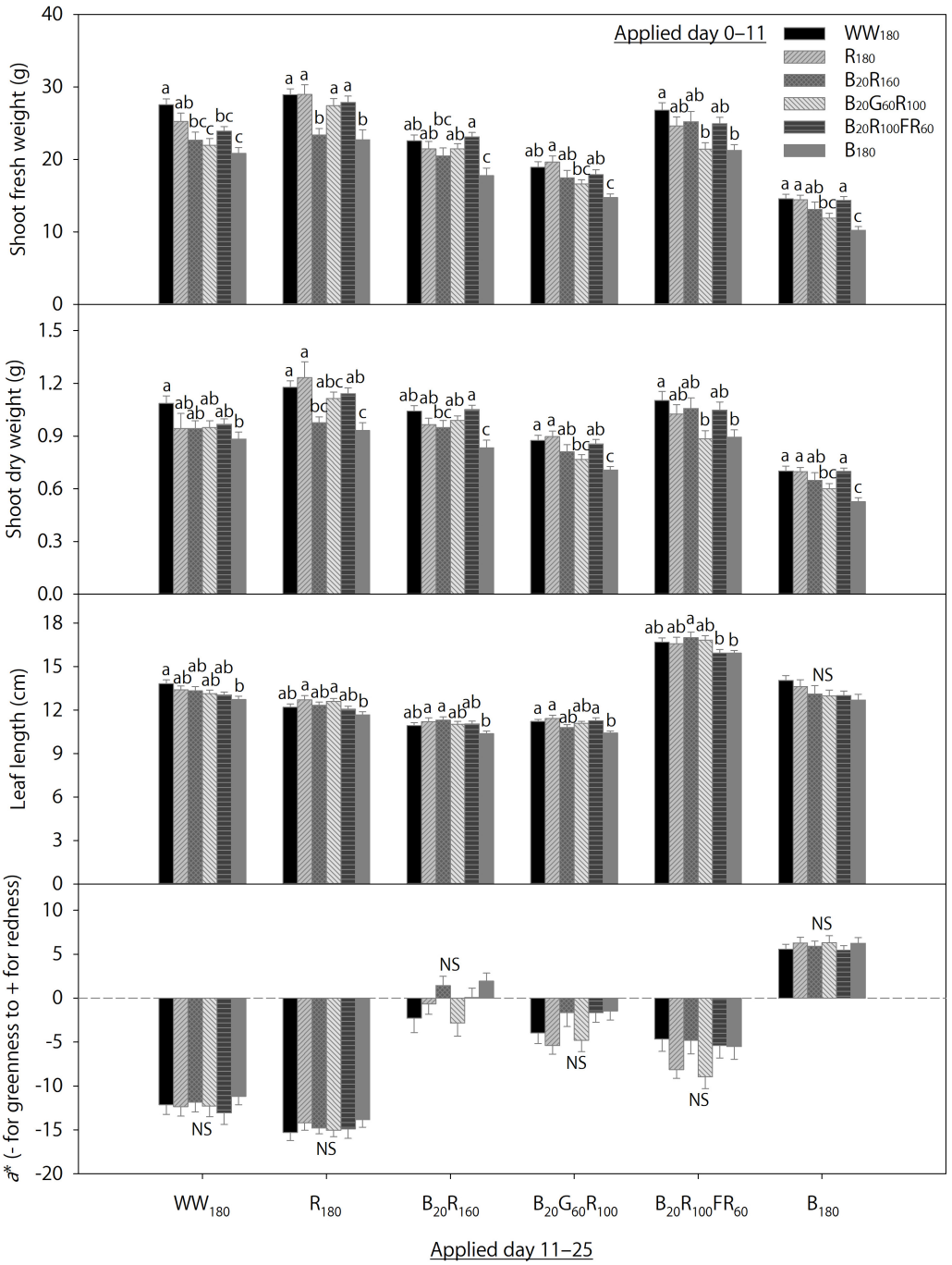

FIGURE 4 | Shoot fresh and dry weights, leaf length, and the a* color space coordinate of lettuce "Rouxai" on day 25. Plants were grown under each of six lighting treatments delivered by warm-white (WW) or mixed blue (B; 400–500 nm), green (G; 500–600 nm), red (R; 600–700 nm), and far-red (FR; 700–800 nm) light-emitting diodes (LEDs) during day 0–11, transferred to all six treatments on day 11, and grown until day 25. The number for each LED type is its photon flux density in $\mu mol \cdot m^{-2} \cdot s^{-1}$. Means followed by different letters within each parameter and treatment applied during day 11–25 are significantly different based on Tukey's honestly significant difference test ($\alpha = 0.05$). NS, non-significant. Error bars show standard errors.

(Zhang and Folta, 2012). Upregulation of anthocyanin accumulation by B radiation is mediated by cryptochrome 1 and reversed by G radiation (Bouly et al., 2007). Although FR radiation increases anthocyanin accumulation during de-etiolation of arabidopsis seedlings through phytochrome A, which stabilizes Long Hypocotyl 5 (HY5) to promote expression of anthocyanin biosynthetic genes (Li et al., 2014; Liu et al., 2015), it can also decrease anthocyanin accumulation through phytochrome

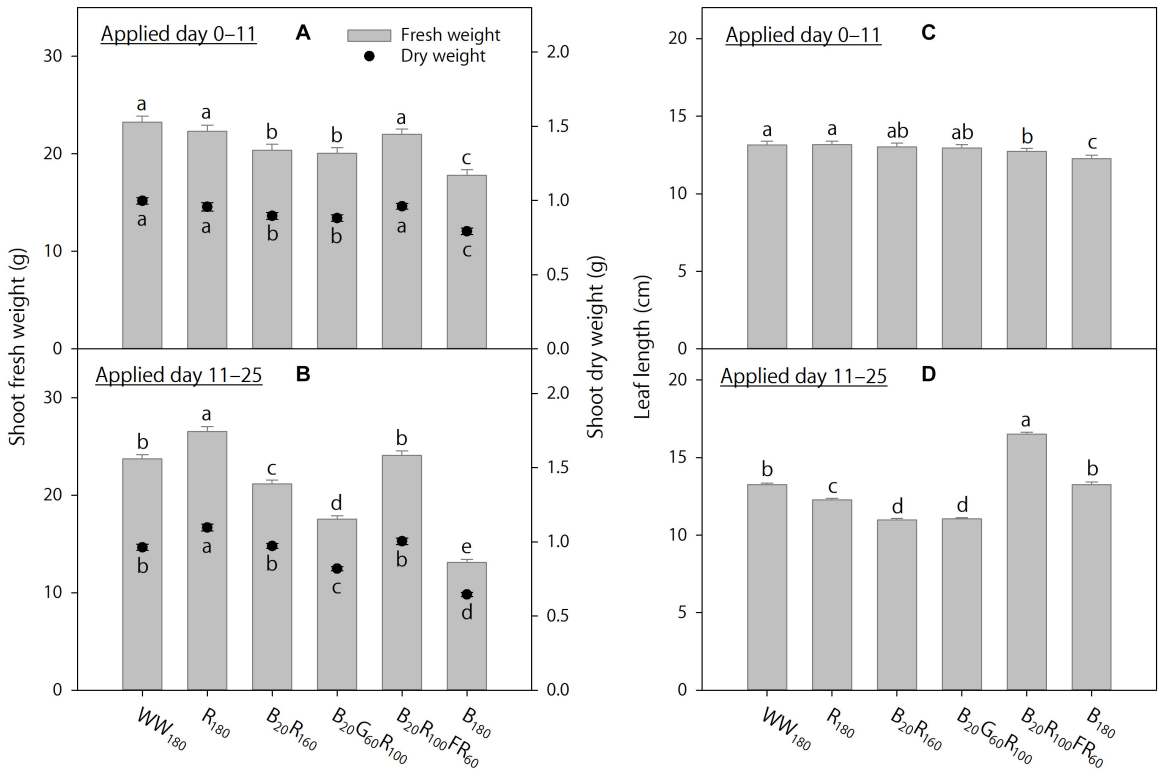

FIGURE 5 | The effects of initial (applied day 0–11) and eventual (applied day 11–25) lighting treatments on pooled final shoot fresh and dry weights and leaf length of lettuce "Rouxai" on day 25. Plants were grown under each of six lighting treatments delivered by warm-white (WW) or mixed blue (B; 400–500 nm), green (G; 500–600 nm), red (R; 600–700 nm), and far-red (FR; 700–800 nm) light-emitting diodes (LEDs) during day 0–11, transferred to all six treatments on day 11, and grown until day 25. The number for LED type is its photon flux density in $\mu mol \cdot m^{-2} \cdot s^{-1}$. Means followed by different letters within each parameter and graph are significantly different based on Tukey's honestly significant difference test ($\alpha = 0.05$). Error bars show standard errors.

B (Zheng et al., 2013). In addition, partial substitution of white radiation with FR radiation decreased anthocyanin concentration of lettuce "Red Cross" (Li and Kubota, 2009). Therefore, G and FR radiation likely antagonize B radiation in regulation of anthocyanin accumulation of red-leaf lettuce through cryptochromes and phytochromes, respectively. Alternatively, with similar total anthocyanin content per leaf, anthocyanin concentration can decrease as leaf area increases with G or FR radiation. Direct biosynthetic regulation and the "dilution" effect could occur concurrently and warrant further investigation.

When lettuce "Rouxai" was grown under different initial treatments day 0–11 but the same eventual treatments day 11–25, initial light quality had a residual effect on final shoot fresh and dry weights, responses of which generally resembled those under static treatments. For example, for plants transferred to the same R_{180} or B_{180} treatment on day 11, final shoot dry weight was greater when initially grown under R_{180} than under B_{180}. In a similar study, when lettuce "Grand Rapids" was transferred from R_{100} to B_{100} or from B_{100} to R_{100} on day 7, shoot dry weight of mature lettuce was primarily influenced by light quality applied before, rather than after, the transfer (Eskins et al., 1995). Contrary to typical B-induced growth inhibition, shoot dry weight and leaf area were consistently greater under B_{100} than under R_{100} applied during seedling development or throughout the experiment (Eskins et al., 1995). Such unique B radiation responses may be species- and cultivar-specific. In addition, a temporal shift of B radiation responses was previously reported in lettuce "Banchu Red Fire," which was grown under fluorescent lamps day 0–10; R_{100}, $B_{50}R_{50}$, or B_{100} day 10–17; and then sunlight with supplemental fluorescent lamps day 17–45 (Johkan et al., 2010). Increasing B:R during the seedling phase decreased leaf area and fresh weight on day 17 but increased them on day 45 (Johkan et al., 2010). Although spectral effects varied in these and our studies, they all showed lasting influences of light quality applied during the seedling phase on subsequent plant growth. A sustained environmental treatment delivered early in seedling development could persist into the mature phase possibly by DNA methylation or irreversible activation or suppression of growth-related genes (Bird, 1993; Eskins et al., 1995). The latency of early light signals was also evident in accelerated flowering of mature snapdragon and petunia (*Petunia* × *hybrida* L.) by additional FR radiation applied during the seedling phase (Park and Runkle, 2017, 2018).

Although light quality during the seedling phase modified shoot fresh and dry weights of mature lettuce, the magnitude of this modification was less pronounced than that by light quality in the mature phase. As the plant underwent the exponential growing phase, light interception increased drastically

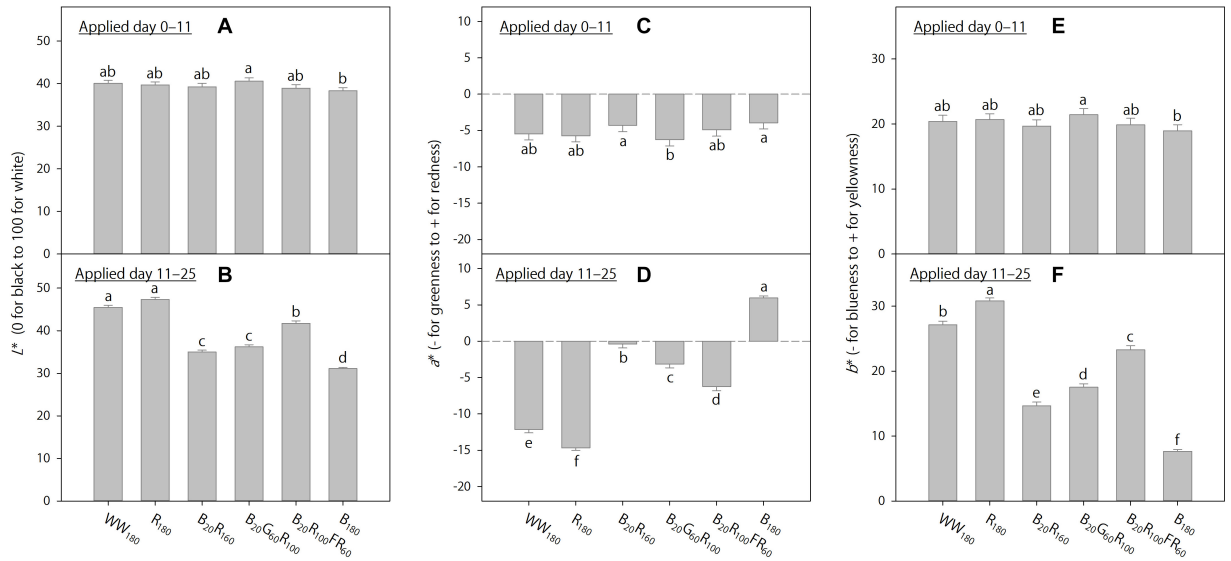

FIGURE 6 | The effects of initial (applied day 0–11) and eventual (applied day 11–25) lighting treatments on pooled final Lab color space parameters of lettuce "Rouxai" on day 25. Plants were grown under each of six lighting treatments delivered by warm-white (WW) or mixed blue (B; 400–500 nm), green (G; 500–600 nm), red (R; 600–700 nm), and far-red (FR; 700–800 nm) light-emitting diodes (LEDs) during day 0–11, transferred to all six treatments on day 11, and grown until day 25. The number for each LED type is its photon flux density in $\mu mol \cdot m^{-2} \cdot s^{-1}$. Means followed by different letters within each graph are significantly different based on Tukey's honestly significant difference test ($\alpha = 0.05$). Error bars show standard errors.

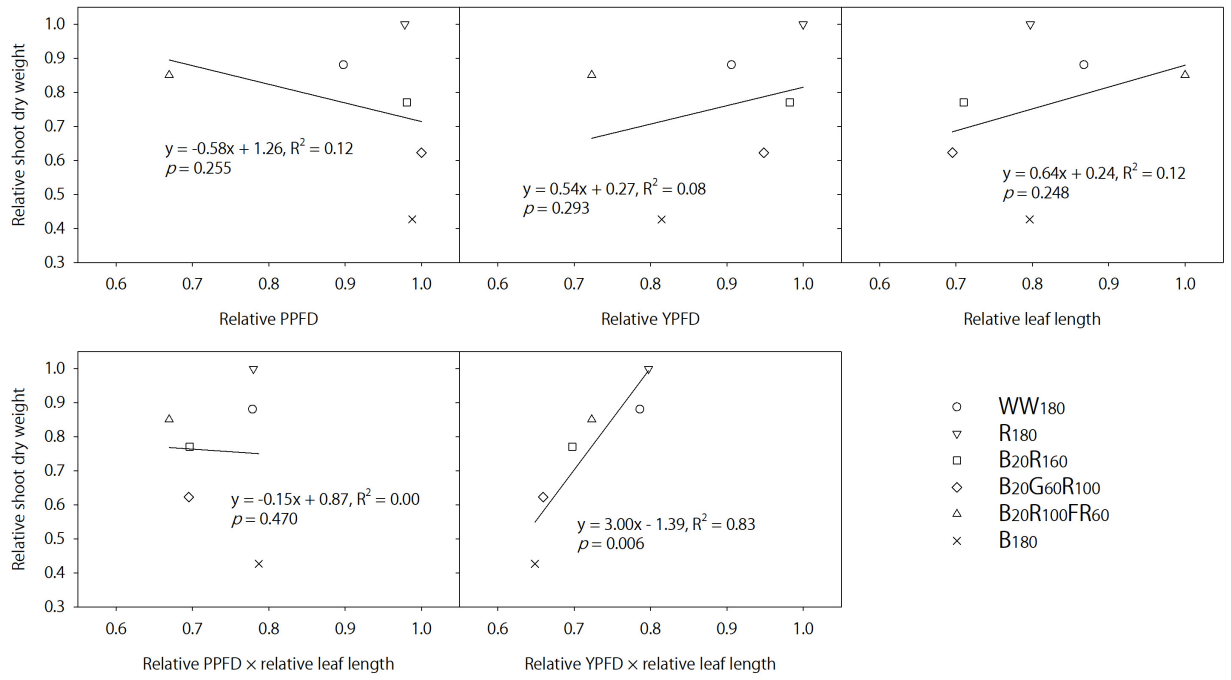

FIGURE 7 | Relative shoot dry weight of lettuce "Rouxai" on day 25 plotted against the relative photosynthetic photon flux density (PPFD), relative yield photon flux density (YPFD), relative leaf length, relative PPFD × relative leaf length, and relative YPFD × relative leaf length. Plants were grown under six static lighting treatments delivered by warm-white (WW) or mixed blue (B; 400–500 nm), green (G; 500–600 nm), red (R; 600–700 nm), and far-red (FR; 700–800 nm) light-emitting diodes (LEDs). The number for each LED type is its photon flux density in $\mu mol \cdot m^{-2} \cdot s^{-1}$. Data were averaged for each lighting treatment from two blocks. Linear regression equations, coefficients of determination, and p-values for slopes are provided. The only significant linear relationship occurs between relative YPFD × relative leaf length and relative shoot dry weight ($\alpha = 0.05$).

with leaf development, which likely led to greater impacts of eventual treatments on photosynthesis and morphology. In addition, leaf length and coloration of mature lettuce were primarily controlled by eventual lighting treatments and negligibly affected by initial ones. The greater influence of eventual light quality on foliage coloration could at least partly be attributed to rapid anthocyanin accumulation in lettuce under light stresses within days (Owen and Lopez, 2015). In general, final lettuce shoot weight, leaf length, and coloration were similar under lighting treatments applied day 0–25 and day 11–25, further highlighting the predominant role of eventual light quality. Nonetheless, the lasting initial spectral effects exerted significant influence on final shoot weight and thus should be considered for growth of both seedlings and mature plants. In another treatment-switching experiment, spectral effects during the seedling (day 0–14) and mature (day 14–28) phases on final growth of lettuce "Crispa" depended on specific lighting combinations (Chang and Chang, 2014). Therefore, dynamic lighting strategies should be based on specific cultivars and potentially interactive environmental factors such as light quality, the PPFD, and temperature.

The following conclusions are in response to the three original hypotheses. First, effects of light quality applied during the seedling phase persisted into the mature phase, although they were less pronounced than those applied during the mature phase. Second, substituting substantial G radiation for R radiation did not influence growth of seedlings but decreased growth of mature lettuce. Third, B radiation alone decreased lettuce shoot weight during both the seedling and mature phases. However, compared to R radiation, B radiation alone suppressed leaf elongation during the seedling phase but promoted it during the mature phase. In addition to testing hypotheses, we conclude temporally alternating light quality improved precision of phenotype control over static lighting. Thus, differential lighting treatments could be delivered at various developmental stages to optimize crop growth and quality attributes. Our results suggest that lettuce biomass can be maximized with WW, R, or B + R + FR radiation during propagation, followed by R radiation during production. End-of-production B radiation can be used to induce anthocyanin accumulation.

DATA AVAILABILITY STATEMENT

The raw data supporting the conclusions of this article will be made available by the authors, without undue reservation.

AUTHOR CONTRIBUTIONS

QM conceived and performed the experiment, collected and analyzed data, and wrote the first draft of the manuscript. ER was the recipient of funds and reviewed experimental design. Both authors contributed to the manuscript revision and approved the final version.

FUNDING

This work was supported by Michigan State University AgBioResearch Project GREEEN GR17-072 and the USDA National Institute of Food and Agriculture, Hatch project 192266.

ACKNOWLEDGMENTS

The authors thank Cary Mitchell, Jennifer Boldt, and Roberto Lopez for manuscript reviews and suggestions; David Hamby, Rodrigo Pereyra, Charles Brunault, Alan Sarkisian, and Dorian Spero from OSRAM Innovation for lighting support; Nathan Kelly for experimental assistance; Steve Brooks for technical assistance; Randy Beaudry, Dan Brainard, and Roberto Lopez for instruments; and material donations from Grodan and JR Peters, Inc.

REFERENCES

Armbruster, U., Carrillo, L. R., Venema, K., Pavlovic, L., Schmidtmann, E., Kornfeld, A., et al. (2014). Ion antiport accelerates photosynthetic acclimation in fluctuating light environments. *Nat. Commun.* 5:5439. doi: 10.1038/ncomms6439

Bird, A. P. (1993). Imprints on islands. *Curr. Biol.* 3, 275–277. doi: 10.1016/0960-9822(93)90177-P

Bouly, J. P., Schleicher, E., Dionisio-Sese, M., Vandenbussche, F., Van Der Straeten, D., Bakrim, N., et al. (2007). Cryptochrome blue light photoreceptors are activated through interconversion of flavin redox states. *J. Biol. Chem.* 282, 9383–9391. doi: 10.1074/jbc.M609842200

Brodersen, C. R., and Vogelmann, T. C. (2010). Do changes in light direction affect absorption profiles in leaves? *Funct. Plant Biol.* 37, 403–412. doi: 10.1071/FP09262

Carvalho, S. D., and Folta, K. M. (2014a). Environmentally modified organisms–expanding genetic potential with light. *Critical Rev. Plant Sci.* 33, 486–508. doi: 10.1080/07352689.2014.929929

Carvalho, S. D., and Folta, K. M. (2014b). Sequential light programs shape kale (*Brassica napus*) sprout appearance and alter metabolic and nutrient content. *Hortic. Res.* 1:8. doi: 10.1038/hortres.2014.8

Cerdán, P. D., and Chory, J. (2003). Regulation of flowering time by light quality. *Nature* 423, 881–885. doi: 10.1038/nature01636

Chang, C. L., and Chang, K. P. (2014). The growth response of leaf lettuce at different stages to multiple wavelength-band light-emitting diode lighting. *Sci. Hortic.* 179, 78–84. doi: 10.1016/j.scienta.2014.09.013

Chen, X. L., Guo, W. Z., Xue, X. Z., Wang, L. C., and Qiao, X. J. (2014). Growth and quality responses of 'Green Oak Leaf' lettuce as affected by monochromic or mixed radiation provided by fluorescent lamp (FL) and light-emitting diode (LED). *Sci. Hortic.* 172, 168–175. doi: 10.1016/j.scienta.2014.04.009

Cope, K. R., Snowden, M. C., and Bugbee, B. (2014). Photobiological interactions of blue light and photosynthetic photon flux: effects of monochromatic and broad-spectrum light sources. *Photochem. Photobiol.* 90, 574–584. doi: 10.1111/php.12233

Demmig-Adams, B., Cohu, C. M., Muller, O., and Adams, W. W. (2012). Modulation of photosynthetic energy conversion efficiency in nature: from seconds to seasons. *Photosynth. Res.* 113, 75–88. doi: 10.1007/s11120-012-9761-6

Eskins, K., Warner, K., and Felker, F. C. (1995). Light quality during early seedling development influences the morphology and bitter taste intensity of mature lettuce (*Lactuca sativa*) leaves. *J. Plant Physiol.* 147, 709–713. doi: 10.1016/S0176-1617(11)81482-3

Folta, K. M., and Maruhnich, S. A. (2007). Green light: a signal to slow down or stop. *J. Exp. Bot.* 58, 3099–3111. doi: 10.1093/jxb/erm130

Franklin, K. A. (2016). Photomorphogenesis: plants feel blue in the shade. *Curr. Biol.* 26, R1275–R1276. doi: 10.1016/j.cub.2016.10.039

Gómez, C., and Jiménez, J. (2020). Effect of end-of-production high-energy radiation on nutritional quality of indoor-grown red-leaf lettuce. *HortScience* 55:7. doi: 10.21273/HORTSCI15030-20

Hernández, R., and Kubota, C. (2016). Physiological responses of cucumber seedlings under different blue and red photon flux ratios using LEDs. *Environ. Exp. Bot.* 121, 66–74. doi: 10.1016/j.envexpbot.2015.04.001

Jishi, T., Kimura, K., Matsuda, R., and Fujiwara, K. (2016). Effects of temporally shifted irradiation of blue and red LED light on cos lettuce growth and morphology. *Sci. Hortic.* 198, 227–232. doi: 10.1016/j.scienta.2015.12.005

Johkan, M., Shoji, K., Goto, F., Hashida, S. N., and Yoshihara, T. (2010). Blue light-emitting diode light irradiation of seedlings improves seedling quality and growth after transplanting in red leaf lettuce. *HortScience* 45, 1809–1814. doi: 10.21273/HORTSCI.45.12.1809

Kang, W. H., Park, J. S., Park, K. S., and Son, J. E. (2016). Leaf photosynthetic rate, growth, and morphology of lettuce under different fractions of red, blue, and green light from light-emitting diodes (LEDs). *Hortic. Environ. Biotechnol.* 57, 573–579. doi: 10.1007/s13580-016-0093-x

Kim, H. H., Goins, G. D., Wheeler, R. M., and Sager, J. C. (2004). Green-light supplementation for enhanced lettuce growth under red-and blue-light-emitting diodes. *HortScience* 39, 1617–1622. doi: 10.21273/HORTSCI.39.7.1617

Kopsell, D. A., Sams, C. E., and Morrow, R. C. (2015). Blue wavelengths from LED lighting increase nutritionally important metabolites in specialty crops. *HortScience* 50, 1285–1288. doi: 10.21273/HORTSCI.50.9.1285

Lee, J. S., Lim, T. G., and Kim, Y. H. (2014). Growth and phytochemicals in lettuce as affected by different ratios of blue to red LED radiation. *Acta Hortic.* 1037, 843–848. doi: 10.17660/ActaHortic.2014.1037.112

Li, Q., and Kubota, C. (2009). Effects of supplemental light quality on growth and phytochemicals of baby leaf lettuce. *Environ. Exp. Bot.* 67, 59–64. doi: 10.1016/j.envexpbot.2009.06.011

Li, T., Jia, K. P., Lian, H. L., Yang, X., Li, L., and Yang, H. Q. (2014). Jasmonic acid enhancement of anthocyanin accumulation is dependent on phytochrome A signaling pathway under far-red light in *Arabidopsis*. *Biochem. Biophys. Res. Commun.* 454, 78–83. doi: 10.1016/j.bbrc.2014.10.059

Liu, X. Y., Chang, T. T., Guo, S. R., Xu, Z. G., and Li, J. (2009). Effect of different light quality of LED on growth and photosynthetic character in cherry tomato seedling. *Acta. Hortic.* 907, 325–330. doi: 10.17660/ActaHortic.2011.907.53

Liu, Z., Zhang, Y., Wang, J., Li, P., Zhao, C., Chen, Y., et al. (2015). Phytochrome-interacting factors PIF4 and PIF5 negatively regulate anthocyanin biosynthesis under red light in *Arabidopsis* seedlings. *Plant Sci.* 238, 64–72. doi: 10.1016/j.plantsci.2015.06.001

McCree, K. J. (1972). The action spectrum, absorptance and quantum yield of photosynthesis in crop plants. *Agric. Meteorol.* 9, 191–216. doi: 10.1016/0002-1571(71)90022-7

Meng, Q., Boldt, J., and Runkle, E. S. (2020). Blue radiation interacts with green radiation to influence growth and predominantly controls quality attributes of lettuce. *J. Am. Soc. Hortic. Sci.* 145, 75–87. doi: 10.21273/JASHS04759-19

Meng, Q., Kelly, N., and Runkle, E. S. (2019). Substituting green or far-red radiation for blue radiation induces shade avoidance and promotes growth in lettuce and kale. *Environ. Exp. Bot.* 162, 383–391. doi: 10.1016/j.envexpbot.2019.03.016

Meng, Q., and Runkle, E. S. (2019). Far-red radiation interacts with relative and absolute blue and red photon flux densities to regulate growth, morphology, and pigmentation of lettuce and basil seedlings. *Sci. Hortic.* 255, 269–280. doi: 10.1016/j.scienta.2019.05.030

Ohashi-Kaneko, K., Takase, M., Kon, N., Fujiwara, K., and Kurata, K. (2007). Effect of light quality on growth and vegetable quality in leaf lettuce, spinach and komatsuna. *Environ. Control Biol.* 45, 189–198. doi: 10.2525/ecb.45.189

Owen, W. G., and Lopez, R. G. (2015). End-of-production supplemental lighting with red and blue light-emitting diodes (LEDs) influences red pigmentation of four lettuce varieties. *HortScience* 50, 676–684. doi: 10.21273/HORTSCI.50.5.676

Park, Y., and Runkle, E. S. (2017). Far-red radiation promotes growth of seedlings by increasing leaf expansion and whole-plant net assimilation. *Environ. Exp. Bot.* 136, 41–49. doi: 10.1016/j.envexpbot.2016.12.013

Park, Y., and Runkle, E. S. (2018). Far-red radiation and photosynthetic photon flux density independently regulate seedling growth but interactively regulate flowering. *Environ. Exp. Bot.* 155, 206–216. doi: 10.1016/j.envexpbot.2018.06.033

Pedmale, U. V., Huang, S. S. C., Zander, M., Cole, B. J., Hetzel, J., Ljung, K., et al. (2016). Cryptochromes interact directly with PIFs to control plant growth in limiting blue light. *Cell* 164, 233–245. doi: 10.1016/j.cell.2015.12.018

Sager, J. C., Smith, W. O., Edwards, J. L., and Cyr, K. L. (1988). Photosynthetic efficiency and phytochrome photoequilibria determination using spectral data. *Trans. Am. Soc. Agric. Eng.* 31, 1882–1889. doi: 10.13031/2013.30952

Snowden, M. C., Cope, K. R., and Bugbee, B. (2016). Sensitivity of seven diverse species to blue and green light: interactions with photon flux. *PLoS One* 11:e0163121. doi: 10.1371/journal.pone.0163121

Son, K. H., Lee, J. H., Oh, Y., Kim, D., Oh, M. M., and In, B. C. (2017). Growth and bioactive compound synthesis in cultivated lettuce subject to light-quality changes. *HortScience* 52, 584–591. doi: 10.21273/HORTSCI11592-16

Son, K. H., and Oh, M. M. (2013). Leaf shape, growth, and antioxidant phenolic compounds of two lettuce cultivars grown under various combinations of blue and red light-emitting diodes. *HortScience* 48, 988–995. doi: 10.21273/HORTSCI.48.8.988

Terashima, I., Fujita, T., Inoue, T., Chow, W. S., and Oguchi, R. (2009). Green light drives leaf photosynthesis more efficiently than red light in strong white light: revisiting the enigmatic question of why leaves are green. *Plant Cell Physiol.* 50, 684–697. doi: 10.1093/pcp/pcp034

Wang, Y., and Folta, K. M. (2013). Contributions of green light to plant growth and development. *Am. J. Bot.* 100, 70–78. doi: 10.3732/ajb.1200354

Wollaeger, H. M., and Runkle, E. S. (2014). Growth of impatiens, petunia, salvia, and tomato seedlings under blue, green, and red light-emitting diodes. *HortScience* 49, 734–740. doi: 10.21273/HORTSCI.49.6.734

Wollaeger, H. M., and Runkle, E. S. (2015). Growth and acclimation of impatiens, salvia, petunia, and tomato seedlings to blue and red light. *HortScience* 50, 522–529. doi: 10.21273/HORTSCI.50.4.522

Zhang, T., and Folta, K. M. (2012). Green light signaling and adaptive response. *Plant Signal. Behav.* 7, 75–78. doi: 10.4161/psb.7.1.18635

Zhang, T., Maruhnich, S. A., and Folta, K. M. (2011). Green light induces shade avoidance symptoms. *Plant Physiol.* 157, 1528–1536. doi: 10.1104/pp.111.180661

Zheng, X., Wu, S., Zhai, H., Zhou, P., Song, M., Su, L., et al. (2013). *Arabidopsis* phytochrome B promotes SPA1 nuclear accumulation to repress photomorphogenesis under far-red light. *Plant Cell* 25, 115–133. doi: 10.1105/tpc.112.107086

Conflict of Interest: The authors declare that the research was conducted in the absence of any commercial or financial relationships that could be construed as a potential conflict of interest.

Copyright © 2020 Meng and Runkle. This is an open-access article distributed under the terms of the Creative Commons Attribution License (CC BY). The use, distribution or reproduction in other forums is permitted, provided the original author(s) and the copyright owner(s) are credited and that the original publication in this journal is cited, in accordance with accepted academic practice. No use, distribution or reproduction is permitted which does not comply with these terms.

frontiers in Plant Science

ORIGINAL RESEARCH
published: 29 October 2020
doi: 10.3389/fpls.2020.594681

UV-B Induced Flavonoids Contribute to Reduced Biotrophic Disease Susceptibility in Lettuce Seedlings

*Emily R. McLay[1,2], Ana Clara Pontaroli[2] and Jason J. Wargent[1,2]**

[1] School of Agriculture and Environment, College of Sciences, Massey University, Palmerston North, New Zealand,
[2] BioLumic Limited, Palmerston North, New Zealand

Biotrophic disease is one of the largest causes of decreased yield in agriculture. While exposure to ultraviolet B (UV-B) light (280–320 nm) has been previously observed to reduce plant susceptibility to disease, there is still a paucity of information regarding underlying biological mechanisms. In addition, recent advances in UV-LED technology raise the prospect of UV light treatments in agriculture which are practical and efficient. Here, we characterized the capability of UV-B LED pre-treatments to reduce susceptibility of a range of lettuce (*Lactuca sativa*) cultivars to downy mildew disease caused by the obligate biotroph *Bremia lactucae*. Innate cultivar susceptibility level did not seem to influence the benefit of a UV-B induced disease reduction with similar reductions as a percentage of the control observed (54–62% decrease in conidia count) across all susceptible cultivars. UV-B-induced reductions to conidia counts were sufficient to significantly reduce the infectivity of the diseased plant. Secondary infections caused by UV-B pre-treated plants exhibited yet further (67%) reduced disease severity. UV-B-induced flavonoids may in part mediate this reduced disease severity phenotype, as *B. lactucae* conidia counts of lettuce plants negatively correlated with flavonoid levels in a UV-B-dependent manner ($r = -0.81$). Liquid chromatography–mass spectrometry (LC-MS) was used to identify metabolic features which contribute to this correlation and, of these, quercetin 3-O-(6”-O-malonyl)-b-D-glucoside had the strongest negative correlation with *B. lactucae* conidia count ($r = -0.68$). When quercetin 3-O-(6”-O-malonyl)-b-D-glucoside was directly infiltrated into lettuce leaves, with those leaves subsequently infected, the *B. lactucae* conidia count was reduced (25–39%) in two susceptible lettuce cultivars. We conclude that UV-B induced phenolics, in particular quercetin flavonoids, may act as phytoanticipins to limit the establishment of biotrophic pathogens thus delaying or reducing their sporulation as measured by conidia count. These findings highlight the opportunity for UV-B morphogenesis to be exploited through the application of UV-LED technology, as part of the development of next-generation, sustainable disease control tools.

Keywords: UV-B, flavonoids, *Bremia lactucae*, LED, photomorphogenesis, disease management, *Lactuca sativa*

OPEN ACCESS

Edited by:
Susana M. P. Carvalho, University of Porto, Portugal

Reviewed by:
Tao Li, Institute of Environment and Sustainable Development in Agriculture (CAAS), China
María Serrano, Miguel Hernández University of Elche, Spain

***Correspondence:**
Jason J. Wargent
J.Wargent@massey.ac.nz

Specialty section:
This article was submitted to Crop and Product Physiology, a section of the journal Frontiers in Plant Science

Received: *14 August 2020*
Accepted: *09 October 2020*
Published: *29 October 2020*

Citation:
McLay ER, Pontaroli AC and Wargent JJ (2020) UV-B Induced Flavonoids Contribute to Reduced Biotrophic Disease Susceptibility in Lettuce Seedlings. Front. Plant Sci. 11:594681. doi: 10.3389/fpls.2020.594681

INTRODUCTION

Plant disease reduces the efficiency of crop production by decreasing potential yield by an estimated average of 16% (Oerke, 2006). Improved disease control techniques can help maximize crop production efficiency by reducing both losses of quality and yield. However, due to the versatility of plant pathogens, improvement of disease control can be an ambitious task. Methods which are highly effective such as chemical sprays and breeding for disease immunity often apply a heavy selection pressure resulting in the evolution of resistant pathogens (Strange and Scott, 2005). An integrated pest management system, which utilizes a combination of different control measures, can provide effect disease control while reducing the potential for development of pathogen resistance. It is therefore important to continue to develop and improve plant disease control tools for sustainable reduction of potential yield loss from disease.

The use of light-emitting diodes (LEDs) to provide a plant with specific light-signaling stimulation, such as ultraviolet B (UV-B; 280–320 nm), is an emerging approach which may be used to induce an increased defense against disease. UV-B is a short wavelength, high energy light that acts as a signal to induce a protective response in plants (Lee, 2016). Plants exposed to UV-B tend to become compacted, with thick leaves and high levels of polyphenols such as flavonoids (Jansen, 2002). UV-B can be recognized by the plant through a UV-B specific photoreceptor; UV-B resistance 8 (UVR8), or through less understood pathways (Jenkins, 2014). The high tolerance phenotype of UV-B-exposed plants may decrease susceptibility to biotic stress such as pathogens and insects (Wargent et al., 2005; Demkura and Ballare, 2012; Mewis et al., 2012; Schenke et al., 2019).

Previous studies reveal many overlaps between the response of a plant to UV-B light and pathogen attack. Ballaré et al. (2012) suggest UV-B acts in tandem with background light, in particular red: far red (R:Fr), to regulate partitioning of resources to vertical growth or defense. In low-competition scenarios, the high level of UV-B light (and R:Fr) acts as a signal to indicate upward growth is not required, and instead allocates resources to protective responses and branching (Mazza and Ballaré, 2015). However, the effect of UV-B exposure on the resistance of a plant to disease is a relatively unexplored area. The mechanism through which UV-B causes this increased resistance is also largely unknown. Demkura and Ballare (2012) conducted the most targeted investigation to date, in which the authors found a UV-B induced defense against *Botrytis cinerea* was UVR8 dependent and likely caused by increases to a syringyl type lignin. In addition to lignin, many phenolic compounds have also been observed to have antibacterial and antifungal activity (Rauha et al., 2000; Zhu et al., 2004; Gatto et al., 2011). A large number of these antimicrobial compounds—most commonly: querticin, and kaempferol flavonoids—are also upregulated by UV-B (Winter and Rostás, 2008; Hectors et al., 2012; Fraser et al., 2017). It is therefore hypothesized that UV-B induced flavonoids may have a role in a UV-B induced protection against disease.

We aimed to address this paucity of research using UV-B LED pre-treatments of seedlings as a potential disease control tool. Lettuce downy mildew caused by *Bremia lactucae* was chosen as a case study, due to past evidence toward a UV-B-induced resistance (Wargent et al., 2005) and the need for improved disease control methods in lettuce downy mildew. In addition, we hypothesized that UV-B pre-treatments can reduce disease severity in lettuce against *B. lactucae* and that UV-B-induced phenolics in part mediate this reduced disease severity phenotype.

MATERIALS AND METHODS

Plant Material and Growth Conditions

Lettuce (*Lactuca sativa*) seeds were sown into seedling trays, with a cell size of 3 cm^2, containing "Daltons Seedling Raising Mix" (Daltons^{TM}, New Zealand). The tray was spread with a single layer of grade 3 medium vermiculite (Auspari Pty Ltd., Australia). Seedlings were grown for 14–17 days in a controlled temperature room (17°C) with a 10 h photoperiod providing 215 $\mu mol\ m^{-2}\ s^{-1}$ from FL58W/965 super daylight deluxe fluorescent tubes (Sylvania Premium Extra, China). Capillary matting beneath the trays was watered daily until wet. Lettuce cultivars used comprised Casino, Pedrola (Terranova Seeds), El Dorado, Iceberg, Pavane, and Salinas (Richard Michelmore, UC Davis, CA, United States).

UV-B Treatments

Light treatments were applied using a proprietary LED luminaire designed by BioLumic Ltd. (Palmerston North, New Zealand). Photosynthetically active radiation (PAR: 400–700 nm) light was supplied through red (630–690 nm) and blue (415–485 nm) light LEDs at a red:blue ratio of 0.8. The total PAR supplied was 215 $\mu mol\ m^{-2}\ s^{-1}$. Our UV-B treatment was selected following an initial dose response study in a single lettuce cultivar (data not shown). UV-B treatment conditions consisted of either control (PAR only) or UV-B (PAR + 0.5 $\mu mol\ m^{-2}\ s^{-1}$ UV-B), whereby the UV-B emission peaked at 300 nm. Light quality and quantity were confirmed with an OL756 double-scanning monochromator spectroradiometer (Optronic Laboratories, Orlando, FL, United States), and a portable spectrometer (Spectrilight ILT950, MA, United States) prior to each treatment. Light treatments were applied to seedlings at the 14 days after sowing stage, for a photoperiod of 10 h over 3 days in total. Following light treatment completion, plants received a darkness period of 14 h. Treatments were conducted in a 17°C controlled temperature room, with the LED luminaire acting as the sole light source. In summary, plants were propagated to 14 days post sowing under the white fluorescent lights, UV-B treatment was applied with the LED luminaire for 3 days, and then plants were returned to the white fluorescent lights for the infection and assessment period.

Pathogen Inoculation and Disease Assessment

Bremia lactucae was isolated from a commercial lettuce production field (Otaki, New Zealand) during summer 2015. The *Bremia* isolate was identified as sextext code

IBEB-C 36-01-00 or EU-B 16-63-40-00 using differential host set C as set by the International Bremia Evaluation Board (IBEB, 2013). Conidia were harvested by washing plants with sporulating tissue in sterile distilled water. The resulting conidia suspension was quantified using a hemocytometer (0.1 mL depth) (BRAND® counting chamber BLAUBRAND® Neubauer improved, Merek, Auckland, New Zealand) and diluted to 10^5 *B. lactucae* conidia mL^{-1} using sterile distilled water. Plants were misted with the conidia solution with a pressure sprayer until plants were saturated. Inoculated plants were kept in a misting tent at a temperature of 17°C and misted twice daily with water to encourage high humidity.

Conidia counts were taken 8, 11, or 12 days post-inoculation (DPI) depending on disease progression speed. Plants were washed in distilled water at a ratio of one plant per 20 mL. Leaves were washed in distilled water at a ratio of one leaf per 5 mL. An aliquot (5 μL) of the resulting suspension was pipetted into a hemocytometer (0.1 mL depth) (BRAND® counting chamber BLAUBRAND® Neubauer improved, Merek, Auckland, New Zealand) and conidia were counted in the four corner squares. The average of these four counts was multiplied by 10,000 to give a measurement in conidia mL^{-1}. A pilot study did not show any UV-B mediated differences in leaf area following UV treatment (data not shown), therefore a focus was placed on conidia counts per plant/leaf. Each experiment was repeated three times. Four plants were washed together for each conidia count (number of conidia counts per light treatment = 13–16).

Secondary Infection Experiments

Secondary infection experiments used two sets of lettuce cv. Casino plants. Inoculum plants ("donor") were treated with PAR + UV-B or PAR alone (control) as defined in Section "UV-B Treatments" and then inoculated with 10^5 conidia mL^{-1} of *B. lactucae*. At 7 DPI, a second set of plants (recipient) were treated with PAR + UV-B or PAR alone (control), and were then placed into the misting tent containing donor plants. Inoculation of recipient plants by donor ones was encouraged by lightly pumping air over the plants followed by misting with water thrice a day for 7 days. Conidia counts of the recipient plants were taken at 11 DPI. Each experiment was repeated four times. Four plants were washed together for each conidia count (number of conidia counts per light treatment = 11).

Quantitative Phenolics Measurements

Plants were measured for generalized flavonoid index using a Dualex leaf-clip instrument (Goulas et al., 2004) [Force A, Orsay; France] during the light treatment and disease period.

At 72 h, between treatment end and inoculation, sample plants were frozen in packets of three in liquid N_2 and stored at −80°C. A modified version of the protocol used by Wargent et al. (2015) used to perform liquid chromatography–mass spectrometry (LC-MS). Frozen foliar material was crushed to a powder in liquid N_2. Powdered leaf samples (150 mg each sample) were incubated overnight at 4°C in 1.5 mL of methanol/MQ/formic acid (80/20/1 v/v/v). Samples were diluted with methanol before analysis by LC-MS at Plant and Food Research, Palmerston North. LC-MS-grade methanol was obtained from Merek (Auckland, New Zealand). Ultrapure water (MQ) was obtained from a Milli-Q Synthesis system (Millipore, Billerica, MA, United States).

The LCHRMS system used was the same as that used in the previous study (Wargent et al., 2015), including a Dionex Ultimate® 3000 Rapid Separation LC and a micrOTOF QII mass spectrometer (Bruker Daltonics, Bremen, Germany) fitted with an electrospray ion source. The LC contained an SRD-3400 solvent rack/degasser, an HPR-3400RS binary pump, a WPS-3000RS thermostated autosampler, and a TCC-3000RS thermostated column compartment. The column used was C68 (Luna Omega C18 100 × 2.1 mm id, 1.6 μm; Agilent, Melbourne, Australia) and it was maintained at 40°C. The flow rate was 0.400 mL min^{-1}. Solvents were A = 0.2% formic acid and B = 100% acetonitrile, which set up a gradient over 20 min. The gradient was set up as 90% A, 10% B, 0–0.5 min; linear gradient to 60% A, 40% B, 0.5–9 min; linear gradient to 5% A, 95% B, 9–14 min; maintained at 5%A, 95%B, 14–18 min; linear gradient to 90%A, 10%B, 18–18.2 min; then returned to original conditions for next sample injection at 20 min. The injection volume was 1 mL. Mass spectrum (micrOTOF QII) parameters were as in Wargent et al. (2015). Each experiment was repeated three times, with all collected samples processed and run through LC-MS together ($n = 9$).

Analysis of raw output was completed by XCMS online (Gowda et al., 2014) to determine molecular features labeled with accurate mass and retention time. XCMS also grouped features into peak groups which likely represent a singular metabolite. Feature groups and representative mass were confirmed manually by curating spectral data using MZMINE (Pluskal et al., 2010). Intensities of features within a peak group were summed to determine feature area intensity. Identification (formula and compound name) of features was determined using MSDIAL and MSFINDER (Tsugawa et al., 2015; Lai et al., 2017). Proposed identification by MSFINDER was given a score of confidence and confirmed by comparison a composite sample MS/MS spectral data (MZMINE) to published spectrum and published literature.

Phenolic Infiltration

Quercetin 3-O-(6"-malonyl-glucoside) (Q) was chosen from the list of candidate metabolites identified by LC-MS as having significant negative correlations with disease severity, as well as a strong certainty of identification. Compound standard of Q was ordered from Sigma–Aldrich (Sigma–Aldrich, Auckland, New Zealand). Published studies on polyphenol content were used to determine a control content of Iceberg/Crisphead type lettuce plant as 1.85 mg/100 g fresh weight Q (DuPont et al., 2000). Concentrations were adjusted for leaf weight, and infiltration volume of plants at 16 days old of each of the three cultivars and dilutions of the standards made to achieve a 1. 5-, 2. 5-, and 4-fold increase in each of El Dorado, Iceberg, and Salinas plants. These fold changes are based on UV-B-induced increases to levels of Q of 1.2–2.6-fold observed in LC-MS. The higher fold increase (x4) was selected to provide

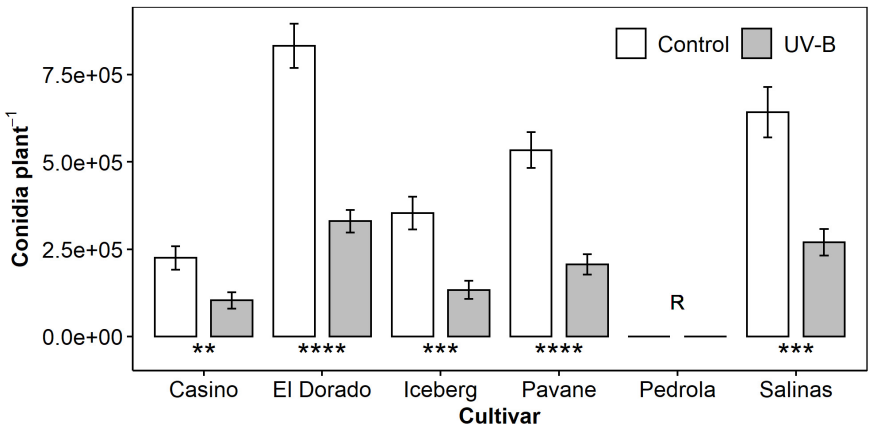

FIGURE 1 | Mean *B. lactucae* conidia per plant was lower in UV-B (white bar)-pre-treated plants than control (gray bar) plants of multiple lettuce (*L. sativa*) cultivars (n = 13–16). Pedrola was completely resistant to *B. lactucae* infection as denoted by the letter R. Lettuce plants were treated with photosynthetically active radiation (PAR) + 0.5 μmol m^{-2} s^{-1} UV-B or PAR only (control) for 3 days and then inoculated with 10^5 conidia mL^{-1} of *B. lactucae*. At 12 days post-inoculation, plants were washed and the resulting conidia suspension counted. Error bars indicate 1 SE. Asterisks indicate significant differences between control and UV-B plants according to a t-test within each cultivar where $^{**}p < 0.005$, $^{***}p < 0.0005$, $^{****}p < 0.00005$.

insight on how further increases to the compound could alter disease susceptibility.

Syringe infiltration is typically used in bacterial infiltration studies; however, it was adapted in this work for infiltration of phenolic compounds. Protocol loosely followed the leaf infiltration technique of Kim and Mackey (2008). Plants (16 days post sowing) were placed in a humid environment for 30 min to encourage stomatal opening. The oldest true leaf of each plant was marked for infiltration with permanent marker at the base of the leaf. Infiltrations were carried out by injections of either sterile distilled water (mock) or the Q solution using a 1 mL needle-less syringe into the back of the leaf at two points (one on each side of the midrib). Plants were infiltrated till the entire leaf had changed color indicating entry of the liquid (approximately 0.8 ± 0.1 mL). Plants were allowed to rest 17 h (5 h light, 12 h dark) prior to inoculation. Inoculation and disease assessment were carried out as described in Section "Pathogen Inoculation and Disease Assessment." Each experiment was repeated four times. Each leaf was washed individually for each conidia count(number of conidia counts per light treatment = 14–52).

Statistical Methods

R-3.6.0 (R Core Team, 2019) was used for statistical analysis, with base statistical package used unless otherwise specified. Graphs were produced using package ggplot2 (Wickham, 2016). Significant differences between means of normally distributed data such as conidia counts, feature area intensity, and dualex measurements were determined with t-tests or ANOVAs with Tukey *post hoc* (multcomp package; Hothorn et al., 2008). P-values of multiple comparisons were unadjusted. Relationships between multiple variables were investigated using linear models, two-way ANOVAs, principal component analysis, and Pearson correlation analysis.

RESULTS

Lettuce Seedlings Exposed to UV-B Prior to Infection Release a Reduced Number of *B. lactucae* Conidia per Plant

We assessed the effect of UV-B pre-treatment on the susceptibility of six lettuce cultivars to downy mildew disease using counts of *B. lactucae* conidia washed from infected plants at 12 DPI (n = 13–16). Cultivars ranged from highly susceptible (El Dorado) to fully resistant (Pedrola). UV-B pre-treatment reduced conidia harvested per plant at a similar level (54–62%) in all cultivars compared to plants exposed to PAR light only (**Figure 1**). Reductions in conidia count indicated a reduction in susceptibility to downy mildew disease.

Secondary Infections Caused by UV-B-Pre-treated Plants Exhibit Enhanced Reduction of Disease Severity

As conidia are the primary inoculum of *B. lactucae* (Fall et al., 2016), UV-B induced reductions in conidia counts suggest a lower potential of secondary infections. To test this hypothesis, UV-B pre-treated or control lettuce plants were used as a source of *B. lactucae* inoculum (donor) to infect a new set of UV-B pre-treated or control plants (recipient). Treatments are described in the format of donor → recipient; e.g., UV→C indicates a UV-B pre-treated inoculum plant (donor) infected control plants (recipient). The disease symptoms of the secondary plant (recipient) were assessed (n = 11).

All secondary infections in which either the donor or the recipient or both plants received a UV-B pre-treatment had significantly lower conidia per plant than those that did not receive a UV-B pre-treatment (C→C) (**Figure 2**). Intermediate treatments reduced conidia count by 35% (C→UV, $p < 0.0005$) and 42% (UV→C, $p < 0.0005$) compared to C→C infections.

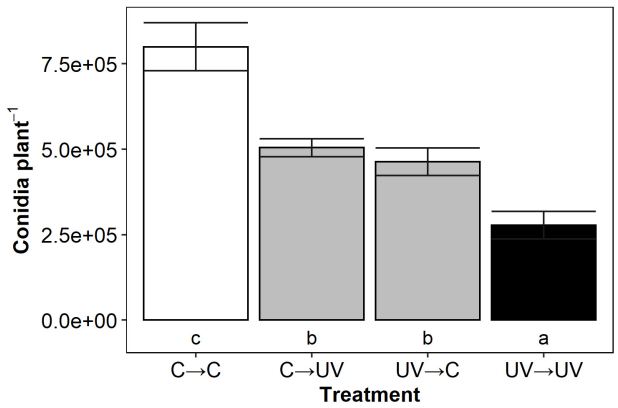

FIGURE 2 | Mean *B. lactucae* conidia per lettuce (*L. sativa*) cv. Casino plant was lower in UV→UV plants than any other treatment combination (n = 11). Donor plants were treated with photosynthetically active radiation (PAR) + UV-B or PAR only (control) and then inoculated with 10^5 conidia mL^{-1} of *B. lactucae*. At 7 days post-inoculation, recipient UV-B or control treated plants were placed in a misting tent with donor plants. At 11 days after being placed in the misting tent, recipient plants were washed and the resulting conidia suspension counted. Treatments are coded in the format of donor→ recipient treatment where C = control and UV = UV-B-pre-treated. Lower case letters indicate significance groups (ANOVA Tukey HSD; $p < 0.05$). Error bars indicate 1 SE.

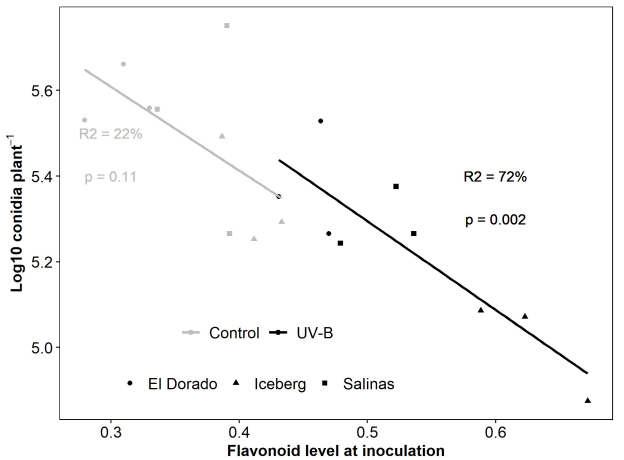

FIGURE 3 | log10 Conidia count of *B. lactucae* decreases as flavonoid level of infected lettuce (*L. sativa*) plants increases. Lettuce plants were treated with photosynthetically active radiation (PAR) + 0.5 μmol m^{-2} s^{-1} UV-B or PAR only (control) for 3 days. Following treatment plants were non-destructively measured for flavonoids using a Dualex and then inoculated with 10^5 conidia mL^{-1} of *B. lactucae*. At 12 days post-inoculation, plants were washed in water and the resulting conidia suspension was counted using a hemocytometer (n = 9). UV-B-pre-treated plants (black points) drive this response with the regression (line) lost when control (gray points) are considered separately. Cultivars are indicated by point shape (El Dorado = circle, Iceberg = diamond, Salinas = square). Regression fit is indicated by the R^2 values and model significance by p-value with text color indicating treatment (control = gray, UV-B = black)

When both donor and recipient plants received a UV-B pre-treatment (UV→UV), disease was further reduced (67%, $p < 0.0005$) compared to controls (C→C infections). Our results showed a progressive effect, where one set of UV-B plants (donor or recipient) caused an intermediate decrease in disease severity; however, when both sets of plants are UV treated (UV→UV), an amplified decrease occurred. This suggests that the amplified disease control effect is caused by the combination of a decreased inoculum from a UV-B pre-treated plant source and the additional UV-B protective response in the secondary plant.

Reductions in Disease Severity Correlated With Increases in Overall UV-B Induced Flavonoids at Time of Inoculation

To determine whether UV-B induction of flavonoids contributed to an increase in disease protection, flavonoid levels were measured using a Dualex throughout the treatment and disease period and correlated with the resulting disease severity of infected plants. Regression analysis showed flavonoid level prior to inoculation negatively correlated with conidia count (24 h; $r = -0.680$, 48 h; $r = -0.805$, $p < 0.05$), however, was strongest at the time of inoculation (72 h) ($r = -0.812$, $p < 0.05$).

UV-B-responsive flavonoids heavily drove this correlation (**Figure 3**). Separate models for UV-B-pre-treated and control plants indicated that although variation in flavonoids explained variation in conidia count in UV-B-pre-treated plants alone (R^2 = 72%, $p < 0.05$), this was not the case for control plants alone (R^2 = 22%, p = 0.11). To add, UV-B-pre-treated plants alone showed a very strong significant negative regression coefficient ($r = -0.844$) whereas control plants displayed a non-significant negative moderate regression coefficient ($r = -0.491$) between flavonoid level and conidia count. As the higher level of flavonoids in UV-B-treated plants can be attributed to UV-B response, we argue that UV-B-responsive flavonoids rather than general flavonoids contributed to the correlation and may have a role in reduction of disease susceptibility as demonstrated by conidia count.

Untargeted Metabolomic Screening Revealed 36 Metabolomic Features Present in Lettuce Seedlings

Analysis of raw LC-MS data with XCMS (Gowda et al., 2014) revealed 1630 metabolic features (combinations of m/z and retention time). These formed 188 peak/feature groups. Using MZ mine (Pluskal et al., 2010) and MS-DIAL (Tsugawa et al., 2015), features with intensities over 1E3 were confirmed through comparison against the blank sample and examination of m/z patterns. The resulting 36 features (**Supplementary Table 1**) were then given putative identities using MS-FINDER or database searches to match precursor MS and resulting MS/MS spectrum using METLIN (Guijas et al., 2018) and MoNA (Horai et al., 2010). Multiple of the putative compounds we putatively identified have also been identified by spectral analysis of lettuce in previous studies (**Supplementary Table 1**). The majority of

the putatively identified compounds were phenylpropanoids, especially flavonoids.

UV-B Increased Level of Several Metabolomic Features

The metabolic features found in lettuce (cv. El Dorado, Iceberg, and Salinas) were expressed at different intensities (**Figure 4**, n = 9). The most intense features, indicating the highest abundance, were feature IDs 2, 6, 17, 19, 34, and 36. Although intensity indicated quantity, it does not necessarily indicate contributory importance of the corresponding metabolite to the disease response. Following UV-B treatment, many features experienced little or no change in feature intensity of UV-B-treated compared to control lettuce plants. Several features (7, 8, 9, 17, 18, 19, and 21) exhibited an overall higher feature intensity in UV-B-treated plants of each cultivar compared to control ($p < 0.05$). Features 2 and 20 were increased by UV-B exposure in cultivar El Dorado only ($p < 0.05$). Features which experienced a general increase by UV-B had a range of putative identities including a phenolic acid, flavonoid, and terpene. UV-B exposure decreased feature intensity across cultivars in very few cases. El Dorado and Iceberg UV-B-exposed plants had a reduced intensity of feature 30 (p = 0.0098 and 0.024, respectively), and UV-B-exposed El Dorado only had a reduced intensity of feature 33 (p = 0.027).

Metabolomic Feature Intensity at the Time of Pathogen Inoculation Negatively Correlated With Conidia Count of Infected Lettuce Plants

A bivariate correlation analysis was run to determine relationships between disease severity and metabolomic feature intensity across all cultivars and treatments. Ten features showed a significant Pearson's correlation (r) over 0.5 (positively or negatively) between conidia count and feature intensity (**Table 1**). All significant correlations (except feature ID 33) were negative indicating increases in feature intensity correlated with decreased disease severity. The feature intensity of feature 33, however, had a positive correlation with conidia count. The strongest negative correlations with conidia count were of features 11, 19, and 20.

The role of UV-B treatment and cultivar in correlations between conidia count and feature intensities was further investigated through a principal component analysis of key metabolic features and conidia count (**Figure 5**). UV-B and control plants were heavily separated diagonally across the first component (PC1) (55.09% of variation) and second component (PC2) (26.16% of variation). This indicated that both PC1 and PC2 can explain the majority (81.25%) of the treatment variation. Features 9, 17, 19, and 20 were separated from conidia count along both PC1 and PC2 suggesting they had a major influence on treatment effect.

The remaining features (11, 22, 24, 27, 29) formed a group high in both PC1 and PC2. These negatively correlated with conidia count along PC1 only. Although partially explained by treatment effect, this loading may also be influenced by cultivar effect. Cultivars El Dorado and Salinas are grouped together, however, heavily separated from Iceberg by PC1. While these features might be important for disease defense, correlations may also be driven by the low disease susceptibility of Iceberg.

Direct Infiltrations of UV-B-Induced Phenolic Compounds Can Result in Decreased Disease Severity

Feature 19, putatively identified as Quercetin 3-O-(6"-O-malonyl)-b-D-glucoside (Q), displayed the strongest negative correlation between intensity and conidia count. To determine if Q had a role in decreasing disease susceptibility, Q solutions were directly infiltrated into a leaf of each lettuce plant followed by inoculation with *B. lactucae* conidia. Infiltrated leaves were individually washed at 8 DPI, and the resulting conidia suspension counted (**Figure 6**) (n = 14–52).

Conidia counts in both El Dorado and Salinas leaves were decreased by addition of Q at 2.5-fold compared to mock infiltration (decrease of 25% in El Dorado; p = 0.029, 39% in Salinas; p = 0.024). Infiltration of El Dorado with fourfold Q also resulted in a significant reduction of leaf conidia compared to mock infiltration (39% decrease; p = 0.001). A non-significant trend suggests that El Dorado conidia count may decrease with increasing Q concentration. However, in Salinas, although leaf conidia count decreased more by an infiltration of 2.5 than 1.5-fold Q, conidia count was increased by fourfold Q infiltration. The peak for optimal Q concentration resulting in conidia decrease may be lower in Salinas than in El Dorado. Iceberg plants were unaffected by infiltration of Q. This is likely due to the low level of susceptibility of Iceberg plants as reflected by a high number (mock = 14% incidence) uninfected plants at 8 DPI compared to other cultivars (El Dorado = 98%, Salinas = 96% incidence in mock plants).

DISCUSSION

UV-B Pre-treatment of Lettuce Plants Reduced Downy Mildew Disease Severity

UV-B Pre-treatment Has Potential to Reduce the Spread of Downy Mildew Disease

Ultraviolet B mediated reduction in *B. lactucae* conidia count of lettuce plants indicates UV-B pre-treated plants have a lower downy mildew disease susceptibility. Reduced conidia number also suggests a reduced inoculum, which in turn lowers potential secondary infections. The level of airborne conidia directly relates to the risk of downy mildew disease development and resulting yield loss (Fall et al., 2015). Lower conidia counts from UV-B-pre-treated plants as compared to untreated plants could be caused by several possibilities: (i) fewer conidiophores or conidia are produced in UV-B-pre-treated plants, (ii) attachment of conidia to conidiophores is increased in UV-B-pre-treated plants, or (iii) conidia are less stable and more likely to burst when produced on UV-B-pre-treated plants. Regardless of mechanism, our findings indicate that UV-B pre-treated plants exhibit

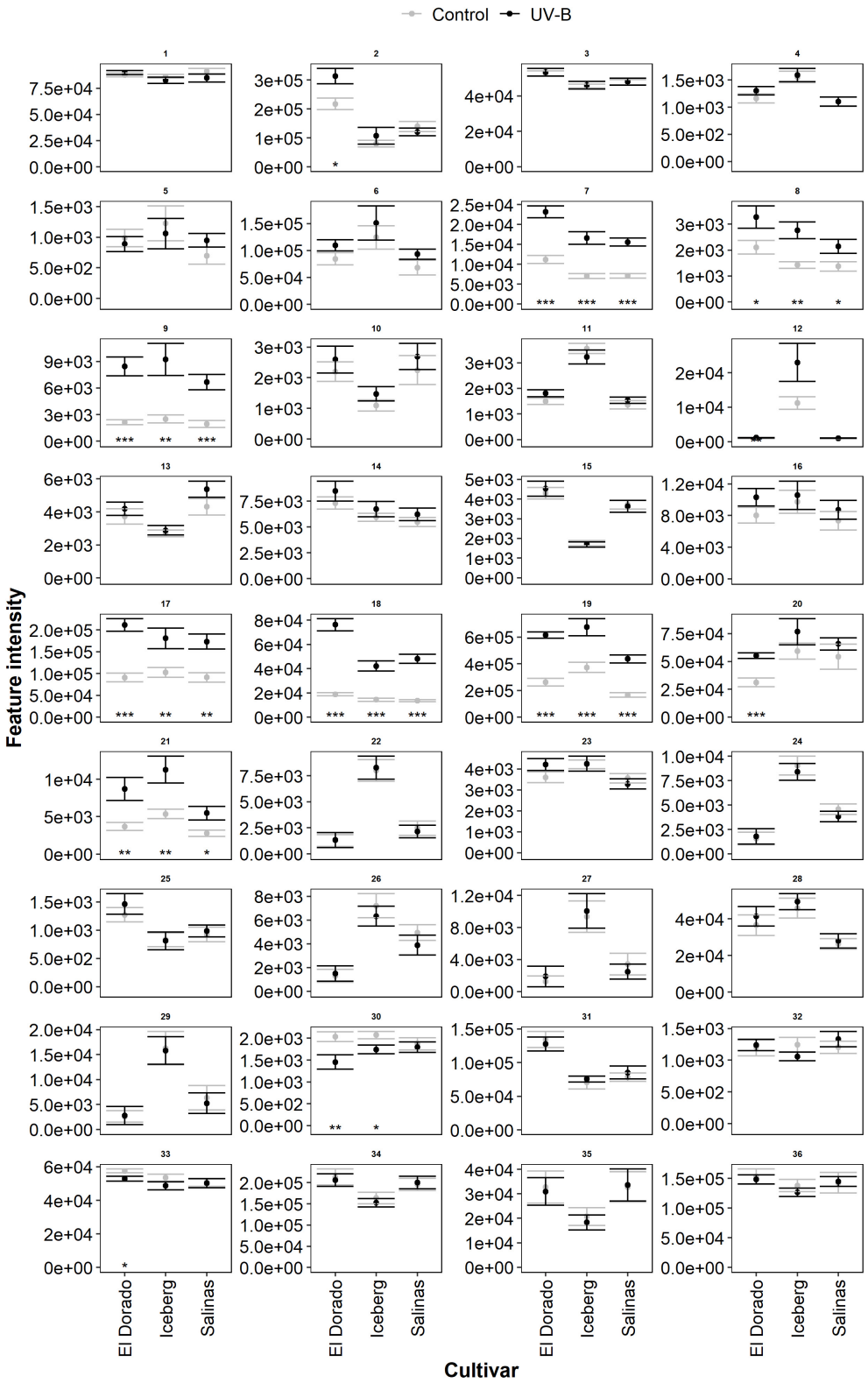

FIGURE 4 | Mean intensity of all metabolomic features (**Supplementary Table 1**) in UV-B (black) and control (gray) plants of lettuce (*L. sativa*) cv.; El Dorado, Iceberg, and Salinas ($n = 9$). Plants were treated with photosynthetically active radiation (PAR)+UV-B or PAR only (control) for 3 days. Following treatment, samples were extracted for liquid chromatography–mass spectrometry (LC-MS) analysis. Significant differences between UV-B and control plants of each feature (panel) are indicated by asterisks (*t*-test, $*p < 0.05$, $**p < 0.005$, $***p < 0.0005$). Error bars are 1 SE.

TABLE 1 | Significant correlations ($p < 0.05$) with a Pearson's value over ±0.5 between feature intensity and conidia count across cultivars and treatments ($n = 9$).

Feature ID	Putative ID	Pearson correlation	Sig. (two-tailed)
9	Chlorogenic acid	−0.51	*
11	Unidentified	−0.62	*
17	Quercetin-3-glucuronide	−0.52	*
19	Quercetin 3-O (6-malonyl)-glucoside	−0.68	**
20	3,5-Dicaffeoylquinic acid	−0.61	*
22	Unidentified	−0.55	*
24	Unidentified	−0.56	*
27	Unidentified	−0.53	*
29	Unidentified	−0.52	*
33	Nitrogen containing lipid	0.55	*

Lettuce (L. sativa) cultivars (El Dorado, Iceberg, and Salinas) were treated with photosynthetically active radiation (PAR)+UV-B or PAR only (control) for 3 days. Following treatment, samples were taken for liquid chromatography–mass spectrometry (LC-MS), with the remaining plants inoculated with 10^5 conidia mL^{-1} of B. lactucae. Plants were harvested for conidia count at 12 days post-inoculation. A bivariate correlation analysis was carried out on all LC-MS features and disease symptoms. Information on feature IDs is provided in ***Supplementary Table 1****. Significance level is indicated by asterisks where *$p < 0.05$, **$p < 0.005$.*

interference with the development of conidiophores/conidia, and/or, UV-B-pre-treated plants have a lower potential risk of downy mildew infection spread, due to reduced levels of airborne *B. lactucae* conidia.

A reduced inoculum (conidia count) from infected UV-B pre-treated plants is sufficient to reduce disease symptoms of a secondary infected plant. When inoculum from a UV-B pre-treated donor plant was used to infect a control recipient plant (UV→C), a significantly lower disease severity was observed as compared with controls (C→C). Although in these experiments intermediate stages in which either the inoculum (donor) or the secondary infection (recipient) plants have experienced UV-B (C→UV or UV→C) displayed a moderate decrease in conidia count, the effect was not as great as when UV-B pre-treatment of both donor and recipient plants was applied. UV-B defense is therefore apparently accumulative, i.e., with greater cycle numbers of UV-B-treated plants that disease is spread through, the weaker disease severity becomes.

Our findings have implications for the agronomically beneficial effects of UV-B pre-treatment on disease spread dynamics in an applied setting. Although only two cycles of UV-B treatment were tested, it presents the possibility that severity of disease will decrease over infection cycles if they occur on UV-B pre-treated plants. Downy mildew disease is polycyclic in lettuce (Fall et al., 2016). Commonly, a small number of plants will be infected, develop symptoms, and become an inoculum source resulting in the infection of a secondary plant. This cycle continues until all nearby plants are infected unless disease control measures are taken. If infected plants were UV-B pre-treated, symptoms are limited, resulting in a reduced amount of inoculum on maturation of disease. Although it is likely secondary infections will still occur, disease may be restricted by UV-B-induced defenses resulting in a further reduced disease level in the recipient plant. The cycle continues with reduced inoculum levels as disease passes through UV-B pre-treated plants. Therefore, over cycles of disease produced on UV-B pre-treated plants, the *B. lactucae* inoculum is reduced, resulting in limitations in speed or area of spread of downy mildew disease.

UV-B Reductions in Conidia Count Are Comparable to the Efficacy of Current Commercial Control Tools

Ultraviolet B induced decreases of *B. lactucae* conidia count were comparable to current control measures of lettuce downy mildew. Cohen et al. (2008) showed that treatment of lettuce with several carboxylic acid amide (CAA) fungicides (mandipropamid, dimethomorph, and iprovalcarb) reduced *B. lactucae* conidia count of lettuce leaf disks by 48–55% when applied post infection. These reductions are slightly lower than the greatest reductions achieved by a UV-B pre-treatment in this work (58% reduction in conidia count). Conidia count reductions were, however, greater in leaf disks post infection treatment with benthiavalicarb (85% reduction) (Cohen et al., 2008) than they were following our UV-B-pre-treatments. These results show that UV-B can be nearly as successful at reducing downy mildew disease (as conidia count) as commercial standards, and with further development and as part of an integrated system, has a place as a disease control tool.

UV-B Induced Flavonoids Contribute to Reductions in Disease Severity

Here, we have provided evidence toward a role of UV-B-induced flavonoids in an increased defense against downy mildew disease in lettuce. Reduction in disease severity (as conidia count) negatively correlated with UV-B-induced flavonoid level at the time of inoculation. LC-MS analysis of UV-B-induced metabolites indicates features which correlated with disease reduction included phenolic compounds such as phenolic acids and flavonoids. Infiltration of one such flavonoid [Quercetin 3-O-(6-O-malonyl)-b-D-glucoside] into lettuce leaves resulted in a decreased leaf conidia count in cultivars El Dorado and Salinas at levels slightly lower than that of UV-B pre-treatment. Therefore, UV-B-induced phenolics, in particular flavonoids, may be involved in mechanisms of UV-B induced reduction of disease severity; however, we cannot conclude they are responsible for the entire reduced susceptibility phenotype. A combination of UV-B morphogenic responses likely underlies the observed reduced conidia count, rather than the action of a single compound.

Quercetin and its derivatives have been associated with increased disease resistance in previous studies. However, a clear mode of action of quercetin in decreasing disease is not well established. Some studies suggest quercetin derivatives can have direct antimicrobial activity against bacterial and fungal pathogens (Rauha et al., 2000; Zhu et al., 2004; Gatto et al., 2011). Tao et al. (2010) suggests that a mechanism of antifungal activity could be through restricting initial spore germination and growth on the plant such as shown by quercetin-3-galactoside inhibition of germtube elongation of *B. cinerea*. Other studies

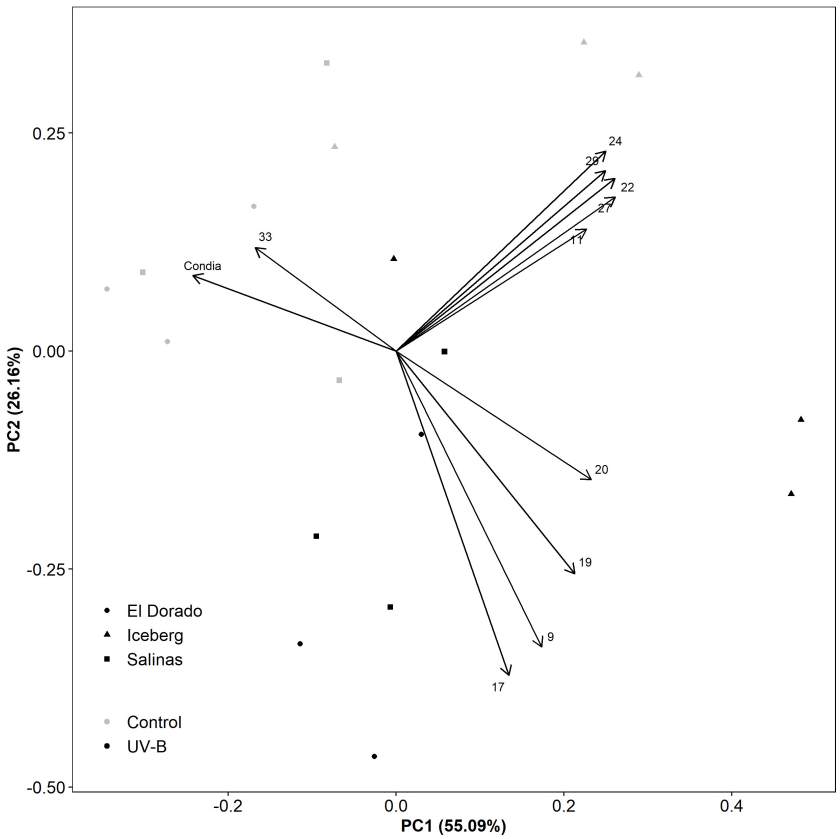

FIGURE 5 | A principal component analysis evaluating disease assessment and key metabolite features of UV-B (black) and control (white) lettuce (*L. sativa*) plants of the cv. El Dorado (circle), Iceberg (diamond), and Salinas (square) (n = 9). Plants were treated with photosynthetically active radiation (PAR)+UV-B or PAR only (control) for 3 days. Following treatment, samples were taken for liquid chromatography–mass spectrometry (LC-MS) and the remaining plants were inoculated with 10^5 conidia mL^{-1} *B. lactucae*. At 12 DPI, plants were also harvested for conidia count.

suggest that quercetin has no direct anti-fungal action (Sanzani et al., 2008), but acts to enhance host resistance such as application of quercetin onto apples enhancing resistance to *P. expansum* (Sanzani et al., 2010). The glycosylated quercetin compound rutin has been shown to activate defenses against *Xanthomonas oryzae* pv. *oryzae*, *Ralstonia solanacearum*, and *Pseudomonas syringae* pv. *tomato* strain DC3000 in rice, tobacco, and *Arabidopsis*, respectively (Yang et al., 2016). This enhanced resistance could be due to quercetin acting as a pro-oxidant (Jia et al., 2010). Quercetin, although more commonly known as an anti-oxidant, can increase H_2O_2 levels resulting in the activation of defensive responses such as PR1 and PAL induction (Jia et al., 2010). Therefore, UV-B-induced upregulation of quercetin may have a direct antimicrobial effect on invading *B. lactucae* conidia or induce a host resistance response resulting in reduced conidia count.

Previous Studies Suggest UV-B-Related Flavonoids Are Suppressed by Biotic Stress

Schenke et al. (2011) summarized and explored the conflicting evidence that while many flavonoids have antimicrobial properties, flavonoids are also commonly downregulated by biotic stressors. Schenke et al. (2019) hypothesize that perhaps flavonoids may have had a role in protection against pathogens in evolutionarily early disease defense pathways, which later evolved into alternative, more successful phenylpropanoid derived defense pathways, such as lignin fortification. This would explain why flavonoids would be downregulated in order to funnel precursors into other branches of the phenylpropanoid pathway. Although as suggested by Schenke et al. (2019), UV-B induced flavonoids can be downregulated by biotic stress, this is not necessarily contradictory to our findings, as regardless of change post-infection, UV-B induced flavonoids present at the time of infection, i.e., induced prior to pathogen introduction, are the key to UV-B enhanced disease resistance in our work.

Host flavonoid response to disease appears to be very contextual with plant-disease system heavily influencing the accumulation of flavonoids. Observations in which flavonoids were downregulated in response to biotic stress commonly used elicitors alone (Lozoya et al., 1991; Logemann and Hahlbrock, 2002; Schenke et al., 2011; Serrano et al., 2012) often in a cell culture environment in which the success of the defense was not observed. Therefore, in these cases, although downregulation of flavonoids occurs, it is difficult to confirm if reduction in flavonoid production contributes toward an increased disease defense. In other cases, the regulation of flavonoids depends on

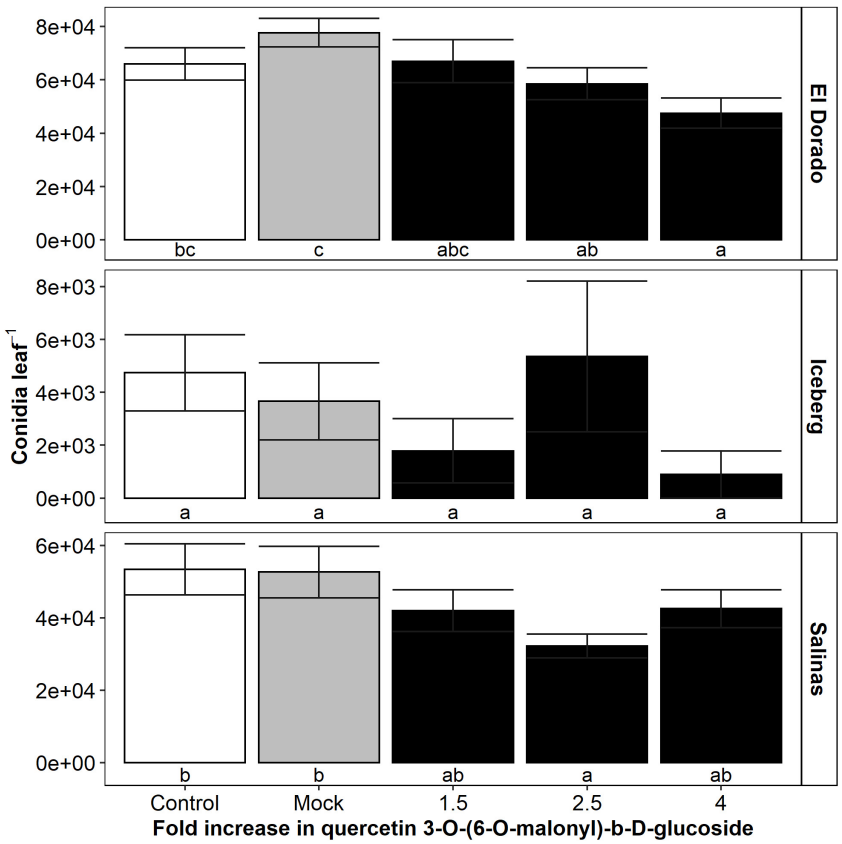

FIGURE 6 | Mean *B. lactucae* conidia counts were reduced in lettuce (*L. sativa*) leaves infiltrated with a 2.5-fold increase in quercetin 3-O-(6-O-malonyl)-b-D-glucoside compared to mock infiltrated leaves in cultivars El Dorado and Salinas (n = 14–52). Lettuce plants were grown to 17 days old and then the oldest true leaf infiltrated with water (mock) or quercetin 3-O-(6-O-malonyl)-b-D-glucoside using a needleless syringe to reach a 1. 5-, 2. 5-, or 4-fold increase compared to a standard crisphead-type lettuce plant. Control plants were not infiltrated. Plants were then inoculated with 10^5 conidia mL^{-1} of *B. lactucae*. At 12 days post-inoculation, the infiltrated leaf was washed in water and the resulting conidia suspension counted. Error bars are 1 SE. Letters indicated significance groupings within each cultivar (ANOVA Tukey HSD; $p < 0.05$).

the pathogen type. For example, confrontation of *Arabidopsis* with the obligate biotroph *Plasmodiophora brassicae* (Päsold et al., 2010) resulted in increases to flavonoids; however, a necrotophic interaction between onion and *Botrytis allii* resulted in flavonoid downregulation (McLusky et al., 1999). The regulation of (UV-B induced) flavonoids in disease defense may therefore not applicable as a broad statement, but rather to plant and pathogen types.

Changes in flavonoids as a response to disease may not always be an indicator of resistance, but as a susceptibility reaction. One method to alleviate some uncertainty about contribution of flavonoids to resistance is to examine the differential expression of flavonoid related genes during an incompatible (resistant host) versus an incompatible (susceptible host) plant–pathogen interaction. One such example was studied by Asai et al. (2014) in a model obligate biotrophic system comparable to that used in our work: *Arabidopsis* infected with pathogenic oomycete *Hyaloperonospora arabidopsidis* (causal agent of *Brassica* downy mildew). One of the major specialization steps in flavonoid synthesis is further differentiation of naringenin into dihydroflavonols. Dihydroflavonols include quercetins, such as Quercetin 3-O-(6"-O-malonyl)-b-D-glucoside found to have a high correlation with disease reduction in our work. An incompatible interaction, in which the plant is resistant to the pathogen, resulted in increased dihydroflavonol synthesis though upregulation of flavanone 3-hydroxylase (F3H) by 1.9-fold change at 1 day post-inoculation (Asai et al., 2014). However, this gene was heavily down regulated (−2.9-fold change) in a compatible interaction (Asai et al., 2014). Therefore, in an *Arabidopsis* downy mildew system, upregulation of F3H can act as a marker for resistance, providing evidence that flavonoids may still be upregulated as part of a successful disease defense. UV-B can also upregulate F3H (4.4-fold change; Ulm et al., 2004) strengthening evidence that UV-B can induce flavonoids that contribute to a biotrophic disease defense.

Disparities in the Involvement of Flavonoids in UV-B Induced Disease Defense May Be Due to Pathogen Lifestyle

Demkura and Ballare (2012) provided evidence against flavonoids contributing to UV-B-induced disease defense in

a necrotrophic interaction. *Arabidopsis* mutants which had reduced function of chalcone synthase (*tt4-1*) and were therefore deficient in flavonoid synthesis maintained a UV-B-induced reduction to lesion size by the necrotrophic pathogen *B. cinerea*. In this case, UV-B-induced flavonoids were not required for UV-B-induced disease resistance. Schenke et al. (2019) provided mixed evidence toward a role of UV-B-induced flavonoids in necrotrophic disease defense. *Arabidopsis* mutants which lacked flavonoids (*chs/f3h*) had greater bacterial growth than wild type plants when infected with *Pseudomonas syringae* pv. *tomato* strain DC3000, indicating flavonoids have an antimicrobial activity; however, photomorphogenic UV-B pre-treatment failed to reduce *P. syringae* pv. *tomato* strain DC3000 growth rate (Schenke et al., 2019). Interestingly, UV-B pre-treatment of *Arabidopsis* plants did decrease the growth rate of *P. syringae hrcQ* mutants (Schenke et al., 2019). Paul et al. (2012) compared the use of UV transparent or opaque plastics to filter the level of UV from ambient sunlight reaching lettuce plants on the impact of both plant growth and biotic interactions (Paul et al., 2012). Exclusion of ambient UV reduced UV absorbing compounds (likely indicating flavonoids); however, this also resulted in decreased downy mildew infection, thus contradicting the disease relationship in our study. Paul et al. (2012) exposed/excluded both the pathogen and the plant from UV, thus the effect of UV on the pathogen itself will influence the resulting downy mildew infection.

The contrasting experimental evidence for flavonoids in a UV-B induced disease defense may be due to pathogen lifestyle. Necrotrophic pathogens tend to release toxic substances and enzymes to kill plant cells and extract nutrients from dead material (Glazebrook, 2005). On the contrary, biotrophic pathogens extract nutrients from living plant tissue; therefore, they must enter the plant less destructively, mostly occupying extracellular space (Hahn and Mendgen, 2001). Hence, biotrophic and necrotrophic pathogens have different invasion strategies and may be defeated by different plant defense responses. In response to biotrophic pathogens, less toxic antimicrobial compounds, such as flavonoids, might have a larger defensive role. To the best of our knowledge, our work is the first to dissect the role of UV-B-induced flavonoids in reducing biotrophic disease susceptibility.

UV-B Induced Flavonoid Phytoanticipins Are the Key to Increased Disease Protection

In our work, we identified that flavonoid level at the time of inoculation was key to increased disease resistance, i.e., the correlation between disease reduction and flavonoid level was highest at the time of inoculation. Therefore, UV-B-induced flavonoids with antimicrobial activity at time of infection (phytoanticipins) may reduce the ability of the pathogen to establish and reduce the severity of the resulting disease. Once the pathogen is recognized by the plant's innate immune systems, downregulation of the flavonoid pathway may occur in some disease systems; however, this does not negate our argument for the importance of flavonoids which were induced by UV-B prior to infection. UV-B upregulation of phytoanticipins would satisfy both arguments that flavonoids contribute to defense against disease regardless of what occurs as part of an induced disease response.

CONCLUSION

Ultraviolet B LED pre-treatments can reduce susceptibility to downy mildew disease caused by *B. lactucae* in lettuce (*L. sativa*). This reduction in disease severity is correlated with increases of phenolic compounds, in particular quercetin flavonoids. While some insights into mechanisms of induced defense are given, this remains a largely unexplored area. UV-B pre-treatments have significant potential to become a commercial tool for disease control, and further scientific investigation will advance the opportunity for commercial exploitation of such "clean green" sustainable disease control tools, as well as the development of UV-B pre-treatments for different crop-disease systems.

DATA AVAILABILITY STATEMENT

The datasets presented in this article are not readily available however raw metabolomic data files can be requested from BioLumic Limited. Requests to access the datasets should be directed to info@biolumic.com.

AUTHOR CONTRIBUTIONS

EM and JW planned and designed the research and analyzed and interpreted the data. EM performed the experiments and carried out metabolomics analyses. EM, AP, and JW co-wrote and approved the manuscript. All authors contributed to the article and approved the submitted version.

FUNDING

This work was supported by a Ph.D. scholarship award from Massey University and BioLumic Limited to EM. The scholarship was funded at 50% by each of the two organizations.

ACKNOWLEDGMENTS

We thank Tony McGhie for assistance with LC-MS analyses of lettuce samples, Leyla Bustamante for informal comments on the manuscript, and Richard Michelmore for providing lettuce lines used in the experiments.

SUPPLEMENTARY MATERIAL

The Supplementary Material for this article can be found online at: https://www.frontiersin.org/articles/10.3389/fpls.2020.594681/full#supplementary-material

REFERENCES

Asai, S., Rallapalli, G., Piquerez, S. J. M., Caillaud, M.-C., Furzer, O. J., Ishaque, N., et al. (2014). Expression profiling during *Arabidopsis*/downy mildew interaction reveals a highly-expressed effector that attenuates responses to salicylic acid. *PLoS Pathog.* 10:e1004443. doi: 10.1371/journal.ppat.1004443

Ballaré, C. L., Mazza, C. A., Austin, A. T., and Pierik, R. (2012). Canopy light and plant health. *Plant Physiol.* 160, 145–155.

Cohen, Y., Rubin, A., and Gotlieb, D. (2008). "Activity of carboxylic acid amide (CAA) fungicides against *Bremia lactucae*," in *The Downy Mildews–Genetics, Molecular Biology and Control*, eds A. Lebeda, P. T. N. Spencer-Phillips, and B. M. Cooke (Dordrecht: Springer), 169–183.

Demkura, P. V., and Ballare, C. L. (2012). UVR8 mediates UV-B-induced *Arabidopsis* defense responses against *Botrytis cinerea* by controlling sinapate accumulation. *Mol. Plant* 5, 642–652. doi: 10.1093/mp/sss025

DuPont, M. S., Mondin, Z., Williamson, G., and Price, K. R. (2000). Effect of variety, processing, and storage on the flavonoid glycoside content and composition of lettuce and endive. *J. Agric. Food Chem.* 48, 3957–3964. doi: 10.1021/jf0002387

Fall, M. L., Van der Heyden, H., Beaulieu, C., and Carisse, O. (2015). *Bremia lactucae* infection efficiency in lettuce is modulated by temperature and leaf wetness duration under Quebec field conditions. *Plant Dis.* 99, 1010–1019. doi: 10.1094/PDIS-05-14-0548-RE

Fall, M. L., Van der Heyden, H., and Carisse, O. (2016). A quantitative dynamic simulation of *Bremia lactucae* airborne conidia concentration above a lettuce canopy. *PLoS One* 11:e0144573. doi: 10.1371/journal.pone.0144573

Fraser, D. P., Sharma, A., Fletcher, T., Budge, S., Moncrieff, C., Dodd, A. N., et al. (2017). UV-B antagonises shade avoidance and increases levels of the flavonoid quercetin in coriander (*Coriandrum sativum*). *Sci. Rep.* 7:17758. doi: 10.1038/s41598-017-18073-8

Gatto, M. A., Ippolito, A., Linsalata, V., Cascarano, N. A., Nigro, F., Vanadia, S., et al. (2011). Activity of extracts from wild edible herbs against postharvest fungal diseases of fruit and vegetables. *Postharv. Biol. Technol.* 61, 72–82. doi: 10.1016/j.postharvbio.2011.02.005

Glazebrook, J. (2005). Contrasting mechanisms of defense against biotrophic and necrotrophic Pathogens. *Annu. Rev. Phytopathol.* 43, 205–227.

Goulas, Y., Cerovic, Z. G., Cartelat, A., and Moya, I. (2004). Dualex: a new instrument for field measurements of epidermal ultraviolet absorbance by chlorophyll fluorescence. *Appl. Opt.* 43, 4488–4496. doi: 10.1364/AO.43.004488

Gowda, H., Ivanisevic, J., Johnson, C. H., Kurczy, M. E., Benton, H. P., Rinehart, D., et al. (2014). Interactive XCMS Online: simplifying advanced metabolomic data processing and subsequent statistical analyses. *Anal. Chem.* 86, 6931–6939. doi: 10.1021/ac500734c

Guijas, C., Montenegro-Burke, J. R., Domingo-Almenara, X., Palermo, A., Warth, B., Hermann, G., et al. (2018). METLIN: a technology platform for identifying knowns and unknowns. *Anal. Chem.* 90, 3156–3164. doi: 10.1021/acs.analchem.7b04424

Hahn, M., and Mendgen, K. (2001). Signal and nutrient exchange at biotrophic plant-fungus interfaces. *Curr. Opin. Plant Biol.* 4, 322–327. doi: 10.1016/S1369-5266(00)00180-1

Hectors, K., van Oevelen, S., Guisez, Y., Prinsen, E., and Jansen, M. A. K. (2012). The phytohormone auxin is a component of the regulatory system that controls UV-mediated accumulation of flavonoids and UV-induced morphogenesis. *Physiol. Plant.* 145, 594–603. doi: 10.1111/j.1399-3054.2012.01590.x

Horai, H., Arita, M., Kanaya, S., Nihei, Y., Ikeda, T., Suwa, K., et al. (2010). MassBank: a public repository for sharing mass spectral data for life sciences. *J. Mass Spectr.* 45, 703–714. doi: 10.1002/jms.1777

Hothorn, T., Bretz, F., and Westfall, P. (2008). Simultaneous inference in general parametric models. *Biometric. J.* 50, 346–363.

IBEB (2013). The International Bremia Evaluation Board (IBEB) Aims to Identify New Races of Bremia lactucae that Pose a Significant Threat to the European lettuce industry. Available online at: https://www.worldseed.org/our-work/plant-health/other-initiatives/ibeb/ (accessed June 10, 2020).

Jansen, M. A. K. (2002). Ultraviolet-B radiation effects on plants: induction of morphogenic responses. *Physiol. Plant.* 116, 423–429. doi: 10.1034/j.1399-3054.2002.1160319.x

Jenkins, G. I. (2014). The UV-B photoreceptor UVR8: from structure to physiology. *Plant Cell* 26, 21–37. doi: 10.1105/tpc.113.119446

Jia, Z., Zou, B., Wang, X., Qiu, J., Ma, H., Gou, Z., et al. (2010). Quercetin-induced H_2O_2 mediates the pathogen resistance against *Pseudomonas syringae* pv. *Tomato DC3000* in *Arabidopsis thaliana*. *Biochem. Biophys. Res. Commun.* 396, 522–527. doi: 10.1016/j.bbrc.2010.04.131

Kim, M. G., and Mackey, D. (2008). Measuring cell-wall-based defenses and their effect on bacterial growth in *Arabidopsis*. *Innate Immun.* 415, 443–452. doi: 10.1007/978-1-59745-570-1_26

Lai, Z., Tsugawa, H., Wohlgemuth, G., Mehta, S., Mueller, M., Zheng, Y., et al. (2017). Identifying metabolites by integrating metabolome databases with mass spectrometry cheminformatics. *Nat. Methods* 15, 53–56. doi: 10.1038/nmeth.4512

Lee, J. H. (2016). UV-B signal transduction pathway in *Arabidopsis*. *J. Plant Biol.* 59, 223–230. doi: 10.1007/s12374-016-0155-8

Logemann, E., and Hahlbrock, K. (2002). Crosstalk among stress responses in plants: pathogen defense overrides UV protection through an inversely regulated ACE/ACE type of light-responsive gene promoter unit. *Proc. Natl. Acad. Sci. U.S.A.* 99, 2428–2432. doi: 10.1073/pnas.042692199

Lozoya, E., Block, A., Lois, R., Hahlbrock, K., and Scheel, D. (1991). Transcriptional repression of light−induced flavonoid synthesis by elicitor treatment of cultured parsley cells. *Plant J.* 1, 227–234. doi: 10.1111/j.1365-313X.1991.00227.x

Mazza, C. A., and Ballaré, C. L. (2015). Photoreceptors UVR8 and phytochrome B cooperate to optimize plant growth and defense in patchy canopies. *New Phytol.* 207, 4–9. doi: 10.1111/nph.13332

McLusky, S. R., Bennett, M. H., Beale, M. H., Lewis, M. J., Gaskin, P., and Mansfield, J. W. (1999). Cell wall alterations and localized accumulation of feruloyl−3'−methoxytyramine in onion epidermis at sites of attempted penetration by *Botrytis allii* are associated with actin polarisation, peroxidase activity and suppression of flavonoid biosynthesis. *Plant J.* 17, 523–534. doi: 10.1046/j.1365-313X.1999.00403.x

Mewis, I., Schreiner, M., Nguyen, C. N., Krumbein, A., Ulrichs, C., Lohse, M., et al. (2012). UV-B irradiation changes specifically the secondary metabolite profile in broccoli sprouts: induced signaling overlaps with defense response to biotic stressors. *Plant Cell Physiol.* 53, 1546–1560.

Oerke, E. C. (2006). Crop losses to pests. *J. Agric. Sci.* 144, 31–43. doi: 10.1017/S0021859605005708

Päsold, S., Siegel, I., Seidel, C., and Ludwig−Müller, J. (2010). Flavonoid accumulation in *Arabidopsis thaliana* root galls caused by the obligate biotrophic pathogen *Plasmodiophora brassicae*. *Mol. Plant Pathol.* 11, 545–562. doi: 10.1111/j.1364-3703.2010.00628.x

Paul, N. D., Moore, J. P., McPherson, M., Lambourne, C., Croft, P., Heaton, J. C., et al. (2012). Ecological responses to UV radiation: interactions between the biological effects of UV on plants and on associated organisms. *Physiol. Plant.* 145, 565–581. doi: 10.1111/j.1399-3054.2011.01553.x

Pluskal, T., Castillo, S., Villar-Briones, A., and Orešič, M. (2010). MZmine 2: modular framework for processing, visualizing, and analyzing mass spectrometry-based molecular profile data. *BMC Bioinform.* 11:395. doi: 10.1186/1471-2105-11-395

R Core Team (2019). *R: A Language and Environment for Statistical Computing*. Vienna: R Foundation for Statistical Computing.

Rauha, J.-P., Remes, S., Heinonen, M., Hopia, A., Kahkonen, M., Kujala, T., et al. (2000). Antimicrobial effects of Finnish plant extracts containing flavonoids and other phenolic compounds. *Int. J. Food Microbiol.* 56, 3–12. doi: 10.1016/s0168-1605(00)00218-x

Sanzani, S. M., Girolamo, A. D., Schena, L., Solfrizzo, M., Ippolito, A., and Visconti, A. (2008). Control of *Penicillium expansum* and patulin accumulation on apples by quercetin and umbelliferone. *Eur. Food Res. Technol.* 228, 381–389. doi: 10.1007/s00217-008-0944-5

Sanzani, S. M., Schena, L., Girolamo, A. D., Ippolito, A., and González-Candelas, L. (2010). Characterization of genes associated with induced resistance against *Penicillium expansum* in apple fruit treated with quercetin. *Postharv. Biol. Technol.* 56, 1–11. doi: 10.1016/j.postharvbio.2009.11.010

Schenke, D., Böttcher, C., and Scheel, D. (2011). Crosstalk between abiotic ultraviolet-B stress and biotic (flg22) stress signalling in *Arabidopsis* prevents flavonol accumulation in favor of pathogen defence compound production. *Plant Cell Environ.* 34, 1849–1864. doi: 10.1111/j.1365-3040.2011.02381.x

Schenke, D., Utami, H. P., Zhou, Z., Gallegos, M.-T., and Cai, D. (2019). Suppression of UV-B stress induced flavonoids by biotic stress: is there

reciprocal crosstalk? *Plant Physiol. Biochem.* 134, 53–63. doi: 10.1016/j.plaphy.2018.06.026

Serrano, M., Kanehara, K., Torres, M., Yamada, K., Tintor, N., Kombrink, E., et al. (2012). Repression of Sucrose/Ultraviolet B light-induced flavonoid accumulation in microbe-associated molecular pattern-triggered immunity in *Arabidopsis*. *Plant Physiol.* 158, 408–422. doi: 10.1104/pp.111.183459

Strange, R. N., and Scott, P. R. (2005). Plant disease: a threat to global food security. *Annu. Rev. Phytopathol.* 43, 83–116.

Tao, S., Zhang, S., Tsao, R., Charles, M. T., Yang, R., and Khanizadeh, S. (2010). In vitro antifungal activity and mode of action of selected polyphenolic antioxidants on *Botrytis cinerea*. *Arch. Phytopathol. Plant Protect.* 43, 1564–1578.

Tsugawa, H., Cajka, T., Kind, T., Ma, Y., Higgins, B., Ikeda, K., et al. (2015). MS-DIAL: data-independent MS/MS deconvolution for comprehensive metabolome analysis. *Nat. Methods* 12, 523–526. doi: 10.1038/nmeth.3393

Ulm, R., Baumann, A., Oravecz, A., Máté, Z., Ádám, É, Oakeley, E., et al. (2004). Genome-wide analysis of gene expression reveals function of the bZIP transcription factor HY5 in the UV-B response of *Arabidopsis*. *Proc. Natl. Acad. Sci. U.S.A.* 101, 1397–1402.

Wargent, J. J., Nelson, B. C. W., McGhie, T. K., and Barnes, P. W. (2015). Acclimation to UV-B radiation and visible light in *Lactuca sativa* involves up-regulation of photosynthetic performance and orchestration of metabolome-wide responses. *Plant Cell Environ.* 38, 929–940. doi: 10.1111/pce.12392

Wargent, J. J., Taylor, A., and Paul, N. D. (2005). UV supplementation for growth regulation and disease control. *V Int. Symp. Artif. Light. Horticult.* 711, 333–338.

Wickham, H. (2016). *ggplot2: Elegant Graphics for Data Analysis*. New York, NY: Springer-Verlag.

Winter, T. R., and Rostás, M. (2008). Ambient ultraviolet radiation induces protective responses in soybean but does not attenuate indirect defense. *Environ. Pollut.* 155, 290–297. doi: 10.1016/j.envpol.2007.11.018

Yang, W., Xu, X., Li, Y., Wang, Y., Li, M., Wang, Y., et al. (2016). Rutin-mediated priming of plant resistance to three bacterial pathogens initiating the early SA signal pathway. *PLoS One* 11:e0146910. doi: 10.1371/journal.pone.0146910

Zhu, X., Zhang, H., and Lo, R. (2004). Phenolic compounds from the leaf extract of artichoke (*Cynara scolymus L.*) and their antimicrobial activities. *J. Agric. Food Chem.* 52, 7272–7278. doi: 10.1021/jf0490192

Conflict of Interest: At the time of experimentation, JW was employed by Massey University and BioLumic Limited. At the time of manuscript submission, all authors were employed by BioLumic Limited, and JW was also employed by Massey University.

The remaining authors declare that this study received partial funding from BioLumic Limited, and BioLumic Limited supplied the UV-B LED luminaires used in the study. BioLumic Limited was not involved itself in study design, collection, analysis, or interpretation of data.

Copyright © 2020 McLay, Pontaroli and Wargent. This is an open-access article distributed under the terms of the Creative Commons Attribution License (CC BY). The use, distribution or reproduction in other forums is permitted, provided the original author(s) and the copyright owner(s) are credited and that the original publication in this journal is cited, in accordance with accepted academic practice. No use, distribution or reproduction is permitted which does not comply with these terms.

frontiers in Plant Science

ORIGINAL RESEARCH
published: 19 November 2020
doi: 10.3389/fpls.2020.597823

Metabolic Profile and Performance Responses of *Ranunculus asiaticus* L. Hybrids as Affected by Light Quality of Photoperiodic Lighting

*Petronia Carillo[1], Emilia Dell'Aversana[1], Giuseppe Carlo Modarelli[2], Giovanna Marta Fusco[1], Stefania De Pascale[2] and Roberta Paradiso[2]**

[1] Department of Environmental, Biological and Pharmaceutical Sciences and Technologies, University of Campania Luigi Vanvitelli, Caserta, Italy, [2] Department of Agricultural Sciences, University of Naples Federico II, Portici, Italy

Ranunculus asiaticus is a quantitative long day plant grown for cut flowers and flowering potted plants production. We evaluated the influence of light spectrum of three light sources for end-of-day photoperiodic treatments, with different phytochrome photoequilibria (PPE) induced at plant level, on the metabolic profiling of two hybrids of *R. asiaticus* L., MBO and MDR, in plants from vernalized tuberous roots. The following treatments were compared with natural day length (NL): white fluorescence lamp (FL, PPE 0.84), light emitting diodes (LEDs) Red:Far Red light at 3:1 ratio (R:FR 3:1, PPE 0.84), and LEDs Red:Far Red light at 1:3 ratio (R:FR 1:3, PPE 0.63). Measurements were carried out to evaluate the time course of carbohydrate, amino acid, and protein levels throughout the growing cycle in tuberous roots and leaves, in relation to the different plant stages (pre-planting, vegetative phase, and flowering). The study of metabolic profiling suggested that the differences between the tuberous root reserves of the two *R. asiaticus* hybrids could be responsible for the capacity of MBO to exert an early flowering. In particular, the proton-consuming synthesis during the pre-planting of two amino acids, alanine and γ-*aminobutyric acid* (GABA), is able to buffer the cytoplasmic acidosis and pH altered by the vernalization process, and GABA itself can efficiently scavenge reactive oxygen species. This fast response to the stress caused by vernalization allows MBO plants to accelerate the process of vegetative development and flowering. Some other changes in metabolites profile were certainly related to the different responses to day length and photoperiodic light quality in the two hybrids, such as dose exerted by low R:FR lighting in both MBO and MDR. However, most of the responses are under a strict genetic control.

Keywords: geophytes, tuberous roots, photosynthetic carbohydrates, amino acids, proteins, alanine, GABA

OPEN ACCESS

Edited by:
Sissel Torre, Norwegian University of Life Sciences, Norway

Reviewed by:
Barbara De Lucia, University of Bari Aldo Moro, Italy
Giacomo Cocetta, University of Milan, Italy

****Correspondence:***
Roberta Paradiso
rparadis@unina.it

Specialty section:
This article was submitted to Crop and Product Physiology, a section of the journal Frontiers in Plant Science

Received: *22 August 2020*
Accepted: *12 October 2020*
Published: *19 November 2020*

Citation:
Carillo P, Dell'Aversana E, Modarelli GC, Fusco GM, De Pascale S and Paradiso R (2020) Metabolic Profile and Performance Responses of Ranunculus asiaticus L. Hybrids as Affected by Light Quality of Photoperiodic Lighting. Front. Plant Sci. 11:597823. doi: 10.3389/fpls.2020.597823

Abbreviations: ABA, abscisic acid; BCAAs, branched-chain amino acids; Chl, chlorophyll; DW, dry weight; EOD, end-of-day; F0, basal fluorescence; FL, fluorescence lamp; Fm, maximal fluorescence in the dark; FR, Far Red light; Fv, difference between the maximal and the basal fluorescence; Fv/Fm, maximal PSII photochemical efficiency; GA, gibberellic acid; *GABA,γ-aminobutyric acid;* GAE, gallic acid equivalents; LD, long day; LEDs, light emitting diodes; MEA, methyl ethanolamine; NL, natural day length; PCs, principal components; Pfr, phytochrome far red; PPE, phytochrome photoequilibria; PPFD, Photosynthetic Photon Flux Density; Pr, phytochrome red; Ptot, total amount of phytochrome; R, red light; ROS, reactive oxygen species.

INTRODUCTION

Ranunculus asiaticus L. (family Ranunculaceae) is an a perennial geophytesgeophyte, native of the Mediterranean basin and Asia Minor, grown as annual crop for flower stems and flowering potted plants production (De Hertogh, 1996). Cultivation of *R. asiaticus* has been rising during the last years all over the world, also thanks to the breeding and the development of many hybrids (Beruto et al., 2018).

In the natural Mediterranean habitat, dormant tuberous roots sprout in autumn, when the first rain rehydrates the dried tissue, and develop a rosette of long petiole leaves, plants flower from February to May, and then enter in dormancy, and the aerial part wilt and disappear during summer (Horovitz, 1985; Meynet, 1993). As many spring flowering geophytes exhibit a summer rest period, *R. asiaticus* requires a warm - -cold - -warm sequence to express active growth and complete its life cycle (Le Nard and De Hertogh, 1993).

Flowering earliness and flower stem production and characteristics (i.e., stem length and flower size) vary widely with the plant genotype, the size of tuberous roots and the procedure of storing and preparation before planting, and the growing conditions. In general, plants from bigger roots show an earlier floral induction and produce more flowers compared to than from smaller roots, due to the greater quantity of reserve starch available for flower stem development (Meynet, 1993).

For production of propagation material, the tuberous roots harvested after plant wilting are dehydrated to less than 15% of moisture content (Meynet, 1993). During growth, plants exhibit a low temperature requirement (night/day regime 5–10/12–25°C, optimum day 16°C) and a medium to high light intensity requirement. Referring to photoperiodic requirements for flowering, *R. asiaticus* is classified as a quantitative long day (LD) plant (Horovitz, 1985). Flowering is influenced by both the thermal history of tuberous roots and the photoperiod during plant growth. Particularly, cold treatments of tuberous roots (vernalization) anticipate sprouting, leaf rosette formation, and flowering (Beruto et al., 2009); therefore, the use of vernalized propagation material is a common practice for production scheduling of cut flowers in ranunculus, similarly, to many flower geophytes.

It is known that the exposure to low temperature promotes the overcoming of bulb dormancy in *Lilium pumilum* by promoting starch degradation and increasing sucrose content and availability (Wang et al., 2018). Besides, since bulb dormancy is regulated by the abscisic acid (ABA) and gibberellic acid (GA) balance (Liu et al., 2011), vernalization releases dormancy by activating the metabolic pathways involved in the downregulation of ABA and priming the biosynthesis of GA active forms (Wang et al., 2018). However, recently, we found that vernalization not only induced a faster hydrolysis of starch in *R. asiaticus* tuberous roots but also promoted a strong accumulation of hexoses and proline, acting as compatible osmolytes and reactive oxygen species (ROS) scavengers (Carillo et al., 2019a). Moreover, minor amino acids, whose accumulation is correlated with that of hexoses under stress (Fritz et al., 2006), can act as antioxidants and/or as alternative electron donors for the mitochondrial electron transport chain, accelerating plant metabolism and flowering (Woodrow et al., 2017; Carillo, 2018).

The influence of light spectrum on plant growth, photosynthesis, and photomorphogenetic responses, including flowering, is well documented (Devlin et al., 2007; Ouzounis et al., 2015; Dueck et al., 2016). Among the plant photoreceptors able to perceive the different light wavelengths to regulate plant development and shaping and metabolism, phytochromes are appointed for the absorption of red (R, 600–700 nm) and far red (FR, 700–800 nm) light. They are present in all plant tissues in two forms with different absorption properties: phytochrome red (Pr, absorption peak at 660 nm) and phytochrome far red (Pfr, absorption peak at 730 nm). R light converts Pr to Pfr, whereas FR light has the opposite effect; hence, changes in spectral light composition influence the ratio between the two forms and the phytochrome photoequilibria (PPE = Pfr/Ptot) (Sager et al., 1988) involved in several physiological functions, such as seed germination, flowering, tuberization, bud dormancy, and shade-avoidance responses (Fukuda, 2019).

Red and Far Red light are perceived at very low light intensity, so that the threshold irradiance in photoperiodic lighting effective to promote flower induction in some herbaceous species is between 0.05 and 0.40 μmol m^{-2} s^{-1} (Whitman et al., 1998). Accordingly, a light intensity between 1 and 3 μmol m^{-2} s^{-1} is adopted by growers for photoperiodic treatments (Zhang and Runkle, 2019).

The importance of the PPE value induced at plant level by R and FR light in the regulation of the flowering process of LD plants has been deepened recently, thanks to the use of light emitting diodes (LEDs) (Craig and Runkle, 2016; Dueck et al., 2016). It has been demonstrated that the light quality of the different light sources for greenhouse photoperiodic lighting affects flowering of LD plants by influencing the PPE in plant. However, light requirement in terms of intensity and quality can vary among the species, and the best light spectrum to promote flowering is known for only a few flower crops. Specifically, R and FR proportion creating an intermediate PPE (0.63–0.80) has been proven to be more effective in some LD species (*Antirrhinum majus*, *Fuchsia* × *hybrida*, *Petunia* × *hybrida*, *Rudbeckia hirta*) than ratios inducing higher PPE (above 0.80) (Craig and Runkle, 2016). Conversely, results obtained in our experiment on *R. asiaticus* in plants from rehydrated and vernalized tuberous roots revealed a stronger advance of flowering under LEDs light with 3:1 R:FR ratio (estimated PPE 0.84) than with 1:3 ratio (estimated PPE 0.63) and highlighted a hybrid specific response (Modarelli et al., 2020b).

As known, underground storage organs in geophytes are modified roots or stems that evolved to survive adverse environmental conditions. Little is known about storage organs composition and metabolism during their rest period in nature or storage in commercial practice. Accumulation of large amounts of reserve carbohydrates in these organs is critical to ensure a supply of carbon and energy for their maintenance during unfavorable conditions and for rapid vegetative growth when sprouting can occur. Starch is the most abundant reserve carbohydrate in geophytes, however, other carbohydrates (e.g., fructan and glucomannan) can be synthesized in place

of or in addition to starch (Ranwala and Miller, 2008), and the carbohydrate composition may differ among species (Miller, 1992). Despite the importance of storage carbohydrate metabolism in ornamental geophytes and their worldwide economic significance, information about their identity and distribution among species is scarce, and most importantly, data on source–sink relationships between storage organs and above-ground plant parts are limited to a few major species. In principle, carbohydrates stored in the under-ground parts are mobilized during resprouting, acting as the major supply of carbon for the early stages of regrowth; accordingly, the carbohydrate content of storage organs varies from time to time and depends on environmental conditions (Addai, 2010). In general, during the early shoot growth of most geophytes (e.g., tulip), when stored reserves are utilized, starch content decreases and subsequently increases after anthesis, and at this point, carbohydrate filling in under-ground organs is rapid. In tulip, low temperature is essential for the mobilization of reserves and the accumulation in bulb scales of soluble constituents, available to be transported into the shoots for elongation and growth (Ohyama et al., 1998). As a consequence, dry weight (DW) of the mother bulb decreases gradually after planting and during sprouting until anthesis.

Conversely to other geophytes or wild ranunculus species (Madsen, 1993; Madsen and Brik, 1997), little is known about the plant metabolism in *R. asiaticus*, and no study seems to be available on the influence of photoperiodic lighting on plant physiology, apart from our recent experiments (Modarelli et al., 2020a,b).

We investigated the influence of light spectrum of three light sources for photoperiodic lighting, inducing different PPE at plant level, in two hybrids of *R. asiaticus* with a different flowering earliness, in plants from rehydrated and vernalized tuberous roots grown in unheated glasshouse. The effects of artificial lighting and of interactions between plant genotype and light duration and quality were studied on leaf net photosynthesis, plant growth, flowering earliness, and duration and metabolic profile. We reported the results of this experiment for photosynthesis, growth, and flowering in Modarelli et al. (2020a). In the same paper, these results were linked to the metabolic profile (starch, soluble sugars, soluble proteins, amino acids, and polyphenols) of only leaves at the sole flowering phase. In the present paper, we show the time course of the above-mentioned metabolites throughout the whole growing cycle in both tuberous roots and leaves, in relation to the different phenological phases (pre-planting, vegetative phase, and flowering). This in-depth analysis aimed to unveil the importance of root–shoot relationship in determining the differences of plant behavior between different genotypes and of plant sensitivity to light environment. To our best knowledge, our results provide the first comprehensive analysis of metabolism of the whole plant, including both storage organ and leaves, in *R. asiaticus*.

MATERIALS AND METHODS

The experiment was carried out in an unheated greenhouse at the Department of Agricultural Sciences of the University of Naples Federico II, located in Portici (Naples, Italy—40°49′N, 14°20′E), from the middle of November 2018 until the end of March 2019.

Plant Materials and Culture

Plants of the hybrids MBO (early flowering) and MDR (medium earliness) (Biancheri Creazioni, Italy)[1] were obtained from tuberous roots of the most common size for each hybrid (3–4 and 4–5 cm, respectively). Dry tuberous roots were subjected to rehydration, followed by vernalization, through exposure at 3.5°C for 2 weeks and then pre-sprouted at 12°C for 2 weeks. Plants were grown in a pot on a mixture of perlite and peat (70:30 in vol.).

The mean values of air temperature and relative humidity (day/night) recorded during the experiment (125 days) were $21.0 \pm 3.0/9.8 \pm 1.9$°C and $59.9 \pm 10.7/71.4 \pm 21.7$%, respectively (hourly measurements; mean value ± standard deviation).

Irrigation was alternated with fertigation (4 pulses per week in total). In the nutrient solution (recipe Hoagland full strength), pH and electrical conductivity were measured with a portable pH–EC multi-parameter sensor (HI9813 series; Hanna Instruments Intl.) and kept at 5.5 and 1.7 dSm^{-1}, respectively.

Light Sources and Photoperiodic Treatments

Photoperiodic lighting was applied as end-of-day (EOD) lighting treatment to extend the day length to 14 h (critical photoperiod for *R. asiaticus* L.) starting from sunset, from December 10 (24 days after planting), when all the tuberous roots were fully sprouted, until the end of the experiment. The duration of lighting treatment to reach 14 h day length was calculated weekly, on the basis of the natural photoperiod, and ranged between approximately 4 h and 30 min in December and about 2 h in March. Four photoperiodic treatments were compared:

- NL: natural day length, ranging from 9:16 (2nd week of December) to 11:54 h (3rd week of March);
- FL: NL + EOD lighting with a compact white fluorescence lamp (Phillips Master 13W, color temperature 2,700°K), estimated PPE 0.84;
- R:FR 3:1: NL + EOD lighting with monochromatic R and FR LEDs at 3:1 ratio (emission peak at 662 and 743 nm, respectively), estimated PPE 0.84;
- R:FR 1:3: NL + EOD lighting with monochromatic R and FR LEDs at 1:3 ratio (emission peak at 662 and 743 nm, respectively), estimated PPE 0.63.

LEDs used for R:FR lighting treatments were FD-39R-Y 3W 740 and FD-33R-Y 3W 660 nm (Shenzhen Fedy Technology Co., Ltd., Guanlan, Shenzhen, China). The light emission spectra of the light sources were determined by an integrating sphere (1 cm diameter opening) coupled with a spectroradiometer OL770 (Optronic Lab. Inc., Orlando, FL, United States) (**Figure 1**). In all photoperiodic lighting treatments, Photosynthetic Photon Flux Density (PPFD) at canopy level was 3–4 $\mu mol\ m^{-2}\ s^{-1}$. The estimated PPE for each lighting treatment was calculated according to Sager et al. (1988).

[1] https://www.bianchericreazioni.it/

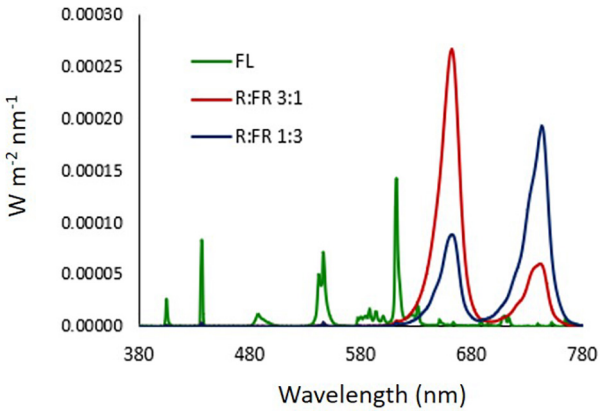

FIGURE 1 | Light emission spectra of light sources. FL: compact white fluorescence lamp (Phillips Master 13W, color temperature 2,700°K); R:FR 3:1: monochromatic red and far red LEDs at ratio 3:1; R:FR 1:3: monochromatic red and far red LEDs at ratio 1:3. LEDs used for R:FR lighting treatments were FD-39R-Y 3W 740 and FD-33R-Y 3W 660 nm (Shenzhen Fedy Technology Co., China).

Sampling

Before planting, three tuberous roots per hybrid were sampled. During cultivation, the tuberous root and three fully expanded leaves per plant, per 3 plants per combination *Hybrid* × x *Lighting treatment*, were sampled in the morning (9:00–11:00), during the 7th week after planting (vegetative phase), and the 15th week after planting (flowering phase). After collection, all samples were immediately frozen in liquid nitrogen prior to storage at −80°C, and before the analysis, they were frozen dried at −50°C for 3 days and powdered in a cooled mortar.

Leaf Photosynthetic Pigments

Photosynthetic pigments were extracted from fully expanded leaves of plants at the 12th week after planting (phase of flowering), on 1 leaf per plants, in 4 plants per combination *Hybrid* × x *Lighting treatment*. Samples of 10 mg lyophilized leaf tissues were homogenized in 1 ml methanol according to Annunziata et al. (2013). The resulting extracts were centrifuged at 4,800*g* for 15 min, and chlorophylls (Chls) *a* and *b* and total carotenoids were estimated by measuring the absorbance of the supernatants at 470, 652, and 665 nm in polypropylene microplates by a microplate reader (Synergy HT; BioTEK Instruments, Bad Friedrichshall, Germany) according to Woodrow et al. (2017).

Starch, Soluble Sugars, Soluble Proteins, Amino Acids, and Polyphenols in Leaves and Tuberous Roots

Starch and soluble sugars were extracted according to Ferchichi et al. (2018) with some modifications. Frozen powdered tuberous roots and leaves (50 mg) were submitted to a first extraction in 300 ml of ethanol (98%, v/v) at 80 °C for 20 min and centrifuged at 14,000 × *g* at 4°C for 10 min. The clear supernatants were collected in 1 ml tubes and stored at 4°C. The remaining pellets were submitted to two subsequent extractions with 150 ml of ethanol 80% (v/v) and 50% (v/v), respectively, at 80°C for 20 min. The tubes were cooled in ice and centrifuged at 14,000 × *g*, for 10 min at 4°C. The clear supernatants of the two following extractions were pooled together with that of first extraction and stored at −20°C until analysis. The pellets of the ethanol extraction were further used for starch determination, by adding to them 250 ml of 0.1 M KOH and heating at 90°C for 2 h. After cooling in ice, the samples were acidified to pH 4.5 by adding 70 ml of 1 M acetic acid. Aliquots of 100 μl of acidified samples, mixed with 100 μl of an enzymatic hydrolysis buffer constituted by sodium acetate 50 mM pH 4.8, α-amylase 2 U/ml, and amyloglucosidase 20 U/ml, were incubated at 37°C for 18 h. The samples were vortexed and then centrifuged at 13,000 × *g* for 10 min at 4°C, and the supernatant containing the glucose derived from hydrolyzed starch was used for measurement. The enzymatic assay of soluble sugars of the ethanolic extracts as well as glucose originating from starch hydrolysis was performed by a FLX-Xenius spectrophotometer (SAFAS, Monaco) according to Carillo et al. (2019c). Soluble proteins were extracted by mixing 20 mg of lyophilized plant material with 0.1 M Tris–HCl 200 mM pH 7.5 containing 500 mM $MgCl_2$ at 4°C for 24 h, the samples were vortexed and then centrifuged at 16,000 × *g*, for 10 min at 4°C, and the clear supernatants were separated from the pellets. Triplicate aliquots of 20 μl of extracts, as well as protein standards prepared according to Carillo et al. (2019b), were dispensed into wells of a polypropylene microplate. The wells contained also 180 μl of Bio-Rad protein assay dye reagent diluted 1:5 with bidistilled water (Bradford, 1976). The solutions were mixed, and then absorbance at 595 nm was recorded on a microplate reader (Synergy HT, BioTEK Instruments, Bad Friedrichshall, Germany). The absorbance of samples was referred to the calibration curve of protein standards used, and the concentration was calculated accounting for dilution factor.

Amino acids were extracted from frozen powdered tuberous roots and leaves by mixing 40 mg samples with 1 ml of ethanol:water in the ratio 40:60 (v/v), incubating overnight at 4°C, and centrifuging at 14, 000 × *g* for 10 min at 4°C (Carillo et al. (2012). The supernatants were pooled and used for the analyses. The primary amino acids were determined by high-performance liquid chromatography (HPLC) according to Ferchichi et al. (2018) using a Shimadzu Nexera X2 UHPLC system (Shimadzu, Italy), after pre-column derivatization of 20 μl of ethanolic extract with 40 μl of o-phthaldialdehyde (OPA) reagent in the an autosampler needle. OPA reagent was prepared by mixing 50 μl of OPA dissolved in methanol (142 mg ml^{-1}) and 37 μl of pure β-mercaptoethanol with 1 ml of 0.8 mM Na-borate buffer, pH 10.4. The derivatized sample was then injected onto the column (ZORBAX Eclipse Plus C18, 250 × 4.6 mm internal diameter; Agilent Technologies Italia S.p.A) and eluted at a flow rate of 1 ml min^{-1} at 25°C with a discontinuous gradient as detailed in Carillo et al. (2019c). The amino acid–OPA derivatives were detected by their fluorescence with an excitation at 330 nm and an emission at 450 nm. The HPLC peaks were identified and quantified by comparing their retention time and area data with those obtained from the standards (Carillo et al., 2019c). Proline was determined from the same ethanolic extract by an

acid ninhydrin method according to Woodrow et al. (2017). The amino acids were expressed as μmol g^{-1} FW.

The total polyphenols content was determined by the Folin–Ciocalteu method according to Singleton et al. (1999) with few modifications. Lyophilized tissues (30 mg) were extracted in 700 μl of 60% methanol (v:v); 35 μl of extract was mixed with 125 μl of the Folin–Ciocalteu reagent diluted with distilled water (1:4 v/v), and, after mixing for 6 min, 650 μl of 3% (w:v) sodium carbonate was added. After 90 min at room 25°C temperature, the absorbance at 760 nm was determined in a microplate reader (Synergy HT, BioTEK Instruments, Bad Friedrichshall, Germany). The polyphenols concentration was expressed as gallic acid equivalents (GAE) as described by Carillo et al. (2019c).

Statistical Analysis

The experiment was conducted on 25 plants per combination *Hybrid* × x *Lighting treatment*. Data were analyzed by ANOVA using the SPSS 25 software package[2], and means were compared by Duncan *post-hoc* test at $p \leq 0.05$. Three different plants were used for each metabolite analysis, and three plants were used for the analysis of plant growth and flowering.

For all the analyzed parameters, principal component analysis (PCA) was conducted on a number of replicates mentioned above, using the Minitab 18.1 statistical software, aimed to extract trends when multiple qualitative variables were used, by formulating new variables correlated with the original ones (Ciarmiello et al., 2015). The PCA outputs included treatment component scores as well as variable loadings (Ferchichi et al., 2018).

The heat map results used in the pathway maps summarizing the effect of light treatments and hybrids on starch, soluble sugars, free amino acids, including branched-chain amino acids (BCAAs) and methyl ethanolamine (MEA), and polyphenols, were calculated as Logarithm base 2 (Log_2) of the value to average (avg.) ratio, and visualized using a false-color scale, with red indicating an increase and blue a decrease of values (according to Carillo et al., 2020).

RESULTS

Leaf Photosynthetic Pigments

At the stage of flowering (**Figure 2**), the contents of Chl a, Chl b, and carotenoids in MBO leaves were on average 0.05, 0.02, and 0.02 mg g^{-1} DW, respectively, independently of the light treatments (**Supplementary Table S2**), and they significantly differed ($p > 0.05$) from MBO at the rosette stage (**Supplementary Table S1**), and from MDR in both the rosette and flowering stages (**Supplementary Tables S3**, **S4**). In particular, MDR showed values of Chl a, Chl b, and carotenoids that did not differ significantly between the rosette and flowering stages and were, on average, 0.12, 0.04, and 0.04 mg g^{-1} DW, respectively.

[2]www.ibm.com/software/analytics/spss

Starch and Soluble Sugars in Tuberous Roots and Leaves

At the pre-planting stage (**Figure 2**), pre-sprouted tuberous roots of MBO and MDR hybrids showed similar starch and soluble sugar contents. In particular, the average values for starch, glucose, fructose, and sucrose were 17.2, 25.0, 29.2, and 12.6 mg g^{-1} DW, respectively (**Supplementary Tables S1**, **S4**). However, later, the starch content decreased differently in the two hybrids, varying also in dependence on the light conditions. In fact, at the rosette stage, the MBO and MDR tuberous roots had an average starch contents of 11.3 and 9.8 mg g^{-1} DW, respectively. In particular, in MBO-NL was present the highest starch content was present in MBO-NL (13.0 mg g^{-1} DW) (**Supplementary Table S1**), whereas the lowest starch value of starch was present in MDR-R:FR 1:3 (7.4 mg g^{-1} DW) (**Supplementary Table S4**). The hexose contents in the tuberous roots of the two hybrids at the rosette stage were similar, but while whereas MBO showed a higher content of glucose, MDR had a higher content of fructose. However, the sucrose content was higher in MDR than in MBO, and in particular, it they were on average 6.0 and 4.3 mg g^{-1} DW, respectively, with the lowest value present in the MDR-R:FR 1:3 (4.0 mg g^{-1} DW). The leaves at the same stage of growth, showed an average content of starch of 16.3 and 13.4 in MBO and MDR, respectively, with the highest and lowest contents of 18.7 and 11.0 mg g^{-1} DW present in MBO-FL and MDR-NL, respectively. However, in the leaves at the rosette stage, the glucose content strongly increased in both hybrids, showing values of 42.4 and 38.7 mg g^{-1} DW in MBO and MDR, respectively (**Supplementary Tables S1**, **S4**).

At the flowering stage, while the starch content was stable in the leaves (e.g., 19.0 and 14.0 mg g^{-1} DW on average in MBO and MDR, respectively), it strongly increased in tuberous roots, getting average values of 29.1 and 31.3 mg g^{-1} DW in MBO and MDR hybrids, respectively. Glucose decreased to values of about 32.4 μmol g^{-1} DW in the leaves of both hybrids, whereas sucrose increased in both tuberous roots (**Supplementary Tables S2**, **S5**).

Proteins and Polyphenols in Tuberous Roots and Leaves

At the pre-planting stage, pre-sprouted tuberous roots of MBO and MDR plants showed protein values of 58.2 and 41.4 mg g^{-1} DW, respectively. The germination caused a strong decrease of proteins, which were on average 21.5 mg g^{-1} DW in tuberous root and leaves of MBO plants (**Supplementary Table S1**), and 21.3 and 28.4 in tuberous root and leaves of MDR plants, respectively (**Supplementary Table S4**). During the flowering stage, the protein content significantly increased in tuberous roots (+56%, on average), whereas it decreased in leaves (−18%) of MBO hybrids (**Supplementary Table S2**) compared with the rosette stage. The highest and lowest values of proteins were present in tuberous roots and leaves, respectively, of both FL and R:FR 3:1 lighting treatments. Protein contents significantly ($p > 0.05$) varied also among lighting treatments in both in tuberous roots and leaves (**Supplementary Table S3**). In MDR plants under the flowering stage, the proteins in leaves did not show any significant change compared with

FIGURE 2 | Plant phenological phases in *Ranunculus asiaticus* L.: pre-planting phase (rehydrated and vernalized tuberous roots), vegetative phase, and flowering phase.

the previous phenological stage, but they significantly differed among lighting treatments (**Supplementary Table S6**). Instead, in tuberous roots under the flowering stage, the proteins significantly increased (+40%) compared with the rosette stage, but their content was independent of lighting treatments (**Supplementary Tables S2**, **S3**).

During the pre-germination stage, polyphenol content contents were 6.0 and 5.4 $\mu g\ g^{-1}$ DW in MBO and MDR tuberous roots, respectively (**Supplementary Tables S1**, **S4**). In the successive rosette stage, the content of this metabolite slightly varied in tuberous roots of MBO plants, whereas it increased to a value of 10.3, on average, in leaves, which was independent of lighting treatments and the phenological stage (**Supplementary Tables S1**, **S2**). During the flowering stage, polyphenols in MBO tuberous roots significantly increased compared with those present in the rosette stage, except for FL lighting treatment, which remained stable (**Supplementary Tables S2**, **S3**). In the MDR hybrid, during the rosette stage, the content of polyphenols underwent the same increase in leaves and tuberous roots up to 10.25 $\mu g\ g^{-1}$ DW, on average, except for the R:FR 1:3 lighting treatment (**Supplementary Table S4**). However, in MDR plants during the flowering stage, the content of polyphenols in tuberous roots significantly ($p < 0.05$) changed in NL (+43%) and FL (−27%) lighting treatments, whereas it remained stable in the other ones. In the MDR leaves slightly but significantly changed, but their average value remained stable (**Supplementary Tables S5**, **S6**).

Free Amino Acids in Tuberous Roots and Leaves

The content of total amino acids was higher in MBO than in MDR hybrid independently of the growth stage and light conditions, except for those present in leaves of MDR plants during the rosette stage independently of lighting treatments (**Supplementary Tables S1**, **S2**, **S4**, **S5**). The main free amino acids in tuberous roots during the pre-planting stage were glutamine (190 and 117 $\mu mol\ g^{-1}$ DW in MBO and MDR, respectively), minor amino acids, as the sum of histidine, isoleucine, leucine, lysine, methionine, phenylalanine, tryptophan, tyrosine, and valine (152 and 62 $\mu mol\ g^{-1}$ DW in MBO and MDR, respectively), and branched chain amino acids (BCAAs), as the sum of isoleucine, leucine and valine (79 and 32 $\mu mol\ g^{-1}$ DW in MBO and MDR, respectively), followed by glutamate, threonine, asparagine, and alanine (**Supplementary Tables S1**, **S4** and **Figures 3A,B**). γ-*Aminobutyric acid* (GABA), alanine, threonine, serine, glutamate, minor amino acids, and total amino acids were 16.3, 9.8, 4.9, 4.2, 2.6, 2.4, and 2.3- fold higher in MBO than in MDR tuberous roots during the pre-planting stage, respectively. During the following growth stages, there was a remodulation of amino acid contents in the plant tissues, however, they remained always higher in tuberous roots than in leaves, independently of the growth stage. In order to obtain an easier overview of the changes of amino acids profile, pathway maps were constructed choosing for the heat maps to make the ratio of single parameter values to the total average values over the hybrid, growth stage, and light treatments to evidence not only the single changes but also the relative ones. The pathway maps were also included carbohydrates, proteins, and polyphenols (**Figures 3**,**4**).

Glutamate and threonine were the only amino acids that strongly increased in leaves of the MDR rosette and MBO flowering stages, respectively, independently of light treatments, peaking the former at NL (39 $\mu mol\ g^{-1}$ DW) (**Supplementary Table S4** and **Figure 3B**) and the latter at R:FR 1:3 light treatments (81 $\mu mol\ g^{-1}$ DW) (**Supplementary Table S2** and **Figure 4A**). On the contrary in tuberous roots, asparagine strongly increased during the rosette stage, and in particular in MBO plants (+722%), independently of light treatments, peaking at R:FR 3:1 with a content of 379 $\mu mol\ g^{-1}$ DW (**Supplementary Tables S1**, **S4** and **Figures 3A,B**). This amino acid remained at high levels in the same tissues in both hybrids, also during the flowering stage, even if it varied among light treatments (**Supplementary Table S2**, **S5** and **Figures 4A,B**). The glycine content of tuberous roots was always higher in the rosette and flowering stage stages than in the pre-germination stage. In

particular, it strongly increased in MBO at the flowering stage in all light conditions (+507%) except for R:FR 1:3. Glutamine was the second more abundant amino acid in tuberous roots during the rosette and flowering stages. However, it peaked in all treatments of MBO plants during the flowering stage except for the MBO-R:FR 1:3 treatment, as glycine (**Supplementary Table S2** and **Figure 4A**).

Principal Component Analysis of the Analyzed Parameters

To obtain an in-depth overview of the metabolites profile of the two hybrids under the different lighting treatments and growth stages, a PCA was conducted for all of the above-mentioned measured parameters for both tuberous roots and leaves (**Figures 5A,B**).

The PCA of all analyzed parameters highlighted that the first three principal components (PCs) were related with eigenvalues higher than 1 and explained 72% of the total variance for tuberous roots, with PC1, PC2, and PC3 accounting for 37.8, 22.0, and 12.1%, respectively, and 74.2% of the total variance for leaves, with PC1, PC2, and PC3 accounting for 31.3, 27.8, and 15.1%, respectively (data not shown). The growth stage contributed to the clear separation on PC1 for tuberous roots and on PC2 for leaves (**Figure 5**). In tuberous roots, PC1 was positively correlated with glutamate, starch, aspartate, threonine, proteins, sucrose, ornithine, and fructose. PC1 was also negatively correlated with asparagine, glucose, BCAAs, and serine. PC2 was negatively correlated with minor amino acids, proline, BCAAs, alanine, total amino acids, GABA, glycine, and serine (**Figure 5A**). In leaves, PC1 was positively correlated with glutamine, total amino acids, alanine, glycine, serine, starch, and asparagine, whereas it was negatively correlated with carotenoids, Chl a, Chl b, proteins, and glucose. PC2 was positively correlated with starch, polyphenols, and sucrose, whereas it was negatively correlated with MEA, ornithine, glutamate, aspartate, and proline (**Figure 5B**). In addition, the MBO-R:FR 3:1 treatment showed the highest minor amino acids content, in particular BCAAs, whereas the MDR-R:FR 3:1 treatment had the highest photosynthetic pigments and polyphenols content (**Figure 5**).

DISCUSSION

MBO and MDR tuberous roots at the pre-germination stage, after vernalization, showed similar contents of starch, soluble

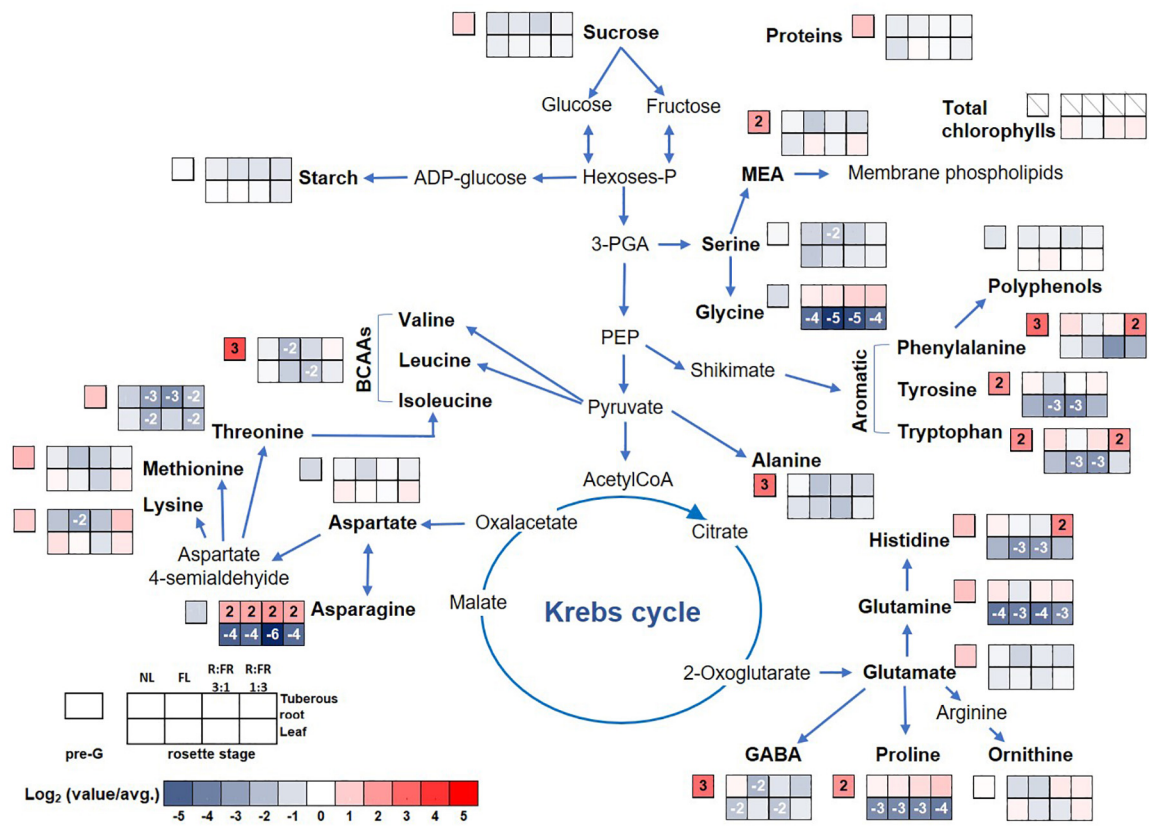

FIGURE 3 | Continued

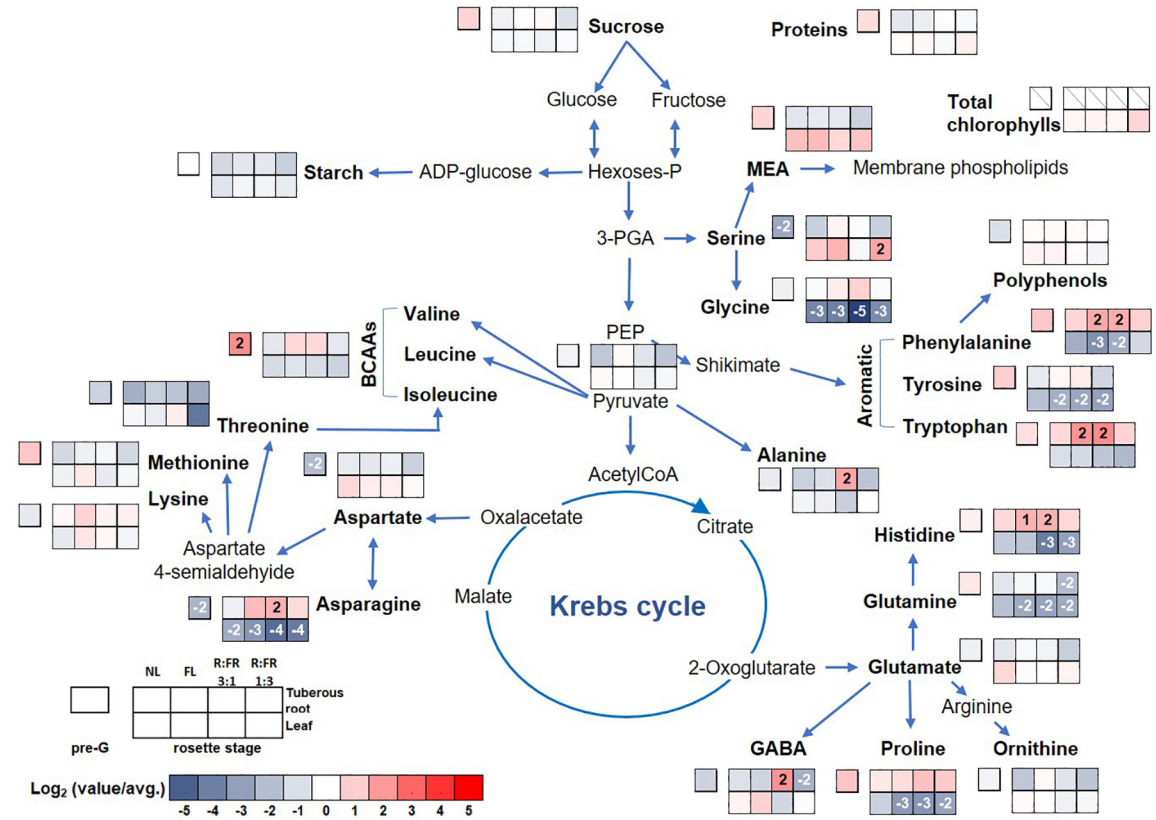

FIGURE 3 | Pathway map summarizing the effect of growth stage (pre-germination and leaf rosette) and photoperiodic lighting treatments: NL, NL + photoperiodic lighting with fluorescence light (FL), NL + photoperiodic lighting with LEDs R:FR 3:1 (R:FR 3:1), and NL + photoperiodic lighting with LEDs R:FR 1:3 (R:FR 1:3), on leaves and tuberous roots of the two hybrids MBO **(A)** and MDR **(B)** of *Ranunculus asiaticus* L. The heat map results were calculated as Logarithm base 1.5 ($Log_{1.5}$) of single values/total average values and visualized using a false-color scale, with red indicating an increase and blue a decrease. The significant ratios were indicated in the squares.

carbohydrates, and polyphenols, but a completely different profile of amino acids. In particular, GABA and alanine strongly increased in MBO tuberous roots compared with MDR ones. Yoshida et al. (1999) demonstrated that cold exposure induces the inactivation of cell H^+-ATPases and the impairment of the H^+ extrusion from cytosol, with the consequent rapid acidification of the cytoplasm and the concomitant alkalization of the vacuoles. In this view, the increases of alanine, deriving from the malic enzyme decarboxylation of malate to pyruvate, and GABA, deriving from the decarboxylation of glutamate catalyzed by glutamate decarboxylase, are proton-consuming reactions able to buffer cytoplasmic acidosis and regulate pH (Carillo, 2018; Carillo et al., 2019c; Van Oosten et al., 2019). Subsequently, after the relief from cold stress, the two amino acids can be converted to intermediates of the TCA cycle and used to produce alpha-keto acids and ATP (Bouché and Fromm, 2004). In addition, GABA exerts a well-known ROS scavenger activity able to stabilize and protect membranes and macromolecules from oxidative stress (Molina-Rueda et al., 2015).

At the germination stage, MBO tuberous roots under NL treatment still retained high contents of starch and glutamine and accumulated MEA, an amino acid derivative important for the synthesis and/or regeneration of phospholipids, derived by the decarboxylation of serine. Instead, all the other MBO tuberous roots exposed to the other light conditions were able to remobilize the N reserves synthetizing the amides asparagine and/or glutamine, amino acids having the highest nitrogen:carbon ratios and used for long-distance transport of nitrogen throughout the plant (Lea et al., 2007).

The increase of polyphenols in MDR tuberous roots during the germination stage evidenced a delayed response to the oxidative stress caused by vernalization (Yanagida et al., 2004). The increase of these metabolites was accompanied by an enhancement of the content of glucose under NL, proline under FL, fructose, sucrose, minor amino acids, and in particular BCAAs under R:FR 3:1, and by high amounts of GABA and alanine in addition to soluble carbohydrates and amino acids under R:FR 1:3 treatments. Both soluble carbohydrates and amino acids can play a

role in protecting membranes and macromolecules by ROS (Woodrow et al., 2017). In particular, the photoperiodic treatment R:FR 3:1 and R:FR 1:3 determined an increase of minor amino acids including BCAAs, which may actively function as antioxidants and alternative electron donors for the mitochondrial electron transport chain (Woodrow et al., 2017), limiting the occurrence of oxidative damages. Their increase appeared to be related to the levels of fructose, in agreement with Fritz et al. (2006) and Carillo et al. (2019a). Moreover, fructose, or glucose itself, can also be used for supplying glucose to the oxidative pentose pathway (OPP) and enhancing NADPH production, which is a major cofactor of the ROS scavenging ascorbate–glutathione pathway (Couée et al., 2006). However, the synthesis and accumulation of these metabolites with a protective function has a very high cost in terms of energy consumption (50–70 mol ATP for mole) (Raven, 1985; Cirillo et al., 2019) and seems to require the intervention of recent photosynthates from leaves. This export of carbohydrates from leaves at the germination stage, necessary for repairing the damages caused by vernalization and not promptly repaired at the pre-germination stage, could be responsible for the delay in growth and flowering in MDR plants.

At the flowering stage, in MBO under R:FR 1:3 light treatment, there was an increase of starch and amino acids, in particular GABA, otherwise Chls, carotenoids, polyphenols, and proteins decreased, while as reported by Modarelli et al. (2020b), leaf area still enlarged. Accordingly, Heraut-Bron et al. (2011) reported that white clover leaves that developed under a low R:FR ratio showed a decrease of photosynthetic pigments without consequences on the net photosynthesis, while leaf area increased. In these conditions, it is probable that the strong increase of GABA could be related to the decrease of protection of the photosynthesis apparatus deriving from the decrease of carotenoids and polyphenols. Both classes of metabolites are well known for their important ROS scavenging activity (Sandmann, 2019). Carotenoids, in particular, avoid photoinhibition under rapid fluctuations in light intensity when photochemical quenching activity is exceeded (Külheim et al., 2002). In addition, carotenoids protect chloroplasts from excess light, modulating the non-radiative dissipation of excess excitation energy and mediating the direct quenching of chlorophyll triplets (3Chl*) (Cazzaniga et al., 2012). The increase of starch proved that the photosynthesis was working quite efficiently and well protected by GABA, but this latter was not used for investing proteins in new leaves (Modarelli

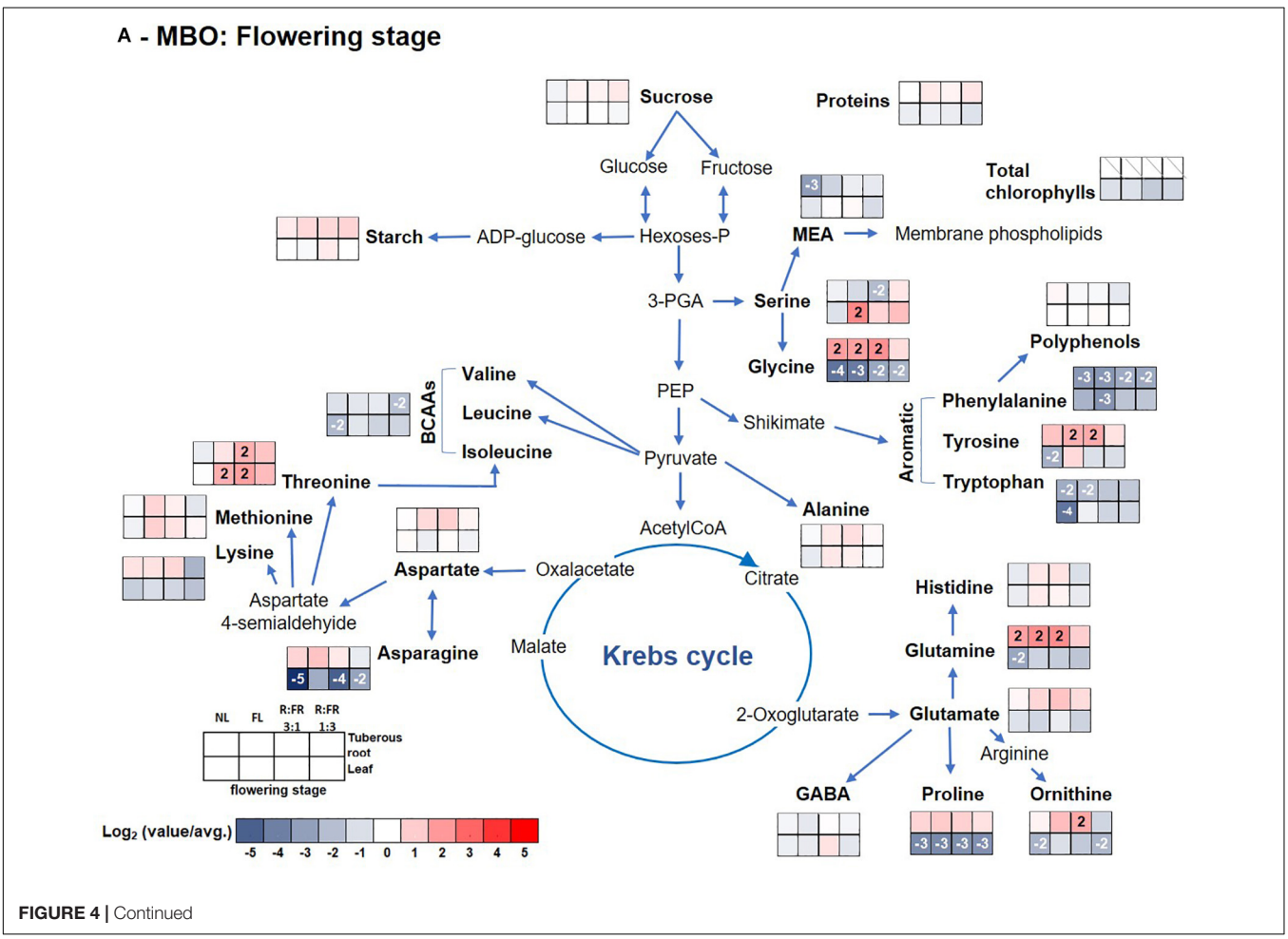

FIGURE 4 | Continued

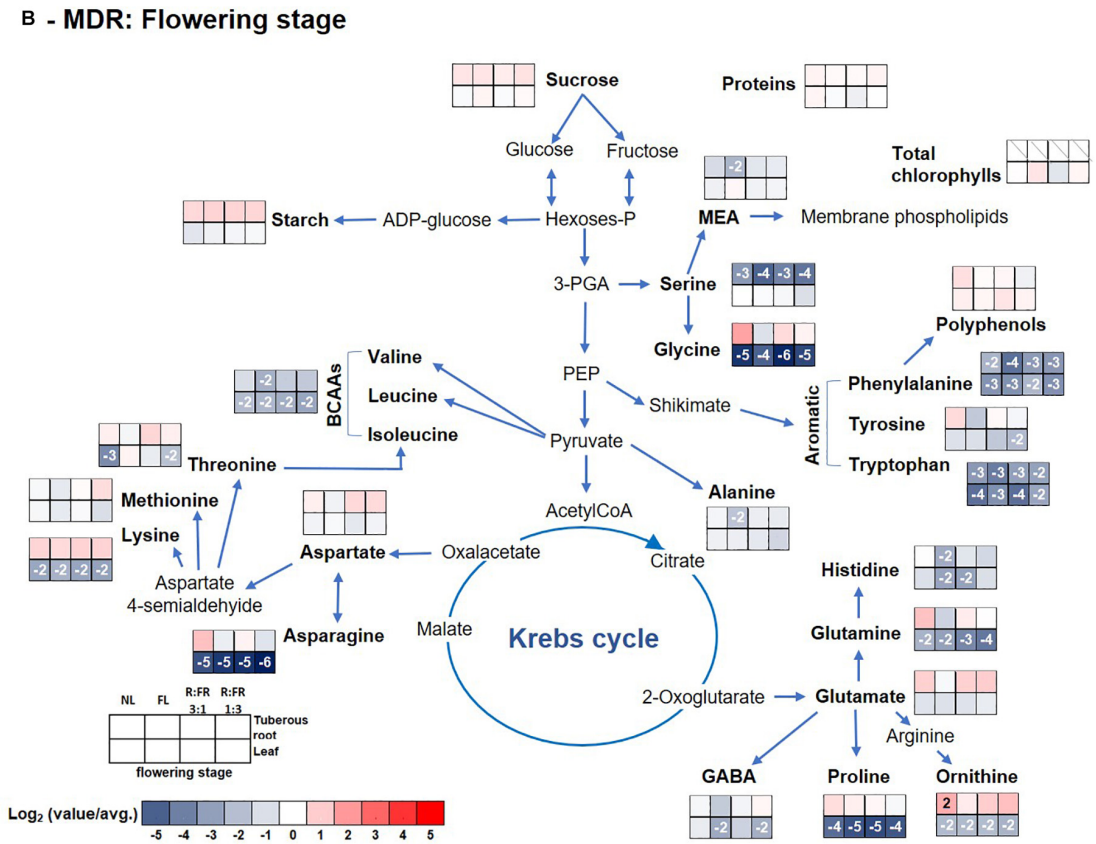

FIGURE 4 | Pathway map summarizing the effect of growth stage (flowering) and photoperiodic lighting treatments: NL, NL + photoperiodic lighting with fluorescence light (FL), NL + photoperiodic lighting with LEDs R:FR 3:1 (R:FR 3:1), and NL + photoperiodic lighting with LEDs R:FR 1:3 (R:FR 1:3), on leaves and tuberous roots of the two hybrids MBO **(A)** and MDR **(B)** of *Ranunculus asiaticus* L. The heat map results were calculated as Logarithm base 1.5 ($Log_{1.5}$) of single values/total average values and visualized using a false-color scale, with red indicating an increase and blue a decrease. The significant ratios were indicated in the squares.

et al., 2020b). Low R:FR is, in fact, perceived by plants as a signal of shade conditions and activates a set of genes related to cell proliferation and/or enlargement among which while decreasing cytokinin in young, middle, and old leaves (Wu et al., 2017). Auxin is well known for its induction of acid growth, in which plant cells and plant cell walls elongate and/or expand quickly without effectively growing (Arsuffi and Braybrook, 2017). Indeed, it is known that the addition of FR to the natural light spectrum (reducing the R:FR ratio and the PPE value at plant level) promotes leaf expansion (Li and Kubota, 2009; Park and Runkle, 2017, 2018; Fukuda, 2019; Meng and Runkle, 2019). These changes in metabolism allow plants to enact a ubiquitous mechanism known as "shade-avoidance syndrome" in which leaves already present are enlarge, and flowering is accelerated (Martínez-García et al., 2014; Modarelli et al., 2020b). In these conditions, large amounts of amino acids are exported to roots but not sugars.

MBO R:FR 3:1 underwent a slower decrease of photosynthetic pigments in leaves, but an equally fast export of amino acids to tuberous roots that were also converted to proteins. MBO NL showed a fast decrease of leaf metabolites, but not an equally and quick filling of the tuberous root reserve. Unexpectedly, FL, the other high R:FR condition, was faster and more efficient than the other MBO lighting conditions to transport sugars and amino acids to tuberous roots and by converting them to starch, proteins, and serine.

Except for MDR R:FR 1:3, that accelerated the export of metabolites from leaves without efficiently replenishing the sugar reserves of tuberous roots, all the other lighting conditions showed the presence of a still active photosynthetic apparatus, as proven by the persistence of photosynthetic pigments and proteins, but an already active export of sugars, soon converted to starch. MDR NL showed the lowest starch content in tuberous roots at the flowering stage but the highest content of glucose and polyphenols.

The study of metabolic profiling confirmed the intrinsic differences between the two *R. asiaticus* hybrids. The different profiles of tuberous root reserves seem responsible for the capacity of MBO to exert a faster overcome of the vernalization stress and an equally fast development of the germination and flowering activities. Some changes in morphological and

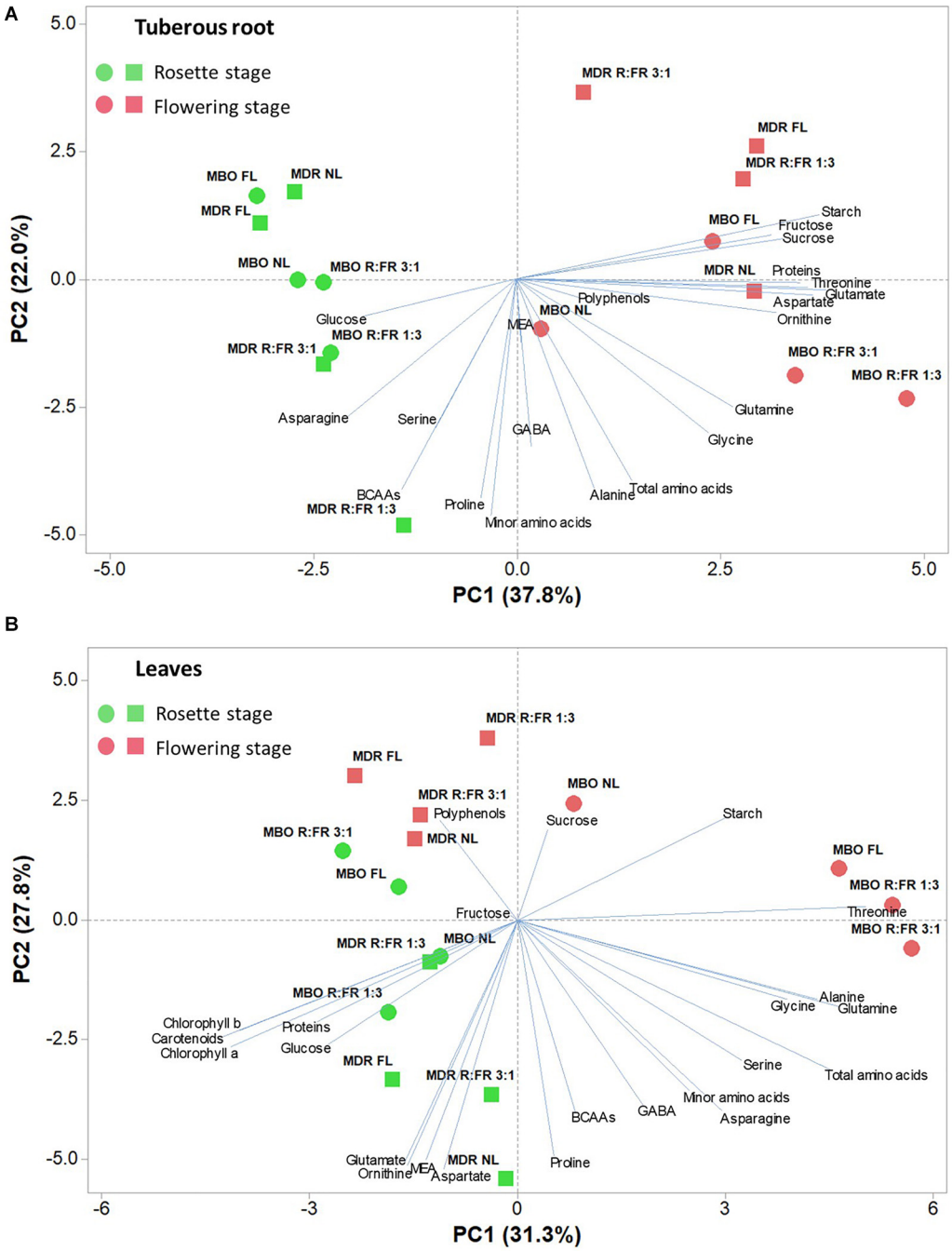

FIGURE 5 | Principal component loading plot and scores of principal component analysis (PCA) of starch, soluble carbohydrates, photosynthetic pigments (only for leaves), polyphenols, soluble proteins, and amino acids of tuberous roots **(A)** and leaves **(B)** of two hybrids (MBO and MDR) of *Ranunculus asiaticus* L. at the growth stage of rosette and flowering. The plants underwent different photoperiodic lighting treatments: NL, NL + photoperiodic lighting with fluorescence light (FL), NL + photoperiodic lighting with LEDs R:FR 3:1 (R:FR 3:1), and NL + photoperiodic lighting with LEDs R:FR 1:3 (R:FR 1:3).

physiological traits were certainly related to the different responses to day length and photoperiodic light quality in the two hybrids, as also observed in plants from rehydrated and vernalized roots (Modarelli et al., 2020a).

Photoperiodic treatments with all the lighting sources were effective to reduce the flowering time in both the hybrids, even though R:FR light at 1:3 ratio was less efficient than the other treatments in MDR. The metabolic pathway and PCA carried out in this work facilitated a broad view of morpho-physiological and biochemical traits and enabled the identification of phenotypic variation patterns associated with *Ranunculus* genotype and/or

lighting conditions, as evidenced also for other species (Carillo et al., 2019a,c).

In conclusion, in its entirety, our work provides information on the different performances of two *R. asiaticus* L. hybrids in a cold glasshouse in a Mediterranean environment and on their response to photoperiodic treatment, in terms of duration and light spectrum. The two hybrids confirmed intrinsic differences in metabolic profile, as already observed in photosynthetic behavior, plant growth, and flowering (Carillo et al., 2019a; Modarelli et al., 2020b,c).

Our results demonstrate that, together with the different behaviors depending on the plant genotype, the different sensitivities of the hybrids to vernalization should be considered for the proper choice of the preparation procedure in production scheduling at large scale. Similarly, the specific response of the hybrids to light environment should be taken into account to optimize lighting protocols and production planning in *R. asiaticus* L.

DATA AVAILABILITY STATEMENT

The raw data supporting the conclusions of this article will be made available by the authors, without undue reservation.

AUTHOR CONTRIBUTIONS

RP and SD designed the experiment. GM carried out the plant cultivation and performed the statistical analysis of data. ED'A and GF performed the pigments and metabolic analyses. PC performed the PCA and constructed the metabolic pathways. RP and PC wrote the manuscript. All authors contributed to the article and approved the submitted version.

FUNDING

This work was carried out within the framework of the Research Doctorate on Food and Agricultural Sciences—XXII cycle, of the University of Naples Federico II. Universitàà degli Studi della Campania Luigi Vanvitelli (grant number VALERE: VAnviteLli pEr la RicErca).

ACKNOWLEDGMENTS

We thank Dr. Mario Rabaglio (Biancheri Creazioni, Italy) for propagation material and technical assistance, Dr. Giuseppe Pesce (University of Naples Federico II) for customizing the LED panels, Dr. Raffaele Garramone (University of Naples Federico II) for their help in setting up the experiment, and Dr. Giuseppe Nenna (ENEA Portici Research Center) for light emission spectra of light source.

SUPPLEMENTARY MATERIAL

The Supplementary Material for this article can be found online at: https://www.frontiersin.org/articles/10.3389/fpls.2020.597823/full#supplementary-material

REFERENCES

Addai, I. K. (2010). *Growth and Biochemistry of the Common Hyacinth (Hyacinthus orientalis L.) and the Lily (Lilium longiflorum L.)*. Doctoral dissertation. Sussex: University of Sussex.

Annunziata, M. G., Carillo, P., Fuggi, A., Troccoli, A., and Woodrow, P. (2013). Metabolic profiling of cauliflower under traditional and reduced tillage systems. *Aust. J. Crop Sci.* 7, 1317–1323.

Arsuffi, G., and Braybrook, S. A. (2017). Acid growth: an ongoing trip. *J. Exp. Bot.* 69, 137–146. doi: 10.1093/jxb/erx390

Beruto, M., Fibiani, M., Rinino, S., Lo Scalzo, R., and Curir, P. (2009). Plant development of *Ranunculus asiaticus* L. tuberous roots is affected by different temperature and oxygen conditions during storage period. *Isr. J. Plant Sci.* 57, 377–388. doi: 10.1560/IJPS.57.4.377

Beruto, M., Rabaglio, M., Viglione, S., Van Labeke, M. C., and Dhooghe, E. (2018). "*Ranunculus*, in ornamental crops," in *Handbook of Plant Breeding*, Vol. 11, ed. J. Van Huylenbroeck (Cham: Springer International Publishing AG), 649–671.

Bouché, N., and Fromm, H. (2004). GABA in plants: just a metabolite? *Trends Plant Sci.* 9, 110–115. doi: 10.1016/j.tplants.2004.01.006

Bradford, M. M. (1976). A rapid and sensitive method for the quantitation of microgram quantities of protein utilizing the principle of protein-dye binding. *Anal. Biochem.* 72, 248–254. doi: 10.1016/0003-2697(76)90527-3

Carillo, P. (2018). GABA shunt in durum wheat. *Front. Plant Sci.* 9:100. doi: 10.3389/fpls.2018.00100

Carillo, P., Arena, C., Modarelli, G. C., De Pascale, S., and Paradiso, R. (2019a). Photosynthesis in *Ranunculus asiaticus* L.: the influence of the hybrid and the preparation procedure of tuberous roots. *Front. Plant Sci.* 10:241. doi: 10.3389/fpls.2019.00241

Carillo, P., Colla, G., El-Nakhel, C., Bonini, P., D'amelia, L., Dell'aversana, E., et al. (2019b). Biostimulant application with a tropical plant extract enhances *Corchorus olitorius* adaptation to sub-optimal nutrient regimens by improving physiological parameters. *Agron* 9:249. doi: 10.3390/agronomy9050249

Carillo, P., Kyriacou, M. C., El-Nakhel, C., Pannico, A., Dell'Aversana, E., D'Amelia, L., et al. (2019c). Sensory and functional quality characterization of protected designation of origin 'Piennolo del Vesuvio' cherry tomato landraces from Campania-Italy. *Food Chem.* 292, 166–175. doi: 10.1016/j.foodchem.2019.04.056

Carillo, P., Cacace, D., De Pascale, S., Rapacciuolo, M., and Fuggi, A. (2012). Organic vs. traditional potato powder. *Food Chem.* 133, 1264–1273. doi: 10.1016/j.foodchem.2011.08.088

Carillo, P., Kyratzis, A., Kyriacou, M. C., Dell-Aversana, E., Fusco, G. M., Corrado, G., et al. (2020). Biostimulatory action of arbuscular mycorrhizal fungi enhances productivity, functional and sensory quality in 'Piennolo del Vesuvio' cherry tomato landraces. *Agronomy* 10:911. doi: 10.3390/agronomy10060911

Cazzaniga, S., Li, Z., Niyogi, K. K., Bassi, R., and Dall'Osto, L. (2012). The *Arabidopsis* szl1 mutant reveals a critical role of β-carotene in photosystem I photoprotection. *Plant Physiol.* 159, 1745–1758. doi: 10.1104/pp.112.201137

Ciarmiello, L. F., Piccirillo, P., Carillo, P., De Luca, A., and Woodrow, P. (2015). Determination of the genetic relatedness of fig (*Ficus carica* L.) accessions using RAPD fingerprint and their agro-morphological characterization. *South Afr. J. Bot.* 97, 40–47. doi: 10.1016/j.sajb.2014.11.012

Cirillo, C., De Micco, V., Arena, C., Carillo, P., Pannico, A., De Pascale, S., et al. (2019). Biochemical, physiological and anatomical mechanisms of adaptation of *Callistemon citrinus* and *Viburnum lucidum* to NaCl and CaCl(2) salinization. *Front. Plant Sci.* 10:742. doi: 10.3389/fpls.2019.00742

Couée, I., Sulmon, C., Gouesbet, G., and El Amrani, A. (2006). Involvement of soluble sugars in reactive oxygen species balance and responses to oxidative stress in plants. *J. Exp. Bot.* 57, 449–459. doi: 10.1093/jxb/erj027

Craig, D. S., and Runkle, E. S. (2016). An intermediate phytochrome photoequilibria from night-interruption lighting optimally promotes flowering of several long-day plants. *Environ. Exp. Bot.* 121, 132–138. doi: 10.1016/j.envexpbot.2015.04.004

De Hertogh, A. (1996). *Holland Bulb Forcer's Guide*, 5th Edn. Leiden: Alkemade Printing BV.

Devlin, P. F., Christie, J. M., and Terry, M. J. (2007). Many hands make light work. *J. Exp. Bot.* 58, 3071–3077. doi: 10.1093/jxb/erm251

Dueck, T., van Ieperen, W., and Taulavuori, K. (2016). Light perception, signalling and plant responses to spectral quality and photoperiod in natural and horticultural environments. *Environ. Exp. Bot.* 121, 1–3. doi: 10.1016/j.envexpbot.2015.06.012

Ferchichi, S., Hessini, K., Dell'Aversana, E., D'Amelia, L., Woodrow, P., Ciarmiello, L. F., et al. (2018). *Hordeum vulgare* and *Hordeum maritimum* respond to extended salinity stress displaying different temporal accumulation pattern of metabolites. *Funct. Plant Biol.* 45, 1096–1109. doi: 10.1071/FP18046

Fritz, C., Mueller, C., Matt, P., Feil, R., and Stitt, M. (2006). Impact of the C-N status on the amino acid profile in tobacco source leaves. *Plant Cell Environ.* 29, 2055–2076. doi: 10.1111/j.1365-3040.2006.01580.x

Fukuda, N. (2019). "Plant growth and physiological responses to light conditions," in *Plant Factory Using Artificial Light*, eds M. Anpo, H. Fukuda, and T. Wada (Amsterdam: Elsevier), 71–77.

Heraut-Bron, V., Robin, C., Varlet-Grancher, C., and Afif, D. (2011). Light quality (red:far-red ratio): does it affect photosynthetic activity, net CO2 assimilation, and morphology of young white clover leaves? *Can. J. Bot.* 77, 1425–1431. doi: 10.1139/b99-099

Horovitz, A. (1985). "Ranunculus," in *Handbook of Flowering*, Vol. 4, ed. A. Halevy (Boca Raton FL: CRC Press), 155–161.

Külheim, C., Agren, J., and Jansson, S. (2002). Rapid regulation of light harvesting and plant fitness in the field. *Science* 297, 91–93. doi: 10.1126/science.1072359

Le Nard, M., and De Hertogh, A. (1993). "The physiology of flower bulbs, Chapter 4," in *Bulb Growth and Development and Flowering*, eds A. De Hertogh and M. Le Nard (Amsterdam: Elsevier).

Lea, P. J., Sodek, L., Parry, M. A. J., Shewry, P. R., and Halford, N. G. (2007). Asparagine in plants. *Ann. App. Biol.* 150, 1–26. doi: 10.1111/j.1744-7348.2006.00104.x

Li, Q., and Kubota, C. (2009). Effects of supplemental light quality on growth and phytochemicals of baby leaf lettuce. *Environ. Exp. Bot.* 67, 59–64. doi: 10.1016/j.envexpbot.2009.06.011

Liu, F., Zhang, H., Wu, G., Sun, J., Hao, L., Ge, X., et al. (2011). Sequence variation and expression analysis of seed dormancy and germination associated ABA and GA related genes in rice cultivars. *Front. Plant Sci.* 2:17. doi: 10.3389/fpls.2011.00017

Madsen, T. V. (1993). Growth and photosynthetic acclimation by *Ranunculus aquatilis* L. in response to inorganic carbon availability. *New Phytol.* 125, 707–715. doi: 10.1111/j.1469-8137.1993.tb03919.x

Madsen, T. V., and Brik, H. (1997). Growth, photosynthesis and acclimation by two submerged macrophytes in relation to temperature. *Oecologia* 110, 320–327. doi: 10.1007/s004420050165

Martínez-García, J. F., Gallemí, M., Molina-Contreras, M. J., Llorente, B., Bevilaqua, M. R. R., and Quail, P. H. (2014). The shade avoidance syndrome in arabidopsis: the antagonistic role of Phytochrome A and B differentiates vegetation proximity and canopy shade. *PLoS One* 9:e109275. doi: 10.1371/journal.pone.0109275

Meng, Q., and Runkle, E. S. (2019). Far-red radiation interacts with relative and absolute blue and red photon flux densities to regulate growth, morphology, and pigmentation of lettuce and basil seedlings. *Sci. Hortic.* 255, 269–280. doi: 10.1016/j.scienta.2019.05.030

Meynet, J. (1993). "Ranunculus," in *Physiology of Flower Bulbs: A Comprehensive Treatise on the Physiology and Utilization of Ornamental Flowering Bulbous and Tuberous Plants*, eds A. A. De Hertogh and M. Le Nard (Amsterdam: Elsevier), 603–610.

Miller, W. B. (1992). A review of carbohydrate metabolism in geophytes. *Acta Hortic.* 325, 239–246. doi: 10.17660/ActaHortic.1992.325.29

Modarelli, G. C., Arena, C., De Pascale, S., and Paradiso, R. (2020a). *Photosynthesis in Ranunculus asiaticus* L.: *Characterization in Two Mediterranean Hybrids Under Fluorescent White Light*. Leuven: International Society for Horticultural Science (ISHS), 163–168.

Modarelli, G. C., Arena, C., De Pascale, S., and Paradiso, R. (2020b). "The influence of the hybrid and the preparation procedure of tuberous roots on plant growth and flowering in *Ranunculus asiaticus* L.," in *Proceedings of the International Symposium on Advanced Technologies and Management for Innovative Greenhouses - GreenSys 2019*. Angers

Modarelli, G. C., Arena, C., Pesce, G., Dell'Aversana, E., Fusco, G. M., Carillo, P., et al. (2020c). The role of light quality of photoperiodic lighting on photosynthesis, flowering and metabolic profiling in *Ranunculus asiaticus* L. *Physiol. Plant* 170, 187–201. doi: 10.1111/ppl.13122

Molina-Rueda, J. J., Pascual, M. B., Pissarra, J., and Gallardo, F. (2015). A putative role for γ-aminobutyric acid (GABA) in vascular development in pine seedlings. *Planta* 241, 257–267. doi: 10.1007/s00425-014-2157-4

Ohyama, T., Ikarashi, T., Matsubara, T., and Baba, A. (1998). Behaviour of carbohydrates in mother and daughter bulbs of tulip. *Soil Sci. Plant Nutr.* 34, 405–415. doi: 10.1080/00380768.1988.10415696

Ouzounis, T., Rosenqvist, E., and Ottosen, C. O. (2015). Spectral effects of artificial light on plant physiology and secondary metabolism: a review. *HortScience* 50, 1128–1135. doi: 10.21273/HORTSCI.50.8.1128

Park, Y., and Runkle, E. S. (2017). Far-red radiation promotes growth of seedlings by increasing leaf expansion and whole-plant net assimilation. *Environ. Exp. Bot.* 136, 41–49. doi: 10.1016/j.envexpbot.2016.12.013

Park, Y., and Runkle, E. S. (2018). Far-red radiation and photosynthetic photon flux density independently regulate seedling growth but interactively regulate flowering. *Environ. Exp. Bot.* 155, 206–216. doi: 10.1016/j.envexpbot.2018.06.033

Ranwala, A. P., and Miller, W. B. (2008). Analysis of nonstructural carbohydrates in storage organs of 30 ornamental geophytes by high performance anion exchange chromatography with pulsed amperometric detection. *New Phytol.* 180, 421–433. doi: 10.1111/j.1469-8137.2008.02585.x

Raven, J. A. (1985). Tansley review no. 2. Regulation of pH and generation of osmolarity in vascular plants: a cost-benefit analysis in relation to efficiency of use of energy, nitrogen and water. *New Phytol.* 101, 25–77.

Sager, J. C., Smith, W. O., Edwards, J. L., and Cry, K. L. (1988). Photosynthetic efficiency and phytochrome photoequilibria determination using spectral data. *Trans. Asae* 31, 1882–1889. doi: 10.13031/2013.30952

Sandmann, G. (2019). Antioxidant protection from UV- and light-stress related to carotenoid structures. *Antioxidants* 8:219. doi: 10.3390/antiox8070219

Singleton, V. L., Orthofer, R., and Lamuela-Raventós, R. M. (1999). Analysis of total phenols and other oxidation substrates and antioxidants by means of Folin-Ciocalteu reagent. *Methods Enzymol.* 299, 152–178. doi: 10.1016/S0076-6879(99)99017-1

Van Oosten, M. J., Dell'aversana, E., Ruggiero, A., Cirillo, V., Gibon, Y., Woodrow, P., et al. (2019). Omeprazole treatment enhances nitrogen use efficiency through increased nitrogen uptake and assimilation in corn. *Front. Plant Sci.* 10:1507. doi: 10.3389/fpls.2019.01507

Wang, W., Su, X., Tian, Z., Liu, Y., Zhou, Y., and He, M. (2018). Transcriptome profiling provides insights into dormancy release during cold storage of *Lilium pumilum*. *BMC Genomics* 19:196. doi: 10.1186/s12864-018-4536-x

Whitman, C. M., Heins, R. D., Cameron, A., and Carlson, W. H. (1998). Lamp type and irradiance level for daylength extensions influence flowering of *Campanula carpatica* "blue clips", *Coreopsis grandiflora* "Early Sunrise", and *Coreopsis verticillata* "Moonbeam.". *J. Am. Soc. Hortic. Sci.* 123, 802–807. doi: 10.21273/JASHS.123.5.802

Woodrow, P., Ciarmiello, L. F., Annunziata, M. G., Pacifico, S., Iannuzzi, F., Mirto, A., et al. (2017). Durum wheat seedling responses to simultaneous high light and salinity involve a fine reconfiguration of amino acids and carbohydrate metabolism. *Physiol. Plant* 159, 290–312. doi: 10.1111/ppl.12513

Wu, Y., Gong, W., and Yang, W. (2017). Shade inhibits leaf size by controlling cell proliferation and enlargement in soybean. *Sci. Rep.* 7:9259. doi: 10.1038/s41598-017-10026-5

Yanagida, M., Mino, M., Iwabuchi, M., and Ogawa, K. (2004). Reduced glutathione is a novel regulator of vernalization-induced bolting in the rosette plant *Eustoma grandiflorum*. *Plant Cell Physiol.* 45, 129–137. doi: 10.1093/pcp/pch030

Yoshida, S., Hotsubo, K., Kawamura, Y., Murai, M., Arakawa, K., and Takezawa, D. (1999). Alterations of intracellular pH in response to low temperature stresses. *J. Plant Res.* 112, 225–236. doi: 10.1007/PL00013879

Zhang, M., and Runkle, E. S. (2019). Regulating flowering and extension growth of *Poinsettia* using red and far-red light-emitting diodes for end-of-day lighting. *HortScience* 54, 323–327. doi: 10.21273/HORTSCI13630-18

Conflict of Interest: The authors declare that the research was conducted in the absence of any commercial or financial relationships that could be construed as a potential conflict of interest.

Copyright © 2020 Carillo, Dell'Aversana, Modarelli, Fusco, De Pascale and Paradiso. This is an open-access article distributed under the terms of the Creative Commons Attribution License (CC BY). The use, distribution or reproduction in other forums is permitted, provided the original author(s) and the copyright owner(s) are credited and that the original publication in this journal is cited, in accordance with accepted academic practice. No use, distribution or reproduction is permitted which does not comply with these terms.

frontiers in Plant Science

ORIGINAL RESEARCH
published: 04 December 2020
doi: 10.3389/fpls.2020.597906

Response of Basil Growth and Morphology to Light Intensity and Spectrum in a Vertical Farm

*Dorthe H. Larsen[1], Ernst J. Woltering[1,2], Celine C. S. Nicole[3] and Leo F. M. Marcelis[1]**

[1] Horticulture and Product Physiology, Department of Plant Sciences, Wageningen University & Research, Wageningen, Netherlands, [2] Postharvest Technology, Wageningen Food and Biobased Research, Wageningen University & Research, Wageningen, Netherlands, [3] Signify, Eindhoven, Netherlands

Vertical farming is becoming increasingly popular for production of leafy vegetables and herbs, with basil (*Ocimum basilicum* L.) as one of the most popular herbs. In basil most research has focused on increasing secondary metabolites with light spectra. However, knowledge about the effect of light intensity (photosynthetic photon flux density, PPFD) and spectra on growth and morphology is key for optimizing quality at harvest. The impact of PPFD and spectrum on plant growth and development is species dependent and currently few studies in basil are available. Understanding the response to End-Of-Production (EOP) light of growth and morphology is important for successful vertical farming. We performed a comprehensive series of experiments, where the effects of EOP PPFD, fraction of blue and their interaction on the growth and morphology were analyzed in two green and one purple basil cultivar. In addition, the impact of different EOP intensities and duration of far-red were investigated. We found that increasing the PPFD increased fresh mass, dry matter content and plant height in all three cultivars. The responses were linear or quadratic depending on the cultivar. A high fraction of blue (>90%) increased plant height and decreased the dry mass partitioning to the leaves. The only interaction found between the fraction of blue and overall PPFD was on plant height in the green cultivar whereas other growth parameters and morphology responded stronger to PPFD than to the fraction of blue light. Plant dry matter production was increased with the addition of far-red. Far-red EOP intensity treatments enhanced the fraction of dry mass partitioned to the leaves, whereas a prolonged far-red treatment enhanced partitioning to the stem. Both plant fresh mass and dry matter content were improved by applying high PPFD shortly before harvest. Light spectra were found to be of less importance than PPFD with respect to plant dry matter content. Light use efficiency (LUE) based on fresh mass decreased with increasing PPFD whereas LUE based on dry mass increased with increasing PPFD, when given as EOP treatments. The overall physiological mechanisms of the light intensity and spectral effects are discussed.

Keywords: basil, LED, spectra, blue light, far-red light, photosynthetic photon flux density, vertical farming

OPEN ACCESS

Edited by:
Oliver Körner,
Leibniz Institute of Vegetable and Ornamental Crops, Germany

Reviewed by:
Cristian Silvestri,
University of Tuscia, Italy
Alberto Pardossi,
University of Pisa, Italy
Paul R. H. Robson,
Aberystwyth University, United Kingdom

***Correspondence:**
Leo F. M. Marcelis
leo.marcelis@wur.nl

Specialty section:
This article was submitted to Crop and Product Physiology, a section of the journal Frontiers in Plant Science

Received: *22 August 2020*
Accepted: *09 November 2020*
Published: *04 December 2020*

Citation:
Larsen DH, Woltering EJ, Nicole CCS and Marcelis LFM (2020) Response of Basil Growth and Morphology to Light Intensity and Spectrum in a Vertical Farm. Front. Plant Sci. 11:597906. doi: 10.3389/fpls.2020.597906

INTRODUCTION

Vertical farming systems, also called plant factories, are indoor growth facilities with plants grown in multiple layers. In a vertical farm, plants are grown in a closed system without the use of pesticides and all climate factors can be controlled (SharathKumar et al., 2020). Controlling the pre-harvest factors can have a great influence on the growth and morphology as well as postharvest quality (Mattheis and Fellman, 1999). Light is the primary source of energy for plants and the dominant light source in a vertical farm is light emitting diodes (LEDs) which makes a vertical farm efficient and allows for year-round production. LEDs are energy efficient, they have a low heat emission, the light intensity can be adjusted and light spectra can be modulated (Kusuma et al., 2020). Leafy vegetables and herbs are often the crops of choice in vertical farms due to fast growth, low plant height, and high retail price (Touliatos et al., 2016). One popular culinary herb is basil (*Ocimum basilicum* L.) that is used for its unique aroma. Besides aroma other important quality parameters include yield, plant morphology and fresh mass and dry matter content (Maness, 2003; Zhou et al., 2012). However, there has been little research on elucidating the response to light intensity and spectra of yield and dry matter content in basil.

Plant development, yield and dry matter content are highly affected by light intensity. Light intensity used for photosynthesis is defined as photosynthetic photon flux density (PPFD) ranging from 400–700 nm (McCree, 1972; Poorter et al., 2019). Increased light intensity generally correlates with an increase in net photosynthesis which can increase plant fresh mass and yield. Furthermore, an increase in light intensity can increase soluble sugars which are part of the dry matter. In basil, plant growth and dry matter content were found to increase under increasing light intensity but only until an optimum after which the plants might be limited by other environmental factors (Pennisi et al., 2020). Yet, Kelly et al. (2020) found in lettuce biomass increased linearly with PPFD. In addition to PPFD, light spectrum is important for morphological features, specifically the partitioning of carbon to leaves vs. stem. Some of the most studied light spectra include ratios of blue (400–500 nm) and red (600–700 nm), and addition of far-red (700–800 nm) to PPFD. While red is the most efficient color for photosynthesis and energy use, 100% red often disturbs normal morphology (i.e., leaf curling, thin, and pale leaves). It is important to add blue to the spectra for optimal morphology. Blue light plays a role in several plant processes such as photomorphogenesis, stomatal opening, and leaf photosynthetic functioning (Hogewoning et al., 2010; Boccalandro et al., 2012). An optimum of blue light could exist for photosynthetic capacity as well as for biomass accumulation (Kaiser et al., 2019). Fresh mass (Li and Kubota, 2009) and dry matter (Kalaitzoglou et al., 2019) can also increase with the addition of far-red. Furthermore, far-red has been associated with increased leaf area and plant height in basil (Carvalho et al., 2016) which could increase light interception. Plant height might also increase under 100% blue light (Heo et al., 2002; Johnson et al., 2020). However, the opposite effect has been reported in several studies where a high fraction of blue light resulted in more compact plants (Hoenecke et al., 1992; Islam et al., 2012; Keuskamp et al., 2012). In basil, contradictory reports exists with respect to the plant growth and morphology response to light spectra. Plant height was neither affected by 100% blue light compared to greenhouse grown basil (Carvalho et al., 2016), nor the addition of blue to a red light spectra (20–60% blue) in a greenhouse (Jensen et al., 2018), or the response to blue light was entangled with addition of far-red (Bantis et al., 2016). Piovene et al. (2015) reported 37% blue had a positive effect while Pennisi et al. (2019) found that a fraction of blue above 30% had a negative effect on fresh mass. However, the optimal PPFD, as well as spectra with respect to fraction of blue and addition of far-red light for plant growth have been found to be highly species dependent (Kim et al., 2006; Colonna et al., 2016).

Several studies have focused on increasing the secondary metabolites in basil, however, fewer studies have elucidated the effect of PPFD, light spectra and the interaction of the two on the growth and morphological features. The primary attribute of crops in a commercial production system is biomass, that is fresh and dry mass of leaves. Other relevant attributes include morphology such as short internodes and increased partitioning of carbon to the leaves. Knowledge of the response of basil to changes in light intensity and spectra will allow for a fully controlled plant production and a desired growth and morphology. To optimize production in vertical farming, it has been proposed to focus the lighting strategy during the first part of cultivation cycle on optimizing biomass increase, while the last period before harvest the lighting strategy should focus on optimizing product quality by End-Of-Production (EOP) treatments (SharathKumar et al., 2020). We aimed at understanding the response of growth and morphology of basil to PPFD, fraction of blue light and far-red. In addition, we wanted to study the response to EOP light applied 5–7 days before harvest. To study this, we set up a comprehensive series of (five) studies, in a vertical farming set-up with green and purple basil cultivars.

MATERIALS AND METHODS

Growth Conditions

Basil (*O. basilicum* L.) was grown in a climate chamber in a vertical farming set-up with twelve compartments of the size 0.8 × 1.3 m in table area and a plant density of 123 plants m^{-2}. Two green cultivars (Emily and Dolly) and one purple cultivar (Rosie) Sweet basil, were used; all cultivars were derived from Enza Zaden, NL. Seeds were germinated under red-white LED light (GreenPower LED production module 120 cm, DeepRedWhite, Phillips Eindhoven, Netherlands) varying between 150 and 200 μmol m^{-2} s^{-1} (**Table 1**). The spectral intensities in Experiment 1–4 were measured with a spectroradiometer (USB2000 spectrometer, Ocean Optics, Duiven, Netherlands), and in Experiment 5 with another spectroradiometer (SS-110; Apogee Instruments, Logan, UT, United States). Phytochrome Photostationary state (PSS) values were calculated according to Sager et al. (1988). PPFD was regularly measured with a quantum sensor (LI-190SB quantum sensor, LI-1400 Datalogger, LI-COR Bioscience, Lincoln, NE, United States) to adjust the height of the light frames during

the growth and maintain a constant light intensity at the top of the plants throughout each experiment. The sides of each compartment were covered with white reflective plastic to increase light uniformity. Seeds were sown in trays with 240 stone wool plugs (Grodan Rockwool B.V., Netherlands) with one seed per plug. After 10–15 days the morphologically most similar plants were selected and transplanted to 7.5 × 7.5 × 6.5 cm stone wool blocks (Grodan Rockwool B.V., Netherlands), one outer row surrounding the plants were border plants and not used for the experiment. Day/night temperature was kept at 25°C, the relative humidity was set at 75% and CO_2 was ambient concentration. Relative humidity and temperature in each light treatment were recorded with either keytag dataloggers (KTL-508, Keytag, NL) or Hanwell data loggers (ML4160, Hanwell Solutions, United Kingdom) with deviations within 10% and 1°C from the set points. To maintain air temperature around 25°C fans were installed in high light treatments above the lamps blowing out of the individual compartments. Plants were kept well-watered through an ebb and flood system based on plant needs and growth stage. For the first 3 weeks of the growth, plants were watered once every second day for 10 min and after that once every day for 10 min. High light and high blue treatments were given an extra round of watering when needed. The nutrient solution consisted of NO_3^- 8.5 mM, SO_4^{2-} 1.5 mM, HPO_4^{2-} 1.5 mM, NH_4^+ 1.5 mM, K^+ 5.5 mM, Ca^{2+} 4.0 mM, Mg^{2+} 1.5 mM, Cl^- 0.2 mM, Fe^{3+}/Fe^{2+} 30 μM, Mn^{2+} 5 μM, Zn^{2+} 5 μM, $H_2BO_3^-$ 35 μM, Cu^+/Cu^{2+} 1 μM, MoO_4^{2-} 1 μM with pH 5.7 and EC 1.7 dS m^{-1} before transplant and with an EC of 2.3 dS m^{-1} after transplant.

Experimental Set-up

Five different experiments were performed (summarized in **Table 1**). In Experiment 1 the response of cultivars Emily and Dolly to different light intensities applied as EOP treatments during 5 days before harvest was investigated. Seeds of both cultivars germinated for 15 days under 150 μmol m^{-2} s^{-1}. After transplant, the light intensity was kept at 150 μmol m^{-2} s^{-1} for another 15 days. During the whole growth period a light spectrum with red-white LED was used and a day length of 18 h. EOP treatments were given for 5 days and included light intensities of 50, 150, 300, and 600 μmol m^{-2} s^{-1}, respectively.

In Experiment 2 the response of cultivar Dolly to different fractions of blue light applied either throughout the growth (25 days) or as EOP treatment during 5 days before harvest were investigated. The different fractions of blue light were created by using different ratios between pure blue (GreenPower LED production module, 120 cm, Blue, Phillips Eindhoven, Netherlands) and red white LEDs. Seeds germinated for 15 days under 150 μmol m^{-2} s^{-1} red white LED light. After transplant the plants were exposed for 25 days to four different blue light (400–500 nm) treatments of 9, 33, 65, and 100% out of the total PPFD of 300 μmol m^{-2} s^{-1}. In three other treatments the plants were grown under red white light of 300 μmol m^{-2} s^{-1} for 20 days after which they were exposed for 5 days to different blue light treatments of 33, 65, and 100%. Day length was 16 h.

In Experiment 3 the response of cultivars Rosie and Dolly to EOP treatments with increased fractions of blue light and the interaction with PPFD during 5 days before harvest were investigated. Seeds of both cultivars germinated under 200 μmol m^{-2} s^{-1} red white LED light for 15 days. After transplant the plants were grown for another 15 days under red white light of 200 μmol m^{-2} s^{-1}. Five days before harvest plants were exposed to treatments of 100 μmol m^{-2} s^{-1} PPFD with 9% blue, 100 μmol m^{-2} s^{-1} PPFD with 90% blue, 300 μmol m^{-2} s^{-1} PPFD with 9% blue and 300 μmol m^{-2} s^{-1} PPFD with 90% blue. The different fractions blue light were created by using different ratios between pure blue (GreenPower LED production module, 120 cm, Blue, Phillips Eindhoven, Netherlands) and red white LEDs. Day length was 18 h.

In Experiment 4 the response of cultivar Emily to EOP treatments with increasing intensities of far-red in addition to the PPFD during 5 days before harvest were investigated. Seeds germinated under 150 μmol m^{-2} s^{-1} red white LED light for 15 days. After transplant the PPFD was increased to 300 μmol m^{-2} s^{-1} of red white LED light for 15 days. EOP treatments were applied 5 days before harvest with 0, 50, or 100 μmol m^{-2} s^{-1} far-red (GreenPower Production module, 120 cm, Far Red, Phillips Eindhoven, Netherlands) added to the 300 μmol m^{-2} s^{-1} of red white LED light. This resulted in treatments with a total photon flux density (PFD) of 303, 350, 400 μmol m^{-2} s^{-1} (400–800 nm). Day length was 16 h.

In Experiment 5 the response of cultivar Emily to different durations of far-red before harvest were investigated. Seeds germinated under 150 μmol m^{-2} s^{-1} red white LED light for 10 days. After transplant the plants continued to grow under 150 μmol m^{-2} s^{-1} red white light for another 21 days. No far-red was applied or additional far-red (GreenPower Production module, 120 cm, Far Red, Phillips Eindhoven, Netherlands) (180 μmol m^{-2} s^{-1}) was applied during 1 week (as EOP treatment) or 3 weeks (throughout the growth). This resulted in treatments with a total PFD of 152, 330, 330 μmol m^{-2} s^{-1} (400–800 nm). Day length was 18 h.

Measurements of Growth and Morphological Parameters

Plant height was measured from the surface of the stone wool block to the height of the apex. Leaves of a minimum size of 1 cm^2 were counted as true leaves, leaf area was measured with a leaf area meter LI-3100C (LICOR, Lincoln, NE, United States). Leaves and stem were separated and weighed for fresh mass and dry mass. Dry mass was measured after drying for 48 h at 80°C.

Daily light integral ($mol_{400-700\,nm}$ m^{-2} d^{-1}) was calculated as:

$$\text{PPFD}\left(\mu\text{mol}\,\text{m}^{-2}\,\text{s}^{-1}\right) \times \text{day length}\ \left(\text{h}\right)\ \times\ 0.0036 \quad (1)$$

Daily radiation integral ($mol_{400-800\,nm}$ m^{-2} d^{-1}) was calculated as:

$$\text{PFD}\left(\mu\text{mol}\,\text{m}^{-2}\,\text{s}^{-1}\right) \times \text{day length}\ \left(\text{h}\right) \times 0.0036 \quad (2)$$

TABLE 1 | Overview of the experiments carried out.

Experiment	Cultivar	PFD (μmol m^{-2} s^{-1})			Spectra during treatments (%)				Treatment duration (d)	Day length (hours)	DLI Initial phase (mol m^{-2} d^{-1})	DLI Treatment (mol m^{-2} d^{-1})	DRI Treatment (mol m^{-2} d^{-1})	PSS treatment
		Initial phase	Treatment		Blue	Green	Red	Far-red						
		PPFD	PPFD	Far-red										
Experiment 1 PPFD	Dolly and Emily	150	50	0	9	19	70	1	5	18	9.7	3.2	3.2	
			150	2								9.7	9.9	0.88
			300	3								19.4	19.6	
			600	6								38.9	39.3	
Experiment 2 Blue light fraction	Dolly	300	300	3	9	19	70	1	5 and 25	16	17.3	17.3	17.5	0.88
				2	33	14	51	1					17.4	0.86
				1	65	7	26	0					17.3	0.82
				0	100	0	0	0					17.3	0.49
Experiment 3 Blue light interaction PPFD	Rosie and Dolly	200	100	1	9	19	70	1	5	18	13	6.5	6.5	0.88
			100	0	90	2	8	0				6.5	6.5	0.7
			300	3	9	19	70	1				19.4	19.6	0.88
			300	0	90	2	8	0				19.4	19.4	0.7
Experiment 4 Far-red PFD	Emily	300	300	3	9	19	70	1	5	16	17.3	17.3	17.5	0.88
			300	50	9	17	60	14					20.2	0.82
			300	100	8	15	53	25					23	0.78
Experiment 5 Far-red duration	Emily	150	150	2	9	19	70	1	21	18	9.7	9.7	9.7	0.88
			150	180	5	9	32	55	7				21.4	0.62
			150	180					21				21.4	0.62

PPFD (400–700 nm) and PFD of far-red (700–800 nm) during the initial phase (i.e., from transplant until start of treatments) and treatments, and spectral composition during the treatments. Fractions of the spectra; blue (400–500 nm), green (500–600 nm), red (600–700 nm), and far-red (700–800 nm) are percentages of the total Photon flux density (PFD) (400–800 nm), treatment duration, the daily light integral (DLI) from 400–700 nm for the initial phase, DLI and daily radiation integral (400–800 nm) and treatments are given. Phytochrome photostationary state (PSS) were calculated according to Sager et al. (1988).

Light use efficiency (g $mol_{400-700\ nm}^{-1}$) was calculated as:

$$\frac{\text{plant mass (g)} \times \text{plant density (plants m}^{-2})}{\text{Daily Light Integral}_{(400-700\,\text{nm})}\ (\text{mol m}^{-2}\,\text{d}^{-1})} \times \text{days of cultivation (d)} \quad (3)$$

Radiation use efficiency (g $mol_{400-800\ nm}^{-1}$) was calculated as:

$$\frac{\text{plant mass (g)} \times \text{plant density (plants m}^{-2})}{\text{Daily Radiation Integral}_{(400-800\,\text{nm})}\ (\text{mol m}^{-2}\,\text{d}^{-1})} \times \text{days of cultivation (d)} \quad (4)$$

Specific leaf area (SLA) ($cm^2\ g^{-1}$) was calculated as:

$$\frac{\text{Leaf area (cm}^2)}{\text{leaf dry mass (g)}} \quad (5)$$

Dry matter content (%) was calculated as:

$$\frac{\text{dry mass (g)}}{\text{fresh mass (g)}} \times 100\% \quad (6)$$

Statistical Set-up and Analysis

The experiments were carried out as complete randomized block designs. Each experiment was repeated in time, which represented the blocks. In each experiment six small compartments were used for plant growth. Each light treatment was done in one compartment and repeated in time. For each repetition the position of the light treatments in the six compartments were randomized. Generally 5 or 6 representative plants from the light compartment were sampled for the analyses. For statistical analyses, the average values of each block were used as one replicate. Experiment 1 and 3 (cv. Dolly) were carried out three times, experiment 3 (cv. Rosie) 4 times and experiment 2, 4, and 5 and two times.

Data was analyzed with Genstat (VSN International, 19th Edition). Experiments on light intensity, blue light and far-red were analyzed with One-way Analysis of Variance (ANOVA), while the blue and blue light × light intensity experiment were analyzed with a two-way ANOVA, followed by *post hoc* LSD test. Treatment effects were tested at a probability level of 5%, unless an experiment had only two blocks in which case probability level of 10% was applied (Ott and Longnecker, 2010). Furthermore, it was tested with the ANOVA if a polynomial model could explain the effect of the light treatment on the tested variates. Significance of the linear or quadratic component were used as proof of treatment having a significant effect (and additionally if this effect was linear or quadratic). Based on the result of the ANOVA a linear or quadratic trendline was added in Excel (Excel, Microsoft Pro Plus 2019). When no interaction was found in the two-way ANOVAs the overall means were shown. Assumptions of homogeneity and normality were met as tested with Bartlett's and Shapiro–Wilk test, respectively.

RESULTS

Response to End-Of-Production PPFD (Experiment 1)

The PPFD during the last 5 days had a significant effect on all growth parameters in cultivars Emily and Dolly. Plant height, plant fresh mass, leaf area and partitioning of dry mass to the leaves all increased with an increase in PPFD (**Figure 1**). The response to PPFD was linear or quadratic depending on the different parameters and cultivars. Plant fresh mass displayed a significant linear response to light intensity for cv. Emily while it was a quadratic response for cv. Dolly, indicating that within this range an optimum PPFD exists for cv. Dolly (**Figure 1B**). A similar trend was found for plant height between the two cultivars (**Figure 1A**), whereas both cultivars had a quadratic response to light for leaf area (**Figure 1C**). Plant dry matter content and partitioning to the leaves increased linearly with increase in PPFD for both cultivars (**Figures 1E,F**). SLA decreased due to a strong increase in dry mass of the leaves for both cultivars (**Figure 1D**). Plants from both cultivars grown under 600 $\mu mol\ m^{-2}\ s^{-1}$ displayed very brittle leaves that easily broke at the petiole and broke easily when handled. For both cultivars light use efficiency (LUE) based on dry mass increased with increasing PPFD, but decreased when based on fresh mass (**Table 2**).

Response to Increasing Fraction Blue Light in the Light Spectrum (Experiment 2)

The response to varying fractions of blue light was studied in a 5 day EOP treatment and as a throughout the growth treatment (25 days) in cv. Dolly. Plants showed a fairly similar response to the fraction of blue light, both to the EOP and throughout the growth treatments. The largest difference was found between the 100% blue treatment and the other treatments which also included red and green light. Plant height increased quadratically while the fraction of dry mass partitioned into the leaves decreased quadratically with increasing blue light (**Figure 2**); in fact it only showed a strong response when the fraction of blue was raised to 100%. The leaf area (**Figure 2C**), leaf fresh and leaf dry mass (**Supplementary Figures 2A,C**) decreased linearly with increasing fraction of blue light. There was no appreciable effect on the dry matter content of the leaves. LUE based on both dry and fresh mass did not significantly change with neither fraction of blue light or number of treatment days (**Table 2**).The only difference found between 5 and 25 days of application of blue light was on leaf area with increases in SLA when grown under 25 days of increased fraction of blue light.

Interaction Between Fraction of Blue Light and PPFD (Experiment 3)

Photosynthetic photon flux density could play an important role in the response to blue light. Therefore the interaction of PPFD and fraction of blue light was studied in a purple (Rosie) and a green cultivar (Dolly) (**Figures 3**, **4**). The green leaved

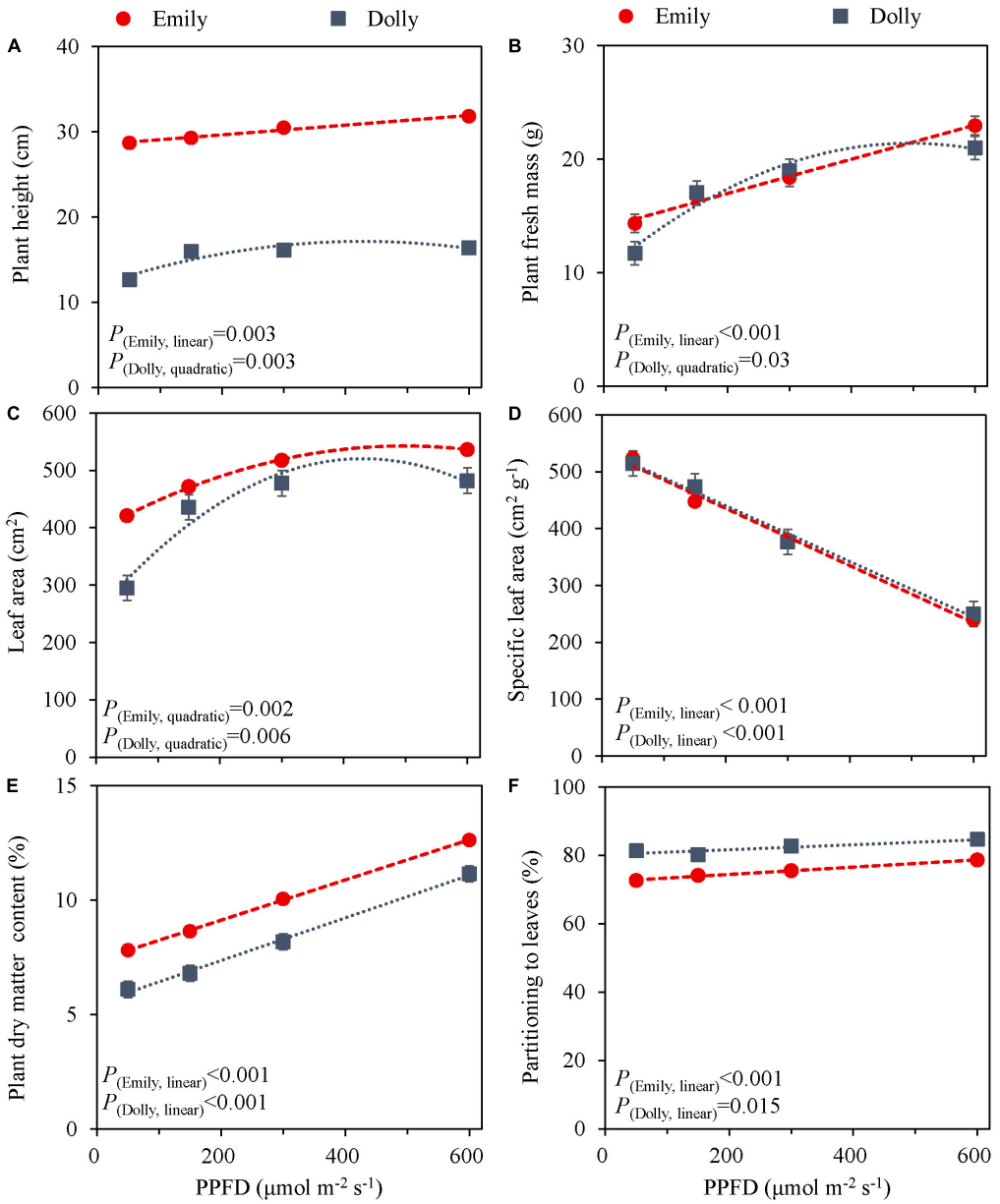

FIGURE 1 | Response of basil cvs. Emily (red circles) and Dolly (gray squares) to different End-Of-Production PPFD (Experiment 1). Plants were grown for 30 days under 150 µmol m^{-2} s^{-1} after which they were exposed to different PPFD (i.e., 50, 150, 300, and 600 µmol m^{-2} s^{-1}) during 5 days before harvest. **(A)** Plant height, **(B)** plant fresh mass, **(C)** leaf area, **(D)** specific leaf area, **(E)** plant dry matter content, **(F)** dry mass partitioning to leaves. Data are means of three blocks (n = 3) each with six replicate plants. Error bars represent standard errors of means, when larger than symbols. For significant quadratic or linear effects of PPFD, trendlines together with the respective p-values (α = 0.05) are depicted.

cultivar (Dolly) showed only a limited response to blue light in Experiment 2, therefore we here extended the experiment with a cultivar with purple leaves. In this way we could test if the response to the light depended on the color (i.e., content of anthocyanins) of the leaves. Plant height (**Figures 3A**, **4A**) was higher at high PPFD compared to low PPFD (100 vs. 300 µmol m^{-2} s^{-1}) and height was higher at 90% compared to 9% blue light for both cultivars. These results were similar as in the experiments where either the PPFD or the fraction blue were studied separately (**Figures 1**, **2**). For cv. Dolly the response of plant height to blue light was greater at a lower PPFD (about 20% increase) than at higher PPFD (10%) whereas for the purple cultivar Rosie no interaction between blue light and PPFD was found. The increase in plant height corresponded to an increase in fresh mass of stems (**Supplementary Figures 3B**, 4B) and a lower dry mass partitioning to the leaves with higher light intensity and fraction of blue (**Figures 3F**, **4F**). Moreover, cv. Rosie responded mainly to the increase in PPFD while cv.

TABLE 2 | Overview of light use efficiency (LUE) for plant fresh and dry mass in response to PPFD and fraction blue (Experiment 1–3).

Experiment	Cultivar	Treatment		LUE (g mol^{-1})	
				Plant fresh mass	Plant dry mass
Experiment 1 PPFD		**PPFD (μmol m^{-2} s^{-1})**			
	Emily	50		10.92 ± 0.39c	0.84 ± 0.03a
		150		10.63 ± 0.39bc	0.91 ± 0.03a
		300		9.33 ± 0.39ab	0.92 ± 0.03a
		600		8.31 ± 0.39a	1.04 ± 0.03b
	Dolly	50		8.92 ± 0.26b	0.55 ± 0.03a
		150		10.82 ± 0.26c	0.74 ± 0.03b
		300		9.62 ± 0.26b	0.79 ± 0.03bc
		600		7.60 ± 0.26a	0.83 ± 0.03c
Experiment 2 Blue light fraction		**days**	**Blue light (%)**		
	Dolly	5	9	9.01 ± 0.65	0.71 ± 0.06
			33	8.40 ± 0.65	0.65 ± 0.06
			65	7.52 ± 0.65	0.61 ± 0.06
			100	7.73 ± 0.65	0.56 ± 0.06
		25	9	9.01 ± 0.65	0.71 ± 0.06
			33	9.27 ± 0.65	0.69 ± 0.06
			65	9.40 ± 0.65	0.70 ± 0.06
			100	8.12 ± 0.65	0.62 ± 0.06
Experiment 3 Blue light interaction PPFD		**PPFD (μmol m^{-2} s^{-1})**	**Blue light (%)**		
	Rosie	100	9	5.12 ± 0.40	0.35 ± 0.04
		100	90	6.01 ± 0.40	0.42 ± 0.04
		300	9	5.09 ± 0.40	0.37 ± 0.04
		300	90	5.75 ± 0.40	0.41 ± 0.04
	Dolly	100	9	10.8 ± 0.27	0.66 ± 0.02a
		100	90	11.31 ± 0.27	0.68 ± 0.02a
		300	9	11.03 ± 0.27	0.78 ± 0.02b
		300	90	11.00 ± 0.27	0.73 ± 0.02b

LUE is based on PPFD incident on the plants accumulated over the initial (i.e., from transplant until start of treatments) and treatment phase. Letters indicate significant differences.

Dolly had an increase in plant dry matter content and dry mass of leaves with an increase in both fraction of blue and PPFD. The LUE based on plant dry mass increased for cv. Dolly when PPFD was increased from 100 to 300 μmol m^{-2} s^{-1}whereas no change in LUE was found for cv. Rosie (**Table 2**).

Response to Increasing Far-Red Intensities and Duration (Experiment 4 and 5)

In an experiment with cv. Emily, 5 days EOP treatments were applied adding 0, 50, or 100 μmol m^{-2} s^{-1} far-red to the PPFD of 300 μmol m^{-2} s^{-1} red-white light (**Figure 5**). In another experiment different durations of (180 μmol m^{-2} s^{-1}) far-red were applied for 0, 1, and 3 weeks (**Figure 6**) on top of 150 μmol m^{-2} s^{-1} red-white light. Plant height increased by 15% with the addition of 100 μmol m^{-2} s^{-1} of far-red and 7 and 36% with the one and 3 weeks duration of far-red, respectively. The increase in plant height was significant as the linear component of the statistical analysis was significant. Other responses to duration and intensity of far-red in terms of fresh, dry mass, dry matter content and SLA differed greatly. Increased intensity of EOP far-red on top of 300 μmol m^{-2} s^{-1} red-white light resulted in a significant decrease in leaf area and s SLA while a small increase in plant dry matter content was observed. Plant fresh mass and partitioning to leaves did not respond to increased intensity of far-red when given on top of 300 μmol m^{-2} s^{-1} red-white light during 5 days. Interestingly plant dry matter content increased with the addition of 100 μmol m^{-2} s^{-1} far-red (**Figure 5E**) due to an increase in dry matter content of both leaves and stem (**Supplementary Figures 5E,F**). Neither LUE nor radiation use efficiency (RUE) based on fresh or dry mass were affected by EOP far-red treatments (**Table 3**).

Plants grown with 1 week of added far-red did not show an increase in plant fresh mass while plant fresh mass increased after 3 weeks (**Figure 6B**). A similar response was found for leaf area (**Figure 6C**), where a quadratic response to duration of far-red was found; after 1 week leaf area decreased while it increased after 3 weeks. SLA did not change when far-red was applied on top of 150 μmol m^{-2} s^{-1} red-white light (**Figure 6D**). The response of LUE based on fresh mass followed the pattern of leaf area (**Table 3**). No differences were found for LUE based on dry mass whereas RUE based on dry and fresh mass decreased when far-red was added (**Table 3**). The dry mass partitioning to the leaves had an overall linear decrease with duration of far-red (**Figure 6F**).

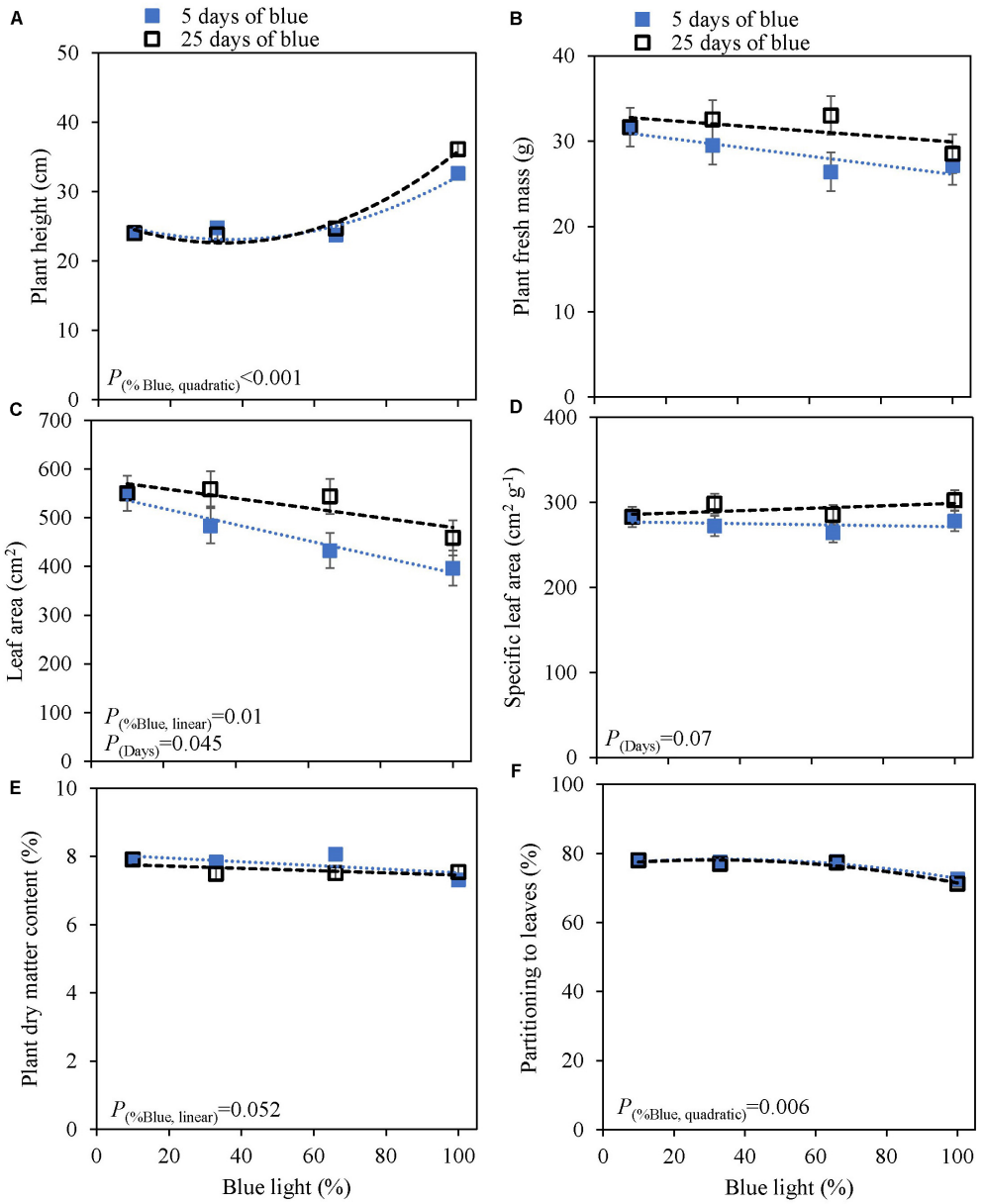

FIGURE 2 | Response of basil cv. Dolly to different blue fractions out of a total PPFD of 300 μmol m^{-2} s^{-1} either applied throughout the growth for 25 days (open squares) or as 5 days End-Of-Production treatments (closed squares) (Experiment 2). The data point 9% blue is shared between 5 and 25 days as 9% blue light also was the initial phase before EOP treatments. **(A)** Plant height, **(B)** plant fresh mass, **(C)** leaf area, **(D)** specific leaf area, **(E)** plant dry matter content, **(F)** dry mass partitioning to leaves. Data are means of two blocks (n = 2) each with six replicate plants. Error bars representing standard errors, when larger than symbol size. For significant quadratic or linear effects of increasing fraction of blue, trendlines together with the respective p-values (α = 0.10) are depicted.

DISCUSSION

Increased PPFD Applied as End-Of-Production Treatment Increases Plant Fresh Mass and Dry Matter Content

The effect of LED light on plant growth has previously been investigated in species such as lettuce (Li and Kubota, 2009), spinach, rocket, microgreens (Colonna et al., 2016), and basil (Carvalho et al., 2016; Jensen et al., 2018; Pennisi et al., 2019). However, the effects of both light spectra and PPFD have been found to be species dependent (Cope and Bugbee, 2013; Colonna et al., 2016), and in lettuce and tomato even cultivar dependent (Ouzounis et al., 2015, 2016; Gomez and Jimenez, 2020). This was also found in the present study where certain responses to PPFD and spectra were shown to be cultivar dependent. While we found that plant dry matter content in two sweet basil cvs., Emily

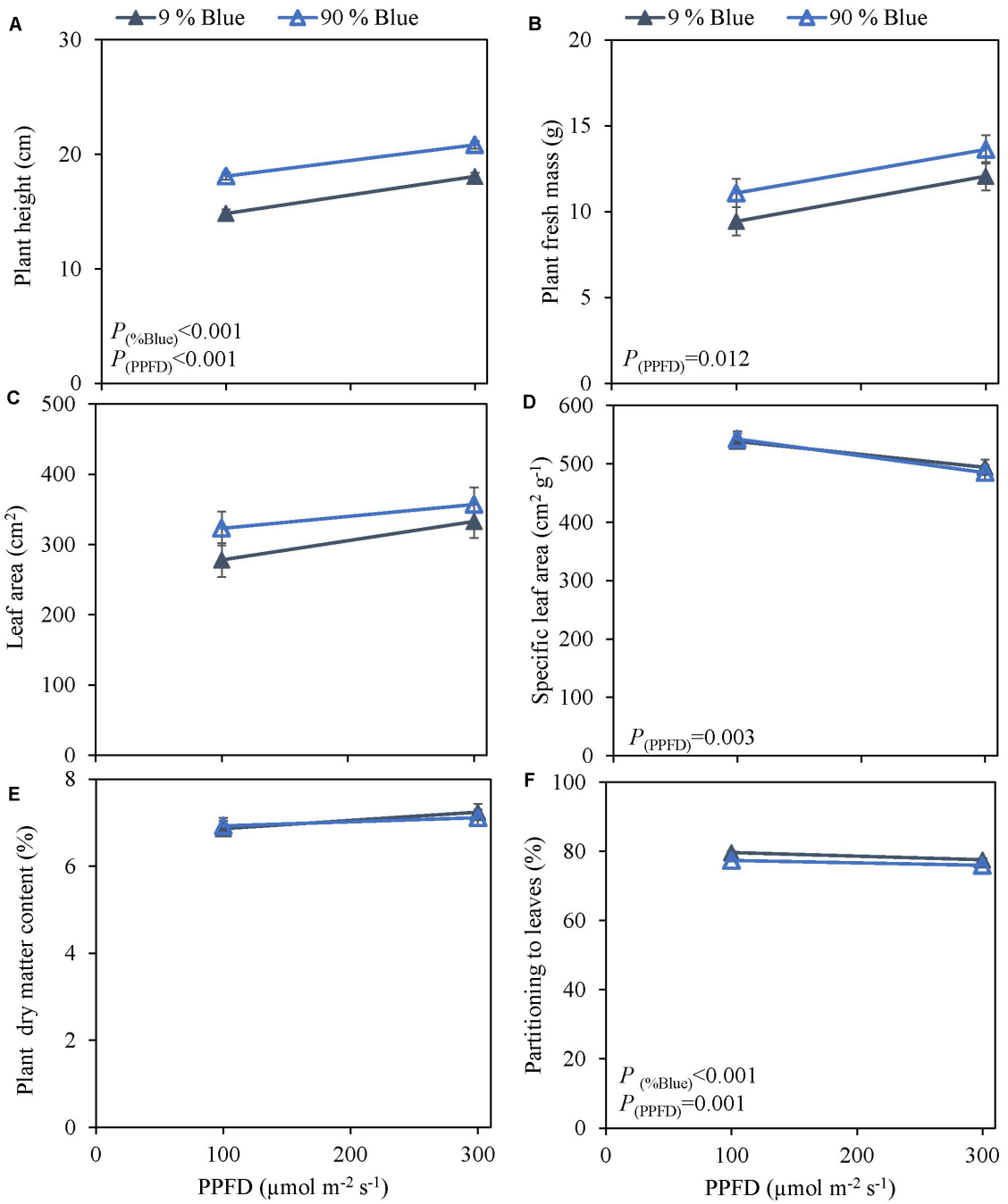

FIGURE 3 | Response of basil cv. Rosie to End-Of-Production blue light and PPFD. Plants were grown for 30 days under red white light (9% blue) and PPFD of 200 µmol m^{-2} s^{-1} (Experiment 3). EOP treatments were applied 5 days before harvest blue light and PPFD were changed to 100 µmol m^{-2} s^{-1} red white with 9% blue or 90% blue, and to 300 µmol m^{-2} s^{-1} red white with 9% blue or 90% blue. Closed triangle 9% blue and open triangle 90% blue. **(A)** Plant height, **(B)** plant fresh mass, **(C)** leaf area, **(D)** specific leaf area, **(E)** plant dry matter content, **(F)** dry mass partitioning to leaves. Data are means of four blocks (n = 4) each with six replicate plants. Error bars representing standard errors, when larger than symbol size. p-Values of main effects % Blue and PPFD (α = 0.05) are depicted.

and Dolly (**Figure 1**) increased linearly with PFFD, a saturation response was found for the fresh mass of leaves (**Supplementary Figure 1A**) in cv. Dolly whereas in cv. Emily a linear response to the increase in PPFD was observed. This is in line with results from Pennisi et al. (2020) where fresh and dry mass of both lettuce and basil saturated at a light intensity of 250 µmol m^{-2} s^{-1}. A light saturation response occurs when plant growth gets limited by other factors, e.g., CO_2, temperature or nutrients (Osmond, 1983). Under high light, photosynthesis becomes CO_2 limited and thus the growth is hampered (Long and Bernacchi, 2003).

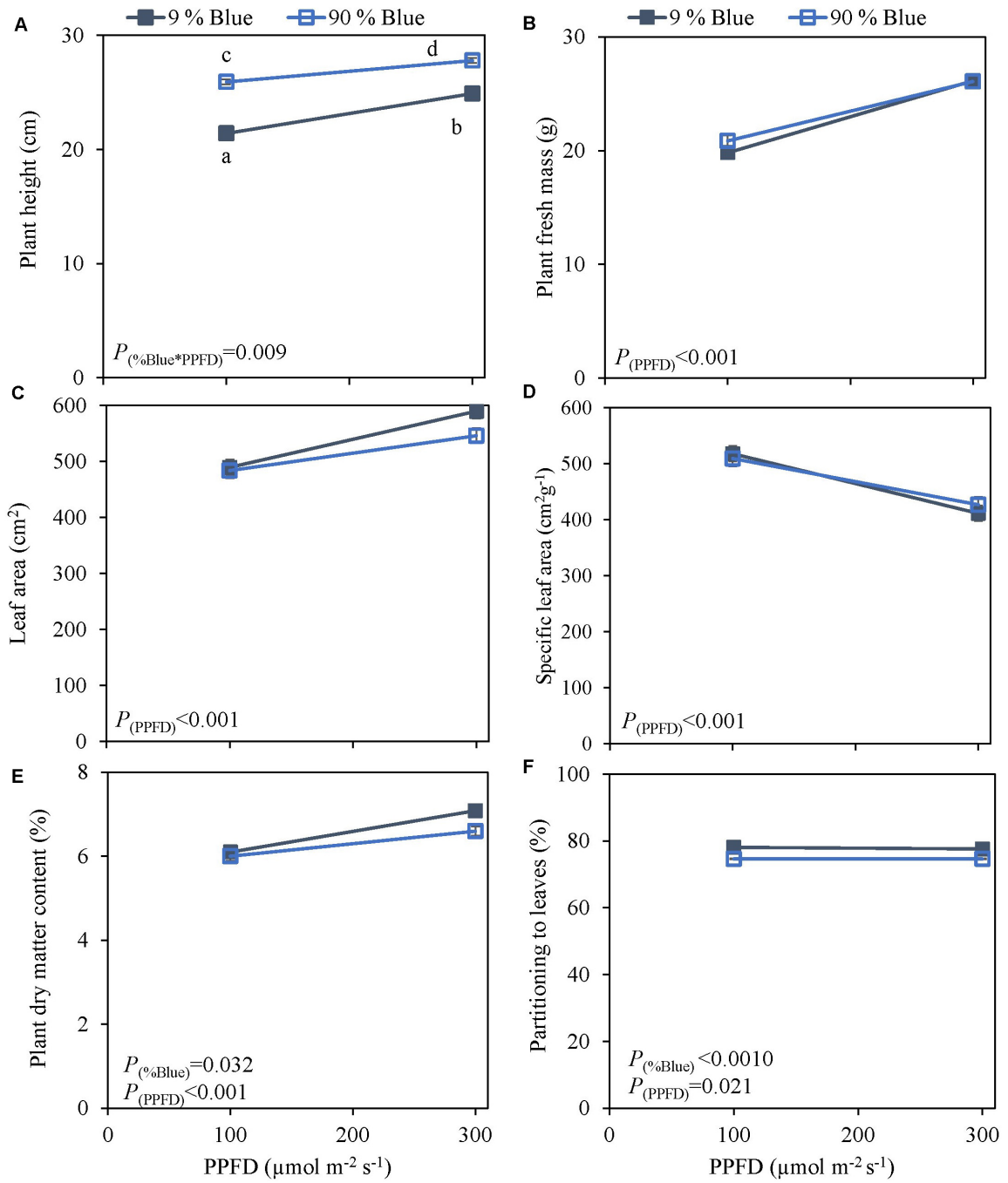

FIGURE 4 | Response of basil cv. Dolly to End-Of-Production blue light and PPFD. Plants were grown for 30 days under red white light (9% blue) and PPFD of 200 µmol m^{-2} s^{-1} (Experiment 3). EOP treatments were applied 5 days before harvest blue light and PPFD were changed to 100 µmol m^{-2} s^{-1} red white with 9% blue or 90% blue, and to 300 µmol m^{-2} s^{-1} red white with 9% blue or 90% blue. Closed squares 9% blue and open squares 90% blue. **(A)** Plant height, **(B)** plant fresh mass, **(C)** leaf area, **(D)** specific leaf area, **(E)** plant dry matter content, **(F)** dry mass partitioning to leaves. Data are means of four blocks (n = 3) each with six replicate plants. Error bars representing standard errors, when larger than symbol size. p-Values of main effects %Blue and PPFD (α = 0.05) are depicted.

However, the light intensity at which net photosynthesis gets light limited is species dependent and dependent on the growth environment. Basil, grown under increasing light intensities from 160–310 µmol m^{-2} s^{-1} showed a saturating net leaf photosynthesis at above 220 µmol m^{-2} s^{-1}, yet shoot fresh mass and dry matter content increased linearly with light intensity (Dou et al., 2018). A high dry matter content, as observed at higher PPFD, implicates higher levels of carbohydrates. In postharvest storage carbohydrates are used for respiration. Therefore, having a large reserve of carbohydrates are beneficial

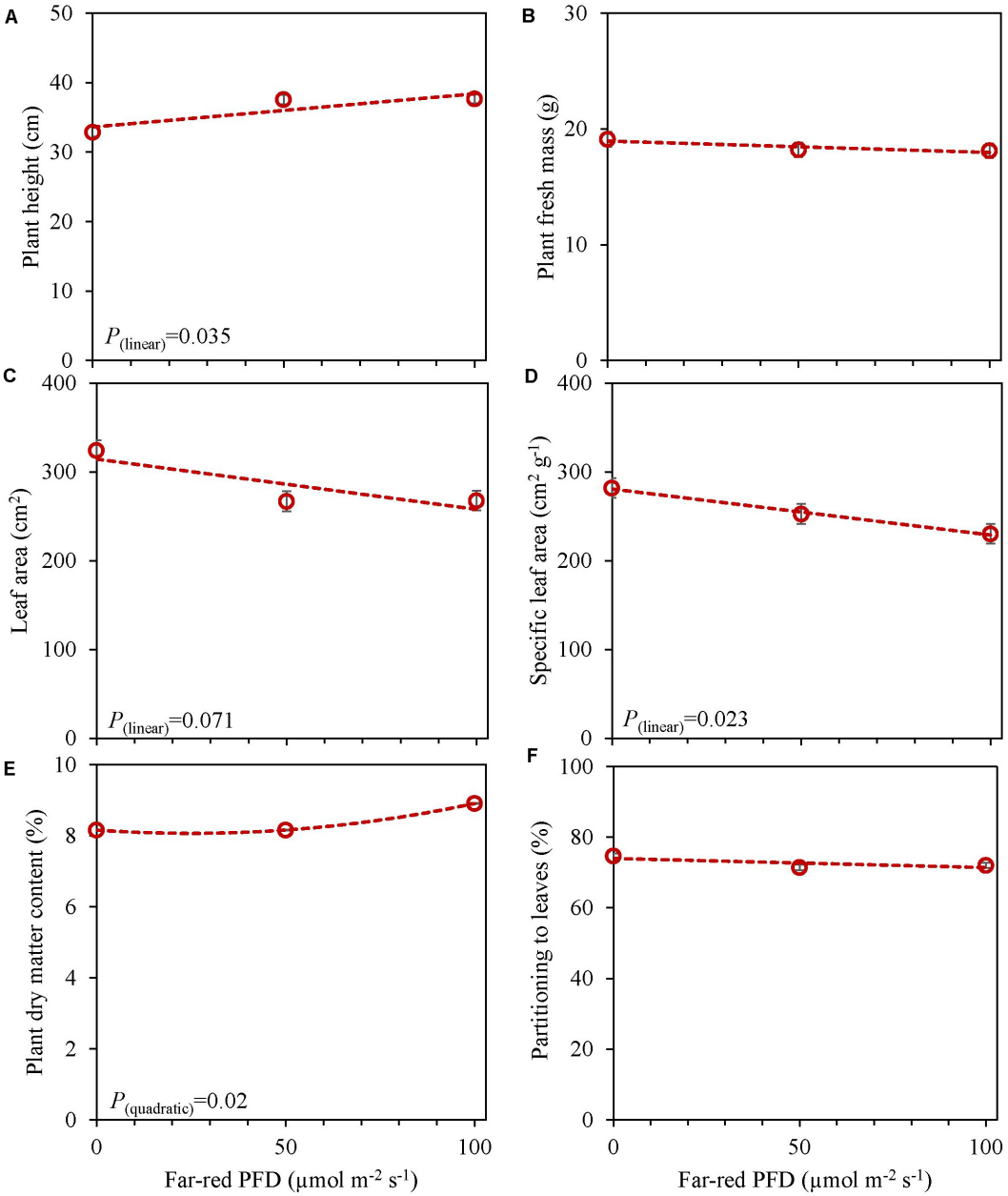

FIGURE 5 | Response of basil cv. Emily to End-Of-Production increased far-red PFD (Experiment 4). Plants were grown for 15 days under PPFD 150 µmol m^{-2} s^{-1}, after transplant for another 15 days of PPFD 300 µmol m^{-2} s^{-1} red white light and exposed to different far-red intensities (i.e., 0, 50, 100 µmol m^{-2} s^{-1}) in addition to 300 µmol m^{-2} s^{-1} red white light applied during 5 days before harvest. **(A)** Plant height, **(B)** plant fresh mass, **(C)** leaf area, **(D)** specific leaf area, **(E)** plant dry matter content, **(F)** dry mass partitioned to leaves. Data are means of two blocks (n = 2) each with five replicate plants. Error bars representing standard errors, when larger than symbol size. For significant quadratic or linear effects of increasing far-red intensity, trendlines together with the respective p-values (α = 0.10) are depicted.

for shelf-life and quality (Dorais et al., 2002; Caleb et al., 2016). This has also been shown in lettuce (Woltering and Witkowska, 2016) and broccoli (Finger et al., 1999). Consequently, basil with a higher dry matter content might have a better postharvest quality.

Optimal PPFD for basil growth (i.e., highest LUE for plant dry mass) has been suggested to be 250 µmol m^{-2} s^{-1} (DLI 14.4 mol m^{-2} d^{-1}) (Pennisi et al., 2020), 224 µmol m^{-2} s^{-1} (DLI 12.9 mol m^{-2} d^{-1}) (Dou et al., 2018) and 500 µmol m^{-2} s^{-1} (DLI 28.8 mol m^{-2} d^{-1}) (Beaman et al., 2009). In our study, the LUE based on dry mass was the highest at 600 µmol m^{-2} s^{-1} for both cv. Emily and cv. Dolly. For growers the LUE based on fresh mass is probably more interesting, however, at 600 µmol m^{-2} s^{-1} LUE based on fresh mass was the lowest for both cultivars (**Table 2**). Furthermore, at 600 µmol m^{-2} s^{-1} the leaves were

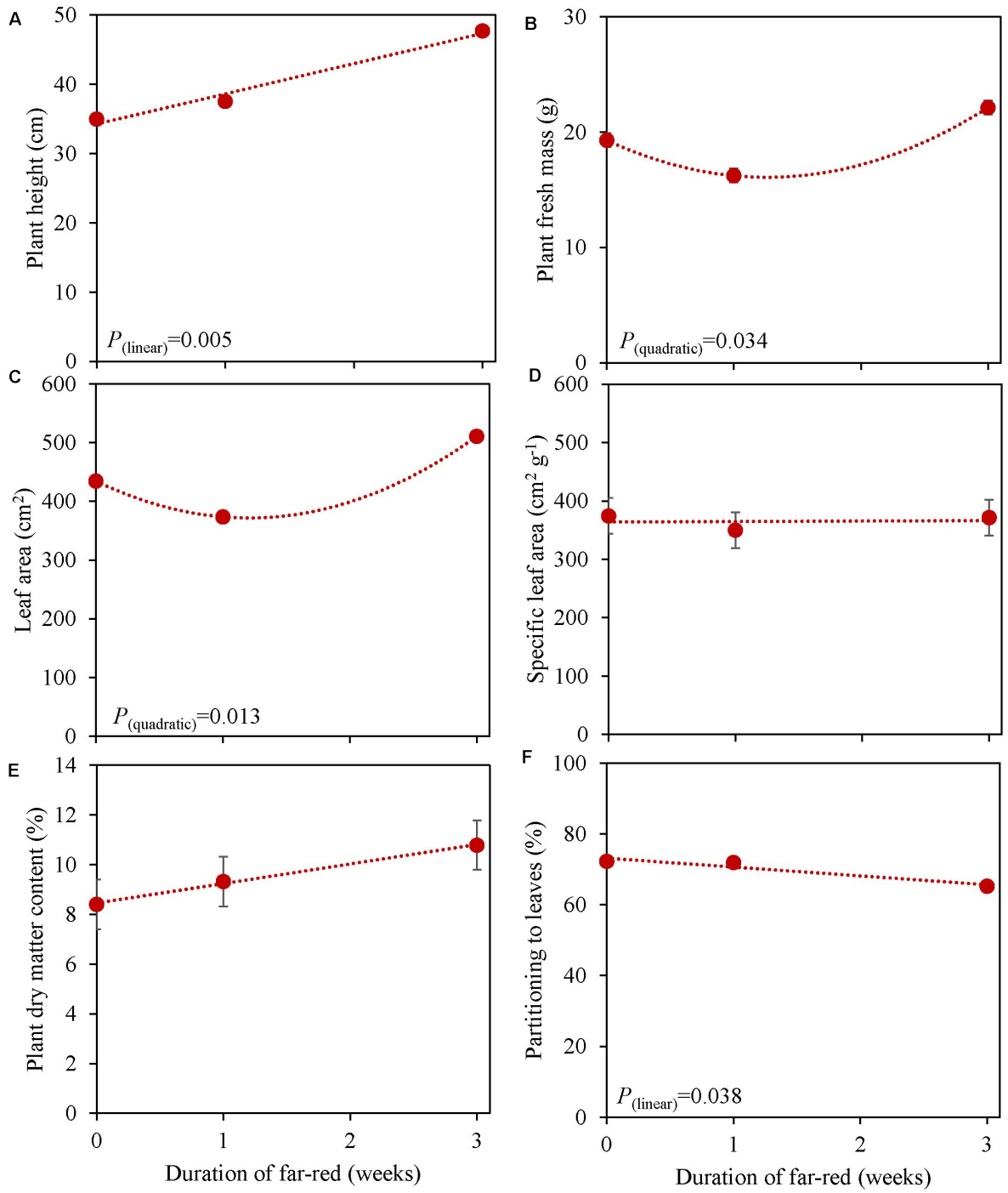

FIGURE 6 | Response of basil cv. Emily to different duration of far-red treatments either throughout the growth for 3 weeks or as 1 week End-Of-Production treatment (Experiment 5). Plants were grown for 31 days under 150 μmol m^{-2} s^{-1} red white light, and additional far-red light (180 μmol m^{-2} s^{-1}) was applied during 0, 1 and 3 weeks before harvest. **(A)** Plant height, **(B)** plant fresh mass, **(C)** leaf area, **(D)** specific leaf area, **(E)** plant dry matter content **(F)** dry mass partitioning to leaves. Data are means of two blocks (n = 2) each with five replicate plants. Error bars representing standard errors, when larger than symbol size. For significant quadratic or linear effects of duration of far-red, trendlines together with the respective p-values (α = 0.10) are depicted.

brittle and broke easily; this high light level can therefore not be considered optimal. The combination of initially raising the plants at a PPFD of 150 μmol m^{-2} s^{-1} and an EOP of 300 μmol m^{-2} s^{-1} resulted in an increase in dry mass partitioning to the leaves for both cvs. Emily and Dolly. Whereas an initial PPFD >150 μmol m^{-2} s^{-1} for cv. Dolly resulted in a

TABLE 3 | Overview of light use efficiency (LUE) for plant fresh and dry mass in response to far-red (Experiment 4 and 5).

Experiment	Cultivar	Treatment	LUE (g mol^{-1})		RUE (g mol^{-1})	
			Plant fresh mass	Plant dry mass	Plant fresh mass	Plant dry mass
Experiment 4 Far-red PFD		**PFD of far-red (μmol m^{-2} s^{-1})**				
	Emily	3	6.79 ± 0.23	0.55 ± 0.02	6.66 ± 0.21	0.54 ± 0.02
		50	6.47 ± 0.23	0.53 ± 0.02	6.22 ± 0.21	0.51 ± 0.02
		100	6.44 ± 0.23	0.57 ± 0.02	6.07 ± 0.21	0.54 ± 0.02
Experiment 5 Far-red duration		**Duration of far-red (d)**				
	Emily	0	11.63 ± 0.37b	0.98 ± 0.10	11.63 ± 0.17c	0.98 ± 0.06b
		7	9.78 ± 0.37a	0.90 ± 0.10	6.99 ± 0.17b	0.65 ± 0.06a
		21	13.33 ± 0.37c	1.36 ± 0.10	6.06 ± 0.17a	0.62 ± 0.06a

LUE is based on PPFD incident on the plants accumulated over the initial (i.e., from transplant until start of treatments) and treatment phase, and the radiation use efficiency (RUE), which is based on PFD incident on the plants. Letters indicate significant differences.

slightly higher dry mass partitioning to the stem. Therefore, we overall consider the combination of initially raising the plants at a PPFD of 150 μmol m^{-2} s^{-1} and an EOP of 300 μmol m^{-2} s^{-1} (DLI 19.4 mol m^{-2} d^{-1}) the optimal growth conditions. This consideration, is based on both LUE parameters and growth and morphological parameters (e.g., dry matter content and leaf area).

Plant Biomass Does Not Respond to the Fraction of Blue Light in the Spectrum

Blue light and red:blue ratio have been intensely studied. Red light is the most efficient color driving photosynthesis but adding blue to a red background improves the overall photosynthesis (Hogewoning et al., 2010). Yet, the optimal fraction of blue light to a growth light spectrum has had varying conclusions. A blue light optimum was found of 12% blue, in tomato, with respect to leaf dry mass (Kaiser et al., 2019). In basil, Pennisi et al. (2019) found that an increase in blue light up to 58% blue reduced plant fresh mass. However, opposite results were found where an increase in blue fraction up to 37% increased plant fresh mass Piovene et al. (2015) and Jensen et al. (2018) found that a fraction of blue of 60% increased the leaf dry matter content. In our experiments, the fraction of blue mostly affected plant height in cv. Dolly as well as in the purple cv. Rosie. In line with this finding, stem fresh mass and dry mass increased at higher fraction of blue. This may have happened at the expense of leaf fresh mass and dry mass (**Supplementary Figure 2**). There were no significant effects of fraction of blue light (range 9–100%) on overall plant fresh mass (**Figures 2B**, **3B**, **4B**) nor on plant dry mass (**Supplementary Figures 2–4**) or plant dry matter content (**Figures 2E**, **3E**). Previous findings by Snowden et al. (2016) indicated that an interaction between light intensity and fraction of blue light existed. In the current experiment we found a limited interaction of blue light and light intensity, i.e., only on the dry mass of the leaves (**Supplementary Figure 4C**) in the green cv. Dolly. For Experiment 3 the purple cv. Rosie was chosen a long with the green cv. Dolly and as in line with results from Dou et al. (2019) the purple cultivar had a lower plant fresh and dry mass of leaves than the green cultivar (**Figures 3B**, **4B** and **Supplementary Figures 3C**, **4C**). However, Dou et al. (2019) found a negative effect of blue light in the purple cultivar and not in green basil whereas blue light did not affect biomass in cv. Rosie in Experiment 3.

Based on our findings a spectrum with 9% blue while the remaining part of the spectrum being 70% red and 19% green can be maintained throughout the growth of basil as an increased amount of blue did not improve the plant fresh mass nor the dry matter content. Furthermore, no differences were found between the EOP and throughout the growth blue light treatment.

A High Fraction of Blue Light Induces SAS Like Responses

Amongst morphological parameters plant height is one that has been recorded in numerous studies. Blue light usually suppresses elongation (Laskowski and Briggs, 1989) but in a number of cases a promotion of stem elongation has been observed (Johnson et al., 2020) depending on the species and fraction of blue in the spectra (90–100%) (Kong et al., 2018). Blue light is sensed by photoreceptors such as cryptochromes, phototropins, and Zeitlupes (Huché-Thélier et al., 2016). However, phytochromes also absorb blue and consequently blue light can affect the PSS value which indicates the active phytochromes out of the total phytochromes (Sager et al., 1988; Casal, 2013; Meng et al., 2019). A low PSS value results in shade avoidance syndrome (SAS). Hundred percent blue light has been found to increase stem elongation due to low phytochrome activity (PSS 0.49) (Kong et al., 2018; Johnson et al., 2020). In accordance with Kong et al. (2018), we also observed increased stem elongation under both 90 and 100% blue light (**Figures 2A**, **3A**, **4A**). This was likely because of the reduced PSS values of 0.7 at 90% blue and 0.49 at 100% blue. Furthermore, the response to blue light on plant height was more pronounced under a low light intensity compared to the high light intensity in cv. Dolly. This finding was also reported by Johnson et al. (2020) although the response was found to be species dependent. In addition, SAS can lead to an increase in leaf area (Demotes-Mainard et al., 2016) but the response is not universal but rather species dependent. Although, 100 and 90% blue induced stem elongation, we found 100% blue to reduce leaf area while 90% blue had no effect. In addition, leaf area decreased overall with increasing fraction of blue light (**Figure 2C**) which is in accordance with Kaiser et al. (2019).

Far-Red Increases Plant Height While Effects on Biomass Depend on Duration of Far-Red Application

Shade avoidance syndrome like responses were also found when we grew plants under additional far-red light (**Figures 5A**, **6A**) where plant height increased with far-red intensity and duration. However, leaf area, similar as in the experiments with blue light EOP, decreased when far-red was applied EOP for 5 days or 1 week (**Figures 5C**, **6C**). Increased leaf area in response to far-red has been found to be more pronounced in the early growth stage (Kalaitzoglou et al., 2019) which is in agreement with the increase in leaf area when far-red was added throughout the growth period (**Figure 6C**). SLA decreased with increasing far-red PFD during the 5-days EOP treatment due the decrease in leaf area and no difference in the dry mass of leaves (**Supplementary Figure 5C**). SLA which is an indicator of the leaf thickness and would be expected to increase with increasing far-red and decreasing PSS values as found in other species (Ji et al., 2019; Zou et al., 2019). Interestingly, cv. Emily grown with a PSS of 0.62 did not have any change in SLA (**Figure 6D**). Therefore, we suggest that SAS response in basil is mostly linked to stem elongation. While plant dry matter content increased quadratically under 5 days of EOP far-red (**Figure 5E**) no increase was found in the longer duration far-red (**Figure 6E**). However, for the plant fresh mass the longer duration of far-red had a significant effect, mainly due to an increase in stem fresh mass (**Supplementary Figure 6B**) which also resulted in a lower dry mass partitioning to the leaves. This is in accordance with previous findings, where stem dry mass increased with far-red (Ji et al., 2019).

Recently, Zhen and Bugbee (2020) suggested far-red photons to be photosynthetically active. They found the magnitude of the increase in net photosynthesis to be species dependent where basil was one of the less responsive species. An increase in net photosynthesis is expected to be reflected in an increase in biomass. This was not the case in either of our experiments as cv. Emily did not increase in plant dry mass after 5 days (total PFD 350–400 μmol m^{-2} $s^{-1)}$ (**Supplementary Figure 5**) or after 1 week of added far-red (total PFD 330 μmol m^{-2} s^{-1}) (**Supplementary Figure 6**). However, when the PPFD increased from 150 to 300 μmol m^{-2} s^{-1} dry mass did increase (**Supplementary Figure 1**). The decrease in fresh mass after 1 week of added far-red and subsequent increase after 3 weeks could indicate an acclimation period (**Figure 6B**). This is supported by our results with increased far-red intensity where no increase in plant fresh mass was found (**Figure 5B**). Although, the radiation use efficiency for plant fresh mass increased by 3 weeks of added far-red (**Table 3**) it decreased based on dry mass with increasing duration of far-red in Experiment 5 while far-red did not affect radiation use efficiency in Experiment 4. Thus, additional far-red, in a small dosages added 5 days before harvest may be beneficial to improve leaf dry matter content whereas a higher dosage throughout the growth does not yield a desired plant morphology as the stem is not a used organ from basil plants.

CONCLUSION

We showed that growth (plant fresh mass, plant dry matter content, and dry mass partitioning to the leaves) and morphology (plant height and leaf area) were significantly affected by EOP increase in PPFD. Interestingly, LUE based on fresh mass decreased with increasing PPFD whereas LUE based on dry mass increased. The plant fresh mass did not respond to the fraction of blue light while plant dry matter content was reduced at the combination high fraction of blue and a high PPFD. When the spectrum consisted of either 90 or 100% blue, either applied as EOP treatments or throughout the growth shade avoidance syndrome was induced and plants grew taller resulting in more fresh and dry mass partitioned to the stem. Therefore, a high fraction of blue in the spectrum is not desirable for basil growth as the leaves are the consumed part.

Addition of far-red for basil during growth is most beneficial when added as EOP treatment before harvest and only in a lower dosage at a high PPFD as it increases dry matter content of both leaves and stem.

DATA AVAILABILITY STATEMENT

The raw data supporting the conclusions of this article will be made available by the authors, without undue reservation.

AUTHOR CONTRIBUTIONS

DL, EW, CN, and LM conceptualized the research plan. DL, EW, and LM designed the experiments. DL carried out the experiments, analyzed the data, and wrote the manuscript. EW and LM provided critical feedback on the manuscript. CN provided critical comments to the overall structure of the manuscript. All authors reviewed and approved the final manuscript.

FUNDING

This work was funded by Signify, Eindhoven, Netherlands.

ACKNOWLEDGMENTS

Technical staff in Klima Gerrit Stunnenberg, Taede Stoker and David Brink at Wageningen University and Research. Furthermore, Xinyuan Ma, Diederick van Kempen, Ruiyun Zhang, Sarah Carton, Jooseop Park, and Malleshaiah Sharath Kumar took part in the experimental work.

SUPPLEMENTARY MATERIAL

The Supplementary Material for this article can be found online at: https://www.frontiersin.org/articles/10.3389/fpls.2020.597906/full#supplementary-material

REFERENCES

Bantis, F., Ouzounis, T., and Radoglou, K. (2016). Artificial LED lighting enhances growth characteristics and total phenolic content of *Ocimum basilicum*, but variably affects transplant success. *Sci. Hortic.* 198, 277–283. doi: 10.1016/j.scienta.2015.11.014

Beaman, A. R., Gladon, R. J., and Schrader, J. A. (2009). Sweet basil requires an irradiance of 500 m mol Á m – 2 Á s – 1 for greatest edible biomass production. *HortScience* 44, 64–67.

Boccalandro, H. E., Giordano, C. V., Ploschuk, E. L., Piccoli, P. N., Bottini, R., and Casal, J. J. (2012). Phototropins but not cryptochromes mediate the blue light-specific promotion of stomatal conductance, while both enhance photosynthesis and transpiration under full sunlight. *Plant Physiol.* 158, 1475–1484. doi: 10.1104/pp.111.187237

Caleb, O. J., Herppich, W. B., and Mahajan, P. V. (2016). *The Basics of Respiration for Horticultural Products*. Amsterdam: Elsevier.

Carvalho, S. D., Schwieterman, M. L., Abrahan, C. E., Colquhoun, T. A., and Folta, K. M. (2016). Light quality dependent changes in morphology, antioxidant capacity, and volatile production in sweet basil (*Ocimum basilicum*). *Front. Plant Sci.* 7:1328. doi: 10.3389/fpls.2016.01328

Casal, J. J. (2013). Photoreceptor signaling networks in plant responses to shade. *Annu. Rev. Plant Biol.* 64, 403–427. doi: 10.1146/annurev-arplant-050312-120221

Colonna, E., Rouphael, Y., Barbieri, G., and De Pascale, S. (2016). Nutritional quality of ten leafy vegetables harvested at two light intensities. *Food Chem.* 199, 702–710. doi: 10.1016/j.foodchem.2015.12.068

Cope, K. R., and Bugbee, B. (2013). Spectral effects of three types of white light-emitting diodes on plant growth and development: absolute versus relative amounts of blue light. *HortScience* 48, 504–509.

Demotes-Mainard, S., Péron, T., Corot, A., Bertheloot, J., Le Gourrierec, J., Pelleschi-Travier, S., et al. (2016). Plant responses to red and far-red lights, applications in horticulture. *Environ. Exp. Bot.* 121, 4–21. doi: 10.1016/j.envexpbot.2015.05.010

Dorais, M., Papadopoulos, A. P., and Gosselin, A. (2002). "Greenhouse tomato fruit quality," in *Horticultural Reviews*, ed. J. Janick, (Hoboken, NJ: John Wiley & Sons).

Dou, H., Niu, G., and Gu, M. (2019). Photosynthesis, morphology, yield, and phytochemical accumulation in basil plants influenced by substituting green light for partial red and/or blue light. *HortScience* 54, 1769–1776. doi: 10.21273/HORTSCI14282-19

Dou, H., Niu, G., Gu, M., and Masabni, J. G. (2018). Responses of sweet basil to different daily light integrals in photosynthesis, morphology, yield, and nutritional quality. *HortScience* 53, 496–503. doi: 10.21273/HORTSCI12785-17

Finger, F. L., Endres, L., Mosquim, P. R., and Puiatti, M. (1999). Physiological changes during postharvest senescence of broccoli. *Pesqui. Agropecu. Bras.* 34, 1565–1569. doi: 10.1590/s0100-204x1999000900006

Gomez, C., and Jimenez, J. (2020). Effect of end-of-production high- energy radiation on nutritional quality of indoor-grown red-leaf lettuce. *HortScience* 55, 1055–1060. doi: 10.21273/HORTSCI15030-20

Heo, J., Lee, C., Chakrabarty, D., and Paek, K. (2002). Growth responses of marigold and salvia bedding plants as affected by monochromic or mixture radiation provided by a light-emitting diode (LED). *Plant Growth Regul.* 38, 225–230. doi: 10.1023/A:1021523832488

Hoenecke, M. E., Bula, R. J., and Tibbitts, T. W. (1992). Importance of "blue" photon levels for lettuce seedlings grown under red-light-emitting diodes. *HortScience* 27, 427–430.

Hogewoning, S. W., Trouwborst, G., Maljaars, H., Poorter, H., van Ieperen, W., and Harbinson, J. (2010). Blue light dose-responses of leaf photosynthesis, morphology, and chemical composition of Cucumis sativus grown under different combinations of red and blue light. *J. Exp. Bot.* 61, 3107–3117. doi: 10.1093/jxb/erq132

Huché-Thélier, L., Crespel, L., Gourrierec, J., Le Morel, P., Sakr, S., and Leduc, N. (2016). Light signaling and plant responses to blue and UV radiations-Perspectives for applications in horticulture. *Environ. Exp. Bot.* 121, 22–38. doi: 10.1016/j.envexpbot.2015.06.009

Islam, M. A., Kuwar, G., Clarke, J. L., Blystad, D. R., Gislerød, H. R., Olsen, J. E., et al. (2012). Artificial light from light emitting diodes (LEDs) with a high portion of blue light results in shorter poinsettias compared to high pressure sodium (HPS) lamps. *Sci. Hortic.* 147, 136–143. doi: 10.1016/j.scienta.2012.08.034

Jensen, N. B., Clausen, M. R., and Kjaer, K. H. (2018). Spectral quality of supplemental LED grow light permanently alters stomatal functioning and chilling tolerance in basil (*Ocimum basilicum* L.). *Sci. Hortic.* 227, 38–47. doi: 10.1016/j.scienta.2017.09.011

Ji, Y., Ouzounis, T., Courbier, S., Kaiser, E., Nguyen, P. T., Schouten, H. J., et al. (2019). Far-red radiation increases dry mass partitioning to fruits but reduces Botrytis cinerea resistance in tomato. *Environ. Exp. Bot.* 168:103889. doi: 10.1016/j.envexpbot.2019.103889

Johnson, R. E., Kong, Y., and Zheng, Y. (2020). Elongation growth mediated by blue light varies with light intensities and plant species: a comparison with red light in arugula and mustard seedlings. *Environ. Exp. Bot.* 169:103898. doi: 10.1016/j.envexpbot.2019.103898

Kaiser, E., Ouzounis, T., Giday, H., Schipper, R., Heuvelink, E., and Marcelis, L. F. M. (2019). Adding blue to red supplemental light increases biomass and yield of greenhouse-grown tomatoes, but only to an optimum. *Front. Plant Sci.* 9:2002. doi: 10.3389/fpls.2018.02002

Kalaitzoglou, P., van Ieperen, W., Harbinson, J., van der Meer, M., Martinakos, S., Weerheim, K., et al. (2019). Effects of continuous or end-of-day far-red light on tomato plant growth, morphology, light absorption, and fruit production. *Front. Plant Sci.* 10:322. doi: 10.3389/fpls.2019.00322

Kelly, N., Choe, D., Meng, Q., and Runkle, E. S. (2020). Promotion of lettuce growth under an increasing daily light integral depends on the combination of the photosynthetic photon flux density and photoperiod. *Sci. Hortic.* 272:109565. doi: 10.1016/j.scienta.2020.109565

Keuskamp, D. H., Keller, M. M., Ballaré, C. L., and Pierik, R. (2012). Blue light regulated shade avoidance. *Plant Signal. Behav.* 7, 514–517. doi: 10.4161/psb.19340

Kim, H. H., Wheeler, R. M., Sager, J. C., Goins, G. D., and Norikane, J. H. (2006). Evaluation of lettuce growth using supplemental green light with red and blue light-emitting diodes in a controlled environment - a review of research at kennedy space center. *Acta Hortic.* 711, 111–119.

Kong, Y., Stasiak, M., Dixon, M. A., and Zheng, Y. (2018). Blue light associated with low phytochrome activity can promote elongation growth as shade-avoidance response: a comparison with red light in four bedding plant species. *Environ. Exp. Bot.* 155, 345–359. doi: 10.1016/j.envexpbot.2018.07.021

Kusuma, P., Pattison, P. M., and Bugbee, B. (2020). From physics to fixtures to food: current and potential LED efficacy. *Hortic. Res.* 7:56. doi: 10.1038/s41438-020-0283-7

Laskowski, M. J., and Briggs, W. R. (1989). Regulation of pea epicotyl elongation by blue light: fluence-response relationships and growth distribution. *Plant Physiol.* 89, 293–298. doi: 10.1104/pp.89.1.293

Li, Q., and Kubota, C. (2009). Effects of supplemental light quality on growth and phytochemicals of baby leaf lettuce. *J. Environ. Exp. Bot.* 67, 59–64. doi: 10.1016/j.envexpbot.2009.06.011

Long, S. P., and Bernacchi, C. J. (2003). Gas exchange measurements, what can they tell us about the underlying limitations to photosynthesis? Procedures and sources of error. *J. Exp. Bot.* 54, 2393–2401. doi: 10.1093/jxb/erg262

Maness, N. (2003). "Soluble and storage carbohydrates," in *Postharvest Physiology and Pathology of Vegetables*, eds J. A. Bertz, and J. K. Brecht, (New York, NY: M. Dekker), 361–382.

Mattheis, J. P., and Fellman, J. K. (1999). Preharvest factors influencing flavor of fresh fruit and vegetables. *Postharvest Biol. Technol.* 15, 227–232. doi: 10.1016/S0925-5214(98)00087-8

McCree, K. J. (1972). The action spectrum, absorptance and quantum yield of photosynthesis in crop plants. *Agric. Meteorol.* 9, 191–216. doi: 10.1016/0002-1571(71)90022-7

Meng, Q., Kelly, N., and Runkle, E. S. (2019). Substituting green or far-red radiation for blue radiation induces shade avoidance and promotes growth in lettuce and kale. *Environ. Exp. Bot.* 162, 383–391. doi: 10.1016/j.envexpbot.2019.03.016

Osmond, C. B. (1983). Interactions between irradiance, nitrogen nutrition, and water stress in the sun-shade responses of Solanum dulcamara. *Oecologia* 57, 316–321. doi: 10.1007/BF00377174

Ott, L., and Longnecker, M. (2010). *An Introduction to Statistical Methods and Data Analysis*, 6th Editio Edn. Belmont, CA: Brooks/Cole.

Ouzounis, T., Heuvelink, E., Ji, Y., Schouten, H. J., Visser, R. G. F., and Marcelis, L. F. M. (2016). Blue and red LED lighting effects on plant biomass, stomatal

conductance, and metabolite content in nine tomato genotypes. *Acta Hortic.* 1134, 251–258. doi: 10.17660/ActaHortic.2016.1134.34

Ouzounis, T., Razi Parjikolaei, B., Fretté, X., Rosenqvist, E., and Ottosen, C.-O. (2015). Predawn and high intensity application of supplemental blue light decreases the quantum yield of PSII and enhances the amount of phenolic acids, flavonoids, and pigments in *Lactuca sativa*. *Front. Plant Sci.* 6:19. doi: 10.3389/fpls.2015.00019

Pennisi, G., Blasioli, S., Cellini, A., Maia, L., Crepaldi, A., Braschi, I., et al. (2019). Unraveling the role of red:blue LED lights on resource use efficiency and nutritional properties of indoor grown sweet basil. *Front. Plant Sci.* 10:305. doi: 10.3389/fpls.2019.00305

Pennisi, G., Pistillo, A., Orsini, F., Cellini, A., Spinelli, F., Nicola, S., et al. (2020). Optimal light intensity for sustainable water and energy use in indoor cultivation of lettuce and basil under red and blue LEDs. *Sci. Hortic.* 272:109508. doi: 10.1016/j.scienta.2020.109508

Piovene, C., Orsini, F., Bosi, S., Sanoubar, R., Bregola, V., Dinelli, G., et al. (2015). Optimal red: blue ratio in led lighting for nutraceutical indoor horticulture. *Sci. Hortic.* 193, 202–208. doi: 10.1016/j.scienta.2015.07.015

Poorter, H., Niinemets, Ü, Ntagkas, N., Siebenkäs, A., Mäenpää, M., Matsubara, S., et al. (2019). A meta-analysis of plant responses to light intensity for 70 traits ranging from molecules to whole plant performance. *New Phytol.* 223, 1073–1105. doi: 10.1111/nph.15754

Sager, J. C., Smith, W. O., Edwards, J. L., and Cyr, K. L. (1988). Photosynthetic efficiency and phytochrome photoequilibria determination using spectral data. *Trans. ASAE* 31, 1882–1889.

SharathKumar, M., Heuvelink, E., and Marcelis, L. F. M. (2020). Trends in plant science forum vertical farming?: moving from genetic to environmental modification trends in plant science. *Trends Plant Sci.* 25, 1–4. doi: 10.1016/j.tplants.2020.05.012

Snowden, M. C., Cope, K. R., and Bugbee, B. (2016). Sensitivity of seven diverse species to blue and green light: interactions with photon flux. *PLoS One* 11:e0163121. doi: 10.1371/journal.pone.0163121

Touliatos, D., Dodd, I. C., and Mcainsh, M. (2016). Vertical farming increases lettuce yield per unit area compared to conventional horizontal hydroponics. *Food Energy Secur.* 5, 184–191. doi: 10.1002/fes3.83

Woltering, E. J., and Witkowska, I. M. (2016). Effects of pre- and postharvest lighting on quality and shelf life of fresh-cut lettuce. *Acta Hortic.* 1134, 357–366. doi: 10.17660/ActaHortic.2016.1134.47

Zhen, S., and Bugbee, B. (2020). Far-red photons have equivalent efficiency to traditional photosynthetic photons: implications for redefining photosynthetically active radiation. *Plant Cell Environ.* 43, 1259–1272. doi: 10.1111/pce.13730

Zhou, W. L., Liu, W. K., and Yang, Q. C. (2012). Quality changes in hydroponic lettuce grown under pre-harvest short-duration continuous light of different intensities. *J. Hortic. Sci. Biotechnol.* 87, 429–434. doi: 10.1080/14620316.2012.11512890

Zou, J., Zhang, Y., Zhang, Y., Bian, Z., Fanourakis, D., Yang, Q., et al. (2019). Morphological and physiological properties of indoor cultivated lettuce in response to additional far-red light. *Sci. Hortic.* 257:108725. doi: 10.1016/j.scienta.2019.108725

Conflict of Interest: CS Nicole was employed by company Signify.

The remaining authors declare that the research was conducted in the absence of any commercial or financial relationships that could be construed as a potential conflict of interest.

Copyright © 2020 Larsen, Woltering, Nicole and Marcelis. This is an open-access article distributed under the terms of the Creative Commons Attribution License (CC BY). The use, distribution or reproduction in other forums is permitted, provided the original author(s) and the copyright owner(s) are credited and that the original publication in this journal is cited, in accordance with accepted academic practice. No use, distribution or reproduction is permitted which does not comply with these terms.

frontiers in Plant Science

ORIGINAL RESEARCH
published: 18 December 2020
doi: 10.3389/fpls.2020.598082

Producing Enhanced Yield and Nutritional Pigmentation in Lollo Rosso Through Manipulating the Irradiance, Duration, and Periodicity of LEDs in the Visible Region of Light

Laura Cammarisano[1,2], Iain S. Donnison[1] and Paul R. H. Robson[1]*

[1] *Institute of Biological, Environmental and Rural Sciences (IBERS), Aberystwyth University, Aberystwyth, United Kingdom,*
[2] *Next-Generation Horticultural Systems, Leibniz-Institute of Vegetable and Ornamental Crops (IGZ), Grossbeeren, Germany*

OPEN ACCESS

Edited by:
Jason Wargent, Massey University, New Zealand

Reviewed by:
Cristina Sgherri, University of Pisa, Italy
Cherubino M. Leonardi, University of Catania, Italy

***Correspondence:**
Laura Cammarisano
cammarisano@igzev.de

Specialty section:
This article was submitted to Crop and Product Physiology, a section of the journal Frontiers in Plant Science

Received: *23 August 2020*
Accepted: *23 November 2020*
Published: *18 December 2020*

Citation:
Cammarisano L, Donnison IS and Robson PRH (2020) Producing Enhanced Yield and Nutritional Pigmentation in Lollo Rosso Through Manipulating the Irradiance, Duration, and Periodicity of LEDs in the Visible Region of Light. Front. Plant Sci. 11:598082. doi: 10.3389/fpls.2020.598082

Pigmented food are an important part of the human diet, and anthocyanins have demonstrable protection against tumor production in mouse models and beneficial effects on human liver chemistry. As such, producing pigmented crops is important for a nutritionally diverse diet. Lollo rosso lettuce is a fast-growing pigmented plant, is rich in phenolic compounds, and represents a suitable system to test optimization strategies for yield and anthocyanin production. High-energy UV wavebands are often used to stimulate increased pigmentation; however, we hypothesized that optimizing visible wavebands would deliver both yield and quality improvements. Growing Lollo rosso under irradiances between 5 and 180 W m^{-2} using visible waveband LEDs produced 0.4 g fresh weight per W m^{-2} in the linear portion of the curve between 5 and 40 W m^{-2} and achieved an approximate asymptote of 20 g fresh weight at around 100–120 W m^{-2} for yield. Anthocyanin content increased linearly with irradiance. We attempted to optimize the visible wavebands by supplementing half the asymptotic energy for 15 days with supplemental red (R) or blue (B) wavebands in the peaks of photosynthetic activity (430–460 and 630–660 nm). R and B affected rosette morphology with no significant impact on yield, but B significantly increased anthocyanin content by 94% compared to R. We therefore focused on further optimizing B by shortening the daily duration of supplemental B. The minimum B treatment that lacked significant pigment induction was 1 h. We hypothesized that short durations would be more active at different times in the diurnal cycle. Supplemental B was applied for 2 h at four different times. A night-break with B produced the highest yield and anthocyanin content. Our research demonstrates new ways to efficiently use readily available LEDs within the PAR wavebands to increase both yield and crop quality in controlled environment agriculture.

Keywords: LED, blue light, anthocyanin, red light, diel cycle, red lettuce

INTRODUCTION

It is expected that available land per capita to cultivate food will decline due to population growth and climate change. Possible alternatives to increase land use efficiency include using efficient closed-environment agriculture which can produce more crop per unit area (Touliatos et al., 2016). A revolution in lighting allows such systems to utilize efficient LEDs which allow potential control over both irradiance and spectra and, when used in completely enclosed environments, photoperiod (Bantis et al., 2018). Lighting represents a major cost, and therefore, it is important to understand how the increased flexibility achievable in new LED lighting may be best utilized to maximize returns from both crop yield and quality.

Increasing the photon flux density (PFD) results in a linear increase in photosynthetic rate (Kelly et al., 2020) until light exceeds photosynthetic capacity and photosynthesis becomes limited by other factors such as CO_2 (Herron and Mauzerall, 1972; Robinson, 2001). Light use efficiency may also be limited by photoprotective strategies that reduce the risk of photo-oxidative damage by limiting the light interception and absorption and by enhancing dissipative routes (Adams and Demmig-Adams, 1992; Takahashi and Badger, 2011). Such strategies evolved in highly variable environments, and plants can therefore generally tolerate a range of light intensities (Ruban, 2009). Indoor cultivation, where artificial lamps are the sole source of illumination, reduces variability and allows growers to adopt optimal irradiance levels for yield, morphology, and energy costs (Kozai, 2013). Growing plants under optimized light conditions can lead to high yield and high-quality produce (Ouzounis et al., 2015). The exact light recipe may require a balance of light that is optimally used for photosynthesis and that also induces other characteristics of commercial value such as pigmentation and morphological changes that under natural conditions are responses to light stress.

Growing plants under monochromatic R or B appears to be unsuitable for most plants tested so far; monochromatic B results in a decline in photosynthetic activity (Lichtenthaler et al., 1980) and monochromatic R in the deleterious red light syndrome (Matsuda et al., 2004). A combination of R and B radiation, with notable variations in the importance of the ratio between R and B, represents a suitable and efficient light spectrum for crop growth and development (Kim et al., 2004; Izzo et al., 2019). However, a broader spectrum may be more beneficial for crop growth (Pennisi et al., 2019) and addition of green light to the growth spectrum enhances plant growth and development (Johkan et al., 2012) and increases light to the lower plant canopy (Terashima et al., 2009). Replacing a part of the broad-spectrum background with an appropriate fraction of B or R light may increase biomass accumulation (Kaiser et al., 2019), produce regular crop morphological and physiological characteristics, and enhance crop quality (Li and Kubota, 2009).

The types of crops predominantly grown in controlled environments under LEDs have tended to be limited to leafy greens and micro herbs (Benke and Tomkins, 2017). Many studies have focused on lettuce as an important global crop that responds well to light treatment (Son and Oh, 2013). Lollo rosso lettuce is rapid growing and red pigmented, the major pigment being the anthocyanidin cyanidin (Ferreres et al., 1997). Anthocyanin showed anti-carcinogenic activity in cell culture models and in animal model tumor systems (Wang and Stoner, 2008), and some pigments can protect lipoproteins and vascular cells from oxidation which is the widely accepted theory for the genesis of atherosclerosis (Wilcox et al., 2003). The importance of pigments has led to the general advice to eat a more varied and colorful diet (WHO-FAO, 2004). Furthermore, anthocyanin accumulation is stimulated by both light intensity (Stutte and Edney, 2009) and quality (Zhang et al., 2018) in red lettuce. As such, Lollo rosso represents a suitable system for cultivation in controlled environment agriculture for studies of both yield and important nutritional quality.

Reports of optimal irradiance for indoor cultivation of lettuce vary between 100 and 600 $\mu mol\ m^{-2}\ s^{-1}$ (Hee and Beom, 2001; Ilieva et al., 2010; Fu et al., 2012; Kang et al., 2013). The ratio of R to B light affects growth in lettuce (Chen et al., 2016; Clavijo-Herrera et al., 2018; Naznin et al., 2019), and there is a clear interaction between the amount of R, B, and W (Son et al., 2016). In addition to the impacts of spectrum, the timing and duration of light treatments may also be significant and although circadian biology is well researched in plant sciences its application to closed environment agriculture is sparse. Many physiological plant processes change over the day in response to environmental signals; others instead follow specific cyclic patterns ascribed as circadian rhythms. Through daily morphological and physiological adaptations, e.g., leaf angle and chloroplast movement, the plant is able to adapt to the fluctuating natural environment by predicting daily changes but also by anticipating regular natural events such as dawn (Dodd et al., 2015). In addition to circadian control, some processes respond cyclically to metabolic feedback; for example, in natural conditions, CO_2 assimilation usually follows a daily pattern characterized by an initial "photosynthesis activation" at dawn, a maximum CO_2 fixation at mid-morning, and a decline from midday (midday depression) (Koyama and Takemoto, 2014; Maai et al., 2019). After the midday depression, the photosynthetic activity declines until the dark when the nocturnal process of starch consumption is under circadian oscillator control (Haydon et al., 2013). In controlled environments lacking daylight, complete control of plant rhythms is possible and may be a route to further optimization of light treatments.

In this study, we used a dose-response curve to assess the relationship between irradiance of a broad-spectrum (PAR) LED array and the yield and pigmentation in Lollo rosso. From this curve, we identified a suitable treatment that produced a good combination of yield and morphology that was used to study the effects of PAR plus supplemental R and B on yield and pigmentation. We used supplemental B to examine the effects of duration and to identify a minimal active treatment for further diel studies. We hypothesized that the effectiveness of supplemental B would vary between different diel treatment periods.

MATERIALS AND METHODS

Plant Material and Growth Conditions

Four separate experiments were performed in the same controlled growth room with an 18-h and 6-h light and dark photoperiod. The walls were covered by white reflective sheets (ORCA grow film, California Grow Films LLC), and atmospheric conditions were monitored using Tinytag Ultra 2 (Gemini Data Loggers, Chichester, United Kingdom) and Rotronic CL11 (Rotronic Instruments Ltd., United Kingdom). The average air temperature was 21.9 ± 0.6°C, relative humidity was 58.5 ± 4.8%, and CO_2 was 470.5 ± 2.4 ppm; averaged environmental values for individual experiments are detailed in **Supplementary Table 1**.

Seeds of red lettuce Lollo rosso (Antonet RZ seeds from Rijk Zwaan, De Lier, Netherlands) were sown in 155 g of sieved John Innes No. 3 soil-based compost. Water-holding "field" capacity of the compost was calculated following the gravimetric method for soil moisture determination (Reynolds, 1970). Pots were filled, saturated with water, covered with plastic film, and left to drain at room temperature (20 ± 5°C). After 24 h, pot weight was noted and pots were incubated in the oven at 105°C. Every 24 h, pots were weighed until stable dry weight was reached. The dry and wet weights were used to estimate the weight of pots, and soil at approximately 0% and 100% water holding capacity and capacities in between these extremes were estimated as a linear proportion of the difference between these values. Pots were individually irrigated to 80% water holding capacity (205 g) every 48 h until harvest at 30 days after sowing (DAS).

Light intensity and spectral composition of the treatments were measured using the spectroradiometer SpectraPen LM 500 (cosine-corrected, 380–780 nm; Photon Systems Instruments, Drásov, Czechia) (**Supplementary Figure 1**).

Broad-Spectrum LED Light Response Curve

Seeds were germinated and grown under two broad-spectrum (PAR) LED arrays (EP006, 380–760 nm, Shenzhen Herifi Technology Co., Ltd., China) (**Supplementary Figure 1A**) for 30 days. A total of twelve irradiance treatments (5, 10, 15, 30, 40, 60, 80, 100, 120, 140, 160, 180 W m^{-2} or 25, 30, 75, 150, 200, 300, 400, 500, 600, 700, 800, 900 μmol m^{-2} s^{-1}) were obtained from the same broad spectrum by adding different layers of muslin cloth as a neutral density filter between source and individual plants. Each treatment was replicated three times and the plants were used for FW determination.

Supplementing Broad-Spectrum (PAR) LED Arrays With Blue and Red LED Light

Seeds were germinated and grown for 15 days under a broad-spectrum PAR LED source (EP006, 380–760 nm, Shenzhen Herifi Technology Co., Ltd., China) with a photosynthetic photon flux density (PPFD) of 300 μmol m^{-2} s^{-1} (P60). After growth under the P60 array, groups of 9 randomly selected plants were moved under different spectral treatments comprising either double the PAR irradiance (P120), the same PAR irradiance supplemented with R LEDs (P60 + R), or the same PAR irradiance supplemented with B LEDs (P60 + B). Supplemental B and R were provided from mixed arrays of two LEDs centered at 430 and 460 nm (B) and 630 and 660 nm (R) (**Supplementary Figures 1B,C**). Treatments P120, P60 + R, and P60 + B provided approximately the same PPFD (500 μmol m^{-2} s^{-1}). Plants were moved to one of the three supplemental treatments either at 15 DAS or 26 DAS, leaving the remainder under P60 radiation, thus plants were grown under supplemental treatments for either 15 days or 4 days.

Supplementing Broad-Spectrum (PAR) LEDs With Different Durations of B LEDs

Seeds were germinated and grown for 15 days under a broad-spectrum PAR LED source (EP006, 380–760 nm, Shenzhen Herifi Technology Co., Ltd., China) with a photosynthetic photon flux density (PPFD) of 300 μmol m^{-2} s^{-1} (P60). Plants were randomly selected to either remain under PAR treatment or were grown under similar PAR LEDs supplemented with B radiation to reach a PPFD of 500 μmol m^{-2} s^{-1} (total B accounted for 44% of the emission spectrum). Supplemental B LED treatments varied from a high daily light integral (DLI) B treatment in which plants were transferred to PAR plus supplemental B for the remaining 15 days of the experiment to a minimal DLI B treatment whereby plants remained under P60 for 29 days and received 1 h of PAR60 plus supplemental B LED treatment on the final day (see **Table 1** for full range of treatments).

Interaction of Supplemental B LED Light and the Diel Cycle

Seeds were germinated and grown for 15 days under a broad-spectrum PAR LED source (EP006, 380–760 nm, Shenzhen Herifi Technology Co., Ltd., China) with a photosynthetic photon

TABLE 1 | Duration, description, and daily light integrals (DLI) of treatment regimes with PAR plus supplemental B applied for different periods across a 30-days growth period.

Treatments	PAR radiation	Supplemental B radiation	Total DLI (mol m^{-2} d^{-1})	Total B DLI (mol m^{-2} d^{-1})
P60	30 days (18 h photoperiod)	–	19.44	6.09
B15D	15 days (18 h photoperiod)	15 days (18 h photoperiod)	26.50	14.09
B4D	26 days (18 h photoperiod)	4 days (18 h photoperiod)	21.30	8.22
B2D	28 days (18 h photoperiod)	2 days (18 h photoperiod)	20.38	7.16
B1D	29 days (18 h photoperiod)	1 day (18 h photoperiod)	19.91	6.62
B9h	29 days + 9 h	9 h	19.68	6.36
B4h	29 days + 14 h	4 h	19.54	6.20
B2h	29 days + 16 h	2 h	19.49	6.15
B1h	29 days + 17 h	1 h	19.47	6.12

Daily light integral (DLI) was calculated by multiplying the instantaneous photon flux density (PFD) (μmol m^{-2} s^{-1}) for the total time of the treatment application, then was divided by the number of growth days (30) in order to obtain the mol of photons per day reaching the plant.

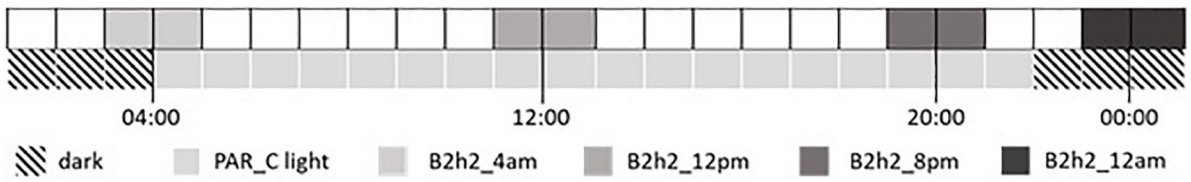

FIGURE 1 | Application times of supplemental B treatment across the diel cycle. The bottom line shows the daily photoperiod of 18 h PAR light (pale gray) and 6 h dark (diagonal stripes). The upper line shows the timing of four supplemental B treatments each applied individually for 2 h.

flux density (PPFD) of 300 μmol m^{-2} s^{-1} (P60). Plants were randomly selected to either remain under PAR treatment or were grown for a further 15 days under similar PAR LEDs supplemented with B LED treatments (PPFD of 800 μmol m^{-2} s^{-1}) for 2 h during different periods of the day–night cycle. Four treatment times were tested placing the 2-h B treatment at the beginning, middle, and end of the 18-h light period and in the middle of the 6-h dark period (**Figure 1**).

Sampling and Measurements of Plant Morphological and Physiological Parameters

Chlorophyll *a* fluorescence was assessed from leaf number four using a portable Handy PEA continuous excitation chlorophyll fluorimeter (Hansatech Instruments Ltd., King's Lynn, United Kingdom). First, light-adapted measurements were taken, then dark-adapted measurements after 30 min of dark adaptation using the manufacturer's leaf clips. Measurements were always in the morning just after 10:00, except when treatments required measurements at different specific times.

Rosette images were taken using a fixed focal length digital camera and stand. Images were used for rosette area determination using the "Shape descriptor" plugin in ImageJ software (version 1.52a) (Schneider et al., 2012). The rosette was harvested from just above the cotyledon node and immediately weighed for fresh weight (FW). The entire rosette was then placed in a paper bag and dried to constant weight at 60°C to determine dry weight (DW).

A random selection of plants not used for yield determination was harvested for biochemical analyses at the end of the experiment (day 30). Fully expanded leaves, developmentally the third and fourth leaves, were excised, the midrib was removed, and tissue was immediately frozen in liquid nitrogen before storage at −80°C until analyzed. Prior to analysis, samples were freeze-dried and cold milled to a fine powder in an automated sample grinder (Labman Automation Ltd., Middlesbrough, United Kingdom) for 90 s at −70°C.

Extraction and Quantification of Anthocyanin Content

Anthocyanins were quantified as a single peak cyanidin 3-malonylglucoside [reported as main anthocyanin in Lollo rosso (Ferreres et al., 1997)] confirmed by fragmentation pattern and mass spectroscopy. Lyophilized powdered leaf material (30 mg) was extracted by shaking in acidified methanol solution (methanol: water: acetic acid; 70: 28.5: 1.5) for 30 min at room temperature. The sample was then centrifuged for 10 min at 1500 × *g*, and the extract was collected and evaporated in a centrifugal evaporator (Jouan, RC 10.22). The concentrated extract was then purified by Solid Phase Extraction using sep-pak cartridges (500 mg Sep-Pak C_{18} 3 cc Vac RC cartridge, Waters Ltd., Elstree, United Kingdom). The final extract was analyzed by reversed-phase HPLC using a Waters system equipped with a 996 photodiode detector array (PDA) and a Nova-Pak C_{18} radial compression column (8 mm × 100 mm, particle size 4 μm; Waters Ltd., Elstree, United Kingdom). The column was equilibrated with 20% solvent A (5% acetic acid) at a flow rate of 2 ml min^{-1}. Compounds were eluted by linear gradient to 60% solvent B (100% methanol) over 20 min and monitored from 240 to 600 nm with the detection wavelength set to 525 nm. Anthocyanins were quantified from peak areas using an external standard curve using a cyanidin chloride standard (Sigma-Aldrich Company Ltd.) which had a very similar retention time.

Statistical Analysis

All the data were statistically analyzed using Microsoft Excel 2016 and R studio [R version 3.5.2 (2018-12-20), "Eggshell Igloo"] with packages agricolae, car, ggplot2, and segmented (Muggeo, 2003; De Mendiburu, 2020; Fox et al., 2020; Wickham et al., 2020). For the measured parameters, data were analyzed by one-way ANOVA and the means were compared by least significance difference (LSD), at 5% significance level.

RESULTS

Yield and Morphological Responses to Varying Irradiance of Broad-Spectrum (PAR) LEDs

Using a broad-spectrum (PAR) LED array, to provide a range of irradiances between 5 and 180 W m^{-2}, demonstrated a highly plastic response in the pigmented lettuce Lollo rosso. Rosette fresh weight (FW) increased logarithmically with increasing irradiance. At lower irradiances, between 5 and 40 W m^{-2}, rosette FW increased linearly with increasing irradiance at an average rate of 0.4 g FW per W m^{-2}. Higher irradiances, between 40 and 80 W m^{-2}, produced 0.1 g per W m^{-2}, while irradiances

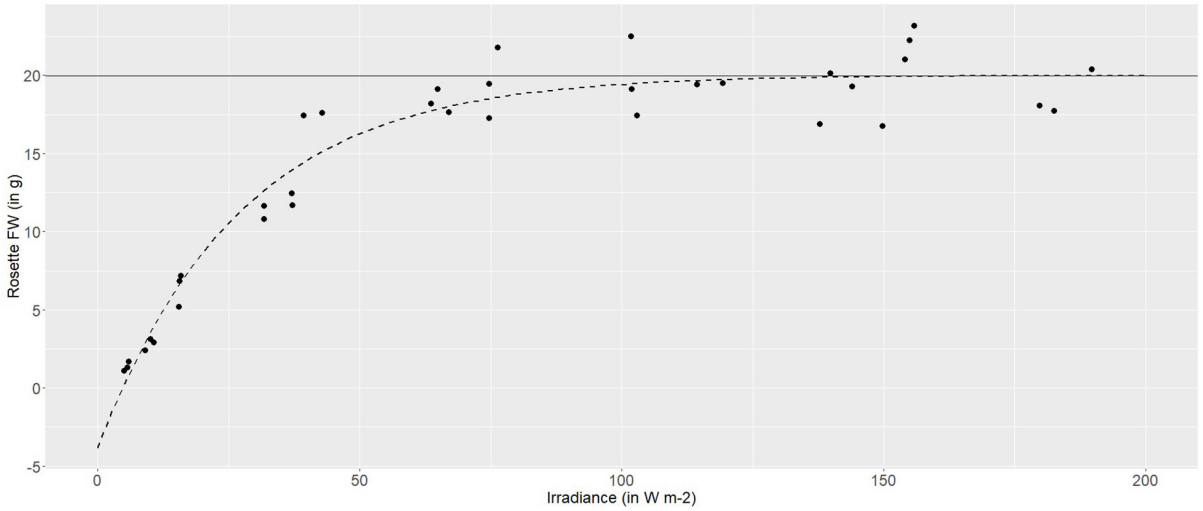

FIGURE 2 | Non-linear (logarithmic) asymptotic regression between the fresh weight (g) of Lollo rosso and irradiance (W m^{-2}). In dark gray is the horizontal asymptote, and in dashed dark gray is the model-based regression curve.

TABLE 2 | Morphological responses of Lollo rosso to varying the incident irradiance of a broad-spectrum (PAR) LED array.

Averaged light treatments (W m^{-2})	Averaged light treatment (μ mol m^{-2} s^{-1})	Leaf number***	Rosette area*** (cm^2)	Anthocyanin*** (mgCYA g^{-1} DW)
5.5	27.0	5.0 ± 0.0^{f}	73.1 ± 12.7^{f}	0.19 ± 0.01^{f}
9.9	48.2	6.3 ± 0.3^{ef}	131.2 ± 14.0^{e}	0.28 ± 0.01^{f}
15.6	75.4	6.7 ± 0.3^{def}	211.7 ± 4.5^{a}	0.18 ± 0.02^{f}
33.5	161.6	7.7 ± 0.3^{de}	171.3 ± 7.1^{cd}	2.07 ± 0.14^{e}
39.7	186.9	8.7 ± 0.3^{cd}	200.1 ± 6.2^{abc}	4.21 ± 0.13^{d}
65.1	329.7	10.7 ± 1.2^{bc}	203.4 ± 5.5^{ab}	5.46 ± 0.08^{c}
75.3	387.1	13.0 ± 0.6^{a}	186.6 ± 9.3^{abcd}	5.72 ± 0.09^{bc}
102.2	387.1	12.7 ± 0.9^{ab}	183.1 ± 10.7^{abcd}	5.75 ± 0.09^{bc}
125.9	517.9	12.7 ± 1.5^{ab}	194.9 ± 16.8^{abc}	6.03 ± 0.53^{abc}
142.4	731.1	11.7 ± 0.3^{ab}	157.2 ± 5.8^{de}	6.55 ± 0.22^{ab}
154.9	800.0	13.0 ± 0.6^{a}	180.8 ± 6.6^{bcd}	6.87 ± 0.63^{a}
184.0	942.4	12.7 ± 0.3^{ab}	141.8 ± 11.1^{e}	6.21 ± 0.74^{abc}

*Values are reported as mean ± standard error of the mean. Different letters within columns indicate significant treatment differences at $P < 0.05$, as determined by analysis of variance (ANOVA) and Fisher's least significant difference (LSD) test. Significance codes: 0.000 "***"; n = 3.*

of 100–120 W m^{-2} produced a maximum rosette FW of 20 g and growth was asymptotic at higher irradiances (**Figure 2**).

Increasing irradiance induced significant changes to morphological responses such as rosette area ($P = 4.7 \times 10^{-8}$), leaf number ($P = 2.9 \times 10^{-9}$), and leaf pigmentation ($P = 4.5 \times 10^{-5}$). Rosette area almost tripled from 5 (73.1 ± 12.7 cm^2) to 15 W m^{-2} (211.7 ± 4.5 cm^2), and plants growing under the lower irradiances displayed a prostrate leaf morphology. Rosette area decreased linearly between light energy of 60 and 180 W m^{-2} to a rosette area of 141.8 ± 11.1 cm^2 (**Table 2**). Anthocyanins were difficult to detect in plants grown under very low irradiance (up to 15 W m^{-2}, 0.18–0.28 mg g^{-1} DW). Light levels of 30 W m^{-2} produced increased accumulation of anthocyanin content (2.07 ± 0.14 mg g^{-1} DW) and reached a maximum under 160 W m^{-2} (6.87 ± 0.63 mg g^{-1} DW) (**Table 2**).

Supplementing Broad-Spectrum (PAR) LED Arrays With Blue and Red LED Light

There was no significant effect on rosette FW and DW of supplementing broad-spectrum (PAR) LED arrays with R and B LEDs at the irradiances tested (**Table 3**), but morphology was affected especially rosette area and leaf pigmentation. Rosette area was reduced by the longer (15 days) supplemental treatments ($P = 0.001$). A 15-days supplementation with B LEDs produced the most compact rosette with the lowest area (167.39 ± 3.13 cm^2), next lowest was 15-days supplementation with PAR LEDs (188.62 ± 6.09), and 15-days supplementation with R LEDs produced a larger rosette area (193.43 ± 4.63). The largest rosette area was produced by Lollo rosso growing under the 4-days supplementation with R LEDs. Accumulation of anthocyanins was enhanced under supplemental B only and was greater in leaves exposed to 4 days than 15 days of supplemental

B LEDs (13.00 ± 0.44 and 9.60 ± 0.65 mg g^{-1} DW after 4 days and 15-days B supplementation, respectively) (**Table 3**) ($P = 2.2 \times 10^{-16}$).

Supplementing Broad-Spectrum (PAR) LEDs With Different Durations of B LEDs

The duration of supplemental B radiation had a significant effect on rosette FW ($P = 1.9 \times 10^{-14}$) and DW ($P = 7.2 \times 10^{-8}$) of Lollo rosso (**Table 4**). Longer durations of supplemental B increased biomass accumulation which was greatest and asymptotic under 1, 2, 4, and 15 days of supplemental B (19.1 to 20.4 g). Rosette DW followed a similar trend to FW, but the greatest DW was measured after 1 day of supplemental B. Rosette area in general decreased with increasing duration of supplemental B. The smallest rosette areas (1.8-fold smaller than rosettes from control plants) were measured in plants treated with the longest duration of supplemental B (15 days, 146.8 ± 8.5 cm^2), and the largest rosette area was measured in plants treated with 1 day of supplemental B (181.3 ± 11.5 cm^2); rosette areas from all the intermediate treatments did not significantly differ (**Table 4**).

Supplemental B did not have a significant effect on chlorophyll *a* fluorescence and the maximum quantum efficiency of PSII photochemistry in the dark (F_V/F_M) approximated to a similar value of 0.83 in all measured plants. The amount of light energy dissipated via non-photochemical quenching generally increased with duration of supplemental B, but the differences were not statistically significant.

All supplemental B treatments greater than 1-h duration resulted in significant increases in anthocyanin content compared to levels in leaves from control plants lacking supplemental B ($P = 3.6 \times 10^{-14}$). The anthocyanin content increased approximately linearly with increasing durations of supplemental B from 2 h (27%) to 4 days (224%) (**Table 4**). Anthocyanin accumulation declined slightly in leaves exposed to the longest, 15-days, supplemental B treatment (187%). The amount of anthocyanin in leaves exposed to the shortest supplemental B treatment (1 h) did not statistically differ from that in control leaves.

TABLE 3 | Fresh and dry weight yield, rosette area, and anthocyanin content of leaf tissue of Lollo rosso lettuce growing under 300 μmol m^{-2} s^{-1} broad-spectrum (PAR) LED (P60) for 15 days and followed by a further 15 days under P60 or P60 plus supplemental PAR, Red (R) or Blue (B) LEDs for either 15 days or 4 days.

Supplemental treatments	Rosette area** (cm^2) (n = 3)	Fresh weight (g) (n = 9)	Dry weight (g) (n = 6)	Anthocyanin*** (mgCYA g^{-1} DW) (n = 3)
–	239.9 ± 14.4^{a}	20.4 ± 1.0	1.46 ± 0.09	4.96 ± 0.20^{c}
15D P60	188.6 ± 6.1^{bc}	17.9 ± 1.2	1.26 ± 0.10	4.14 ± 0.16^{cd}
4D P60	240.6 ± 11.3^{a}	19.9 ± 0.7	1.47 ± 0.05	4.42 ± 0.15^{cd}
15D R	193.4 ± 4.6^{bc}	21.7 ± 1.1	1.50 ± 0.18	3.77 ± 0.40^{d}
4D R	246.3 ± 21.4^{a}	19.8 ± 1.6	1.45 ± 0.09	3.75 ± 0.49^{d}
15D B	167.4 ± 3.1^{c}	20.3 ± 0.5	1.44 ± 0.04	9.60 ± 0.65^{b}
4D B	221.1 ± 7.0^{ab}	19.8 ± 0.7	1.67 ± 0.08	13.00 ± 0.44^{a}

*Values are reported as mean ± standard error of the mean. Different letters within columns indicate significant treatment differences at P < 0.05, as determined by analysis of variance (ANOVA) and Fisher's least significant difference (LSD) test. Significance codes: 0.000 "***," 0.001 "**".*

TABLE 4 | Fresh and dry weight yield, rosette area, and anthocyanin content of leaf tissue of Lollo rosso lettuce growing under 300 μmol m^{-2} s^{-1} broad-spectrum (PAR) LED (P60) for 15 days and then a further 15 days under P60 with different durations of supplemental Blue (B) LEDs.

Treatments	Rosette area* (cm^2) (N = 3)	Fresh weight*** (g) (N = 8)	Dry weight*** (g) (N = 4)	Anthocyanin*** (mgCYA g^{-1} DW) (N = 3)
P60	202.9 ± 19.4^{a}	11.8 ± 0.5^{c}	0.85 ± 0.13^{d}	3.98 ± 0.21^{g}
B15D	146.8 ± 8.5^{c}	20.4 ± 0.5^{a}	1.46 ± 0.07^{bc}	11.44 ± 0.39^{b}
B4D	174.9 ± 1.5^{b}	20.2 ± 0.7^{a}	1.60 ± 0.08^{abc}	12.91 ± 0.43^{a}
B2D	169.7 ± 5.1^{bc}	20.3 ± 1.3^{a}	1.72 ± 0.10^{ab}	8.48 ± 0.48^{c}
B1D	181.3 ± 11.5^{ab}	19.1 ± 1.6^{a}	1.76 ± 0.21^{a}	7.53 ± 0.29^{d}
B9h	166.2 ± 2.7^{bc}	15.4 ± 0.8^{b}	1.44 ± 0.06^{bc}	7.09 ± 0.09^{de}
B4h	168.8 ± 4.3^{bc}	15.7 ± 0.7^{b}	1.35 ± 0.06^{c}	6.44 ± 0.05^{e}
B2h	161.4 ± 3.7^{bc}	11.2 ± 0.4^{c}	0.79 ± 0.03^{d}	5.04 ± 0.15^{f}
B1h	170.0 ± 4.0^{bc}	12.0 ± 0.6^{c}	0.85 ± 0.06^{d}	3.69 ± 0.04^{g}

*Values are reported as mean ± standard error of the mean. Different letters within columns indicate significant treatment differences at P < 0.05, as determined by analysis of variance (ANOVA) and Fisher's least significant difference (LSD) test. Significance codes: 0.000 "***," 0.01 "*".*

Interaction of Supplemental B LED Light and the Diel Cycle

When Lollo rosso was grown in an 18-h light, 6-h dark cycle, the timing of a 2-h supplemental B treatment within the light and dark periods had a significant effect on rosette FW ($P = 0.008$). When supplemental B was applied in the middle of the dark period (12 am), rosette FW was greatest. When supplemental B was applied at the end of the light cycle (8 pm), rosette FW was lowest and did not significantly differ from control plants lacking supplemental B. Similar trends were seen in rosette DW ($P = 0.05$) (**Table 5**).

Anthocyanin content was significantly higher when supplemental B was supplied in the middle of the dark period (9.81 ± 0.37 mg g^{-1} DW) than all other treatment and control plants ($P = 3.7 \times 10^{-8}$) (**Table 5**). Supplementing with 2-h B at the beginning (4 am) and middle (12 pm) of the light cycle (6.60 ± 0.29 mg g^{-1} DW and 7.50 ± 0.48 mg g^{-1} DW, respectively) resulted in significantly higher anthocyanin accumulation than control plants (4.00 ± 0.14 mg g^{-1} DW), but anthocyanin contents of control plants and plants treated with supplemental B at the end of the light cycle were not significantly different.

F_V/F_M was similar between differently treated plants and approximated the optimal value. Maximum operating efficiency of PSII photochemistry in the light (F_V/F_M') was lowest under midday supplementation and highest under midnight supplementation ($P = 0.010$). Performance index (PI) was similar across the diverse treatments, except the significantly lower values measured when supplementation was applied at the end of the light cycle ($P \geq 0.000$). Non-photochemical quenching (NPQ) was low and similar in leaves grown in control (P60) and

TABLE 5 | Fresh and dry weight yield, and anthocyanin content of leaf tissue of Lollo rosso lettuce growing under 300 μmol m^{-2} s^{-1} broad-spectrum (PAR) LED (P60) for 15 days and then a further 15 days under P60 and P60 supplemented with Blue (B) LEDs for 2 h at four different periods.

Treatments	Fresh weight** (g) (*n* = 8)	Dry weight· (g) (*n* = 4)	Anthocyanin*** (mgCYA g^{-1} DW) (*n* = 4)
P60	10.6 ± 0.6^{b}	0.79 ± 0.09^{ab}	4.00 ± 0.14^{c}
P60 + 2hB (12 am)	12.4 ± 0.4^{a}	0.92 ± 0.04^{a}	9.81 ± 0.32^{a}
P60 + 2hB (4 am)	10.1 ± 0.7^{b}	0.73 ± 0.06^{b}	6.60 ± 0.29^{b}
P60 + 2hB (12 pm)	11.0 ± 0.4^{ab}	0.75 ± 0.04^{ab}	7.50 ± 0.48^{b}
P60 + 2hB (8 pm)	9.6 ± 0.6^{b}	0.71 ± 0.03^{b}	4.43 ± 0.44^{c}

*Values are reported as mean ± standard error of the mean. Different letters within columns indicate significant treatment differences at P < 0.05, as determined by analysis of variance (ANOVA) and Fisher's least significant difference (LSD) test. Significance codes: 0.000 "***," 0.001 "***," and 0.05 "·".*

TABLE 6 | Chlorophyll fluorescence parameters of leaf tissue of Lollo rosso lettuce growing under 300 μmol m^{-2} s^{-1} broad-spectrum (PAR) LED (P60) for 15 days and then a further 15 days under P60 and P60 supplemented with Blue (B) LEDs for 2 h at four different periods.

Treatments	F_V/F_M'*	F_V/F_M	PI**	NPQ*
P60	0.77 ± 0.01^{ab}	0.85 ± 0.01	3.01 ± 0.30^{a}	0.28 ± 0.02^{bc}
P60 + 2h B (12 am)	0.77 ± 0.01^{a}	0.85 ± 0.00	3.70 ± 0.22^{a}	0.23 ± 0.05^{c}
P60 + 2h B (4 am)	0.75 ± 0.01^{bc}	0.84 ± 0.00	3.08 ± 0.43^{a}	0.40 ± 0.04^{ab}
P60 + 2h B (12 pm)	0.74 ± 0.01^{c}	0.84 ± 0.01	3.77 ± 0.38^{a}	0.50 ± 0.06^{a}
P60 + 2h B (8 pm)	0.74 ± 0.02^{bc}	0.84 ± 0.01	1.74 ± 0.11^{b}	0.43 ± 0.08^{ab}

*Values are reported as mean ± standard error of the mean. Different letters within columns indicate significant treatment differences at P < 0.05, as determined by analysis of variance (ANOVA) and Fisher's least significant difference (LSD) test. Significance codes: 0.001 "**," 0.01 "*"; n = 4.*

midnight supplemental B treatments but was significantly higher in all three treatments when B was supplemented during the light cycle ($P = 0.015$) (**Table 6**).

DISCUSSION

The use of LED lighting is revolutionizing the provision of light to controlled environment agriculture (Pattison et al., 2018). Light intensity has a significant effect on plant growth and morphology (Poorter et al., 2019), and to fully exploit the flexibility afforded by new LED-based lighting systems will involve investigation of the interactions between crop production and variation in irradiance and spectrum (Gómez and Izzo, 2018). Less is known about the potential for further optimization through interactions between light and other factors such as temperature (Franklin et al., 2014) and circadian rhythms (Belbin et al., 2017).

Here we used Lollo rosso, a fast-growing commercial lettuce variety, as a model system to study how irradiance, spectrum, duration, and rhythm of LED light may be used to affect crop growth. We studied aspects of both yield and quality, the latter through the accumulation of anthocyanin pigment. By growing Lollo rosso under a range of PAR irradiance levels, limiting, optimal, and saturating light levels were identified. Light intensity of over 100 W m^{-2} (PAR ∼ 520 μmol m^{-2} s^{-1}) produced asymptotic growth, suggesting that photosynthesis and or partitioning of photosynthate into harvestable yield is saturated at such high irradiances. Light exceeding the limiting light levels is more likely to activate photoprotective responses (Robinson, 2001), and light not directly converted to harvestable yield may impact crop quality through alterations in morphology and composition. Rosette area, for instance, decreased in response to irradiance. Under low irradiance light conditions (5–15 W m^{-2}), a pale loose-leaf head developed which lacked measurable levels of anthocyanins; such phenotypes are associated with shade conditions to optimize light capture (Björkman and Demmig-Adams, 1995). A more compact rosette head formed and anthocyanin content doubled at moderate light levels (30–40 W m^{-2}). At higher irradiances, the rosette area decreased, resulting in more compact rosettes, presumably as a result of hypocotyl length and leaf angle reduction, both traits reported to be protective strategies that decrease incident light interception (Rama Das, 2006; Arsovski et al., 2012). Combining assessments of yield and morphology we concluded that PAR LEDs at 60 W m^{-2} (approximately 300 μmol m^{-2} s^{-1}) produced a good combination of yield and morphology in Lollo rosso, and this treatment was chosen to examine supplementing broad spectrum LED light with additional narrow-band LEDs.

Maximal leaf absorbance occurs in the B and R wavelengths due to the absorption peaks of chlorophylls a and b (428–453 and 642–661 nm) and carotenoids (400–500 nm) (McCree, 1971; Barber, 2009). Hence, the previously identified PAR LED irradiance level was supplemented with R or B radiation to reach a higher, but not saturating, light intensity (approximately 500 μmol m^{-2} s^{-1}). Our results demonstrated that supplementation of a PAR LED array with additional R or B LEDs had no significant effect on Lollo rosso biomass accumulation. However, supplemental B was effective at stimulating other desirable plant traits including rosette area and anthocyanin content. The reduced rosette area under supplemental B probably resulted from previously demonstrated effects of B inhibiting stem elongation and controlling leaf orientation (Huché-thélier et al., 2016). The increase in cyanidin content compared to PAR treatments lacking supplemental B was greater in the shorter B treatment. In contrast, NPQ increased with duration of supplemental B and a similar contrast was reported in young leaves of *Acmena acuminatissima* in contrasting seasons by Zhu et al. (2018). The phenotype of decreasing pigmentation and increasing stress may be due to alternative acclimation responses (Nogués et al., 1998), with the plant investing more in internal and constitutive protective mechanisms such as energy dissipation as heat through the xanthophyll cycle or rearrangements of photosystem machinery, rather than adopting largely preventive strategies through increased pigmentation (Steyn et al., 2002; Bailey et al., 2004; Li et al., 2009).

Having established the potential for shorter-duration supplemental B to improve pigmentation and morphology,

we next determined the relationship between duration of supplemental B treatment and pigmentation to identify a minimal treatment condition. Identifying a short enough treatment would enable us to further investigate the interaction of supplementation and the diel growth cycle. If absorbed by plants, the highly energetic photons of short wavelength light may increase photoprotection responses and negatively impact plant growth (Landi et al., 2015). UV radiation, for example, has been widely studied in this respect and stimulates the accumulation of secondary metabolites in plants (Schreiner et al., 2012) and inhibits growth in many plant species including lettuce (Tsormpatsidis et al., 2010; Lee et al., 2013). In contrast to UV, B wavelengths are photosynthetically active (Zhu et al., 2018), B LEDs are readily available commercially and can produce light at a higher efficiency (93%) compared with 81% for R LEDs (Kusuma et al., 2020). Thus, supplementation with B LEDs represents a suitable system to examine ways to increase photoassimilation and increase pigmentation while minimizing the negative impacts of phototoxicity, non-photochemical quenching, and consequent reduction in yield.

Exposing Lollo rosso to supplemental B for decreasing periods of time (from 15 days to 1 h) produced a distinct dose–response effect on the measured variables. Leaf anthocyanin content increased linearly from 2 h to 4 days of B supplementation. Rosette area and NPQ increased proportionally with treatment duration. The plateau in yield at around 1 day of supplemental B treatment suggests that the extra B photons were no longer contributing to net biomass accumulation at longer durations and the decrease in leaf anthocyanin content after the longest B treatment may be caused by acclimation of the plant to the high light environment. A similar response was reported by Taulavuoria et al. (2016) in which many compounds in basil decreased after B treatment for 48 days compared to a shorter 36-days treatment.

A minimal treatment of 2-h supplemental B was sufficient to significantly increase cyanidin content but had no significant effect on biomass. Thus, in the next test, the 2-h B treatment was adjusted to deliver an equivalent DLI to the most effective 4 days treatment ($\sim$21.3 mol m^{-2} d^{-1}, **Table 4**) and broad-spectrum PAR LEDs were supplemented with the resulting 2-h B at different times in the diel cycle. Increasing daily light integral (DLI), or the total sum of radiation in a 24-h period, allows higher radiation sums with lower PPFD, thus avoiding negative effects of saturating light levels and increasing lettuce fresh and dry mass (Kelly et al., 2020). Supplemental B at midday resulted in the highest NPQ which could be associated with midday depression of photosynthesis, stomatal closure, and reduced ability to dissipate light energy photochemically (Koyama and Takemoto, 2014). The lower total PPFD in the night break treatment (545 compared to 830 μmol m^{-2} s^{-1}) may allow most incident B photons to be photochemically quenched explaining the high and unaffected F_V/F_M' and the low level of NPQ. B light application in the night period was reported to increase carbon export and enhance fruit production (Lanoue et al., 2019), and the night break produced the highest biomass of our diel treatments. The higher percentage of B in the total PPF, 100% in the midnight treatment compared to 75% in PAR LEDs supplemented with B radiation, may explain the greater effectiveness at inducing anthocyanins of the supplemental B night break since anthocyanin content has been reported to increase with the percentage of B (Hernández et al., 2016).

Our data demonstrates the effectivity of supplemental B LEDs in stimulating leaf cyanidin accumulation while enhancing plant growth in Lollo rosso. Our results suggest that application of short-duration supplemental B LED light to PAR arrays has beneficial effects on Lollo rosso yield, morphology, and pigmentation and further that shorter duration supplementation may be made even more effective if applied during night breaks. Such studies will help producers improve crop quality and maximize returns on energy input from supplemental LED lighting utilizing visible wavelengths.

DATA AVAILABILITY STATEMENT

The original contributions presented in the study are included in the article/**Supplementary Material**, further inquiries can be directed to the corresponding author.

AUTHOR CONTRIBUTIONS

LC: conceptualization, methodology, investigation, formal analysis, writing – original draft, and writing – reviewing and editing. ID: funding acquisition and supervision. PR: funding acquisition, conceptualization, resources, writing – original draft, writing – reviewing and editing, and supervision. All authors contributed to the article and approved the submitted version.

FUNDING

LC was funded by an Aberystwyth University studentship. ID and PR by the BBSRC Core Strategic Programme in Resilient Crops BBS/E/W/0012843A.

ACKNOWLEDGMENTS

We thank Dr. Ana Winters and Dr. Barbara Hauck (Aberystwyth University) for their assistance in anthocyanin extraction and analysis.

SUPPLEMENTARY MATERIAL

The Supplementary Material for this article can be found online at: https://www.frontiersin.org/articles/10.3389/fpls.2020.598082/full#supplementary-material

Supplementary Figure 1 | Light spectral composition of the PAR array (**A**, solid line in pink), the blue LEDs (**B**, dashed line in blue), and the red LEDs (**C**, dotted

line in red). Each line represents the average of three measurements recorded at different spots of the plant canopy.

Supplementary Table 1 | Environmental data for the experiments reported. Values are reported as mean ± standard error of the mean.

Supplementary Table 2 | Maximum quantum efficiency of PSII (F_V/F_M) and non-photochemical quenching (NPQ) of Lollo rosso leaf growing under 60 W m^{-2} broad spectrum (PAR) LED (P60) for 15 days and followed by a further 15 days under P60 or P60 plus supplemental PAR, Red (R) or Blue (B) LEDs for either 15 days or 4 days. Values are reported as mean ± standard error of the mean.

REFERENCES

Adams, W. W., and Demmig-Adams, B. (1992). Operation of the xanthophyll cycle in higher plants in response to diurnal changes in incident sunlight. *Planta* 186, 390–398. doi: 10.1007/BF00195320

Arsovski, A. A., Galstyan, A., Guseman, J. M., and Nemhauser, J. L. (2012). Photomorphogenesis. *Am. Soc. Plant Biol.* 150, 202–212. doi: 10.1199/tab.0147

Bailey, S., Horton, P., and Walters, R. G. (2004). Acclimation of *Arabidopsis thaliana* to the light environment: the relationship between photosynthetic function and chloroplast composition. *Planta* 218, 793–802. doi: 10.1007/s00425-003-1158-5

Bantis, F., Smirnakou, S., Ouzounis, T., and Koukounaras, A. (2018). Current status and recent achievements in the fi eld of horticulture with the use of light-emitting diodes (LEDs). *Sci. Horticult.* 235, 437–451. doi: 10.1016/j.scienta.2018.02.058

Barber, J. (2009). Photosynthetic energy conversion: natural and artificial. *Chem. Soc. Rev.* 38, 185–196. doi: 10.1039/b802262n

Belbin, F. E., Noordally, Z. B., Wetherill, S. J., Atkins, K. A., Franklin, K. A., and Dodd, A. N. (2017). Integration of light and circadian signals that regulate chloroplast transcription by a nuclear-encoded sigma factor. *New Phytol.* 213, 727–738. doi: 10.1111/nph.14176

Benke, K., and Tomkins, B. (2017). Future food-production systems: vertical farming and controlled-environment agriculture. *Sustainability* 13, 13–26. doi: 10.1080/15487733.2017.1394054

Björkman, O., and Demmig-Adams, B. (1995). "Regulation of photosynthetic light energy capture, conversion, and dissipation in leaves of higher plants," in *BT – Ecophysiology of Photosynthesis*, Vol. 100, eds E.-D. Schulze and M. M. Caldwell (Berlin: Springer). doi: 10.1007/978-3-642-79354-7_2

Chen, X., Xue, X., Guo, W., Wang, L., and Qiao, X. (2016). Growth and nutritional properties of lettuce affected by mixed irradiation of white and supplemental light provided by light-emitting diode. *Sci. Horticult.* 200, 111–118. doi: 10.1016/j.scienta.2016.01.007

Clavijo-Herrera, J., Van Santen, E., and Gómez, C. (2018). Growth, water-use efficiency, stomatal conductance, and nitrogen uptake of two lettuce cultivars grown under different percentages of blue and red light. *Horticulturae* 4:16. doi: 10.3390/horticulturae4030016

De Mendiburu, F. (2020). *Package 'agricolae'*. Available online at: https://CRAN.R-project.org/package=agricolae (accessed June 7, 2020).

Dodd, A. N., Belbin, F. E., Frank, A., and Webb, A. A. R. (2015). Interactions between circadian clocks and photosynthesis for the temporal and spatial coordination of metabolism. *Front. Plant Sci.* 6:245. doi: 10.3389/fpls.2015.00245

Ferreres, F., Gil, M. I., Castañer, M., and Tomás-Barberán, F. A. (1997). Phenolic metabolites in red pigmented lettuce (Lactuca sativa). Changes with minimal processing and cold storage. *J. Agricult. Food Chem.* 45, 4249–4254. doi: 10.1021/jf970399j

Fox, J., Weisberg, S., Price, B., Adler, D., Bates, D., Baud-bovy, G., et al. (2020). *Package 'Car'*. Available online at: https://CRAN.R-project.org/package=car (accessed September 29, 2020).

Franklin, K. A., Toledo-Ortiz, G., Pyott, D. E., and Halliday, K. J. (2014). Interaction of light and temperature signalling. *J. Exp. Bot.* 65, 2859–2871. doi: 10.1093/jxb/eru059

Fu, W., Li, P., and Wu, Y. (2012). Effects of different light intensities on chlorophyll fluorescence characteristics and yield in lettuce. *Sci. Horticult.* 135, 45–51. doi: 10.1016/j.scienta.2011.12.004

Gómez, C., and Izzo, L. G. (2018). Increasing efficiency of crop production with LEDs. *AIMS Agricult. Food* 3, 135–153. doi: 10.3934/agrfood.2018.2.135

Haydon, M. J., Hearn, T. J., Bell, L. J., Hannah, M. A., and Webb, A. A. R. (2013). Metabolic regulation of circadian clocks. *Semin. Cell Dev. Biol.* 24, 414–421. doi: 10.1016/j.semcdb.2013.03.007

Hee, P., and Beom, L. (2001). Effects of CO2 concentration, light intensity and nutrient level on growth of leaf lettuce in a plant factory. *Acta Horticult.* 548, 377–383.

Hernández, R., Eguchi, T., Deveci, M., and Kubota, C. (2016). Tomato seedling physiological responses under different percentages of blue and red photon flux ratios using LEDs and cool white fluorescent lamps. *Sci. Horticult.* 213, 270–280. doi: 10.1016/j.scienta.2016.11.005

Herron, A. H. A., and Mauzerall, D. (1972). The development of photosynthesis in a greening mutant of chlorella and an analysis of the light saturation curve. *Plant Physiol.* 50, 141–148.

Huché-thélier, L., Crespel, L., Le, J., Morel, P., Sakr, S., and Leduc, N. (2016). Light signaling and plant responses to blue and UV radiations — Perspectives for applications in horticulture. *Environ. Exp. Bot.* 121, 22–38. doi: 10.1016/j.envexpbot.2015.06.009

Ilieva, I., Ivanova, T., Naydenov, Y., Dandolov, I., and Stefanov, D. (2010). Plant experiments with light-emitting diode module in Svet space greenhouse. *Adv. Space Res.* 46, 840–845. doi: 10.1016/j.asr.2010.05.009

Izzo, L. G., Arena, C., De Micco, V., Capozzi, F., and Aronne, G. (2019). Light quality shapes morpho-functional traits and pigment content of green and red leaf cultivars of Atriplex hortensis. *Sci. Horticult.* 246, 942–950. doi: 10.1016/j.scienta.2018.11.076

Johkan, M., Shoji, K., Goto, F., Hahida, S., and Yoshihara, T. (2012). Effect of green light wavelength and intensity on photomorphogenesis and photosynthesis in *Lactuca sativa*. *Environ. Exp. Bot.* 75, 128–133. doi: 10.1016/j.envexpbot.2011.08.010

Kaiser, E., Ouzounis, T., Giday, H., Schipper, R., Heuvelink, E., and Marcelis, L. F. M. (2019). Adding blue to red supplemental light increases biomass and yield of greenhouse-grown tomatoes, but only to an optimum. *Front. Plant Sci.* 9:2002. doi: 10.3389/fpls.2018.02002

Kang, J. H., Krishna Kumar, S., and Atulba, S. (2013). Light Intensity and photoperiod influence the growth and development of hydroponically grown leaf lettuce in a closed-type plant factory system. *Horticult. Environ. Biotechnol.* 54, 501–509. doi: 10.1007/s13580-013-0109-8

Kelly, N., Choe, D., Meng, Q., and Runkle, E. S. (2020). Promotion of lettuce growth under an increasing daily light integral depends on the combination of the photosynthetic photon flux density and photoperiod. *Sci. Horticult.* 272:109565. doi: 10.1016/j.scienta.2020.109565

Kim, S. J., Hahn, E. J., Heo, J. W., and Paek, K. (2004). Effects of LEDs on net photosynthetic rate, growth and leaf stomata of chrysanthemum plantlets in vitro. *Sci. Horticult.* 101, 143–151. doi: 10.1016/j.scienta.2003.10.003

Koyama, K., and Takemoto, S. (2014). Morning reduction of photosynthetic capacity before midday depression. *Sci. Rep.* 4, 1–6. doi: 10.1038/srep04389

Kozai, T. (2013). Resource use efficiency of closed plant production system with artificial light: concept, estimation and application to plant factory. *Proc. Jpn. Acad. Ser. B Phys. Biol. Sci.* 89, 447–461. doi: 10.2183/pjab.89.447

Kusuma, P., Pattison, P. M., and Bugbee, B. (2020). From physics to fixtures to food: current and potential LED efficacy. *Horticult. Res.* 7:56. doi: 10.1038/s41438-020-0283-7

Landi, M., Tattini, M., and Gould, K. S. (2015). Multiple functional roles of anthocyanins in plant-environment interactions. *Environ. Exp. Bot.* 119, 4–17. doi: 10.1016/j.envexpbot.2015.05.012

Lanoue, J., Zheng, J., Little, C., Thibodeau, A., Grodzinski, B., and Hao, X. (2019). Alternating red and blue light-emitting diodes allows for injury-free tomato production with continuous lighting. *Front. Plant Sci.* 10:1114. doi: 10.3389/fpls.2019.01114

Lee, S., Seo, J. M., Lee, M. K., Chun, J. H., Antonisamy, P., Arasu, M. V., et al. (2013). Influence of different LED lamps on the production of phenolic compounds in common and Tartary buckwheat sprouts. *Indust. Crops Product.* 54, 320–326. doi: 10.1016/j.indcrop.2014.01.024

Li, Q., and Kubota, C. (2009). Effects of supplemental light quality on growth and phytochemicals of baby leaf lettuce. *Environ. Exp. Bot.* 67, 59–64. doi: 10.1016/j.envexpbot.2009.06.011

Li, Z., Wakao, S., Fischer, B. B., and Niyogi, K. N. (2009). Sensing and responding to excess light. *Ann. Rev. Plant Biol.* 60, 239–260. doi: 10.1146/annurev.arplant.58.032806.103844

Lichtenthaler, H. K., Buschmann, C., and Rahmsdorf, U. (1980). "The Importance of blue light for the development of sun-type chloroplasts," in *The Blue Light Syndrome. Proceedings in Life Sciences*, ed. H. Senger (Berlin: Springer).

Maai, E., Nishimura, K., Takisawa, R., and Nakazaki, T. (2019). Light stress-induced chloroplast movement and midday depression of photosynthesis in sorghum leaves. *Plant Product. Sci.* 00, 1–10. doi: 10.1080/1343943X.2019.1673666

Matsuda, R., Ohashi-Kaneko, K., Fujiwara, K., Goto, E., and Kurata, K. (2004). Photosynthetic characteristics of rice leaves grown under red light with or without supplemental blue light. *Plant Cell Physiol.* 45, 1870–1874. doi: 10.1093/pcp/pch203

McCree, K. J. (1971). The action spectrum, absorptance and quantum yield of photosynthesis in crop plants. *Agricult. Meteorol.* 9, 191–216. doi: 10.1016/0002-1571(71)90022-7

Muggeo, V. M. R. (2003). Estimating regression models with unknown break-points. *Statistic. Med.* 22, 3055–3071. doi: 10.1002/sim.1545

Naznin, M. T., Lefsrud, M., Gravel, V., and Azad, M. O. K. (2019). Blue light added with red LEDs enhance growth characteristics, pigments content, and antioxidant capacity in lettuce, Spinach, Kale, Basil, and sweet pepper in a controlled environment. *Plants* 8:93. doi: 10.3390/plants8040093

Nogués, S., Allen, D. J. D., Morison, J. J. I. L., Baker, N. N. R., Nogués, S., Allen, D. J. D., et al. (1998). Ultraviolet-B radiation effects on water relations, leaf development, and photosynthesis in droughted pea plants. *Plant Physiol.* 117, 173–181. doi: 10.1104/pp.117.1.173

Ouzounis, T., Rosenqvist, E., and Ottosen, C. O. (2015). Spectral effects of artificial light on plant physiology and secondary metabolism: a review. *HortScience* 50, 1128–1135. doi: 10.21273/hortsci.50.8.1128

Pattison, P. M., Tsao, J. Y., Brainard, G. C., and Bugbee, B. (2018). LEDs for photons, physiology and food. *Nature* 563, 493–500. doi: 10.1038/s41586-018-0706-x

Pennisi, G., Blasioli, S., Cellini, A., Maia, L., Crepaldi, A., Braschi, I., et al. (2019). Unraveling the role of red: blue LED lights on resource use efficiency and nutritional properties of indoor grown sweet Basil. *Front. Plant Sci.* 10:305. doi: 10.3389/fpls.2019.00305

Poorter, H., Niinemets, U., Ntagkas, N., Siebenkas, A., Maenpaa, M., Matsubara, S., et al. (2019). A meta-analysis of plant responses to light intensity for 70 traits ranging from molecules to whole plant performance. *New Phytol.* 223, 1073–1105. doi: 10.1111/nph.15754

Rama Das, V. S. (2006). Photosynthesis. Regulation under varying light regimes. *Photosynthetica* 44:364. doi: 10.1007/s11099-006-0037-2

Reynolds, S. G. (1970). Gravimetric meth of soil moisture determination. *J. Hydrol.* 11, 258–273.

Robinson, S. A. (2001). Plant light stress. *Encycl. Life Sci.* 1, 1–5.

Ruban, A. V. (2009). Plants in light. *Comun. Interact. Biol.* 889, 50–55. doi: 10.4161/cib.2.1.7504

Schneider, C. A., Rasband, W. S., and Eliceiri, K. W. (2012). NIH Image to ImageJ: 25 years of image analysis. *Nat. Methods* 9, 671–675. doi: 10.1007/978-1-84882-087-6_9

Schreiner, M., Mewis, I., Huyskens-Keil, S., Jansen, M. A. K., Zrenner, R., Winkler, J. B., et al. (2012). UV-B-induced secondary plant metabolites – potential benefits for plant and human health. *Crit. Rev. Plant Sci.* 31, 229–240. doi: 10.1080/07352689.2012.664979

Son, K. H., Jeon, Y. M., and Oh, M. M. (2016). Application of supplementary white and pulsed light-emitting diodes to lettuce grown in a plant factory with artificial lighting. *Horticult. Environ. Biotechnol.* 57, 560–572. doi: 10.1007/s13580-016-0068-y

Son, K. H., and Oh, M. M. (2013). Leaf shape, growth, and antioxidant phenolic compounds of two lettuce cultivars grown under various combinations of blue and red light-emitting diodes. *HortScience* 48, 988–995. doi: 10.21273/hortsci.48.8.988

Steyn, W. J., Wand, S. J. E., Holcroft, D. M., and Jacobs, G. (2002). Anthocyanins in vegetative tissues: a proposed unified function in photoprotection. *New Phytol.* 155, 349–361. doi: 10.1046/j.1469-8137.2002.00482.x

Stutte, G. W., and Edney, S. (2009). Photoregulation of bioprotectant content of red leaf lettuce with light-emitting diodes. *HortScience* 9, 79–82.

Takahashi, S., and Badger, M. R. (2011). Photoprotection in plants: a new light on photosystem II damage. *Trends Plant Sci.* 16, 53–60. doi: 10.1016/j.tplants.2010.10.001

Taulavuoria, K., Hyökya, V., Oksanena, J., Taulavuoria, E., and Julkunen-Tiittob, R. (2016). Species-specific differences in synthesis of flavonoids and phenolic acids under increasing periods of enhanced blue light. *Environ. Exp. Bot.* 121, 145–150. doi: 10.1016/j.envexpbot.2015.04.002

Terashima, I., Fujita, T., Inoue, T., Chow, W. S., and Oguchi, R. (2009). Green light drives leaf photosynthesis more efficiently than red light in strong white light: revisiting the enigmatic question of why leaves are green. *Plant Cell Physiol.* 50, 684–697. doi: 10.1093/pcp/pcp034

Touliatos, D., Dodd, I. C., and Mcainsh, M. (2016). Vertical farming increases lettuce yield per unit area compared to conventional horizontal hydroponics. *Food Energy Secur.* 5, 184–191. doi: 10.1002/fes3.83

Tsormpatsidis, E., Henbest, R. G. C., Battey, N. H., and Hadley, P. (2010). The influence of ultraviolet radiation on growth, photosynthesis and phenolic levels of green and red lettuce: Potential for exploiting effects of ultraviolet radiation in a production system. *Ann. Appl. Biol.* 156, 357–366. doi: 10.1111/j.1744-7348.2010.00393.x

Wang, L. S., and Stoner, G. D. (2008). Anthocyanins and their role in cancer prevention. *Cancer Lett.* 269, 281–290. doi: 10.1016/j.canlet.2008.05.020

WHO-FAO (2004). Fruit and vegetable for health: report of a joint FAO/WHO workshop, 1-3 september 2004, Kobe, Japan. *Handbook Plant Food Phytochem.* 4, 105–137. doi: 10.1002/9781118464717.ch5

Wickham, H., Chang, W., Hermy, L., Pedersen, T. L., Takahashi, K., Wilke, C., et al. (2020). *Package 'ggplot2'*. Available Online at: https://CRAN.R-project.org/package=ggplot2 (accessed June 19, 2020).

Wilcox, J. K., Catignani, G. L., and Lazarus, C. (2003). Tomatoes and cardiovascular health. *Food Sci.* 43, 1–18.

Zhang, Y., Xu, S., Cheng, Y., Peng, Z., and Han, J. (2018). Transcriptome profiling of anthocyaninrelated genes reveals effects of light intensity on anthocyanin biosynthesis in red leaf lettuce. *PeerJ* 2018, 1–18. doi: 10.7717/peerj.4607

Zhu, H., Zhang, T. J., Zheng, J., Huang, X. D., Yu, Z. C., and Peng, C. L. (2018). Anthocyanins function as a light attenuator to compensate for insufficient photoprotection mediated by nonphotochemical quenching in young leaves of *Acmena acuminatissima* in winter. *Photosynthetica* 56, 445–454. doi: 10.1007/s11099-017-0740-1

Conflict of Interest: The authors declare that the research was conducted in the absence of any commercial or financial relationships that could be construed as a potential conflict of interest.

Copyright © 2020 Cammarisano, Donnison and Robson. This is an open-access article distributed under the terms of the Creative Commons Attribution License (CC BY). The use, distribution or reproduction in other forums is permitted, provided the original author(s) and the copyright owner(s) are credited and that the original publication in this journal is cited, in accordance with accepted academic practice. No use, distribution or reproduction is permitted which does not comply with these terms.

frontiers in Plant Science

ORIGINAL RESEARCH
published: 23 December 2020
doi: 10.3389/fpls.2020.599982

Regulation of Early Plant Development by Red and Blue Light: A Comparative Analysis Between *Arabidopsis thaliana* and *Solanum lycopersicum*

*Kiki Spaninks[1], Jelmer van Lieshout[1], Wim van Ieperen[2] and Remko Offringa[1]**

[1] Plant Developmental Genetics, Institute for Biology Leiden, Leiden University, Leiden, Netherlands, [2] Horticulture and Product Physiology Group, Wageningen University and Research, Wageningen, Netherlands

In vertical farming, plants are grown in multi-layered growth chambers supplied with energy-efficient LEDs that produce less heat and can thus be placed in close proximity to the plants. The spectral quality control allowed by LED lighting potentially enables steering plant development toward desired phenotypes. However, this requires detailed knowledge on how light quality affects different developmental processes per plant species or even cultivar, and how well information from model plants translates to horticultural crops. Here we have grown the model dicot *Arabidopsis thaliana* (Arabidopsis) and the crop plant *Solanum lycopersicum* (tomato) under white or monochromatic red or blue LED conditions. In addition, seedlings were grown *in vitro* in either light-grown roots (LGR) or dark-grown roots (DGR) LED conditions. Our results present an overview of phenotypic traits that are sensitive to red or blue light, which may be used as a basis for application by tomato nurseries. Our comparative analysis showed that young tomato plants were remarkably indifferent to the LED conditions, with red and blue light effects on primary growth, but not on organ formation or flowering. In contrast, Arabidopsis appeared to be highly sensitive to light quality, as dramatic differences in shoot and root elongation, organ formation, and developmental phase transitions were observed between red, blue, and white LED conditions. Our results highlight once more that growth responses to environmental conditions can differ significantly between model and crop species. Understanding the molecular basis for this difference will be important for designing lighting systems tailored for specific crops.

Keywords: tomato, *Arabidopis thaliana*, LED lighting, growth, development, R/B light ratio, floral transition

OPEN ACCESS

Edited by:
Eiji Goto,
Chiba University, Japan

Reviewed by:
Paolo Bonini,
Ngalab, Spain
Pradeep Kumar,
Central Arid Zone Research Institute (ICAR), India

***Correspondence:**
Remko Offringa
r.offringa@biology.leidenuniv.nl

Specialty section:
This article was submitted to Crop and Product Physiology, a section of the journal Frontiers in Plant Science

Received: *28 August 2020*
Accepted: *02 December 2020*
Published: *23 December 2020*

Citation:
Spaninks K, van Lieshout J, van Ieperen W and Offringa R (2020) Regulation of Early Plant Development by Red and Blue Light: A Comparative Analysis Between Arabidopsis thaliana and Solanum lycopersicum. Front. Plant Sci. 11:599982. doi: 10.3389/fpls.2020.599982

INTRODUCTION

To ensure optimal plant performance in horticultural crops, it is required to understand how growth and development are affected by environmental factors. Light is a key environmental factor that not only affects the available sugars through photosynthesis, but also steers development through processes such as photomorphogenesis, phototropism, and shade avoidance (Nemhauser and Chory, 2002; Goyal et al., 2013; Ballaré and Pierik, 2017). Studies have shown that light

intensity can be used to modulate plant growth and ultimately yield in different species (Smeets and Garretsen, 1986; Zhou et al., 2009; Lu et al., 2017; Viršilė et al., 2019). Aside from its intensity, the spectral quality of light influences plant development by activating different families of photoreceptors that can detect light, ranging from UV-B to far-red. Blue light-activated receptor families include cryptochromes (CRYs) (Yu et al., 2010), phototropins (Christie, 2007), and Zeitlupes (ZTLs) (Suetsugu and Wada, 2013), whereas phytochromes (PHYs) respond to red and far-red light (Galvão and Fankhauser, 2015). Many artificial lights that are used in horticulture try to loosely mimic the spectrum of sunlight by including fractions of all the spectral colors. However, the development of LED technology has created new possibilities for spectral control that may lead to more energy efficient and economic lighting. For example, matching the LED spectral output to specific photoreceptor families can ensure optimal plant performance without wasting energy on non-productive wavelengths. Aside from spectral control, LEDs are more energy-efficient than traditional artificial lighting systems and are less detrimental to the environment when discarded, since they contain no toxic metals such as mercury (Morrow, 2008). Finally, LEDs produce less heat and are thus suitable for application in multi-layered vertical farming (SharathKumar et al., 2020).

To implement LED lighting in horticulture it is important to understand how the different colors in the spectrum influence all aspects of plant growth and development. Furthermore, developmental effects of specific LED spectra have been shown to vary between species (Dougher and Bugbee, 2001), suggesting that there are optimal light recipes for different species and even for different ecotypes or cultivars within these species. So far, most studies on spectral properties of light have focused on changes in the red/far-red (R/FR) ratio within the spectrum. At the top of the canopy, R/FR ratios are high, whereas low R/FR fractions are found lower in the canopy (Ballaré et al., 1990). In *Solanum lycopersicum* (tomato), LEDs have been used to add extra far-red light to the spectrum to study shade avoidance (Schrager-Lavelle et al., 2016), plant growth and yield (Ji et al., 2019; Kalaitzoglou et al., 2019) and vitamin production (Ntagkas et al., 2019) among others. Aside from studying R/FR ratios, LED lights can be used to study plant development in response to monochromatic light (red, far-red, yellow, green, or blue) or differential red/blue (R/B) light ratios. So far, most of these studies have been performed in crop species. For example, in tomato, light quality has been found to influence leaf development, assimilates, gas exchange, and biomass (Fan et al., 2013; Lanoue et al., 2017, 2018). However, most of these studies have focused on one crop species, one wavelength, or only on one developmental trait. Moreover, photoreceptor function and downstream pathways have been studied extensively in *Arabidopsis thaliana* (Arabidopsis) (Wang et al., 2016; Lim et al., 2018; Schumacher et al., 2018), but only a small fraction of these pathways have been investigated in commercial crops. In contrast, many light-induced physiological traits have been studied in different crops (Kaiser et al., 2019; Pennisi et al., 2019; Song et al., 2019) but not in Arabidopsis.

Here we performed a comparative analysis between the commercial crop tomato and the genetic model dicot Arabidopsis, studying how monochromatic red or blue LED lighting, compared to white LED lighting, affects early plant development in these species by monitoring several morphological and developmental traits. Although monochromatic red or blue conditions are unlikely to be used in horticulture, this set-up allowed us to obtain more insights into the wavelength-specific effects on plant traits compared to when using different R/B light ratios. Our analyses showed that monochromatic red or blue LED treatments resulted in significant differences in primary growth of both Arabidopsis and tomato, when compared to white LED conditions. However, whereas red and blue light could be used to steer developmental phase transitions in Arabidopsis, in tomato these traits appeared to be surprisingly indifferent to the type of LED treatment. Our results offer an overview of phenotypic traits in young plants that are regulated by red or blue light, and also provide new insights in the conservation and divergence of these traits with respect to their light sensitivity between two plant species from different families.

MATERIALS AND METHODS

Growth Conditions and LED Treatments

In all experiments, plants were grown at a 16 h photoperiod, under white, deep red, or blue Philips Greenpower LED research modules (Signify B.V., Eindhoven, Netherlands) with a measured photon flux density of 120 ± 10 μmol $m^{-2}s^{-1}$ at the top of the canopy, a temperature of 21°C, and 70% relative humidity. The percentages of blue, green, red, and far-red wavelengths for the different LED modules are listed in **Supplementary Table S1**. Experiments with the different LED treatments were performed simultaneously in the same growth chamber in separate compartments enclosed by white plastic screens with a proximal distance of 50 cm to the plants. For *in vitro* analysis of seedling development, two different light treatments were used in all three LED conditions: (1) seedlings were grown completely exposed to light (light-grown roots or LGR); or (2) seedlings were grown in a more "natural" light environment with shoots exposed to light and roots shielded from light using black paper covers (dark-grown roots or DGR) (based on Silva-Navas et al., 2015).

Plant Lines and Seed Germination

Arabidopsis wild-type ecotypes Columbia (Col-0) and Landsberg *erecta* (L*er*) and tomato cultivar Moneymaker (MM) and the commercial hybrid Foundation (FO) were used in all experiments. This study includes both *in vitro* experiments where seedlings were grown on sterile growth medium as well as experiments where the plants were grown on soil. For *in vitro* experiments, Arabidopsis and tomato seeds were surface sterilized by incubating for 1 min in 70% ethanol and 10 min in a 2-fold diluted commercial bleach solution (1% chlorine). Subsequently the seeds were washed five times with sterile water. Arabidopsis seeds were stratified for 5 days at 4°C in

darkness and germinated on square plates (#688102, Greiner Bio-One™) containing MA medium (Masson and Paszkowski, 1992) supplemented with 1% (w/v) sucrose and 0.8% (w/v) Daishin agar. For efficient and simultaneous germination, plates with Arabidopsis seeds were placed vertically in white light for 1 day and then moved to the LED conditions (**Supplementary Figure S1A**). Sterile tomato seeds were placed on sterilized, wet Whatman filter paper using forceps. Tomato seeds showed optimal germination in darkness (**Supplementary Figure S1B**) and were therefore kept in darkness at 21°C until 5 days after sowing. Geminated seeds were moved from the filter to square plates containing solid MA medium and placed vertically in the LED conditions. For *on soil* experiments, Arabidopsis seeds were sown on the soil surface and stratified for 5 days at 4°C in darkness. Subsequently the seeds were moved to white light to allow simultaneous germination. After 1 day in white light, the pots were placed in the LED conditions. Tomato seeds were placed approximately 2 cm under the soil surface and pots were directly placed in the LED conditions. The age of tomato plants was therefore expressed as days after sowing (DAS), instead of days after germination (DAG) used for Arabidopsis.

In vitro Analysis of Seedling Development

At 7 days after germination (DAG), Arabidopsis seedlings were photographed, and primary root length and hypocotyl length were measured. Tomato seedlings were photographed at 5 DAG for primary root length and hypocotyl length measurements. All measurements were performed with ImageJ (Fiji) (Schindelin et al., 2012). The shoot-root ratio was calculated based on the measured primary root length and hypocotyl length. At 14 DAG, Arabidopsis seedlings were photographed, and the number of emerged lateral roots was counted using binoculars. Lateral roots could not be counted for tomato since tomato seedlings older than 6 DAG outgrew the square plates.

Analysis of Leaf Appearance and Morphology

The leaf appearance rate was measured throughout the experiment once or twice per week for tomato and Arabidopsis, respectively. Leaves were counted from the moment they were visible by eye. For Arabidopsis, the plants were grown until bolting. At this time, the rosettes were photographed and rosette surface area (RSA) was measured. Individual rosette leaves were removed and photographed separately for length and width measurements of the leaf blade. Length/width ratio of rosette leaves was calculated based on these measurements. For tomato plants, compound leaves were removed at 45 DAS and photographed individually. Leaf surface area was measured for leaf #4 (fully developed, mature leaf) and leaf #6 (developing, young leaf). All of these measurements were performed with ImageJ (Fiji) (Schindelin et al., 2012).

Analysis of Flowering Time

Arabidopsis flowering time was measured in number of days until bolting, or until the moment that the first flower buds were visible by eye. For tomato measurements, toothpicks were used to carefully push aside the young leaves from the apex. Flowering time was determined as the day on which small inflorescences became visible near the shoot apex. Individual plants were photographed at 1 week after bolting for Arabidopsis and 30 DAS for tomato.

Analysis of Stem Development

After Arabidopsis plants became reproductive, plant height measurements commenced. Plant height was measured twice a week until termination of the primary inflorescence meristem. At this time point, individual plants were photographed and the number of branches from the primary inflorescence were counted. Branches were categorized into primary shoots, secondary shoots and tertiary shoots, as previously described (Li et al., 2017). For tomato plants, hypocotyl length, epicotyl length and stem length were measured once a week until 45 DAS. At this time point, individual plants were photographed.

Statistical Analysis and Figures

All experiments were performed with 20 or 30 biologically independent plants for tomato or Arabidopsis, respectively. For destructive measurements, 10 representative biological replicates were used. Data was obtained from either two or three independent experiments for *on soil* or *in vitro* experiments, respectively. Measurements under different LED conditions, or comparing different ecotypes or cultivars, were statistically analyzed using a one-way ANOVA followed by a Tukey's honestly significant different (HSD) *post hoc* test. When comparing results from monochromatic (red or blue) with white (control) LED conditions, a two-sided Student's *t*-test was used. For *in vitro* experiments, LGR and DGR treatments using the same LED condition were also compared using a two-sided Student's *t*-test. All measurements were plotted into graphs using GraphPad Prism 5 software. In the graphs, the colors of the dots, bars and lines indicate white, red, and blue LED conditions. All photographs were taken with a Nikon D5300 camera and edited in ImageJ (Fiji). Final figures were assembled using Microsoft PowerPoint.

RESULTS

Red and Blue Light Influence *in vitro* Development of Arabidopsis and Tomato Seedlings

Arabidopsis and tomato seedlings were grown in white, red, or blue LED conditions with either light-grown roots (LGR) or dark-grown roots (DGR). Treatment with monochromatic red or blue light strongly affected seedling growth of Arabidopsis ecotypes Col-0 (**Figure 1A**) and L*er* (**Supplementary Figure S4A**) and tomato cultivars MM (**Figure 1B**) and FO (**Supplementary Figure S5A**). Hypocotyl growth was strongly enhanced in red light and reduced in blue light compared to white light, in both Arabidopsis and tomato seedlings grown either in DGR (**Figure 1C**) or LGR (**Supplementary Figures S2A,C**)

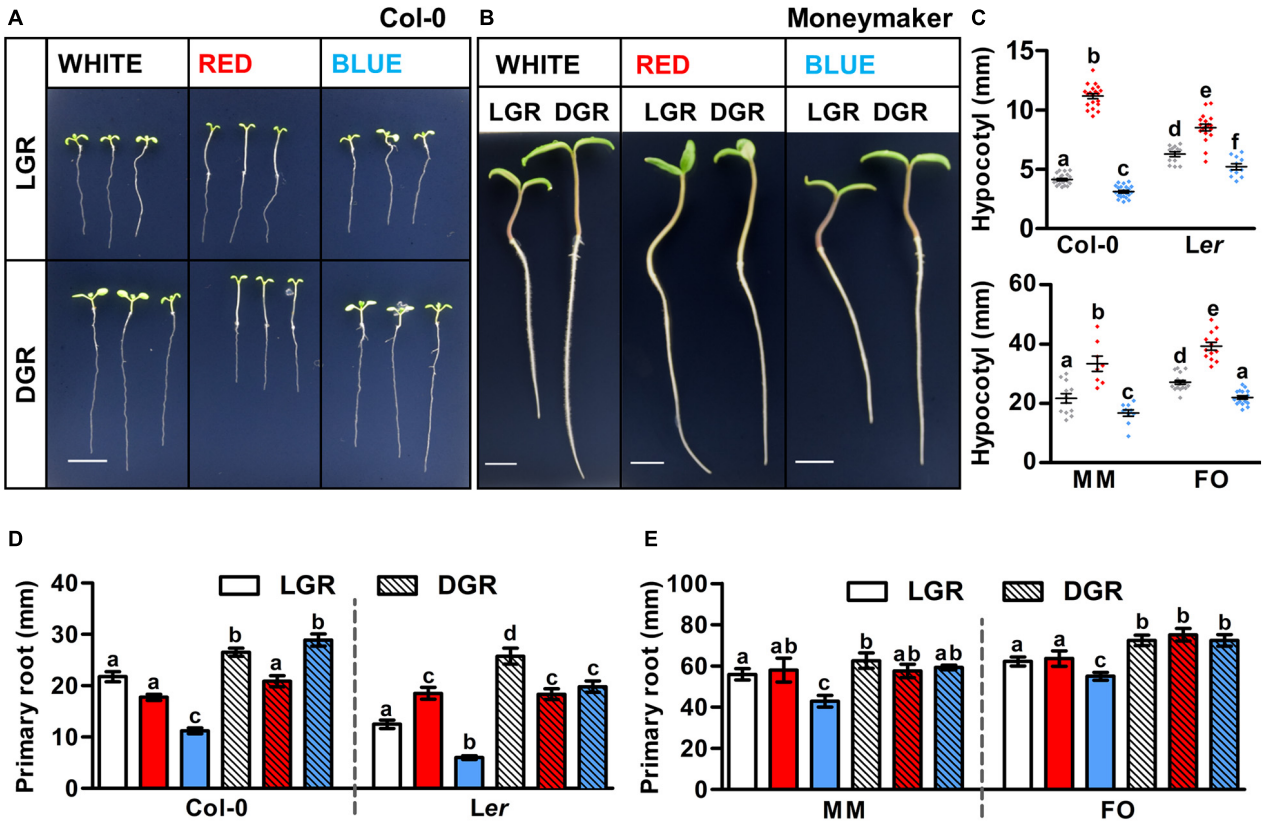

FIGURE 1 | The effect of red and blue light on primary growth of Arabidopsis and tomato seedlings. **(A,B)** Representative 7 day old Arabidopsis and 5 day old tomato seedlings grown in white, red, or blue LED conditions. Seedlings of Arabidopsis ecotype Columbia (Col-0) **(A)** and tomato cultivar Moneymaker (MM) **(B)** were grown in light-grown roots (LGR) and dark-grown roots (DGR) LED conditions. For presentation purposes, seedlings were transferred to black agarose plates before photographing. Scale bars indicate 1 cm. **(C–E)** Quantification of the hypocotyl length of DGR seedlings **(C)** and the primary root length of LGR and DGR seedlings **(D,E)** of Arabidopsis ecotypes Col-0 and Landsberg *erecta* (L*er*) and tomato cultivars MM and Foundation (FO) as shown in (**A,B**, and **Supplementary Figures S4A**, **S5A**), respectively. LED conditions and ecotypes or cultivars were compared using a one-way ANOVA followed by a Tukey's test (letters a–f indicate statistically significant differences values, $p < 0.05$) in **(C–E)**. Error bars represent standard error of the mean in **(C–E)** ($n = 30$). Similar results were obtained in three independent experiments.

conditions, making it the most conserved trait regulated by light quality. Red- or blue light-induced alterations of primary root growth were only partially conserved between the two species. In both Arabidopsis (**Figure 1D**) and tomato (**Figure 1E**), seedlings grown in monochromatic blue LGR conditions had shorter roots than in white LGR conditions, whereas there was no difference between blue and white DGR conditions (with the exception of L*er* DGR seedlings). This suggests that blue light inhibits root growth locally, and not through shoot-to-root signaling. In monochromatic red light, Arabidopsis, but not tomato seedlings, showed reduced primary root growth compared to white light in DGR conditions, but not in LGR conditions (**Figures 1D,E**), suggesting that in Arabidopsis red LED conditions hamper root growth by shoot-to-root signaling. In conclusion, our results show that *in vitro* growth of both Arabidopsis and tomato seedlings can be altered by light quality. The local effect of light quality on primary root, and hypocotyl growth seems conserved between these two species, whereas the effect of light quality mediated by shoot-to-root signaling seems more species- or cultivar-dependent. In addition, our results suggest that light conditions with higher rather than lower R/B ratios, and dark-grown roots are optimal for *in vitro* seedling development.

Red Light Promotes Shoot Elongation in Arabidopsis and Young Tomato Plants

The height of a plant determines its ability to compete for light and therefore often correlates with leaf mass, seed production and longevity among others (Moles et al., 2009). For monopodial species such as Arabidopsis, stem growth is initiated once the plant becomes reproductive and continues until termination of the inflorescence meristems (IMs) (Schmitz and Theres, 1999). To investigate if shoot elongation can be modulated by light quality, Arabidopsis plants were grown in white, red, or blue LED conditions, until termination of the primary IM (Col-0: **Figure 2A** and L*er*: **Supplementary Figure S4E**). At this time, plant height of Col-0 and L*er* ecotypes was significantly reduced in blue light and increased in red light, compared to white light (**Figure 2C**). In a series of weekly measurements, we observed that the primary IM of plants grown in monochromatic blue or

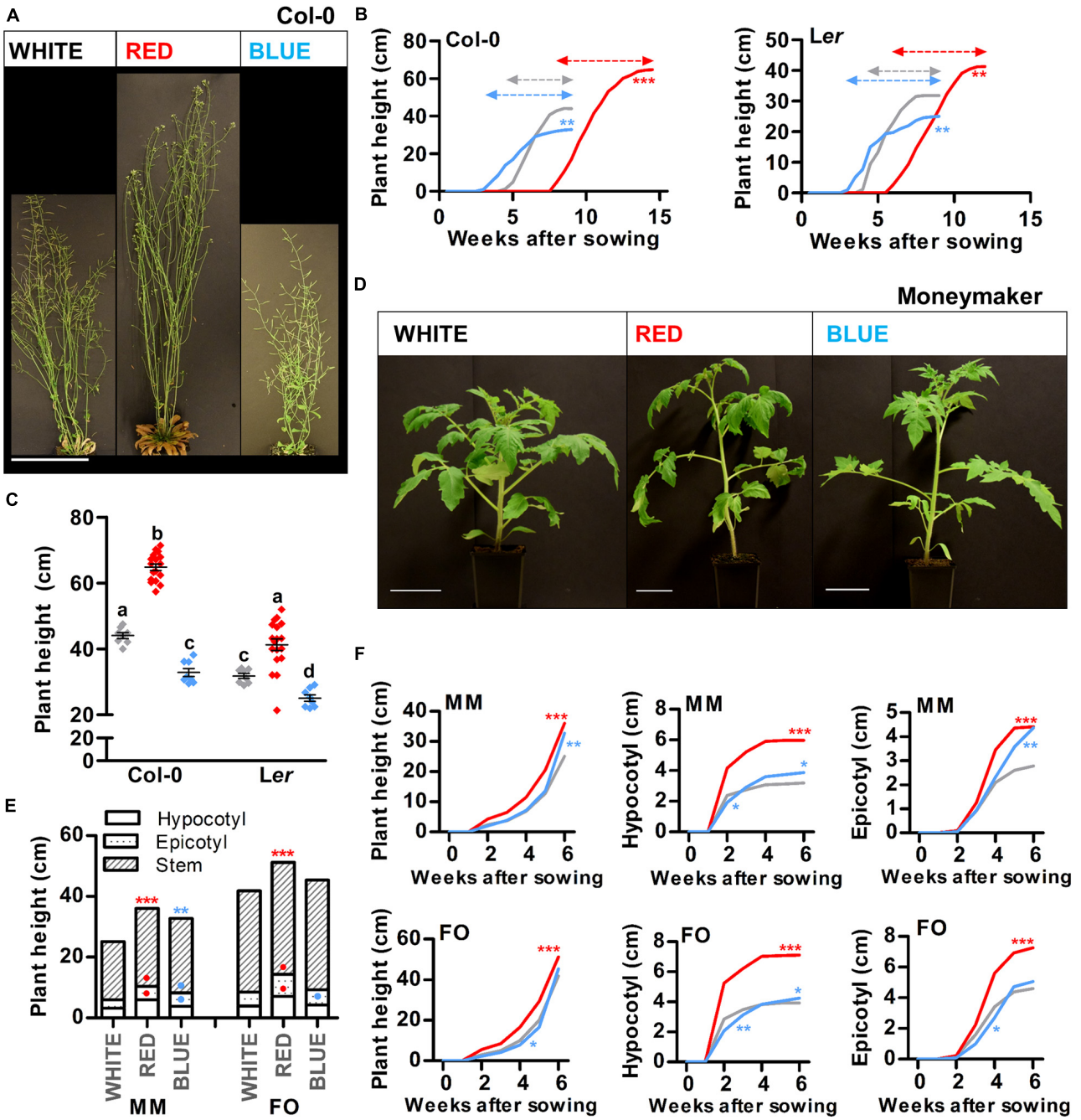

FIGURE 2 | Red light promotes shoot growth in Arabidopsis and young tomato plants. **(A)** Representative Arabidopsis Columbia (Col-0) plants grown in white, red, or blue LED conditions until 4 weeks after bolting. **(B,C)** Quantification of the plant height over time **(B)** or the plant height after termination of the primary inflorescence **(C)** of Arabidopsis Col-0 or Landsberg *erecta* (*Ler*) plants as shown in (**A** and **Supplementary Figure S4E**), respectively. **(D)** Representative tomato Moneymaker (MM) plants grown in white, red, or blue LED conditions until 45 days after sowing (DAS). **(E,F)** Quantification of the plant height at 45 DAS **(E)**, or the plant height, hypocotyl length, or epicotyl length over time **(F)** of tomato MM or Foundation (FO) plants as shown in (**D** and **Supplementary Figure S5D**), respectively. LED conditions and ecotypes or cultivars were compared using a one-way ANOVA followed by a Tukey's test (letters a–d indicate statistically significant differences, $p < 0.05$) in **(C)**. In **(B,E,F)**, monochromatic LED conditions (red or blue) were compared to white (control) using a two-sided Student's *t*-test (asterisks indicate significant differences ($p < 0.05$) in time series in **(B,F)**, or in plant height in **(E)**, bullets indicate significant differences ($p < 0.05$) in hypocotyl or epicotyl length in **(E)**. Error bars represent standard error of the mean in **(C),** standard errors for **(B,E,F)** are listed in **Supplementary Table S2** ($n = 20$). Dashed arrows in **(B)** represent the time from bolting until termination of the primary inflorescence. For presentation purposes, pots were placed in front of a black background in **(A,D)** before photographing. Scale bars indicate 10 cm in **(A)**, and 5 cm in **(D)**. Similar results were obtained in two independent experiments.

red light produced flowers for approximately 6 weeks, whereas in white light grown plants the primary IM terminated after approximately 5 weeks (**Figure 2B**, dashed arrows). This slight extension of the reproductive phase in blue light compared to white light, indicated that the reduction of plant height in blue light is caused by reduced elongation of the shoot, and not by a shorter growth phase. In contrast, the elongated plants in red light might be caused by both enhanced elongation growth, and the extended reproductive phase, when compared to white light. As a sympodial plant, tomato initiates stem growth already during the vegetative growth phase (Schmitz and Theres, 1999). To investigate shoot elongation of tomato plants grown in white, red, or blue LED conditions, we measured hypocotyl length, epicotyl length and stem length (from epicotyl to SAM) every week for up to 45 days after sowing (DAS). At 45 DAS, red light grown plants of both cultivars were taller than white light grown plants (MM and FO: **Figures 2D–F** and **Supplementary Figure S5D**). Also at earlier timepoints, tomato plants grown in red light had a significantly longer hypocotyl, epicotyl, and stem than white light grown plants (**Figure 2F**). At 45 DAS, MM plants grown in blue light were significantly taller than those grown in white light (**Figures 2D,E**), whereas FO plants only showed a significant increase in hypocotyl length in blue light (**Figure 2E** and **Supplementary Figure S5D**). However, during our weekly measurements we observed that, at earlier time points (mainly before the appearance of inflorescence meristems), blue light grown plants of both cultivars had shorter hypocotyls, epicotyls and stems compared to white light grown plants (**Figure 2F**). This shows that, in tomato, the effects of monochromatic blue light treatment on shoot elongation are dependent on both cultivar and developmental stage. Taken together, our results show that the enhanced shoot elongation in monochromatic red LED conditions is conserved between Arabidopsis and tomato, whereas the effect of monochromatic blue light seems to vary between species and cultivars.

Monochromatic Red Light Promotes Shoot Growth and Inhibits Root Branching in Arabidopsis

In nature, the balance between shoot growth to increase photosynthetic capacity, and root growth to compete for soil nutrients is tightly controlled and dependent on the growth conditions and nutrient and water availability (Puig et al., 2012). In greenhouses, however, the growth conditions and availability of water and nutrients are generally good, making development of the root system less relevant. As a result, plant breeders of fruit-producing species have spent decades to optimize the growth and development of above-ground organs (Van der Ploeg et al., 2007), often at the cost of root development. In our *in vitro* experiments, monochromatic red conditions, either LGR or DGR, significantly enhanced the shoot-root ratio of both Arabidopsis and tomato seedlings (**Figure 3A** and **Supplementary Figures S2B,D**). A mildly opposite effect was observed in seedlings grown under monochromatic blue LED DGR conditions (**Figure 3A**). In LGR conditions, however, Arabidopsis seedlings showed a slightly increased shoot-root ratio (**Supplementary Figures S2B,D**), which is most likely the result of the strong local inhibition of primary root growth in monochromatic blue light (**Figures 1D,E**). This suggests that the balance between shoot and root elongation in Arabidopsis and tomato seedlings can be controlled by the R/B light ratio in the spectrum. Interestingly, analysis of the number of branches on the primary Arabidopsis inflorescence showed that bud formation from axillary meristems is greatly enhanced in red light compared to white light conditions (**Figure 3B**). In contrast, red light grown Arabidopsis seedlings showed a significant decrease in lateral root density compared to those grown in white light, in both LGR and DGR conditions (**Figure 3C** and **Supplementary Figure S3**). In monochromatic blue light, branching of the primary inflorescence was significantly reduced compared to white light (**Figure 3B**). The lateral root density of blue light DGR Arabidopsis seedlings was unaffected (**Figure 3C** and **Supplementary Figure S3**), but was increased in LGR seedlings, most likely as a result of primary root growth inhibition in blue LGR conditions (**Figures 1D,E**, **3C**). To summarize, our results show that Arabidopsis plants grown in monochromatic red LED conditions show increased shoot elongation and branching, and decreased root branching compared to white light grown plants. In contrast, the effect of monochromatic blue light is relatively mild, except for the strong inhibitory effect on root growth in LGR conditions. Tomato plants show the same increased shoot-root ratio in monochromatic red compared to white light, and a similar mild effect of monochromatic blue light, but the effects of red light on lateral organ formation in tomato shoots and roots remain to be determined.

Developmental Phase Transitions in Arabidopsis Are Promoted by Blue Light and Delayed by Red Light

To ensure a high yield in crops, it is important that leaves are produced at an optimal rate and that the morphology of the leaf allows for optimal exposure to light (Mathan et al., 2016). Moreover, optimizing the timing of flowering is crucial to ensure either a long vegetative phase (for leaf production in crop species such as lettuce or cabbage) or a short vegetative phase (for rapid breeding cycles or for fruit-producing species such as tomato). Previous studies that used light filters or continuous lighting indicated that developmental phase transitions in Arabidopsis can be modulated by light quality (Eskins, 1992; Guo et al., 1998). To investigate if similar phenotypes could be obtained using a LED setup with a 16/8 h day/night cycle, Arabidopsis plants were grown on soil in white, red, or blue LED conditions. In monochromatic blue light, the rosette size, expressed as rosette surface area (RSA), was greatly reduced, whereas white light grown plants showed a regular rosette development, and monochromatic red light grown plants developed large rosettes resembling those of Arabidopsis plants grown in short-day conditions (**Figures 4A,B** and **Supplementary Figure S4B**; Brandt et al., 2018). Both the increase of RSA in red LED conditions and the decrease of RSA in blue LED conditions correlated with significant changes in the timing of the plant's floral transition (Col-0: **Figures 4C–E**

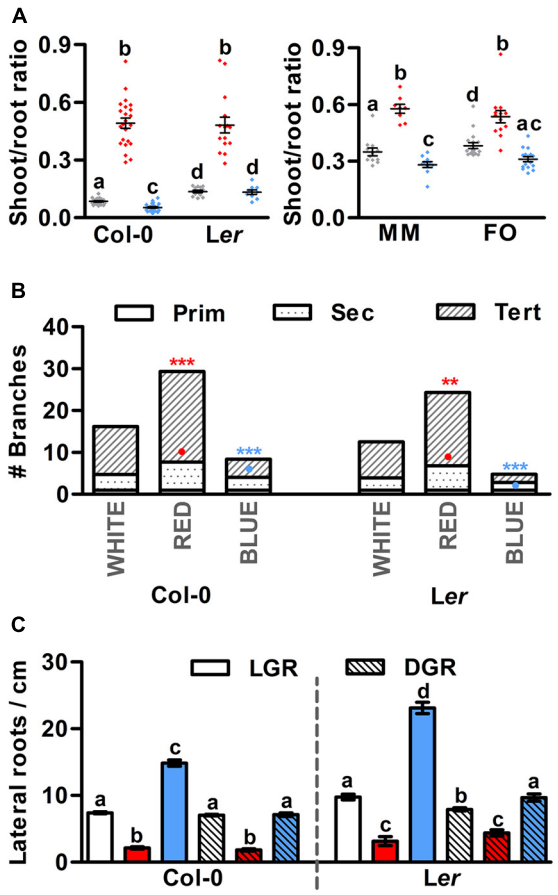

FIGURE 3 | Monochromatic red light promotes shoot growth and inhibits root branching in Arabidopsis. **(A)** Shoot-root ratio of 7 day old Arabidopsis seedlings (left) and 5 day old tomato seedlings (right), grown in white, red, or blue LED conditions. Arabidopsis ecotypes Columbia (Col-0) and Landsberg *erecta* (L*er*), and tomato cultivars Moneymaker (MM) and Foundation (FO) were grown in dark-grown roots (DGR) LED conditions. **(B)** Number of primary (Prim), secondary (Sec) and tertiary (Tert) branches from the primary inflorescence of Arabidopsis Col-0 and L*er* plants grown in LED conditions until termination of the primary inflorescence. **(C)** Lateral root density of 14-day old Col-0 and L*er* seedlings grown in light-grown roots (LGR) and DGR LED conditions. Graph colors represent the LED conditions in **(A,C)**. LED conditions and ecotypes or cultivars were compared using a one-way ANOVA followed by a Tukey's test (letters a–d indicate statistically significant differences, $p < 0.05$) in **(A**,**C)**. In **(B)**, monochromatic LED conditions (red or blue) were compared to white (control) using a two-sided Student's *t*-test [bullets indicate significant differences in secondary branches ($p < 0.05$), asterisks indicate significant differences in tertiary branches (***$p < 0.001$, **$p < 0.01$)]. Error bars represent standard error from mean in **(A,C)** ($n = 30$), standard errors for **(B)** are listed in **Supplementary Table S2** ($n = 20$). Similar results were obtained in three **(A,C)** or two **(B)** independent experiments.

and L*er*: **Supplementary Figure S4D**). Col-0 and L*er* plants that were grown in blue light produced a limited number of rosette leaves as they flowered extremely early, whereas plants that were grown in red light developed many rosette leaves during an extended vegetative phase due to late flowering (**Figures 4D,E**). In Arabidopsis, the floral transition is preceded by the juvenile-to-adult or vegetative phase transition, the occurrence of which can be determined by leaf heteroblasty. Juvenile leaves consist of a round leaf blade with a long petiole, with a length/width ratio of approximately 1, whereas adult leaves have a more serrated leaf blade with a short petiole, and with a length/width ratio of approximately 1.7 (Telfer et al., 1997). Based on their length/width ratio, leaves of blue light grown plants seemed to mature significantly faster, although in L*er*, no completely adult leaves were formed before the plants switched to the reproductive phase (Col-0: **Figure 4F** and L*er*: **Supplementary Figure S4C**). In red light grown plants, the timing of the vegetative phase changes did not differ significantly from that of white light grown plants, suggesting that, in contrast to the reproductive phase transition, the vegetative phase transition was not delayed by the monochromatic red light treatment. Altogether, our results show that especially the floral transition but also the vegetative phase transition in Arabidopsis are sensitive to light quality and can thus be modulated not only by day length but also by the R/B light ratio in the spectrum.

Developmental Phase Transitions in Tomato Are Indifferent to the R/B Light Ratio

To investigate if developmental phase transitions can be modulated by red and blue light in tomato as well, MM and FO plants were grown on soil in white, red, or blue LED conditions until the start of the reproductive phase, which was defined as the moment that the first inflorescences appeared near the shoot apex (**Figure 5A**). MM and FO plants became reproductive at approximately 30 and 32 DAS, respectively, in all three LED conditions (**Figure 5B**). In addition, the appearance rate of new compound leaves was the same in all three LED conditions and in both cultivars (**Figure 5C**). These results are in contrast to our observations in Arabidopsis and imply that developmental phase shifts in tomato are completely indifferent to the R/B light ratio. To investigate the sensitivity of tomato leaf morphology to red and blue light, MM and FO plants were grown in the three different LED conditions until 45 DAS. We used leaf #4 as a representative for fully developed leaves (MM: **Figure 5D** and FO: **Supplementary Figure S5B**), and leaf #6 as a representative for young, not fully developed leaves (MM: **Figure 5E** and FO: **Supplementary Figure S5C**) for leaf surface area (LSA) measurements. The LSA of leaf #4 was similar for plants grown in white and blue LED conditions (**Figure 5F**). However, leaf #6 of blue light grown FO plants showed a decreased LSA, which is most likely a result of a slight delay in leaf development specific for this cultivar, and not a true effect of monochromatic blue light on leaf morphology. In contrast, monochromatic red LED conditions led to a significant decrease in LSA of leaf #4 in both cultivars (**Figure 5F**). Moreover, leaves of plants grown in red light showed epinasty (**Figures 5D,E** and **Supplementary Figures S5B,C**), thus further reducing the effective LSA for photosynthesis. In conclusion, light quality does have an effect on leaf morphology, and may alter photosynthetic capacity in tomato. However, these changes in leaf morphology do not influence the formation rate of new leaves or flowering time. Although developmental phase transitions in Arabidopsis are

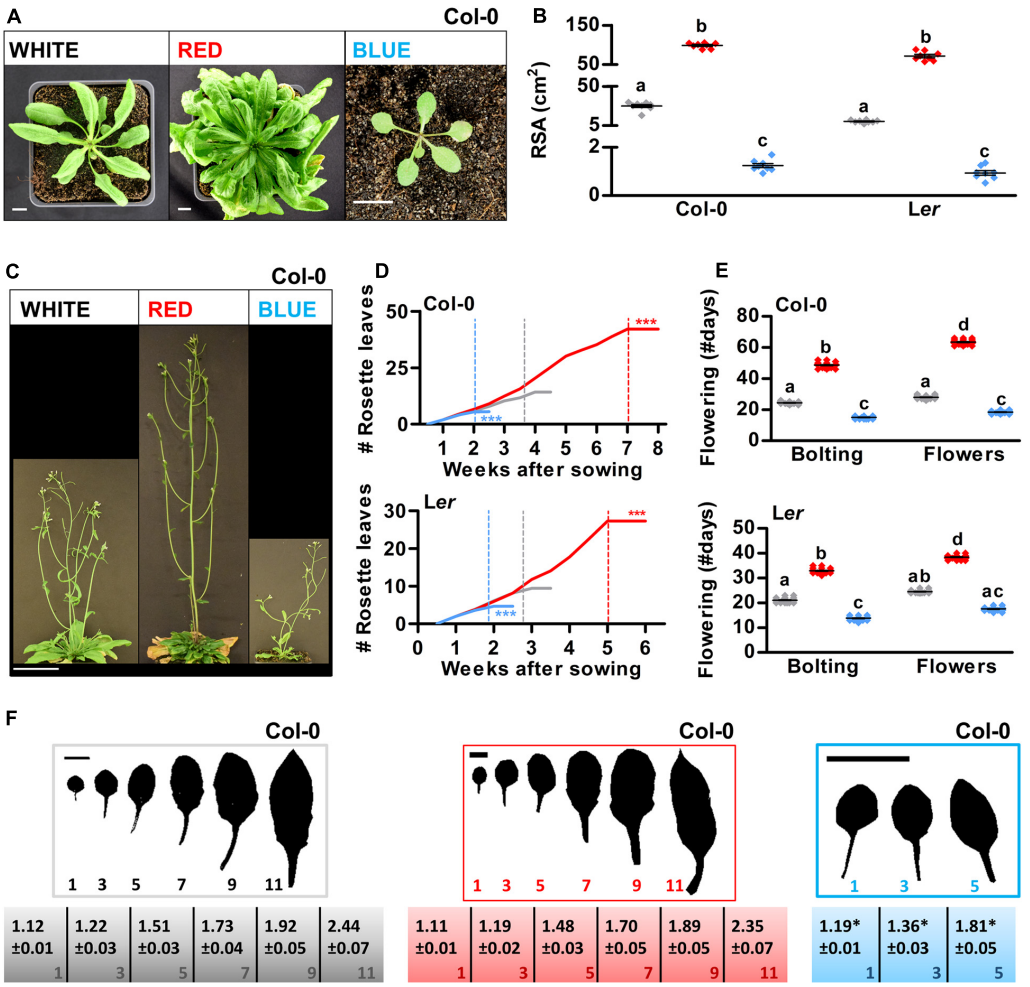

FIGURE 4 | Developmental phase transitions in Arabidopsis are promoted by blue light and delayed by red light. **(A)** Rosette phenotype of representative Arabidopsis plants of ecotype Columbia (Col-0) grown in white, red, or blue LED conditions. **(B)** Quantification of rosette surface area (RSA) of Col-0 or Landsberg *erecta* (*Ler*) plants as shown in (**A** and **Supplementary Figure S4B**), respectively. **(C)** Representative Arabidopsis Col-0 plants grown in LED conditions until 1 week after flowering. **(D)** Rosette leaf appearance in Col-0 and *Ler* plants over time. **(E)** Flowering time (until bolting, or until the appearance of flower buds) of Col-0 and *Ler* plants in number of days. **(F)** Rosette leaves of representative Col-0 plants and length/width ratios of the leaf blade (± SE, $n = 10$). Scale bars represent 1 cm in **(A**,**F)**, and 10 cm in **(C)**. Graph colors represent the LED conditions in **(B,D,E)**. LED conditions and ecotypes were compared using a one-way ANOVA followed by a Tukey's test (letters a–d indicate statistically significant differences, $p < 0.05$) in **(B,E)**. In **(D,F)**, monochromatic LED conditions (red or blue) were compared to white (control) using a two-sided Student's *t*-test [asterisks indicate significant differences ($*p < 0.05$, $***p < 0.001$)]. Error bars represent standard error of the mean in **(B,E)** ($n = 30$), standard errors for **(D)** are listed in **Supplementary Table S2** ($n = 30$). Dashed lines in **(D)** represent the time of bolting. Similar results were obtained in two independent experiments.

highly sensitive to light quality, to our surprise the same phase transitions in tomato appeared to be completely indifferent to the R/B light ratio.

DISCUSSION

Recent developments in LED technology have created new possibilities for spectral control that allow us to use light quality to steer plant development (Morrow, 2008). Here we present an overview of the phenotypes that arise from growing Arabidopsis and young tomato plants in white or monochromatic red or blue LED lighting. During *in vitro* seedling development, hypocotyls were significantly more elongated in red light and shorter in blue light, compared to white light grown Arabidopsis and tomato seedlings. This confirmed previously published results that were obtained with the use of light filters (Ballaré et al., 1995), or with lighting setups in which the light intensity differed greatly between LED conditions (Jensen et al., 1998). At later developmental stages, Arabidopsis and tomato plant height were significantly increased in monochromatic red light and decreased in monochromatic blue light. In tomato, however, the reduced plant elongation in monochromatic blue light was limited to early stages of plant development. These results are in line with previous studies in wheat (Monostori et al., 2018) and chili peppers (Gangadhar et al., 2012), and a recent greenhouse

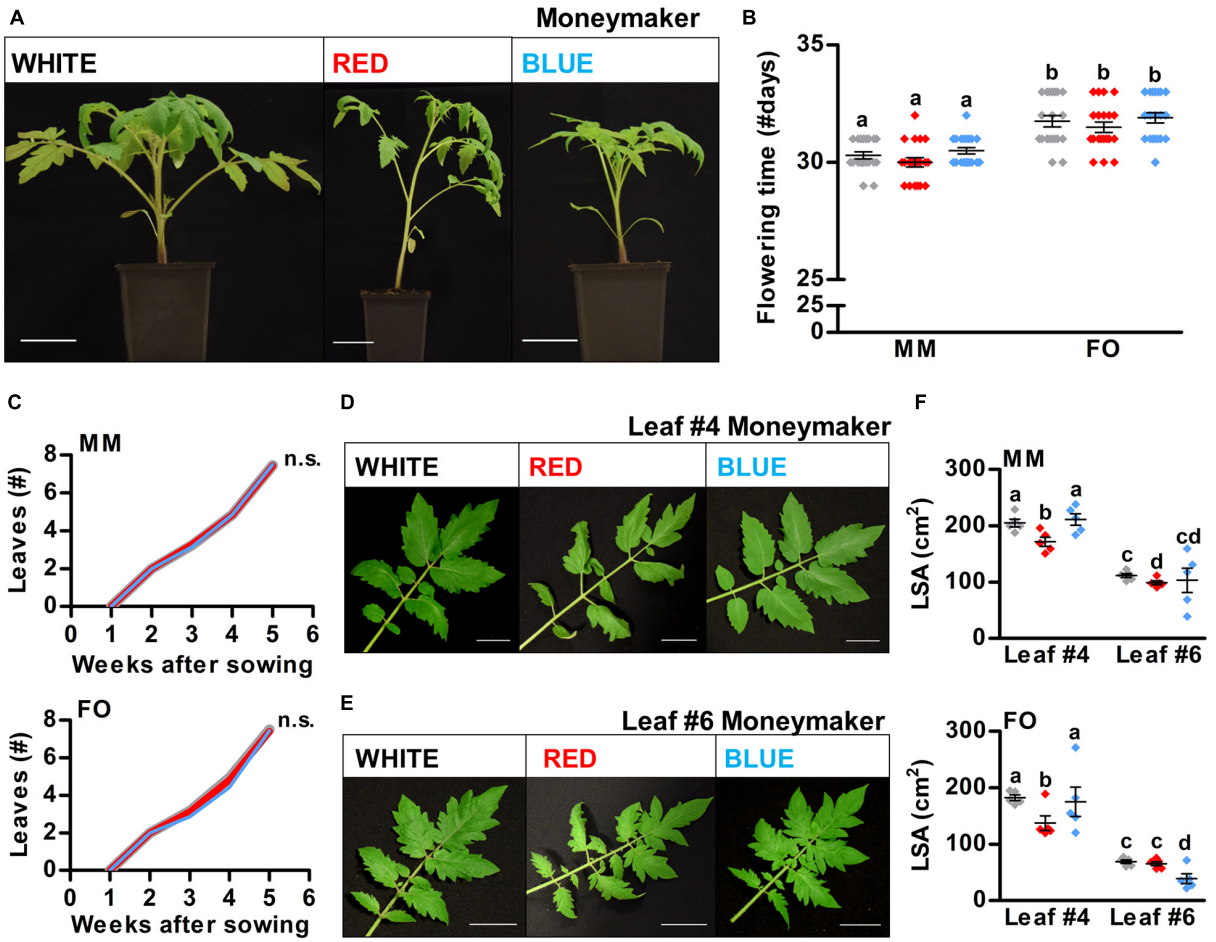

FIGURE 5 | Developmental phase transitions in tomato are indifferent to R/B light ratios. **(A)** Representative tomato plants of cultivar Moneymaker (MM) grown in white, red, or blue LED conditions until 30 days after sowing (DAS). **(B)** Flowering time of MM and Foundation (FO) plants in number of days. **(C)** Leaf appearance over time in MM and FO plants. **(D,E)** Representative compound leaves from MM plants grown in LED conditions until 45 DAS: leaf #4 **(D)** and leaf #6 **(E)**. For presentation purposes, leaves were removed, flattened, and placed on black paper. **(F)** Quantification of leaf surface area (LSA) of MM and FO leaves shown in (**D,E**, and **Supplementary Figures S5B,C**), respectively. Scale bars represent 5 cm in **(A,D,E)**. Graph colors represent the LED conditions in **(B,C,F)**. LED conditions and cultivars were compared using a one-way ANOVA followed by a Tukey's test (letters a–d indicate statistically significant differences, $p < 0.05$) in **(B,F)**. In **(C)**, monochromatic LED conditions (red or blue) were compared to white (control) using a two-sided Student's *t*-test [n.s. indicates no significant differences between LED conditions ($p < 0.05$)]. Error bars represent standard error of the mean in **(B**,**F)** ($n = 20$), standard errors for **(C)** are listed in **Supplementary Table S2** ($n = 20$). Similar results were obtained in two independent experiments.

study in tomato where LEDs were used as supplemental lighting (Dieleman et al., 2019). However, monochromatic blue light has been reported to enhance hypocotyl growth in cucumber, indicating that there are species-specific differences (Hernández and Kubota, 2016). Primary shoot growth in white light grown seedlings and plants was intermediate between that in monochromatic red or blue light grown seedlings and plants, suggesting an antagonistic effect of both light conditions, with red light promoting and blue light inhibiting shoot growth. Since auxin, ethylene, gibberellic acid and brassinosteroids are the main phytohormones that regulate hypocotyl and stem elongation in response to light (Vandenbussche et al., 2005; Kurepin and Pharis, 2014), it is likely that red- and blue light-responsive photoreceptors interact with the corresponding hormone signaling pathways. We also observed a significant effect of red and blue light on primary root growth in Arabidopsis and tomato seedlings. By combining the different LED conditions with LGR (light-grown roots) and DGR (dark-grown roots) conditions, we were able to show that the reduced primary root growth in monochromatic blue light is caused by a local light-induced inhibition of root growth. As auxin and cytokinin are the main regulators of primary root growth (Su et al., 2011), we expect that activation of root-localized photoreceptors affects cytokinin levels and auxin gradients in the root apical meristem. In contrast, we observed reduced primary root growth in Arabidopsis seedlings grown in red DGR, but not LGR conditions, suggesting that red LED conditions inhibit root growth by altering the shoot to root signaling. In this case, we expect that activation of shoot-localized photoreceptors influences shoot to root transport of key signaling molecules

such as HY5, HYH or auxin to modulate primary root growth (Chen et al., 2016; Van Gelderen et al., 2018). To summarize, our results show that primary growth of Arabidopsis and tomato can be modulated by changing the light quality at different developmental stages, and in different ecotypes or cultivars (**Table 1**). In this way, light quality may be used to steer primary growth toward compact and sturdy crop plants which can be grown in multi-layered growth chambers.

In Arabidopsis, we observed a considerable increase in the shoot-root ratio in monochromatic red light, and a slight decrease in the shoot-root ratio in monochromatic blue light, which resulted from light-induced changes in hypocotyl growth and, to a lesser extent, primary root growth. Moreover, the lateral organ density in roots was greatly decreased in red LED conditions. Since the far-red light-activated phytochrome A has been shown to promote lateral root formation (Salisbury et al., 2007), it is likely that the low number of lateral roots in monochromatic red light results from red light-inactivation of this photoreceptor. Previous studies have shown that blue light photoreceptors suppress lateral root formation (Zeng et al., 2010; Moni et al., 2015). In contrast, we observed an increase in lateral root density in monochromatic blue light. We suspect that the strong decrease in primary root growth in blue LED conditions is responsible for an indirect increase in lateral root density similar to in white LED conditions. In contrast to the roots, shoot branching was significantly enhanced in monochromatic red light, and significantly decreased in monochromatic blue light, whereas white light grown plants showed an intermediate phenotype. Shoot branching is promoted by cytokinin, and inhibited by strigolactones, either directly or through interactions with auxin (Domagalska and Leyser, 2011; Brewer et al., 2013). This suggests that red light might either enhance cytokinin signaling, or inhibit strigolactones, to promote shoot branching, and that an opposite effect on these phytohormones might be expected for blue light. This hypothesis is in line with previous studies that show that the blue light photoreceptor cryptochrome 1 inhibits shoot branching, and that the red light-inducible phytochrome B promotes shoot branching through auxin signaling (Reddy and Finlayson, 2014; Zhai et al., 2020). Although we demonstrate that the balance between shoot and root development can be steered by the light quality in Arabidopsis, additional research is required for horticultural application.

Our comparative analysis identified a remarkable difference in the regulation of developmental phase transitions by light quality between Arabidopsis and tomato. We observed that Arabidopsis plants grown in monochromatic blue light developed very small rosettes and flowered early, whereas plants grown in monochromatic red light developed extremely big rosettes due to late flowering. Our results confirm previous studies in which light filters were used, or where plants were grown under continuous LED illumination, which excludes the effect of day-length (Eskins, 1992; Guo et al., 1998). The light-induced changes in leaf length/width ratios, leaf formation and RSA in Arabidopsis are most likely the result of light quality-induced changes in both the juvenile to adult vegetative and the adult vegetative to reproductive phase transition (also referred to as the vegetative phase change and the floral transition, respectively). Strikingly, in contrast to Arabidopsis, these phase transitions in tomato were completely indifferent to red and blue light (**Table 2**). This might be a result of fundamental differences in plant architecture

TABLE 1 | Primary growth of Arabidopsis and tomato is regulated by red and blue light.

	Arabidopsis		Tomato	
	Red	**Blue**	**Red**	**Blue**
Primary root growth	*Similar to W	Shorter root	Similar to W	Shorter root
Hypocotyl length	Longer hypocotyl	Shorter hypocotyl	Longer hypocotyl	Shorter hypocotyl
Shoot/root ratio	Higher S/R ratio	*Similar to W	Higher S/R ratio	Similar to W
Epicotyl length	N/A	N/A	Longer epicotyl	*Shorter epicotyl
Plant height	Taller plants	Shorter plants	Taller plants	**Shorter/taller plants

Summary of the Arabidopsis and tomato primary growth phenotypes that were induced by monochromatic red or blue light in LGR conditions. Statistically significant differences between white light (control) and monochromatic LED conditions (red or blue) are indicated in this table ($p < 0.05$). When no statistical differences were found between LED conditions, it is indicated as "similar to white (W)." Asterisks indicate results that are ecotype-, or cultivar-dependent. Double Asterisks indicate results that are time-dependent.

TABLE 2 | Developmental phase transitions are modulated by red and blue light in Arabidopsis, but not in tomato.

	Arabidopsis		Tomato	
	Red	**Blue**	**Red**	**Blue**
Leaf formation	More leaves	Less leaves	Similar to W	Similar to W
Leaf morphology	Bigger leaves/bigger rosette	Smaller leaves/smaller rosette	Smaller leaves	Similar to W
Flowering time	Late	Early	Similar to W	Similar to W

Summary of the Arabidopsis and tomato developmental phenotypes that were induced by monochromatic red or blue light. Statistically significant differences between white light (control) and monochromatic LED conditions (red or blue) are indicated in this table ($p < 0.05$). When no statistical differences were found between monochromatic light and white light, it is indicated as "similar to white (W)."

(monopodial vs. sympodial growth), daylength sensitivity (long-day vs. day-neutral) or life history (annual vs. semi-perennial) between Arabidopsis and tomato, respectively. Similar to the phenotypes that we observed in Arabidopsis, strawberry and petunia have been shown to flower early in blue light and late in red light (Fukuda et al., 2012; Fukuda et al., 2016; Yoshida et al., 2016). Petunia and tomato are both members of the *Solanaceae* family and are categorized as sympodial, semi-perennial plants. However, in contrast to tomato, petunia is not a day-neutral plant but a long-day plant, suggesting that photoperiodic sensitivity is a key characteristic of plants for which developmental phase transitions are sensitive to red or blue light. Because Arabidopsis plants grown in white light show an intermediate phenotype compared to those grown in either monochromatic red or blue LED conditions, a separate phase transition-promoting effect of blue light and a phase transition-delaying effect of red light should be considered. Previous studies have shown that blue light promotes flowering through photoreceptors of the cryptochrome and Zeitlupe families. In response to blue light, these photoreceptors enhance expression of *CONSTANS* (*CO*). As a main integrator of circadian clock components and light signaling, CO promotes flowering through the florigen *FLOWERING LOCUS T,* in response to day length (Valverde, 2011). In day-neutral plant species, components of the photoperiodic pathway are likely non-existent, or unresponsive (Mizoguchi et al., 2007), which might explain the indifference of tomato plants to LED conditions that lack blue light. Although red light has been shown to inhibit flowering through targeted degradation of CO proteins (Lazaro et al., 2015), we do not expect that the flower-delaying effect of red light relies solely on photoperiodicity. Based on the length/width ratios of leaf blades, we suggest that meristems of plants grown in monochromatic blue light may mature faster, whereas meristems of plants grown in monochromatic red light mature at the same rate as those in white light. This suggests that red light might inhibit the aging pathway, in addition to the photoperiodic pathway, to delay the floral transition. Therefore, LED conditions that lack red light would result in an early vegetative phase transition and early flowering. To summarize, our observations in Arabidopsis suggest a possibility to identify more (long-day) species in which developmental phase transitions can be steered by light quality, whereas our experiments in tomato demonstrate that tomato growers may change the R/B light ratio toward desired phenotypes, without affecting the timing of the developmental phase transitions. If we wish to apply the R/B light ratio to steer the timing of developmental phase transitions in horticulture, it will be necessary to further investigate the LED phenotypes in Arabidopsis, and to verify whether these are conserved in other species from the same or from different families. However, changes in the LED spectrum are likely to simultaneously modulate the activity of multiple photoreceptors, and the interplay between photoreceptors and their downstream targets adds another layer of complexity. For example, it has been shown that blue light-activated cryptochromes physically interact with the far-red/red light-inducible phytochromes, and with their downstream targets (Mas et al., 2000; Pedmale et al., 2016). Nonetheless, identification of the key photoreceptors, phytohormones, and downstream signaling targets that underly the phenotypes that we observed in this study will be the next step toward optimizing light quality-induced phenotypic traits for horticultural application, and to understand the divergence of these traits between plant species.

CONCLUSION

Our results demonstrate that light quality modulates different aspects of the growth and early development of Arabidopsis and tomato. In Arabidopsis, treatment with monochromatic red light resulted in increased shoot growth and development (sometimes at the cost of root development), and delayed flowering, whereas plants grown in monochromatic blue light showed reduced shoot growth and development, and early flowering. In tomato plants grown in monochromatic red light we observed increased shoot growth and development, and a decrease in leaf surface area, whereas tomato plants grown in blue LED conditions showed reduced shoot growth in vegetative plants and increased shoot growth in flowering plants. Our comparative analysis showed that most of the primary growth responses to light quality were conserved between Arabidopsis and tomato (**Table 1**). In contrast, developmental phase transitions in Arabidopsis were highly sensitive to light quality, whereas these transitions in tomato were completely indifferent to red and blue light (**Table 2**).

DATA AVAILABILITY STATEMENT

The original contributions presented in the study are included in the article/**Supplementary Material**, further inquiries can be directed to the corresponding author/s.

AUTHOR CONTRIBUTIONS

KS, WI, and RO conceived and designed the experiments and analyzed the results. KS and JL performed the experiments. KS performed the statistical analysis. KS and RO wrote the manuscript. All authors contributed to manuscript revision and read and approved the submitted version.

FUNDING

This work was part of the research program "LED it be 50%" with project number 14212, which was partly financed by the Dutch Research Council (NWO).

ACKNOWLEDGMENTS

We would like to thank Nunhems Netherlands BV for providing seeds of their commercial tomato hybrid line Foundation and Signify for providing the LED modules. We thank Fred Schenkel

and Emiel Wiegers for help with design and construction of the LED lighting set-up, and Daliá Alves Carvalho for photon flux measurements and helpful suggestions. We acknowledge Jeroen Nels and Nakisa Echobardo for help with initial germination assays.

SUPPLEMENTARY MATERIAL

The Supplementary Material for this article can be found online at: https://www.frontiersin.org/articles/10.3389/fpls.2020.599982/full#supplementary-material

REFERENCES

Ballaré, C. L., Barnes, P. W., and Flint, S. D. (1995). Inhibition of hypocotyl elongation by ultraviolet−B radiation in de−etiolating tomato seedlings. I. The photoreceptor. *Physiol. Plant.* 93, 584–592. doi: 10.1111/j.1399-3054.1995.tb05104.x

Ballaré, C. L., and Pierik, R. (2017). The shade-avoidance syndrome: multiple signals and ecological consequences. *Plant Cell Environ.* 40, 2530–2543. doi: 10.1111/pce.12914

Ballaré, C. L., Scopel, A. L., and Sánchez, R. A. (1990). Far-red radiation reflected from adjacent leaves: AN early signal of competition in plant canopies. *Science* 247, 329–332. doi: 10.1126/science.247.4940.329

Brandt, S., Fachinger, S., Tohge, T., Fernie, A. R., Braun, H. P., and Hildebrandt, T. M. (2018). Extended darkness induces internal turnover of glucosinolates in *Arabidopsis thaliana* leaves. *PLoS One* 13:e0202153. doi: 10.1371/journal.pone.0202153

Brewer, P. B., Koltai, H., and Beveridge, C. A. (2013). Diverse roles of strigolactones in plant development. *Mol. Plant* 6, 18–28. doi: 10.1093/mp/sss130

Chen, X., Yao, Q., Gao, X., Jiang, C., Harberd, N. P., and Fu, X. (2016). Shoot-to-root mobile transcription factor HY5 coordinates plant carbon and nitrogen acquisition. *Curr. Biol.* 26, 640–646. doi: 10.1016/j.cub.2015.12.066

Christie, J. M. (2007). Phototropin blue-light receptors. *Annu. Rev. Plant Biol.* 58, 21–45. doi: 10.1146/annurev.arplant.58.032806.103951

Dieleman, J. A., De Visser, P. H. B., Meinen, E., Grit, J. G., and Dueck, T. A. (2019). Integrating morphological and physiological responses of tomato plants to light quality to the crop level by 3D modeling. *Front. Plant Sci.* 10:839. doi: 10.3389/fpls.2019.00839

Domagalska, M. A., and Leyser, O. (2011). Signal integration in the control of shoot branching. *Nat. Rev. Mol. Cell Biol.* 12, 211–221. doi: 10.1038/nrm3088

Dougher, T. A. O., and Bugbee, B. (2001). Differences in the response of wheat, soybean and lettuce to reduced blue radiation. *Photochem. Photobiol.* 73:199. doi: 10.1562/0031-86552001073<0199:ditrow<2.0.co;2

Eskins, K. (1992). Light−quality effects on *Arabidopsis* development. Red, blue and far−red regulation of flowering and morphology. *Physiol. Plant.* 86, 439–444. doi: 10.1111/j.1399-3054.1992.tb01341.x

Fan, X. X., Xu, Z. G., Liu, X. Y., Tang, C. M., Wang, L. W., and Han, X. L. (2013). Effects of light intensity on the growth and leaf development of young tomato plants grown under a combination of red and blue light. *Sci. Hortic.* 153, 50–55. doi: 10.1016/j.scienta.2013.01.017

Fukuda, N., Ajima, C., Yukawa, T., and Olsen, J. E. (2016). Antagonistic action of blue and red light on shoot elongation in petunia depends on gibberellin, but the effects on flowering are not generally linked to gibberellin. *Environ. Exp. Bot.* 121, 102–111. doi: 10.1016/j.envexpbot.2015.06.014

Fukuda, N., Yoshida, T., Olsen, J. E., Senaha, C., Jikumaru, Y. and Kamiya, Y. (2012). Short main shoot length and inhibition of floral bud development under red light can be recovered by application of gibberellin and cytokinin. *Acta Hortic.* 956, 215–222. doi: 10.17660/ActaHortic.2012.956.23

Galvão, V. C., and Fankhauser, C. (2015). Sensing the light environment in plants: Photoreceptors and early signaling steps. *Curr. Opin. Neurobiol.* 34, 46–53. doi: 10.1016/j.conb.2015.01.013

Gangadhar, B. H., Mishra, R. K., Pandian, G., and Park, S. W. (2012). Comparative study of color, pungency, and biochemical composition in chili pepper (*Capsicum annuum*) under different light-emitting diode treatments. *HortScience* 47, 1729–1735. doi: 10.21273/hortsci.47.12.1729

Goyal, A., Szarzynska, B., and Fankhauser, C. (2013). Phototropism: At the crossroads of light-signaling pathways. *Trends Plant Sci.* 18, 393–401. doi: 10.1016/j.tplants.2013.03.002

Guo, H., Yang, H., Mockler, T. C., and Lin, C. (1998). Regulation of flowering time by *Arabidopsis* photoreceptors. *Science* 279, 1360–1363. doi: 10.1126/science.279.5355.1360

Hernández, R., and Kubota, C. (2016). Physiological responses of cucumber seedlings under different blue and red photon flux ratios using LEDs. *Environ. Exp. Bot.* 121, 66–74. doi: 10.1016/j.envexpbot.2015.04.001

Jensen, P. J., Hangarter, R. P., and Estelle, M. (1998). Auxin transport is required for hypocotyl elongation in light-grown but not dark-grown *Arabidopsis*. *Plant Physiol.* 116, 455–462. doi: 10.1104/pp.116.2.455

Ji, Y., Ouzounis, T., Courbier, S., Kaiser, E., Nguyen, P. T., Schouten, H. J., et al. (2019). Far-red radiation increases dry mass partitioning to fruits but reduces *Botrytis cinerea* resistance in tomato. *Environ. Exp. Bot.* 168:103889. doi: 10.1016/j.envexpbot.2019.103889

Kaiser, E., Ouzounis, T., Giday, H., Schipper, R., Heuvelink, E., and Marcelis, L. F. M. (2019). Adding blue to red supplemental light increases biomass and yield of greenhouse-grown tomatoes, but only to an optimum. *Front. Plant Sci.* 9:2002. doi: 10.3389/fpls.2018.02002

Kalaitzoglou, P., van Ieperen, W., Harbinson, J., van der Meer, M., Martinakos, S., Weerheim, K., et al. (2019). Effects of continuous or end-of-day far-red light on tomato plant growth, morphology, light absorption, and fruit production. *Front. Plant Sci.* 10:322. doi: 10.3389/fpls.2019.00322

Kurepin, L. V., and Pharis, R. P. (2014). Light signaling and the phytohormonal regulation of shoot growth. *Plant Sci.* 229, 280–289. doi: 10.1016/j.plantsci.2014.10.006

Lanoue, J., Leonardos, E. D., and Grodzinski, B. (2018). Effects of light quality and intensity on diurnal patterns and rates of photo-assimilate translocation and transpiration in tomato leaves. *Front. Plant Sci.* 9:756. doi: 10.3389/fpls.2018.00756

Lanoue, J., Leonardos, E. D., Ma, X., and Grodzinski, B. (2017). The effect of spectral quality on daily patterns of gas exchange, biomass gain, and water-use-efficiency in tomatoes and lisianthus: an assessment of whole plant measurements. *Front. Plant Sci.* 8:1076. doi: 10.3389/fpls.2017.01076

Lazaro, A., Mouriz, A., Piñeiro, M., and Jarillo, J. A. (2015). Red light-mediated degradation of constans by the e3 ubiquitin ligase hos1 regulates photoperiodic flowering in *Arabidopsis*. *Plant Cell* 27, 2437–2454. doi: 10.1105/tpc.15.00529

Li, F., De Storme, N., and Geelen, D. (2017). Dynamics of male meiotic recombination frequency during plant development using fluorescent tagged lines in *Arabidopsis thaliana*. *Sci. Rep.* 7, 1–9. doi: 10.1038/srep42535

Lim, J., Park, J. H., Jung, S., Hwang, D., Nam, H. G., and Hong, S. (2018). Antagonistic roles of phyA and phyB in far-red light-dependent leaf senescence in *Arabidopsis thaliana*. *Plant Cell Physiol.* 59, 1753–1764. doi: 10.1093/pcp/pcy153

Lu, T., Meng, Z., Zhang, G., Qi, M., Sun, Z., Liu, Y., et al. (2017). Sub-high temperature and high light intensity induced irreversible inhibition on photosynthesis system of tomato plant (*Solanum lycopersicum L.*). *Front. Plant Sci.* 8:365. doi: 10.3389/fpls.2017.00365

Mas, P., Devlin, P. F., Panda, S., and Kay, S. A. (2000). Functional interaction of phytochrome B and cryptochrome 2. *Nature* 408, 207–211. doi: 10.1038/35041583

Masson, J., and Paszkowski, J. (1992). The culture response of *Arabidopsis thaliana* protoplasts is determined by the growth conditions of donor plants. *Plant J.* 2, 829–833. doi: 10.1111/j.1365-313X.1992.tb00153.x

Mathan, J., Bhattacharya, J., and Ranjan, A. (2016). Enhancing crop yield by optimizing plant developmental features. *Dev.* 143, 3283–3294. doi: 10.1242/dev.134072

Mizoguchi, T., Niinuma, K., and Yoshida, R. (2007). Day-neutral response of photoperiodic flowering in tomatoes: possible implications based on recent

molecular genetics of *Arabidopsis* and rice. *Plant Biotechnol.* 24, 83–86. doi: 10.5511/plantbiotechnology.24.83

Moles, A. T., Warton, D. I., Warman, L., Swenson, N. G., Laffan, S. W., Zanne, A. E., et al. (2009). Global patterns in plant height. *J. Ecol.* 97, 923–932. doi: 10.1111/j.1365-2745.2009.01526.x

Moni, A., Lee, A. Y., Briggs, W. R., and Han, I. S. (2015). The blue light receptor phototropin 1 suppresses lateral root growth by controlling cell elongation. *Plant Biol.* 17, 34–40. doi: 10.1111/plb.12187

Monostori, I., Heilmann, M., Kocsy, G., Rakszegi, M., Ahres, M., Altenbach, S. B., et al. (2018). LED lighting – modification of growth, metabolism, yield and flour composition in wheat by spectral quality and intensity. *Front. Plant Sci.* 9:605. doi: 10.3389/fpls.2018.00605

Morrow, R. C. (2008). LED lighting in horticulture. *HortScience* 43, 1947–1950. doi: 10.21273/hortsci.43.7.1947

Nemhauser, J., and Chory, J. (2002). Photomorphogenesis. *Arab. B.* 1:e0054. doi: 10.1199/tab.0054

Ntagkas, N., Woltering, E., Bouras, S., De Vos, R. C., Dieleman, J. A., Nicole, C. C. S., et al. (2019). Light-induced vitamin C accumulation in tomato fruits is independent of carbohydrate availability. *Plants* 8, 1–12. doi: 10.3390/plants8040086

Pedmale, U. V., Huang, S. S. C., Zander, M., Cole, B. J., Hetzel, J., Ljung, K., et al. (2016). Cryptochromes interact directly with PIFs to control plant growth in limiting blue light. *Cell* 164, 233–245. doi: 10.1016/j.cell.2015.12.018

Pennisi, G., Blasioli, S., Cellini, A., Maia, L., Crepaldi, A., Braschi, I., et al. (2019). Unraveling the role of red:blue LED lights on resource use efficiency and nutritional properties of indoor grown sweet basil. *Front. Plant Sci.* 10:305. doi: 10.3389/fpls.2019.00305

Puig, J., Pauluzzi, G., Guiderdoni, E., and Gantet, P. (2012). Regulation of shoot and root development through mutual signaling. *Mol. Plant* 5, 974–983. doi: 10.1093/mp/sss047

Reddy, S. K., and Finlayson, S. A. (2014). Phytochrome B promotes branching in *Arabidopsis* by suppressing auxin signaling. *Plant Physiol.* 164, 1542–1550. doi: 10.1104/pp.113.234021

Salisbury, F. J., Hall, A., Grierson, C. S., and Halliday, K. J. (2007). Phytochrome coordinates *Arabidopsis* shoot and root development. *Plant J.* 50, 429–438. doi: 10.1111/j.1365-313X.2007.03059.x

Schindelin, J., Arganda-Carreras, I., Frise, E., Kaynig, V., Longair, M., Pietzsch, T., et al. (2012). Fiji: an open-source platform for biological-image analysis. *Nat. Methods* 9, 676–682. doi: 10.1038/nmeth.2019

Schmitz, G., and Theres, K. (1999). Genetic control of branching in *Arabidopsis* and tomato. *Curr. Opin. Plant Biol.* 2, 51–55. doi: 10.1016/S1369-5266(99)80010-7

Schrager-Lavelle, A., Herrera, L. A., and Maloof, J. N. (2016). Tomato phyE is required for shade avoidance in the absence of phyB1 and phyB2. *Front. Plant Sci.* 7:1275. doi: 10.3389/fpls.2016.01275

Schumacher, P., Demarsy, E., Waridel, P., Petrolati, L. A., Trevisan, M., and Fankhauser, C. (2018). A phosphorylation switch turns a positive regulator of phototropism into an inhibitor of the process. *Nat. Commun.* 9, 1–9. doi: 10.1038/s41467-018-04752-1

SharathKumar, M., Heuvelink, E., and Marcelis, L. F. M. (2020). Vertical farming: moving from genetic to environmental modification. *Trends Plant Sci.* 25, 724–727. doi: 10.1016/j.tplants.2020.05.012

Silva-Navas, J., Moreno-Risueno, M. A., Manzano, C., Pallero-Baena, M., Navarro-Neila, S., Téllez-Robledo, B., et al. (2015). D-Root: a system for cultivating plants with the roots in darkness or under different light conditions. *Plant J.* 84, 244–255. doi: 10.1111/tpj.12998

Smeets, L., and Garretsen, F. (1986). Growth analyses of tomato genotypes grown under low night temperatures and low light intensity. *Euphytica* 35, 701–715. doi: 10.1007/BF00028578

Song, J., Cao, K., Hao, Y., Song, S., Su, W., and Liu, H. (2019). Hypocotyl elongation is regulated by supplemental blue and red light in cucumber seedling. *Gene* 707, 117–125. doi: 10.1016/j.gene.2019.04.070

Su, Y. H., Liu, Y. B., and Zhang, X. S. (2011). Auxin-cytokinin interaction regulates meristem development. *Mol. Plant* 4, 616–625. doi: 10.1093/mp/ssr007

Suetsugu, N., and Wada, M. (2013). Evolution of three LOV blue light receptor families in green plants and photosynthetic stramenopiles: phototropin, ZTL/FKF1/LKP2 and aureochrome. *Plant Cell Physiol.* 54, 8–23. doi: 10.1093/pcp/pcs165

Telfer, A., Bollman, K. M., and Poethig, R. S. (1997). Phase change and the regulation of trichome distribution in *Arabidopsis thaliana*. *Development* 124, 645–654.

Valverde, F. (2011). CONSTANS and the evolutionary origin of photoperiodic timing of flowering. *J. Exp. Bot.* 62, 2453–2463. doi: 10.1093/jxb/erq449

Van der Ploeg, A., Van der Meer, M., and Heuvelink, E. (2007). Breeding for a more energy efficient greenhouse tomato: Past and future perspectives. *Euphytica* 158, 129–138. doi: 10.1007/s10681-007-9437-z

Van Gelderen, K., Kang, C., and Pierik, R. (2018). Light signaling, root development, and plasticity. *Plant Physiol.* 176, 1049–1060. doi: 10.1104/pp.17.01079

Vandenbussche, F., Verbelen, J. P., and Van Der Straeten, D. (2005). Of light and length: regulation of hypocotyl growth in *Arabidopsis*. *BioEssays* 27, 275–284. doi: 10.1002/bies.20199

Viršilė, A., Brazaitytė, A., Vaštakaitė-Kairienė, V., Miliauskienė, J., Jankauskienė, J., Novičkovas, A., et al. (2019). Lighting intensity and photoperiod serves tailoring nitrate assimilation indices in red and green baby leaf lettuce. *J. Sci. Food Agric.* 99, 6608–6619. doi: 10.1002/jsfa.9948

Wang, Q., Zuo, Z., Wang, X., Gu, L., Yoshizumi, T., Yang, Z., et al. (2016). Photoactivation and inactivation of *Arabidopsis* cryptochrome 2. *Science* 354, 343–347. doi: 10.1126/science.aaf9030

Yoshida, H., Mizuta, D., Fukuda, N., Hikosaka, S., and Goto, E. (2016). Effects of varying light quality from single-peak blue and red light-emitting diodes during nursery period on flowering,photosynthesis,growth,and fruit yield of everbearing strawberry. *Plant Biotechnol.* 33, 267–276. doi: 10.5511/plantbiotechnology.16.0216a

Yu, X., Liu, H., Klejnot, J., and Lin, C. (2010). The cryptochrome blue light receptors. *Arab. B.* 8:e0135. doi: 10.1199/tab.0135

Zeng, J., Wang, Q., Lin, J., Deng, K., Zhao, X., Tang, D., et al. (2010). *Arabidopsis* cryptochrome-1 restrains lateral roots growth by inhibiting auxin transport. *J. Plant Physiol.* 167, 670–673. doi: 10.1016/j.jplph.2009.12.003

Zhai, H., Xiong, L., Li, H., Lyu, X., Yang, G., Zhao, T., et al. (2020). Cryptochrome 1 inhibits shoot branching by repressing the self-activated transciption loop of PIF4 in *Arabidopsis*. *Plant Commun.* 1:100042. doi: 10.1016/j.xplc.2020.100042

Zhou, Y. H., Zhang, Y. Y., Zhao, X., Yu, H. J., Shi, K., and Yu, J. Q. (2009). Impact of light variation on development of photoprotection, antioxidants, and nutritional value in *Lactuca sativa L. J. Agric. Food Chem.* 57, 5494–5500. doi: 10.1021/jf8040325

Conflict of Interest: The authors declare that the research was conducted in the absence of any commercial or financial relationships that could be construed as a potential conflict of interest.

Copyright © 2020 Spaninks, van Lieshout, van Ieperen and Offringa. This is an open-access article distributed under the terms of the Creative Commons Attribution License (CC BY). The use, distribution or reproduction in other forums is permitted, provided the original author(s) and the copyright owner(s) are credited and that the original publication in this journal is cited, in accordance with accepted academic practice. No use, distribution or reproduction is permitted which does not comply with these terms.

frontiers in Plant Science

ORIGINAL RESEARCH
published: 05 January 2021
doi: 10.3389/fpls.2020.610011

Spectral Composition of Light Affects Sensitivity to UV-B and Photoinhibition in Cucumber

Carolina Falcato Fialho Palma[1], Victor Castro-Alves[2], Luis Orlando Morales[2], Eva Rosenqvist[3], Carl-Otto Ottosen[1] and Åke Strid[2]*

[1] Department of Food Science, Plant, Food & Climate, Aarhus University, Aarhus, Denmark, [2] School of Science and Technology, Örebro Life Science Centre, Örebro University, Örebro, Sweden, [3] Department of Plant and Environmental Sciences, Crop Sciences, University of Copenhagen, Taastrup, Denmark

Ultraviolet B (UV-B) (280–315 nm) and ultraviolet A (UV-A) (315–400 nm) radiation comprise small portions of the solar radiation but regulate many aspects of plant development, physiology and metabolism. Until now, how plants respond to UV-B in the presence of different light qualities is poorly understood. This study aimed to assess the effects of a low UV-B dose (0.912 ± 0.074 kJ m^{-2} day^{-1}, at a 6 h daily UV exposure) in combination with four light treatments (blue, green, red and broadband white at 210 μmol m^{-2} s^{-1} Photosynthetically active radiation [PAR]) on morphological and physiological responses of cucumber (*Cucumis sativus* cv. "Lausanna RZ F1"). We explored the effects of light quality backgrounds on plant morphology, leaf gas exchange, chlorophyll fluorescence, epidermal pigment accumulation, and on acclimation ability to saturating light intensity. Our results showed that supplementary UV-B significantly decreased biomass accumulation in the presence of broad band white, blue and green light, but not under red light. UV-B also reduced the photosynthetic efficiency of CO_2 fixation (α) when combined with blue light. These plants, despite showing high accumulation of anthocyanins, were unable to cope with saturating light conditions. No significant effects of UV-B in combination with green light were observed for gas exchange and chlorophyll fluorescence parameters, but supplementary UV-B significantly increased chlorophyll and flavonol contents in the leaf epidermis. Plants grown under red light and UV-B significantly increased maximum photosynthetic rate and dark respiration compared to pure red light. Additionally, red and UV-B treated plants exposed to saturating light intensity showed higher quantum yield of photosystem II (PSII), fraction of open PSII centres and electron transport rate and showed no effect on the apparent maximum quantum efficiency of PSII photochemistry (F_v/F_m) or non-photochemical quenching, in contrast to solely red-light conditions. These findings provide new insights into how plants respond to UV-B radiation in the presence of different light spectra.

Keywords: UV-B, LEDs, light quality, chlorophyll fluorescence, gas exchange, cucumber, morphology

OPEN ACCESS

Edited by:
Sissel Torre, Norwegian University of Life Sciences, Norway

Reviewed by:
Sasan Aliniaeifard, University of Tehran, Iran
Mauricio Hunsche, University of Bonn, Germany

****Correspondence:***
Carl-Otto Ottosen
coo@food.au.dk

Specialty section:
This article was submitted to Crop and Product Physiology, a section of the journal Frontiers in Plant Science

Received: *24 September 2020*
Accepted: *23 November 2020*
Published: *05 January 2021*

Citation:
Palma CFF, Castro-Alves V, Morales LO, Rosenqvist E, Ottosen CO and Strid Å (2021) Spectral Composition of Light Affects Sensitivity to UV-B and Photoinhibition in Cucumber. Front. Plant Sci. 11:610011. doi: 10.3389/fpls.2020.610011

INTRODUCTION

Plants perceive signals from their surrounding environment and regulate their growth and development accordingly (Smith, 1982; Huché-Thélier et al., 2016). Plants are highly sensitive to the spectral distribution of light and perceive changes in the light spectra and intensity through several protein photoreceptors (Fankhauser and Chory, 1997). These photoreceptors are sensitive to specific regions of the spectrum and overlap of action spectra of different plant photoreceptors occur, allowing the plant to detect a wider and more complex range of changes in their light environment (Heijde and Ulm, 2012). Cryptochromes and phototropins are sensitive to blue light (400–500 nm) and ultraviolet (UV) radiation A (UV-A) (315–400 nm), whereas phytochromes perceive red (600–700 nm) and far-red (700–800 nm) light. Moreover, phytochromes and cryptochromes also absorb light in the green wavelength region (500–600 nm) (Folta and Maruhnich, 2007), although the response of these photoreceptors to green light is extremely weak compared to red and blue radiation, respectively.

Ultraviolet B (UV-B) radiation (290–315 nm) comprises a small but energetic portion of the solar radiation that also reaches the surface of the Earth. UV-B perceived through the photoreceptor UV RESISTANCE LOCUS 8 (UVR8) (Rizzini et al., 2011) largely affects plant morphology and metabolism (Jenkins, 2017). Plant responses to UV-B radiation are highly dependent on UV-B dosage and are also affected by whether or not the plants have previously been UV-B acclimated (Huché-Thélier et al., 2016; Jenkins, 2017), as well as by the accumulation of photosynthetic pigments and phenolic compounds in the leaf epidermis. In addition, the levels of the photosynthetically active radiation (PAR) (400–700 nm) and the PAR/UV-B ratio are factors that strongly influence plant UV-B responses (Krizek, 2004; Lidon et al., 2012; Jenkins, 2017).

Exposure to high doses of UV-B may also induce (di)stress responses in plants, triggering the formation of free radicals [reactive oxygen species (ROS)] that cause oxidative damage (Day and Vogelmann, 1995; Jansen et al., 1998; Hideg et al., 2013). Plant responses to UV-B are highly species specific and morphological responses can be either positive (increase in plant growth) or negative (decrease in plant growth) (Huché-Thélier et al., 2016). UV-B can also reduce stem extension and leaf expansion and affect leaf thickness, leaf curling and auxiliary branching (Jansen, 2002; Wargent et al., 2009; Klem et al., 2012; Jenkins, 2017; Qian et al., 2020). Moreover, under low doses, UV-B radiation can promote the accumulation of photoprotective compounds in the leaf tissue (Day et al., 1993). For instance, an increase in the accumulation of flavonoid glycosides in response to UV-B has been described both under artificial and natural conditions (Krizek et al., 1997; Demkura and Ballaré, 2012; Zhao et al., 2020), although in some instances UV-B had no effect or even led to decreased flavonoid accumulation (Huché-Thélier et al., 2016). Flavonoids, particularly anthocyanins, are mainly accumulated in vacuoles in the upper layer of the leaf epidermis although they can also be found in the cell wall, chloroplast envelope and cell nucleus (Hideg and Strid, 2017). Apart from having a strong free-radical scavenging activity (Lattanzio et al., 2006; Agati and Tattini, 2010), flavonoids absorb radiation in the UV range of the spectrum (280–340 nm), functioning as sunscreen compounds to protect plants from further UV induced damage (Day et al., 1993).

Contradicting results in UV-B research often derive from methodological differences among studies or from species or ecotype differences (Kalbina and Strid, 2006). Different UV-B doses, light environments (natural sunlight vs. artificial lighting), other abiotic factors and species-specific responses cause variation between studies. Additionally, most UV-B research has been performed using broadband white light background under controlled conditions. Hence, there is a lack of studies depicting the effects of UV-B radiation on whole plant responses under monochromatic light backgrounds. This type of research is important to assess plant responses triggered by crosstalk between different light qualities and their impact on plant growth and development. With the development of light emitting diode (LED) technology, the use of LED lighting for horticultural production is increasing. Because of the high energy efficiency, customizable light environment and low radiant heat that allows for the placement of the lamps close to the canopy (Bourget, 2008; Darko et al., 2014; Singh et al., 2015), an interest in the use of LED lights in multilayer production has emerged. Multilayer systems allow the production of the same number of plants in a smaller area and could be relevant to use for intensive production systems such as germination of seedlings or rooting of cuttings. These production systems, although not yet economically feasible in all geographical regions when compared to normal greenhouse production (Graamans et al., 2018), rely on the sole use of LEDs and provide a unique environment for investigating new opportunities of LED lighting use, such as in monochromatic illumination and the use of UV to manipulate plant growth and development.

Blue light perception is often involved in physiological processes such as photomorphogenesis, phototropism (de Carbonnel et al., 2010), stomatal opening (Briggs and Huala, 1999; Boccalandro et al., 2012) and chlorophyll formation. Moreover, blue light induces an accumulation of several phytonutrients in the leaves, such as phenolic acids and flavonoids (Ohashi-Kaneko et al., 2007; Li and Kubota, 2009; Nascimento et al., 2013; Ouzounis et al., 2014, 2015). Red light can regulate vegetative development and plant architecture by influencing phototropism and shade-avoidance syndrome (SAS) (Fankhauser and Chory, 1997; Demotes-Mainard et al., 2016) and promote the accumulation of anthocyanins in the leaf epidermis (Mizuno et al., 2011; Zoratti et al., 2014; Garrett Owen and Lopez, 2015). Green light can inhibit stomatal opening stimulated

Abbreviations: α, apparent quantum yield of photosynthesis; θ, curvature; A_n, net photosynthetic rate; A_{max}, maximum net assimilation rate; C_i, intracellular CO_2 concentration; CO_2, carbon dioxide; DM%, Dry mass percentage; DM, Dry mass; E, transpiration rate; ETR, electron transport rate; FM, fresh mass; F_v/F_m, maximum photochemical efficiency of PSII; F_q'/F_m', quantum yield or operation efficiency of PSII; g_s, stomatal conductance; ILA, individual leaf area; INL internode length; LCP, light compensation point; LMR, leaf mass ratio; NPQ, non-photochemical quenching; PAR, photosynthetically active radiation; q_L, fraction of open PSII centres; PSII, photosystem II; R_{dark}, dark respiration; ROS, reactive oxygen species; SLM, specific leaf mass; TLA, total leaf area; UV-B, Ultraviolet B; Ø, stem diameter.

by blue light (Frechilla et al., 2000; Smith et al., 2017) and promote early stem elongation (Folta, 2004). These observations suggest that different monochromatic light spectra not only have a different impact on plant growth, but could also influence plants ability to cope with abiotic stress (e.g., high light) due to a wavelength-driven accumulation of photoprotective compounds (Bayat et al., 2018).

Cucumber (*Cucumis sativus* L.), is an important food crop with fast growth and high sensitivity toward the spectral composition of the light environment. These aspects make cucumber an interesting crop for studying light-driven responses in plants, such as responses to UV radiation (Qian et al., 2019, 2020). The aim of this study was to investigate the effects of supplementary UV-B on growth, morphology and physiology of cucumber plants grown under different monochromatic light backgrounds. We hypothesized that: (I) different monochromatic lights have different impacts on plant morphology and (II) the response of cucumber to UV-B radiation is highly dependent on individual monochromatic light backgrounds.

MATERIALS AND METHODS

Plant Material and Growing Conditions

Cucumber seeds (*cv*. "Lausanna RZ F1," Semenco, Asmundtorp, Sweden) were individually sown in 8 × 8 cm pots filled with peat substrate (Grön Torvmull 50-liter, SW Horto, Hasselfors Garden, Örebro, Sweden). The seeds were germinated under artificial light at 200 μmol m^{-2} s^{-1} PAR provided by metal halide lamps (MASTER HPI-T Plus 400 W/645, Phillips) during a 16 h photoperiod (6:00 to 22:00). The germination took place at room temperature of 22 ± 1/18 ± 1°C day/night and 60 ± 5% relative humidity. Immediately after germination and opening of the cotyledons, the seedlings were randomly transferred to a room without natural light and placed in four 2 m high custom-made trolleys with an 80 × 170 cm ebb/flow watering table. Each trolley had a unique light spectral treatment (four trolleys in total) and contained 72 treatment plants. These plants were later randomly divided into 36 control plants per treatment that were only exposed to one of four different light spectra in the PAR region and 36 plants that in addition to the different light spectra were exposed to low levels of UV-B (for both treatment types, see description below). Plants remained under four different LED light treatments for 23 days at a constant light intensity of 200–215 μmol m^{-2} s^{-1} PAR and 16 h photoperiod (6:00 to 22:00). The climate conditions in the room were maintained at 22 ± 1/18 ± 1°C day/night and RH of 60 ± 5%. No external supply of carbon dioxide (CO_2) was used. The cucumber plants were watered daily by flood irrigation containing commercial mineral nutrient solution (composition: 3.1 g NO_3^-, 2.0 g NH_4^+, 1.0 g P, 4.3 g K, 0.4 g S, 0.3 g Ca, 0.4 g Mg, 35 mg Fe, 20 mg Mn, 10 mg B, 3.0 mg Zn, 1.5 mg Cu, 0.4 mg Mo; pH 6.5 and EC 1.4 mS cm^{-1}; Blomstra växtnäring, Orkla, Solna, Sweden). A portable data logger (Tinytag, Gemini Data Loggers Ltd., Chichester, United Kingdom) placed within the canopy recorded the temperature and relative humidity of each light treatment (**Supplementary Figure S2**).

Light Treatments

From cotyledon stage until the final harvest, plants were grown under four light treatments created in the trolleys by using FL300 LED luminaires (Senmatic, Søndersø, Denmark). The white light was created by the commercially available white broadband FL300 Sunlight (33% blue [400–500 nm], 40% green [500–600 nm] and 27% red [600–700 nm]), while the monochromatic FL300 were custom made: blue (wavelength peak at 448 nm), green (528 nm), and red (660 nm). The lamps were adjusted to give 200–215 μmol m^{-2} s^{-1} PAR at plant height (**Table 1**), creating a daily light integral (DLI) of approx. 10.5 mol m^{-2} d^{-1}. Because of the comparatively low photosynthetic photon flux efficacy from green LEDs the green FL300 lamp was complemented by two custom-made narrow, green luminaires (Fluence Bioengineering, Austin, TX, United States). To eliminate stray light the sides of the trolleys were covered with non-transparent black/white plastic with the white side facing inward. Additionally, the position effect within each treatment was minimized by randomizing the treatment pots daily.

The cucumber seedlings were exposed to UV-B radiation 9 days after the start of the light treatments, when the first true leaf was fully expanded. Two open top, front and backside Perspex boxes (OTFB boxes; *c.f.* Qian et al., 2019) were used in each trolley to filter the UV radiation. The open top, front and backsides of the OTFB boxes were covered with sheets of Perspex to block all UV radiation for the exposure of control plants, while 0.13 mm cellulose diacetate (CA) sheets (Nordbergs Tekniska AB, Vallentuna, Sweden) were used for the UV-treated plants to block mainly UV-C radiation (<292 nm). The UV was provided by fluorescent tubes (Philips TL20/12 UV, Eindhoven, Netherlands). The spectra of both UV and the visible light were measured inside the OTFB boxes, with an OL756 double monochromator spectroradiometer (Optronic Laboratories, Orlando, FL, United States) with the orifice of the upward-directed integrating sphere placed approximately 20 cm above the table, at plant height (**Figures 1A,B**). The plant-weighted UV normalized to 300 nm (Thimijan et al., 1978; Yu and Björn, 1997; Kalbina et al., 2008) shows that the UV provided is biologically active in plants almost exclusively in the UV-B range (280–315 nm) (**Figure 1B**). The plant-weighted UV normalized to 300 nm was quantified to 42.4 ± 3.4 mW m^{-2}, corresponding to 0.912 ± 0.074 kJ m^{-2} day^{-1} (at a 6 h daily UV exposure). Plants were exposed to UV-B

TABLE 1 | Photosynthetically active radiation of four different light backgrounds (broadband White, Blue, Green, and Red).

Light treatment	White	Blue	Green	Red
PAR [400–800 nm] (μmol m^{-2} s^{-1})	214	212	201/180[#]	211

The values represent averages.

[#]*Due to the extra green LEDs and the resulting architecture of the light equipment, the UV tube was hanging lower and partly shaded the green lights, thus giving lower PAR in the CA box than in the "Perspex only" box. This shading effect was not happening in the three other light qualities.*

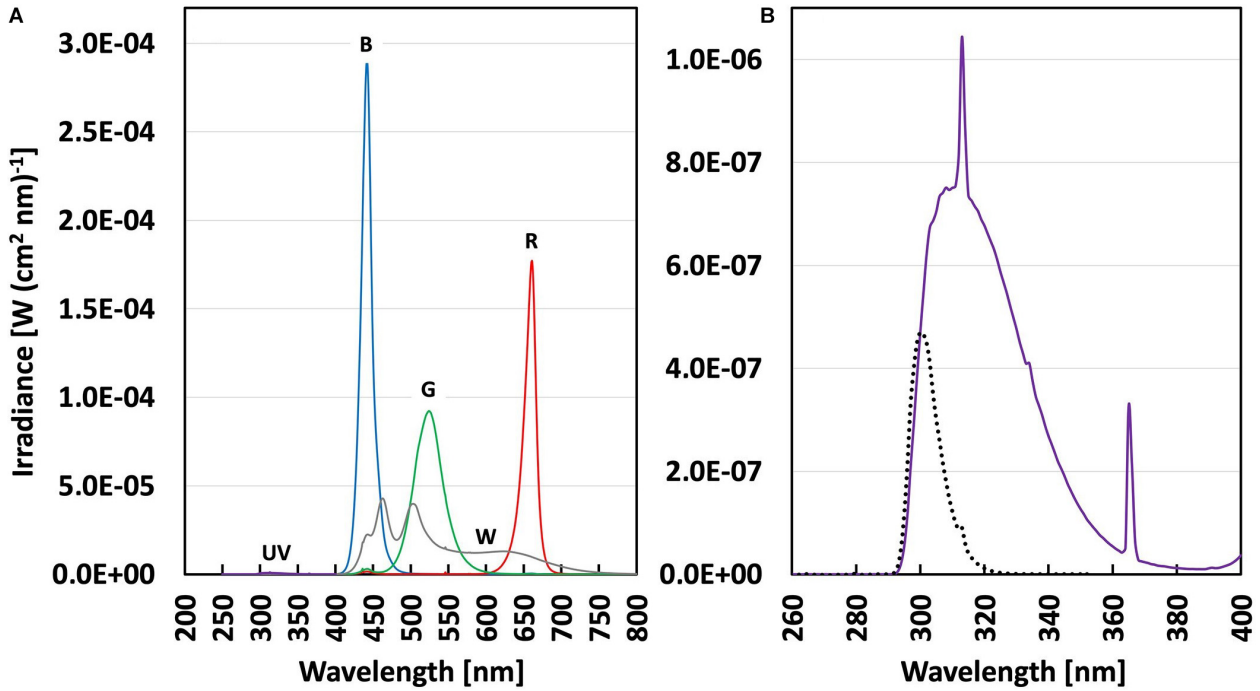

FIGURE 1 | (A) Spectral irradiance (in W(cm^2 nm)$^{-1}$) in Perspex covered (control) and cellulose acetate covered (UV-B) boxes under four different PAR backgrounds (**Table 1**); broadband White (gray line), Blue, Green, Red (with lines of respective color) and UV-B (violet line). **(B)** Spectral irradiance in the UV range (violet line) with enlarged scale and the plant-weighted UV dose (black dotted line) in the UV-B treatments.

radiation for 14 days. Thereafter 22 plants per treatment were measured and harvested (see below). To investigate whether the different light acclimation regimens induced a difference in the ability to cope with photoinhibition, the remaining treatment plants were subjected to a saturating light treatment for 5 h at 1600 μmol m^{-2} s^{-1} PAR provided by two FL300 Sunlight luminaires, delivering an additional light integral of 29 mol m^{-2} 5 h^{-1}.

Plant Growth and Development

Plant growth was assessed for 5–7 plants per treatment through destructive harvest at the end of the UV-B radiation treatment. The plant height was measured from the stem base to the apical meristem and the stem diameter (Ø) 1 cm above the soil using a digital slide caliper (Biltema, Linköping, Sweden). The number of true leaves and leaf area (LA) was measured on scanned leaves using the Image J software (version 1.52a) (Wayne Rasband, National Institute of Health, United States). After each harvest, leaf and stem fresh mass (LFM and SFM) and dry mass (LDM and SDM) were determined after drying for 3 days at 80°C. Specific leaf mass (SLM = leaf DM/LA), leaf mass ratio (LMR = leaf DM/total DM), individual leaf area (ILA = LA/leaf number), internode length (INL = height/leaf number) and dry mass per cent (DM% = total DM/total FM) were calculated.

Gas Exchange Measurements

The photosynthetic CO_2 assimilation rate (A_n), transpiration rate (E), stomatal conductance (g_s) and intracellular CO_2 concentration (C_i) were estimated in seven plants per treatment by gas exchange (CIRAS-2 with PLC6(U) with a LED light source, PP Systems, Amesbury, United States) on the last fully expanded leaf on day 9 to 12 of the UV-B treatment. The conditions during measurement were 22°C leaf temperature, 400 ppm CO_2 and 0.9 ± 1.0 Pa kPa^{-1} vapor pressure deficit (VPD). The light response curve covered 12 light levels starting at a PAR of 250 μmol m^{-2} s^{-1}, decreasing in steps to 20 μmol m^{-2} s^{-1} and again from 250 increasing in steps to 1800 μmol m^{-2} s^{-1}. Data were logged every 5 s and the mean value of 1 min of steady-state was averaged for each light level. The light response curves were fitted by Solver in Excel to a non-rectangular hyperbola (Ögren, 1993) to determine plant dark respiration rate (R_{dark}), the apparent quantum yield of CO_2 assimilation based on incident light (α), the light compensation point (LCP), maximum net assimilation rate at light saturation (A_{max}), and the convexity (θ) of the light response curve.

Chlorophyll Fluorescence Measurements

Chlorophyll fluorescence was measured using a Mini-PAM with leaf clips (Walz, Effeltrich, Germany) on day 13 to 14 of UV-B radiation and after the subsequent saturating light treatment (1600 m^{-2} s^{-1}) that was used to induce photoinhibition. Randomized measurements were performed in the afternoon (13:00–16:00) in 4–5 biological replicates per treatment. The F_o and F_m were measured for maximum photochemical efficiency of PSII (F_v/F_m = (F_m–F_o)/F_m) after 30 min dark adaptation with aluminum foil on the last fully expanded leaf. The

site of measurement was marked on the leaf and the plant was placed under saturating PAR (1600 ± 100 μmol m^{-2} s^{-1}) from a KL 1500 electronic halogen lamp (SCHOTT AG Lighting and Imaging, Mainz, Germany) for 30 min to reach steady-state photosynthesis. Thereafter, the leaf clip was placed on the marked spot, F′ and Fm′ were measured and the operation efficiency of PSII (Fq′/Fm′), the electron transport rate (ETR), the fraction of open PSII centres (q_L) and the non-photochemical quenching (NPQ) were calculated (Murchie and Lawson, 2013).

Non-destructive Optical Absorbance Measurements

Non-destructive measurements of chlorophyll, flavonol and anthocyanin contents were assessed on the adaxial side of the last fully developed leaf with a Dualex+ (FORCE-A, Centre Universitaire Paris Sud, Cedex, France). The four replicates per treatment were measured immediately after the daily UV-B exposure.

Statistical Analysis

All data analyzed was collected from three independent experiments. Statistical analyses were performed in R (version 3.3.1., R Core Development Team, 2017). Linear mixed effects models were fitted using the *lme* function in the *nlme* package (Pinheiro and Bates, 2000) and with experimental replicate as a random component. The effect of the different PAR backgrounds (White, Blue, Green, Red) on plant growth, morphology and physiology was assessed using ANOVA. In case significant differences were identified among treatments, contrasts between the four PAR backgrounds were fitted using the function *fit.contrasts* from the *gmodels* package (Warnes et al., 2018). The resulting *p*-values were adjusted using the function *p.adjust* (Holm, 1979) (**Supplementary Table S3**). Additionally, the effect of supplementary UV-B irradiation was tested solely within the same PAR background and no comparison between light backgrounds was made. Differences between control and UV-B plants within the same light environment were tested using linear mixed effects models with experimental replicate as a random factor. Differences between control and UV-B-treated plants were assessed using ANOVA (**Supplementary Table S4**).

RESULTS

Monochromatic Light Qualities Within the PAR Spectrum Differentially Regulate Growth and Development

To investigate the spectral effect on growth and development of cucumber plants, we analyzed non-UV-B (control plants) grown under different PAR spectra 24 days after germination (**Figure 2**). Plants grown under blue and green light were tallest compared to plants grown under the other light spectra (**Figure 2A**). INL followed the same pattern with decreasing length of internodes from blue to white growth light (**Figure 2B**). Plants grown under red light showed lower total dry mass (TDM) compared to plants grown under the other light spectra, whilst green light plants had the highest TDM (**Figure 2C**). Plants grown under green light had the largest total leaf area (TLA) whilst the plants under broadband white light had the smallest (**Figure 2D**). The white-light-grown plants had a higher SLM compared to plants grown under the other light spectra (**Figure 2E**). Plants grown under green light had the largest leaf number while blue-light plants had the smallest leaf number, compared with the other light treatments (**Figure 2F**).

Green and Red Light Reduce Photosynthesis in Cucumber Leaves

Light response curves were measured in the UV-control plants 9–12 days after the start of the UV-B treatment (**Figure 3A**). For control treatments in the absence of UV-B, plants grown under white and blue light had higher A_{max} followed by the green-light grown plants, whereas the lowest A_{max} was observed in plants grown under red light (**Figure 3B**). The white- and blue-light-grown plants had higher R_{dark} than those grown under green or red light (**Figure 3C**). Furthermore, plants grown under white light had the significantly highest LCP and green-light-grown plants the lowest (**Figure 3D**). The α was significantly lower in plants grown under red light compared to those grown under the other light qualities (**Figure 3E**). Finally, plants grown under red light had the highest θ while those grown under blue light had the lowest (**Figure 3F**).

Monochromatic Light Qualities Induce Different Sensitivity to Saturating Light Conditions

Chlorophyll fluorescence was measured prior to and immediately after the potentially photoinhibitory saturating light treatment (5 h at a PPFD of 1600 μmol m^{-2} s^{-1}) to assess the light stress tolerance of plants grown under different light spectra. Prior to the saturating light treatment, the red-light-grown control plants had significantly lower F_v/F_m compared to plants grown under the other light spectra (**Figure 4A**). After the saturating light treatment, plants grown under white light had the highest F_v/F_m, followed by plants grown under blue, green and red monochromatic light, in descending order (**Figure 4A**). Prior to the saturating light treatment, the ETR and q_L were significantly highest in plants grown in white or blue light, while red light-grown plants had the significantly lowest values (**Figures 4B,C**). Finally, prior to saturating light application, plants grown under red light had significantly lower NPQ than plants grown under the other spectra, whereas after the saturating light treatment, plants grown under white light were the only ones showing significantly higher NPQ compared with plants grown under the other spectra (**Figure 4D**).

Non-destructive Measurements of Chlorophyll and Epidermal Flavonols

Plants grown under white light had a higher chlorophyll content compared to plants grown under blue or green light.

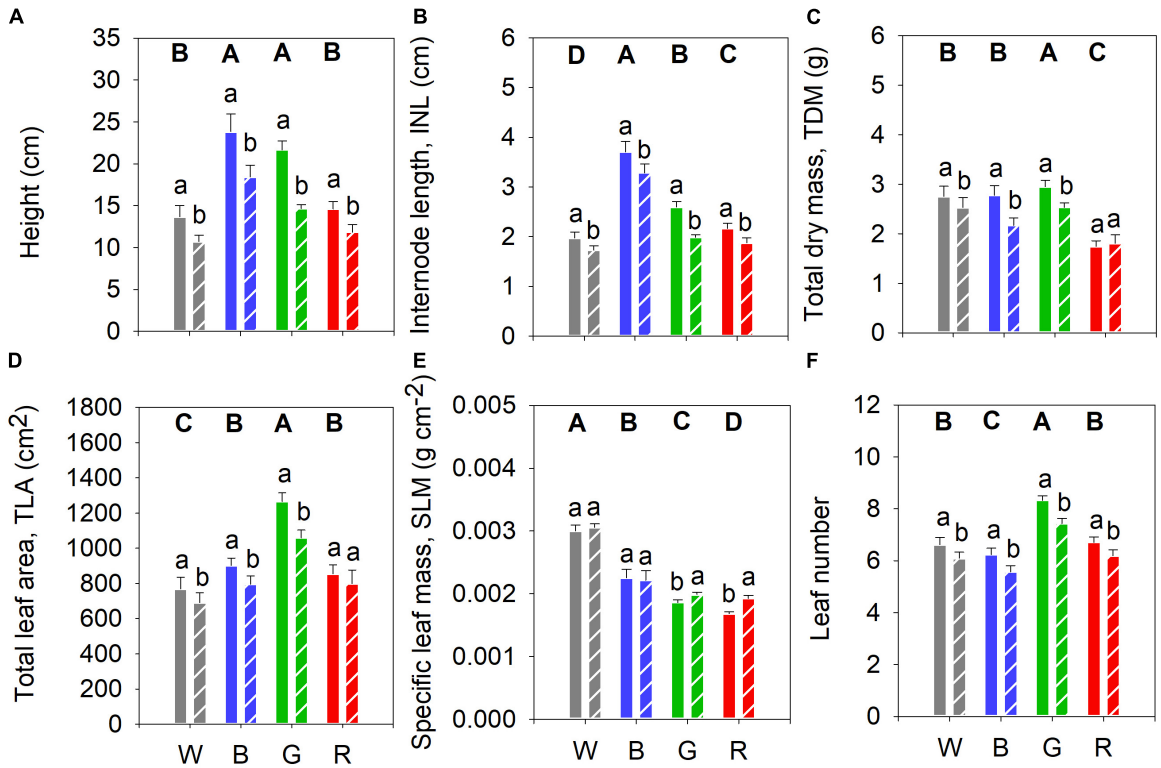

FIGURE 2 | Biomass accumulation of cucumber plants grown under four PAR backgrounds after 14 days without (solid bars) or with (dashed bars) exposure to supplementary UV-B irradiation. **(A)** Height (cm); **(B)** Internode length (INL, cm); **(C)** Total dry mass (TDM, g); **(D)** Total leaf area (TLA, cm^2); **(E)** Specific leaf mass (SLM, g cm^{-2}); **(F)** Leaf number. Data are mean values ($n = 21 \pm$ SE). Capital letters indicate significant differences between growth light qualities without UV-B and lower-case letters between non-UV-B-exposed plants and UV-B-exposed plants within the same light backgrounds, both at $P < 0.05$.

Red light-grown plants exhibited an even lower chlorophyll content (**Figure 5A**). Cucumber seedlings grown under white and blue light had the highest content of epidermal flavonols, while plants grown under red and green light had the lowest concentrations (**Figure 5B**). Moreover, plants grown under red light showed the significantly highest anthocyanin content with leaf concentrations decreasing in the following order of light spectra: blue > green > white (**Figure 5C**).

UV-B-Induced Effects on Plant Morphology Is Dependent on Monochromatic Light Background

We also analyzed the influence of different monochromatic growth light qualities on UV-induced plant responses. Supplementary UV-B led to a decrease in plant height and INL compared to the corresponding controls (**Figures 2A,B**, respectively). UV-B also generally reduced plant TDM, except in plants grown under red light (**Figure 2C**). Moreover, after UV-B exposure, plant TLA decreased significantly in all treatments except for those grown under red light (**Figure 2D**). Finally, SLM increased in UV-B-treated plants grown in green and red light backgrounds (**Figure 2E**), whereas leaf number was decreased in all cases (**Figure 2F**).

Supplementary UV-B Boosted Photosynthesis in Cucumber Grown Under Red Light

The light response curves of plants grown in the control and UV-B OFTB boxes were compared in order to investigate the effects of supplementary UV-B on photosynthesis parameters in cucumber plants grown under the different spectra (**Figure 3A**). Only UV-B-exposed plants grown under red light had a statistically significant increase in A_{max}, whereas A_{max} was unaltered in all other plants (**Figure 3B**), which in turn resulted in a similar pattern for the R_{dark} and LCP parameters (**Figures 3C,D**, respectively). α significantly decreased after UV-B exposure in plants grown under white or blue light, whilst no significant differences were observed in red or green light (**Figure 3E**). The UV-B exposure of cucumber led to significant decreases in θ in plants grown under white or red light, whereas no significant differences were observed in plants grown under blue or green light (**Figure 3F**).

The PAR Spectrum Changes the Effect of UV-B and the Susceptibility to Photoinhibition

To investigate the effect of UV-B on the susceptibility to photoinhibition, plants from all treatments were exposed to 5 h

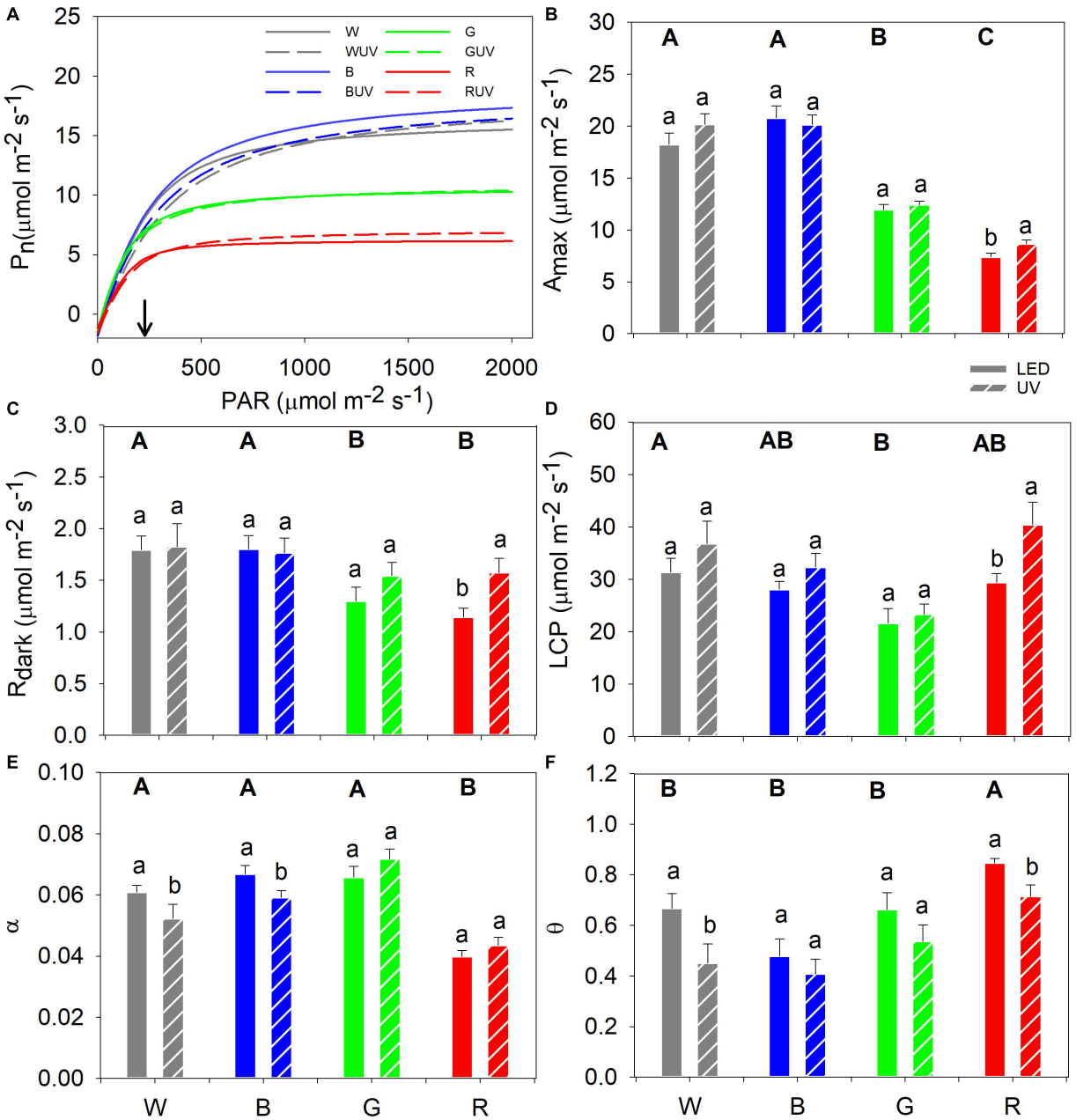

FIGURE 3 | (A) Fitted light response curves of cucumber grown under four LED light backgrounds (White, Blue, Green, and Red) without (solid bars) and with (dashed bars) exposure to supplementary UV-B radiation for 14 days [for variation of the data at light saturation refer from panels **(B–F)**], where the arrow indicates the growth PAR. Curve fitted parameters: **(B)** Maximum net assimilation rate (A_{max}); **(C)** Dark respiration (R_{dark}); **(D)** Light compensation point (LCP); **(E)** Apparent quantum yield of photosynthesis (α); and **(F)** convexity (θ). Bars represent the mean values (n = 21 ± SE). Capital letters indicate significant differences between growth light qualities without UV-B and lower-case letters between non-UV-B-exposed plants and UV-B-exposed plants within the same PAR background, both at $P < 0.05$.

of saturating light after the last day of exposure to UV-B. Prior to the saturating light treatment, only plants grown under white light had a small but significant decrease in F_v/F_m after UV-B exposure (**Figure 4A**). The F_v/F_m of plants grown under the other light qualities was unaffected by UV-B. After the saturating light treatment, however, plants grown under the red PAR background showed no significant effect of UV-B on F_v/F_m, whilst the other PAR backgrounds led to significant decreases in F_v/F_m by UV-B (**Figure 4A**). Prior to the exposure to saturating light, ETR and q_L were reduced after UV-B irradiation in plants grown under white and blue PAR, whereas plants grown under green PAR were unaffected. UV-B exposed plants grown under red PAR were boosted (but non-significantly for ETR) (**Figures 4B,C,** respectively). After the saturating light treatment, plants that had

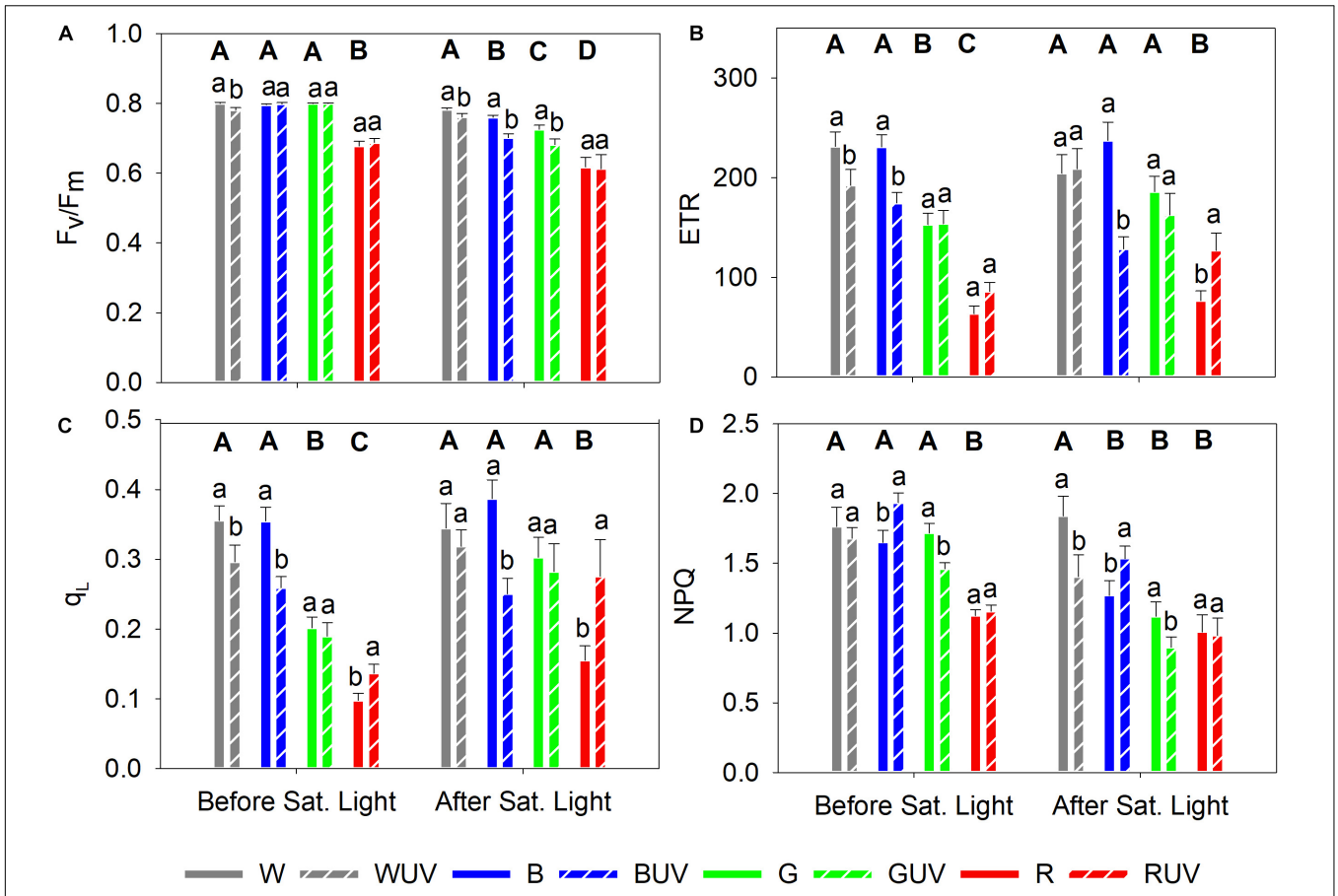

FIGURE 4 | Chlorophyll fluorescence parameters measured in cucumber plants grown under four different PAR qualities (White, Blue, Green, and Red) and without (solid bars) or with (dashed bars) exposure to supplementary UV-B radiation for 14 days, prior to and after a 5 h saturating light treatment (1600 μmol m^{-2} s^{-1}). **(A)** Maximum photochemical efficiency (F_v/F_m); **(B)** Apparent electron transport rate (ETR); **(C)** Fraction of oxidized PSII (q_L), **(D)** Non-photochemical quenching (NPQ). Bars represent mean values (Before saturating light: $n = 21 \pm$ SE; After saturating light $n = 15 \pm$ SE). Capital letters indicate significant differences between growth light qualities without UV-B and lower-case letters between non-UV-B-exposed plants and UV-B exposed plants within the same PAR background, both at $P < 0.05$.

been exposed to UV-B showed a significant decrease in ETR when grown under blue PAR, while ETR was boosted by UV-B in plants that had red background PAR (**Figure 4B**). Finally, prior to the saturating light treatment, UV-B increased NPQ in plants grown under blue PAR and decreased in plants grown under green PAR (**Figure 4D**). After the saturating light treatment, however, UV-B decreased NPQ in white light-grown plants, while NPQ increased in plants grown under blue PAR (**Figure 4D**).

UV-B Has a Limited Effect on Pigment Accumulation

After the UV-B treatment, the chlorophyll content increased significantly in plants grown under white and green light compared to their controls (**Figure 5A**). The strong decrease in epidermal flavonol content seen in plants grown in green or red light, compared with plants grown in white or blue light, was slightly mitigated by UV-B exposure in plants grown in green light (**Figure 5B**). UV-B exposure of plants grown in blue light led to a significant increase in the anthocyanin content compared to the control, whereas for plants grown under the other light spectra the UV-B did not have any significant effect (**Figure 5C**).

DISCUSSION

Monochromatic Light Differentially Affects Plant Development and Photosynthesis

Development and physiology of cucumber plants grown under white, blue, green or red light differed substantially. Plants grown under white light were more compact, had smaller and thicker leaves compared to plants grown under the other light qualities, yet retained a high biomass accumulation. Notably, plants grown under blue light had a high biomass accumulation and had longer stems and larger leaves. It has been previously shown that blue light effects on growth were dependent on both the plant species studied and the growth conditions. While blue light inhibited stem elongation and leaf expansion, through

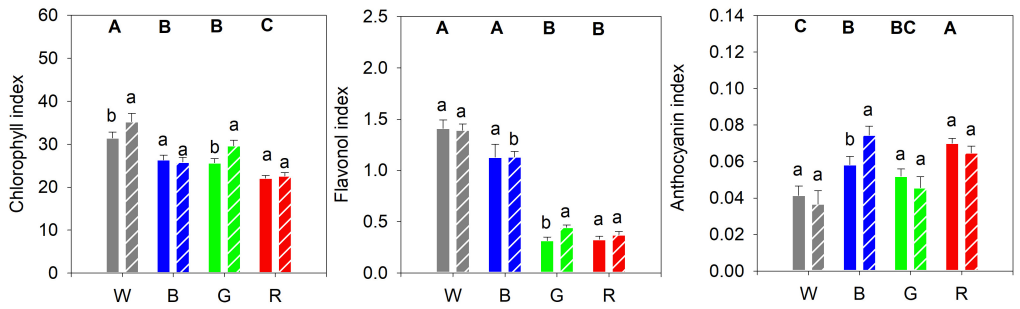

FIGURE 5 | (A) Epidermal chlorophyll, **(B)** flavonol and **(C)** anthocyanin content of cucumber plants, as measured with a DUALEX instrument, and grown under different light quality backgrounds (White, Blue, Green, and Red) and without (solid bars) or with (dashed bars) exposure to supplementary UV-B radiation for 14 days. Data are mean values (n = 15 ± SE). Capital letters indicate significant differences between growth light qualities without UV-B and lower-case letters between non-UV-B-exposed plants and UV-B exposed plants within the same PAR background, both at $P < 0.05$.

a reduction in cell expansion (Cosgrove, 1981), other reports instead inferred increased stem elongation and leaf expansion under this light quality (Ahmad and Cashmore, 1997; Hernández and Kubota, 2016). This blue light induction of growth was previously associated to lack of co-action between phytochromes and cryptochromes (Ahmad and Cashmore, 1997; Hernández and Kubota, 2016) and could explain the increased INL and ILA observed in blue-light-grown plants in our study. Plants grown under either broadband white or blue light had similar photosynthetic responses, suggesting that monochromatic blue light was enough to maintain photosynthetic activity. Similar levels of NPQ, ETR, F_q'/F_m' (data not shown) and q_L of plants grown under blue or white light support this (**Figure 4**). Therefore, blue-light-grown plants are able to efficiently use photosynthates for growth.

Our data show that cucumber plants grown under green light had a higher leaf number than plants grown under any of the other light qualities, indicating an increased developmental rate in green PAR. Johkan et al. (2012) showed that small shifts in green wavelengths (510, 520, and 530 nm) had remarkable effects on growth and morphology in red leaf lettuce, and that under a moderate light intensity (300 μmol m^{-2} s^{-1}), green light induced a higher biomass accumulation and larger leaf expansion than in plants grown under broadband white light. Green PAR is perceived by both phytochromes and cryptochromes. However, compared with the strong absorption of red and blue wavelengths, respectively, green wavelengths are poorly absorbed by both photoreceptors (Folta and Maruhnich, 2007). Green PAR penetrates deeper into leaf mesophyll than other wavelengths (Smith et al., 2017), increasing absorption of green quanta in light-depleted environments (Sun et al., 1998). The thinner and larger leaves of plants grown under green light could indicate that plants are trying to optimize light absorption by increasing both the light intercepting area and the light transmission to lower levels in the canopy since light scattering in leaves improves light penetration into the leaf especially in the green part of the spectrum (DeLucia et al., 1996). Also, absorption of green light triggered both large and fast biomass accumulation (**Figure 2**). In fact, green-light-grown plants had slightly larger biomass than plants grown under white or blue light, although A_n was lower than in the white- or blue-light-grown plants (**Supplementary Figure S1**). Thus, plants grown under monochromatic green light managed to sustain growth and development due to improved light absorption at the canopy level as a result of a combination of larger and thinner leaves and improved light transmission. A limitation of this study was that the measurement of photosynthesis was made on the first fully developed leaf (sun leaf) from the top. It shows the acclimation of photosynthesis to the spectrum but does not give a full picture of the canopy photosynthesis. However, it could be expected that the efficient penetration of green light into leaves (DeLucia et al., 1996; Smith et al., 2017) and the distribution of the photosynthetic machinery over large and thin leaves measured under green PAR would allow efficient canopy light absorption and efficient photosynthesis also at the lower leaf levels. If comparing plants grown in white or green light by putting the values of TDM, TLA and A_{max} to 1 for white-light-grown plants, the relative values for the green-light-grown plants will be TDM = 1.07, TLA = 1.65, and A_{max} = 0.65. If these numbers are used to calculate a very crude estimation of the total canopy A_{max}, without taking internal shading and light acclimation into consideration, the white-light-grown plants will have canopy A_{max} of 1 × 1 = 1, while the green-light-grown plants will have 1.65 × 0.65 = 1.07. This crude relative photosynthesis rate at light saturation on canopy level actually fits to the relative TDM for the green-light-grown plants.

In nature, a green-light-enriched environment is an indication of overgrowing vegetation triggering a shade-avoidance response resulting in stem elongation and upward leaf orientation (Zhang et al., 2011; Zhang and Folta, 2012; Wang et al., 2015). Moreover, Folta (2004) suggested that supplementary green light irradiation induces early hypocotyl elongation. Inhibition of stem elongation is a phytochrome-dependent response, and the wavelengths of our green growth light fall precisely outside the range of the phytochrome action spectrum, thus simulating a light environment lacking the red wavelengths. In our study, green light grown plants were significantly taller than the plants grown under red and broadband white light. This suggests that plants grown under green light, in addition to having thinner and larger leaves, also tried to optimize light absorption by growing taller in response to a red-depleted light environment.

While blue growth light did not change any of the plants' photosynthetic parameters compared with plants grown in white light, plants grown under green light showed decreased A_{max}, R_{dark}, and LCP, while maintaining α and θ at the same levels as plants grown in white or blue light (**Figure 3**). All these changes correspond to low-light acclimation of photosynthesis (Givnish, 1988), accompanied by lower ETR and q_L, and maintained NPQ, resulting in an NPQ increase in proportion to ETR. Plants grown under green light showed a large decrease in the light saturated A_{max} compared with plants grown in white light. However, at the lower growth irradiance (210 μmol m^{-2} s^{-1}) the decrease of A_n was considerably smaller. Since the total biomass production was even higher in plants grown under green light than in plants grown under white PAR, this suggests that the green-light-grown-plants were not source limited.

Generally, plants grown under monochromatic red PAR cannot sustain normal photosynthetic activity (Hogewoning et al., 2010; Trouwborst et al., 2010). Red-light-grown plants had a severely decreased A_{max} so that the growth was source limited with a much decreased A_n and a lower biomass production. For plants grown under red light, A_{max} decreased more than in plants grown under green light, and when R_{dark} decreased, so did α, leaving LCP unaffected. Plants grown under red PAR were the only ones showing a lower α, which deviates from the normal pattern of acclimation to low light level (Givnish, 1988). It could be expected a lower α during stomatal limitation of A_n, but this was not the case since C_i was unaffected (**Supplementary Figure S1**), suggesting instead a strong biochemical limitation. A decrease in α could also be an indication of photoinhibition (Ögren and Sjöström, 1990). Indeed, F_v/F_m was significantly lower in plants grown under red PAR than in those grown under white light which agrees with previous studies showing dysfunctional photosynthesis in cucumber grown in the absence of blue PAR during growth (Hogewoning et al., 2010). NPQ is a protective mechanism through which plants dissipate excessive energy in the form of heat (Maxwell and Johnson, 2000). The low NPQ of red-light-grown cucumber suggests a low heat dissipation, which could be associated with a strong down-regulation of the photosynthetic process. Furthermore, impairment of photosynthesis could explain the growth inhibition observed in cucumber grown under red light, manifested as plants with the smallest stem Ø and lowest biomass accumulation (LDM, SDM, and TDM) compared with plants grown under the other light qualities. Red-light-grown cucumber also had highest LMR, suggesting that the plants allocated as many resources as possible toward leaves to mitigate growth inhibition.

To evaluate how light acclimation affected general light stress tolerance, plants were subjected to a 5-h photoinhibitory treatment. The applied high light stress decreased F_v/F_m in all treatments. However, white-light-grown plants had the smallest decrease, suggesting a better ability to cope with saturating light conditions. Plants grown under blue, green or red light showed gradually lower F_v/F_m, indicating increasing sensitivity toward saturating light in that order. ETR and q_L also gradually decreased in the same order, although it was only plants grown under red light that showed a statistically significant change (**Supplementary Table S3**). NPQ decreased in plants grown under all different monochromatic light qualities, indicating that energy dissipation due to down-regulation of PSII increased. This was manifested as a lower F_v/F_m, at the expense of light-regulated heat dissipation (NPQ), particularly in red-light-grown plants.

Metabolite Composition Is Affected by Spectral Composition

We show a relation between the spectral composition and accumulation of secondary metabolites. The non-destructive measurements showed that plants grown under white light had the highest total chlorophyll content, followed by plants grown under blue, green and red light in decreasing order. This indicates the importance of blue light in the light environment for chlorophyll formation in cucumber during growth. The effects of broadband white on flavonoid content differs between plant species, but in our study, the cucumber plants grown under white PAR had the highest leaf epidermal flavonol content followed by plants grown under blue light. Plants grown under green or red light had significantly lower leaf epidermal flavonol content. In fact, Ouzounis et al. (2014) showed an increase in flavonoid content of roses, campanulas and chrysanthemums with an increasing proportion of blue light in a red background light, in contrast to a low flavonoid content in plants grown under monochromatic red light.

Anthocyanins often function as photoprotective pigments, reducing the amount of light that penetrates the leaf epidermis and preventing damage caused by excessive incident light (Day et al., 1993). In our study, red-light-grown plants had the highest anthocyanin content, followed by plants grown in blue, green and white light, respectively. This suggests that plants grown under red PAR induced anthocyanin accumulation in the leaf epidermis in order to reduce incident light and protect the photosynthetic system from further damage. An increased anthocyanin accumulation in plants grown under red light has previously been reported in red cabbage (Mizuno et al., 2011), bilberries (Zoratti et al., 2014), and lettuce (Garrett Owen and Lopez, 2015). The accumulation of anthocyanins, as well as the decreased F_v/F_m and α suggest that the red light is a stress factor in cucumber, but that the accumulated anthocyanins were insufficient to protect the leaves from light stress by the red growth light.

Monochromatic Light Treatments Modify UV-B Responses in Cucumber

We found that a lower than ambient level of supplementary UV-B exposure led to decreased extension growth (height and INL) that mostly affected plants grown in green and red PAR, in which SLM increased. This indicates that plants developed shorter stems and thicker leaves to acclimate to UV-B (Jenkins, 2017). Moreover, a clear partitioning of biomass from stem to leaves were observed in plants grown under all light qualities after exposure to UV-B, manifested as a higher LMR. The height, leaf number and TDM were reduced and the effects were smallest in plants grown under red light. This either suggests that red-light-grown plants are less sensitive to the low UV-B level used with

regards to morphology, or that growth inhibition caused by red growth light itself overrides the effects of supplementary UV-B. It should also be noted that the effects of UV-B are dose dependent and high doses of UV-B radiation, much higher than those used in this study, can cause distress and reduce plant growth and development (Hideg et al., 2013). Low level supplementary UV-B exposures reduced α in plants grown in white light although A_{max} remained unaltered. In addition, supplementary UV-B led to decreased F_v/F_m, ETR, and q_L, while no effects on NPQ were observed in white-light-grown plants, suggesting a slight down-regulation of photosynthesis compared with the corresponding control plants. UV-B radiation can decrease photosynthetic capacity through a number of high dose mechanisms targeting for instance both the donor and the acceptor sides of Photosystem II or Rubisco (Jordan et al., 2016). Other such mechanisms include photodegradation of light-absorbing pigments (Prasad et al., 2004), such as chlorophyll (Strid and Porra, 1992; Nedunchezhian and Kulandaivelu, 1997) and carotenoids. However, we show that the chlorophyll content increases in cucumber grown in white light treated with UV-B compared with the corresponding control, contributing to the contradicting conclusions described in literature (Jordan et al., 2016). This may be due to different levels of UV-B used in in different studies, as well as the use of different UV-B to PAR ratios.

The use of blue light may prevent damage caused by high UV-B levels (Hoffmann et al., 2015; Escobar-Bravo et al., 2017). Hoffmann et al. (2015) demonstrated that high intensities of blue light (300 μmol m^{-2} s^{-1}) improved the photosynthetic performance of pepper plants exposed to UV-B. The reduced UV-B damage could be explained by reduced degradation of photosynthetic pigments and by increased accumulation of epidermal UV-absorbing flavonoids synergistically induced by blue light and UV-B (Nascimento et al., 2013; Ouzounis et al., 2014; Hoffmann et al., 2015). However, this was not observed in our study using low level UV-B. Together with an unchanged A_{max}, decreased ETR and q_L, as well as an increased NPQ in plants grown under blue PAR, we show that monochromatic blue light does not improve plant acclimation or increase photoprotection to UV-B. The production of anthocyanins has previously been shown to increase by a combination of blue PAR and UV-A in turnip seedlings (Wang et al., 2012) and apple (Arakawa et al., 1985). This agrees with our results.

Cucumbers appear less susceptible to low levels of UV-B when grown in green light, since a decrease in NPQ was the only significant UV-B-induced change in the photosynthesis parameters, suggesting a slightly increased energy flow to photochemistry. This was accompanied by higher concentrations of chlorophyll and flavonols. Most interestingly, adding UV-B to red PAR growth light boosted photosynthesis of cucumber plants compared with the corresponding red PAR control. Although a higher A_{max}, LCP, and R_{dark} indicated increased photosynthesis, this was not due to improved photochemistry (no increase in α), but rather due to a positive effect on the biochemical processes regulating CO_2 assimilation. Moreover, supplementary UV-B had no negative effect on F_v/F_m and did not induce any additional stress to the photosynthetic machinery of red-light-grown plants. Additionally, no changes in epidermal pigment content (chlorophyll, flavonol, and anthocyanin) were observed when supplementary UV-B was added to a red PAR growth light. The positive effects on photosynthesis may explain the lack of growth inhibition caused by UV-B in a background of red growth light.

Light Spectra and UV-B Affects the Susceptibility to Photoinhibition

The use of realistic levels of UV-B radiation play an important role in enhancing photoprotection under saturating light (Wargent et al., 2015), rather than causing further damage to the photosynthetic apparatus. After photoinhibition, plants grown under all different light qualities (but without UV-B) showed a lowered F_v/F_m along a distinct gradient with the smallest effect in plants grown in white light, via blue- and green-light-grown plants, to the largest effect in plants grown in red light. In addition, supplementary UV-B lowered F_v/F_m even further in plants grown in each different light quality, except for red-light-grown plants, where F_v/F_m was unaffected. This is of particular interest since ETR and q_L decreased after 2 weeks of UV-B exposure prior to photoinhibitory treatment in blue-light-grown plants (unaffected A_{max}; **Figure 3**), remained the same in green-light-grown plants (slightly reduced A_{max}), but increased in red-light-grown cucumber (strongly reduced A_{max}; lower F_v/F_m). We suggest that the low UV-B levels used in our study create eustress to activate defense systems, e.g., antioxidants, which put the plants in a state of "low alert" toward other stresses that may involve oxidative stress (Hideg et al., 2013), including photoinhibition. Obviously, addition of UV-B is not enough to fully overcome stress induced by red light given in the growth phase, but both A_{max} and q_L are significantly higher in UV-B-treated photoinhibited plants than in plants that had been grown solely in red light before photoinhibition (with a clear trend also in ETR). In fact, absolute levels of q_L and ETR in UV-B-treated photoinhibited red-light-grown plants were similar as in UV-B-treated photoinhibited green- or blue-light-grown plants. If the UV-B treatment induces a low-level alert against other stresses (Jansen et al., 2019), it seems that such another stress (in this case photoinhibition) has to be of a certain magnitude for a plant to benefit from the UV-B treatment. Thus, the effect of UV-B mitigating a second stress, such as photoinhibition, follows a gradient from no beneficial effect at all in non-stressed leaves to a beneficial effect in already light stressed leaves.

CONCLUSION

In agreement with our first hypothesis, we show that different monochromatic light backgrounds exert different responses in growth and physiology in cucumber. Monochromatic green and blue growth light, but not red, enabled normal photosynthetic functioning of leaves of cucumber plants without compromising biomass accumulation. Despite being exposed to the same light level, plants grown in green light showed low light acclimation of photosynthesis, but because of the changed canopy architecture with larger and thinner leaves these plants had the highest total biomass production. On the other hand, in plants grown in

red light, the low light acclimation was more pronounced and accompanied by light stress symptoms that reduced F_v/F_m and also led to reduced growth.

Our data confirmed our second hypothesis that cucumber responses to UV-B are highly dependent of the spectrum of monochromatic growth light. Supplementary UV-B radiation decreased plant growth and development in plants grown under blue, green and white but not under red light. Although the results suggest dysfunctional photosynthesis in plants grown under red light, UV-B boosted some photosynthetic parameters, actually increasing the potential carbon gain. Thus, UV-B and red light could act synergistically on priming the plant antioxidant capacity and diminish negative effects of photoinhibition. However, a more in-depth study of the metabolic and molecular pathways and antioxidants triggered by the treatments is required to fully explain our findings.

The findings presented here could have a positive impact on horticultural settings. By using the right monochromatic light in early stages of cucumber production, plant development may be accelerated and thus decreasing overall production time.

DATA AVAILABILITY STATEMENT

The original contributions presented in the study are included in the article/**Supplementary Material**. Further inquiries can be directed to the corresponding author/s.

AUTHOR CONTRIBUTIONS

CP performed the experiment and most of the analysis, and prepared the manuscript. VC-A commented on the manuscript. LM assisted with analysis and worked on the manuscript. ER helped analyzing data and edited the manuscript. C-OO worked with editing of the manuscript. ÅS prepared spectral figures and edited the manuscript. All authors contributed to the article and approved the submitted version.

FUNDING

The project was funded by GUDP (Danish Ministry of Food, Agriculture and Fisheries) for the project Dynamic light, Interreg North Sea project SMARTGREEN and research center iFood. This project was also funded by research grants from the Knowledge Foundation (http://kks.se; grant #20130164), and the Swedish Research Council Formas (http://formas.se/en; grant #942-2015-516). The project was also supported by the Faculty for Business, Science and Technology at Örebro University and by Örebro University Vice Chancellor's strategic research programme on 'Food and Health'. Furthermore, part of the Ph.D. project was covered by the Research School for Science and Technology and iFood (Aarhus University Centre for Innovative Food Research).

ACKNOWLEDGMENTS

The authors would like to thank Dr. Irina Kalbina for the technical assistance and guidance. We also thank Nikolaj Bjerring Jensen and Dr. Rong Zhou for the helpful discussion and critical evaluation of the manuscript.

SUPPLEMENTARY MATERIAL

The Supplementary Material for this article can be found online at: https://www.frontiersin.org/articles/10.3389/fpls.2020.610011/full#supplementary-material

REFERENCES

Agati, G., and Tattini, M. (2010). Multiple functional roles of flavonoids in photoprotection. *New Phytol.* 186, 786–793. doi: 10.1111/j.1469-8137.2010.03269.x

Ahmad, M., and Cashmore, A. R. (1997). The blue-light receptor cryptochrome 1 shows functional dependence on phytochrome A or phytochrome B in *Arabidopsis thaliana*. *Plant J.* 11, 421–427. doi: 10.1046/j.1365-313X.1997.11030421.x

Arakawa, O., Hori, Y., and Ogata, R. (1985). Relative effectiveness and interaction of ultraviolet−B, red and blue light in anthocyanin synthesis of apple fruit. *Physiol. Plant.* 64, 323–327. doi: 10.1111/j.1399-3054.1985.tb03347.x

Bayat, L., Arab, M., Aliniaeifard, S., Seif, M., Lastochkina, O., and Li, T. (2018). Effects of growth under different light spectra on the subsequent high light tolerance in rose plants. *AoB Plants* 10, 1–17. doi: 10.1093/aobpla/ply052

Boccalandro, H. E., Giordano, C. V., Ploschuk, E. L., Piccoli, P. N., Bottini, R., and Casal, J. J. (2012). Phototropins but not cryptochromes mediate the blue light-specific promotion of stomatal conductance, while both enhance photosynthesis and transpiration under full sunlight. *Plant Physiol.* 158, 1475–1484. doi: 10.1104/pp.111.187237

Bourget, C. M. (2008). An introduction to light-emitting diodes. *HortScience* 43, 1944–1946. doi: 10.21273/hortsci.43.7.1944

Briggs, W. R., and Huala, E. (1999). Blue-light photoreceptors in higher plants. *Annu. Rev. Cell Dev. Biol.* 15, 33–62. doi: 10.1146/annurev.cellbio.15.1.33

Cosgrove, D. J. (1981). Rapid suppression of growth by blue light. *Plant Physiol.* 67, 584–590. doi: 10.1104/pp.68.6.1447

Darko, E., Heydarizadeh, P., Schoefs, B., and Sabzalian, M. R. (2014). Photosynthesis under artificial light: the shift in primary and secondary metabolism. *Philos. Trans. R. Soc. London Ser. B Biol. Sci.* 369:20130243. doi: 10.1098/rstb.2013.0243

Day, T. A., Martin, G., and Vogelmann, T. C. (1993). Penetration of UV−B radiation in foliage: evidence that the epidermis behaves as a non−uniform filter. *Plant. Cell Environ.* 16, 735–741. doi: 10.1111/j.1365-3040.1993.tb00493.x

Day, T. A., and Vogelmann, T. C. (1995). Alterations in photosynthesis and pigment distributions in pea leaves following UV−B exposure. *Physiol. Plant.* 94, 433–440. doi: 10.1111/j.1399-3054.1995.tb00950.x

de Carbonnel, M., Davis, P., Roelfsema, M. R. G., Inoue, S.-I., Schepens, I., Lariguet, P., et al. (2010). The *Arabidopsis* PHYTOCHROME KINASE SUBSTRATE2 protein is a phototropin signaling element that regulates leaf flattening and leaf positioning. *Plant Physiol.* 152, 1391–1405. doi: 10.1104/pp.109.150441

DeLucia, E. H., Nelson, K., Vogelmann, T. C., and Smith, W. K. (1996). Contribution of intercellular reflectance to photosynthesis in shade leaves. *Plant Cell Environ.* 19, 159–170. doi: 10.1111/j.1365-3040.1996.tb00237.x

Demkura, P. V., and Ballaré, C. L. (2012). UVR8 mediates UV-B-induced *Arabidopsis* defense responses against *Botrytis cinerea* by controlling sinapate accumulation. *Mol. Plant* 5, 642–652. doi: 10.1093/mp/sss025

Demotes-Mainard, S., Péron, T., Corot, A., Bertheloot, J., Le Gourrierec, J., Pelleschi-Travier, S., et al. (2016). Plant responses to red and far-red lights, applications in horticulture. *Environ. Exp. Bot.* 121, 4–21. doi: 10.1016/j.envexpbot.2015.05.010

Escobar-Bravo, R., Klinkhamer, P. G. L., and Leiss, K. A. (2017). Interactive effects of UV-B light with abiotic factors on plant growth and chemistry, and their consequences for defense against arthropod herbivores. *Front. Plant Sci.* 8:278. doi: 10.3389/fpls.2017.00278

Fankhauser, C., and Chory, J. (1997). Light control of plant development. *Annu. Rev. Cell Dev. Biol.* 13, 203–229. doi: 10.1146/annurev.cellbio.13.1.203

Folta, K. M. (2004). Green light stimulates early stem elongation. *Plant Physiol.* 135, 1407–1416. doi: 10.1104/pp.104.038893.1

Folta, K. M., and Maruhnich, S. A. (2007). Green light: a signal to slow down or stop. *J. Exp. Bot.* 58, 3099–3111. doi: 10.1093/jxb/erm130

Frechilla, S., Talbott, L. D., Bogomolni, R. A., and Zeiger, E. (2000). Reversal of blue light-stimulated stomatal opening by green light. *Plant Cell Physiol.* 41, 171–176. doi: 10.1093/pcp/41.2.171

Garrett Owen, W., and Lopez, R. G. (2015). End-of-production supplemental lighting with red and blue light-emitting diodes (LEDs) influences red pigmentation of four lettuce varieties. *HortScience* 50, 676–684. doi: 10.21273/hortsci.50.5.676

Givnish, T. J. (1988). Adaptation to sun and shade: a whole-plant perspective. *Aust. J. Plant Physiol.* 15, 63–92. doi: 10.1071/pp9880063

Graamans, L., Baeza, E., van den Dobbelsteen, A., Tsafaras, I., and Stanghellini, C. (2018). Plant factories versus greenhouses: comparison of resource use efficiency. *Agric. Syst.* 160, 31–43. doi: 10.1016/j.agsy.2017.11.003

Heijde, M., and Ulm, R. (2012). UV-B photoreceptor-mediated signalling in plants. *Trends Plant Sci.* 17, 230–237. doi: 10.1016/j.tplants.2012.01.007

Hernández, R., and Kubota, C. (2016). Physiological responses of cucumber seedlings under different blue and red photon flux ratios using LEDs. *Environ. Exp. Bot.* 121, 66–74. doi: 10.1016/j.envexpbot.2015.04.001

Hideg, É, Jansen, M. A. K., and Strid, Å (2013). UV-B exposure, ROS, and stress: inseparable companions or loosely linked associates? *Trends Plant Sci.* 18, 107–115. doi: 10.1016/j.tplants.2012.09.003

Hideg, É, and Strid, A. (2017). "The effects of UV-B on the biochemistry and metabolism of plants," in *UV-B Radiation and Plant Life. Molecular Biology and Ecology*, ed. B. R. Jordan (Wallingford: CAB International), 90–110. doi: 10.1079/9781780648590.0090

Hoffmann, A. M., Noga, G., and Hunsche, M. (2015). High blue light improves acclimation and photosynthetic recovery of pepper plants exposed to UV stress. *Environ. Exp. Bot.* 109, 254–263. doi: 10.1016/j.envexpbot.2014.06.017

Hogewoning, S. W., Trouwborst, G., Maljaars, H., Poorter, H., van Ieperen, W., and Harbinson, J. (2010). Blue light dose-responses of leaf photosynthesis, morphology, and chemical composition of *Cucumis sativus* grown under different combinations of red and blue light. *J. Exp. Bot.* 61, 3107–3117. doi: 10.1093/jxb/erq132

Holm, S. (1979). A simple sequentially rejective multiple test procedure. *Scand. J. Stat.* 6, 65–70.

Huché-Thélier, L., Crespel, L., Gourrierec, J. L., Morel, P., Sakr, S., and Leduc, N. (2016). Light signaling and plant responses to blue and UV radiations – perspectives for applications in horticulture. *Environ. Exp. Bot.* 121, 22–38. doi: 10.1016/j.envexpbot.2015.06.009

Jansen, M. A. K. (2002). Ultraviolet-B radiation effects on plants: induction of morphogenic responses. *Physiol. Plant.* 116, 423–429. doi: 10.1034/j.1399-3054.2002.1160319.x

Jansen, M. A. K., Bilger, W., Hideg, É, Strid, Å, Aphalo, P., Brelsford, C., et al. (2019). Editorial: interactive effects of UV-B radiation in a complex environment. *Plant Physiol. Biochem.* 134, 1–8. doi: 10.1016/j.plaphy.2018.10.021

Jansen, M. A. K., Gaba, V., and Greenberg, B. M. (1998). Higher plants and UV-B radiation: balancing damage, repair and acclimation. *Trends Plant Sci.* 3, 131–135. doi: 10.1016/S1360-1385(98)01215-1

Jenkins, G. I. (2017). Photomorphogenic responses to ultraviolet-B light. *Plant Cell Environ.* 40, 2544–2557. doi: 10.1111/pce.12934

Johkan, M., Shoji, K., Goto, F., Hahida, S., and Yoshihara, T. (2012). Effect of green light wavelength and intensity on photomorphogenesis and photosynthesis in *Lactuca sativa*. *Environ. Exp. Bot.* 75, 128–133. doi: 10.1016/j.envexpbot.2011.08.010

Jordan, B. R., Strid, Å., and Wargent, J. J. (2016). "What role does UVB play in determining photosynthesis?," in *Handbook of Photosynthesis* (Boca Raton: CRC Press), 275–286. doi: 10.1201/9781315372136-16

Kalbina, I., Li, S., Kalbin, G., Björn, L. O., and Strid, Å (2008). Two separate UV-B radiation wavelength regions control expression of different molecular markers in *Arabidopsis thaliana*. *Funct. Plant Biol.* 35, 222–227. doi: 10.1071/FP07197

Kalbina, I., and Strid, Å (2006). Supplementary ultraviolet-B irradiation reveals differences in stress responses between *Arabidopsis thaliana* ecotypes. *Plant Cell Environ.* 29, 754–763. doi: 10.1111/j.1365-3040.2005.01436.x

Klem, K., Ač, A., Holub, P., Kováč, D., Špunda, V., Robson, T. M., et al. (2012). Interactive effects of PAR and UV radiation on the physiology, morphology and leaf optical properties of two barley varieties. *Environ. Exp. Bot.* 75, 52–64. doi: 10.1016/j.envexpbot.2011.08.008

Krizek, D. T. (2004). Influence of PAR and UV-A in determining plant sensitivity and photomorphogenic responses to UV-B radiation. *Photochem. Photobiol.* 79:307. doi: 10.1562/2004-01-27-ir.1

Krizek, D. T., Mirecki, R. M., and Britz, S. J. (1997). Inhibitory effects of ambient levels of solar UV-A and UV-B radiation on growth of cucumber. *Physiol. Plant.* 100, 886–893. doi: 10.1111/j.1399-3054.1997.tb00014.x

Lattanzio, V., Lattanzio, V. M. T., Cardinali, A., and Amendola, V. (2006). Role of phenolics in the resistance mechanisms of plants against fungal pathogens and insects. *Phytochemistry* 37, 23–67.

Li, Q., and Kubota, C. (2009). Effects of supplemental light quality on growth and phytochemicals of baby leaf lettuce. *Environ. Exp. Bot.* 67, 59–64. doi: 10.1016/j.envexpbot.2009.06.011

Lidon, F. J. C., Reboredo, F. H., Leitão, A. E., Silva, M. M. A., Duarte, M. P., and Ramalho, J. C. (2012). Impact of UV-B radiation on photosynthesis - an overview. *Emirates J. Food Agric.* 24, 546–556. doi: 10.9755/ejfa.v24i6.14673

Maxwell, K., and Johnson, G. N. (2000). Chlorophyll fluorescence—a practical guide. *J. Exp. Bot.* 51, 659–668. doi: 10.1093/jexbot/51.345.659

Mizuno, T., Amaki, W., and Watanabe, H. (2011). Effects of monochromatic light irradiation by LED on the growth and anthocyanin contents in leaves of cabbage seedlings. *Acta Hortic.* 907, 179–184. doi: 10.17660/ActaHortic.2011.907.25

Murchie, E. H., and Lawson, T. (2013). Chlorophyll fluorescence analysis: a guide to good practice and understanding some new applications. *J. Exp. Bot.* 64, 3983–3998. doi: 10.1093/jxb/ert208

Nascimento, L. B. S., Leal-Costa, M. V., Coutinho, M. A. S., Moreira, N. D. S., Lage, C. L. S., Barbi, N. D. S., et al. (2013). Increased antioxidant activity and changes in phenolic profile of *Kalanchoe pinnata* (Lamarck) *persoon* (Crassulaceae) specimens grown under supplemental blue light. *Photochem. Photobiol.* 89, 391–399. doi: 10.1111/php.12006

Nedunchezhian, N., and Kulandaivelu, G. (1997). Changes induced by ultraviolet-B (280-320 nm) radiation to vegetative growth and photosynthetic characteristics in field grown *Vigna unguiculata* L. *Plant Sci.* 123, 85–92. doi: 10.1016/S0168-9452(97)04583-4

Ögren, E. (1993). Convexity of the photosynthetic light-response curve in relation to intensity and direction of light during growth. *Plant Physiol.* 101, 1013–1019. doi: 10.1104/pp.101.3.1013

Ögren, E., and Sjöström, M. (1990). Estimation of the effect of photoinhibition on the carbon gain in leaves of a willow canopy. *Planta* 181, 560–567. doi: 10.1007/BF00193011

Ohashi-Kaneko, K., Takase, M., Kon, N., Fujiwara, K., and Kurata, K. (2007). Effect of light quality on growth and vegetable quality in leaf lettuce, spinach and komatsuna. *Environ. Control Biol.* 45, 189–198. doi: 10.2525/ecb.45.189

Ouzounis, T., Fretté, X., Rosenqvist, E., and Ottosen, C. O. (2014). Spectral effects of supplementary lighting on the secondary metabolites in roses, chrysanthemums, and campanulas. *J. Plant Physiol.* 171, 1491–1499. doi: 10.1016/j.jplph.2014.06.012

Ouzounis, T., Razi Parjikolaei, B., Fretté, X., Rosenqvist, E., and Ottosen, C.-O. (2015). Predawn and high intensity application of supplemental blue light decreases the quantum yield of PSII and enhances the amount of phenolic acids, flavonoids, and pigments in *Lactuca sativa*. *Front. Plant Sci.* 6:19. doi: 10.3389/fpls.2015.00019

Pinheiro, J., and Bates, D. M. (2000). "Linear mixed-effects models: basic concepts and examples," in *Mixed-Effects Models in S and S-PLUS*, eds J. C. Pinheiro, J. Pinheiro, and D. Bates (New York, NY: Springer), 3–56. doi: 10.1007/0-387-22747-4_1

Prasad, S. M., Dwivedi, R., Zeeshan, M., and Singh, R. (2004). UV-B and cadmium induced changes in pigments, photosynthetic electron transport activity, antioxidant levels and antioxidative enzyme activities of *Riccia* sp. *Acta Physiol. Plant.* 26, 423–430. doi: 10.1007/s11738-004-0033-8

Qian, M., Kalbina, I., Rosenqvist, E., Jansen, M. A. K., Teng, Y., and Strid, Å (2019). UV regulates the expression of phenylpropanoid biosynthesis genes in cucumber (*Cucumis sativus* L.) in an organ and spectrum dependent manner. *Photochem. Photobiol. Sci.* 18, 424–433. doi: 10.1039/C8PP00480C

Qian, M., Rosenqvist, E., Flygare, A. M., Kalbina, I., Teng, Y., Jansen, M. A. K., et al. (2020). UV-A light induces a robust and dwarfed phenotype in cucumber plants (*Cucumis sativus* L.) without affecting fruit yield. *Sci. Hortic.* 263:109110. doi: 10.1016/j.scienta.2019.109110

Rizzini, L., Favory, J. J., Cloix, C., Faggionato, D., O'Hara, A., Kaiserli, E., et al. (2011). Perception of UV-B by the *Arabidopsis* UVR8 protein. *Science* 332, 103–106. doi: 10.1126/science.1200660

Singh, D., Basu, C., Meinhardt-Wollweber, M., and Roth, B. (2015). LEDs for energy efficient greenhouse lighting. *Renew. Sustain. Energy Rev.* 49, 139–147. doi: 10.1016/j.rser.2015.04.117

Smith, H. (1982). Light quality, photoperception, and plant strategy. *Annu. Rev. Plant Physiol.* 33, 481–518. doi: 10.1146/annurev.pp.33.060182.002405

Smith, H., McAusland, L., and Murchie, E. H. (2017). Don't ignore the green light: exploring diverse roles in plant processes. *J. Exp. Bot.* 68, 2099–2110. doi: 10.1093/jxb/erx098

Strid, Å, and Porra, R. J. (1992). Alterations in pigment content in leaves of *Pisum sativum* after exposure to supplementary UV-B. *Plant Cell Physiol.* 33, 1015–1023. doi: 10.1093/oxfordjournals.pcp.a078325

Sun, J., Nishio, J. N., and Vogelmann, T. C. (1998). Green light drives CO2 fixation deep within leaves. *Plant Cell Physiol.* 39, 1020–1026. doi: 10.1093/oxfordjournals.pcp.a029298

Thimijan, R. W., Carns, H. R., and Campbell, L. E. (1978). *Final Report (EPA-IAG-D6-0168): Radiation Sources and Relative Environmental Control for Biological and Climatic Effects of UV Research (BACER)*. Washington D.C.: USDA-ETA.

Trouwborst, G., Oosterkamp, J., Hogewoning, S. W., Harbinson, J., and van Ieperen, W. (2010). The responses of light interception, photosynthesis and fruit yield of cucumber to LED-lighting within the canopy. *Physiol. Plant.* 138, 289–300. doi: 10.1111/j.1399-3054.2009.01333.x

Wang, Y., Zhang, T., and Folta, K. M. (2015). Green light augments far-red-light-induced shade response. *Plant Growth Regul.* 77, 147–155. doi: 10.1007/s10725-015-0046-x

Wang, Y., Zhou, B., Sun, M., Li, Y., and Kawabata, S. (2012). UV-A light induces anthocyanin biosynthesis in a manner distinct from synergistic blue + UV-B light and UV-A/blue light responses in different parts of the hypocotyls in turnip seedlings. *Plant Cell Physiol.* 53, 1470–1480. doi: 10.1093/pcp/pcs088

Wargent, J. J., Moore, J. P., Roland Ennos, A., and Paul, N. D. (2009). Ultraviolet radiation as a limiting factor in leaf expansion and development. *Photochem. Photobiol.* 85, 279–286. doi: 10.1111/j.1751-1097.2008.00433.x

Wargent, J. J., Nelson, B. C. W., Mcghie, T. K., and Barnes, P. W. (2015). Acclimation to UV-B radiation and visible light in *Lactuca sativa* involves up-regulation of photosynthetic performance and orchestration of metabolome-wide responses. *Plant Cell Environ.* 38, 929–940. doi: 10.1111/pce.12392

Warnes, A. G. R., Bolker, B., Lumley, T., and Randall, C. (2018). *Package 'gmodels*. Vienna: R Foundation for Statistical Computing.

Yu, S. G., and Björn, L. O. (1997). Effects of UVB radiation on light-dependent and light-independent protein phosphorylation in thylakoid proteins. *J. Photochem. Photobiol. B Biol.* 37, 212–218. doi: 10.1016/S1011-1344(96)07409-X

Zhang, T., and Folta, K. M. (2012). Green light signaling and adaptive response. *Plant Signal. Behav.* 7, 75–78. doi: 10.4161/psb.7.1.18635

Zhang, T., Maruhnich, S. A., and Folta, K. M. (2011). Green light induces shade avoidance symptoms. *Plant Physiol.* 157, 1528–1536. doi: 10.1104/pp.111.180661

Zhao, B., Wang, L., Pang, S., Jia, Z., Wang, L., Li, W., et al. (2020). UV-B promotes flavonoid synthesis in *Ginkgo biloba* leaves. *Ind. Crops Prod.* 151:112483. doi: 10.1016/j.indcrop.2020.112483

Zoratti, L., Sarala, M., Carvalho, E., Karppinen, K., Martens, S., Giongo, L., et al. (2014). Monochromatic light increases anthocyanin content during fruit development in bilberry. *BMC Plant Biol.* 14:377. doi: 10.1186/s12870-014-0377-1

Conflict of Interest: The authors declare that the research was conducted in the absence of any commercial or financial relationships that could be construed as a potential conflict of interest.

Copyright © 2021 Palma, Castro-Alves, Morales, Rosenqvist, Ottosen and Strid. This is an open-access article distributed under the terms of the Creative Commons Attribution License (CC BY). The use, distribution or reproduction in other forums is permitted, provided the original author(s) and the copyright owner(s) are credited and that the original publication in this journal is cited, in accordance with accepted academic practice. No use, distribution or reproduction is permitted which does not comply with these terms.

frontiers in Plant Science

ORIGINAL RESEARCH
published: 13 January 2021
doi: 10.3389/fpls.2020.614714

Dissecting the Genotypic Variation of Growth Responses to Far-Red Radiation in Tomato

Yongran Ji[1], Theoharis Ouzounis[1], Henk J. Schouten[2], Richard G. F. Visser[2], Leo F. M. Marcelis[1] and Ep Heuvelink[1]*

[1] Horticulture and Product Physiology, Department of Plant Sciences, Wageningen University & Research, Wageningen, Netherlands, [2] Plant Breeding, Department of Plant Sciences, Wageningen University & Research, Wageningen, Netherlands

OPEN ACCESS

Edited by:
María Serrano, Miguel Hernández University of Elche, Spain

Reviewed by:
Bodie Pennisi, University of Georgia, United States
Mohammad R. Sabzalian, Isfahan University of Technology, Iran
Gerhard Buck-Sorlin, Agrocampus Ouest, France

***Correspondence:**
Leo F. M. Marcelis
leo.marcelis@wur.nl

Specialty section:
This article was submitted to Crop and Product Physiology, a section of the journal Frontiers in Plant Science

Received: *06 October 2020*
Accepted: *11 December 2020*
Published: *13 January 2021*

Citation:
Ji Y, Ouzounis T, Schouten HJ, Visser RGF, Marcelis LFM and Heuvelink E (2021) Dissecting the Genotypic Variation of Growth Responses to Far-Red Radiation in Tomato. Front. Plant Sci. 11:614714. doi: 10.3389/fpls.2020.614714

The recent development of light-emitting diodes (LEDs) and their application in modern horticulture stimulated studies demonstrating that additional far-red (FR) radiation (700–800 nm) increases plant dry mass. This effect of FR has been explained by improved photosynthesis and/or plant architecture. However, the genotypic variation in this response is largely unknown. Here, we aim to explore and explain the genotypic variation in growth responses to additional FR. We expected the genotypic variation in the responses of plant dry mass to additional FR. Further, we hypothesized that a significant improvement of both net assimilation rate (NAR) and leaf area ratio (LAR) is responsible for a strong dry mass increase under additional FR, while some genotypes respond only marginally or even negatively in NAR or LAR under FR, thus resulting in a weak FR effect on plant dry mass. To test these hypotheses, we grew 33 different tomato genotypes for 21 days with 0, 25, or 100 μmol m^{-2} s^{-1} of FR added to a common white + red LED background lighting of 150 μmol m^{-2} s^{-1}. Genotypes responded similarly with respect to plant height, stem dry mass, and shoot:root ratio; i.e., they all increased with increasing FR. However, the response of total plant dry mass varied among genotypes. We categorized the genotypes into three groups (strongly, moderately, and weakly responding groups) based on their relative response in total plant dry mass to FR. Growth component analysis revealed that the strongly responding genotypes increased strongly in NAR rather than LAR. The weakly responding genotypes, however, showed a substantial increase in LAR but not NAR. The increase in LAR was due to the increase in specific leaf area. Leaf mass fraction, which is the other component of LAR, decreased with FR and did not differ between groups. In conclusion, tomato genotypes that increased strongly in NAR in response to FR were able to achieve a more substantial increase in dry mass than did other genotypes. This is the first study to explain the differences in growth responses of a large number of tomato genotypes toward FR in their light environment.

Keywords: far red, genotypic variation, growth analysis, LED lighting, *Solanum lycopersicum*

INTRODUCTION

Far-red (FR) radiation (700–800 nm) is an important light signal perceived by plants via the phytochrome photoreceptor family. Phytochromes exist as two photo-interconvertible isoforms, that is, the red (R)-absorbing biologically inactive P_r and the FR-absorbing active P_{fr} (Chen et al., 2005). A low R:FR ratio causes the equilibrium between the two isoforms of phytochromes to shift toward Pr, resulting in a set of morphological and physiological changes collectively known as the shade-avoidance syndrome (SAS). SAS responses such as stem elongation, leaf hyponasty, and flowering acceleration enable the plant to compete for more light capture and to secure reproductive success, as decreased R:FR ratio occurs naturally when plants are shaded (Huber and Wiggerman, 1997; Devlin, 1998; Yang et al., 2016; Michaud et al., 2017).

In the past decades, light-emitting diodes (LEDs) gained popularity in modern horticulture, a development that stimulated the study of spectral effects on plant growth and development. Plant photosynthesis is driven by photosynthetically active radiation (PAR; 400–700 nm). FR is not commonly considered to be part of PAR, as monochromatic FR drives neither CO_2 assimilation nor O_2 evolution from photosynthesis (Kono et al., 2020). When added to PAR, however, FR radiation may increase not only yield (Ji et al., 2019, 2020) but also total plant biomass production (Li and Kubota, 2009; Park and Runkle, 2017; Zhen and van Iersel, 2017). Much effort has been made to explain FR-enhanced plant growth. It has been found that FR-induced changes in plant architecture increase light interception (Kalaitzoglou et al., 2019). For a long time, FR effect on leaf photosynthesis has been described as the Emerson enhancement effect: radiation at shorter wavelengths enhances the quantum yield of radiation at longer wavelengths (Emerson et al., 1957; Emerson and Rabinowitch, 1960; Govindjee et al., 1964). Several recent studies revisited this concept and proposed the reverse interpretation: FR radiation enhances the quantum yield of PAR (Zhen and van Iersel, 2017). Furthermore, Zhen and Bugbee (2020) demonstrated in an experiment with 14 species of both C_3 and C_4 crops that FR can be as efficient in driving photosynthesis as PAR, not by itself but when provided in addition to PAR.

Modern horticultural production can benefit from a deeper understanding of plants' responses to different light spectra. More importantly, it is crucial to explore the genotypic variation in such responses. For example, Ouzounis et al. (2016) showed genotypic differences in growth and physiological parameters when plants were grown in a red LED background with or without 12% of blue LED lighting. Plant's response to FR is a new way to increase crop production and resource use efficiency (Demotes-Mainard et al., 2016). However, the genotypic variation in plants' responses to additional FR is largely unknown due to the often-limited numbers of genotypes used in FR-related research. Here, we aim to evaluate and explain the similarities and differences between tomato genotypes in growth responses under additional FR. We hypothesize that not all genotypes respond the same way in their dry mass production under additional FR. Further, we hypothesize that this variation is the result of different morphological or physiological responses in the components of dry mass production under additional FR. To test these hypotheses, we conducted a climate chamber experiment where 33 tomato genotypes were grown for 21 days with 0, 25, or 100 μmol m^{-2} s^{-1} of FR added to a common white + red LED lighting background of 150 μmol m^{-2} s^{-1}. Growth component analysis, which subdivides growth into underlying morphological and physiological components (Jolliffe and Courtney, 1984), is a useful tool to dissect the effect of FR on dry mass production (Higashide and Heuvelink, 2019). Here, growth components such as relative growth rate (RGR), net assimilation rate (NAR), leaf area ratio (LAR), specific leaf area (SLA), and leaf mass fraction (LMF) were determined, and the contribution of the different growth components to the genotypic variation in growth response was evaluated.

MATERIALS AND METHODS

Plant Materials and Growth Conditions

The experiment was conducted in a fully controlled climate chamber at Wageningen University (Wageningen, Netherlands). The air temperature was maintained at 22°C, and the relative humidity was 70%. In this climate chamber, seeds of 33 tomato (*Solanum lycopersicum*, **Table 1**) genotypes, varying in genetic background and morphological traits (Aflitos et al., 2014), were germinated under white fluorescent light (Philips, Eindhoven, Netherlands) with 16 h photoperiod. Ten days after sowing, eight uniform seedlings of each genotype were individually transplanted into 10.5-cm-diameter plastic pots filled with sterilized river sand and placed onto the experimental bench equipped with an ebb-and-flow system. The plants were irrigated daily with nutrient solution (electrical conductivity 2.0 dS m^{-1}, pH 5.5) containing 1.2 mM of NH_4^+, 7.2 mM of K^+, 4.0 mM of Ca^{2+}, 1.8 mM of Mg^{2+}, 12.4 mM of NO_3^-, 3.3 mM of SO_4^{2-}, 1.0 mM of PO_4^{2-}, 35 μM of Fe^{3+}, 8.0 μM of Mn^{2+}, 5.0 μM of Zn^{2+}, 20 μM of B, 0.5 μM of Cu^{2+}, and 0.5 μM of MoO_4^{2-}.

Light Treatment

A deep red + white light at 150 μmol m^{-2} s^{-1} with 0.16 W m^{-2} of UV-B of was used as the control light treatment, and two light treatments were applied from transplanting (10 days after sowing). There were three FR treatments: 0, 25, or 100 μmol m^{-2} s^{-1} of FR radiation was added to a common background of red + white LED light of 150 μmol m^{-2} s^{-1} with 0.16 W m^{-2} of UV-B. The UV-B radiation was included to mimic the UV dosage in natural solar radiation. All lighting was provided by LED modules (Control: 3× GreenPower LED-TL-DR/W-MB-VISN; FR: 15 or 60× GreenPower LED-RM-FR, Philips, Eindhoven, Netherlands) except for UV-B (2× TL 20W/12 RS Ultraviolet-B, Philips). Light modules were placed 1.3 m above the experimental bench. Spectral distribution (**Supplementary Figure S1**) and photon flux density (PFD) of the LED lighting (**Table 2**) was measured at canopy height at transplanting with a spectroradiometer (USB 2000+ UV-VIS, Ocean Optics, Duiven, Netherlands) on 30 evenly distributed spots on the experimental

TABLE 1 | List of genotypes used in the experiment and their relative response in total dry mass to increasing far red and their corresponding growth response groups.

No.	Code	Name	Source or identification[1]	Relative response (μmol^{-1} m^{-2} s^{-1})	Group
1	RF-1	Moneymaker	LA2706/EA00840/EA02936/	0.0073	Strong
2	RF-102		LA4133/TR00026	0.0092	Strong
3	RF-15	Momotaro	TR00003	0.0075	Strong
4	RF-16	Rote Beere	LYC11/EA01965/CGN15464	0.0177	Strong
5	RF-2	Alisa Craig	LA2838A/EA01101/EA00240/	0.0094	Strong
6	RF-23		PI272654/EA05170	0.0104	Strong
7	RF-29	Black Cherry	LA4451/EA00027	0.0080	Strong
8	RF-3	Gardeners delight	EA06086/PI406760	0.0109	Strong
9	RF-7	Katinka Cherry	EA00375	0.0083	Strong
10	RF-94	Marmande	TR00022	0.0089	Strong
11	RZ-CAP	Cappricia	Rijk Zwaan	0.0093	Strong
12	BJ-HB1	Hybrid-1	Bejo Zaden	0.0073	Moderate
13	RF-11	Allround	LA2463/LYC1365/EA02617	0.0050	Moderate
14	RF-20		LYC3153/EA03221	0.0055	Moderate
15	RF-22		PI129097/EA04710	0.0050	Moderate
16	RF-226		EA05721	0.0070	Moderate
17	RF-27	Cal J Tm VF	EA02054/CGN20815	0.0039	Moderate
18	RF-34	Tiffen Mennonite	EA01088	0.0038	Moderate
19	RF-40	ES 58 Heinz	LYC1410/EA02655	0.0063	Moderate
20	RF-43		LYC2910/EA03058/T115	0.0071	Moderate
21	RF-89	Brandywine	EA01019	0.0053	Moderate
22	RF-97	Watermelon beefsteak	EA01640	0.0073	Moderate
23	BJ-HB2	Hybrid-2	Bejo Zaden	-0.0014	Weak
24	N-9008	Foundation	Nunhems	0.0037	Weak
25	N-9098	9098	Nunhems	0.0004	Weak
26	N-FM001	FM001	Nunhems	0.0009	Weak
27	RF-103		LA1421/TR00027	-0.0021	Weak
28	RF-206		EA00915	0.0034	Weak
29	RF-229		EA05979	0.0026	Weak
30	RF-4	Rutgers	LA1090/EA00465	0.0003	Weak
31	RF-91	Giant Belgium	EA01037	-0.0006	Weak
32	RF-93	Kentucky Beefsteak	TR00021	0.0037	Weak
33	RZ-CAL	Caldino	Rijk Zwaan	0.0036	Weak

[1] *Identification starting with "EA," "LA," "LYC," "PI," and "TR" are genotypes registered by "EU-SOL tomato core collection database" (Aflitos et al., 2014), while others are provided by the corresponding company.*

bench. Based on these measurements, values of phytochrome photostationary state (PSS) were calculated as described in Sager et al. (1988).

TABLE 2 | Photosynthetic photon flux density (PPFD), photon flux density (PFD) of far red, red:far red ratio, and phytochrome photostationary state (PSS) of the LED light measured at the top of canopy.

Light treatment	PPFD ($\mu mol\ m^{-2}\ s^{-1}$)	Far red ($\mu mol\ m^{-2}\ s^{-1}$)	R:FR[1]	PSS
White + red	151 ± 2[2]	3 ± 0.2	35 ± 1.3	0.87
White + red + 25 FR	152 ± 3	28 ± 0.9	3 ± 0.1	0.80
White + red + 100 FR	155 ± 5	95 ± 3.6	1 ± 0.1	0.69

[1] *For the calculation of ratios, PFD was integrated over 100-nm intervals for red (600–700 nm) and far red (700–800 nm).*

[2] *All values are means ± standard error of means (SEM). SEM of PSS was very small (<0.001) and therefore not shown.*

Data Collection

Non-destructive Measurement

After 14 days of growth, stomatal conductance and chlorophyll index on the first fully expanded leaf of each experimental plant were determined. Stomatal conductance was measured with a SC-1 leaf porometer (Decagon Devices, Inc., Pullman, WA, United States), and chlorophyll index was measured using a Dualex leaf-clip sensor (Force-A, Orsay, France). For the chlorophyll measurement, the values measured from both sides of the leaf were averaged.

Destructive Measurement

After 21 days from transplanting, a final destructive harvest was carried out. Each experimental plant was carefully cleaned to remove any remaining river sand from the roots. Excess water was wiped clean with tissue paper, and the plant height was measured immediately, after which the plant was separated into roots, stem, and leaves. Total leaf area was measured using an area

meter (LI-3100, Li-Cor Biosciences, Lincoln, NE, United States). Leaves, stems, and roots were dried in a ventilated oven for 72 h at 105°C to obtain the dry mass. For each genotype, the initial dry mass at transplanting was measured using seedlings of each genotype germinated in the same conditions as the experimental plants.

Growth Component Analysis

A linear relation was fitted between the total dry mass and PFD of FR for each genotype. Then, the relative response of each genotype was calculated as the ratio between the slope of this line and the absolute total plant dry mass (TDM) in the control light treatment. All 33 genotypes were then ranked by their relative response to increasing FR in total dry mass, and three response groups were distinguished, i.e., the strongly, moderately, and weakly responding groups, with 11 genotypes in each group. Effects of additional FR on RGR were analyzed using a growth component analysis, which separates RGR from its underlying components (**Figure 1**) (Hunt et al., 2002). RGR is the product of NAR and LAR, as shown in Eq. 1. NAR was calculated by dividing RGR by LAR.

$$NAR = RGR/LAR \quad (1)$$

Relative growth rate was calculated according to Eq. 2 using the initial plant dry mass ($DW_{initial}$) and the final plant dry mass (DW_{final}) of each plant after 21 days of growth.

$$RGR = (ln(DW_{final}) - ln(DW_{initial}))/21 \quad (2)$$

Further, LAR was analyzed as the product of SLA and LMF as indicated by Eq. 3.

$$LAR = SLA * LMF \quad (3)$$

Leaf area ratio, SLA, and LMF were calculated from the measured total leaf area (LA_{plant}), final plant dry mass (DW_{final}), and leaf dry mass per plant (DW_{leaf}) using Eqs 4–6.

$$LAR = LA_{plant}/DW_{final} \quad (4)$$

$$SLA = LA_{plant}/DW_{leaf} \quad (5)$$

$$LMF = DW_{leaf}/DW_{final} \quad (6)$$

Experimental Setup and Statistical Analysis

Each experiment with one light treatment was conducted consecutively in the same fully controlled climate room. For each light treatment, eight blocks were designed according to the light distribution over the bench, and one plant per genotype was randomly placed in each block. The experiment with 25 μmol m^{-2} s^{-1} of FR was repeated in time for one extra time (again with eight blocks). To prevent border effects, *S. lycopersicum* cv. Moneymaker plants were grown around the experimental plants as border plants. Responsiveness of plant dry mass and RGR to additional FR was quantified as the slope of a linear regression with the FR PFD as the regressor. For the growth component analysis, statistical differences for the FR effect in each group were tested with paired sample *t*-test (genotypes defining the pairs). All statistics were performed in Genstat (18th Edition, VSN International Ltd., Hemel Hempstead, United Kingdom) at $\alpha = 0.05$.

RESULTS

Effect of Far-Red Radiation on Growth Parameters

Effects of additional FR varied among genotypes and among growth parameters studied (**Figure 2**). Plant height, stem dry mass, and shoot:root ratio increased in all genotypes with increasing FR. Chlorophyll index showed a minor decrease by adding 25 μmol m^{-2} s^{-1} of FR and a stronger and universal decrease in all genotypes by adding 100 μmol m^{-2} s^{-1} of FR. Responses of plant dry mass, leaf dry mass, root dry mass, and leaf area to increasing FR varied among genotypes. For plant dry mass, 58% of the genotypes showed a positive response under 25 μmol m^{-2} s^{-1} of FR, and this percentage increased to 70% under 100 μmol m^{-2} s^{-1} of FR. For leaf dry mass and root dry mass, about 30–40% of the genotypes responded positively to increasing FR, most of which belong to the strongly responding group (genotypes whose total dry mass increased relatively strong with FR). For stomatal conductance, half of the genotypes responded positively to 25 μmol m^{-2} s^{-1} of additional of FR, while this fraction decreased to 21% under 100 μmol m^{-2} s^{-1} of additional FR. Absolute numbers of each parameter are shown in **Supplementary Table S1**.

Growth Component Analysis

In order to explain the variation in the FR effect on plant dry mass production, we categorized the genotypes into three groups (i.e., strongly, moderately, and weakly responding groups; 11 genotypes in each group) based on their relative response to increasing FR in TDM (**Figure 3A** and **Table 1**). RGR, which is a common parameter used for growth component analysis, showed a similar pattern to TDM in response to increasing FR (**Figure 3B**). Slopes of the regression models fitted for both total dry mass and RGR showed significant differences between the three groups.

This similarity facilitates using a growth component analysis of RGR to explain the genotypic variation in the FR effect on total dry mass (**Figure 4**). When 25 μmol m^{-2} s^{-1} of FR was provided, RGR and NAR increased in the strongly responding group, while both were not significantly affected in the moderately and weakly responding groups. LAR showed an opposite response to FR with a decrease in the strongly responding group and an increase in the weakly responding group. LAR was further

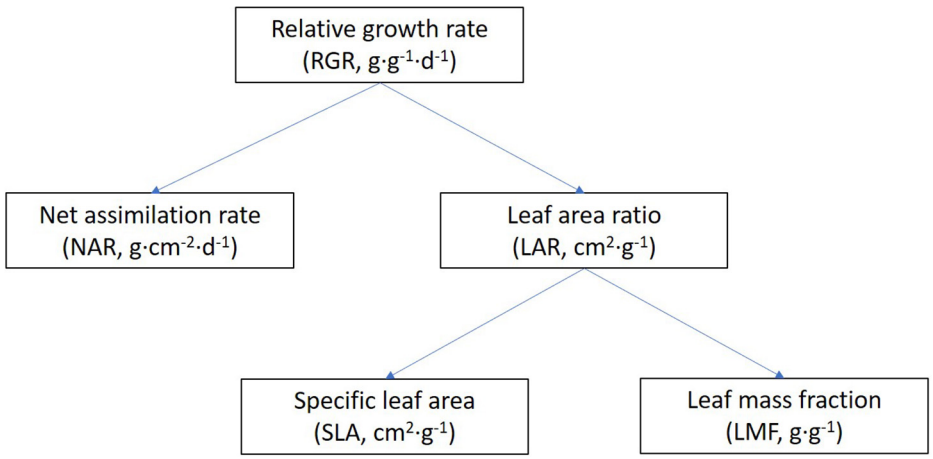

FIGURE 1 | General scheme of a growth component analysis of relative growth rate. Abbreviations and units are included in brackets. RGR is the product of NAR and LAR, and LAR is the product of SLA and LMF.

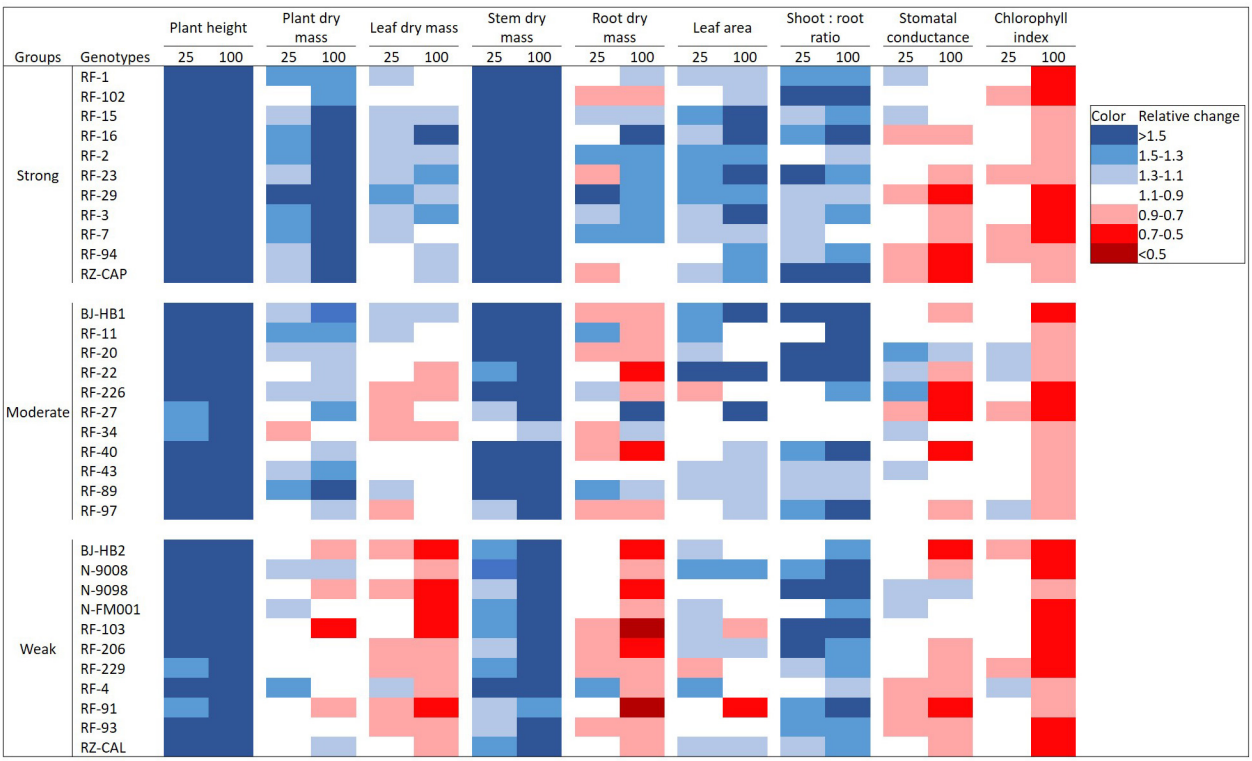

FIGURE 2 | Effects of adding 25 or 100 μmol m^{-2} s^{-1} of far-red (FR) radiation on plant height, plant dry mass, leaf dry mass, stem dry mass, root dry mass, leaf area, shoot:root ratio, stomatal conductance, and chlorophyll index in 33 tomato genotypes. Genotypes were categorized into three groups (strongly, moderately, and weakly responding groups) based on their relative responses in total plant dry mass to FR. Color scales represent relative changes of parameters when compared with the control light treatment without FR, with blue indicating an increase under FR and red representing a decrease.

divided into SLA and LMF. LMF decreased in all three groups by a comparable magnitude, while SLA increased with FR with the weakly responding group showing the strongest increase, followed by moderately and strongly responding groups. Similar responses of the growth components were observed when additional FR increased from 25 to 100 μmol m^{-2} s^{-1}. Here, an additional 100 μmol m^{-2} s^{-1} of FR resulted in a significant increase in RGR and NAR in the strong and moderate groups, while those in the weak group were not statistically significant. Also, 100 μmol m^{-2} s^{-1} of FR decreased the LAR in the

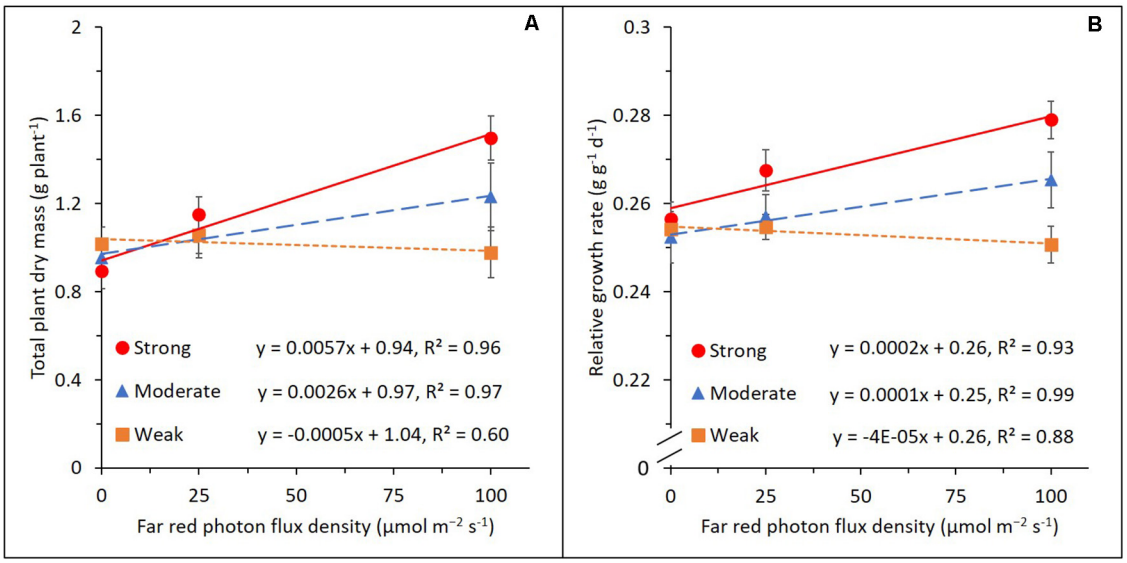

FIGURE 3 | Effects of adding 25 or 100 μmol m^{-2} s^{-1} of far-red (FR) radiation on total plant dry mass **(A)** and relative plant growth rate **(B)** in the strongly (red circle), moderately (blue triangle), and weakly (orange rectangle) responding groups of genotypes. Lines represent linear regression. Error bars represent standard error of means (n = 8 for 0 and 100 μmol m^{-2} s^{-1} of FR and n = 16 for 25 μmol m^{-2} s^{-1} of FR).

strong and moderate groups while increasing that in the weak group. This was due to the difference in the increasingly large response in SLA from strong to weak group. LMF strongly decreased with FR with only marginal differences between the three groups. For all parameters, there was a clear dosage effect as the responses became more substantial as FR increased from 25 to 100 μmol m^{-2} s^{-1}. The absolute numbers of the parameters used in the component analysis are presented in **Supplementary Table S2**.

DISCUSSION

Genotypic Similarities and Variations in Growth Response to Far Red

This study is the first to analyze the differences in growth responses of a large number of tomato genotypes toward FR in their light environment (**Figure 2**). The most distinct response to FR in many species is stem elongation, which has been reported in many species (Kasperbauer, 1971; Franklin and Quail, 2010; Kalaitzoglou et al., 2019; Shibuya et al., 2019). In agreement with this, we observed a universal increase of plant height in all 33 genotypes, and this increase in plant height was dosage dependent. Corresponding to the FR-induced stem elongation, stem dry mass also increased with FR in all genotypes, and this agreed well with other studies (Ji et al., 2019; Zhang et al., 2019). In general, responses of leaf growth to FR may vary between species and genotypes (Casal and Smith, 1989). Also in tomato, both positive (Cao et al., 2018; Zhang et al., 2019) and negative (Ji et al., 2019; Kim et al., 2019) effects of FR on leaf dry mass have been reported. Similarly, we observed that the response of leaf dry mass to FR varied among genotypes, ranging from negative to positive response when grown with FR, with a negative response being more frequent. FR stimulates the dry mass to be distributed more to the above ground, thus increasing the shoot:root ratio (Kasperbauer, 1987; Lee et al., 2016; Cao et al., 2018). In line with these results, we observed that all genotypes responded positively to increasing FR in shoot:root ratio, which may be a combined result of higher shoot (mainly stem) dry mass and a lower root dry mass. In this study, we noticed that the increase in shoot:root ratio for the strongly responding genotypes was likely due to an increase in shoot dry mass that was stronger than the increase in root dry mass. For moderately and weakly responding genotypes, this was a result of an increase in shoot dry mass combined with a decrease in root dry mass. Interestingly, FR decreased the chlorophyll index, which indicates that FR reduces chlorophyll content and suggests that photosynthetic capacity may be reduced. Similarly, decrease in chlorophyll content was also reported both in young tomato and fruiting tomato plants (Cao et al., 2018; Kalaitzoglou et al., 2019; Kim et al., 2019) as well as other crops (Tucker, 1981; Casal and Aphalo, 1989; Li and Kubota, 2009). Furthermore, despite a trend of increased TDM due to FR, the genotypic variation in the response was very noticeable when comparing the magnitude of this FR effect.

Genotypes Achieved a Stronger Increase in Dry Mass Production by the Increase in Net Assimilation Rate

We categorized the genotypes into three groups (i.e., strongly, moderately, and weakly responding groups) based on their relative response in TDM to FR (**Table 1**) to conduct a growth component analysis based on the breakdown of RGR (Hunt et al., 2002). RGR is the product of NAR and LAR. The strongly responding genotypes substantially increased their RGR under

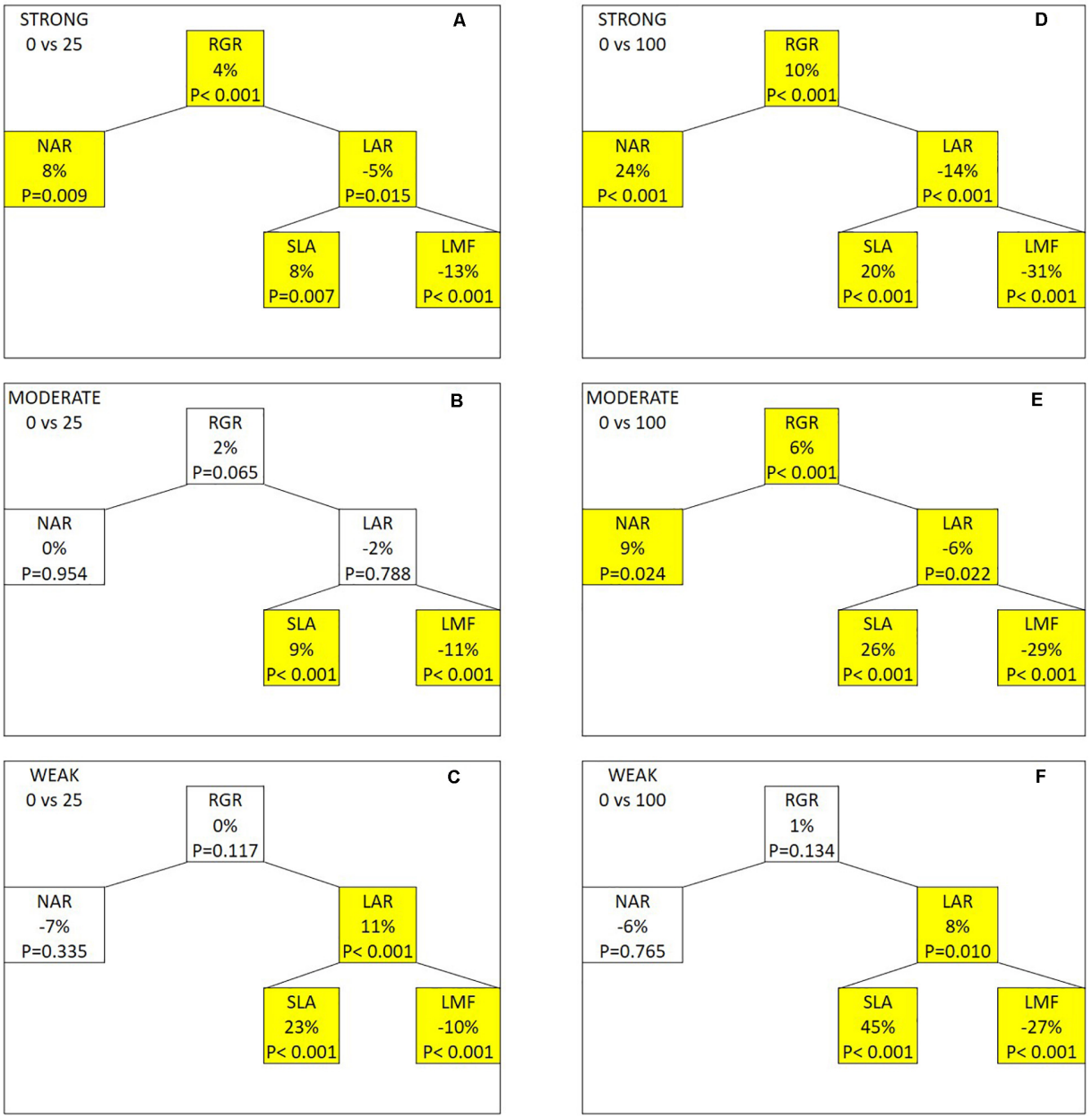

FIGURE 4 | Effects of adding 25 **(A–C)** or 100 μmol m^{-2} s^{-1} of far-red (FR) radiation **(D–F)** on the growth components in the strongly, moderately, and weakly responding groups of genotypes. Abbreviations in this figure: RGR, relative growth rate; NAR, net assimilation rate; LAR, leaf area ratio; SLA, specific leaf area; LMF, leaf mass fraction. The percentage represents the relative change in the components when compared between the FR treatment and the control treatment. *P*-value of the paired *t*-test is indicated in each component with a significant difference ($P < 0.05$) being highlighted in yellow.

additional FR, followed by the moderately responding genotypes, while the weakly responding genotypes showed no significant changes in their RGR under FR (**Figure 4**). The increase in RGR of the strongly responding genotypes under FR was the result of an increase in NAR, but not in LAR, as it decreased with FR. FR was reported by Ji et al. (2019) and Kalaitzoglou et al. (2019) to increased SLA. Here, we found that the weakly responding genotypes showed a stronger increase in SLA than did other genotypes. LMF, the other component of LAR, was significantly decreased for all groups, and the response did not differ between groups and was only dependent on the amount of FR. The dry mass partitioning between organs is regulated by the relative sink strength of the organs (Marcelis, 1996). The decreased LMF may be due to the strong enhancement of stem sink strength under FR, causing less dry mass to be partitioned to the leaves. For both the strongly and weakly responding groups, their responses to FR were in accordance with the known SAS responses. Our result suggests that when grown

under additional FR, tomato plants are not likely to be able to increase NAR and LAR simultaneously, and that the genotypes with a strong increase in NAR under FR allowed them to achieve a stronger increase in RGR than did other genotypes.

Possible Mechanism of Far-Red Enhancement in Net Assimilation Rate

One explanation for the FR-increased NAR may be that the morphology of plants grown with FR contributed to better vertical distribution of light. FR increases the internode length in tomato, which may lead to a more open plant architecture. Indeed, up to 10% of increase in canopy photosynthesis was achieved in a model simulation by increasing internode length in tomato (Sarlikioti et al., 2011). Also, NAR represents largely the net carbon gain from photosynthesis (Poorter and Remkes, 1990). FR enhances the quantum yield of PAR (400–700 nm) in various species (Zhen and van Iersel, 2017; Zhen and Bugbee, 2020). Such an improvement in photosynthesis agrees with our finding that FR increases NAR. However, their studies focused on short-term light treatments. Experiments with plants grown or adapted to additional FR showed varying results. For example, Kalaitzoglou et al. (2019) found that a 4-week growth period with additional FR resulted in a higher net leaf photosynthesis rate (A) when 50 μmol m^{-2} s^{-1} of FR was added to 150 μmol m^{-2} s^{-1} PAR. Cao et al. (2018), however, reported no significant differences in A using a comparable spectrum. In addition, no significant FR effect on A was reported for tomato plants grown with prolonged exposure to additional FR until fruiting stage (Ji et al., 2019; Zhang et al., 2019). This may indicate that the short-term FR enhancement in photosynthesis cannot fully explain the increase in NAR either, especially when considering the decrease in chlorophyll index (**Figure 2**; Li and Kubota, 2009; Cao et al., 2018; Kalaitzoglou et al., 2019) and a decreased photosynthetic capacity (Ji et al., 2019). FR may also reduce the photosynthetic rate via the *phyB*-mediated downregulation of genes such as *FAMA* and *TMM* in *Arabidopsis*, leading to the reduction of stomata development (Boccalandro et al., 2009). This reduction, however, may be compensated by the increase in water-use efficiency. To date, there is still insufficient evidence to fully dissect the effect of FR on the NAR due to the complex interaction between the underlying morphological and physiological components. We do, however, speculate that the effect of FR (positive, neutral, or negative) on net photosynthesis rate, light interception, and light distribution varies and that it is the combined effect that determines the NAR.

CONCLUSION

Genotypes responded similarly with respect to plant height, stem dry mass, and shoot:root ratio. However, the response of TDM varied among genotypes. Here, we demonstrated that it was the differences in genotype's responses in NAR and LAR that explain the genotypic variation in response to total dry mass. Genotypes with a strong increase in RGR with increasing FR showed a strong increase in NAR rather than LAR. The weakly responding genotypes, however, showed a substantial increase in LAR but not NAR. The genotypic differences in the increase in LAR were mainly due to the genotypic differences in the increase in SLA, while the responses of LMF to FR were conserved between genotypes.

DATA AVAILABILITY STATEMENT

The raw data supporting the conclusions of this article will be made available by the authors, without undue reservation.

AUTHOR CONTRIBUTIONS

YJ wrote the manuscript. YJ and TO conducted the experiment and conducted the analysis. LM and EH initiated this work and obtained funding for this research, provided guidance in the experimental design and data analysis, and provided critical comments on the manuscript. HS and RV provided critical comments to the overall structure of the manuscript. All authors reviewed and approved the final manuscript.

FUNDING

This research is part of the "LED it be 50%" program and was supported by Glastuinbouw Nederland, BASF Vegetable Seeds, Rijk Zwaan, Signify, WUR Greenhouse Horticulture, and the Netherlands Organization for Scientific Research (NWO), which is partly funded by the Ministry of Economic Affairs.

ACKNOWLEDGMENTS

We thank E. de Beer, E. Nieland, and E. Onac of Signify for the support in the design of the LED lighting system. We thank A. Maassen, S. Geurts, G. Versteeg, W. van der Slikke, T. Stoker, G. Stunnenberg, and C. Tebarts for their technical support.

SUPPLEMENTARY MATERIAL

The Supplementary Material for this article can be found online at: https://www.frontiersin.org/articles/10.3389/fpls.2020.614714/full#supplementary-material

REFERENCES

Aflitos, S., Schijlen, E., De Jong, H., De Ridder, D., Smit, S., Finkers, R., et al. (2014). Exploring genetic variation in the tomato (*Solanum* Section *Lycopersicon*) clade by whole-genome sequencing. *Plant J.* 80, 136–148. doi: 10.1111/tpj.12616

Boccalandro, H. E., Rugnone, M. L., Moreno, J. E., Ploschuk, E. L., Serna, L., Yanovsky, M. J., et al. (2009). Phytochrome B enhances photosynthesis at the

expense of water-use efficiency in *Arabidopsis*. *Plant Physiol.* 150, 1083–1092. doi: 10.1104/pp.109.135509

Cao, K., Yu, J., Xu, D., Ai, K., Bao, E., and Zou, Z. (2018). Exposure to lower red to far-red light ratios improve tomato tolerance to salt stress. *BMC Plant Biol.* 18:92. doi: 10.1186/s12870-018-1310-9

Casal, J. J., and Aphalo, P. J. (1989). Phytochrome control of chlorophyll content in mature attached leaves of petunia axillaris. *Ann. Bot.* 63, 595–598. doi: 10.1093/oxfordjournals.aob.a087785

Casal, J. J., and Smith, H. (1989). The function, action and adaptive significance of phytochrome in light-grown plants. *Plant Cell Environ.* 12, 855–862. doi: 10.1111/j.1365-3040.1989.tb01966.x

Chen, M., Tao, Y., Lim, J., Shaw, A., and Chory, J. (2005). Regulation of phytochrome B nuclear localization through light-dependent unmasking of nuclear-localization signals. *Curr. Biol.* 15, 637–642. doi: 10.1016/j.cub.2005.02.028

Demotes-Mainard, S., Péron, T., Corot, A., Bertheloot, J., Le Gourrierec, J., Pelleschi-Travier, S., et al. (2016). Plant responses to red and far-red lights, applications in horticulture. *Environ. Exp. Bot.* 121, 4–21. doi: 10.1016/j.envexpbot.2015.05.010

Devlin, P. F. (1998). Phytochrome E influences internode elongation and flowering time in *Arabidopsis*. *Plant Cell Online* 10, 1479–1488. doi: 10.1105/tpc.10.9.1479

Emerson, R., Chalmers, R., and Cederstrand, C. (1957). Some factors influencing the long-wave limit of photosynthesis. *Proc. Natl. Acad. Sci. U.S.A.* 43, 133–143. doi: 10.1073/pnas.43.1.133

Emerson, R., and Rabinowitch, E. (1960). Red drop and role of auxiliary pigments in photosynthesis. *Plant Physiol.* 35, 477–485. doi: 10.1104/pp.35.4.477

Franklin, K. A., and Quail, P. H. (2010). Phytochrome functions in *Arabidopsis* development. *J. Exp. Bot.* 61, 11–24. doi: 10.1093/jxb/erp304

Govindjee, R., Govindjee, and Hoch, G. (1964). Emerson enhancement effect in chloroplast reactions. *Plant Physiol.* 39, 10–14. doi: 10.1104/pp.39.1.10

Higashide, T., and Heuvelink, E. (2019). Physiological and morphological changes over the past 50 years in yield components in tomato. *J. Am. Soc. Hortic. Sci.* 134, 460–465. doi: 10.21273/jashs.134.4.460

Huber, H., and Wiggerman, L. (1997). Shade avoidance in the clonal herb *Trifolium fragiferum*: a field study with experimentally manipulated vegetation height. *Plant Ecol.* 130, 53–62. doi: 10.1023/A:1009702611270

Hunt, R., Causton, D. R., Shipley, B., and Askew, A. P. (2002). A modern tool for classical plant growth analysis. *Ann. Bot.* 90, 485–488. doi: 10.1093/aob/mcf214

Ji, Y., Nuñez Ocaña, D., Choe, D., Larsen, D. H., Marcelis, L. F. M., and Heuvelink, E. (2020). Far-red radiation stimulates dry mass partitioning to fruits by increasing fruit sink strength in tomato. *New Phytol.* 228, 1914–1925. doi: 10.1111/nph.16805

Ji, Y., Ouzounis, T., Courbier, S., Kaiser, E., Nguyen, P. T., Schouten, H. J., et al. (2019). Far-red radiation increases dry mass partitioning to fruits but reduces *Botrytis cinerea* resistance in tomato. *Environ. Exp. Bot.* 168:103889. doi: 10.1016/j.envexpbot.2019.103889

Jolliffe, P. A., and Courtney, W. H. (1984). Plant growth analysis: additive and multiplicative components of growth. *Ann. Bot.* 54, 243–254. doi: 10.1093/oxfordjournals.aob.a086788

Kalaitzoglou, P., van Ieperen, W., Harbinson, J., van der Meer, M., Martinakos, S., Weerheim, K., et al. (2019). Effects of continuous or end-of-day far-red light on tomato plant growth, morphology, light absorption, and fruit production. *Front. Plant Sci.* 10:322. doi: 10.3389/fpls.2019.00322

Kasperbauer, M. J. (1971). Spectral distribution of light in a tobacco canopy and effects of end-of-day light quality on growth and development. *Plant Physiol.* 47, 775–778. doi: 10.1104/pp.47.6.775

Kasperbauer, M. J. (1987). Far-Red light reflection from green leaves and effects on phytochrome-mediated assimilate partitioning under field conditions. *Plant Physiol.* 85, 350–354. doi: 10.1104/pp.85.2.350

Kim, H. J., Lin, M. Y., and Mitchell, C. A. (2019). Light spectral and thermal properties govern biomass allocation in tomato through morphological and physiological changes. *Environ. Exp. Bot.* 157, 228–240. doi: 10.1016/j.envexpbot.2018.10.019

Kono, M., Kawaguchi, H., Mizusawa, N., Yamori, W., Suzuki, Y., and Terashima, I. (2020). Far-Red light accelerates photosynthesis in the low-light phases of fluctuating light. *Plant Cell Physiol.* 61, 192–202. doi: 10.1093/pcp/pcz191

Lee, M. J., Son, K. H., and Oh, M. M. (2016). Increase in biomass and bioactive compounds in lettuce under various ratios of red to far-red LED light supplemented with blue LED light. *Hortic. Environ. Biotechnol.* 57, 139–147. doi: 10.1007/s13580-016-0133-6

Li, Q., and Kubota, C. (2009). Effects of supplemental light quality on growth and phytochemicals of baby leaf lettuce. *Environ. Exp. Bot.* 67, 59–64. doi: 10.1016/j.envexpbot.2009.06.011

Marcelis, L. F. M. (1996). Sink strength as a determinant of dry matter partitioning in the whole plant. *J. Exp. Bot.* 47, 1281–1291. doi: 10.1093/jxb/47.Special_Issue.1281

Michaud, O., Fiorucci, A.-S., Xenarios, I., and Fankhauser, C. (2017). Local auxin production underlies a spatially restricted neighbor-detection response in *Arabidopsis*. *Proc. Natl. Acad. Sci.U.S.A.* 114, 7444–7449. doi: 10.1073/pnas.1702276114

Ouzounis, T., Heuvelink, E., Ji, Y., Schouten, H. J., Visser, R. G. F., and Marcelis, L. F. M. (2016). Blue and red LED lighting effects on plant biomass, stomatal conductance, and metabolite content in nine tomato genotypes. *Acta Hortic.* 1134, 251–258. doi: 10.17660/ActaHortic.2016.1134.34

Park, Y., and Runkle, E. S. (2017). Far-red radiation promotes growth of seedlings by increasing leaf expansion and whole-plant net assimilation. *Environ. Exp. Bot.* 136, 41–49. doi: 10.1016/j.envexpbot.2016.12.013

Poorter, H., and Remkes, C. (1990). Leaf area ratio and net assimilation rate of 24 wild species differing in relative growth rate. *Oecologia* 83, 553–559.

Sager, J. C., Smith, W. O., Edwards, J. L., and Cyr, K. L. (1988). Photosynthetic efficiency and phytochrome photoequilibria determination using spectral data. *Trans. Am. Soc. Agric. Eng.* 31, 1882–1889. doi: 10.13031/2013.30952

Sarlikioti, V., de Visser, P. H. B., Buck-Sorlin, G. H., and Marcelis, L. F. M. (2011). How plant architecture affects light absorption and photosynthesis in tomato: towards an ideotype for plant architecture using a functional–structural plant model. *Ann. Bot.* 108, 1065–1073. doi: 10.1093/aob/mcr221

Shibuya, T., Kishigami, S., Endo, R., and Matsuda, R. (2019). Interaction between red to far-red ratio of light and vapor-pressure deficit on extension growth of cucumber seedlings. *Sci. Hortic. (Amsterdam)* 248, 98–104. doi: 10.1016/j.scienta.2018.12.049

Tucker, D. J. (1981). Phytochrome regulation of leaf senescence in cucumber and tomato. *Plant Sci. Lett.* 23, 103–108. doi: 10.1016/0304-4211(81)90031-6

Yang, D., Seaton, D. D., Krahmer, J., and Halliday, K. J. (2016). Photoreceptor effects on plant biomass, resource allocation, and metabolic state. *Proc. Natl. Acad. Sci.U.S.A.* 113, 7667–7672. doi: 10.1073/pnas.1601309113

Zhang, Y., Zhang, Y., Yang, Q., and Li, T. (2019). Overhead supplemental far-red light stimulates tomato growth under intra-canopy lighting with LEDs. *J. Integr. Agric.* 18, 62–69. doi: 10.1016/S2095-3119(18)62130-6

Zhen, S., and Bugbee, B. (2020). Far-red photons have equivalent efficiency to traditional photosynthetic photons: Implications for redefining photosynthetically active radiation. *Plant Cell Environ.* 43, 1259–1272. doi: 10.1111/pce.13730

Zhen, S., and van Iersel, M. W. (2017). Far-red light is needed for efficient photochemistry and photosynthesis. *J. Plant Physiol.* 209, 115–122. doi: 10.1016/j.jplph.2016.12.004

Conflict of Interest: The authors declare that the research was conducted in the absence of any commercial or financial relationships that could be construed as a potential conflict of interest.

Copyright © 2021 Ji, Ouzounis, Schouten, Visser, Marcelis and Heuvelink. This is an open-access article distributed under the terms of the Creative Commons Attribution License (CC BY). The use, distribution or reproduction in other forums is permitted, provided the original author(s) and the copyright owner(s) are credited and that the original publication in this journal is cited, in accordance with accepted academic practice. No use, distribution or reproduction is permitted which does not comply with these terms.

frontiers in Plant Science

ORIGINAL RESEARCH
published: 13 January 2021
doi: 10.3389/fpls.2020.610046

LED Lighting Strategies Affect Physiology and Resilience to Pathogens and Pests in Eggplant (*Solanum melongena* L.)

J. Anja Dieleman, H. Marjolein Kruidhof, Kees Weerheim and Kirsten Leiss*

Business Unit Greenhouse Horticulture, Wageningen University & Research, Wageningen, Netherlands

Over the last decade, LED lighting has gained considerable interest as an energy-efficient supplemental light source in greenhouse horticulture that can change rapidly in intensity and spectral composition. Spectral composition not only affects crop physiology but may also affect the biology of pathogens, pests, and their natural enemies, both directly and indirectly through an impact on induced plant resistance. In this study, we investigated the effects of light spectrum against a background of sunlight on growth and development of *Solanum melongena*. These effects were related to the spectral effects on the establishment of populations of the predatory mite *Amblyseius swirskii* and plant resilience against the biotrophic fungus powdery mildew, the necrotrophic fungus botrytis, and the herbivorous arthropod Western flower thrips. The effects of a reduced red/far-red (R:FR) ratio were studied under two ratios of red to blue light. Far-red light either was supplied additionally to the photosynthetic photon flux density (PPFD) or partially replaced PPFD, while maintaining total photon flux density (PFD). Effects of white light or additional UV-B light on plant resilience was tested, compared to the reference (5% blue, 5% green, and 90% red light). Plant biomass in the vegetative phase increased when additional far-red light was supplied. Stem length increased with far-red, irrespective of PPFD and the percentage of blue light. In the generative phase, total shoot biomass and fruit fresh weights were higher under additional far-red light, followed by the treatments where far-red partly replaced PPFD. Far-red light increased biomass partitioning into the fruits, at the expense of the leaves. There were no differences in population growth of *A. swirskii* mites between light treatments, nor did light treatment have an effect on the vertical distribution of these predatory mites in the plants. The treatments with additional far-red light reduced the infection rate of powdery mildew, but increased botrytis infection. These differences might be due to the plant defenses acting against these pathogens evolving from two different regulatory pathways. These results show that positive effects of altered spectral compositions on physiological responses were only moderately compensated by increased susceptibility to fungal pathogens, which offers perspective for a sustainable greenhouse horticulture.

Keywords: Botrytis cinera, far-red light, blue light, shade avoidance, defense response, *Solanum melongena* (L.)

OPEN ACCESS

Edited by:
Sissel Torre,
Norwegian University of Life Sciences, Norway

Reviewed by:
Francesco Orsini,
University of Bologna, Italy
Niels Holst,
Aarhus University, Denmark

****Correspondence:***
J. Anja Dieleman
anja.dieleman@wur.nl

Specialty section:
This article was submitted to Crop and Product Physiology, a section of the journal Frontiers in Plant Science

Received: *24 September 2020*
Accepted: *30 November 2020*
Published: *13 January 2021*

Citation:
Anja Dieleman J, Marjolein Kruidhof H, Weerheim K and Leiss K (2021) LED Lighting Strategies Affect Physiology and Resilience to Pathogens and Pests in Eggplant (Solanum melongena L.). Front. Plant Sci. 11:610046. doi: 10.3389/fpls.2020.610046

INTRODUCTION

Light is considered to be the most important environmental factor affecting plant development, growth, and production in greenhouse horticulture. In northern latitudes, solar light levels during the winter can be insufficient to maintain production levels and product quality, due to the low light intensities and short photoperiods (Davis and Burns, 2016). The potential of supplemental lighting to foster off-seasonal production in the Mediterranean region is also now under investigation (Palmitessa et al., 2020; Paucek et al., 2020). Under low-light conditions, natural light can be supplemented by artificial lighting, with high pressure sodium (HPS) fixtures currently being the predominant greenhouse lighting source. However, the introduction of LED lighting systems has received considerable attention over the last decade. Benefits of LED lighting are the high efficiency with which they convert electricity into light, low heat emission, and long lifetime. Where HPS emits a fixed spectrum of approximately 4% blue, 34% green, 50% red, and 12% far-red light, LEDs can emit narrow-bandwidth light allowing the design and optimization of a dedicated light spectrum for plant growth and development (Morrow, 2008). However, before the full potential of LEDs as light source for plant production in greenhouses can be used, plant responses to spectral composition of the light as well as the effects on the biology of pathogens, pests, and their natural enemies have to be quantified.

Red photons are well absorbed by leaves, photosynthetically highly efficient (McCree, 1972), and efficiently generated by LEDs. Therefore, red is the basis light color in most commercially used light sources in protected cultivation of plants (Kusuma et al., 2020). Some blue light (ranging from 5 to 10%) is typically added to improve growth and prevent excessive stem elongation (Hernández and Kubota, 2016). Adding far-red light to a red/blue light spectrum was recently shown to increase fruit production in fruit vegetable crops such as tomato (Ji et al., 2019; Kalaitzoglou et al., 2019). A decreased ratio of red to far-red light by adding far-red light to the spectrum initiates shade avoidance symptoms, leading to increased internode and petiole elongation (Franklin and Quail, 2010), upward leaf movement (hyponasty; Keuskamp et al., 2010), reduced branching (Finlayson et al., 2010), and accelerated flowering, as reviewed by Demotes-Mainard et al. (2016). The positive effect of a reduced red/far-red ratio on plant biomass may be explained by an increase in light interception due to the altered plant architecture (Heraut-Bron et al., 2001; Sarlikioti et al., 2011), increased rate of photosynthesis (Zhen and van Iersel, 2017; Zhen and Bugbee, 2020), and biomass partitioning in favor of the generative plant parts (Ji et al., 2020). To which extent the addition of far-red light has comparable effects in other fruit vegetable crops such as eggplant (*Solanum melongena*) still has to be determined. In most studies, positive effects of far-red light were established by giving far-red additional to the PAR light spectrum. However, this implies that the total photon flux density (PFD) is increased and thereby also the electricity consumption of the LED lighting system. From a sustainability perspective, the question would be whether comparable effects of far-red light can be achieved by replacing part of the PAR light by far-red, thereby maintaining the PFD and, under the assumption that photons with different wavelengths are produced equally efficient, the energy input in the greenhouse system. Recent results have shown that far-red photons are equally efficient at driving canopy photosynthesis when acting synergistically with traditionally defined photosynthetic photons (Zhen and Bugbee, 2020). This opens the discussion to which extent the definition of PAR should be adjusted, incorporating wavelengths up to 750 nm. In contrast to the effects of far-red, blue light reduces plant height and leaf expansion in nearly all species (Huché-Thélier et al., 2016; Dieleman et al., 2019). Runkle and Heins (2001) showed that an environment deficient in blue promoted stem extension in all long day species tested, independent of the red/far-red ratio. This offers perspectives to suppress an expected stem elongation as a consequence of a low red/far-red ratio by decreasing the red/blue ratio. Increasing the proportion of blue light increases the rate of leaf photosynthesis (Hogewoning et al., 2010), which might be related to the increased concentration of photosynthetically active pigments such as chlorophyll (Meng and Runkle, 2019). To which extent an increased proportion of blue light compensates for far-red-mediated plant responses in eggplant remains to be established.

The spectral composition of the light not only influences crop growth and development but also affects the biology of pathogens, pests, and their natural enemies. Until recently, however, these effects have rarely been investigated. Light spectrum can influence pests and pathogens directly or indirectly, via host plant resistance. UV-B, for example, is almost absent in most of the light spectra to which greenhouse crops are exposed, as this part of the natural sunlight spectrum is largely filtered out by most cladding materials. The response of plants to UV-B is regulated by a UV-B-specific photoreceptor called UV RESISTANT LOCUS (UVR8). Apart from steering the expression of genes that code for inhibition of hypocotyl elongation and DNA repair, UVR8 also codes for genes involved in antioxidative defenses and the production of phenols that can play a role in plant defense against pests and diseases (Rizzini et al., 2011; Escobar-Bravo et al., 2017). Indeed, several studies indicate that deficiency in UV-B in greenhouse environments can lead to increased susceptibility of plants for pests and diseases (Caldwell et al., 2003; Ballaré et al., 2011; Kuhlmann and Muller, 2011; Demkura and Ballaré, 2012; Ballaré, 2014; Huché- Thélier et al., 2016). In addition to short-wavelength UV-B light, light with longer wavelengths can also influence plant defenses against pathogens and pests. Young cucumber plants grown under red monochromatic LEDs, for example, had lower incidence of powdery mildew than plants grown under white and other monochromatic lights (Wang et al., 2013). Moreover, monochromatic red and blue LEDs inhibited *B. cinerea* infection in grapevine through an increase of plant defense-related stilbenes (Ahn et al., 2015).

These effects of light on plant resistance show that defense pathways interact with and are influenced by light-dependent processes (Kangasjärvi et al., 2012), whereby light has emerged as a key modulator of plant immunity (Ballaré et al., 2012; Ballaré, 2014). There are two major pathways involved in plant immune responses: the salicylic acid (SA) pathway and the

jasmonic acid (JA) pathway. The SA and JA defense pathways each induce different sets of responsive genes and are often mutually antagonistic, which enables the plant to fine-tune their defense response to a specific pathogen (Pieterse et al., 2012). The SA pathway is activated predominantly to fend off biotrophic pathogens, while the JA pathway is mainly activated in response to necrotrophic pathogens and herbivorous insects. Light is required for SA biosynthesis and activation (Genoud et al., 2002). Exposure of germinating soybean sprouts to monochromatic red light resulted in seedlings with higher levels of SA and stronger expression of SA-related defense genes that were more resistant against bacterial rotting disease (Dhakal et al., 2015). The red/far-red ratio (R:FR) is a key modulator of defense expression by which plants resolve the trade-off between resource allocation to growth or defense. Low R:FR, which signals a high risk of competition in plant canopies, represses both jasmonate-induced and salicylic acid-induced defense responses, thus redirecting resource allocation from defense to rapid plant elongation (de Wit et al., 2013; Leone et al., 2014; Ballaré and Pierik, 2017). Several studies have shown that a relatively low R:FR ratio can cause a decrease in plant resistance to necrotrophic pathogens (Cerrudo et al., 2012; Cargnel et al., 2014; Ji et al., 2019), pests (Izaguirre et al., 2006; Moreno et al., 2009), as well as biotrophic and hemibiotrophic pathogens (Shibuya et al., 2011; de Wit et al., 2013).

Apart from impacting pathogens and pests through plant-mediated effects, light can also exert a direct effect on plant attackers as well as their natural enemies. Just as plants, arthropods, and fungi possess photoreceptors, and they use light as signals for steering important developmental and/or behavioral processes (Avalos and Estrada, 2010; Johansen et al., 2011; Schumacher, 2017). Filamentous fungi maintain a complex regulatory network of photoreceptors and signal transduction pathways that enable them to use light (quantity, quality, and direction) as a signal to produce protective metabolites (e.g., carotenoids), to gear growth (direction) and development (e.g., sporulation), and to regulate their biological clock (Herrera-Estrella and Horwitz, 2007; Rodriguez-Romero et al., 2010). Arthropod photoreceptors typically have optima in the UV-A, green, and sometimes blue parts of the light spectrum (Kelber, 2001; Warrant and Nilsson, 2006). It is important to note that arthropods do not perceive light in the red and far-red part of the spectrum. Therefore, a large discrepancy exists in the perception and usage of light between arthropods and plants.

When regarding direct effects of light on arthropod pests and natural enemies, UV-A light plays a major role. Multiple studies have shown that in semi-open greenhouses that allow for UV-A to penetrate the cladding material, crops suffer from higher pest densities than in similar greenhouses with UV-absorbing cladding materials (Antignus et al., 1996; Costa and Robb, 1999; Chyzik et al., 2003; Raviv and Antignus, 2004; Legarrea et al., 2010). Direct exposure of arthropods and plant pathogens to UV-B, on the other hand, can negatively impact development and survival (Suthaparan et al., 2016; Tanaka et al., 2016; Johansen et al., 2017). Moreover, changes in light quality within the PAR spectrum can also directly affect pathogens and arthropods. The anthocorid predatory bug *Orius sauteri* developed 40 and 18% slower, respectively, and had reduced fecundity, under monochromatic red and blue light in comparison to white, green, or yellow light (Wang et al., 2013). This may have been caused by lower perceived light intensity by these arthropods due to the absence of photoreceptors in the red and blue parts of the spectrum. Indeed, the same study showed that developmental time of *O. sauteri* increased with decreasing light intensity (Wang et al., 2013). No published studies have evaluated the effect of PAR spectral composition on life history parameters and/or population growth of predatory mites. Unpublished work of Shipp, however, indicates that egg–egg development of *Amblyseius swirskii* is significantly faster under HPS supplemental lighting compared to red and blue LED lights (Buitenhuis et al., 2015). Moreover, Zilahl-Balogh et al. (2007) showed that the oviposition rate of the predatory mite *Neoseiulus cucumeris* was reduced under low light intensity, while the predation activity of this mite remained unaffected by light intensity.

In the experiments described in this paper, we grew three *S. melongena* (eggplant) genotypes under seven different LED light spectra against a background of low-intensity sunlight. We aimed to quantify the growth and development of these genotypes and tested host plant resistance against the necrotrophic pathogen *Botrytis cinerea*, the biotrophic pathogen powdery mildew (*Oidium lycopersicum*), and the herbivorous arthropod Western flower thrips (*Frankliniella occidentalis*) during both the vegetative and fruit-bearing stage. Moreover, we assessed the population growth and vertical distribution of *A. swirskii* predatory mites under a subset of four light spectra. Based on studies in the fruit vegetable crop tomato, we hypothesized that the addition of far-red light would increase stem elongation, biomass production, and assimilate partitioning toward the fruits. However, we assumed this would come at the expense of plant resistance to the abovementioned plant attackers. The expected stem elongation as a consequence of the addition of far-red light might be suppressed or overcome by decreasing the red/blue ratio. Decreasing the red/blue ratio might also reduce the expected negative effects of additional far-red light on plant resistance to pathogens and pests. Furthermore, we hypothesized that the addition of a low dose of UV-B light may increase plant resistance to pests and fungal pathogens. We expected the highest population growth of *A. swirskii* predatory mites to occur under the light spectrum with the highest proportion of green light, since mites possess photoreceptors for green light, whereas they cannot perceive light in the red part of the light spectrum. The implications of these results for greenhouse horticulture will be discussed.

MATERIALS AND METHODS

Plant Material and Light Treatments

The experiment was conducted in a greenhouse compartment of 9.6 m × 15 m with 14 tables of 4 m × 1.8 m, each having a ceiling of dynamic LED modules (Philips GreenPower LED production modules Dynamic, Signify, Eindhoven, Netherlands). These modules are tunable in blue (B; peak at 446 nm), white [broad

spectrum with large proportion of green (G) light with peak emission at 571 nm], red (R; 660 nm), and far-red (FR; 730 nm). In one of the treatments, UV light (UV; peak at 312 nm) was given at an intensity of 0.5 and 1 kJ m^{-2} day^{-1} for 30 min per day at noon during the vegetative and generative stage, respectively. The incidence of sunlight was controlled by the use of an energy screen (LS Ultra, Ludvig Svensson, Kinna, Sweden) with a transmission of 38% and a blackout screen (LS Obscura, Ludvig Svensson, Kinna, Sweden). The greenhouse was air conditioned, allowing the realization of winter conditions throughout the year. The average realized temperature was 22.0°C with a day/night temperature of 22.8 and 19.8°C, respectively, a VPD of 3.4 kPa, and a CO_2 concentration of 631 ppm.

On July 16, 2019, eggplant cvs Tracey, Beyoncé, and Lemmy plants were transplanted on rockwool cubes (Grodan Plantop, Roermond, Netherlands) on the tables at a planting density of 20 plants/m^2. Tracey and Beyoncé plants were sown on June 14, grafted on the rootstock Kaiser on July 3, and topped on July 15 to maintain two stems per plant. Lemmy plants were sown on June 17, grafted on July 3, and topped on July 18. The plants were placed under seven lighting strategies (**Figure 1** and **Table 1**; one treatment per table, $n = 2$) at a light intensity of 100 μmol m^{-2} s^{-1}, which was gradually increased to 140 μmol m^{-2} s^{-1} on August 30 [45 days after transplanting (DAT)] and to 180 μmol m^{-2} s^{-1} 62 DAT, at a photoperiod of 18 h. For the two treatments with additional far-red light, these PFD values were 115, 161, and 207 μmol m^{-2} s^{-1}, respectively. The increase in light intensity was applied based on an expected assimilate demand based on the gradually increasing biomass of vegetative and generative organs. To prevent light pollution between treatments, tables were separated by white plastic sheets. To prevent air stratification and ensure that temperature setpoints were reached, conditioned air was distributed from top to bottom of all 14 tables through a perpendicularly located perforated sleeve. During the trial, the plants received a DLI (daily light integral) of sunlight and LED light of 8.6 mol m^{-2} s^{-1}. The contributions of LED

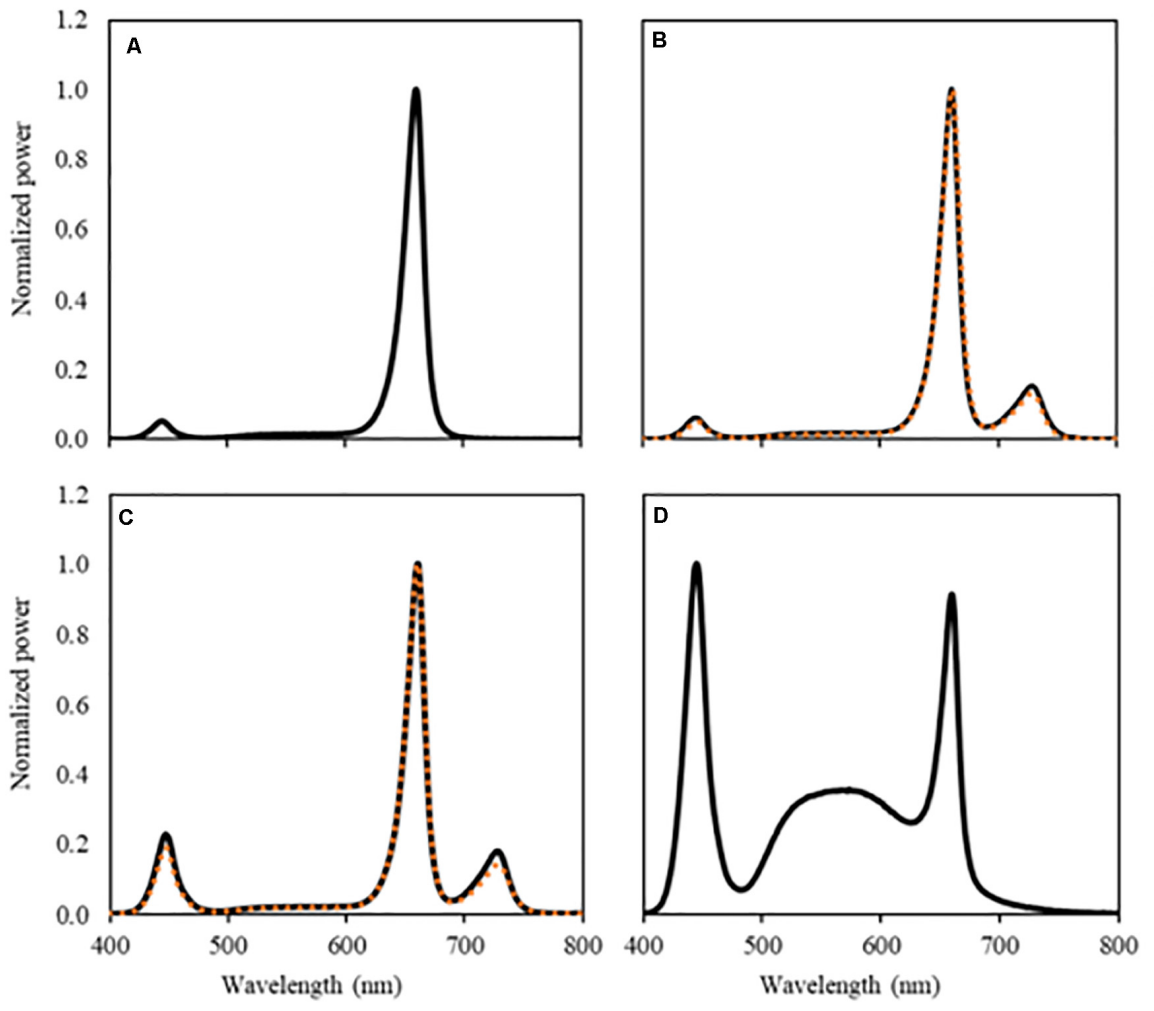

FIGURE 1 | Spectral composition of the light treatments, UV-B light excluded. **(A)** RWB, **(B)** RWB FR (orange dotted line) and RWB + FR (black solid line), **(C)** RWhB FR (orange dotted line) and RWhB + FR (black solid line), and **(D)** White provided by the LEDs measured at the top of the canopy.

TABLE 1 | Spectral compositions of the light treatments.

Treatment	Blue (%)	Green (%)	Red (%)	Far-red (%)	PFD* (μmol m^{-2} s^{-1})
RWB	5	5	90	0	100–180
RWB UV	5	5	90	0	100–180
RWB FR	5	5	75	15	100–180
RWhB FR	15	5	65	15	100–180
RWB + FR	5	5	90	15	115–207
RWhB + FR	15	5	80	15	115–207
White	30	35	35	0	100–180

*Spectral compositions consist of blue light (400–500 nm; peak at 446 nm), green light (500–600 nm, obtained by a white broadband spectrum with a large proportion of green light with peak emission at 571 nm), red light (500–600 nm; peak at 660 nm), and far-red light (700–800 nm; peak at 730 nm). In the treatment RWB UV, UV light (peak of 312 nm) is given during 30 min per day at an intensity of 0.5–1 kJ m^{-2} day^{-1}. *PFD is photon flux density (μmol m^{-2} s^{-1}) and was 100 μmol m^{-2} s^{-1} at transplanting (115 μmol m^{-2} s^{-1} for treatments with additional FR). PFD gradually increased to 140 μmol m^{-2} s^{-1} (161 μmol m^{-2} s^{-1} 45 DAT) and to 180 μmol m^{-2} s^{-1} (207 μmol m^{-2} s^{-1} 62 DAT).*

light and sunlight to the DLI were 79 and 21%, respectively, for the vegetative phase (DAT 0–24) and 88 and 12%, respectively, for the generative phase (DAT 25–90). The vegetative phase ended 24 DAT for Tracey and Beyoncé and 27 DAT for Lemmy with a final destructive harvest of three plants per table (n = 2, 6 plants per treatment). Thereafter, plants of the varieties Tracey and Beyoncé were placed on rockwool slabs (Grodan, Roermond, The Netherlands) at a density of three plants/m^2 in two rows per table for the generative phase. The generative phase ended 85 DAT for variety Beyonce and 90 DAT for variety Tracey with a final destructive harvest.

Plant Measurements

Photosynthesis and Stomatal Conductance

Light response curves of photosynthesis of Tracey leaves were measured 71 and 86 DAT in the treatments RWB and RWB + FR. Measurements were taken of four individual plants per measuring date per light treatment. The uppermost fully expanded leaf (enclosed leaf area of 6 cm^2) was enclosed in the leaf chamber of the LI-6800 portable photosynthesis system equipped with the fluorometer chamber (LI-COR, Lincoln, NE, United States). The light spectrum during the measurements consisted of 10% blue and 90% red light. Since the light spectrum in the leaf chamber was identical for both light treatments measured, the results indicate the effects of structural changes in the leaf due to the light treatments. The block temperature was set to 25°C, CO_2 concentration was 600 ppm, and VPD was 0.9 kPa. Light intensities applied were 1,500, 1,200, 1,000, 800, 600, 400, 300, 200, 100, 50, and 0 μmol m^{-2} s^{-1}. At every light intensity, the photosynthesis, conductance, and fluorescence were measured after matching the infrared gas analyzers. The fluorescence was measured with a Multiphase protocol, with a red light target of 8,000 μmol m^{-2} s^{-1}, in three phases for a total duration of 0.9 s. The quantum yield of photosystem II (ΦPSII) was calculated based on fluorescence yield data (Genty et al., 1989). The effect of light intensity on rate of photosynthesis rate, not taking into account the effect of CO_2 concentration, can be described with a curve that reaches a plateau at high light intensity (Farquhar et al., 1980):

$$Ass = \left(\varepsilon R + (A_{\max} + R_d) - \sqrt{\left((\varepsilon R + A_{\max} + R_d)^2 - 4\Theta\varepsilon R\,(A_{\max} + R_d)\right)}\right) / (2\Theta)$$

in which

Ass: rate of gross CO_2 assimilation (μmol m^{-2} s^{-1})

$A_{\max}$: asymptotic value of net CO_2 assimilation rate at high light intensity (μmol m^{-2} s^{-1})

R_d: day respiration (μmol m^{-2} s^{-1}) (in this formula, R_d has a negative value)

ε: initial light use efficiency (mol CO_2 m^{-2} s^{-1}/mol PAR m^{-2} s^{-1})

Θ: curvature factor

R: photosynthetically active radiation (μmol m^{-2} s^{-1})

Each photosynthesis light response curve was fitted to this non-rectangular hyperbola, and a two-way analysis of variance (ANOVA) with month of observation (two levels) and light treatment (two levels) was done for each of the parameters of the light response curve. In addition, a one-way ANOVA was performed for all light intensities on net assimilation rate, stomatal conductance, and ΦPSII with month of observation (two levels) as block factor.

Plant Morphology, Flowering, and Biomass

At the end of the vegetative phase, 24 DAT (Tracey and Beyoncé) or 27 DAT (Lemmy), three plants per table (n = 2; 6 plants per treatment) per variety were harvested destructively, and stem lengths, leaf area, and fresh and dry weights of stems and leaves were determined. Specific leaf area (SLA) was calculated by dividing the leaf area per plant by the dry leaf mass. In the generative phase, flowers were labeled to determine fruit growth duration (from anthesis until harvest). Ripe fruits of six plants per table were harvested twice per week in the period of 57–90 DAT (n = 2; 12 plants per treatment), and fresh weights and numbers of harvested fruits were recorded. Periodically, dry matter percentage of the fruits was determined by placing them in stoves at 80°C for at least 3 days. At the final destructive harvest, 90 DAT, three plants per table (n = 2; 6 plants per treatment) per variety were harvested destructively, and stem lengths, leaf area, and fresh and dry weights of stems, leaves, and fruits were determined. SLA was calculated by dividing the leaf area per plant by the dry leaf mass. Total fruit dry weight was calculated by multiplying the fresh weight of the harvested fruits with the dry matter percentage of these fruits and adding the dry weights of the fruits on the plant at the destructive harvest. Total shoot biomass production was calculated by adding the dry weights of the stems and leaves at the destructive harvest and the total fruit dry weight. The biomass partitioning between stems, leaves, and fruits was determined by dividing the weight of the relevant organ by the total shoot biomass. Data were analyzed by means of the statistical package GenStat (19th edition) with a two-factor ANOVA using variety and light treatments as factors. Fisher's unprotected least significance test was used to make *post hoc* multiple comparisons among means.

P values <0.05 were considered as significantly different for the pairwise comparisons.

Population Development of *A. swirskii*

The population growth of *A. swirskii* predatory mites, as well as their vertical distribution on *S. melongena* plants, was assessed for a subset of four LED treatments, namely, the RWB, RWB UV, RWhB + FR, and White (see **Table 1**). Six of the plants on each of the two tables of the respective light treatments were used for this experiment (n = 2, 12 plants per treatment). One of the stems of these plants was topped to create plants with a single stem. *A. swirskii* was introduced 23 DAT at the base of the stem (80 predatory mites/plant). On the same day, as well as in each subsequent week, Typha pollen (Nutrimite®, Biobest) were dispersed equally over the entire plant. On 55 DAT, three leaves from each of the six plants on a table were harvested divided over three vertical layers: one leaf in layer A (1st and 2nd youngest fully grown leaves), one leaf in layer B (3rd and 4th youngest fully grown leaves), and one leaf in layer C (5th and 6th youngest fully grown leaves). On each leaf, the number of *A. swirskii* eggs, nymphs, and adults were counted (n = 2; 12 plants per light treatment per leaf position). The effect of light treatment and leaf position and their interaction on the number of *A. swirskii* individuals (eggs + nymphs + adults) were analyzed in Genstat 19th edition. A generalized linear mixed model with Poisson data distribution was used, and plant replicate nested within table was introduced as a random factor into the model.

Bioassays of Host Plant Resistance

Effects on plant health were examined using leaf disc biossays with gray mold (*B. cinerea*) as a necrotroph and powdery mildew (*O. lycopersicum*) as a biotroph fungus as well as Western flower thrips (*F. occidentalis*) as a sucking insect being representatives of economically important pests and diseases in eggplant. For each table and variety, three plants were sampled (n = 2; 6 plants per treatment). Leaf discs with a diameter of 5 cm were taken from a medium-aged leaf (9th leaf from below) at the end of the vegetative phase as well as in the generative phase. Discs were placed on 1% water agar in 9-cm-diameter petri dishes to prevent desiccation. Subsequently, the leaf discs were inoculated with spore suspensions of 10^5 spores/ml for botrytis obtained from a stock of strain *Botrytis* B05.10 and 10^6 spores/ml for powdery mildew obtained from a rearing on tomato (variety Moneymaker). For the thrips bioassay, leaf discs were infested with five adult thrips each derived from a rearing on chrysanthemum (variety Miramar). The petri dishes were randomly placed in a climate room (20°C, 60% RH, fluorescent tubes 23 μmol m^{-2} s^{-1}). Four days after inoculation, incidence of *B. cinerea* was measured as diameter of necrotic lesions (mm^2). Incidence of powdery mildew was measured 10 days after inoculation as Spencer index with a range of 1–5 whereby 0 represents no infection and 1, 2, 3, 4, and 5 represent 1, 2–5, 6–20, 20–40, and >40% infection, respectively. Toward the end of the experiment, a natural infection with powdery mildew occurred. Therefore, at the end of the experiment, four whole plants per table and variety were scored for mildew infection using the Spencer index (n = 2, 8 plants per treatment). Thrips damage was scored as silver damage (mm^2) 5 days after infestation. Data for *B. cinerea* were analyzed with a two-factor ANOVA using variety and light treatments as factors, whereas data for powdery mildew were analyzed with a χ^2 test.

RESULTS

Plant Growth, Development, and Biomass Partitioning

At the end of the vegetative phase, plants that received far-red light were taller than the treatments without far-red light (**Table 2**). Total plant dry weight was higher for the treatments with additional far-red light (RWB + FR and RWhB + FR), primarily due to the increased leaf dry weight. Leaf area did not differ between treatments for the varieties Tracey and Beyoncé, whereas in Lemmy, leaf area was higher (**Table 2**). SLA was lower for the treatments with additional far-red light, implying that they are capable of intercepting more light with a comparable leaf biomass.

Total fresh fruit production (kg m^{-2}) in the generative phase for both varieties was highest for the treatment RWB + FR, followed by RWhB + FR (**Table 3**). Fruit production in the treatments where far-red light was given at the expense of PAR light (RWB FR and RWhB FR) also had a higher production than the reference treatment. Production differences were due to the total number of harvested fruits and the average fruit fresh weight (g $fruit^{-1}$). Fruit growth duration from anthesis to harvest in the treatments White and RWB ranged from 21 days for Beyoncé to 23–25 days for Tracey (**Table 3**). In the treatments with additional far-red light, fruit growth duration was shortened by 4 to 7 days. The number of harvested fruits was highest in RWB + FR, followed by RWhB + FR, for both varieties (**Table 3**). In the treatments where far-red replaced part of the PAR light (RWB FR and RWhB FR), the number of harvested fruits was lower than when far-red light was given additionally. The number of fruits harvested was lowest in the reference treatment (RWB), as well as the average fruit weight (**Table 3**). Fruits from the treatments with far-red FR light had the highest dry matter percentage (**Table 3**), although the dry matter percentage of fruits from RWhB FR did not differ significantly from the treatments RWB, RWB UV, and White. As at the end of the vegetative phase, stem length at the end of the generative phase was highest for the treatments with far-red light (data not shown). Leaf area or SLA differed between treatments for either variety (P = 0.20 and P = 0.44, respectively; data not shown). At the final destructive harvest, dry weights of the stems, leaves, and fruits on the plants were determined, and the dry weights of the harvested fruits (calculated by FW × dry matter percentage of a sample of fruits) were added to determine total shoot biomass. Total shoot dry weight was highest for the treatments with additional far-red light (RWB + FR and FWhB + FR), followed by the other treatments with far-red light in the spectrum (RWB FR, RWhB FR, and White). Treatments with far-red partitioned a larger part of their biomass into the fruits, at the expense of the leaves (**Table 4**).

TABLE 2 | Effects of spectral composition on vegetative eggplant traits.

Variety treatment	Stem length (cm)	Leaf dry weight (g plant^{-1})	Stem dry weight (g plant^{-1})	Shoot dry weight (g plant^{-1})	Leaf area (10^{-3} m^2 plant^{-1})	SLA (m^2 kg^{-1})
Tracey						
RWB	10.7 b	7.4 b	0.9 c	8.2 b	2.4 a	32.9 a
RWB UV	11.2 b	8.0 b	1.0 c	8.9 b	2.5 a	33.0 a
RWB FR	19.2 a	7.7 b	1.6 ab	9.3 b	2.4 a	32.5 a
RWhB FR	18.6 a	6.3 b	1.3 b	7.6 b	2.2 a	35.9 a
RWB + FR	17.3 a	9.4 a	1.9 a	11.3 a	2.5 a	26.2 b
RWhB + FR	18.0 a	9.8 a	1.6 ab	11.4 a	2.6 a	25.2 b
White	10.3 b	7.7 b	0.9 c	8.7 b	2.6 a	32.1 a
Beyoncé						
RWB	12.3 b	7.8 c	0.8 b	8.6 b	2.5 a	34.3 a
RWB UV	10.6 b	8.1 c	1.0 b	9.1 b	2.5 a	31.8 ab
RWB FR	19.3 a	8.0 c	1.5 a	9.5 b	2.5 a	30.2 bc
RWhB FR	17.8 a	8.5 c	1.5 a	9.9 b	2.6 a	29.9 bc
RWB + FR	18.3 a	10.5 a	1.8 a	12.3 a	2.6 a	24.0 d
RWhB + FR	17.3 a	9.9 ab	1.6 a	11.5 a	2.6 a	27.5 cd
White	11.9 b	8.6 bc	1.0 b	9.6 b	2.6 a	29.7 bc
Lemmy						
RWB	10.7 c	8.4 a	1.0 b	9.4 a	2.6 a	32.4 b
RWB UV	10.3 c	6.6 bc	0.8 b	7.4 b	2.2 b	36.3 a
RWB FR	22.0 a	6.1 c	1.4 a	7.5 b	2.1 b	36.5 a
RWhB FR	21.1 a	6.5 bc	1.5 a	7.9 ab	2.4 ab	38.1 a
RWB + FR	18.9 b	7.6 ab	1.7 a	9.3 a	2.4 ab	32.2 b
RWhB + FR	19.3 b	7.6 ab	1.6 a	9.2 a	2.5 ab	32.8 b
White	11.8 c	6.3 bc	0.9 b	7.2 b	2.2 b	36.9 a
Two-way ANOVA						
Treatment	***	***	***	***	n.s.	***
Variety	n.s.	***	n.s.	***	*	***
Treatment × variety	n.s.	*	n.s.	n.s.	n.s.	n.s.

*Light treatments (see **Table 1**) were maintained during 25 days on stem length (average length of two stems per plant), shoot dry weight (sum of stem dry weight and leaf dry weight per shoot), leaf area per shoot, and specific leaf area, calculated as the leaf dry weight divided by the leaf area (n = 2, 6 plants per treatment). Different letters per variety within columns indicate significant differences ($P < 0.05$). The means are tested with two-way analysis of variance (ANOVA) for significant effects of treatment, variety, and the interaction between treatment and variety. Fisher's unprotected least significance test was used to make post hoc multiple comparisons among means. Significant differences are indicated: *$P < 0.05$; ***$P < 0.001$; n.s., non-significant.*

Analysis of the light response curves of photosynthesis for the variety Tracey showed that the addition of far-red light to the RWB spectrum did not have a significant effect on any of the four parameters describing the non-rectangular hyperbolas ($P = 0.49$ for A_{max}, $P = 0.69$ for R_d, $P = 0.44$ for ε, and $P = 0.19$ for Θ; **Figure 2A**). Comparisons between treatments per individually measured light intensity showed significant differences in rate of photosynthesis between 300 and 800 μmol m^{-2} s^{-1} ($P = 0.041$). Stomatal conductance was lower in the treatment with additional far-red light between 600 and 1,000 μmol m^{-2} s^{-1} ($P = 0.047$) (**Figure 2B**). ΦPSII efficiency was higher in the treatment with additional far-red light (**Figure 2C**). Between 300 and 1,500 μmol m^{-2} s^{-1}, ΦPSII was up to 43% higher in the treatment RWB + FR compared to RWB ($P = 0.019$). The observed rates of photosynthesis are low, which might be due to the varying levels of chlorosis in the leaves during measurements. Between 600 and 800 μmol m^{-2} s^{-1}, stomatal conductance was higher in the RWB treatment compared to RWB + FR treatment, but assimilation rates were lower, indicating that conductance was not limiting assimilation rate.

Population Development of *A. swirskii*

The light treatments did not significantly affect population size of *A. swirskii*, measured as number of individuals (eggs + nymphs + adults) per leaf, at the time of evaluation ($P = 0.99$; **Figure 3**). Leaf position, however, did affect the population size ($P < 0.001$), with lower numbers of predatory mites per leaf on the leaves of the upper leaf layer (on average 42 individuals/leaf) compared to the leaves of the middle and lower leaf layers (on average 74 and 73 mites/leaf, respectively). The difference in *A. swirskii* number between leaf layers did not depend on the light treatment ($P = 0.22$).

Host Plant Resistance Against Botrytis, Powdery Mildew, and Thrips

For the vegetative phase, no differences between varieties in infestation with *B. cinerea* or powdery mildew could be observed

TABLE 3 | Effects of spectral composition on fruit production of eggplant.

Variety treatment	Fresh fruit production (kg m^{-2})	Fruit growth duration (days) $plant^{-1}$)	Number of harvested fruits (-)	Average fruit weight (g $fruit^{-1}$)	Dry matter percentage of the harvested fruits (%)
Tracey					
RWB	3.2 d	23 ab	40 c	254 b	4.9 b
RWB UV	3.4 d	24 ab	40 c	269 ab	4.9 b
RWB FR	4.4 b	21 ab	49 b	286 a	5.2 ab
RWhB FR	4.5 b	20 b	49 b	293 a	5.3 a
RWB + FR	5.2 a	20 b	57 a	290 a	5.1 ab
RWhB + FR	4.9 ab	18 c	52 b	300 a	5.3 a
White	3.8 c	25 a	43 c	280 ab	5.0 ab
Beyoncé					
RWB	2.9 e	21 ab	33 d	279 c	4.9 b
RWB UV	3.3 d	23 a	37 c	289 bc	5.0 b
RWB FR	4.2 c	18 bc	44 b	300 bc	5.3 a
RWhB FR	4.2 c	18 bc	44 b	302 bc	5.0 ab
RWB + FR	5.5 a	19 abc	55 a	318 a	5.3 a
RWhB + FR	5.0 b	17 c	51 a	310 ab	5.2 ab
White	3.3 de	21 ab	37 c	284 bc	5.1 ab
Two-way ANOVA					
Treatment	***	**	***	**	*
Variety	n.s.	*	***	**	n.s.
Treatment × variety	n.s.	n.s.	n.s.	n.s.	n.s.

*Light treatment (see **Table 1**) effects on fresh fruit production (kg m^{-2}) in the period of 57 to 90 days after transplanting for the varieties Tracey and Beyoncé (n = 2, measured on 12 plants per treatment). Different letters per variety within columns indicate significant differences ($P < 0.05$). The means are tested with two-way analysis of variance (ANOVA) for significant effects of treatment, variety, and the interaction between treatment and variety. Fisher's unprotected least significance test was used to make post hoc multiple comparisons among means. Significant differences are indicated: *$P < 0.05$; **$P < 0.01$; ***$P < 0.001$; n.s., non-significant.*

TABLE 4 | Effects of spectral composition on assimilate partitioning of eggplant.

Variety	Treatment	Shoot biomass (g $plant^{-1}$)	Partitioning to the leaves (%)	Partitioning to the stem (%)	Partitioning to the fruits (%)
Beyoncé	RWB	157 d	43 a	15 a	42 b
	RWB UV	181 cd	42 a	15 a	43 b
	RWB FR	198 bc	32 b	17 a	51 a
	RWhB FR	193 c	33 b	17 a	50 a
	RWB + FR	241 a	30 b	16 a	54 a
	RWhB + FR	222 ab	31 b	16 a	52 a
	White	174 cd	40 a	17 a	43 b
Tracey	RWB	159 d	38 a	16 bc	45 b
	RWB UV	165 d	39 a	16 c	45 b
	RWB FR	203 bc	31 b	17 bc	52 a
	RWhB FR	201 bc	28 b	20 a	52 a
	RWB + FR	218 ab	30 b	18 abc	52 a
	RWhB + FR	229 a	31 b	19 ab	50 a
	White	180 cd	38 a	17 bc	45 b
Two-way ANOVA	Treatment	***	***	*	***
	Variety	n.s.	**	**	n.s.
	Treatment × variety	n.s.	n.s.	n.s.	n.s.

*Effect of spectral composition on total shoot dry weight (including harvested fruits) at the destructive harvest (90 days after transplanting) and assimilate partitioning over leaves, stems, and fruits for the varieties Tracey and Beyoncé (n = 2; measured on 6 plants per treatment). Different letters per variety per column indicate statistical differences. The means are tested with two-way analysis of variance (ANOVA) for significant effects of treatment, variety, and the interaction between treatment and variety. Fisher's unprotected least significance test was used to make post hoc multiple comparisons among means. Significant differences are indicated: *$P < 0.05$; **$P < 0.01$; ***$P < 0.001$; n.s., non-significant.*

(data not shown). Thrips damage, however, was significantly higher in the variety Lemmy (average area of 50 ± 4 mm^2) than in the varieties Tracy and Beyoncé with average areas of 39 ± 3 mm^2 and 38 ± 4 mm^2, respectively ($P = 0.04$; data not shown). In the generative phase, no differences in incidence of *B. cinerea* or thrips infestation occurred between varieties (data not shown).

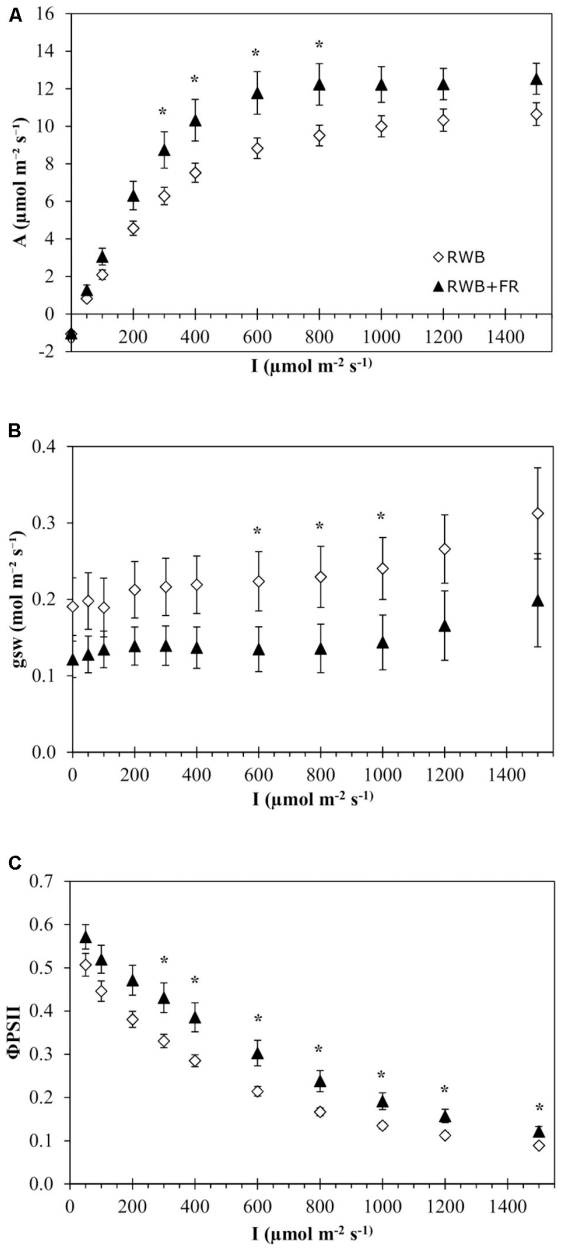

FIGURE 2 | Effect of the light treatments RWB and RWB + FR on the pattern of **(A)** net photosynthetic response, **(B)** stomatal conductance, and **(C)** ΦPSII to a series of light intensities (0–1,500 µmol m^{-2} s^{-1}) of the uppermost unshaded leaves of *Solanum melongena*, variety Tracey. Each data point represents the mean of two series of measurements on four individual plants per treatment (n = 2; 8 plants per treatment) ± standard error of the mean. Data were analyzed with a one-way ANOVA for all light month of observation (two levels) as block factor. Significant differences ($P \leq 0.05$) between treatments are indicated with asterisk (*).

However, the area infected by powdery mildew in the variety Tracey was three times larger compared to Beyoncé ($P \leq 0.001$; data not shown). Infection of *B. cinerea* in the vegetative phase was significantly higher under RWhB + FR ($P = 0.05$) compared to the other light treatments (**Figure 4A**), but did not differ in the generative phase (**Figure 4B**). In contrast, infection of powdery mildew was lower ($P = 0.05$) under RWB + FR in the vegetative phase (**Figure 4C**) and under RWB + FR as well as RWhB + FR ($P = 0.007$) in the generative phase (**Figure 4D**). Infection of powdery mildew on whole plants that were naturally infected was strongly reduced under RWB UV ($P \leq 0.001$; data not shown). Thrips damage was not different between light treatments in the vegetative and the generative phase (data not shown).

DISCUSSION

In this study, the effects of a range of spectral compositions of LED light on plant growth and development, plant resilience to fungal diseases, and the establishment of *A. swirskii* predatory mites were quantified. Plant biomass and fruit production were favorably affected by increasing the contribution of far-red light in the spectrum, which was only moderately compensated for by an increased susceptibility to fungal pathogens. The observations underlying these conclusions and the implications of these results are discussed below.

Additional Far-Red Increases Biomass and Partitioning to the Fruits

Providing additional far-red light in eggplant increased fruit fresh production, total biomass, and partitioning to the fruits, in accordance with earlier findings in tomato (Ji et al., 2019; Kalaitzoglou et al., 2019). In the vegetative stage, additional FR resulted in longer stems and a more open plant structure (**Table 2**). This may have positively affected light interception and thereby crop photosynthesis, as indicated by 3D model simulations (Sarlikioti et al., 2011). Indeed, total shoot biomass at the end of the vegetative phase was increased by additional far-red light (**Table 2**), which corroborates findings of Park and Runkle (2017). In the generative phase, total fruit production increased when additional far-red light was supplied. The increased fraction of dry matter partitioned to the fruits was primarily due to the increased number of fruits and the shorter fruit growth duration. This is in accordance with general effects of far-red light on flowering (Demotes-Mainard et al., 2016) and fruit set (Ji et al., 2019). Exposure to far-red light may increase the efficiency of photosystem II electron transport by balancing the excitation of both photosystems, thereby increasing the net photosynthesis rate. This effect has been described as the Emerson enhancement effect (Emerson et al., 1957; Zhen and van Iersel, 2017). This effect directly contributes to rate of leaf photosynthesis during the hours of the day that no natural far-red light from the sun is present, which in our experiment was between midnight and 8:30 a.m. This effect was quantified by Kalaitzoglou et al. (2019), who reported an increase in rate of photosynthesis of 15% when 54 µmol m^{-2} s^{-1} far-red was added to a red/blue spectrum. However, in our trial, only indirect effects of the light spectra on rate of photosynthesis were determined, since photosynthesis measurements were performed under a fixed red/blue spectrum in the leaf chamber of the LI-6800. We observed a positive trend of the far-red light treatment on the capacity for CO_2 fixation per unit leaf area (**Figure 2**), although

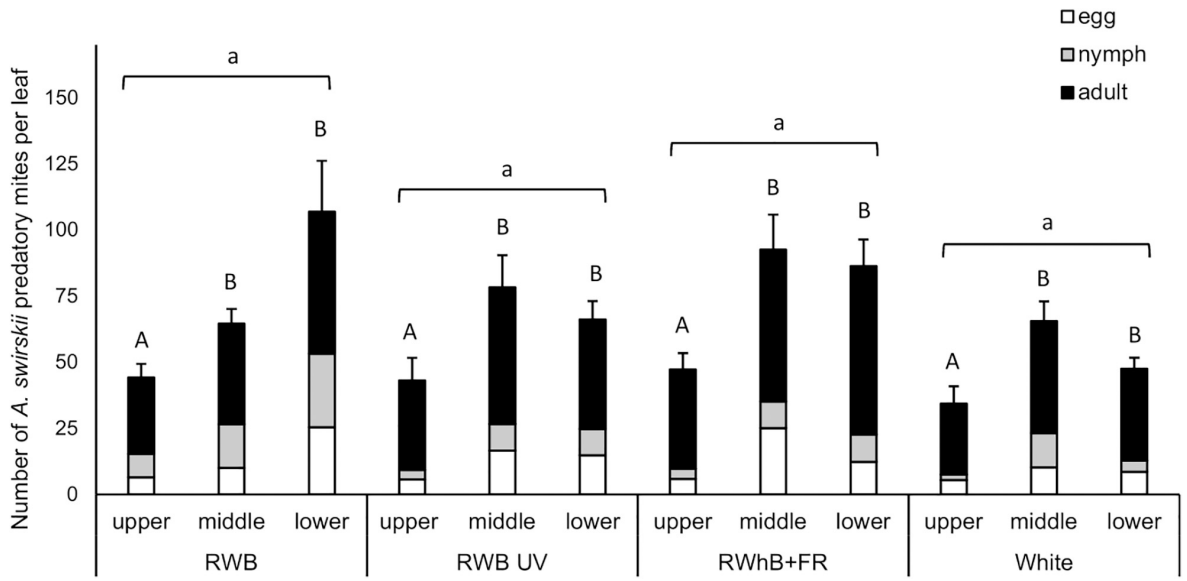

FIGURE 3 | Effect of the light treatments RWB, RWB UV, RWhB + FR, and White on the average number of *Amblyseius swirskii* individuals per leaf (± standard error of the mean), subdivided into average numbers of eggs, nymphs, and adults, in the upper, middle, and lower leaf layers ($n = 2$; 12 plants per treatment). Data were analyzed with a generalized linear mixed model with Poisson data distribution where plant replicate nested within table was introduced as a random factor into the model. Different small letters indicate significant differences ($P < 0.05$) between light treatments and different capital letters indicate significant differences ($P < 0.05$) between leaf layers.

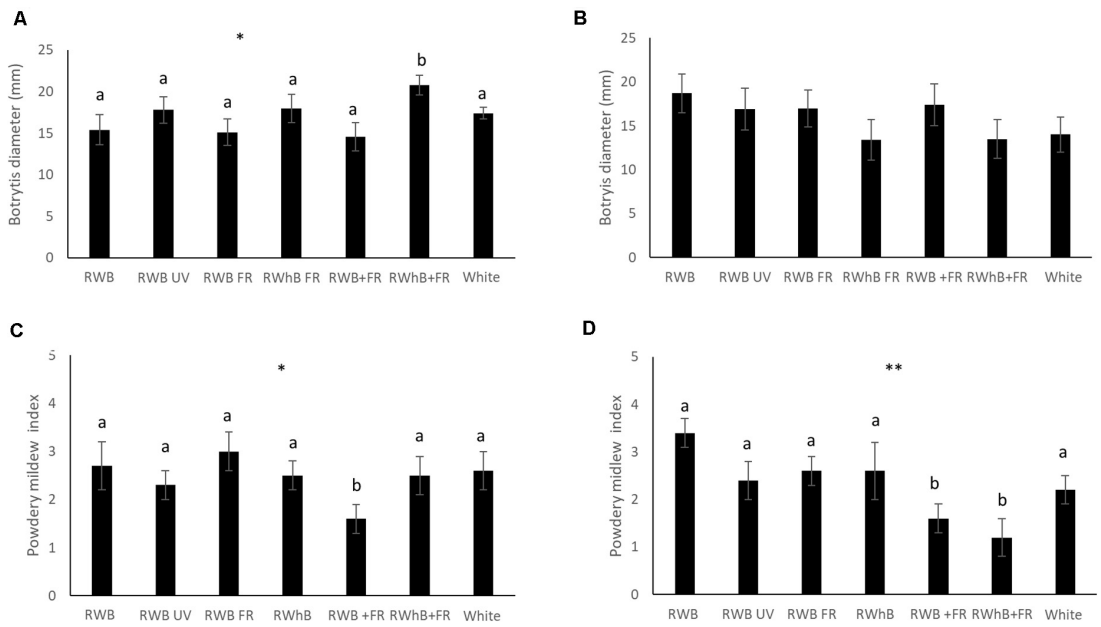

FIGURE 4 | Effect of spectral composition on eggplant host plant resistance (varieties Tracy, Beyoncé, and Lemmy) to *B. cinerea* in panel **(A)** the vegetative and **(B)** the generative phase, and to powdery mildew (*Oidium lycopersicum*) in panel **(C)** the vegetative and **(D)** the generative phase. Data represent the mean ($n = 2$, 6 plants per treatment per variety) ± standard error of the mean. Data were analyzed with ANOVA for botrytis and with a χ^2 test for powdery mildew. Different letters denote significant differences between treatments at $^*P \leq 0.05$ and $^{**}P \leq 0.01$.

none of the parameters of the photosynthesis response curves that were fitted were significantly different. However, when net assimilation rate was analyzed per light intensity measured, rates were significantly higher in the RWB + FR treatment compared to the reference (RWB), between 300 and 800 μmol m^{-2} s^{-1}. Since far-red photons preferentially excite PSI reaction centers, leaf acclimation can result in an increased PSII/PSI ratio (Hogewoning et al., 2012). Indeed, stomatal conductance was not

different between treatments, but the ΦPSII was higher for the treatment with additional far-red light, indicating acclimation of leaf photosystem composition. However, the net assimilation rates were low for both treatments. Romanatti et al. (2019) reported an assimilation rate of 15.1 μmol CO_2 m^{-2} s^{-1} at a light intensity of 700 μmol m^{-2} s^{-1} and 390ppm CO_2, whereas we measured 12.0 and 9.0 μmol CO_2 m^{-2} s^{-1} at a light intensity of 800 μmol m^{-2} s^{-1} for the RWB + FR and RWB treatments, respectively. This indicates that the photosynthetic performance under the LED treatments was suboptimal and further research toward a sustainable cultivation method that includes LED lighting is required.

So far, all studies in which the effects of altered R:FR ratios in horticultural systems were examined added additional far-red light to the PAR light sum (Ji et al., 2019; Kalaitzoglou et al., 2019; Zhang et al., 2019; Zhen and Bugbee, 2020). When additional far-red light is supplied, the total photon flux (PDF) increases, as well as the electricity consumption of the lighting system. From a sustainability perspective, it would be relevant to know the effects of a spectrum that includes far-red light compared to a reference spectrum with the same PFD. Therefore, we investigated the effects of replacing part of the PAR light by far-red on plant growth and crop resilience, while maintaining PFD. In the vegetative phase, replacing part of the PAR light by far-red resulted in lower leaf and shoot dry weights compared to the treatments with additional far-red, due to the lower level of PAR light. However, direct shade avoidance effects such as plant height and leaf size (Evans and Poorter, 2001) did not differ between the treatments with additional far-red light or in which far-red replaced part of the PAR light. In spite of the lower level of PAR light, the treatments where far-red replaced part of the PAR light (RWB FR and RWhB FR), shoot biomass was comparable to the reference, indicating that far-red light positively affected light interception and thereby crop photosynthesis. In the generative phase, shoot biomass in the treatments where part of the PAR light was replaced by far-red was lower than in the treatments with additional far-red light, although the biomass partitioning between leaves, stems, and fruits was comparable (**Table 3**). Early fruit production in the treatments where PAR was partly replaced by far-red light was 45% higher than in the reference treatment. This shows that altering the spectral composition of the light while maintaining the PFD is favorable for biomass accumulation and fruit production. This offers perspectives in the design of energy-efficient greenhouse cultivation systems.

In general, decreased ratios of red to blue radiation reduce biomass accumulation and extension growth, but enhance pigmentation and nutritional value (Huché- Thélier et al., 2016), although growth responses to R:B can vary depending on species (Hernández and Kubota, 2016). In our study, we applied two levels of red/blue ratio, assuming that the increased percentage of blue light might counteract some of the far-red light effects (Runkle and Heins, 2001). However, increasing the percentage of blue light in the presence of far-red light did not have any effect on plant height or shoot weight in the vegetative phase, which is in agreement with findings of Meng and Runkle (2019) for shoot dry weight and hypocotyl length in lettuce and basil. In the generative phase, a higher percentage of blue light reduced the fruit growth duration and increased the fruit production only in the treatments with additional far-red (RWhB + FR compared to RWB + FR), thereby indicating an interaction with PAR levels. Kaiser et al. (2019a) also reported a favorable effect of blue light on fruit production, with an optimum of 6–12%. In line with findings in tomato (Kaiser et al., 2019b), the white light treatment containing a higher proportion of green light showed a tendency toward increased biomass production compared to the reference treatment.

Light Spectrum Affects Host Plant Resistance to Pathogens

In all eggplant genotypes, the treatments with far-red light induced shade avoidance responses such as increased stem length and led to a higher shoot biomass and fruit production. However, the treatments with far-red light did not show negative effects on host plant resistance to *B. cinerea*, except for the vegetative plants under high blue and additional far-red light (RWhB + FR). It seems that more resource allocation to growth in vegetative eggplant only marginally compromised allocation to defense, while it did not affect fruit-bearing eggplant at all. This is in contrast to the findings in Arabidopsis (Cerrudo et al., 2012; Cargnel et al., 2014) and tomato (Ji et al., 2019) where low R:FR repressed jasmonate-induced defense leading to increased *B. cinerea* infection. While vegetative Arabidopsis rosettes were subjected to a R:FR ratio of 0.55, environmental factors including R:FR ratio, PAR level, and photoperiod used in tomato (Ji et al., 2019) were comparable to our study. Effects of low R:FR on defense may thus possibly depend on plant species. For both genotypes and growth stages, additional far-red light increased plant resistance to powdery mildew as a biotroph, irrespective of the proportion of blue light. This effect was not observed in the treatments where far-red light replaced part of the PAR light, which resulted in lower PAR levels than in the treatments with additional far-red light. Lower PAR can potentially lead to lower host plant resistance as has been shown in tomato (Escobar-Bravo et al., 2018). Opposite to our results, de Wit et al. (2013) observed that low R:FR ratio enhanced susceptibility to the hemibiotroph pathogen *Pseudomonas syringae* in Arabidopsis. There is, however, one major difference between their experimental setup and ours. In our study, exposure of the plants to the light treatments preceded the inoculation with the pathogen, while in the study of de Wit et al. (2013), inoculation of the pathogen preceded the exposure of plants to the light treatments. This difference in the order in which plants were challenged by pathogen attack and low R:FR light treatment may be part of the explanation why a low R:FR light treatment led to these opposite results. Our findings that low R:FR ratio marginally restrained host plant resistance to *B. cinerea* while resistance to powdery mildew was increased may be explained by a shift between the mutually antagonistic JA and SA defense pathways. Gene expression studies of major SA- and JA-dependent genes in response to low R:FR treatments would be useful for subsequent investigations of host plant resistance in eggplant. Meanwhile, our results point out that altering the spectral composition of LED light could offer the potential to not

only increase plant growth and production but also enhance host plant resistance to diseases.

Treatment with UV-B did not increase plant resistance to powdery mildew, but seemed to have a strong direct effect on this pathogen. This observation, however, was based on a spontaneous natural mildew infection without standardized inoculation. Direct effects of UV-B on mildew have been reported in cucumber (Suthaparan et al., 2014) and tomato (Suthaparan et al., 2016). Powdery mildew is an ecto-parasite, whose colorless hyphae without pigmentation are likely to be especially vulnerable to UV treatment. Plants treated with additional far-red light did not show reduction of powdery mildew infection, although the leaf bioassays had shown enhanced host plant resistance. Possibly, the natural infection was much stronger than the inoculated one, diminishing any plant resistance effect. Host plant resistance to thrips or *B. cinerea* was affected by UV-B treatment. A strong reduction of thrips silver damage was reported by Escobar-Bravo et al. (2019a) using the same UV-B intensity in tomato as in our trial. Doubling of this UV-B intensity was needed to increase resistance to thrips in chrysanthemum whereby effects were genotype dependent (Escobar-Bravo et al., 2019b). Although eggplant belongs to the plant family of the Solanaceae, as does tomato, it appears that UV-B treatments to increase host plant resistance may be species specific, especially seen in the relatively low window of effective UV-B ranges (Escobar-Bravo et al., 2019a). This is supported by the fact the UV-B intensity used for increasing plant resistance to *B. cinerea* in Arabidopsis was 18-fold higher compared to the one used in tomato (Demkura and Ballaré, 2012).

Light Spectrum Does Not Affect Population Development of *A. swirskii*

In this study, no effect of LED spectrum on population growth of *A. swirskii* could be observed. This is contrary to our hypothesis that *A. swirskii* would reproduce faster under the light spectrum with the highest proportion of green light, which was based on the premise that predatory mites can only perceive light in the green and UV-A parts of the spectrum. It differs from the results of the unpublished work of Shipp that indicates that *A. swirskii* develops faster under supplemental lighting with HPS lamps compared to red and blue LED lights (Buitenhuis et al., 2015). It also contrasts the work of Wang et al. (2013) on the predatory bug *O. sauteri* that shows that the developmental time of *O. sauteri* increased and fecundity decreased under monochromatic red light compared to white light. In our study, however, LED spectra were supplied against a background of low-intensity natural sunlight, whereas Wang et al. (2013) used monochromatic LED treatments and Buitenhuis et al. (2015) did not mention the conditions under which the study of Shipp was performed. Whether the lack of an influence of light spectrum against a background of low-intensity sunlight on the population growth of *A. swirskii* can also be extrapolated to other climate conditions or predatory mite species remains to be investigated. The study of Zilahl-Balogh et al. (2007) showed that oviposition rate of the predatory mite *Amblyseius cucumeris* was reduced under low light intensity, and this effect tended to be more pronounced under lower temperature (20°C) and short day conditions (8 h light) than at higher temperature (24°C) and long day conditions (16 h). We can therefore not exclude the possibility that the effect of light spectrum on *A. swirskii* is dependent on the temperature and daylength conditions. UV-B irradiation has been previously observed to exert an inhibiting effect on the population growth of spider mites (Tanaka et al., 2016). A major difference between the study of Tanaka et al. (2016) and our study is the use of light reflection sheets that increased the UV-B irradiation on the abaxial side of the leaves. In our study, UV-B only reached the plants from above, thus allowing *A. swirskii* to hide from the UV-B irradiation. Moreover, the light spectra tested did not exert any effect on the vertical distribution of these predatory mites over the crop. In all four light treatments, less mites were present on the upper leaf layer compared to the lower leaf layers, which is in accordance with the findings of Messelink et al. (2006).

Conclusion

Our results demonstrate that including far-red light in the supplementary lighting spectrum significantly increased eggplant fruit fresh and dry mass production. This increase was due to the increase of the fraction of dry mass partitioned to the fruits, due to the reduced fruit growth duration and increased number of harvested fruits. A crucial element in the design of sustainable LED lighting strategies for greenhouse horticulture is their effect on pathogens, pests, and their natural enemies. Adding far-red light to the spectrum reduced host plant resistance to *Botrytis*, but increased the resistance to powdery mildew. No effects of light spectrum on the population development of *A. swirskii* or resistance to thrips were observed. These combined results indicate that LED lighting strategies should be developed for crops, depending on the major pathogens and pests occurring in those crops.

DATA AVAILABILITY STATEMENT

The raw data supporting the conclusions of this article will be made available by the authors, without undue reservation.

AUTHOR CONTRIBUTIONS

JA, KL, HM, and KW: conception and design of the experiments. KW, HM, and KL: execution of the experiments and analysis of the data. JA, HM, and KL: writing of the manuscript. All authors contributed to the article and approved the submitted version.

FUNDING

The results presented were obtained within the project "Sustainable cultivation systems with LEDs," funded by the innovation and action program "Greenhouse as a source of energy" of the Dutch growers association Glastuinbouw Nederland and the Ministry of Agriculture, Nature and Food Quality.

ACKNOWLEDGMENTS

We are grateful to Signify for providing us with the multi-channel LED systems used in the experiments. We thank Marianne Noordam, Suzanne Breeuwsma, and Huei Ming Huisman for their technical assistance in regard to the bioassays. We would like to thank Dr. Anne Elings for analyzing the photosynthesis light response curves.

REFERENCES

Ahn, S. Y., Kim, S. A., and Yun, H. K. (2015). Inhibition of *Botrytis cinerea* and accumulation of stilbene compounds by light-emitting diodes of grapevine leaves and differential expression of defense-related genes. *Eur. J. Plant Pathol.* 143, 753–765. doi: 10.1007/s10658-015-0725-5

Antignus, Y., Mor, N., Joseph, R. B., Lapidot, M., and Cohen, S. (1996). Ultraviolet-absorbing plastic sheets protect crops from insect pests and from virus diseases vectored by insects. *Environ. Entom.* 25, 919–924. doi: 10.1093/ee/25.5.919

Avalos, J., and Estrada, A. F. (2010). Regulation by light in *Fusarium*. *Fungal Gen. Biol.* 47, 930–938. doi: 10.1016/j.fgb.2010.05.001

Ballaré, C. L. (2014). Light regulation of plant defense. *Ann. Rev. Plant Biol.* 65, 335–363. doi: 10.1146/annurev-arplant-050213-040145

Ballaré, C. L., Caldwell, M. M., Flint, S. D., Robinson, A., and Bornman, J. F. (2011). Effects of solar ultraviolet radiation on terrestrial ecosystems. Patterns, mechanisms, and interactions with climate change. *Photoch. Photobiol. Sci.* 10, 226–241. doi: 10.1039/c0pp90035d

Ballaré, C. L., Mazza, C. A., Austin, A. T., and Pierik, R. (2012). Canopy light and plant health. *Plant Physiol.* 160, 145–155. doi: 10.1104/pp.112.200733

Ballaré, C. L., and Pierik, R. (2017). The shade-avoidance syndrome: multiple signals and ecological consequences. *Plant Cell Environ.* 40, 2530–2543. doi: 10.1111/pce.12914

Buitenhuis, R., Murphy, G., Shipp, L., and Scott-Dupree, C. (2015). Amblyseius swirskii in greenhouse production systems: a floricultural perspective. *Exp. App. Acarol.* 65, 451–464. doi: 10.1007/s10493-014-9869-9

Caldwell, M. M., Ballaré, C. L., Bornman, J. F., Flint, S. D., Bjorn, L. O., Teramura, A. H., et al. (2003). Terrestrial ecosystems increased solar ultraviolet radiation and interactions with other climatic change factors. *Photochem. Photobio. Sci.* 2, 29–38. doi: 10.1039/B700019G

Cargnel, M. D., Demkura, P. V., and Ballaré, C. L. (2014). Linking phytochrome to plant immunity: low red; far-red ratios increase Arabidopsis susceptibility to *Botryis cinerea* by reducing the biosynthesis of indolic glucosinulates and camlexin. *New Phytol.* 204, 342–354. doi: 10.1111/nph.13032

Cerrudo, I., Keller, M. M., Cargnel, M. D., Demkura, P. V., De Wit, M., Patitucii, M. S., et al. (2012). Low red/far-red ratios reduce *Arabidopsis* resistance to *Botrytis cinerea* and jasmonate responses via a COII-JAZ10-dependent, salicylic acid-independent mechanism. *Plant Physiol.* 158, 2042–2052. doi: 10.1104/pp.112.193359

Chyzik, R., Dobrinin, S., and Antignus, Y. (2003). Effect of a UV-deficient environment on the biology and flight activity of *Myzus persicae* and its hymenopterous parasite aphidius matricariae. *Phytoparasitica* 31, 467–477. doi: 10.1007/BF02979740

Costa, H. S., and Robb, K. L. (1999). Effects of ultraviolet-absorbing greenhouse plastic films on flight behavior of *Bemisia argentifolii* (Homoptera : Aleyrodidae) and *Frankliniella occidentalis* (Thysanoptera : Thripidae). *J. Econ. Entom.* 92, 557–562. doi: 10.1093/jee/92.3.557

Davis, P. A., and Burns, C. (2016). Photobiology in protected horticulture. *Food Energy Secur.* 5, 223–238. doi: 10.1002/fes3.97

de Wit, M., Spoel, T. H., Sanches-Perez, G. F., Gommers, C. M. M., Pieterse, C. M. J., Voesenek, L. A. C. J., et al. (2013). Perception of low red:far-red ratio compromises both salicylic acid- and jasmonic acid- dependent pathogen defences in *Arabidopsis*. *Plant J.* 75, 90–103. doi: 10.1111/tpj.12203

Demkura, P., and Ballaré, C. L. (2012). UVR8 mediates UV-B induced Arabidopsis defence responses against *Botrytis cinerea* by controlling sinapate accumulation. *Mol. Plant* 5, 642–652. doi: 10.1093/mp/sss025

Demotes-Mainard, S., Péron, T., Corot, A., Bertheloot, J., Le Gourrierec, J., Pelleschi-Travier, S., et al. (2016). Plant responses to red and far-red lights, applications in horticulture. *Environ. Exp. Bot.* 121, 4–21. doi: 10.1016/j.envexpbot.2015.05.010

Dhakal, R., Park, E., Lee, S.-W., and Baek, H.-H. (2015). Soybean (*Glycine max* L.Merr.) sprouts germinated under red light irradiation induce resistance against bacterial rotting disease. *PLoS One* 10:e0117712. doi: 10.1371/journal.pone.0117712

Dieleman, J. A., De Visser, P. H. B., Meinen, E., Grit, J., and Dueck, T. A. (2019). Integrating morphological and physiological responses of tomato plants to light quality to the crop level by 3D modeling. *Front. Plant Sci.* 10:839. doi: 10.3389/fpls.2019.00839

Emerson, R., Chalmers, R., and Cederstrand, C. (1957). Some factors influencing the long-wave limit of photosynthesis. *Proc. Natl. Acad. Sci. U. S. A.* 43, 133–143. doi: 10.1073/pnas.43.1.133

Escobar-Bravo, R., Chen, G., Kim, H. K., Grosser, K., Leiss, K. A., and Klinkhamer, P. G. (2019a). Ultraviolet radiation exposure time and intensity modulate tomato resistance to herbivory through activation of jasmonic acid signaling. *J. Exp. Bot.* 70, 315–327. doi: 10.1093/jxb/ery347

Escobar-Bravo, R., Klinkhamer, P. G. L., and Leiss, K. A. (2017). Interactive effects of UV-B light with abiotic factors on plant growth and chemistry, and their consequences for defense against arthropod herbivores. *Front. Plant Sci.* 8:278. doi: 10.3389/fpls.2017.00278

Escobar-Bravo, R., Nederpel, C., Naranjo, S., Kim, H. K., Rodriguez-López, M. J., Chen, G., et al. (2019b). Ultraviolet radiation modulates bot constitutive and inducible plant defences against thrips but is dose and plant genotype dependent. *J. Pest Sci.* doi: 10.1007/s10340-019-01166-w

Escobar-Bravo, R., Ruijgrok, J., Kim, H. K., Grosser, K., van Dam, N. M., Klinhamer, P. G. L., et al. (2018). Light intensity-mediated induction of trichome-associated allelochemicals increases resistance against thrips in tomato. *Plant Cell Physiol.* 59, 2462–2475. doi: 10.1093/pcp/pcy166

Evans, J. R., and Poorter, H. (2001). Photosynthetic acclimation of plants to growth irradiance: the relative importance of specific leaf area and nitrogen partitioning in maximizing carbon gain. *Plant Cell Environ.* 24, 755–767. doi: 10.1046/j.1365-3040.2001.00724.x

Farquhar, G. D., von Caemmerer, S., and Berry, J. A. (1980). A biochemical model of photosynthetic CO_2 assimilation in leaves of C3 species. *Planta* 149, 78–90. doi: 10.1007/BF00386231

Finlayson, S. A., Krishnareddy, S. R., Kebrom, T. H., and Casal, J. J. (2010). Phytochrome regulation of branching in Arabidopsis. *Plant Physiol.* 152, 1914–1927. doi: 10.1104/pp.109.148833

Franklin, K. A., and Quail, P. H. (2010). Phytochrome functions in Arabidopsis development. *J. Exp. Bot.* 61, 11–24. doi: 10.1093/jxb/erp304

Genoud, T., Buchala, A. J., Chua, N. H., and Metraux, J. P. (2002). Phtyochrome signalling modulates the SA-perceptive pathway in *Arabidopsis*. *Plant J.* 31, 87–95. doi: 10.1046/j.1365-313x.2002.01338.x

Genty, B., Briantais, J. M., and Baker, N. R. (1989). The relationship between the quantum yield of photosynthetic electron transport and quenching of chlorophyll fluorescence. *Biochim. Biophys. Acta Gen. Sub.* 990, 87–92. doi: 10.1016/S0304-4165(89)80016-9

Heraut-Bron, V., Robin, C., Varlet-Grancher, C., and Guckert, A. (2001). Phytochrome mediated effects on leaves of white clover: consequences for light interception by the plant under competition for light. *Ann. Bot.* 88, 737–743. doi: 10.1006/anbo.2001.1510

Hernández, R., and Kubota, C. (2016). Physiological responses of cucumber seedlings under different blue and red photon flux ratios using LEDs. *Envir. Exp. Bot.* 121, 66–74. doi: 10.1016/j.envexpbot.2015.04.001

Herrera-Estrella, A., and Horwitz, B. A. (2007). Looking through the eyes of fungi: molecular genetics of photoreception. *Mol. Microbiol.* 64, 5–15. doi: 10.1111/j.1365-2958.2007.05632.x

Hogewoning, S. W., Trouwborst, G., Maljaars, H., Poorter, H., Van Ieperen, W., and Harbinson, J. (2010). Blue light dose-responses on leaf photosynthesis, morphology and chemical composition of *Cucumis sativus* grown under different combinations of red and blue light. *J. Exp. Bot.* 61, 3107–3117. doi: 10.1093/jxb/erq132

Hogewoning, S. W., Wientjes, E., Douwstra, P., Trouwborst, G., Van Ieperen, W., Croce, R., et al. (2012). Photosynthetic quantum yield dynamics: from

photosystems to leaves. *Plant Cell* 24, 1921–1935. doi: 10.1105/tpc.112.097972

Huché- Thélier, L., Crespel, L., Le Gourrierec, J., Morel, P., Sakr, S., and Leduc, N. (2016). Light signalling and plant responses to blue and UV-radiations – Perspectives for applications in horticulture. *Envir. Exp. Bot.* 121, 22–38. doi: 10.1016/j.envexpbot.2015.06.009

Izaguirre, M. M., Mazza, C. A., Biondini, M., Baldwin, I. T., and Ballaré, C. L. (2006). Remote sensing of future competitors: impacts on plant defenses. *Proc. Nat. Acad. Sci. U. S. A.* 103, 7170–7174. doi: 10.1073/pnas.0509805103

Ji, Y., Nuñez Ocaña, D., Choe, D., Larsen, D. H., Marcelis, L. F. M., and Heuvelink, E. (2020). Far-red radiation stimulates dry mass partitioning to fruits by increasing fruit sink strength in tomato. *New Phytol.* 228, 1914–1925. doi: 10.1111/nph.16805

Ji, Y., Ouzounis, T., Courbier, S., Kaiser, E., Nguyen, P. T., Schouten, H. J., et al. (2019). Far-red radiation increases dry mass partioning to fruits but reduces *Botrytis cinerea* resistance in tomato. *Envir. Exp. Bot.* 168:103889. doi: 10.1016/j.envexpbot.2019.103889

Johansen, N. S., Tadesse, B. A., Suthaparan, A., Stensvand, A., From, P. J., and Gadoury, D. M. (2017). Nighttime treatments of ultraviolet (UV) light targeting powdery mildews also suppress the two-spotted spider mite (*Tetranychus urticae*). *Phytopath* 107, 77–77.

Johansen, N. S., Vanninen, I., Pinto, D. M., NIssinen, A. I., and Shipp, L. (2011). In the light of new greenhouse technologies: 2. Direct effects of artificial lighting on arthropods and integrated pest management in greenhouse crops. *Ann. Appl. Biol.* 159, 1–27. doi: 10.1111/j.1744-7348.2011.00483.x

Kaiser, E., Ouzounis, T., Giday, H., Schipper, R., Heuvelink, E., and Marcelis, L. F. M. (2019a). Adding blue to red supplemental light increases biomass and yield of greenhouse-grown tomatoes, but only to an optimum. *Front. Plant Sci.* 9:2002. doi: 10.3389/fpls.2018.02002

Kaiser, E., Weerheim, K., Schipper, R., and Dieleman, J. A. (2019b). Partial replacement of red and blue by green light increases biomass and yield in tomato. *Sci. Hort.* 249, 271–279. doi: 10.1016/j.scienta.2019.02.005

Kalaitzoglou, P., van Ieperen, W., Harbinson, J., van der Meer, M., Martinakos, S., Weerheim, K., et al. (2019). Effects of continuous or end-of-day far-red light on tomato plant growth, morphology, light absorption, and fruit production. *Front. Plant Sci.* 10:322. doi: 10.3389/fpls.2019.00322

Kangasjärvi, S., Neukermans, J., Li, S., Aro, E. M., and Noctor, G. (2012). Photosynthesis, photorespiration, and light signalling in defence responses. *J. Exp. Bot.* 63, 1619–1636. doi: 10.1093/jxb/err402

Kelber, A. (2001). Receptor based models for spontaneous colour choices in flies and butterflies. *Ent. Exp. Appl.* 99, 231–244. doi: 10.1046/j.1570-7458.2001.00822.x

Keuskamp, D. H., Sasidharan, R., and Pierik, R. (2010). Physiological regulation and functional significance of shade avoidance responses to neighbours. *Plant Signal Behav.* 5, 655–662. doi: 10.4161/psb.5.6.11401

Kuhlmann, F., and Muller, C. (2011). Impacts of ultraviolet radiation on interactions between plants and herbivorous insects: a chemo-ecological perspective. *Progr. Bot.* 72, 305–347. doi: 10.1007/978-3-642-13145-5_12

Kusuma, P., Pattison, P. M., and Bugbee, B. (2020). From physics to fixtures to food: current and potential LED efficacy. *Hort. Res.* 7:56. doi: 10.1038/s41438-020-0283-7

Legarrea, S., Karnieli, A., Fereres, A., and Weintraub, P. G. (2010). Comparison of UV-absorbing nets in pepper crops: spectral properties, effects on plants and pest control. *Photochem. Photobiol.* 86, 324–330. doi: 10.1111/j.1751-1097.2009.00657.x

Leone, M., Keller, M. M., Cerrudo, I., and Ballaré, C. L. (2014). To grow of defend? Low red:far-red ratios reduce jasmonate sensitivity in Arabidopsis seedlings by promoting DELLA degradation and increasing JAZ10 stability. *New Phytol.* 204, 355–367. doi: 10.1111/nph.12971

McCree, K. J. (1972). The action spectrum, absorbance and quantum yield of photosynthesis in crop plants. *Agric. Meteor.* 9, 191–216. doi: 10.1016/0002-1571(71)90022-7

Meng, Q., and Runkle, E. S. (2019). Far-red radiation interacts with relative and absolute blue and red photon flux densities to regulate growth, morphology, and pigmentation of lettuce and basil seedlings. *Sci. Hort.* 255, 269–280. doi: 10.1016/j.scienta.2019.05.030

Messelink, G. J., van Steenpaal, S. E. F., and Ramakers, P. M. J. (2006). Evaluation of phytoseiid predators for control of western flower thrips on greenhouse cucumber. *BioControl* 51, 753–768. doi: 10.1007/s10526-006-9013-9

Moreno, J. E., Tao, Y., Chory, J., and Ballaré, C. L. (2009). Ecological modulation of plant defense via phytochrome control of jasmonate sensitivity. *Proc. Natl. Acad. Sci. U. S. A.* 106, 4935–4940. doi: 10.1073/pnas.0900701106

Morrow, R. C. (2008). LED lighting in horticulture. *HortScience* 43, 1947–1950. doi: 10.21273/hortsci.43.7.1947

Palmitessa, O. D., Paciello, P., and Santamaria, P. (2020). Supplemental LED increases tomato yield in Mediterranean semi-closed greenhouse. *Agronomy* 10:1353. doi: 10.3390/agronomy10091353

Park, Y., and Runkle, E. S. (2017). Far-red radiation promotes growth of seedlings by increasing leaf expansion and whole-plant net assimilation. *Environ. Exp. Bot.* 136, 41–49. doi: 10.1016/j.envexpbot.2016.12.013

Paucek, I., Pennisi, G., Pistillo, A., Appolloni, E., Crepaldi, A., Calegari, B., et al. (2020). Supplementary LED interlighting improves yield and precocity of greenhouse tomatoes in the Mediterranean. *Agronomy* 10:1002. doi: 10.3390/agronomy10071002

Pieterse, C. M. J., Van der Does, D., Zamioudis, C., Leon-Reye, A., and Van Wees, S. C. M. (2012). Hormonal modulation of plant immunity. *Ann. Rev. Cel Dev. Biol.* 28, 489–521. doi: 10.1146/annurev-cellbio-092910-154055

Raviv, M., and Antignus, Y. (2004). UV radiation effects on pathogens and insect pests of greenhouse-grown crops. *Photochem. Photobiol.* 79, 219–226. doi: 10.1111/j.1751-1097.2004.tb00388.x

Rizzini, L., Favory, J. J., Cloix, C., Faggionato, D., O'Hara, A., Kaiserli, E., et al. (2011). Perception of UV-B by the Arabidopsis UVR8 Protein. *Science* 332, 103–106. doi: 10.1126/science.1200660

Rodriguez-Romero, J., Hedtke, M., Kastner, C., Muller, S., and Fischer, R. (2010). Fungi, hidden in soil or up in the air: light makes a difference. *Ann. Rev. Microbiol.* 64, 585–610. doi: 10.1146/annurev.micro.112408.134000

Romanatti, P. V., Rocha, G. A., Veroneze Júnior, V., Santos Filho, P. R., de Souza, T. C., Pereira, F. J., et al. (2019). Limitation to photosynthesis in leaves of eggplant under UVB according to anatomical changes and alterations on the antioxidant system. *Sci. Hort.* 249, 449–454. doi: 10.1016/j.scienta.2019.01.060

Runkle, E. S., and Heins, R. D. (2001). Specific functions of red, far red, and blue light in flowering and stem extension of long-day plants. *J. Am. Soc. Hort. Sci.* 126, 275–283. doi: 10.21273/JASHS.126.3.275

Sarlikioti, V., De Visser, P. H. B., Buck-Sorlin, G. H., and Marcelis, L. F. M. (2011). How plant architecture affects light absorption and photosynthesis in tomato: towards an ideotype for plant architecture using a functional-structural plant model. *Ann. Bot.* 108, 1065–1073. doi: 10.1093/aob/mcr221

Schumacher, J. (2017). How light affects the life of Botrytis. *Fung. Gen. Biol.* 106, 26–41. doi: 10.1016/j.fgb.2017.06.002

Shibuya, T., Itagaki, K., Tojo, M., Endo, R., and Kitaya, Y. (2011). Fluorescent illumination with high red-to-far-red ratio improves resistance of cucumber seedlings to powdery mildew. *Hortscience* 46, 429–431. doi: 10.21273/HORTSCI.46.3.429

Suthaparan, A., Solhaug, K. A., Stensvand, A., and Gislerød, H. R. (2016). Determination of UV action spectra affecting the infection process of *Oidium neolycopersici*, the cause of tomato powdery mildew. *J. Photochem. Photbiol. B Biol.* 156, 41–49. doi: 10.1016/j.jphotobiol.2016.01.009

Suthaparan, A., Stensvand, A., Solhaug, K. A., Torre, S., Telfer, K. H., Ruud, A. K., et al. (2014). Suppression of cucumber powdery mildew by supplemental UV-B-radiation in greenhouses can be augmented or reduced by background radiation quality. *Plant Dis.* 98, 1349–1357. doi: 10.1094/PDIS-03-13-0222-RE

Tanaka, M., Yase, J., Aoki, S., Sakurai, T., Kanto, T., and Osakabe, M. (2016). Physical control of spider mites using Ultraviolet-B with light reflection sheets in greenhouse strawberries. *J. Econ. Entom.* 109, 1758–1765. doi: 10.1093/jee/tow096

Wang, S., Tan, X. L., Michaud, J. P., Zhang, F., and Guo, X. (2013). Light intensity and wavelength influence development, reproduction and locomotor activity in the predatory flower bug *Orius sauteri* (Poppius) (Hemiptera: Anthocoridae). *Biocontrol* 58, 667–674. doi: 10.1007/s10526-013-9522-2

Warrant, E. J., and Nilsson, D. E. (2006). Invertebrate Vision. Cambridge: University Press.

Zhang, Y., Zhang, Y., Yang, Q., and Li, T. (2019). Overhead supplemental far-red light stimulates tomato growth under intra-canopy lighting with LEDs. *J. Integr. Agric.* 18, 62–69. doi: 10.1016/S2095-3119(18)62130-6

Zhen, S., and Bugbee, B. (2020). Far-red photons have equivalent efficiency to traditional photosynthetic photons: implications for redefining photosynthetically active radiation. *Plant Cell Environ.* 43, 1259–1272. doi: 10.1111/pce.13730

Zhen, S., and van Iersel, M. W. (2017). Far-red light is needed for efficient photochemistry and photosynthesis. *J. Plant Physiol.* 209, 115–122.

Zilahl-Balogh, G. M. G., Shipp, J. L., Cloutier, C., and Brodeur, J. (2007). Predation by *Neoseiulus cucumeris* on western flower thrips, and its oviposition on greenhouse cucumber under winter vs. summer conditions in a temperate climate. *Biol. Contr.* 40, 160–167. doi: 10.1016/j.biocontrol.2006.10.011

Conflict of Interest: The authors declare that the research was conducted in the absence of any commercial or financial relationships that could be construed as a potential conflict of interest.

Copyright © 2021 Anja Dieleman, Marjolein Kruidhof, Weerheim and Leiss. This is an open-access article distributed under the terms of the Creative Commons Attribution License (CC BY). The use, distribution or reproduction in other forums is permitted, provided the original author(s) and the copyright owner(s) are credited and that the original publication in this journal is cited, in accordance with accepted academic practice. No use, distribution or reproduction is permitted which does not comply with these terms.

frontiers in Plant Science

ORIGINAL RESEARCH
published: 15 January 2021
doi: 10.3389/fpls.2020.609977

Adding Far-Red to Red-Blue Light-Emitting Diode Light Promotes Yield of Lettuce at Different Planting Densities

*Wenqing Jin[1,2], Jorge Leigh Urbina[1], Ep Heuvelink[1] and Leo F. M. Marcelis[1]**

[1] Horticulture and Product Physiology, Department of Plant Sciences, Wageningen University and Research, Wageningen, Netherlands, [2] Priva, De Lier, Netherlands

The economic viability and energy use of vertical farms strongly depend on the efficiency of the use of light. Increasing far-red radiation (FR, 700–800 nm) relative to photosynthetically active radiation (PAR, 400–700 nm) may induce shade avoidance responses including stem elongation and leaf expansion, which would benefit light interception, and FR might even be photosynthetically active when used in combination with PAR. The aims of this study are to investigate the interaction between FR and planting density and to quantify the underlying components of the FR effects on growth. Lettuce (*Lactuca sativa* cv. Expertise RZ) was grown in a climate chamber under two FR treatments (0 or 52 μmol m^{-2} s^{-1}) and three planting densities (23, 37, and 51 plants m^{-2}). PAR of 89% red and 11% blue was kept at 218 μmol m^{-2} s^{-1}. Adding FR increased plant dry weight after 4 weeks by 46–77% (largest effect at lowest planting density) and leaf area by 58–75% (largest effect at middle planting density). Radiation use efficiency (RUE: plant dry weight per unit of incident radiation, 400–800 nm) increased by 17–42% and incident light use efficiency (LUE_{inc}: plant dry weight per unit of incident PAR, 400–700 nm) increased by 46–77% by adding FR; the largest FR effects were observed at the lowest planting density. Intercepted light use efficiency (LUE_{int}: plant dry weight per unit of intercepted PAR) increased by adding FR (8–23%). Neither specific leaf area nor net leaf photosynthetic rate was influenced by FR. We conclude that supplemental FR increased plant biomass production mainly by faster leaf area expansion, which increased light interception. The effects of FR on plant dry weight are stronger at low than at high planting density. Additionally, an increased LUE_{int} may contribute to the increased biomass production.

Keywords: vertical farm, LED, far-red, lettuce, light use efficiency, yield component analysis

OPEN ACCESS

Edited by:
Stefania De Pascale, University of Naples Federico II, Italy

Reviewed by:
Yun Kong, University of Guelph, Canada
Jung Eek Son, Seoul National University, South Korea

***Correspondence:**
Leo F. M. Marcelis
leo.marcelis@wur.nl

Specialty section:
This article was submitted to Crop and Product Physiology, a section of the journal Frontiers in Plant Science

Received: *24 September 2020*
Accepted: *17 December 2020*
Published: *15 January 2021*

Citation:
Jin W, Urbina JL, Heuvelink E and Marcelis LFM (2021) Adding Far-Red to Red-Blue Light-Emitting Diode Light Promotes Yield of Lettuce at Different Planting Densities. Front. Plant Sci. 11:609977. doi: 10.3389/fpls.2020.609977

INTRODUCTION

Vertical farming is a relatively new plant production system, where plants are grown without solar light in many layers above each other. Plants receive light from lamps (usually light-emitting diodes, LEDs) and all growth conditions can be fully controlled. This production system scores high on sustainability since crops can be grown without the use of pesticides, without nutrient

emission, and with high water and land use efficiencies (SharathKumar et al., 2020). However, the energy consumption is high, especially for lighting. Therefore, there is an urgent need for increased light use efficiency.

Light use efficiency (LUE) can be defined in several ways. For overall performance of vertical farming, the fresh yield of harvested product per unit of emitted light by light source is the most relevant definition. The efficiency of the lighting may also refer to the ratio between plant dry weight and total photon flux incident on the canopy, which is called radiation use efficiency (RUE, g mol^{-1}), or the ratio between plant dry weight and total photosynthetic photon flux intercepted by the canopy, which is called intercepted light use efficiency (LUE_{int}, g mol^{-1}). RUE is directly connected to the energy use efficiency (Pennisi et al., 2020) and LUE_{int} indicates the efficiency of the plants transforming intercepted photons into biomass.

Far-red radiation (FR, 700–800 nm) is relatively little absorbed by leaves and mostly reflected or transmitted (Taiz et al., 2015). In nature where the sun is the sole light source, the ratio between red (R) and FR (R/FR ratio) perceived by leaves decreases when vegetation proximity or shading by leaves occurs. R/FR ratio determines the equilibrium of Pfr and Pr in plant (Pierik and De Wit, 2014). Pr and Pfr are two photo-convertible isomers of phytochrome, which could transform to each other by absorbing R or FR (Demotes-Mainard et al., 2016). A rebalanced equilibrium by lowered R/FR ratio induces shade avoidance syndrome (SAS), which includes responses such as increased stem length and/or leaf elongation, leaf moving upward (hyponasty), a higher fraction of assimilate partitioning to stem, and/or increased specific leaf area (Franklin, 2008; Vos et al., 2010; Bongers et al., 2014).

As the application of light-emitting diodes (LEDs) expanded in the past decade, several studies on FR have been conducted for further understanding its effect on crop growth. Park and Runkle (2017) reported 28–50% shoot dry weight increase by adding 16–64 μmol m^{-2} s^{-1} FR on top of 128 μmol m^{-2} s^{-1} R, and 32 μmol m^{-2} s^{-1} blue in geranium and snapdragon. Zou et al. (2019) observed a 49% leaf area increase and 39% biomass production increase by addition of 50 μmol m^{-2} s^{-1} FR during the whole photoperiod in lettuce with the background 200 μmol m^{-2} s^{-1} R and B (R/B = 7:1). Thus, adding FR is a possible approach to increase plant light interception and biomass production.

Planting density affects R/FR ratio as well, since R will be mostly absorbed by plants but FR only to a small extent. A lowered R/FR ratio will be perceived by plants in a higher planting density. In addition, adding FR to photosynthetically active radiation (PAR, 400–700 nm) may increase the efficiency of photosystem II electron transport and thus increase the net instantaneous photosynthesis rate (Zhen and van Iersel, 2017; Zou et al., 2019). Some authors even proposed to consider a part of FR (700–750 nm) as PAR (Zhen and Bugbee, 2020) when it is applied in combination with PAR such as R and B, although some others did not find an increment in instantaneous net photosynthesis rate when plants acclimated to FR-enriched light were compared with plants under light without FR (Ji et al., 2019; Zhang et al., 2019). Although several studies on the effect of FR on lettuce growth have been conducted (Meng and Runkle, 2019; Zou et al., 2019), a study quantifying the contribution of underlying components on FR improved crop growth is lacking.

Yield component analysis has been used to quantify contributions of underlying components of yield in several studies (Higashide and Heuvelink, 2009; Li et al., 2014; Ji et al., 2019). The aims of this study are to investigate the interaction between FR and planting density and to quantify the underlying components of the FR effects on growth. We hypothesize that FR addition increases the partitioning to the shoot, resulting in an increased biomass production by enlarged leaf area and hence light interception. We expected that the effects on light interception are in particular of importance when plants are widely spaced. For testing this hypothesis, a climate room experiment was conducted with lettuce applying two levels of FR at three planting densities.

MATERIALS AND METHODS

Plant Material and Experimental Setup

Lettuce (*Lactuca sativa* cv. Expertise RZ) was grown in a climate room with six compartments divided by white plastic screens (treatment distribution see **Supplementary Table S1**). Seeds were sown in 108-cell plug trays filled with a mix of peat and perlite (Lentse Potgrond, Horticoop, Netherlands). Germination procedure involved 2 days in dark followed by 5 days in light at 18 h light/6 h dark with a light intensity of 132 ± 1.5 μmol m^{-2} s^{-1} provided by red (R) and blue (B) LEDs (89% R and 11% B) (GreenPower LED production module, 2nd generation, Philips). Seven days after sowing, seedlings with two cotyledons were transplanted to individual pots (9 × 9 × 10 cm, L × W × H) filled by expanded clay grid (4–8 mm; Jongkind hydrocorns, Netherlands) and were grown for 28 days. Light and planting density treatments started at the same time. Pots were always in 1.5–2.0 cm layer of nutrient solution. Nutrient solution [electrical conductivity (EC) 2.3 dS m^{-1} and pH 5.8], containing 0.38 mM NH_4^+, 8.82 mM K^+, 4.22 mM Ca^{2+}, 1.15 mM Mg^{2+}, 12.92 mM NO_3^-, 1.53 mM Cl^-, 1.53 mM SO_4^{2-}, 0.12 mM HCO_3^-, 1.53 mM $H_2PO_4^-$, 0.38 mM SiO_3^{2-}, 30.67 μM Fe^{3+}, 3.83 μM Mn^{2+}, 3.83 μM Zn^{2+}, 38.33 μM B, 0.77 μM Cu^{2+}, and 0.38 μM Mo, was applied from the second day after transplanting. Nutrient solution was completely renewed twice a week to keep EC, composition, and pH stable. During the whole cultivating period, temperature and relative humidity (RH) were maintained at 22 ± 0.0°C and 75 ± 0.1% for photoperiod and 20 ± 0.0°C and 79 ± 0.2% for dark period, respectively. CO_2 concentration was kept at 752 ± 6.2 ppm. These data are average with standard errors of means of three blocks (replications in time).

Light and Planting Density Treatments

Two far-red (FR) treatments (with FR and without FR: RB + FR and RB, respectively) in combination with three planting densities [23 (low), 37 (middle), and 51 (high) plants m^{-2}] were applied. PAR was 218 ± 0.5 μmol m^{-2} s^{-1} and 219 ± 1.5 μmol m^{-2} s^{-1} (89% R and 11% B, GreenPower LED production module, 2nd generation, Philips) for treatment with

and without FR, respectively. In the treatment with FR, the FR intensity (700–800 nm) was 52 ± 0.2 μmol m^{-2} s^{-1} provided by GreenPower LED production module, Philips (**Figure 1**). These intensities of R, B, and FR resulted in phytochrome stationary state (PSS) of 0.83 (RB + FR) and 0.88 (RB) as calculated by the procedure of Sager et al. (1988). The choice for light intensity, photoperiod, and red/blue ratio of the light was based on what is commonly used in vertical farms. The FR level was chosen such that a distinct effect on plant growth could be expected, but not so high that it would never be realistic for a vertical farm. Light measurements were done at pot height using a quantum sensor (LI-COR, LI-250A Lincoln, United States) and with a spectroradiometer (Apogee Instruments model SS-110, Utah, United States). In each of the three blocks, the light intensity was measured at 24 locations per plot. The presented average values and their standard errors were based on three blocks per treatment.

Plants were distributed equidistantly following a chess board pattern. The outer row of plants in each plot was considered as border plants and not used for measurements. After each destructive harvest, plants were relocated to keep the original planting density.

Biomass and Leaf Net Photosynthesis Rate

Destructive measurements were conducted at 0, 7, 14, 21, and 28 days after transplanting (DAT). Individual plant pictures from the top were taken before destructive measurement for estimation of projected leaf area (PLA) at 14, 21, and 28 DAT. Leaf area was measured by a leaf area meter (LI-3100 Area Meter, LI-COR, Lincoln, United Kingdom). Fresh and dry weights (forced air oven at 105°C for 24 h) of shoot and root were determined. As the stem of this cultivar was extremely small, leaf dry weight was considered to be equal to the shoot dry weight.

At 20 DAT, leaf net photosynthesis rate was measured with a portable gas exchange system (LI-6400; LI-COR, Lincoln, United Kingdom) using a transparent cuvette under the following growing conditions: incident light intensity: 220 μmol m^{-2} s^{-1} with 90% R and 10% B, 22°C for the temperature, 75% for relative humidity, and CO_2 concentration for 700 ppm. Measurements were performed on fully expanded and unshaded leaves.

Light Interception and Use Efficiency of Light

Floor coverage fraction was calculated based on individual plant projected leaf area and planting density. Daily floor coverage fraction was calculated by linear interpolation between measurement days at 14, 21, and 28 DAT. Floor coverage fraction at 0 DAT was assumed to be zero. Daily light interception was calculated as the product of incident light intensity and floor coverage fraction at that day. For these calculations, the incident light intensity was measured before start of the experiment at half the final height of the plants. Considering the small height of the lettuce plants, this is a reasonable estimate of the average light intensity.

Radiation use efficiency (RUE) was calculated by dividing plant total dry weight by the cumulative incident radiation, including PAR and FR (400–800 nm), at canopy top level. Incident light use efficiency (LUE_{inc}) was calculated as the ratio between plant total dry weight and cumulative incident PAR (400–700 nm). Intercepted light use efficiency (LUE_{int}) was calculated as the ratio between plant total dry weight and cumulative intercepted PAR.

Yield Component Analysis

Treatment effects can be analyzed by breaking down fresh weight into underlying components (**Figure 2**). In this analysis, leaf fresh weight (FW_{leaf}) is the product of leaf dry weight

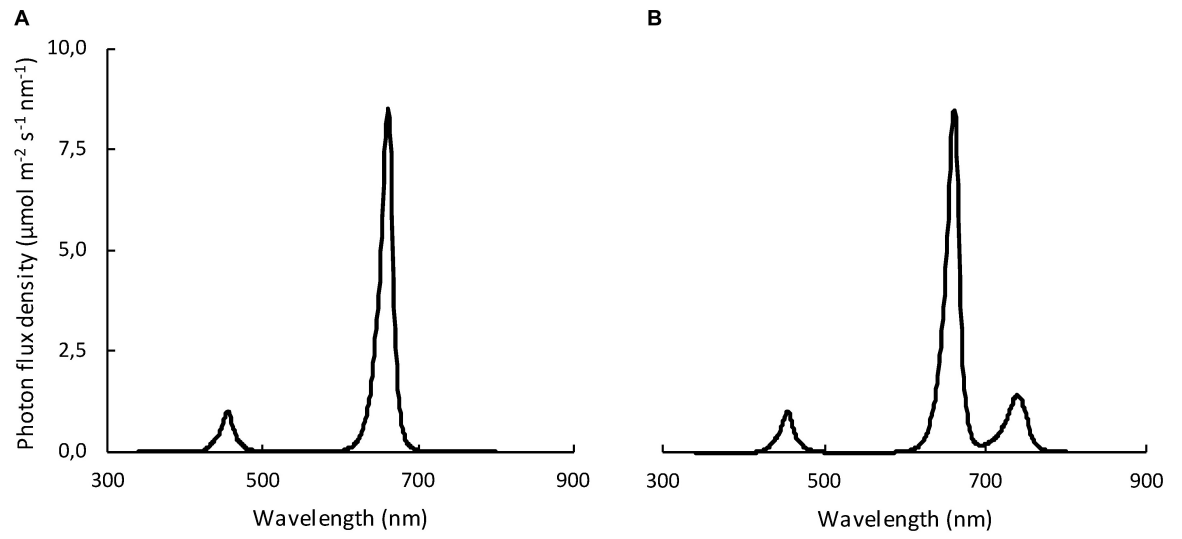

FIGURE 1 | Spectral distribution of the two light treatments: **(A)** without far-red (RB); **(B)** with far-red (RB + FR). Spectra were recorded and averaged on 21 locations along the cultivated area at pot level, measured by a spectroradiometer.

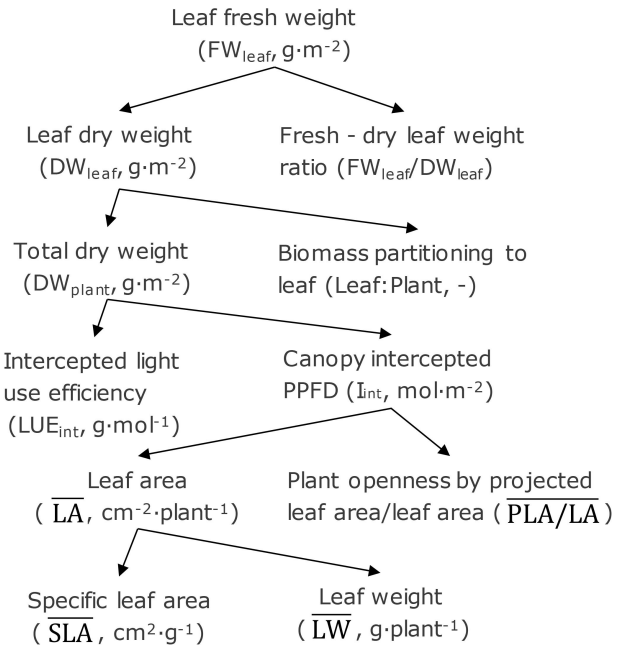

FIGURE 2 | Leaf fresh weight separated into underlying components. Abbreviation and unit are given in between brackets.

(DW_{leaf}) and the fresh/dry leaf weight ratio (FW_{leaf}/DW_{leaf}). Leaf dry weight is the product of total dry weight (DW_{plant}) and fraction of biomass partitioning to leaf (leaf/plant). Canopy-intercepted photosynthetic photon flux density (PPFD) (I_{int}), which is the cumulative PPFD interception during the whole cultivating period (0–28 DAT), and the dry weight production per unit intercepted PPFD (LUE_{int}) determine the total dry weight. Canopy-intercepted PPFD was calculated based on projected leaf area, which is determined by leaf area per plant ($\overline{LA}$) and plant openness defined as the ratio between projected leaf area and leaf area ($\overline{PLA/LA}$). Leaf dry weight ($\overline{LW}$) and specific leaf area ($\overline{SLA}$) determine the leaf area. The $\overline{LA}$, $\overline{PLA/LA}$, $\overline{SLA}$, and $\overline{LW}$ were averaged over 14, 21, and 28 DAT representing the average levels of all parameters during the whole cultivating period (0–28 DAT).

Statistical Setup and Analysis

A randomized complete block design was applied. The experiment was repeated three times, with repetitions in time representing three blocks ($n = 3$). At 28 DAT for high planting density and no additional FR, only data from two blocks were used. The third block gave an extreme outlier for leaf/root ratio, 15 instead of 4–6; therefore, these measurements were not included in the final analysis. There were four–six replicate plants per block for each destructive measurement and three for photosynthesis. For each block, a new randomization of the light treatment positions was done. Analysis of variance was used to determine treatment effects using Genstat software (18th edition, United Kingdom). Normality of the residuals was tested using the Shapiro–Wilk test, and equal variances were assumed as this could not be tested with only three repetitions. Mean separation was done with Fisher's protected least significant difference (LSD) test ($P < 0.05$ or $P < 0.10$). In each repetition, the measurements were based on three–six replicate plants, as indicated in the description of the measurements.

FR effects were tested for each planting density separately using a one-way ANOVA in component analysis. Since for such a test the total number of experimental units was only six, a level of significance of 0.10 was applied as is normal in such cases (Ott and Longnecker, 2010). FR effects were also tested together with planting density using a two-way ANOVA in other figures and results with the level of significance of 0.05.

RESULTS

Biomass, Leaf Area, Leaf/Root Ratio, Intercepted PPFD, LUE_{inc}, LUE_{int}, RUE, and SLA

At all three planting densities, plant dry weight and leaf area were higher when FR was added (**Figure 3**). Neither plant dry weight nor leaf area per plant was affected by planting density when no FR was present. Dry weight per plant in the presence of FR was lower at higher planting density. The effects of FR on plant dry weight and leaf area were smaller at higher planting density. Adding FR increased plant dry weight after 4 weeks by 46–77% (largest effect at lowest planting density) and leaf area by 58–75% (largest effect at middle planting density).

Leaf/root ratio increased during plant development. FR increased leaf/root ratio significantly at 14 and 21 DAT (**Figure 4**). Planting density did not significantly affect leaf/root ratio.

Canopy-intercepted PPFD increased with time (**Figure 5**), which was related to the increase in leaf area. Intercepted PPFD was larger for plants grown with FR compared to plants grown without FR, at all three planting densities.

FR significantly increased incident light use efficiency (LUE_{inc}, **Figure 6A**) and radiation use efficiency (RUE, **Figure 6B**) at all three planting densities. Radiation use efficiency (RUE: plant dry weight per unit of incident radiation, 400–800 nm) increased by 17–42% and incident light use efficiency (LUE_{inc}: plant dry weight per unit of incident PAR, 400–700 nm) increased by 46–77% by FR; the largest FR effects were observed at the lowest planting density. Intercepted light use efficiency (LUE_{int}: plant dry weight per unit of intercepted PAR) also increased by FR, but to a lesser extent (8–23%) (**Figure 6C**).

No difference of specific leaf area (SLA) among treatments was observed at 14 and 21 DAT (**Figure 7**). At 28 DAT, SLA was significantly affected by planting densities but not by FR (**Figure 7**). Similarly, the increment in SLA during the final cultivating week, from 21 to 28 DAT, was significantly different among planting densities and not affected by FR (not shown).

Yield Component Analysis

FR increased leaf fresh weight (FW_{leaf}) for all planting densities by 42–61%. This was the result of increased leaf dry weight (DW_{leaf}) and not a higher fresh/dry weight ratio

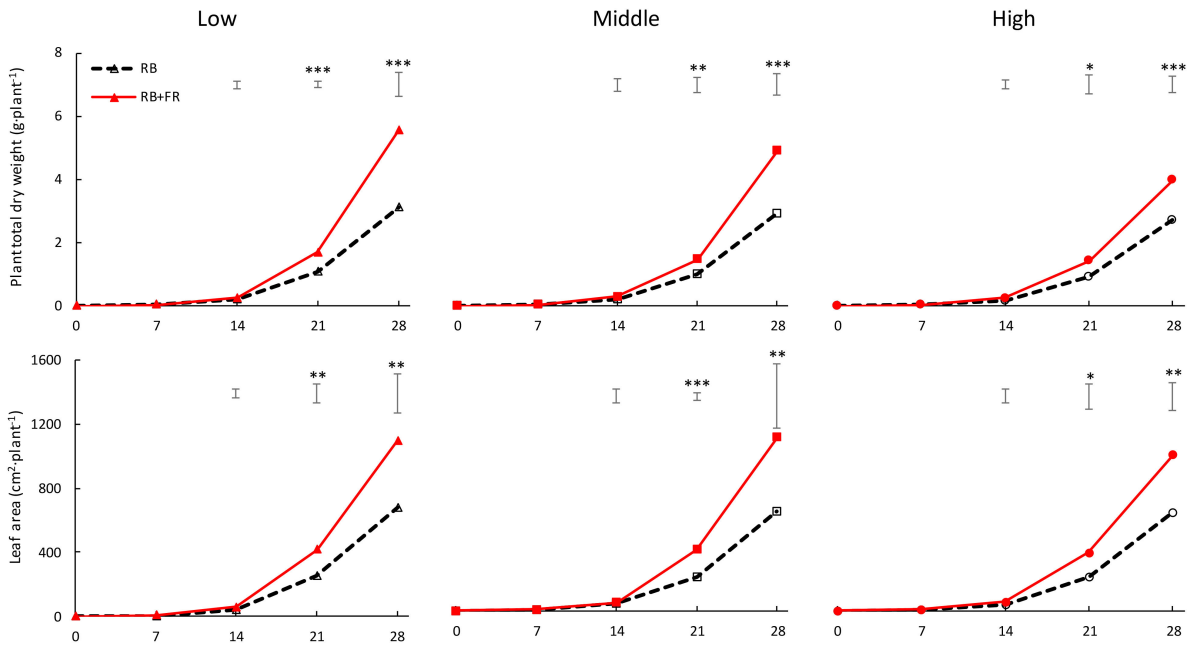

FIGURE 3 | Time course of total dry weight of lettuce plants (g plant^{-1}, upper layer) and plant leaf area (cm^2 plant^{-1}, lower layer) when grown without (RB) or with (RB + FR) 52 μmol m^{-2} s^{-1} far-red radiation (FR) intensity, at three planting densities (low, middle, and high being 23, 37, and 51 plants m^{-2}, respectively). Solid lines represent RB + FR treatment and dashed lines indicate RB treatment. Bars on top of each day represent least significant difference. Significant effect of FR: $^*P < 0.10$, $^{**}P < 0.05$, and $^{***}P < 0.01$ Data are means of three blocks ($n = 3$) each with four–six replicate plants.

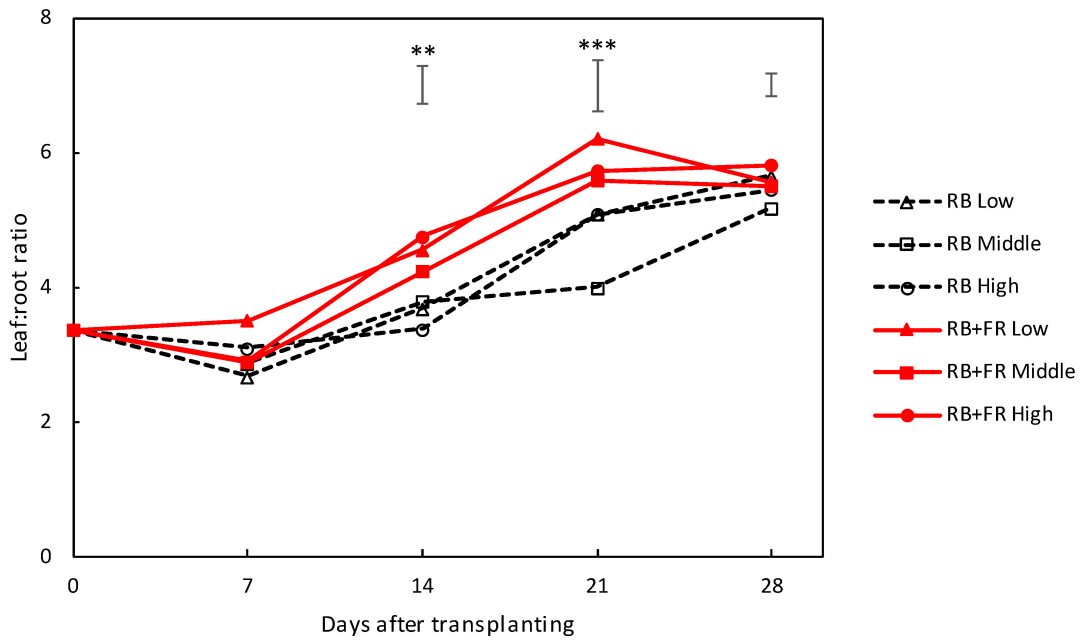

FIGURE 4 | Pattern of leaf/root ratio over time for lettuce plants grown with or without far-red radiation (FR) at three planting densities (low, middle, and high being 23, 37, and 51 plants m^{-2}, respectively). Solid lines represent RB + FR treatment and dashed lines indicate RB treatment. Bars on top of each day represent least significant difference. Significant FR effect: $^{**}P < 0.05$ and $^{***}P < 0.01$. Data are means of two ($n = 2$) or three blocks ($n = 3$) each with four–six replicate plants.

(FW_{leaf}/DW_{leaf}); this ratio actually was lower at RB + FR at the low planting density. FR increased DW_{plant} by 46–77%, which was mainly due to a higher canopy-intercepted PPFD (I_{int}), which increased by 29–64%, and to a smaller extent (8–23%) by higher intercepted light use efficiency (LUE_{int}). The higher I_{int} was caused by an increased average leaf area

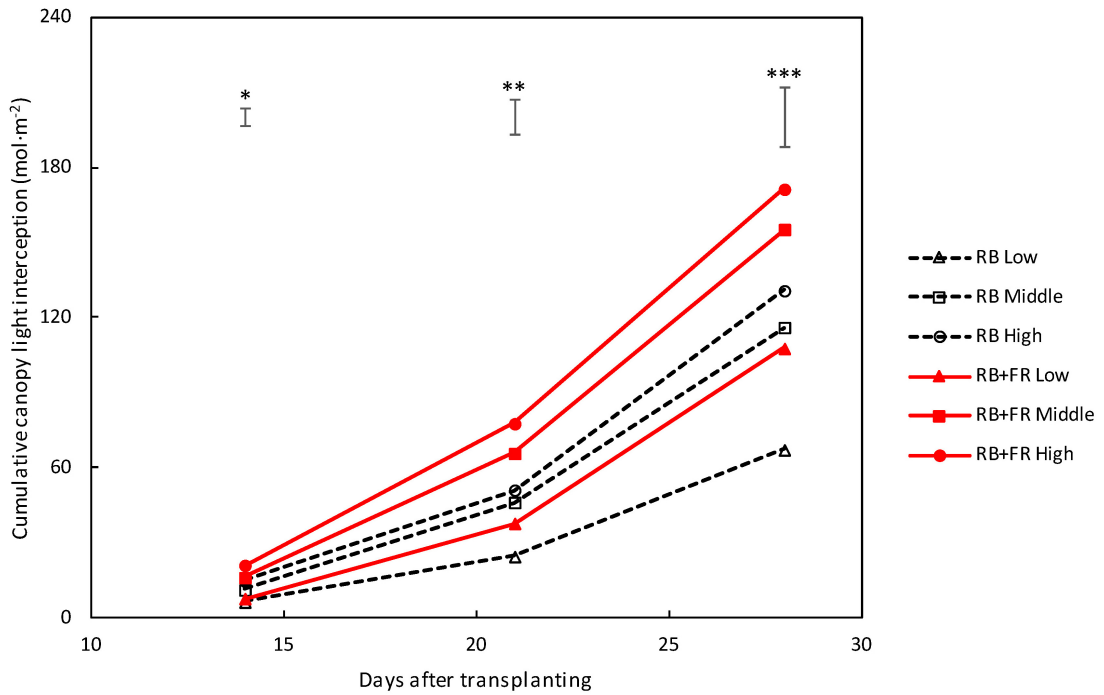

FIGURE 5 | Intercepted photosynthetic photon flux density (PPFD) of lettuce canopy grown at three planting densities (low, middle, and high being 23, 37, and 51 plants m^{-2}). Solid lines represent with far-red radiation (FR) treatment (52 μmol m^{-2} s^{-1} FR) and dashed lines indicate treatment without FR. Light was cumulated from 14 to 28 DAT. Bars on top of each day represent least significant difference. Significant FR effect: $^{*}P < 0.10$, $^{**}P < 0.05$ and, $^{***}P < 0.01$. Data are means of two blocks ($n = 2$) each with four–six replicate plants.

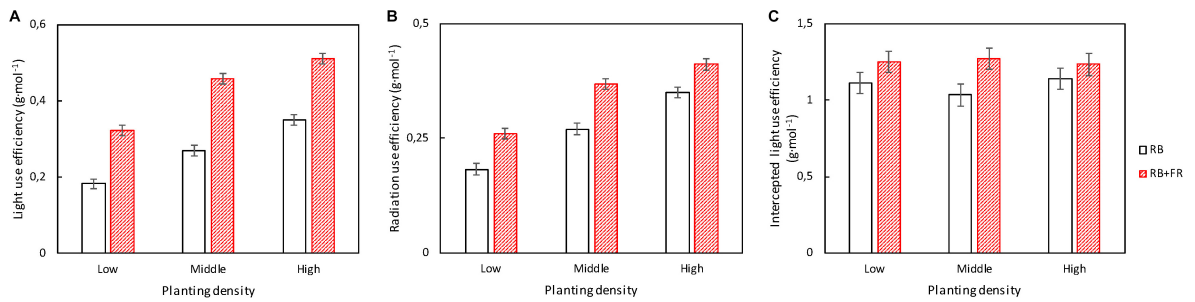

FIGURE 6 | (A) Incident light use efficiency [LUE_{inc}, which is plant dry weight per unit of incident photosynthetically active radiation (PAR)]; **(B)** radiation use efficiency [RUE, which is plant dry weight per unit of incident radiation including PAR and far-red radiation (FR)]; and **(C)** intercepted light use efficiency [LUE_{int}, which is the plant dry weight per unit of canopy-intercepted photosynthetic photon flux density (PPFD)] of lettuce plants grown at three planting densities (23, 37, and 51 plants m^{-2}), with (52 μmol m^{-2} s^{-1}) and without FR at 28 days after transplanting (DAT). Error bars indicate standard errors of means. None of these three parameters showed a significant interaction between FR and planting density ($P > 0.25$). For incident light use efficiency **(A)** and radiation use efficiency **(B)**, effects of both FR [least significant difference (LSD) = 0.024 and LSD = 0.022, respectively, $n = 3$] and planting density (LSD = 0.030 and LSD = 0.027, respectively, $n = 2$) were significant ($P < 0.001$). For intercepted light use efficiency **(C)**, planting density effect was not significant ($P = 0.87$) and FR effect was significant ($P = 0.043$; LSD = 0.15; $n = 2$). Data are means of two ($n = 2$) or three blocks ($n = 3$) each with four–six replicate plants.

(LA_{plant}) by 58–67%, rather than plant openness (PLA/LA), which varied little between treatments with and without FR. FR increased overall biomass partitioning to leaf (**Figure 4**), which led to a higher leaf area with a relative constant specific leaf area (SLA). The overall reasoning based on the component analysis (**Figure 8**) was supported by the correlation analysis (**Supplementary Table S2**).

DISCUSSION

Higher efficiencies of the photochemistry of photosystem II (PSII) and I (PSI), which are maximumly excited at 680 and 700 nm, respectively, contribute to a higher photosynthesis rate (Baker, 2008). Due to Emerson enhancement effect, the PSII efficiency might be increased by adding FR, hence the net

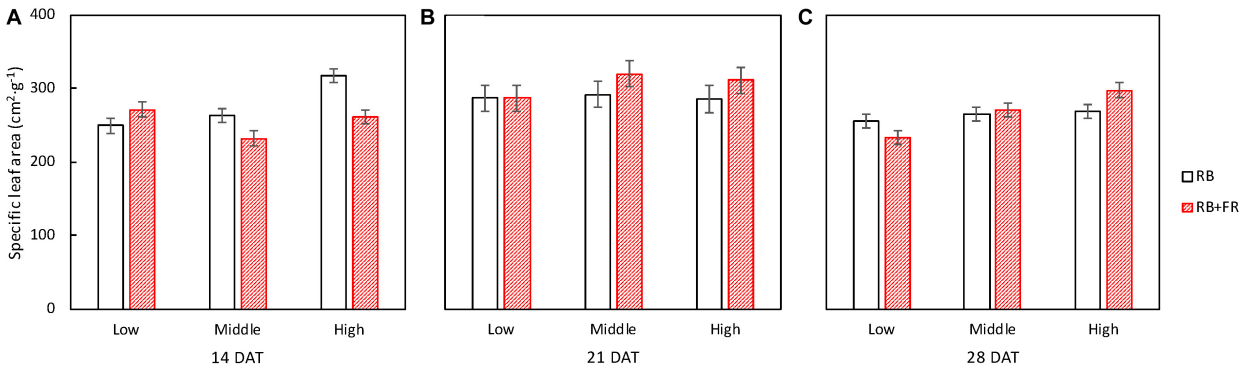

FIGURE 7 | Specific leaf area (SLA) of lettuce plants grown at three planting densities (23, 37, and 51 plants m^{-2}), with (52 μmol m^{-2} s^{-1}) and without far-red radiation (FR) at 14 **(A)**, 21 **(B)**, and 28 **(C)** days after transplanting (DAT). Error bars indicate standard errors of means. For 14 DAT, a significant interaction between FR and planting density was observed ($P = 0.027$; $n = 2$). For 21 DAT, no significant interaction ($P = 0.70$) between effect of planting density ($P = 0.59$) and effect of FR ($P = 0.26$) was found. For 28 DAT, there was a significant interaction ($P = 0.055$; $n = 3$). Data are means of two ($n = 2$) or three blocks ($n = 3$) each with four–six replicate plants.

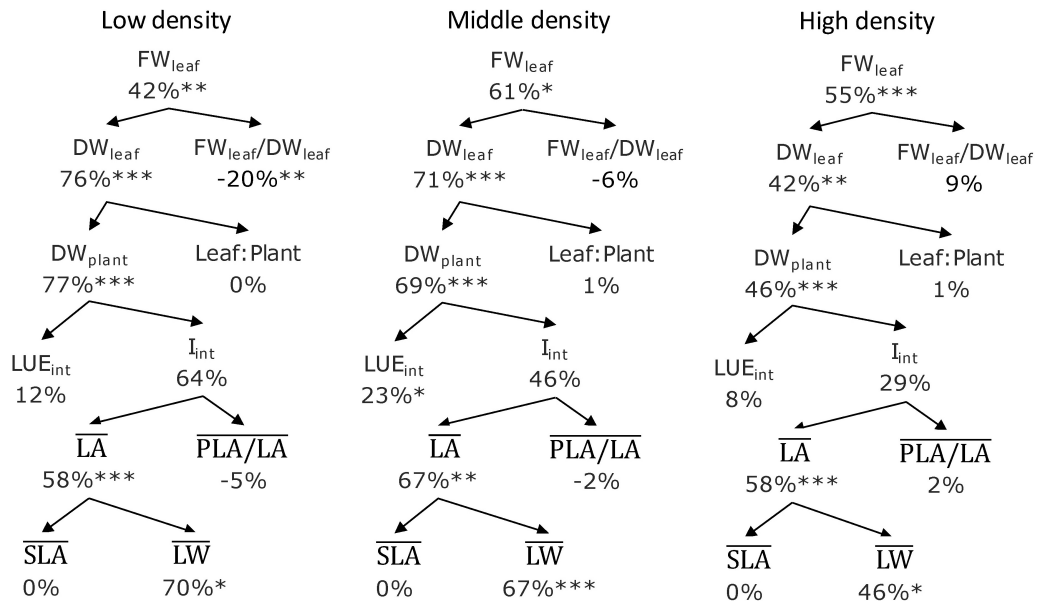

FIGURE 8 | Effect of adding far-red radiation (FR) on top of red and blue at three planting densities. Percentages are the RB + FR increment on top of RB. Abbreviations within schemes are as follows: FW$_{leaf}$, leaf fresh weight; DW$_{leaf}$, leaf dry weight; FW$_{leaf}$/DW$_{leaf}$, leaf fresh/dry weight ratio; DW$_{plant}$, plant total dry weight; Leaf:Plant, ratio of leaf dry weight in total plant; LUE$_{int}$, intercepted light use efficiency; I_{int}, canopy-intercepted photosynthetic photon flux density; $\overline{LA}$, plant leaf area; $\overline{PLA/LA}$, projected leaf area and leaf area ratio; $\overline{SLA}$, specific leaf area; $\overline{LW}$, leaf weight. The $\overline{LA}$, $\overline{PLA/LA}$, $\overline{SLA}$, and $\overline{LW}$ are all averaged values over 14, 21, and 28 days after transplanting (DAT) representing cumulative values during the whole cultivating period (0–28 DAT). *$P < 0.10$, **$P < 0.05$, and ***$P < 0.01$. Data are means of two ($n = 2$) or three blocks ($n = 3$) each with four–six replicate plants.

photosynthetic rate increases in short term (Emerson et al., 1957). Zou et al. (2019) observed a 7–10% immediate increment in net photosynthesis rate by adding FR on top of plants acclimated to environments with and without FR. However, due to a lower chlorophyll and total nitrogen content as well as lower leaf absorbance, FR-acclimated plant's photosynthetic capacity decreased in the long-term (Ji et al., 2019; Zou et al., 2019). In the present study, we did not find an effect of FR on leaf net photosynthesis rate, 9.8 ± 0.2 μmol (CO_2) m^{-2} s^{-1}in average (**Supplementary Table S3**), when measured under the light conditions. The plants were grown at 20 DAT, which resulted in similar results as reported by Ji et al. (2019) and Zhang et al. (2019) in tomato. There is a possible cancelling out of a positive instantaneous effect on net photosynthesis rate (Emerson enhancement effect) and lowered chlorophyll content per unit leaf area by FR-enriched environment acclimation. Plants acclimate to the growing light environment by adapting photochemistry system under RB or RB + FR conditions to utilize absorbed photons efficiently (Walters, 2005; Zhen et al., 2019). As shown by Ji et al. (2019) and Kalaitzoglou et al. (2019) in

tomato, on the long run, the effect of FR on plant growth via affecting leaf photosynthesis rate is limited. The significantly higher biomass production is rather due to a substantial increment of photosynthetic leaf area by adding FR (**Figure 3**).

Adding FR on top of red and blue increased plant fresh weight significantly at all three planting densities (**Figures 3**, **8**). This resulted from a higher total plant dry weight (DW_{plant}) as well as leaf dry weight (DW_{leaf}) in agreement with previous studies (Meng et al., 2019; Zou et al., 2019). The significantly higher DW_{leaf} when FR was added was due to a substantially higher leaf area (**Figure 3**). Several papers (Franklin, 2008; Vos et al., 2010; Bongers et al., 2014) have reviewed the effect of lowered R/FR, which typically happens in vegetation proximity where red (R) photons were mainly absorbed and thus the ratio between R and FR decreases. Lowering R/FR may result in more expansion of leaf area but not increases in the leaf number (**Supplementary Table S3**). In our experiment, an increase in expansion of leaf area by FR resulted in a cumulative advantage in intercepting a much higher fraction of incident light, resulting in an increase in plant dry weight (**Figures 3**, **8**) at all planting densities. The more rapid expansion of leaf area resulted in a larger fraction of floor cover and consequently a higher light interception for the RB + FR treatment (**Figure 5**). The incident light use efficiency (LUE_{inc}: plant dry weight per unit of cumulative incident PPFD) was consequently increased by adding FR. Radiation use efficiency (RUE: plant dry weight per unit of cumulative incident PFD) was also improved due to the strong increase in radiation interception by the enhanced leaf area expansion, which is in agreement with the lettuce experiment of Zou et al. (2019). The intercepted light use efficiency (LUE_{int}: plant dry weight per unit of canopy-intercepted PPFD) was significantly increased by FR but no planting density effect was observed, which was in line with the results of instantaneous net photosynthesis rate increase when adding FR on top of R and B (Zou et al., 2019). The effects of FR on plant dry weight were stronger at low planting density, which could be explained by the fact that at low planting density, the light interception is lower and therefore an increase in light interception will have a larger effect on plant growth. Surprisingly, this stronger effect at low planting density was not observed for fresh weight, as the ratio of fresh to dry weight was strongly reduced at low planting density. Unexpectedly, this ratio did not decrease by FR at high planting density. In basil plants, the fresh-to-dry ratio was also reduced by FR (Larsen et al., 2020). A higher fraction of biomass partitioning to the shoot is one of the effect of lowered R/FR (Vos et al., 2010; Bongers et al., 2014). In case of lettuce, which has only a very small stem, it is the leaf that benefits from this. The increase of leaf/root ratio under FR suggests the relative sink strength of leaves had increased compared to that of the root (Marcelis, 1996; Heuvelink, 1997). Specific leaf area (SLA) has often been found to increase by additional FR or a lowered R/FR, which normally happens in vegetation proximity (Ballaré and Pierik, 2017), but not in the current research (**Figure 8**). Therefore, a higher fraction of biomass partitioned to the leaf resulted in a larger leaf area.

Considering that FR resulted in a higher biomass partitioning to the shoot, a higher leaf area, and improved light interception, the data suggest that adding FR on top of PAR is likely more efficient for dry weight production than adding same intensity PAR. The radiation use efficiency was indeed higher for plants grown with additional FR compared to no FR. It would be worthwhile to grow plants with and without FR, but with same total radiation, in order to test if the addition of FR is more efficient in promoting growth than addition of extra PAR.

CONCLUSION

Our results demonstrate that adding FR on top of red and blue light increased lettuce fresh and dry weight significantly at three planting densities. The effects on dry weight were strongest at low planting density. The increased plant growth by adding FR was caused by a higher light interception by an enlarged leaf area resulting from a higher biomass partitioning to shoot, rather than from a higher leaf photosynthesis rate or specific leaf area. FR increased incident light use efficiency and radiation use efficiency, while it increased intercepted light use efficiency to a lesser extent.

DATA AVAILABILITY STATEMENT

The original contributions presented in the study are included in the article/**Supplementary Material**, further inquiries can be directed to the corresponding author/s.

AUTHOR CONTRIBUTIONS

WJ, EH, and LM conceived and designed the experiments. WJ and JU performed the experiments. WJ and EH performed statistical analysis. WJ wrote the manuscript. EH and LM revised and edited the manuscript. All authors contributed to manuscript revision and read and approved the submitted version.

FUNDING

This project was funded by Priva, De Lier, Netherlands.

ACKNOWLEDGMENTS

We would like to thank Gerrit Stunnenberg, Taede Stoker, and David Brink for their technical assistance. Emilio Villar Allegria, Julia Winkeler, and Michele Butturini for their help in all measurements; and Elias Kaiser and Maarten Wassenaar for instrumentation training.

SUPPLEMENTARY MATERIAL

The Supplementary Material for this article can be found online at: https://www.frontiersin.org/articles/10.3389/fpls.2020.609977/full#supplementary-material

REFERENCES

Baker, N. R. (2008). Chlorophyll fluorescence: a probe of photosynthesis in vivo. *Annu. Rev. Plant Biol.* 59, 89–113. doi: 10.1146/annurev.arplant.59.032607.092759

Ballaré, C. L., and Pierik, R. (2017). The shade-avoidance syndrome: multiple signals and ecological consequences. *Plant Cell Environ.* 40, 2530–2543. doi: 10.1111/pce.12914

Bongers, F. J., Evers, J. B., Anten, N. P. R., and Pierik, R. (2014). From shade avoidance responses to plant performance at vegetation level: using virtual plant modelling as a tool. *New Phytol.* 204, 268–272. doi: 10.1111/nph.13041

Demotes-Mainard, S., Péron, T., Corot, A., Bertheloot, J., Le Gourrierec, J., Pelleschi-Travier, S., et al. (2016). Plant responses to red and far-red lights, applications in horticulture. *Environ. Exp. Bot.* 121, 4–21. doi: 10.1016/j.envexpbot.2015.05.010

Emerson, R., Chalmers, R., and Cederstrand, C. (1957). Some factors influencing the long-wave limit of photosynthesis. *Proc. Natl. Acad. Sci. U.S.A.* 43, 133–143. doi: 10.1073/pnas.43.1.133

Franklin, K. A. (2008). Shade avoidance. *New Phytol.* 179, 930–944. doi: 10.1111/j.1469-8137.2008.02507.x

Heuvelink, E. (1997). Effect of fruit load on dry matter partitioning in tomato. *Sci. Hortic.* 69, 51–59. doi: 10.1016/S0304-4238(96)00993-4

Higashide, T., and Heuvelink, E. (2009). Physiological and morphological changes over the past 50 years in yield components in tomato. *J. Am. Soc. Hortic. Sci.* 134, 460–465.

Ji, Y., Ouzounis, T., Courbier, S., Kaiser, E., Nguyen, P. T., Schouten, H. J., et al. (2019). Far-red radiation increases dry mass partitioning to fruits but reduces *Botrytis cinerea* resistance in tomato. *Environ. Exp. Bot.* 168:103889. doi: 10.1016/j.envexpbot.2019.103889

Kalaitzoglou, P., van Ieperen, W., Harbinson, J., van der Meer, M., Martinakos, S., Weerheim, K., et al. (2019). Effects of continuous or end-of-day far-red light on tomato plant growth, morphology, light absorption, and fruit production. *Front. Plant Sci.* 10:332. doi: 10.3389/fpls.2019.00322

Larsen, D. H., Woltering, E. J., Nicole, C. C. S., and Marcelis, L. F. M. (2020). Response of basil growth and morphology to light intensity and spectrum in a vertical farm. *Front. Plant Sci.* 11:597906. doi: 10.3389/fpls.2020.597906

Li, T., Heuvelink, E., Dueck, T. A., Janse, J., Gort, G., and Marcelis, L. F. M. (2014). Enhancement of crop photosynthesis by diffuse light: quantifying the contributing factors. *Ann. Bot.* 114, 145–156. doi: 10.1093/aob/mcu071

Marcelis, L. F. M. (1996). Sink strength as a determinant of dry matter partitioning in the whole plant. *J. Exp. Bot.* 47, 1281–1291.

Meng, Q., and Runkle, E. S. (2019). Far-red radiation interacts with relative and absolute blue and red photon flux densities to regulate growth, morphology, and pigmentation of lettuce and basil seedlings. *Sci. Hortic.* 255, 269–280. doi: 10.1016/j.scienta.2019.05.030

Meng, Q., Kelly, N., and Runkle, E. S. (2019). Substituting green or far-red radiation for blue radiation induces shade avoidance and promotes growth in lettuce and kale. *Environ. Exp. Bot.* 162, 383–391. doi: 10.1016/j.envexpbot.2019.03.016

Ott, L. R., and Longnecker, M. T. (2010). *An Introduction to Statistical and Data Analysis*. Belmont, CA: Brooks/Cole.

Park, Y., and Runkle, E. S. (2017). Far-red radiation promotes growth of seedlings by increasing leaf expansion and whole-plant net assimilation. *Environ. Exp. Bot.* 136, 41–49. doi: 10.1016/j.envexpbot.2016.12.013

Pennisi, G., Pistillo, A., Orsini, F., Cellini, A., Spinelli, F., Nicola, S., et al. (2020). Optimal light intensity for sustainable water and energy use in indoor cultivation of lettuce and basil under red and blue LEDs. *Sci. Hortic.* 272:109508. doi: 10.1016/j.scienta.2020.109508

Pierik, R., and De Wit, M. (2014). Shade avoidance: phytochrome signalling and other aboveground neighbour detection cues. *J. Exp. Bot.* 65, 2815–2824. doi: 10.1093/jxb/ert389

Sager, J. C., Smith, W. O., Edwards, J. L., and Cyr, K. L. (1988). Photosynthetic efficiency and phytochrome photoequilibria determination using spectral data. *Trans. ASAE* 31, 1882–1889. doi: 10.13031/2013.30952

SharathKumar, M., Heuvelink, E., and Marcelis, L. F. M. (2020). Vertical farming: moving from genetic to environmental modification. *Trends Plant Sci.* 25, 724–727. doi: 10.1016/j.tplants.2020.05.012

Taiz, L., Zeiger, E., Møller, I. M., and Murphy, A. (2015). *Plant Physiology and Development, 2015*, 6th Edn. Sunderland, MA: Sinauer Assotiates.

Vos, J., Evers, J. B., Buck-Sorlin, G. H., Andrieu, B., Chelle, M., and De Visser, P. H. B. (2010). Functional-structural plant modelling: a new versatile tool in crop science. *J. Exp. Bot.* 61, 2101–2115. doi: 10.1093/jxb/erp345

Walters, R. G. (2005). Towards an understanding of photosynthetic acclimation. *J. Exp. Bot.* 56, 435–447. doi: 10.1093/jxb/eri060

Zhang, Y., Zhang, Y., Yang, Q., and Li, T. (2019). Overhead supplemental far-red light stimulates tomato growth under intra-canopy lighting with LEDs. *J. Integr. Agric.* 18, 62–69. doi: 10.1016/S2095-3119(18)62130-6

Zhen, S., and Bugbee, B. (2020). Far-red photons have equivalent efficiency to traditional photosynthetic photons: implications for redefining photosynthetically active radiation. *Plant Cell Environ.* 43, 1259–1272. doi: 10.1111/pce.13730

Zhen, S., and van Iersel, M. W. (2017). Far-red light is needed for efficient photochemistry and photosynthesis. *J. Plant Physiol.* 209, 115–122. doi: 10.1016/j.jplph.2016.12.004

Zhen, S., Haidekker, M., and van Iersel, M. W. (2019). Far-red light enhances photochemical efficiency in a wavelength-dependent manner. *Physiol. Plant.* 167, 21–33. doi: 10.1111/ppl.12834

Zou, J., Zhang, Y., Zhang, Y., Bian, Z., Fanourakis, D., and Yang, Q. (2019). Morphological and physiological properties of indoor cultivated lettuce in response to additional far-red light. *Sci. Hortic.* 257:108725. doi: 10.1016/j.scienta.2019.108725

Conflict of Interest: The authors declare that this study received funding from Priva, De Lier, Netherlands. The funder was not involved in the study design, collection, analysis, interpretation of data, the writing of this article or the decision to submit it for publication.

The authors declare that the research was conducted in the absence of any commercial or financial relationships that could be construed as a potential conflict of interest.

Copyright © 2021 Jin, Urbina, Heuvelink and Marcelis. This is an open-access article distributed under the terms of the Creative Commons Attribution License (CC BY). The use, distribution or reproduction in other forums is permitted, provided the original author(s) and the copyright owner(s) are credited and that the original publication in this journal is cited, in accordance with accepted academic practice. No use, distribution or reproduction is permitted which does not comply with these terms.

frontiers in Plant Science

ORIGINAL RESEARCH
published: 25 January 2021
doi: 10.3389/fpls.2020.610041

Floral Induction in the Short-Day Plant Chrysanthemum Under Blue and Red Extended Long-Days

*Malleshaiah SharathKumar, Ep Heuvelink, Leo F. M. Marcelis and Wim van Ieperen**

Horticulture and Product Physiology, Wageningen University and Research, Wageningen, Netherlands

Shorter photoperiod and lower daily light integral (DLI) limit the winter greenhouse production. Extending the photoperiod by supplemental light increases biomass production but inhibits flowering in short-day plants such as *Chrysanthemum morifolium*. Previously, we reported that flowering in growth-chamber grown chrysanthemum with red (R) and blue (B) LED-light could also be induced in long photoperiods by applying only blue light during the last 4 h of 15 h long-days. This study investigates the possibility to induce flowering by extending short-days in greenhouses with 4 h of blue light. Furthermore, flower induction after 4 h of red light extension was tested after short-days RB-LED light in a growth-chamber and after natural solar light in a greenhouse. Plants were grown at 11 h of sole source RB light (60:40) in a growth-chamber or solar light in the greenhouse (short-days). Additionally, plants were grown under long-days, which either consisted of short-days as described above extended with 4 h of B or R light to long-days or of 15 h continuous RB light or natural solar light. Flower initiation and normal capitulum development occurred in the blue-extended long-days in the growth-chamber after 11 h of sole source RB, similarly as in short-days. However, when the blue extension was applied after 11 h of full-spectrum solar light in a greenhouse, no flower initiation occurred. With red-extended long-days after 11 h RB (growth-chamber) flower initiation occurred, but capitulum development was hindered. No flower initiation occurred in red-extended long-days in the greenhouse. These results indicate that multiple components of the daylight spectrum influence different phases in photoperiodic flowering in chrysanthemum in a time-dependent manner. This research shows that smart use of LED-light can open avenues for a more efficient year-round cultivation of chrysanthemum by circumventing the short-day requirement for flowering when applied in emerging vertical farm or plant factories that operate without natural solar light. In current year-round greenhouses' production, however, extension of the natural solar light during the first 11 h of the photoperiod with either red or blue sole LED light, did inhibit flowering.

Keywords: blue extended long-day, chrysanthemum, photoperiodic flowering, morphology, supplemental lighting, vertical farm

OPEN ACCESS

Edited by:
Petronia Carillo, University of Campania Luigi Vanvitelli, Italy

Reviewed by:
Federico Apelt, Max Planck Institute of Molecular Plant Physiology, Germany
Antonio Ferrante, University of Milan, Italy

****Correspondence:***
Wim van Ieperen
wim.vanieperen@wur.nl

Specialty section:
This article was submitted to Crop and Product Physiology, a section of the journal Frontiers in Plant Science

Received: *24 September 2020*
Accepted: *30 December 2020*
Published: *25 January 2021*

Citation:
SharathKumar M, Heuvelink E, Marcelis LFM and van Ieperen W (2021) Floral Induction in the Short-Day Plant Chrysanthemum Under Blue and Red Extended Long-Days. Front. Plant Sci. 11:610041. doi: 10.3389/fpls.2020.610041

INTRODUCTION

Flowering time is governed by various internal and external factors including developmental competence, circadian rhythms, temperature, and photoperiod (Srikanth and Schmid, 2011; Cho et al., 2017). Many plant species monitor seasonal changes in the light environment (photoperiod, light intensity, direction, and spectral composition) to optimize their growth and development (Thomas, 2006). Photoperiod influences floral induction and flowering rate in many flowering plant species. Based on photoperiod requirement plants are classified into short-day (SD) and long-day (LD) plants (Garner and Allard, 1920). However, short- and long-night plants would be more accurate as it is the length of the dark period that is decisive for flower induction (Borthwick et al., 1952). The perception of photoperiod takes place in leaves *via* photoreceptors that are well described in model plant species (Song et al., 2015). Additionally, differences in the light spectrum are perceived by a distinct set of photoreceptors; red/far-red [phytochromes (PHY)], blue/UV-A [cryptochromes (CRY)], [phototropins (PHOT), ZTL/ FKF_1/LKP_2], and UV-B light (UVR8). Most of the flowering plants possess several of these photoreceptors and together these photoreceptors influence and regulate flowering, through a complex network of regulatory genes (Andrés and Coupland, 2012; Viczián et al., 2020). Photoperiodic flowering is controlled, in part, by light signals that entrain the circadian clock, which is an essential component of the mechanism for day-length sensing by plants and is involved in the regulation of flowering as explained by the "external coincidence" model for flowering (Johansson and Staiger, 2015). The control of photoperiodic flowering operates by upregulation of florigen – *FLOWERING LOCUS T* (*FT*) and downregulation of anti-florigenic *FT* (*AFT*) / *TERMINAL FLOWER 1* (*TFL1*) under inductive photoperiod and this mechanism is conserved in both LD and SD plants (Higuchi, 2018).

In addition to photoperiod, light spectrum plays a regulatory role in flowering in both short-day and long-day plants (Cerdán and Chory, 2003; Song et al., 2015). In many long-day species, blue and far-red light accelerates flower induction (Song et al., 2015; Zhang et al., 2020), and the presence of far-red light during the daily photoperiod or given at end-of-day accelerates flowering (Lane et al., 1965; Vince, 1965; Runkle and Heins, 2003). Long-day plants grown under a far-red deficient environment delayed floral initiation and development in crops such as lisianthus, snapdragon (van Haeringen et al., 1998), tussock bellflower (*Campanula carpatica*), tickseed (*Coreopsis grandifora*; Runkle and Heins, 2001), and petunia (*Petunia hybrida*; Kim et al., 2002). In the short-day plant's such as poinsettia (Zhang and Runkle, 2019), garden strawberry (Fragaria × ananassa), and chrysanthemum illumination with end-of-day far-red delayed flowering (Hisamatsu et al., 2008). Red light is typically effective in inhibiting the flowering of short-day plants. Various photoperiod studies demonstrated that a red light night-break could inhibit flowering of cocklebur (*Xanthium strumarium*), soybean (*Glycine max*), and chrysanthemum, and a subsequent far-red exposure could reverse the flowering inhibition (Borthwick et al., 1952; Downs, 1956; Cathey and Borthwick, 1957; Thomas and Vince-Prue, 1996). Similar flowering inhibition was also observed in dahlia (*Dahlia hortensis*), and marigold (*Tagetes erecta*) under 4 h night-break by red (Craig and Runkle, 2013). Furthermore, the combination of far-red with red light, delivered as night-break, were effective both for inhibiting flowering in short-day plant (marigold) and for promoting flowering of long-day plants (petunia and snapdragon; Craig and Runkle, 2013). Besides red and far-red, blue light is known for flower promoting effects (Guo et al., 1998; Song et al., 2012). Blue light delivered as night-break or daylength-extension promoted flowering of long-day plants compared to the short-days (Goto et al., 1991; Yamada et al., 2011; Lopez et al., 2020), whereas in the short-day plants perilla (*Perilla ocymoides*) and rice (Hamamoto et al., 2003; Ishikawa et al., 2009), its delayed flowering. Therefore, flowering responses vary depending on the quality of light, photoperiodic lighting (daylength-extension or night-break), and on species.

Chrysanthemum is a commercially important species that occupies a large share of the global market of cut-flower production (Higuchi, 2018). To meet the global demand for marketable flowers throughout the year, the flowering time of this obligate short-day plant is highly regulated by supplemental lighting by daylength-extension or by night-breaks to prevent premature flowering (Higuchi et al., 2013; Park and Jeong, 2020). For many years, most of the light spectrum studies on chrysanthemum flowering regulation are confined to the effect of the light spectrum during night-breaks (Cathey and Borthwick, 1957; Borthwick and Cathey, 1962; Kadman-Zahavi and Ephrat, 1971, 1973; Horridge and Cockshull, 1989; Higuchi et al., 2012; Liao et al., 2014; Park and Jeong, 2020). Supplemental lighting is also used for photosynthesis and growth enhancement during short days, while it is particularly needed to avoid substantial flowering delays when daily light integrals are low (Langton, 1992). An earlier study in a growth chamber experiment in our lab demonstrated the possibility of inducing flowering under long-days (15 h) by extending red-blue short-days with 4 h of photosynthetic active blue light (Jeong et al., 2014). Such a treatment would be highly interesting if it could be used in the commercial greenhouse industry, where solar light instead of red-blue light is present during the short-day period. This is not certain as it has been shown that the composition of the light spectrum during the short-day period may alter the night-break flowering responses to light spectrum in chrysanthemum (Higuchi et al., 2012). Therefore, in the present study, we investigated whether it is possible to induce flowering by extending short-days to long-days with 4 h of blue LED light after short-days of natural full-spectrum daylight in greenhouses. Additionally, flower induction after 4 h of red daylight extension was tested after short-days of RB (growth-chamber) or natural full-spectrum daylight (greenhouse).

MATERIALS AND METHODS

Plant Material and Growth Conditions

Peat block-rooted cuttings of *Chrysanthemum morifolium* cv. "Radost" (Deliflor Chrysanten B.V, Netherlands) were transplanted in 8 cm × 8 cm × 10 cm plastic pots containing

a peat-based horticultural substrate (Lentse Potgrond, Horticoop), which contains 810 g m^{-3} N-P-K in the ratio of 15-10-20 and had a pH = 5.7 and EC = 0.8 dS m^{-1}. The transplanted cuttings were placed in a greenhouse and grown with a 15 h long-day photoperiod (solar light) for 7 days. The day/night temperature was 23/18 ± 4°C, the relative humidity 60–72%, and the CO_2 concentration was ambient. Water was supplied every other day *via* overhead irrigation. After 7 days, the plants were moved to the experimental greenhouse or the growth-chamber with the final spectral light treatments and grown for 6 weeks. Each spectral light treatment had 125 plants including 34 border plants. Realized day/night temperatures were 22/18°C ± 2°C (greenhouse) and 20/18°C ± 0.2°C (growth-chamber). Relative humidity was 60–72% (greenhouse) and 65 ± 2% (growth-chamber). CO_2 concentration was ambient. To achieve uniform climate conditions, six small electric fans per light treatment were installed in each plot in the growth-chamber. Plants were irrigated *via* overhead irrigation every other day, with a nutrient solution (Hoagland, pH = 5.9 ± 0.2, EC = 1.2 dS m^{-1}).

Lighting Treatments

Greenhouse Experiment: Four light treatments were applied, in which in each treatment the photoperiod started with 11 h of natural full-spectrum solar light (SL; **Figure 1A**): (1) solar

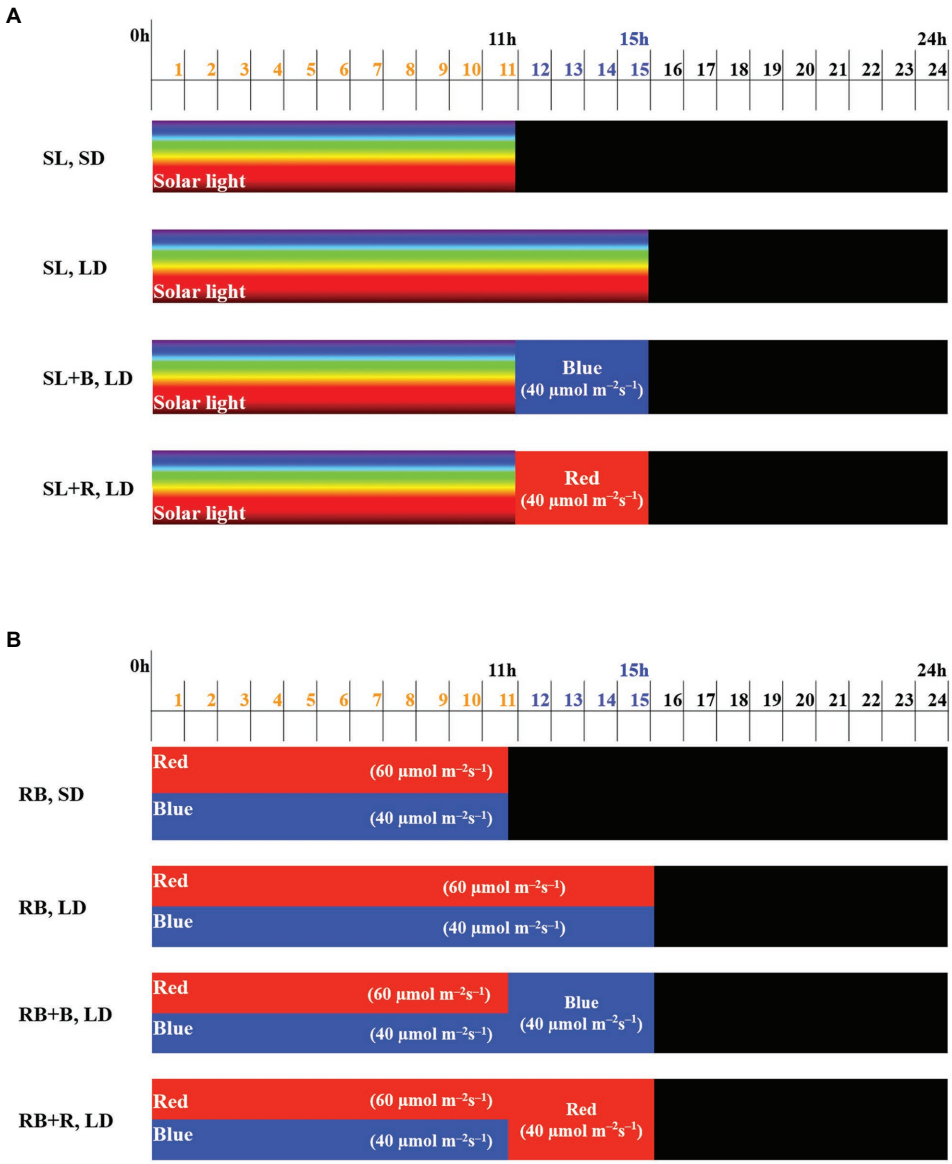

FIGURE 1 | Schematic representation of light treatments applied in **(A)** greenhouse or **(B)** climate chamber. Multicolor or red or blue colors indicate day light period; black color indicates dark period. The numbers in parenthesis indicate the light intensities supplied by red and blue LEDs (µmol m^{-2} s^{-1}). SL light intensity in the greenhouse varied between and within days according to season and weather.

light, SD – 11 h of natural full-spectrum solar light; (2) solar light, LD – 15 h of natural full-spectrum solar light; (3) solar light + B, LD – 11 h of natural full-spectrum solar light, extended by 4 h of blue light; and (4) solar light + R, LD – 11 h of natural full-spectrum solar light, extended by 4 h of red light. Obviously, the light intensity during the first 11 h of each light treatment (during 15 h in the solar LD treatment) varied with solar irradiance outside the greenhouse. Incidental light measurements at plant level in experimental plots indicated light integrals that were of the same order of magnitude as in the growth chamber experiment (described below). Detailed global solar radiation data over the full experimental period (measured outside the greenhouse) are provided in the **Supplementary Material**. The greenhouse compartment was divided into 16 plots of 1.0 × 1.3 m^2. Light treatments were repeated four times randomized over these 16 plots. To avoid light interference between light treatments, we used double-layered white plastic screens. The experiment was executed during summer, and to achieve a precise photoperiod of short-day (11 h) and long-day (15 h), solar light was blocked by black-out screens. To achieve the red or blue light day extensions, plants were illuminated by red or blue LEDs (Signify GreenPower LEDs research modules) with a peak wavelength of 450 (blue) and 660 nm (red; **Figure 2**). LEDs were positioned ∼1 m above the plants. The photosynthetic photon flux density (PPFD) during blue or red light photoperiod extension was 40 µmol m^{-2} s^{-1}. The LED light intensity was kept constant at plant height by adjusting twice per week to correct for an increase in plant height. Light spectra (**Figure 2**) and PPFD of LED light were measured using a spectroradiometer (Specbos 1211, Jeti Technische Instrumente GmbH, Jena, Germany). Solar light intensity in the greenhouse varied between and within days according to season and weather.

Growth-Chamber Experiment: Four light treatments were applied, in which in each treatment the photoperiod started with 11 h of red (R) and blue (B) light mixture at a 60:40 ratio (**Figure 1B**): (1) RB, SD – 11 h of mixed red and blue light; (2) RB, LD – 15 h of mixed red-blue light; (3) RB+B, LD – 11 h of mixed red and blue light, extended by 4 h of blue light; and (4) RB+R, LD – 11 h of mixed red and blue light, extended by 4 h of red light. Light treatments were repeated four times simultaneously in three different climate rooms (four treatments in each of two climate rooms, four treatments in two replicates in the same climate room in parallel). To avoid light interference among light treatment, we used double-layered white plastic screens between plots. Custom-built illumination systems containing red and blue LEDs (Signify GreenPower LEDs research modules) were used with a peak wavelength of either 450 (blue) or 660 nm (red; **Figure 2**). Illumination systems were suspended ∼1 m above the plants. All plants received a PPFD of 100 ± 5 µmol m^{-2} s^{-1} during the first 11 h of each light treatment and 40 µmol m^{-2} s^{-1} during red or blue light day extensions. The PPFD during the RB, LD treatment was 100 µmol m^{-2} s^{-1}. The PPFD was kept constant at plant height by adjusting twice per week to correct for plant growth.

Flowering Observations

The developmental stages of chrysanthemum shoot apical meristem (SAM) up to the visible flower bud stage were microscopically examined and described (**Figure 3**). To detect the number of days for floral initiation, every other day stereoscopic SAM dissections were conducted on two randomly selected plants per light treatment from day 8 until day 28 after the start of light treatments. Three centimeter long shoot apices were excised and immediately dissected to reach the SAMs by carefully peeling off leaves and removing leaf primordia with a surgical knife under a stereoscope. Images of developing stages of SAMs were acquired on a Zeiss Stereo Discovery-V12 microscope equipped with a Plan S 1.0 lens and an Axiocam MRc5 camera controlled by Axio Vision 4.8.1.0 software. Dissected SAMs with distinctive developmental stages of floral transition were imaged to assess the number of days for floral initiation. Floral initiation was confirmed when the SAM

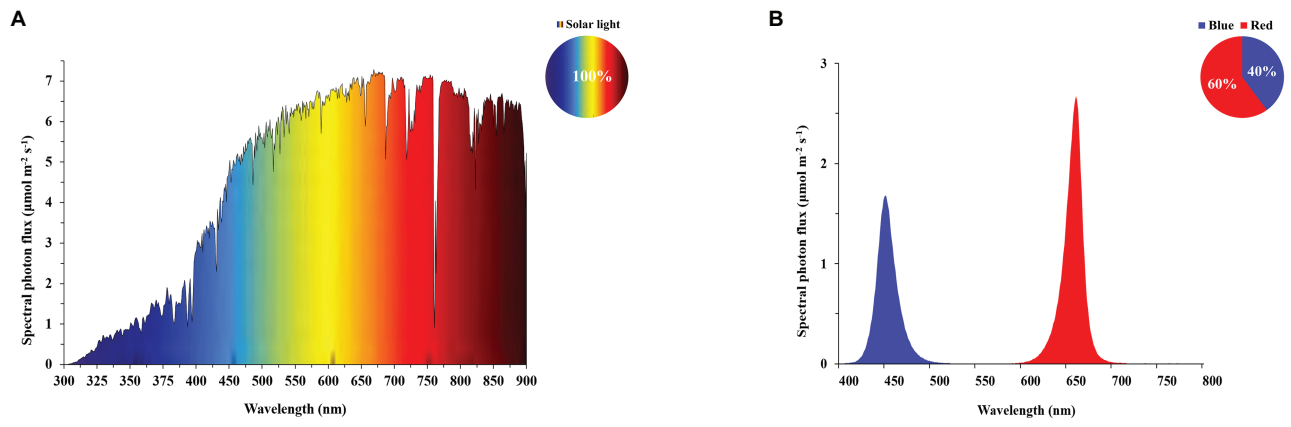

FIGURE 2 | Spectral photon distribution of **(A)** solar light, measured at a representative day in the greenhouse at noon, and **(B)** measured in a mixed RB treatment in the growth chamber. The separate spectral photon distributions in R and B reflect the wavelength distribution of the supplied narrow-band R and B light during daylength extensions in the greenhouse as well as in the growth chamber.

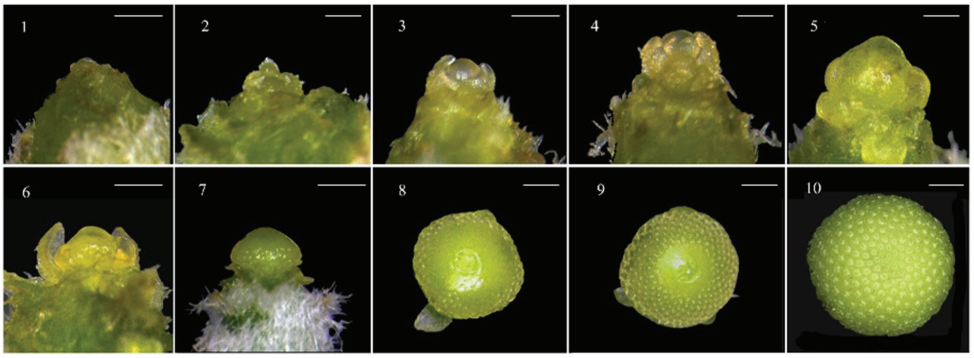

FIGURE 3 | Developmental stages of floral transition in *Chrysanthemum morifolium* cv. Radost. Stage-1 (vegetative phase), – the flat shoot apical meristem (SAM). Stage-2, – between the leaf primordia, a barely perceptible bulge of SAM happens. Stage-3, – the bulge is larger and the leaf primordia begin to deviate. Stage-4, – the first bracts are visible under the leaf primordia. Stage-5, – the bracts cover the dome. Stage-6 (floral initiation phase) – first floral primordia visible. Stage-7 (floral development phase) – one to four rings of floral primordia visible. Stage-8, – multiple rings of floral primordia visible (<half of area of flower head). Stage-9, – multiple rings of floral primordia visible (>half of area of flower head); Stage-10, – entire bud covered with floral primordia (visible bud emerges). Images were taken from a stereoscope with 80.0x magnification. When the diameter of apex was more than 2 mm (image 8–10), a lower magnification (from 30 to 70 x) was used to fit whole apex in the field of view. White lines at the left top side of each image indicate the length of 1 mm.

attained floral developmental stage 6 (first floral primordia initiation stage; **Figure 3**). Based on the linear regression between flower developmental stage and time, it was deduced when stage 6 was reached. The obtained value was considered as the number of days taken for floral initiation. Derived values for each of the light treatments were subjected to one-way ANOVA. Daily recording of the number of days for visible flower bud appearance started 8 days after the start of the light treatments on 10 plants per plot. The number of buds per plant and flowering (%) were recorded until day 42. Additionally, 10 plants were used to follow capitulum development and anthesis until day 55.

Growth and Morphology Observations

Growth and morphology were measured on day 42 after the onset of light treatments. Ten plants per plot were used to record stem length (cm), number of internodes and leaves and the leaf area (LI-COR 3100 area meter). Dry weights of leaves, stem, and flower buds were measured after oven-drying at 105°C for 24 h and used to calculate the total shoot dry weight.

Statistical Design and Analysis

In both experiments, four-light treatments were arranged in a randomized design over 16 plots. Hence, four replicate plots were used per light treatment. Out of 125 plants per plot, 34 were border plants, for SAM dissections, two plants per observation day starting from day 8 to day 28 (22 plants per plot), and on day 42, 10 plants per plot were used for growth and morphology observations, and on day 55, 10 plants per plot were used for observing flower capitulum. All statistical analyses were performed using Genstat (18th edition; VSN International Ltd., Herts, United Kingdom). One-way ANOVA, according to a complete randomized design, was applied to test for light treatment effect (p = 0.05). Mean separation was done by Fisher's Protected LSD test (p = 0.05).

RESULTS

Short-Day Light Spectrum Influenced Flowering Under Red and Blue Extended Long-Days

Under constant sole source red and blue lighting and natural solar light, chrysanthemum flowered in short-days and not in long-days (**Figures 4, 5**). Extending the short-days of solar light in a greenhouse with either blue or red light to long-days did not result in flowering (**Figures 4A, 5A**), while the same daylight extensions (with either red or blue) after a short-day with sole source red and blue light resulted in floral initiation (**Figure 4**). However, full capitulum development and anthesis occurred only when these short-days were extended with blue light (**Figures 6C,D**). All plants, which were grown under red-blue short-day (RB, SD) and red-blue short days extended to long days with blue light (RB + B, LD) reached the floral initiation within 14 days from the start of the light treatment, while the plants that were grown under red-blue short-days extended with red light (RB + R, LD) reached the final floral initiation stage 5–6 days later (**Figure 5B**). Plants grown under 11 h red-blue extended with 4 h blue succeeded in attaining visible bud stage in 22–23 days, which was only 1–2 days later than in red-blue short-day (**Figures 5B, 6C**) and produced the same number of flower buds as plants grown under red-blue short-day (**Figure 5D**). Flower buds of RB, SD and RB + B, LD plants weighed almost equal (**Figure 5H**). All plants, which were grown under short-day (red-blue and solar light) and blue extended long-day (RB + B, LD) recorded 100% flowering (**Figures 5E,F**).

Plant Morphology and Growth Under Red and Blue Extended Long-Days

In the greenhouse experiment, stem length was higher in plants that were grown under solar light extended with blue

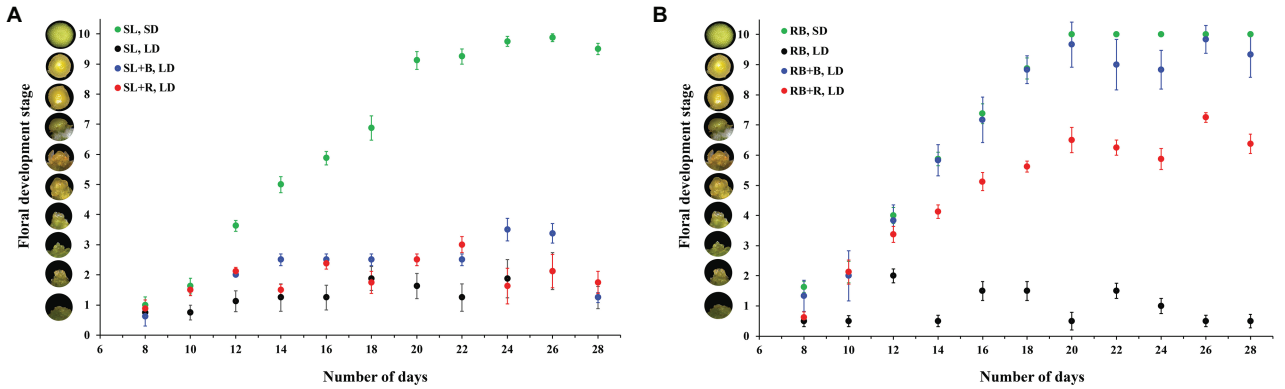

FIGURE 4 | Effect of different light treatments on floral initiation of *Chrysanthemum morifolium* cv. Radost. Floral initiation and development of shoot apical meristem in greenhouse **(A)** and climate room **(B)** scored as per the floral developmental stages of Chrysanthemum (see the **Figure 3**), stage 6 is considered as floral initiation attainment [data are represented as mean ± SE (n = 8)].

light (SL + B, LD) than under solar light short-day (SL, SD) and solar light extended with red light (SL + R, LD; **Figure 7A**). The number of internodes and leaves was higher in solar light long-day treatments compared to solar light short-day and solar light extended with 4 h of either blue or red light treatments (**Figure 7C**). Plants grown under 15 h long-day solar light photoperiod had a larger leaf area compared to 11 h short-day photoperiod (**Figure 7E**). Under 15 h solar light, the specific leaf area was lower than under solar light short-day and solar light extended with 4 h of either blue or red light treatments (**Figure 7E**). The total dry weight did not exhibit a significant difference between solar light short-day and photoperiods extended by red and blue, but plants grown under solar light LD had higher total dry weight (**Figure 7G**).

Some of the morphological responses were slightly different between the greenhouse and the climate chamber experiments. Increasing the photoperiod from 11 h sole source red-blue light to 15 h always resulted in an increased stem length, as was also observed in the greenhouse experiment, but the contrasts among the long-day treatments differed from the results obtained in the greenhouse (**Figure 7B**). The number of internodes and leaves in the blue and red extended long-day treatments (RB + R, LD and RB + B, LD) was not lower than in the short-day (RB, SD) treatment (**Figure 7D**), as was the case in the greenhouse experiment under solar light. In the climate chamber, only the extension of the day with red-blue light resulted in a larger leaf area (RB, LD; **Figure 7F**), whereas in the greenhouse experiment leaf area increased in all long-day treatments compared to the short-day treatment. Specific leaf area showed similar responses as in the greenhouse experiment and was lower in the short-day treatment than the long-day treatments. Similar to the greenhouse experiment, the only long-day treatment with a higher total dry weight at harvest was the normal long-day (RB, LD), but the relative increase was larger than in the greenhouse (**Figure 7H**).

DISCUSSION

Growing short-day chrysanthemum in 11 h of red-blue extended with 4 h of monochromatic blue (100% artificial light) resulted in flowering despite the 15 h long photoperiod (**Figures 5B, 6C,D**). This confirms the earlier study by our lab (Jeong et al., 2014). However, plants grown in a greenhouse under 11 h of solar light extended with 4 h of monochromatic blue or red light failed to flower (**Figures 5A, 6A,B**). This could have been due to several aspects that differed in the light climates between the growth chamber and greenhouse, among which differences in light intensity and differences in spectral composition of the light received by the plants during light periods before the day-length extension (the first 11 h of each light period).

Last decade, important steps were made in unraveling molecular mechanisms underlying photoperiodic flowering in Chrysanthemum: altered light signals influence the signal transduction pathway of important flower regulatory genes in *Chrysanthemum morifolium* (floral inhibiting antiflorigen *CmAFT* and floral stimulating florigen *CmFTL3*) of which the expression levels are clock regulated, daylength dependent, and control photoperiodic flowering (Oda et al., 2012; Higuchi et al., 2013). Much of this progress is the result of loss-of-function studies in the diploid *C. seticuspe*, which is much easier to transform, than the hexaploid *C. morifolium* that is commonly used in commercial production of chrysanthemum. However, even in *C. seticuspe*, it is still largely uncertain, how *CsFTL3* and *CsAFT* are regulated by light to define the critical night length for flowering (Oda et al., 2020).

Potential Effects of Light Intensity Differences Between Greenhouse and Growth Chamber

An adequate carbon supply is vital for developmental transitions, such as flowering in plants, and can be sensed through sugar signaling (Wingler, 2018). In Arabidopsis, for instance, trehalose-6-phosphate (T6P) is involved in sugar

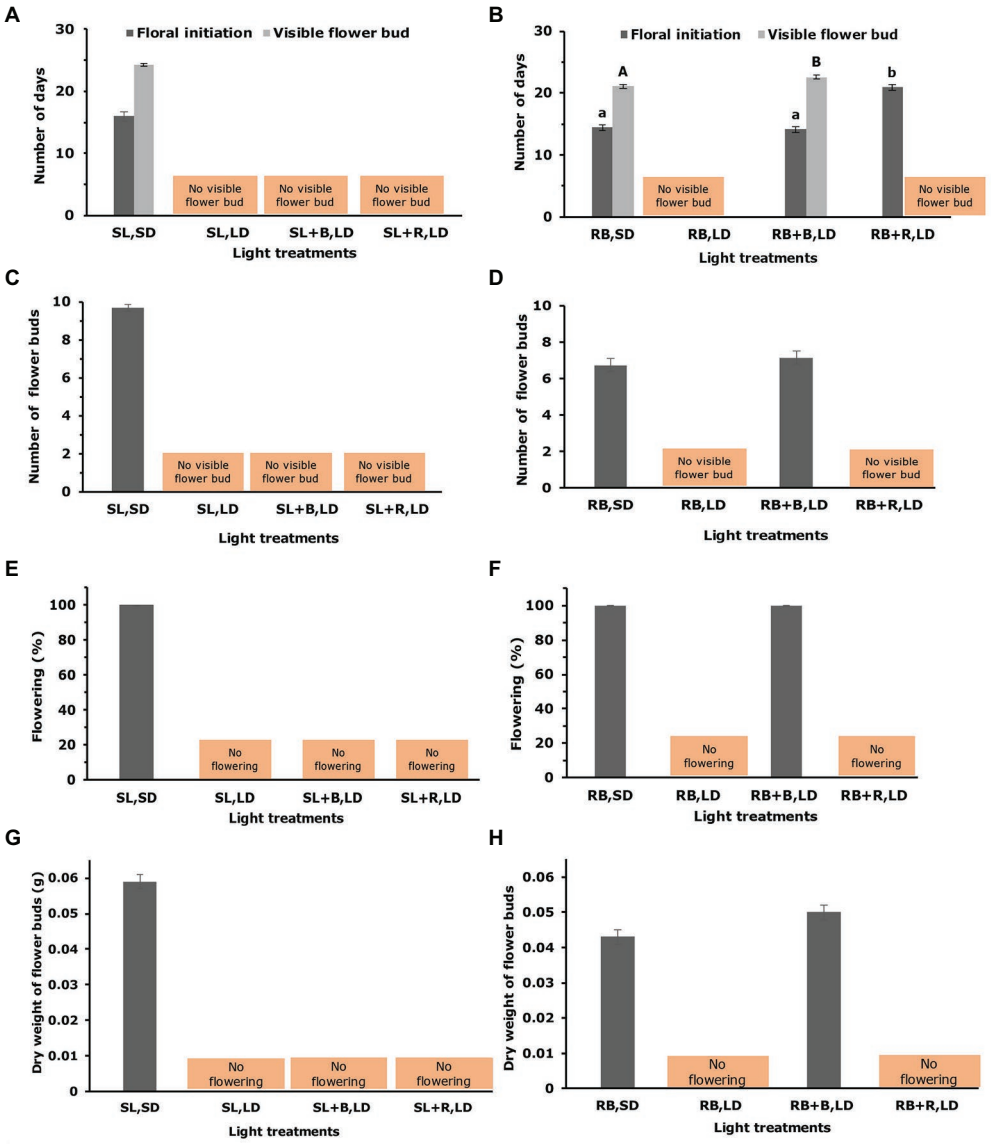

FIGURE 5 | Effect of different light treatments on flowering response of *Chrysanthemum morifolium* cv. Radost. Number of days until floral initiation and visible flower buds **(A,B)**; number of flower buds per plant **(C,D)**; percentage of flowering plants **(E,F)**; dry weight of flower buds **(G,H)** on the 42th day after start of light treatments. Panel **(A,C,E,G)** under solar light in greenhouse experiment and panel **(B,D,F,H)** under sole source red-blue LEDs lighting in growth chamber experiment [data are represented as mean ± SE (n = 10)]. Different letters indicate that means differed significantly (Fisher's Protected LSD test, p = 0.05). No letters indicate that means not differed significantly. Light treatment label details: see **Figure 1**.

status sensing and also required for the expression of FT and flowering (Wahl et al., 2013). Differences in light intensity between the growth chamber and greenhouse experiments influencing carbon availability to the plants might therefore be important. Other than in the growth chamber experiment, the light intensity in the greenhouse varied with natural solar light over and between the days (see **Supplementary Material**). The daily light integrals of photosynthetic active radiation (DLI) outside the greenhouse were much higher than the DLIs in the growth chamber, but due to the low transmissivity of the research greenhouse, and the use of light screens to avoid stray light between plots, light intensity in the greenhouse plots was strongly reduced. Because the overall transmissivity variated with the changing angle of incidence of solar radiation over the day, it is impossible to estimate DLIs at plant level from the outside radiation measurements. Incidental measurements in the greenhouse plots, conducted around noon, yielded light intensities that were slightly higher than those in the growth chamber plots (results not shown). However, based on the almost similar dry weight of the plants after 42 days of growth in the SD-treatments in the greenhouse and in the

FIGURE 6 | Flower buds **(A,C)** and flower capitulum **(B,D)** of *Chrysanthemum morifolium* cv. Radost on 25 **(A,C)** and 55 **(B,D)** days after start of eight different light treatments at different photoperiods and spectral composition. Panel **(A,B)** under solar light (SL) in greenhouse experiment and panel **(C,D)** sole source red-blue LEDs lighting (RB) in growth chamber. The label in each image denotes the specific light treatment, with comparable daylength and spectral composition (in case of daylength extension) in the same column.

growth chamber (**Figures 7G,H**), it is reasonable to assume that the total light integrals in the growth chamber and greenhouse experiment were not very different. It is well-known that low light integral delays flower initiation and retards flower development in chrysanthemum. Langton (1992) showed that the number of inductive SD's required for flowering exponentially increases below 4.6–6.9 mol PAR m^{-2} d^{-1} (depending on cultivar). The light integral in the growth chamber SD-treatment was approximately 4 mol PAR m^{-2} d^{-1}. Therefore, the very small difference in days until floral initiation between plants in the SD-treatments in greenhouse and growth chamber (**Figures 5A,B**) also indicate a not more than small difference in light integral. How low light integrals influence the timing of flowering in chrysanthemum still needs to be elucidated. It has been indicated by RNA-sequencing that sugar sensing through T6P might be involved in flowering of the summer-flowering chrysanthemum variety "Yuuka," which flowers under SD and LD, though only under LDs (Ren et al., 2016). Later experiments with sucrose application on leaves supported this restriction to LDs, while in a strict SD-flowering variety, no effect of sucrose application on leaves on flowering was observed (Sun et al., 2017). Taking this all together, it is not very likely that there were substantial differences in light integral between the growth chamber and greenhouse experiments in the present study. Light integrals were low, but not that low that they strongly influenced the time to flowering. Additionally, the strong differences in response to the B-extended long days, with flowering in the growth chamber and no flowering in the greenhouse, occurred at substantially higher light integrals than in the SD-treatments, which both flowered.

Flowering of Chrysanthemum in Long Photoperiods With Diurnal Spectra Variations

Previously it has been shown in chrysanthemum, that the light spectrum during a short photoperiod can strongly influence and even reverse the effectiveness of night-break of a certain color: blue or far-red night-breaks were effective in inhibiting flowering when plants were grown under a short photoperiod with monochromatic blue light, but not when they were applied after a short photoperiod with white light (Higuchi et al., 2012). Blue light increases the fraction of deactivated phytochrome similar to far-red (Sager et al., 1988). In the same study (Higuchi et al., 2012), the effect of far-red during

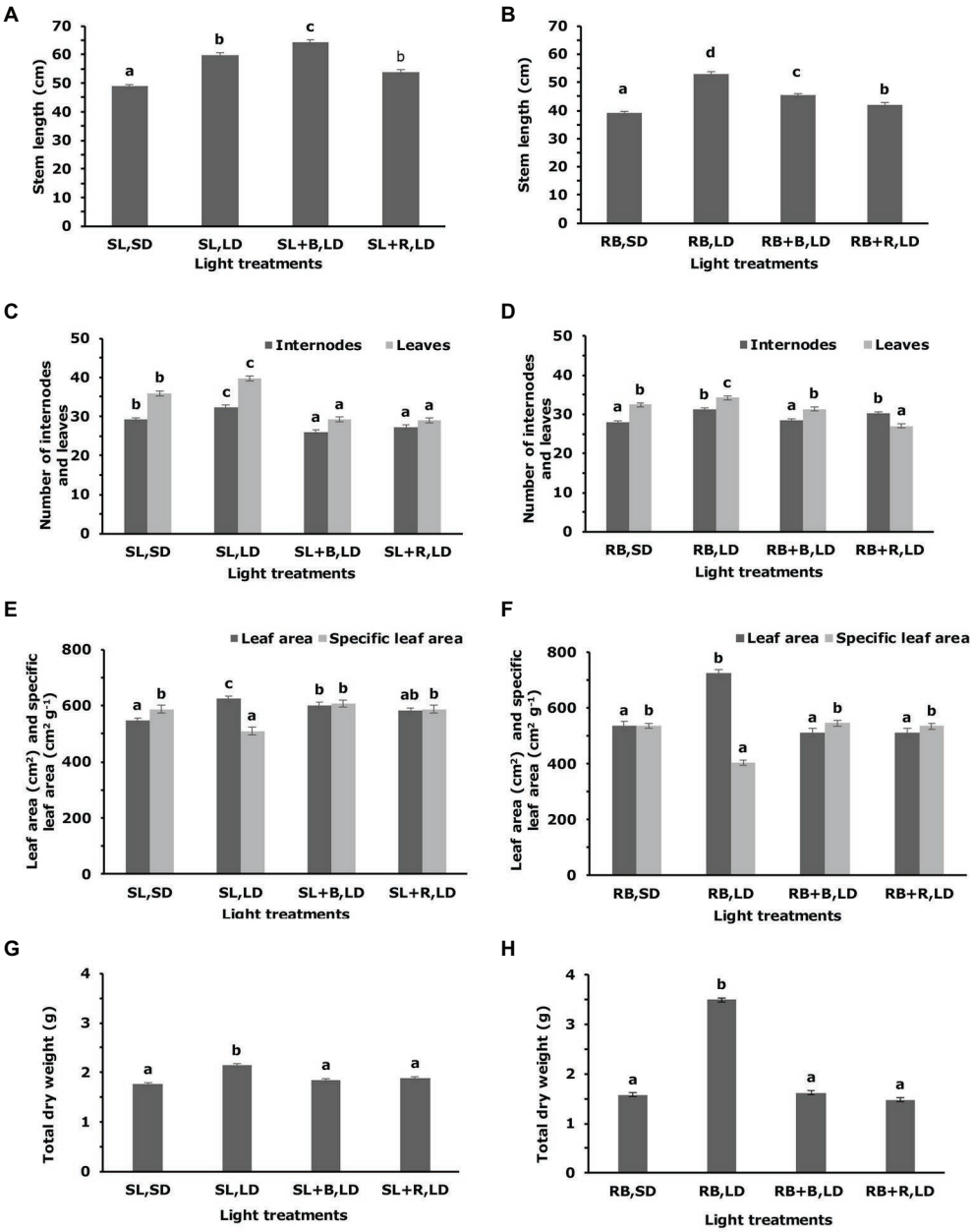

FIGURE 7 | Effect of spectrally different daylength extensions on plant growth of *Chrysanthemum morifolium* cv. Radost in a greenhouse and growth chamber. Stem length **(A,B)**; number of internodes and leaves **(C,D)**; leaf area and specific leaf area **(E,F)**; total dry weight **(G,H)**; on the 42th day after start of light treatments. Panel **(A,C,E,G)** under solar light in greenhouse experiment and panel **(B,D,F,H)** under sole source re-blue LEDs lighting in growth chamber experiment [data are represented as mean ± SE (n = 10)]. Different letters indicate that means differed significantly (Fisher's Protected LSD test, p = 0.05). Light treatment label details: see **Figure 1**.

night-break was exposure-time dependent and night-breaks with blue or far-red became ineffective in the inhibition of flowering when short day light spectrum was a mixture of red and blue light. Therefore, these authors suggested a role of at least two phytochromes (PHYA and PHYB) in the regulation of flowering in Chrysanthemum, but at the same time could not exclude a role for cryptochromes.

Interestingly, we observed that 11 h of red-blue daylight extended with 4 h of red triggered floral initiation, but that further capitulum development was arrested (**Figures 4B, 5B**), while a daylength extension with red in the greenhouse showed no stimulation of floral initiation at all (SL + R, LD). This shows, similar to comparing blue extended long days in climate room and greenhouse, that the light spectrum during the first

11 h of the day period influences the effect of the light spectrum after the first 11 h on flower initiation.

A large difference between solar light in the greenhouse and red-blue LEDs in the growth chamber during the first 11 h of the photoperiod is the lack of green and far-red wavelengths in the LED-lighting. It may therefore be well possible that this lack of green and/or far-red is responsible for the different flowering responses in the growth chamber experiments compared to the greenhouse. Green light can influence the photoperiodic flowering of long-day and short-day plants (as reviewed by Zhang and Folta, 2012). The inhibitory effect of green light on flowering was shown by delivering green as a night-break in many short-day plants such as *Cosmos bipinnatus, Perilla ocymoides*, *Abelmoschus esculentus* and *Abelmoschus moschatus* ssp. *tuberosus* (Hamamoto et al., 2003; Hamamoto and Yamazaki, 2009), and chrysanthemum (Sumitomo et al., 2012). Likewise, chrysanthemum grown under a 12 h white fluorescent light photoperiod extended with 4 h of green (518 nm) failed to flower (Jeong et al., 2012). Green light responses might be mediated by blue sensing cryptochromes (Zhang and Folta, 2012; Smith et al., 2017). In *Arabidopsis*, plants grown under simultaneous blue-green failed to flower, because the presence of green nullified the strong blue-induced flowering by reducing the *FT* levels. Green light reversed the blue-induced floral induction by CRY2 degradation and suppressing *FT* expression in *Arabidopsis* (Banerjee et al., 2007). In chrysanthemum, a 30 min night-break with green (530 nm) light delayed flowering by 17 days compared to short-day by suppressing the expression of *CmFTL3* (Sumitomo et al., 2012). As of yet, it is not clear whether the presence of green light during the daylight spectrum interferes with the possible promotive effects of 4 h of blue light day extension in chrysanthemum.

Another possible reason for non-flowering under short-days with solar light extended with either blue or red light could be a high fraction of far-red, during the photoperiod. Similar flowering inhibition due to higher far-red (735 nm) light at the end of the day was reported in short-day plants, *Phabitis nil* (Fredericq, 1964) and rice (Ikeda, 1985). Far-red at the end of the day may be responsible for non-flowering due to altered phytochrome state. The inhibitory action of far-red light may be associated with the lowered level of phytochrome P_{fr} that is essential to start the dark reactions responsible in triggering the floral induction. In other terms, a high P_{fr} is needed for floral stimuli/florigen during inductive darkness (Higuchi et al., 2012). This inhibitory effect of far-red light was reported in other short-day plants such as duckweed (*Lemna paucicostata*) and *Xanthium pennsylvanicum* (Salisbury, 1965; Ohtani and Ishiguri, 1979). From our study, short-days of natural full-spectrum daylight followed by 4 h blue or red day extension was obviously not enough to increase the amount of P_{fr} to stop floral inhibition. It can thus be suggested that the relative amounts of green or far-red during the daily photoperiod can possibly influence flowering genes to regulate photoperiodic flowering under solar light extended with 4 h of blue or red day extension. Thus, chrysanthemum appears to be particularly sensitive to the spectral composition of 11 h of daylight to flower under blue or red extended long-days. The present study suggests that, besides daylength, the spectral composition of the short-day photoperiod also influences the flowering responses.

Growth and Morphology of Chrysanthemum in Long Photoperiods With Diurnal Spectra Variations

Extending the day with blue light promoted stem length due to internode elongation (**Figures 7A,B**), in agreement with Jeong et al. (2014). Similar effects of narrow-band blue light on stem elongation have been reported in other species such as petunia, salvia, and marigold (Heo et al., 2002; Fukuda et al., 2016). Narrow-band blue light is seen as a strong signal in enhancing shoot elongation, through modulation of gibberellin content (Fukuda et al., 2016). Stem elongation is strongly correlated with both internode appearance rate and internode elongation (Carvalho et al., 2002). Plants that were grown under short photoperiods (solar and red-blue) were shorter than their long-photoperiod counterparts in both growth environments (greenhouse and growth chamber). The length difference was caused by a lower number of internodes due to floral initiation, whereas average internode length was not affected (results not shown). The lower stem length in the RB + B, LD treatment compared to the RB long-day treatment can also be explained by a lower number of internodes due to flowering (**Figures 7B,D**) because the shift of the vegetative shoot apical meristem into a floral meristem stops the initiation of new leaves and new internodes on the main stem. Day-length extensions with R and B increased stem length compared to SDs in both the greenhouse and growth chamber experiments due to effects on internode elongation alone (**Figures 7A,B**), as in all day-extension treatments the number of internodes per stem remained similar (after 11 h RB) or even slightly decreased (after 11 h of SL).

Longer photoperiods increase the daily available light for the plant, which enhances total dry weight as observed under 15 h of solar light and red-blue long-day photoperiod (**Figures 7G,H**). These results are consistent with Kurilčik et al. (2008), who reported a continuous increase in dry weight and leaf number in chrysanthemum with increased photoperiod duration from 8 to 24 h. In contrast, to the observations made by Jeong et al. (2014) present results do not show a significant positive effect on dry weight in the blue extended long-day treatments, most likely due to the lower intensity of blue during day extension in present experiment. Similarly, stem length (an important quality attribute of chrysanthemum cut flower) differed between red-blue short-days and blue extended long-days (Jeong et al., 2014). Higher growth rate is often achieved by an increase in the net assimilation rate (Adams and Langton, 2005). Therefore, plants grown under red-blue long-day photoperiod showed higher total dry weight and leaf area compared to red-blue short-day and red-blue extended with either 4 h of blue or red (**Figures 7G,H**). This is most likely because plants under red-blue extension received a higher PPFD of 100 $\mu mol\, m^{-2}\, s^{-1}$ compared to 40 $\mu mol\, m^{-2}\, s^{-1}$ under 4 h of blue during daylight extension. Additionally, mixed red-blue light is known to increase total dry weight and leaf area in

plants by increasing the net assimilation rate, compared to that by monochromatic blue or red light (Kim et al., 2004).

CONCLUSION

Sole source red-blue short-day extended with 4 h of sole blue resulted in complete flowering, while extension with 4 h of sole red resulted in floral initiation but no further flower development took place. In contrast, plants in solar light short-day extended with 4 h of blue or red light failed to flower. Our results show that, besides photoperiod, the spectral composition of the short-day part of the photoperiod influences the effect of the light spectrum thereafter on flowering. This limits the application of blue daylength extension in commercial greenhouse production of chrysanthemum. However, the smart use of LED-light opens up new avenues for a more efficient year round production of short-day plants in vertical farms or plant factories that operate without solar light.

Taken together, multiple components of the daylight spectrum may influence the mechanism of photoperiodic flowering in chrysanthemum in a time-dependent manner. Furthermore, more fundamental knowledge is needed about diurnal effects of light quality on the cascade of processes (from floral evocation to anthesis) to fully take advantage of the possibilities of LEDs in plant production systems. For this, the involvement of photoreceptors in the molecular framework of flowering regulatory genes such as florigen (*CmFTL3*) and antiflorigen (*CmAFT*) needs to be elucidated.

This study shows that not only day-length *per se* but also the spectral composition of the first 11 h of a long photoperiod influences the flowering responses in chrysanthemum.

DATA AVAILABILITY STATEMENT

The raw data supporting the conclusions of this article will be made available by the authors, without undue reservation.

AUTHOR CONTRIBUTIONS

WI, EH, MS, and LM conceptualized the research idea and designed the experiments. MS performed the experiments and wrote the first version of the manuscript. MS, EH, and WI performed data analysis and all authors discussed the results and the interpretation of the data. MS, EH, and WI revised the manuscript according to the helpful comments of the reviewers. All authors contributed to the article and approved the submitted version.

FUNDING

This work was partly funded by Deliflor Chrysanten B.V, Netherlands and Government of Karnataka, India for PhD fellowship.

ACKNOWLEDGMENTS

We thank Geert van Geest, Robert Stoker, and Aike Post of Deliflor for the fruitful discussions and kindly providing chrysanthemum plant material. For technical assistance in SAMs imaging the authors like to acknowledge dr NCA de Ruijter from the Wageningen Light Microscopy Centre at the Laboratory of Cell Biology of Wageningen University and Research. We also thank the technical staff of Klima: Taede Stoker, Gerrit Stunnenberg, and David Brink at Wageningen University and Research. Furthermore, MSc thesis students Paul Poullaidis and Xun Su for participating in the experimental work.

SUPPLEMENTARY MATERIAL

The Supplementary Material for this article can be found online at: https://www.frontiersin.org/articles/10.3389/fpls.2020.610041/full#supplementary-material

REFERENCES

Adams, S. R., and Langton, F. A. (2005). Photoperiod and plant growth: a review. *J. Hortic. Sci. Biotechnol.* 80, 2–10. doi: 10.1080/14620316.2005.11511882.

Andrés, F., and Coupland, G. (2012). The genetic basis of flowering responses to seasonal cues. *Nat. Rev. Genet.* 13, 627–639. doi: 10.1038/nrg3291

Banerjee, R., Schleicher, E., Meier, S., Viana, R. M., Pokorny, R., Ahmad, M., et al. (2007). The signaling state of Arabidopsis cryptochrome 2 contains flavin semiquinone. *J. Biol. Chem.* 282, 14916–14922. doi: 10.1074/jbc.M700616200

Borthwick, H. A., and Cathey, H. M. (1962). Role of phytochrome in control of flowering of chrysanthemum. *Bot. Gaz.* 123, 155–162. doi: 10.1086/336143

Borthwick, H. A., Hendricks, S. B., and Parker, M. W. (1952). The reaction controlling floral initiation. *Proc. Natl. Acad. Sci. U. S. A.* 38, 929–934. doi: 10.1073/pnas.38.11.929

Carvalho, S. M. P., Heuvelink, E., Cascais, R., and Van Kooten, O. (2002). Effect of day and night temperature on internode and stem length in chrysanthemum: is everything explained by DIF? *Ann. Bot.* 90, 111–118. doi: 10.1093/aob/mcf154

Cathey, M., and Borthwick, H. A. (1957). Photoreversibility of floral initiation in chrysanthemum. *Bot. Gaz.* 119, 71–76. doi: 10.1086/335964

Cerdán, P. D., and Chory, J. (2003). Regulation of flowering time by light quality. *Nature* 423, 881–885. doi: 10.1038/nature01636

Cho, L. H., Yoon, J., and An, G. (2017). The control of flowering time by environmental factors. *Plant J.* 90, 708–719. doi: 10.1111/tpj.13461

Craig, D. S., and Runkle, E. S. (2013). A moderate to high red to far-red light ratio from light-emitting diodes controls flowering of short-day plants. *J. Am. Soc. Hortic. Sci.* 138, 167–172. doi: 10.21273/jashs.138.3.167.

Downs, R. J. (1956). Photoreversibility of flower initiation. *Plant Physiol.* 31, 279–284. doi: 10.1104/pp.31.4.279

Fredericq, H. (1964). Conditions determining effects of far-red and red irradiations on flowering response of Pharbitis nil. *Plant Physiol.* 39, 812–816. doi: 10.1104/pp.39.5.812

Fukuda, N., Ajima, C., Yukawa, T., and Olsen, J. E. (2016). Antagonistic action of blue and red light on shoot elongation in petunia depends on gibberellin, but the effects on flowering are not generally linked to gibberellin. *Environ. Exp. Bot.* 121, 102–111. doi: 10.1016/j.envexpbot.2015.06.014

Garner, W. W., and Allard, H. A. (1920). Agricultural United States Department of Agriculture and for the association. *J. Agric. Res.* XVIII, 553–606.

Goto, N., Kumagai, T., and Koornneef, M. (1991). Flowering responses to light-breaks in photomorphogenic mutants of *Arabidopsis thaliana*, a long-day plant. *Physiol. Plant.* 83, 209–215. doi: 10.1111/j.1399-3054.1991.tb02144.x

Guo, H., Yang, H., Mockler, T. C., and Lin, C. (1998). Regulation of flowering time by *Arabidopsis* photoreceptors. *Science* 279, 11360–11363. doi: 10.1126/science.279.5355.1360.

Hamamoto, H., Shimaji, H., and Higashide, T. (2003). Budding and bolting responses of horticultural plants to night-break treatments with LEDs of various colors. *J. Agric. Meterol.* 59, 103–110. doi: 10.2480/agrmet.59.103

Hamamoto, H., and Yamazaki, K. (2009). Reproductive response of okra and native rosella to long-day treatment with red, blue, and green light-emitting diode lights. *HortScience* 44, 1494–1497. doi: 10.21273/HORTSCI.44.5.1494

Heo, J., Lee, C., Chakrabarty, D., and Paek, K. (2002). Growth responses of marigold and salvia bedding plants as affected by monochromic or mixture radiation provided by a light-emitting diode (LED). *Plant Growth Regul.* 38, 225–230. doi: 10.1023/A:1021523832488

Higuchi, Y. (2018). Florigen and anti-florigen: flowering regulation in horticultural crops. *Breed. Sci.* 68, 109–118. doi: 10.1270/jsbbs.17084

Higuchi, Y., Narumi, T., Oda, A., Nakano, Y., Sumitomo, K., Fukai, S., et al. (2013). The gated induction system of a systemic floral inhibitor, antiflorigen, determines obligate short-day flowering in chrysanthemums. *Proc. Natl. Acad. Sci. U. S. A.* 110, 17137–17142. doi: 10.1073/pnas.1307617110

Higuchi, Y., Sumitomo, K., Oda, A., Shimizu, H., and Hisamatsu, T. (2012). Day light quality affects the night-break response in the short-day plant chrysanthemum, suggesting differential phytochrome-mediated regulation of flowering. *J. Plant Physiol.* 169, 1789–1796. doi: 10.1016/j.jplph.2012.07.003

Hisamatsu, T., Sumitomo, K., and Shimizu, H. (2008). End-of-day far-red treatment enhances responsiveness to gibberellins and promotes stem extension in chrysanthemum. *J. Hortic. Sci. Biotechnol.* 83, 695–700. doi: 10.1080/14620316.2008.11512446.

Horridge, J. S., and Cockshull, K. E. (1989). The effect of the timing of a night-break on flower initiation in *Chrysanthemum morifolium* Ramat. *J. Hortic. Sci* 64, 183–188. doi: 10.1080/14620316.1989.11515943.

Ikeda, K. (1985). Photoperiodic flower induction in rice plants as influenced by light intensity and quality. *JARQ. Japan Agric. Res. Q.* 18, 164–170.

Ishikawa, R., Shinomura, T., Takano, M., and Shimamoto, K. (2009). Phytochrome dependent quantitative control of Hd3a transcription is the basis of the night breakeffect in rice flowering. *Genes Genet. Syst.* 84, 179–184. doi: 10.1266/ggs.84.179

Jeong, S. W., Hogewoning, S. W., and van Ieperen, W. (2014). Responses of supplemental blue light on flowering and stem extension growth of cut chrysanthemum. *Sci. Hortic.* 165, 69–74. doi: 10.1016/j.scienta.2013.11.006

Jeong, S. W., Park, S., Jin, J. S., Seo, O. N., Kim, G. S., Kim, Y. H., et al. (2012). Influences of four different light-emitting diode lights on flowering and polyphenol variations in the leaves of chrysanthemum (*Chrysanthemum morifolium*). *J. Agric. Food Chem.* 60, 9793–9800. doi: 10.1021/jf302272x

Johansson, M., and Staiger, D. (2015). Time to flower: interplay between photoperiod and the circadian clock. *J. Exp. Bot.* 66, 719–730. doi: 10.1093/jxb/eru441

Kadman-Zahavi, A., and Ephrat, E. (1971). Phytochrome effects in night-break illuminations on flowering of chrysanthemum. *Physiol. Plant.* 25, 90–93. doi: 10.1111/j.1399-3054.1971.tb01094.x

Kadman-Zahavi, A., and Ephrat, E. (1973). Effect of red and far-red illuminations at the end of short days and their interaction with night-break illuminations, on flowering of *Chrysanthemum morifolium* plants. *Plant Cell Physiol.* 14, 409–411. doi: 10.1093/oxfordjournals.pcp.a074873.

Kim, S., Hahn, E., Heo, J., and Paek, K. (2004). Effects of LEDs on net photosynthetic rate, growth and leaf stomata of chrysanthemum plantlets in vitro. *Sci. Hortic.* 101, 143–151.

Kim, H. H., Heins, R. D., and Carlson, W. H. (2002). Development and flowering of petunia grown in a far-red deficient light environment. *Acta Hortic.* 580, 127–135. doi: 10.17660/ActaHortic.2002.580.15.

Kurilčik, A., Miklušytė-čanova, R., Dapkūnienė, S., Žilinskaitė, S., Kurilčik, G., Tamulaitis, G., et al. (2008). *In vitro* culture of *Chrysanthemum* plantlets using light-emitting diodes. *Cent. Eur. J. Biol.* 3, 161–167.

Lane, H. C., Cathey, H. M., and Evans, L. T. (1965). The dependence of flowering in several long-day plants on the spectral composition of light extending the photoperiod. *Am. J. Bot.* 52:1006. doi: 10.1002/j.1537-2197.1965.tb07278.x

Langton, F. A. (1992). Interrupted lighting of chrysanthemums: monitoring of average daily light integral as an aid to timing. *Sci. Hortic.* 49, 147–157. doi: 10.1016/0304-4238(92)90151-2

Liao, Y., Suzuki, K., Yu, W., Zhuang, D., Takai, Y., Ogasawara, R., et al. (2014). Night break effect of led light with different wavelengths on floral bud differentiation of *Chrysanthemum morifolium* ramat "jimba" and "iwa no hakusen." *Environ. Control. Biol.* 52, 45–50. doi: 10.2525/ecb.52.45

Lopez, R. G., Meng, Q., and Runkle, E. S. (2020). Blue radiation signals and saturates photoperiodic flowering of several long-day plants at crop-specific photon flux densities. *Sci. Hortic.* 271, 2–6. doi: 10.1016/j.scienta.2020.109470.

Oda, A., Higuchi, Y., and Hisamatsu, T. (2020). Constitutive expression of CsGI alters critical night length for flowering by changing the photo-sensitive phase of anti-florigen induction in chrysanthemum. *Plant Sci.* 293:110417. doi: 10.1016/j.plantsci.2020.110417

Oda, A., Narumi, T., Li, T., Kando, T., Higuchi, Y., Sumitomo, K., et al. (2012). CsFTL3, a chrysanthemum FLOWERING LOCUS T-like gene, is a key regulator of photoperiodic flowering in chrysanthemums. *J. Exp. Bot.* 63, 1461–1477. doi: 10.1093/jxb/err387

Ohtani, T., and Ishiguri, Y. (1979). Inhibitory action of blue and far-red light in the flowering of *Lemna paucicostata*. *Physiol. Plant.* 47, 255–259. doi: 10.1111/j.1399-3054.1979.tb06523.x

Park, Y. G., and Jeong, B. R. (2020). Both the quality and positioning of the night interruption light are important for flowering and plant extension growth. *J. Plant Growth Regul.* 39, 583–593. doi: 10.1007/s00344-019-10002-5

Ren, L., Liu, T., Cheng, Y., Sun, J., Gao, J., Dong, B., et al. (2016). Transcriptomic analysis of differentially expressed genes in the floral transition of the summer flowering chrysanthemum. *BMC Genomics* 17:673. doi: 10.1186/s12864-016-3024-4

Runkle, E. S., and Heins, R. D. (2001). Specific functions of red, far red, and blue light in flowering and stem extension of long-day plants. *J. Am. Soc. Hortic. Sci.* 126, 275–282. doi: 10.21273/JASHS.126.3.275

Runkle, E. S., and Heins, R. D. (2003). Photocontrol of flowering and extension growth in the long-day plant pansy. *J. Am. Soc. Hortic. Sci.* 128, 479–485. doi: 10.21273/JASHS.128.4.0479

Sager, J. C., Smith, W. O., Edwards, J. L., and Cyr, K. L. (1988). Photosynthetic efficiency and phytochrome photoequilibria determination using spectral data. *Trans. ASAE* 31, 1882–1889.

Salisbury, F. B. (1965). Time measurement and the light period in flowering. *Planta* 26, 1–26.

Smith, H. L., Mcausland, L., and Murchie, E. H. (2017). Don't ignore the green light: exploring diverse roles in plant processes. *J. Exp. Bot.* 68, 2099–2110. doi: 10.1093/jxb/erx098

Song, Y. H., Shim, J. S., Kinmonth-Schultz, H. A., and Imaizumi, T. (2015). Photoperiodic flowering: time measurement mechanisms in leaves. *Annu. Rev. Plant Biol.* 66, 441–464. doi: 10.1146/annurev-arplant-043014-115555

Song, Y. H., Smith, R. W., To, B. J., Millar, A. J., and Imaizumi, T. (2012). FKF1 conveys timing information for CONSTANS stabilization in photoperiodic flowering. *Science* 1045, 1045–1050. doi: 10.1126/science.1219644

Srikanth, A., and Schmid, M. (2011). Regulation of flowering time: all roads lead to Rome. *Cell. Mol. Life Sci.* 68, 2013–2037. doi: 10.1007/s00018-011-0673-y

Sumitomo, K., Higuchi, Y., Aoki, K., Miyamae, H., Oda, A., Ishiwata, M., et al. (2012). Spectral sensitivity of flowering and FT-like gene expression in response to night-break light treatments in the chrysanthemum cultivar, "Reagan". *J. Hortic. Sci. Biotechnol.* 87, 461–469. doi: 10.1080/14620316.2012.11512896.

Sun, J., Wang, H., Ren, L., Chen, S., Chen, F., and Jiang, J. (2017). CmFTL2 is involved in the photoperiod- and sucrose-mediated control of flowering time in chrysanthemum. *Hort. Res.* 4:17001. doi: 10.1038/hortres.2017.1

Thomas, B. (2006). Light signals and flowering. *J. Exp. Bot.* 57, 3387–3393. doi: 10.1093/jxb/erl071

Thomas, B., and Vince-Prue, D. (1996). *Daylength perception in short-day plants. 2nd Edn*. London: Academic Press.

van Haeringen, C. J., West, J. S., Davis, F. J., Gilbert, A., Hadley, P., Pearson, S., et al. (1998). The development of solid spectral filters for the regulation of plant growth. *Photochem. Photobiol.* 67:407. doi: 10.1111/j.1751-1097.1998.tb05219.x

Viczián, A., Ádám, É., Staudt, A. M., Lambert, D., Klement, E., Romero Montepaone, S., et al. (2020). Differential phosphorylation of the N-terminal extension regulates phytochrome B signaling. *New Phytol.* 225, 1635–1650. doi: 10.1111/nph.16243

Vince, D. (1965). The promoting effect of far-red light on flowering in the long day plant *Lolium temulentum*. *Physiol. Plant.* 18, 474–482. doi: 10.1111/j.1399-3054.1965.tb06910.x

Wahl, V., Ponnu, J., Schlereth, A., Arrivault, S., Langenecker, T., Franke, A., et al. (2013). Regulation of flowering by Trehalose-6-phosphate signaling in *Arabidopsis thaliana*. *Science* 339, 704–707. doi: 10.1126/science.1230406

Wingler, A. (2018). Transitioning to the next phase: the role of sugar signaling throughout the plant life cycle. *Plant Physiol.* 176, 1075–1084. doi: 10.1104/pp.17.01229

Yamada, A., Tanigawa, T., Suyama, T., Matsuno, T., and Kunitake, T. (2011). Effects of red:far-red light ratio of night-break treatments on growth and flowering of *Eustoma grandiflorum* (Raf.) shinn. *Acta Hortic.* 907, 313–318. doi: 10.17660/ActaHortic.2011.907.51

Zhang, T., and Folta, K. M. (2012). Green light signaling and adaptive response. *Plant Signal. Behav.* 7, 1–4. doi: 10.4161/psb.7.1.18635.

Zhang, M., Park, Y., and Runkle, E. S. (2020). Regulation of extension growth and flowering of seedlings by blue radiation and the red to far-red ratio of sole-source lighting. *Sci. Hortic.* 272:109478. doi: 10.1016/j.scienta.2020.109478

Zhang, M., and Runkle, E. S. (2019). Regulating flowering and extension growth of poinsettia using red and far-red light-emitting diodes for end-of-day lighting. *HortScience* 54, 323–327. doi: 10.21273/HORTSCI13630-18

Conflict of Interest: The authors declare that the research was conducted in the absence of any commercial or financial relationships that could be construed as a potential conflict of interest.

Copyright © 2021 SharathKumar, Heuvelink, Marcelis and van Ieperen. This is an open-access article distributed under the terms of the Creative Commons Attribution License (CC BY). The use, distribution or reproduction in other forums is permitted, provided the original author(s) and the copyright owner(s) are credited and that the original publication in this journal is cited, in accordance with accepted academic practice. No use, distribution or reproduction is permitted which does not comply with these terms.

frontiers in Plant Science

ORIGINAL RESEARCH
published: 28 January 2021
doi: 10.3389/fpls.2021.615355

High Light Intensity Applied Shortly Before Harvest Improves Lettuce Nutritional Quality and Extends the Shelf Life

Qianxixi Min[1], Leo F. M. Marcelis[1], Celine C. S. Nicole[2] and Ernst J. Woltering[1,3]**

[1] Horticulture and Product Physiology Group, Wageningen University and Research, Wageningen, Netherlands, [2] Signify Research Laboratories, Eindhoven, Netherlands, [3] Food and Biobased Research, Wageningen University and Research, Wageningen, Netherlands

The effect of light intensity applied shortly before harvest on the nutritional quality, postharvest performance, and shelf life of loose-leaf lettuce (*Lactuca sativa* L. cv. Expertise RZ Salanova®) was investigated. Lettuce was grown either in a greenhouse with supplemental high-pressure sodium light (Experiment 1, EXP 1) or in a climate room under white LED light (Experiment 2, EXP 2). In both experiments full grown plants were transferred to a climate room for the End of Production (EoP) light treatments during the last week of cultivation. During EoP lighting plants were exposed to different intensities (0, 110, and 270 μmol m^{-2} s^{-1} in EXP 1; 50, 210, and 470 μmol m^{-2} s^{-1} in EXP 2) from white-red LEDs for 6 (EXP 2) or 7 days (EXP 1). Mature leaves were then harvested and stored in darkness at 10°C to study the postharvest performance. Changes in dry matter content, total ascorbic acid, and carbohydrates (including glucose, fructose sucrose, and starch) levels were determined during EoP lighting and during the subsequent shelf life as indicators of lettuce nutritional quality. Quality aspects (appearance, texture, and odor) were accessed during the shelf life as indicators of postharvest performance. In both experiments, high light intensities applied in EoP lighting increased dry matter percentage and contents of ascorbic acid (AsA) and carbohydrates at harvest and these increased levels were maintained during the shelf life. Increased light intensity in EoP treatment also extended the shelf life. The levels of AsA and carbohydrates at harvest correlated positively with the subsequent shelf life, indicating that the prolonged shelf life relies on the improved energy and antioxidant status of the crop at harvest.

Keywords: LED, lettuce, vertical farm, carbohydrates, ascorbic acid, overall visual quality, shelf life, End of Production lighting

OPEN ACCESS

Edited by:
Oliver Körner, Leibniz Institute of Vegetable and Ornamental Crops, Germany

Reviewed by:
Youssef Rouphael, University of Naples Federico II, Italy
Giedrė Samuolienė, Institute of Horticulture, Lithuanian Research Centre for Agriculture and Forestry, Lithuania

****Correspondence:***
Qianxixi Min
xixi.min@wur.nl;
xixi.minqian@gmail.com
Ernst J. Woltering
ernst.woltering@wur.nl

Specialty section:
This article was submitted to Crop and Product Physiology, a section of the journal Frontiers in Plant Science

Received: *08 October 2020*
Accepted: *12 January 2021*
Published: *28 January 2021*

Citation:
Min Q, Marcelis LFM, Nicole CCS and Woltering EJ (2021) High Light Intensity Applied Shortly Before Harvest Improves Lettuce Nutritional Quality and Extends the Shelf Life. Front. Plant Sci. 12:615355. doi: 10.3389/fpls.2021.615355

INTRODUCTION

Leafy vegetables generally have a short postharvest life due to mechanical damage and the lack of light during storage and transportation. Postharvest performance is related to both nutritional quality (measured as the levels of health and flavor related compounds) and sensorial quality (accessed as visual quality scores, texture, and odor). A negative nutritional image and

unattractive visual quality aspects decreases the shelf life and reduces consumer purchases of fresh products. Therefore, improving nutritional and visual quality is important for achieving a good postharvest performance.

Important nutritional elements and quality markers include the levels of carbohydrates (sucrose, fructose, glucose, and starch) and vitamin C. Carbohydrates may relate to the sensorial quality of leafy vegetables by providing sweeter or less bitter taste and delaying crop texture deterioration (shape and crispness) and discoloration (Lin et al., 2013; Hasperué et al., 2015). Vitamin C is defined as the total ascorbic acid (TAsA), which is the sum of ascorbic acid (AsA), and dehydroascorbic acid (DHA). TAsA is the major antioxidants group in leafy lettuce and is involved in balancing redox status and eliminating enzymatic pinking and browning. Hence, high levels of carbohydrates and TAsA are potentially beneficial for postharvest performance.

Both carbohydrates and TAsA levels are affected by light conditions (Ntagkas et al., 2018). The production of carbohydrates is directly related to the photosynthetic rate, which is dependent on light. Carbohydrates content at harvest significantly increases by increasing light levels during growth of leafy vegetables in both greenhouses and vertical farms (Zhou et al., 2009; Pérez-López et al., 2015). However, excess light during growth may also induce an unbalanced redox status (Zhou et al., 2009). In such a situation, TAsA is rapidly produced and acts as a strong antioxidant to scavenge the reactive oxygen species (ROS; Yabuta et al., 2007; Zhou et al., 2009, Zhou et al., 2012). Therefore, carbohydrates and TAsA levels can be increased by increasing light intensity during growth, which can potentially lead to a better postharvest performance of leafy vegetables.

Light exposure during the postharvest phase may also preserve plants nutritional quality and protects plants from visual quality deterioration (Büchert et al., 2011; Woltering and Witkowska, 2016). Postharvest lighting delayed sugars decrease, enlarged antioxidants capacity (accumulated AsA), delayed chlorophyll degradation, lowered the browning index and suppression of browning-related enzyme activities (polyphenol oxidase, PPO and peroxidase, POD) in leaves (Toledo et al., 2003; Zhan et al., 2012a,b, 2013; Hasperué et al., 2016b). However, postharvest lighting also stimulates stomata opening and may lead to loss of fresh weight and texture (Noichinda et al., 2007; Olarte et al., 2009; Hasperué et al., 2016a). If postharvest lighting has positive effects on quality of lettuce, it remains a question whether high light levels applied as End of Production (EoP) lighting can also promote postharvest quality. Lettuce harvested with improved initial quality may better resist unfavorable postharvest conditions and thus present a better postharvest performance.

The objective of this study was to investigate the effect of light treatments applied before harvest on postharvest performance in lettuce, as a representative crop of leafy vegetables. We tested two hypotheses: (1) short-term light treatment with high light intensity applied to the plants before harvest increases the carbohydrates and TAsA levels at harvest, and (2) the increased carbohydrates and TAsA levels at harvest improve postharvest visual and nutritional quality and extends the shelf life. To this end, full grown lettuce plants that were grown either in a greenhouse (EXP 1) or vertical farm (EXP 2) were subjected for up to 1 week to different EoP LED light intensities in a climate room. Lettuce leaves were sampled pre-harvest and during postharvest storage to measure the nutritional and sensorial quality traits (sucrose, fructose, glucose, starch, TAsA, and sonsorial arttrubutes) and to assess their shelf life (days till unacceptable quality).

MATERIALS AND METHODS

Plant Material and Cultivation Conditions

Lettuce Expertise (*Lactuca sativa* L. cv. Expertise RZ Salanova®) was grown either in a greenhouse (EXP 1, Wageningen, Netherland) or in a climate chamber (EXP 2, Eindhoven, Netherland) for approximately 5 weeks. In both experiments, approximately 1 week before commercial harvest, plants were transferred into a climate chamber for the EoP light treatment. The main cultivation conditions for both experiments are summarized in **Table 1**.

In EXP 1, seeds were sown in potting soil, given a 2-days pre-cold treatment at 4°C in dark and then followed by 2 weeks gemination period (from 27th January 2016 to 10th February 2016) in the greenhouse at 16°C. Uniform seedlings were selected and transplanted into rock wool cubes (8 cm × 8 cm × 6.5 cm, Grodan Rockwool B.V., Netherlands). Plants were grown in the greenhouse for 5 weeks with a density of 25 plants m^{-2}. The irrigation solution contained NO_3^-, 10.9; NH_4^+, 1.2; $H_2PO_4^-$, 1.1; K^+, 6.12; Ca^{2+}, 2.5; Mg^{2+}, 0.84; SO_4^{2-}, 0.56; Cl^-, 1.53 mmol L^{-1}; Fe^{3+}, 25; B^{3+}, 20; Cu^{2+}, 0.5; Zn^{2+}, 5; Mn^{2+}, 8; and Mo^+, 0.5 μmol L^{-1} (pH = 5.8 and EC = 1.5 mS cm^{-1}). This is the composition used in commercial practice when irrigation water is taken into account. Temperature was set at 20 and 18°C for day and night, respectively. The average photosynthetic photon flux density (PPFD) in the growth phase was estimated as 237 ± 19.6 μmol m^{-2} s^{-1} during the day, a value representing the daily average light intensity of the light period during the entire growth phase. This was calculated from global radiation outside the greenhouse considering 62% transmission and 50% photosynthetically active radiation. Either shading screen or high pressure sodium (HPS) light was applied 16 h a day from 5:00 am to 21:00 pm. Six plants in a group were rotated every 2 days to assure a uniform illumination over the plants.

In EXP 2, seeds were sown in rock wool plugs (Grodan Rockwool B.V., Netherlands) and germinated under LED lighting [GreenPower LED research module DR/W (**Supplementary Table 1**), Philips, Netherlands] with 140 μmol m^{-2} s^{-1} and 18 h photoperiod (24:00 am to 18:00 pm) for 6 days. Seedlings were then transferred into rock wool cubes (7 cm × 7 cm × 6.5 cm, Grodan Rockwool B.V., Netherlands) and grown for 5 weeks with a density of 32 plants m^{-2} and under same LED modules with intensity of 211 ± 6 μmol m^{-2} s^{-1} and a photoperiod of 18 h. Far-red light was added only during the first 4 weeks (13.6 ± 0.31 μmol s^{-1} m^{-2}, Research module far-red, Philips, Netherlands). Light was measured as the mean of 15 measurements that were equally distributed over the illuminated area. Day/night temperature was set at 23/22°C. The irrigation solution was supplied through ebb and flood system and had the

TABLE 1 | Cultivation conditions for Expertise lettuce cv. Expertise in 2 experiments.

Conditions	Experiment 1 (EXP 1)	Experiment 2 (EXP 2)
Cultivation environment	Greenhouse	Vertical farm (Climate chamber)
Substrate	Rockwool 8 cm × 8 cm × 6.5 cm	Rockwool 8 cm × 8 cm × 6.5 cm
Light intensity [a] in growth phase (PPFD [b], before EoP treatments)	237 ± 19.6 μmol m^{-2} s^{-1}	210 ± 6 μmol m^{-2} s^{-1}
Photoperiod	16 h	18 h
Light source in growth phase (before EoP treatments)	Natural light HPS lamps	White LED light Far-red LED light (first 4 weeks)
Density	25 plant m^{-2}	32 plant m^{-2}
Day/night temp	20/18°C	23/22°C
CO_2 concentration	Ambient level	1,000 ppm
Relative air humidity (light / dark period)	–	70%/80%

[a]*Average light intensity in light period before short-term pre-harvest light treatment applied.* [b]*PPFD, photosynthetic photon flux density (400–700 nm) measured at plant level.*

TABLE 2 | Measured light conditions during the End of Production (EoP) light treatments.

	Light source used in EoP treatments	PPFD[a] (μ mol s^{-1} m^{-2})	PSS[b]	Photoperiod (hours)	Treatment duration (d)
EXP 1	Red and white LEDs (GreenPower LED toplight module DR/W_Vision MB, Philips, Netherlands)	0 ± 0	–	–	7
		109 ± 12.32	0.88	16	7
		266 ± 7.21	0.87	16	7
EXP 2		49 ± 1.46	0.87	18	6
		211 ± 6.02	0.87	18	6
		469 ± 17.58	0.87	18	6

Photosynthetic photon flux density (PPFD) and phytochrome stationary state (PSS) data represent the mean of 25 measurements equally distributed over the illuminated area in each treatment compartment. [a]*PPFD, photosynthetic photon flux density (400–700 nm).* [b]*PSS, phytochrome stationary state.*

following composition: NO_3^-, 12.91; NH_4^+, 0.38; $H_2PO_4^-$, 1.53; K^+, 8.82; Ca^{2+}, 4.22; Mg^{2+}, 1.15; SO_4^{2-}, 1.53; Cl^-,1.53 mmol L^{-1}; Fe^{3+}, 30.67; B^{3+}, 38.33; Cu^{2+}, 0.77; Zn^{2+}, 3.83; Mn^{2+}, 3.83; and Mo^+, 0.38 μmol L^{-1} (pH = 6 and EC = 2.3 mS cm^{-1}). This is the composition used in commercial practice when considered irrigation water. Daily average relative humidity was maintained at 70 and 80% for light and dark period, CO_2 concentration was supplied at 1,000 ppm during light period.

End of Production Light Treatments

In both experiments, 5 weeks old lettuce plants were transferred to the climate chamber and randomly distributed over EoP light treatments with different light intensities for 7 days in EXP 1, and 6 days in EXP 2. In both experiments, different light intensities were applied by red and white LEDs (GreenPower LED toplight module DR/W_Vision MB, Philips, Netherlands) in isolated compartments. In EXP 1 plants were held under 0 (darkness), 110 and 270 μmol m^{-2} s^{-1}; in EXP 2 under 50, 210, and 470 μmol m^{-2} s^{-1} light treatments. Experimental set up and specifics of the light treatments and spectral properties are summarized in **Table 2** and **Figures 1**, **2**. Light intensity, spectrum and light distribution were measured at plant level (approximately 55 cm from LED lamps) using spectroradiometer (USB2000, Ocean Optics, Duiven, Netherlands). Light profile of EoP light treatments were measured as the mean of 25 and 15 measurements that were equally distributed over the illuminated area, respectively, in EXP 1 EXP 2. Phytochrome stationary state (PSS) was calculated by Eq. 1 (Sager et al., 1988), where N_λ stand for photon flux at wavelength λ nm, $\sigma_{r\lambda}$ stands for photochemical cross-section of red absorbing phytochrome state and $\sigma_{fr\lambda}$ stands for photochemical cross-section of far-red absorbing phytochrome state.

$$PSS = \left(\sum_{300}^{800} N_\lambda \sigma_{r\lambda}\right) \Big/ \left(\sum_{300}^{800} N_\lambda \sigma_{r\lambda} + \sum_{300}^{800} N_\lambda \sigma_{fr\lambda}\right) \quad (1)$$

Plants were rotated within each compartment every 2 days to ensure homogeneous illumination. Temperature, photoperiod, and irrigation were kept the same as the conditions during the previous growth period in each experiment. During the EoP light treatments relative humidity was 70 and 80% for light and dark period, CO_2 concentration was at ambient level. Air temperature was measured at canopy level using *k*-type thermocouples (shielded with aluminum foil to avoid the direct radiation from LED lamps) on TC-80 data loggers (Picotechnology LETD., Cambridge, United Kingdom). The air temperature differences between each compartment were less than 1°C (data not shown).

Leaf Sampling and Postharvest Conditions

Fully expanded lettuce leaves were sampled for carbohydrates and TAsA analysis during the EoP light treatment (day 0, 1, 4, and 7 in EXP 1 and day 0 and 6 in EXP 2) and during subsequent shelf life (day 3, 7, 10, 13, and 16 in EXP 2). Leaves were always selected from the middle "whorls" and sampled approximately 10 h after start of light period. At each sampling time, per light treatment, 16 leaves were selected randomly from 16 plants (1 leaf per plant) and pooled into 4 replicates with 4 leaves each. In each pooled sample, leaves were halved along the mid rib into two equal parts for either carbohydrates or TAsA analysis. These samples were immediately frozen in liquid nitrogen and stored at −80°C.

Additionally, four pooled samples with intact leaves were taken before (day 0) and at the end of the light treatments (day 6 or 7) to determine the dry matter content. Following weighing (fresh weight, FW), samples were oven dried at 70°C for 3 days to determine the dry weight (DW).

For overall visual quality (OVQ) and shelf life assessment, leaves harvested at the last day of the light treatment were stored in darkness at 10°C. For each light treatment, 16 mature

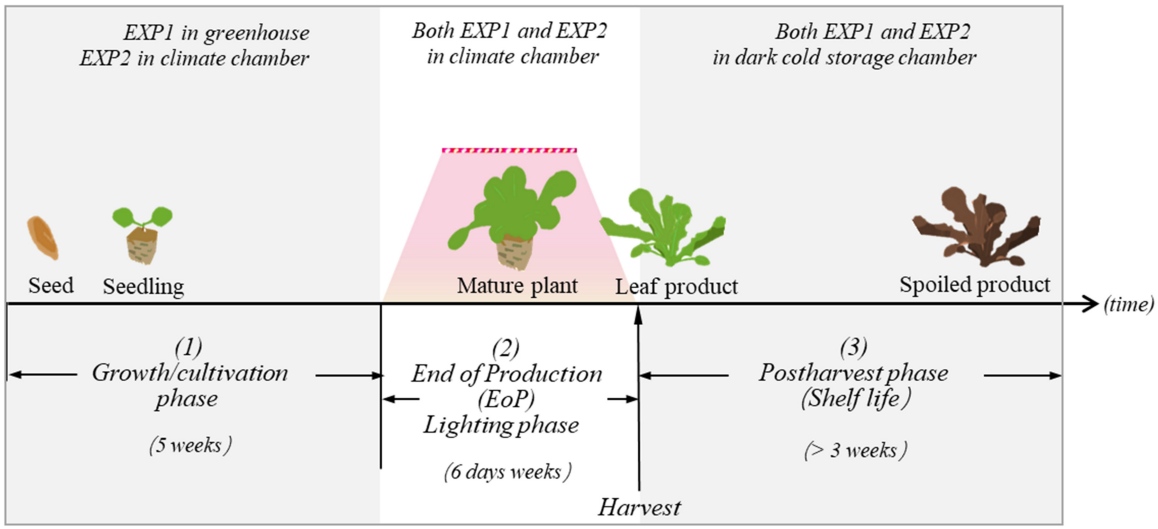

FIGURE 1 | In both EXP1 and EXP2, lettuce plants were exposed to three different experimental phases: (1) the growth/cultivation phase, (2) the EoP light treatment phase, and (3) the harvest and postharvest phase. The aim of our study is to investigate how different level of light intensity in the EoP phase affects the nutritional contents and quality performance of lettuce during the postharvest phase.

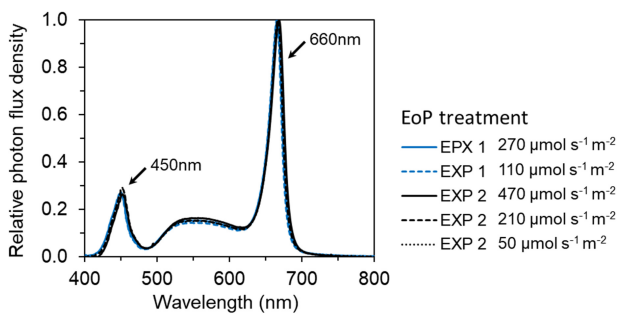

FIGURE 2 | The spectral distribution of red and white LEDs (GreenPower LED toplight module DR/W_Vision MB, Philips, Netherlands) used in EoP light treatments in both EXP 1 and EXP 2. The relative photon distribution of 6 EoP light treatments were same and overlapped on each other.

leaves were selected randomly from 16 plants (1 leaf per plant) and pooled into 4 replicates of 4 leaves each. Each pooled sample of four leaves was assigned to one plastic box (18 L × 13 W × 6.5 H cm), where a double layered wet filter paper was placed underneath. The box was covered by a lid with 12 punched pinholes in order to maintain a high relative humidity but allow sufficient air exchange. Every day (EXP 1) or every 2 days (EXP 2), 4 sample boxes from each treatment were taken to assess the OVQ scores.

Determination of Overall Visual Quality and Shelf Life

The OVQ of lettuce leaves was evaluated by a panel of two experienced assessors, according to ratings scale (Kader et al., 1973), modified for cultivar Expertise (**Table 3**). At each sampling time, sample boxes from all treatments without information on treatment were presented to assessors in a random order, at room temperature. The assessors evaluated quality parameters including appearance (yellowing, senescence browning, and wound browning/pinking), texture (crispness), and odor (smell; **Supplementary Table 2**). Evaluations were carried out under same white fluorescent light. All the quality parameters were scored with a structured scale from 1 (very bad) to 9 (excellent) and score 6 marking the lower limit of consumer acceptance. The shelf life was calculated as number of days from harvest till OVQ scores drop below 6.

Determination of Total Ascorbic Acid Content

Ascorbic acid was measured according to the method by Davey et al. (2003) with modifications. 300 mg fine ground sample from each pooled sample was extracted with 1.5 mL ice-cold 3.3% meta-phosphoric acid (MPA) and thawed on ice. The mixed solution was vortexed for 20 s and placed in ultrasonic bath at 0°C for 10 min in darkness. After 10 min centrifugation (25,000 rcf) at 4°C, 1 mL extract filtering through 0.45 µm filter was used for HPLC analysis of AsA. 100 µL filtered extraction was mixed with 50 µL of 5 mM dithiothreitol (DTT, in 400 mM Tris base) for converting DHA to AsA. After 15 min incubation in darkness and room temperature, 50 µl of 8.5% o-phosphoric acid was added into the mix to stop the reaction.

The concentration of AsA was analyzed using a HPLC consisting of a P580 pump (Dionex), a 340S UV-VIS detector (Dionex), and a MIDAS autosampler (Spark Holland) equipped with a ProntoSIL 120-3 C18 AQ, 250 × 3 mm column (Knauer) The column was eluted at a flow rate of 0.35 mL min^{-1} with 400 µL L^{-1} H_3PO_4 + 2.5 mL L^{-1} MeOH + 0.1 mM EDTA in H_2O followed by a wash step with 30% acetonitrile in H_2O. AsA was detected at 243 nm. The system was calibrated with standard AsA

TABLE 3 | The description of overall visual quality (OVQ) scoring scale for lettuce leaves (cv. Expertise).

9- Excellent	Bright and typical natural color of leaf blade and petiole; no browning was shown; firm and crispy with fresh grass like smell. All samples meet score = 9 in appearance, texture, and odor.
8- Very good	One slightly discolored or browning or pinking feature are shown at the leaf cut edge or blade. Leaves are firm and crisp and fresh grass like smell. All samples meet score ≥8 in appearance, texture, and odor.
7- Good	Few slightly discolored leaves and brown edges are allowed. leaves still crisp, reduced fresh smell. All samples meet score ≥7 in appearance, texture, and odor.
6- Satisfactory	The defined consumer acceptance threshold Slightly discolored leaves and moderate brown edges are allowed. No unpleasant odor or texture decay. All samples meet score ≥ 6 and no sample below score 6 in appearance, texture, and odor.
5- Mediocre	Some yellowing and browning of leaf blade; slightly brown petiole; darker brown cut edge; texture decay but still acceptable; slightly unpleasant odor emerged. One or more samples meet score 5 in appearance, texture, and odor.
4- Borderline	Obvious discolouration on leaf blades; browning of leaf blade and petiole; clearly mild soft in texture; unpleasant odor. One or more samples meet score 4 in appearance, texture, and odor.
3- Poor	Strong discolouration, browning of leaves; wilted texture; obvious unpleasant odor. One or more samples meet score 3 in appearance, texture, and odor.
2- Bad	Complete yellow or brown leaf; texture decay with liquid leakage; strong off-odor. One or more samples meet score 2 in appearance, texture, and odor.
1- Very bad	Complete discolored leaf; liquid leaking from leaf material; fermented smell. One or more samples meet score 1 in appearance, texture, and odor.

OVQ is scored as intuitional sensorial feeling that integrates quality parameters of appearance (yellowing, senescence browning, and wound browning /pinking), texture (crispness), and odor (smell; details are described in ***Supplementary Table 2****).*

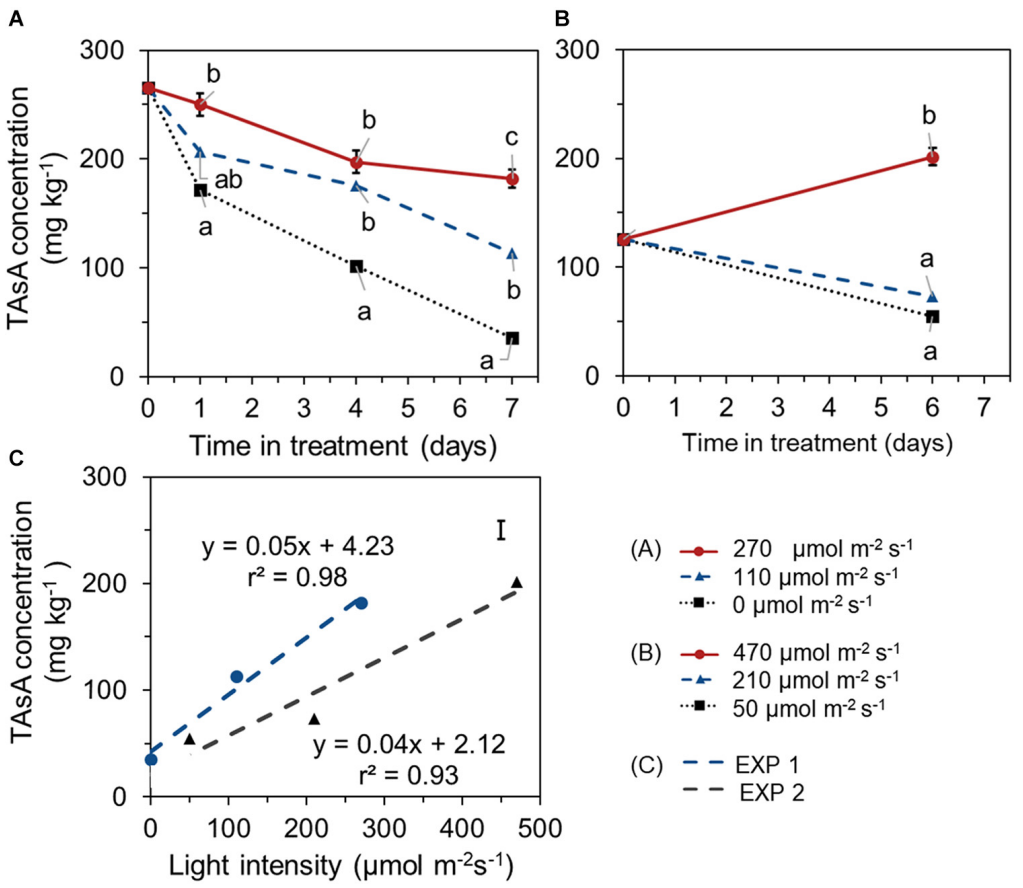

FIGURE 3 | Time course of TAsA concentration (expressed on a fresh weight bases) of lettuce plants grown under different light intensities for the last 7 days in EXP 1 **(A)** or 6 days in EXP 2 **(B)** and the correlation between final TAsA concentration and light intensity **(C)**. EoP Light treatments started when plants were 5 weeks old. Data points represent means of 4 samples ($n = 4$), each consisting of leaves from 4 plants. Within each experiment, significant differences (at $P < 0.01$) are indicated by different letters when comparing different treatments at the same time point. Vertical bars represent standard errors of means [in panels **(A,B)** error bar only given in the highest line; in panel **(C)** error bar is given at right upper corner].

solution (prepared in 3% MPA/1 mM, stabilized with 2.5 mM DTT). The TAsA were calculated as the sum of the AsA directly measured and the AsA converted from DHA.

Determination of Carbohydrate Content

Soluble sugars and starch were measured using a modified method according to van Geest et al. (2016). Carbohydrates were extracted from 15 mg freeze dried, fine ground sample with 5 mL 80% ethanol at 80°C in a shaking water bath for 20 min. After extraction, tubes were centrifuged (8,800 rcf) at 4°C and 1 mL supernatant was vacuum dried in a vacuum centrifuge (Savant SpeedVac SPD2010, Thermo Fisher Inc., Waltham, MA, United States) at 45°C and 5.1 mbar for 105 min. Then, 2 mL 0.01 M hydrochloric acid was added to re-dissolve the carbohydrates using an ultrasonic water bath (Branson 2200, Branson Ultrasonics, Danbury, CT, United States) at room temperature for 10 min. The solution was eluted over a HyperSep SCX cartridge, 100 mg/1 mL (Thermo Scientific, United States) to remove amino compounds and diluted 10 times with Milli-Q water for determination of glucose, fructose, and sucrose. The remaining pellets were stored in 80% ethanol at -20°C for starch analysis. The pellet was washed 3 times with 80% ethanol and then vacuum dried in a vacuum centrifuge at 45°C and 5.1 mbar for 25 min. 2 mL 1 g L^{-1} thermostable α-amylase (SERVA Electrophoresis GmbH, Heidelberg, Germany) was added to the dried pellet and incubated for 30 min at 90°C. After that, 1 mL solution of amyloglucosidase from *Aspergillus niger* (Sigma 10115, Sigma, St Louis, MO, United States; 0.5 mg mL^{-1} in 50 Mm citrate buffer, pH = 4.6) was added. After incubation at 60°C for 15 min, the solution was centrifuged (8,800 rcf) and diluted 20 times with Milli-Q water for quantification of the glucose. All soluble sugars were quantified using High Performance Anion Exchange Chromatography with Pulsed Amperometric Detection (HPAEC-PAD; Dionex ICS5000, Thermo Fisher Inc.), equipped with a Dionex CarboPac1 column (250 × 2 mm; Thermo Fisher), eluted with 100 mM NaOH at 0.25 mL min^{-1}. Carbohydrates data before harvest were expressed on a fresh weight bases (g kg^{-1}) similar to the TAsA level. Carbohydrate levels during postharvest were expressed on a dry weight bases (g kg^{-1}) as fresh weight is subject to rapid changes when quality deteriorates in the later phase of storage which may obscure changes in absolute levels.

Statistical Analysis

One-way analysis of variance (ANOVA) was used to test the effects of the light intensity on DM, FW, DM%, carbohydrates (sucrose, fructose, glucose, and starch) and TAsA for EXP 1 and EXP 2 when comparing different treatments at same time after treatment or time in shelf life. Normality of the variables was tested applying the Shapiro–Wilk test. Bartlett's test was carried out to test homogeneity of variances. Fisher's protected LSD was carried out for multiple comparison tests ($P \leq 0.01$). Individual pooled samples consisted of 4 leaves from 4 different plants were considered as independent replicates, all measurements were based on four replicate samples. As there was only one compartment in the climate room per treatment, we may have underestimated the random variance. Therefore, the tests have been conducted at P = 99% instead of the commonly used P = 95%.

The Weibull distribution was fitted to the visual quality data according to Eq. 2 (Hertog, 2002; Ares et al., 2008) and were based on the average of 4 replicates in each treatments for OVQ scores (**Figure 5**) and on the individual replicates for individual visual quality traits (cut edge browning, senescence browning, yellowing/discoloring, odor/smell, and texture in **Table 2**).

$$F\left(t;\ b,\ c,\ d,\ e\right) = c + \left(d - c\right) \left\{1 - \exp\left\{-\exp\left[b\left(\log\left(t\right) - \log\left(e\right)\right)\right]\right\}\right\} \quad (2)$$

Where t is the time after harvest; b, c, d and e are the model parameter estimates. Shelf life ($t_{\text{shelf life}}$) is calculated as the results when $F\left(t;\ b,\ c,\ d,\ e\right)$ equals to 6 and are based on the individual replicates in each treatment. Statistical analysis was performed using the R software (R 3.4.3; R Project for Statistical Computing, Vienna, Austria).

RESULTS

TAsA and Carbohydrate Levels at Harvest

During the 1 week EoP light treatment, higher light intensity resulted in higher level of TAsA in lettuce leaves in both experiments. In EXP 1, TAsA concentration decreased over time of 7 days EoP light treatment at all light intensities compared to its start level at day 0. However, the decrease of TAsA concentration was stronger the lower the light intensity (**Figure 3A**). In EXP 2, plants from treatment with 210 μmol m^{-2} s^{-1} intensity (same light intensity as during growth) showed a decrease in TAsA level over treatment time. Only at the highest light intensity (470 μmol $s^{-1}m^{-2}$ for 6 days), TAsA was significantly increased at the end of the EoP light treatment (**Figure 3B**). A linear relation was found between the light intensity (applied as EoP lighting) and the level of TAsA at the end of the light treatment (**Figure 3C**).

Different EoP light intensities also affected the level of total carbohydrates (glucose + fructose + sucrose + starch). In EXP 1, carbohydrates concentration in leaves showed a decreasing trend in all treatments and reached significant lower values at day 7 compared to its start level at day 0. Carbohydrates reduction was less under higher light intensity (270 μmol s^{-1} m^{-2}). A steep decline in carbohydrates was observed in darkness (**Figure 4A**). In EXP 2, for lettuce that was grown under 210 μmol s^{-1} m^{-2} light during both the initial stage and EoP lighting stage, no significant changes in carbohydrates level were shown with crop development during the EoP light treatment. At the highest light intensity (470 μmol s^{-1} m^{-2}), the carbohydrate level substantially increased (**Figure 4B**). Carbohydrate levels at the end of EoP light treatments were linearly correlated with applied light intensities in both experiments (**Figure 4C**). Glucose, sucrose, fructose, and starch levels showed similar responses to light intensity as the total carbohydrates level (**Supplementary Figure 1**).

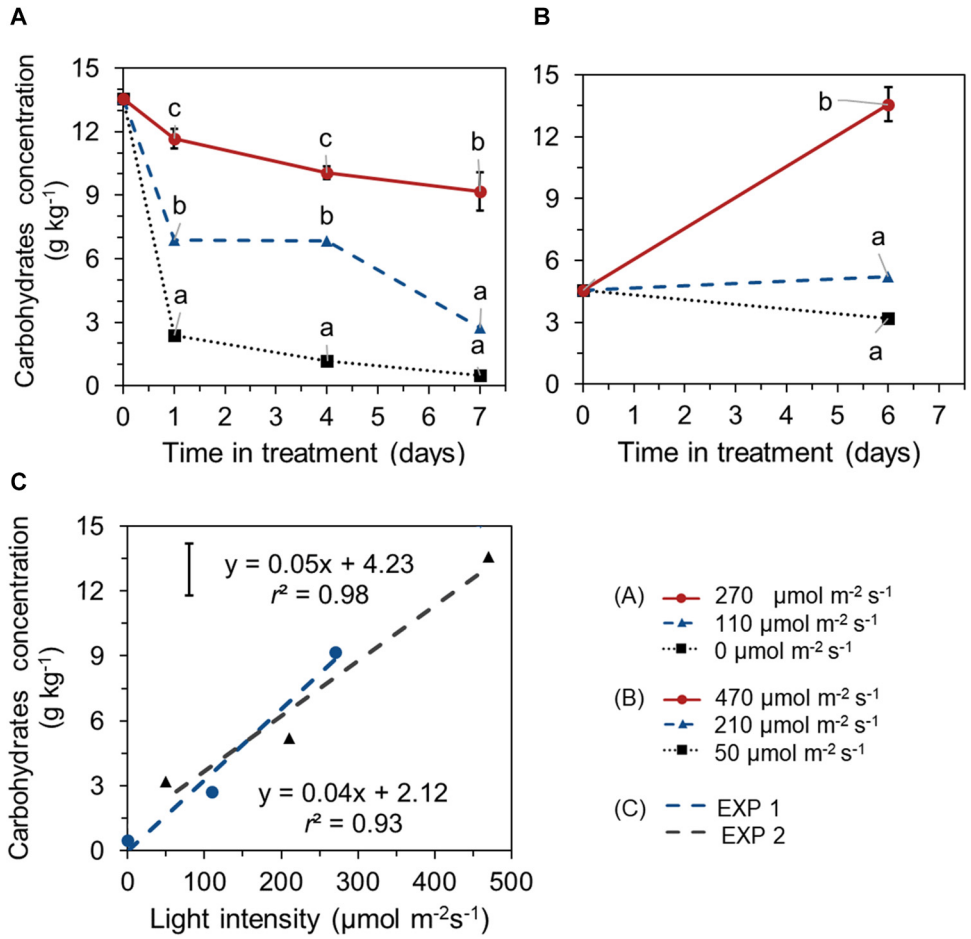

FIGURE 4 | Time course of total carbohydrate concentration (sum of glucose, sucrose, fructose, and starch, expressed on a fresh weight bases) of lettuce plants grown under different light intensities for the last 7 days in EXP 1 **(A)** or 6 days EXP 2 **(B)** and the correlation between final carbohydrate level and light intensity **(C)**. Light treatments started when plants were 5 weeks old. Data points represent means of 4 samples (n = 4), each consisting of leaves from 4 plants. Within each experiment, significant differences (at $P < 0.01$) are indicated by different letters comparing different treatments at the same time point. Vertical bars represent standard errors of means [in panels **(A,B)** error bar only given in the highest line; in panel **(C)** error bar is given at left upper corner].

In both experiments, increased light intensity during the last week of cultivation significantly increased the dry weight and dry matter percentage of lettuce leaves, where fresh weight only showed a slight increase in EXP 2 (**Supplementary Figure 2**).

TAsA and Carbohydrate Levels During Shelf Life in Darkness

Both TAsA and total carbohydrate levels declined during the shelf life in darkness. The leaves harvested from plants that received the highest pre-harvest light intensities, maintained a significant higher TAsA and total carbohydrate level during the whole shelf life period until the end of storage (**Figures 5A,B**). Postharvest levels of glucose, sucrose, fructose, and starch showed similar trends as the total carbohydrate levels (**Supplementary Figure 3**).

Overall Visual Quality and Shelf Life

In both experiments, the decline of OVQ was suppressed by applying increased light intensity in the last week before harvest. This resulted in a significantly extended shelf life. Pre-harvest light intensity of 110–270 µmol m^{-2} s^{-1} increased the shelf life by 3–4 days compared to darkness in EXP 1 (**Figure 6A**) and increasing light intensity to 470 µmol m^{-2} s^{-1} increased the shelf life by 6 days compared to low light condition (50 µmol m^{-2} s^{-1}) and by 3 days compared to moderate light condition (210 µmol m^{-2} s^{-1}) in EXP 2 (**Figure 6B**).

In EXP 2, the dynamics of individual quality aspects was further analyzed. **Table 4** shows the time that respective quality aspects reach the consumer acceptance limit. Shelf life (based on OVQ) appeared to be primarily determined by leaf yellowing and senescence browning.

Pre-harvest Light Intensity and Nutritional Quality at Harvest Is Positively Corelated With Shelf Life

In both EXP 1 and EXP 2, the shelf life was positively correlated with the EoP light level and with the nutritional quality

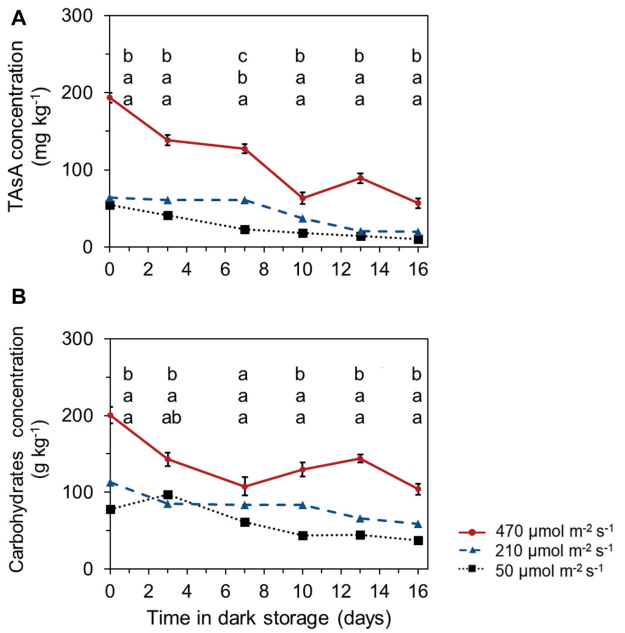

FIGURE 5 | Time course of TAsA **(A)** and total carbohydrate (glucose + fructose + sucrose + starch) levels **(B)** during shelf life at 10°C in darkness. The TAsA concentration was expressed on fresh weight bases; carbohydrate concentration was expressed on a dry weight bases. Samples were derived from plants that received different pre-harvest lighting intensities (50, 210 and 470 µmol m^{-2} s^{-1}) for 6 days (EXP 2). Data points represent means of 4 samples (n = 4), each consisting of leaves from 4 plants. Within each experiment, significant differences (at $P < 0.01$) are indicated by different letters comparing different treatments at the same time point. Vertical bars represent standard errors of means (only given in the highest line).

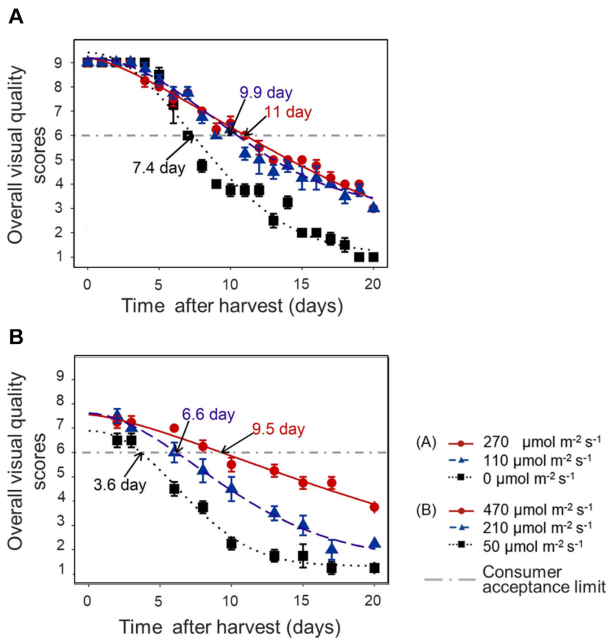

FIGURE 6 | Time course of lettuce OVQ changes during shelf life at 10°C in darkness in EXP 1 **(A)** and EXP 2 **(B)**. End of Production (EoP) light treatment was applied to 5 weeks old plants and lasted 7 (EXP 1) or 6 days (EXP 2). Data points represent means of 4 samples (n = 4), each sample consisting of 4 leaves from 4 plants. The curves show the fitted model according to Eq. 2 and are based on the average of 4 replicates in each treatment. The horizontal dash-dot line indicates the defined consumer acceptance threshold (OVQ score = 6). Shelf life was calculated from the intersection of fitted Weibull curves and consumer acceptance threshold, numbers indicated by arrows are average of 4 estimated shelf life figures. Error bars indicates standard error of the mean measured value.

level at harvest, both with respect to the levels of TAsA and total carbohydrates (**Figure 7**). Similar correlations were found between shelf life and the levels of individual soluble sugars and total soluble sugar at harvest (**Supplementary Figure 4**; glucose 2/J, fructose 3/J, sucrose 4/J, and total soluble sugar 5/J). In addition, a good correlation was observed between the shelf life and the dry matter percentage at harvest (**Figure 7D**), the latter being directly related to the improved levels of carbohydrates.

DISCUSSION

Most of the previous research on the effects of light intensity on end product quality has been done using different light levels applied during the entire cultivation period. Here we focussed on applying different light levels only at the days before harvest. This has the advantage that the light treatments have limited influence on crop growth, yield and morphology. In addition, EoP lighting limits the energy input required for higher light intensities compared to prolonged lighting.

We showed that short-term (6 or 7 days) high light intensity applied in the days before harvest significantly increases the nutritional quality in lettuce. This is reflected in higher levels of carbohydrates and TAsA. The improved nutritional quality is maintained during the postharvest phase and positively affects postharvest performance and the shelf life.

High End of Production Light Intensity Improves Nutritional Status at Harvest

The effects of high light during growth on plant nutritional quality at harvest have been studied before (Zhou et al., 2009; Locato et al., 2013). For instance, lettuce grown under light intensities above 200 µmol m^{-2} s^{-1} (red and blue LEDs) showed increased antioxidants capacity and higher phenolic and flavonoids levels at harvest compared to plants grown under light intensities of 100 and 150 µmol m^{-2} s^{-1} (Pennisi et al., 2020).

High light intensities applied as EoP lighting was shown before to improve the nutritional status at harvest. Carbohydrates and chlorophyll content in harvested lettuce were increased when increasing the light intensity from 400 to 700 µmol m^{-2} s^{-1} in the 4 days before harvest (light source not mentioned; Pérez-López et al., 2015). The level of soluble sugars and starch in lettuce increased 1.5 times at harvest when additional supplemental lighting (1,000–1,200 µmol m^{-2} s^{-1} from HPS lamps) is applied in greenhouse 10 days before harvest (Zhou et al., 2009). Samuolienė et al. (2011) showed

TABLE 4 | Effect of pre-harvest light intensity on time until consumer acceptance limit was reached according to scores of different quality traits in EXP 2.

Light intensity (μ mol m^{-2} s^{-1})	Time to consumer acceptance limit (days)					
	OVQ	Cut edge browning	Senescence browning	Yellowing/Discoloring	Odor/Smell	Texture
50	3.6 ± 0.50	6.4 ± 0.59	4.2 ± 0.58	3.0 ± 1.02	4.9 ± 0.71	4.4 ± 0.84
210	6.6 ± 0.72	7.0 ± 0.77	7.1 ± 0.44	5.8 ± 0.95	6.0 ± 1.26	7.7 ± 0.37
470	9.5 ± 0.52	11.2 ± 2.48	8.5 ± 0.98	8.1 ± 0.74	10.8 ± 1.35	12.4 ± 0.54

Values represent the average of 4 estimated values (n = 4) according to fitted Weibull curve; each value is based on a pooled sample consisting of leaves from 4 plants. Values are mean ± standard error of the mean measured value.

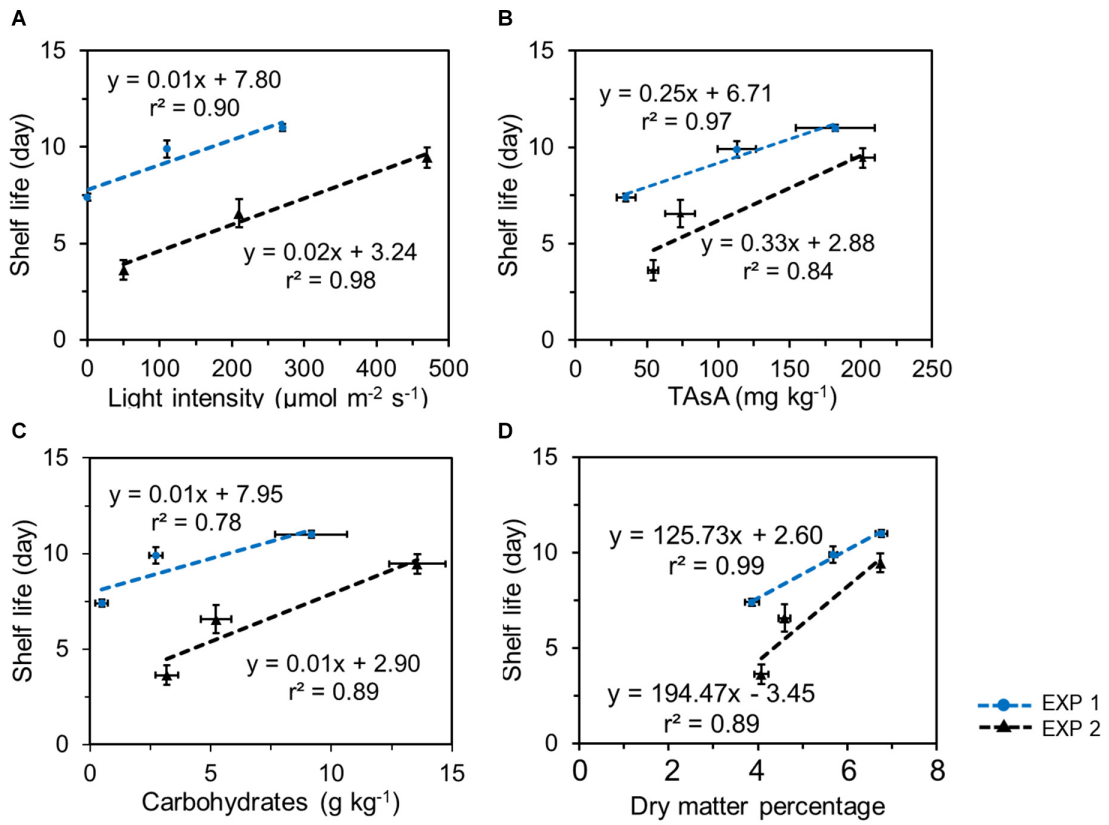

FIGURE 7 | Correlations between lettuce shelf life and light intensity applied in pre-harvest treatment **(A)**, the total ascorbic acid level (**B**, expressed on a fresh weight bases), the total carbohydrates (glucose + fructose + sucrose + starch) levels (**C**, expressed on a fresh weight bases), and dry matter percentage **(D)** in lettuce at harvest in 2 experiments. Plotted values represent the average value of 4 samples (*n* = 4) each consisting of leaves derived from 4 different plants. Vertical bars indicate standard errors of the mean estimated shelf life; horizontal error bars indicate standard errors of the mean carbohydrate content and of dry matter percentage.

that application of supplemental red LEDs (300 μmol m^{-2} s^{-1}) during last 3 days before harvest observed increasing TAsA in lettuce at harvest.

In our results, we found a positive correlation between carbohydrates level and TAsA level. This was also found in previous research about light regulation of TAsA (Nishikawa et al., 2005; Zhou et al., 2009; Schmitz et al., 2014; Pérez-López et al., 2015), however, the causal connection between carbohydrates levels and the increases in TAsA has not yet been proven (Yabuta et al., 2007). Although glucose is the starting point for AsA biosynthesis, more sugars does not automatically lead to more AsA (Ntagkas et al., 2019). The activities and expression of many enzymes and genes involved in TAsA biosynthesis and recycling pathway are induced under high light intensity in both leaves and in fruits (Bartoli et al., 2006; Dowdle et al., 2007; Yabuta et al., 2007). The light regulation of these enzymes and genes is suggested to be mediated by photosynthesis (through its effect on the plastoquinone state) and by respiration (Bartoli et al., 2006; Ntagkas et al., 2018). Both the increase in carbohydrate and AsA during high intensity EoP lighting may therefore result from the increased photosynthetic activity.

High EoP Light Improves the Postharvest Performance and Shelf Life

Our results showed that in all treatments, carbohydrates and TAsA levels decreased during dark storage. However, plants which had received high light intensity before harvest, showed higher starting levels of these compounds and maintained higher levels throughout the entire storage period (**Figure 6**). This resulted in an improved visual quality and a longer shelf life.

The rapid deterioration that occurs in leafy material during dark storage is due to a phenomenon called "dark induced senescence," primarily induced by a developing shortage of carbohydrates (Van Doorn, 2004a). Senescence itself is a form of programmed cell death in which the cells degrade their contents to sustain energy production before they die (Van Doorn and Woltering, 2004). The later phase of senescence is often accompanied by an increased production of ROS and associated loss of membrane integrity (Van Doorn and Woltering, 2005). These processes lead to a sequential loss of organelles, chlorophyll, proteins and other compounds and finally death of the cells. This is reflected in loss of sensorial quality (e.g., loss greenness, loss of shininess and crispness, tissue collapse, and browning; Thimann et al., 1977; Büchert et al., 2011). A higher nutritional status at the start may postpone such deteriorative processes during storage.

The reduction of TAsA after harvest is caused by both increased consumption and decreased biosynthesis (Smirnoff and Wheeler, 2000). On the one hand, TAsA is used to scavenge ROS, which are usually generated under postharvest conditions (e.g., sugar starvation, wounding and leaf senescence; Smirnoff, 2000; Nishikawa et al., 2003; Couée et al., 2006; Baxter et al., 2014). In this way TAsA can protect against oxidative stress. On the other hand, substrates for TAsA biosynthesis may be limited during dark storage, possibly due to absence of photosynthesis, chloroplast disintegration, and interruption of carbohydrates allocation from source leaves (Nishikawa et al., 2003). Limited carbohydrate availability may suppress AsA biosynthesis and recycling through suppression of the genes involved in AsA biosynthesis and recycling (Millar, 2003; Nishikawa et al., 2005).

We found positive correlations between the shelf life and the contents of carbohydrates and TAsA at harvest (**Figure 7**), indicating that the higher nutritional quality indeed postponed the deteriorative processes during postharvest storage. Previous studies showed that higher sugar levels in plants suppressed yellowing in broccoli florets (Coupe et al., 2003; Nishikawa et al., 2005), reduced petal senescence and increased keeping quality in cut flowers (Fjeld et al., 1994; Van Doorn, 2004b; Fanourakis et al., 2013; Pattaravayo et al., 2013). Additionally, visual quality deterioration in lettuce was greatly delayed when the product was stored under low light intensities (5 to 30 μmol m^{-2} s^{-1} provided by fluorescent tubes or narrow band red, blue, red + blue, or green LEDs) compared to dark storage (Zhan et al., 2013; Woltering et al., 2015, 2016; Woltering and Witkowska, 2016), and this was found to be associated with increased levels of sugars and TAsA under postharvest lighting.

In our research, cut edge browning and senescence browning was suppressed in leaves that contained higher levels of TAsA as a result of high light intensity applied in EoP light treatment (**Supplementary Figure 4**. 1/L and 1/M). The anti-browning effects of TAsA have been shown in previous research on fruit and leaves (Soliva-Fortuny and Martín-Belloso, 2003; Degl'Innocenti et al., 2005). TAsA inhibits enzymatic browning (pink/brown coloration mainly on cut surface) by competing with PPO and reducing colored quinones products to colorless diphenols (Couture et al., 1993; Degl'Innocenti et al., 2005, 2007).

The improved postharvest performance and prolonged shelf life of the leaves from high intensity EoP lighting is likely a direct result of the higher levels of carbohydrates and TAsA. Both compounds postpone deteriorative processes connected to senescence and AsA, in addition, may play a role in limiting tissue browning.

Future Perspective

End of Production light treatments seem a feasible way to improve plant nutritional and health related properties and can be employed to improve postharvest performance and shelf life of leafy vegetables. Here we studied the effect of EoP light intensity (red – white LEDs) during 1 week and a photoperiod of 16–18 h. Other light factors, such as photoperiod and spectrum and the optimal EoP light duration need to be studied to further elucidate the underlying mechanisms of light effects on crop nutritional status and postharvest performance.

CONCLUSION

Increased light intensity at the EoP phase increased the levels of carbohydrates, TAsA and the percentage of dry matter at harvest, indicating an improved nutritional quality of the lettuce. The response to EoP lighting was independent on the cultivation history in either a greenhouse or vertical farm. The improved nutritional status of the lettuce was maintained during the subsequent postharvest storage. The higher levels of carbohydrates and TAsA postpone deteriorative processes connected to senescence, in addition, TAsA may play a role in limiting tissue browning. The improved nutritional status at harvest resulted in a better postharvest performance and extended the shelf life.

DATA AVAILABILITY STATEMENT

The raw data supporting the conclusions of this article will be made available by the authors, without undue reservation.

AUTHOR CONTRIBUTIONS

QM, EW, CN, and LM conceptualized the research plan. QM, EW, and LM designed the experiments and QM carried out the experiments, analyzed the data, and wrote the manuscript. EW and LM provided critical feedback on the manuscript. CN provided critical comments to the overall structure of the manuscript. All authors reviewed and approved the final manuscript.

FUNDING

This work was supported by the China Scholarship Council (CSC; Grant No. 201507720013) and Signify B.V. (Previously known as Philips Lighting).

ACKNOWLEDGMENTS

We thank to Ms. Amanda M. Lewis, Ms. Yiming Ji, and Unifarm staff for valuable help and contributions to the experiment to Dr. Ningyi Zhang for valuable discussion and instructive advice in manuscript writing and to Arjen van de Peppel for technical assistance and to Rijk Zwaan for providing the lettuce seeds.

SUPPLEMENTARY MATERIAL

The Supplementary Material for this article can be found online at: https://www.frontiersin.org/articles/10.3389/fpls.2021.615355/full#supplementary-material

REFERENCES

Ares, G., Giménez, A., and Gámbaro, A. (2008). Sensory shelf life estimation of minimally processed lettuce considering two stages of consumers' decision-making process. *Appetite* 50, 529–535. doi: 10.1016/j.appet.2007.11.002

Bartoli, C. G., Yu, J., Gómez, F., Fernández, L., McIntosh, L., and Foyer, C. H. (2006). Inter-relationships between light and respiration in the control of ascorbic acid synthesis and accumulation in *Arabidopsis thaliana* leaves. *J. Exp. Bot.* 57, 1621–1631. doi: 10.1093/jxb/erl005

Baxter, A., Mittler, R., and Suzuki, N. (2014). ROS as key players in plant stress signalling. *J. Exp. Bot.* 65, 1229–1240. doi: 10.1093/jxb/ert375

Büchert, A. M., Gómez Lobato, M. E., Villarreal, N. M., Civello, P. M., and Martínez, G. A. (2011). Effect of visible light treatments on postharvest senescence of broccoli (*Brassica oleracea* L.). *J. Sci. Food Agric.* 91, 355–361. doi: 10.1002/jsfa.4193

Couée, I., Sulmon, C., Gouesbet, G., and El Amrani, A. (2006). Involvement of soluble sugars in reactive oxygen species balance and responses to oxidative stress in plants. *J. Exp. Bot.* 57, 449–459. doi: 10.1093/jxb/erj027

Coupe, S. A., Sinclair, B. K., Watson, L. M., Heyes, J. A., and Eason, J. R. (2003). Identification of dehydration-responsive cysteine proteases during post-harvest senescence of broccoli florets. *J. Exp. Bot.* 54, 1045–1056. doi: 10.1093/jxb/erg105

Couture, R., Cantwell, M. I., Ke, D., and Saltveit, M. E. (1993). Physiological attributes related to quality attributes and storage life of minimally processed lettuce. *HortScience* 28, 723–725. doi: 10.21273/hortsci.28.7.723

Davey, M. W., Dekempeneer, E., and Keulemans, J. (2003). Rocket-powered high-performance liquid chromatographic analysis of plant ascorbate and glutathione. *Anal. Biochem.* 316, 74–81. doi: 10.1016/S0003-2697(03)00047-2

Degl'Innocenti, E., Guidi, L., Pardossi, A., and Tognoni, F. (2005). Biochemical study of leaf browning in minimally processed leaves of lettuce (*Lactuca sativa* L. *var. acephala*). *J. Agric. Food Chem.* 53, 9980–9984. doi: 10.1021/jf050927o

Degl'Innocenti, E., Pardossi, A., Tognoni, F., and Guidi, L. (2007). Physiological basis of sensitivity to enzymatic browning in "lettuce", "escarole" and "rocket salad" when stored as fresh-cut products. *Food Chem.* 104, 209–215. doi: 10.1016/j.foodchem.2006.11.026

Dowdle, J., Ishikawa, T., Gatzek, S., Rolinski, S., and Smirnoff, N. (2007). Two genes in *Arabidopsis thaliana* encoding GDP-l-galactose phosphorylase are required for ascorbate biosynthesis and seedling viability. *Plant J.* 52, 673–689. doi: 10.1111/j.1365-313X.2007.03266.x

Fanourakis, D., Pieruschka, R., Savvides, A., Macnish, A. J., Sarlikioti, V., and Woltering, E. J. (2013). Sources of vase life variation in cut roses: a review. *Postharvest Biol. Technol.* 78, 1–15. doi: 10.1016/j.postharvbio.2012.12.001

Fjeld, T., Gislerød, H. R., Revhaug, V., and Mortensen, L. M. (1994). Keeping quality of cut roses as affected by high supplementary irradiation. *Sci. Hortic. (Amsterdam).* 57, 157–164. doi: 10.1016/0304-4238(94)90043-4

Hasperué, J. H., Guardianelli, L., Rodoni, L. M., Chaves, A. R., and Martínez, G. A. (2016a). Continuous white-blue LED light exposition delays postharvest senescence of broccoli. *LWT Food Sci. Technol.* 65, 495–502. doi: 10.1016/j.lwt.2015.08.041

Hasperué, J. H., Lemoine, L., Vicente, A. R., Chaves, A. R., and Martínez, G. A. (2015). Postharvest senescence of florets from primary and secondary broccoli inflorescences. *Postharvest Biol. Technol.* 104, 42–47. doi: 10.1016/j.postharvbio.2015.02.015

Hasperué, J. H., Rodoni, L. M., Guardianelli, L. M., Chaves, A. R., and Martínez, G. A. (2016b). Use of LED light for Brussels sprouts postharvest conservation. *Sci. Hortic. (Amsterdam)* 213, 281–286. doi: 10.1016/j.scienta.2016.11.004

Hertog, M. L. A. T. M. (2002). The impact of biological variation on postharvest population dynamics. *Postharvest Biol. Technol.* 26, 253–263. doi: 10.1016/S0925-5214(02)00044-3

Kader, A., Lipton, W., and Morris, L. (1973). Systems for scoring quality of harvested lettuce. *HortSci* 8, 408–409.

Lin, K., Huang, M., Huang, W., Hsu, M., Yang, Z., and Yang, C. (2013). The effects of red, blue, and white light-emitting diodes on the growth, development, and edible quality of hydroponically grown lettuce (*Lactuca sativa L. var. capitata). Sci. Hortic. (Amsterdam)* 150, 86–91. doi: 10.1016/j.scienta.2012.10.002

Locato, V., Cimini, S., and De Gara, L. (2013). Strategies to increase vitamin C in plants: from plant defense perspective to food biofortification. *Front. Plant Sci.* 4:152. doi: 10.3389/fpls.2013.00152

Millar, A. H. (2003). Control of ascorbate synthesis by respiration and its implications for stress responses. *Plant Physiol.* 133, 443–447. doi: 10.1104/pp.103.028399

Nishikawa, F., Kato, M., Hyodo, H., Ikoma, Y., Sugiura, M., and Yano, M. (2003). Ascorbate metabolism in harvested broccoli. *J. Exp. Bot.* 54, 2439–2448. doi: 10.1093/jxb/erg283

Nishikawa, F., Kato, M., Hyodo, H., Ikoma, Y., Sugiura, M., and Yano, M. (2005). Effect of sucrose on ascorbate level and expression of genes involved in the ascorbate biosynthesis and recycling pathway in harvested broccoli florets. *J. Exp. Bot.* 56, 65–72. doi: 10.1093/jxb/eri007

Noichinda, S., Bodhipadma, K., Mahamontri, C., Narongruk, T., and Ketsa, S. (2007). Light during storage prevents loss of ascorbic acid, and increases glucose and fructose levels in Chinese kale (*Brassica oleracea var. alboglabra*). *Postharvest Biol. Technol.* 44, 312–315. doi: 10.1016/j.postharvbio.2006.12.006

Ntagkas, N., Woltering, E. J., and Marcelis, L. F. M. (2018). Light regulates ascorbate in plants: an integrated view on physiology and biochemistry. *Environ. Exp. Bot.* 147, 271–280. doi: 10.1016/j.envexpbot.2017.10.009

Ntagkas, N., Woltering, E., Bouras, S., De Vos, R. C., Dieleman, J. A., Nicole, C. C., et al. (2019). Light-induced vitamin C accumulation in tomato fruits is independent of carbohydrate availability. *Plants* 8, 1–12. doi: 10.3390/plants8040086

Olarte, C., Sanz, S., Federico Echávarri, J., and Ayala, F. (2009). Effect of plastic permeability and exposure to light during storage on the quality of minimally processed broccoli and cauliflower. *LWT Food Sci. Technol.* 42, 402–411. doi: 10.1016/j.lwt.2008.07.001

Pattaravayo, R., Ketsa, S., and van Doorn, W. G. (2013). Sucrose feeding of cut *Dendrobium* inflorescences promotes bud opening, inhibits abscission of open flowers, and delays tepal senescence. *Postharvest Biol. Technol.* 77, 7–10. doi: 10.1016/j.postharvbio.2012.09.014

Pennisi, G., Pistillo, A., Orsini, F., Cellini, A., Spinelli, F., Nicola, S., et al. (2020). Optimal light intensity for sustainable water and energy use in indoor cultivation of lettuce and basil under red and blue LEDs. *Sci. Hortic. (Amsterdam)* 272:109508. doi: 10.1016/j.scienta.2020.109508

Pérez-López, U., Miranda-Apodaca, J., Muñoz-Rueda, A., and Mena-Petite, A. (2015). Interacting effects of high light and elevated CO2 on the nutraceutical quality of two differently pigmented *Lactuca sativa* cultivars (Blonde of Paris Batavia and Oak Leaf). *Sci. Hortic. (Amsterdam)* 191, 38–48. doi: 10.1016/j.scienta.2015.04.030

Sager, J. C., Smith, W. O., Edwards, J. L., and Cyr, K. L. (1988). Photosynthetic efficiency and phytochrome photoequilibria determination using spectral data. *Trans. ASAE* 31, 1882–1889. doi: 10.13031/2013.30952

Samuolienë, G., Brazaityte, A., Sirtautas, R., Novičkovas, A., and Duchovskis, P. (2011). Supplementary red-LED lighting affects phytochemicals and nitrate of baby leaf lettuce. *J. Food Agric. Environ.* 9, 271–274.

Schmitz, J., Heinrichs, L., Scossa, F., Fernie, A. R., Oelze, M.-L., Dietz, K.-J., et al. (2014). The essential role of sugar metabolism in the acclimation response of *Arabidopsis thaliana* to high light intensities. *J. Exp. Bot.* 65, 1619–1636. doi: 10.1093/jxb/eru027

Smirnoff, N. (2000). Ascorbate biosynthesis and function in photoprotection. *Philos. Trans. R. Soc. London Ser. B Biol. Sci.* 355, 1455–1464. doi: 10.1098/rstb.2000.0706

Smirnoff, N., and Wheeler, G. L. (2000). Ascorbic acid in plants: biosynthesis and function. *Crit. Rev. Biochem. Mol. Biol.* 35, 291–314. doi: 10.1080/07352680091139231

Soliva-Fortuny, R. C., and Martín-Belloso, O. (2003). New advances in extending the shelf-life of fresh-cut fruits: a review. *Trends Food Sci. Technol.* 14, 341–353. doi: 10.1016/S0924-2244(03)00054-2

Thimann, K. V., Tetley, R. M., and Krivak, B. M. (1977). Metabolism of Oat leaves during senescence: V. Senescence in light. *Plant Physiol.* 59, 448–454. doi: 10.1104/pp.59.3.448

Toledo, M. E. A., Ueda, Y., Imahori, Y., and Ayaki, M. (2003). l-ascorbic acid metabolism in spinach (*Spinacia oleracea* L.) during postharvest storage in light and dark. *Postharvest Biol. Technol.* 28, 47–57. doi: 10.1016/S0925-5214(02)00121-7

Van Doorn, W. G. (2004a). Is petal senescence due to sugar starvation? *Plant Physiol.* 134, 35–42. doi: 10.1104/pp.103.033084.COMPARISON

Van Doorn, W. G. (2004b). Update on senescence is petal senescence due to sugar starvation? *Plant Physiol.* 134, 35–42. doi: 10.1104/pp.103.033084.compounds

Van Doorn, W. G., and Woltering, E. J. (2004). Senescence and programmed cell death: substance or semantics? *J. Exp. Bot.* 55, 2147–2153. doi: 10.1093/jxb/erh264

Van Doorn, W. G., and Woltering, E. J. (2005). Many ways to exit? Cell death categories in plants. *Trends Plant Sci.* 10, 117–122. doi: 10.1016/j.tplants.2005.01.006

van Geest, G., Choi, Y. H., Arens, P., Post, A., Liu, Y., and van Meeteren, U. (2016). Genotypic differences in metabolomic changes during storage induced-degreening of *Chrysanthemum* disk florets. *Postharvest Biol. Technol.* 115, 48–59. doi: 10.1016/j.postharvbio.2015.12.008

Woltering, E. J., and Witkowska, I. M. (2016). Effects of pre-and postharvest lighting on quality and shelf life of fresh-cut lettuce. *Acta Hortic.* 1134, 357–365. doi: 10.17660/ActaHortic.2016.1134.47

Woltering, E. J., Seifu, Y. W., Supply, H., and Group, C. (2015). Low intensity monochromatic red, blue or green light increases the carbohydrate levels and substantially extends the shelf life of fresh- cut lettuce. *Acta Hortic.* 1079, 257–264. doi: 10.17660/actahortic.2015.1079.30

Woltering, E. J., Wang, J. F., and Seifu, Y. W. (2016). Storage of fresh-cut lettuce at light levels below the light compensation point increases sugar levels and greatly prolongs the shelf-life. *Acta Hortic.* 1141, 357–364. doi: 10.17660/ActaHortic.2016.1141.45

Yabuta, Y., Mieda, T., Rapolu, M., Nakamura, A., Motoki, T., Maruta, T., et al. (2007). Light regulation of ascorbate biosynthesis is dependent on the photosynthetic electron transport chain but independent of sugars in *Arabidopsis*. *J. Exp. Bot.* 58, 2661–2671. doi: 10.1093/jxb/erm124

Zhan, L., Hu, J., Ai, Z., Pang, L., Li, Y., and Zhu, M. (2013). Light exposure during storage preserving soluble sugar and l-ascorbic acid content of minimally processed romaine lettuce (*Lactuca sativa L.var. longifolia*). *Food Chem.* 136, 273–278. doi: 10.1016/j.foodchem.2012.07.123

Zhan, L., Hu, J., Li, Y., and Pang, L. (2012a). Combination of light exposure and low temperature in preserving quality and extending shelf-life of fresh-cut broccoli (*Brassica oleracea* L.). *Postharvest Biol. Technol.* 72, 76–81. doi: 10.1016/j.postharvbio.2012.05.001

Zhan, L., Li, Y., Hu, J., Pang, L., and Fan, H. (2012b). Browning inhibition and quality preservation of fresh-cut romaine lettuce exposed to high intensity light. *Innov. Food Sci. Emerg. Technol.* 14, 70–76. doi: 10.1016/j.ifset.2012.02.004

Zhou, W. L., Liu, W. K., Yang, Q. C. (2012). Quality changes in hydroponic lettuce grown under pre-harvest short-duration continuous light of different intensities. *J. Hortic. Sci. Biotechnol.* 87, 429–434. doi: 10.1080/14620316.2012.11512890

Zhou, Y. H., Zhang, Y. Y., Zhao, X., Yu, H. J., Shi, K., and Yu, J. Q. (2009). Impact of light variation on development of photoprotection, antioxidants, and nutritional value in *Lactuca sativa* L. *J. Agric. Food Chem.* 57, 5494–5500. doi: 10.1021/jf8040325

Conflict of Interest: The authors declare that the research was conducted in the absence of any commercial or financial relationships that could be construed as a potential conflict of interest.

Copyright © 2021 Min, Marcelis, Nicole and Woltering. This is an open-access article distributed under the terms of the Creative Commons Attribution License (CC BY). The use, distribution or reproduction in other forums is permitted, provided the original author(s) and the copyright owner(s) are credited and that the original publication in this journal is cited, in accordance with accepted academic practice. No use, distribution or reproduction is permitted which does not comply with these terms.

frontiers in Plant Science

ORIGINAL RESEARCH
published: 28 January 2021
doi: 10.3389/fpls.2021.619973

Only Extreme Fluctuations in Light Levels Reduce Lettuce Growth Under Sole Source Lighting

Ruqayah Bhuiyan and Marc W. van Iersel*

Horticultural Physiology Laboratory, Department of Horticulture, University of Georgia, Athens, GA, United States

The cost of providing lighting in greenhouses and plant factories can be high. In the case of variable electricity prices, providing most of the light when electricity prices are low can reduce costs. However, it is not clear how plants respond to the resulting fluctuating light levels. We hypothesized that plants that receive a constant photosynthetic photon flux density (PPFD) will produce more biomass than those grown under fluctuating light levels. To understand potential growth reductions caused by fluctuating light levels, we quantified the effects of fluctuating PPFD on the photosynthetic physiology, morphology, and growth of 'Little Gem' and 'Green Salad Bowl' lettuce. Plants were grown in a growth chamber with dimmable white LED bars, alternating between high and low PPFDs every 15 min. The PPFDs were ∼400/0, 360/40, 320/80, 280/120, 240/160, and 200/200 $\mu mol \cdot m^{-2} \cdot s^{-1}$, with a photoperiod of 16 h and a DLI of ∼11.5 $mol \cdot m^{-2} \cdot day^{-1}$ in all treatments. CO_2 was ∼800 $\mu mol \cdot mol^{-1}$. Plants in the 400/0 $\mu mol \cdot m^{-2} \cdot s^{-1}$ treatment had ∼69% lower $A_{n,30}$ (net assimilation averaged over 15 min at high and 15 min at low PPFD) than plants grown at a PPFD of 320/80 $\mu mol \cdot m^{-2} \cdot s^{-1}$ (or treatments with smaller PPFD fluctuations). The low $A_{n,30}$ in the 400/0, and to a lesser extent the 360/40 $\mu mol \cdot m^{-2} \cdot s^{-1}$ treatment was caused by low net assimilation at 360 and 400 $\mu mol \cdot m^{-2} \cdot s^{-1}$. Plants grown at 400/0 $\mu mol \cdot m^{-2} \cdot s^{-1}$ also had fewer leaves and lower chlorophyll content compared to those in other treatments. The four treatments with the smallest PPFD fluctuations produced plants with similar numbers of leaves, chlorophyll content, specific leaf area (SLA), dry mass, and leaf area. Chlorophyll content, $A_{n,30}$, and dry mass were positively correlated with each other. Our results show that lettuce tolerates a wide range of fluctuating PPFD without negative effects on growth and development. However, when fluctuations in PPFD are extreme (400/0 or 360/40 $\mu mol \cdot m^{-2} \cdot s^{-1}$), chlorophyll levels and $A_{n,30}$ are low, which can explain the low poor growth in these treatments. The ability of lettuce to tolerate a wide range of fluctuating light levels suggests that PPFD can be adjusted in response to variable electricity pricing.

Keywords: assimilation, chlorophyll, *Lactuca sativa*, light-emitting diodes, photosynthesis, photosynthetic photon flux density, variable electricity prices

OPEN ACCESS

Edited by:
Jason Wargent,
Massey University, New Zealand

Reviewed by:
Daniele Massa,
Council for Agricultural and Economics Research (CREA), Italy
Cristian Silvestri,
University of Tuscia, Italy

****Correspondence:***
Ruqayah Bhuiyan
rhb58017@uga.edu;
ruqayahhb@gmail.com

Specialty section:
This article was submitted to Crop and Product Physiology, a section of the journal Frontiers in Plant Science

Received: *21 October 2020*
Accepted: *06 January 2021*
Published: *28 January 2021*

Citation:
Bhuiyan R and van Iersel MW (2021) Only Extreme Fluctuations in Light Levels Reduce Lettuce Growth Under Sole Source Lighting. Front. Plant Sci. 12:619973. doi: 10.3389/fpls.2021.619973

INTRODUCTION

Increased year-round demand for fresh fruits and vegetables has increased the need for productive and profitable controlled environment growing operations, such as greenhouses and plant factories. Among the most popular crops for controlled environment agriculture are various leafy greens, including lettuce (Agrylist, 2017). Because of large day-to-day and seasonal fluctuations in the daily light integral (DLI) from sunlight (Albright et al., 2000), consistent, year-round greenhouse production of lettuce may require supplemental lighting from Fall through Spring. This is especially important at higher latitudes, where seasonal fluctuations in DLI from sun are greatest (Faust and Logan, 2018). However, the light environment in greenhouses is often poorly controlled (van Iersel and Gianino, 2017) and the variable light environment makes greenhouse production less predictable. The capital and operating costs of supplemental lighting are high (Albright et al., 2000). Lighting accounts for up to 30% of total operating costs in greenhouses (van Iersel and Gianino, 2017) and 40–50% in plant factories, either to provide the light or to remove the heat generated by the light fixtures (Watanabe, 2011; Zeidler and Schubert, 2014). Reducing the cost of lighting in controlled environment agriculture can reduce operating costs and increase profitability. One potential approach to decrease the cost of supplemental lighting is the use of photovoltaic greenhouses, where part of the greenhouse roof is covered with solar panels (Emmott et al., 2015; Cossu et al., 2017). However, the resulting shading of the greenhouse crop can reduce yields (Cossu et al., 2020). In addition, photovoltaic panels generate most electricity when there is ample sunlight, so there is a disconnect between the availability of electricity from photovoltaic panels and the need for supplemental lighting. Although the power generated by photovoltaic panels can be stored in batteries, this is expensive.

One obvious option for reducing electricity costs is to take advantage of variable electricity prices. The Light and Shade System Implementation (LASSI) algorithm can account for variable electricity prices and was shown to reduce electricity costs of greenhouse production by 8–37% as compared to threshold lighting control, where lights are controlled based on PPFD readings. The magnitude of the cost savings depended on location and which threshold control algorithm LASSI was compared to Harbick et al. (2016). Sørensen et al. (2016) used a multi-objective evolutionary algorithm in their DynaGrow control system to optimize greenhouse temperature, CO_2, and supplemental lighting, based on the greenhouse environment, electricity price forecasts, and weather forecasts. DynaGrow successfully reduced energy use and cost, while resulting in similar quality plants as a standard lighting control approach. Based on this prior work, accounting for energy prices in control algorithms for supplemental light can reduce energy costs. However, Kjaer et al. (2011) showed that an irregular greenhouse light environment resulted in poor flowering of *Campanula*, which could be prevented by assuring that the photoperiod was the same each day.

How fluctuating light levels affect photosynthetic physiology in controlled environments is not clear. Leaves in outdoor canopies experience changes in PPFD in the form of sunflecks, lasting anywhere from a few seconds to a few minutes, and shadeflecks, due to cloud cover, which can last hours (Knapp and Smith, 1987). The occurrence of sunflecks is dependent on movement of the sun and/or leaves higher in the canopy. Understory plants have adapted to the occurrence of sunflecks and have developed photosynthetic machinery to facilitate efficient use of this high PPFD (Chazdon and Pearcy, 1991). When plants are exposed to high light after periods of low light or darkness, it can take 10–40 min for leaves to acclimate and reach steady state photosynthesis, and is dependent on the duration and timing of those sunflecks (Chazdon and Pearcy, 1986, 1991). Vice versa (Kromdijk et al., 2016) showed that downregulation of photoprotective mechanisms as sunlit leaves are suddenly shaded can be slow, reducing photosynthesis of those shaded leaves. Upregulating the expression of genes encoding violaxanthin de-epoxidase, zeaxanthin epoxidase, and PSII subunit S allowed plants to respond more quickly to sudden reductions in sunlight increased dry matter production of tobacco (*Nicotiana tabacum*) by 15%.

Vialet-Chabrand et al. (2017) compared the photosynthetic physiology and growth of *Arabidopsis thaliana* under four different lighting treatments, constant high or low PPFD during the entire photoperiod vs. natural fluctuations in PPFD, resulting in the same DLI. Plants grown with a greater DLI had a higher light-saturated rate of photosynthesis, but whether that DLI was provided with constant or fluctuating PPFD had little impact on the photosynthetic physiology. However, fluctuating PPFD resulted in thinner leaves, decreased leaf area, and shoot biomass, and increased specific leaf area (SLA), as compared to constant PPFD with the same DLI. This reduction in growth under fluctuating PPFD was at least partly explained by a greater daily net carbon gain (photosynthesis minus respiration) under constant as compared to fluctuating PPFD (Vialet-Chabrand et al., 2017). These differences in daily net carbon gain are likely caused by multiple factors. First, under fluctuating PPFD conditions, plants are required to constantly acclimate to a changing light environment, which can reduce photosynthetic efficiency and growth (Kromdijk et al., 2016). Secondly, because of the asymptotic shape of photosynthesis-light response curves (Vialet-Chabrand et al., 2017), the total photosynthesis over the course of a day, given a specific DLI, is achieved under constant PPFD conditions (Sims and Pearcy, 1993). Likewise, the daily electron transport rate, the photosynthetic process most directly impacted by light, with a specific DLI increases as PPFD fluctuations decrease (Weaver and van Iersel, 2019).

Our objective was to quantify the photosynthesis and growth of lettuce in response to fluctuating PPFD levels. We hypothesized that plant biomass would decrease as the magnitude of PPFD fluctuations increased, because of the effect of such fluctuations on photosynthesis and carbon gain. By quantifying the effects of fluctuating PPFD on plant physiological parameters and crop growth, we aimed to determine whether it is possible to take advantage of variable electricity prices to provide light to controlled environment agriculture crops.

MATERIALS AND METHODS

Growing Conditions

The study was conducted in a 54 m^3 walk-in growth chamber. The chamber contained three racks with three shelves each. Each shelf was divided into two 0.74 m^2 growing areas. Each growing area was outfitted with two dimmable LED bars (SPYDRx with Physiospec indoor spectrum, Fluence Bioengineering, Austin, TX, United States). Environmental conditions were monitored with a temperature/humidity probe (HMP50, Vaisala, Helsinki, Finland) and a CO_2 sensor (GMC20, Vaisala, Vantaa, Finland) connected to a datalogger (CR6, Campbell Scientific, Logan, UT, United States), which calculated the vapor pressure deficit (VPD) from the temperature and relative humidity measurements. The datalogger controlled CO_2 levels by opening a valve connected to a compressed CO_2 cylinder for 0.1 s, whenever the measured CO_2 dropped below 800 $\mu mol \cdot mol^{-1}$. CO_2 enrichment was used because it can make supplemental lighting more economical by increasing photosynthesis and growth more than supplemental lighting by itself (Both et al., 1997; Ferentinos et al., 2000). Excess water vapor was removed using a dehumidifier (FAD704DWD13, Electrolux, Charlotte, NC, United States). The temperature was 19.7 ± 0.8°C, CO_2 concentration was 797 ± 47 $\mu mol \cdot mol^{-1}$, and the VPD was 0.99 ± 0.17 kPa (mean ± *SD*).

Plant Material

Lettuce 'Green Salad Bowl' and 'Little Gem' were seeded into 10-cm square pots filled with peat-perlite substrate (Fafard 2P; Sun Gro Horticulture, Agawam, MA, United States). Seedlings were thinned to one plant per pot at 6 days after seeding. Plants were sub-irrigated as needed using a water-soluble fertilizer solution with a nitrogen concentration of 100 $mg \cdot L^{-1}$ (Peters Excel 15-5-15 CalMag Special, ICL, Summerville, SC, United States). The experimental unit was a group of 15 plants of one cultivar, with three replications, and six treatments (PPFD fluctuations). The plants were grown over a 6 weeks period.

Treatments

Plants were grown under six different fluctuating lighting treatments with the photosynthetic photon flux density (PPFD) switching from high to low PPFD every 15 min throughout the photoperiod. The PPFDs in the different treatments were approximately 400/0, 360/40, 320/80, 280/120, 240/160, and 200/200 $\mu mol \cdot m^{-2} \cdot s^{-1}$, with a photoperiod of 16 h. The DLI in all treatments was ∼11.5 $mol \cdot m^{-2} \cdot day^{-1}$. The actual PPFD was not exactly equal to the target PPFD and measured using a spectroradiometer (SS-110, Apogee, Logan, UT) (**Table 1**). Measurements were taken at 9 cm height from the ebb-and-flow tray, 3 cm above the soil line at the center of each 15-unit tray.

TABLE 1 | Target PPFDs (mean ± *SD*; *n* = 3) and actual measured PPFDs for each fluctuating lighting treatment.

Target high and low PPFD ($\mu mol \cdot m^{-2} \cdot s^{-1}$)	High PPFD ($\mu mol \cdot m^{-2} \cdot s^{-1}$)	Low PPFD ($\mu mol \cdot m^{-2} \cdot s^{-1}$)
200/200	211 ± 5	211 ± 5
240/160	249 ± 4	167 ± 4
280/120	283 ± 5	123 ± 3
320/80	341 ± 8	86 ± 2
360/40	367 ± 19	41 ± 2
400/0	420 ± 16	0.2 ± 0.1

Data was collected at canopy level.

Data Collection and Analysis

Canopy images of trays with 15 plants were taken weekly after seedling emergence [16, 23, 30, and 37 days after planting (DAP)]. We used a monochrome camera (CM3-U3-31S4M-CS, Flir, Wilsonville, OR, United States) outfitted with a 680 nm long-pass filter (Midwest Optics, Palatine, IL, United States) mounted inside a light-proof grow tent. Plants were illuminated with a blue LED (225 ultrathin grow light, Yescom United States, City of Industry, CA, United States). The camera took images of the fluorescence emitted by the leaves, excited by the blue light, resulting in grayscale images, with the canopy light and the background dark. The projected canopy size for each tray of plants was determined using threshold separation in ImageJ (Narayanan et al., 2019).

Gas exchange data was collected on one 'Green Salad Bowl' plant per experimental unit at 35–37 DAP to determine the photosynthesis of plants within each treatment using a portable leaf gas exchange system (CIRAS-3, PP Systems, Inc., Amesbury, MA). The youngest fully expanded leaf was used for these measurements. The leaf gas exchange system was programmed to run for 45 min; 15 min of low PPFD (as an acclimation period), followed by 15 min of high and 15 min of low PPFD. Built in white LEDs were programmed to set the target PPFDs in the leaf cuvette. Cuvette temperature, CO_2 concentration, and VPD were similar to conditions in the growth chamber. The net assimilation data for each 15 min period were averaged ($A_{n,15}$), as were the data from the 30 min period, which included 15 min of both high and low PPFD ($A_{n,30}$). Stomatal conductance was measured as well.

'Green Salad Bowl' was harvested at 40 DAP and 'Little Gem' was harvested at 43 DAP. The chlorophyll content index (CCI) (Opti-Sciences, CCM-200plus, Hudson, NH), number of leaves, length and width of the longest leaf, total leaf area, and shoot dry weight were measured on the three plants in the center of each tray. SLA was calculated as leaf area/shoot dry weight. Dry mass measurements were collected from the 12 remaining border plants for calculating total dry mass.

Experimental Design and Statistical Analysis

The study was set up as a randomized complete block with three replications and a split-plot (cultivar). Data was analyzed

using both linear and non-linear regression (SigmaPlot 11, Systat Software, Inc., San Jose, CA).

RESULTS

Crop Growth and Morphology

Projected canopy size at 16 DAP was low and not affected by PPFD fluctuations for either cultivar. At all subsequent times, PPFD fluctuations did affect projected canopy size, with 400/0 $\mu mol \cdot m^{-2} \cdot s^{-1}$ fluctuations resulting in the smallest canopy size in both cultivars. In 'Green Salad Bowl,' the 360/40 $\mu mol \cdot m^{-2} \cdot s^{-1}$ treatment resulted in slightly lower projected canopy size than treatments with smaller PPFD fluctuations at 23 and 30 DAP, but no longer at 37 DAP (**Figure 1**).

Projected canopy size of 'Green Salad Bowl' was more sensitive to PPFD fluctuations than that of 'Little Gem'; at 37 DAP, projected canopy size of 'Little Gem' was 32% lower with 400/0 $\mu mol \cdot m^{-2} \cdot s^{-1}$ fluctuations than in the other treatments, while for 'Green Salad Bowl,' this reduction was 64%. In treatments with PPFD fluctuations of 360/40 $\mu mol \cdot m^{-2} \cdot s^{-1}$ or less, 'Little Gem' had a ∼12.5% smaller projected canopy than 'Green Salad Bowl' at 37 DAP (**Figure 1**). This is consistent with the growth habits of these two cultivars; 'Green Salad Bowl' is a loose-leaf lettuce, while 'Little Gem' forms a small head.

In both cultivars, there was an asymptotic increase in leaf number, length, width, and chlorophyll content index. 'Green Salad Bowl' plants averaged 6.7 leaves in the 400/0 $\mu mol \cdot m^{-2} \cdot s^{-1}$ treatment, compared to 12.3 leaves in the other treatments (**Figure 2**). For 'Little Gem,' plants in the 400/0 $\mu mol \cdot m^{-2} \cdot s^{-1}$ treatment averaged 11.6 leaves, increasing to 14.3 leaves in the 360/40 $\mu mol \cdot m^{-2} \cdot s^{-1}$ treatment and 17.4 leaves in the other treatments (**Figure 2**). Leaf length of 'Green Salad Bowl' averaged 12.5 cm in the 400/0 $\mu mol \cdot m^{-2} \cdot s^{-1}$ treatment, compared to 19.4 cm in the other treatments. 'Little Gem' plants in the 400/0 $\mu mol \cdot m^{-2} \cdot s^{-1}$ treatment averaged a leaf length of 10.5 cm, increasing to 14.4 cm in the 360/40 $\mu mol \cdot m^{-2} \cdot s^{-1}$ and 16.6 cm for the other treatments (**Figure 2**). Leaf width for 'Green Salad Bowl' averaged 5.8 cm in the 400/0 $\mu mol \cdot m^{-2} \cdot s^{-1}$ treatment, increasing to 13.1 cm in the 360/40 $\mu mol \cdot m^{-2} \cdot s^{-1}$ treatments and 15.1 cm in all other treatments. For 'Little Gem,' the 400/0 $\mu mol \cdot m^{-2} \cdot s^{-1}$ treatment resulted in a leaf width of 7.0 cm, increasing to 8.6 cm in the other treatments (**Figure 2**).

'Green Salad Bowl' had an ∼67% lower chlorophyll content index than 'Little Gem.' Plants grown under the 400/0 $\mu mol \cdot m^{-2} \cdot s^{-1}$ treatment had an ∼65 and ∼75% lower chlorophyll content index as compared to the other treatments in 'Green Salad Bowl' and 'Little Gem,' respectively. 'Green Salad Bowl' had larger but fewer leaves than 'Little Gem' and the number of leaves increased more gradually, from ∼12 to 18, for 'Little Gem than for Green Salad Bowl' (∼7–12 leaves), as PPFD fluctuations decreased (**Figure 2** and **Supplementary Figure S1**).

On average, 'Little Gem' had an ∼8% larger leaf area than 'Green Salad Bowl' (**Figure 3**), which contrasts with the substantially larger projected canopy size of 'Green Salad Bowl.' This is likely related to the compact and head-forming 'Little Gem' having smaller but more leaves (**Figure 2**), which overlap each other more than the leaves of the loose-leaf 'Green Salad Bowl' lettuce.

Leaf area and total dry mass of both cultivars increased asymptotically as the lower PPFD increased from 0 to 200 $\mu mol \cdot m^{-2} \cdot s^{-1}$. 'Green Salad Bowl' plants in the 400/0 $\mu mol \cdot m^{-2} \cdot s^{-1}$ and 360/40 $\mu mol \cdot m^{-2} \cdot s^{-1}$ treatments, had a ∼90 and ∼28% lower dry mass and an ∼83 and

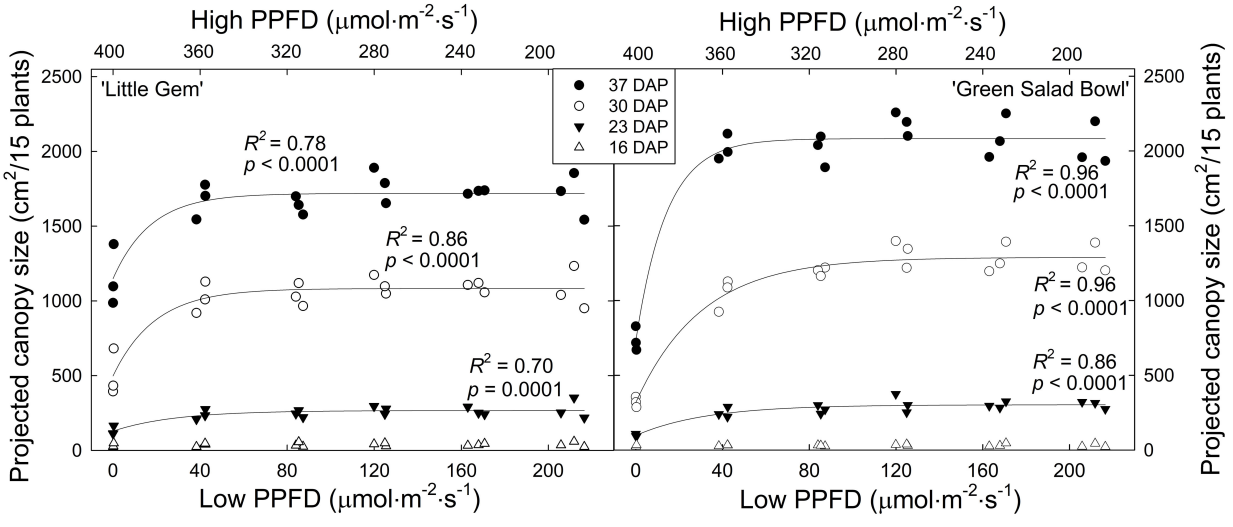

FIGURE 1 | Projected canopy size of 'Little Gem' and 'Green Salad Bowl' lettuce (*Lactuca sativa*) at 16, 23, 30, and 37 days after planting (DAP), measured on experimental units consisting of 15 plants. Plants were grown under fluctuating photosynthetic photon flux density (PPFD), with PPFD changing every 15 min between high and low intensities (∼400/0, 360/40, 320/80, 280/120, 240/160, and 200/200 $\mu mol \cdot m^{-2} \cdot s^{-1}$). Identical symbols represent the three replications of each treatment.

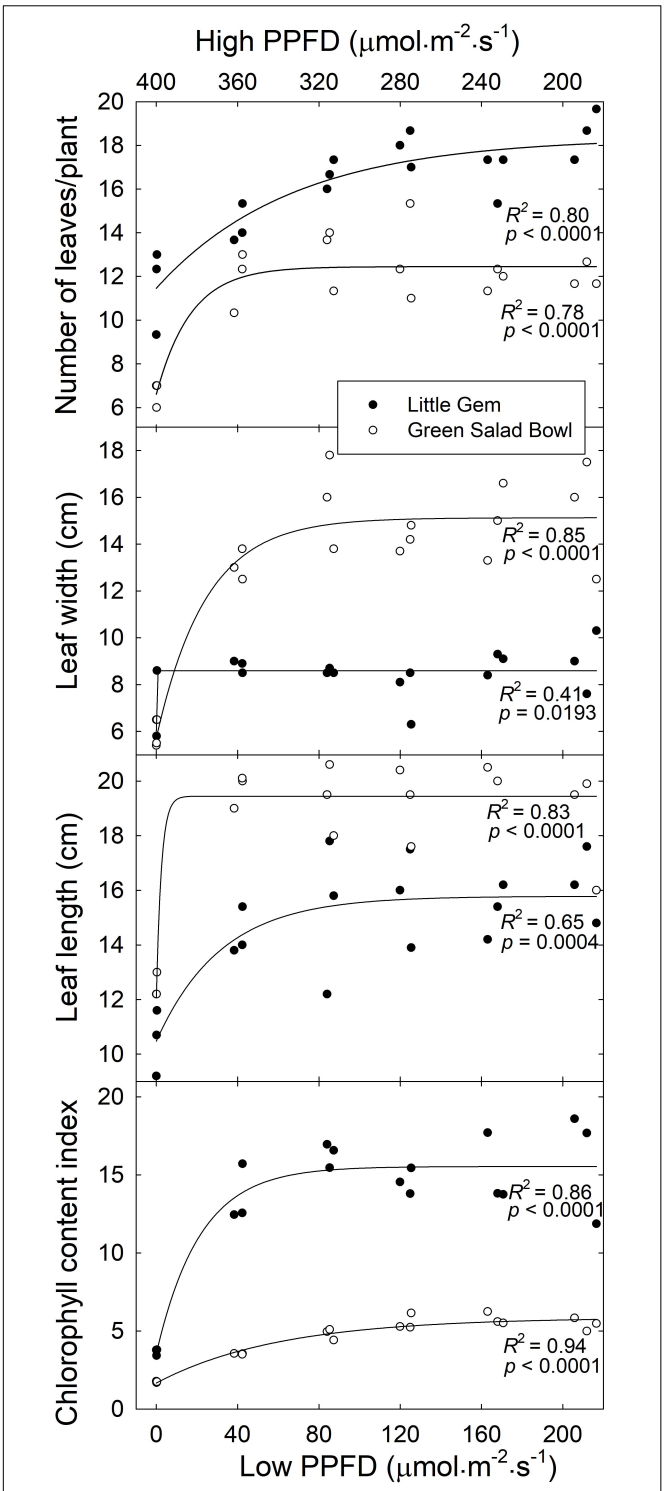

FIGURE 2 | Number of leaves per plant, leaf width, leaf length, and chlorophyll content index as a function of treatment (*x*-axis indicates lower *PPFD*). Symbols (three replications per treatment) represent cultivars 'Green Salad Bowl' (open symbols) and 'Little Gem' (closed symbols) of lettuce (*Lactuca sativa*). Measurements are from the three center plants from each tray. Plants were grown under fluctuating photosynthetic photon flux density (*PPFD*), with *PPFD* changing every 15 min between high and low intensities (~400/0, 360/40, 320/80, 280/120, 240/160, and 200/200 $\mu mol \cdot m^{-2} \cdot s^{-1}$).

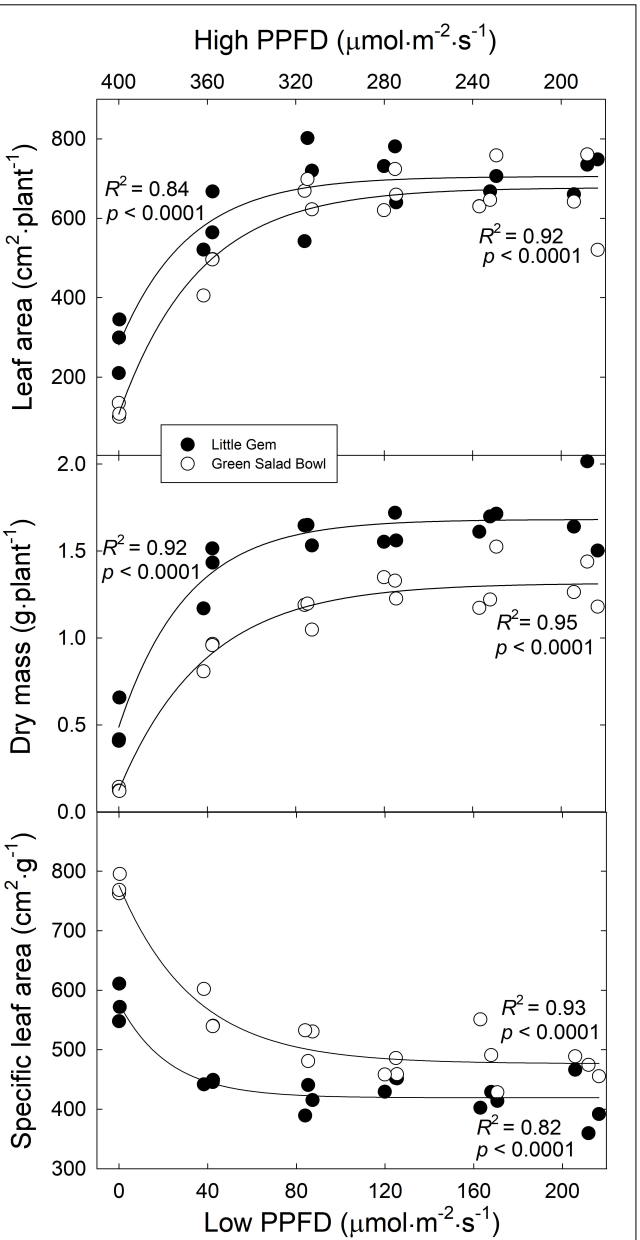

FIGURE 3 | Leaf area per plant, dry mass per plant, and specific leaf area as a function of the treatments (*x*-axis indicates lower PPFD). Symbols (three replications per treatment) represent cultivars 'Green Salad Bowl' (open symbols) and 'Little Gem' (closed symbols) of lettuce (*Lactuca sativa*). Measurements from the three center plants from each tray. Plants were grown under fluctuating photosynthetic photon flux density (PPFD), with PPFD changing every 15 min between high and low intensities (~00/0, 360/40, 320/80, 280/120, 240/160, and 200/200 $\mu mol \cdot m^{-2} \cdot s^{-1}$).

~30% lower leaf area compared to the other treatments (**Figure 3**). 'Little Gem' plants in the 400/0 $\mu mol \cdot m^{-2} \cdot s^{-1}$ and 360/40 $\mu mol \cdot m^{-2} \cdot s^{-1}$ treatments, had a ~70 and ~22% lower dry mass and an ~59 and ~16% lower leaf area compared to the other treatments. 'Green Salad Bowl' had

a ∼12% lower dry mass and ∼28% lower leaf area than 'Little Gem' (**Figure 3**).

Specific leaf area decreased exponentially as the lower PPFD increased from 0 to 200 $\mu mol \cdot m^{-2} \cdot s^{-1}$, suggesting thinner leaves with large PPFD fluctuations in both lettuce cultivars. The SLA of 'Green Salad Bowl' plants in the 360/40 $\mu mol \cdot m^{-2} \cdot s^{-1}$ treatment was ∼28%, and in those with smaller PPFD fluctuations ∼37%, lower than in the 400/0 $\mu mol \cdot m^{-2} \cdot s^{-1}$ treatment (**Figure 3**). 'Little Gem' SLA in the 360/40 $\mu mol \cdot m^{-2} \cdot s^{-1}$ treatment was ∼23%, and in the other treatments ∼27% lower than in the 400/0 $\mu mol \cdot m^{-2} \cdot s^{-1}$ treatment. 'Little Gem' had a ∼18% lower SLA than 'Green Salad Bowl' (**Figure 3**).

Leaf Assimilation Rates

Net assimilation rates of 'Green Salad Bowl' lettuce in most treatments increased rapidly as the PPFD was changed from low to high. However, plants in the 400/0 $\mu mol \cdot m^{-2} \cdot s^{-1}$ treatment, and to a lesser extent the 360/40 $\mu mol \cdot m^{-2} \cdot s^{-1}$ treatment, showed a more gradual initial increase in A_n (for about 5 min) following exposure to high PPFD. Net assimilation did not reach a steady state during the 15 min at high PPFD in the 400/0 and 360/40 $\mu mol \cdot m^{-2} \cdot s^{-1}$ treatments, but instead kept increasing slowly (**Figure 4**). This suggests that the plants may have been trying to acclimate to the high PPFD but were not able to fully do so before the PPFD was lowered again. In all other treatments, stable A_n was reached within 2 min at high PPFD. After switching from high to low PPFD, A_n stabilized quickly in all treatments. The 200/200 $\mu mol \cdot m^{-2} \cdot s^{-1}$ treatment resulted in consistent A_n over the 30 min period, ranging between 8.1 and 8.6 $\mu mol \cdot m^{-2} \cdot s^{-1}$ (**Figure 4**).

The $A_{n,15}$ of 'Green Salad Bowl' lettuce increased linearly, from ∼-1 to 14 $\mu mol \cdot m^{-2} \cdot s^{-1}$, as PPFD increased from 0 to 320 $\mu mol \cdot m^{-2} \cdot s^{-1}$ and decreased rapidly at even higher PPFDs. At 400 $\mu mol \cdot m^{-2} \cdot s^{-1}$, $A_{n,15}$ averaged only ∼4 $\mu mol \cdot m^{-2} \cdot s^{-1}$, ∼9.1 $\mu mol \cdot m^{-2} \cdot s^{-1}$ lower than at a PPFD of 320 $\mu mol \cdot m^{-2} \cdot s^{-1}$ (**Figure 5**), indicating that the extreme PPFD fluctuations in the 400/0 $\mu mol \cdot m^{-2} \cdot s^{-1}$ treatment seriously impaired the photosynthetic physiology.

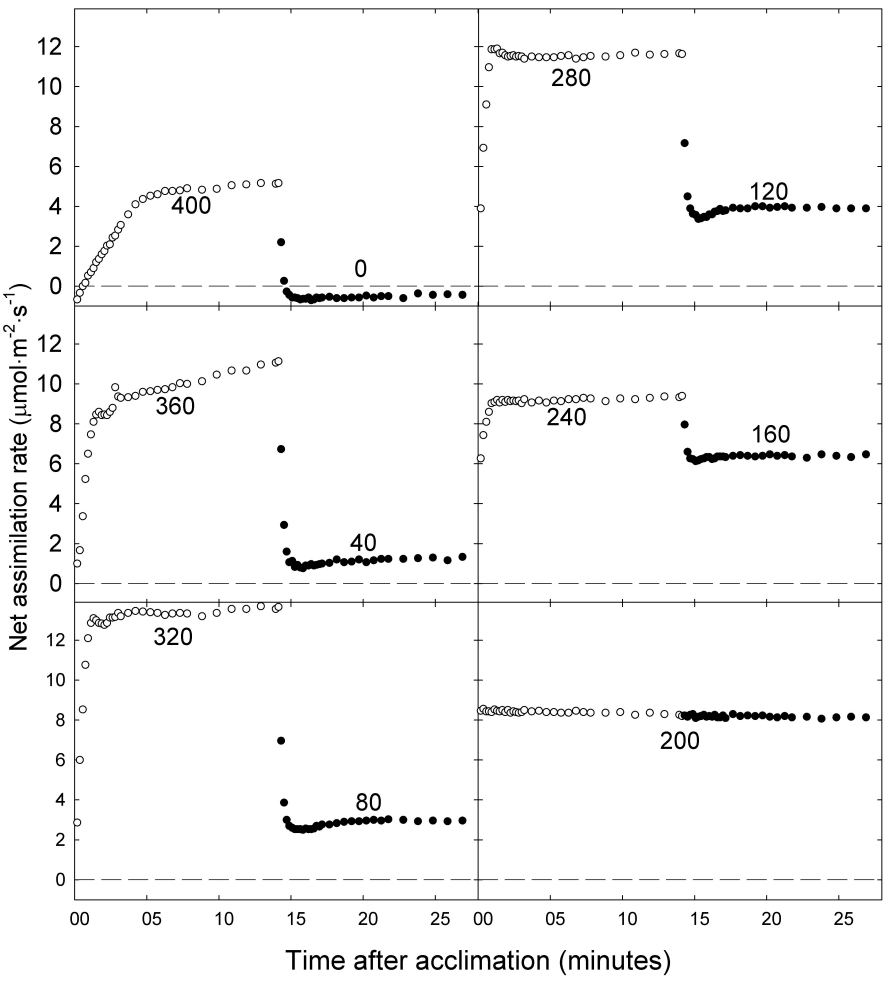

FIGURE 4 | Net photosynthetic rate of 'Green Salad Bowl' lettuce (*Lactuca sativa*) during a 15 min high photosynthetic photon flux density (PPFD) period followed by a 15 min low PPFD period (400/0, 360/40, 320/80, 280/120, 240/160, and 200/200 $\mu mol \cdot m^{-2} \cdot s^{-1}$). Open circles represent high PPFD, and closed circles low PPFD. Values in each graph indicate the PPFD.

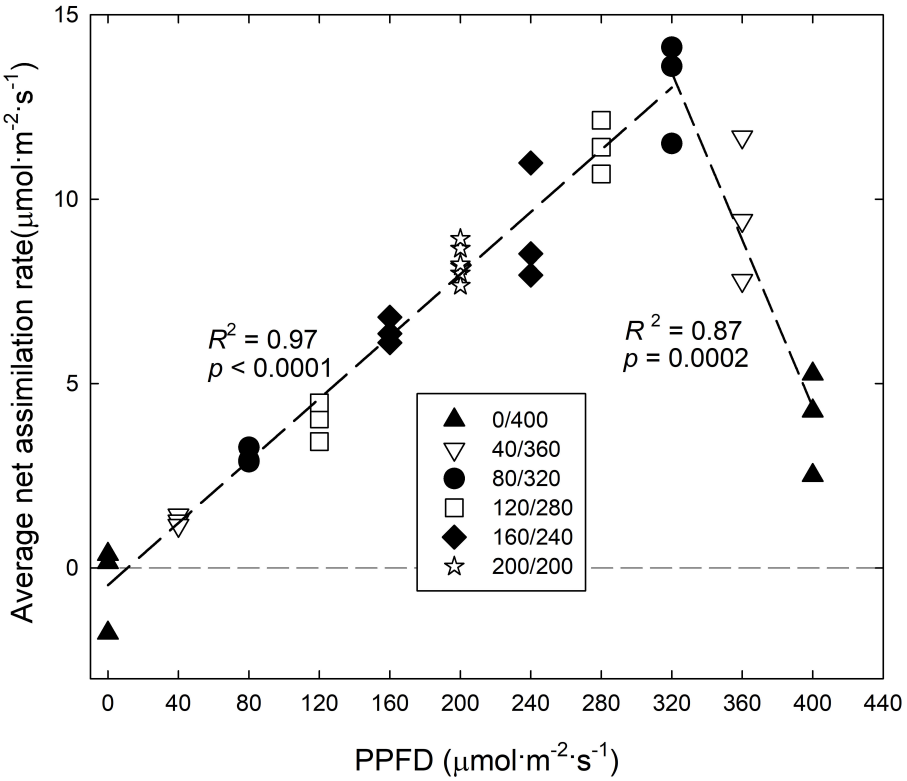

FIGURE 5 | Average net assimilation rate over 15 min ($A_{n,15}$) of 'Green Salad Bowl' lettuce (*Lactuca sativa*) as a function of photosynthetic photon flux density (PPFD). Photosynthesis was measured for 15 min under high PPFD, followed by 15 min under low PPFD (see **Figure 2**). Plants were grown under fluctuating PPFD, changing every 15 min between high and low PPFD (~400/0, 360/40, 320/80, 280/120, 240/160, and 200/200 μmol·m^{-2}·s^{-1}).

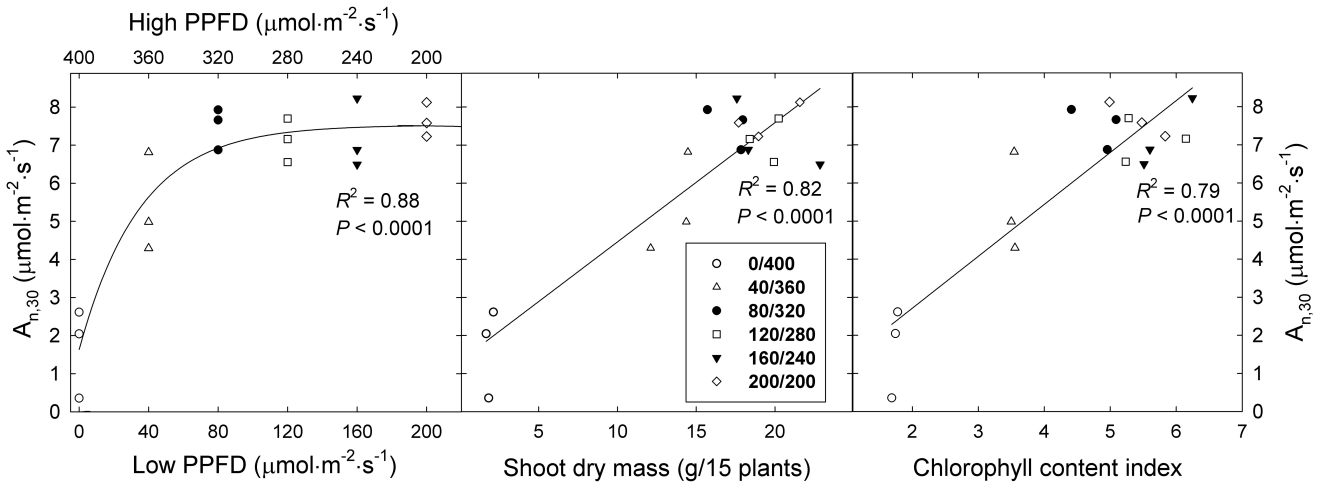

FIGURE 6 | Average net assimilation rate over 30 min ($A_{n,30}$) of 'Green Salad Bowl' lettuce (*Lactuca sativa*) as a function of fluctuating photosynthetic photon flux density (PPFD), total dry mass, and chlorophyll content index. Symbols represent data from each lighting treatment (three replications per treatment). Plants were grown under fluctuating PPFD, changing every 15 min between high and low PPFD (~400/0, 360/40, 320/80, 280/120, 240/160, and 200/200 μmol·m^{-2}·s^{-1}).

The $A_{n,30}$ of 'Green Salad Bowl' lettuce increased asymptotically as the lower PPFD increased from 0 to 200 μmol·m^{-2}·s^{-1} (and the high PPFD decreased from 400 to 200 μmol·m^{-2}·s^{-1}), with little or no difference among the 320/80, 280/120, 240/160, and 200/200 μmol·m^{-2}·s^{-1} treatments (**Figure 6**). The linear relationship between $A_{n,15}$ at PPFDs from 0 to 320 μmol·m^{-2}·s^{-1} (**Figure 5**) explains the lack of differences $A_{n,30}$ among these four treatments (**Figure 6**).

The $A_{n,30}$ in the 360/40 and 400/0 treatments was ∼27 and 69% lower compared to the other treatments with smaller PPFD fluctuations. The rapid decrease in $A_{n,15}$ at a PPFD above of 320 μmol·m^{-2}·s^{-1} (**Figure 5**) explains the low $A_{n,30}$ in the two treatments with the greatest PPFD fluctuations.

The $A_{n,30}$ data follow the same trends as the dry mass and leaf area data (**Figure 3**). There was a strong positive correlation between the $A_{n,30}$ and shoot dry mass of 'Green Salad Bowl' lettuce, largely due to the low $A_{n,30}$ and dry mass in the 400/0 μmol·m^{-2}·s^{-1} treatment (**Figure 6**). Since A_n underlies dry mass production, this correlation is not surprising. The $A_{n,30}$ of 'Green Salad Bowl' lettuce also was positively correlated with the leaf chlorophyll content index (**Figure 6**), suggesting that the low A_n and dry mass of plants grown under a PPFD of 400/0 μmol·m^{-2}·s^{-1} were at least partly due to the low chlorophyll levels in the leaves of these plants.

SLA of 'Green Salad Bowl' lettuce was negatively correlated with both $A_{n,30}$ and CCI (**Figure 7**). High SLA suggests thinner leaves with fewer and/or smaller mesophyll cells, where most of the carbon assimilation occurs. As the SLA decreased from ∼780 cm^2·g^{-1} (in the 400/0 μmol·m^{-2}·s^{-1} treatment) to 460 cm^2·g^{-1}, $A_{n,30}$ increased from 1.9 to 7.6 μmol·m^{-2}·s^{-1} and CCI increased from 1.7 to 5.4 (**Figure 7**).

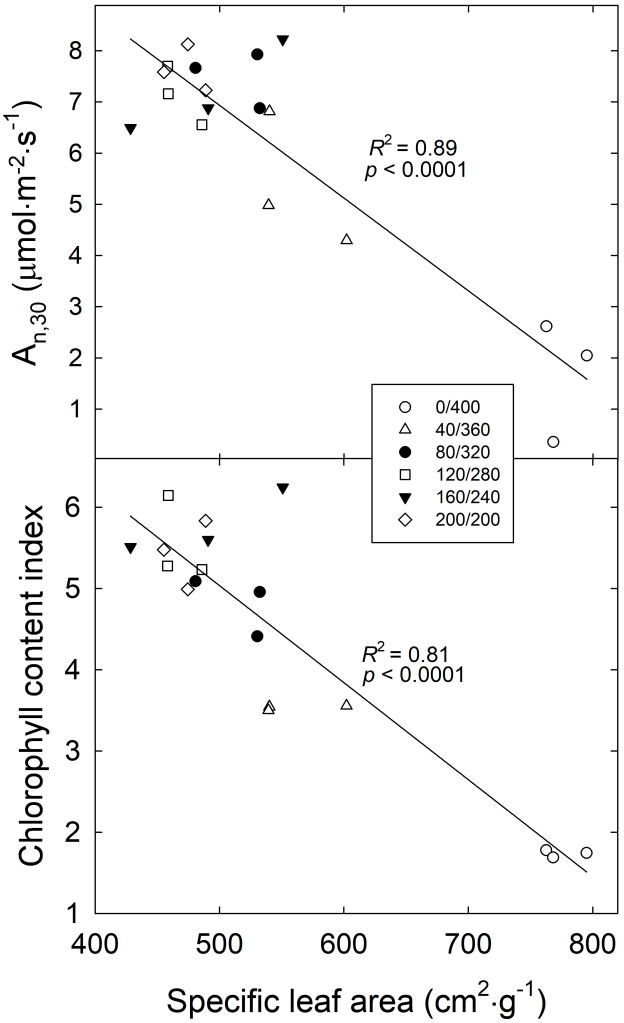

FIGURE 7 | Average net photosynthesis over a 30 min period ($A_{n,30}$) and chlorophyll content index of 'Green Salad Bowl' lettuce (*Lactuca sativa*) as a function of specific leaf area. Symbols represent each treatment, with three replications per treatment. Plants were grown and measured under fluctuating PPFD, changing every 15 min between high and low PPFD (∼ 400/0, 360/40, 320/80, 280/120, 240/160, and 200/200 μmol·m^{-2}·s^{-1}).

DISCUSSION

The Importance of Canopy Size

Projected canopy size (PCS) is a good indicator of the amount of light a canopy intercepts (Klassen et al., 2004) and of morphological changes in response to environmental conditions, in this case fluctuations in PPFD. When taken over a growing period, it provides information on growth rates from seed to maturity. In the 400/0 μmol·m^{-2}·s^{-1} treatment for both cultivars, the plants had a lower PCS than those in other treatments throughout the growing period from 23 DAP until the end of the study (**Figure 1**). A lower projected canopy size reduces the amount of incident light, canopy photosynthesis, and growth (Klassen et al., 2004). Projected canopy sizes in all other treatments were similar, indicating that lettuce canopy development tolerates wide fluctuations in PPFD.

The PCS of 'Green Salad Bowl' was more sensitive to large PPFD fluctuations than that of 'Little Gem.' At 30 and 37 DAP, 'Green Salad Bowl' had a larger PCS than 'Little Gem' in treatments with relatively small PPFD fluctuations (200/200 to 320/80 μmol·m^{-2}·s^{-1}), while 'Green Salad Bowl' had a smaller PCS in the 400/0 μmol·m^{-2}·s^{-1}. This indicates that genetic factors play a role in determining both PCS, as well as cultivar responses to fluctuating PPFD. 'Green Salad Bowl' produces larger leaves than 'Little Gem,' a small head-forming lettuce (**Figure 2**). The importance of PCS in determining crop growth is evident from the positive correlation between PCS at 23, 30, and 37 DAP and final dry mass (**Figure 8**). Our results suggest that measurements of PCS during the growing cycle can provide an early indication of final dry mass production in response to different lighting treatments. Similar correlations between PCS and final dry mass were reported by Elkins and van Iersel (2020) in response to different PPFD and photoperiod treatments, all with the same DLI. Differences in growth among lettuce cultivars are also strongly correlated with differences in canopy size early in the growing cycle (Kim and van Iersel, 2019).

The effects of fluctuating light levels on PCS were consistent with effects on leaf number, length, width, and total leaf area in both cultivars (**Figures 2**, **3**). These treatment effects tended to be larger in 'Green Salad Bowl' than in 'Little Gem.' The reductions in these morphological parameters in response to the 400/0 μmol·m^{-2}·s^{-1}, and to a lesser extent in the 360/40 μmol·m^{-2}·s^{-1} treatments, may be the result the low $A_{n,30}$ (**Figure 6**) and the resulting limited carbohydrate supply for new growth. Plants in 400/0 μmol·m^{-2}·s^{-1} treatment had a higher SLA than

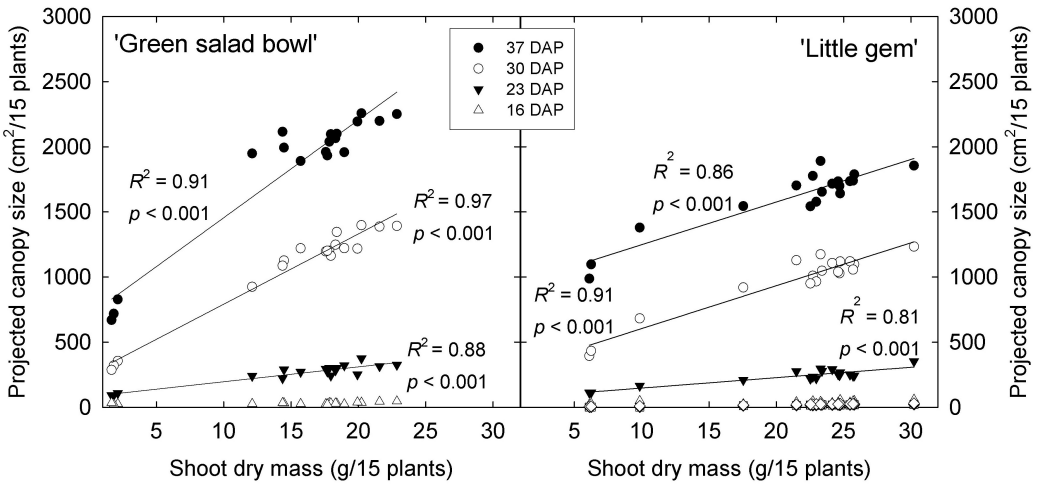

FIGURE 8 | Projected canopy size of 'Green Salad Bowl' and 'Little Gem' lettuce (*Lactuca sativa*) at 16, 23, 30, and 37 days after planting (DAP) vs. shoot dry mass of 15 plants. Symbols represent DAP. Plants were grown under fluctuating *PPFD*, with *PPFD* changing every 15 min between high and low intensities (~400/0, 360/40, 320/80, 280/120, 240/160, and 200/200 $\mu mol \cdot m^{-2} \cdot s^{-1}$).

those in treatments with smaller PPFD fluctuations, possibly in an attempt to produce as much leaf as possible with the limited carbohydrate supply. Smaller leaf area and reduced leaf number in response to a fluctuation light levels (900–90 $\mu mol \cdot m^{-2} \cdot s^{-1}$ every 4 min, compared to a constant PPFD of 250 $\mu mol \cdot m^{-2} \cdot s^{-1}$) has also been reported in *Arabidopsis thaliana* (Kaiser et al., 2020).

Fluctuating Light and Photosynthesis

Since plants in our study were exposed to fluctuating PPFD, their photosynthetic processes had to constantly respond to those changing conditions. Steady state A_n is typically achieved within 5–10 min of exposure to high PPFD (Kalaji et al., 2014). In our study, steady-state A_n was achieved within 2 min after exposure to a high PPFD in the 240/160, 280/120, and 320/80 $\mu mol \cdot m^{-2} \cdot s^{-1}$ treatments (**Figure 4**). This fast response to a change from low to high PPFD suggests that the photosynthetic apparatus in those plants was adequately activated under low PPFD to allow for a rapid response to an increase in PPFD. However, when PPFD was increased from 0 to 400 $\mu mol \cdot m^{-2} \cdot s^{-1}$ or from 40 to 360 $\mu mol \cdot m^{-2} \cdot s^{-1}$, A_n initially increased rapidly, followed by a more gradual increase during the remainder of the 15 min period, never reaching a steady state (**Figure 4**), suggesting that activation of the photosynthetic apparatus in response to a rapid change in PPFD depends on the magnitude of the change in PPFD. Sims and Pearcy (1993) grew the understory species *Alocasia macrorrhiza* with sunflecks for 10–12 min every hour (PPFD of ~280 $\mu mol \cdot m^{-2} \cdot s^{-1}$ sunflecks alternating with ~16 $\mu mol \cdot m^{-2} \cdot s^{-1}$ during the remainder of the hour) and without sunflecks. Plants in both treatments receiving a similar DLI. Induction of full photosynthetic activity in response to a sunfleck required ~40 min, consistent with our observation that plants in the 400/0 and 360/40 $\mu mol \cdot m^{-2} \cdot s^{-1}$ treatments did not achieve steady-state photosynthesis during the 15 min at high PPFD. Exposing plants to sunflecks reduced leaf carbon gain, dry mass (by 89%) and increased SLA (Sims and Pearcy, 1993), similar to our findings in the 400/0 and 360/40 $\mu mol \cdot m^{-2} \cdot s^{-1}$ treatments.

Surprisingly, $A_{n,15}$ decreased as PPFD increased from 320 to 400 $\mu mol \cdot m^{-2} \cdot s^{-1}$ (**Figure 5**). This indicates that large PPFD fluctuations negatively affect the photosynthetic performance of lettuce leaves. Leaf A_n depends on light harvesting, subsequent electron transport in the light reactions of photosynthesis, and the ability of Calvin cycle enzymes to use the products of the light reactions to assimilate CO_2. Pigments in the thylakoid membrane of chloroplasts absorb light energy (photons) and that energy is used to drive electron transport. This results in the reduction of ferredoxin, followed by the reduction of $NADP^+$ to NADPH (Pinnola, 2019) and the formation of a hydrogen gradient across the thylakoid membrane. This hydrogen gradient facilitates the synthesis of ATP. The rate of the light reactions depends on how much light is absorbed by photosynthetic pigments. The CCI was lower in the 400/0 and 360/40 $\mu mol \cdot m^{-2} \cdot s^{-1}$ treatments as compared to the treatments with smaller light fluctuations (**Figure 6**). A low CCI is associated with low leaf absorptance (Bauerle et al., 2004) and would thus be expected to result in low electron transport rates, which may result in low rates of NADPH and ATP production. This is supported by Wei et al. (2020), who reported that fluctuating light inhibits photosystem I and II activity through upregulation of non-photochemical quenching in rice (*Oryza sativa*). This resulted in decreased electron transport and lower ATP synthase activity. Fluctuating light also interfered with stacking of the thylakoid membrane. Thus fluctuating PPFDs can have a strong impact on the light reactions of photosynthesis.

The low chlorophyll levels in the treatments with large PPFD fluctuations may be due to light-dependent nature of chlorophyll biosynthesis. A key step in chlorophyll biosynthesis

is the conversion of protochlorophyllide to chlorophyllide, the immediate precursor to chlorophyll *a* and chlorophyll *b*. This process that is both NADPH- and light-dependent (via the enzyme protochlorophyllide oxidoreductase, POR) (Reinbothe and Reinbothe, 1996). The activation of POR is unique in that its activation depends on the absorption of photons by its substrate protochlorophyllide. This induces a conformational change in the enzyme, activating it. Further complicating the effect of light on POR activity is that plants have multiple POR genes. In *Arabidopsis thaliana*, PORA is expressed in the dark and its expression is strongly inhibited in the light, through a phytochrome mediated process. PORB and PORC, on the other hand have low expression levels in the dark, and expression of PORC is upregulated in the light, through phytochrome-interacting factors (Gabruk and Mysliwa-Kurdziel, 2015). Thus, both the transcript levels and activity of POR are light-dependent and it seems plausible that production of chlorophyll cannot proceed normally when leaves are exposed to constant large light fluctuations, consistent with the low CCI in the 400/0 $\mu mol \cdot m^{-2} \cdot s^{-1}$ treatment (**Figure 2**). The idea that the low $A_{n,15}$ at PPFDs of 360 and 400 $\mu mol \cdot m^{-2} \cdot s^{-1}$ was due at least in part due to poor light absorptance is supported by the positive correlation between CCI and $A_{n,30}$ (**Figure 6**). The low CCI in the 400/0 $\mu mol \cdot m^{-2} \cdot s^{-1}$ treatment may also have been caused partly by leaf morphological effects. Plants in the 400/0 $\mu mol \cdot m^{-2} \cdot s^{-1}$ treatment had a high SLA, i.e., low biomass per unit leaf area. Since CCI is an indicator of the amount of chlorophyll per unit leaf area, a high SLA is likely associated a low CCI. We did indeed find strong negative correlations between SLA and both CCI and $A_{n,30}$ (**Figure 7**), consistent with prior findings (Brodersen and Vogelmann, 2010).

Large fluctuations in PPFD may also affect Calvin cycle activity. The activation of key Calvin cycle enzymes and the biochemical reactions of the Calvin cycle themselves depend on products of the light reactions. Specifically, activation of fructose-1,6-bisphosphatase, sedoheptulose-1,7-bisphosphatase, glyceraldehyde-3-phosphate dehydrogenase, and phosphoribulokinase requires thioredoxin, produced from reduced ferredoxin, for the reduction of regulatory disulfides (Michelet et al., 2013). Low activity of these enzymes can limit photosynthesis by limiting the regeneration of ribulose 1,5-bisphosphate (RuBP). In addition, Rubisco activase is light-dependent, since it relies on a high stroma pH, which results from hydrogen transport from the stroma into the lumen in the light reactions. Rubisco activase activity depends on NADPH and thus on the light reactions (Kleczkowski, 1994). Rubsico is inactive in the dark because of the binding of metabolites to its active site and depends on Rubisco activase to remove those metabolites (Zhang and Portis, 1999).

Thus, light is not only required to drive the light reactions, but also controls the production and activity of chlorophyll and Calvin cycle enzymes. Although our data do not shed light on which enzymatic processes may have been affected by large PPFD fluctuations, it seems likely that such fluctuations interfere with the development of photosynthetic machinery and normal CO_2 assimilation. The low $A_{n,15}$ at PPFDs of 360 and 400 $\mu mol \cdot m^{-2} \cdot s^{-1}$ resulted in low $A_{n,30}$ in the 360/40 and especially 400/0 $\mu mol \cdot m^{-2} \cdot s^{-1}$ treatments. That low A_n was likely partly responsible for the relatively poor growth in the 360/40 and 400/0 $\mu mol \cdot m^{-2} \cdot s^{-1}$ treatments, since $A_{n,30}$ was strongly and positively correlated with shoot dry mass (**Figure 6**).

Stomatal conductance was also greatly affected by the light treatments (**Supplementary Figure S2**), with conductance decreasing with increasing PPFD fluctuations. Interestingly, conductance was not very responsive to the PPFD fluctuations themselves and remained stable during 15 min at high, followed by 15 min at low PPFD. The results may suggest that the low $A_{n,30}$ in the 400/0 and 360/40 $\mu mol \cdot m^{-2} \cdot s^{-1}$ treatments may have been partly due to the low stomatal conductance in these treatments. However, that appears unlikely, given that the leaf internal CO_2 concentration was 568 to 738 $\mu mol \cdot mol^{-1}$ and not affected by treatment. These relatively high leaf internal CO_2 concentrations are unlikely to seriously limit CO_2 assimilation. The differences in stomatal conductance thus seem to have been the result, rather than the cause, of the differences in $A_{n,30}$.

Practical Implications

'Little Gem' and 'Green Salad Bowl' lettuce tolerate fluctuating light levels, as long as the fluctuations are not extreme. This is consistent with the findings of Sørensen et al. (2016) and suggests that regulating supplemental light in response to real-time electricity prices is feasible for controlled environment agriculture. Our research was limited to two lettuce cultivars, which generally behaved similarly. Follow-up research on spreading (e.g., strawberry) and vine crops (e.g., tomato bell peppers, cucumbers) is needed to determine how other crops respond. In addition, we only tested fluctuations at 15 min intervals and how plants respond to different intervals is not clear. Although we did not answer all questions related to fluctuating lights, this research indicates that there is potential to reduce the electricity costs associated with supplemental lighting in response to real-time electricity price fluctuations. Dynamic algorithms that control supplemental lighting in response to variable sunlight conditions (Seginer et al., 2006) could be updated to incorporate real time pricing and implemented in the greenhouse industry. Such algorithms have been described (Clausen et al., 2015; Harbick et al., 2016; Sørensen et al., 2016), but it is not clear if they have been implemented in commercial greenhouses.

CONCLUDING REMARKS

Our results indicate that lettuce can tolerate a wide range of fluctuating light levels. A constant PPFD is not needed to maintain proper growth and development of 'Little Gem' and 'Green Salad Bowl.' Extreme fluctuations, 400/0 $\mu mol \cdot m^{-2} \cdot s^{-1}$ and to a lesser extent the 360/40 $\mu mol \cdot m^{-2} \cdot s^{-1}$ treatments, resulted in plants with fewer and smaller leaves, lower chlorophyll content, and lower assimilation rates compared to those in

all other treatments. However, results with smaller PPFD fluctuations indicate that growers can take advantage of variable electricity prices to provide light in controlled environment operations. This can aid growers in reducing operating costs and increase profitability.

DATA AVAILABILITY STATEMENT

The raw data supporting the conclusions of this article will be made available by the authors, without undue reservation.

AUTHOR CONTRIBUTIONS

RB and MI designed the experiment, discussed the data, and revised the manuscript. RB performed the experiment, analyzed the data, and prepared the first draft. Both authors contributed to the article and approved the submitted version.

FUNDING

This study was funded by the USDA-NIFA-SCRI award number 2018-51181-28365, project Lighting Approaches to Maximize Profits.

SUPPLEMENTARY MATERIAL

The Supplementary Material for this article can be found online at: https://www.frontiersin.org/articles/10.3389/fpls.2021.619973/full#supplementary-material

Supplementary Figure 1 | Images of 'Little Gem' (left and middle top) and 'Green Salad Bowl' (right and middle bottom) lettuce (*Lactuca sativa*) grown at PPFDs of 200/200 and 400/0 $\mu mol \cdot m^{-2} \cdot s^{-1}$ treatments, fluctuating at 15 min intervals.

Supplementary Figure 2 | Stomatal conductance of 'Green Salad Bowl' lettuce (*Lactuca sativa*) during a 15 min high PPFD period followed by a 15 min low *PPFD* period (~400/0, 360/40, 320/80, 280/120, 240/160, and 200/200 $\mu mol \cdot m^{-2} \cdot s^{-1}$).

REFERENCES

Agrylist (2017). *State of Indoor Farming*. New York, NY: Agrylist, 39.

Albright, L., Both, A., and Chiu, A. (2000). Controlling greenhouse light to a consistent daily integral. *Trans. ASAE* 43, 421–431. doi: 10.13031/2013.2721

Bauerle, W. L., Weston, D. J., Bowden, J. D., Dudley, J. B., and Toler, J. E. (2004). Leaf absorptance of photosynthetically active radiation in relation to chlorophyll meter estimates among woody plant species. *Sci. Hortic.* 101, 169–178. doi: 10.1016/j.scienta.2003.09.010

Both, A.-J., Albright, L., and Langhans, R. (1997). Coordinated management of daily PAR integral and carbon dioxide for hydroponic lettuce production. *II Model. Plant Growth Environ. Control Farm Manage. Prot. Cultiv.* 456, 45–52. doi: 10.17660/actahortic.1998.456.3

Brodersen, C. R., and Vogelmann, T. C. (2010). Do changes in light direction affect absorption profiles in leaves? *Funct. Plant Biol.* 37, 403–412. doi: 10.1071/FP09262

Chazdon, R. L., and Pearcy, R. W. (1986). Photosynthetic responses to light variation in rainforest species. II. Carbon gain and photosynthetic efficiency during lightflecks. *Oecologia* 69, 524–531. doi: 10.1007/bf00410358

Chazdon, R. L., and Pearcy, R. W. (1991). The importance of sunflecks for forest understory plants. *Bioscience* 41, 760–766. doi: 10.2307/1311725

Clausen, A., Maersk-Moeller, H. M., Soerensen, J. C., Joergensen, B. N., Kjaer, K. H., and Ottosen, C. O. (2015). "Integrating commercial greenhouses in the smart grid with demand response based control of supplemental lighting," in *Proceedings of the 2015 International Conference on Industrial Technology and Management Science (ITMS 2015)*, Tianjin.

Cossu, M., Ledda, L., Urracci, G., Sirigu, A., Cossu, A., Murgia, L., et al. (2017). An algorithm for the calculation of the light distribution in photovoltaic greenhouses. *Sol. Energy* 141, 38–48. doi: 10.1016/j.solener.2016.11.024

Cossu, M., Yano, A., Solinas, S., Deligios, P. A., Tiloca, M. T., Cossu, A., et al. (2020). Agricultural sustainability estimation of the European photovoltaic greenhouses. *Eur. J. Agron.* 118:126074. doi: 10.1016/j.eja.2020.126074

Elkins, C., and van Iersel, M. W. (2020). Longer photoperiods with the same daily light integral increase daily electron transport through photosystem II in lettuce. *Plants* 9:1172. doi: 10.3390/plants9091172

Emmott, C. J., Röhr, J. A., Campoy-Quiles, M., Kirchartz, T., Urbina, A., Ekins-Daukes, N. J., et al. (2015). Organic photovoltaic greenhouses: a unique application for semi-transparent PV? *Energy Environ. Sci.* 8, 1317–1328. doi: 10.1039/c4ee03132f

Faust, J. E., and Logan, J. (2018). Daily light integral: a research review and high-resolution maps of the United States. *HortScience* 53, 1250–1257. doi: 10.21273/hortsci13144-18

Ferentinos, K., Albright, L., and Ramani, D. (2000). SE—structures and environment: optimal light integral and carbon dioxide concentration combinations for lettuce in ventilated greenhouses. *J. Agric. Eng. Res.* 77, 309–315.

Gabruk, M., and Mysliwa-Kurdziel, B. (2015). Light-dependent protochlorophyllide oxidoreductase: phylogeny, regulation, and catalytic properties. *Biochemistry* 54, 5255–5262. doi: 10.1021/acs.biochem.5b00704

Harbick, K., Albright, L. D., and Mattson, N. S. (2016). "Electrical savings comparison of supplemental lighting control systems in greenhouse environments," in *Proceedings of the 2016 ASABE Annual International Meeting*, Vol. 1, (St. Joseph, MI: American Society of Agricultural and Biological Engineers), 8. doi: 10.13031/aim.20162460478

Kaiser, E., Walther, D., and Armbruster, U. (2020). Growth under fluctuating light reveals large trait variation in a panel of *Arabidopsis* accessions. *Plants* 9:316. doi: 10.3390/plants9030316

Kalaji, H. M., Schansker, G., Ladle, R. J., Goltsev, V., Bosa, K., Allakhverdiev, S. I., et al. (2014). Frequently asked questions about in vivo chlorophyll fluorescence: practical issues. *Photosynth. Res.* 122, 121–158. doi: 10.1007/s11120-014-0024-6

Kim, C., and van Iersel, M. W. (2019). "Morphological and physiological screening for growth differences among 11 lettuce cultivars," in *Proceedings of the Annual Conference of the American-Society-for-Horticultural-Science*, (Alexandria, VA: Amer Soc Horticultural Science), S89–S90.

Kjaer, K. H., Ottosen, C.-O., and Jørgensen, B. N. (2011). Cost-efficient light control for production of two campanula species. *Sci. Hortic.* 129, 825–831. doi: 10.1016/j.scienta.2011.05.003

Klassen, S., Ritchie, G., Frantz, J., Pinnock, D., and Bugbee, B. (2004). "Real−time imaging of ground cover: relationships with radiation capture, canopy photosynthesis, and daily growth rate," in *Digital Imaging and Spectral Techniques: Applications to Precision Agriculture and Crop Physiology*, Vol. 66, eds T. VanToai, D. Major, M. McDonald, J. Schepers, and L. Tarpley (Madison,WI: ASA Special Publications), 1–14. doi: 10.2134/asaspecpub66.c1

Kleczkowski, L. A. (1994). Inhibitors of photosynthetic enzymes/carriers and metabolism. *Annu. Rev. Plant Biol.* 45, 339–367. doi: 10.1146/annurev.pp.45.060194.002011

Knapp, A., and Smith, W. (1987). Stomatal and photosynthetic responses during sun/shade transitions in subalpine plants: influence on water use efficiency. *Oecologia* 74, 62–67. doi: 10.1007/bf00377346

Kromdijk, J., Głowacka, K., Leonelli, L., Gabilly, S. T., Iwai, M., Niyogi, K. K., et al. (2016). Improving photosynthesis and crop productivity by accelerating recovery from photoprotection. *Science* 354, 857–861. doi: 10.1126/science.aai8878

Michelet, L., Zaffagnini, M., Morisse, S., Sparla, F., Pérez-Pérez, M. E., Francia, F., et al. (2013). Redox regulation of the Calvin–Benson cycle: something old, something new. *Front. Plant Sci.* 4:470. doi: 10.3389/fpls.2013.00470

Narayanan, M., van Iersel, M. W., and Haidekker, M. (2019). "Chlorophyll fluorescence imaging: a novel, simple and non-destructive method for canopy size imaging," in *Proceedings of the 2019 ASHS Annual Conference*, (Alexandria, VA: ASHS).

Pinnola, A. (2019). The rise and fall of light-harvesting complex stress-related proteins as photoprotection agents during evolution. *J. Exp. Bot.* 70, 5527–5535. doi: 10.1093/jxb/erz317

Reinbothe, S., and Reinbothe, C. (1996). The regulation of enzymes involved in chlorophyll biosynthesis. *Eur. J. Biochem.* 237, 323–343. doi: 10.1111/j.1432-1033.1996.00323.x

Seginer, I., Albright, L. D., and Ioslovich, I. (2006). Improved strategy for a constant daily light integral in greenhouses. *Biosyst. Eng.* 93, 69–80. doi: 10.1016/j.biosystemseng.2005.09.007

Sims, D., and Pearcy, R. (1993). Sunfleck frequency and duration affects growth rate of the understorey plant, Alocasia macrorrhiza. *Funct. Ecol.* 7, 683–689. doi: 10.2307/2390189

Sørensen, J. C., Kjær, K. H., Ottosen, C.-O., and Jørgensen, B. N. (2016). "DynaGrow-Multi-objective optimization for energy cost-efficient control of supplemental light in greenhouses," in *Proceedings of the 8th International Joint Conference on Computational Intelligence (IJCCI 2016)*, (Belgium: ECTA), 41–48.

van Iersel, M. W., and Gianino, D. (2017). An adaptive control approach for light-emitting diode lights can reduce the energy costs of supplemental lighting in greenhouses. *HortScience* 52, 72–77. doi: 10.21273/hortsci11385-16

Vialet-Chabrand, S., Matthews, J. S., Simkin, A. J., Raines, C. A., and Lawson, T. (2017). Importance of fluctuations in light on plant photosynthetic acclimation. *Plant Physiol.* 173, 2163–2179. doi: 10.1104/pp.16.01767

Watanabe, H. (2011). "Light-controlled plant cultivation system in Japan-development of a vegetable factory using LEDs as a light source for plants," in *Paper presented at the VI International Symposium on Light in Horticulture*, Tsukuba, 37–44. doi: 10.17660/ActaHortic.2011.907.2

Weaver, G., and van Iersel, M. W. (2019). Photochemical characterization of greenhouse-grown lettuce (*Lactuca sativa* L.'Green Towers') with applications for supplemental lighting control. *HortScience* 54, 317–322. doi: 10.21273/HORTSCI13553-18

Wei, Z., Duan, F., Sun, X., Song, X., and Zhou, W. (2020). Leaf photosynthetic and anatomical insights into mechanisms of acclimation in rice in response to long-term fluctuating light. *Plant Cell Environ.* doi: 10.1111/pce.13954

Zeidler, C., and Schubert, D. (2014). "From bioregenerative life support systems for space to vertical farming on earth - the 100% spin-off," in *Paper presented at the Life in Space for Life on Earth Symposium*, Waterloo, ONT.

Zhang, N., and Portis, A. R. (1999). Mechanism of light regulation of Rubisco: a specific role for the larger Rubisco activase isoform involving reductive activation by thioredoxin-f. *Proc. Natl. Acad. Sci. U.S.A.* 96, 9438–9443. doi: 10.1073/pnas.96.16.9438

Conflict of Interest: The authors declare that the research was conducted in the absence of any commercial or financial relationships that could be construed as a potential conflict of interest.

Copyright © 2021 Bhuiyan and van Iersel. This is an open-access article distributed under the terms of the Creative Commons Attribution License (CC BY). The use, distribution or reproduction in other forums is permitted, provided the original author(s) and the copyright owner(s) are credited and that the original publication in this journal is cited, in accordance with accepted academic practice. No use, distribution or reproduction is permitted which does not comply with these terms.

frontiers in Plant Science

ORIGINAL RESEARCH
published: 28 January 2021
doi: 10.3389/fpls.2020.592171

Plant Factories Are Heating Up: Hunting for the Best Combination of Light Intensity, Air Temperature and Root-Zone Temperature in Lettuce Production

Laura Carotti[1], Luuk Graamans[2], Federico Puksic[3], Michele Butturini[3], Esther Meinen[2], Ep Heuvelink[3] and Cecilia Stanghellini[2]*

[1] Department of Biological, Geological and Environmental Sciences, Alma Mater Studiorum, University of Bologna, Bologna, Italy, [2] Greenhouse Horticulture, Wageningen University and Research, Wageningen, Netherlands, [3] Horticulture and Product Physiology, Wageningen University and Research, Wageningen, Netherlands

OPEN ACCESS

Edited by:
Bruce Bugbee, Utah State University, United States

Reviewed by:
Shardendu Kumar Singh, AeroFarms, United States
Tao Li, Institute of Environment and Sustainable Development in Agriculture (CAAS), China
Erik Runkle, Michigan State University, United States

***Correspondence:**
Luuk Graamans
luuk.graamans@wur.nl

Specialty section:
This article was submitted to Crop and Product Physiology, a section of the journal Frontiers in Plant Science

Received: *06 August 2020*
Accepted: *21 December 2020*
Published: *28 January 2021*

Citation:
Carotti L, Graamans L, Puksic F, Butturini M, Meinen E, Heuvelink E and Stanghellini C (2021) Plant Factories Are Heating Up: Hunting for the Best Combination of Light Intensity, Air Temperature and Root-Zone Temperature in Lettuce Production. Front. Plant Sci. 11:592171. doi: 10.3389/fpls.2020.592171

This study analyzed interactions among photon flux density (PPFD), air temperature, root-zone temperature for growth of lettuce with non-limiting water, nutrient, and CO_2 concentration. We measured growth parameters in 48 combinations of a PPFD of 200, 400, and 750 μmol m^{-2} s^{-1} (16 h daylength), with air and root-zone temperatures of 20, 24, 28, and 32°C. Lettuce (*Lactuca sativa cv*. Batavia Othilie) was grown for four cycles (29 days after transplanting). Eight combinations with low root-zone (20 and 24°C), high air temperature (28 and 32°C) and high PPFD (400 and 750 μmol m^{-2} s^{-1}) resulted in an excessive incidence of tip-burn and were not included in further analysis. Dry mass increased with increasing photon flux to a PPFD of 750 μmol m^{-2} s^{-1}. The photon conversion efficiency (both dry and fresh weight) decreased with increasing photon flux: 29, 27, and 21 g FW shoot and 1.01, 0.87, and 0.76 g DW shoot per mol incident light at 200, 400, and 750 μmol m^{-2} s^{-1}, respectively, averaged over all temperature combinations, following a concurrent decrease in specific leaf area (SLA). The highest efficiency was achieved at 200 μmol m^{-2} s^{-1}, 24°C air temperature and 28°C root-zone temperature: 44 g FW and 1.23 g DW per mol incident light. The effect of air temperature on fresh yield was linked to all leaf expansion processes. SLA, shoot mass allocation and water content of leaves showed the same trend for air temperature with a maximum around 24°C. The effect of root temperature was less prominent with an optimum around 28°C in nearly all conditions. With this combination of temperatures, market size (fresh weight shoot = 250 g) was achieved in 26, 20, and 18 days, at 200, 400, and 750 μmol m^{-2} s^{-1}, respectively, with a corresponding shoot dry matter content of 2.6, 3.8, and 4.2%. In conclusion, three factors determine the "optimal" PPFD: capital and operational costs of light intensity vs the value of reducing cropping time, and the market value of higher dry matter contents.

Keywords: climate management, dry matter allocation, efficiency, leaf expansion, production climate, resource use efficiency, vertical farm, light use efficiency

INTRODUCTION

Recent social developments have increased the allure of locally produced food and urban horticulture is increasingly seen as an option to produce locally (Benke and Tomkins, 2017; Shamshiri et al., 2018). However, an economically viable exploitation of expensive urban land for agriculture is only possible for high-value, high-yield crops. Plant factories, also known as vertical farms, are capable of cultivating crops on multiple layers and achieving high crop productivity and uniformity, without any need for crop protection chemicals (Graamans et al., 2018; SharathKumar et al., 2020). Such production systems are completely insulated from the exterior climate and control light (spectrum, intensity, and photoperiod), temperature, relative humidity, and CO_2 concentration. They are typically used to produce small, "stackable" plants with a short production cycle, such as leafy vegetables and herbs, seedlings and high-value medicinal crops (Kozai, 2013). Production costs in plant factories are higher than in any other agricultural system relying on sunlight, with estimates by the Rabobank (Van Rijswick, 2018) projecting at least twice the production cost in comparison with the nearest competitor: the high-tech, heated glasshouse. As the energy requirement for climatization (lighting, cooling, and dehumidification) is a major component of the production costs, climate management should be optimized to balance marginal yield, and marginal energy requirement. Systems with full climate control, such as plant factories, allow for the optimization of the production climate when the crop response to different climate factors is known.

The response of plant development and growth to environmental conditions, known as phenotypic plasticity, is species-specific (Sultan, 2003). Light intensity, CO_2 concentration and, to a lesser extent, temperature are the main environmental factors that determine photosynthesis and therefore crop growth and production. The ability of leaves to intercept light is determined by the leaf area, orientation and optical properties (Héraut-Bron et al., 2001). Plants have evolved different mechanisms to adapt to the light environment. For instance, plants grown in low light maximize light interception by partitioning a high proportion of assimilates toward the leaves (Shoot Mass Fraction, SMF, Poorter and Nagel, 2000) and by increasing their specific leaf area (SLA, leaf area per unit dry matter; Fan et al., 2013). Leaf area extension consists of two components: an increase in volume (by cell expansion) and an increase in dry matter, also known as structural growth (by leaf initiation and cell multiplication; Pantin et al., 2011).

Crop photosynthesis does not depend much on temperature, provided it is within a "reasonable range" (Körner et al., 2009). High temperature stress can induce changes in, e.g., water relations, osmolyte accumulation, photosynthetic activity, hormone production, and cell membrane thermostability (Waraich et al., 2012). Furthermore, temperature directly determines the rate of development of new organs in a species-specific way (Hatfield and Prueger, 2015). This influences marketable yield, which is determined by the amount of dry matter and the water content of the harvestable product. The amount of dry matter is determined by the dry matter production (net assimilation) and its allocation among organs (sinks; e.g., Marcelis et al., 1998). A reduced water content of the harvestable product is often an indicator of better quality (e.g., Acharya et al., 2017). The role of temperature in the aforementioned processes has been investigated in greater depth for leaf and air temperature than for root-zone temperature. Nonetheless, for lettuce there are indications that cooling the root zone may have a mitigating effect under high air temperatures (Thompson et al., 1998; He et al., 2001) and that the optimal root-zone temperature may increase with light intensity (Gosselin and Trudel, 1984; Frantz et al., 2004).

The lack of obvious conclusions above is probably the reason for most existing models of leafy crops (such as Van Henten, 1994) to have a SMF, SLA and shoot water content as parameters, and furthermore to not take into account possible effects of root zone temperature on crop growth (**Figure 1**).

Understanding the relationship between light, air temperature and root-zone temperature and lettuce growth allows for the optimization of the growing conditions for the plants. This optimization is particularly interesting for systems with extensive climate control, such as plant factories. Such closed systems need cooling whenever light is supplied, whereas maintaining a high CO_2 concentration is relatively cheap. Therefore, it makes economic sense to explore yield response to climate conditions that are not typical of more conventional growing environments (including heated greenhouses with natural ventilation) where there is always a high correlation among factors such as solar radiation, air and root-zone temperature. Therefore the objective of this paper is to extend our knowledge about plant processes, such as leaf expansion and dry matter allocation, in order to determine whether and how they could be manipulated through climate management. In view of the extended climate

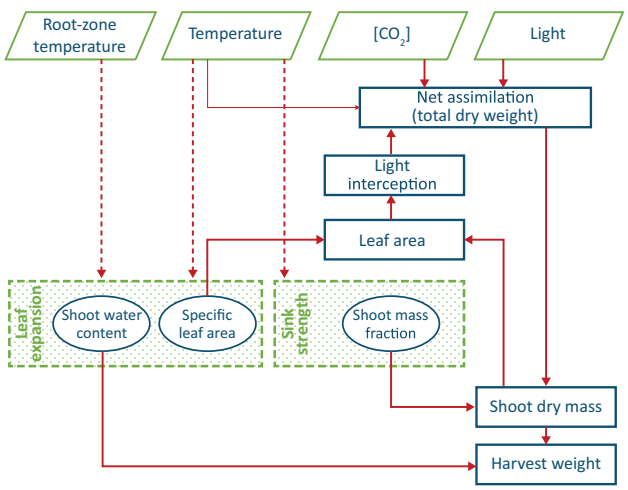

FIGURE 1 | Conceptual model of production of a leafy vegetable, such as lettuce. Thick arrows indicate well-known causal relationships, thin arrows a weak relationship and dashed arrows circumstantial evidence. The two shaded processes are not yet fully understood, and the three encircled 'entities' are often regarded as constant values. Water and nutrient supply are assumed not to be limiting and thus do not appear in the scheme.

manipulation options in a vertical farm, we have also considered "unnatural" combinations of light intensity and root zone and ambient temperature independently. Our assumption was that production increases with light intensity, as long as other factors are not limiting. We also expected a higher optimal temperature at higher light intensity to maintain a balance between source and sink strength (Gent and Seginer, 2012).

MATERIALS AND METHODS

Growth Conditions, Treatments and Analysis

Plants of *Lactuca sativa* cv. Batavia Othilie were grown in two climate rooms at Wageningen University & Research (Netherlands) in a hydroponic (deep water culture) system (**Figure 2**) with different combinations of air temperature (20, 24, 28, and 32°C), root-zone temperature (20, 24, 28, and 32°C) and light intensity (200, 400, and 750 μmol m^{-2} s^{-1}). Four sequential growth cycles were conducted from December 2018 to May 2019, for a total of 48 treatments. The photoperiod was 16/8 h (day/night) throughout the entire cycle and CO_2 concentration was kept constant at 1,200 μmol mol^{-1}. Air was continuously circulated, resulting in an air exchange rate of approximately 40 times per hour. The relative humidity was adjusted based on the temperature, to keep similar vapor pressure deficit among the various treatments (about 5.8 and 3.4 hPa, day and night, respectively, that is a higher relative humidity in the dark period).

Lettuce seeds were sown in stonewool cubes (4 × 4 cm; Rockwool Grodan, Roermond, Netherlands) and covered with plastic (dark and at 18°C) in a separate, germination room. After 2 to 3 days, the seeds germinated and the plastic was removed. Temperature was maintained at 20°C, vapor pressure deficit 5.8 and 3.5 hPa during light and dark period, respectively, and a photosynthetic photon flux density (PPFD) of 200 μmol m^{-2} s^{-1} (photoperiod 16 h) was provided by fluorescent tubes. The temperature of the germination room was increased gradually over the course of 3 days to acclimate the plants to the air temperatures of 28 and 32°C. In all cases uniform lettuce seedlings were selected after 19 days before being transplanted at random into the floaters of the deep water culture system (each floater 20 × 80 cm, 4 plants). After transplanting, the air temperature and root zone temperatures were gradually increased over the course of 48 h to reach the final temperatures for the treatment 32°C. The treatment with the highest light intensity (750 μmol m^{-2} s^{-1}) was shaded for 48 h to allow the plants to acclimate to the light levels.

Each climate cell contained six production layers, three on the left side and three on the right side (**Figure 2**). On each layer a deep flow tank (8 cm deep) contained 15 floating trays of 4 plants each, resulting in a density of 25 plants m^{-2}. The nutrient solution had an electronic conductivity (EC) of 2.0 dS m^{-1} and was composed of the following ions in mmol L^{-1}: 12 NO_3^-, 1 NH_4^+, 6 K^+, 3 Ca^{2+}, 0.84 Mg^{2+}, 1.1 $H_2PO_4^-$, 0.79 SO_4^{2-}, and in μmol L^{-1}: 50 Fe, 8 Mn, 5 Zn, 40 B, 0.5 Cu, and 0.5 Mo. A new solution using the same recipe was prepared for each cycle and any refill. EC and pH were checked weekly

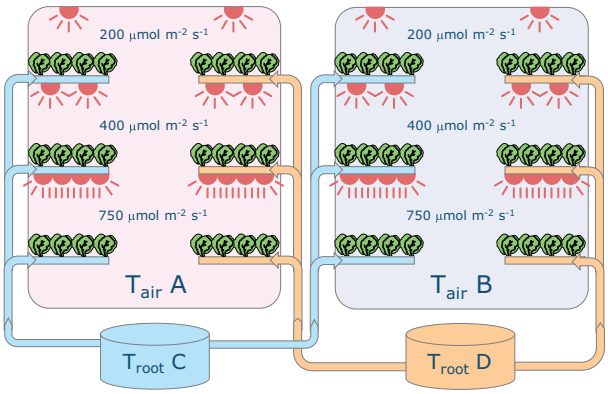

FIGURE 2 | Schematic representation of the experimental set-up. Each of the two climate rooms had three light intensity levels installed (200, 400 and 750 μmol m^{-2} s^{-1}) and featured two root-zone temperatures. All combinations of 20, 24, 28, 32°C for air and root-zone temperatures were tested in four successive crop cycles. The lights were on-off for 16–8 hours, respectively and temperature was maintained constant. Carbon dioxide concentration was 1200 μmol mol^{-1} throughout.

and the actual concentration was measured halfway through the each cycle to check whether corrections were needed[1]. The dissolved oxygen was maintained at saturation with a water oxygenator and root-zone temperature set-point was maintained using a heat exchanger in each of the two nutrient solution tanks. The tanks were placed outside of the climate rooms to exclude heat exchange.

The climate rooms were thermally insulated and the air temperature, humidity levels and CO_2 concentration was managed per room. The temperature of the nutrient solution for the root zone was varied per side of the climate room and the light intensity was varied per production layer. Four air and root zone temperatures (20, 24, 28, or 32°C) and three light intensities (200, 400, or 750 μmol m^{-2} s^{-1}, corresponding to Daily Light Integrals of 11.5, 23.0, and 43.2 mol m^{-2} d^{-1}, respectively) were used during the experiment. Each production layer, characterized by a specific combination of air temperature, root zone temperature and light intensity, corresponded to a treatment.

Air temperature, root-zone temperature and relative humidity were continuously monitored from the day of transplanting (19 DAS). Each climate room was provided with 6 ventilated sensors, one for each layer (Sensirion SHT75, WiSensys, Wireless Value, Netherlands) measuring air temperature (±0.3°C) and relative humidity (±1.8%) and with 4 sensors (two for each side, top and bottom layer, SHT71, WiSensys, Wireless Value, Netherlands) for the root-zone temperature (±0.3°C). CO_2 was measured and controlled using the central climate control box. Measurements were recorded at 5 min intervals. PPFD was provided with two different types of LED modules: For the 200 μmol m^{-2} s^{-1} treatment the Philips GP LED production module (2.2 DR/W 150 cm LB HO) and for the 400 and 750 μmol m^{-2} s^{-1} treatments the Philips GP LED Toplight (1.2 DR/W LB

[1]Corrections were not required during any of the treatments.

400V) were used. The application of different lighting modules was necessary to ensure the required light intensities, as well as an adequate spatial distribution. These factors were considered to be more consequential for the experiment than the resulting minor difference in spectral distribution (see **Supplementary Figure 1**). Light intensity was measured using a quantum sensor (LI-190) at the start of the cycle, on 36 spots on each layer, at the height of the top of transplanted plants. Light spectrum was measured using a spectroradiometer (Jeti specbos 1211).

Crop Measurements and Statistical Analysis

Each crop cycle lasted 29 days after transplanting (DAT), which gave heads of market size (250 g) in the 200 μmol m^{-2} s^{-1} treatments. Destructive harvests for determining leaf, stem and root fresh and dry weight (ventilated oven, 24 h at 70°C followed by 24 h at 105°C) and leaf area per plant (LI-31000C, LI-COR Biosciences, United States) were conducted twice a week, for a total of nine harvests. Tip-burn occurrence (% of plants affected to any extent) was evaluated each time but no severity scale was used. The external 3 floaters at each side of a layer were considered as border floaters. The central 9 floaters contained the experimental plants for each layer. The central floater was extracted each time and the four plants (replicas) were destructively measured (**Figure 3**). The remaining floaters were slid to the center to ensure uniformity and maintain a continuous canopy and density.

Eight combinations ($T_{air} \geq 28$°C, $T_{root} \leq 24$°C, and PPFD $\geq$ 400 μmol m^{-2} s^{-1}) resulted in excessive (>50%) incidence of tip-burn from DAT 6 and were therefore excluded from further analysis. Data of 4 replicate plants were averaged and represent one experimental unit. An Analysis of Variance (ANOVA; SPSS 26th edition) was conducted on final total dry weight, shoot/root ratio, SLA, and light use efficiency, treating the data from the four experiments as a 3-way full-factorial incomplete randomized design. Sources of variance were the main effects of light intensity, air temperature and root-zone temperature and their 2-way interactions whereas the 3-way interaction was taken as a residual term, because each combination of a light intensity, a root temperature and an air temperature was conducted only once.

FIGURE 3 | One of the final harvests in the 750 μmol m^{-2} s^{-1} treatment.

RESULTS

Treatments

The realized climate conditions were maintained within 3% (average temperature) and 6% (light intensity) of the desired setpoints (**Table 1**) and the standard deviation was never more than 5% (air temperature); 2% (root temperature); and 6% (spatial distribution of light intensity).

The limited nature of tip-burn observations (fraction of plants affected) did not allow for a detailed analysis, but indicated that vapor condensation on the growing tip was the most likely cause in the combinations that had to be discarded. In all cases, tip-burn occurrence increased with air temperature.

Yield

Yield increased with light intensity as expected, and there was an obvious effect of air temperature, as 24°C resulted in the highest yield and 32°C the lowest at all light intensities. The effect of root temperature (not shown) was smaller in all cases and less uniform. **Figure 4** shows the combined effect of air temperature and light intensity on fresh weight of shoot, at a root zone temperature of 28°C (the one that warranted the highest weight in most cases). Raising light intensity from 200 to 400 μmol m^{-2} s^{-1} could shorten the time needed to reach market weight by 8 days at an air temperature of 20°C, 5 days at 24°C, and 3 at 28°C. Raising it further, to 750 μmol m^{-2} s^{-1} would shave off only another 2 days in all cases.

The trend of total plant dry weight (TDW) was similar. Nevertheless, both air and root zone temperatures influenced TDW. The effect of air temperature is illustrated in **Figure 5** for a root-zone temperature of 28°C. At equal air and root-zone temperature (not shown), the highest final dry weights were observed at 24°C (10.0, 16.3, and 28.1 g $plant^{-1}$ at 200, 400, and 750 μmol m^{-2} s^{-1}, respectively) and the lowest weights at 32°C (8.3; 11.2 and 17.9 g $plant^{-1}$ at 200, 400 and 750 μmol m^{-2} s^{-1},

TABLE 1 | Average ± standard deviation of the measured temperature and light levels for each setpoint.

Set-point (°C)	20	24	28	32
Measured air temperature (°C)	19.3 ± 1.0	23.6 ± 0.8	28.6 ± 1.4	32.6 ± 1.3
Measured root temperature (°C)	20.2 ± 0.2	24.1 ± 0.4	27.8 ± 0.6	31.4 ± 0.2
Set-point PPFD (μmol m^{-2} s^{-1})	200	400	750	
Measured PPFD (μmol m^{-2} s^{-1})	197 ± 8	425 ± 24	741 ± 24	

The listed measured air temperature is the mean of six sensors per climate room. The listed root-zone temperature is the mean of four sensors per climate room, two per side. Temperature data was recorded at an interval of 5 min and was averaged over the full growth cycle, during each experiment. Light intensity was measured at 36 spots on each layer, at crop height, before the cycles.

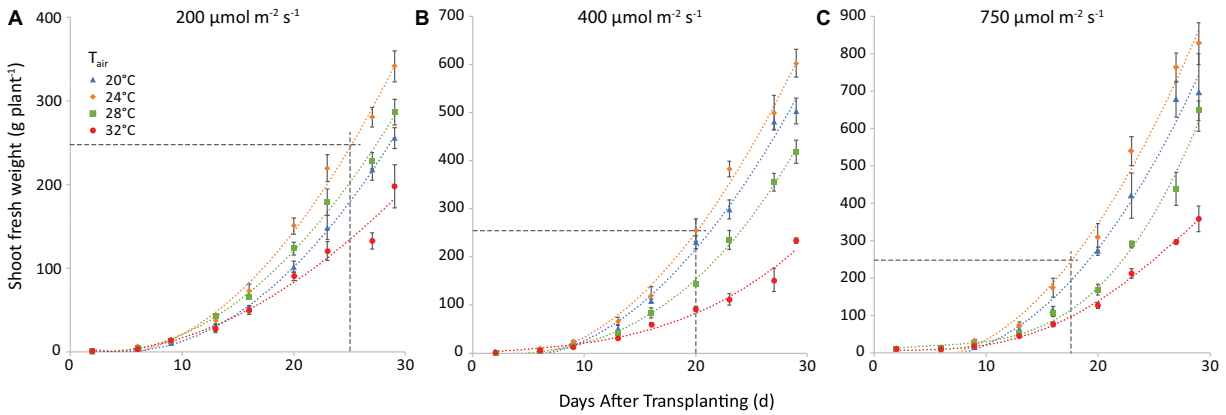

FIGURE 4 | Shoot fresh weight (g plant^{-1}) at a root temperature of 28°C, at light intensities of 200 **(A)**, 400 **(B)** and 750 **(C)** µmol m^{-2} s^{-1} and at air temperatures as indicated. The points represent the values at the different harvests (days after transplanting) and are the average of four plants, shown with the standard error of the mean. Note that the *y*-axis scale differs among the 3 panels, the horizonal line gives in each case the market size of 250 g. The curves are polynomials to increase legibility.

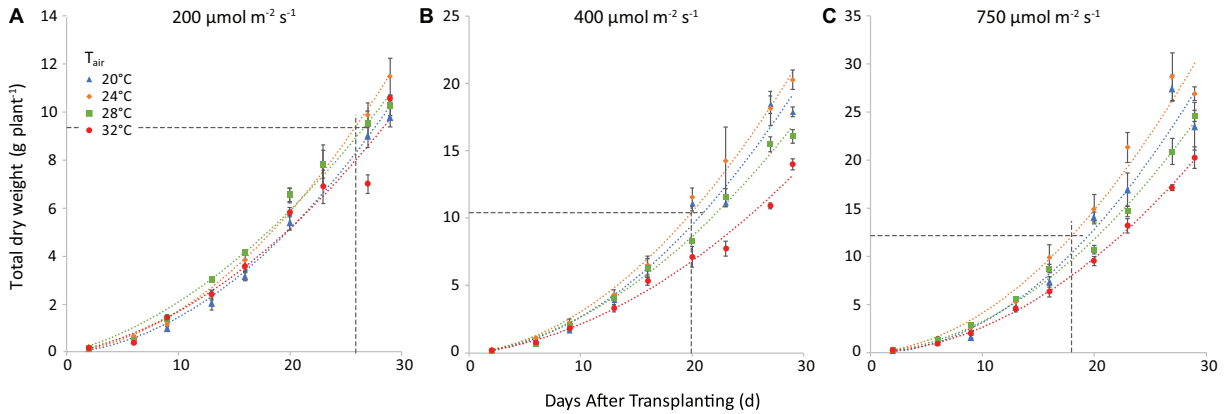

FIGURE 5 | Total plant dry weight (g plant^{-1}) at a root-zone temperature of 28řC and light intensities of 200 **(A)**, 400 **(B)** and 750 **(C)** µmol m^{-2} s^{-1}. The four air temperatures are represented by different symbols/colors. The data points represent the values at the different harvests (days after transplanting) and are the average of four plants, shown with the standard error of the mean. The dashed lines represent the day when shoot market yield was reached (see **Figure 4**) and the corresponding total dry weight. Note that the *y*-axis scale differs among the 3 panels. The curves are polynomials to increase legibility.

respectively). The effect of air temperature on TDW at the final harvest was non-significant at 200 µmol m^{-2} s^{-1}. At 400 and at 750 µmol m^{-2} s^{-1}, however, the effect of air temperature on the dry matter production became increasingly significant for nearly all temperature combinations. The interaction between air and root-zone temperature was slightly significant ($P = 0.036$) and the plants grown at 20°C root zone temperature produced the lowest final dry weight, in all cases.

When the market weight was reached, shoot dry matter was 2.6, 3.8, and 4.2% at 200, 400, and 750 µmol m^{-2} s^{-1}, respectively.

Shoot Mass Fraction

Light intensity did not influence the allocation of dry matter to the shoot, as shown at air and root zone temperature of 24°C (**Figure 6**). Note that the best-fit lines were not forced through the origin, to account for preferential allocation to roots in the very early stages. The intercept with the *x*-axis is an estimate of the total weight at the end of this phase.

The difference in regression lines under different light intensities was minimal for each combination of equal air and root zone temperature (**Figure 6** and **Supplementary Table 1**). A single equation was fitted that combined the plants grown under different intensities. Both the effect of root temperature (examined at T_{air} = 24°C) and of air temperature (at T_{root} = 28°C) were minimal, but statistically significant (not shown). The joint effect was also minimal, yet visible at T_{root} = T_{air} (**Figure 7** and **Supplementary Figure 2**) and statistically significant ($P = 0.028$).

Specific Leaf Area

The slope of the regression line of leaf area against leaf dry weight (**Figure 8**) is the specific leaf area (SLA, cm^2 g^{-1}). Increasing light intensity notably reduced SLA. This trend was the same for

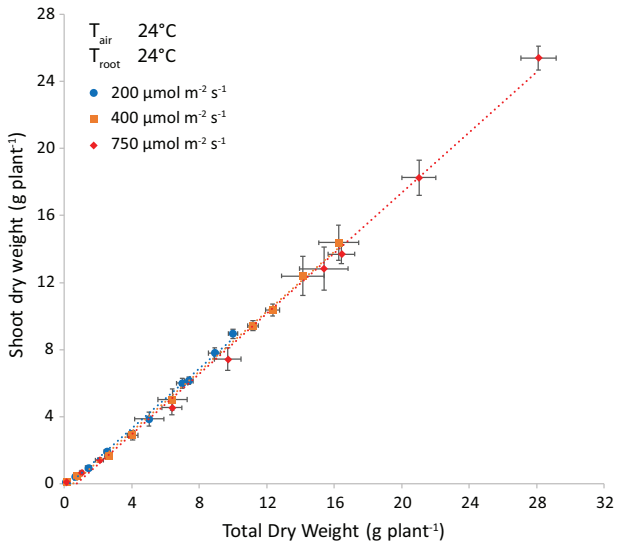

FIGURE 6 | Shoot dry weight (g plant^{-1}) plotted versus the total plant dry weight (g plant^{-1}) and the corresponding trendlines at both air and root-zone temperatures of 24°C. Each symbol represents a different light intensity (200, 400 or 750 µmol m^{-2} s^{-1}). The points are the average of four plants shown with the standard error of the mean.

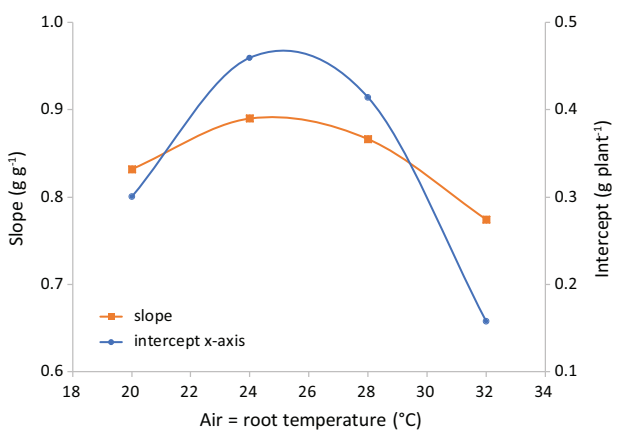

FIGURE 7 | Representation of the parameters of the best-fit lines shown in **Figure 6**. Light intensities have been combined and root = air temperature. The slope is the shoot mass fraction (left axis) and the intercept with the *x*-axis (right axis) is an indication of the total plant dry weight at the end of the phase of preferential allocation to the roots.

all investigated combinations of air and root-zone temperature. Temperatures had a minor effect on SLA, where air temperature had a greater effect than root-zone temperature (**Figure 9**). At all light intensities the highest SLA was obtained at an air temperature of 24°C. A root-zone temperature of 28°C generally resulted in the highest SLA and 32°C in the lowest, but effects were minor. An increase in light intensity decreased SLA and reduced the influence of air temperature on SLA.

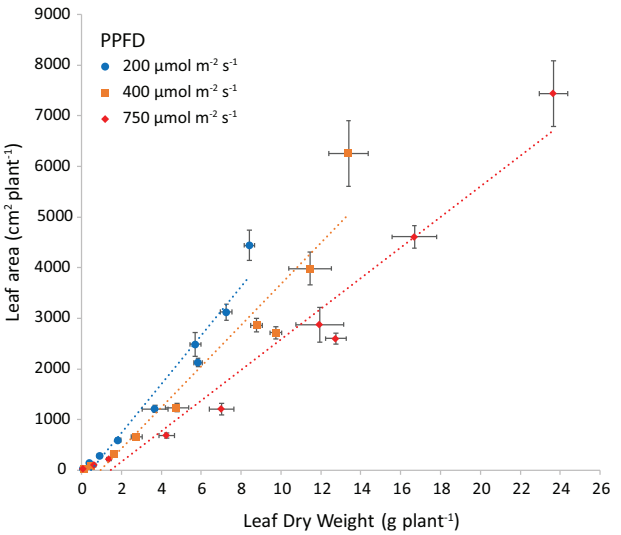

FIGURE 8 | Leaf area (cm^2 plant^{-1}) plotted versus the leaf dry weight (g plant^{-1}) at both air and root zone temperatures of 24°C and the three light intensities as indicated. The dotted lines represent the linear regression equations: at 200 µmol m^{-2} s^{-1} $y = 444x$ ($R^2 = 0.9487$), at 400 µmol m^{-2} s^{-1} $y = 367x$ ($R^2 = 0.9112$) and at 750 µmol m^{-2} s^{-1} $y = 274x$ ($R^2 = 0.9474$). The points are the average of four plants shown with the standard error of the mean.

Fresh Weight vs Dry Weight

The ratio of fresh to dry weight (the slope of the linear relationship between leaf fresh weight and leaf dry weight) showed a high R^2 (>0.95) for any combination of PPFD, T_{air} and T_{root} (**Supplementary Table 2**). The lines were not forced through the origin, to account for the higher dry matter content of young plants.

Figure 10 shows the leaf fresh weight vs leaf dry weight at an air temperature of 24°C, for all light intensities and root zone temperatures. **Supplementary Figure 3** shows the fresh weight results of the four combinations with equal air and root zone temperature at all PPFD's. **Supplementary Figure 4** complements **Figure 10** with the remaining air temperatures. Light intensity had little effect on leaf dry matter content. **Figure 11** illustrates the slopes calculated by pooling light intensities together at a given combination of air and root zone temperature, as well as the corresponding leaf dry matter content.

Light Use Efficiency

A main factor determining the feasibility of vertical farming is the ratio "fresh produce (g m^{-2}) per unit of incident light (mol m^{-2})" (LUE_{FW}, **Figure 12**). Averaged over all air and root-zone temperature combinations, the LUE_{FW} was 29, 27, and 21 g FW per mol incident light at 200, 400, and 750 µmol m^{-2} s^{-1}, respectively. LUE_{FW} was highest at 24°C air temperature and lowest at 32°C for all 3 light intensities. Root-zone temperature also had a clear effect, where 28°C generally resulted in the highest LUE_{FW} and 32°C the lowest.

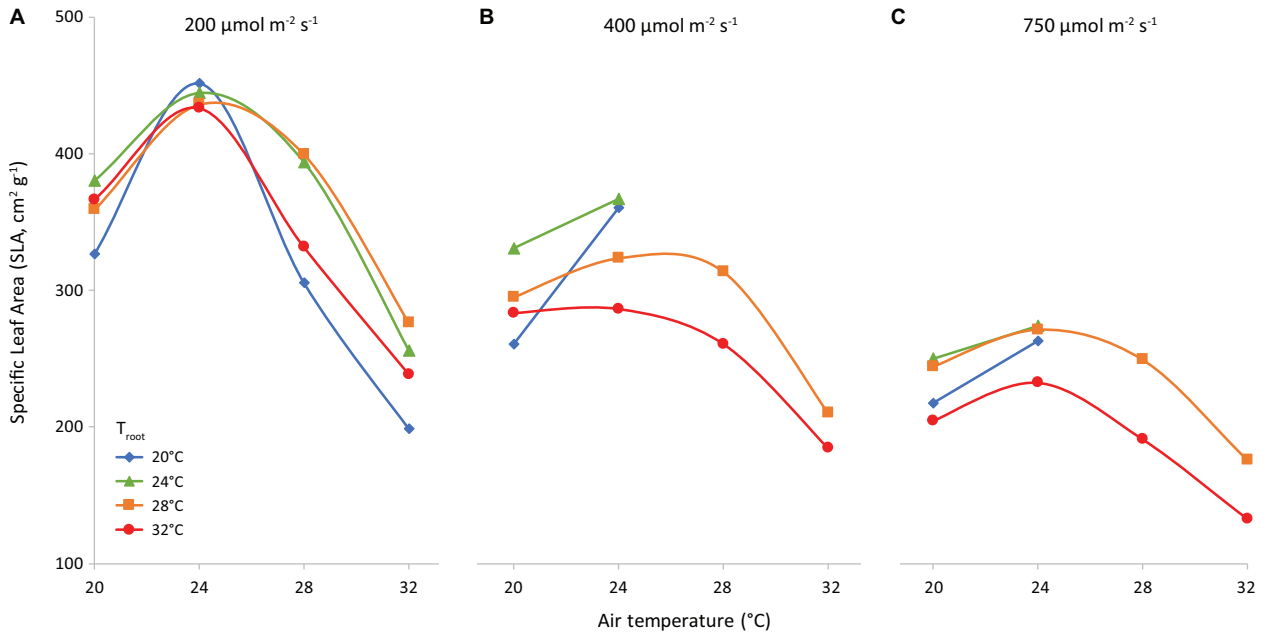

FIGURE 9 | Specific Leaf Area (cm^2 g^{-1}) as affected by air temperature (*x*-axis) and root temperature (colors/symbols). Light intensities are 200 **(A)**, 400 **(B)** and 750 **(C)** µmol m^{-2} s^{-1}, as indicated.

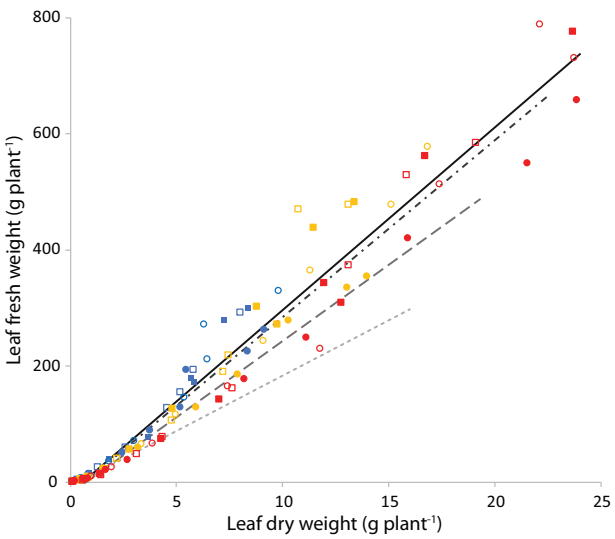

FIGURE 10 | Leaf fresh weight (g $plant^{-1}$) as a function of leaf dry weight (g $plant^{-1}$) at an air temperature of 24°C. Blue is light intensity of 200 µmol m^{-2} s^{-1}, yellow 400 and red 750 µmol m^{-2} s^{-1}. The symbols indicate the root zone temperature, as follows: □ = 20°C; ■ = 24°C; ○ = 28°C and ● = 32°C. The continuous line is the best fit of the points displayed (T_{air} = 24°C). The dashed lines are the best fit calculated for similar plots (see **Supplementary Figure 4**) with a T_{air} of 20°C (dash-dot), 28°C (long dash) and 32°C (short dash).

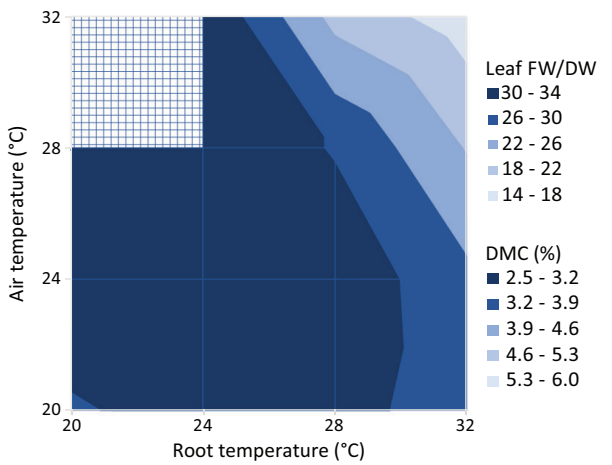

FIGURE 11 | Ratio of leaf fresh to dry weight (Leaf FW/DW) and corresponding dry matter content (DMC, the ratio of leaf dry mass to leaf fresh mass in %). Values represent the slope of the regression line between the leaf fresh weight and leaf dry weight for all possible combinations of air and root zone temperature, while pooling light intensities together.

The combination of air and root-zone temperature had little to no effect on the dry matter per unit of incident light (LUE_{DW}). The effect of increasing light intensity on LUE_{DW} was about as large as on LUE_{FW} (1.01, 0.87, and 0.76 g DW per mol incident light at 200, 400, and 750 µmol m^{-2} s^{-1}, respectively).

DISCUSSION

This study was aimed at providing quantitative information on lettuce crop growth that is relevant for good climate management

in plant factories. The final aim was to explain yield response to light intensity (other than assimilation), air temperature and root zone temperature, which was mediated through the effect of these variables on biomass allocation, SLA and fresh weight accumulation (**Figure 1**). The high incidence of tip burn in the treatments that combined the two highest air temperatures with the two lowest root temperatures at the middle and high light intensity did not allow us to explore all planned combinations of these variables (8 out of 48 were excluded). Nevertheless, we believe that our results provided useful information for climate management in plant factories and advanced our knowledge about relevant processes, particularly the accumulation of fresh weight.

Biomass Production and Light Use Efficiency

The light use efficiency of shoot dry matter production (LUE_{DW}) was 1.01, 0.87, and 0.76 g mol^{-1} incident light at 200, 400, and 750 $\mu mol\ m^{-2}\ s^{-1}$, respectively, when averaged over all temperature combinations. A decrease in LUE_{DW} at increased light intensity was also observed by Fu et al. (2012) for 200 up to 800 $\mu mol\ m^{-2}\ s^{-1}$. This decrease can be explained by the saturation-type photosynthesis-light response curve. This also explains why Kelly et al. (2020) did not find a decrease in LUE_{DW} as their PPFD levels were much lower (120 to 270 $\mu mol\ m^{-2}\ s^{-1}$ at 16 h daylength) than in our experiment. Here the highest LUE was achieved at 200 $\mu mol\ m^{-2}\ s^{-1}$, 24°C air temperature and 28°C root temperature: 44 g FW and 1.23 g DW per mol incident light. This was approximately 30% higher than Pennisi et al. (2020), who observed a LUE of about 0.9 g DW per mol incident light at 200 $\mu mol\ m^{-2}\ s^{-1}$. Although they had a shorter crop cycle and an exclusively red-blue spectrum, we reason that the difference in CO_2 concentration is the most likely cause: Pennisi et al. (2020) grew lettuce at 450 $\mu mol\ mol^{-1}$ CO_2, whereas we used 1,200 $\mu mol\ mol^{-1}$. An increase in LUE of 30% as a result of this difference is plausible (Nederhoff, 1994). Zou et al. (2019) reported an even lower LUE of only 0.6 g DW per mol incident light at 200 $\mu mol\ m^{-2}\ s^{-1}$ and ambient CO_2.

The yield in the experiments of Pennisi et al. (2020) did not increase for light intensities exceeding 250 $\mu mol\ m^{-2}\ s^{-1}$, which indicates that CO_2 concentration may have been the limiting factor. Fu et al. (2012) also observed no difference is shoot weight between PPFD 400 and 600 $\mu mol\ m^{-2}\ s^{-1}$ and a lower shoot weight at 800 $\mu mol\ m^{-2}\ s^{-1}$ for lettuce grown at 400 $\mu mol\ mol^{-1}$ CO_2. Indeed, Pérez-López et al. (2013) observed that an individual or combined increase in light intensity (from 400 to 700 $\mu mol\ m^{-2}\ s^{-1}$) and CO_2 concentration (from 400 to 700 $\mu mol\ mol^{-1}$) could significantly increase yield of a Batavia variety of lettuce (up to 77%). Duggan-Jones and Nichols (2014) did not observe saturation with light up to 480 $\mu mol\ m^{-2}\ s^{-1}$ in lettuce at 1,000 $\mu mol\ mol^{-1}$ CO_2. Frantz et al. (2004) observed an increase of dry matter production even up to their maximum PPFD of 1,000 $\mu mol\ m^{-2}\ s^{-1}$, with a CO_2 concentration of 1,200 $\mu mol\ mol^{-1}$.

In our experiment total dry mass increased with light intensity up to our highest intensity (750 $\mu mol\ m^{-2}\ s^{-1}$), although the relative increase was lower at higher light intensities. It was of course rather unfortunate that the light spectrum was not identical at all intensities (section "Growth conditions, treatments and analysis" and **Supplementary Figure 1**). Nevertheless, as the spectrum was the same for the two highest light intensities, we can safely conclude that light was the limiting factor in well-managed lettuce production, even at a high light intensity of 750 $\mu mol\ m^{-2}\ s^{-1}$ (DLI of 43.2 $mol\ m^{-2}\ d^{-1}$).

Shoot Mass Fraction and Specific Leaf Area

An important parameter in understanding the amount of fresh weight produced per mol of incident light is the fraction of light intercepted, which depends on the leaf area index. The formation of thin leaves (high SLA) results in more leaf area for the same leaf dry mass and hence a quicker build-up of light interception and higher plant growth rate [e.g., shown by Heuvelink (1989) for young tomato plants]. Furthermore, the partitioning of a high proportion of assimilates toward the leaves is also important to quickly build up leaf area index in the early stages of crop growth. In our case, SMF was not influenced by light intensity (**Figure 6**), whereas we would expect a higher SMF at low light intensity according to the functional equilibrium (Poorter and Nagel, 2000). However, in their meta-analyses, Poorter et al. (2012, 2019), reported a minimal effect on mass allocation of Daily Light Integrals above approximately 10 $mol\ m^{-2}\ d^{-1}$. As the lowest light intensity in our experiment was equivalent to 11.5 $mol\ m^{-2}\ d^{-1}$, this might explain the absence of a light intensity effect on SMF.

Increasing light interception may be attained more efficiently at no cost to the root system, by making "thinner" leaves and consequently increasing SLA. In our experiment, SLA was lower at higher light intensity (**Figures 8**, **9**). This is a well-known response (meta-analysis by Evans and Poorter, 2001) and was also shown by Kitaya et al. (1998) in lettuce grown in a growth chamber. A decrease in SLA negates the positive effect of light intensity on total dry matter production. Light intensity did not have an effect on leaf area for up to 15 days after transplanting as a result of the adaptation in SLA (**Supplementary Figure 5**). The effect of temperature on SLA (**Figure 9**) is less documented, although Rosbakh et al. (2015) revealed a very weak positive SLA-temperature correlation. However, there is evidence that SLA across species correlates with the temperature of their habitat (Atkin et al., 2006). Low rates of cell expansion at low temperatures may lead to a large number of small cells per unit area, resulting in smaller and denser leaves on plants in cold habitats (Poorter et al., 2009). By transplanting plants of the same genotype at three different heights in the Bavarian Alps, Scheepens et al. (2010) demonstrated that temperature can cause intraspecific variation in SLA. Frantz et al. (2004) showed a strong influence of air temperature on leaf expansion in lettuce grown in a growth chamber (600 $\mu mol\ m^{-2}\ s^{-1}$; 34.6 $mol\ m^{-2}\ d^{-1}$; and 1,200 $\mu mol\ mol^{-1}CO_2$ concentration), the highest expansion rate being at 27 and 30°C, and the lowest at 33°C. Even though expansion rate is not exactly SLA, one can conclude that literature corroborates the observed trend of

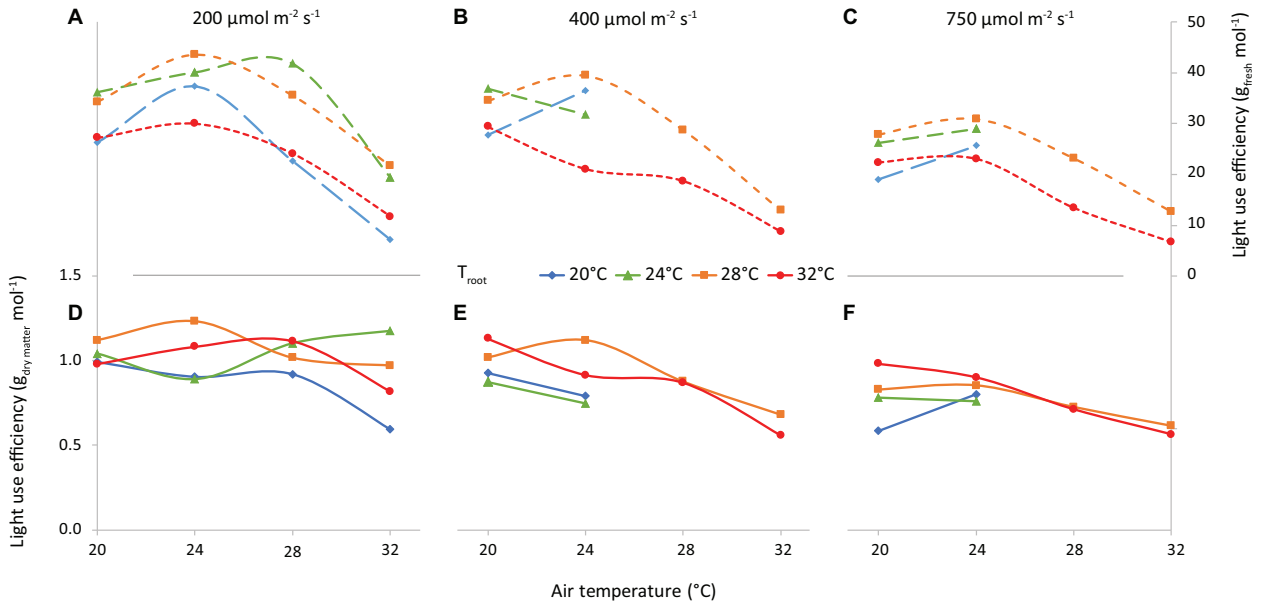

FIGURE 12 | Light Use Efficiency vs air temperature, for light intensities of 200 **(A,D)**, 400 **(B,E)** and 750 **(C,F)** µmol m^{-2} s^{-1}, as indicated. The colors/symbols represent the root-zone temperatures. The top graphs **(A–C)** illustrate shoot fresh weight and the bottom graphs **(D–F)** illustrate shoot dry weight production per unit of incident light (g mol^{-1}).

the SLA temperature relationship. The temperature at which the maximum SLA is attained differs from literature and might well depend on cultivar.

Leaf Fresh to Dry Weight Ratio

The only variable that affected the ratio of leaf fresh weight to dry weight was air temperature (**Figure 10**). The observed trend with a maximum at 24°C was similar to the trend of SLA with temperature (**Figure 9**). The correlation between temperature and cell size of lettuce has been known since Bensink (1971) demonstrated that an increase in temperature from 10 to 30°C increased average cell diameter by 68% without an effect on cell number. Conversely, light intensity did increase cell number while decreasing cell size. Bensink (1971) concluded that "growth increments are entirely due to a proportional increase in cell size," which is either caused by or correlated with temperature. This explains the similarity of the temperature trend of SLA with the trend of water content (**Figure 10**), assuming that cell dry matter does not increase proportionally with size. As the response of SMF to temperature (**Figure 7**) is very similar, there seems to be a correlation between sink strength and leaf expansion. Altogether, the temperature effect on these partial processes of leaf area development and mass allocation explains the (small) temperature effect observed on total dry matter production.

Climate Management

Our results confirmed the optimal day-time temperature for lettuce production of 24°C (Marsh and Albright, 1991; Thompson et al., 1998). In spite of the small decrease of yield observed at 28°C, the 30°C optimal temperature proposed by Frantz et al. (2004) is certainly beyond the limit (of this cultivar).

Even though root-zone temperature had a limited effect on the dry weight production, it had some effect on the water-related processes (**Figure 11**), and ultimately on the light use efficiency of fresh weight (**Figure 12**). The fact that the occurrence of tip burn was highest at 32°C (T_{air} = T_{root}, not shown) would be caution enough against high root zone temperatures. He and Lee (1998) found no direct effect of root zone temperature (15–25°C) in all indicators of growth of three lettuce cultivars, either shaded or unshaded, but growth was much reduced when there was no root zone temperature control, in the tropical conditions of Singapore. Furthermore, we certainly cannot state that optimal root temperature depends on light intensity [as Gosselin and Trudel (1984) observed with tomato] since T_{root} = 28°C seems optimal for nearly all performance indicators at all light intensities. Nevertheless, in the hydroponic growing systems typical of lettuce in plant factories, a most reasonable compromise would be T_{root} = T_{air} = 24°C, which disposes of the need for heating the nutrient solution.

The yield per mol of incident light was determined by several plant parameters (**Figure 12**). The ratio between fresh and dry shoot weight was not influenced by light intensity nor root zone temperature, but was reduced at higher air temperatures (**Figure 10**). Therefore an air temperature not exceeding 24°C seems to warrant the highest amount of water for a given quantity of dry matter in the leaves. On the other hand, the lack of an effect of PPFD on leaf area (until about 15 days after transplanting) implied that the decrease in SLA perfectly balanced the increase in shoot dry matter (see **Figure 1**). To this end, the positive feedback of dry matter production and light interception is broken and the fraction of light that is intercepted by young plants is independent of light intensity.

CONCLUSION

This study was aimed at providing quantitative information that is relevant for good climate management of lettuce crops in plant factories. In particular, we have analyzed the relationship between light intensity, air temperature and root-zone temperature and lettuce growth, at non-limiting CO_2 concentration.

When other factors are not limiting, dry weight production increases with increasing light intensity until the maximum investigated PPFD of 750 μmol m^{-2} s^{-1}. Nevertheless, as the efficiency of light use for both dry and fresh weight production decreased with increasing light intensity, the optimal light intensity has to be determined in view of the value of the crop and the capital and running cost of light. Fresh and dry yield, SLA, shoot mass allocation and water content of leaves showed the same trend with air temperature, with a maximum around 24°C. On the other hand, the effect of root temperature was less prominent, with an optimum around 28°C in nearly all conditions.

DATA AVAILABILITY STATEMENT

The raw data supporting the conclusions of this article will be made available by the authors, without undue reservation.

AUTHOR CONTRIBUTIONS

The experiment was designed by LG (who obtained the funding) and EM. EM prepared the protocol for the measurements. FP and LC executed the experiments, with the help and supervision of MB and LG. LC and FP performed the first analysis of the results and LC drafted the manuscript. EH and CS supervised the analysis and wrote the discussion. The final version of the manuscript has been reviewed and completed by each author. All authors contributed to the article and approved the submitted version.

FUNDING

This work was supported jointly by the EU-H2020 project "Food systems in European Cities" (FoodE, grant 862663) and by the strategic fund of the Business Unit Greenhouse Horticulture of Wageningen Research. However, no endorsement of the results and conclusions by the European Commission nor of Wageningen Research is hereby implied.

ACKNOWLEDGMENTS

We are grateful to Bartian Bosch and Tobias Glimmerveen for their assistance with the experiment and data processing, to Ilias Tsafaras for installing and logging the wireless sensors and to Francesco Orsini for commenting on the manuscript. The stay in Wageningen of LC was sponsored by the Erasmus+ program.

SUPPLEMENTARY MATERIAL

The Supplementary Material for this article can be found online at: https://www.frontiersin.org/articles/10.3389/fpls.2020.592171/full#supplementary-material

Supplementary Figure 1 | Spectral distribution of the two types of lamps used. The spectrum of the two highest intensities was measured separately and found to be identical. The value in the *y*-axis is normalized so that $\int_{\lambda=400}^{\lambda=800}$ measured intensity $d\lambda = 1$.

Supplementary Figure 2 | Shoot dry weight (g $plant^{-1}$) plotted vs total plant dry weight (g $plant^{-1}$) at equal air and root zone temperature. Each color represents all light intensities at a different temperature combination. R^2 was in all cases above 0.995. Regression lines were not forced through the origin and all are statically different at 99% confidence interval, except for the ones at 24/24°C and 28/28°C that are different at 95% confidence interval.

Supplementary Figure 3 | Leaf fresh weight (g $plant^{-1}$) as a function of leaf dry weight (g $plant^{-1}$) for the combinations with same air temperature and root zone temperature, pooled for light intensity. Each trendline represents a different temperature combination: 20/20°C $y = 0.0358x$ ($R^2 = 0.9622$), 24/24°C $y = 0.0308x$ ($R^2 = 0.9555$), 28/28°C $y = 0.035\ 8x$ ($R^2 = 0.9622$), 32/32°C $y = 0.0643x$ ($R^2 = 0.9822$).

Supplementary Figure 4 | Leaf fresh weight (g $plant^{-1}$) as a function of leaf dry weight (g $plant^{-1}$) at air temperatures 20 **(A)**, 28 **(B)** and 32°C **(C)**, as indicated. Blue is light intensity of 200, yellow 400 and red 750 μmol m^{-2} s^{-1}. The symbols indicate the root zone temperature, as follows: □ = 20°C; ■ = 24°C; ○ = 28° and ● = 32°C. The full line is the best fit of all points displayed, and is reported in **Figure 9** in the main text.

Supplementary Figure 5 | Evolution in time (Days after Transplanting) of Leaf area (cm^2 $plant^{-1}$), for the "best" temperature combination (T_{air} 24 and T_{root} 28°C), at the three light intensities, as indicated.

Supplementary Table 1 | Linear regression equations for SDW vs TDW at the same air and root zone temperature, for the different light intensities. The intercept with the *x*-axis is an indication of the total dry weight at the end of the phase with preferential allocation to roots. Within the same temperature the regression lines do not statically differ at 99% confidence interval.

Supplementary Table 2 | Linear equations for leaf fresh weight vs leaf dry weight at different light intensities at equal air and root zone temperatures.

REFERENCES

Acharya, U. K., Subedi, P. P., and Walsh, K. B. (2017). Robustness of tomato quality evaluation using a portable Vis-SWNIRS for dry matter and colour. *Int. J. Anal. Chem.* 2017:2863454. doi: 10.1155/2017/2863454

Atkin, K., Loveys, R., Atkinson, J., and Pons, L. (2006). Phenotypic plasticity and growth temperature: understanding interspecific variability. *J. Exp. Bot.* 57, 267–281. doi: 10.1093/jxb/erj029

Benke, K., and Tomkins, B. (2017). Future food-production systems: vertical farming and controlled-environment agriculture. *Sustainability* 13, 13–26. doi: 10.1080/15487733.2017.1394054

Bensink, J. (1971). *On morphogenesis of Lettuce Leaves in Relation to Light and Temperature*. Doctoral dissertation, Wageningen University, Wageningen.

Duggan-Jones, D. I., and Nichols, M. A. (2014). Determining the optimum temperature, irradiation and CO2 enrichment on the growth of lettuce and

cabbage seedlings in plant factories. *Acta Horticult.* 1107, 187–194. doi: 10.17660/ActaHortic.2015.1107.25

Evans, J., and Poorter, H. (2001). Photosynthetic acclimation of plants to growth irradiance: the relative importance of specific leaf area and nitrogen partitioning in maximizing carbon gain. *Plant Cell Environ.* 24, 755–767. doi: 10.1046/j.1365-3040.2001.00724.x

Fan, X. X., Xu, Z. G., Liu, X. Y., Tang, C. M., Wang, L. W., and Han, X. L. (2013). Effects of light intensity on the growth and leaf development of young tomato plants grown under a combination of red and blue light. *Sci. Horticult.* 153, 50–55. doi: 10.1016/j.scienta.2013.01.017

Frantz, J. M., Ritchie, G., Cometti, N. N., Robinson, J., and Bugbee, B. (2004). Exploring the limits of crop productivity: beyond the limits of tipburn in lettuce. *J. Am. Soc. Horticult. Sci.* 129, 331–338. doi: 10.21273/JASHS.129.3.0331

Fu, W., Li, P., and Wu, Y. (2012). Effects of different light intensities on chlorophyll fluorescence characteristics and yield in lettuce. *Sci. Horticult.* 135, 45–51. doi: 10.1016/j.scienta.2011.12.004

Gent, M. P., and Seginer, I. D. O. (2012). A carbohydrate supply and demand model of vegetative growth: response to temperature and light. *Plant Cell Environ.* 35, 1274–1286.

Gosselin, A., and Trudel, M. J. (1984). Interactions between root-zone temperature and light levels on growth, development and photosynthesis of Lycopersicon esculentum Mill. cultivar 'Vendor'. *Sci. Horticult.* 23, 313–321. doi: 10.1016/0304-4238(84)90027-X

Graamans, L., Baeza, E., Van Den Dobbelsteen, A., Tsafaras, I., and Stanghellini, C. (2018). Plant factories versus greenhouses: comparison of resource use efficiency. *Agricult. Syst.* 160, 31–43. doi: 10.1016/j.agsy.2017.11.003

Hatfield, J. L., and Prueger, J. H. (2015). Temperature extremes: Effect on plant growth and development. *Weather Clim. Ext.* 10, 4–10. doi: 10.1016/j.wace.2015.08.001

He, J., and Lee, S. K. (1998). Growth and photosynthetic responses of three aeroponically grown Lettuce cultivars (*Lactuca sativa* L.) to different rootzone temperatures and growth irradiances under tropical aerial conditions. *J. Horticult. Sci. Biotechnol.* 73, 173–180. doi: 10.1080/14620316.1998.11510961

He, J., Lee, S. K., and Dodd, I. C. (2001). Limitations to photosynthesis of lettuce grown under tropical conditions: alleviation by root-zone cooling. *J. Exp. Bot.* 52, 1323–1330. doi: 10.1093/jexbot/52.359.1323

Héraut-Bron, V., Robin, C., Varlet-Grancher, C., and Guckert, A. (2001). Phytochrome mediated effects on leaves of white clover: consequences for light interception by the plant under competition for light. *Ann. Bot.* 88, 737–743. doi: 10.1006/anbo.2001.1510

Heuvelink, E. (1989). Influence of day and night temperature on the growth of young tomato plants. *Sci. Horticult.* 38, 11–22.

Kelly, N., Choe, D., Meng, Q., and Runkle, E. S. (2020). Promotion of lettuce growth under an increasing daily light integral depends on the combination of the photosynthetic photon flux density and photoperiod. *Sci. Hortic.* 272:109565. doi: 10.1016/j.scienta.2020.109565

Kitaya, Y., Niu, G., Kozai, T., and Ohashi, M. (1998). Photosynthetic photon flux, photoperiod, and CO2 concentration affect growth and morphology of lettuce plug transplants. *HortScience* 33, 988l–999l.

Körner, O., Heuvelink, E., and Niu, Q. (2009). Quantification of temperature, CO2, and light effects on crop photosynthesis as a basis for model-based greenhouse climate control. *J. Horticult. Sci. Biotechnol.* 84, 233–239. doi: 10.1016/j.jplph.2013.06.004

Kozai, T. (2013). Sustainable plant factory: closed plant production systems with artificial light for high resource use efficiencies and quality produce. *Acta Horticult.* 1004, 27–40. doi: 10.17660/ActaHortic.2013.1004.2

Marcelis, L. F., Heuvelink, E., and Goudriaan, J. (1998). Modelling biomass production and yield of horticultural crops: a review. *Sci. Horticult.* 74, 83–111. doi: 10.1016/S0304-4238(98)00083-1

Marsh, L. S., and Albright, L. D. (1991). Economically optimum day temperatures for greenhouse hydroponic lettuce production part I: a computer model. *Transact. ASAE* 34, 550–0556. doi: 10.13031/2013.31698

Nederhoff, E. M. (1994). *Effects of CO2 Concentration on Photosynthesis, Transpiration and Production of Greenhouse Fruit Vegetable Crops*. Doctoral dissertation, Wageningen University, Wageningen.

Pantin, F., Simonneau, T., Rolland, G., Dauzat, M., and Muller, B. (2011). Control of leaf expansion: a developmental switch from metabolics to hydraulics. *Plant Physiol.* 156, 803–815. doi: 10.1104/pp.111.176289

Pennisi, G., Pistillo, A., Orsini, F., Cellini, A., Spinelli, F., Nicola, S., et al. (2020). Optimal light intensity for sustainable water and energy use in indoor cultivation of lettuce and basil under red and blue LEDs. *Sci. Horticult.* 272:109508. doi: 10.1016/j.scienta.2020.109508

Pérez-López, U., Miranda-Apodaca, J., Muñoz-Rueda, A., and Mena-Petite, A. (2013). Lettuce production and antioxidant capacity are differentially modified by salt stress and light intensity under ambient and elevated CO2. *J Plant Physiol.* 170, 1517–1525. doi: 10.1016/j.jplph.2013.06.004

Poorter, H., and Nagel, O. (2000). The role of biomass allocation in the growth response of plants to different levels of light, CO2, nutrients and water: a quantitative review. *Funct. Plant Biol.* 27, 1191–1191. doi: 10.1071/PP99173_CO

Poorter, H., Niinemets, Ü, Ntagkas, N., Siebenkäs, A., Mäenpää, M., Matsubara, S., et al. (2019). A meta-analysis of plant responses to light intensity for 70 traits ranging from molecules to whole plant performance. *New Phytol.* 223, 1073–1105. doi: 10.1111/nph.15754

Poorter, H., Niinemets, Ü, Poorter, L., Wright, I. J., and Villar, R. (2009). Causes and consequences of variation in leaf mass per area (LMA): a meta-analysis. *New Phytol.* 182, 565–588. doi: 10.1111/j.1469-8137.2009.02830.x

Poorter, H., Niklas, K. J., Reich, P. B., Oleksyn, J., Poot, P., and Mommer, L. (2012). Biomass allocation to leaves, stems and roots: meta-analyses of interspecific variation and environmental control. *New Phytol.* 193, 30–50. doi: 10.1111/j.1469-8137.2011.03952.x

Rosbakh, S., Römermann, C., and Poschlod, P. (2015). Specific leaf area correlates with temperature: new evidence of trait variation at the population, species and community levels. *Alpine Bot.* 125, 79–86. doi: 10.1007/s00035-015-0150-6

Scheepens, J. F., Frei, E. S., and Stöcklin, J. (2010). Genotypic and environmental variation in specific leaf area in a widespread Alpine plant after transplantation to different altitudes. *Oecologia* 164, 141–150. doi: 10.1007/s00442-010-1650-0

Shamshiri, R., Kalantari, F., Ting, K. C., Thorp, K. R., Hameed, I. A., Weltzien, et al. (2018). Advances in greenhouse automation and controlled environment agriculture: a transition to plant factories and urban agriculture. *Int. J. Agricult. Biol. Eng.* 11, 1–22. doi: 10.25165/j.ijabe.20181101.3210

SharathKumar, M., Heuvelink, E., and Marcelis, L. F. (2020). Vertical Farming: moving from genetic to environmental modification. *Trends Plant Sci.* 25, 724–727. doi: 10.1016/j.tplants.2020.05.012

Sultan, S. E. (2003). Phenotypic plasticity in plants: a case study in ecological development. *Evolut. Dev.* 5, 25–33. doi: 10.1046/j.1525-142x.2003.03005.x

Thompson, H. C., Langhans, R. W., Both, A. J., and Albright, L. D. (1998). Shoot and root temperature effects on lettuce growth in a floating hydroponic system. *J. Am. Soc. Horticult. Sci.* 123, 361–364. doi: 10.21273/JASHS.123.3.361

Van Henten, E. J. (1994). Validation of a dynamic lettuce growth model for greenhouse climate control. *Agricult. Syst.* 45, 55–72.

Van Rijswick, C. (2018). *Hoge Kosten Bottleneck Voor 'Vertical Farms'*. Available online at: https://www.rabobank.com/nl/raboworld/articles/high-costs-make-it-hard-for-vertical-farms-to-compete (accessed July 22, 2020).

Waraich, E. A., Ahmad, R., Halim, A., and Aziz, T. (2012). Alleviation of temperature stress by nutrient management in crop plants: a review. *J. Soil Sci. Plant Nutr.* 12, 221–244. doi: 10.4067/S0718-95162012000200003

Zou, J., Zhang, Y., Zhang, Y., Bian, Z., Fanourakis, D., Yang, Q., et al. (2019). Morphological and physiological properties of indoor cultivated lettuce in response to additional far-red light. *Sci. Horticult.* 257:108725. doi: 10.1016/j.scienta.2019.108725

Conflict of Interest: The authors declare that the research was conducted in the absence of any commercial or financial relationships that could be construed as a potential conflict of interest.

Copyright © 2021 Carotti, Graamans, Puksic, Butturini, Meinen, Heuvelink and Stanghellini. This is an open-access article distributed under the terms of the Creative Commons Attribution License (CC BY). The use, distribution or reproduction in other forums is permitted, provided the original author(s) and the copyright owner(s) are credited and that the original publication in this journal is cited, in accordance with accepted academic practice. No use, distribution or reproduction is permitted which does not comply with these terms.

frontiers in Plant Science

ORIGINAL RESEARCH
published: 18 February 2021
doi: 10.3389/fpls.2021.603411

The Effect of Red & Blue Rich LEDs vs Fluorescent Light on Lollo Rosso Lettuce Morphology and Physiology

Laura Cammarisano[1,2], Iain S. Donnison[1] and Paul R. H. Robson[1]*

[1] IBERS, Aberystwyth University, Aberystwyth, United Kingdom, [2] Next-Generation Horticultural Systems, Leibniz-Institute of Vegetable and Ornamental Crops (IGZ), Grossbeeren, Germany

The challenges of feeding an increasing population, an increasingly urban population and within an increasingly challenging global environment have focused ideas on new ways to grow food. Growing food in a controlled environment (CE) is not new but new technologies such as broad-spectrum LEDs and robotics are generating new opportunities. Growth recipes can be tailored to plant species in a CE and plasticity in plant responses to the environment may be utilized to make growth systems more efficient for improved yield and crop quality. Light use efficiency within CE must consider energy requirements, yield and impacts on quality. We hypothesized that understanding how plants change their morphology and physiology in response to light will allow us to identify routes to make light more efficient for delivery of high-quality produce. We focused on responses to light in Lollo rosso lettuce which produces compact, crinkly and highly pigmented leaves. We compared the spectra of the commonly used artificial light sources in indoor farming (compact fluorescence tubes, FL, and broad-spectrum light-emitting diodes, LEDs) at two irradiance levels (270 and 570 μmol m^{-2} s^{-1}). We discovered LEDs (λ_P: 451, 634, and 665 nm) produced the same amount of produce for half the incident energy of FL (T5). At higher irradiances LEDs produced 9% thicker leaves, 13% larger rosettes and 15% greater carotenoid content. Leaves differed in light absorptance with plants grown under lower FL absorbing 30% less of mid-range wavelengths. We show that the relative efficiencies of LED and FL is a function of the irradiances compared and demonstrate the importance of understanding the asymptotes of yield and quality traits. Increasing our understanding of structural and biochemical changes that occur under different combination of wavelengths may allow us to better optimize light delivery, select for different ranges of plasticity in crop plants and further optimize light recipes.

Keywords: LED – light emitting diode, fluorescent light, red lettuce, light spectral composition, irradiance, leaf optical properties, leaf structural and functional traits, light adaptation

OPEN ACCESS

Edited by:
Bernard Grodzinski, University of Guelph, Canada

Reviewed by:
Raymond M. Wheeler, National Aeronautics and Space Administration (NASA), United States
Francesco Di Gioia, Pennsylvania State University (PSU), United States

****Correspondence:***
Laura Cammarisano
cammarisano@igzev.de

Specialty section:
This article was submitted to Crop and Product Physiology, a section of the journal Frontiers in Plant Science

Received: *06 September 2020*
Accepted: *28 January 2021*
Published: *18 February 2021*

Citation:
Cammarisano L, Donnison IS and Robson PRH (2021) The Effect of Red & Blue Rich LEDs vs Fluorescent Light on Lollo Rosso Lettuce Morphology and Physiology. Front. Plant Sci. 12:603411. doi: 10.3389/fpls.2021.603411

INTRODUCTION

Incident light provides both energy and information by powering and regulating plant growth and development. The use of focused light treatments, with direct effects on physiological processes, allows fine manipulation of the plant phenotype (Carvalho and Folta, 2015). When absorption of photosynthetically active photons exceeds the photosystems capacity to utilize excitation energy,

dissipation of the excess energy is necessary to avoid or to reduce the risk of photooxidative damage. The excess excitation energy can be re-emitted as radiation energy and particularly chlorophyll a fluorescence or as non-radiative energy that can be dissipated thermally via non-photochemical quenching (NPQ) (Niyogi, 2000; Ruban et al., 2007; Kalaji et al., 2017; Kress and Jahns, 2017).

Plants optimize light capture and prevent photodamage in fluctuating light conditions. Adaptations act across different scales from macro scale to the micro scale (Bjorkman and Demmig-Adams, 1995). Adjustments at plant/leaf level affect light interception and absorption through changes in plant compactness, stem elongation, leaf movement, protective pigment synthesis (e.g., anthocyanins), protective leaf layers (e.g., wax or trichomes) and leaf area. Further adjustments include changes in leaf ultrastructure, i.e., the number of cells or airspaces, chloroplast movement and more in-depth changes in photosystem stoichiometry and synthesis of antioxidants to scavenge reactive oxygen species (Bensink, 1971; Štroch et al., 2004; Terashima et al., 2009; Davis et al., 2011).

Not all incident photons are absorbed because of differences in intrinsic absorption levels of different wavelengths of light. This means that, regardless of the amount of light reaching the leaf, the capture of photons and the energy conversion efficacy of radiant energy into biomass depends on the wavelength of the photon (Hoover, 1937; McCree, 1981). Photon energy is inversely proportional to the wavelength (E = h c/λ), consequently energy decreases across the electromagnetic spectrum, photons with longer wavelengths (>750 nm) have too little energy for photochemistry (1.8 eV, equivalent to the energy of a red photon) and the short wavelengths photons have excessive energy (Zhu et al., 2008; Barber, 2009; Thapper et al., 2009; Kusuma et al., 2020). Plant adaptive mechanisms to incident radiation can be indicative of light stress, too little or too much, but also include desirable plant quality traits. For instance, in red lettuce, leaf pigmentation is a plant stress response and is an important characteristic for visual and nutritional quality of lettuce (Becker et al., 2014).

Controlled Environment Agriculture (CEA) may produce optimal growth conditions to obtain the best yield all year-round (Kozai, 2013). Plant factories could include environmental stresses in growth recipes to enhance crop quality. Furthermore, plant biochemical and biophysical responses to the environment may change the way light is absorbed and could be exploited to further enhance plant performance (Ustin and Jacquemoud, 2020). Characterizing plant responses, especially at leaf level, to light intensity and spectral quality has great potential for the rapidly evolving indoor farming including environmental optimization of stress application and manipulation of plant morphology (Carter and Knapp, 2001; Carvalho and Folta, 2015; Bergstrand et al., 2016).

The aim of this work was to characterize some of the adaptive morphological and physiological responses to light in the pigmented Lollo rosso lettuce. Morphological responses at plant level (e.g., rosette compactness) and leaf level (e.g., pigmentation, thickness, leaf structural anatomy) were studied in combination with chlorophyll fluorescence and leaf absorptance to investigate plant adaptations to irradiance and light quality. We compared Lollo rosso growing in the same controlled environment (CE) cabinet under two efficient light sources, fluorescent and LEDs, at two irradiances to better understand the relative adaptations and efficacy of the light sources and the interactions between their different light spectra and yield and crop quality.

MATERIALS AND METHODS

Plant Material and Growth Conditions

Red lettuce Lollo rosso seeds (Antonet RZ seeds from RijkZwaan, De Lier, The Netherlands) were sown in 155 g of sieved John Innes No. 3 soil-based compost. Water holding "field" capacity of the compost was calculated following the gravimetric method for soil moisture determination (Reynolds, 1970). Pots (7 cm × 7 cm × 10 cm) were filled, saturated with water, covered with plastic film and left to drain at room temperature (20 ± 5°C). After 24 h pot weight was noted and pots were dried in the oven at 105°C. Every 24 h pots were weighed until stable dry weight (DW) was reached. The dry and wet weights were used to estimate the weight of pots and soil at approximately 0 and 100% field capacity and water content in between these extremes was estimated as a linear proportion of the difference between these values. Pots with plants were individually irrigated to 80% field capacity (205 g) every 48 h until harvest at day 30. The 48 pots containing seeds were placed into the experimental system (Fitotron, growth cabinet) which was partitioned in two halves separated by white reflective sheets (ORCA grow film, California Grow Films LLC). One side of the cabinet was equipped with fluorescent tubes [FL, compact fluorescent tubes spectrum (T5, F28W/835, 3,500 K), with a spectral composition of blue (401–498 nm): green–yellow (499–609 nm): red (610–699 nm): far-red (700–750 nm) of 15: 44: 35: 6%, respectively) and the other half with a photosynthetically active radiation (PAR) customized LED array (EP006, 380–760 nm, Shenzhen Herifi Co., Ltd., China, with a spectral composition of blue (401–498 nm): green–yellow (499–609 nm): red (610–99 nm): far-red (700–750 nm) of 19: 5: 65: 11%, respectively). Two shelves (each shelf was 0.27 m^2, with 12 plant replicates) were arranged in each side of the cabinet at different heights to generate two irradiance levels (270 and 570 μmol m^{-2} s^{-1}) for a total of four light treatments [FL(270) (270 μmol m^{-2} s^{-1}), FL(570) (570 μmol m^{-2} s^{-1}), LED(270) (270 μmol m^{-2} s^{-1}), LED(570) (570 μmol m^{-2} s^{-1})]. Environmental conditions were monitored by four Tinytag Ultra 2 (Gemini Data Loggers, Chichester, United Kingdom) placed in each of the treatment areas. Photoperiod was 18 h, temperature was maintained at an average of 22°C, relative humidity 50% and ambient CO_2 (environmental data from the individual treatment areas is in **Table 1**). Irradiance and light spectral composition of the treatments were measured (**Figure 1**) using the spectroradiometer SpectraPen LM 500 (cosine-corrected, 380–780 nm; Photon Systems International, Drasov, Czech Republic).

TABLE 1 | Environmental data for the treatments reported.

Treatments	Temperature (°C)	Relative humidity (%)
FL(270)	21.6 ± 0.2	50.1 ± 0.6
FL(570)	22.7 ± 0.1	46.1 ± 0.4
LED(270)	22.0 ± 0.2	49.1 ± 0.5
LED(570)	23.3 ± 0.2	45.7 ± 0.4

Values are reported as mean ± standard error of the mean.

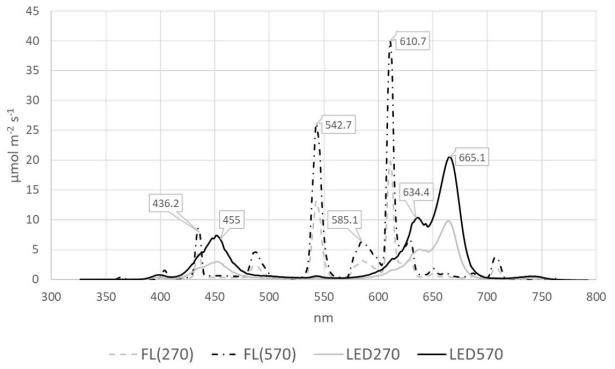

FIGURE 1 | Spectral distribution including peak wavelengths of the four light treatments, FL(270) in dashed gray, FL(570) in dashed black, LED(270) in gray and LED(570) in black. Fluorescent (FL) light provided by T5 fluorescent lamps. LEDs radiation provided by PAR customized LED array (diodes emitting in the blue: 410, 430, and 460 nm and, diodes emitting in the red: 610, 630, and 660 nm).

Sampling and Measurements of Plant Morphological, Physiological and Optical Parameters

Chlorophyll a fluorescence was assessed from leaf number four using a portable HandyPEA continuous excitation chlorophyll fluorimeter (Hansatech, King's Lynn, United Kingdom). First, light-adapted measurements to determine maximum operating efficiency of PSII photochemistry in the light [$F_V/F_M' = (F_M' - F_0')/F_M'$] were taken, then dark-adapted measurements were taken after 30 min of dark-adaptation using the manufacturer's leaf clips and maximum quantum efficiency of PSII photochemistry in the dark [$F_V/F_M = (F_M - F_0)/F_M$], non-photochemical quenching [NPQ = $(F_M - F_M')/F_M'$] and performance index [PI = $[1 - (F_0/F_M)/M_0/V_J] \times [(F_M - F_0)/F_0] \times [1 - V_J)/V_J)]$ were determined for four replicates.

The spectral properties of leaf number four were measured (Ocean Optics Jaz-SpectroClip-TR combined instrument, Ocean Optics, Dunedin, FL, United States) on the adaxial and abaxial leaf surface on day 30. Measurements were taken on the same leaf position in three plant replicates per treatment (on the right side of the midrib toward the leaf four apex). The leaf was illuminated by a standardized light source (Halogen lamp) through an optical fiber, and the transmitted and reflected light was analyzed with respect to its spectral composition.

Rosette images (examples in **Figure 2**) were taken using a fixed focal length digital camera and fixed-lighting stand. Images were used for rosette area, measured as canopy cover, determination using the Shape descriptor plug in in ImageJ software (version 1.52a) (Schneider et al., 2012). Rosette shoots were harvested from just above the cotyledons node and immediately weighed to determine fresh weight (FW). Of the 12 plant replicates used to determine FW, eight were then placed in a paper bag and dried to constant weight at 60°C to determine DW.

A random selection of 3 plants were harvested for biochemical analyses at the end of the experiment (day 30). Fully expanded leaves, developmentally the third and fourth leaf, were excised, the midrib was removed and tissue immediately frozen in liquid nitrogen before storage at -80°C until analyzed. Prior to analysis, samples were freeze-dried and cold milled to a fine powder in an automated sample grinder (Labman Automation Ltd., Middlesbrough, United Kingdom) for 90 s at −70°C.

Imaging of Leaf Disks by Light Microscopy and Transmission Electron Microscopy

Leaf disks of 1 cm^2 were obtained from the fourth leaf (on the right side of the midrib toward the leaf apex) of four plant replicates and transferred to cold 2.5% glutaraldehyde in 0.1 M sodium cacodylate at pH 7.2, after vacuum infiltration discs were stored at 4°C. After a series of buffered washes, leaves were dehydrated in an aqueous alcohol (ethanol) series before being fixed in LR White (Hard grade) resin and were cut in 2–5 µm light microscopy (LM) sections on a Reichert-Jung Ultracut E Ultramicrotome, dried and blue stained. LM micrographs were taken using a Leica DM6000 microscope fitted with a Hitachi HV-D20 camera. Ultrathin 60 – 80 nm sections of interest were cut on a Ultramicrotome (Reichert-Jung Ultracut E) with a diamond knife (Diatome 21 Ultra 45°) and collected on Gilder GS2 × 0.5 3.05 mm diameter nickel or copper slot grids (Gilder Grids, Grantham, United Kingdom) float-coated with Butvar B98 polymer (Agar Scientific) films. transmission electron microscopy (TEM) sections were double-stained with uranyl acetate (Agar Scientific) and Reynold's lead citrate (TAAB Laboratories Equipment Ltd., Aldermaston, United Kingdom) and observed using a JEOL JEM1010 transmission electron microscope (JEOL Ltd., Tokyo, Japan) at 80 kV. The resulting images were photographed using Carestream 4489 electron microscope film (Agar Scientific) and developed in Kodak D-19 developer. The derived negatives were scanned with an Epson Perfection V800 film scanner and converted to positive images (example images shown in **Supplementary Figure 1**). Leaf anatomy characteristics (leaf thickness, cell wall thickness and intercellular airspaces area) was measured on the images by digital analysis of the leaf-cross sections using ImageJ.

Relative Water Content Determination

Leaf disks (1 cm^2), cut from the right side of the midrib toward the leaf number four apex of four plant replicates, were used to determine the relative water content (RWC), calculated using the formula: [(FW-DW)/(TW-DW)]*100, where FW is FW, DW is DW. TW, is turgid weight, which were obtained by leaving

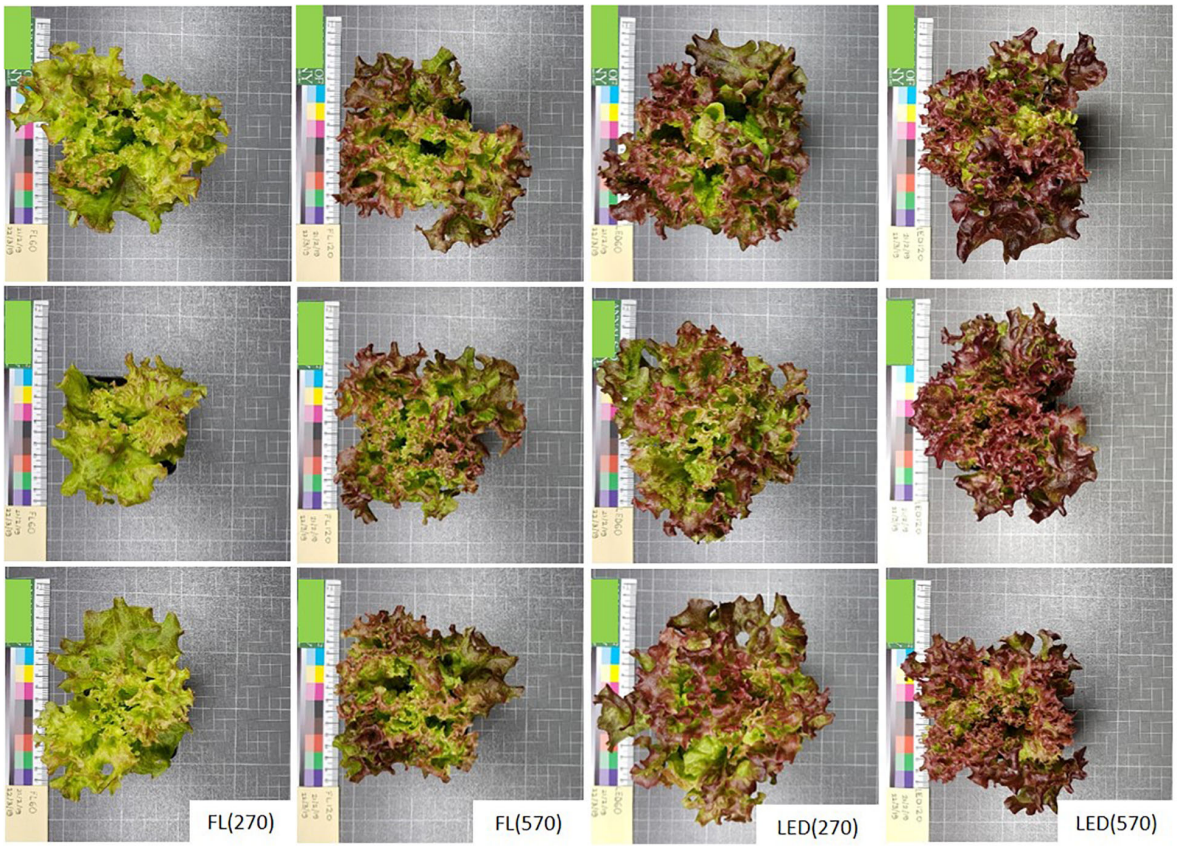

FIGURE 2 | Representative pictures of three of the lettuce replicates treated with different light. Plants grown under fluorescent light (FL) and LEDs at two irradiance levels [270 and 570 μmol m^{-2} s^{-1}) (FL(270), FL(570), LED(270), and LED(570)], showing differences in plant area, crinkliness and pigmentation. Pictures taken 30 days after sowing (DAS).

the leaf disk under distilled water in dark conditions for 24 h (Smart and Bingham, 1974).

Estimation of Foliar Anthocyanin Content From Reflectance Spectra

Reflectance measurements, recorded on the leaf adaxial and abaxial surface on day 30, were used to assess red pigmentation due to the presence of anthocyanins. A three-band approach, mARI $[(R_{530-570}{}^{-1}\text{-}R_{690-710}{}^{-1})*\text{RNIR}$, where R was the reflectance at 530, 570, 690, and 790 nm and RNIR was the reflectance between 700 and 1000 nm] (Gitelson et al., 2006), was used to estimate leaf anthocyanin content. The red-edge band accounts for the variability derived from chlorophyll content and the NIR band for variability related to leaf structure and composition (Croft and Chen, 2018).

Extraction and Quantification of Leaf Chlorophyll and Carotenoid Content

Lyophilized powdered leaf (15 mg) was extracted in three consecutive washes with 95% ethanol. After 48 h, absorbance of the collected extract was read at 470, 649, and 664 nm against the same amount of blank solution in a 96 well half area microplate ensuring a 1 cm pathlength using a UV/VIS spectrophotometer (UV 3100 PC Spectrophotometer, VWR, Belgium). Pigments concentration were determined using equations reported in Lichtenthaler and Buschmann (2001).

Statistical Analysis

All the data were statistically analyzed using Microsoft Excel 2016 and R studio (R version 3.5.2 (2018-12-20), "Eggshell Igloo") with packages: agricolae, car, ggplot2, Mendiburu (2010), Wickham (2016), and Fox and Weisberg (2019). For the effect of the light treatment on the measured parameters data were analyzed by one-way analysis of variance (ANOVA) and the means were compared by Least Significance Difference (LSD), at 5% significance level. The effects of two factors, "irradiance" and "light source," and their interaction were tested by two-way analysis of variance (ANOVA) (Muggeo, 2003).

RESULTS

Yield and Morphological Responses

Interaction effect was detected between irradiance and light source on the averaged FWs and DWs of red lettuce (p = 0.003

and 0.017, respectively). Light treatments had a significant effect on FW and DW ($p = 0.000$ and $p = 7.0 \times 10^{-5}$, respectively) of Lollo rosso lettuce growing in the same environment but under two different light sources at two different irradiances (**Table 2**). Increasing irradiance of FL significantly increased shoot FW (69%) and DW (98%) of "Lollo rosso." Increasing irradiance under LED treatment did not significantly increase FW or DW and biomass values of both LED treatments were grouped with the higher FL treatment by *post hoc* test.

Rosette area (canopy cover) was significantly different between different light treatments ($p = 0.004$) (**Table 2**). Rosettes growing under treatment FL(270) were the smallest, resulting 12% smaller than rosettes grown under FL(570). In contrast, increasing irradiance under LEDs decreased rosette area. The largest rosettes of any treatments were from plants growing under LED(270), rosette area under the higher LED irradiance (LED570) was 13% lower but still greater than either FL treatment.

Light treatment had a significant effect on leaf thickness measured on cross-sections of the fourth leaf ($p = 2.2 \times 10^{-5}$). The thickest leaves were from plants growing under higher LED treatments [LED(570)] and the thinnest from FL(270) plants (**Table 2** and **Supplementary Figure 1**). Light treatment did not have a significant effect on the leaf water status of Lollo rosso lettuce (**Supplementary Table 1**). Intercellular airspace doubled from FL(270) to FL(570) leaves which exhibited the highest values overall ($p = 0.004$) (**Table 2**).

Chlorophyll Fluorescence, Leaf Optical Properties, and Pigments

Light treatment had a significant effect on the maximum operating efficiency of PSII photochemistry in the light, F_V/F_M', and the maximum quantum efficiency of PSII photochemistry in the dark, F_V/F_M, ($p = 0.017$ and $p = 0.030$) (**Table 3**). The highest F_V/F_M' was measured in leaves under FL(270), while the lowest was measured in leaves under LED(270). There was very little difference but LSD *post hoc* test separated measurements of F_V/F_M in leaves grown in FL(270) from the rest of the treatments was slightly higher compared to an average of 0.84 from the other three treatments. No statistical difference was found for PI and NPQ (**Supplementary Table 1**). However, it was notable that the lowest levels of NPQ values were detected from leaves grown under treatment FL(270) and NPQ was two-fold higher in treatment LED(270).

Light treatment did not have a significant effect on levels of the main reaction center pigment chlorophyll a ($p = 0.079$) but did have a significant effect on levels of the main pigment of the light harvesting complex, chlorophyll b, ($p = 0.013$) (**Table 3**). Two-way ANOVA reported a significant effect of both light source ($p = 0.020$) and irradiance ($p = 0.008$) on chlorophyll b content. The lowest chlorophyll b content was in FL(570) leaves while LED(270) leaves contained the greatest chlorophyll b content. The ratio of chlorophylls a and b of the LED grown plants was significantly affected by the light treatment ($p = 0.007$). Leaves grown under FL(270) and LED(270) treatments had the lowest ratio, i.e., greater light harvesting chlorophyll per reaction center, and leaves grown under the higher irradiance [FL(570) and LED(570)] had 11 and 13% greater chlorophyll a:b ratio. Light treatment had a significant effect on levels of the ancillary light harvesting and photoprotective carotenoid pigments ($p = 0.014$). Carotenoid content of leaves grown under the highest irradiance of LED treatment was significantly higher (15%) than the other three light treatments, which were statistically similar.

Two-way ANOVA demonstrated the light source had a significant effect on all the photosynthetic and pigment parameters measured except for chlorophyll a:b ratio and irradiance significantly affected pigments; chlorophyll b and carotenoid contents and chlorophyll a:b ratio. There was no detectable significant interaction effect on any of the measured parameters.

Absorptance measurements from the fourth leaf of "Lollo rosso" lettuce plants were influenced by light treatment (**Figures 3A,B**). Absorptance across the whole PAR region was affected by both light source ($p = 0.001$) and irradiance ($p = 4.5 \times 10^{-5}$). Leaf absorptance was significantly lower in FL(270) samples (∼10% less) than in the other three treatments in the PAR region (400–700 nm) ($p = 3.3 \times 10^{-6}$). Absorptance in the middle wavebands, exemplified by 560 nm, was significantly lower in FL(270) grown leaves (∼20% less) than all other leaves ($p = 6.6 \times 10^{-6}$). There was a significant interaction effect between light source and irradiance on the leaf absorptance at 560 nm ($p = 0.001$). Absorptance levels were similar from the adaxial and abaxial surfaces but the abaxial absorptance was always slightly lower. The modified anthocyanin reflectance index (mARI) of Lollo rosso lettuce leaves was significantly affected by both the light intensity ($p = 0.026$) and source ($p = 0.040$) (**Table 4**). In FL(270) leaves mARI values were half of those of all other treatments ($p = 0.013$), values increased in the order FL(570) < LED(270) < LED(570) but differences were not statistically significant. The normalized photochemical reflectance index [$PRI_N = PRI/[RDVI^*(R_{700}/R_{670})]$, where RDVI is the renormalized difference vegetation index and, R_{670} and R_{700} the reflectance at 670 and 700 nm, respectively (Zarco-Tejada et al., 2013) was statistically different between light source treatments ($p = 1.1 \times 10^{-9}$). PRI_N was almost five-fold higher in LED treated plants (**Table 4**).

DISCUSSION

Conventional incandescent sources for lighting are inefficient due to the significant production of heat rather than light, heat being an undesirable biproduct in most lighting situations particularly but not always in horticulture (Both et al., 2017). Improved efficiency was achieved from fluorescent lighting (FL) which in domestic systems was formulated as tubes and compact lighting (Mile, 2009) and fluorescent lamps have been used for over 50 years for plant growth (Thomas and Dunn, 1967; Tibbitts et al., 1983; Knight and Mitchell, 1988). Light emitting diode (LED) lighting is even more efficient in terms of reduced heat production and has additional benefits such as compact size, longer life span, greater luminous efficacy, affordable cost and allows greater control of spectra due to the narrow wavebands achievable from differently

coated LEDs (Pattison et al., 2018). Thanks to the relatively rapid improvements and the possibility to adjust the spectral emission according to plant needs, LEDs are becoming an increasingly popular light source for plant growth both in greenhouse and closed CEs for industry and research (Mitchell et al., 2015). The light technology is being used for varied purposes including as growth light, to investigate light effects, to increase the daily light integral (DLI) or to environmentally modify the plant and is speeding up advances in horticulture (Bantis et al., 2018).

We made a direct comparison of two efficient light sources, fluorescent and LED, within the same CE cabinet. The light sources differed in their spectra and were applied at two light intensity levels (270 and 570 μmol m^{-2} s^{-1}) to reduce the possibility that all treatments produced responses that were asymptotic in Lollo rosso lettuce.

The same lower irradiance (270 μmol m^{-2} s^{-1}) provided by fluorescent and LED lights produced approximately twice the wet and DWs when delivered from LEDs. At equal PPF regimes, the major difference in the tested light treatments was in the proportions of different wavebands emitted by the two light sources (**Figure 1**). We detected no statistical difference in leaf temperature (23.2 ± 0.2°C) between treatments and thus the effect of the same photosynthetically photon flux densities (PPFDs) may be attributed to spectra perhaps through stimulation of photomorphogenic adaptations.

Optimized spectrum LEDs focused around the red and blue wavebands (red peaks at 634 and 665 nm and blue peak at 451 nm in our case) are highly efficient for plant growth (Matsuda et al., 2004; Zheng and Van Labeke, 2017), and also impact photomorphogenesis (Izzo et al., 2019). Rosette area (canopy cover) for example, a morphological adaptation supposedly resulting from the combination of multiple responses to light such as hypocotyl length, leaf angle and leaf shape (Hoenecke et al., 1992; Cammarisano et al., 2020), responded mainly to light source and antithetically under the tested light sources. If under FL rosettes tended to expand with increasing irradiance, under LEDs increasing irradiance produced more compacted rosettes. This response of rosettes impacts light interception, indicating that under low fluorescent light morphology alters to increase light interception, whereas under high LED interception is reduced probably due to light saturation of photosynthesis for Lollo rosso lettuce under the tested growth conditions.

Leaf anthocyanin content responded in parallel to rosette morphology and increased under high light. The photoprotective and antioxidant capacity of anthocyanins reduces light absorptance by chlorophyll and reduces photodamage by scavenging active oxygen resulting from the photo-excitation

TABLE 2 | Growth responses and leaf structural traits of Lollo rosso lettuce (30 DAS) growing under the same high and low irradiances of fluorescent, FL(270) and FL(570), and LED, LED(270), and LED(570), light.

Treatments	Rosette area** (cm^2) (*n* = 3)	Fresh weight*** (g/head) (*n* = 12)	Dry weight*** (g/head) (*n* = 8)	Leaf thickness*** (mm) (*n* = 18)	Air spaces** (μm^2) (*n* = 9)
FL(270)	181.9 ± 18.8^{c}	10.2 ± 1.1^{b}	0.62 ± 0.07^{b}	0.18 ± 0.01^{c}	1.89 ± 0.20^{b}
FL(570)	$202.8 \pm 2.8^{b,c}$	17.3 ± 0.9^{a}	1.23 ± 0.05^{a}	0.22 ± 0.00^{b}	4.11 ± 0.63^{a}
LED(270)	259.3 ± 6.8^{a}	18.6 ± 1.5^{a}	1.25 ± 0.14^{a}	0.21 ± 0.00^{b}	2.67 ± 0.24^{b}
LED(570)	$229.5 \pm 13.1^{a,b}$	17.6 ± 1.6^{a}	1.27 ± 0.17^{a}	0.24 ± 0.00^{a}	2.33 ± 0.44^{b}
Two-way	ANOVA				
Irradiance		*	*	***	*
Light source	**	**	**	***	
Interaction		**	*		

*Values are reported as mean ± standard error of the mean. Different letters within columns indicate significant treatment differences at P < 0.05, as determined by Fisher's least significant difference (LSD) test, with a > b > c. Significance codes (ANOVA): 0.000 "***," 0.001 "**," 0.01 "*."*

TABLE 3 | Chlorophyll fluorescence and chlorophyll and carotenoid pigment content of Lollo rosso lettuce growing under the same high and low irradiances of fluorescent, FL(270) and FL(570), and LED, LED(270), and LED(570), light for 30 days.

Treatments	F_V/F_M'* (*n* = 4)	F_V/F_M* (*n* = 4)	Chlorophyll a (mg g^{-1}) (*n* = 3)	Chlorophyll b* (mg g^{-1}) (*n* = 3)	Chlorophyll a:b** (*n* = 3)	Carotenoids* (mg g^{-1}) (*n* = 3)
FL(270)	0.79 ± 0.01^{a}	0.86 ± 0.00^{a}	6.18 ± 0.07	$2.04 \pm 0.07^{a,b}$	3.03 ± 0.13^{b}	1.46 ± 0.01^{b}
FL(570)	0.75 ± 0.01^{ab}	0.85 ± 0.00^{ab}	5.99 ± 0.32	1.78 ± 0.09^{c}	3.37 ± 0.02^{a}	1.50 ± 0.07^{b}
LED(270)	0.70 ± 0.04^{b}	0.84 ± 0.01^{b}	6.80 ± 0.15	2.30 ± 0.07^{a}	2.96 ± 0.03^{b}	1.55 ± 0.05^{b}
LED(570)	0.72 ± 0.01^{ab}	0.83 ± 0.01^{b}	6.67 ± 0.23	$1.99 \pm 0.09^{b,c}$	3.35 ± 0.04^{a}	1.72 ± 0.01^{a}
Two-way	ANOVA					
Irradiance				**	**	*
Light source	*	*	*	*		**
Interaction						

*Values are reported as mean ± standard error of the mean. Different letters within columns indicate significant treatment differences at P < 0.05, as determined by Fisher's least significant difference (LSD) test, with a > b > c. Significance codes (ANOVA): 0.001 "**," 0.01 "*."*

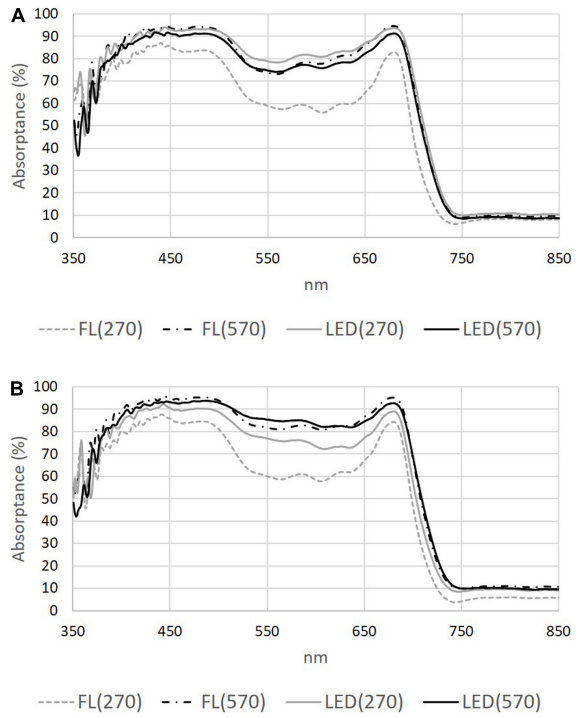

FIGURE 3 | Leaf absorptance from 350 to 850 nm of red lettuce grown under different light sources (FL, compact fluorescence tubes and LED) at two irradiance levels (270 and 570 μmol m^{-2} s^{-1}). **(A)** measurements taken on the adaxial side of leaf number four, **(B)** measurements taken on the abaxial side of leaf number four (N = 3). Absorptance was determined from reflectance and transmittance data measured on the leaf at 30 DAS using a Halogen lamp.

of chlorophyll (Gould et al., 2002; Kyparissis et al., 2007). Anthocyanin content, here estimated as mARI, increased under all light treatments compared with low FL. Bioactive compound accumulation increases in response to blue light (Ouzounis et al., 2015), while red and blue LEDs enhance both quality and yield in lettuce compared to FL lamps (Stutte et al., 2009). The FL source had major emission peaks around 560 and 610 nm and green–yellow radiation is reported to suppress lettuce growth (Dougher and Bugbee, 2001). Plants growing under low intensity FL had the lowest absorptance across the PAR region and when 560 nm was examined specifically (**Table 4**). Thus, the adaptive responses induced under low FL may be unable to efficiently utilize the available photons because this light is poorly intercepted. This is also in accordance with the plants grown under low FL appearing green indicating a lack of compounds absorbing in the mid-wavebands. "Weakly absorbed wavelengths" absorptance can be increased by lengthening of the light path in the leaf by the détour effect (Terashima et al., 2009). Plants under high FL produced the largest intercellular air spaces, a response that is characteristic of low light conditions (Ustin and Jacquemoud, 2020). The expansion of the intercellular air spaces increases light diffusion and the probability for a photon to be captured. The same was not observed in FL(270) leaves, supposedly to avoid negative consequences associated with air spaces such as reduced mesophyll conductance to CO_2 (Gorton et al., 2003).

At higher irradiances there was no longer a difference between the biomass accumulated in plants growing under different light sources. Chlorophyll a:b ratio increased under higher intensity treatments regardless of the source [FL(570) and LED(570)] reflecting a decrease in light harvesting chlorophyll b in favor of reaction centers (Friedland et al., 2019). The observed adaptations in the chl a:b, responding mainly to light intensity this time, indicated an enhanced light use efficiency under higher PPFD. Additionally, leaf thickness was greater under LED(570), this response is known to increase in response to high light (Poorter et al., 2019) and is an adaptive strategy that enhanced water use efficiency (Yun and Taylor, 1986).

The increase in leaf carotenoid content in LED(570) confirmed the likely formation of excessive radiative energy and suggested these accessory pigments could enhance energy dissipation (Kress and Jahns, 2017). The higher carotenoid content was not reflected in higher NPQ suggesting that the photoprotective mechanisms induced including greater chlorophyll a:b ratio, carotenoid and anthocyanin content and reduced rosette area were sufficient to regulate light absorption and mitigate against phototoxicity derived from excess of light energy.

Our results show LEDs spectrum to potentially deliver more energy efficiently by producing twice the DW accumulated under

TABLE 4 | Percentage absorptance in the PAR region (400–700 nm) and at 560 nm and the modified anthocyanin reflectance index (mARI) and normalized photochemical reflectance index (PRI_N) of cv. Lollo rosso lettuce leaves grown under the same high and low irradiances of fluorescent, FL(270) and FL(570), and LED, LED(270), and LED(570), light for 30 days.

Treatments	Absorptance PAR*** (%) (n = 6)	Absorptance at 560nm*** (%) (n = 6)	mARI* (n = 6)	PRI_N*** (N = 6)
FL(270)	71.00 ± 1.94^b	58.20 ± 2.52^b	1.33 ± 0.13^b	0.0025 ± 0.0000^b
FL(570)	86.50 ± 1.54^a	76.96 ± 2.36^a	2.61 ± 0.27^a	0.0035 ± 0.0002^b
LED(270)	84.13 ± 1.58^a	78.71 ± 2.00^a	2.68 ± 0.53^a	0.0153 ± 0.0021^a
LED(570)	85.53 ± 1.41^a	79.48 ± 2.63^a	2.80 ± 0.20^a	0.0125 ± 0.0015^a
Two-way	ANOVA			
Irradiance	***	**	*	
Light source	**	***	*	***
Interaction	***	**		

*Values are reported as mean ± standard error of the mean. Different letters within columns indicate significant treatment differences at $P < 0.05$, as determined by Fisher's least significant difference (LSD) test, with $a > b > c$. Significance codes (ANOVA): 0.000 "***," 0.001 "**," 0.01 "*."*

the same photon flux emitted by FL. We hypothesize the light composition, and more precisely the differing proportions of blue, green–yellow, red and far-red photons, have differently excited the photosynthetic pigments of Lollo rosso lettuce altering its saturation threshold for yield and consequently determining the adaptive strategies implemented to enhance the use of the available light.

Thus, in efficiently exploiting LED light sources it is vital to identify the point at which the relationships between irradiance and desirable crop qualities become asymptotic in various environments in order to avoid energy wastage and especially negative influences on plant photosynthetic capacity and biomass accumulation. The inefficiency of the tested compact fluorescence tubes as a light source for Lollo rosso lettuce growth may also derive from the lack of a response that increases utilization of other available wavebands in this light. This presumably has little evolutionary impact but it may be that constitutively pigmented crops lack an appreciable benefit from artificial light sources.

We conclude that the stated increased efficacy of LED versus FL is a function of the irradiances compared and, at the higher irradiances compared here LEDs are no more efficient than fluorescent light. The presented results demonstrate the importance of the light source and its spectral quality plus the interaction with irradiance in controlling plant growth and quality, both in terms of morphology and nutritional content.

DATA AVAILABILITY STATEMENT

The original contributions presented in the study are included in the article/**Supplementary Material**, further inquiries can be directed to the corresponding author/s.

AUTHOR CONTRIBUTIONS

LC: conceptualization, methodology, investigation, formal analysis, writing – original draft, and writing – reviewing and editing. ID: funding acquisition, supervision. PR: funding acquisition, conceptualization, resources, writing – original draft, writing – reviewing, and editing, supervision. All authors contributed to the article and approved the submitted version.

FUNDING

LC was funded by an Aberystwyth University studentship. ID and PR by the BBSRC Core Strategic Programme in Resilient Crops BBS/E/W/0012843A.

ACKNOWLEDGMENTS

We wish to thank Dr. Alan Coockson (Aberystwyth University) for his technical assistance in the imaging of leaf disks by microscopy techniques, and Alan Gay (Aberystwyth University) for his kind support in the optical study of leaf properties.

SUPPLEMENTARY MATERIAL

The Supplementary Material for this article can be found online at: https://www.frontiersin.org/articles/10.3389/fpls.2021.603411/full#supplementary-material

Supplementary Figure 1 | Leaf cross-sections of red lettuce plants grown under two irradiance treatments (270 and 570 μmol m^{-2} s^{-1}) emitted by two different light sources (Fluorescent light and LEDs). Images of leaf cross-sections are at the same magnification.

Supplementary Table 1 | Effect of two irradiance treatments (270 and 570 μmol m^{-2} s^{-1}) emitted by fluorescent tubes (FL) and LEDs on leaf disk relative water content (RWC), cell wall thickness, performance index (PI) and non-photochemical quenching (NPQ) of Lollo rosso lettuce at 30 DAS.

REFERENCES

Bantis, F., Smirnakou, S., Ouzounis, T., and Koukounaras, A. (2018). Current status and recent achievements in the field of horticulture with the use of light-emitting diodes (LEDs). *Sci. Hortic.* 235, 437–451. doi: 10.1016/j.scienta.2018.02.058

Barber, J. (2009). Photosynthetic energy conversion: natural and artificial. *Chem. Soc. Rev.* 38, 185–196. doi: 10.1039/b802262n

Becker, C., Klaering, H. P., Schreiner, M., Kroh, L. W., and Krumbein, A. (2014). Unlike quercetin glycosides, cyanidin glycoside in red leaf lettuce responds more sensitively to increasing low radiation intensity before than after head formation has started. *J. Agric. Food Chem.* 62, 6911–6917. doi: 10.1021/jf404782n

Bensink, J. (1971). *On Morphogenesis of Lettuce Leaves in Relation to Light and Temperature*. Wageningen: Veenman.

Bergstrand, K. J., Mortensen, L. M., Suthaparan, A., and Gislerød, H. R. (2016). Acclimatisation of greenhouse crops to differing light quality. *Sci. Hortic.* 204, 1–7. doi: 10.1016/j.scienta.2016.03.035

Bjorkman, O., and Demmig-Adams, B. (1995). "Regulation of photosynthetic light energy capture, conversion, and dissipation in leaves of higher plants," in *Ecophysiology of Photosynthesis. Springer Study Edition*, Vol. 100, eds E. D. Schulze, and M. M. Caldwell, (Berlin: Springer).

Both, A., Bugbee, B., Kubota, C., Lopez, R. G., Mitchell, C., Runkle, E. S., et al. (2017). Proposed product label for electric lamps used in the plant sciences. *HortTechnology* 32, 544–549. doi: 10.21273/HORTTECH03648-16

Cammarisano, L., Donnison, I. S., and Robson, P. R. H. (2020). Producing enhanced yield and nutritional pigmentation in lollo rosso through manipulating the irradiance, duration, and periodicity of LEDs in the visible region of light. *Front. Plant Sci.* 11:82. doi: 10.3389/fpls.2020.598082

Carter, G. A., and Knapp, A. K. (2001). Leaf optical properties in higher plants: linking spectral characteristics to stress and chlorophyll concentration. *Am. J. Bot.* 88, 677–684. doi: 10.2307/2657068

Carvalho, S. D., and Folta, K. M. (2015). Expanding genetic potential with light environmentally modified organisms. *Crit. Rev. Plant Sci.* 2689, 486–508. doi: 10.1080/07352689.2014.929929

Croft, H., and Chen, J. M. (2018). "Leaf pigment content," in *Comprehensive Remote Sensing*, ed. S. Liang, (Oxford: Elsevier). doi: 10.1016/B978-0-12-409548-9.10547-0

Davis, P. A., Caylor, S., Whippo, C. W., and Hangarter, R. P. (2011). Changes in leaf optical properties associated with light-dependent chloroplast movements. *Plant Cell Environ.* 34, 2047–2059. doi: 10.1111/j.1365-3040.2011.02402.x

Dougher, T. A. O., and Bugbee, B. (2001). Evidence for yellow light suppression of lettuce growth. *Photochem. Photobiol.* 73:208. doi: 10.1562/0031-86552001073<0208:efylso<2.0.co;2

Fox, J., and Weisberg, S. (2019). *An R Companion to Applied Regression*. Available online at: https://socialsciences.mcmaster.ca/jfox/Books/Companion/.

Friedland, N., Negi, S., Vinogradova-Shah, T., Wu, G., Ma, L., Flynn, S., et al. (2019). Fine-tuning the photosynthetic light harvesting apparatus for improved photosynthetic efficiency and biomass yield. *Sci. Rep.* 9, 1–12. doi: 10.1038/s41598-019-49545-8

Gitelson, A. A., Keydan, G. P., and Merzlyak, M. N. (2006). Three-band model for noninvasive estimation of chlorophyll, carotenoids, and anthocyanin contents in higher plant leaves. *Geophys. Res. Lett.* 33, 2–6. doi: 10.1029/2006GL026457

Gorton, H. L., Herbert, S. K., and Vogelmann, T. C. (2003). Photoacoustic analysis indicates that chloroplast movement does not alter liquid-phase CO2 diffusion in leaves of *Alocasia brisbanensis*. *Plant Physiol.* 132, 1529–1539. doi: 10.1104/pp.102.019612

Gould, K. S., McKelvie, J., and Markham, K. R. (2002). Do anthocyanins function as antioxidants in leaves? Imaging of H2O2 in red and green leaves after mechanical injury. *Plant Cell Environ.* 25, 1261–1269. doi: 10.1046/j.1365-3040.2002.00905.x

Hoenecke, M. E., Bula, R. J., and Tibbitts, T. W. (1992). Importance of "blue" photon levels for lettuce seedlings grown under red-light-emitting diodes. *HortScience* 27, 427–430. doi: 10.21273/hortsci.27.5.427

Hoover, W. H. (1937). *The Dependence of Carbon Dioxide Assimilation in a Higher Plant on Wave Length of Radiation*, Vol. 95. Washington, DC: Smithsonian Institution.

Izzo, L. G., Arena, C., De Micco, V., Capozzi, F., and Aronne, G. (2019). Light quality shapes morpho-functional traits and pigment content of green and red leaf cultivars of *Atriplex hortensis*. *Sci. Hortic.* 246, 942–950. doi: 10.1016/j.scienta.2018.11.076

Kalaji, H. M., Schansker, G., Brestic, M., Bussotti, F., Calatayud, A., Ferroni, L., et al. (2017). Frequently asked questions about chlorophyll fluorescence, the sequel. *Photosynthesis Res.* 132, 13–66. doi: 10.1007/s11120-016-0318-y

Knight, S. L., and Mitchell, C. A. (1988). Effects of incandescent radiation on photosynthesis, growth rate and yield of waldmann's green' leaflettuce. *Sci. Hortic.* 35, 37–49. doi: 10.1016/0304-4238(88)90035-0

Kozai, T. (2013). Resource use efficiency of closed plant production system with artificial light: concept, estimation and application to plant factory. *Proc. Japan Acad. B Phys. Biol. Sci.* 89, 447–461. doi: 10.2183/pjab.89.447

Kress, E., and Jahns, P. (2017). The dynamics of energy dissipation and xanthophyll conversion in arabidopsis indicate an indirect photoprotective role of zeaxanthin in slowly inducible and relaxing components of non-photochemical quenching of excitation energy. *Front. Plant Sci.* 8:2094. doi: 10.3389/fpls.2017.02094

Kusuma, P., Pattison, P., and Bugbee, B. (2020). From physics to fixtures to food: current and potential LED efficacy. *Hortic. Res.* 7:56. doi: 10.1038/s41438-020-0283-7

Kyparissis, A., Grammatikopoulos, G., and Manetas, Y. (2007). Leaf morphological and physiological adjustments to the spectrally selective shade imposed by anthocyanins in *Prunus cerasifera*. *Tree Physiol.* 27, 849–857. doi: 10.1093/treephys/27.6.849

Lichtenthaler, H. K., and Buschmann, C. (2001). Chlorophylls and carotenoids: measurement and characterization by UV-VIS spectroscopy. *Curr. Protoc. Food Anal. Chem.* 1, F4.3.1–F4.3.8. doi: 10.1002/0471142913.faf0403s01

Matsuda, R., Ohashi-Kaneko, K., Fujiwara, K., Goto, E., and Kurata, K. (2004). Photosynthetic characteristics of rice leaves grown under red light with or without supplemental blue light. *Plant Cell Physiol.* 45, 1870–1874. doi: 10.1093/pcp/pch203

McCree, K. J. (1981). "Photosynthetically active radiation," in *Physiological Plant Ecology I: Responses to the Physical Environment*, eds O. L. Lange, P. S. Nobel, C. B. Osmond, and H. Ziegler, (Berlin: Springer). doi: 10.1007/978-3-642-68090-8_3

Mendiburu, F. (2010). Agricolae: statistical procedures for agricultural research. *R Package Version* 1, 1–8.

Mile, B. J. (2009). Lamps for improving the energy efficiency of domestic lighting. *Lighting Res. Technol.* 41, 219–228. doi: 10.1177/1477153509339610

Mitchell, C. A., Dzakovich, M. P., Gomez, C., Lopez, R., Burr, J. F., Hernández, R., et al. (2015). Light-emitting diodes in horticulture. *Hortic. Rev.* 43, 1–88. doi: 10.1002/9781119107781.ch01

Muggeo, V. M. R. (2003). Estimating regression models with unknown break-points. *Stat. Med.* 22, 3055–3071. doi: 10.1002/sim.1545

Niyogi, K. K. (2000). Safety valves for photosynthesis. *Curr. Opin. Plant Biol.* 3, 455–460. doi: 10.1016/S1369-5266(00)00113-8

Ouzounis, T., Parjikolaei, B. R., Frette, X., Rosenqvist, E., and Ottosen, C. O. (2015). Predawn and high intensity application of supplemental blue light decreases the quantum yield of PSII and enhances the amount of phenolic acids, flavonoids, and pigments in *Lactuca sativa*. *Front. Plant Sci.* 6:19. doi: 10.3389/fpls.2015.00019

Pattison, P. M., Tsao, J. Y., Brainard, G. C., and Bugbee, B. (2018). LEDs for photons, physiology and food. *Nature* 563, 493–500. doi: 10.1038/s41586-018-0706-x

Poorter, H., Niinemets, U., Ntagkas, N., Siebenkas, A., Maenpaa, M., Matsubara, S., et al. (2019). A meta-analysis of plant responses to light intensity for 70 traits ranging from molecules to whole plant performance. *New Phytol.* 223, 1073–1105. doi: 10.1111/nph.15754

Reynolds, S. G. (1970). Gravimetric meth of soil moisture determination. *J. Hydrol.* 11, 258–273.

Ruban, A. V., Berera, R., Ilioaia, C., Van Stokkum, I. H. M., Kennis, J. T. M., Pascal, A. A., et al. (2007). Identification of a mechanism of photoprotective energy dissipation in higher plants. *Nature* 450, 575–578. doi: 10.1038/nature06262

Schneider, C. A., Rasband, W. S., and Eliceiri, K. W. (2012). NIH image to imageJ: 25 years of image analysis. *Nature Methods* 9, 671–675. doi: 10.1007/978-1-84882-087-6_9

Smart, R. E., and Bingham, G. E. (1974). Rapid estimates of relative water content. *Plant Physiol.* 53, 258–260. doi: 10.1104/pp.53.2.258

Štroch, M., Špunda, V., and Kurasová, I. (2004). Non-radiative dissipation of absorbed excitation energy within photosynthetic apparatus of higher plants. *Photosynthetica* 42, 323–337. doi: 10.1023/B:PHOT.0000046149.97220.18

Stutte, G. W., Edney, S., and Skerritt, T. (2009). Photoregulation of bioprotectant content of red leaf lettuce with light-emitting diodes. *HortScience* 44, 79–82. doi: 10.21273/hortsci.44.1.79

Terashima, I., Fujita, T., Inoue, T., Chow, W. S., and Oguchi, R. (2009). Green light drives leaf photosynthesis more efficiently than red light in strong white light: revisiting the enigmatic question of why leaves are green. *Plant Cell Physiol.* 50, 684–697. doi: 10.1093/pcp/pcp034

Thapper, A., Mamedov, F., Mokvist, F., Hammarstrom, L., and Styring, S. (2009). Defining the far-red limit of photosystem II in Spinach. *Plant Cell Online* 21, 2391–2401. doi: 10.1105/tpc.108.064154

Thomas, A. S., and Dunn, S. (1967). Plant growth with new fluorescent lamps. *Planta* 212, 208–212.

Tibbitts, T. W., Morgan, D. C., and Warrington, I. J. (1983). Growth of lettuce, spinach, mustard, and wheat plants under for combinations of high-pressure sodium, metal halide, and tungsten halogen lamps at equal PPFD. *J. Am. Soc. Hortic. Sci.* 108, 622–630.

Ustin, S. L., and Jacquemoud, S. (2020). "How the optical properties of leaves modify the absorption and scattering of energy and enhance leaf functionality," in *Remote Sensing of Plant Biodiversity*, eds J. Cavender-Bares, J. A. Gamon, and P. A. Townsend, (Cham: Springer). doi: 10.1007/978-3-030-33157-3

Wickham, H. (2016). *ggplot2, Elegant Graphics for Data Analysis*. New York, NY: Springer, doi: 10.1007/978-3-319-24277-4

Yun, J. I., and Taylor, S. E. (1986). Adaptive implications of leaf thickness for sun- and shade-grown abutilon theophrasti. *Ecol. Soc. Am.* 67, 1314–1318. doi: 10.2307/1938687

Zarco-Tejada, P. J., González-dugo, V., Williams, L. E., Suárez, L., Berni, J. A. J., Goldhamer, D., et al. (2013). Remote sensing of environment a PRI-based water stress index combining structural and chlorophyll effects : assessment using diurnal narrow-band airborne imagery and the CWSI thermal index. *Remote Sensing Environ.* 138, 38–50. doi: 10.1016/j.rse.2013.07.024

Zheng, L., and Van Labeke, M. C. (2017). Long-term effects of red- and blue-light emitting diodes on leaf anatomy and photosynthetic efficiency of three ornamental pot plants. *Front. Plant Sci.* 8:917. doi: 10.3389/fpls.2017.00917

Zhu, X., Long, P. S., and Ort, D. R. (2008). What is the maximum efficiency with which photosynthesis can convert solar energy into biomass? *Curr. Opin. Biotechnol.* 19, 153–159. doi: 10.1016/j.copbio.2008.02.004

Conflict of Interest: The authors declare that the research was conducted in the absence of any commercial or financial relationships that could be construed as a potential conflict of interest.

Copyright © 2021 Cammarisano, Donnison and Robson. This is an open-access article distributed under the terms of the Creative Commons Attribution License (CC BY). The use, distribution or reproduction in other forums is permitted, provided the original author(s) and the copyright owner(s) are credited and that the original publication in this journal is cited, in accordance with accepted academic practice. No use, distribution or reproduction is permitted which does not comply with these terms.

frontiers in Plant Science

ORIGINAL RESEARCH
published: 03 March 2021
doi: 10.3389/fpls.2021.615853

Impact of Different Daily Light Integrals and Carbon Dioxide Concentrations on the Growth, Morphology, and Production Efficiency of Tomato Seedlings

*Brandon M. Huber, Frank J. Louws and Ricardo Hernández**

Department of Horticultural Sciences, North Carolina State University, Raleigh, NC, United States

Indoor growing systems with light-emitting diodes offer advantages for the growth of tomato seedlings through uniform and optimized environmental conditions which increase consistency between plants and growing cycles. CO_2 enrichment has been shown to improve the yield of crops. Thus, this research aimed to characterize the effects of varied light intensities and CO_2 enrichment on the growth, morphology, and production efficiency of tomato seedlings in indoor growing systems. Four tomato cultivars, "Florida-47 R," "Rebelski," "Maxifort," and "Shin Cheong Gang," were subjected to three different daily light integrals (DLIs) of 6.5, 9.7, and 13 mol m^{-2} d^{-1} with a percent photon flux ratio of 40 blue:60 red and an end-of-day far-red treatment of 5 mmol m^{-2} d^{-1}. The plants were also subjected to three different CO_2 concentrations: 448 ± 32 (400-ambient), 1010 ± 45 (1000), and 1568 ± 129 (1600) μmol mol^{-1}. Temperature was maintained at 24.3°C ± 0.48/16.8°C ± 1.1 (day/dark; 22.4°C average) and relative humidity at 52.56 ± 8.2%. Plant density was 1000 plants m^{-2} until canopy closure. Morphological measurements were conducted daily to observe the growth response over time. In addition, data was collected to quantify the effects of each treatment. The results showed increases in growth rate with increases in the DLI and CO_2 concentration. In addition, CO_2 enrichment to 1000–1600 μmol mol^{-1} increased the light use efficiency (g_{DM} mol^{-1} $_{applied}$) by 38–44%, and CO_2 enrichment to 1600 μmol mol^{-1} did not result in any additional increase on shoot fresh mass, shoot dry mass, and stem extension. However, the net photosynthetic rate obtained with 1600 μmol mol^{-1} was 31 and 68% higher than those obtained with 1000 and 400 μmol mol^{-1}, respectively. Furthermore, the comparison of the light and CO_2 treatment combinations with the control (13 mol m^{-2} d^{-1}–400CO_2) revealed that the plants subjected to 6.5DLI–1600CO_2, 9.7DLI–1000CO_2, and 9.7DLI–1600CO_2 treatment combinations exhibited the same growth rate as the control plants but with 25–50% less DLI. Furthermore, two treatment combinations (13.0DLI–1000CO_2 and 13.0DLI–1600CO_2) were associated with the consumption of comparable amount of energy but increased plant growth by 24–33%.

Keywords: carbon dioxide, PPFD, controlled environment agriculture, vertical farm, light-emitting diodes, energy consumption, production cost

OPEN ACCESS

Edited by:
Bernard Grodzinski, University of Guelph, Canada

Reviewed by:
Theoharis Ouzounis, Fluence Bioengineering, Inc., United States
Jason Lanoue, Agriculture and Agri-Food Canada (AAFC), Canada

****Correspondence:***
Ricardo Hernández
ricardo_hernandez@ncsu.edu

Specialty section:
This article was submitted to Crop and Product Physiology, a section of the journal Frontiers in Plant Science

Received: *10 October 2020*
Accepted: *08 February 2021*
Published: *03 March 2021*

Citation:
Huber BM, Louws FJ and Hernández R (2021) Impact of Different Daily Light Integrals and Carbon Dioxide Concentrations on the Growth, Morphology, and Production Efficiency of Tomato Seedlings. Front. Plant Sci. 12:615853. doi: 10.3389/fpls.2021.615853

INTRODUCTION

High-quality transplants include seedlings that are free of disease/pests, that are compact but have high fresh and dry masses, and that exhibit high uniformity in both morphology and development (Kozai, 2005; Kubota et al., 2008). Currently, tomato seedlings are commonly grown in greenhouses or high tunnels, but these systems are subject to fluctuations in external weather, seasonality and solar radiation and thus could lead to seedlings that exhibit low uniformity. Indoor controlled environment (indoor CE) systems that use light-emitting diodes (LEDs) as the sole source of light have several advantages over other controlled environments. For example, indoor CE systems exhibit higher control of all environmental conditions, including temperature, radiation, spectrum, CO_2 concentration, air velocity, photoperiod, and vapor pressure deficit. In addition, spectral customization can enhance the biomass and growth of tomato seedlings (Hernández et al., 2016). When combined, these environmental components that are controlled in indoor CE systems can increase the resource and energy use efficiency of plants. In addition, indoor CE systems provide consistent plant quality independent of the weather and increase the spatial and temporal uniformity of the plants (Ohyama et al., 2000; Kozai, 2005; Kubota et al., 2008). Although these systems have a higher electrical energy use, the high planting density, and short production cycle make them economically feasible (Ohyama et al., 2003; Kozai, 2007, 2013; Kubota et al., 2008).

Tomato (*Solanum lycopersicum* Mill.) is widely grown around the world and is the second most valuable vegetable crop in the United States (U.S. Department of Agriculture, 2016). It is also one of the most consumed vegetables in the world and provides healthy nutrients and antioxidants (Shi and Le Maguer, 2000). In addition, the vast majority of the tomato seedlings grown are started in specialized nurseries and transplanted to greenhouses and the field (Lewis et al., 2014). Furthermore, the use of grafted tomato plants has become an essential cultivation strategy in many parts of the world (Singh et al., 2017). For example, grafted tomato plants represent a significant percentage of the total tomato plants grown in Netherlands (75%), France (50%), Japan (40%), Korea (25%), and Vietnam (33%; Singh et al., 2017), and millions of grafted transplants are used in the United States, Italy, and Spain (Singh et al., 2017). Grafted tomato plants are utilized to increase plant vigor and thus achieve longer production cycles (Oda, 1999; Khah et al., 2006; Yarsi, 2011) and to confer disease resistance in tomato crops grown (Kaskavalci et al., 2009; Louws et al., 2010; Rivard et al., 2010; McAvoy et al., 2012). However, the propagation of grafted tomato plants at a large scale is a challenging process because the environmental conditions have to be adjusted to produce two plants (rootstock and scion) at the same growth rate to ensure proper stem matching (Kubota et al., 2008; Hu et al., 2016). Therefore, tomato transplants, including grafted seedlings, are suitable for indoor CE systems (Ohyama et al., 2003; Kozai, 2005; Nanfelt, 2016).

The light environment needs to be optimized to ensure desirable growth and reduce electricity consumption in indoor CE systems. The effects of the light intensity or photosynthetic photon flux density (PPFD) on the growth of tomato seedlings (Fan et al., 2013; O'Carrigan et al., 2014) and mature fruiting plants (Dorais, 2003; Torres and Lopez, 2011; Hao et al., 2017) have been studied. In general, an increase in the PPFD or daily light integral (DLI) increases the biomass and flower developmental rate (Uzun, 2006; Fan et al., 2013; Gómez and Mitchell, 2015). For example, in a growth chamber study, Fan et al. (2013) found that the shoot dry mass of tomato seedlings increased by 230% when the DLI was increased from 2.2 to 23.0 mol m^{-2} d^{-1} and by 51% when the DLI was increased from 6.5 to 13.0 mol m^{-2} d^{-1}. Similarly, the use of supplemental lighting in a greenhouse to increase the DLI by 5.1 mol m^{-2} d^{-1} increased the shoot dry mass of tomato seedlings by 200% (Gómez and Mitchell, 2015). Although increasing the DLI generally increases growth, it is important to provide an adequate DLI to increase the production efficacy (growth per kilowatt hour). Fan et al. (2013) found that the best light level for tomato transplants was 13.0 mol m^{-2} d^{-1} because increasing the DLI beyond 23.0 mol m^{-2} d^{-1} resulted in only slight increases in the dry mass and no increase in the photosynthetic rate (Fan et al., 2013). Similarly, in tomato seedlings, O'Carrigan et al. (2014) showed that increasing the DLI from 17 to 27 mol m^{-2} d^{-1} only increased the shoot dry mass by 7%.

CO_2 is often supplemented in indoor CE systems (Kozai, 2018) and CO_2 enrichment is inexpensive under low room air exchange (0.001–0.1 h^{-1}), which is common for indoor CE systems (Ohyama and Kozai, 1998). Although ambient CO_2 levels (415 μmol mol^{-1}) are acceptable for plant growth, enrichment is often necessary in indoor CE systems because a fully developed canopy can decrease the CO_2 level to less than 200 μmol mol^{-1} (Bauerle, 1984; Both et al., 2017). CO_2 enrichment to levels higher than the ambient conditions increases the yield and fruit quality of mature tomato plants (Calvert and Slack, 1975; Enoch et al., 1976; Nilsen et al., 1983; Fierro et al., 1994; Reinert et al., 1997; Li et al., 2007b; Khan et al., 2013; Mamatha et al., 2014; Pan et al., 2019). Although many studies have focused on the benefits of individual factors (light or CO_2), fewer studies have highlighted the beneficial interaction of supplemental light and CO_2 enrichment (Labeke and Dambre, 1998; Naing et al., 2016; Ting et al., 2017; Pan et al., 2019). Furthermore, prior studies have also suggested that high CO_2 levels could partially compensate for a lower PPFD through comparable growth and dry mass (Mortensen and Moe, 1983) by increasing the net photosynthetic rate (Bencze et al., 2011; Ting et al., 2017).

Research reports have shown an increase in net photosynthetic rate and growth at CO_2 enrichment concentrations of 700–900 μmol mol^{-1} and suggested that higher concentrations provide little improvement in growth (Behboudian and Lai, 1994; Fierro et al., 1994; Mamatha et al., 2014; Zheng et al., 2019). However, we hypothesize that CO_2 enrichment above recommended values will have a significant positive impact in tomato seedlings' net photosynthetic rate, growth, morphology due to: (1) seedlings are on the exponential growth stage with no competition; (2) the seedlings have a short growing period; and (3) CO_2 enrichment is provided under relatively low DLI. Seedlings under optimal growing conditions show exponential growth. Once plants increase in size and plant competition is

evident (canopy closure), the exponential growth phase changes to linear growth (Kirschbaum, 2011). During the exponential growth phase, plants show greater responses to high CO_2 concentrations (Monje and Bugbee, 1998; Lewis et al., 2002). In the present study, tomato seedlings are in the exponential growth phase with no plant-to-plant competition. Research has also demonstrated long term adaptation to elevated CO_2 concentration, including photosynthetic acclimation and leaf anatomy changes (i.e., lower stomatal density and conductance; Ziska et al., 1995; Zheng et al., 2019). However, these changes often take several days to occur (Ziska et al., 1995). Tomato seedlings in the present study were grown for 16–18 days (to the grafting stage) and 10–11 days from cotyledon expansion, which reduces the time for long term anatomical adaptation and photosynthetic acclimation to high CO_2. Studies have shown down-regulation of photosynthesis under elevated CO_2 (Kirschbaum, 2011). Studies have also shown that the down-regulation of photosynthetic rate under high CO_2 concentrations can be affected by the DLI of the previous day (Bunce and Sicher, 2003), where high DLI in the previous day has a down-regulation effect on the following day, while lower DLI on the previous day does not. Young tomato seedlings in the present study were grown under constant relatively low DLI and therefore the down-regulation effect of previous day is minimized.

In the present study, the first objective was to study the effects of CO_2 enrichment with DLI level of 6.5, 9.7, or 13.0 mol m^{-2} d^{-1} (relatively low PPFD of 100–200 μmol m^{-2} s^{-1}) on the production of tomato seedlings. The second objective was to determine whether CO_2 enrichment can maintain desirable plant growth under reduced light levels while maintaining comparable energy consumption, production cost, and high-quality seedlings. The third objective was to determine whether CO_2 enrichment can reduce the production time of tomato transplants through an increased growth rate. In addition, calculations of the costs associated with different DLI and CO_2 combinations were also performed and compared.

MATERIALS AND METHODS

Plant Material and Growing Conditions

Four tomato cultivars were selected for this study: (1) "Rebelski" (*Solanum lycopersicum*; De Ruiter Seeds, Bergschenhoek, Netherlands), a popular indeterminate variety used in high tunnels and greenhouses for fresh-market tomatoes; (2) "Florida-47 R" (*Solanum lycopersicum*; Seminis Vegetable Seeds, St. Louis, MO, United States), a determinate variety used for field production; (3) "Maxifort" (*Solanum lycopersicum* x *Solanum habrochaites*; De Ruiter Seeds, Bergschenhoek, Netherlands), a vigorous rootstock that confers resistance to multiple soil-borne pathogens; and (4) "Shin Cheong Gang" (*Solanum lycopersicum*; De Ruiter Seeds, Bergschenhoek, Netherlands), an option for growers needing plants with disease resistance specifically against Fusarium race 3 and bacterial wilt. The seeds were sown in trays of Grodan Kiem rockwool plugs (27 × 20 mm; Grodan, Delta, Canada), and one seed was planted per cell at a density of 1000 plants m^{-2}. The seeds were covered with vermiculite, and the trays were sub-irrigated until full saturation. Following irrigation, the trays were placed into a germination chamber at 28°C under darkness. Once radical emergence was evident (24–48 h depending on the cultivar), the trays were moved into three growth chambers subjected to the respective treatments. The temperature was set to 24°C during the day and 16°C at night to obtain a daily temperature average of 22°C. The relative humidity (RH) was maintained at 50–55% in all the treatments. The temperature and RH were monitored and logged every minute (HOBO onset UX100-023, Onset Computer Corporation, Bourne, MA, United States) during the experiment, and a summary is presented in **Table 1**. Dehumidifiers were included in each chamber to help manage the humidity. The plants were watered manually by sub-irrigating the trays twice daily using a nutrient solution composed of 90 mg L^{-1} N, 47 mg L^{-1} P, 144 mg L^{-1} K, 160 mg L^{-1} Ca, 60 mg L^{-1} Mg, 113 mg L^{-1} S, 105 mg L^{-1} Cl, and micronutrients (Jensen and Malter, 1995). The EC and pH of the nutrient solution were recorded daily (Hanna Instruments, Limena, Italy; **Table 1**).

CO_2 Treatments

Three separate growth chambers had different CO_2 level set points of 448 ± 32 (400-ambient), 1010 ± 45 (1000), and 1568 ± 129 (1600) μmol mol^{-1}. The chambers were of identical size (width of 2.4 m, depth of 1.2 m, and height of 2.1 m) and had identical controls. The CO_2 level was logged every minute and monitored (Viasala GMW115, Vantaa, Finland) to maintain sufficient levels (**Table 1**). During the dark period, all the chambers were ventilated to return the CO_2 concentration to the ambient level of ∼400 μmol mol^{-1}. The chambers used for the treatments were randomized before each of the three repeated experiments.

Light Quality and Intensity

Research has suggested that the best spectral quality for producing a tomato transplant is a blue:red ratio of 1:1 (Liu et al., 2011; Hernández et al., 2016). This ratio results in an increased photosynthetic rate (Kim et al., 2004; Li et al., 2007b; Liu et al., 2011), high plant compactness, and high fresh and dry masses (Hernández et al., 2016). However, some cultivars of tomato rootstocks have shown susceptibility to intumescence when grown under conditions lacking UV-B (Lang and Tibbitts, 1983; Craver, 2014). Further research has indicated that the inclusion of end-of-day far-red (EOD-FR) treatment combined with a spectrum of high blue PFD can be an effective strategy to mitigate intumescence (Eguchi et al., 2016). In addition, EOD-FR treatment also increases the hypocotyl length of tomato seedlings, which is desirable for tomato grafting (Chia and Kubota, 2010). With respect to EOD-FR treatment, research has shown that the saturation dose for hypocotyl extension and intumescence reduction is 5 mmol m^{-2} d^{-1}, which can be achieved by exposure to 3.5 μmol m^{-2} s^{-1} for 24 min (Chia and Kubota, 2010; Eguchi et al., 2016). The LED fixtures used in this study (GE ARIZE, GEHL48HPPB1, GE Current, Boston, MA, United States) comprised a 42% blue (B) and 58% red (R) photon flux (PFD; close to the recommended 1B:1R ratio) with peaks at 448 nm (B) and 662 nm (R), both with a full

TABLE 1 | Environmental parameters measured inside the growth chamber[z].

Treatment	6.5DLI–400CO_2	9.7DLI–400CO_2	13.0DLI–400CO_2	6.5DLI–1000CO_2	9.7DLI–1000CO_2	13.0DLI–1000CO_2	6.5DLI–1600CO_2	9.7DLI–1600CO_2	13.0DLI–1600CO_2
DLI[y] (mol m^{-2} d^{-1})	6.5	9.7	13.0	6.5	9.7	13.0	6.5	9.7	13.0
PPFD (μmol m^{-2} s^{-1})	100 ± 7	149 ± 9	200 ± 14	100 ± 6	150 ± 11	199 ± 15	100 ± 7	150 ± 8	200 ± 14
EOD-FR (mmol m^{-2} d^{-1})	13.5 ± 10	12.6 ± 8	12.5 ± 8	13.9 ± 11	12.8 ± 10	13.9 ± 11	15.8 ± 12	14.5 ± 11	14.1 ± 11
CO_2 (μmol mol^{-1})		448 ± 32			1010 ± 45			1568 ± 129	
Day temp °C		24.4 ± 0.5			24.3 ± 0.4			24.2 ± 0.5	
Night temp °C		16.8 ± 1			16.9 ± 1			16.9 ± 1	
Relative humidity (%)		50.7 ± 7			51.9 ± 9			55.1 ± 8	
Photoperiod (h)					18				
pH					6.2 ± 0.1				
EC (dS m^{-1})					1.9 ± 0.1				

[z]*Averages and standard deviations from the three repetitions.* [y]*Daily light integral.*

width at half maximum (FWHM) value of 18 nm (**Figure 1**). Fixtures were installed inside each chamber to produce three light levels, namely, 100, 150, and 200 μmol m^{-2} s^{-1} PPFD, with an 18-h photoperiod.

The treatments within the chamber were separated from each other to ensure that the LED beam angle did not interfere with the other treatments. Light maps were produced for each treatment to ensure that the treatments exhibited minimal variation within each light intensity. The fixtures were set to an 18-h photoperiod (06:00–0:00) to provide three DLI treatments of 6.5, 9.7, and 13.0 mol m^{-2} d^{-1} for 100, 150, and 200 μmol m^{-2} s^{-1} PPFD, respectively (**Table 1**). EOD-FR treatment at 7.6 μmol m^{-2} s^{-1} PF with a peak at 737 nm with a FWHM of 29 nm (Phillips Greenpower LED Research Module Far Red, 929000632103, Amsterdam, Netherlands) was provided evenly to all the treatments for 30 min after the end of the photoperiod (0:00–0:30). The average EOD-FR dosage per treatment is presented in **Table 1** and is above the saturation point. The photoperiodic and EOD lighting was measured with a spectroradiometer (PS-300, Apogee instruments, Logan, UT, United States) before and after each experimental run to measure the quality and quantity of PFD. The light measurements were averaged from eight locations from each treatment and are shown in **Table 1**. Height adjustable lights and growing tables were installed to maintain the same PFD at the top of the canopy throughout the experiment. To account for variations in the light gradient within a light treatment, the trays were systematically rotated daily.

Measurement and Experimental Design

To track the growth of the stem diameter, total height, and leaf count, daily measurements were obtained from a subsample of 15 plants subjected to each treatment starting at day 10 until the final data collection. Commercially, tomato seedlings are typically spaced out (lower plant density) or grafted when plants reach canopy closure (∼3 true leaves and stem diameter of 1.8 mm). Therefore, a stem diameter of 1.8 mm was used as a threshold for data collection. Destructive data collections were performed when the last treatment reached a stem diameter of 1.8 mm. Averages from the subsamples of each experimental replication were obtained. The measurements included the stem diameter, hypocotyl length, epicotyl length, total height, leaf number, and fresh mass. The stem diameter was measured using a caliper (Mitutoyo Absolute Digimatic Caliper, Aurora, IL, United States), and the hypocotyl, epicotyl, and total heights were measured with a ruler. The number of leaves above a 1-cm threshold was counted, and the leaf area, including that of leaves greater than 1 cm, was also recorded using a leaf area meter (LI-3100, LI-COR Biosciences, Lincoln, NE, United States). Fresh samples were dried at 70°C and then weighed to record the dry mass.

The chlorophyll concentration was quantified as described by Moran and Porath (1980): two 56.6-mm^2 leaf disks were cut from each plant of three subsamples per treatment per repetition. The gas exchange was measured at the end of the experiment using a portable photosynthesis machine (LI-6800, LI-COR Biosciences, Lincoln, NE, United States), and the results from three subsamples from each treatment were averaged.

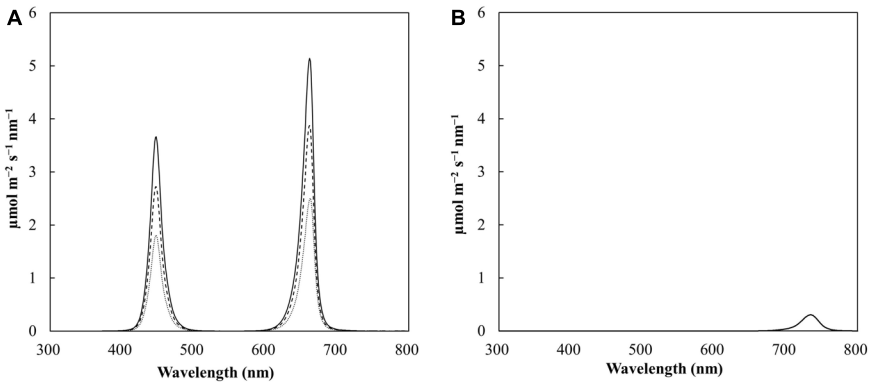

FIGURE 1 | Spectral scan of the photoperiod at light intensities of 100 (dotted line), 150 (dashed line), and 200 (solid line) µmol m^{-2} s^{-1} **(A)** and spectral scan of the end of day (EOD) treatment (5 mmol m^{-2} d^{-1}); **(B)** during the experiment. The data are averaged across the treatments. The photoperiod was 18 h (06:00-0:00), and the EOD-far-red (FR) treatment was delivered for 30 min (0:00-0:30).

Measurements were performed on the youngest fully expanded leaf for all treatments and tomato cultivars. Environmental conditions for the measurements were 22°C, 60% RH and light levels and CO_2 concentrations that matched the light and CO_2 treatments (**Table 1**).

Statistical analyses were conducted to compare the treatments using JMP software 14.2 (SAS Institute, Cary, NC, United States). The experimental design was a split-plot design, the CO_2 treatments were in different climate rooms and the three light levels were in each CO_2 climate room. Light levels were randomized in each climate room for each of the three independent experiments. Also, climate rooms were randomized for each CO_2 treatment at each of the three independent experiments. The treatment effects were run by cultivar and all cultivars had the same treatment response; therefore, the data for all cultivars was combined.

Linear regression was applied to the quantitative response to increasing the DLI at each CO_2 concentration (all measured parameters) and to increasing CO_2 for each DLI level (dry mass). To compare the slopes of the linear fit, a GLM procedure with Indicator Parameterization Estimates was used. Analysis of variance and mean separations via the Tukey-Kramer HSD test (alpha = 0.05) were computed when comparing the different CO_2 treatments within each light level (**Figure 3**). Dunnett's test was used to compare the treatments with different DLI and CO_2 conditions to the 13.0DLI–400CO_2 control treatment. The experiment was conducted three times.

Evaluation of the Cost of Electrical Lighting and CO_2 Enrichment

A summary of the variables, values, and units for the following calculations is shown in **Table 2**.

The number of fixtures needed (N) to reach a set intensity can be described by Eq. (1) adapted from Aldrich and Bartock (1994), where PPFD is the desired PPFD (100, 150, or 200 µmol m^{-2} s^{-1} in our experiment), A is the total growing area (length × width; 1 m^2 for ease of calculation), UF is the utilization factor [value that considers the beam angle distribution, growing area geometry, and reflectivity; 0.9 based on the information reported by Hernández and Kubota (2015)], MF is the maintenance factor [decrease in the fixture photon output over time; 0.9 based on the information reported by Hernández and Kubota (2015)], LPE is the lighting photon efficiency based on current technology (3.0 µmol J^{-1} or µmol W^{-1} s^{-1}; GE current, Boston, MA, United States), and WF is the wattage required to power each fixture (30.5 W).

$$N = \frac{PPFD \times A}{LPE \times WF \times UF \times MF} \quad (1)$$

The area electric power consumption (APC; W m^{-2}) of lamps can be expressed by an Eq. (2) Hernández and Kubota (2015), which does not include the cost of HVAC cooling:

$$APC = \frac{N \times WF}{A} \quad (2)$$

The daily electrical cost (DEC; \$ d^{-1} m^{-2}) can be expressed with Eq. (3), where APC (2) is multiplied by the photoperiod (P; h), divided by 1000 to convert from W h to kW h and then multiplied by the electricity rate Er (\$ kWh^{-1}), which varies by region. In this study, a rate of \$0.09 was used based on the average in the United States (Lewis et al., 2014).

$$DEC = \frac{APC \times P}{1000} \times Er \quad (3)$$

The final calculation was the total electricity cost (TEC; \$ m^{-2}), which is expressed by Eq. (4), where DEC is multiplied by the duration (D) to reach canopy closure and stem diameter of 1.8 mm (15–18 days depending on the cultivar and treatments used in this experiment).

$$TEC = DEC \times D \quad (4)$$

The usage of CO_2 (B; kg CO_2 d^{-1}) can be described by Eq. (5; Ohyama and Kozai, 1998), where (P_n) is the CO_2 level per square meter of transplant growing area per hour (kg CO_2 m^{-2} h^{-1}), which was calculated based on the measured photosynthetic

TABLE 2 | Symbols, descriptions, values, and units used in the calculations.

Symbol	Description	Value	Unit
A	Total growing area	1	m^2
APC	Areal electric power consumption	41.2–82.3	W m^{-2}
B	Usage of CO_2 per day	0.020–0.057	kg CO_2 d^{-1}
CC	Cost of CO_2	0.58	\$ kg^{-1}
C_{in}	CO_2 concentration inside the chamber	0.0004–0.0016	mol mol^{-1}
C_{out}	CO_2 concentration outside the chamber	0.0004	mol mol^{-1}
D	Growing days per cycle	15–18	d
DEC	Daily electrical cost	0.07–0.13	\$ d^{-1} m^{-2}
DEN	Planting density	1000	plants m^{-2}
E	Air exchange rate	0.10	h^{-1}
E_r	Electricity rate (United States)	0.09	\$ kW h
K_m	Volume to mass conversion for CO_2 (22°C)	1.79	kg CO_2 m^{-3}
LPE	Lighting photon efficacy	3.0	μmol J^{-1}
MF	Maintenance factor	0.90	–
N	Number of lamps	1.3–2.7	lamps m^{-2}
P_n	Net photosynthetic rate per LAI	0.001–0.003	kg m^{-2} h^{-1}
P	Photoperiod	18	h
LAI	Leaf area index	1.9	m^2 m^{-2}
PPC	Per plant cost	0.0014–0.0026	\$
PPFD	Photosynthetic photon flux density	100–200	μmol m^{-2} s^{-1}
TCC	Total CO_2 cost per production cycle	0.21–0.50	\$ m^{-2}
TEC	Total electricity cost per production cycle	1.13–2.26	\$ m^{-2}
UF	Utilization factor	0.90	–
V	Volume of growing facility	1	m^3
WF	Wattage per fixture	30.5	W

rate for each treatment combination using the youngest fully expanded leaf. The single leaf photosynthesis measurements (μmol m^{-2} s^{-1}) were extrapolated to photosynthetic rate per meter square area using total leaf area per plant (19 cm^2), plant density of 1000 plants m^{-2}, photoperiod of 18 h, and the final LAI (Pn: 3.7–9.8 μmol m^{-2} s^{-1}; LAI: 1.9). The other components of the equation include the following: K_m is the conversion factor from volume to mass for CO_2 (1.79 kg CO_2 m^{-3}, at 22°C), E is the number of air exchanges per hour (0.1 h^{-1}) which is considered an upper level exchange rate for enclosed controlled environments (0.001–0.1 h^{-1}; Ohyama and Kozai, 1998), V is the volume of the growing area (1 m^3 for ease of calculation), C_{in} is the desired setpoint CO_2 concentration inside the facility, which varies between 400 and 1600 μmol mol^{-1} (0.0004–0.0016 mol mol^{-1}) depending on the treatment, and C_{out} is the CO_2 level outside the facility, which is typically near ambient levels (0.0004 mol mol^{-1}). Pp represents the photoperiod (18 h).

$$B = (A \times P_n + K_m \times E \times V\ (C_{in} - C_{out})) \times P_p \quad (5)$$

The total CO_2 cost (TCC; \$ m^{-2}) is expressed by Eq. (6). As described in the equation, B (kg CO_2 d^{-1}, affected by the CO_2 level, and PPFD) is multiplied by D (15–18 days depending on the treatments used in this experiment) and multiplied by the cost of CO_2 (CC, \$0.58 per kg, small volume price, Airgas, Radner, PA, United States).

$$TCC = B \times D \times CC \quad (6)$$

The total production cost per square meter (PPC; \$ m^{-2}) can then be described by Eq. (7), which involves the addition of TEC (\$ m^{-2}; 4) and TCC (\$ m^{-2}; 6):

$$PPC = TEC + TCC \quad (7)$$

RESULTS AND DISCUSSION

Plant Growth (Fresh and Dry Masses and Net Photosynthetic Rate)

For all light treatments, the fresh mass increased linearly with increases in the DLI for each level of CO_2 (**Figure 2A**). CO_2 enrichment to 1000 μmol mol^{-1} and 1600 μmol mol^{-1} resulted in the same rate of increase (slope) in the fresh mass as that obtained with increasing the DLI, and higher rates of increase in the fresh mass with increases in the DLI were observed under CO_2-enriched conditions to 1600 μmol mol^{-1} than at 400 μmol mol^{-1} (**Figure 2A**). In general, under all CO_2 treatments, the fresh mass increased by 16% with an increase in the DLI from 6.5 to 13.0 mol m^{-2} d^{-1}. On average, under all DLI treatments, the fresh mass increased by 20% after CO_2 enrichment to 1600 μmol mol^{-1} from 400 μmol mol^{-1}. The combination of increasing the DLI from 6.5 mol m^{-2} d^{-1} to 13.0 mol m^{-2} d^{-1} and CO_2 enrichment from 400 μmol mol^{-1} to 1600 μmol mol^{-1} increased the fresh mass by 36%.

Previous research studies on transplants have shown the impact of increasing the DLI on the fresh mass (Fan et al., 2013; Hernández and Kubota, 2014; Garcia and Lopez, 2020; Xu and Hernández, 2020). For example, Fan et al. (2013) showed a 27% increase in the fresh mass of tomato seedlings when the DLI was increased from 6.5 to 13.0 mol m^{-2} d^{-1} under LEDs (50B:50R, 12 h photoperiod) in a growth chamber. In a study of tomato, pepper, and cucumber transplants, Garcia and Lopez (2020) found fresh mass increases of 17, 33, and 18%, respectively, when the DLI was increased from 6.1 to 11.8 mol m^{-2} d^{-1} using supplemental high-pressure sodium (HPS) lighting in a greenhouse. In addition, Hernández and Kubota (2014) found a 28% increase in the fresh mass of cucumber seedlings when the DLI in a greenhouse was increased from 5.2 to 8.7 mol m^{-2} d^{-1} using supplemental LED lighting (0B:100R, 4B:96R, 16B:84R, and 18 h photoperiod).

The impacts of CO_2 enrichment on the fresh mass of tomato seedlings have not been reported. However, many studies have demonstrated that CO_2 enrichment increases the fresh fruit yield of tomato in a range of 19–124% when CO_2 is increased to a range of 700–1400 μmol mol^{-1} separately from that of supplemental lighting (Calvert and Slack, 1975; Nilsen et al., 1983; Reinert et al., 1997; Khan et al., 2013; Mamatha et al., 2014; Pan et al., 2019).

The dry mass increased linearly with increases in the DLI, and this finding was obtained with all light treatments (**Figure 2B**).

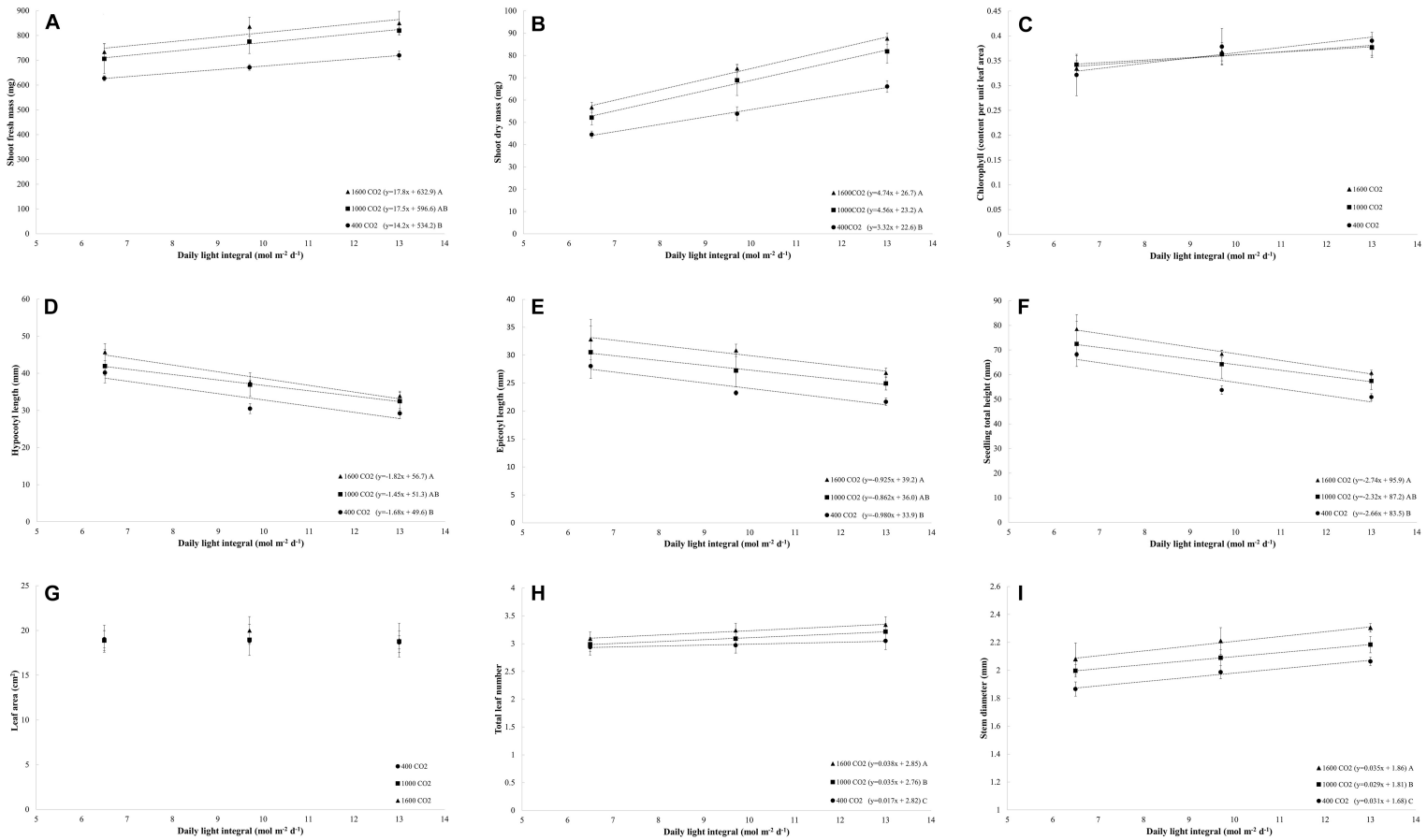

FIGURE 2 | (A–I) Effects of the daily light integrals (DLIs: 6.5, 9.7, and 13 mol m^{-2} d^{-1}) and CO_2 levels (400, 1000, and 1600 μmol mol^{-1}) on the morphology, physiology, and growth rate of four cultivars of tomato (average of all cultivars) at day 18. The dotted lines represent significant linear regressions, and the equations are shown in parentheses. Different letters represent significant differences of the slopes.

CO_2 enrichment to 1000 μmol mol^{-1} and 1600 μmol mol^{-1} resulted in the same rate of increase (slope) in the dry mass as that obtained with increases in the DLI, and both CO_2-enriched levels resulted in a higher rate of increase (slope) in the dry mass with increases in the DLI compared with that found with a CO_2 concentration of 400 μmol mol^{-1} (slope; **Figure 2B**). Under all CO_2 treatments, the dry mass increased by 53% when the DLI was increased from 6.5 to 13.0 mol m^{-2} d^{-1}, whereas under all DLI treatments, the dry mass increased by 33% in response to enrichment to 1000–1600 μmol mol^{-1} from 400 μmol mol^{-1}. The simultaneous increase in the DLI from 6.5 mol m^{-2} d^{-1} to 13.0 mol m^{-2} d^{-1} and CO_2 enrichment from 400 μmol mol^{-1} to 1600 μmol mol^{-1} increased the dry mass by 165%.

When comparing dry mass plant response to CO_2 enrichment (all light levels combined), the dry mass increased linearly with increases in the CO_2 level (y = 0.02x + 50.1; R^2 = 0.29; and p = 0.0008). However, when analyzing the responses by DLI (**Figure 3**), a trend is present that at higher DLI levels, the dry mass response to CO_2 is reaching a saturation point while at lower DLI the response is linear. Research studies have shown similar response (Bencze et al., 2011; Ting et al., 2017).

The comparison of dry mass response per cumulative photon flux (**Figure 4**) showed that plants under CO_2-enrichment (1000–1600 μmol mol^{-1}) conditions produce 0.25–0.26 grams of dry mass per mole of light (g mol^{-1}), whereas 0.18 g mol^{-1} is obtained under ambient CO_2 conditions, which indicates that CO_2 enrichment results in a 38–44% increase in light efficiency (g mol^{-1}).

Previous research on transplants have shown the impact of increasing the DLI on dry mass (Fierro et al., 1994; Pramuk and Runkle, 2005; Fan et al., 2013; Hernández and Kubota, 2014; Pan et al., 2019; Garcia and Lopez, 2020; Xu and Hernández, 2020). In tomato seedlings, Fan et al. (2013) found a dry mass increase of 51% when the DLI was increased from 6.5 to 13.0 mol m^{-2} d^{-1} under LEDs (50B:50R, 12 h photoperiod). In greenhouses, Hernández and Kubota (2014) found a 47% increase in the cucumber seedling dry mass when the DLI was increased from 5.2 to 8.7 mol m^{-2} d^{-1} under LEDs (0B:100R, 4B:96R, 16B:84R, and 18 h photoperiod). In addition, Garcia and Lopez (2020) found an increase in the dry masses of tomato, pepper, and cucumber transplants ranging from 107 to 183% when the DLI was increased from 6.1 to 11.8 mol m^{-2} d^{-1} using HPS lighting in a greenhouse.

Previous research on tomato has also shown the impact of CO_2 enrichment on the dry mass (Behboudian and Lai, 1994; Fierro et al., 1994; Li et al., 2007a; Wang et al., 2009; Pan et al., 2019). For example, studies have focused on the impact of increasing the CO_2 concentration from an ambient level to 700–800 μmol mol^{-1}, and this enrichment results in an increase in the dry mass of tomato plants of 27% when grown under florescent lamps (135 PPFD, 12 h photoperiod; Wang et al., 2009). A similar impact was shown under ambient greenhouse conditions by increasing the CO_2 concentration from an ambient level to 700–800 μmol mol^{-1} resulting in a 16–27% increase of dry mass (Behboudian and Lai, 1994; Pan et al., 2019).

The net photosynthetic rate increased linearly with increases in the PPFD, and this finding was obtained with all light treatments (p = 0.005; **Figure 5**). Similarly, the net photosynthetic rate also increased linearly with increases in the CO_2 level (y = 0.002x + 4.24; R^2 = 0.36; and p = 0.008; data not shown). Plants exposed to a CO_2 concentration of 1000 μmol mol^{-1} exhibited a higher rate of increase in their photosynthetic rate per increase (slope) in the PPFD than plants grown at 400 μmol mol^{-1} (**Figure 5**). In addition, CO_2 enrichment to 1600 μmol mol^{-1} was associated with a higher rate of increase in the photosynthetic rate per PPFD than those obtained with CO_2 levels of 400 and 1000 μmol mol^{-1} (**Figure 5**). In general, under all CO_2 treatments, the net photosynthesis increased by 66% with an increase in the PPFD from 100 to 200 μmol m^{-2} s^{-1}. On average, under all PPFD levels, the photosynthesis rate increased by 52% in response to CO_2 enrichment to 1600 μmol mol^{-1} from 400 μmol mol^{-1}. The combination of increasing the PPFD from 100 μmol m^{-2} s^{-1} to 200 μmol m^{-2} s^{-1} and CO_2 level from 400 μmol mol^{-1} to 1600 μmol mol^{-1} increased the net photosynthesis rate by 165%.

Previous studies with transplants have shown that increasing the PPFD and CO_2 concentration increases the photosynthetic rate (Fan et al., 2013; Hernández and Kubota, 2014; Lanoue et al., 2018; Pan et al., 2019). For example, tomato seedlings exhibit an increase in their photosynthetic rate of 90% when the PPFD is increased from 150 to 300 μmol m^{-2} s^{-1} (50B:50R, 12 h photoperiod; Fan et al., 2013). In greenhouse tomato transplant production, Pan et al. (2019) found a 21–39% increase in the photosynthetic rate with an increase in the PPFD of 200 μmol m^{-2} s^{-1} with HPS lighting. With cucumber transplants, a 20% increase in the photosynthetic rate was observed when the PPFD was increased by 54 μmol m^{-2} s^{-1} in a greenhouse with supplemental LEDs (0B:100R, 4B:96R, 16B:84R, and 18 h photoperiod; Hernández and Kubota, 2014). In response to CO_2 enrichment to 1000 μmol mol^{-1} from 400 μmol mol^{-1}, Lanoue et al. (2018) found a 52% increase in the photosynthetic rate of tomato seedlings. Similarly, Pan et al. (2019) showed that the photosynthetic rate of tomato seedlings increased by 9–27% with the enrichment of CO_2 to 800 μmol mol^{-1} from 400 μmol mol^{-1}.

In the present study, increasing the PPFD and CO_2 concentrations increased the net photosynthetic rate and consequently resulted in more growth (increases in fresh and dry mass). In general, the plant responses to increases in the PPFD follow a logarithmic curve: increases in photosynthesis are observed until a saturation point is reached (Lopez and Runkle, 2017; Eichhorn-Bilodeau et al., 2019), and after this light saturation point, photosynthesis no longer increases with increases in the PPFD due to limitations of the Calvin cycle (Lopez and Runkle, 2017), and more specifically the enzyme activity and concentration of Rubisco (Bjorkman, 1981; Sukenik et al., 1987; Rivkin, 1990; Orellana and Perry, 1992; Geider and McIntyre, 2002). At the seedling stage of tomato, the saturation point for PPFD has been reported to be approximately 1200 μmol m^2 s^{-1}; however, this saturation point is affected by other conditions, including the CO_2 level (Ting et al., 2017). In our

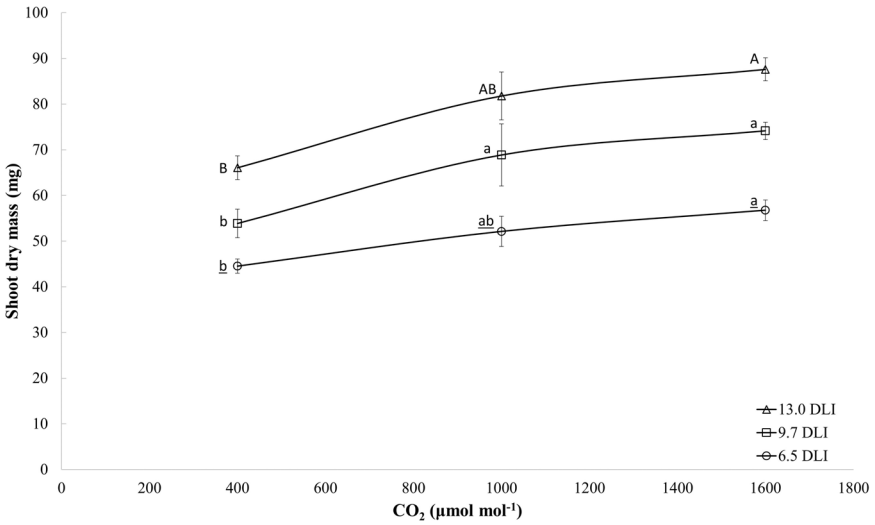

FIGURE 3 | Effects of the CO_2 enrichment treatments (400, 1000, 1600 μmol mol^{-1}) and light levels (DLIs: 6.5, 9.7, and 13 mol m^{-2} d^{-1}) on dry mass of four cultivars of tomato (average of all cultivars) at day 18. The letters represent significant differences within each light level.

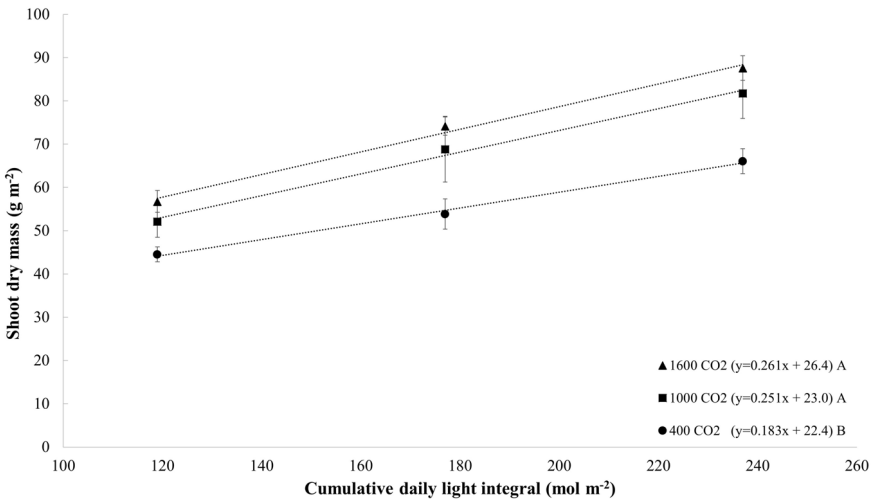

FIGURE 4 | Dry mass (g m^{-2}) of tomato (all cultivars) grown with different cumulative photon flux (119, 177, and 237 mol m^{-2}) and CO_2 levels (400, 1000, and 1600 μmol mol^{-1}). The dotted lines represent significant linear regressions, and the equations are shown in parentheses. Different letters indicate significant differences of the slopes.

study of tomato seedlings, the PPFD levels used (100–200 μmol m^{-2} s^{-1}) did not reach the light saturation point.

Similar to the PPFD, there is a saturation point regarding the benefits of CO_2 enrichment on the net photosynthetic rate. Studies have indicated that the CO_2 saturation point for tomato is approximately 1200–1500 μmol mol^{-1} at the late-seedling stage (Wang et al., 2013; Ting et al., 2017). For example, Ting et al. (2017) found that the maximum photosynthetic rate of tomato seedlings is 1500 μmol mol^{-1} with a PPFD of 600 μmol m^{-2} s^{-1}; however, under a PPFD of 900 μmol m^{-2} s^{-1}, a CO_2 level of 1200 μmol mol^{-1} reached the photosynthetic rate threshold. In the present study, the net photosynthetic rate was not saturated at a PPFD of 200 μmol m^{-2} s^{-1} and a CO_2 level of 1600 μmol mol^{-1}, which suggested that the light intensity and CO_2 concentration can be further increased to increase the photosynthetic rate. However, no additional increase in the dry mass was observed in the present study when the CO_2 level was enriched above 1000 μmol mol^{-1}. Since a similar leaf area was obtained with all light and CO_2 treatments (same canopy light capture), an increase in the dry mass was expected with the increase in the net photosynthetic rate at a CO_2 concentration of 1600 μmol mol^{-1}. Several studies have reported a greater increase in leaf photosynthetic rate and a lower increase in plant dry mass with CO_2 enrichment (Monje and Bugbee, 1998; Bunce and Sicher, 2003; Kirschbaum, 2011). A possible explanation is that the additional photoassimilates were partitioned to

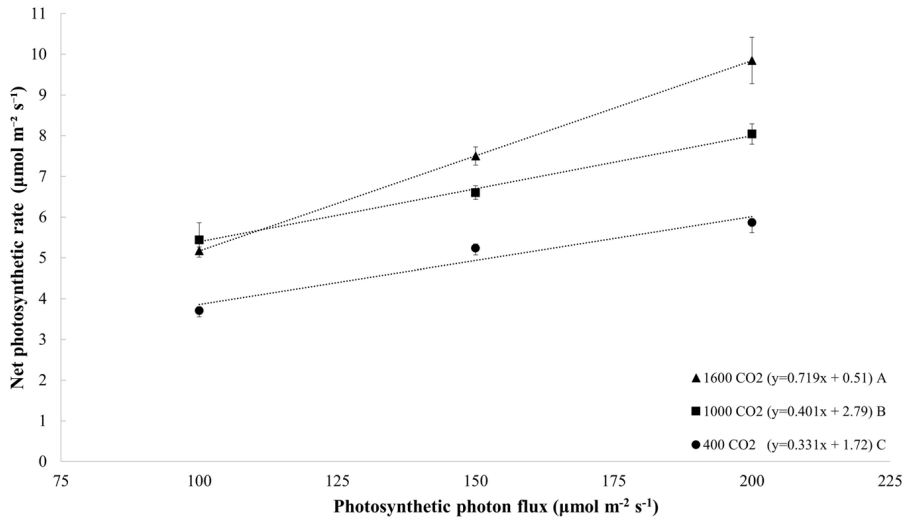

FIGURE 5 | Net photosynthetic rate (µmol m^{-2} s^{-1}) of tomato (all cultivars) at day 20 measured at different photosynthetic photon flux densities (100, 150, and 200 µmol m^{-2} s^{-1}); and CO_2 levels (400, 1000, and 1600 µmol mol^{-1}). The dotted lines represent significant linear fit and the equations are shown in parentheses. Different letters indicate significant differences in the slopes.

increase root growth or phytochemical biosynthesis, such as the biosynthesis of anthocyanin, and these effects were not quantified in the present study. Another possible explanation is that the increased amount of carbohydrates produced by higher photosynthetic rate could not be utilized by the plant (sink limitations) and are stored in the leaves as starch and sugars (Kirschbaum, 2011; Zheng et al., 2019).

Studies on seedlings have focused on the plant responses to either variations in the DLI or in the CO_2 concentration independently, and fewer studies have investigated the responses of plants to variations in both environmental factors (Desjardins et al., 1990; Fierro et al., 1994; Pan et al., 2019). In the present study, an increase in the CO_2 concentration to 1000–1600 µmol mol^{-1} from ambient conditions increased the light use efficiency (grams of dry mass per mole of light applied) by 38–44%; in addition, the comparison of the lowest light and CO_2 treatment with the highest light and CO_2 treatment showed an increase in the plant dry mass of 165% (**Figures 2B**, **4**). Therefore, CO_2 enrichment could be a strategy to increase the growth of young plants while reducing their energy consumption and production time (see section "Stem diameter and impact on production time"). Alternatively, CO_2 enrichment to 1000–1600 µmol mol^{-1} and under the standard DLI (13 mol m^{-2} d^{-1}) can also increase production efficiency by reducing production time and increase overall seedling growth in indoor growing systems.

The benefits of optimizing both the DLI and CO_2 concentration have been shown in previous research, in which the DLIs were usually higher than 13 mol m^{-2} d^{-1}. To our knowledge, the benefits of CO_2 enrichment (greater than 1000 µmol mol^{-1}) under lower DLIs (below 13 mol m^{-2} d^{-1}) have not been previously assessed. Our study highlights the benefits of CO_2 enrichment to high levels (1000–1600 µmol mol^{-1}) under relatively low DLIs ranging from 6.5 to 13.0 mol m^{-2} d^{-1}, and our findings highlight the potential of decreasing the light requirement of plants (25–50%) through CO_2 enrichment without affecting the quality of the transplants.

Chlorophyll Content

The chlorophyll content increased linearly with increases in the DLI, and this finding was obtained with all light treatments (**Figure 2C**). In general, the chlorophyll content per unit leaf area increased by 16% with an increase in the DLI from 6.5 to 13.0 mol m^{-2} d^{-1}. However, in this study, an increase in the CO_2 concentration did not affect the chlorophyll content per unit leaf area (Ct/leaf area; **Figure 2C**).

Research with transplants have shown that an increase in the DLI increases the chlorophyll concentration per leaf area (Hernández and Kubota, 2014; Pan et al., 2019). For example, in cucumber, Hernández and Kubota (2014) found a 27% increase in the chlorophyll concentration on a leaf area basis when the DLI was increased from 5.2 to 8.7 mol m^{-2} d^{-1}. In addition, in tomato transplants, Pan et al. (2019) found a 41% increase in the chlorophyll content with an increase in the DLI of 2.9 mol m^{-2} d^{-1}. This effect is generally attributed to an increase in the palisade rows found in thicker leaves with a lower specific leaf area as a result of a higher light intensity (Lichtenhaler et al., 1981), which allows for adaptation of the photosynthetic apparatus to capture more light when available (Boardman et al., 1975; Lichtenhaler et al., 1981).

Previous studies on CO_2 enrichment have also reported a decrease in the chlorophyll content per leaf area with an increase in the CO_2 concentration. For example, in tomato seedlings, CO_2 enrichment to 700 µmol mol^{-1} and 1000 µmol mol^{-1} decreased the total chlorophyll content (Mamatha et al., 2014; Lanoue et al., 2018), whereas in rice and wheat, no increase in the chlorophyll content was observed after CO_2 enrichment (Mulholland et al., 1997; Kim and You, 2010). In citrus, CO_2 enrichment also reduced the chlorophyll content per unit leaf

area by 5%, but this reduction under elevated CO_2 was overcome by an increase in the total leaf number (Idso et al., 1996). This decrease in the chlorophyll content as a result of CO_2 enrichment is generally explained by an increase in the starch content and the presence of enlarged starch granules in leaves, which is thought to decrease chloroplast structure and function and thus decrease chlorophyll production (Cave et al., 1981; Yelle et al., 1990).

Plant Morphology

Hypocotyl Length, Epicotyl Length, and Seedling Total Height

The hypocotyl, epicotyl, and total heights of the seedlings decreased linearly with increases in the DLI, and this finding was obtained with all light treatments (**Figures 2D–F**). In addition, the hypocotyl, epicotyl, and total heights increased linearly with increases in the CO_2 level (plant height: $y = 0.01x + 54.2$; $R^2 = 0.31$; and $p < 0.001$; data not shown). The plants grown under CO_2 concentrations of 1600 μmol mol^{-1} exhibited higher rates of increases (slope) in the hypocotyl, epicotyl, and total heights per increase in the DLI than those grown under a CO_2 concentration of 400 μmol mol^{-1} (**Figures 2D–F**). In general, under all CO_2 treatments, the hypocotyl, epicotyl, and total heights increased by 25–34% when the DLI increased from 6.5 to 13.0 mol m^{-2} d^{-1}. On average, the hypocotyl, epicotyl, and total heights increased by 24% in response to CO_2 enrichment to 1600 μmol mol^{-1} from 400 μmol mol^{-1}.

Numerous studies have shown that increasing the DLI decreases the plant height, including the hypocotyl, epicotyl, and total heights (Fan et al., 2013; Hernández and Kubota, 2014; Gómez and Mitchell, 2015; Garcia and Lopez, 2020). For example, Garcia and Lopez (2020) found that the hypocotyl height of tomato decreased by 10% when the DLI was increased from 6.1 to 11.8 mol m^2 d^{-1}. Fan et al. (2013) found a 47% decrease in the total height of tomato seedlings when the DLI was increased from 2.2 to 13.0 mol m^{-2} d^{-1}.

Previous studies have also shown that CO_2 enrichment increases the overall height of transplants (Li et al., 2007b; Khan et al., 2013; Mamatha et al., 2014). For example, Li et al. (2007b) found a 22% increase in the plant height of tomato seedlings in response to CO_2 enrichment to 700 μmol mol^{-1} from 360 μmol mol^{-1} CO_2 in indoor systems. Similarly, a 54% increase in the total height of tomato seedlings was found after CO_2 enrichment to 1000 μmol mol^{-1} from 400 μmol mol^{-1} (Lanoue et al., 2018). In greenhouse-grown tomato seedlings, Mamatha et al. (2014) found a 25% increase in the plant height after CO_2 enrichment to 700 μmol mol^{-1} from 400 μmol mol^{-1}. Similarly, Fan et al. (2013) found a 22% increase in the plant height in response to CO_2 enrichment to 1000 μmol mol^{-1} from 400 μmol mol^{-1}.

The decrease in plant height observed with increasing light intensity is an expected adaptive response of plants (Zhang et al., 2003). Low light intensities initiate shade-avoidance responses and increase stem extension to maximize light capture (Schmitt et al., 1999). Therefore, the increase in plant height triggered by increased light intensity in this study was expected. In addition, an increase in plant height with an increase in the CO_2 level has been reported in the literature (Downton et al., 1990; Pushnik et al., 1995; Slafer and Rawson, 1997), and this effect is normally attributed to the increase in the growth rate leading to an overall larger plant (taller with a higher dry mass; Pritchard et al., 1999). However, in the present study, CO_2 enrichment increased stem extension independently of the plant growth rate because the plant hypocotyl length and plant height were 26% higher at the same dry mass (**Table 3**). Therefore, the increase in the stem length obtained with CO_2 enrichment can also be attributed to an increase in cell expansion due to cell wall loosening and cell water/solute uptake (Cosgrove, 1993; Ferris and Taylor, 1994; Taylor et al., 1994; Ranasinghe and Taylor, 1996; Cosgrove, 1997).

The EOD-FR light used in this study increased hypocotyl, epicotyl, and total plant heights. Therefore, the plant heights obtained with all the treatments in this study would have been reduced if the EOD-FR treatment was not included. The application of EOD-FR has been shown to increase the hypocotyl length of tomato seedlings by 12–34% (Chia and Kubota, 2010) and is a strategy used to achieve a longer hypocotyl length to compensate for the excessive compactness caused by a high blue PF in the LED spectrum. However, based on the results of this study, high CO_2 levels could eliminate the need for applying EOD-FR treatment if the only goal is to manage hypocotyl extension.

Leaf Area and Leaf Number

The total leaf area per plant was not affected by increases in the DLI or CO_2 level (**Figure 2G**), and the leaf number marginally increased with increases in the DLI ($p = 0.002$; **Figure 2H**) and increased linearly with increases in the CO_2 level ($y = 0.0002x + 2.91$; $R^2 = 0.56$; and $p < 0.001$; data not shown). The plants grown under CO_2 concentrations of 1600 μmol mol^{-1} exhibited the higher rate of increase (slope) in the leaf number with increases in the DLI, and this rate of increase was higher than that observed in the plants grown under a CO_2 concentration of 1000 μmol mol^{-1} and 400 μmol mol^{-1} (**Figure 2H**). Similarly, plants in 1000 μmol mol^{-1} also showed a higher rate of increase (slope) then plants in 400 μmol mol^{-1} (**Figure 2H**). In general, under all CO_2 treatments, the leaf number increased by 7% with an increase in the DLI from 6.5 to 13 mol m^{-2} d^{-1}, and on average, under all DLI treatments, the leaf number increased by 8% in response to CO_2 enrichment to 1600 μmol mol^{-1} from 400 μmol mol^{-1}.

Although the leaf number was affected by CO_2 enrichment and the DLI, the leaf area was not affected in this experiment. It was expected that plants grown under a lower DLI would increase their leaf area as a response to capture more light. Although the leaf area obtained with the different treatments was comparable, the treatments with higher CO_2 and DLI resulted in a higher dry mass. Therefore, in this experiment, the increase in growth rate obtained with higher DLI and CO_2 can be mainly attributed to a higher photosynthetic rate and not to an increase in the leaf area for enhanced light capture [see section "Plant growth (fresh and dry masses and net photosynthetic rate)"].

Vegetable transplant research has shown similar results where increases in the DLI had no impact on the leaf area (Currey and Lopez, 2013; Garcia and Lopez, 2020). For example, cucumber seedlings grown in a greenhouse showed no increase in leaf area

TABLE 3 | Comparison of the plant physiological responses to different DLI and CO_2 treatments with those obtained with the control treatment (13.0DLI–400CO_2).

Physiological parameter	Control	6.5DLI 400CO_2	9.7DLI 400CO_2	6.5DLI 1000CO_2	9.7DLI 1000CO_2	13.0DLI 1000CO_2	6.5DLI 1600CO_2	9.7DLI 1600CO_2	13.0DLI 1600CO_2
Stem diameter (mm)	13.0DLI–400CO_2	−10%	=	=	=	+6%	=	+7%	+12%
Hypocotyl length (mm)	13.0DLI–400CO_2	+37%	=	+44%	+26%	=	+56%	+29%	=
Epicotyl length (mm)	13.0DLI–400CO_2	+29%	=	+41%	=	=	+52%	+43%	=
Total height (mm)	13.0DLI–400CO_2	+34%	=	+42%	+26%	=	+54%	+35	+19%
Leaf area (cm^2)	13.0DLI–400CO_2	=	=	=	=	=	=	=	=
Leaf number	13.0DLI–400CO_2	=	=	=	=	=	=	=	+9%
Fresh mass (mg)	13.0DLI–400CO_2	=	=	=	=	=	=	=	=
Dry mass (mg)	13.0DLI–400CO_2	-33%	−18%	−21%	=	+24%	=	=	+33%
Chlorophyll per leaf area (g m^{-2})	13.0DLI–400CO_2	-19%	=	−14%	=	=	−15%	=	=
Photosynthetic rate	13.0DLI–400CO_2	−37%	=	=	=	+37%	=	+28%	+68%

For the various treatments, the symbols "–" and "+" indicate whether the values obtained are lower or higher (and the corresponding percentages) than the value obtained with the 13.0DLI–400CO_2 treatment, and the symbol "=" indicates that no difference was found between the respective treatment and the 13.0DLI–400CO_2 treatment. The statistical analysis was based on comparison with the 13.0DLI–400CO_2 (control) treatment and was performed using Dunnett's method with $p \leq 0.05$.

when the DLI was increased from 6.1 to 11.8 mol m^{-2} d^{-1} using supplemental HPS lighting (Garcia and Lopez, 2020). Similarly, ornamental plugs in a greenhouse showed no increase in leaf area when the DLI was increased from 4.5 to 9.5 mol m^{-2} d^{-1} using supplemental LEDs (Currey and Lopez, 2013). However, there are conflictive results when comparing the response of leaf area specifically to CO_2 enrichment. For example, Pritchard et al. (1999) reviewed 63 studies and found that 57% of the studies reported an increase in the leaf area with increase in the CO_2 levels, whereas 10% of the studies showed a decrease in the leaf area, and the remaining 33% observed no effect.

Another possible explanation for the lack of differences in the leaf area between the treatments could be attributed to the EOD-FR treatment used in the present study. All the plants were exposed to a EOD-FR treatment based on the reported daily dosage (intensity × duration) required to maximize (90%) hypocotyl cell extension, which consequently will also increase leaf area (Chia and Kubota, 2010; Eguchi et al., 2016); therefore, it is plausible that leaf expansion was maximized by the EOD treatment in all DLI/CO_2 treatments.

Previous studies with vegetable transplants have also shown an increase in the leaf number with increases in the DLI and CO_2 level (Hernández and Kubota, 2014; Mamatha et al., 2014; Pan et al., 2019; Garcia and Lopez, 2020). For example, Hernández and Kubota (2014) showed an 11% increase in the leaf number of cucumber seedlings when the DLI was increased from 5.2–8.7 mol m^{-2} d^{-1}. In tomato seedlings, Pan et al. (2019) found an increase of 12% in the leaf number in response to an increase in the DLI by 2.9 mol m^{-2} d^{-1} in a greenhouse. Similarly, Garcia and Lopez (2020) found a 16% increase in the leaf number of tomato seedlings when the DLI was increased from 6.1 to 11.8 mol m^{-2} d^{-1}. In response to CO_2 enrichment from 380 to 700 μmol mol^{-1}, Mamatha et al. (2014) found a 24% increase in the leaf number of tomato plants. In addition, Pan et al. (2019) found an increase in the leaf number of 18% in a greenhouse in response to CO_2 enrichment (800 μmol mol^{-1}), but this increase was dependent on a sufficient DLI through supplemental lighting (>2.9 mol m^{-2} d^{-1}). These increases in the leaf number observed with increases in the DLI and CO_2 level can be explained by the increased growth rate.

Stem Diameter and Impact on Production Time

The stem diameter of tomato seedlings increased with increases in the DLI, and this effect was observed with all light treatments ($p < 0.001$; **Figure 2I**). Similarly, the stem diameter increased linearly with increases in the CO_2 concentration ($y = 0.0002x + 1.9$; $R^2 = 0.55$; and $p < 0.001$; data not shown). Plants grown under a CO_2 concentration of 1600 μmol mol^{-1} exhibited a higher rate of increase (slope) in the stem diameter per increase in the DLI than those grown under CO_2 concentrations of 400 and 1000 μmol mol^{-1}; similarly, the plants grown under a CO_2 concentration of 1000 μmol mol^{-1} exhibited higher rate of increase in the stem diameter as those grown with 400 μmol mol^{-1} CO_2 (**Figure 2I**). In general, under all CO_2 treatments, the stem diameter increased by 10% with an increase in the DLI from 6.5 to 13.0 mol m^{-2} d^{-1}, and on average, under all DLI treatments, the stem diameter increased by 11% in response to

CO_2 enrichment to 1600 μmol mol^{-1} from 400 μmol mol^{-1}. The combination of increasing the DLI from 6.5 mol m^{-2} d^{-1} to 13.0 mol m^{-2} d^{-1} and the CO_2 concentration from 400 to 1600 μmol mol^{-1} increased the stem diameter by 24%.

At the seedling density used in this study (1000 plants m^{-2}), the plants are grown until canopy closure and are then spaced to lower plant densities to prevent plant-to-plant competition and undesirable stretching. Several morphological factors serve as a threshold for reducing the plant density to prevent competition. For example, in tomato grafting, a stem diameter of 1.8 mm is often used as a threshold for both plant grafting and plant spacing. Therefore, the sooner the plant reaches this threshold, the shorter the production time. In the present study, the combination of different DLI and CO_2 treatments affected the production time (time to reach 1.8 mm) of tomato seedlings (**Figures 6**, **7**). The fastest growth rate was observed under the 13DLI–1600CO_2 treatment, and these plants reached the threshold in a 12% shorter time than the control plants (**Figure 6**). The plants subjected to the 9.7DLI–1600CO_2 and 13DLI–1000CO_2 treatments reached the threshold in a 6% shorter time than the control plants (**Figure 6**). Comparable growth rates to the control plants were observed under the 6.5DLI–1600CO_2 and 9.7DLI–1000CO_2 treatments, and all of these plants needed 17 days to reach the threshold (**Figure 6**). The plants exposed to the 6.5DLI–1000CO_2 and 9.7DLI–400CO_2 treatments needed a 6% longer duration than the control plants to reach the threshold (**Figure 6**). These treatments with slower growth rates (6.5DLI–1000CO_2, 9.7DLI–400CO_2, and 6.5DLI–400CO_2) also resulted in poor plant quality (lower shoot dry mass, smaller stem diameter, and lower chlorophyll content) and were deemed unsuitable growing conditions for transplants. The treatments that were superior or comparable to the control (13DLI–1600CO_2, 9.7DLI–1600CO_2, 13DLI–1000CO_2, 6.5DLI–1600CO_2, and 9.7DLI–1000CO_2) provided suitable growing conditions for the production of high-quality tomato transplants. Based on our results, the tomato seedlings exposed to CO_2-enriched concentrations of 1000 and 1600 μmol mol^{-1} reached the targeted stem diameter at the same time as the control plants (13 mol m^{-2} d^{-1}, 400 μmol mol^{-1}) despite 25–50% less light (6.5 to 9.7 mol m^{-2} d^{-1} DLI). Furthermore, using conditions consisting of CO_2 enrichment to 1000–1600 μmol mol^{-1} and a DLI of 13 mol m^{-2} d^{-1}, tomato seedlings can be produced at 6–12% faster rate than under the control conditions (**Figure 6**).

Studies have shown that increasing the DLI increases the stem diameter of transplants (Fan et al., 2013; Hernández and Kubota, 2014; Pan et al., 2019; Garcia and Lopez, 2020). For example, in indoor CEs, Fan et al. (2013) found a 16% increase in the stem diameter of tomato transplants when the DLI was increased from 2.2 to 13.0 mol m^{-2} d^{-1}. Similarly, in cucumber transplants, Hernández and Kubota (2014) found a 20% increase in the stem diameter when the DLI was increased from 5.2 to 8.7 mol m^{-2} d^{-1}, and in pepper transplants, Garcia and Lopez (2020) found a 20% increase in the stem diameter when the DLI was increased from 6.1 to 11.8 mol m^{-2} d^{-1}.

CO_2 enrichment studies have also shown an increase in the stem diameter of transplants (Egli et al., 1997; Li et al., 2007b; Khan et al., 2013). For example, in tomato transplants, Li et al. (2007b) found a 16% increase in the stem diameter in response to CO_2 enrichment from 360 to 720 μmol mol^{-1}. Similarly, in tomato, a 24% increase in the stem diameter was found after increasing the CO_2 level from 400 to 1000 μmol mol^{-1} (Khan et al., 2013). Increases in the stem diameter have also shown benefits post-transplant. For example, an increased stem diameter of tomato transplants results in earlier yields (Liptay et al., 1981). Specifically, Liptay et al. (1981) found that transplants with stem diameters of 4.0–4.8 mm produced 32% more fruit at early harvest and thus exhibited a higher early yield than those with stem diameters of 3.2–4.0 mm. The observed increase in the stem diameter is expected and is explained by an overall increase in the plant biomass obtained under higher light (Grimstad, 1987; Dorais et al., 1991; McCall, 1992) and CO_2 conditions (Bencze et al., 2011; Wang et al., 2013; Ting et al., 2017).

Effect of Treatment Combinations on Plant Growth, Morphology and Sustainability

Table 3 presents the effects of the interaction of the DLI and CO_2 level on plant growth and morphology. The combination treatments and their impact on plant growth and morphology were compared with standard growing conditions (13DLI–400CO_2). Compared with the control (13DLI–400CO_2) treatment, the 6.5DLI–400CO_2 treatment, which involves 50% less light and the same CO_2 level, produced a stretched plant (hypocotyl, epicotyl, and plant height) with a 33% lower dry mass and reduced values for the stem diameter, chlorophyll content, and photosynthetic rate (**Table 3** and **Figure 7**). Decreasing the DLI from 13.0 to 9.7 mol m^{-2} d^{-1} while maintaining the same CO_2 concentration (9.7DLI–400CO_2) produced a plant with similar morphological characteristics (stem diameter, stem extension, and chlorophyll content) to the control plants with 25% less light but with a lower dry mass (18%), which was expected due to the reduction in the DLI (**Table 3** and **Figure 7**).

Plants exposed to the 6.5DLI–1000CO_2 treatment, which involves a 50% lower DLI and 150% higher CO_2 level than the control treatment, produced stretched plants, and the total plant height was even greater than that of the plants under the 6.5DLI–400CO_2 treatment, which highlights the contribution of CO_2 enrichment on stem extension (**Table 3** and **Figure 7**). The plants subjected to this treatment still showed a growth rate penalty (−21%) compared with the control plants, which was also attributed to the lower DLI.

The 9.7DLI–1000CO_2 treatment, which involves a 25% lower DLI and 150% greater CO_2 level than the control treatment, produced taller plants with no penalty in the growth rate (**Table 3** and **Figure 7**). Even though the plants subjected to this treatment exhibited a higher plant height, this effect was solely due to a longer hypocotyl, which is likely affected by the EOD-FR treatment used in the experiment. The benefit of CO_2 enrichment mitigated the impact of the reduced DLI, resulting in a similar growth rate. Therefore, this DLI and CO_2 combination is suitable

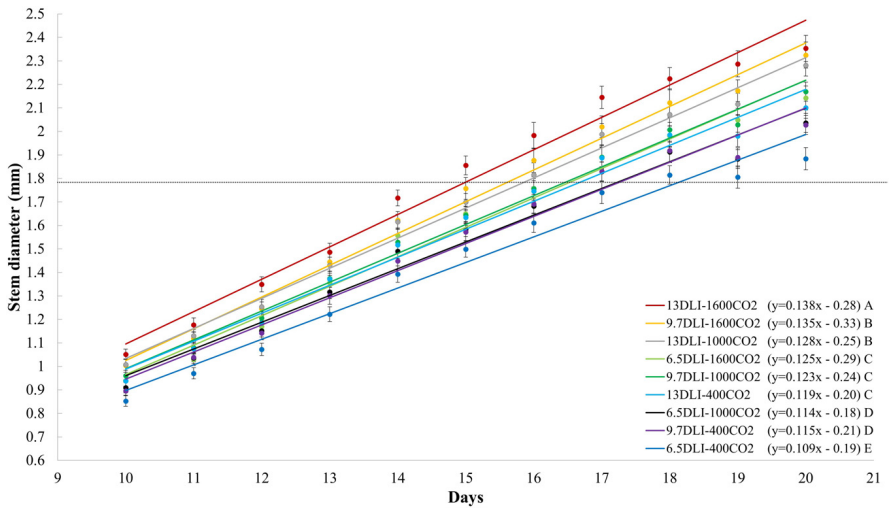

FIGURE 6 | Daily stem diameter (mm) of tomato seedlings (all cultivars) subjected to treatments with daily light integrals (DLIs: 6.5, 9.7, and 13.0 mol m^{-2} d^{-1}) and CO_2 levels (400, 1000, and 1600 μmol mol^{-1}). Lines represent significant linear fit. The regression equation for each treatment is shown in parentheses. Different letters indicate significant differences in slope (rate of stem diameter increase).

for reducing light requirements while maintaining plant quality to meet commercial standards.

The 13DLI–1000CO_2 treatment, which involves the same DLI and a 150% greater CO_2 level compared with the control treatment, resulted in plants with similar morphological characteristics as the control plants but an increased growth rate (24%), highlighting the benefits of CO_2 enrichment on growth (**Table 3** and **Figure 7**). Therefore, this DLI and CO_2 combination is suitable for reducing the production time while maintaining plant quality to meet commercial standards.

The 6.5DLI–1600CO_2 treatment, which consisted of a 50% lower DLI and a 300% greater CO_2 level, produced taller plants with no penalty in the growth rate compared with the control treatment (**Table 3** and **Figure 7**). The total plant height obtained with the 6.5DLI–1600CO_2 treatment was greater than that obtained with the 6.5DLI–400CO_2 and 6.5DLI–1000CO_2 treatments, highlighting the contribution of CO_2 enrichment to stem extension. Similar to the results obtained with the 9.7DLI–1000CO_2 treatment, the benefit of CO_2 enrichment mitigated the impact of the reduced DLI in the 6.5DLI–1600CO_2 treatment, which resulted in a similar growth rate with half of the light. Even though the plants subjected to this treatment exhibited a higher plant height, the increased hypocotyl length is beneficial in the production of grafted plants. Therefore, this DLI and CO_2 combination is suitable for reducing light requirements and maintaining plant quality to meet commercial standards.

The 9.7DLI–1600CO_2 treatment, which involved a 25% lower DLI and a 300% greater CO_2 level than the control treatment, produced taller plants with no penalty in the growth rate (**Table 3** and **Figure 7**). The plants presented an increased plant height compared with the control plants, highlighting the contribution of CO_2 enrichment to stem extension (**Table 3** and **Figure 7**). Although the plants exposed to this treatment showed no penalty in the growth rate, an increase in the stem diameter was observed. Therefore, this DLI and CO_2 combination is suitable for reducing both the light requirements and production time while maintaining plant quality to meet commercial standards. Moreover, the 13DLI–1600CO_2 treatment, which consists of the same DLI and a 300% greater CO_2 level than the control treatment, resulted in an increased total height with an increased growth rate (33%), highlighting the benefits of CO_2 enrichment on growth (**Table 3** and **Figure 7**). This increase in the total height is likely due to the increased growth rate and was not specific to the hypocotyl or epicotyl. Therefore, this DLI and CO_2 combination is suitable for reducing the production time and increasing plant quality above commercial standards.

The reported impacts of CO_2 enrichment on plant growth and morphology in this study utilize a spectrum (1B:1R) recommended for tomato transplant production based on previous research (Liu et al., 2011; Hernández et al., 2016) which optimizes photosynthetic rate (Kim et al., 2004; Li et al., 2007b; Liu et al., 2011), fresh and dry masses (Hernández et al., 2016), and produces a compact plant. Therefore, CO_2 enrichment using other light spectrums during the photoperiod would be expected to impact the results due to altered growth rates, morphology, and photosynthetic rates. Furthermore, the use of EOD-FR also impacted this response. For example, the use of EOD-FR in our study contributed to 63% longer hypocotyl length (reduced excessive compactness) and reduced intumescence (preliminary study) making them commercially acceptable. Without the use of EOD-FR; however, plants for grafting would be commercially unacceptable due to compact internodes using the current spectrum.

Though the four cultivars used in this study showed no interaction of growth or plant morphology, growth rate differences were observed for cultivar independently of those from light and CO_2 as shown with tomato seedlings (Hu et al.,

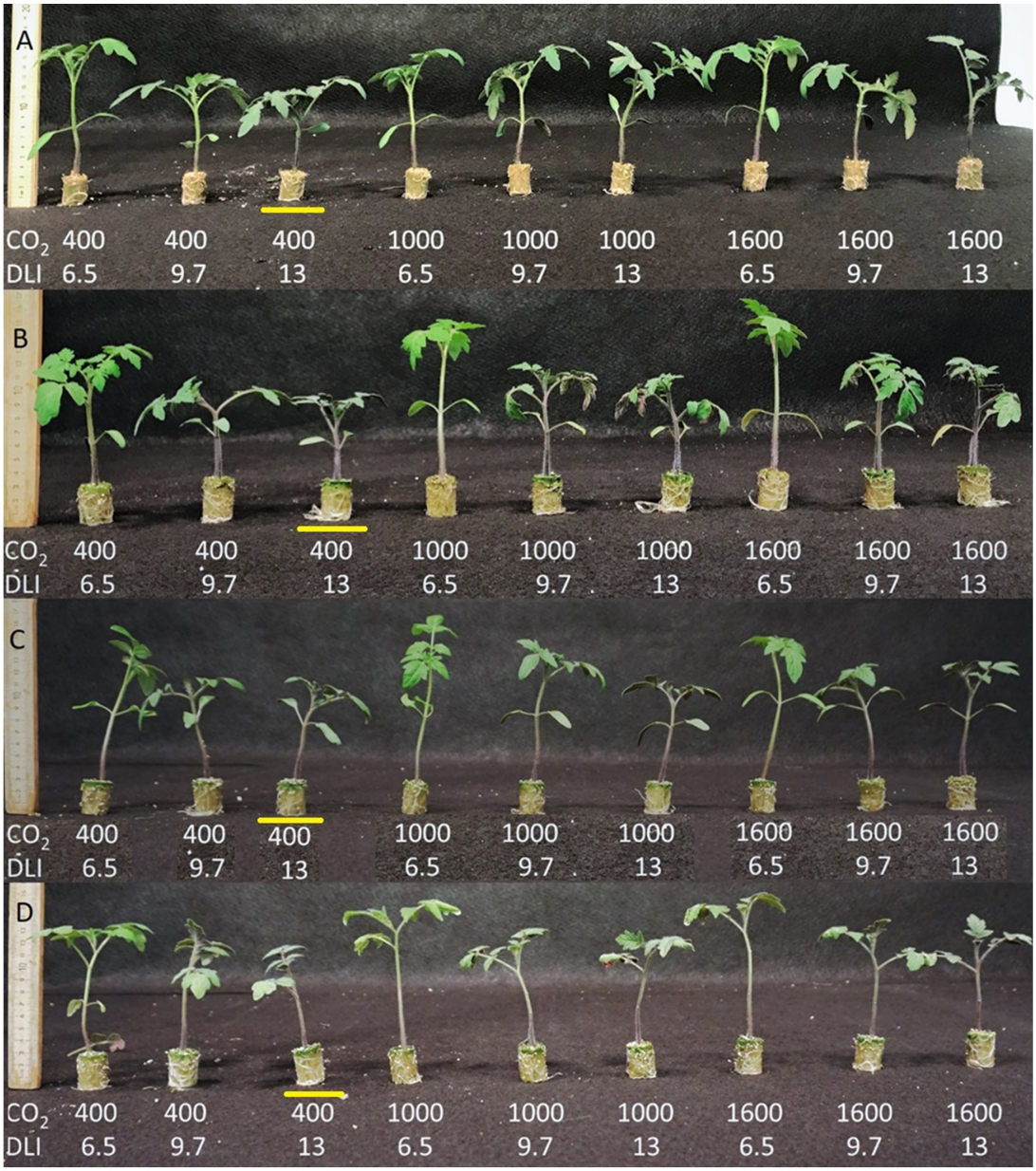

FIGURE 7 | Seedlings of the tomato cultivars Florida 47 **(A)**, Shin Cheong Gang **(B)**, Rebelski **(C)**, and Maxifort **(D)** grown under various DLI and CO_2 conditions. All the plants were harvested when the last DLI/CO_2 treatment reached 1.8 mm (18–20 days). Commercial expected plant morphologies are shown in the control treatment 13DLI/400CO_2 which are highlighted in the image for each cultivar.

2015). For example, in our study "Shin Cheong Gang" reached a 1.8 mm stem diameter (grafting threshold) at day 16, whereas "Florida-47 R" required 18 days when grown under 13DLI–400CO_2. In addition, at day 18 "Shin Cheong Gang" shoot dry mass was 52 mg, whereas "Florida-47 R" was 77 mg under the same environmental conditions highlighting the difference in biomass accumulation between cultivars. Therefore, growth rate and other plant morphological differences may be observed when different cultivars are used. In addition, the physiological disorder intumescence was cultivar specific in our study affecting only "Maxifort" with 39% symptomatic foliage, whereas "Florida-47 R," "Rebelski," and "Shin Cheong Gang" showed no symptoms. The susceptibility of interspecific tomato rootstocks such as "Maxifort" to intumescence was previously reported (Eguchi et al., 2016). Without the use of EOD-FR, intumescence severity may further impact plant growth and decrease plant quality of susceptible cultivars.

In addition to the impacts on plant growth and morphology, varying the light and CO_2 levels also offers an opportunity to optimize sustainability. According to the United States

TABLE 4 | Growing time (15–18 days), calculated energy usage of light-emitting diodes (LEDs; efficacy of LEDs used for the calculation is 3.0 μmol J^{-1}; kWh per growing cycle), estimated operational cost of energy required to power LEDs ($ m^{-2} per cycle), estimated total CO_2 consumption (kg CO_2 per cycle), estimated operational cost of CO_2 consumption ($ m^{-2} per cycle), and total operational cost for light and CO_2 per cycle per square meter of growing area.

Treatment	Days to 1.8 mm	Total energy for lighting kWh	Lighting cost $ m^{-2}	Total CO_2 kg CO_2	CO_2 cost $ m^{-2}	Total cost $ m^{-2}
6.5DLI–400CO_2	18	13.33	$1.20	0.36	$0.21	$1.41
9.7DLI–400CO_2	17	18.89	$1.70	0.48	$0.28	$1.98
13.0DLI–400CO_2	17	25.19	$2.26	0.54	$0.31	$2.57
6.5DLI–1000CO_2	17	12.59	$1.13	0.53	$0.31	$1.44
9.7DLI–1000CO_2	17	18.89	$1.70	0.64	$0.37	$2.07
13.0DLI–1000CO_2	16	23.70	$2.13	0.73	$0.42	$2.55
6.5DLI–1600CO_2	17	12.59	$1.13	0.54	$0.32	$1.45
9.7DLI–1600CO_2	16	17.78	$1.60	0.71	$0.41	$2.01
13.0DLI–1600CO_2	15	22.22	$2.00	0.86	$0.50	$2.50

Department of Agriculture, sustainability involves five different components: (1) efficient use of nonrenewable resources, (2) enhanced environmental quality, (3) sustained economic viability, (4) satisfactory human food and fiber needs, and (5) enhanced quality of life of producers. A comprehensive evaluation of the components was not performed in this study, but the results regarding the usage of energy and CO_2 (sustainability components 1 and 2) and the overall cost of light and CO_2 (sustainability component 3) are presented in **Table 4**. The calculation of CO_2 usage utilized a room air exchange rate of 0.1 h^{-1}, which is still a very low ventilation rate. Therefore, most of the CO_2 provided is used for plant growth and is not released outside the growing environment.

The total energy and the total CO_2 consumed to meet the different DLI and CO_2 conditions are provided per square meter and growing cycle for every treatment combination (**Table 4**). When considering energy usage, production cost, and plant quality (growth and morphology) combined, the 9.7DLI–1000CO_2, 13DLI–1000CO_2, 6.5DLI–1600CO_2, 9.7DLI–1600CO_2, and 13DLI–1600CO_2 treatment combinations are suitable for improving the sustainability of the current production practices (13DLI–400CO_2). For example, the 9.7DLI–1000CO_2, 6.5DLI–1600CO_2, and 9.7DLI–1600CO_2 treatments resulted in reductions in the energy usage of 19, 44, and 22%, respectively, which led to reductions in the production cost of 19, 44, and 22%, respectively, compared with the control treatment. The treatments with the same DLI as the control but a higher level of CO_2 (13DLI–1000CO_2 and 13DLI–1600CO_2) also resulted in a small reduction in the production cost (1–3%) while reducing production time (6–12%) and increasing plant growth (24–33%). The cost of CO_2 enrichment to 1600 μmol mol^{-1} is minimal in contained systems (0.1 h^{-1}). Although the most economical treatment per cycle might be desirable, growers may benefit in producing more cycles per year based on the 13DLI–1600CO_2 treatment.

CONCLUSION

Despite the use of DLIs below the commercial standards (13.0 mol m^{-2} d^{-1}), CO_2 enrichment showed benefits on the growth and morphology of tomato transplants and maintained plant quality. Due to CO_2 enrichment, the DLI requirements for producing tomato transplants can be reduced by 25–50% without affecting plant quality, which would reduce the production costs by up to 44%. Although hypocotyl elongation was observed with the treatments consisted of a lower DLI, this morphological characteristic can be controlled by the light spectrum. Alternatively, if a bigger plant with lower production time is desired, then maintaining a DLI of 13.0 mol m^{-2} d^{-1}, CO_2 enrichment at 1600 μmol mol^{-1} can reduce the production time by 12% and produce plants with a similar morphology and reduce costs by 3%.

With the increase in the light efficacy of LED lights, it is now possible to increase the production efficacy and sustainability of indoor systems by environmental optimization. The present study details the responses of tomato plants to two environmental components (light and CO_2) and highlights an opportunity to optimize production based on selected goals. For example, large-scale tomato production can be optimized based on one or several of the following priorities: increase plant growth, reduce the production time, obtain a desired plant architecture, reduce energy usage, and/or increase affordability.

Future studies should investigate the post-transplant acclimation of these plants to field conditions and should focus on optimizing other environmental conditions to further optimize controlled environment systems.

DATA AVAILABILITY STATEMENT

The raw data supporting the conclusions of this article will be made available by the authors, without undue reservation.

AUTHOR CONTRIBUTIONS

BH: study conception and design, acquisition of data, analysis and interpretation of data, and drafting of manuscript. FL: analysis and interpretation of data, drafting of manuscript, critical revision, and funding acquisition. RH: study conception and design, analysis and interpretation of data, drafting of

manuscript, critical revision, and funding acquisition. All authors contributed to the article and approved the submitted version.

FUNDING

Funding for this research was provided by a USDA-NIFA specialty crop research initiative, growing new roots: Grafting to enhance resiliency in U.S. vegetable industries under award number 2016-51181-25404.

ACKNOWLEDGMENTS

The authors would like to express gratitude to Cristian Collado, Hans Spalholz, Xiangnan Xu, and the NCSU Phytotron staff for their assistance with this research.

REFERENCES

Aldrich, R. A., and Bartock, J. W. (1994). *Greenhouse Engineering; NRAES-Natural Resources, Agriculture, and Engineering Service*, Vol. 33. Ithaca, NY: Northeast Regional Agricultural Engineering Service.

Bauerle, W. L. (1984). Bag culture production of greenhouse tomatoes. *Ohio State Univ. Spec. Circ.* 108:7.

Behboudian, M. H., and Lai, R. (1994). Carbon dioxide enrichment in 'Virosa' tomato plant: responses to enrichment duration and to temperature. *HortScience* 29, 1456–1459. doi: 10.21273/hortsci.29.12.1456

Bencze, S., Keresztenyi, I., Varga, B., Koszegi, B., Balla, K., Gemesne-Juhasz, A., et al. (2011). Effect of CO_2 enrichment on canopy photosynthesis, water use efficiency and early development of tomato and pepper hybrids. *Acta Agronom. Hungar.* 59, 275–284. doi: 10.1556/aagr.59.2011.3.12

Bjorkman, O. (1981). "Responses to different quantum flux densities," in *Physiological Plant Ecology 1. Responses to the Physical Environment*, eds O. L. Lange, P. S. Nobel, C. B. Osmond, and H. Ziegler (Berlin: Springer-Verlag), 57–107. doi: 10.1007/978-3-642-68090-8_4

Boardman, N. K., Björkman, O., Anderson, J. M., Goodchild, D. J., and Thorne, S. W. (1975). Photosynthetic adaptation of higher plants to light intensity: relationship between chloroplast structure, composition of the photosystems and photosynthetic rates. *Photosynth. Res.* 3, 1809–1827.

Both, A. J., Frantz, J. M., and Bugbee, B. (2017). "Carbon dioxide enrichment in controlled environments," in *Light Management in Controlled Environments*, eds R. Lopez and E. Runkle (Willoughby, OH: Meister Media), 82–90.

Bunce, J. A., and Sicher, R. C. (2003). Daily irradiance and feedback inhibition of photosynthesis at elevated carbon dioxide concentration in brassica oleracea. *Photosynthetica* 41, 481–488. doi: 10.1023/b:phot.0000027511.44995.66

Calvert, A., and Slack, G. (1975). Effects of carbon dioxide enrichment on growth, development and yield of glasshouse tomatoes. I. Responses to controlled concentrations. *HortScience* 50, 61–71. doi: 10.1080/00221589.1975.11514604

Cave, G., Tolley, L. C., and Strain, B. R. (1981). Effect of carbon dioxide enrichment on chlorophyll content, starch content and starch grain structure in *Trifolium subterraneum* leaves. *Physiol. Plant.* 51, 171–174. doi: 10.1111/j.1399-3054.1981.tb02694.x

Chia, P. L., and Kubota, C. (2010). End-of-day far-red light quality and dose requirements for tomato rootstock hypocotyl elongation. *HortScience* 45, 1501–1506. doi: 10.21273/hortsci.45.10.1501

Cosgrove, D. J. (1993). Wall extensibility: its nature, measurement, and relationship to plant cell growth. *New Phytol.* 124, 1–23. doi: 10.1111/j.1469-8137.1993.tb03795.x

Cosgrove, D. J. (1997). Relaxation in a high-stress environment: the molecular bases of extensible cell walls and cell enlargement. *Plant Cell* 9, 1031–1041. doi: 10.1105/tpc.9.7.1031

Craver, J. K. (2014). *The Effects of UVB Radiation on Intumescence Development and the Characterization of Lesions from Physiological Disorders on Ornamental Sweet Potato (Ipomoea batatas) Tomato (Solanum lycopersicum) and Interspecific Geranium (Pelargonium spp.)*. MS thesis, Kansas State University, Manhattan, KS.

Currey, C. J., and Lopez, R. (2013). Cuttings of impatiens, pelargonium, and petunia propagated under light-emitting diodes and high-pressure sodium lamps have comparable growth, morphology, gas exchange, and posttransplant performance. *HortScience* 48, 428–434. doi: 10.21273/HORTSCI.48.4.428

Desjardins, Y., Gosselin, A., and Lamarre, M. (1990). Growth of transplants and in vitro-cultured clones of asparagus in response to CO_2 enrichment and supplemental lighting. *HortScience* 115, 364–368. doi: 10.21273/jashs.115.3.364

Dorais, M. (2003). "The use of supplemental lighting for vegetable crop production: light intensity, crop response, nutrition, crop management, cultural practices," in *Proceedingsof the Canadian Greenhouse Conference Toronto, Ontario. 23 May 2013*. Available online at: http://www.agrireseau.qc.ca/legumesdeserre/Documents/CGC-Dorais2003fin2.PDF (accessed October 9, 2003).

Dorais, M., Gosselin, A., and Trudel, M. J. (1991). Annual greenhouse tomato production under a sequential intercropping system using supplemental light. *Sci. Horticult.*45, 225–234. doi: 10.1016/0304-4238(91)90067-9

Downton, W. J. S., Grant, W. J. R., and Chako, E. K. (1990). Effect of elevated carbon dioxide on the photosynthesis and early growth of mangosteen (*Garcinia mangostana* L.). *Sci. Horticult.* 44, 215–225. doi: 10.1016/0304-4238(90)90121-T

Egli, P., Maurer, S., Gunthardt-Goerg, M. S., and Korner, C. (1997). Effects of elevated CO_2 and soil quality on leaf gas exhange and above-ground growth in beech-spruce model ecosystems. *New Phytol.* 140, 185–196. doi: 10.1046/j.1469-8137.1998.00276.x

Eguchi, T., Hernández, R., and Kubota, C. (2016). Far-red and blue light synergistically mitigate intumescence injury of tomato plants grown under ultraviolet-deficit light environment. *HortScience* 51, 712–719. doi: 10.21273/hortsci.51.6.712

Eichhorn-Bilodeau, B. S., Wu, B. S., Rufyikiri, A. S., MacPherson, S., and Lefsrud, M. (2019). An update on plant photobiology and implications for cannabis production. *Front. Plant Sci.* 10:296. doi: 10.3389/fpls.2019.00296

Enoch, H. Z., Rylski, I., and Spigelman, M. (1976). CO_2 enrichment of strawberry and cucumber plants growing in unheated greenhouses in Israel. *Sci. Horticult.* 5, 33–41. doi: 10.1016/0304-4238(76)90020-0

Fan, X., Xu, Z., Liu, X., Tang, C., Wang, L., and Han, X. (2013). Effects of light intensity on the growth and leaf development of young tomato plants grown under a combination of red and blue light. *Sci. Horticult.* 153, 50–55. doi: 10.1016/j.scienta.2013.01.017

Ferris, R., and Taylor, G. (1994). Elevated CO_2, water relations and biophysics of leaf extension in four chalk grassland herbs. *New Phytol.* 127, 297–307. doi: 10.1111/j.1469-8137.1994.tb04280.x

Fierro, A., Gosselin, A., and Tremblay, N. (1994). Supplemental carbon dioxide and light improved tomato and pepper seedling growth and yield. *HortScience* 29, 152–154. doi: 10.21273/HORTSCI.29.3.152

Garcia, C., and Lopez, R. G. (2020). Supplemental radiation quality influences cucumber, tomato, and pepper transplant growth and development. *HortScience* 55, 804–811. doi: 10.21273/hortsci14820-20

Geider, R. J., and McIntyre, H. L. (2002). "Physiology and biochemistry of photosynthesis and algal carbon acquisition," in *Phytoplankton Productivity: Carbon, Assimilation in Marine and Freshwater Ecosystems*, eds P. J. Williams, D. N. Thomas, and C. S. Reynolds (Oxford: Blackwell), 44–77. doi: 10.1063/1.39754

Gómez, C., and Mitchell, C. A. (2015). Growth responses of tomato seedlings to different spectra of supplemental lighting. *HortScience* 50, 112–118. doi: 10.21273/hortsci.50.1.112

Grimstad, S. O. (1987). Supplementary lighting of early tomatoes after planting out in glass and acrylic greenhouses. *Sci. Horticult.*33, 189–196. doi: 10.1016/0304-4238(87)90066-5

Hao, X. Y., Li, P., Li, H. Y., Zong, Y. Z., Zhang, B., Zhao, J. Z., et al. (2017). Elevated CO_2 increased photosynthesis and yield without decreasing stomatal

conductance in broomcorn millet. *Photosynthetica* 55, 176–183. doi: 10.1007/s11099-016-0226-6

Hernández, R., Eguchi, T., Deveci, M., and Kubota, C. (2016). Tomato seedling physiological responses under different percentages of blue and red photon flux ratios using LEDs and cool white fluorescent lamps. *Sci. Horticult.* 213, 270–280. doi: 10.1016/j.scienta.2016.11.005

Hernández, R., and Kubota, C. (2014). Growth and morphological response of cucumber seedlings to supplemental red and blue photon flux ratios under varied solar daily light integrals. *Sci. Horticult.* 173, 92–99. doi: 10.1016/j.scienta.2014.04.035

Hernández, R., and Kubota, C. (2015). Physiological responses of cucumber seedlings under different blue and red photon flux ratios using LEDs. *Environ. Exp. Bot.* 121, 66–74. doi: 10.1016/j.envexpbot.2015.04.001

Hu, B., Bennett, M. A., and Kleinhenz, M. D. (2016). A new method to estimate vegetable seedling vigor, piloted with tomato, for use in grafting and other contexts. *HortTechnology* 26, 767–775. doi: 10.21273/horttech03485-16

Hu, B., Moyseenko, J., Short, S., Walker, S., and Kleinhenz, M. D. (2015). *Eighteen Rootstock and Five Scion Tomato Varieties: Seedling Growth Rates Before Grafting and Success in Grafting the Ninety Variety Combinations. Purdue Fruit and Vegetable Research Reports. Paper 95*. Available online at: https://docs.lib.purdue.edu/fvtrials/95 (accessed September 12, 2020).

Idso, S. B., Kimball, B. A., and Hendrix, D. L. (1996). Effects of atmospheric CO_2 enrichment on chlorophyll and nitrogen concentrations of sour orange tree leaves. *Environ. Exp. Bot.* 36, 323–331. doi: 10.1016/0098-8472(96)01018-0

Jensen, M. H., and Malter, A. J. (1995). *Protected Agriculture: A Global Review*. Washington, DC: World Bank Technical Paper No. 253. 157.

Kaskavalci, G., Tuzel, Y., Dura, O., and Oztekin, G. B. (2009). Effects of alternative control methods against *Meloidogyne incognita* in organic tomato production. *Ekoloji* 18, 23–31. doi: 10.5053/ekoloji.2009.724

Khah, E. M., Kakava, E., Mavromatis, A., Chachalis, D., and Goulas, G. (2006). Effect of grafting on growth and yield of tomato (*Lycopersicon esculentum* Mill.) in greenhouse and open field. *J. Appl. Horticult.* 8, 3–7. doi: 10.37855/jah.2006.v08i01.01

Khan, I., Azam, A., and Mahmood, A. (2013). The impact of enhanced atmospheric carbon dioxide on yield, proximate composition, elemental concentration, fatty acid and vitamin C contents of tomato (*Lycopersicon esculentum*). *Environ. Monitor. Asses.* 185, 205–214. doi: 10.1007/s10661-012-2544-x

Kim, H. R., and You, Y. H. (2010). The effects of the elevated CO_2 concentration and increased temperature on growth, yield, and physiological responses of Rice (*Oryza sativa* L. cv. Junam). *Adv. Biores.* 1, 46–50.

Kim, S. J., Hahn, E. J., Heo, J. W., and Paek, K. Y. (2004). Effects of LEDs on net photosynthetic rate, growth, and leaf stomata of chrysanthemum plantlets in vitro. *Sci. Horticult.* 101, 143–151. doi: 10.1016/j.scienta.2003.10.003

Kirschbaum, M. U. F. (2011). Does enhanced photosynthesis enhance growth? Lessons learned from CO_2 enrichment studies. *Plant Physiol.* 155, 117–124. doi: 10.1104/pp.110.166819

Kozai, T. (2005). "Closed systems for high quality transplants using minimum resources," in *Plant Culture Engineering*, eds S. D. Gupta and Y. Ibaraki (Berlin: Springer), 275–312. doi: 10.1007/1-4020-3694-9_15

Kozai, T. (2007). Propagation, grafting, and transplant production in closed systems with artificial lighting for commercialization in Japan. *J. Ornam. Plants* 7, 145–149.

Kozai, T. (2013). Resource use efficiency of closed plant production system with artificial light: concept, estimation and application to plant factory. *Proc. Jpn. Acad. Ser. B* 89, 447–461. doi: 10.2183/pjab.89.447

Kozai, T. (2018). *Smart Plant Factory: Next-Generation Indoor Vertical Farms*. Singapore: Springer. doi: 10.1007/978-981-13-1065-2

Kubota, C., McClure, M. A., Kokalis-Burelle, N., Bausher, M. G., and Rosskopf, E. N. (2008). Vegetable grafting: history, use, and current technology status in North America. *HortScience* 43, 1664–1669. doi: 10.21273/hortsci.43.6.1664

Labeke, M. C. V., and Dambre, P. (1998). Effect of supplementary lighting and CO_2 enrichment on yield and flower stem quality of Alstroemeria cultivars. *Sci. Horticult.* 74, 269–278. doi: 10.1016/s0304-4238(98)00091-0

Lang, S. P., and Tibbitts, T. W. (1983). Factors controlling intumescence development on tomato plants. *HortScience* 108, 93–98.

Lanoue, J., Leonardos, E. D., Khosia, S., Hao, X., and Grodzinski, B. (2018). Effect of elevated CO_2 and spectral quality on whole plant gas exchange patterns in tomatoes. *PLoS One* 13:e0205861. doi: 10.1371/journal.pone.0205861

Lewis, J. D., Wang, X. Z., Griffin, K. L., and Tissue, D. T. (2002). Effects of age and ontogeny on photosynthetic responses of a determinate annual plant to elevated CO_2 concentrations. *Plant Cell Environ.* 25, 359–368. doi: 10.1046/j.0016-8025.2001.00815.x

Lewis, M., Kubota, C., Tronstad, R., and Son, Y. (2014). Scenario-based cost analysis for vegetable grafting nurseries of diffeernt technologies and sizes. *HortScience* 49, 917–930. doi: 10.21273/HORTSCI.49.7.917

Li, J., Zhou, J., Duan, Z. Q., Du, C. W., and Wang, H. Y. (2007a). Effect of CO_2 enrichment on the growth and nutrient uptake of tomato seedlings. *Pedosphere* 17, 343–351. doi: 10.1016/S1002-0160(07)60041-1

Li, J., Zhou, J. M., and Duan, Z. Q. (2007b). Effects of elevated CO_2 concentration on growth and water usage of tomato seedlings under different ammonium/nitrate ratios. *J. Environ. Sci.* 19, 1100–1107. doi: 10.1016/S1001-0742(07)60179-X

Lichtenhaler, H. K., Buschmann, C., Doll, M., Fietz, H. J., Bach, T., Kozel, U., et al. (1981). Photosynthetic activity, chloroplast ultrastructure, and leaf charateristics of high-light and low-light plants and of sun and shade leaves. *Photosynth. Res.* 2, 115–141. doi: 10.1007/bf00028752

Liptay, A., Jaworski, C. A., and Phatak, S. C. (1981). Effect of tomato transplant stem diameter and ethephon treatment on tomato yield, fruit size and number. *Canad. J. Plant Sci.* 61, 413–415. doi: 10.4141/cjps81-056

Liu, X. Y., Chang, T. T., Guo, S. R., Xu, Z. G., and Li, J. (2011). Effect of different light quality of LED on growth and photosynthetic character in cherry tomato seedling. *Acta Hort* 907, 325–330. doi: 10.17660/actahortic.2011.907.53

Lopez, R., and Runkle, E. S. (2017). *Light Management in Controlled Environments*. Willoughby, OH: Meister Media Worldwide.

Louws, F. J., Rivard, C. L., and Kubota, C. (2010). Grafting fruiting vegetables to manage soilborne pathogens, foliar pathogens arthropods and weeds. *Sci. Horticult.* 127, 127–146. doi: 10.1016/j.scienta.2010.09.023

Mamatha, H., Rao, N. K. S., Laxman, R. H., Shivashankara, K. S., Bhatt, R. M., and Pavithra, K. C. (2014). Impact of elevated CO_2 on growth, physiology, yield, and quality of tomato (*Lycopersicon esculentum* Mill) cv. Arka Ashish. *Photosynthetica* 52, 519–528. doi: 10.1007/s11099-014-0059-0

McAvoy, T., Freeman, J. H., Rideout, S. L., Olson, S. M., and Paret, M. L. (2012). Evaluation of grafting using hybrid rootstocks for management of bacterial wilt in field tomato production. *HortScience* 47, 621–625. doi: 10.21273/hortsci.47.5.621

McCall, D. (1992). Effect of supplementary light on the tomato transplant growth, and the after-effects on yield. *Sci. Horticult.* 51, 65–70. doi: 10.1016/0304-4238(92)90104-k

Monje, O., and Bugbee, B. (1998). Adaptation to high CO_2 concentration in an optimal environment: radiation capture, canopy quantum yield and carbon use efficiency. *Plant Cell Environ.* 21, 315–324. doi: 10.1046/j.1365-3040.1998.00284.x

Moran, R., and Porath, D. (1980). Chlorophyll determination in intact tissues using N, N-dimethylformamide. *Plant Physiol.* 65, 478–479. doi: 10.1104/pp.65.3.478

Mortensen, L., and Moe, R. (1983). Growth responses of some greenhouse plants to environment. V. Effect of CO_2, O2 and light on net photosynthetic rate in *Chrysanthemum morifolium* Ramat. *Sci. Horticult.* 19, 133–140. doi: 10.1016/0304-4238(83)90053-5

Mulholland, B. J., Craigon, J., Black, C. R., Colls, J. J., Atherton, J., and Landon, G. (1997). Impact of elevated atmospheric CO_2 and O_3 on gas exchange and chlorophyll content in spring wheat (*Triticum aestivum* L.). *J. Exp. Bot.* 48, 1853–1863. doi: 10.1093/jexbot/48.315.1853

Naing, A. H., Jeon, S. M., Park, J. S., and Kim, C. K. (2016). Combined effects of supplementary light and CO_2 on rose growth and the production of good quality cut flowers. *Canad. J. Plant Sci.* 96, 503–510. doi: 10.1139/cjps-2015-0304

Nanfelt, M. (2016). *Hydroponic Crop Farming, IBISWorld Industry Report OD4012*. Washington, DC: World Bank Group.

Nilsen, E. T., Sharifi, M. R., Rundel, P. W., Jarrell, W. M., and Virginia, R. (1983). Diurnal and seasonal water relations of the desert phreatophyte *Prosopis glandulosa* (honey mesquite) in the Sonoran Desert of California. *Ecology* 64, 1381–1393. doi: 10.2307/1937492

O'Carrigan, A., Hinde, E., Lu, N., Xu, X. Q., Duan, H. L., Huang, G. M., et al. (2014). Effects of light irradiance on stomatal regulation and growth of tomato. *Environ. Exp. Bot.* 98, 65–73. doi: 10.1016/j.envexpbot.2013.10.007

Oda, M. (1999). Grafting of vegetables to improve greenhouse production. *Food Fertil. Technol. Center Exten. Bul.* 480, 1–11.

Ohyama, K., and Kozai, T. (1998). Estimating electric energy consumption and its cost in a transplant production factory with artificial lighting: a case study. *Shokubutsu Kojo Gakkaishi* 10, 96–107. doi: 10.2525/jshita.10.96

Ohyama, K., Kozai, T., and Chun, C. (2003). Development and application of closed transplant production system (in Japanese). *J Shita* 15, 1–10.

Ohyama, K., Kozai, T., and Yoshinaga, K. (2000). "Electric energy, water and carbon dioxide utilization efficiencies of closed-type transplant production system," in *Transplant production in the 21st Century*, eds C. Kubota and C. Chun (Dordrecht: Kluwer Academic), 28–32.

Orellana, M. V., and Perry, M. J. (1992). An immunoprobe to measure Rubisco concentrations and maximal photosynthesis rates of individual phytoplankton cells. *Limnol. Oceanogr.* 37, 978–990. doi: 10.4319/lo.1992.37.3.0478

Pan, T. H., Ding, J. J., Qin, G. G., Wang, Y. L., Xi, L. J., Yang, J. W., et al. (2019). Interaction of supplementary light and CO_2 enrichment improves growth, photosynthesis, yield, and quality of tomato in autumn through spring greenhouse production. *Hortscience* 54, 246–252. doi: 10.21273/HORTSCI13709-18

Pramuk, L. A., and Runkle, E. S. (2005). Photosynthetic daily light integral during the seedling stage influences subsequent growth and flowering of celosia, impatiens, salvia, tagetes, and viola. *HortScience* 40, 1099C–1099C. doi: 10.21273/hortsci.40.4.1099c

Pritchard, S. G., Rogers, H. H., Prior, S. A., and Peterson, C. M. (1999). Elevated CO_2 and plant structure: a review. *Glob. Change Biol.* 5, 807–837. doi: 10.1046/j.1365-2486.1999.00268.x

Pushnik, J., Demaree, R., Houpis, J., Flory, W., Bauer, S., and Anderson, P. (1995). The effect of elevated carbon dioxide on a Sierra-Nevadan dominant species: Pinus ponderosa. *J. Biogeogr.* 22, 249–254. doi: 10.2307/2845918

Ranasinghe, S., and Taylor, G. (1996). Mechanism for increased leaf growth in elevated CO_2. *J. Exp. Bot.* 47, 349–358. doi: 10.1093/jxb/47.3.349

Reinert, R. A., Eason, G., and Barton, J. (1997). Growth and fruiting of tomato as influenced by elevated carbon dioxide and ozone. *New Phytol.* 137, 411–420. doi: 10.1046/j.1469-8137.1997.00846.x

Rivard, C. L., O'Connell, S., Peet, M., and Louws, F. J. (2010). Grafting tomato with interspecific rootstock to manage diseases caused by *Sclerotium rolfsii* and southern root-knot nematode. *Plant Dis.* 94, 1015–1021. doi: 10.1094/PDIS-94-8-1015

Rivkin, R. B. (1990). Photoadaptation in marine phytoplakton: variations in ribulose 1,5-bisphosphate activity. *Mar. Ecol. Progr. Ser.* 62, 61–72. doi: 10.3354/meps062061

Schmitt, J., Dudley, S. A., and Pigliucci, M. (1999). Manipulative approaches to testing adaptive plasticity: phytochrome-mediated shade-avoidance responses in plants. *Am. Natural.* 154, S43–S54. doi: 10.1086/303282

Shi, J., and Le Maguer, M. (2000). Lycopene in tomatoes: chemical and physical properties affected by food processing. *Crit. Rev. Biotechnol.* 20, 293–334. doi: 10.1080/07388550091144212

Singh, H., Kumar, P., Chaudhari, S., and Edelstein, M. (2017). Tomato grafting: a global perspective. *HortScience* 52, 1328–1336. doi: 10.21273/HORTSCI11996-17

Slafer, G. A., and Rawson, H. M. (1997). CO_2 effects on phasic development, leaf number and rate of leaf appearance in wheat. *Ann. Bot.* 79, 75–81. doi: 10.1006/anbo.1996.0305

Sukenik, A., Bennett, J., and Falkowski, P. (1987). Light-saturated photosynthesis-Limitation by electron transport or carbon fixation? *Biochim. Biophys. Acta Bioenerg.* 891, 205–215.

Taylor, G., Ranasinghe, S., Bosac, C., Gardner, S. D. L., and Ferris, R. (1994). Elevated CO_2 and plant growth: cellular mechanisms and responses of whole plants. *J. Exp. Bot.* 45, 1761–1774. doi: 10.1093/jxb/45.special_issue.1761

Ting, L., Yuhan, K., Man, Z., Sha, S., and Minzan, L. (2017). Universality of an improved photosynthesis prediction model based on PSO-SVM at all growth stages of tomato. *Int. J. Agricult. Biol.* 10, 63–73.

Torres, A., and Lopez, R. (2011). *Commercial Greenhouse Production. Measuring Daily Light Integral in a Greenhouse*. West Lafayette, IN: Purdue Extension.

U.S. Department of Agriculture (2016). *Vegetables 2015 Summary*. Available online at: https://www.nass.usda.gov/Publications/Todays_Reports/reports/vegean17.pdf (accessed December 19, 2016).

Uzun, S. (2006). The quantitative effects of temperature and light on the number of leaves preceding the first fruiting inflorescence on the stem of tomato (*Lycopersicon esculentum*, Mill.) and aubergine (*Solanum leongena* L.). *Sci. Horticult.* 109, 142–146. doi: 10.1016/j.scienta.2006.04.006

Wang, H., Gu, M., Cui, J., Shi, K., Zhou, Y., and Yu, J. (2009). Effects of light quality on CO_2 assimilation, chlorophyll-fluorescence quenching, expression of calvin cycle genes and carbohydrate accumulation in *Cucumis sativus*. *J. Photochem. Photobiol.* 96, 30–37. doi: 10.1016/j.jphotobiol.2009.03.010

Wang, W. Z., Zhang, M., Liu, C. H., Li, M. Z., and Liu, G. (2013). Real-time monitoring of environmental information and modeling of the photosynthetic rate of tomato plants under greenhouse conditions. *Appl. Eng. Agric.* 29, 783–792. doi: 10.13031/aea.29.9743

Xu, X., and Hernández, R. (2020). The effect of light intensity on vegetative propagation efficacy, growth, and morphology of "Albion" strawberry plants in a precision indoor propagation system. *Appl. Sci.* 10:1044. doi: 10.3390/app10031044

Yarsi, G. (2011). Effects of grafted seedling use on yield, growth and quality parameters of tomato growing in greenhouse. *Acta Hort* 923, 311–314. doi: 10.17660/ActaHortic.2011.923.46

Yelle, S., Beeson, R. C. Jr., Trudel, M. J., and Gosselin, A. (1990). Duration of CO_2 enrichment influences growth, yield, and gas exchange of two tomato species. *HortScience* 115, 52–57. doi: 10.21273/jashs.115.1.52

Zhang, S., Ma, K., and Chen, L. (2003). Response of photosynthetic plasticity of *Paeonia suffruticosa* to changed light environments. *Environ. Exp. Bot.* 49, 121–133. doi: 10.1016/s0098-8472(02)00063-1

Zheng, Y., Li, F., Hao, L., Yu, J., Guo, L., Zhou, H., et al. (2019). Elevated CO_2 concentration induces photosynthetic down-regulation with changes in leaf structure, non-structural carbohydrates and nitrogen content of soybean. *BMC Plant Biol.* 19:255. doi: 10.1186/s12870-019-1788-9

Ziska, L. H., Sicher, R. C., and Kremer, D. F. (1995). Reversibility of photosynthetic acclimation of swiss chard and sugarbeet grown at elevated concentrations of CO_2. *Physiol. Plant.* 95, 355–364. doi: 10.1034/j.1399-3054.1995.950304.x

Conflict of Interest: The authors declare that the research was conducted in the absence of any commercial or financial relationships that could be construed as a potential conflict of interest.

Copyright © 2021 Huber, Louws and Hernández. This is an open-access article distributed under the terms of the Creative Commons Attribution License (CC BY). The use, distribution or reproduction in other forums is permitted, provided the original author(s) and the copyright owner(s) are credited and that the original publication in this journal is cited, in accordance with accepted academic practice. No use, distribution or reproduction is permitted which does not comply with these terms.

frontiers in Plant Science

ORIGINAL RESEARCH
published: 05 March 2021
doi: 10.3389/fpls.2021.619987

Photosynthetic Physiology of Blue, Green, and Red Light: Light Intensity Effects and Underlying Mechanisms

Jun Liu and Marc W. van Iersel*

Horticultural Physiology Laboratory, Department of Horticulture, University of Georgia, Athens, GA, United States

Red and blue light are traditionally believed to have a higher quantum yield of CO_2 assimilation (*QY,* moles of CO_2 assimilated per mole of photons) than green light, because green light is absorbed less efficiently. However, because of its lower absorptance, green light can penetrate deeper and excite chlorophyll deeper in leaves. We hypothesized that, at high photosynthetic photon flux density (*PPFD*), green light may achieve higher *QY* and net CO_2 assimilation rate (A_n) than red or blue light, because of its more uniform absorption throughtout leaves. To test the interactive effects of *PPFD* and light spectrum on photosynthesis, we measured leaf A_n of "Green Tower" lettuce (*Lactuca sativa*) under red, blue, and green light, and combinations of those at *PPFD*s from 30 to 1,300 $\mu mol \cdot m^{-2} \cdot s^{-1}$. The electron transport rates (*J*) and the maximum Rubisco carboxylation rate ($V_{c,max}$) at low (200 $\mu mol \cdot m^{-2} \cdot s^{-1}$) and high *PPFD* (1,000 $\mu mol \cdot m^{-2} \cdot s^{-1}$) were estimated from photosynthetic CO_2 response curves. Both $QY_{m,inc}$ (maximum *QY* on incident *PPFD* basis) and *J* at low *PPFD* were higher under red light than under blue and green light. Factoring in light absorption, $QY_{m,abs}$ (the maximum *QY* on absorbed *PPFD* basis) under green and red light were both higher than under blue light, indicating that the low $QY_{m,inc}$ under green light was due to lower absorptance, while absorbed blue photons were used inherently least efficiently. At high *PPFD*, the QY_{inc} [gross CO_2 assimilation (A_g)/incident *PPFD*] and *J* under red and green light were similar, and higher than under blue light, confirming our hypothesis. $V_{c,max}$ may not limit photosynthesis at a *PPFD* of 200 $\mu mol\ m^{-2}\ s^{-1}$ and was largely unaffected by light spectrum at 1,000 $\mu mol \cdot m^{-2} \cdot s^{-1}$. A_g and *J* under different spectra were positively correlated, suggesting that the interactive effect between light spectrum and *PPFD* on photosynthesis was due to effects on *J*. No interaction between the three colors of light was detected. In summary, at low *PPFD*, green light had the lowest photosynthetic efficiency because of its low absorptance. Contrary, at high *PPFD*, QY_{inc} under green light was among the highest, likely resulting from more uniform distribution of green light in leaves.

Keywords: photosynthesis, quantum yield of CO_2 assimilation, light spectrum, photosynthetic photon flux density, electron transport, $V_{c,max}$, light intensity, light quality

OPEN ACCESS

Edited by:
Bernard Grodzinski, University of Guelph, Canada

Reviewed by:
Jan Graefe, Leibniz Institute of Vegetable and Ornamental Crops, Germany
Cristian Silvestri, University of Tuscia, Italy

****Correspondence:***
Jun Liu
jun.liu26@uga.edu

Specialty section:
This article was submitted to Crop and Product Physiology, a section of the journal Frontiers in Plant Science

Received: *21 October 2020*
Accepted: *11 February 2021*
Published: *05 March 2021*

Citation:
Liu J and van Iersel MW (2021) Photosynthetic Physiology of Blue, Green, and Red Light: Light Intensity Effects and Underlying Mechanisms. Front. Plant Sci. 12:619987. doi: 10.3389/fpls.2021.619987

Abbreviations: *PPFD*, photosynthetic photon flux density; RuBP, ribulose 1,5-bisphosphate; Rubisco, ribulose-1,5-bisphosphate carboxylase/oxygenase; VPD, vapor pressure deficit; FWHM, full width at half maximum; A_n, net CO_2 assimilation rate; R_d, dark respiration rate; $QY_{m,inc}$, maximum quantum yield of CO_2 assimilation; $A_{g,max}$, light-saturated gross assimilation rate; $QY_{m,abs}$, maximum quantum yield of CO_2 assimilation on absorbed light base; QY_{inc}, quantum yield of CO_2 assimilation based on incident *PPFD*; A_g, gross CO_2 assimilation rate; QY_{abs}, quantum yield of CO_2 assimilation on absorbed light base; *QY*, quantum yield of CO_2 assimilation; *A/Ci* curve, assimilation – internal leaf CO_2 response curve; RACiR, rapid A/C_i response technique; $V_{c,max}$, maximum rate of Rubisco carboxylation; *J*, rate of electron transport; CA1P, 2-carboxy-D-arabinitol-1-phosphate; NPQ, non-photochemical quenching.

INTRODUCTION

The photosynthetic activity of light is wavelength dependent. Based on McCree's work (McCree, 1971, 1972), photosynthetically active radiation is typically defined as light with a wavelength range from 400 to 700 nm. Light with a wavelength shorter than 400 nm or longer than 700 nm was considered as unimportant for photosynthesis, due to its low quantum yield of CO_2 assimilation, when applied as a single waveband (**Figure 1**). Within the 400–700 nm range, McCree (1971) showed that light in the red region (600–700 nm) resulted in the highest quantum yield of CO_2 assimilation of plants. Light in the green region (500–600 nm) generally resulted in a slightly higher quantum yield than light in the blue region (400–500 nm) (**Figure 1**; McCree, 1971). The low absorptance of green light is partly responsible for its low quantum yield of CO_2 assimilation. Within the visible spectrum, green leaves have the highest absorptance in the blue region, followed by red. Green light is least absorbed by green leaves, which gives leaves their green appearance (McCree, 1971; Zhen et al., 2019).

Since red and blue light are absorbed more strongly by photosynthetic pigments than green light, they are predominantly absorbed by the top few cell layers, while green light can penetrate deeper into leaf tissues (Nishio, 2000; Vogelmann and Evans, 2002; Terashima et al., 2009; Brodersen and Vogelmann, 2010), thus giving it the potential to excite photosystems in deeper cell layers. Leaf photosynthesis may benefit from the more uniform light distribution throughout a leaf under green light. Absorption of photons by chloroplasts near the adaxial surface may induce heat dissipation of excess excitation energy in those chloroplasts, while chloroplasts deeper into the leaf receive little excitation energy (Sun et al., 1998; Nishio, 2000). Blue and red photons, therefore, may be used less efficiently and are more likely to be dissipated as heat than green photons.

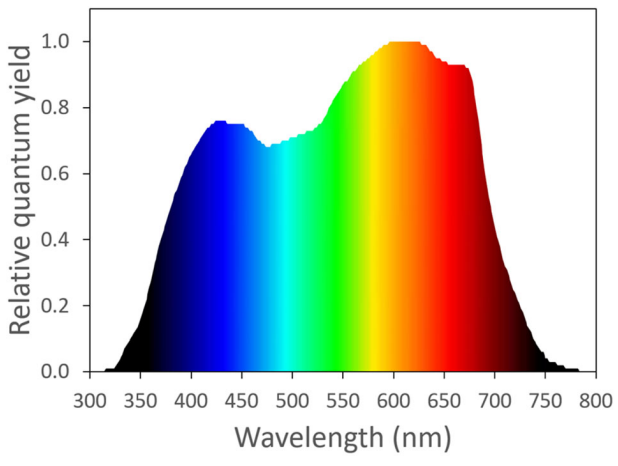

FIGURE 1 | The normalized action spectrum of the maximum quantum yield of CO_2 assimilation for narrow wavebands of light from ultra-violet to far-red wavelengths (McCree, 1971). Redrawn using data from Sager et al. (1988).

The misconception that red and blue light are used more efficiently by plants than green light still occasionally appears (Singh et al., 2015), often citing McCree's action spectrum or the poor absorption of green light by chlorophyll extracts. The limitations of McCree's action spectrum were explained in his original paper: the quantum yield was measured under low photosynthetic photon flux density (*PPFD*), using narrow waveband light, and expressed on an incident light basis (McCree, 1971), but these limitations are sometimes ignored. The importance of green light for photosynthesis has been well established in more recent studies (Sun et al., 1998; Nishio, 2000; Terashima et al., 2009; Hogewoning et al., 2012; Smith et al., 2017).

From those studies, one trend has emerged that has not received much attention: there is an interactive effect of light quality and intensity on photosynthesis (Sun et al., 1998; Evans and Vogelmann, 2003; Terashima et al., 2009). At low *PPFD*, green light has the lowest QY_{inc} (quantum yield of CO_2 assimilation on incident light basis) because of its low absorptance; at high *PPFD*, on the other hand, red and blue light have a lower QY_{inc} than green light, because of their high absorptance by photosynthetic pigments, which shifts much of the light absorption closer to the upper leaf surface. This reduces both the quantum yield of CO_2 assimilation in cells in the upper part of a leaf and light availability in the bottom part of a leaf.

The interactive effect between light quality and intensity was illustrated in an elegant study that quantified the differential quantum yield, or the increase in leaf CO_2 assimilation per unit of additional light (Terashima et al., 2009). The differential quantum yield was measured by adding red or green light to a background illumination of white light of different intensities. At low background white light levels, the differential quantum yield of red light was higher than that of green light, due to the low absorptance of green light. But as the background light level increased, the differential quantum yield of green light decreased more slowly than that of red light, and was eventually higher than that of red light (Terashima et al., 2009). The red light was absorbed efficiently by the chloroplasts in the upper part of leaves. With a high background level of white light, those chloroplasts already received a large amount of excitation energy from white light and up-regulated non-photochemical quenching (NPQ) to dissipate excess excitation energy as heat, causing the additional red light to be used inefficiently. Green light, on the other hand, was able to reach the chloroplasts deeper in the mesophyll and excited those chloroplasts that received relatively little excitation energy from white light. Therefore, with high background white light intensity, additional green light increased leaf photosynthesis more efficiently than red light (Terashima et al., 2009).

In this paper, we present a comprehensive study to explore potential interactive effect of light intensity and light quality on C_3 photosynthesis and underlying processes. We quantified the photosynthetic response of plants to blue, green, and red light over a wide *PPFD* range to better describe how light intensity and waveband interact. In addition, we examined potential interactions among blue, green, and red light, using light with different ratios and intensities of the three

narrow waveband lights. To get a better understanding of the biochemical reasons for the effects of light spectrum and intensity on CO_2 assimilation, we constructed assimilation – internal leaf CO_2 (C_i) response curves (A/C_i curves) under blue, green, and red light, as well as combinations of the three narrow waveband lights at both high and low *PPFD*. We hypothesized that effects of different light spectra would be reflected in the electron transport rate (J) required to regenerate consumed ribulose 1,5-bisphosphate (RuBP), rather than the maximum carboxylation rate of ribulose-1,5-bisphosphate carboxylase/oxygenase (Rubisco) ($V_{c,max}$).

MATERIALS AND METHODS

Plant Material

Lettuce "Green Towers" plants were grown from seed in 1.7 L round pots filled with soilless substrate (Fafard 4P Mix, Sun Gro Horticulture, Agawam, MA, United States). The plants were grown in a growth chamber (E15, Conviron, Winnipeg, Manitoba, Canada) at 23.2 ± 0.8°C (mean ± SD), under white fluorescent light with a 14-hr photoperiod, vapor pressure deficit (VPD) of 1.20 ± 0.43 kPa and a *PPFD* of 200–230 $\mu mol \cdot m^{-2} \cdot s^{-1}$ at the floor level, and ambient CO_2 concentration. Plants were sub-irrigated when necessary with a nutrient solution containing 100 $mg \cdot L^{-1}$ N, made with a complete, water-soluble fertilizer (Peter's Excel 15-5-15 Cal-Mag fertilizer, Everris, Marysville, OH, United States).

Leaf Absorptance, Transmittance, and Reflectance

Leaf absorptance was determined using a method similar to that of Zhen et al. (2019). Three plants were randomly selected. A newly expanded leaf from each plant was illuminated with a broad-spectrum halogen bulb (70W; Sylvania, Wilmington, MA, United States) for leaf transmittance measurement. Transmittance was measured with a spectroradiometer (SS-110, Apogee, Logan, UT, United States). The halogen light spectrum was taken as reference measurement with the spectroradiometer placed directly under the halogen bulb in a dark room. Then, a lettuce leaf was placed between the halogen bulb and spectroradiometer, with its adaxial side facing the halogen bulb and transmitted light was measured. Leaf transmittance was then calculated on 1 nm resolution. Light reflectance of the leaves was measured using a spectrometer with a leaf clip (UniSpec, PP systems, Amesbury, MA, United States). Light absorptance was calculated as $1 - reflectance - transmittance$. We verified that this method results in similar absorptance spectra as the use of an integrating sphere. Absorptance of each of the nine light spectra used in this study were calculated from the overall leaf absorptance spectrum and the spectra of the red, green, and blue LEDs.

Leaf Photosynthesis Measurements

All gas exchange measurements were made with a leaf gas exchange system (CIRAS-3, PP Systems). Light was provided by the LEDs built into the chlorophyll fluorescence module (CFM-3, PP Systems). This module has dimmable LED arrays of different colors, with peaks at 653 nm [red, full width at half maximum (FWHM) of 17 nm], 523 nm (green, FWHM of 36 nm), and 446 nm (blue, FWHM of 16 nm). Nine different combinations of red, green, and blue light were used in this study (**Table 1**). Throughout the measurements, the environmental conditions inside the cuvette were controlled by the leaf gas exchange system. Leaf temperature was 23.0 ± 0.1°C, CO_2 concentration was 400.5 ± 4.1 $\mu mol \cdot mol^{-1}$, and the VPD of air in the leaf cuvette was 1.8 ± 0.3 kPa (mean ± SD).

Photosynthesis – Light Response Curves

To explore photosynthetic efficiency of light with different spectra, we constructed light response curves for lettuce plants using each light spectrum. Lettuce plants were exposed to 10 *PPFD* levels ranging from 30 to 1,300 $\mu mol \cdot m^{-2} \cdot s^{-1}$ (30, 60, 90, 120, 200, 350, 500, 700, 1,000, and 1,300 $\mu mol \cdot m^{-2} \cdot s^{-1}$) in ascending orders for light response curves. Photosynthetic measurements were taken on 40–66 days old lettuce plants. Lettuce plants were taken out of the growth chamber and dark-adapted for 30 min. Starting from the lowest *PPFD*, one newly expanded leaf was exposed to all nine spectra. Net CO_2 assimilation rate (A_n) of the leaf was measured using the leaf gas exchange system. Under each light spectrum, three A_n readings were recorded at 10 s intervals after readings were stable (about 4–20 min depending on *PPFD* after changing *PPFD* and spectrum). The three A_n readings were averaged for analysis. After A_n measurements under all nine light spectra were taken, the leaf was exposed to the next *PPFD* level and A_n measurements were taken with the light spectra in the same order, until measurements were completed at all *PPFD* levels. Throughout the light response curves, C_i decreased with increasing *PPFD*, from 396 ± 10 $\mu mol \cdot mol^{-1}$ at a *PPFD* of 30 $\mu mol \cdot m^{-2} \cdot s^{-1}$ to 242 ± 44 $\mu mol \cdot mol^{-1}$ at a *PPFD* of 1,300 $\mu mol \cdot m^{-2} \cdot s^{-1}$. To account for the potential effect of plants and the order of the spectra on assimilation rates, the order of the different spectra was re-randomized for each light response curve, using a Latin square design with plant and spectrum as the blocking factors. Data were collected on nine different plants.

TABLE 1 | List of light spectrum abbreviations and their spectral composition.

Light spectrum	Fraction of total photon flux (%)		
	Blue	Green	Red
100B	100	0	0
80B20G	80	20	0
20B80G	20	80	0
100G	0	100	0
80G20R	0	80	20
20G80R	0	20	80
100R	0	0	100
20B80R	20	0	80
16B20G64R	16	20	64

Regression curves (exponential rise to maximum) were fitted to the data for each light spectrum and replication (plant):

$$A_n = A_{g,max} \times (1 - e^{-QY_{m,inc} \frac{PPFD}{A_{g,max}}}) - R_d \quad (1)$$

where R_d is the dark respiration rate, $QY_{m,inc}$ is the maximum quantum yield of CO_2 assimilation (initial slope of light response curve, mol of CO_2 fixed per mol of incident photons) and $A_{g,max}$ is the light-saturated gross assimilation rate. The $A_{n,max}$ is the light-saturated net assimilation rate and was calculated as $A_{n,max} = A_{g,max} - R_d$. The maximum quantum yield of CO_2 assimilation was also calculated on absorbed light basis as $QY_{m,abs} = \frac{QY_{m,inc}}{light\ absorptance}$.

The instantaneous quantum yield of CO_2 assimilation based on incident *PPFD* (QY_{inc}) was calculated as $\frac{A_g}{PPFD}$ for each *PPFD* at which A_n was measured, where the gross CO_2 assimilation rate (A_g) was calculated as $A_g = A_n + R_d$. To account for differences in absorptance among the different light spectra, the quantum yield of CO_2 assimilation was also calculated based on absorbed light base, as $QY_{abs} = \frac{A_g}{PPFD \times light\ absorptance}$, where light absorptance is the absorptance of lettuce leaves for each specific light spectrum. The *differential QY*, the increase in assimilation rate per unit of additional incident *PPFD*, was calculated as the derivative of Eq. 1:

$$Differential\ QY = QY_{m,inc} \times e^{-QY_{m,inc} \frac{PPFD}{A_{g,max}}} \quad (2)$$

Photosynthesis – Internal CO_2 Response (A/C_i) Curves

To explore the underlying physiological mechanisms of assimilation responses to different light spectra, we constructed A/C_i curves. Typically, A/C_i curves are collected under saturating *PPFD*. We collected A/C_i curves at two *PPFD*s (200 and 1,000 $\mu mol \cdot m^{-2} \cdot s^{-1}$) to explore interactive effects of light spectrum and *PPFD* on the assimilation rate. At a *PPFD* of 200 $\mu mol \cdot m^{-2} \cdot s^{-1}$, red light has the highest A_n and green light the lowest A_n, while at *PPFD* of 1,000 $\mu mol \cdot m^{-2} \cdot s^{-1}$, red and green light resulted in the highest A_n and blue light in the lowest A_n.

We used the rapid A/C_i response (RACiR) technique that greatly accelerates the process of constructing A/C_i curves (Stinziano et al., 2017). We used a Latin square design, similar to the light response curves. A/C_i curves were measured under the same nine spectra used for the light response curves. Nine lettuce plants were used as replicates. For each A/C_i curve, CO_2 concentration in the leaf cuvette started from 0 $\mu mol \cdot mol^{-1}$, steadily ramping to 1,200 $\mu mol \cdot mol^{-1}$ over 6 min. A reference measurement was also taken at the beginning of each replication with an empty cuvette to correct for the reaction time of the leaf gas exchange system. Post-ramp data processing was used to calculate the real A and C_i with the spreadsheet provided by PP systems, which yielded the actual A/C_i curves with C_i range of about 100–950 $\mu mol\ mol^{-1}$. Throughout the data collection, leaf temperature was 24.4 ± 1.3°C and VPD in the cuvette was 1.4 ± 0.2 kPa.

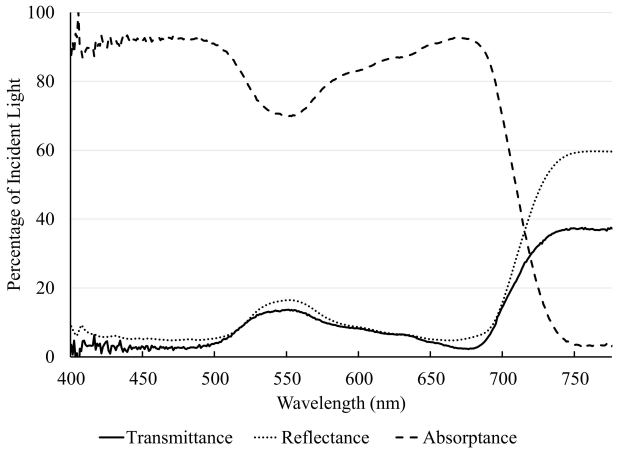

FIGURE 2 | Light absorptance, reflectance, and transmittance spectrum of a newly fully expanded "Green Towers" lettuce leaf.

Curve fitting for A/C_i curves was done by minimizing the residual sum of squares, following the protocol developed by Sharkey et al. (2007). Among our nine replicates, four plants did not show clear Rubisco limitations at low *PPFD* and for those plants Rubisco limitation ($V_{c,max}$) was not included in the model (Sharkey et al., 2007). We therefore report $V_{c,max}$ values for high *PPFD* only. The J was determined for all light spectra at both *PPFD*s. We therefore report $V_{c,max}$ was determined for all light spectra only at high *PPFD*. The quantum yield of electron transport [$QY(J)$] was calculated on both incident and absorbed *PPFD* basis as $QY(J)_{inc} = \frac{J}{PPFD}$ and $QY(J)_{abs} = \frac{QY(J)_{inc}}{light\ absorptance}$, respectively. We did not estimate triose phosphate utilization, because the A/C_i curves often did not show a clear plateau.

Data Analysis

The $QY_{m,inc}$, $QY_{m,abs}$, and $A_{g,max}$ were analyzed with ANOVA to determine the effects of light spectrum using SAS (SAS University Edition; SAS Institute, Cary, NC, United States). A_n, QY_{inc}, and QY_{abs} at each *PPFD* level and $V_{c,max}$ and J estimated from A/C_i curves were similarly analyzed with ANOVA using SAS. A_n at different *PPFD* levels were analyzed with regression analysis to detect interactive effect of blue, green, and red light on leaf assimilation rates using the fractions of red, blue, and green light as explanatory variables (JMP Pro 15, SAS Institute).

RESULTS

Leaf Absorptance

A representative spectrum of light absorptance, reflectance and transmittance of a newly fully expanded lettuce leaf is shown in **Figure 2**. In the blue region, 400–500 nm, the absorptance by "Green Towers" lettuce leaves was high and fairly constant, averaging 91.6%. The leaf absorptance decreased as the wavelength increased from 500 to 551 nm where the absorptance

minimum was 69.8%. Absorptance increased again at longer wavelengths, with a second peak at 666 nm (92.6%). Above 675 nm, the absorptance decreased steadily to <5% at 747 nm (**Figure 2**). The absorptance spectrum of our lettuce leaves is similar to what McCree (1971) obtained for growth chamber-grown lettuce, with the exception of slightly higher absorptance in the green part of the spectrum in our lettuce plants. Using this spectrum, the absorptance of the blue, green, and red LED lights were calculated to be 93.2 ± 1.0%, 81.1 ± 1.9% and 91.6 ± 1.1%, respectively. Absorptance of all nine spectra was calculated based on their ratios of red, green, and blue light (**Table 2**).

Light Quality and Intensity Effects on Photosynthetic Parameters

Light response curves of lettuce under all nine spectra are shown in **Figure 3**, with regression coefficients in **Supplementary Table 1**. It is worth noting that a few plants showed photoinhibition under 100B (decrease in A_n with *PPFD* > 1,000 $\mu mol \cdot m^{-2} \cdot s^{-1}$). Those data were excluded in curve fitting for light response curves to better estimate asymptotes. Photoinhibition was not observed under other spectra.

The $QY_{m,inc}$ of lettuce plants was 22 and 27% higher under red light (74.3 $mmol \cdot mol^{-1}$) than under either 100G (60.8 $mmol \cdot mol^{-1}$) or 100B (58.4 $mmol \cdot mol^{-1}$), respectively (**Figure 4A** and **Supplementary Table 1**). Spectra with a high fraction of red light (64% or more) resulted in a high $QY_{m,inc}$ (**Figure 4A**), while 80G20R resulted in an intermediate $QY_{m,inc}$ (**Figure 4A**). To determine whether differences in $QY_{m,inc}$ were due to differences in absorptance or in the ability of plants to use the absorbed photons for CO_2 assimilation, we also calculated $QY_{m,abs}$. On an absorbed light basis, 100B light still resulted in the lowest $QY_{m,abs}$ (62.7 $mmol \cdot mol^{-1}$) and red light resulted in the highest $QY_{m,abs}$ (81.1 $mmol \cdot mol^{-1}$) among narrow waveband lights (**Figure 4B**). Green light resulted in a $QY_{m,abs}$ (74.9 $mmol \cdot mol^{-1}$) similar to that under red light, but significantly higher than that of blue light (**Figure 4B**). We did not find any interactions (synergism or antagonism) between lights of different colors, with all physiological responses under mixed spectra being similar to the weighted average of responses under single colors. Thus, for the rest of the results we focus on the three narrow waveband spectra.

Among the three narrow waveband lights, 100G resulted in the highest $A_{g,max}$ (20.0 $\mu mol \cdot m^{-2} \cdot s^{-1}$), followed by red (18.9 $\mu mol \cdot m^{-2} \cdot s^{-1}$), and blue light (17.0 $\mu mol \cdot m^{-2} \cdot s^{-1}$) (**Figure 5** and **Supplementary Table 1**). As with $QY_{m,inc}$ and $QY_{m,abs}$, combining two or three colors of light resulted in an $A_{g,max}$ similar to the weighted averages of individual light colors.

QY_{inc} initially increased with increasing *PPFD* and peaked at 90–200 $\mu mol \cdot m^{-2} \cdot s^{-1}$, then decreased at higher *PPFDs* (**Figure 6A**). The QY_{inc} under 100R was higher than under either green or blue light at low *PPFD* (≤300 $\mu mol \cdot m^{-2} \cdot s^{-1}$). Although 100G resulted in lower QY_{inc} than 100B at low *PPFD* (≤300 $\mu mol \cdot m^{-2} \cdot s^{-1}$), the decrease in QY_{inc} under 100G with increasing *PPFD* was slower than that with 100B or 100R. Above 500 $\mu mol\ m^{-2}\ s^{-1}$, the QY_{inc} with 100G was comparable to the QY_{inc} with 100R, and higher than with 100B (**Figure 6A**). The QY_{abs} with 100R was higher than that with either 100G or 100B at *PPFDs* from 60 to 120 $\mu mol \cdot m^{-2} \cdot s^{-1}$ ($p < 0.05$). The QY_{abs} with 100G was similar to 100B at low *PPFD*, but decreased slower than that with either 100R or 100B as *PPFD* increased. At *PPFD* ≥ 500 $\mu mol \cdot m^{-2} \cdot s^{-1}$, QY_{abs} was lowest under 100B among the three monochromatic lights ($p < 0.05$) (**Figure 6B**).

The differential *QY*, which quantifies the increase in CO_2 assimilation per unit of additional *PPFD*, decreased with increasing *PPFD*. The differential *QY* with 100R was higher than those with 100B and 100G at low *PPFD*. At a *PPFD* of 30 $\mu mol \cdot m^{-2} \cdot s^{-1}$, the differential *QY* was 70.5 $mmol \cdot mol^{-1}$ for 100R, 59.4 $mmol \cdot mol^{-1}$ for 100G, and 55.8 $mmol \cdot mol^{-1}$ for 100B (**Figure 7**). However, the differential *QY* with 100R decreased rapidly with increasing *PPFD* and was lower than the differential *QY* with 100G at high *PPFD* (**Figure 7**). At high *PPFD*, the differential *QY* with 100G was highest among three monochromatic light (**Figure 7**). For instance, at a *PPFD* of 1,300 $\mu mol \cdot m^{-2} \cdot s^{-1}$, the differential *QY* with 100G was 1.09 $mmol \cdot mol^{-1}$, while those with 100B and 100R were 0.64 $mmol \cdot mol^{-1}$ and 0.46 $mmol \cdot mol^{-1}$, respectively (**Figure 7**).

TABLE 2 | Light absorptance and transmittance of new fully expanded "Green towers" lettuce leaves under nine light spectra.

Light spectrum*	Light absorptance (%)	Light transmittance (%)
100B	93.2	2.2
80B20G	90.8	3.6
20B80G	83.6	7.8
100G	81.1	9.1
80G20R	83.2	8.1
20G80R	89.5	4.9
100R	91.6	3.9
20B80R	91.9	3.5
16B20G64R	89.8	4.7

*See **Figure 2** for the leaf absorptance spectrum.*
See spectral composition in **Table 1.*

Effect of Light Spectrum and Intensity on *J* and $V_{c,max}$

J of lettuce leaves at low *PPFD* was lowest under 100G (47.4 $\mu mol \cdot m^{-2} \cdot s^{-1}$), followed by 100B (56.1 $\mu mol \cdot m^{-2} \cdot s^{-1}$), and highest under 100R (64.1 $\mu mol \cdot m^{-2} \cdot s^{-1}$) (**Figure 8A**). At high *PPFD*, on the other hand, *J* of leaves exposed to 100G (115.3 $\mu mol \cdot m^{-2} \cdot s^{-1}$) and 100R (112.1 $\mu mol \cdot m^{-2} \cdot s^{-1}$) were among the highest, while *J* of leaves under 100B was the lowest (97.0 $\mu mol \cdot m^{-2} \cdot s^{-1}$) (**Figure 8A**). At high *PPFD*, $V_{c,max}$ of leaves under blue light (59.3 $\mu mol \cdot m^{-2} \cdot s^{-1}$) was lower than $V_{c,max}$ of leaves under 16B20G64R light (72.1 $\mu mol \cdot m^{-2} \cdot s^{-1}$), but none of the other treatments differed significantly (**Figure 8**). When *PPFD* increased from 200 to 1,000 $\mu mol \cdot m^{-2} \cdot s^{-1}$, *J* under green light increased by 143%, while *J* under blue and red light increased by 73% and 75%, respectively (**Figure 8A**). *J* and $V_{c,max}$ at high *PPFD* were strongly correlated ($R^2 = 0.82$) (**Supplementary Figure 3**).

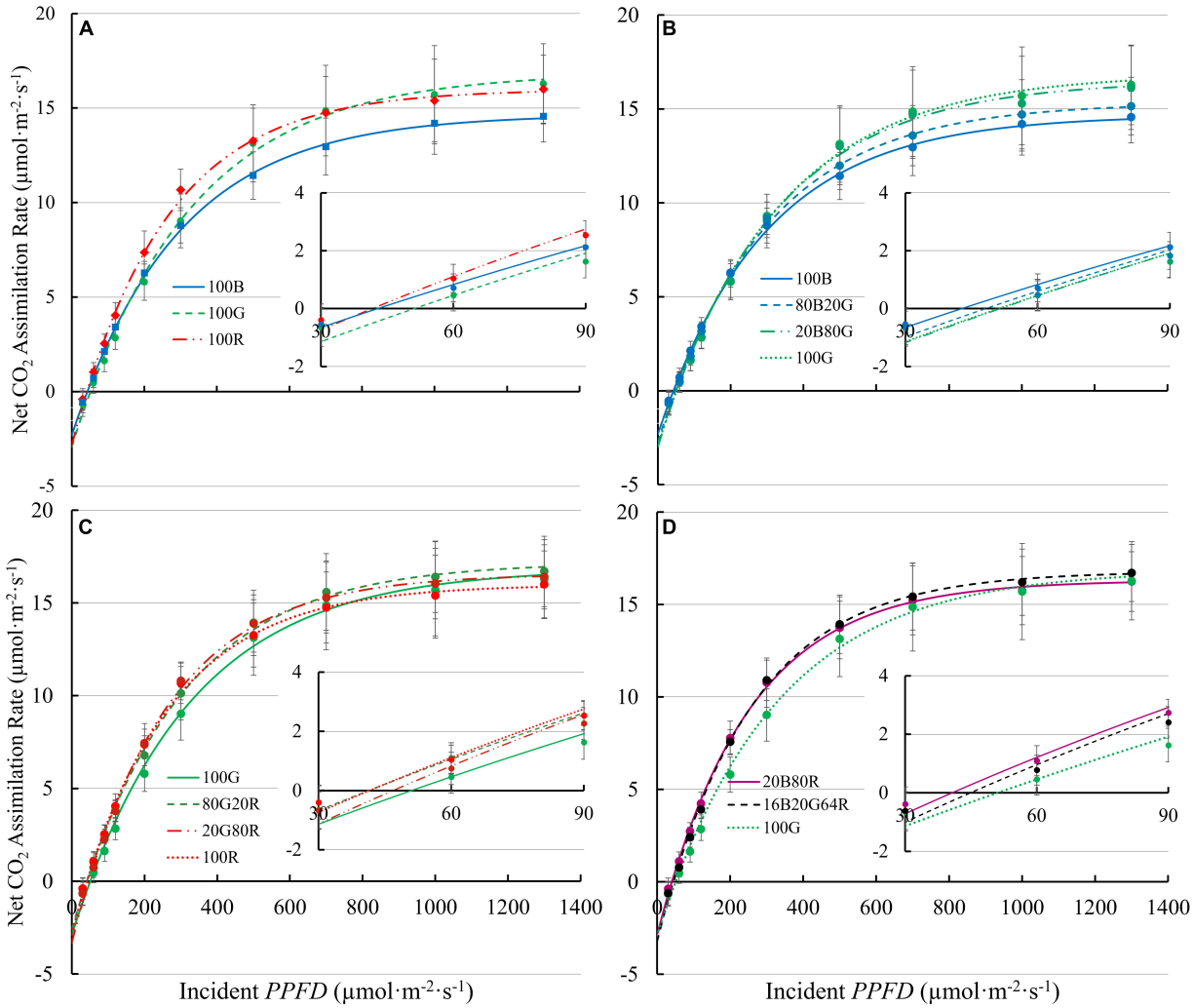

FIGURE 3 | Net assimilation (A_n) – light response curves of "Green Towers" lettuce under nine light spectra. Error bars represent the standard deviation (n = 9). Inserts show A_n against *PPFD* of 30-90 μmol·m^{-2}·s^{-1}s to better show the initial slopes of curves. The composition of the nine light spectra is shown in **Table 1**. The light spectra in the graphs are **(A)** 100B, 100G, and 100R; **(B)** 100B, 80B20G, 20B80G, and 100G; **(C)** 100G, 80G20R, 20G80R, and 100R; and **(D)** 20B80R, 16B20G64R, and 100G.

DISCUSSION

Interactive Effect of Light Spectrum and *PPFD* on Photosynthesis

There was an interactive effect of light spectrum and *PPFD* on photosynthetic properties of lettuce. Under low light conditions (≤200 μmol·m^{-2}·s^{-1}), the QY_{inc} of lettuce leaves under green light was lowest among blue, green, and red light (**Figure 6A**), due to its lower absorptance by lettuce leaves. After accounting for absorptance, green photons were used at similar efficiency as blue photons, while red photons were used most efficiently (**Figure 6B**). The $QY_{m,abs}$ under green and red light were higher than under blue light (**Figure 4B**). At high *PPFD*, green and red light had similar quantum yield, higher than that of blue light, both on an absorbed and incident light basis (**Figure 6A**). Multiple factors contributed to the interactive effect of light spectrum and *PPFD* on quantum yield and photosynthesis.

Light Absorptance and Non-Photosynthetic Pigments Determine Assimilation at Low *PPFD*

$QY_{m,inc}$ with blue and green light was lower than with red light (**Figure 4A**), consistent with McCree's action spectrum (McCree, 1971). But when taking leaf absorptance into account, $QY_{m,abs}$ was similar under green and red light and lower under blue light (**Figure 4B**). Similarly, at low *PPFD* (≤200 μmol·m^{-2}·s^{-1}), QY_{inc} of lettuce leaves was highest under red, intermediate under blue, and lowest under green light. When accounting for leaf absorptance, QY_{abs} under red light remained highest and QY_{abs} under both green and blue light were similar at low *PPFD* (**Figure 6A**). Consistent with our data, previous studies

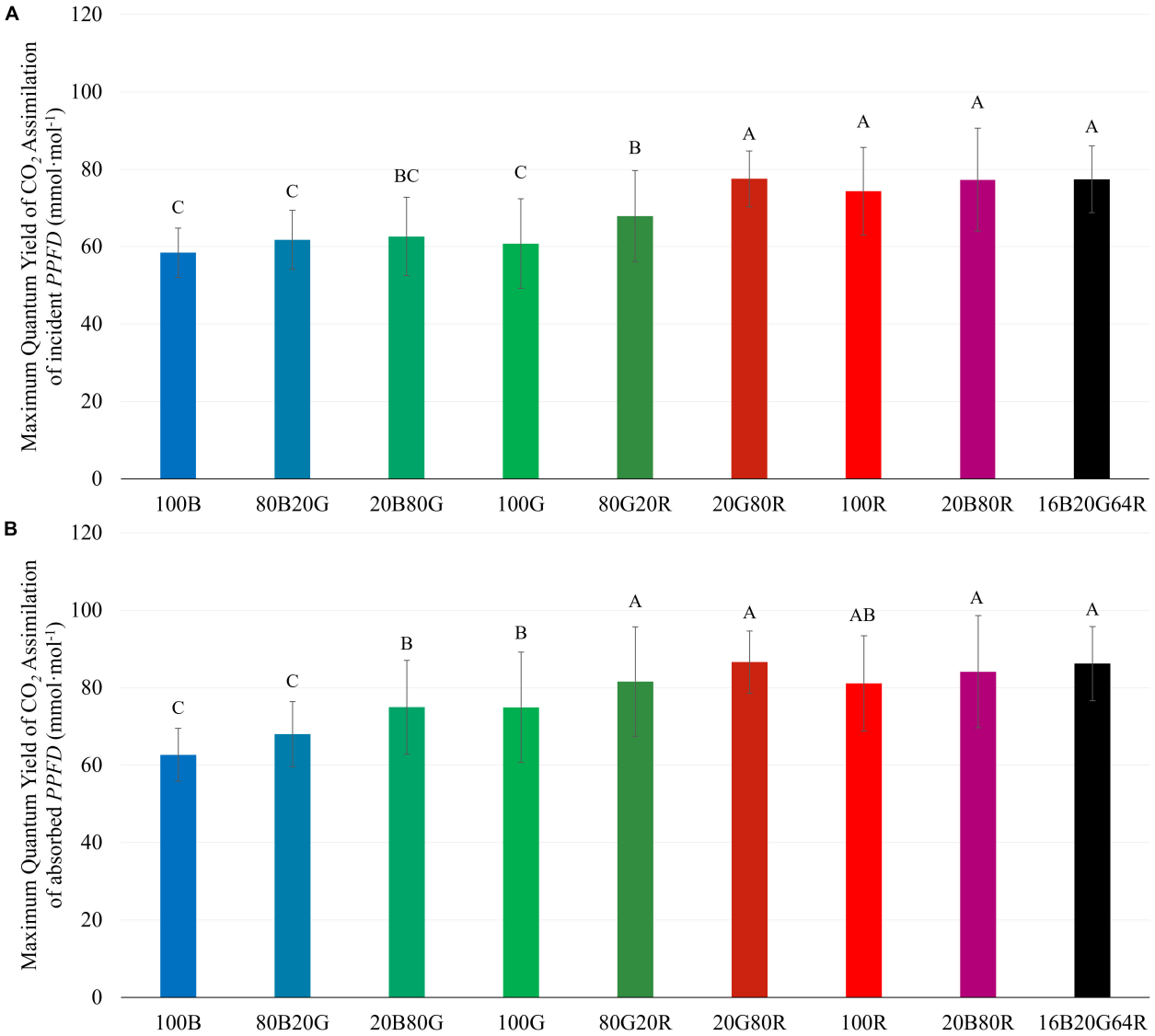

FIGURE 4 | Maximum quantum yield of CO_2 assimilation of "Green Towers" lettuce based on incident ($QY_{m,inc}$) **(A)** and absorbed light ($QY_{m,abs}$) **(B)** under nine different light spectra. Values are calculated as the initial slope of the light response curves of corresponding light spectra (see **Figure 3**). Bars with the same letter are not statistically different ($p \leq 0.05$). Error bars represent the standard deviation ($n = 9$). The composition of the nine light spectra is shown in **Table 1**.

also documented that, once absorbed, green light can drive photosynthesis efficiently at low *PPFD* (Balegh and Biddulph, 1970; McCree, 1971; Evans, 1987; Sun et al., 1998; Nishio, 2000; Terashima et al., 2009; Hogewoning et al., 2012; Vogelmann and Gorton, 2014). For example, the $QY_{m,abs}$ of spinach (*Spinacia oleracea*) and cabbage (*Brassica oleracea L.*) was highest under red light, followed by that under green light and lowest with blue light. But on incident light basis, $QY_{m,inc}$ of under green light was lower than under red or blue light (Sun et al., 1998).

Both our data (**Figure 4B**) and those of Sun et al. (1998) show that $QY_{m,abs}$ with blue light is lower than that with red and green light, indicating that blue light is used intrinsically less efficiently by lettuce. Blue light, and, to a lesser extent, green light is absorbed not just by chlorophyll, but also by flavonoids and carotenoids (Sun et al., 1998). Those pigments can divert energy away from photochemistry and thus reduce the QY_{abs} under blue light. Flavonoids (e.g., anthocyanins) are primarily located in the vacuole and cannot transfer absorbed light energy to photosynthetic pigments (Sun et al., 1998). Likewise, free carotenoids do not contribute to photochemistry (Hogewoning et al., 2012). Carotenoids in light-harvesting antennae and reaction centers channel light energy to photochemistry, but with lower transfer efficiency than chlorophylls (Croce et al., 2001; de Weerd et al., 2003a,b; Wientjes et al., 2011; Hogewoning et al., 2012). Therefore, absorption of blue light by flavonoids and carotenoids reduces the quantum yield of CO_2 assimilation. Thus, even with the high absorptance of blue light by green leaves, $QY_{m,abs}$ of leaves under blue light was the lowest among

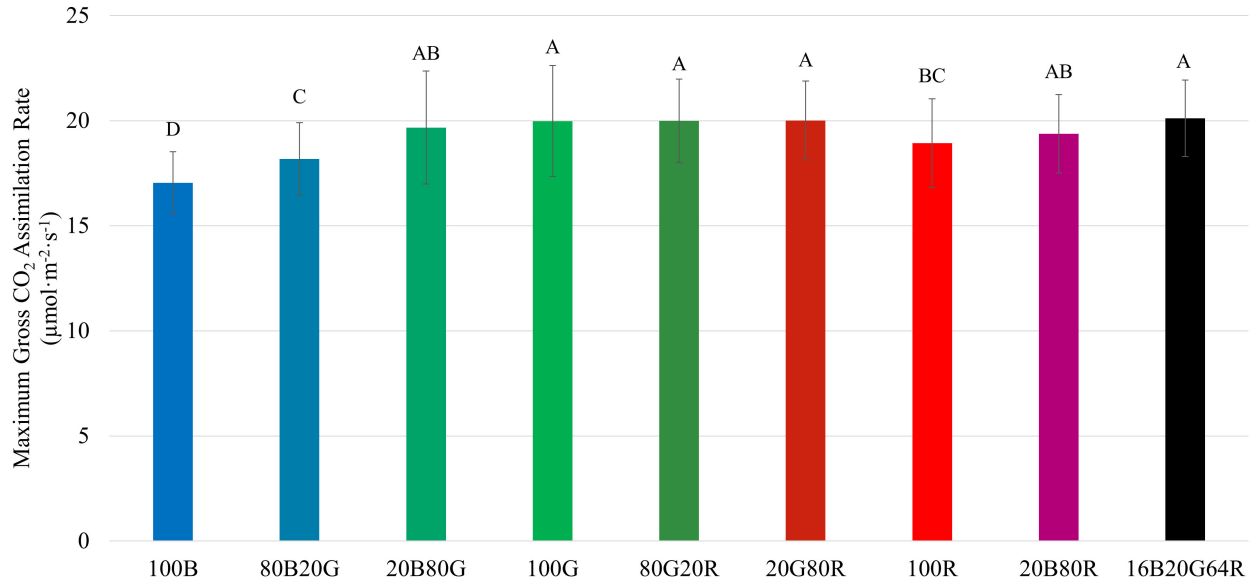

FIGURE 5 | Maximum gross assimilation rate ($A_{g,max}$) of "Green Towers" lettuce under different light spectra, calculated from the light response curves. Bars with the same letter are not statistically different ($p \leq 0.05$). Error bars represent standard deviation ($n = 9$). The composition of the nine light spectra is shown in **Table 1**.

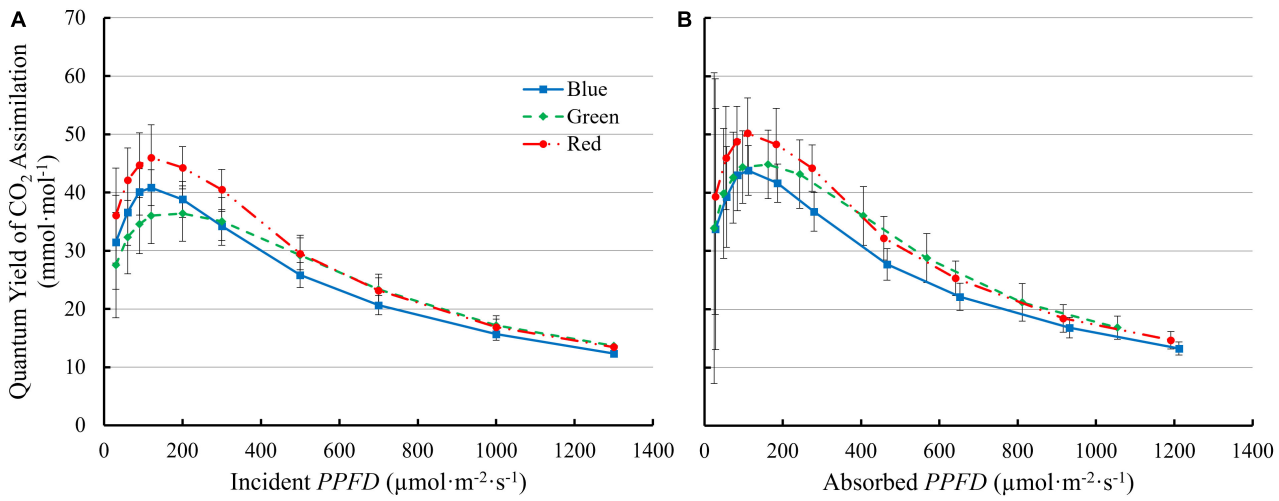

FIGURE 6 | The quantum yield of CO_2 assimilation of "Green Towers" lettuce as a function of incident (QY_{inc}) **(A)** and absorbed *PPFD* (QY_{abs}) **(B)** under blue, green, and red LED light. Error bars represent the standard deviation ($n = 9$).

the three monochromatic lights (**Figure 4B**). It is likely that the lower QY_{abs} under green light than that under red light was also due to absorption of green light by carotenoids and flavonoids (Hogewoning et al., 2012). At high *PPFD*, absorption of blue light by flavonoids and carotenoids still occurs, but this is less of a limiting factor for photosynthesis, since light availability is not limiting under high *PPFD*.

Light Dependence of Respiration and Rubisco Activity May Reduce the Quantum Yield at Low *PPFD*

At *PPFD*s below 200 $\mu mol \cdot m^{-2} \cdot s^{-1}$, the QY_{inc} and QY_{abs} of lettuce showed an unexpected pattern in response to *PPFD* (**Figure 6**). Unlike the quantum yield of PSII, which decreases exponentially with increasing *PPFD* (Weaver and van Iersel, 2019), QY_{inc} and QY_{abs} increased initially with increasing *PPFD* (**Figure 6**). A similar pattern was previously observed by Craver et al. (2020) in petunia (*Petunia* × *hybrida*) seedlings. This pattern could result from light-dependent regulation of respiration (Croce et al., 2001), alternative electron sinks such as nitrate reduction (Skillman, 2008; Nunes-Nesi et al., 2010), or Rubisco activity (Campbell and Ogren, 1992; Zhang and Portis, 1999). In our calculations, we assumed that the leaf respiration in the light was the same as R_d. However, leaf respiration in the light is lower than in the dark, in a *PPFD*-dependent manner

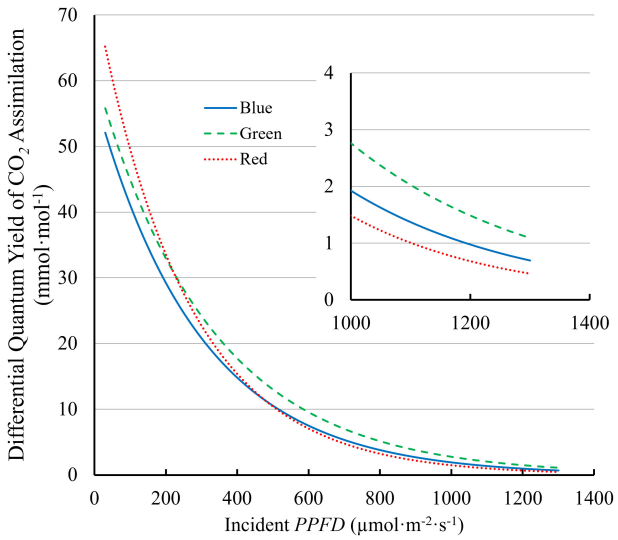

FIGURE 7 | The differential quantum yield of CO_2 assimilation (*differential QY*) of "Green Towers" lettuce under blue, green, and red LED light as a function of the *PPFD*. The *differential QY* is the increase in net assimilation per unit additional *PPFD* and was calculated as the first derivate of the light response curves (**Figure 3**). The insert shows the differential quantum yield plotted at *PPFDs* of 1,000–1,300 μmol m^{-2} s^{-1}s to better show differences at high *PPFD* (note the different *y*-axis scale).

(Brooks and Farquhar, 1985; Atkin et al., 1997), which can lead to overestimation of A_g with increasing *PPFD*. When we accounted for this down-regulation of respiration, using the model by Müller et al. (2005) to correct A_g, QY_{inc}, and QY_{abs}, we found that depression of respiration by light did not explain the initial increase in QY_{inc} and QY_{abs} we observed (**Supplementary Figure 4**). Alternative electron sinks in the chloroplasts that are upregulated in response to light can explain the low QY_{inc}, and QY_{abs} at low *PPFD*, because they compete with the Calvin cycle for reducing power (ferredoxin/NADPH). Such processes include photorespiration (Krall and Edwards, 1992), nitrate assimilation (Nunes-Nesi et al., 2010), sulfate assimilation (Takahashi et al., 2011) and the Mehler reaction (Badger et al., 2000) and their effect on QY_{inc}, and QY_{abs} would be especially notable under low *PPFD* (**Supplementary Figure 5**).

Upregulation of Rubisco activity by Rubisco activase in the light may also have contributed to the increase in QY_{inc} and QY_{abs} at low *PPFD* (Campbell and Ogren, 1992; Zhang and Portis, 1999). In the dark, 2-carboxy-D-arabinitol-1-phosphate (CA1P) or RuBP binds strongly to the active sites of Rubisco, preventing carboxylation activity. In the light, Rubisco activase releases the inhibitory CA1P or RuBP from the catalytic site of Rubisco, in a light-dependent manner (Campbell and Ogren, 1992; Zhang and Portis, 1999; Parry et al., 2008). At *PPFD* < 120 μmol·m^{-2}·s^{-1}, low Rubisco activity may have limited photosynthesis.

Light Distribution Within Leaves Affects *QY* at High *PPFD*

Except for the initial increase at low *PPFD*, both QY_{inc} and QY_{abs} decreased with increasing *PPFD*. QY_{inc} decreased slower under green than under red or blue light (**Figure 6A**). At a *PPFD* ≥ 500 μmol·m^{-2}·s^{-1}, QY_{inc} under green light was higher than that under blue light (**Figure 6A**). Accordingly, A_n under blue light was lower than under green and red light at *PPFD*s above 500 μmol·m^{-2}·s^{-1} (**Figure 3A**). The lower QY_{inc} under blue light than under green and red light at high *PPFD* can be explained by disparities in the light distribution within leaves.

Blue and red light were strongly absorbed by lettuce leaves (93.2 and 91.6%, respectively), while green light was absorbed less (81.1%) (**Table 2**). Similar low green absorptance was found in sunflower (*Helianthus annuus* L.), snapdragon (*Antirrhínum majus* L.) (Brodersen and Vogelmann, 2010), and spinach (Vogelmann and Han, 2000). In leaves of those species, absorption of red and blue light peaked in the upper 20% of leaves, and declined sharply further into the leaf. Absorption of red light decreased slower with increasing depth than that of blue light (Vogelmann and Han, 2000; Brodersen and Vogelmann, 2010). Green light absorption peaked deeper into leaves, and was more evenly distributed throughout leaves, because of low absorption of green light by chlorophyll (Vogelmann and Han, 2000; Brodersen and Vogelmann, 2010). The more even distribution of green light within leaves, as compared to red and blue light, can explain the interactive effects between *PPFD* and light spectrum on leaf photosynthesis. It was estimated that less than 10% of blue light traveled through the palisade mesophyll and reached the spongy mesophyll in spinach, while about 35% of green light and 25% of red light did so (Vogelmann and Evans, 2002). It was also estimated that chlorophyll in the lowermost chloroplasts of spinach leaves absorbed about 10% of green and <2% of blue light, compared to chlorophyll in the uppermost chloroplasts (Vogelmann and Evans, 2002; Terashima et al., 2009).

The more uniform green light distribution within leaves may be a key contributor to higher leaf level QY_{inc} under high *PPFD* because less heat dissipation of excess light energy is needed (Nishio, 2000; Terashima et al., 2009). Reaction centers near the adaxial leaf surface receive more excitation energy under blue, and to a lesser extent under red light, than under green light, because of the differences in absorptance. Consequently, under high intensity blue light, NPQ is up-regulated in the chloroplasts near the adaxial leaf surface to dissipate some of the excitation energy (Sun et al., 1998; Nishio, 2000), lowering the QY_{inc} under blue light. Since less green light is absorbed near the adaxial surface, less heat dissipation is required. When incident light increased from 150 to 600 μmol·m^{-2}·s^{-1}, the fraction of whole leaf CO_2 assimilation that occurred in the top half of spinach leaves remained the same under green light (58%), but decreased from 87 to 73% under blue light. This indicates more upregulation of heat dissipation in the top of the leaves under blue, than under green light (Evans and Vogelmann, 2003). On the other hand, the bottom half of the leaves can still utilize the available light with relatively high QY_{inc}, since the amount of light reaching the bottom half is relatively low, even under high *PPFD* (Nishio, 2000). By channeling more light to the under-utilized bottom part of leaves, leaves could achieve higher QY_{inc} even under high intensity green light. In our study, high QY_{inc} under green light and low QY_{inc} under blue light at high

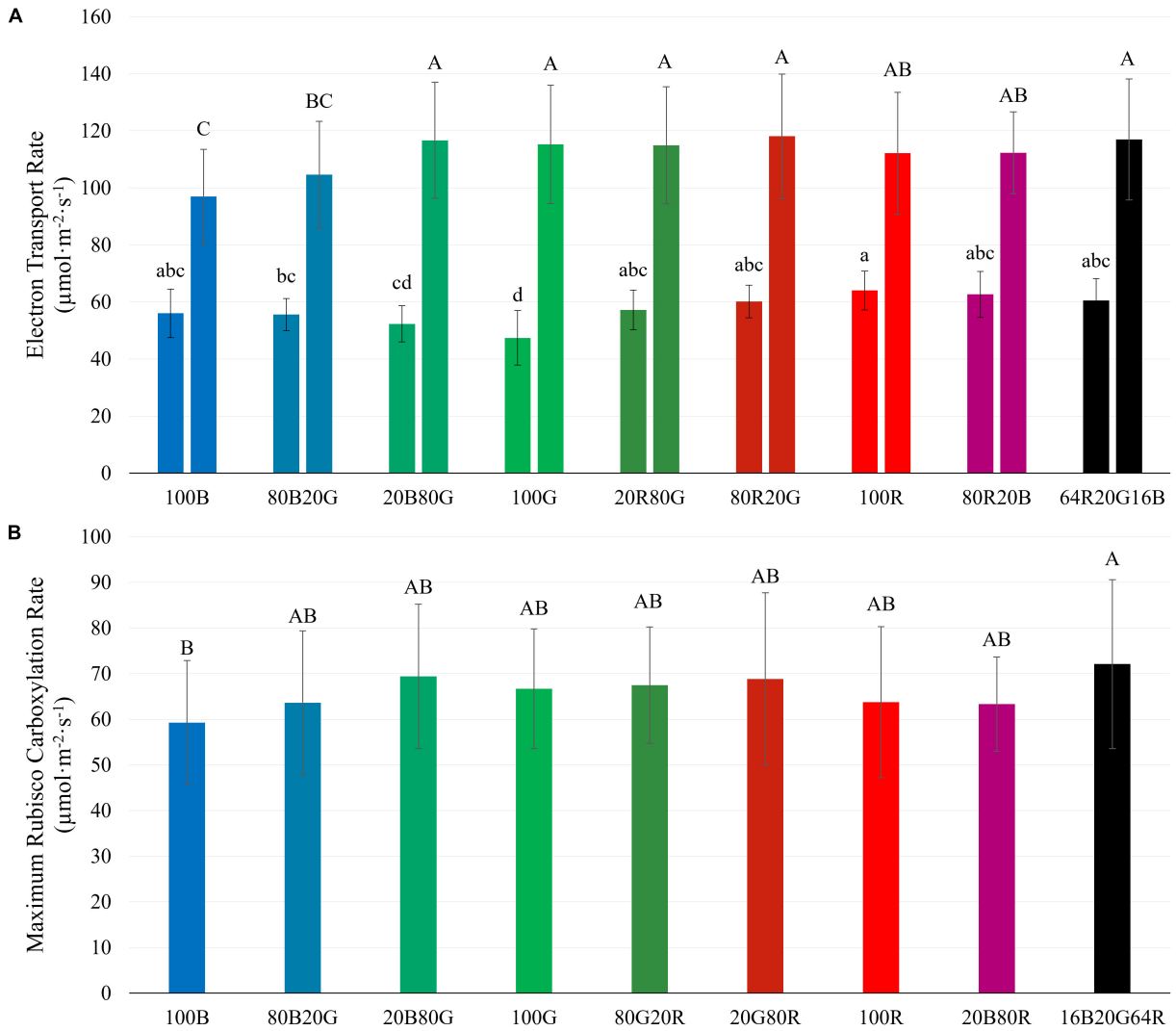

FIGURE 8 | Electron transport rate (*J*) at *PPFD*s of 200 (left bars) and 1,000 μmol m^{-2} s^{-1} (right bars) **(A)** and maximum Rubisco carboxylation rate ($V_{c,max}$) at a *PPFD* of 1,000 μmol m^{-2} s^{-1} **(B)** of "Green Towers" lettuce, as estimated from A/C_i curves under different light spectra. Bars with the same letter are not statistically different ($p \leq 0.05$). Error bars represent the standard deviation ($n = 9$). The light composition of the nine light spectra is shown in **Table 1**.

PPFD (**Figure 6**) can be thus explained by the large disparities in the light environment in chloroplasts from the adaxial to the abaxial side of leaves due to differences in leaf absorptance. Similarly, differential *QY* of lettuce leaves was highest under green light and lower under blue and red light at high *PPFD* (>300 μmol·m^{-2}·s^{-1}) (**Figure 7**), also potentially because of the more uniform distribution of green light and the uneven distribution of blue and red light in leaves.

Along the same line, A_n of lettuce leaves was the lowest under blue light at *PPFD* > 500 μmol·m^{-2}·s^{-1} (**Figure 3**). Also, A_n of lettuce leaves approached light saturation at lower *PPFD*s under blue and red light, than under green light (**Figure 3A**). Under blue, green, and red light, lettuce leaves reached 95% of $A_{n,max}$ at *PPFD*s of 954, 1,110 and 856 μmol·m^{-2}·s^{-1}, respectively. This can be seen more clearly in the differential *QY* at high *PPFD* (**Figure 7**). At a *PPFD* of 1,300 μmol·m^{-2}·s^{-1}, green light had a differential *QY* of 1.09 mmol·mol^{-1}, while that of red and blue light was only 0.46 and 0.69 mmol·mol^{-1}, respectively (**Figure 7**). Green light also resulted in a higher $A_{g,max}$ (22.9 μmol·m^{-2}·s^{-1}) than red and blue light (21.8 and 19.3 μmol·m^{-2}·s^{-1}, respectively) (**Figure 5**). As discussed before, the high $A_{g,max}$ under green light resulted from the more uniform light distribution under green light, allowing deeper cell layers to photosynthesize more. Previous research similarly found that at high *PPFD* (>500 μmol·m^{-2}·s^{-1}), A_n of both spinach and cabbage were lower under blue light than under white, red and green light (Sun et al., 1998). Overall, under high *PPFD*, the differences in light distribution throughout a leaf are important to quantum yield and assimilation rate, since it affects NPQ up-regulation (Sun et al., 1998; Nishio, 2000). However, light distribution within a leaf is less important at low than at high *PPFD*,

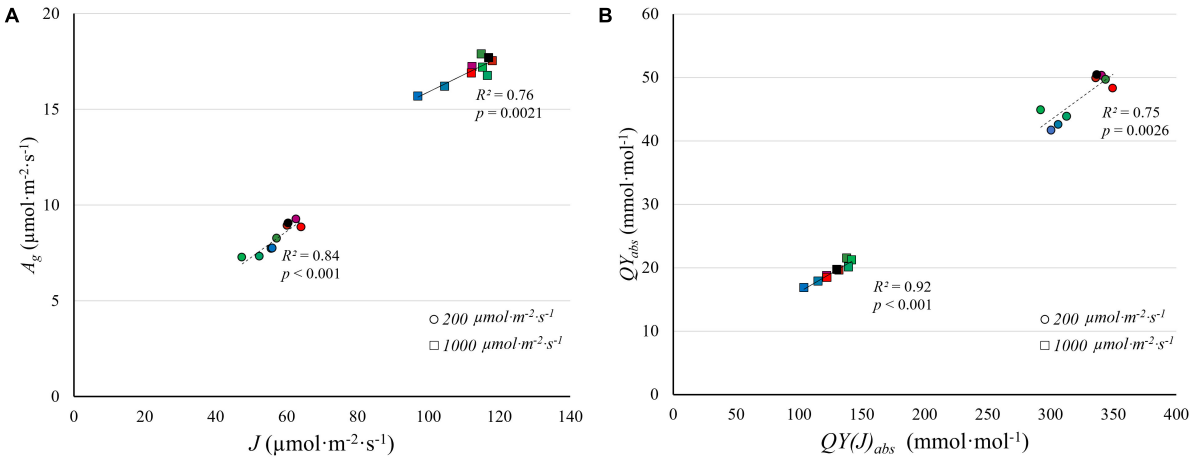

FIGURE 9 | The correlation between gross CO_2 assimilation rate (A_g) estimated from light response curves and electron transport rate (J) estimated from A/C_i curves **(A)**, and between the quantum yield of CO_2 assimilation (QY_{abs}) and the quantum yield of electron transport on an absorbed light basis [$QY(J)_{abs}$] **(B)**, under low *PPFD* (200 μmol m^{-2} s^{-1}) and high *PPFD* (1,000 μmol m^{-2} s^{-1}) under nine light spectra averaged over nine "Green Towers" lettuce plants. The color scheme representing the nine spectra is the same as **Figure 8**.

because upregulation of NPQ increases with increasing *PPFD* (Zhen and van Iersel, 2017).

Light Spectrum Affects *J*, but Not $V_{c,max}$

We examined the effect of light quality and intensity on J and $V_{c,max}$ (**Figure 8**). For the light-dependent reactions, the interactive effect between light spectra and *PPFD* found for CO_2 assimilation and quantum yield was also observed for J (**Figure 8A**). At low *PPFD* (200 $\mu mol \cdot m^{-2} \cdot s^{-1}$), green light resulted in the lowest J and red light in the highest J among single waveband spectra. But at a *PPFD* of 1,000 $\mu mol \cdot m^{-2} \cdot s^{-1}$, red and green light resulted in the highest J and blue light in the lowest J (**Figure 8A**), similar to the differences in A_g.

There was no clear evidence of Rubisco limitations to photosynthesis at a *PPFD* of 200 $\mu mol \cdot m^{-2} \cdot s^{-1}$, so the rate of the light-dependent reactions likely limited photosynthesis. This is corroborated by the strong correlation between A_g and J at a *PPFD* of 200 $\mu mol \cdot m^{-2} \cdot s^{-1}$. Although Rubisco limitations to photosynthesis were observed at a *PPFD* of 1,000 $\mu mol \cdot m^{-2} \cdot s^{-1}$, there were no meaningful differences in $V_{c,max}$ in response to light spectrum, in contrast to J (**Figure 8**).

When *PPFD* increased 5×, from 200 to 1,000 $\mu mol \cdot m^{-2} \cdot s^{-1}$, there was only a 1.7 to 2.4× increase in J, indicating a lower $QY(J)_{inc}$ at higher *PPFD*. This matches the lower QY_{inc} and the asymptotic increase in A_n in response to increasing *PPFD* (**Figure 3**). The relative increase of J under green light (143%) was greater than that under both blue and red light (73 and 75%, respectively) as *PPFD* increased. This similarly can be attributed to a more uniform energy distribution of green light among reaction centers throughout a leaf and weaker upregulation of non-photochemical quenching with increasing green light intensity (Sun et al., 1998; Nishio, 2000; Evans and Vogelmann, 2003), as discussed before.

There was a strong correlation between J and A_g under the nine light spectra at both *PPFD* levels (**Figure 9A**). QY_{abs} and $QY(J)_{abs}$ are similarly strongly correlated (**Figure 9B**). Unlike J, $V_{c,max}$ was largely unaffected by light spectra (**Figure 8B**) and was not correlated with A_g (data not shown). There was, however, a strong correlation between J and $V_{c,max}$ at a *PPFD* of 1,000 $\mu mol \cdot m^{-2} \cdot s^{-1}$ ($R^2 = 0.82$, **Supplementary Figure 3**), suggesting that J and $V_{c,max}$ are co-regulated. Similarly, Wullschleger (1993) noted a strong linear relationship between J and $V_{c,max}$ across 109 C_3 species. The ratio between J and $V_{c,max}$ in our study (1.5–2.0) similar to the ratio found by Wullschleger (1993). These results suggest that the interactive effect of light spectra and *PPFD* resulted from effects on J, which is associated with light energy harvesting by reaction centers, rather than from $V_{c,max}$.

No Interactive Effects Among Blue, Green, and Red Light

The Emerson enhancement effect describes a synergistic effect between lights of different wavebands (red and far-red) on photosynthesis (Emerson, 1957). McCree (1971) attempted to account for interactions between light with different spectra when developing photosynthetic action spectra and applied low intensity monochromatic lights from 350 to 725 nm with white background light to plants. His results showed no interactive effect between those monochromatic lights and white light (McCree, 1971). We tested different ratios of blue, green, and red light and different *PPFD*s, and similarly did not find any synergistic or antagonistic effect of different wavebands on any physiological parameters measured or calculated.

Importance of Interactions Between *PPFD* and Light Quality and Its Applications

The interactive effect between *PPFD* and light quality demonstrates a remarkable adaptation of plants to different light intensities. By not absorbing green light strongly, plants open up a "green window," as Terashima et al. (2009) called it, to excite chloroplasts deeper into leaves, and thus facilitating

CO_2 assimilation throughout the leaf. While red light resulted in relatively high QY_{inc}, QY_{abs} and A_n at both high and low *PPFD* (**Figures 3**, **6**), it is still mainly absorbed in the upper part of leaves (Sun et al., 1998; Brodersen and Vogelmann, 2010). Green light can penetrate deeper into leaves (Brodersen and Vogelmann, 2010) and help plants drive efficient CO_2 assimilation at high *PPFD* (**Figures 3**, **5**).

Many early photosynthesis studies investigated the absorptance and action spectrum of photosynthesis of green algae, e.g., Haxo and Blinks (1950) or chlorophyll or chloroplasts extracts, e.g., Chen (1952). Extrapolating light absorptance of green algae and suspension of chlorophyll or chloroplast to whole leaves from can lead to an underestimation of absorptance of green light by whole leaves and the belief that green light has little photosynthetic activity (Moss and Loomis, 1952; Smith et al., 2017). Photosynthetic action spectra developed on whole leaves of higher plants, however, have long shown that green light effectively contributes to CO_2 assimilation, although with lower QY_{inc} than red light (Hoover, 1937; McCree, 1971; Inada, 1976; Evans, 1987). The importance of green light for photosynthesis was clearly established in more recent studies, emphasizing its role in more uniformly exciting all chloroplasts, which especially important under high *PPFD* (Sun et al., 1998; Nishio, 2000; Terashima et al., 2009; Hogewoning et al., 2012; Smith et al., 2017). The idea that red and blue light are more efficient at driving photosynthesis, unfortunately, still lingers, e.g., Singh et al. (2015).

Light-emitting diodes (LEDs) have received wide attention in recent years for use in controlled environment agriculture, as they now have superior efficacy over traditional lighting technologies (Pattison et al., 2018). LEDs can have a narrow spectrum and great controllability. This provides unprecedented opportunities to fine tune light spectra and *PPFD* to manipulate crop growth and development. Blue and red LEDs have higher efficacy than white and green LEDs (Kusuma et al., 2020). By coincidence, McCree's action spectrum (**Figure 1**; McCree, 1971) also has peaks in the red and blue region, although the peak in the blue region is substantially lower than the one in the red region. Therefore, red and blue LEDs are sometimes considered optimal for driving photosynthesis. This claim holds true only under low *PPFD*. Green light plays an important role in photosynthesis, as it helps plants to adapt to different light intensities. The wavelength-dependent absorptance of chlorophylls channels green light deeper into leaves, resulting in more uniform light absorption throughout leaves and providing excitation energy to cells further from the adaxial surface. Under high *PPFD*, this can increase leaf photosynthesis. Plant evolved under sunlight for hundreds of millions of years, and it seems likely that the relatively low absorptance of green light contributes to the overall photosynthetic efficiency of plants (Nishio, 2000).

CONCLUSION

There was an interactive effect of light spectrum and *PPFD* on leaf photosynthesis. Under low *PPFD*, QY_{inc} was lowest under green and highest under red light. The low QY_{inc} under green light at low *PPFD* was due to low absorptance. In contrast, at high *PPFD*, green and red light achieved similar QY_{inc}, higher than that of blue light. The strong absorption of blue light by chlorophyll creates a large light gradient from the top to the bottom of leaves. The large amount of excitation energy near the adaxial side of a leaf results in upregulation of nonphotochemical quenching, while chloroplasts near the bottom of a leaf receive little excitation energy under blue light. The more uniform distribution of green light absorption within leaves reduces the need for nonphotochemical quenching near the top of the leaf, while providing more excitation energy to cells near the bottom of the leaf. We also found that the interactive effect of light spectrum and *PPFD* on photosynthesis was a result of the light-dependent reactions; gross assimilation and *J* were strongly correlated. We detected no synergistic or antagonistic interactions between blue, green, and red light.

DATA AVAILABILITY STATEMENT

The raw data supporting the conclusions of this article will be made available by the authors, without undue reservation.

AUTHOR CONTRIBUTIONS

JL and MI designed the experiment, discussed the data, and revised the manuscript. JL performed the experiment, analyzed data, and prepared the first draft. Both authors contributed to the article and approved the submitted version.

FUNDING

This study was funded by the USDA-NIFA-SCRI award number 2018-51181-28365, project Lighting Approaches to Maximize Profits.

SUPPLEMENTARY MATERIAL

The Supplementary Material for this article can be found online at: https://www.frontiersin.org/articles/10.3389/fpls.2021.619987/full#supplementary-material

Supplementary Figure 1 | (Related to **Figure 6**) Quantum yield of CO_2 assimilation of "Green Towers" lettuce as a function of incident (QY_{inc}) **(A,C,E,G)** and absorbed *PPFD* (QY_{abs}) **(B,D,F,H)** under nine light spectra (see **Table 1**). Error bars represent standard deviation ($n = 9$).

Supplementary Figure 2 | (Related to **Figure 7**) Differential quantum yield of CO_2 assimilation (*differential QY*) of "Green Towers" lettuce under nine light spectra as a function of the *PPFD*. Inserts show *differential QY* at *PPFD*s of 1,000–1,300 $\mu mol \cdot m^{-2}\ s^{-1}$s to better show differences at high *PPFD* (note the different *y*-axis scale). The composition of the nine light spectra is shown in **Table 1**. The light spectra in the graphs are **(A)** 100B, 100G and 100R; **(B)** 100B, 80B20G, 20B80G and 100G; **(C)** 100G, 80G20R, 20G80R and 100R; and **(D)** 20B80R, 16B20G64R and 100G.

Supplementary Figure 3 | (Related to **Figure 6**) The correlation between electron transport (*J*) and maximum Rubisco carboxylation rate ($V_{c,max}$) of "Green Towers" lettuce estimated from A/C_i curves under *PPFD* (1000 $\mu mol\ m^{-2}\ s^{-1}$) under nine light spectra ($p < 0.001$).

Supplementary Figure 4 | (Related to **Figure 6**) The comparison between QY_{inc} before **(A)** and after **(B)** correcting for light-suppression of respiration under blue, green, and red LED light. Note that the initial increase in QY_{inc} became more pronounced after correction of light suppressed respiration.

Supplementary Figure 5 | The comparison between QY_{abs} before **(A)** and after **(B)** correcting for alternative electron sinks under blue, green, and red LED light. Assuming a simplified electron sink that diverts energy of 15 μmol m^{-2} s^{-1} of absorbed photons (an arbitrary value used for illustrative purposes only) away from the Calvin cycle under all *PPFD*s, the corrected QY_{abs} was calculated based on remaining photons available to support Calvin cycle processes **(B)**. Note that the pattern of QY_{inc} after correcting of alternative electron sink **(B)** is similar to quantum yield of PSII measured by chlorophyll fluorescence by Weaver and van Iersel (2019).

Supplementary Table 1 | Dark respiration rate (R_d), maximum quantum yield of CO_2 assimilation ($QY_{m,inc}$) and maximum gross assimilation rate ($A_{g,max}$) of "Green towers" lettuce derived from the light response curves for nine different spectra using Eq. 1. The light response curves are shown in **Figure 3**. *See light composition of nine lights presented here in **Table 1**.

REFERENCES

Atkin, O. K., Westbeek, M., Cambridge, M. L., Lambers, H., and Pons, T. L. (1997). Leaf respiration in light and darkness (A comparison of slow- and fast-growing *Poa* species). *Plant Physiol.* 113, 961–965. doi: 10.1104/pp.113.3.961

Badger, M. R., von Caemmerer, S., Ruuska, S., and Nakano, H. (2000). Electron flow to oxygen in higher plants and algae: rates and control of direct photoreduction (Mehler reaction) and rubisco oxygenase. *Philos. Trans. R. Soc. Lond. B Biol. Sci.* 355, 1433–1446. doi: 10.1098/rstb.2000.0704

Balegh, S. E., and Biddulph, O. (1970). The photosynthetic action spectrum of the bean plant. *Plant Physiol.* 46, 1–5. doi: 10.1104/pp.46.1.1

Brodersen, C. R., and Vogelmann, T. C. (2010). Do changes in light direction affect absorption profiles in leaves? *Funct. Plant Biol.* 37, 403–412. doi: 10.1071/fp09262

Brooks, A., and Farquhar, G. D. (1985). Effect of temperature on the CO2/O2 specificity of ribulose-1,5-bisphosphate carboxylase/oxygenase and the rate of respiration in the light. *Planta* 165, 397–406. doi: 10.1007/BF00392238

Campbell, W. J., and Ogren, W. L. (1992). Light activation of rubisco by rubisco activase and thylakoid membranes. *Plant Cell Physiol.* 33, 751–756. doi: 10.1093/oxfordjournals.pcp.a078314

Chen, S. L. (1952). The action spectrum for the photochemical evolution of oxygen by isolated chloroplasts. *Plant Physiol.* 27, 35–48. doi: 10.1104/pp.27.1.35

Craver, J. K., Nemali, K. S., and Lopez, R. G. (2020). Acclimation of growth and photosynthesis in *Petunia* seedlings exposed to high-intensity blue radiation. *J. Am. Soc. Hortic. Sci.* 145, 152–161. doi: 10.21273/jashs04799-19

Croce, R., Müller, M. G., Bassi, R., and Holzwarth, A. R. (2001). Carotenoid-to-chlorophyll energy transfer in recombinant major light-harvesting complex (LHCII) of higher plants. I. Femtosecond transient absorption measurements. *Biophys. J.* 80, 901–915. doi: 10.1016/S0006-3495(01)76069-9

de Weerd, F. L., Dekker, J. P., and van Grondelle, R. (2003a). Dynamics of β-carotene-to-chlorophyll singlet energy transfer in the core of photosystem II. *J. Phys. Chem. B* 107, 6214–6220. doi: 10.1021/jp027737q

de Weerd, F. L., Kennis, J. T., Dekker, J. P., and van Grondelle, R. (2003b). β-Carotene to chlorophyll singlet energy transfer in the photosystem I core of *Synechococcus elongatus* proceeds via the β-carotene S2 and S1 states. *J. Phys. Chem. B* 107, 5995–6002. doi: 10.1021/jp027758k

Emerson, R. (1957). Dependence of yield of photosynthesis in long-wave red on wavelength and intensity of supplementary light. *Science* 125, 746–746. doi: 10.1126/science.125.3251.746

Evans, J. (1987). The dependence of quantum yield on wavelength and growth irradiance. *Funct. Plant Biol.* 14, 69–79. doi: 10.1071/PP9870069

Evans, J., and Vogelmann, T. C. (2003). Profiles of 14C fixation through spinach leaves in relation to light absorption and photosynthetic capacity. *Plant Cell Environ.* 26, 547–560. doi: 10.1046/j.1365-3040.2003.00985.x

Haxo, F. T., and Blinks, L. (1950). Photosynthetic action spectra of marine algae. *J. Gen. Physiol.* 33, 389–422. doi: 10.1085/jgp.33.4.389

Hogewoning, S. W., Wientjes, E., Douwstra, P., Trouwborst, G., Van Ieperen, W., Croce, R., et al. (2012). Photosynthetic quantum yield dynamics: from photosystems to leaves. *Plant Cell* 24, 1921–1935. doi: 10.1105/tpc.112.097972

Hoover, W. H. (1937). The dependence of carbon dioxide assimilation in a higher plant on wave length of radiation. *Smithson. Misc. Collect.* 95, 1–13.

Inada, K. (1976). Action spectra for photosynthesis in higher plants. *Plant Cell Physiol.* 17, 355–365. doi: 10.1093/oxfordjournals.pcp.a075288

Krall, J. P., and Edwards, G. E. (1992). Relationship between photosystem II activity and CO2 fixation in leaves. *Physiol. Plant.* 86, 180–187. doi: 10.1111/j.1399-3054.1992.tb01328.x

Kusuma, P., Pattison, P. M., and Bugbee, B. (2020). From physics to fixtures to food: current and potential LED efficacy. *Hortic. Res.* 7:56. doi: 10.1038/s41438-020-0283-7

McCree, K. J. (1971). The action spectrum, absorptance and quantum yield of photosynthesis in crop plants. *Agric. Meteorol.* 9, 191–216. doi: 10.1016/0002-1571(71)90022-7

McCree, K. J. (1972). Test of current definitions of photosynthetically active radiation against leaf photosynthesis data. *Agric. Meteorol.* 10, 443–453. doi: 10.1016/0002-1571(72)90045-3

Moss, R. A., and Loomis, W. E. (1952). Absorption spectra of leaves. I. the visible spectrum. *Plant Physiol.* 27, 370–391. doi: 10.1104/pp.27.2.370

Müller, J., Wernecke, P., and Diepenbrock, W. (2005). LEAFC3-N: a nitrogen-sensitive extension of the CO_2 and H_2O gas exchange model LEAFC3 parameterised and tested for winter wheat (Triticum aestivum L.). *Ecol. Modell.* 183, 183–210. doi: 10.1016/j.ecolmodel.2004.07.025

Nishio, J. (2000). Why are higher plants green? Evolution of the higher plant photosynthetic pigment complement. *Plant Cell Environ.* 23, 539–548. doi: 10.1046/j.1365-3040.2000.00563.x

Nunes-Nesi, A., Fernie, A. R., and Stitt, M. (2010). Metabolic and signaling aspects underpinning the regulation of plant carbon nitrogen interactions. *Mol. plant* 3, 973–996.

Parry, M. A., Keys, A. J., Madgwick, P. J., Carmo-Silva, A. E., and Andralojc, P. J. (2008). Rubisco regulation: a role for inhibitors. *J. Exp. Bot.* 59, 1569–1580. doi: 10.1093/jxb/ern084

Pattison, P., Lee, K., Stober, K., and Yamada, M. (2018). *Energy Savings Potential of SSL in Horticultural Applications*. Washington, DC: U.S. Department of Energy, Office of Scientific and Technical Information.

Sharkey, T. D., Bernacchi, C. J., Farquhar, G. D., and Singsaas, E. L. (2007). Fitting photosynthetic carbon dioxide response curves for C3 leaves. *Plant Cell Environ.* 30, 1035–1040. doi: 10.1111/j.1365-3040.2007.01710.x

Singh, D., Basu, C., Meinhardt-Wollweber, M., and Roth, B. (2015). LEDs for energy efficient greenhouse lighting. *Renew. Sustain. Energy Rev.* 49, 139–147.

Skillman, J. B. (2008). Quantum yield variation across the three pathways of photosynthesis: not yet out of the dark. *J. Exp. Bot.* 59, 1647–1661. doi: 10.1093/jxb/ern029

Smith, H. L., McAusland, L., and Murchie, E. H. (2017). Don't ignore the green light: exploring diverse roles in plant processes. *J. Exp. Bot.* 68, 2099–2110. doi: 10.1093/jxb/erx098

Stinziano, J. R., Morgan, P. B., Lynch, D. J., Saathoff, A. J., McDermitt, D. K., and Hanson, D. T. (2017). The rapid A–Ci response: photosynthesis in the phenomic era. *Plant Cell Environ.* 40, 1256–1262. doi: 10.1111/pce.12911

Sun, J., Nishio, J. N., and Vogelmann, T. C. (1998). Green light drives CO2 fixation deep within leaves. *Plant Cell Physiol.* 39, 1020–1026. doi: 10.1093/oxfordjournals.pcp.a029298

Takahashi, H., Kopriva, S., Giordano, M., Saito, K., and Hell, R. (2011). Sulfur assimilation in photosynthetic organisms: molecular functions and regulations of transporters and assimilatory enzymes. *Annu. Rev. Plant Biol.* 62, 157–184. doi: 10.1146/annurev-arplant-042110-103921

Terashima, I., Fujita, T., Inoue, T., Chow, W. S., and Oguchi, R. (2009). Green light drives leaf photosynthesis more efficiently than red light in strong white light: revisiting the enigmatic question of why leaves are green. *Plant cell physiol.* 50, 684–697. doi: 10.1093/pcp/pcp034

Vogelmann, T., and Han, T. (2000). Measurement of gradients of absorbed light in spinach leaves from chlorophyll fluorescence profiles. *Plant Cell Environ.* 23, 1303–1311. doi: 10.1046/j.1365-3040.2000.00649.x

Vogelmann, T. C., and Evans, J. (2002). Profiles of light absorption and chlorophyll within spinach leaves from chlorophyll fluorescence. *Plant Cell Environ.* 25, 1313–1323. doi: 10.1046/j.1365-3040.2002.00910.x

Vogelmann, T. C., and Gorton, H. L. (2014). "Leaf: light capture in the photosynthetic organ," in *The Structural Basis of Biological Energy Generation*, ed. M. F. Hohmann-Marriott, (Dordrecht: Springer Netherlands), 363–377.

Weaver, G., and van Iersel, M. W. (2019). Photochemical characterization of greenhouse-grown Lettuce (*Lactuca sativa* L. 'Green Towers') with applications for supplemental lighting control. *HortScience* 54, 317–322. doi: 10.21273/hortsci13553-18

Wientjes, E., van Stokkum, I. H., van Amerongen, H., and Croce, R. (2011). The role of the individual Lhcas in photosystem I excitation energy trapping. *Biophys. J.* 101, 745–754. doi: 10.1016/j.bpj.2011.06.045

Wullschleger, S. D. (1993). Biochemical limitations to carbon assimilation in C3 Plants—a retrospective analysis of the A/Ci curves from 109 species. *J. Exp. Bot.* 44, 907–920. doi: 10.1093/jxb/44.5.907

Zhang, N., and Portis, A. R. (1999). Mechanism of light regulation of rubisco: a specific role for the larger rubisco activase isoform involving reductive activation by thioredoxin-f. *Proc. Natl. Acad. Sci. U.S.A.* 96, 9438–9443. doi: 10.1073/pnas.96.16.9438

Zhen, S., Haidekker, M., and van Iersel, M. W. (2019). Far−red light enhances photochemical efficiency in a wavelength−dependent manner. *Physiol. Plant.* 167, 21–33. doi: 10.1111/ppl.12834

Zhen, S., and van Iersel, M. W. (2017). Photochemical acclimation of three contrasting species to different light levels: implications for optimizing supplemental lighting. *J. Am. Soc. Hortic. Sci.* 142, 346–354. doi: 10.21273/jashs04188-17

Conflict of Interest: The authors declare that the research was conducted in the absence of any commercial or financial relationships that could be construed as a potential conflict of interest.

Copyright © 2021 Liu and van Iersel. This is an open-access article distributed under the terms of the Creative Commons Attribution License (CC BY). The use, distribution or reproduction in other forums is permitted, provided the original author(s) and the copyright owner(s) are credited and that the original publication in this journal is cited, in accordance with accepted academic practice. No use, distribution or reproduction is permitted which does not comply with these terms.

frontiers in Plant Science

ORIGINAL RESEARCH
published: 06 April 2021
doi: 10.3389/fpls.2021.609975

Seasonal Efficiency of Supplemental LED Lighting on Growth and Photomorphogenesis of Sweet Basil

Jan Andreas Solbach, Andreas Fricke and Hartmut Stützel*

Vegetable Systems Modelling Section, Institute of Horticultural Production Systems, University of Hannover, Hannover, Germany

For decisions on supplemental lighting a quantitative knowledge of the plants' responses to light under varying conditions is fundamental. In this study, we developed light dose-response curves of growth and morphological traits for *Ocimum basilicum* L. and examined the effects of light color (blue, red, and white plus far-red) and natural environment (season) on these curves. Four greenhouse experiments were conducted throughout the year to determine the efficiencies of the light regimes on growth and their effects on plant morphology. A special aspect was the photosynthetic efficiency of far-red light. Linear and monomolecular relationships were found for the relationships between plant traits and supplemental light dose. Traits related to biomass productivity increased linearly with light dose whereas some morphological characters showed a saturation behavior. Red light and white plus far-red light were more efficient in plant dry weight production than blue light, and the plants adapted differently to the light qualities: higher biomass under red light was related to a plant architecture more favorable for light capture, i.e., taller plants and bigger leaves. White plus far-red light, on the other hand, increased leaf mass per area (LMA) and light use efficiency (LUE). Blue light resulted in lowest plant light interception and LUE. Considering photosynthetic effects of near-infrared light ($PPFD_{800}$, 400–800 nm) instead of photosynthetic photon flux density ($PPFD_{700}$, 400–700 nm) led to strongly reduced efficiencies. Traits related to photosynthesis such as dry weight, LMA and LUE were particularly affected by $PPFD_{800}$. There were no interactions between the efficiencies of the different light colors and the seasons. Efficiencies of all light regimes were significantly lower during summer compared to spring and winter. Higher dry weight production during summer compared to winter and spring were a consequence of increased light interception rather than changes in LUE. The observed differences in seasonal efficiencies were directly linked to the amount of natural light present as indicated by changes in the ratio of supplemental to natural light.

Keywords: Basil (*Ocimum basilicum* L.), light dose-response curves, light interception, light use efficiency, photomorphogenesis, supplemental lighting, light emitting diode (LED), far-red light

OPEN ACCESS

Edited by:
Leo Marcelis, Wageningen University and Research, Netherlands

Reviewed by:
Giuseppina Pennisi, University of Bologna, Italy
Agnieszka Klimek-Kopyra, University of Agriculture in Krakow, Poland

****Correspondence:***
Jan Andreas Solbach
solbach@gem.uni-hannover.de

Specialty section:
This article was submitted to Crop and Product Physiology, a section of the journal Frontiers in Plant Science

Received: *24 September 2020*
Accepted: *10 March 2021*
Published: *06 April 2021*

Citation:
Solbach JA, Fricke A and Stützel H (2021) Seasonal Efficiency of Supplemental LED Lighting on Growth and Photomorphogenesis of Sweet Basil. Front. Plant Sci. 12:609975. doi: 10.3389/fpls.2021.609975

INTRODUCTION

Growth and morphology of plants are strongly influenced by the light environment under which they are grown. Light spectrum, light dose, photoperiod, and the growing period are major determinants of the plant's adaptation to the environment (Goto, 2003). In general, plants grow under natural daylight that strongly varies in light spectrum and intensity depending on the weather, time of day, season and atmospheric conditions. For example, an overcast sky leads to increased proportions of blue light, whereas the ratio of red to far-red (R/FR) has been shown to vary little with weather conditions and season and is roughly 1.2 in natural daylight. Changes in R/FR occur during sunrise and sunset as well as when the light penetrates the plant canopy (Smith, 1982). A reduction in R/FR induces photomorphogenetic effects, known as shade-avoidance responses, that are usually characterized by a rapid elongation of stems and leaves (for comprehensive reviews on shade-avoidance see: Franklin and Whitelam, 2005; Vandenbussche et al., 2005; Franklin, 2008).

Red light (600–700 nm) is considered the most efficient in driving plant photosynthesis (e.g., McCree, 1972; Hogewoning et al., 2012) although the "red light syndrome" is commonly observed in studies under controlled environments. The syndrome is characterized by reduced plant growth and development (e.g., Goins et al., 1997; Yorio et al., 2001) due to decreased photosynthetic capacity, leaf thickness and nitrogen. The addition of blue light (400–500 nm) may alleviate the symptoms (Hogewoning et al., 2010; Ouzounis et al., 2016; Trouwborst et al., 2016). Blue light is involved in a number of physiological processes including the development of sun-type chloroplasts (Lichtenthaler et al., 1980), chloroplast movement (Banaś et al., 2012) and stomatal movement (Shimazaki et al., 2007). Blue light mediates stomatal opening, but this may be reversed by adequate amounts of green light (Frechilla et al., 2000; Talbott et al., 2002, 2006). Furthermore, it has been shown that green light (500–600 nm) may drive photosynthesis more efficiently than red light in white background light (Terashima et al., 2009). Moreover, recent studies suggest that far-red photons (701–750 nm) may drive photosynthesis equally efficiently as photons in the PAR (400–700 nm) region (Zhen and Bugbee, 2020a,b).

As previously pointed out (Hemming, 2011), most LED lighting studies investigating plant responses to light quality were conducted in controlled environments under completely artificial light, rather than under greenhouse conditions with natural background radiation. Sunlight is composed of different wavelengths ranging from ultraviolet to infrared and approximately equal proportions (∼20–25%) of blue, green, and red photons (Smith et al., 2017). Results from artificial environments may therefore not always be directly transferable to greenhouse production conditions although they certainly help to broaden our understanding of the principles of plant responses to light. On the other hand, since light intensity and spectra continuously fluctuate in natural sunlight, light quality, and dose effects of supplemental LED lighting may vastly vary in size which makes the interpretation of results and the comparison of studies difficult. Hence, a clear distinction between light intensity or spectral effects is often not possible. Several studies reported no quality effects of supplemental LED lighting during greenhouse production of ornamentals and vegetables (Hernández and Kubota, 2012, 2014; Bergstrand and Schüssler, 2013). Bergstrand and Schüssler (2013) supposed that during greenhouse production the effect of supplemental light quality depends on the amount of natural radiation present, and Hernández and Kubota (2012, 2014) concluded that the natural light environment already meets quantitative blue light requirements. Recent findings showed that the lack of blue light in the supplementing light source did not induce symptoms of the "red light syndrome" indicating that there might be such a blue light threshold as mentioned by Hernández and Kubota (2012, 2014) although adding increased proportions of blue light increased biomass and yield of tomato to an optimum under greenhouse conditions (Kaiser et al., 2019).

These inconsistent and partially contradictory results of the effects of supplemental LED lighting under solar background make it difficult to predict plant responses to the applied supplemental light spectrum. In particular, little is known about the influence of seasonally varying natural light environments on the effects of supplemental LED lighting in greenhouse production.

Thus, the present study aims to investigate the following questions:

(1) How does light dose affect the efficiency of supplemental radiation for plant growth and its effects on plant morphology?
(2) Do trait value dose-responses follow the same pattern among light colors?
(3) How does the background radiation (season) affect the efficiency of supplemental lighting?
(4) How do efficiencies change when near-infrared is considered photosynthetically active, i.e., when $PPFD_{800}$ (400–800 nm) is used instead of $PPFD_{700}$ (400–700 nm)?

To answer these questions, we analyzed the efficiency of supplemental LED lighting under greenhouse conditions on growth and morphological traits of sweet basil under blue, red and white plus far-red LEDs as dependent on the level of supplemental and natural light.

MATERIALS AND METHODS

Plant Material and Growing Conditions

Four greenhouse experiments were conducted at the Institute of Horticultural Production Systems, Leibniz University Hannover, Germany (lat. 52°23′N, long. 9°39′E) in 2018. The first trial was carried out from February 8 to March 19 (Late Winter), the second from March 13 to April 16 (Mid Spring), the third from May 22 to June 27 (Early Summer) and the fourth from August 2 to September 11 (Late Summer). Growing parameters and environmental conditions that prevailed during the experiments are shown in **Table 1**. In each trial, *Ocimum basilicum* L. cv. "Edwina" seeds (Enza Zaden Beheer B.V., Enkhuizen, Netherlands) were sown in 10-cell trays (5 cm H × 4.5 cm W × 4.5 cm L per hole) in a fertilized peat substrate

(Potgrond H, Klasmann-Deilmann GmbH, Geeste, Germany) and germinated in a greenhouse without supplemental lighting. Each tray included one plant per cell. When the seedlings emerged at the substrate surface, they were subjected to the supplemental lighting treatments (see next section). Seeds that did not germinate were replaced by transplants to restock the canopy. Plants were irrigated and fertigated when necessary with a 2 g L^{-1} concentrated nutrient solution (Ferty®Mega 2, Planta Düngemittel GmbH, Regenstauf, Germany). Greenhouse day/night temperatures were set to 20/16°C and ventilation opened at 24°C.

Supplemental Lighting Setup and Treatments

Three light quality treatments were arranged in a randomized complete block design on two benches (4.8 m × 2 m), each of them was evenly divided into three compartments (1.6 m × 2 m).

TABLE 1 | Overview of the growing conditions in the greenhouse.

	Experiment (Season)							
	Late Winter		Mid Spring		Early Summer		Late Summer	
Harvest point	**Int[u]**	**Final**	**Int**	**Final**	**Int**	**Final**	**Int**	**Final**
Growing period[v] [d]	18	32	20	28	15	29	14	33
Mean air temperature [°C]	19.3		20.6		24.4		24.1	
Temperature sum[w] [°Cd]	159.4	290.2	191.4	277.5	228.6	401.4	202.3	446.3
Mean relative humidity [%]	34.8		43.8		53.9		49.4	
Mean natural DLI[x] [mol PAR m^{-2} d^{-1}]	7.1		9.8		15.7		13.8	
Cumulated light sum[y] [mol PAR m^{-2}]	127.7	226.8	186.1	274.5	254.0	454.9	217.8	456.6
SL/NL[z]	1.72		1.24		0.78		0.88	

[u]Int, Intermediate; [v]Counted from the start of the supplemental lighting treatment; [w]Calculated following McMaster and Wilhelm (1997). T_{base} for basil was taken as 11°C (Walters and Currey, 2019); [x]DLI, Daily light integral; [y]Calculated by cumulating DLI's each day from the start of the supplemental lighting treatment; [z]SL/NL, Ratio of supplemental light to natural light directly under the LEDs calculated over the growing period.

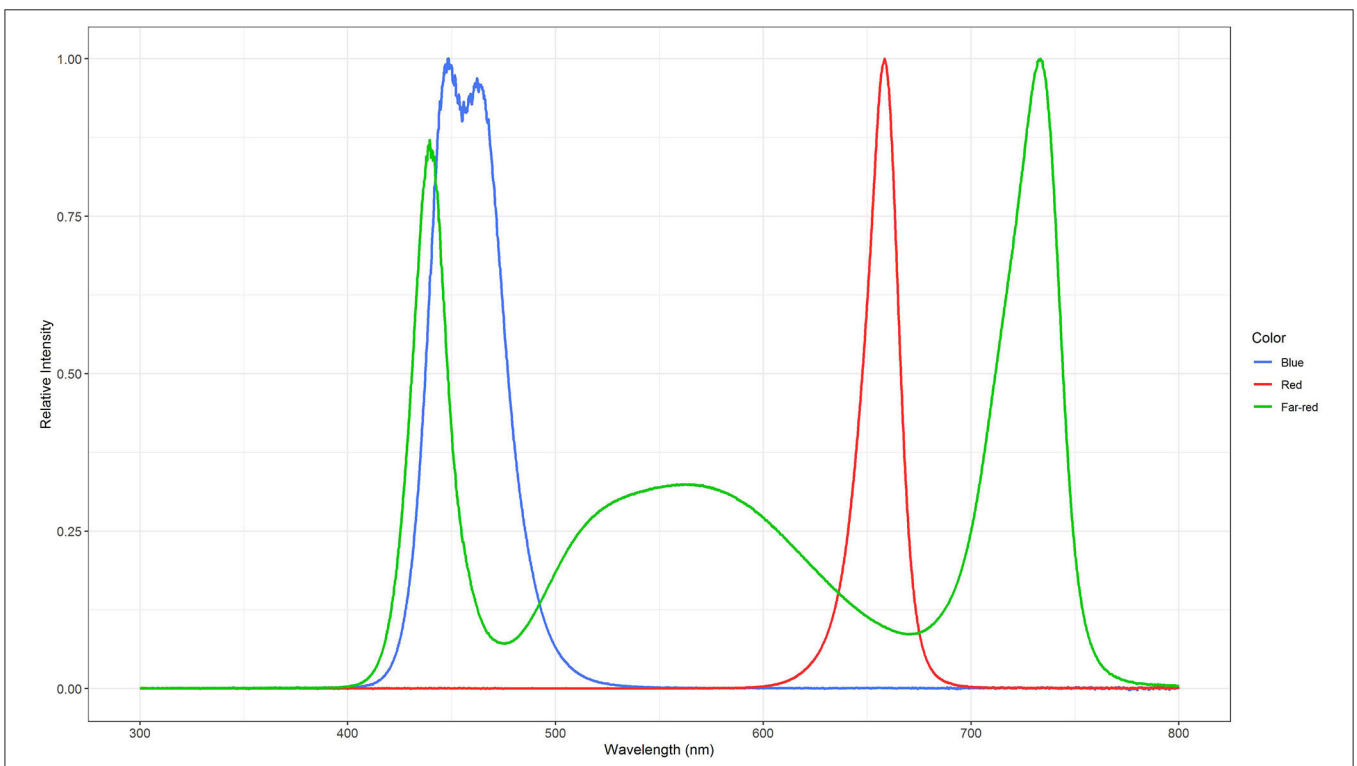

FIGURE 1 | Normalized spectral distributions of the blue (440 + 470 nm), red (660 nm), and far-red (730 nm) light treatments. The far-red light treatment included white light (400–700 nm) to ensure the same $PPFD_{700}$ in all treatments.

On each bench, a full repetition of the experiment was carried out. The distance between the two benches was 2.7 m and the compartments were separated at the eastern and western edges through 2 m × 0.40 m double layered 0.08 mm black plastic films (Lux Baufolie, Emil Lux GmbH & Co. KG, Wermelskirchen, Germany) to eliminate light pollution among treatments and to interfere as little as possible with the natural radiation. Each compartment included one LED lamp (LED-KE 300, DH Licht GmbH, Wülfrath, Germany) that could be adjusted in light color and intensity via a software (VisuSpectrum v2.0, RAM GmbH Mess- und Regeltechnik, Herrsching am Ammersee, Germany). Light quality treatments were: blue (440 + 470 nm), red (660 nm), and far-red (730 nm, **Figure 1**). The far-red treatment additionally included white light (6,500 K, 400–700 nm) to ensure the same PPFD ($PPFD_{700,}$ 400–700 nm) in all treatments and resulted in a red to far-red ratio (calculated according to Franklin, 2008) of 0.1. We additionally defined photon flux density ($PPFD_{800}$, 400–800 nm) of the far-red light treatment. LEDs were turned on at 4 a.m. and turned off at 10 p.m. (18 h day/6 h night). The LEDs were mounted centrally in 0.60 m distance from the bench's surface at the northern edges of each compartment to create a continuous supplemental light gradient ranging from ∼230 µmol $PPFD_{700}$ m^{-2} s^{-1} directly below the LED lamp to <1 µmol $PPFD_{700}$ m^{-2} s^{-1} at the edge of the compartment. In each light color treatment, trays with a total of 240 basil plants were arranged in a straight line from beneath the LED lamp to the end of the treatment over the whole compartment to cover the entire length of the light gradient. A distinct specific supplemental light dose was assigned to each plant within the gradient. Furthermore, two harvest dates, namely intermediate and final harvest, were arranged within the gradient by splitting it in the middle (120 plants in both harvests), and thereby mirroring the gradient on two sides (**Figure 2**). The positions of the light quality treatments and harvests were randomized in each season. In addition, border rows were arranged to eliminate edge effects. Border rows were moved toward the center to close the canopy after the intermediate harvest.

Light Measurements and Unit Conversion

Greenhouse light transmission was determined to be 0.55 by relating $PPFD_{700}$ inside the greenhouse to outside $PPFD_{700}$. PAR quantum sensors connected to a data logger (LI-1100 DataLogger, LI-COR Inc., USA) were used to collect the inside light data at plant height and natural radiation was recorded by a weather station next to the greenhouse throughout the experiments. An average of five days was taken to calculate the transmission factor. $PPFD_{700}$, $PPFD_{800}$ and light spectra of the LED treatments were measured under exclusion of natural radiation with a spectroradiometer (USB4000, OceanInsight, formerly OceanOptics, USA) equipped with a 3,900 µm optical

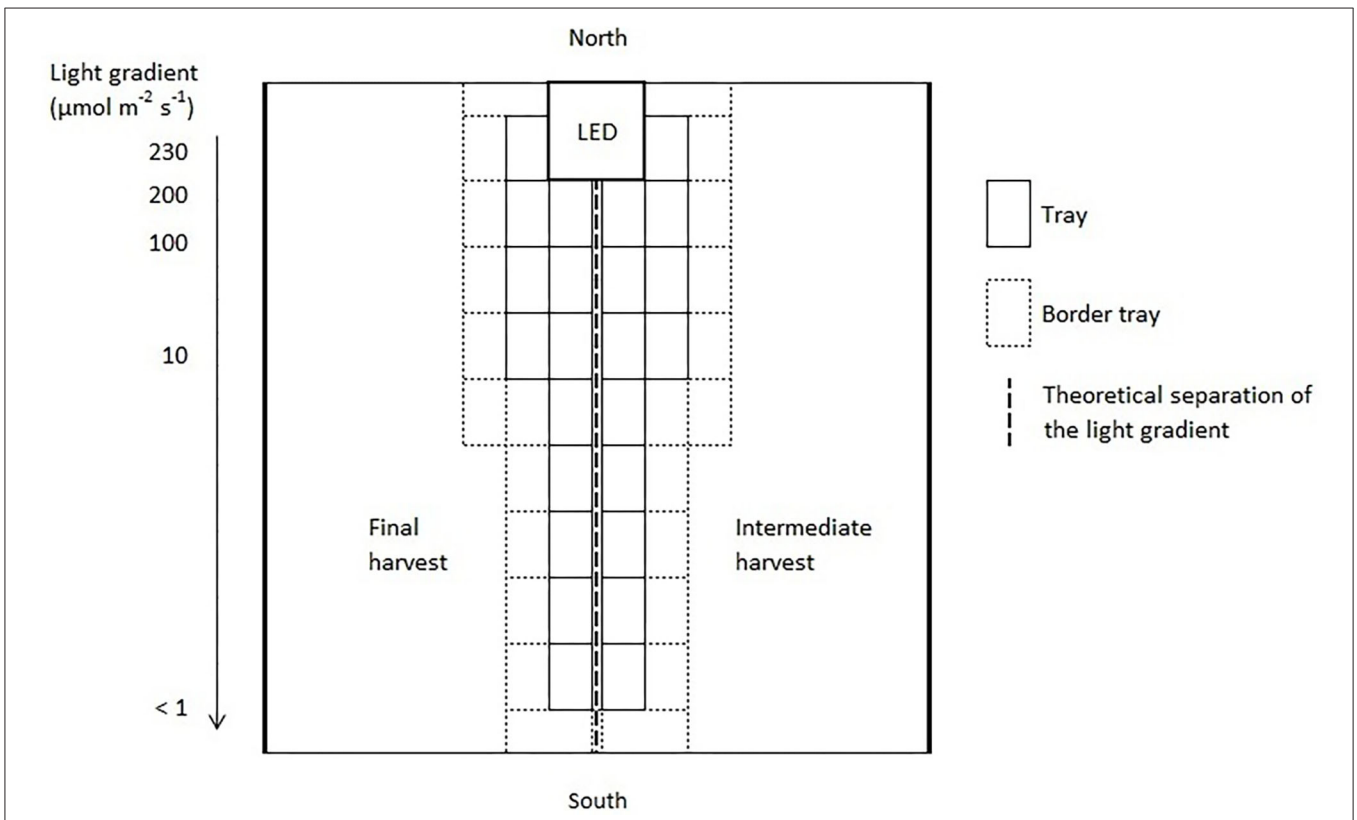

FIGURE 2 | Schematic representation of one light quality treatment of the supplemental lighting setup. The positions of the light quality treatments and harvests were randomized in each replication and season.

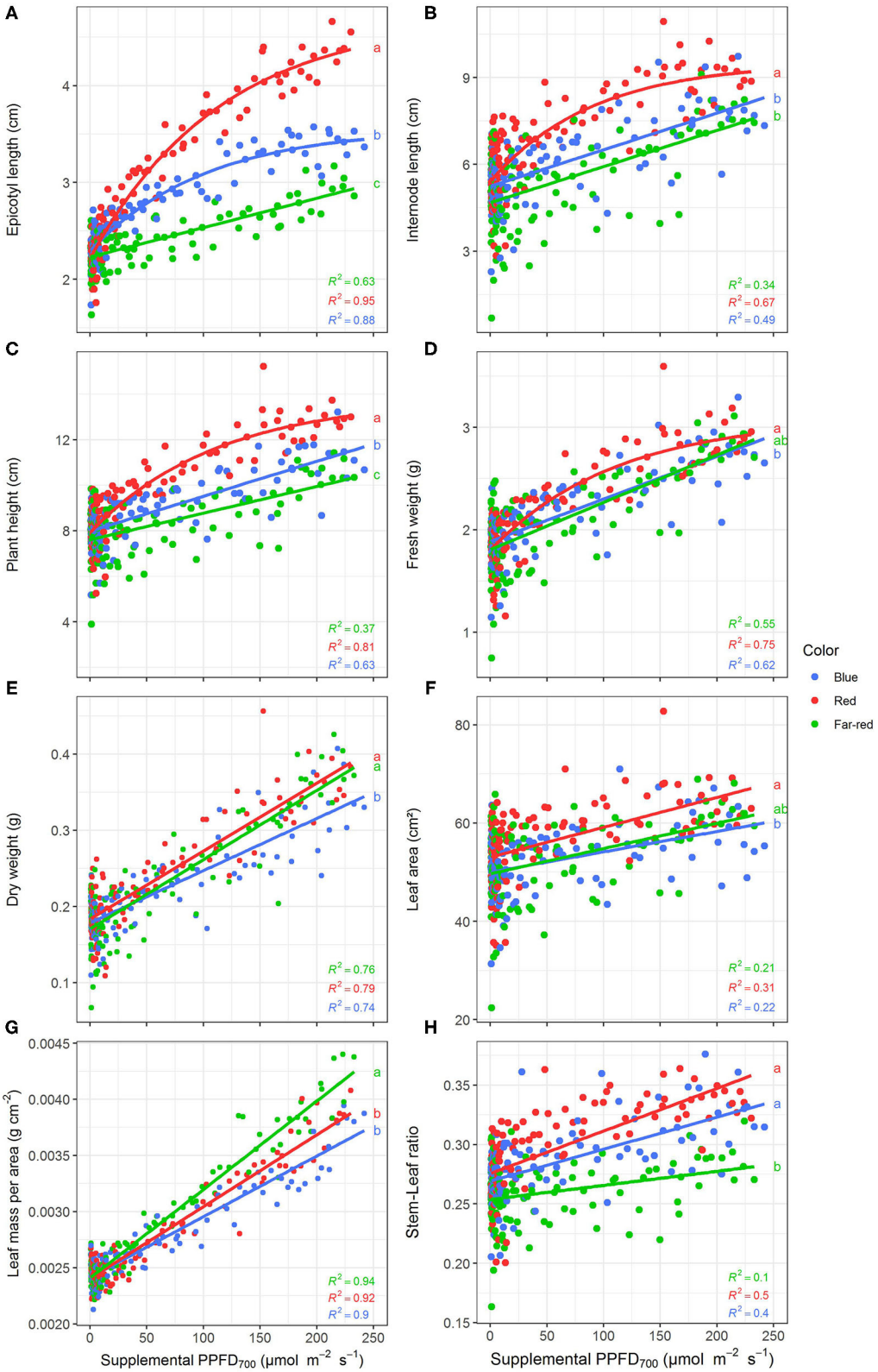

FIGURE 3 | Effect of supplemental $PPFD_{700}$ (400–700 nm) with different spectra on epicotyl length **(A)**, total internode length **(B)**, height **(C)**, fresh weight **(D)**, dry weight **(E)**, leaf area **(F)**, leaf mass per area **(G)**, and stem-leaf ratio **(H)** of *Ocimum basilicum* L. cv. "Edwina" cultivated under greenhouse conditions. Different

(Continued)

FIGURE 3 | lower-case letters indicate significant differences in slopes between colors ($p < 0.05$). Linear or monomolecular regression lines of each light color are indicated. Regressions are based on 120 plants per treatment, each with a specific light dose. Each data point shows an average of the four seasons, two harvest points and two experimental repetitions.

fiber and a cosine corrector (CC-3-UV-S, OceanInsight, formerly OceanOptics, USA). Quantum flux (μmol PAR m^{-2} s^{-1}) was converted into daily light energy integral (MJ PAR m^{-2} d^{-1}) integrating over the light period and using a conversion factor of 0.219 (Thimijan and Heins, 1983).

Growth and Morphological Measurements

Data were collected at two harvest points (**Table 1**) from individual plants. Shoots were cut at the soil surface and partitioned into stems and leaves. Fresh weights of the two organs were taken and subsequently leaf and stem samples were dried in an oven (TU-2, Heraeus Holding GmbH, Hanau, Germany) at 70°C for at least 72 h to determine dry weights. Leaf area was determined with a leaf area meter (LI-3100C, LI-COR Inc., USA) prior to leaf drying. Leaf mass per area (LMA, leaf dry weight divided by leaf area) and stem to leaf ratio (stem-leaf ratio, stem dry weight divided by leaf dry) were calculated. Furthermore, hypocotyl, epicotyl, and internode lengths were measured with a ruler. Plant height was defined as the sum of these lengths.

Estimation of Light and Energy Use Efficiency

The amount of daily absorbed $PPFD_{700}$ and $PPFD_{800}$ (Q_{daily}, MJ m^{-2} d^{-1}) of a plant was calculated as described by Monsi and Saeki (2005) following Beer–Lambert's law, respectively:

$$Q_{daily} = I \times (1 - e^{-k \times LAI}) \quad (1)$$

where I is the daily recorded $PPFD_{700}$ and $PPFD_{800}$ (MJ m^{-2} d^{-1}) above the plant, respectively, LAI is the leaf area index (m^2 leaf area per m^2 ground area, the ground area is defined here as 0.002025 m^2 per $plant^{-1}$) and k is the light extinction coefficient, assumed as 0.8 for basil. I is the sum of supplemental and natural $PPFD_{700}$ or $PPFD_{800}$ inside the greenhouse. As leaf areas could only be measured at the two harvests, leaf areas between the start of the supplemental lighting treatment and harvest 1, and between the two harvests were interpolated on the basis of temperature sum [°Cd, calculated following McMaster and Wilhelm (1997); T_{base} for basil was taken as 11°C (Walters and Currey, 2019)] based on three data points: the measured leaf area at intermediate and final harvest, and the zero point at the start of the supplemental light treatment (day 0). The three data points were log-transformed and a linear regression was fitted to the data to estimate leaf areas for each day starting from the beginning of the supplemental lighting treatment. Subsequently, logarithmic estimated leaf areas were back transformed to follow an exponential function. In experiment 3 and 4, two linear regressions (the first based on zero point and intermediate harvest, and the second based on intermediate and final harvest) were fitted to estimate daily leaf areas instead because estimation on three data points deviated >25% from the measured data points.

The total amount of absorbed $PPFD_{700}$ and $PPFD_{800}$ (Q_{total}, MJ m^{-2}) of a plant was then calculated by accumulating Q_{daily} from the beginning of the supplemental lighting treatment until the intermediate and final harvest, respectively.

The light use efficiency (LUE, g MJ^{-1}) of a canopy was expressed as the quotient of the dry weight (DW, g) of the plant to Q_{total} at intermediate and final harvests:

$$LUE = \frac{DW}{Q_{total}} \quad (2)$$

Potential energy use efficiency (EUE, g MJ^{-1}) was calculated by dividing the dry weight of a plant produced by the supplemental light only (DW_{SL}, g m^{-2}) by the supplemental light received by it (SL, MJ m^{-2}) and multiplying it by the electrical conversion efficacy (μ):

$$EUE = \frac{DW_{SL}}{SL} \times \mu \quad (3)$$

where conversion efficacies of blue, red, and white plus far-red were 0.37, 0.63, and 0.37 MJ MJ^{-1}, respectively. Conversion efficacies were calculated by relating the total light output of the LED lamp to its power consumption for each light color.

Statistical Analysis

Linear regressions of growth and photomorphological responses on light intensity were calculated to derive regression coefficients (i.e., slopes and intercepts) based on 120 biologically distinct plants, each with a specific light dose, for each replication of each treatment separately. Response and explanatory variables were log and square root transformed, respectively, prior to calculation of regression lines to approximate normal distribution and homogeneity of data.

Slopes and intercepts were then evaluated with a linear mixed-effects model

$$y = (c + s + h)^2 + RS + RSC + RSCH + e \quad (4)$$

where y is the response (i.e., slopes and intercepts), c is the supplement light color (blue, red, and white plus far-red), s is the season (Late Winter, Mid Spring, Early Summer, and Late Summer), h is the harvest point (intermediate and final), and RS, RSC, and $RSCH$ describe the randomization units which include the replication per season, replication per season per color and replication per season per color per harvest, respectively, and e is the residual error. Fixed effects are presented in lower case letters and random effects in capital letters. Analyses were conducted in RStudio (RStudio Team., 2016), an integrated development for R (R Core Team., 2020), using *lmer* function of the lme4 package (Bates et al., 2015) to fit the linear mixed-effects model to the data. The *anova* function was used to examine differences between the fixed effects as well as their two-way interactions ($p < 0.05$). Estimated marginal means were computed based on

the fitted model using the *emmeans* function of the emmeans package (Lenth, 2020). When the data showed a saturating trend, monomolecular functions were fitted and compared to the linear model using a *F*-test.

RESULTS

Effects of $PPFD_{700}$ and Light Color on Plant Growth and Morphology

All investigated efficiencies (slopes) of growth and morphological traits were significantly ($p < 0.05$) affected by light quality but there were no interactions between light color and season as well as light color and harvest point (**Supplementary Table 1**). Positive linear or monomolecular relationships were found between all plant parameters and supplemental light intensity, except for LUE and EUE which were negatively correlated with supplemental $PPFD_{700}$ dose (**Figures 3**, **4**). Monomolecular relationships indicating a saturating light response were mainly observed under red light and on plant traits resulting from expansive processes such as epicotyl and internode elongation (**Figures 3A,B**), rather than traits related to plant productivity which showed linear responses to supplemental light throughout (**Figure 3E**).

Red light stimulated the elongation of the plant axes (i.e., epicotyl, internode length, and plant height, **Figures 3A–C**) more than far-red and blue light. For shoot dry weight production, red and white plus far-red light had steeper slopes, i.e., were more efficient (**Figure 3E**) than blue light. The high dry weight production under red light was associated with the highest leaf area (**Figure 3F**) and high stem-leaf ratio (**Figure 3H**)

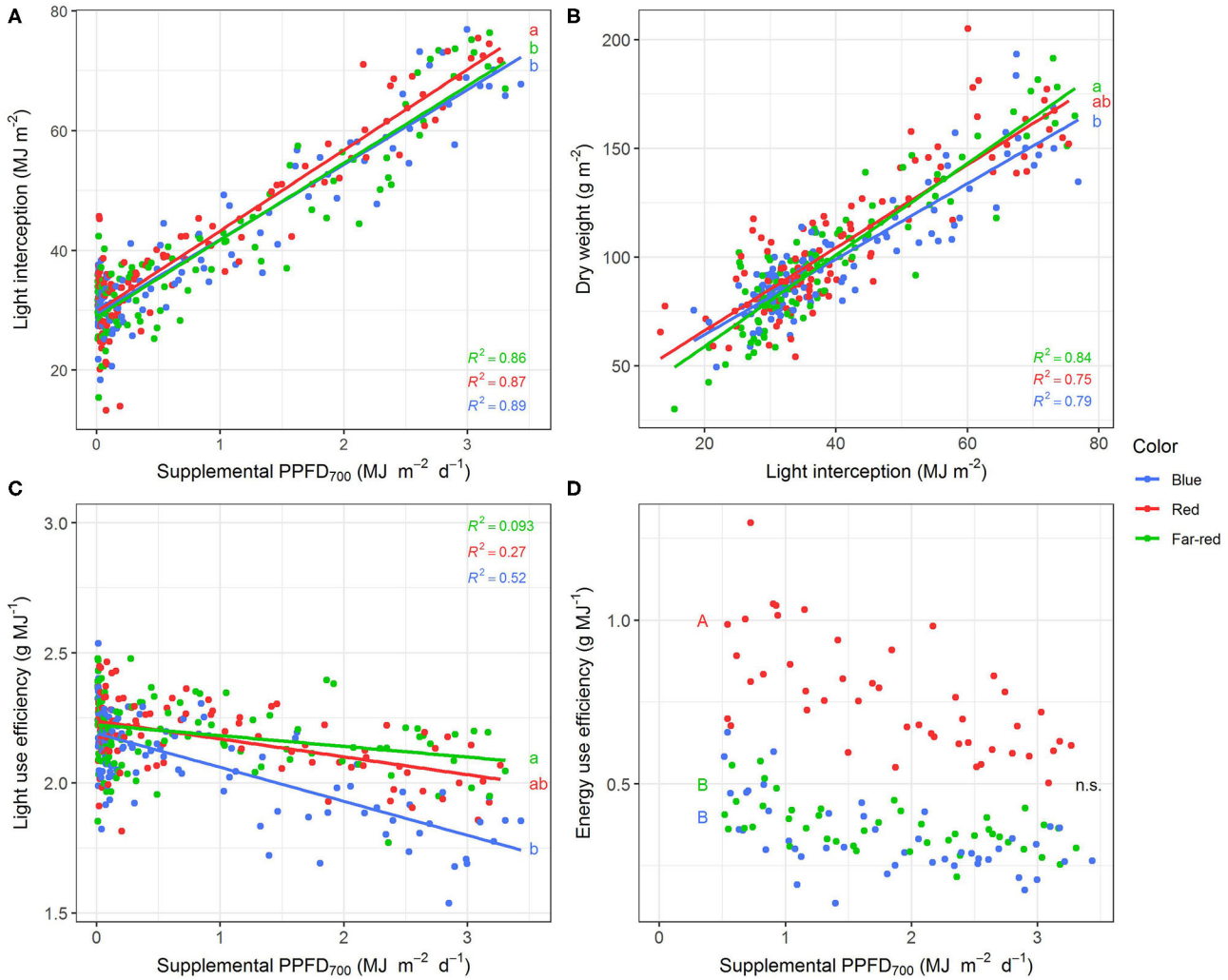

FIGURE 4 | Effect of supplemental $PPFD_{700}$ (400–700 nm) with different spectra on light interception **(A)**, dry weight **(B)**, light use efficiency **(C)**, and energy use efficiency **(D)** of *Ocimum basilicum* L. cv. "Edwina" cultivated under greenhouse conditions. Different lower-case and upper-case letters indicate significant differences in slopes and intercepts between colors ($p < 0.05$; n.s., non-significant), respectively. Intercepts of **(A–C)** were not significant. Linear regression lines of each light color are indicated. Regressions are based on 120 plants per treatment, each with a specific light dose. Each data point shows an average of the four seasons, two harvest points and two experimental repetitions.

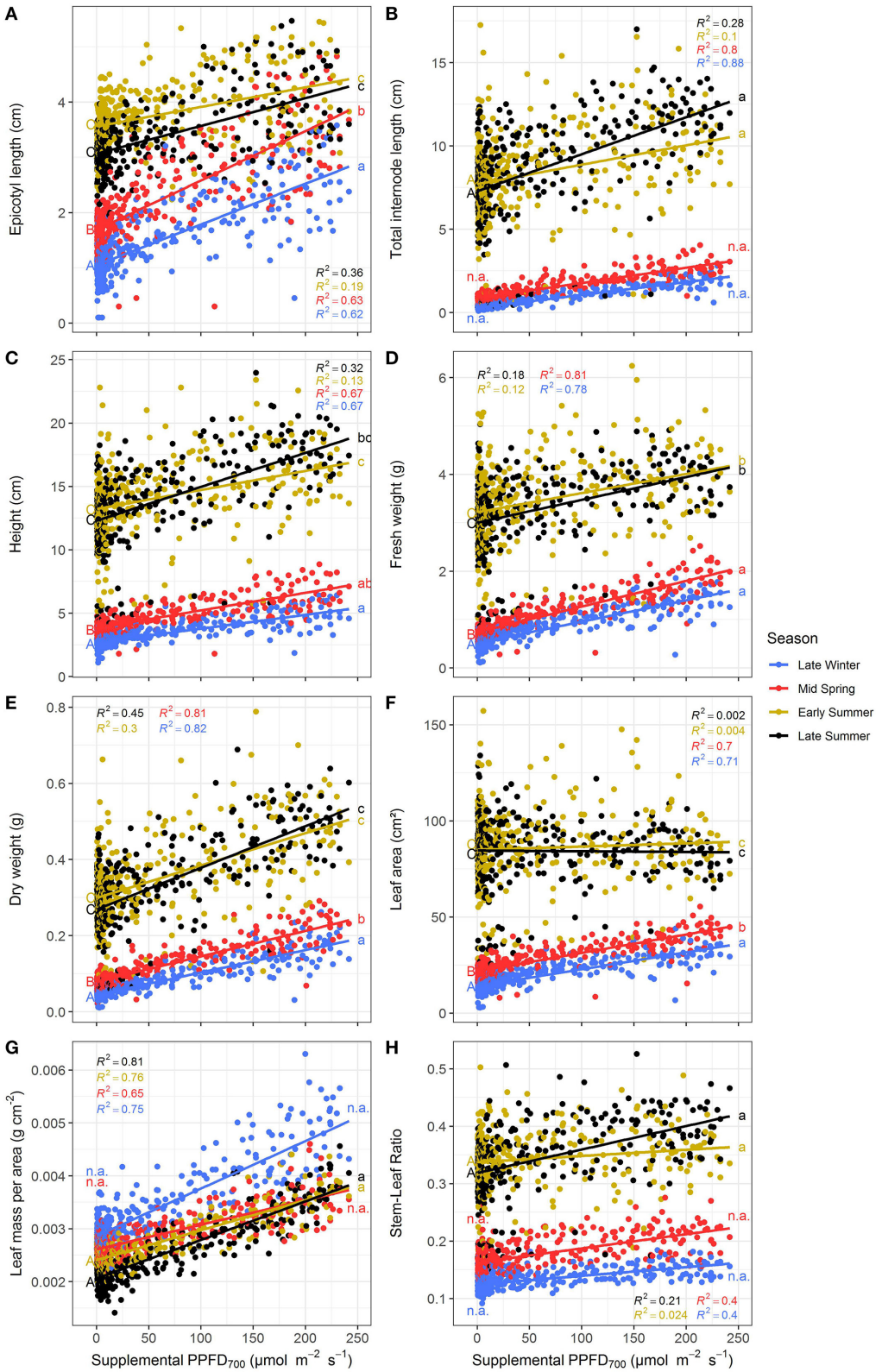

FIGURE 5 | Effect of the season on epicotyl length **(A),** total internode length **(B)**, height **(C)**, fresh weight **(D),** dry weight **(E),** leaf area **(F)**, leaf mass per area **(G)**, and stem-leaf ratio **(H)** of *Ocimum basilicum* L. cv. "Edwina" cultivated under greenhouse conditions. Different lower-case and upper-case letters indicate significant

(Continued)

FIGURE 5 | differences in slopes and intercepts between seasons ($p < 0.05$; n.a., non-estimable), respectively. Linear regression lines of each light color are indicated. Regressions are based on 120 plants per treatment, each with a specific light dose. Each data point shows an average of the three light colors, two harvest points and two experimental repetitions.

which were more favorable for light interception (**Figure 4A**). On the other hand, plants grown under white plus far-red light invested a higher proportion of dry weight into leaves (**Figure 3H**). Increasing LMA (**Figure 3G**) resulted in a better photosynthetic utilization of the incident light, i.e., higher LUE (**Figures 4B,C**) indicating a higher photosynthetic capacity of the leaves. Blue light was least efficient for plant dry weight production (**Figure 3E**) which was due to a low light interception (**Figure 4A**) accompanied by a poor LUE (**Figures 4B,C**). Electrical energy use efficiency (EUE) was about two-fold higher for the plants grown under red light compared to the other two treatments (**Figure 4D**) and mainly related to differences in electrical energy conversion efficacy among light colors.

Seasonal Influences on the Efficiencies of Supplemental LED Lighting

The efficiencies (slopes) and magnitudes (intercepts) of all plant parameters showed significant ($p < 0.05$) differences between the four seasonal environments except for LUE and EUE (**Supplementary Tables 1**, **2**). Efficiencies of the different light colors were not affected by the seasons. It could clearly be observed that the efficiencies of supplemental LED lighting were lower during early and late summer compared to winter and spring, whereas effect magnitudes were higher in summer than in winter (**Figures 5**, **6**). Although the growing periods until intermediate (14–20 days) and final harvest (28–33 days) were similar in all seasons, environmental conditions inside the greenhouse largely differed between the experiments (**Table 1**). Temperatures during winter and spring experiments were roughly 5°C lower than in summer and natural day light integral (DLI) approximately doubled from 7.1 mol m^{-2} d^{-1} in late winter to 15.7 mol m^{-2} d^{-1} in early summer. Differences in natural DLI were associated with differences in SL/NL that decreased with an increase in natural light. Plants in summer were taller (**Figures 5A–C**) and had larger leaves (**Figure 5F**) compared to plants grown in winter and spring. Furthermore, plants invested roughly three to four times more dry matter into the stem than into the leaves during summer (**Figure 5H**). At the same time, lower LMA's were observed (**Figure 5G**). The increased amount of light during summer, coupled with the altered plant morphology was associated with increased light interception (**Figure 6A**) leading to an overall higher biomass production compared to winter and spring (**Figures 5D,E**). LUE was not affected by the seasons (**Figures 6B,C**) although it tended to be lower during both summer experiments (**Figure 6C**).

Effect of $PPFD_{800}$ on Supplemental LED Lighting Efficiencies

Efficiencies of supplemental LED lighting were significantly altered when dry matter was related to $PPFD_{800}$ (**Figures 7**, **8**) instead of $PPFD_{700}$ (**Figures 3**, **4**). Lighting efficiency on plant dry weight production was strongly reduced when far-red was considered photosynthetic active (**Figure 7E**). Changes in dry weight production were mainly linked to a severely reduced LUE (**Figures 8B,C**) rather than light interception (**Figure 8A**) under $PPFD_{800}$ compared to $PPFD_{700}$. The lower LUE was primarily associated with altered morphological traits related to photosynthesis such as leaf area (**Figure 7F**) and LMA (**Figure 7G**).

DISCUSSION

Efficiencies of LED lighting on plant growth and morphology were determined under the same amount of supplemented $PPFD_{700}$ in all light treatments to allow a clear distinction between supplemental light quality and quantity effects. Light spectra and natural environments (seasons) had significant effects on the efficiencies. However, the different light spectra lead to unexpected plant responses. Furthermore, considering $PPFD_{800}$ instead of $PPFD_{700}$ resulted in reduced efficiencies. Possible causes and implications are discussed below.

Significance of the Light Color on the Plants Adaption Strategies to Light

It was striking that, contrary to our expectations and literature on basil cultivars "Eleonora" and "Emily" (Dörr et al., 2020, Larsen et al., 2020) the plants in our study did not show typical shade avoidance reactions, but had increased stem elongation under red light. Morgan and Smith (1979) showed that stem extension rate and petiole length are negatively related to an increase in phytochrome photostationary state (number of active phytochromes to total phytochromes) in most species. However, the species *Oxalis acetosella* L. exhibited a clear opposite response in their study indicating a species-specific behavior. Moreover, it has been shown that cultivars of the same species may react differently toward the light quality under that they are grown (e.g., Ohashi-Kaneko et al., 2006). Consequently, the observed reaction to R/FR seems to be a cultivar-specific rather than a species-specific response.

It was reported that during early photomorphogensis of tomato seedlings monochromatic red light stimulated plant elongation whereas monochromatic blue light induced a more compact size (Izzo et al., 2020). Our results concur with this observation during early plant growth as plants in our trials were already more elongated and had higher leaf areas under red light than under far-red and blue light during the intermediate harvest (data not shown). Moreover, reducing the plant density under the same experimental setup resulted in less elongated plants endorsing the above suggested line of thought (**Supplementary Figure 1**). Hence, we presume that the stimulated early seedling growth under red light had resulted in an earlier canopy closure compared to the other light treatments

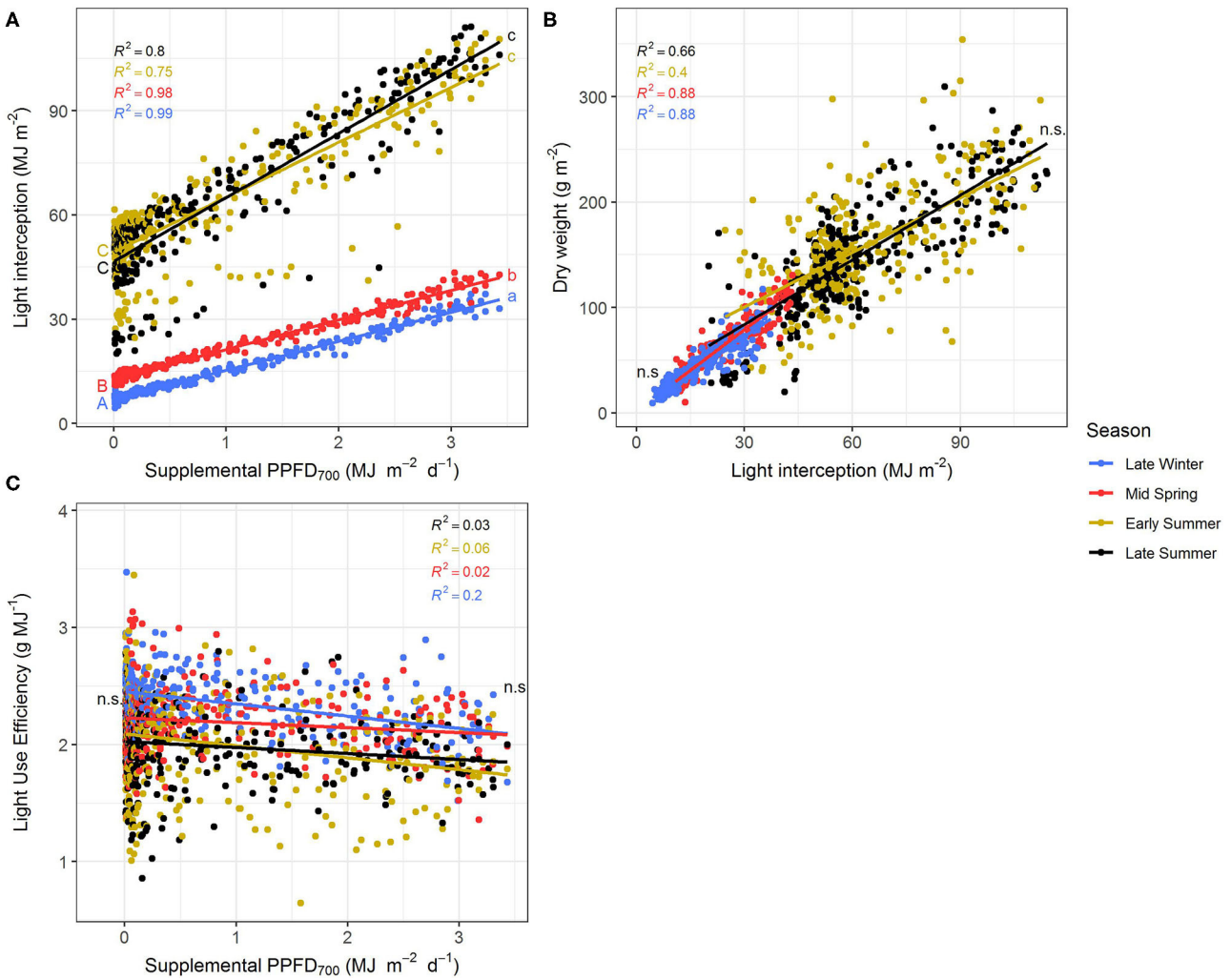

FIGURE 6 | Effect of the season on light interception **(A)**, dry weight **(B)**, and light use efficiency **(C)** of *Ocimum basilicum* L. cv. "Edwina" cultivated under greenhouse conditions. Different lower-case and upper-case letters indicate significant differences in slopes and intercepts between seasons ($p < 0.05$; n.s., non-significant), respectively. Linear regression lines of each light color are indicated. Regressions are based on 120 plants per treatment, each with a specific light dose. Each data point shows an average of the three light colors, two harvest points, and two experimental repetitions.

which, as a consequence, lead to early competition for light and thus further facilitated plant elongation growth.

Another interesting aspect is that stem elongation was also more promoted by blue light than by far-red light. There are reports ranging from promotion (Heo et al., 2002; Johnson et al., 2020; Larsen et al., 2020) to reduction (Hoenecke et al., 1992; Islam et al., 2012, Izzo et al., 2020) of elongation growth by blue light. It was suggested that promoted plant elongation by blue light is a shade avoidance response which is attributed to lower phytochrome activity (Kong et al., 2018). Moreover, the elongation response to blue light varies among plant species (Kong et al., 2018, Johnson et al., 2020). Larsen et al. (2020) found promotion of stem elongation in basil under 90 and 100% blue light during the production in a vertical farm which was most likely related to reduced phytochrome activity. Hence, the observed increased elongation under blue light was likely related to reduced phytochrome activity in our study as well.

Light Dose Effects on Growth Efficiency of Supplemental Radiation

The effects of light quality on plant growth and morphology in this study are striking. The high efficiency of red light in promoting stem elongation and leaf area was associated with significantly increased light interception compared to the other light quality treatments, and thereby contributed to the high efficiency of plant biomass production. An increase in leaf area and stem length is more favorable for light capture due to a higher light penetration in the canopy and increased light absorption (Sarlikioti et al., 2011). Blue light was the least efficient in promoting biomass. An increase in blue light fraction is often associated with a decreased leaf area (Hernández and Kubota,

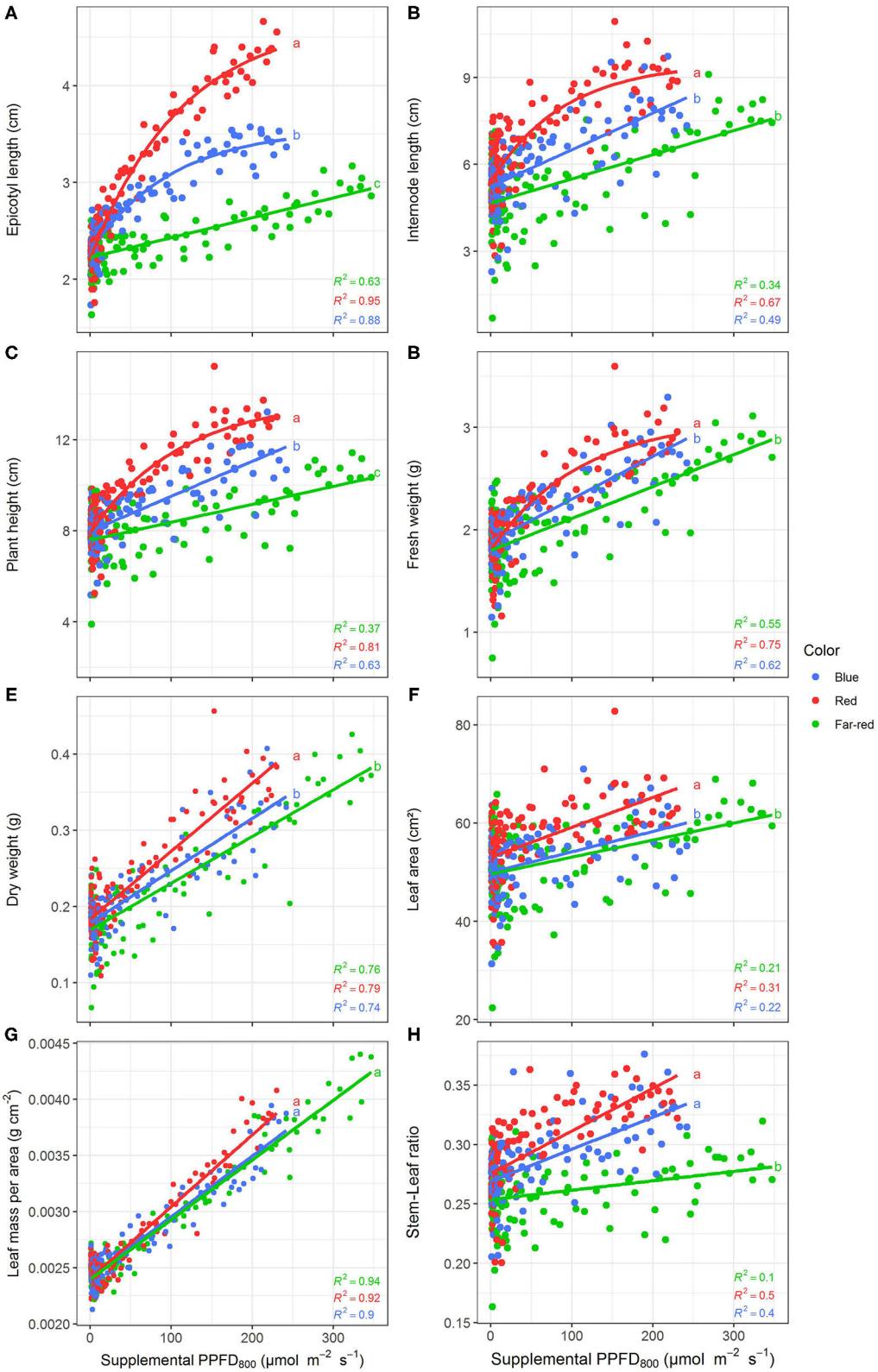

FIGURE 7 | Effect of supplemental $PPFD_{800}$ (400–800 nm) with different spectra on epicotyl length **(A)**, total internode length **(B)**, height **(C)**, fresh weight **(D)**, dry weight **(E)**, leaf area **(F)**, leaf mass per area **(G)**, and stem-leaf ratio **(H)** of *Ocimum basilicum* L. cv. "Edwina" cultivated under greenhouse conditions. Different

(Continued)

FIGURE 7 | lower-case letters indicate significant differences in slopes between colors ($p < 0.05$). Linear or monomolecular regression lines of each light color are indicated. Regressions are based on 120 plants per treatment, each with a specific light dose. Each data point shows an average of the four seasons, two harvest points and two experimental repetitions.

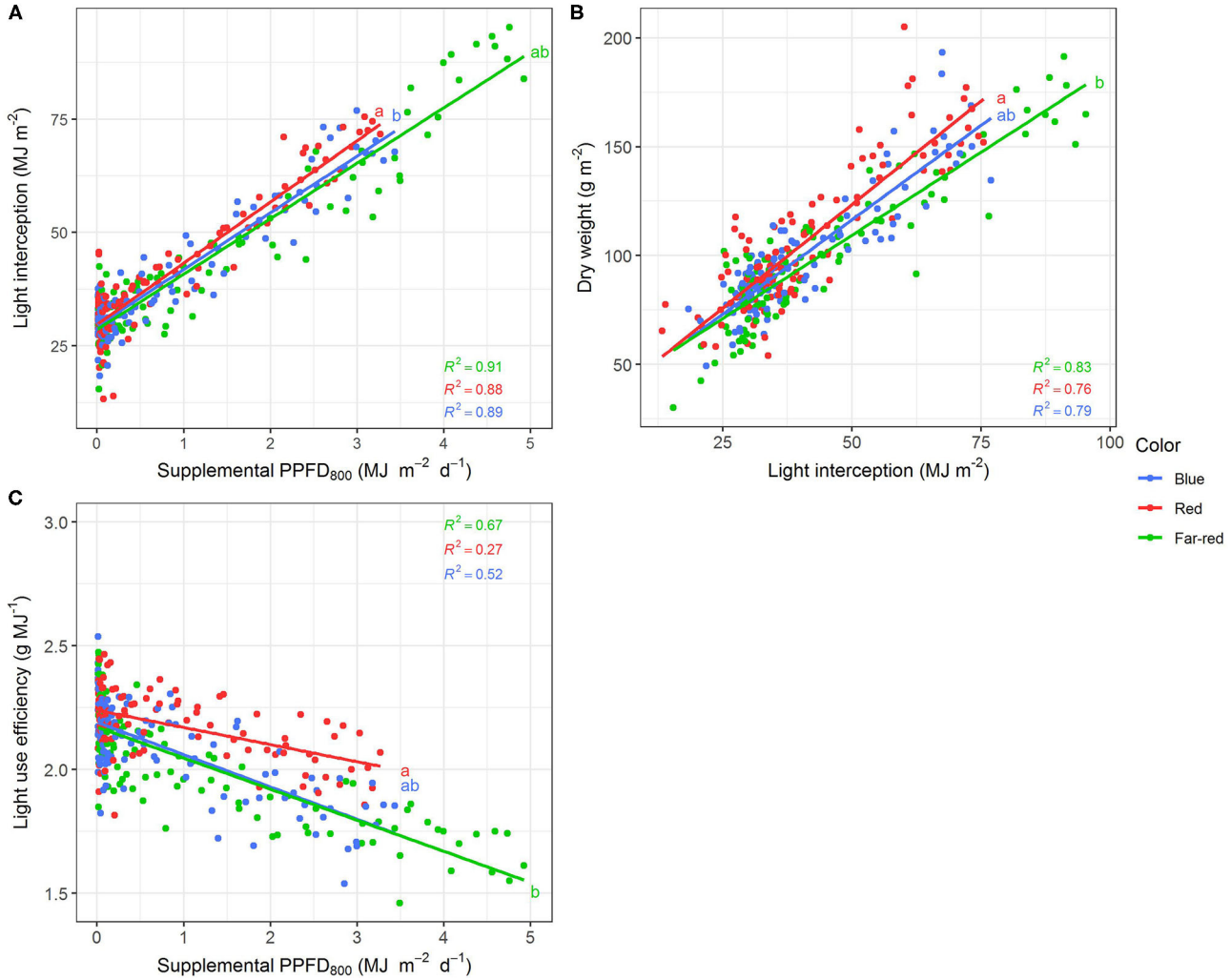

FIGURE 8 | Effect of supplemental $PPFD_{800}$ (400–800 nm) with different spectra on light interception **(A)**, dry weight **(B)** and light use efficiency **(C)** of *Ocimum basilicum* L. cv. "Edwina" cultivated under greenhouse conditions. Different lower-case letters indicate significant differences in slopes between colors ($p < 0.05$). Linear regression lines of each light color are indicated. Regressions are based on 120 plants per treatment, each with a specific light dose. Each data point shows an average of the four seasons, two harvest points and two experimental repetitions.

2014, 2016; Kaiser et al., 2019; Larsen et al., 2020) and radiation capture rather than changes in net-assimilation per unit leaf area (Snowden et al., 2016). In our study, however, the lower biomass of plants grown under blue LEDs appears to be mainly a result of the lower LUE instead of effects on light capture even though light interception was quite low as well. Although blue light is essential for proper functioning of photosynthesis (Hogewoning et al., 2010; Trouwborst et al., 2016), it is less efficiently used for photosynthesis in leaves (McCree, 1972; Hogewoning et al., 2012). The low LUE was accompanied by a low LMA under blue light. Increasing proportions of blue light are usually associated with the development of sun-type leaf characteristics with high LMA and high photosynthetic capacity (e.g., Buschmann et al., 1978; Lichtenthaler et al., 1980; Matsuda et al., 2008; Kaiser et al., 2019). However, increasing proportions of blue light did not affect LMA in rice (Ohashi-Kaneko et al., 2006) and basil (Larsen et al., 2020). Hence, the low LMA likely explains the lower light utilization by the leaves. The aforementioned train of thought that the observed changes in LUE are related to altered leaf morphology that affect leaf photosynthetic capacity

(Oguchi et al., 2003), and in our case that the low LMA may explain the lower LUE under blue light, is consistent with the observed increase in LMA and LUE in the far-red light treatment. Increasing LMA was previously associated with a higher far-red fraction in the light source (Dörr et al., 2020) and increasing far-red light dose (Larsen et al., 2020) in basil although an opposite response toward an increase in far-red photons or lowered R/FR was reported in other species (Kalaitzoglou et al., 2019; Zou et al., 2019).

Importance of Seasonality on Supplemental LED Lighting Effects

The variation in solar DLI (**Table 1**) mainly explains the observed seasonal differences in growth and morphology. Plants grown in winter were not only significantly shorter, but also had lower leaf area and weight compared to plants cultivated in summer which can be explained by reduced rates of photosynthesis (Chang et al., 2008; Dou et al., 2018). Dou et al. (2018) suggested a DLI of 12.9 mol m^{-2} d^{-1} for optimal commercial production of basil in indoor farming. This suggests that the summer sets were operating largely under light saturation, explaining the lack of differences between the two sets. Temperature was likely the most important factor for variation in LMA. It has been demonstrated that a decrease in LMA is a common response to elevated temperature (Poorter et al., 2009a,b; Poorter et al., 2010) which was observed in basil as well (Chang et al., 2005; Walters and Currey, 2019). The seasonal variation in dry mass production in our trials was rather a consequence of changes in DLI than of light utilization efficiency, as it could be expected from the decreased LMA. The altered plant architecture was more favorable for light interception and whole-canopy photosynthesis (Buck-Sorlin et al., 2011; Sarlikioti et al., 2011; Song et al., 2013; Chen et al., 2014).

Impact of Supplemental $PPFD_{800}$ Under Solar Radiation

Latest studies revised the Emerson enhancement effect (Emerson et al., 1957) showing that far-red photons have positive, synergetic effects on photosynthesis in combination with shorter wavelength (Hogewoning et al., 2012; Zhen and van Iersel, 2017; Murakami et al., 2018; Zhen et al., 2018; Kono et al., 2020). Besides the positive effect on photosynthesis it was even demonstrated that far-red photons have equal photon efficiency in combination with shorter wavelengths (Zhen and Bugbee, 2020a) and it was thus suggested that far-red photons (701–750 nm) should be included in the definition of PAR (Zhen and Bugbee, 2020a,b). As it is to be expected, efficiencies in the far-red treatment decreased considerably when growth and morphological traits were related to $PPFD_{800}$ instead of $PPFD_{700}$ as the amount of total photons was far greater in the far-red light regime compared to the others. Parameters associated with photosynthesis such as dry weight, LMA, biomass partitioning and LUE were particularly affected. Hence, for future investigations it would be interesting to compare efficiencies of different light regimes with the same $PPFD_{800}$.

Perspectives and Implications of the Efficiency of Supplemental LED Lighting for Future Applications

Greenhouse production in northern latitudes is mainly limited by low incident light and short photoperiods during winter. Thus, supplemental lighting has been used to enable a year-round production of crops (Davis and Burns, 2016). Our results add to this demonstrating that the efficiency of supplemental LED lighting is significantly affected by seasonal variations. Efficiencies were significantly higher during low light conditions (Late Winter and Mid Spring) compared to high light conditions (Early and Late Summer) and associated with changes in the ratio of supplemental to natural light. A more precise application of supplemental lighting taking SL/NL into account may contribute to energy saving and cost-reduction during greenhouse cultivation under solar radiation. Hence, we suggest that it may be used as an indicator to assess and evaluate supplemental lighting effects under solar background radiation, and would allow a better comparison among research studies.

CONCLUSIONS

The present study demonstrated that there are striking differences in the efficiencies among light qualities highlighting the importance of the choice of the light color during greenhouse production and the plants strategy to cope with the growing environment. Plant responses to the different light qualities were mainly associated with two adaptation strategies: increased light interception due to a plant architecture more favorable for light capture under red light and changed LUE due to altered leaf morphology under far-red light. Blue light was the least efficient color in affecting plant growth and morphology. However, efficiencies were significantly reduced when $PPFD_{800}$ was considered instead of $PPFD_{700}$. Furthermore, our results underline the significance of the natural growth environment (seasons) on the efficiency of supplemental LED lighting as indicated by the altered efficiencies with changing natural light conditions. Seasonal changes in biomass production were attributed to increased light interception due to altered crop architecture more favorable for light absorption rather than changes in light use efficiency. Finally, it is suggested that the ratio of supplemental to natural light is a good indicator to quantitatively evaluate plant responses to supplemental LED lighting during greenhouse production throughout the year.

DATA AVAILABILITY STATEMENT

The raw data supporting the conclusions of this article will be made available by the authors, without undue reservation.

AUTHOR CONTRIBUTIONS

This study was designed by JS, AF, and HS. JS acquired the data, performed the analyses, drafted the manuscript, and discussed with AF and HS. All authors revised the article and approved the final version to be submitted.

FUNDING

This work was funded by the Ministry of Food, Agriculture, and Consumer Protection of Lower Saxony, Germany.

ACKNOWLEDGMENTS

The authors are grateful to Ulrich Hering for his technical assistance during the experimental setup, Dr. Frank Schaarschmidt for his help with the statistical analysis and Abdallah Medini, Moritz Nickels, Asha Devcota, and Seyed Mahdi Nezam Abadi for their assistance during peaks of workload. The authors thank Leibniz University Hannover's Open Access Publishing Fund for covering the publication cost.

SUPPLEMENTARY MATERIAL

The Supplementary Material for this article can be found online at: https://www.frontiersin.org/articles/10.3389/fpls.2021.609975/full#supplementary-material

REFERENCES

Banaś, A. K., Aggarwal, C., Łabuz, J., Sztatelman, O., and Gabryś, H. (2012). Blue light signalling in chloroplast movements. *J. Exp. Bot*. 63, 1559–1574. doi: 10.1093/jxb/err429

Bates, D., Mächler, M., Bolker, B., and Walker, S. (2015). Fitting linear mixed-effects models using lme4. *J. Stat. Softw*. 67, 1–48. doi: 10.18637/jss.v067.i01

Bergstrand, K.-J., and Schüssler, H. K. (2013). Growth, development and photosynthesis of some horticultural plants as affected by different supplementary lighting technologies. *Europ. J. Hort. Sci*. 78, 119–125.

Buck-Sorlin, G., Visser, P. H. B., Henke, M., Sarlikioti, V., van der Heijden, G. W. A. M., Marcelis, L. F. M., et al. (2011). Towards a functional-structural plant model of cut-rose: simulation of light environment, light absorption, photosynthesis and interference with the plant structure. *Ann. Bot*. 108, 1121–1134. doi: 10.1093/aob/mcr190

Buschmann, C., Meier, D., Kleudgen, H. K., and Lichtenthaler, H. K. (1978). Regulation of chloroplast development by red and blue light. *Photochem. Photobiol*. 27, 195–198. doi: 10.1111/j.1751-1097.1978.tb07587.x

Chang, X., Alderson, P. G., and Wright, C. J. (2005). Effect of temperature integration on the growth and volatile oil content of basil (*Ocimum basilicum* L.). *J. Hortic. Sci. Biotechnol*. 80, 593–598. doi: 10.1080/14620316.2005.11511983

Chang, X., Alderson, P. G., and Wright, C. J. (2008). Solar irradiance level alters the growth of basil (*Ocimum basilicum* L.) and its content of volatile oils. *Environ. Exp. Bot*. 63, 216–223. doi: 10.1016/j.envexpbot.2007.10.017

Chen, T. W., Nguyen, T. M., Kahlen, K., and Stützel, H. (2014). Quantification of the effects of architectural traits on dry mass production and light interception of tomato canopy under different temperature regimes using a dynamic functional-structural plant model. *J. Exp. Bot*. 65, 6399–6410. doi: 10.1093/jxb/eru356

Davis, P. A., and Burns, C. (2016). Photobiology in protected horticulture. *Food Energy Secur*. 5, 223–238. doi: 10.1002/fes3.97

Dörr, O. S., Brezina, S., Rauhut, D., and Mibus, H. (2020). Plant architecture and phytochemical composition of basil (*Ocimum basilicum* L.) under the influence of light from microwave plasma and high-pressure sodium lamps. *J. Photochem. Photobiol. B*. 202:111678. doi: 10.1016/j.jphotobiol.2019.111678

Dou, H., Niu, G., Gu, M., and Masabni, J. (2018). Responses of sweet basil to different daily light integrals in photosynthesis, morphology, yield, and nutritional quality. *HortScience* 53, 496–503. doi: 10.21273/HORTSCI12785-17

Emerson, R., Chalmers, R., and Cederstrand, C. (1957). Some factors influencing the long-wave limit of photosynthesis. *Proc. Natl. Acad. Sci. U.S.A*. 43, 133–143. doi: 10.1073/pnas.43.1.133

Franklin, K. A. (2008). Shade avoidance. *New Phytol*. 179, 930–944. doi: 10.1111/j.1469-8137.2008.02507.x

Franklin, K. A., and Whitelam, G. C. (2005). Phytochromes and shade-avoidance responses in plants. *Ann. Bot*. 96, 169–175. doi: 10.1093/aob/mci165

Frechilla, S., Talbott, L. D., Bogomolni, R. A., and Zeiger, E. (2000). Reversal of blue light-stimulated stomatal opening by green light. *Plant Cell Physiol*. 41, 171–176. doi: 10.1093/pcp/41.2.171

Goins, G. D., Yorio, N. C., Sanwo, M. M., and Brown, C. S. (1997). Photomorphogenesis, photosynthesis, and seed yield of wheat plants grown under red light-emitting diodes (LEDs) with and without supplemental blue lighting. *J. Exp. Bot*. 48, 1407–1413. doi: 10.1093/jxb/48.7.1407

Goto, E. (2003). Effects of light quality on growth of crop plants under artificial lighting. *Environ. Control Biol*. 41, 121–132. doi: 10.2525/ecb1963.41.121

Hemming, S. (2011). Use of natural and artificial light in horticulture - Interaction of plant and technology. *Acta Hortic*. 907, 25–35. doi: 10.17660/ActaHortic.2011.907.1

Heo, J., Lee, C., Chakrabarty, D., and Paek, K. (2002). Growth responses of marigold and salvia bedding plants as affected by monochromic or mixture radiation provided by a light-emitting diode (LED). *Plant Growth Regul*. 38, 225–230. doi: 10.1023/A:1021523832488

Hernández, R., and Kubota, C. (2012). Tomato seedling growth and morphological responses to supplemental LED lighting red:blue ratios under varied daily solar light integrals. *Acta Hortic*. 956, 187–194. doi: 10.17660/ActaHortic.2012.956.19

Hernández, R., and Kubota, C. (2014). Growth and morphological response of cucumber seedlings to supplemental red and blue photon flux ratios under varied solar daily light integrals. *Sci. Hortic*. 173, 92–99. doi: 10.1016/j.scienta.2014.04.035

Hernández, R., and Kubota, C. (2016). Physiological responses of cucumber seedlings under different blue and red photon flux ratios using LEDs. *Environ. Exp. Bot*. 121, 66–74. doi: 10.1016/j.envexpbot.2015.04.001

Hoenecke, M. E., Bula, R. J., and Tibbitts, T. W. (1992). Importance of "blue" photon levels for lettuce seedlings grown under red-light-emitting diodes. *HortScience* 27, 427–430. doi: 10.21273/HORTSCI.27.5.427

Hogewoning, S. W., Trouwborst, G., Maljaars, H., Poorter, H., van Ieperen, W., and Harbinson, J. (2010). Blue light dose-responses of leaf photosynthesis, morphology, and chemical composition of *Cucumis sativus* grown under different combinations of red and blue light. *J. Exp. Bot*. 61, 3107–3117. doi: 10.1093/jxb/erq132

Hogewoning, S. W., Wientjes, E., Douwstra, P., Trouwborst, G., van Ieperen, W., Croce, R., et al. (2012). Photosynthetic quantum yield dynamics: from photosystems to leaves. *Plant Cell* 24, 1921–1935. doi: 10.1105/tpc.112.097972

Islam, M. A., Kuwar, G., Clarke, J. L., Blystad, D. R., Gislerød, H. R., Olsen, J. E., et al. (2012). Artificial light from light emitting diodes (LEDs) with a high portion of blue light results in shorter poinsettias compared to high pressure sodium (HPS) lamps. *Sci. Hortic*. 147, 136–143. doi: 10.1016/j.scienta.2012.08.034

Izzo, L. G., Hay Mele, B., Vitale, L., Vitale, E., and Arena, C. (2020). The role of monochromatic red and blue light in tomato early photomorphogenesis and photosynthetic traits. *Environ. Exp. Bot*. 179:104195. doi: 10.1016/j.envexpbot.2020.104195

Johnson, R. E., Kong, Y., and Zheng, Y. (2020). Elongation growth mediated by blue light varies with light intensities and plant species: a comparison with red light in arugula and mustard seedlings. *Environ. Exp. Bot*. 169:103898. doi: 10.1016/j.envexpbot.2019.103898

Kaiser, E., Ouzounis, T., Giday, H., Schipper, R., Heuvelink, E., and Marcelis, L. F. M. (2019). Adding blue to red supplemental light increases biomass and yield of

greenhouse-grown tomatoes, but only to an optimum. *Front. Plant Sci*. 9:2002. doi: 10.3389/fpls.2018.02002

Kalaitzoglou, P., van Ieperen, W., Harbinson, J., van der Meer, M., Martinakos, S., Weerheim, K., et al. (2019). Effects of continuous or end-of-day far-red light on tomato plant growth, morphology, light absorption, and fruit production. *Front. Plant Sci*. 10:322. doi: 10.3389/fpls.2019.00322

Kong, Y., Stasiak, M., Dixon, M. A., and Zheng, Y. (2018). Blue light associated with low phytochrome activity can promote elongation growth as shade-avoidance response: a comparison with red light in four bedding plant species. *Environ. Exp. Bot*. 155, 345–359. doi: 10.1016/j.envexpbot.2018.07.021

Kono, M., Kawaguchi, H., Mizusawa, N., Yamori, W., Suzuki, Y., and Terashima, I. (2020). Far-red light accelerates photosynthesis in the low-light phases of fluctuating light. *Plant Cell Physiol*. 61, 192–202. doi: 10.1093/pcp/pcz191

Larsen, D. H., Woltering, E. J., Nicole, C. C. S., and Marcelis, L. F. M. (2020). Response of basil growth and morphology to light intensity and spectrum in a vertical farm. *Front. Plant Sci*. 11:597906. doi: 10.3389/fpls.2020.597906

Lenth, R. (2020). *emmeans: Estimated Marginal Means, aka Least-Squares Means*. R packageversion 1.4.5. Available online at: https://CRAN.R-project.org/package=emmeans

Lichtenthaler, H., Buschmann, C., and Rahmsdorf, U. (1980). "The importance of blue light for the development of sun-type chloroplasts," in *The Blue Light Syndrome*, ed. H. Senger (Berlin: Springer-Verlag), 485–494.

Matsuda, R., Ohashi-Kaneko, K., Fujiwara, K., and Kurata, K. (2008). Effects of blue light deficiency on acclimation of light energy partitioning in PSII and CO_2 assimilation capacity to high irradiance in spinach leaves. *Plant Cell Physiol*. 49, 664–670. doi: 10.1093/pcp/pcn041

McCree, K. J. (1972). The action spectrum, absorptance and quantum yield of photosynthesis in crop plants. *Agric. Meteorol*. 9, 191–216. doi: 10.1016/0002-1571(71)90022-7

McMaster, G. S., and Wilhelm, W. W. (1997). Growing degree-days: one equation, two interpretations. *Agric. For. Meteorol*. 87, 291–300. doi: 10.1016/S0168-1923(97)00027-0

Monsi, M., and Saeki, T. (2005). On the factor light in plant communities and its importance for matter production. *Ann. Bot*. 95, 549–567. doi: 10.1093/aob/mci052

Morgan, D. C., and Smith, H. (1979). A systematic relationship between phytochrome-controlled development and species habitat for plants grown in simulated natural radiation. *Planta*. 145, 253–258. doi: 10.1007/BF00454449

Murakami, K., Matsuda, R., and Fujiwara, K. (2018). A mathematical model of photosynthetic electron transport in response to the light spectrum based on excitation energy distributed to photosystems. *Plant Cell Physiol*. 59, 1643–1651. doi: 10.1093/pcp/pcy085

Oguchi, R., Hikosaka, K., and Hirose, T. (2003). Does the photosynthetic light-acclimation need change in leaf anatomy? *Plant Cell Environ*. 26, 505–512. doi: 10.1046/j.1365-3040.2003.00981.x

Ohashi-Kaneko, K., Matsuda, R., Goto, E., Fujiwara, K., and Kurata, K. (2006). Growth of rice plants under red light with or without supplemental blue light. *Soil Sci. Plant Nutr*. 52, 444–452. doi: 10.1111/j.1747-0765.2006.00063.x

Ouzounis, T., Heuvelink, E., Ji, Y., Schouten, H. J., Visser, R. G. F., and Marcelis, L. F. M. (2016). Blue and red LED lighting effects on plant biomass, stomatal conductance, and metabolite content in nine tomato genotypes. *Acta Hortic*. 1134, 251–258. doi: 10.17660/ActaHortic.2016.1134.34

Poorter, H., Niinemets, U., Poorter, L., Wright, I. J., and Villar, R. (2009a). Causes and consequences of variation in leaf mass per area (LMA): a meta-analysis. *New Phytol*. 182, 565–588. doi: 10.1111/j.1469-8137.2009.02830.x

Poorter, H., Niinemets, U., Poorter, L., Wright, I. J., and Villar, R. (2009b). Causes and consequences of variation in leaf mass per area (LMA): a meta-analysis. *Erratum. New Phytol*. 183:1222.

Poorter, H., Niinemets, U., Walter, A., Fiorani, F., and Schurr, U. (2010). A method to construct dose-response curves for a wide range of environmental factors and plant traits by means of a meta-analysis of phenotypic data. *J. Exp. Bot*. 61, 2043–2055. doi: 10.1093/jxb/erp358

R Core Team. (2020). *R: A Language and Environment for Statistical Computing*. Vienna: R Foundation for Statistical Computing.

RStudio Team. (2016). *RStudio: Integrated Development for R*. RStudio, Inc., Boston, MA.

Sarlikioti, V., de Visser, P. H. B., Buck-Sorlin, G. H., and Marcelis, L. F. M. (2011). How plant architecture affects light absorption and photosynthesis in tomato: towards an ideotype for plant architecture using a functional-structural plant model. *Ann. Bot*. 108, 1065–1073. doi: 10.1093/aob/mcr221

Shimazaki, K., Doi, M., Assmann, S. M., and Kinoshita, T. (2007). Light regulation of stomatal movement. *Annu. Rev. Plant Biol*. 58, 219–247. doi: 10.1146/annurev.arplant.57.032905.105434

Smith, H. (1982). Light quality, photoperception, and plant strategy. *Ann. Rev. Plant Physiol*. 33, 481–518. doi: 10.1146/annurev.pp.33.060182.002405

Smith, H. L., McAusland, L., and Murchie, E. H. (2017). Don't ignore the green light: exploring diverse roles in plant processes. *J. Exp. Bot*. 68, 2099–2110. doi: 10.1093/jxb/erx098

Snowden, M. C., Cope, K. R., and Bugbee, B. (2016). Sensitivity of seven diverse species to blue and green light: interactions with photon flux. *PLoS One* 11:e0163121. doi: 10.1371/journal.pone.0163121

Song, Q., Zhang, G., and Zhu, X.-G. (2013). Optimal crop canopy architecture to maximise canopy photosynthetic CO_2 uptake under elevated CO_2 - a theoretical study using a mechanistic model of canopy photosynthesis. *Funct. Plant Biol*. 40, 109–124. doi: 10.1071/FP12056

Talbott, L. D., Hammad, J. W., Harn, L. C., Nguyen, V. H., Patel, J., and Zeiger, E. (2006). Reversal by green light of blue light-stimulated stomatal opening in intact, attached leaves of Arabidopsis operates only in the potassium-dependent, morning phase of movement. *Plant Cell Physiol*. 47, 332–339. doi: 10.1093/pcp/pci249

Talbott, L. D., Nikolova, G., Ortiz, A., Shmayevich, I., and Zeiger, E. (2002). Green light reversal of blue-light-stimulated stomatal opening is found in a diversity of plant species. *Am. J. Bot*. 89, 366–368. doi: 10.3732/ajb.89.2.366

Terashima, I., Fujita, T., Inoue, T., Chow, W. S., and Oguchi, R. (2009). Green light drives leaf photosynthesis more efficiently than red light in strong white light: revisiting the enigmatic question of why leaves are green. *Plant Cell Physiol*. 50, 684–697. doi: 10.1093/pcp/pcp034

Thimijan, R., and Heins, R. (1983). Photometric, radiometric, and quantum light units of measure: a review of procedures for interconversion. *HortScience* 18, 818–822.

Trouwborst, G., Hogewoning, S. W., van Kooten, O., Harbinson, J., and van Ieperen, W. (2016). Plasticity of photosynthesis after the 'red light syndrome' in cucumber. *Environ. Exp. Bot*. 121, 75–82. doi: 10.1016/j.envexpbot.2015.05.002

Vandenbussche, F., Pierik, R., Millenaar, F. F., Voesenek, L. A., and Van Der Straeten, D. (2005). Reaching out of the shade. *Curr. Opin. Plant Biol*. 8, 462–468. doi: 10.1016/j.pbi.2005.07.007

Walters, K., and Currey, C. (2019). Growth and development of basil species in response to temperature. *HortScience* 54, 1915–1920. doi: 10.21273/HORTSCI12976-18

Yorio, N. C., Goins, G. D., Kagie, H. R., Wheeler, R. M., and Sager, J. C. (2001). Improving spinach, radish, and lettuce growth under red light-emitting diodes (LEDs) with blue light supplementation. *HortScience* 36, 380–383. doi: 10.21273/HORTSCI.36.2.380

Zhen, S., and Bugbee, B. (2020a). Far-red photons have equivalent efficiency to traditional photosynthetic photons: Implications for redefining photosynthetically active radiation. *Plant Cell Environ*. 43, 1259–1272. doi: 10.1111/pce.13730

Zhen, S., and Bugbee, B. (2020b). Substituting far-red for traditionally defined photosynthetic photons results in equal canopy quantum yield for CO2 fixation and increased photon capture during long-term studies: Implications for re-defining PAR. *Front. Plant Sci*. 11:581156. doi: 10.3389/fpls.2020.581156

Zhen, S., Haidekker, M., and van Iersel, M. W. (2018). Far-red light enhances photochemical efficiency in a wavelength-dependent manner. *Physiol. Plant*. 167, 21–33. doi: 10.1111/ppl.12834

Zhen, S., and van Iersel, M. W. (2017). Far-red light is needed for efficient photochemistry and photosynthesis. *J. Plant Physiol*. 209, 115–122. doi: 10.1016/j.jplph.2016.12.004

Zou, J., Zhang, Y., Zhang, Y., Bian, Z., Fanourakis, D., Yang, Q., et al. (2019). Morphological and physiological properties

of indoor cultivated lettuce in response to additional far-red light. *Sci. Hortic.* 257:108725. doi: 10.1016/j.scienta.2019.108725

Conflict of Interest: The authors declare that the research was conducted in the absence of any commercial or financial relationships that could be construed as a potential conflict of interest.

Copyright © 2021 Solbach, Fricke and Stützel. This is an open-access article distributed under the terms of the Creative Commons Attribution License (CC BY). The use, distribution or reproduction in other forums is permitted, provided the original author(s) and the copyright owner(s) are credited and that the original publication in this journal is cited, in accordance with accepted academic practice. No use, distribution or reproduction is permitted which does not comply with these terms.

frontiers in Plant Science

SYSTEMATIC REVIEW
published: 29 April 2021
doi: 10.3389/fpls.2021.596927

Supplemental LED Lighting Effectively Enhances the Yield and Quality of Greenhouse Truss Tomato Production: Results of a Meta-Analysis

Elisa Appolloni[1], *Francesco Orsini*[1]*, *Giuseppina Pennisi*[1], *Xavier Gabarrell Durany*[2,3], *Ivan Paucek*[1] *and Giorgio Gianquinto*[1]

[1] DISTAL – Department of Agricultural and Food Sciences, Alma Mater Studiorum – Università di Bologna, Bologna, Italy, [2] María de Maeztu Unit of Excellence, Institut de Ciència i Tecnologia Ambientals (ICTA-UAB), Universitat Autònoma de Barcelona, Barcelona, Spain, [3] Chemical, Biological and Environmental Engineering Department, Universitat Autònoma de Barcelona, Barcelona, Spain

OPEN ACCESS

Edited by:
Bernard Grodzinski, University of Guelph, Canada

Reviewed by:
Mark Lefsrud, McGill University, Canada
Jason Lanoue, Agriculture and Agri-Food Canada (AAFC), Canada

***Correspondence:**
Francesco Orsini
f.orsini@unibo.it

Specialty section:
This article was submitted to Crop and Product Physiology, a section of the journal Frontiers in Plant Science

Received: *20 August 2020*
Accepted: *06 April 2021*
Published: *29 April 2021*

Citation:
Appolloni E, Orsini F, Pennisi G, Gabarrell Durany X, Paucek I and Gianquinto G (2021) Supplemental LED Lighting Effectively Enhances the Yield and Quality of Greenhouse Truss Tomato Production: Results of a Meta-Analysis. Front. Plant Sci. 12:596927. doi: 10.3389/fpls.2021.596927

Intensive growing systems used for greenhouse tomato production, together with light interception by cladding materials or other devices, may induce intracanopy mutual shading and create suboptimal environmental conditions for plant growth. There are a large number of published peer-reviewed studies assessing the effects of supplemental light-emitting diode (LED) lighting on improving light distribution in plant canopies, increasing crop yields and producing qualitative traits. However, the research results are often contradictory, as the lighting parameters (e.g., photoperiod, intensity, and quality) and environmental conditions vary among conducted experiments. This research presents a global overview of supplemental LED lighting applications for greenhouse tomato production deepened by a meta-analysis aimed at answering the following research question: does supplemental LED lighting enhance the yield and qualitative traits of greenhouse truss tomato production? The meta-analysis was based on the differences among independent groups by comparing a control value (featuring either background solar light or solar + HPS light) with a treatment value (solar + supplemental LED light or solar + HPS + supplemental LED light, respectively) and included 31 published papers and 100 total observations. The meta-analysis results revealed the statistically significant positive effects (p-value < 0.001) of supplemental LED lighting on enhancing the yield (+40%), soluble solid (+6%) and ascorbic acid (+11%) contents, leaf chlorophyll content (+31%), photosynthetic capacity (+50%), and leaf area (+9%) compared to the control conditions. In contrast, supplemental LED lighting did not show a statistically significant effect on the leaf stomatal conductance (p-value $= 0.171$). In conclusion, in addition to some partial inconsistencies among the considered studies, the present research enables us to assert that supplemental LED lighting ameliorates the quantitative and qualitative aspects of greenhouse tomato production.

Keywords: supplemental light, LED, greenhouse, *Solanum lycopersicum*, interlighting

INTRODUCTION

In greenhouse tomato (*Solanum lycopersicum*) production, photosynthesis and carbon sequestration may be hindered by cloud cover, shading systems, and variable solar radiation, as well as by plant mutual shading (e.g., when high vertical stem training or increased crop densities are used) (Zhang et al., 2015; Tewolde et al., 2018). Considering the non-uniform distribution of solar radiation around the world, limitations may also occur in cases of high-latitude countries such as Canada, Japan, Norway, as well as in the northern areas of China and the United States, where long winters and low DLIs (daily light integrals) may affect greenhouse production (Garland et al., 2010; Deram et al., 2014; Sun et al., 2015; Tewolde et al., 2016; Paponov et al., 2019). Supplemental artificial lighting can be applied to increase greenhouse yields and ensure stable year-round production regardless of environmental conditions (Ohashi-Kaneko et al., 2007), even in regions with high DLIs, such as the Mediterranean and Jordan Valley (Israel) (Joshi et al., 2019; Paucek et al., 2020). Today, light-emitting diode (LED) lamps represent the most advantageous artificial lighting systems in terms of energy use efficiency, with foreseen expectations for further reducing investments and running costs in the near future (Olle and Viršile, 2013). Additional advantages also involve the functional aspects of LEDs that make the technology suitable for cultivation, particularly thanks to their possible miniaturization, light weight, and limited radiant heat emissions (Ibaraki, 2017). Accordingly, LED lamps can be used in proximity to plant canopies without excessively increasing the leaf temperature (Morrow, 2008), enabling inter-lighting applications that reduce intracanopy shading conditions in high-stem-density plants (Jokinen et al., 2012, Gómez and Mitchell, 2016a; Kumar et al., 2016; Hao et al., 2017).

LED application can enable the fine tuning of combinations between light spectral compositions and light intensities, with direct consequences not only on yield but also on structural and physiological plant aspects (Ouzounis et al., 2015; Hao et al., 2017; Ibaraki, 2017). In fact, the responses of plants to light characteristics are regulated by photoreceptors that reading specific wavelengths, intensities or photoperiods can trigger signals that modify plant metabolism (Christie et al., 2015). Accordingly, light environmental management can lead to interesting commercial results. For instance, red light can promote flower development (Liao et al., 2014), while the blue-violet spectrum can increase plant protection from diseases (Tokuno et al., 2012; Hui et al., 2017), preserving postharvest conservation and food safety through the inactivation of pathogen action (D'Souza et al., 2015). Moreover, specific light spectra can improve the qualitative and nutraceutical aspects of plants (Mempel and Wittmann, 2019), such as enhancing antioxidant compound biosynthesis (e.g., flavonoids, ascorbic acid) in various species (e.g., lettuce, basil, tomato) (Ebisawa et al., 2008; Carvalho et al., 2016; Jiang et al., 2017; Pennisi et al., 2019a,b).

Stomatal conductance is a specific physiological response that is guided by light. The wavelength mainly involved in this process is blue light (450 and 495 n), which is also implicated in other mechanisms, such as phototropism, chloroplast migration, photomorphogenesis, and chlorophyll production (O'Carrigan et al., 2014b). Cryptochromes and phototropins are the main photoreceptors stimulated by blue light (Christie et al., 2015); these photoreceptors go through a phosphorylation process and bind protein to trigger proton extrusion and K^+ uptake in stomatal guard cells, with the consequent cell turgidity and stomatal opening enabling gas exchange (Roelfsema and Hedrich, 2005: Shimazaki et al., 2007). Apparently, green and red light may also play roles in gas exchange by inducing stomatal closure, as green light may stop soluble uptake in guard cells (Talbott et al., 2002), while red light may lead to K^+ and solute losses (Zeiger, 1990). In tomato plants, studies that have applied blue, red, and green lighting in closed chambers seem to confirm such observations (O'Carrigan et al., 2014b; Bian et al., 2019), opening the possibility of integrating green LED lighting to reduce drought stress in tomato plants (Bian et al., 2019). However, it is important to consider that what is observed in growing chamber experiments is not always transferable to the processes occurring in productive systems, where different environmental factors may affect plant responses.

Greenhouse tomatoes represent one of the most relevant horticultural crops worldwide (Deram et al., 2014; FAO, 2018). In intensive greenhouse tomato production, high-wire single-truss training systems are normally applied to enable labor reductions, multiple harvests and possible automation (Giniger et al., 1988; Okano et al., 2001). Nonetheless, the high plant density required for these systems can limit light penetration within canopies with consequences on fruit quality and yield (Wada et al., 2006). In this context, several studies have already reported the usefulness of LED lighting system applications for qualitative and quantitative improvements in greenhouse truss tomato production (Tewolde et al., 2016; Dzakovich et al., 2017; Jiang et al., 2017; Kim et al., 2019). However, inconsistencies among studies are also present; non-significant effects of supplemental LED lighting, especially on qualitative parameters (e.g., soluble solids, ascorbic acid) (Lu et al., 2012b; Hao et al., 2016), have been found. In most studies to date, researchers have integrated supplemental LED lighting technologies either in greenhouses where no supplemental lighting was formerly present or as additional lighting sources in greenhouses where top artificial lights (e.g., high-pressure sodium lights, HPSs, lamps) were already installed and in operation. Accordingly, this study aims to offer an overview of the recent topic of supplemental LED lighting for greenhouse tomato production through the use of a meta-analysis as a statistical tool to summarize the results of published studies and understand the effectiveness of supplementary LED lighting in influencing the qualitative-quantitative aspects of truss tomatoes. Consequently, the meta-analysis aims to answer the following research question: does supplemental LED lighting enhance the yield and qualitative traits of greenhouse truss tomato production?

MATERIALS AND METHODS

Data Collection

Article collection was conducted during the first half of 2020 using online databases (e.g., Google Scholar and Scopus). The

following search string was applied to identify publications: LED *AND* supplemental light* *AND* tomato* *AND* greenhouse. Only accessible published material in the English language was collected, including scientific articles, conference papers, book chapters, and thesis dissertations. The literature search results were then filtered to reduce heterogeneity in the studies and to include only *Solanum lycopersicum* species cultivated in greenhouses with supplemental LED lighting or supplemental LED lighting combined with HPS lamps. All cultivar types, growing systems and greenhouse typologies were considered. Given that the presence of solar radiation was a requisite of the research question (targeting the effect of supplemental LEDs in greenhouses), studies of indoor cultivation in which only artificial lighting sources (e.g., indoor farming) were applied were not considered in the research. Overhead, intracanopy and bottom lighting supplies were all included, as well as nighttime, end-of-the-day, and continuous lighting treatments. Only one case of night-break lighting supply was excluded from the research (Cao et al., 2016). Furthermore, studies reporting evaluations on seedlings or transplants with short treatment periods were also excluded; only mature and productive plants were considered to accomplish the upstream objective of evaluating the qualitative and quantitative effects of supplemental LED lighting on tomato production.

The collected data included both general information related to trial conditions and more specific data used in the meta-analysis. In particular, the general data were represented by intrinsic or environmental trial features (cultivar, location, maximum and minimum temperatures, relative humidity, nutrient solution electrical conductivity (EC) and pH, plant density, greenhouse typology, and growing system), as well as by the LED treatment characteristics (light spectrum, intensity and photoperiod, treatment duration, and other eventual specific experimental conditions, e.g., nighttime treatments). All these general data were used in the descriptive statistical analysis and to identify factors of heterogeneity among different experiments during the meta-analysis. The natural lighting amount (e.g., DLI) was not considered due to the scarcity of articles reporting this information. The specific data referred to precise information that was needed for the development of the meta-analysis, including the treatment and control mean outcomes as well as the sample size (or replicate number, in cases in which the sample size was not available). Studies not reporting specific data were not used for the meta-analysis development. The outcomes, also called the effect sizes or response ratios [R] (Hedges et al., 1999), used in the meta-analysis consisted of the fresh fruit mass yield (yield, expressed as kg plant^{-1} of fresh fruit mass), soluble solid content (TSS, expressed as °Brix), ascorbic acid content (Asc, expressed as mg Asc 100 g^{-1} of fruit fresh weight), chlorophyll content (Chl, expressed as Chl index), net photosynthesis (PN, expressed as μmol CO_2 m^{-2} s^{-1}), stomatal conductance (g_s, expressed as mmol H_2O m^{-2} s^{-1}), and leaf area (LA, expressed as m^2 per plant). Only physiological and vegetative outcomes directly influencing tomato productivity and quality were considered, while other information (e.g., stem diameter, internode length) was not investigated. Outcome values were extracted from both tables and graphs, integrating textual information in cases of general descriptive data relative to the trials. **Figure 1** shows the flow diagram applied for the data selection and evaluation.

Meta-Analysis

The response ratio [R] considered in the meta-analysis was represented by the influence of supplemental LED lighting on the Yield, TSS, Asc, Chl, PN, g_s, and LA of greenhouse-grown tomato plants. Since each study accounted for more than one treatment, each trial was examined as a separate observation (k). Accordingly, each study could have more than one observation. For instance, if an article compared two different supplemental LED lighting treatments, one with a red spectrum and the other with a blue spectrum, each treatment was considered an individual observation. Each treatment value was compared with a control value from the same article to perform a meta-analysis based on the differences among independent groups. In the current study, the applied control treatment may be of two types: solar light only or solar light + HPS light. In the first case, the control was compared with solar light + supplemental LED light, while in the second case, the comparison involved solar light + HPS light + supplemental LED light. Only observations reporting a control, either with solar or solar + HPS light, were used for the meta-analysis after a second selection phase. In one case (Deram et al., 2014), the comparison between the control and treatment showed extremely high values compared to other results. In this case, the data were considered outliers and were excluded from the meta-analysis.

The [R] of each observation was calculated as follows:

$$\ln R = \ln (R) = \frac{\ln m_t}{\ln m_c} = \ln m_t \ \ln m_c$$

where m_t and m_c represent the mean outcomes of the treatment and control, respectively (Hedges et al., 1999; Borenstein et al., 2009). Since most of the considered publications did not display standard error (SE), variance (Var), or standard deviation (S) values, an unweighted meta-analysis was applied to equally weight each observation (McDaniel et al., 2014; Qin et al., 2015). The data were analyzed using the online available software Meta-Essential (Suurmond et al., 2017). A random effect model was chosen for each response value (Yield, TSS, Asc, Chl, PN, g_s, and LA). The heterogeneity value (I^2) was used to evaluate the percentage of variation among studies (Hak et al., 2016). Cases reporting I^2 values higher than 25% were further investigated by applying a subgroup analysis (Borenstein et al., 2009; Hak et al., 2016). The subgroup analysis divided the observations into six categories: solar light or solar light + HPS used as a control; pure supplemental LED light or supplemental LED light + HPS; artificial light supply (e.g., DLI ≥10 or <10 mol m^{-2} d^{-1}); seasonality (whether the hours of natural light were increasing, e.g., during spring in the Northern Hemisphere, or decreasing, e.g., during fall in Northern Hemisphere, along the experiment); photoperiod ≥16 or <16 h d^{-1}; lighting supplied as intracanopy or others. In the last case, "others" were intended to include overhead, bottom or combined lighting supplies, which were grouped together due to the low number of singular categories.

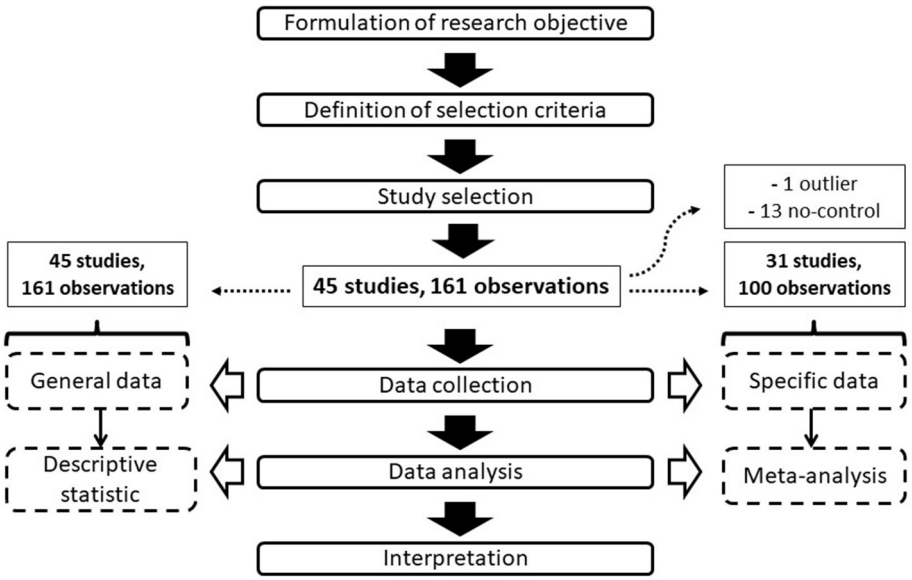

FIGURE 1 | Flow diagram showing the steps of the study selection and analysis.

Hedges' *g* was applied as the measurement of the effect size in the meta-analysis model. The [*R*] value was accepted as significant with a *p*-value < 0.05, considering a confidence interval (CI) of 95%. Since the results showed high heterogeneity, no publication bias analysis was performed, assuming its absence (Hak et al., 2016). A graphic representation of the study distribution per year and country was realized using Gephi software (Bastian et al., 2009) (**Figure 2**).

RESULTS

The literature search results are included in **Supplementary Material 1**, attached as an Excel file to the present manuscript. The preliminary literature search resulted in 45 studies following the selection criteria. These publications were used for the descriptive statistical analysis. The results showed that the majority of trials took place in North America, with 38% of the total cases (USA $n = 9$, Canada $n = 8$), while Europe (Netherlands $n = 8$, Norway $n = 3$, Poland $n = 2$, Belgium $n = 1$, Germany $n = 1$, and Italy $n = 1$) and Asia (Japan $n = 6$, China $n = 4$, and South Korea $n = 2$) reported frequencies of 35 and 27%, respectively. No cases were registered in other continents. No collected publication was released before 2011, and the collected studies showed the highest frequencies in 2019 (29%) and 2016 (18%) (**Figure 2**).

Although not always stated, most experiments were conducted in technologically advanced greenhouses applying soilless growing methods, and the studies often mentioned controlled environmental systems. When reported, the highest-frequency growing methods reported were substrate cultivation on slabs (61% of 36 cases reported this growing method). Slab materials were mainly represented by rockwool, although two cases of coir use were also reported. Pot employment was also registered, occurring for 22% of cited cases with sand, perlite, vermiculite or peat applied as growing substrates. The use of bags filled with substrate (peat, vermiculite or perlite) was also identified in 3 out of 36 cases. Finally, only two soil-based cultivation cases and one nutrient film technique (NFT) case were reported.

Concerning the planting density, the 45 studies showed a mean of ∼5 plants m^{-2}, a mode of 2.7 plants m^{-2} and a median of 2.7 plants m^{-2}, with values ranging from 1.5 to 16.6 plants m^{-2}. The average maximum and minimum temperatures were 23 and 19°C, respectively, while the average relative humidity was 69%. The applied nutrient solutions had a mean EC value of 2.4 dS m^{-1} and a mean pH value of 6. Different cultivars of truss tomato were used in the trials (33), and the highest recurrence was observed for *Solanum lycopersicum* cv Komeett (De Ruiter, Amstelveen, The Netherlands), which was mentioned in 10 publications.

In total, 161 supplemental LED lighting treatments were observed within the 45 collected publications. Of those treatments, 57% applied intracanopy LED lighting, 8% applied bottom lighting, 17% applied overhead lamps, 13% applied a combination of supply methods (e.g., intracanopy + overhead lighting), and 6% of cases did not clearly report the type of lighting supply. Furthermore, 20% of revised observations applied a combination of LED and HPS lighting as the supplemental treatment. Regarding the daily lighting duration, the mean photoperiod used was 15 h d^{-1}, while the mode and median durations were both 16 h d^{-1}. Within the collected literature, two extreme cases of 24 h of continuous lighting and 2 h of end-of-the-day lighting were also found. The average photosynthetic photon flux density (PPFD) and DLI supplied through lighting were also registered, showing values of 165 μmol m^{-2} s^{-1} and 9.5 mol m^{-2} d^{-1}, respectively, while the mode

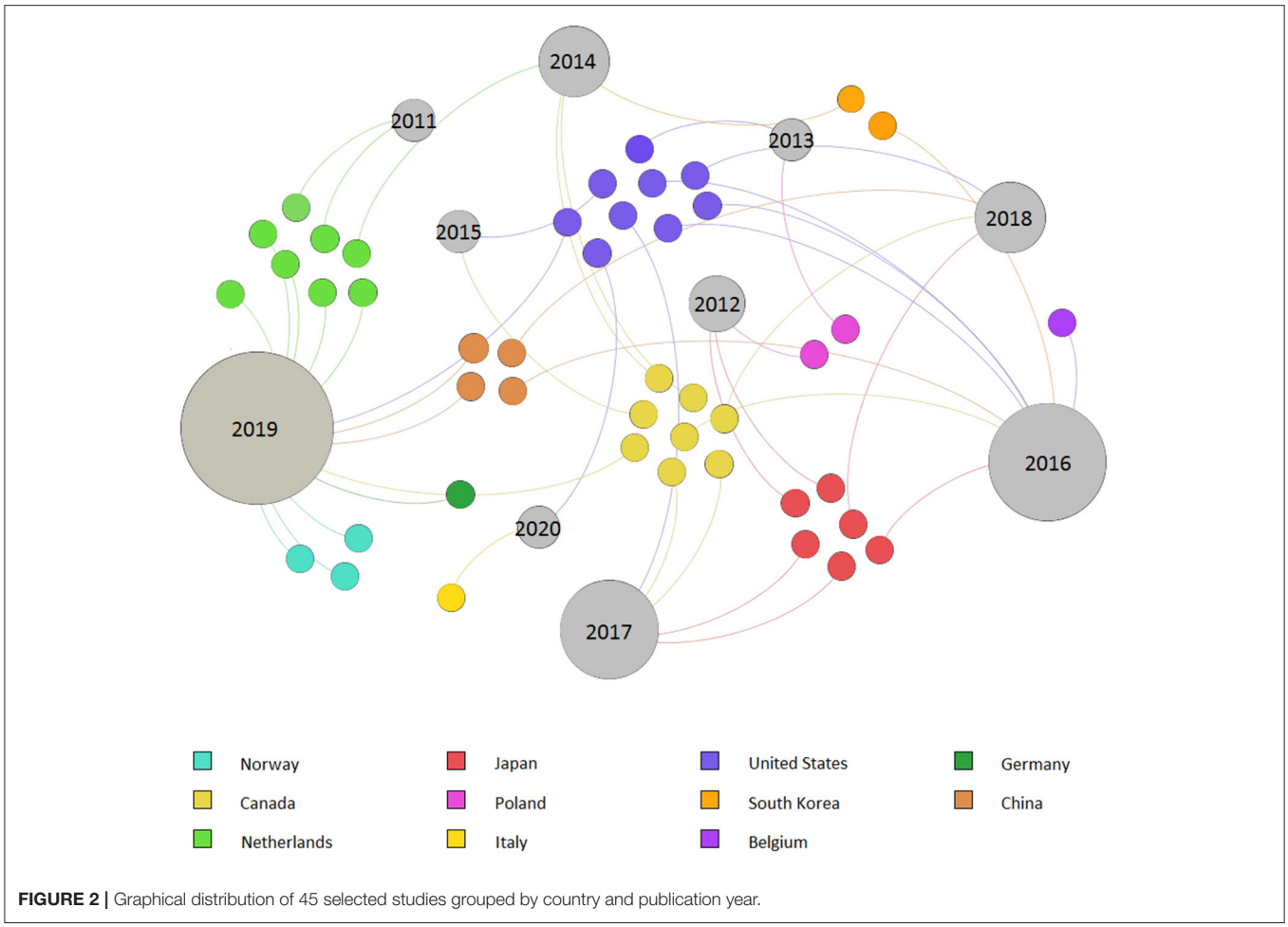

FIGURE 2 | Graphical distribution of 45 selected studies grouped by country and publication year.

and median were 160 and 165 μmol m^{-2} s^{-1} for PPFD and 11.5 and 9.8 mol m^{-2} d^{-1} for DLI, respectively. Spectral compositions occurred in numerous combinations and ratios depending on the trial. The absolute frequencies of the red, blue, white, far-red, and UV spectral components were registered separately, and each component was counted each time it appeared in a treatment independently from the combinations. The count resulted in red light supplies recurring in 128 cases, while light in the blue, white and far-red spectra were adopted 115, 24 and 20 times, respectively. UV application was only used 3 times, while green light occurred once. Both UV and green light were always applied in combination with other light spectral components. Furthermore, 68% of the reviewed observations used a combination of red and blue diodes, while monochromatic red or blue diodes were applied in 6 and 2% of total observations, respectively. The average duration of treatments was 5 months, with the durations ranging from 2 to 8 months.

After a second selection phase, 10 studies not reporting any control, as well as one outlier case concerning the reported yield values (Deram et al., 2014), were excluded from the meta-analysis. This selection resulted in 31 studies, and 100 total observations were used for the further analyses. The results revealed the generally positive effects of supplemental LED lighting, although different tendencies and significances were observed depending on the evaluated [*R*] (**Figure 3**). PN ($k = 45$) and Yield ($k = 68$) were the parameters most affected by supplemental LED treatments, reporting the highest standardized mean differences (Hedges' g) of 2.70 and 1.75, respectively. Both response ratios were significantly influenced by supplemental lighting, with one-tailed p-values < 0.001. Conversely, g_s ($k = 26$) showed a standardized mean difference of 0.83, although no significant effect was reported ($p = 0.171$). Asc ($k = 20$) and TSS ($k = 38$) presented standardized mean differences of 0.81 and 0.34, with significant p-values of 0.001 and <0.001, respectively. Finally, Chl ($k = 40$) and LA ($k = 38$) recorded similar values, showing Hedges' g values of 0.74 and 0.75, respectively, while the p-values were <0.001 for both cases. **Figure 3** displays a summary of the combined effect sizes.

The I^2 value, which describes the percentage of variation among studies, was the main investigated factor used to understand the heterogeneity in the results (Hak et al., 2016). In particular, fruit yield (Yield) showed a heterogeneity of 89.18%. The qualitative effects, measured as TSS and Asc, reported I^2 values of 29.27 and 75.97%, respectively. The physiological parameters showed I^2 values equal to 91.66% for g_s, 91.15% for PN, and 73.23% for Chl. Finally, the LA heterogeneity

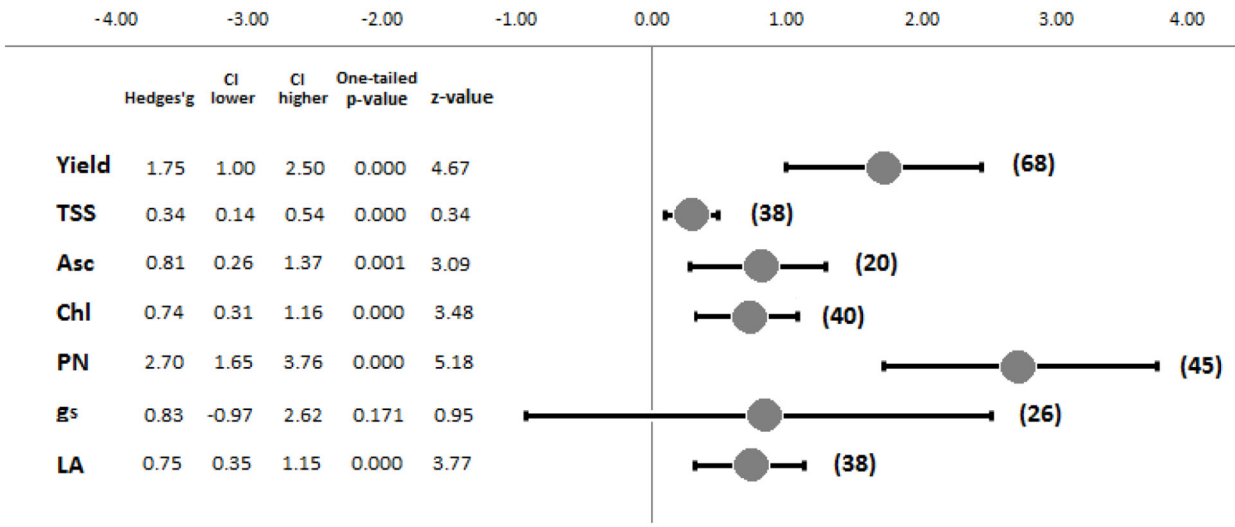

FIGURE 3 | Forest plot showing the combined effect sizes and main meta-analysis parameters of the investigated response ratios (*Yield*, Yield; *TSS*, soluble solid content; *Asc,* ascorbic acid content; *Chl,* chlorophyll content; *PN,* photosynthetic capacity; g_s, stomatal conductance; *LA*, leaf area). Numbers within brackets refer to *k* response ratios. The meta-analysis parameters are the effect size value (Hedges'*g*), low and high confidence intervals (CI), and tests of the null hypothesis (one-tailed *p*-value and *z*-value) (Hak et al., 2016).

TABLE 1 | Heterogeneity evaluation of response ratios.

	Q	p_q	I^2	T^2	*T*
Yield	619	<0.001	89.18	3.45	1.86
TSS	52.31	0.049	29.27	0.10	0.31
Asc	79.07	<0.001	75.97	0.86	0.93
g_s	299.70	<0.001	91.66	4.07	2.02
PN	497.14	<0.001	91.15	4.18	2.05
Chl	145.67	<0.001	73.23	0.76	0.87
LA	185.33	<0.001	80.04	1.09	1.05

Yield, Yield; TSS, soluble solid content; Asc, ascorbic acid content; Chl, chlorophyll content; PN, photosynthetic capacity; g_s, stomatal conductance; LA, leaf area.
Q, The heterogeneity parameters are the weighted sum-of-squared differences between the observed effects and the weighted-average effects; p_q, the test of the null hypothesis; I^2, the measure of the proportion of observed variance that reflects the real differences in the effect size; T^2 and T, the measure of the dispersion of the true effect sizes between studies in terms of the scale of the effect size (Hak et al., 2016).

was 80.04%. The other parameters explaining heterogeneity are reported in **Table 1**.

All response ratios showed high heterogeneity, with I^2 values >25%. Accordingly, a subgroup analysis was performed for each outcome. Low heterogeneity was observed for Yield in cases of light supplies different from intracanopy supplies (I^2 = 18.7%) and cases using solar + HPS lighting as controls (I^2 = 12.7%); for TSS in cases with increased natural lighting (I^2 = 21.2%) and lighting supplies other than intracanopy supplies (I^2 = 0.0%); and for Chl in cases with decreased natural lighting (I^2 = 0.0%). **Table 2** shows the I^2 heterogeneity values identified for each [*R*] value and subgroup, as well as the percentages of each subgroup both relative to the single response ratios and to the total number of meta-analysis observations. Cases not reporting a sufficient number of observations ($k \geq 5$) within each subgroup division were not reported.

DISCUSSION

The worldwide distribution of the 45 identified studies showed a prevalence of trials in countries of the boreal hemisphere occurring at latitudes above 43°N, falling within the temperate climatic zone (Fischer et al., 2012). Geographical latitude is one of the main factors constraining daily solar radiation during the year, thus affecting the minimal light requirements of most horticultural crops (~2.34 kWh m^{-2} d^{-1}, which translates to ~8.5 MJ m^{-2} day^{-1}) and, consequently, affecting climatic suitability for greenhouse cultivation (Castilla and Baeza, 2013). Accordingly, supplemental lighting can be particularly appropriate to guarantee better light distributions and longer cultivation spans in high-tech greenhouses in northern countries, although useful applications were also observed within the Mediterranean area (Paucek et al., 2020). Although Mediterranean greenhouse cultivation is mainly

TABLE 2 | Subgroup analysis reporting heterogeneity (I^2) and percentage (P) by response ratio (Yield, Yield; TSS, soluble solid content; Asc, ascorbic acid content; Chl, chlorophyll content; PN, photosynthetic capacity; g_s, stomatal conductance; LA, leaf area) and total percentage (Tot P) of subgroups considering 104 total observations used in the meta-analysis.

	Yield ($k = 68$)		**TSS ($k = 38$)**		**Asc ($k = 20$)**		**g_s ($k = 26$)**		**PN ($k = 45$)**		**Chl ($k = 40$)**		**LA ($k = 38$)**		**Tot ($k = 104$)**
	I^2 (%)	**P(%)**	**I^2 (%)**	**P (%)**	**I^2 (%)**	**P (%)**	**I^2 (%)**	**P(%)**	**I^2 (%)**	**P (%)**	**I^2 (%)**	**P(%)**	**I^2 (%)**	**P(%)**	**Tot P (%)**
Control type															
Solar light	92.2	69.1	-	97.4	-	85.0	-	100.0	-	97.8	-	90.0	79.8	86.8	80
Solar + HPS	**12.7**	30.9	-	2.6	-	15.0	-	0.0	-	2.2	-	10.0	77.5	13.2	20
Lamp type															
LED	92.6	64.7	-	94.7	-	80.0	-	92.3	-	93.3	75.1	87.5	78.9	86.8	76
LED+HPS	28.9	35.3	-	5.3	-	20.0	-	7.7	-	6.7	49.9	12.5	67.5	13.2	24
DLI															
<10	76.9	52.9	34.4	44.1	81.6	45.0	88.1	65.4	87.6	55.6	81.1	50.0	72.5	50.0	42
>=10	93.2	47.1	36.7	55.9	71.2	55.0	93.7	34.6	92.2	44.4	56.9	50.0	83.5	50.0	58
Photoperiod															
<16	80.8	35.3	45.5	41.9	84.4	45.0	92.8	34.6	90.3	37.8	88.5	30.0	35.8	34.2	30
>=16	91.1	64.7	28.6	58.1	71.3	55.0	91.4	65.4	90.4	62.2	43.2	70.0	84.9	65.8	70
Natural light															
Decreasing	86.6	30.5	52.9	33.3	84.9	38.9	91.2	28.0	95.8	27.0	**0.0**	16.1	-	11.1	30
Increasing	91.2	69.5	**21.2**	66.7	67.7	61.1	90.4	72.0	83.2	73.0	66.2	83.9	-	88.9	70
Light supply															
Intracanopy	91.9	72.1	36.9	84.2	-	80.0	92.6	62.2	92.9	68.9	73.4	57.5	86.7	57.9	77
Others	**7.4**	27.9	**0.0**	15.8	-	20.0	84.7	30.8	81.6	31.1	71.7	42.5	45.0	42.1	23

I^2 values <25% are reported in bold.

characterized by applications of low-tech solutions (Fernández et al., 2018), some examples of technologically advanced high-density greenhouse farms also exist in this region (Meneses and Castilla, 2009; Tuzel and Oztekin, 2014). In these cases, supplemental lighting may be applied to improve off-season production. Indeed, research on the application of supplemental LED lighting in the Mediterranean region has already demonstrated the capability of this technology to improve yields and anticipate the ripening of truss tomatoes during spring and summer (Paucek et al., 2020), although further research should be conducted in the fall season. Furthermore, it is important to consider that Mediterranean greenhouse cultivation can suffer from excessive sun radiation and temperatures during summertime, making external shading a necessary technique to ensure good internal growing conditions (Castilla et al., 2002). However, sunlight screening may also reduce plant photosynthesis, especially in cases of low-cost permanent solutions (e.g., whitewashing) (Garcia et al., 2011). Tewolde et al. (2018) demonstrated the feasibility of supplemental LED inter-lighting on tomato production in cases of shading cover applications, obtaining the same qualitative-quantitative performances as those observed in the naturally lighted control. Although LED use was identified as an effective artificial lighting source for horticultural purposes (Heuvelink and Gonzalez-Real, 2007; Gupta and Agarwal, 2017), research on greenhouse-grown tomato production using supplemental LED lighting seems to be relatively recent, as evidenced by the higher number of studies published during the last 5 years (**Figure 2**). Nevertheless, earlier studies on seedlings and transplants are also present (Brazaityte et al., 2009; Suzuki et al., 2009), though they were not considered within this research.

High-tech solutions characterized by the use of soilless cultivation systems, controlled climates and high plant densities were mainly adopted in the evaluated trials. Although not always mentioned, some studies reported high-wire growing methods based on plant lowering, allowing for production throughout several seasons (Kubota et al., 2018). This training system, in association with advanced protected growing technologies, can ensure increased productivity despite flourishing vegetation causing inner canopy shading (Hamamoto and Yamazaki, 2009) and light quality modifications that occur due to both greenhouse cladding materials and shading items (Kittas et al., 1999; Petropoulos et al., 2019). An economic analysis demonstrated that these highly productive systems, together with efficient lighting technologies, can make supplemental lighting more effective for greenhouse tomato production than for the production of other species (Kubota et al., 2016). With reference to both the technical and environmental aspects of trial management, the analysis of the results showed that most supplemental LED lighting studies followed the optimal growth conditions suggested for intensive greenhouse tomato production (Schwarz et al., 2014; Kubota et al., 2018). For instance, rockwool was found to be the most-applied growing substrate, as is commonly observed in greenhouse tomato soilless cultivation systems (Kubota et al., 2018). The environmental growth conditions also followed the recommendations for the fruit production phase, suggesting a mean temperature of 21–18°C, with nutrient solutions featuring ECs of 2.7–4.0 dS m^{-1} and a pH value of 5.8 (OMAFRA, 2001). When a supplemental LED lighting system is adopted, temperature management becomes a key factor. Dueck et al. (2011) observed that tomato plants grown under LED lighting receive less radiative energy than when other lamp typologies (such as HPS lamps) are used, thus requiring more thermal heat during cold seasons to maintain an optimal temperature within the greenhouse. On the other hand, Verheula et al. (2019) pointed out that the addition of supplemental LED inter-lighting to HPS lamps can increase the temperature by 1–2°C, leading to increased ventilation requirements for greenhouse production during summer. Furthermore, considering that the lifespans of LED lamps are halved when the working temperature increases by 10°C, a cooling system may also be necessary (Nelson and Bugbee, 2014; Hinov et al., 2019). The average planting density value adopted in the considered studies was higher than the suggested greenhouse standards (2.5 plants m^{-2} for northern Europe) (Kubota et al., 2018), even reaching 16.6 plants m^{-2} in some studies (Song et al., 2016; Johkan et al., 2017). Elevated planting densities may negatively affect light absorption in tomato plants (Sarlikioti et al., 2011), but the use of supplemental lighting can compensate for the lower light availability caused by an increased planting density, also enabling higher annual production compared to systems with lower planting densities (Dorais et al., 1991).

The lighting distribution is a fundamental factor associated with optimizing the effectiveness of supplemental lighting systems. Traditionally, overhead lamps were used in greenhouse production systems, resulting in increased upper leaf interception and intracanopy shading (Gomez et al., 2013). Although an overhead lighting supply may be preferred by growers due to both its easy installation in greenhouses and reduced labor requirements for crop management (Gunnlaugsson and Adalsteinsson, 2005), intracanopy lighting can increase light interception within a canopy, enhance light use efficiency thanks to better lighting distribution and maintain the photosynthetic capacities of lower leaves (Trouwborst et al., 2011). The efficacy of intracanopy lighting on tomato production has already been ascertained by using HPS and fluorescent lamps (Gunnlaugsson and Adalsteinsson, 2005; Lu et al., 2012a), although its feasibility for technological uptake emerged only after the introduction of low-surface-temperature LEDs (Hao et al., 2012; Guo et al., 2016). In our research, the majority of considered trials applied intracanopy LED lighting alone, sometimes combined with overhead HPS lamps. However, few cases of overhead LED lighting alone against a control were also registered. Although not statistically significant differences could be observed, intracanopy lighting tended to have a larger impact on yield than overhead lighting alone when compared to the controls. Finally, LEDs can also be applied as below-canopy lighting. Supplemental lighting strategies have been shown to increase photosynthesis both below and within the canopy. However, two studies comparing intracanopy light with below-canopy lighting found that the latter technology can promote CO_2 assimilation and stomatal

conductance by providing stable light penetration even at low canopy levels (Song et al., 2016; Johkan et al., 2017).

Deram et al. (2014) observed that the responses of plants to supplemental lighting also depended on the spectral components of the lighting system adopted. Red and blue wavelengths, alone or combined in different ratios, were mainly used in the studies evaluated in our research. In general, red light was mostly efficient in enhancing photosynthesis (McCree, 1971; Kaiser et al., 2019a), while blue light was shown to play an important role in controlling plant morphology, biomass accumulation and stomatal conductance (Ménard et al., 2005; Johkan et al., 2010; Ieperen et al., 2012). Monochromatic lighting may be less effective than a combination of red and blue light, since combined blue light can mitigate the so-called "red light syndrome" (seen with monochromatic red lighting), which manifests itself in reduced leaf growth and decreased stomatal conductance and photosynthetic capacity (Miao et al., 2019). Lu et al. (2012b) observed the effects of monochromatic supplemental lighting on greenhouse truss tomato plants, showing higher yields in cases of red light application compared to pure blue light application. However, good results were also obtained by using white light containing both red and blue spectral regions in addition to an abundant presence of green light, which may favor light penetration within a canopy and be particularly suitable for single-truss growing systems (Lu et al., 2012b). Deram et al. (2014) and Kaiser et al. (2019a) highlighted the effectiveness of red and blue combinations for tomato production, suggesting red:blue = 4 and red:blue = 1.2–2.4 as optimal ratios for yield improvement, respectively. Kaiser et al. (2019b) also evaluated the partial replacement of red:blue LED lights with different percentages of green light (7, 20, and 39%) in cases of greenhouse tomato production with supplemental artificial lighting. The results showed that the highest studied green percentage (39%), which was similar to the sunlight spectrum, showed the best effects on plant biomass and yield, suggesting that plants may use sunlight-combined wavelengths more efficiently for growth than other wavelength combinations (Kaiser et al., 2019b). The far-red wavelength was also investigated by several studies on greenhouse tomato supplemental LED lighting (Pepin et al., 2014; Hao et al., 2015, 2016; Gómez and Mitchell, 2016b; Song et al., 2016; Dzakovich et al., 2017; Fanwoua et al., 2019; Ji et al., 2019; Kalaitzoglou et al., 2019; Kim et al., 2019, 2020; Zhang et al., 2019). The far-red ratio, particularly the red:far-red ratio, influences phytochrome regulation and has effects on plant architectural development, flower induction, germination, photosynthetic capacity, and nutrition (Demotes-Mainard et al., 2016). Zhang et al. (2019) evaluated the effects of different durations of the far-red lighting supply (namely, 0.5, 1.5, or 12 h day^{-1}) on greenhouse tomato cultivation, concluding that even when adopting the lowest supply time, plant stem elongation was stimulated, thus enhancing light penetration within the canopy. Kalaitzoglou et al. (2019) also highlighted similar far-red-induced morphological and productive effects on tomato plants, although pointing out the necessity for long-term far-red supplies during the day to obtain optimal performances. Furthermore, far-red light may also improve the hedonic perception of tomato fruit (Kim et al., 2020), despite the potential reduction of resistance to *Botrytis cinerea* (Ji et al., 2019). Finally, Hao et al. (2018) investigated the effects of UV light on tomato yield and did not confirm any significant increase compared to other wavelengths. It should be noted that UV light is traditionally not considered within photosynthetic active radiation (PAR), although recent studies have also attributed the capacity of UV light to foster photosynthesis and growth in plants, e.g., in basil (Dou et al., 2019). Moreover, Tokuno et al. (2012) demonstrated the effectiveness of supplemental UV LED radiation in reducing phytopathological diseases in greenhouse tomato plants. Further research should also specifically target the effect of UV radiation on inducing secondary metabolite production in greenhouse-grown tomato plants, as already observed in several crops (Schreiner et al., 2014).

In addition to lighting quality, the intensity and photoperiod of lighting are also fundamental aspects. Deram et al. (2014) investigated different supplemental LED lighting intensities (135, 115, and 100 $\mu mol\ m^{-2}\ s^{-1}$), although no statistically significant differences in plant productivity were observed. However, studies on light intensity are still limited, and further investigations of the optimization of plant photosynthetic responses while minimizing energy costs are needed (Weaver et al., 2019). Concerning the photoperiod, the tomato is a photosensitive species with an optimal photoperiod identified at ∼14 h d^{-1} (Dorais et al., 1996; Demers et al., 1998; Demers and Gosselin, 2000). Continuous lighting (24 h d^{-1}) for 5–7 weeks may improve tomato plant growth and tomato yield, while a longer supply period can have negative effects, likely caused by accumulations of sucrose and starch affecting the maximum quantum efficiency of photosystem II (PSII) with consequent leaf chlorosis (Demers et al., 1998; Demers and Gosselin, 2000; Velez-Ramirez et al., 2017). However, the alternation of red and blue continuous LED lighting was reported to reduce plant injuries, with potential applications for long-term yield improvements (Lanoue et al., 2019). Additionally, the period of the day (daytime or nighttime) in which additional lighting is supplied may affect plant production. Particularly, Tewolde et al. (2016) confronted daytime vs. nighttime (applying light from 4:00 am to 4:00 pm in the case of daytime supply and from 10:00 am to 10:00 pm for nighttime treatment) supplemental LED lighting applications, reporting a significant increase in yield, as well as of soluble solids and ascorbic acid, during wintertime in the case of nighttime supply and also observing better cost-effectiveness of nighttime supply compared to diurnal applications.

The meta-analysis results showed that the application of supplemental LED lighting on greenhouse tomato plants has a statistically significant tendency toward enhancing Yield, TSS, Asc, Chl, PN, and LA, while no significant results were observed for g_s (**Figure 3**). With reference to Yield, although the tendency revealed a global positive effect (with an average yield increase of +40% from the control conditions), some studies reported negative or equal output values compared with their control treatments. These inconsistencies may be attributed to different trial management aspects and should be considered to obtain the best tomato cultivation performance using supplemental LED lighting. Tewolde et al. (2016) observed that daytime LED inter-lighting during summer may reduce

tomato yield compared to a solar light control, probably due to the excessive temperature and radiation around the mid-canopy area caused by lamps. A similar effect was also observed by Verheula et al. (2019), equally pointing out the need for ventilation during summer, although with lower energy savings. Additionally, Gómez et al. (2016) reinforced these observations, concluding that supplemental LED lighting may not be a feasible solution during summer even when a root cooling system is used.

Looking at qualitative parameters, while most of the analyzed studies associated supplemental lighting with positive effects (increasing TSS by 6% and Asc by 11%), some inconsistent results were also found. Accordingly, Dzakovich et al. (2015, 2017) reported that supplemental lighting did not increase the TSS values. Similarly, supplemental lighting on tomato plants was not associated with increased TSS values or Asc contents (Lu et al., 2012b) or with the sugar or acid contents, according to Gautier et al. (2005). However, it is important to consider that in addition to light access, other factors may affect the qualitative parameters of tomato fruits (e.g., genotype, environmental conditions, nutrient solution EC) (Kubota et al., 2012; Dzakovich et al., 2015; Ouzounis et al., 2016). Furthermore, it must be acknowledged that the parameters used for the purpose of this research (e.g., TSS and Asc) do not entirely describe tomato fruit quality from a sensorial or nutraceutical standpoint. For instance, due to the scarcity of studies, some qualitative aspects (e.g., antioxidant content) were not evaluated in the present research. Further research on the antioxidant response to supplemental LED lighting is therefore needed, also considering that a potential increase in carotenoids induced by using far-red light has already been reported (Hao et al., 2016).

In this study, the leaf response to supplemental LED lighting was evaluated in terms of Chl, PN, LA, and g_s. As already presented within the results (**Figure 3**), the response ratios [*R*] for Chl, PN, and LA globally reported statistically significant increases when supplemental LED lighting was applied (on average, increasing Chl by 31%, PN by 50%, and LA by 9%). Additionally, for these parameters, however, inconsistencies were observed among studies. In particular, Kim et al. (2019) observed reductions in Chl and LA in plants treated with low red:far-red levels for long durations, which may be attributed to major biomass allocations in reproductive structures during plant growth and development. Other authors also observed non-statistically significant differences in both the chlorophyll content and total leaf area (Jiang et al., 2017) or in the leaf area only (Gómez and Mitchell, 2016b) when applying supplemental lighting treatments. No statistically significant effect of supplemental LED lighting application on PN was observed by Gajc-Wolska et al. (2013) or by Gómez et al. (2016) compared to the control conditions. From the meta-analysis, a non-significant effect of supplemental lighting on g_s was observed, possibly suggesting that excessive light irradiance could also lead to stomatal closure (O'Carrigan et al., 2014a).

The evaluation of heterogeneity among the studies showed high values for each response ratio [*R*] (**Table 1**). Such results were, however, expected, considering not only the variability in trial management (e.g., diverse locations and technologies, light qualities, intensities, growing systems, etc.) but also the absence of common meta-data protocols for data collection and presentation. The last can be seen as one of the main issues hindering the development of agricultural meta-analyses, and this challenge should be overcome by always presenting all the statistical values needed for a meta-analysis evaluation (e.g., the standard error, standard deviation, variance, and sample size), as well as by applying common measurement methods (Eagle et al., 2017). The lower heterogeneity observed for TSS than for the other factors may be attributed to different measuring systems or units, while the other evaluated effect sizes utilized different measurement standards that required unit conversions in some cases. Concerning the subgroup analysis, most of the confronted group showed high heterogeneity, indicating the absence of influences determined by specific trial characteristics. However, low heterogeneity was observed for Yield in cases of lighting supplies different from intracanopy lighting or pure HPS lamps used as controls, for TSS in cases of increased natural light or other lighting supplies, and for Chl in cases of decreased natural lighting. Accordingly, the analysis revealed common trends of results in these specific subgroups. However, further targeted assumptions regarding the effect of specific LED lighting features (e.g., decreasing or increasing natural sunlight; intracanopy or other light supplies) on the combined effect sizes cannot be hypothesized due to the absence of homogeneity in the confronted group.

CONCLUSION

Despite some limitations commonly occurring in agricultural meta-analyses, the research conducted herein revealed that supplemental LED lighting may be effective in improving the quantitative and qualitative aspects of greenhouse-grown truss tomato production. Significant positive results were observed for both direct qualitative-quantitative parameters (Yield, TSS, Asc) and crop photosynthetic properties (Chl, PN, LA), while only stomatal conductance (g_s) was not significantly affected by supplemental LED lighting. Further research is needed regarding product quality, particularly focusing on the unexplored effects of LED lighting on nutraceutical properties and organoleptic features. Moreover, most studies considered herein applied red and blue spectra, although preliminary studies have also introduced promising results by applying UV or green light. Finally, the collected studies were mainly concentrated in the northern part of the boreal hemisphere, where the presence of technologically advanced greenhouses, as well as some favorable environmental conditions due to lower temperatures and sun radiation, have induced the wide uptake of horticultural LED technology. However, interesting applications may also be hypothesized for milder climates such as those of the Mediterranean area, in which supplemental LED lighting could improve the quantitative and qualitative aspects of greenhouse tomato plants both during the off-season and when extremely hot summers occur and intensive shading is needed.

DATA AVAILABILITY STATEMENT

The authors confirm that the data supporting the findings of this study are available within the article and its **Supplementary Materials**.

AUTHOR CONTRIBUTIONS

EA designed and performed the data collection and meta data analysis, and drafted the manuscript. GP and FO contributed to the research design and the drafting of the manuscript. IP revised the manuscript. XG and GG supervised the research and critically revised the manuscript. All authors contributed to the article and approved the submitted version.

FUNDING

The research leading to this publication has received funding from the European Union's Horizon 2020 research and innovation programme under grant agreement No 862663.

SUPPLEMENTARY MATERIAL

The Supplementary Material for this article can be found online at: https://www.frontiersin.org/articles/10.3389/fpls.2021.596927/full#supplementary-material

REFERENCES

Bastian, M., Heymann, S., and Jacomy, M. (2009). "*Gephi: an open source software for exploring and manipulating networks*," in *International AAAI Conference on Weblogs and Social Media* (San Jose, CA).

Bian, Z., Zhang, X., Wang, Y., and Lu, C. (2019). Improving drought tolerance by altering the photosynthetic rate and stomatal aperture via green light in tomato (Solanum lycopersicum L.) seedlings under drought conditions. *Environ. Exp. Bot*. 167:103844. doi: 10.1016/j.envexpbot.2019.103844

Borenstein, M., Hedges, L. V., Higgins, J. P. T., and Rothstein, H. R. (2009). *Introduction to Meta-Analysis*. Chichester: Wiley. doi: 10.1002/9780470743386

Brazaityte, A., Duchovskis, P., Urbonavičiute, A., Samuoliene, G., Jankauskiene, J., Kazenas, V., et al. (2009). After-effect of light-emitting diodes lighting on tomato growth and yield in greenhouse. *Sodininkyste ir darŽininkyste* 28, 115–126.

Cao, K., Cui, L., Ye, L., Zhou, X., Bao, E., Zhao, H., et al. (2016). Effects of red light night break treatment on growth and flowering of tomato plants. *Front. Plant Sci.* 7:527. doi: 10.3389/fpls.2016.00527

Carvalho, S. D., Schwieterman, M. L., Abrahan, C. E., Colquhoun, T. A., and Folta, K. M. (2016). Light quality dependent changes in morphology, antioxidant capacity, and volatile production in sweet basil (*Ocimum basilicum*). *Front. Plant Sci.* 7:1328. doi: 10.3389/fpls.2016.01328

Castilla, N., and Baeza, E. (2013). *Greenhouse site selection. Good Agricultural Practices for greenhouse vegetable crops: principles for mediterranean climate areas*. FAO plant production and protection paper, FAO, 21–34.

Castilla, N., Hernández, J., and Abou-Hadid, A. F. (2002). Strategic crop and greenhouse management in mild winter climate areas. *Acta Hortic.* 633, 183–196. doi: 10.17660/actahortic.2004.633.22

Christie, J. M., Blackwood, L., Petersen, J., and Sullivan, S. (2015). Plant flavoprotein photoreceptors. *Plant Cell Physiol.* 56, 401–413. doi: 10.1093/pcp/pcu196

Demers, D. A., Dorais, M., Wien, C. H., and Gosselin, A. (1998). Effects of supplemental light duration on greenhouse tomato (*Lycopersicon esculentum* Mill.) plants and fruit yields. *Sci. Hortic.* 74, 295–306. doi: 10.1016/s0304-4238(98)00097-1

Demers, D. A., and Gosselin, A. (2000). Growing greenhouse tomato and sweet pepper under supplemental lighting: optimal photoperiod, negative effects of long photoperiod and their causes. *Acta Hortic.* 580, 83–88. doi: 10.17660/actahortic.2002.580.9

Demotes-Mainard, S., Péron, T., Corot, A., Bertheloot, J., Le Gourrierec, J., and Pelleschi-Travier, S., et al. (2016). Plant responses to red and far-red lights, applications in horticulture. *Environ. Exp. Bot.* 121, 4–21. doi: 10.1016/j.envexpbot.2015.05.010

Deram, P., Lefsrud, M. G., and Orsat, V. (2014). Supplemental lighting orientation and red-to-blue ratio of light-emitting diodes for greenhouse tomato production. *HortScience* 49, 448–452. doi: 10.21273/hortsci.49.4.448

Dorais, M., Gosselin, A., and Trudel, M. J. (1991). Annual greenhouse tomato production under a sequential intercropping system using supplemental light. *Sci. Hortic.* 45, 225–234. doi: 10.1016/0304-4238(91)90067-9

Dorais, M., Yelle, S., and Gosselin, A. (1996). Influence of extended photoperiod on photosynthate partitioning and export in tomato and pepper plants. *N. Z. J. Crop Hort.* 24, 29–37. doi: 10.1080/01140671.1996.9513932

Dou, H., Niu, G., and Gu, M. (2019). Pre-harvest UV-B radiation and photosynthetic photon flux density interactively affect plant photosynthesis, growth, and secondary metabolites accumulation in basil (*Ocimum basilicum*) plants. *Agronomy* 9:434. doi: 10.3390/agronomy9080434

D'Souza, C., Yuk, H. G., Khoo, G. H., and Zhou, W. (2015). Application of light-emitting diodes in food production, postharvest preservation, and microbiological food safety. *Compr. Rev. Food Sci. F* 14, 719–740. doi: 10.1111/1541-4337.12155

Dueck, T. A., Janse, J., Eveleens, B. A., Kempkes, F. L. K., and Marcelis, L. F. M. (2011). Growth of tomatoes under hybrid LED and HPS lighting. *Acta Hortic.* 952, 335–342. doi: 10.17660/actahortic.2012.952

Dzakovich, M. P., Gómez, C., Ferruzzi, M. G., and Mitchell, C. A. (2017). Chemical and sensory properties of greenhouse tomatoes remain unchanged in response to Red, Blue, and Far Red supplemental light from Light-Emitting Diodes. *HortScience* 52, 1734–1741. doi: 10.21273/hortsci12469-17

Dzakovich, M. P., Gómez, C., and Mitchell, C. A. (2015). Tomatoes grown with light-emitting diodes or high-pressure sodium supplemental lights have similar fruit-quality attributes. *HortScience* 50, 1498–1502. doi: 10.21273/hortsci.50.10.1498

Eagle, A. J., Christianson, L. E., Cook, R. L., Harmel, R. D., Miguez, F. E., and Qian, S. S., et al. (2017). Meta-analysis constrained by data: recommendations to improve relevance of nutrient management research. *J. Agron.* 109, 2441–2449. doi: 10.2134/agronj2017.04.0215

Ebisawa, M., Shoji, K., Kato, M., Shimomura, K., Goto, F., and Yoshihara, T. (2008). Supplementary ultraviolet radiation B together with blue light at night increased quercetin content and flavonol synthase gene expression in leaf lettuce (*Lactuca sativa* L.). *Environ. Control Biol.* 46, 1–11. doi: 10.2525/ecb.46.1

Fanwoua, J., Vercambre, G., Buck-Sorlin, G., Dieleman, J. A., de Visser, P., and Génard, M. (2019). Supplemental LED lighting affects the dynamics of tomato fruit growth and composition. *Sci. Hortic.* 256:108571. doi: 10.1016/j.scienta.2019.108571

FAO (2018). *FAOSTAT database collections*. Rome: Food and Agriculture Organization of the United Nations. Available online at: http://faostat.fao.org (accessed June 24, 2020).

Fernández, J. A., Orsini, F., Baeza, E., Oztekin, G. B., Muñoz, P., Contreras, J., et al. (2018). Current trends in protected cultivation in Mediterranean climates. *Eur. J. Hortic. Sci.* 83, 294–305. doi: 10.17660/ejhs.2018/83.5.3

Fischer, G., Nachtergaele, F. O., Prieler, S., Teixeira, E., Tóth, G., and Van Velthuizen, H., et al. (2012). *Global agro-ecological zones (GAEZ v3. 0) - Model Documentation*. IIASA, FAO, Rome, Italy.

Gajc-Wolska, J., Kowalczyk, K., Metera, A., Mazur, K., Bujalski, D., and Hemka, L. (2013). Effect of supplementary lighting on selected physiological

parameters and yielding of tomato plants. *Folia Horticult.* 25, 153–159. doi: 10.2478/fhort-2013-0017

Garcia, M. L., Medrano, E., Sanchez-Guerrero, M. C., and Lorenzo, P. (2011). Climatic effects of two cooling systems in greenhouses in the Mediterranean area: external mobile shading and fog system. *Biosyst. Eng.* 108, 133–143. doi: 10.1016/j.biosystemseng.2010.11.006

Garland, K. F., Burnett, S. E., Stack, L. B., and Zhang, D. (2010). Minimum daily light integral for growing high-quality coleus. *Horttechnology* 20, 929–933. doi: 10.21273/HORTTECH.20.5.929

Gautier, H., Rocci, A., Buret, M., Grasselly, D., Dumas, Y., and Causse, M. (2005). Effect of photoselective filters on the physical and chemical traits of vine-ripened tomato fruits. *Can. J. Plant Sci.* 85, 439–446. doi: 10.4141/p03-163

Giniger, M. S., McAvoy, R. J., Giacomelli, G. A., and Janes, H. W. (1988). Computer simulation of a single truss tomato cropping system. *Trans. ASAE* 31, 1176–1179. doi: 10.13031/2013.30840

Gómez, C., Clark, M., and Mitchell, C. A. (2016). Effect of intracanopy lighting and/or root-zone temperature on high-wire tomato production under supra-optimal air temperature. *Acta Hortic.* 1134, 63–70. doi: 10.17660/ActaHortic.2016.1134.9

Gómez, C., and Mitchell, C. A. (2016a). Physiological and productivity responses of high-wire tomato as affected by supplemental light source and distribution within the canopy. *J. Am. Soc. Hortic. Sci.* 141, 196–208. doi: 10.21273/jashs.141.2.196

Gómez, C., and Mitchell, C. A. (2016b). In search of an optimized supplemental lighting spectrum for greenhouse tomato production with intracanopy lighting. *Acta Hortic.* 1134, 57–62. doi: 10.17660/actahortic.2016.1134.8

Gomez, C., Morrow, R. C., Bourget, C. M., Massa, G. D., and Mitchell, C. A. (2013). Comparison of intracanopy light-emitting diode towers and overhead high-pressure sodium lamps for supplemental lighting of greenhouse-grown tomatoes. *Horttechnology* 23, 93–98. doi: 10.21273/HORTTECH.23.1.93

Gunnlaugsson, B., and Adalsteinsson, S. (2005). Interlight and plant density in year-round production of tomato at northern latitudes. *Acta Hortic.* 711, 71–76. doi: 10.17660/actahortic.2006.711.6

Guo, X., Hao, X., Khosla, S., Kumar, K. G. S., Cao, R., and Bennett, N. (2016). Effect of LED interlighting combined with overhead HPS light on fruit yield and quality of year-round sweet pepper in commercial greenhouse. *Acta Hortic.* 1134, 71–78. doi: 10.17660/actahortic.2016.1134.10

Gupta, S. D., and Agarwal, A. (2017). "Artificial lighting system for plant growth and development: Chronological advancement, working principles, and comparative assessmen," in *Light Emitting Diodes for Agriculture*, ed S. D. Gupta (Singapore: Springer), 1–25. doi: 10.1007/978-981-10-5807-3_1

Hak, T., Van Rhee, H. J., and Suurmond, R. (2016). *How to Interpret Results of Meta-Analysis. (Version 1.3)*. **Rotterdam**: Erasmus Rotterdam Institute of Management. doi: 10.2139/ssrn.3241367

Hamamoto, H., and Yamazaki, K. (2009). Supplemental lighting inside the plant canopy increased the yield and quality of three-truss-ordered tomato. *Acta Hortic.* 907, 283–286. doi: 10.17660/actahortic.2011.907.45

Hao, X., Cao, R., Zheng, J., Little, C., Kholsa, S., and Yelton, M. (2018). Optimizing vertical light spectral distribution to improve yield and quality in greenhouse fruit vegetable production. *Acta Hortic.* 1271, 141–148. doi: 10.17660/actahortic.2020.1271.20

Hao, X., Guo, X., Lanoue, J., Zhang, Y., Cao, R., Zheng, J., et al. (2017). A review on smart application of supplemental lighting in greenhouse fruiting vegetable production. *Acta Hortic.* 1227, 499–506. doi: 10.17660/ActaHortic.2018.1227.63

Hao, X., Guo, X., Zheng, J., Celeste, L., Kholsa, S., and Chen, X. (2015). Response of greenhouse tomato to different vertical spectra of LED lighting under overhead high pressure sodium and plasma lighting. *Acta Hortic.* 1170, 1003–1110. doi: 10.17660/actahortic.2017.1170.129

Hao, X., Little, C., Zheng, J. M., and Cao, R. (2016). Far-red LEDs improve fruit production in greenhouse tomato grown under high-pressure sodium lighting. *Acta Hortic.* 1134, 95–102. doi: 10.17660/actahortic.2016.1134.13

Hao, X., Zheng, J., Little, C., and Khosla, S. (2012). LED inter-lighting in year-round greenhouse mini-cucumber production. *Acta Hortic.* 956, 335–340. doi: 10.17660/ActaHortic.2012.956.38

Hedges, L. V., Gurevitch, J., and Curtis, P. S. (1999). The meta-analysis of response ratios in experimental ecology. *Ecology* 80, 1150–1156. doi: 10.1890/0012-9658(1999)080[1150:TMAORR]2.0.CO;2

Heuvelink, E., and Gonzalez-Real, M. M. (2007). Innovation in plant-greenhouse interactions and crop management. *Acta Hortic.* 80, 63–74. doi: 10.17660/actahortic.2008.801.2

Hinov, N., Tsankov, P., and Ibrishimov, H. (2019). "Innovative LED lighting," in *2019 International Conference on Creative Business for Smart and Sustainable Growth (CREBUS)* (Sandanski), 1–5. doi: 10.1109/CREBUS.2019.8840095

Hui, X., Fu, Y. N., Li, T. L., and Rui, W. (2017). Effects of different LED light wavelengths on the resistance of tomato against *Botrytis cinerea* and the corresponding physiological mechanisms. *J. Integr. Agric.* 16, 106–114. doi: 10.1016/s2095-3119(16)61435-1

Ibaraki, Y. (2017). "LED supplementary lighting," in *Light Emitting Diodes for Agriculture*, ed S. D. Gupta (Singapore: Springer), 27–36. doi: 10.1007/978-981-10-5807-3_2

Ieperen, W. V., Savvides, A., and Fanourakis, D. (2012). Red and blue light effects during growth on hydraulic and stomatal conductance in leaves of young cucumber plants. *Acta Hortic.* 956, 223–230. doi: 10.17660/actahortic.2012.956.24

Ji, Y., Ouzounis, T., Courbier, S., Kaiser, E., Nguyen, P. T., Schouten, H. J., et al. (2019). Far-red radiation increases dry mass partitioning to fruits but reduces *Botrytis cinerea* resistance in tomato. *Environ. Exp. Bot.* 168:103889. doi: 10.1016/j.envexpbot.2019.103889

Jiang, C., Johkan, M., Hohjo, M., Tsukagoshi, S., Ebihara, M., Nakaminami, A., et al. (2017). Photosynthesis, plant growth, and fruit production of single-truss tomato improves with supplemental lighting provided from underneath or within the inner canopy. *Sci. Hort.* 222, 221–229. doi: 10.1016/j.scienta.2017.04.026

Johkan, M., Hohjo, T., Tsukagoshi, S., Ebihara, M., Nakaminami, A., Maruo, M., et al. (2017). Supplemental lighting applied within or underneath the canopy enhances leaf photosynthesis, stomatal regulation and plant development of tomato under limiting light conditions. *Acta Hortic.* 1227, 645–652. doi: 10.17660/actahortic.2018.1227.82

Johkan, M., Shoji, K., Goto, F., Hashida, S. N., and Yoshihara, T. (2010). Blue light-emitting diode light irradiation of seedlings improves seedling quality and growth after transplanting in red leaf lettuce. *HortScience* 45, 1809–1814. doi: 10.21273/hortsci.45.12.1809

Jokinen, K., Särkkä, L. E., and Näkkilä, J. (2012). Improving sweet pepper productivity by LED interlighting. *Acta Hortic.* 956, 59–66. doi: 10.17660/actahortic.2012.956.4

Joshi, N. C., Ratner, K., Eidelman, O., Bednarczyk, D., Zur, N., Many, Y., et al. (2019). Effects of daytime intra-canopy LED illumination on photosynthesis and productivity of bell pepper grown in protected cultivation. *Sci. Hort.* 250, 81–88. doi: 10.1016/j.scienta.2019.02.039

Kaiser, E., Ouzounis, T., Giday, H., Schipper, R., Heuvelink, E., and Marcelis, L. F. (2019a). Adding blue to red supplemental light increases biomass and yield of greenhouse-grown tomatoes, but only to an optimum. *Front. Plant Sci.* 9:2002. doi: 10.3389/fpls.2018.02002

Kaiser, E., Weerheim, K., Schipper, R., and Dieleman, J. A. (2019b). Partial replacement of red and blue by green light increases biomass and yield in tomato. *Sci. Hort.* 249, 271–279. doi: 10.1016/j.scienta.2019.02.005

Kalaitzoglou, P., Van Ieperen, W., Harbinson, J., van der Meer, M., Martinakos, S., Weerheim, K., et al. (2019). Effects of continuous or end-of-day far-red light on tomato plant growth, morphology, light absorption and fruit production. *Front. Plant Sci.* 10:322. doi: 10.3389/fpls.2019.00322

Kim, H. J., Lin, M. Y., and Mitchell, C. A. (2019). Light spectral and thermal properties govern biomass allocation in tomato through morphological and physiological changes. *Environ. Exp. Bot.* 157, 228–240. doi: 10.1016/j.envexpbot.2018.10.019

Kim, H. J., Yang, T., Choi, S., Wang, Y. J., Lin, M. Y., and Liceaga, A. M. (2020). Supplemental intracanopy far-red radiation to red LED light improves fruit quality attributes of greenhouse tomatoes. *Sci. Hort.* 261:108985. doi: 10.1016/j.scienta.2019.108985

Kittas, C., Baille, A., and Giaglaras, P. (1999). Influence of covering material and shading on the spectral distribution of light in greenhouses. *J. Agric. Eng. Res.* 73, 341–351. doi: 10.1006/jaer.1999.0420

Kubota, C., de Gelder, A., and Peet, M. M. (2018). "Greenhouse tomato production," in *Tomatoes*, ed E. Heuvelink (Wageningen: CABI), 276–314. doi: 10.1079/9781780641935.0276

Kubota, C., Kroggel, M., Both, A. J., Burr, J. F., and Whalen, M. (2016). Does supplemental lighting make sense for my crop? – empirical evaluations. *Acta Hortic.* 1134, 403–412. doi: 10.17660/actahortic.2016.1134.52

Kubota, C., Kroggel, M., Torabi, M., Dietrich, K. A., Kim, H. J., Fonseca, J., et al. (2012). Changes in selected quality attributes of greenhouse tomato fruit as affected by pre-and postharvest environmental conditions in year-round production. *HortScience* 47, 1698–1704. doi: 10.21273/hortsci.47.12.1698

Kumar, K. G. S., Hao, X., Khosla, S., Guo, X., and Bennett, N. (2016). Comparison of HPS lighting and hybrid lighting with top HPS and intra-canopy LED lighting for high-wire mini-cucumber production. *Acta Hortic.* 1134, 111–118. doi: 10.17660/actahortic.2016.1134.15

Lanoue, J., Zheng, J., Little, C., Thibodeau, A., Grodzinski, B., and Hao, X. (2019). Alternating Red and Blue Light-Emitting Diodes allows for injury-free tomato production with continuous lighting. *Front. Plant Sci.* 10:1114. doi: 10.3389/fpls.2019.01114

Liao, Y., Suzuki, K., Yu, W., Zhuang, D., Takai, Y., Ogasawara, R., et al. (2014). Night break effect of LED light with different wavelengths on floral bud differentiation of *Chrysanthemum morifolium* ramat 'Jimba'and Iwa no hakusen. *Environ. Exp. Bot.* 52, 45–50. doi: 10.2525/ecb.52.45

Lu, N., Maruo, T., Johkan, M., Hohjo, M., Tsukagoshi, S., Ito, Y., et al. (2012a). Effects of supplemental lighting within the canopy at different developing stages on tomato yield and quality of single-truss tomato plants grown at high density. *Environ. Exp. Bot.* 50, 1–11. doi: 10.2525/ecb.50.1

Lu, N., Maruo, T., Johkan, M., Hohjo, M., Tsukagoshi, S., Ito, Y., et al. (2012b). Effects of supplemental lighting with light-emitting diodes (LEDs) on tomato yield and quality of single-truss tomato plants grown at high planting density. *Environ. Exp. Bot.* 50, 63–74. doi: 10.2525/ecb.50.63

McCree, K. J. (1971). The action spectrum, absorptance and quantum yield of photosynthesis in crop plants. *J. Agric. Meteorol.* 9, 191–216. doi: 10.1016/0002-1571(71)90022-7

McDaniel, M. D., Tiemann, L. K., and Grandy, A. S. (2014). Does agricultural crop diversity enhance soil microbial biomass and organic matter dynamics? A meta-analysis. *Ecol. Appl.* 24, 560–570. doi: 10.1890/13-0616.1

Mempel, H., and Wittmann, S. (2019). Potential and use of artificial lighting in horticulture. *Light Eng.* 27, 31–41.

Ménard, C., Dorais, M., Hovi, T., and Gosselin, A. (2005). Developmental and physiological responses of tomato and cucumber to additional blue light. *Acta Hortic.* 711, 291–296. doi: 10.17660/actahortic.2006.711.39

Meneses, J. F., and Castilla, N. (2009). Protected cultivation in Iberian horticulture. *Chron. Horticult.* 49, 37–39.

Miao, Y., Chen, Q., Qu, M., Gao, L., and Hou, L. (2019). Blue light alleviates 'red light syndrome' by regulating chloroplast ultrastructure, photosynthetic traits and nutrient accumulation in cucumber plants. *Sci. Hort.* 257:108680. doi: 10.1016/j.scienta.2019.108680

Morrow, R. C. (2008). LED lighting in horticulture. *HortScience* 43, 1947–1950. doi: 10.21273/hortsci.43.7.1947

Nelson, J. A., and Bugbee, B. (2014). Economic analysis of greenhouse lighting: light emitting diodes vs. high intensity discharge fixtures. *PLoS ONE* 9:e99010. doi: 10.1371/journal.pone.0099010

O'Carrigan, A., Babla, M., Wang, F., Liu, X., Mak, M., Thomas, R., et al. (2014b). Analysis of gas exchange, stomatal behaviour and micronutrients uncovers dynamic response and adaptation of tomato plants to monochromatic light treatments. *Plant Physiol. Biochem.* 82, 105–115. doi: 10.1016/j.plaphy.2014.05.012

O'Carrigan, A., Hinde, E., Lu, N., Xu, X. Q., Duan, H., Huang, G., et al. (2014a). Effects of light irradiance on stomatal regulation and growth of tomato. *Environ. Exp. Bot.* 98, 65–73. doi: 10.1016/j.envexpbot.2013.10.007

Ohashi-Kaneko, K., Takase, M., Kon, N., Fujiwara, K., and Kurata, K. (2007). Effect of light quality on growth and vegetable quality in leaf lettuce, spinach and komatsuna. *Envrion. Control Biol.* 45, 189–198. doi: 10.2525/ecb.45.189

Okano, K., Nakano, Y., and Watanabe, S. I. (2001). Single-truss tomato system—a labor-saving management system for tomato production. *Jpn. Agr. Res. Q.* 35, 177–184. doi: 10.6090/jarq.35.177

Olle, M., and Viršile, A. (2013). The effects of light-emitting diode lighting on greenhouse plant growth and quality. *Agr. Food Sci.* 22, 223–234. doi: 10.23986/afsci.7897

OMAFRA (2001). *Growing Greenhouse Vegetables*. Publication 371. Ontario Ministry of Agriculture, Food and Rural Affairs, Toronto, Canada, 116.

Ouzounis, T., Heuvelink, E., Ji, Y., Schouten, H. J., Visser, R. G. F., and Marcelis, L. F. M. (2016). Blue and red LED lighting effects on plant biomass, stomatal conductance, and metabolite content in nine tomato genotypes. *Acta Hortic.* 1134, 251–258. doi: 10.17660/actahortic.2016.1134.34

Ouzounis, T., Rosenqvist, E., and Ottosen, C. O. (2015). Spectral effects of artificial light on plant physiology and secondary metabolism: a review. *HortScience* 50, 1128–1135. doi: 10.21273/hortsci.50.8.1128

Paponov, M., Kechasov, D., Lacek, J., Verheul, M., and Paponov, I. A. (2019). Supplemental LED inter-lighting increases tomato fruit growth through enhanced photosynthetic light use efficiency and modulated root activity. *Front. Plant Sci.* 10:1656. doi: 10.3389/fpls.2019.01656

Paucek, I., Pennisi, G., Pistillo, A., Appolloni, E., Crepaldi, A., Calegari, B., et al. (2020). Supplementary LED interlighting improves yield and precocity of greenhouse tomatoes in the mediterranean. *Agron* 10:1002. doi: 10.3390/agronomy10071002

Pennisi, G., Blasioli, S., Cellini, A., Maia, L., Crepaldi, A., Braschi, I., et al. (2019b). Unravelling the role of red:blue LED lights on resource use efficiency and nutritional properties of indoor grown sweet basil. *Front. Plant Sci.* 10: 305. doi: 10.3389/fpls.2019.00305

Pennisi, G., Orsini, F., Blasioli, S., Cellini, A., Crepaldi, A., Braschi, I., et al. (2019a). Resource use efficiency of indoor lettuce (*Lactuca sativa* L.) cultivation as affected by red:blue ratio provided by LED lighting. *Sci. Rep.* 9:14127. doi: 10.1038/s41598-019-50783-z

Pepin, S., Fortier, E., Béchard-Dubé, S. A., Dorais, M., Ménard, C., and Bacon, R. (2014). Beneficial effects of using a 3-D LED interlighting system for organic greenhouse tomato grown in Canada under low natural light conditions. *Acta Hortic.* 1041, 239–246. doi: 10.17660/actahortic.2014.1041.28

Petropoulos, S. A., Fernandes, Â., Katsoulas, N., Barros, L., and Ferreira, I. C. (2019). The effect of covering material on the yield, quality and chemical composition of greenhouse-grown tomato fruit. *J. Sci. Food Agric.* 99, 3057–3068. doi: 10.1002/jsfa.9519

Qin, W., Hu, C., and Oenema, O. (2015). Soil mulching significantly enhances yields and water and nitrogen use efficiencies of maize and wheat: a meta-analysis. *Sci. Rep.* 5:16210. doi: 10.1038/srep16210

Roelfsema, M. R. G., and Hedrich, R. (2005). In the light of stomatal opening: new insights into 'the Watergate'. *New Phytol.* 167, 665–691. doi: 10.1111/j.1469-8137.2005.01460.x

Sarlikioti, V., de Visser, P. H., Buck-Sorlin, G. H., and Marcelis, L. F. M. (2011). How plant architecture affects light absorption and photosynthesis in tomato: towards an ideotype for plant architecture using a functional–structural plant model. *Ann. Bot.* 108, 1065–1073. doi: 10.1093/aob/mcr221

Schreiner, M., Martínez-Abaigar, J., Glaab, J., and Jansen, M. (2014). UV-B induced secondary plant metabolites: potential benefits for plant and human health. *Optik (Stuttg)* 9, 34–37. doi: 10.1002/opph.201400048

Schwarz, D., Thompson, A. J., and Kläring, H. P. (2014). Guidelines to use tomato in experiments with a controlled environment. *Front. Plant Sci.* 5:625. doi: 10.3389/fpls.2014.00625

Shimazaki, K. I., Doi, M., Assmann, S. M., and Kinoshita, T. (2007). Light regulation of stomatal movement. *Ann. Rev. Plant Biol.* 58, 219–247. doi: 10.1146/annurev.arplant.57.032905.105434

Song, Y., Jiang, C., and Gao, L. (2016). Polychromatic supplemental lighting from underneath canopy is more effective to enhance tomato plant development by improving leaf photosynthesis and stomatal regulation. *Front. Plant Sci.* 7:1832. doi: 10.3389/fpls.2016.01832

Sun, Y., Sun, Y., Sun, Z., Li, P., and Li, C. (2015). "*Mapping monthly distribution of daily light integrals across China*," in *Annual Conference of ASHS* (New Orleans).

Suurmond, R., van Rhee, H., and Hak, T. (2017). Introduction, comparison and validation of Meta-Essentials: a free and simple tool for meta-analysis. *Res. Synth. Methods* 8, 537–553. doi: 10.1002/jrsm.1260

Suzuki, K., Yasuba, K., Takaichi, M., Takahashi, T., and Hoshi, T. (2009). Effect of the supplemental lighting on the growth of young plants in second nursery in tomato. *Acta Hortic.* 907, 269–276. doi: 10.17660/actahortic.2011.907.43

Talbott, L. D., Nikolova, G., Ortiz, A., Shmayevich, I., and Zeiger, E. (2002). Green light reversal of blue-light-stimulated stomatal opening is found in a diversity of plant species. *Am. J. Bot.* 89, 366–368. doi: 10.3732/ajb.89.2.366

Tewolde, F. T., Lu, N., Shiina, K., Maruo, T., Takagaki, M., Kozai, T., et al. (2016). Nighttime supplemental LED inter-lighting improves growth and yield of single-truss tomatoes by enhancing photosynthesis in both winter and summer. *Front. Plant Sci.* 7:448. doi: 10.3389/fpls.2016.00448

Tewolde, F. T., Shiina, K., Maruo, T., Takagaki, M., Kozai, T., and Yamori, W. (2018). Supplemental LED inter-lighting compensates for a shortage of light for plant growth and yield under the lack of sunshine. *PLoS ONE* 13:e0206592. doi: 10.1371/journal.pone.0206592

Tokuno, A., Iaraki, Y., Ito, S. I., Araki, H., Yoshimura, K., and Osaki, K. (2012). Disease suppression in greenhouse tomato by supplementary lighting with 405 nm LED. *Environ. Control. Biol.* 50, 19–29. doi: 10.2525/ecb.50.19

Trouwborst, G., Sander, W. H., Harbinson, J., and Wim Van, I. (2011). The influence of light intensity and leaf age on the photosynthetic capacity of leaves within a tomato canopy. *J. Hortic. Sci. Biotech.* 86, 403–407. doi: 10.1080/14620316.2011.11512781

Tuzel, Y., and Oztekin, G. B. (2014). Recent developments of vegetables protected cultivation in Turkey. *Acta Hortic.* 1142, 435–442. doi: 10.17660/actahortic.2016.1142.66

Velez-Ramirez, A. I., Carreño-Quintero, N., Vreugdenhil, D., Millenaar, F. F., and van Ieperen, W. (2017). Sucrose and starch content negatively correlates with PSII maximum quantum efficiency in tomato (*Solanum lycopersicum*) exposed to abnormal light/dark cycles and continuous light. *Plant Cell Physiol.* 58, 1339–1349. doi: 10.1093/pcp/pcx068

Verheula, M. J., Maessen, H. F. R., Panosyan, A., Paponov, M., and Paponov, I. A. (2019). *Effects of supplemental light and temperature on summer production of tomato in Norway*. Available online at: https://vb.northsearegion.eu/public/files/repository/20190925153007_2019-10m%C3%B8de.pdf (accessed June 24, 2020).

Wada, T., Ikeda, H., Matsushita, K., Kambara, A., Hirai, H., and Abe, K. (2006). Effect of shading in summer on yield and quality of tomatoes grown on a single-truss system. *J. Jpn. Soc. Hortic. Sci.* 75, 51–58. doi: 10.2503/jjshs.75.51

Weaver, G. M., van Iersel, M. W., and Velni, J. M. (2019). A photochemistry-based method for optimising greenhouse supplemental light intensity. *Biosyst. Eng.* 182, 123–137. doi: 10.1016/j.biosystemseng.2019.03.008

Zeiger, E. (1990). Light perception in guard cells. *Plant, Cell Environ.* 13, 739–744. doi: 10.1111/j.1365-3040.1990.tb01088.x

Zhang, G., Shen, S., Takagaki, M., Kozai, T., and Yamori, W. (2015). Supplemental upward lighting from underneath to obtain higher marketable lettuce (*Lactuca sativa*) leaf fresh weight by retarding senescence of outer leaves. *Front. Plant Sci.* 6:1110. doi: 10.3389/fpls.2015.01110

Zhang, Y. T., Zhang, Y. Q., Yang, Q. C., and Tao, L. I. (2019). Overhead supplemental far-red light stimulates tomato growth under intra-canopy lighting with LEDs. *J. Integr. Agric.* 18, 62–69. doi: 10.1016/s2095-3119(18)62130-6

Disclaimer: The publication reflects the author's views. The Research Executive Agency (REA) is not liable for any use that may be made of the information contained therein.

Conflict of Interest: The authors declare that the research was conducted in the absence of any commercial or financial relationships that could be construed as a potential conflict of interest.

Copyright © 2021 Appolloni, Orsini, Pennisi, Gabarrell Durany, Paucek and Gianquinto. This is an open-access article distributed under the terms of the Creative Commons Attribution License (CC BY). The use, distribution or reproduction in other forums is permitted, provided the original author(s) and the copyright owner(s) are credited and that the original publication in this journal is cited, in accordance with accepted academic practice. No use, distribution or reproduction is permitted which does not comply with these terms.

frontiers in Plant Science

ORIGINAL RESEARCH
published: 24 May 2021
doi: 10.3389/fpls.2021.596943

Improving the Predictive Value of Phytochrome Photoequilibrium: Consideration of Spectral Distortion Within a Leaf

Paul Kusuma and Bruce Bugbee*

Crop Physiology Laboratory, Utah State University, Logan, UT, United States

The ratio of active phytochrome (Pfr) to total phytochrome (Pr + Pfr), called phytochrome photo-equilibrium (PPE; also called phytochrome photostationary state, PSS) has been used to explain shade avoidance responses in both natural and controlled environments. PPE is commonly estimated using measurements of the spectral photon distribution (SPD) above the canopy and photoconversion coefficients. This approach has effectively predicted morphological responses when only red and far-red (FR) photon fluxes have varied, but controlled environment research often utilizes unique ratios of wavelengths so a more rigorous evaluation of the predictive ability of PPE on morphology is warranted. Estimations of PPE have rarely incorporated the optical effects of spectral distortion within a leaf caused by pigment absorbance and photon scattering. We studied stem elongation rate in the model plant cucumber under diverse spectral backgrounds over a range of one to 45% FR (total photon flux density, 400–750 nm, of 400 μmol m^{-2} s^{-1}) and found that PPE was not predictive when blue and green varied. Preferential absorption of red and blue photons by chlorophyll results in an SPD that is relatively enriched in green and FR at the phytochrome molecule within a cell. This can be described by spectral distortion functions for specific layers of a leaf. Multiplying the photoconversion coefficients by these distortion functions yields photoconversion weighting factors that predict phytochrome conversion at the site of photon perception within leaf tissue. Incorporating spectral distortion improved the predictive value of PPE when phytochrome was assumed to be homogeneously distributed within the whole leaf. In a supporting study, the herbicide norflurazon was used to remove chlorophyll in seedlings. Using distortion functions unique to either green or white cotyledons, we came to the same conclusions as with whole plants in the longer-term study. Leaves of most species have similar spectral absorbance so this approach for predicting PPE should be broadly applicable. We provide a table of the photoconversion weighting factors. Our analysis indicates that the simple, intuitive ratio of FR (700–750 nm) to total photon flux (far-red fraction) is also a reliable predictor of morphological responses like stem length.

Keywords: phytochrome, morphology, photobiology, far-red, photostationary state, phytochrome photoequilibrium

OPEN ACCESS

Edited by:
Oliver Körner,
Leibniz Institute of Vegetable and Ornamental Crops, Germany

Reviewed by:
Tao Li,
Institute of Environment and Sustainable Development in Agriculture, Chinese Academy of Agricultural Sciences, China
Shardendu Kumar Singh,
AeroFarms, United States

****Correspondence:***
Paul Kusuma
paul.kusuma@aggiemail.usu.edu

Specialty section:
This article was submitted to Crop and Product Physiology, a section of the journal Frontiers in Plant Science

Received: *20 August 2020*
Accepted: *28 April 2021*
Published: *24 May 2021*

Citation:
Kusuma P and Bugbee B (2021) Improving the Predictive Value of Phytochrome Photoequilibrium: Consideration of Spectral Distortion Within a Leaf. Front. Plant Sci. 12:596943. doi: 10.3389/fpls.2021.596943

INTRODUCTION

Light-emitting diodes (LEDs) provide a high degree of control over spectral output, which can be utilized to manipulate plant photoreceptors, but this manipulation requires an understanding of the photoreceptor activity. The action of phytochrome, the most well studied photoreceptor, has been extensively modeled (Sage, 1992), and our understanding continues to evolve (Sellaro et al., 2019; Smith and Fleck, 2019). In addition to predicting plant morphology in the field, phytochrome models must be able to predict morphology in controlled environments that can have unique background spectra.

Here we describe the historic and evolving modeling of phytochrome action that is largely based on stem/hypocotyl elongation. We discuss how these models have mostly ignored the issue spectral distortion by chlorophyll screening in green plants, and show that accounting for spectral distortion within leaves improves the predictive capability of classic phytochrome models.

A Historic Review of Phytochrome Modeling

Models of phytochrome action were developed in parallel with its discovery. The first models included the photon absorbing pigment phytochrome and reaction partners (Borthwick et al., 1952), where two forms of phytochrome were interconverted by red (R) and far-red (FR) photons. Later, Hartmann (1966) provided a hypothesis to explain how phytochrome controlled the high irradiance response. He simultaneously irradiated hypocotyls with photons at two wavelengths, and explained the results with an estimate of the ratio of Pfr to Ptotal [called phytochrome photoequilibrium (PPE) or the photostationary state (PSS)], where Ptotal is the sum of Pr plus Pfr.

Hartmann's work was praised by Smith (1973, 1975), who hypothesized that the PPE ratio explained phytochrome regulated responses in mature plants in the natural environment. Morgan and Smith (1976) provided evidence for this hypothesis by showing a direct linear relationship between PPE and the log of the stem extension rate. Morgan and Smith (1979) went on to show that this log linear relationship generally held for multiple species that evolved in a range of environments with the exception of understory plants that evolved in woodland areas, which had either a reduced or absent response. Child and Smith (1987) further built upon this hypothesis, showing that the rapid percentage increase in stem extension rate after applying FR was linearly correlated with PPE.

Smith and collaborators either measured PPE directly in etiolated tissue (Morgan and Smith, 1976; Smith, 1990) or estimated it with the R:FR ratio (Morgan and Smith, 1978, 1979). It is now common to predict PPE from the spectral photon distribution (SPD) above the canopy and photoconversion coefficients: σ_R for the conversion of Pr $\rightarrow$ Pfr, and σ_{FR} for the conversion of Pfr $\rightarrow$ Pr. These coefficients are essentially probability functions that predict the likelihood of photon absorbance at a given wavelength and subsequent conversion to the other form. The calculation to estimate PPE following this method is as follows:

$$\mathrm{PPE} = \frac{\mathrm{Pfr}}{\mathrm{Ptotal}} = \frac{\sum_{\lambda=300\ \mathrm{nm}}^{\lambda=800\ \mathrm{nm}} I_\lambda\ \sigma_{R,\lambda}}{\sum_{\lambda=300\ \mathrm{nm}}^{\lambda=800\ \mathrm{nm}} I_\lambda\ \sigma_{R,\lambda} + \sum_{\lambda=300\ \mathrm{nm}}^{\lambda=800\ \mathrm{nm}} I_\lambda\ \sigma_{FR,\lambda}} \quad (1)$$

Where I_λ is the incident photon flux density at wavelength, λ. Photoconversion coefficients are calculated from *in vitro* measurements of the photochemical properties of phytochrome including: (1) absorbance spectra, (2) an estimation/calculation of PPE under actinic red photons, (3) the extinction coefficient of Pr at the peak in the red region (about 668 nm), and (4) quantum yields of Pr $\rightarrow$ Pfr and Pfr $\rightarrow$ Pr. Different photochemical properties are provided in at least ten publications (see Mancinelli, 1986, 1988, 1994; Lagarias et al., 1987). Thus it is possible to derive different photoconversion coefficients (Here, the term photoconversion coefficient refers to what has historically been called the photochemical/photoconversion cross-section, whereas the term photoconversion coefficient historically refers to the photochemical cross-section divided by the natural log of 10. Because coefficient is a more friendly term we use this term instead of cross-section).

These photoconversion coefficients, however, are primarily based on phytochrome-A (phyA) and not phyB. The phyB photoreceptor is the primary phytochrome photoreceptor responsible for sensing and responding to shade in the natural environment (Legris et al., 2019). Although phyA plays a larger role during de-etiolation (Mazzella and Casal, 2001), only monogenic mutants deficient in phyB (compared to monogenic mutants deficient in phyA, phyC, phyD, or phyE) appear elongated when grown in white light indicating the dominant role of phyB past the stage of de-etiolation (Whitelam et al., 1993; Aukerman et al., 1997; Devlin et al., 1998, 1999; Franklin et al., 2003; Franklin and Quail, 2010). Some limited evidence suggests that the photochemical properties of phyA and phyB may be similar (Ruddat et al., 1997; Eichenberg et al., 2000). If so, the fact that the photoconversion coefficients are derived primarily from phyA may not be a significant concern.

Estimates of PPE using photoconversion coefficients and the SPD above the leaf were used by Park and Runkle (2017, 2018, 2019) whose data shows a linear (as opposed to log linear) relationship between estimated PPE and stem length in several ornamental species. Overall, PPE estimates have resulted in a negative relationship with stem length. One limitation of most previous studies is that they are typically performed under a single background SPD, and treatments often only change the amount of FR and occasionally the amount of R. Thus, the full extent of the reliability of estimated PPE to predict morphology has not been determined.

Recent PPE Modeling Efforts

The Three-State Model

The model described above (PPE = Pfr / Ptotal) is called *the two-state model*. A more complex model considers the dimerization of the phytochrome molecule in which the two arms of the dimer are activated independently. This is called *the three-state model*. It assumes only the Pfr–Pfr homodimer (called D_2) is

the active form, while the Pr–Pr homodimer (D_0) and the Pr–Pfr heterodimer (D_1) are both inactive. Therefore *the three-state model* at photoequilibrium is equal to $D_2/(D_0+D_1+D_2)$, which can be calculated by squaring PPE calculated by *the two-state model* (PPE^2; Mancinelli, 1988, 1994). Although there is sufficient evidence to suggest that phytochrome exists as a dimer (Jones and Quail, 1986; Brockmann et al., 1987; Rockwell et al., 2006) the evidence that D_2 is the only active form is at present only based on mathematical analysis (Klose et al., 2015), and further investigation is required.

The Cellular Model

Thermal reversion, phytochrome destruction and nuclear body association/disassociation can either reduce or stabilize the pool of active phytochrome (Rausenberger et al., 2010; Klose et al., 2015). When these factors are considered the model is referred to as *the cellular model*. Sellaro et al. (2019) described that these other factors mainly play a role at low photon fluxes and/or high temperature, while only photoconversions apply at sufficiently high photon fluxes and low enough temperature. This model is thoroughly described in Smith and Fleck (2019). These complex models have yet to be used in applied research.

Spectral Distortion Within Leaves

Leaves/cotyledons, and not stems/hypocotyls, were shown to be the primary site of red and far-red perception in *Cucumis sativus* (Black and Shuttleworth, 1974), *Sinapis alba* (Casal and Smith, 1988a), *Arabidopsis thaliana* (Tanaka et al., 2002; Endo et al., 2005), and *Brassica rapa* (Procko et al., 2014), while both organs were shown to be perceptive in a separate study in *Sinapis alba* (Casal and Smith, 1988b) and the epicotyl was shown to be the primary site of perception in *Vigna sinensis* (García-Martínez et al., 1987). Upon far-red perception in leaves/cotyledons, signals (including auxin) are transported to the stem/hypocotyl to induce elongation (Tanaka et al., 2002; Procko et al., 2014). From these data, it seems likely that phytochrome in the leaves/cotyledons play a dominant role in controlling stem elongation, with stems/hypocotyls playing a secondary role.

A major issue with using photoconversion coefficients to estimate PPE is that they are applied to the SPD above the leaf, and not the SPD at the phytochrome molecule, which is distorted by chlorophyll and other pigments, as well as cell walls. Photons are scattered within leaves making the light diffuse within leaves (**Figure 1**). Due to this internal reflection, refraction and diffraction, leaves act as "light traps" wherein the photon intensity in the epidermis can exceed the intensity above the leaf by several fold (Seyfried and Fukshansky, 1983; Vogelmann, 1994). Because the term attenuation specifically refers to a decrease in the photon intensity, we use the term distortion to describe spectral changes in leaves.

Both Morgan and Smith (1978) and Gardner and Graceffo (1982) discuss chlorophyll screening issues stating that estimates of PPE (above the leaf) are only accurate for the top epidermal layer of cells within a leaf. Gardner and Graceffo (1982) suggested that the functional layer of phytochrome must be near the outer epidermal layer because of the linear relationship between PPE and the log stem extension rate seen in Morgan and Smith (1976). These assumptions are invalid because spectral distortions still occur in the epidermis, and additionally, several studies have shown that the peaks of phytochrome regulated action spectra shift to lower wavelengths than the peak absorbance of extracted phytochrome, indicating that some degree of spectral distortion occurs within leaves. For example, Kasperbauer et al. (1963) observed that inhibition of flowering in *Chenopodium rubrum* was most affected by night break lighting at 645 nm, instead of the expected 660 (or 668) nm, an effect they attributed to spectral filtering by chlorophyll. Similarly, Jose and Schäfer (1978) found that 630 nm photons induced the shortest hypocotyls and internodes in green tissue.

Several attempts have been made to account for spectral distortion within a leaf, especially via Kubelka-Munk theory. The Kubelka-Munk theory describes light propagation within a scattering medium like a leaf (Vogelmann, 1994). It simplifies to the Beer-Lambert law if extinction and scattering coefficients are assumed to be constant and not dependent on fractional distance through the leaf (Evans, 1995). Holmes and Fukshansky (1979) modeled PPE through a green leaf using the Kubelka-Munk theory and estimated that PPE decreased by about 40% as it moved through a leaf under full sunlight. Later, Kazarinova-Fukshansky et al. (1985) used the Kubelka-Munk theory to develop distortion functions that describe photon gradients within zucchini cotyledons. These distortion functions can be multiplied by the phytochrome photoconversion coefficients to develop weighting factors that can be used to predict the action spectra of phytochrome conversions within a certain layer of cotyledon tissue based on the incident photon flux above the leaf. Little has been done to test predictions of PPE with these weighting factors using experimental data. As such, despite the efforts of Kazarinova-Fukshansky et al. (1985), above-the-leaf estimates are still regularly employed.

Because the degree of spectral distortion depends on the specific layer of the leaf, it is important to ask whether all phytochrome is "functional". The epidermis has been shown to control the rate of elongation (Kutschera and Niklas, 2007; Savaldi-Goldstein et al., 2007), but whether the epidermis is where the light signals are perceived, especially in leaf/cotyledon tissue, remains undetermined. Phytochrome is expressed in all tissue (Somers and Quail, 1995), but Kim et al. (2016) concluded that only phytochrome in epidermal tissue (of the hypocotyl) controlled elongation under continuous R light and end-of-day FR. This conclusion was based on transgenic lines of *Arabidopsis thaliana* that controlled *PHYB* expression using hypocotyl-tissue-specific promoters, effectively limiting phyB to specific layers of hypocotyl tissue (i.e., epidermis, cortex, endodermis, and vasculature). Endo et al. (2005) similarly expressed phytochrome in tissue specific organs and found that mesophyll-located phytochrome (in the cotyledons) controlled elongation.

Our objective was to use models of spectral distortion within a leaf (for both epidermal-located phytochrome and homogeneously distributed phytochrome) to improve the predictive relationship between PPE and morphological parameters.

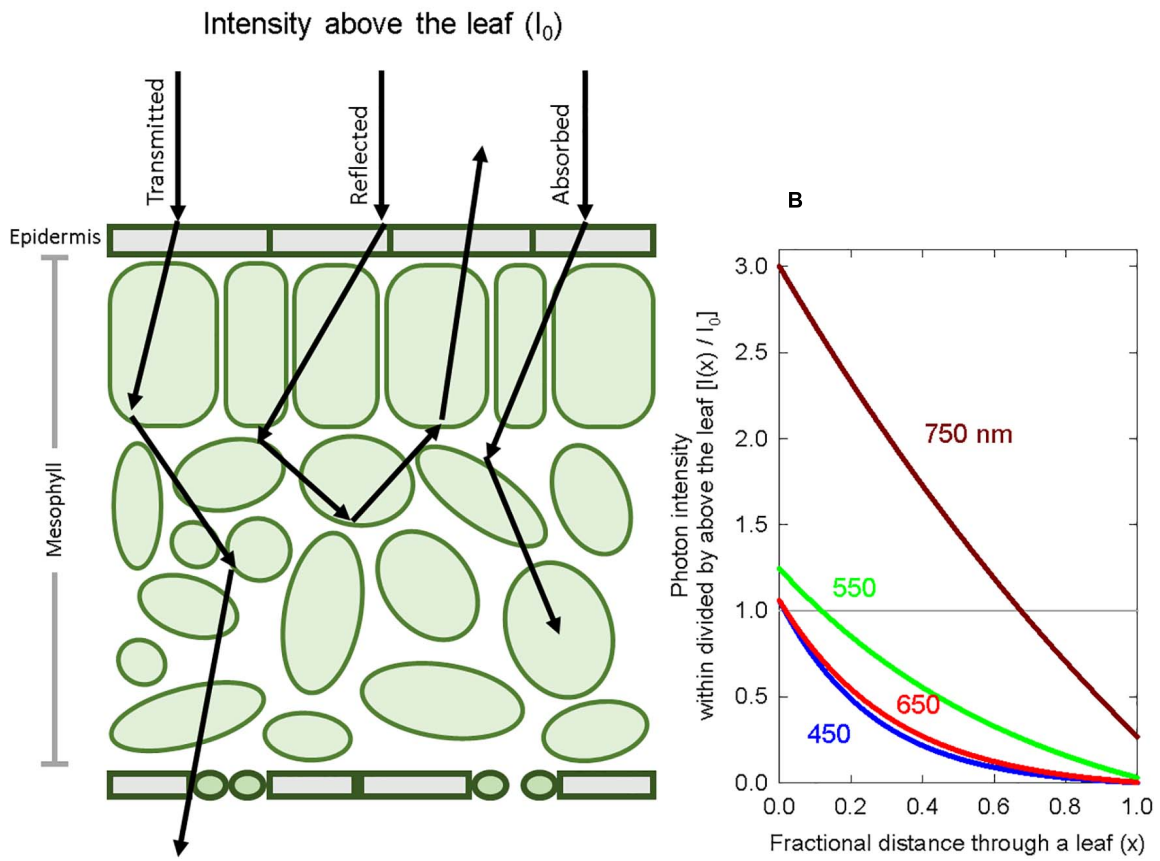

FIGURE 1 | Basic principles of spectral distortion and photon scattering within a leaf. **(A)** A diagram of a cross section of a leaf showing the scattering of photons, which are eventually transmitted, reflected or absorbed. **(B)** A graphical representation of photon intensity at wavelengths 450, 550, 650, and 750 nm as a function of leaf depth. Because of reflection, diffraction and refraction, the photon intensity in the top layers of a leaf can exceed the intensity above the leaf. The Kubelka-Munk theory was used to calculate photon intensity with depth. The grey horizontal line represents the photon intensity just above the leaf.

MATERIALS AND METHODS

Two studies were conducted:

1. Cucumber plants were grown for 10–15 days in growth chambers with unique spectral backgrounds and different doses of FR (long-term study).
2. Elongation of photobleached and green cucumber seedlings were compared after 2 days in the growth chambers with a gradient of FR (short-term photobleaching study).

In both studies, multiple models of spectral distortion were used to predict PPE in specific layers of tissue.

Plant Materials

Long-Term Study

Tomato, lettuce, spinach, soybean, and cucumber were screened for sensitivity to FR by applying either a low dose or no added FR. Cucumber was the most sensitive species to FR and was selected for further study (example data from one tomato study is shown in **Supplementary Figure 1**).

Seeds of cucumber (*Cucumis sativus* cv. Straight Eight) were planted into 1.7 L pots with a 1:1 mixture of peat/vermiculite by volume amended with 1.6 g per liter of dolomitic lime and 0.8 g per liter Gypsum ($CaSO_4$). Cotyledons emerged 4 days after planting and pots were moved from the greenhouse to the growth chambers (**Supplementary Figure 2**).

Short-Term Photobleaching Study

Nine cucumber seeds were germinated on black felt saturated with nutrient solution (Utah hydroponic refill solution for dicots, USU Crop Physiology Laboratory, 2020) in each of 22 germination boxes (18 × 16.5 cm^2) at 21°C. Black felt was used to minimize ground reflection so photons would primarily enter the cotyledons from above (**Supplementary Figure 3**). After 3 days the radicle had emerged, and nutrient solution was re-applied, with half of the germination boxes (11 boxes) receiving 50 μM norflurazon in the nutrient solution. Norflurazon is an herbicide that blocks the synthesis of carotenoids, leading to

photobleaching in high light, eventually killing the plant. Seeds were then moved into pretreatment conditions: two norflurazon treated and two non-treated boxes were moved into the dark and the remainder of the boxes were moved into a growth chamber with a continuous photosynthetic photon flux density (PPFD) of about 500 µmol m^{-2} s^{-1} (**Supplementary Figure 4**) and a temperature of 20°C to finish emerging. 12% of the seeds either did not germinate or were not vigorous and all boxes had at least 6 seedlings. After 3 days in the pretreatment the norflurazon treated seedlings appeared white with an average hypocotyl length of 1.4 cm and the non-photobleached seedlings had an average hypocotyl length of 1.2 cm. 3 days in continuous light reduces the concentration of highly light-labile phyA, which was shown to be reduced by 50- to 100-fold after 12 h under low red photon flux and was below detectable limits after 7 days in white light (Sharrock and Clack, 2002). This ensured that responses were primarily caused by phyB. The germination boxes were placed in seedling trays with one photobleached and one non-photobleached germination box in each tray. Trays were then placed in the growth chambers for 48 h. This was repeated four times.

Environmental Conditions

Long-Term Study

Temperature was maintained at 27/22°C day/night. Plants were watered as needed (typically every 2–3 days) with a complete nutrient solution at a concentration of 120 mg N per L (Peter's professional 20-10-20, 20N-4.4P-16.6K; Allentown, PA). Potassium silicate (AgSil16H; Certis United States; Columbia, MD, United States) was added to the nutrient solution at 0.3 mM Si. Chambers were enriched to 850 ppm CO_2. All studies contained six replicate plants per treatment. Plants were rotated every other day to minimize any position effects in the chamber. Individual plants were analyzed as replicates. Plant density was 20 plants per square meter.

Short-Term Photobleaching Study

Temperature was maintained at a constant 20°C. The norflurazon treated seedlings lost turgor at low humidity so water was added to the tray and the tray was covered to raise the humidity. Condensation formed on the lid of the seedling trays.

Spectral Treatments

Spectral measurements were made with a spectroradiometer (PS-300; Apogee instruments; Logan, UT, United States). For both the long-term and the short-term studies, three growth chambers (1.25 × 0.9 × 1.2 m^3, L × W × H) provided separate background SPD from either cool white LED fixtures, 400-W high-pressure sodium (HPS) fixtures, or white + red LED fixtures. These background spectral distributions are common in controlled environment agriculture and are referred to here as high blue (cool white LED), high green (HPS) and high red (white + red LED). Spectral data for these background spectra are provided in **Table 1** and **Figure 2**.

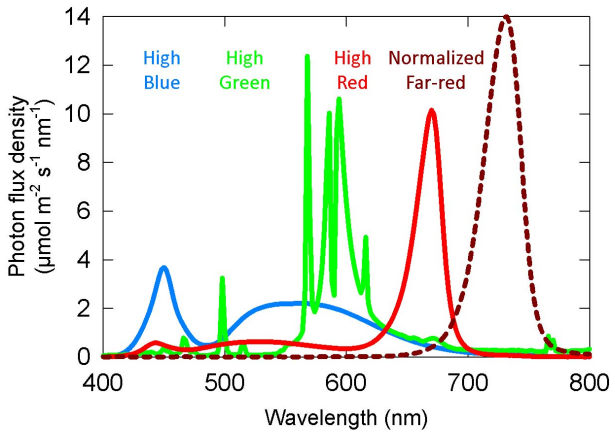

FIGURE 2 | Representative spectral photon distributions (SPD) of the high blue, high green, and high red spectra used in both the long-term and short-term studies. The dashed dark red line is the SPD of the far-red, which was variable among studies.

TABLE 1 | Ratios of colors for the three spectral backgrounds.

Treatment	% BLUE ∑ 400 –499 nm / ∑ 400 –700 nm	% GREEN ∑ 500 –599 nm / ∑ 400 –700 nm	% RED ∑ 600 –699 nm / ∑ 400 –700 nm	Total
HIGH BLUE	29	48	23	100
HIGH GREEN	6	52	42	100
HIGH RED	7	12	81	100

Long-Term Study

Each chamber was separated in half with a white reflective board to provide a higher and lower level of FR from LEDs (peak of 730–735 nm). This allowed for two fractions of FR in each trial in time. Cucumber plants in the chambers at the end of one of these studies are shown in **Figure 3A**. The FR fraction was then varied among trials to achieve a collective range of one to 45% FR across seven replicate trials for a total of 14 doses of FR in each spectral background. Using regression analysis with plant rotation, this provided 84 replicates (six replicate plants × 14 doses of FR) for each spectral background.

Percent far-red (FR fraction) was calculated as:

$$\text{Percent far red} = \frac{\text{FR flux } (701 - 750 \text{ nm})}{\text{ePPFD } (400 - 750 \text{ nm})} \times 100 \qquad (2)$$

Because FR photons are photosynthetically active (Zhen and van Iersel, 2017; Zhen and Bugbee, 2020), the extended photosynthetic photon flux density (ePPFD: 400–750 nm) was kept constant among studies. This meant that as FR increased, the traditional PPFD (400–700 nm) decreased. For ePPFD, a cut-off wavelength of 750 nm may slightly overestimate photosynthetic photons (Zhen et al., 2018), but this definition is adequate for FR from LEDs. The average ePPFD was 400 and carefully adjusted so that it varied less than 10 µmol m^{-2} s^{-1} among the background spectra in each study. The

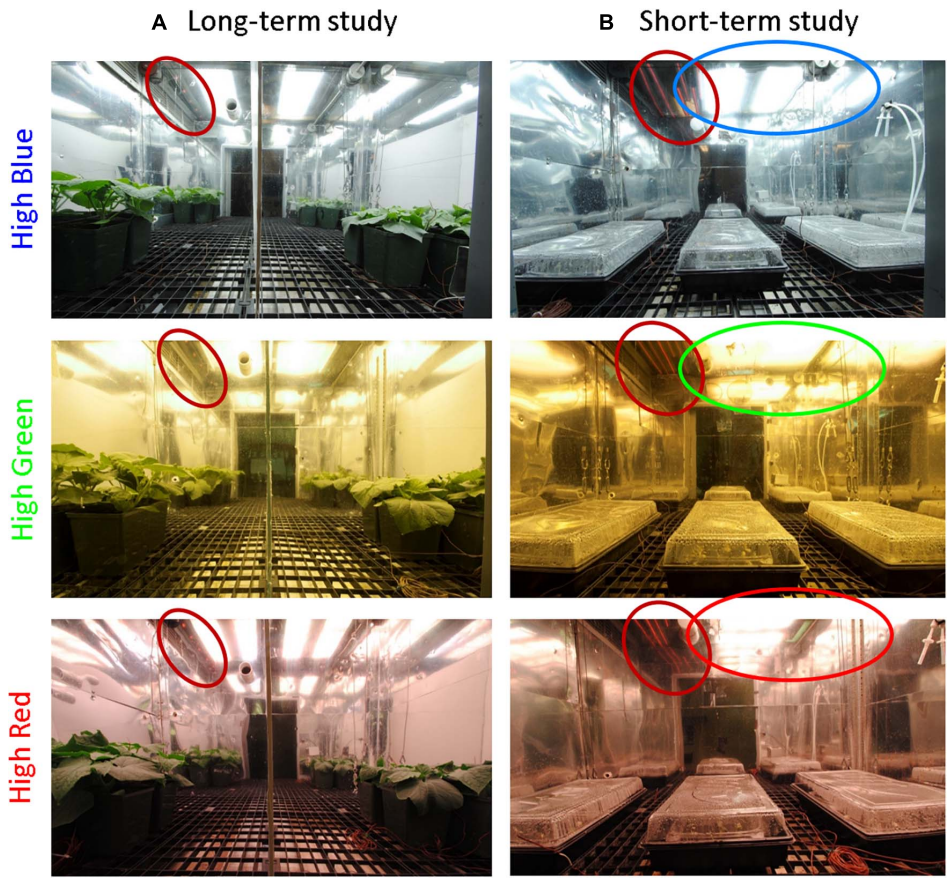

FIGURE 3 | (A) Example photo of the plants in the high blue, green, and red chambers from the long-term studies. In this example there was no added far-red (FR) on the right side in each chamber. Treatments were randomized among studies. Each chamber was divided in half to supply two doses of FR. FR LEDs are circled in red. There is a second FR LED on the other side of the background LED (out of view, see **Supplementary Figure 2**) to improve the uniformity of FR. Additionally, in studies with higher fractions of FR, LEDs were placed across the top of the chamber. Uniformity within and between treatments was ensured by dimming lamps with either power supply capabilities or neutral density window screen. To achieve uniformity of SPD and extended photosynthetic photon flux density (ePPFD), the plants were grown on the sides of each half-chamber. **(B)** Photo of the experimental set-up for short-term photobleaching seedling study. Each chamber was provided with a high dose of FR on one side of the chamber and the background light source on the other side of the chamber. This provided a gradient of percent far-red decreasing from left to right. FR LEDs are circled in red, and the background light source is circled in its respective color. Seedlings (in germination boxes) were kept in seedling trays that were brought to a high relative humidity by placing water in the bottom of the tray.

photoperiod was 16 h. Detailed spectral information showing the 1–45% FR is provided in **Supplementary Table 1** and **Supplementary Figure 5**.

Short-Term Photobleaching Study

The background light fixtures were placed at the top of one side of the chamber and FR LED bars were placed on the other side of the chamber to provide a gradient of FR that increased from right to left while the PPFD increased from left to right. Seedling trays were placed on the left, middle and right sides of the chamber to obtain about 18, 31, and 50% FR for each background spectrum. A photo of the experimental set-up is provided in **Figure 3B**. The average ePPFD in these studies was 300 μmol m^{-2} s^{-1} and varied less than 15 μmol m^{-2} s^{-1} among the background spectra. The SPDs for these studies are shown in **Supplementary Figure 6**. Light was applied continuously for the whole 48 h treatment period.

Estimation of PPE

We calculated PPE (assuming *the two-state model*) following Eq. 1. We used the photoconversion coefficients derived from the photochemical properties in Lagarias et al. (1987). These are different than other commonly-used photoconversion coefficients (Kelly and Lagarias, 1985; Sager et al., 1988) on an absolute scale, but are similar when normalized to the Pr peak. The absolute magnitudes of the photoconversion coefficients are only important if other rates of phytochrome dynamics, like thermal reversions, are considered.

Estimation of the Three-State Model

We did not account for the additional factors in *the cellular model* proposed by Rausenberger et al. (2010) and modified

by Klose et al. (2015). Sellaro et al. (2019) reported that when the temperature is 25°C, the cellular model reaches 99% of *the three-state model* (assuming only photoconversions) at a PPFD of about 450 μmol m^{-2} s^{-1}, and when the temperature is 20°C, the cellular model reaches 99% of *the three-state model* at a PPFD of about 350 μmol m^{-2} s^{-1}. These conditions are close to the environmental conditions used in these experiments. Therefore, we used the simplified *three-state model* assuming the temperature effects on phytochrome reversion were negligible. As mentioned previously, *the three-state model* is simply calculated by squaring PPE calculated by Eq. 1 (Mancinelli, 1988).

Modeling Spectral Distortion Within a Leaf

We use spectral distortion functions derived from Kazarinova-Fukshansky et al. (1985) to predict spectral distortion at the phytochrome molecule under the assumption that "functional" phytochrome is either (1) only located in the epidermis (top 1% of the leaf), or (2) homogeneously distributed within all layers of the leaf. All curves from Kazarinova-Fukshansky et al. (1985) were obtained using GetData Graph Digitizer[1]. Kazarinova-Fukshansky et al. (1985) modeled spectral distortion using the Kubelka-Munk theory within 7 days old *Cucurbita pepo* cv. "Senator" (zucchini), a species closely related to cucumber.

The Kubelka-Munk theory-based distortion functions use transmittance and reflectance measurements, so we include this data in **Figure 4A** for etiolated and green zucchini seedlings (Kazarinova-Fukshansky et al., 1985). **Figure 4B** shows the distortion functions for green plants assuming "functional" phytochrome is (1) only in the epidermal tissue (orange lines) or (2) homogenously distributed throughout the whole leaf (purple lines). **Figure 4C** shows the same distortion functions in etiolated tissue.

The photoconversion coefficients derived from Lagarias et al. (1987) were multiplied by the distortion functions to obtain modeled estimates of phytochrome conversion weighting factors (or action spectra) in specific layers of tissue (Eq. 3).

$$\text{Photoconversion weighting factor for Pr}(\lambda) = \sigma_R(\lambda) \times \text{Distortion coefficient }(\lambda)$$

$$\text{Photoconversion weighting factor for Pfr}(\lambda) = \sigma_{FR}(\lambda) \times \text{Distortion coefficient }(\lambda) \quad (3)$$

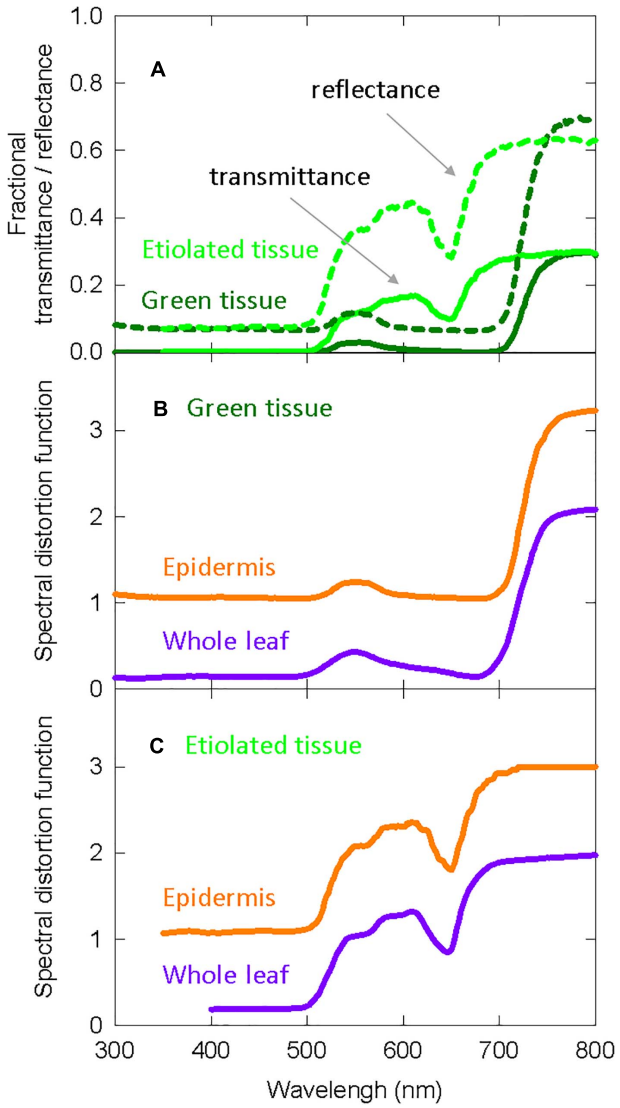

FIGURE 4 | Spectral distortion functions developed from zucchini that were used in both the long-term and the short-term studies on elongation in cucumber. **(A)** Fractional transmittance (solid) and reflectance (dashed) spectra of green and etiolated zucchini cotyledons. Etiolated cotyledons represented norflurazon treated cotyledons. **(B)** Derived spectral distortion functions for green plants in epidermal tissue (orange) or the whole leaf (purple). **(C)** Derived spectral distortion functions in etiolated/white seedlings for epidermal tissue (orange) or the whole leaf (purple). All data are derived from Kazarinova-Fukshansky et al. (1985).

Plant Measurements

Long-Term Study

Plants were harvested when the stem length in the highest FR treatment was 25–30 cm long; this occurred 10–15 days after emergence. Stem length, petiole length and leaf area were recorded. Leaf area was measured with a leaf area meter (model Li-3000, LI-COR, Lincoln NE). Leaves, cotyledons and stems were separated and dried at 80°C for 2 days, after which dry mass was measured and percent leaf and percent stem dry mass were calculated by dividing the respective dry mass by the total dry mass.

Stems typically elongate following a sigmoidal curve (Fisher et al., 1996; Björkman, 1999) with exponential elongation in young plants (Morgan and Smith, 1978), followed by linear elongation, and finally, exponential rise to a maximum. This

[1]http://getdata-graph-digitizer.com

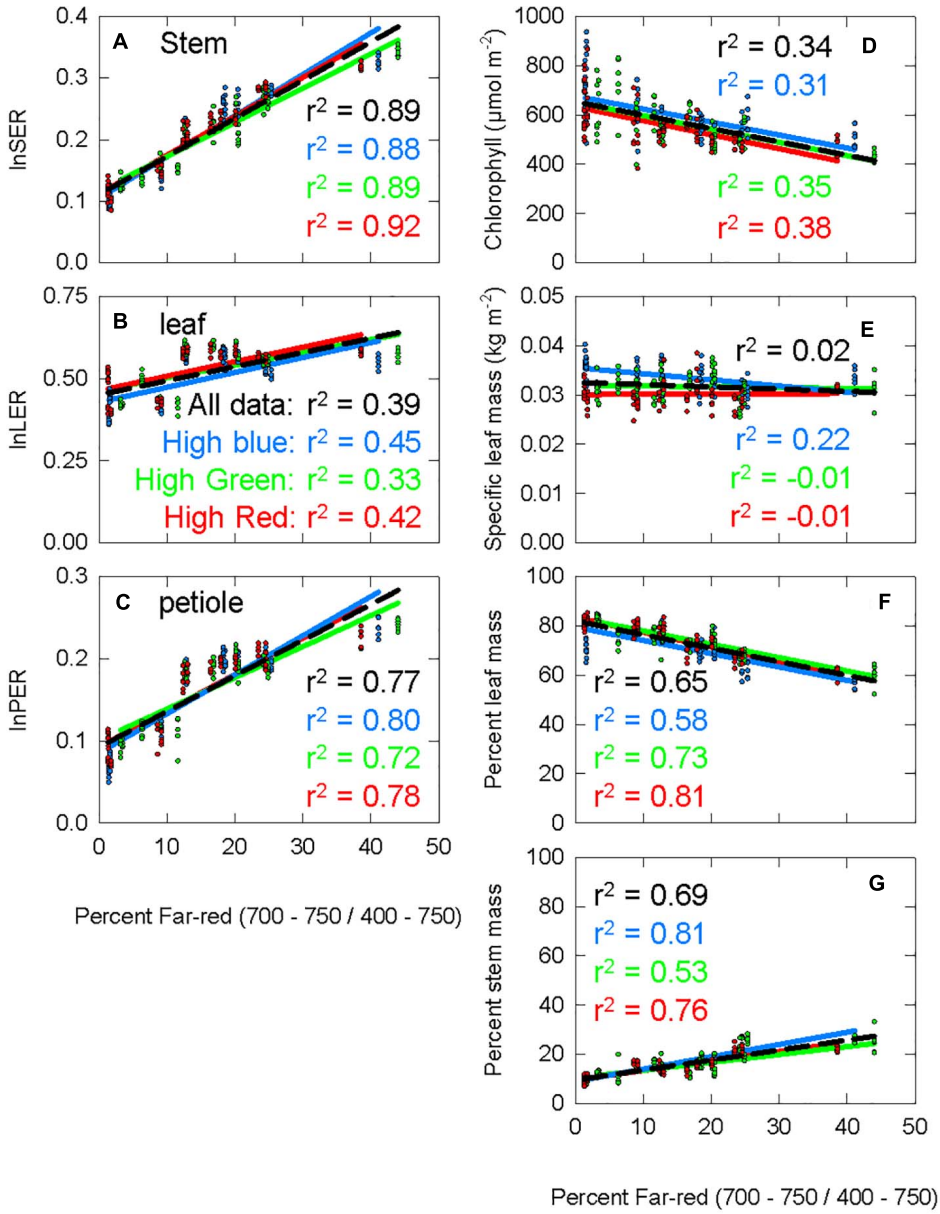

FIGURE 5 | The response of seven physiological parameters to increasing percent far-red. The blue data and lines come from the chamber with spectral background containing a high portion of blue photons (high blue), the green data comes from the high green chamber, and the red data comes from the high red chamber. The r^2 value for each background is shown with the respective color. The black dashed line is a trend line running through all the data from all three background light sources, with the corresponding r^2 shown in black. **(A)** The stem extension rate constant (the natural log of the stem extension rate, log of the stem extension rate (lnSER); described in Eqs 4, 5). **(B)** The leaf expansion rate constant, calculated following the same method as lnSER, but using leaf area at harvest instead of stem length. **(C)** Petiole extension rate constant, calculated following the same method as lnSER, but using petiole length at harvest instead of stem length. **(D)** Chlorophyll concentration at harvest. **(E)** Specific leaf mass, leaf mass divided by leaf area. **(F)** Percent leaf mass, leaf mass divided by total shoot mass **(G)** percent stem mass, stem mass divided by total shoot mass.

means that elongation is best described as a natural log function in the early stages of growth. For this reason early studies regularly used log-linear stem elongation rates to predict elongation as a function of PPE (Morgan and Smith, 1976, 1978, 1979). Thus in young plants, stem length at day (t) would be equal to:

$$\text{Stem length}\,(t) = \text{Stem length}\,(i)\,e^{kt} \tag{4}$$

Where Stem length (i) is the initial length. We can then calculate the exponential extension coefficient (the natural log of the stem extension rate; lnSER or k in Eq. 4), assuming the initial stem length was equal to one, as follows:

$$\text{lnSER} = \frac{\ln\left(\text{Stem length at harvest}\right)}{\text{days to harvest}} \tag{5}$$

This equation was also used to calculate the leaf expansion coefficient (natural log of the leaf expansion rate; lnLER) and the petiole extension coefficient (natural log of the petiole extension rate; lnPER). Chlorophyll concentration was measured with a chlorophyll meter (model MC-100, Apogee Instruments, Logan, UT, United States).

Short-Term Photobleaching Study

Cucumber hypocotyl lengths were measured with a ruler to the nearest 0.5 mm before and after they were moved into the treatments. The change in hypocotyl length over 48 h was normalized to the elongation of the respective dark control:

$$\text{Elongation relative to the control} = \frac{L_f - L_i}{L_{c,t2} - L_{c,t1}} \quad (6)$$

Where L_f is the final hypocotyl length, L_i is the initial hypocotyl length, and $L_{c,t1}$ and $L_{c,t2}$ are the average hypocotyl lengths of the dark controls before or after the cucumber seedlings were placed in the treatments. The change in hypocotyl length was normalized to its respective control (with or without applied norflurazon) due to the finding of Casal (1995) in which norflurazon treated seedlings grown in the dark were 15–20% shorter than untreated seedlings. For each replicate in time, the elongation relative to the control for all the seedlings in each treatment were averaged together.

Statistics

All data was analyzed using R statistical software (R Foundation for Statistical Computing; Vienna, Austria). Correlations were determined by calculating the r^2 value of a trend-line through the data. Trend-lines used either linear or exponential decay functions. Data was analyzed using a mixed effect linear model using *lmer* and *Anova* functions with the F statistic judged to be significant at $p < 0.05$. The background spectra (e.g., high blue) were treated as a categorical variable, while different methods for analyzing the effect of FR were treated as a continuous variable. Two examples of methods for analyzing the effects of far-red include percent FR and PPE modeled above the leaf. Chambers and replicates were treated as random factors.

RESULTS

Long-Term Study

The percent far-red ranged from less than 2% (which is only obtainable under LEDs) to 45% (typical of canopy shade). **Figure 5** shows the response of seven morphological parameters to increasing percent FR under three diverse spectral backgrounds. lnSER, lnLER, lnPER, and percent stem mass all increased with increasing percent FR (**Figures 5A–C,G**). Chlorophyll concentration and percent leaf mass both decreased with increasing percent FR (**Figures 5D,F**). Specific leaf mass, which is calculated by dividing leaf mass by leaf area and is an indicator of leaf thickness, was unaffected by percent FR (p = 0.19, **Figure 5E**). Because lnSER had the highest correlation with percent FR, it was used as the response variable for models of PPE within leaf tissue.

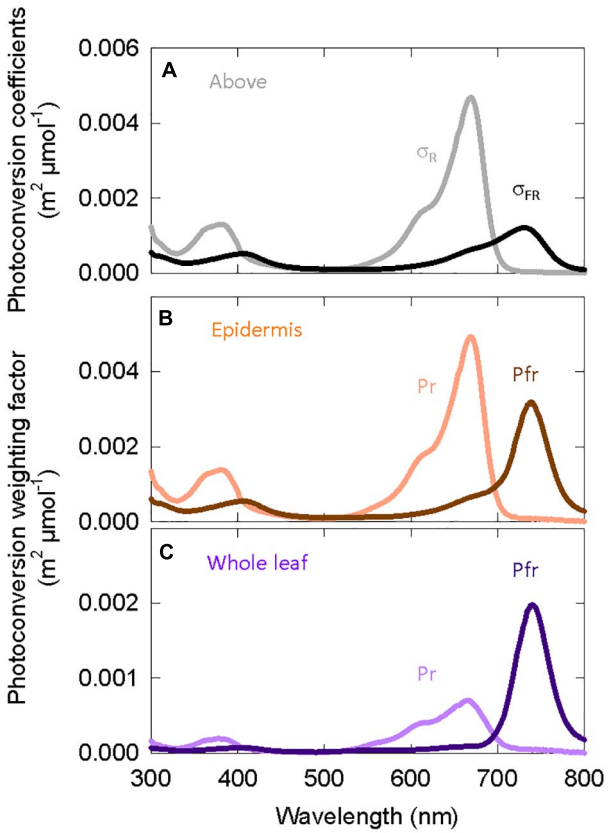

FIGURE 6 | (A) Photoconversion coefficients derived from Lagarias et al. (1987). These are used to estimate PPE above the canopy. The other two graphs are the photoconversion weighting factors for phytochrome that is **(B)** only in epidermal tissue or **(C)** homogeneously distributed through all leaf/cotyledon tissue.

Accounting for Spectral Distortions in Predictions of PPE

Multiplying the spectral distortion functions (**Figure 4B**) by the photoconversion coefficients (Eq. 3) provides weighting factors that predict local phytochrome conversions within a specific layer of tissue for a given SPD above the leaf (**Figure 6**). It is important to note that (a) the photochemical properties of phytochrome, and thus the photoconversion coefficients, have not changed and that (b) if no spectral distortion occurs within a leaf, then the photoconversion weighting factors are equal to the photoconversion coefficients.

Figure 6 shows that weighting factors for Pfr (Pfr → Pr) increase relative to Pr (Pr → Pfr) as the location of phytochrome moves from the epidermis to all leaf/cotyledon tissue. The weighting factors for Pr do not significantly shift the peak of action away from about 668 nm.

Using σ_R and σ_{FR} (**Figure 6A**) in Eq. 1 or substituting them with the Pr and Pfr weighing factors (**Figures 6B,C**) produces estimates PPE in three layers: PPE_{above}, $PPE_{epidermis}$, and $PPE_{wholeleaf}$. We fit the lnSER data in **Figure 5A** to the estimates of PPE in these three layers assuming the commonly used *two-state model* (**Figure 7**). There was a high correlation between PPE estimated above the leaf (PPE_{above}) and lnSER for any single background SPD (**Figure 7A**; r^2 = 0.91, 0.89, and 0.85 for high blue, high green and high red, respectively). This relationship declines if PPE is compared to all the data (all three background spectra, dashed line, r^2 = 0.47). The correlation between PPE and lnSER for any single background spectrum remained relatively unchanged when PPE was estimated in the epidermal leaf tissue ($PPE_{epidermis}$) or the whole leaf ($PPE_{wholeleaf}$), but the relationship with all the data was improved when predicted within the leaf (**Figures 7B,C**). $PPE_{wholeleaf}$ produced the highest correlation between PPE and lnSER of all the data (r^2 = 0.75, **Figure 7C**).

Comparison Between the Two-State and Three-State Models

The two-state and *three-state models* of phytochrome were compared assuming the active phytochrome was (a) in the epidermis and (b) homogeneously distributed in all the leaf tissue (**Figure 8** compared to **Figures 7B,C**). Using regression analysis through all three spectral backgrounds, *the three-state model* did not improve the predictive power over the commonly used *two-state model* for any of the three assumed locations of phytochrome (r^2 = 0.58 and 0.72 for $PPE_{epidermis}$ and $PPE_{wholeleaf}$, respectively).

To further investigate differences between these four estimates of PPE (**Figures 7B,C**, **8**), the slopes and offsets for the three individual background spectra (blue, green, and red lines) were compared using a linear mixed effects model, with the estimates of PPE as a continuous variable and the background spectrum as a categorical variable. There was a significant effect of the background spectrum on the prediction of lnSER for all four estimates of PPE, indicating that the offsets for the linear models were significantly different ($p < 0.0001$ in all cases). In the linear mixed effects model, an interaction effect between PPE and the background spectrum indicates that the slopes of the three lines are significantly different. This was the case for every model with the exception of only $PPE_{wholeleaf}$ using *the three-state model* (p = 0.25 compared to p = 0.033 for $PPE_{wholeleaf}$ using the *two-state model*, and $p < 0.0001$ for $PPE_{epidermis}$ using both the *two* and *three-state models*). This means that the three lines (blue, green, and red) in this model of PPE ($PPE_{wholeleaf}$ using *the three-state model*) are not significantly different (nearly parallel).

Short-Term Photobleaching Study

To further investigate the role spectral distortion by chlorophyll on estimates of PPE and subsequent stem or hypocotyl elongation, seedlings were grown with or without chlorophyll using the herbicide norflurazon.

The photobleaching of the norflurazon treated seedlings was visually apparent, although some seedlings had chlorophyll at the tips of the cotyledons (**Figure 9**). Over the 48 h treatment period, the dark-grown norflurazon treated seedlings elongated an average of 8.5 cm, while the non-treated seedlings elongated an average of 9 cm. Elongation of seedlings in the light treatments relative to the dark controls are plotted as a function of percent FR in **Figure 10**. The photobleached seedlings elongated significantly less than the green seedlings, but a higher fraction of FR induced more elongation in both green and photobleached seedlings.

Spectral distortion functions for etiolated seedlings (**Figure 4C**) were used to calculate weighting factors for phytochrome conversions in either the epidermis or the whole leaf (**Supplementary Figure 7**). The photoconversion coefficients (**Figure 6A**) were substituted with the weighting factors for specific locations in green or etiolated cotyledons (**Figures 6B,C** and **Supplementary Figure 7**) in Eq. 1 to estimate PPE in these treatments.

Figure 11 models the data in **Figure 10** with these estimates of PPE. For this analysis, both the green and photobleached seedlings grown under a single spectral background (e.g., high blue) were combined together for regression analysis. Similar to the long-term study, PPE estimated above the cotyledon produced a poor correlation when run through all the data from all three spectral backgrounds (r^2 = 0.20; **Figure 11A**), but unlike the long-term study, the regression through the data for a single spectral background also produced a poor correlation (r^2 = 0.12, 0.13, and 0.30 for high blue, high green and high red, respectively). Compared to PPE estimated above the cotyledon (PPE_{above}), the estimate of PPE within the epidermal tissue ($PPE_{epidermis}$) provided a slight improvement in predictive ability (**Figure 11B**). Corroborating the results of the long-term study, the assumptions that "functional" phytochrome is homogeneously distributed within the whole leaf ($PPE_{wholeleaf}$) provided the best correlations between PPE and elongation relative to the dark controls (**Figure 11C**). This was true for both correlations using all the data and correlations using each individual background spectrum.

Similar to the comparison between *the three-state* and *the two-state models* in the long-term study, there was little difference between the correlation between PPE and elongation relative to the control in a specific layer of tissue using either model. *The three-state model* for homogenously distributed "functional" phytochrome required non-linear models to fit the data, and this resulted in a strong relationship (**Figure 11E**).

DISCUSSION

Effects of Spectral Distortion on the Action Spectrum of Phytochrome Conversion

Kazarinova-Fukshansky et al. (1985) previously estimated the weighting factors for *in vivo* (either green or etiolated tissue) phytochrome photoconversions based on *in vitro* determinations of the photoconversion coefficients and their spectral distortion functions. They used the original photoconversion coefficients from Butler et al. (1964), which are based on partially degraded 60 kDa phytochrome rather than *native* 124 kDa phytochrome (Mancinelli, 1986). Therefore, the weighting factors

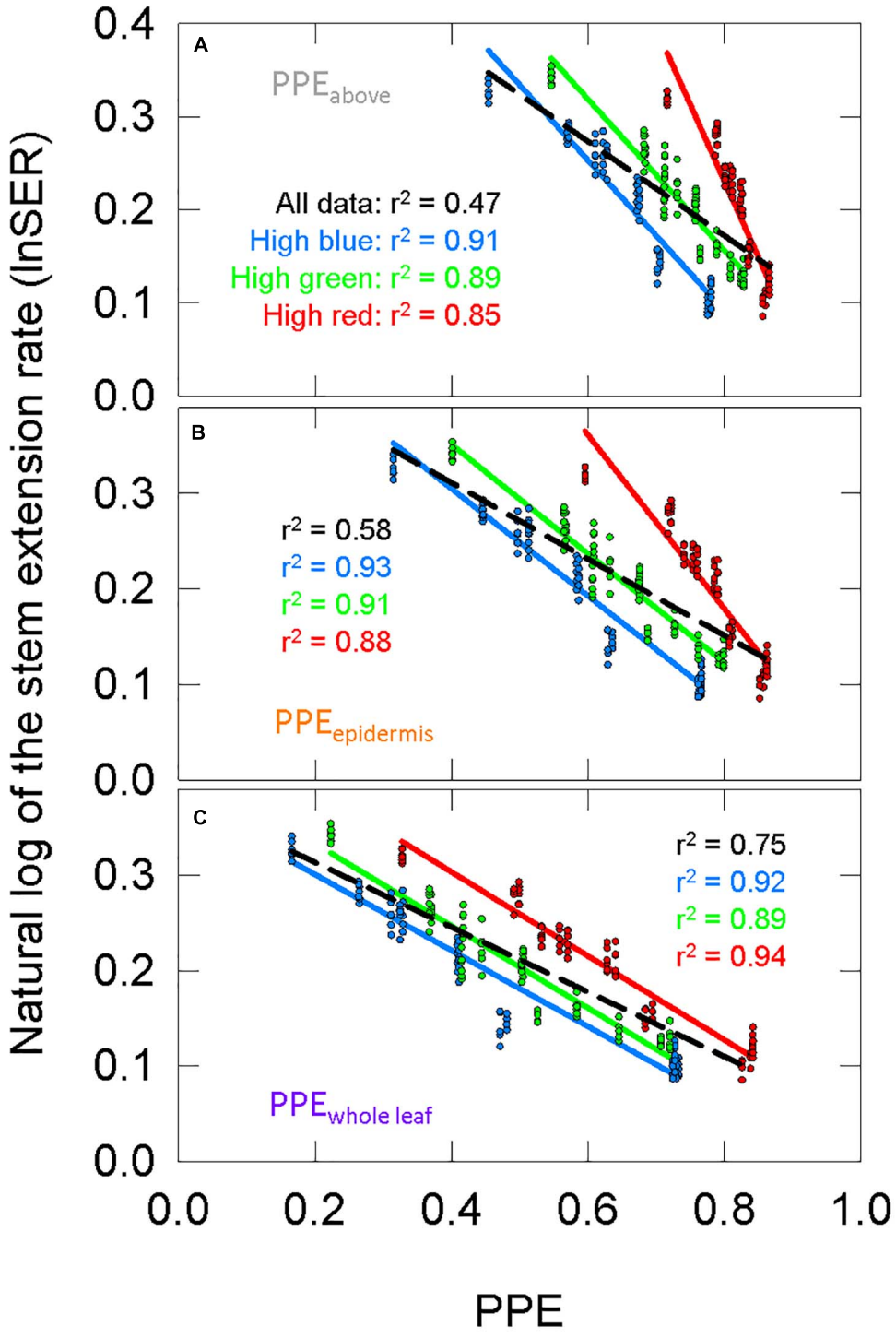

FIGURE 7 | The response of the natural lnSER to changes in the estimate of phytochrome photoequilibrium (PPE) in multiple layers of tissue. PPE is calculated with *the two-state model*. See **Figure 5** for an explanation of colors. **(A)** The relationship between PPE_{above} and lnSER. This is the most common method to model phytochrome activity using the spectral photon distribution above the leaf. Panels **(B,C)** use estimates of PPE for phytochrome that is **(B)** in epidermal tissue or **(C)** homogeneously distributed through the whole leaf.

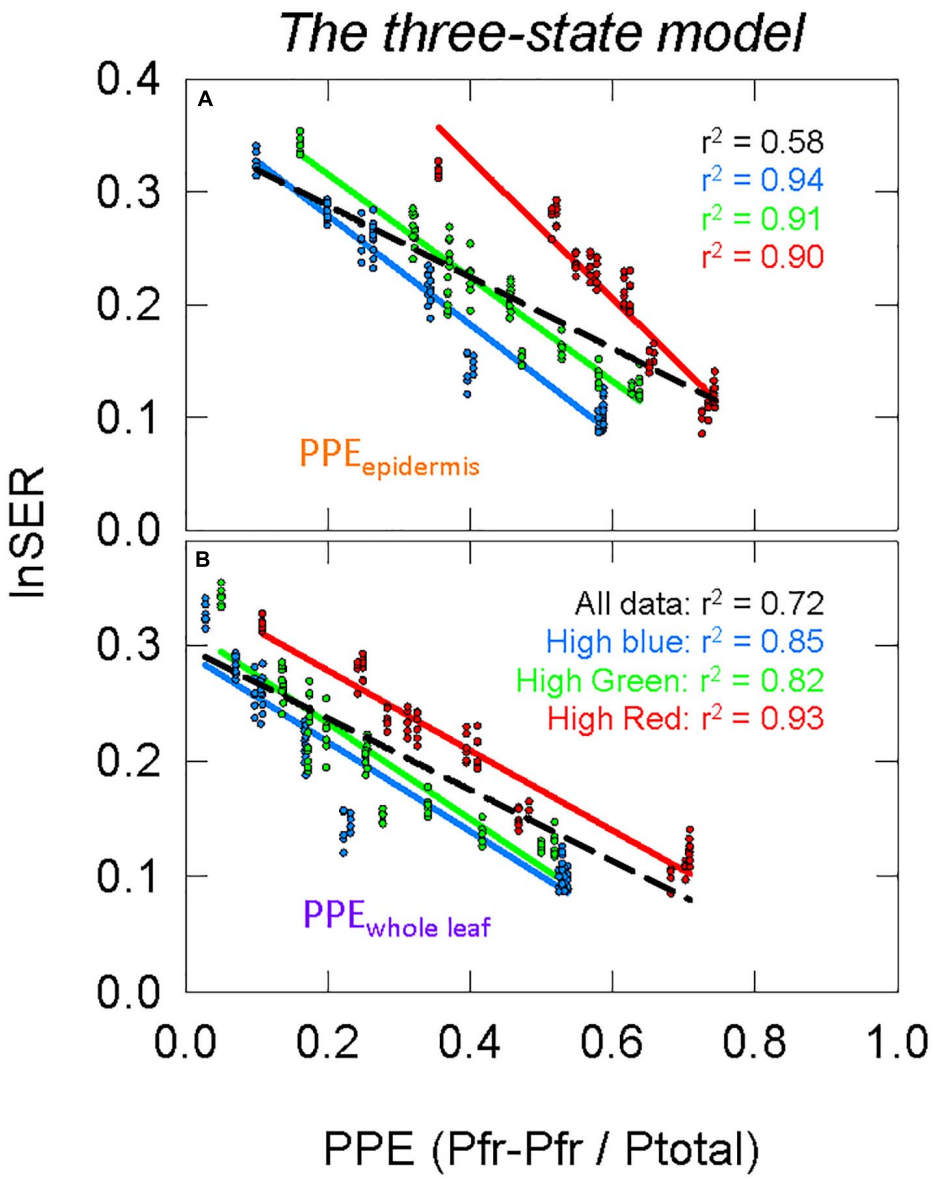

FIGURE 8 | Modeling phytochrome activity with *the three-state model*. For this analysis, only phytochrome that is **(A)** in the epidermis or **(B)** homogeneously distributed within the whole leaf were considered. See **Figure 5** for an explanation of colors.

from Kazarinova-Fukshansky et al. (1985) required updating using the most accurate photoconversion coefficients. Here, photoconversion coefficients calculated from the photochemical properties in Lagarias et al. (1987) were used.

The application of photoconversion weighting factors did not significantly shift of the Pr peak away from 668 nm. Therefore, we could not explain why Kasperbauer et al. (1963) or Jose and Schäfer (1978) observed shifts to 645 and 630 nm, respectively.

Analysis of Phytochrome Models

The high correlations between PPE_{above} and lnSER for each individual background in the long-term study is similar to previous reports that kept the background spectrum constant, and only adjusted levels of R or FR (Morgan and Smith, 1976, 1978, 1979; Park and Runkle, 2017, 2018), but there is a low correlation when using PPE_{above} to broadly estimate lnSER under any spectral background (**Figure 7A**). By comparison, the convergence of lnSER data in **Figures 7B,C** indicate that models that account for spectral distortion within a leaf better predict phytochrome mediated plant responses under a broader range of spectral backgrounds.

Morgan and Smith (1978) found a linear relationship between PPE and lnSER when PPE was estimated under a leaf with a low chlorophyll concentration (380 μmol m^{-2}), but they reported a departure from linearity at a high chlorophyll concentration (660 μmol m^{-2}). Here, chlorophyll concentration

FIGURE 9 | Representative plants at harvest from the short-term photobleaching study. Green seedlings are shown on the left and norflurazon-treated photobleached seedlings are shown on the right. There was some chlorophyll at the tips of some of the photobleached seedlings.

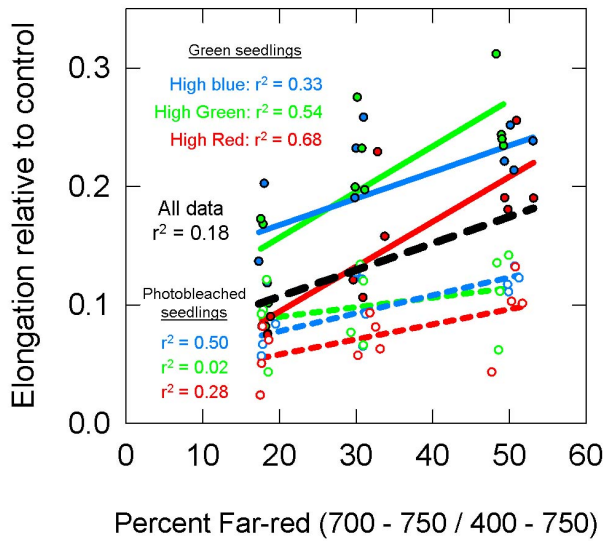

FIGURE 10 | Elongation of green (closed circles, solid lines) and photobleached (open circles, dashed lines) seedlings over a 48 h period relative to dark controls. See **Figure 5** for an explanation of colors. Data show that photobleached seedlings elongated less then green seedlings.

in the leaves averaged 574 μmol m^{-2} across all treatments, although it ranged from 383 to 937 μmol m^{-2} and decreased as percent FR increased (**Figure 5D**). Using only the transmitted spectrum, the relationship between PPE and lnSER was non-linear (**Supplementary Figure 8**). Phytochrome in the upper layers of a leaf would have a lower "effective" chlorophyll concentration, and may be thought of as similar to the low chlorophyll leaf in Morgan and Smith (1978). Thus, the linear relationship between PPE and lnSER in the upper layers of leaf tissue ($PPE_{epidermis}$) is similar to previous findings (**Figure 7B**).

Results from our short-term photobleaching study were similar to Holmes and Wagner (1981), who measured the percent inhibition of elongation (relative to dark controls) of green and norflurazon-treated *Chenopodium rubrum* seedlings grown under a single spectral background with added R or FR. As PPE increased from 0.3 to 0.8 in their study, inhibition of hypocotyl elongation increased (i.e., shorter hypocotyls) for both the treated and untreated seedlings, although the effect appeared reduced in the green seedlings. Additionally, when white light was applied along with R and FR, the green seedlings were taller than the norflurazon treated seedlings. Broadly, their results are similar to ours (**Figures 10**, **11A**).

It is difficult to determine whether the relationship between PPE and lnSER should be linear (e.g., **Figure 7C**) or non-linear (e.g., **Figure 11E**). Activated phyB (Pfr) is translocated from the cytosol to the nucleus, where it interacts with numerous transcription factors including phytochrome interacting factors (PIFs), often inactivating or phosphorylating them (Legris et al., 2019). PIFs transcriptionally promote the expression of genes related to auxins, gibberellins, and cell walls, effectively leading to increased cell expansion (de Lucas and Prat, 2014). Thus, the down regulation of PIFs caused by higher relative concentrations of phyB–Pfr (high PPE) will cause a decrease in stem elongation, but with so many contributing factors, the exact relationship is difficult to determine. Additionally, post-transcriptional and translation regulation by phytochrome (Legris et al., 2019), the circadian control of phyB protein accumulation (Sharrock and Clack, 2002), and cytoplasmic roles of phytochrome (Hughes, 2013) all further complicate this relationship.

The assumption that "functional" phytochrome was homogeneously distributed throughout all leaf layers (whole leaf) provided better correlations with elongation than the assumption that "functional" phytochrome was only in the epidermis (**Figures 7**, **11**). This corroborates the findings of Endo et al. (2005) who found that phyB expression in the mesophyll of the cotyledons restored the wild-type morphology in a *phyB* mutant. Kim et al. (2016) concluded that only phytochrome in the epidermis (of the hypocotyl) contributes to the control of hypocotyl elongation, but their results show a potential role for both epidermal and cortex located phytochrome in the control of hypocotyl elongation. Cortex and mesophyll cells are both "ground" tissue, comprising the majority of plant

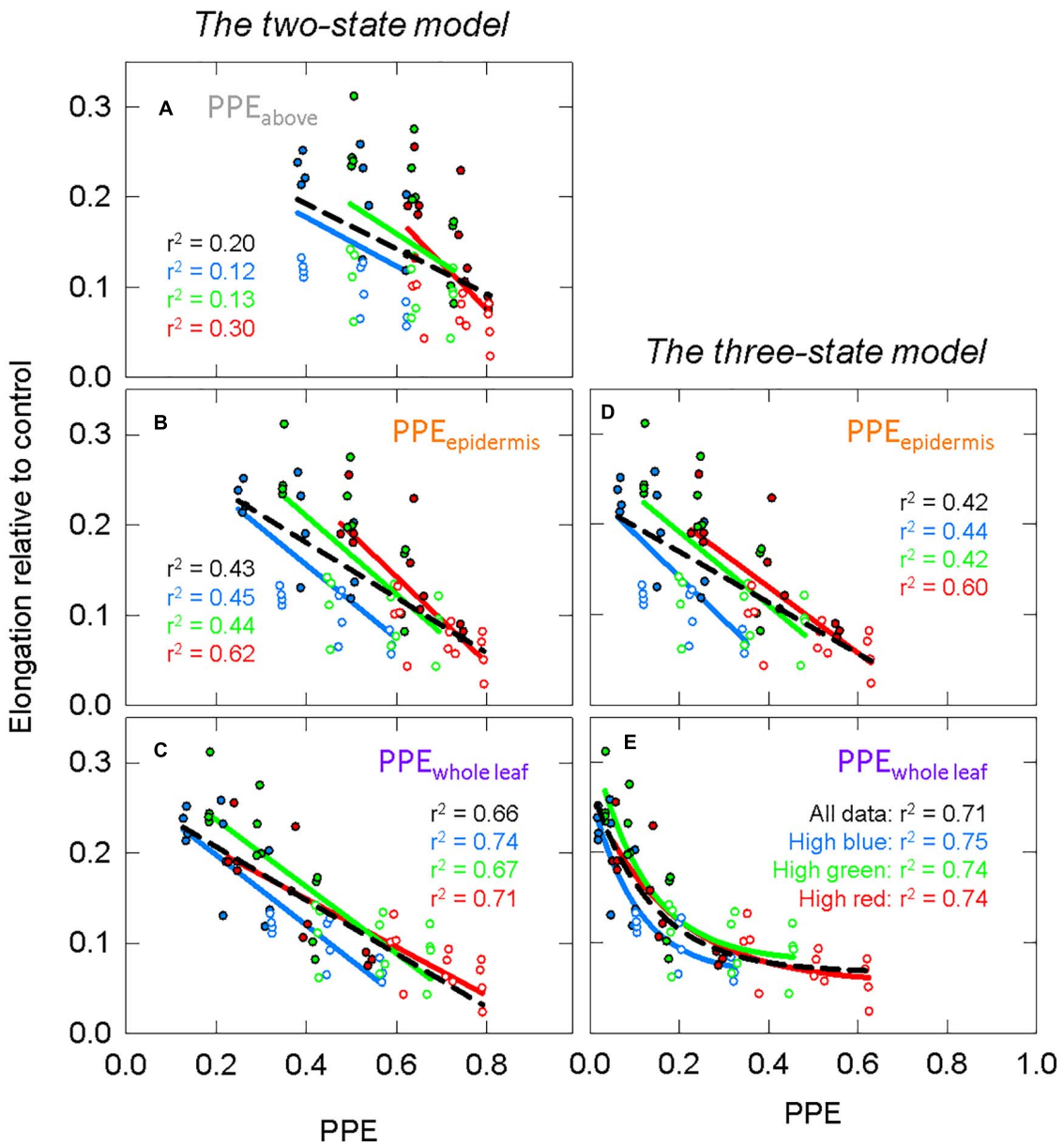

FIGURE 11 | The response of green (closed circles) and photobleached (open circles) seedlings to models of PPE in specific leaf layers, using the same models as **Figures 7**, **8**. See **Figure 5** for an explanation of colors. Estimates of PPE are calculated using green or etiolated weighting factors. The green and photobleached seedlings from a single spectral treatment were combined for analysis. Panels **(A)** through **(C)** use estimates of PPE based on *the two-state model* for phytochrome that is **(A)** above the leaf, **(B)** in epidermal tissue or **(C)** homogeneously distributed in the whole cotyledon. Panels **(D,E)** use estimates of PPE based on *the three-state model* for phytochrome that is **(D)** in epidermal tissue or **(E)** homogeneously distributed in the whole cotyledons. All models use linear regression with the exception of **(E)**, which fits the date with exponential decay functions. Each point represents an average of 6–9 seedlings. There were four replications in time.

biomass. It seems likely that phytochrome in these cells (and the epidermis) modulate development in response to light signals, while phytochrome in vascular tissue does not (Endo et al., 2005; Kim et al., 2016).

The data presented here indicate that PPE estimated above a leaf is an inappropriate method for predicting phytochrome action. Under electric lights, above-the-leaf estimates of PPE are often above 0.8, which is higher than in sunlight. Some authors have concluded that the biological responses to treatments with PPE_{above} ranging from about 0.8 to 0.88 were likely not caused by phytochrome because it did not vary to a large degree (Barnes and Bugbee, 1992; Dougher and Bugbee, 2001a,b; Cope and Bugbee, 2013). The proposed method of modifying the SPD that reaches phytochrome molecules demonstrates a high attenuation of R photons, resulting in lower rates of Pr → Pfr conversion than expected by

above-the-leaf estimates. A re-evaluation of previous studies may be warranted.

Consideration of More Recent Models: Three-State and Cellular Models

In the studies reported here, the intensity was kept close to the threshold intensities for a given temperature described by Sellaro et al. (2019) in order to minimize the contribution of thermal reversion on phytochrome dynamics. This simplified the estimates of PPE to only photoconversions, and therefore *the cellular model*, which accounts for other phytochrome dynamics, could be ignored.

The three-state model could still be investigated by simply squaring PPE calculated by *the two-state model* (Mancinelli, 1988). The correlations between PPE and elongation were not greatly changed when using *the three-state* over the *two-state model* (**Figures 7B,C** compared to **Figures 8**, **11B,C** compared to **Figures 11D,E**), but the linear models between PPE and lnSER for the estimate of phytochrome homogenously distributed in the whole leaf using *the three-state model* produced nearly parallel lines (more specifically, the slopes were not determined to be significantly different) for the three spectral backgrounds (**Figure 8B**). This means that a change in PPE is predicted to result in identical changes in elongation for the three spectral backgrounds. These results suggest that *the three-state* model for $PPE_{wholeleaf}$ best predicts phytochrome action.

The three-state model assuming phytochrome is homogeneously distributed in all leaf tissue provided non-linear relationship between PPE and elongation in the short-term photobleaching study, and while linear responses may be more satisfying, it is possible that the response of stem extension to changes in PPE is non-linear (described above). Overall, it is difficult to conclude anything further regarding *the two-state* vs. *the three-state models*.

Based on the principles of *the cellular model*, an interaction between intensity and percent far-red is expected (i.e., increasing percent far-red should have a more pronounced effect on stem elongation at lower intensities than higher intensities). Although specific effects of intensity have been well documented in the literature (Smith, 1982), the interactions between intensity and percent far-red on the stem length or stem extension rate have been less well documented.

Hitz et al. (2019) applied three FR fractions (1, 7, and 20% FR) to a PPFD of 100 μmol m^{-2} s^{-1} and a PPFD of 400 μmol m^{-2} s^{-1}, and saw an increase in stem length both when the percent FR was increased and when the PPFD was decreased, as *the cellular model* would generally predict. However, when the data from Hitz et al. (2019) is considered as a percent increase from the treatments with no added FR, there appears to be no effect of intensity (**Supplementary Figure 9**). Child and Smith (1987) saw no difference in the relationship between PPE and the change in stem extension rate at intensities between 50 and 150 μmol m^{-2} s^{-1} of white light. Smith (1990) saw only transient changes in stem extension rate when rapidly increasing or decreasing the total intensity while keeping the R:FR ratio constant. Park and Runkle (2018) did not observe an interaction between PPE and intensity on stem length in petunia, geranium or coleus, but they did observe an independent effect of intensity on petunia stem length. These contradictions are difficult to explain because intensity in these studies, unlike our own, dropped below the thresholds described by Sellaro et al. (2019). Our study may not be representative of a traditional cucumber propagation environment because of the high intensity utilized to minimize this thermal reversion. Further studies at various intensities are required to test the robustness of *the cellular model*.

Blue and Green Responses

Although stem and hypocotyl elongating were primarily explained by changes in PPE, it cannot be ruled out the background spectra would not have significantly different effects on elongation. The high green and high red treatments had roughly the same percentage of blue photons, which make them comparable to each other, but less comparable to the high blue treatment (**Table 1**), especially on a PPE basis. This is because the blue light receptors, cryptochromes, must be considered. Blue photons decrease stem elongation in cucumbers (Hernández and Kubota, 2016; Snowden et al., 2016). When the data from both the long-term and short-term studies were plotted with PPE (*two-state* or *three-state*) as the independent variable (**Figures 7**, **8**, **11**) the background spectral treatments generally increased in elongation in the order of high blue, high green then high red at the same value of PPE. This indicates a role of blue photons (through cryptochrome), and possibly green photons, in shifting the offset of the PPE model. These results are consistent with Park and Runkle (2019).

Research in the last 15 years has indicated that blue and green photons, sensed through the photoreceptor cryptochrome, act in a similarly antagonistic manner as R and FR. For example, green photons were found to reverse the blue induced decrease in hypocotyl elongation (Bouly et al., 2007). This has led to models of cryptochrome action similar to the phytochrome models described above (Procopio et al., 2016). It might be expected that green photons would increase stem elongation similar to FR, but neither Hernández and Kubota (2016) nor Snowden et al. (2016) saw this response in cucumber. Additionally, although Sellaro et al. (2010) demonstrated that a blue/green ratio reliably predicted hypocotyl lengths, their data showed that increasing the flux of green photons, like blue photons, also decreased hypocotyl elongation, but to a lesser extent than the blue photons. It is difficult to determine what caused this green induced decrease in hypocotyl length, but this effect may explain the differences in offsets for the high blue and high green data compared to high red data (**Figures 7**, **8**, **11**).

Future Directions and Potential Improvements

Kusuma and Bugbee (2021) recently outlined six issues with using PPE as a model to predict morphological responses. These included (1) differences in photoconversion coefficients from different studies, (2) multiple phytochromes, (3) thermal reversions, (4) phytochrome intermediates, (5) fluctuations in Ptotal, and (6) spectral distortion by chlorophyll. In this study,

photoconversion coefficients derived from measurements of highly pure phytochrome *in vitro* from Lagarias et al. (1987) were used. Our experiments were constructed to primarily obtain effects from phyB and minimize contributions of thermal reversion, but fluctuations in Ptotal and the formation of intermediates were not accounted for. Finally, the results presented here provide evidence that spectral distortion by chlorophyll must be considered in estimating PPE, but several further considerations could improve the robustness of PPE prediction of morphology based on spectral measurements.

As discussed previously, the leaves and cotyledons are likely the primary location of photon perception by phytochrome, but hypocotyls also contribute to photon perception. The planting density in the long-term study was 20 plants per m^2, which likely led to additional FR enrichment caused by reflection by neighboring plants. Because FR induced auxin signals can move within the plant (Roig-Villanova and Martinez-Garcia, 2016) it is important to determine how FR signals are integrated across different tissues across the plant.

The spectral distortion functions used in this study were derived from Kazarinova-Fukshansky et al. (1985). These distortion functions were calculated from transmission and reflectance measurements using the Kubelka-Munk theory from Kazarinova-Fukshansky et al. (1985), who made their measurements in 7 days old zucchini seedlings grown under 16,000 lx of white light (it is difficult to determine what this is in PPFD, but we estimate that it is about 250–300 $\mu mol\ m^{-2}\ s^{-1}$). Because spectral reflectance and transmittance have roughly the same shape for all plants with chlorophyll, these distortion functions may have relatively universal utility, but environmental conditions contribute to a few key changes in plant internal structure that could decrease the reliability of the presented distortion functions.

Potential Shifts in Spectral Distortion Functions

Increasing the FR fraction (decreasing PPE) decreased the leaf chlorophyll concentration (**Figure 5D**), and there was no effect of percent FR on specific leaf mass, with the exception of a small effect in the high blue treatment (**Figure 5E**). This means that this change in chlorophyll concentration (μmol per square meter of leaf) was unlikely caused by changes in leaf thickness, but rather was caused by differences in chlorophyll synthesis or retention. Decreasing the concentration of chlorophyll within the leaves is expected to increase the penetration of photons into deeper layers of tissue, increasing the average photon intensity within a leaf. This would result in spectral distortion functions (and thus photoconversion weighting factors) that are intermediate between the epidermis and whole leaf estimates (**Figures 4B**, **6B,C**).

The change in the spectral distortion function with changing chlorophyll concentrations will depend on the distribution of the chlorophyll within the leaves. Nishio et al. (1993) reported that carotenoid and chlorophyll concentrations peaked halfway through a spinach leaf if the plants were grown in sunlight, but peaked at a depth of about 30% through the leaf when grown in the shade. When chlorophyll/carotenoids are concentrated toward the adaxial side of the leaf, photons in the will be attenuated more rapidly, decreasing the average photon flux within the leaf. It seems unlikely that the shade (FR) induced changes in both chlorophyll concentration and chlorophyll distribution will perfectly offset each other, but nonetheless the two effects would antagonistically alter the average SPD within the leaf. If chlorophyll distributions favor the adaxial side under higher FR, this may mean that the FR induced decrease in chlorophyll concentration will minimally affect the average spectral distortion within the leaf.

High photon intensity and blue photons can increase leaf thickness and reorient chloroplasts. Cui et al. (1991) suggested that increased leaf thickness via palisade elongation promoted photon penetration deeper into leaf tissue, although there was little difference in fractional leaf penetration between thick and thin leaves in their study. Chloroplast orientation along the sides of cell walls at high photon intensity induces a sieve effect allowing photon penetration deeper into leaf tissue (Davis et al., 2011; Parry et al., 2014). Again, this results in spectral distortion functions intermediate between the whole leaf and epidermis estimates (**Figure 4B**).

Developing leaves tend to have lower chlorophyll concentrations than mature leaves. As plants mature and chlorophyll concentrations increase, the average fluxes of blue and red photons within a leaf will decrease. This means that the phytochrome dynamics in older leaves would shift to lower average Pfr concentrations than younger leaves under identical SPD. Younger leaves were more receptive to far-red than older cotyledons in Casal and Smith (1988b). This response is the opposite of what would be expected assuming chlorophyll concentrations were higher in older cotyledon tissue compared to younger leaf tissue. Therefore, younger leaves may be more receptive to photon signals than older leaves. Nonetheless, as these younger leaves develop and chlorophyll concentrations increase, photon penetration into leaves will decrease, shifting the spectral distortion functions from similar to the epidermis estimate to lower than the whole leaf estimate (**Figure 4B**).

The combined effects of photon quality and quantity on leaf internal structure and chlorophyll concentration/distribution could result in changes in the internal SPD. Modifications to the spectral distortion functions to account for these changes could improve the model. Additional research is warranted.

A Simpler Intuitive Metric: The FR Fraction

Phytochrome and cryptochrome, when activated, interact with some of the same transcription factors (de Wit et al., 2016). The chromophore at the center of the photoreceptor cryptochrome is a flavin adenine dinucleotide (FAD) molecule, a coenzyme associated with numerous proteins. FAD absorbs photons in the UV-A and blue regions of the spectrum. FAD absorbance drops substantially around 500 nm (Banerjee et al., 2007; Procopio et al., 2016). The inactive form of phytochrome absorbs across the entire biologically active spectrum (300–800 nm), but is primarily activated by red photons. Chlorophyll-induced spectral distortions may mean that phytochrome is also significantly activated by (longer wavelength) green photons (**Figure 6C**).

Therefore, blue, green and red photons may push back against FR photons to affect morphology. Percent far-red (FR fraction) was shown to be an excellent predictor of lnSER in the long-term study (r^2 = 0.89, **Figure 5A**), although the expected blue (and possibly green) offsets are not present. Percent far-red did not appear to be a good predictor of morphology in seedlings (**Figure 10**).

Due to the issues with PPE outlines above, Kusuma and Bugbee (2021) suggested that environmental signals may be more reliable than photo-molecular models, like PPE. Environmental pressure drives evolution, and thus genetically regulated molecular machinery could be expected to conform to the incoming signals (in so much as it provides a survival advantage). The R:FR ratio is often used as a metric to describe the degree of shade, but percent far-red may be a better ratio because it integrates the action of multiple photoreceptors that co-evolved to detect the extent of shade. Although our improvements to the PPE model indicate some important mechanistic aspects of photon perception within a leaf, the FR fraction is a simple intuitive metric that may be widely applicable across many conditions.

SUMMARY

Phytochrome photoequilibrium is generally estimated from the SPD above the leaf, which does not account for the spectral distortion caused by absorbance and scattering within a leaf, and is thus an inadequate metric for estimating phytochrome induced morphology. Estimates of PPE for phytochrome that is homogeneously distributed throughout the whole leaf accounted for spectral distortions and was a better predictor of morphological responses. The distortion functions used here were from a different species than species investigated and yet improved predictions. We thus believe the distortion functions used here have universal utility. We provide both the distortion functions and photoconversion weighting factors in **Supplementary Data**.

Percent far-red is an intuitive environmental metric that accounts for photon effects from 400 to 750 nm on stem elongation rate, possibly because it accounts for cryptochrome and phytochrome action. This is an empirical metric but it appears to have excellent predictive power.

The use of LEDs in controlled environments allows an unprecedented opportunity to manipulate plant growth. FR LEDs have a high efficacy and may thus contribute to these manipulations, but the phytochrome mediated responses to FR must be better understood to utilize their potential.

DATA AVAILABILITY STATEMENT

All datasets presented in this study are included in the article/**Supplementary Material**.

AUTHOR CONTRIBUTIONS

PK and BB contributed to the design of the study, analysis of data, and writing of the manuscript. Both authors contributed to the article and approved the submitted version.

FUNDING

This work was supported by the Utah Agricultural Experiment Station, Utah State University (journal paper number 9381), the USDA-NIFA-SCRI (Grant Number 2018-51181-28365) (LAMP Project) NASA-CUBES (Grant Number NNX17AJ31G).

ACKNOWLEDGMENTS

We thank William Wheeler and Shuyang Zhen for their helpful review and comments. We thank Logan Banner and Wyatt Johnson for their laboratory assistance. We thank BIOS Lighting (Melbourne, FL, United States), Philips Lighting (Amsterdam, Netherlands), and Fluence by Osram (Austin, TX, United States) for their donation of LEDs used in this research.

SUPPLEMENTARY MATERIAL

The Supplementary Material for this article can be found online at: https://www.frontiersin.org/articles/10.3389/fpls.2021.596943/full#supplementary-material

REFERENCES

Aukerman, M. J., Hirschfeld, M., Wester, L., Weaver, M., Clack, T., Amasino, R. M., et al. (1997). A deletion in the PHYD gene of the Arabidopsis Wassilewskija ecotype defines a role for phytochrome D in red/far-red light sensing. *Plant Cell* 9, 1317–1326. doi: 10.1105/tpc.9.8.1317

Banerjee, R., Schleicher, E., Meier, S., Muñoz Viana, R., Pokorny, R., Ahmad, M., et al. (2007). The signaling state of Arabidopsis cryptochrome 2 contains flavin semiquinone. *J. Biol. Chem.* 282, 14916–14922. doi: 10.1074/jbc.M700616200

Barnes, C., and Bugbee, B. (1992). Morphological responses of wheat to blue light. *J. Plant Physiol.* 139, 339–342. doi: 10.1016/S0176-1617(11)80347-0

Björkman, T. (1999). Dose and timing of brushing to control excessive hypocotyl elongation in cucumber transplants. *HortTechnology* 9, 224–226. doi: 10.21273/HORTTECH.9.2.224

Black, M., and Shuttleworth, J. E. (1974). The role of the cotyledons in the photocontrol of hypocotyl extension in Cucumis sativus L. *Planta* 117, 57–66. doi: 10.1007/BF00388678

Borthwick, H. A., Hendricks, S. B., Parker, M. W., Toole, E. H., and Toole, V. K. (1952). A reversible photoreaction controlling seed germination. *Proc. Natl. Acad. Sci. U.S.A.* 38, 662–666. doi: 10.1073/pnas.38.8.662

Bouly, J. P., Schleicher, E., Dionisio-Sese, M., Vandenbussche, F., Van Der Straeten, D., Bakrim, N., et al. (2007). Cryptochrome bluelight photoreceptors are activated through interconversion of flavinredox states. *J. Biol. Chem.* 282, 9383–9391. doi: 10.1074/jbc.M609842200

Brockmann, J., Rieble, S., Kazarinova-Fukshansky, N., Seyfried, M., and Schäfer, E. (1987). Phytochrome behaves as a dimer in vivo. *Plant Cell Environ.* 10, 105–111. doi: 10.1111/1365-3040.ep11602037

Butler, W. L., Hendricks, S. B., and Siegelman, H. W. (1964). Action spectra of phytochrome in vitro. *Photochem. Photobiol.* 3, 521–528. doi: 10.1111/j.1751-1097.1964.tb08171.x

Casal, J. J. (1995). Coupling of phytochrome B to the control of hypocotyl growth in Arabidopsis. *Planta* 196, 23–29. doi: 10.1007/BF00193213

Casal, J. J., and Smith, H. (1988a). Persistent effects of changes in phytochrome status on internode growth in light-grown mustard: occurrence, kinetics and locus of perception. *Planta* 175, 214–220. doi: 10.1007/BF00392430

Casal, J. J., and Smith, H. (1988b). The loci of perception for phytochrome control of internode growth in light-grown mustard: promotion by low phytochrome photoequilibria in the internode is enhanced by blue light perceived by the leaves. *Planta* 176, 277–282. doi: 10.1007/BF00392456

Child, R., and Smith, H. (1987). Phytochrome action in light-grown mustard: kinetics, fluence-rate compensation and ecological significance. *Planta* 172, 219–229. doi: 10.1007/BF00394591

Cope, K. R., and Bugbee, B. (2013). Spectral effects of three types of white light-emitting diodes on plant growth and development: absolute versus relative amounts of blue light. *HortScience* 48, 504–509. doi: 10.21273/HORTSCI.48.4.504

Cui, M., Vogelmann, T. C., and Smith, W. K. (1991). Chlorophyll and light gradients in sun and shade leaves of Spinacia oleracea. *Plant Cell Environ.* 14, 493–500. doi: 10.1111/j.1365-3040.1991.tb01519.x

Davis, P. A., Caylor, S., Whippo, C. W., and Hangarter, R. P. (2011). Changes in leaf optical properties associated with light-dependent chloroplast movement. *Plant Cell Environ.* 34, 2047–2059. doi: 10.1111/j.1365-3040.2011.02402.x

de Lucas, M., and Prat, S. (2014). PIFs get BRright: PHYTOCHROME INTERACTING FACTORs as integrators of light and hormonal signals. *New Phytol.* 202, 1126–1141. doi: 10.1111/nph.12725

de Wit, M., Keuskamp, D. H., Bongers, F. J., Hornitschek, P., Gommers, C. M., Reinen, E., et al. (2016). Integration of phytochrome and cryptochrome signals determines plant growth during competition for light. *Curr. Biol.* 26, 3320–3326. doi: 10.1016/j.cub.2016.10.031

Devlin, P. F., Patel, S. R., and Whitelam, G. C. (1998). Phytochrome E influences internode elongation and flowering time in Arabidopsis. *Plant Cell* 10, 1479–1487. doi: 10.1105/tpc.10.9.1479

Devlin, P. F., Robson, P. R., Patel, S. R., Goosey, L., Sharrock, R. A., and Whitelam, G. C. (1999). Phytochrome D acts in the shade-avoidance syndrome in Arabidopsis by controlling elongation growth and flowering time. *Plant Physiol.* 119, 909–916. doi: 10.1104/pp.119.3.909

Dougher, T. A., and Bugbee, B. (2001a). Differences in the Response of Wheat, Soybean and Lettuce to Reduced Blue Radiation. Photochem. *Photobiol.* 73, 199–207. doi: 10.1562/0031-865520010730199DITROW2.0.CO2

Dougher, T. A., and Bugbee, B. (2001b). Evidence for yellow light suppression of lettuce growth. *Photochem. Photobiol.* 73, 208–212. doi: 10.1562/0031-865520010730208EFYLSO2.0.CO2

Eichenberg, K., Bäurle, I., Paulo, N., Sharrock, R. A., Rüdiger, W., and Schäfer, E. (2000). Arabidopsis phytochromes C and E have different spectral characteristics from those of phytochromes A and B. *FEBS Lett.* 470, 107–112. doi: 10.1016/S0014-5793(00)01301-6

Endo, M., Nakamura, S., Araki, T., Mochizuki, N., and Nagatani, A. (2005). Phytochrome B in the mesophyll delays flowering by suppressing FLOWERING LOCUS T expression in Arabidopsis vascular bundles. *Plant Cell* 17, 1941–1952. doi: 10.1105/tpc.105.032342

Evans, J. R. (1995). Carbon fixation profiles do reflect light absorption profiles in leaves. *Aust. J. Plant Physiol.* 22, 865–873. doi: 10.1071/PP9950865

Fisher, P. R., Heins, R. D., and Lieth, J. H. (1996). Quantifying the relationship between phases of stem elongation and flower initiation in poinsettia. *J. Am. Soc. Hort. Sci.* 121, 686–693. doi: 10.21273/JASHS.121.4.686

Franklin, K. A., Davis, S. J., Stoddart, M. W., Vierstra, R. D., and Whitelam, G. C. (2003). Mutant analyses define multiple roles for phytochrome C in Arabidopsis photomorphogenesis. *Plant Cell* 15, 1981–1989. doi: 10.1105/tpc.015164

Franklin, K. A., and Quail, P. H. (2010). Phytochrome functions in Arabidopsis development. *J. Expt. Bot.* 61, 11–24. doi: 10.1093/jxb/erp304

García-Martínez, J. L., Keith, B., Bonner, B. A., Stafford, A. E., and Rappaport, L. (1987). Phytochrome regulation of the response to exogenous gibberellins by epicotyls of Vigna sinensis. *Plant Physiol.* 85, 212–216. doi: 10.1104/pp.85.1.212

Gardner, G., and Graceffo, M. A. (1982). The use of a computerized spectroradiometer to predict phytochrome photoequilibria under polychromatic irradiation. *Photochem. Photobiol.* 36, 349–354. doi: 10.1111/j.1751-1097.1982.tb04385.x

Hartmann, K. M. (1966). A general hypothesis to interpret 'high energy phenomena' of photomorphogenesis on the basis of phytochrome. *Photochem. Photobiol.* 5, 349–365. doi: 10.1111/j.1751-1097.1966.tb05937.x

Hernández, R., and Kubota, C. (2016). Physiological responses of cucumber seedlings under different blue and red photon flux ratios using LEDs. *Environ. Exp. Bot.* 121, 66–74. doi: 10.1016/j.envexpbot.2015.04.001

Hitz, T., Hartung, J., Graeff-Hönninger, S., and Munz, S. (2019). Morphological response of soybean (*Glycine max* (L.) Merr.) cultivars to light intensity and red to far-red ratio. *Agronomy* 9, 428. doi: 10.3390/agronomy9080428

Holmes, M. G., and Fukshansky, L. (1979). Phytochrome photoequilibria in green leaves under polychromatic radiation: a theoretical approach. *Plant Cell Environ.* 2, 59–65. doi: 10.1111/j.1365-3040.1979.tb00774.x

Holmes, M. G., and Wagner, E. (1981). Phytochrome control of hypocotyl extension in light-grown Chenopodium rubrum. *Physiologia Plantarum* 53, 233–238. doi: 10.1111/j.1399-3054.1981.tb04492.x

Hughes, J. (2013). Phytochrome cytoplasmic signaling. *Annu. Rev. Plant Biol.* 64, 377–402. doi: 10.1146/annurev-arplant-050312-120045

Jones, A. M., and Quail, P. H. (1986). Quaternary structure of 124-kilodalton phytochrome from *Avena sativa* L. *Biochemistry* 25, 2987–2995. doi: 10.1021/bi00358a038

Jose, A. M., and Schäfer, E. (1978). Distorted phytochrome action spectra in green plants. *Planta* 138, 25–28. doi: 10.1007/BF00392909

Kasperbauer, M. J., Borthwick, H. A., and Hendricks, S. B. (1963). Inhibition of flowering of Chenopodium rubrum by prolonged far-red radiation. *Bot. Gaz.* 124, 444–451. doi: 10.1086/336234

Kazarinova-Fukshansky, N., Seyfried, M., and Schäfer, E. (1985). Distortion of action spectra in photomorphogenesis by light gradients within the plant tissue. *Photochem. Photobiol.* 41, 689–702. doi: 10.1111/j.1751-1097.1985.tb03624.x

Kelly, J. M., and Lagarias, J. C. (1985). Photochemistry of 124-kilodalton avena phytochrome under constant illumination in vitro. *Biochemistry* 24, 6003–6010. doi: 10.1021/bi00342a047

Kim, J., Song, K., Park, E., Kim, K., Bae, G., and Choi, G. (2016). Epidermal phytochrome B inhibits hypocotyl negative gravitropism non-cell-autonomously. *Plant Cell* 28, 2770–2785. doi: 10.1105/tpc.16.00487

Klose, C., Venezia, F., Hussong, A., Kircher, S., Schäfer, E., and Fleck, C. (2015). Systematic analysis of how phytochrome B dimerization determines its specificity. *Nat. Plants* 1, 15090. doi: 10.1038/nplants.2015.90

Kusuma, P., and Bugbee, B. (2021). Far-red Fraction: an improved metric for characterizing phytochrome effects on morphology. *J. Am. Soc. Hort. Sci.* 146, 3–13. doi: 10.21273/JASHS05002-20

Kutschera, U., and Niklas, K. J. (2007). The epidermal-growth-control theory of stem elongation: an old and a new perspective. *J. Plant Physiol.* 164, 1395–1409. doi: 10.1016/j.jplph.2007.08.002

Lagarias, J. C., Kelly, J. M., Cyr, K. L., and Smith, W. O. Jr. (1987). Comparative photochemical analysis of highly purified 124 kilodalton oat and rye phytochromes in vitro. *Photochem. Photobiol.* 46, 5–13. doi: 10.1111/j.1751-1097.1987.tb04729.x

Legris, M., Ince, Y. Ç, and Fankhauser, C. (2019). Molecular mechanisms underlying phytochrome-controlled morphogenesis in plants. *Nat. Commun.* 10:5219. doi: 10.1038/s41467-019-13045-0

Mancinelli, A. L. (1986). Comparison of spectral properties of phytochromes from different preparations. *Plant physiol.* 82, 956–961. doi: 10.1104/pp.82.4.956

Mancinelli, A. L. (1988). Some thoughts about the use of predicted values of the state of phytochrome in plant photomorphogenesis research. *Plant Cell Environ.* 11, 429–439. doi: 10.1111/j.1365-3040.1988.tb01780.x

Mancinelli, A. L. (1994). "The physiology of phytochrome action," in *Photomorphogenesis in Plants*, eds R. E. Kendrick and G. H. M. Kronenberg (Netherlands: Springer), 211–269. doi: 10.1007/978-94-011-1884-2_10

Mazzella, M. A., and Casal, J. J. (2001). Interactive signalling by phytochromes and cryptochromes generates de-etiolation homeostasis in Arabidopsis thaliana. *Plant Cell Environ.* 24, 155–161. doi: 10.1111/j.1365-3040.2001.00653.x

Morgan, D., and Smith, H. (1978). The relationship between phytochrome-photoequilibrium and development in light grown *Chenopodium album* L. *Planta* 142, 187–193. doi: 10.1007/BF00388211

Morgan, D. C., and Smith, H. (1976). Linear relationship between phytochrome photo-equilibrium and growth in plants under simulated natural radiation. *Nature* 262, 210–212. doi: 10.1038/262210a0

Morgan, D. C., and Smith, H. (1979). A systematic relationship between phytochrome controlled development and species habitat. *Planta* 145, 253–258. doi: 10.1007/BF00454449

Nishio, J. N., Sun, J. D., and Vogelmann, T. C. (1993). Carbon fixation gradients across spinach leaves do not follow internal light gradients. *Plant Cell* 5, 953–961. doi: 10.1105/tpc.5.8.953

Park, Y., and Runkle, E. S. (2017). Far-red radiation promotes growth of seedling by increasing leaf expansion and whole-plant net assimilation. *Environ. Exp. Bot.* 136, 41–49. doi: 10.1016/j.envexpbot.2016.12.013

Park, Y., and Runkle, E. S. (2018). Far-red radiation and photosynthetic photon flux density independently regulate seedling growth but interactively regulate flowering. *Environ. Exp. Bot.* 155, 206–216. doi: 10.1016/j.envexpbot.2018.06.033

Park, Y., and Runkle, E. S. (2019). Blue radiation attenuates the effects of the red to far-red ratio on extension growth but not on flowering. *Environ. Exp. Bot.* 168:103871. doi: 10.1016/j.envexpbot.2019.103871

Parry, C., Blonquist, J. M., and Bugbee, B. (2014). In situ measurement of leaf chlorophyll concentration: analysis of the optical/absolute relationship. *Plant Cell Environ.* 37, 2508–2520. doi: 10.1111/pce.12324

Procko, C., Crenshaw, C. M., Ljung, K., Noel, J. P., and Chory, J. (2014). Cotyledon-generated auxin is required for shade-induced hypocotyl growth in Brassica rapa. *Plant Physiol.* 165, 1285–1301. doi: 10.1104/pp.114.241844

Procopio, M., Link, J., Engle, D., Witczak, J., Ritz, T., and Ahmad, M. (2016). Kinetic modeling of the Arabidopsis cryptochrome photocycle: FADH accumulation correlates with biological activity. *Front. Plant Sci.* 7:888. doi: 10.3389/fpls.2016.00888

Rausenberger, J., Hussong, A., Kircher, S., Kirchenbauer, D., Timmer, J., Nagy, F., et al. (2010). An integrative model for phytochrome B mediated photomorphogenesis: from protein dynamics to physiology. *PLoS One* 5:e10721. doi: 10.1371/annotation/4563eaf4-e45b-4d9e-ab06-5f1794bf11e3

Rockwell, N. C., Su, Y., and Lagarias, J. C. (2006). Phytochrome structure and signaling mechnaisms. *Annu. Rev. Plant Biol.* 57, 837–858. doi: 10.1146/annurev.arplant.56.032604.144208

Roig-Villanova, I., and Martinez-Garcia, J. F. (2016). Plant responses to vegetation proximity: a whole life avoiding shade. *Front. Plant Sci.* 7:236. doi: 10.3389/fpls.2016.00236

Ruddat, A., Schmidt, P., Gatz, C., Braslavsky, S. E., Gärtner, W., and Schaffner, K. (1997). Recombinant type A and B phytochromes from potato. Transient absorption spectroscopy. *Biochemistry* 36, 103–111. doi: 10.1021/bi962012w

Sage, L. C. (1992). *Pigment of the Imagination*. Boston: Academic Press, 562.

Sager, J. C., Smith, W. O., Edwards, J. L., and Cyr, K. L. (1988). Photosynthetic efficiency and phytochrome photoequilibria determination using spectral data. *Trans. ASAE* 31, 1882–1889. doi: 10.13031/2013.30952

Savaldi-Goldstein, S., Peto, C., and Chory, J. (2007). The epidermis both drives and restricts plant shoot growth. *Nature* 446, 199–202. doi: 10.1038/nature05618

Sellaro, R., Crepy, M., Trupkin, S. A., Karayekov, E., Buchovsky, A. S., Rossi, C., et al. (2010). Cryptochrome as a sensor of the blue/green ratio of natural radiation in Arabidopsis. *Plant Physiol.* 154, 401–409. doi: 10.1104/pp.110.160820

Sellaro, R., Smith, R. W., Legris, M., Fleck, C., and Casal, J. J. (2019). Phytochrome B dynamics departs from photoequilibrium in the field. *Plant Cell Environ.* 42, 606–617. doi: 10.1111/pce.13445

Seyfried, M., and Fukshansky, L. (1983). Light gradients in plant tissue. *Appl. Optics* 22, 1402–1408. doi: 10.1364/AO.22.001402

Sharrock, R. A., and Clack, T. (2002). Patterns of expression and normalized levels of the five Arabidopsis phytochromes. *Plant Physiol.* 130, 442–456. doi: 10.1104/pp.005389

Smith, H. (1973). "Light quality and germination: ecological implications," in *Seed ecology*, ed. W. Heydecker (Butterworths), 219–231.

Smith, H. (1975). "The photomorphogenic response systems and their photoreceptors," in *Phytochrome and Photomorphogenesis*, ed. H. Smith (London: McGraw-Hill), 22–53.

Smith, H. (1982). Light quality, photoperception, and plant strategy. *Annu. Rev. Plant Physiol.* 33, 481–518. doi: 10.1146/annurev.pp.33.060182.002405

Smith, H. (1990). Phytochrome action at high photon fluence rates: rapid extension rate responses of light-grown mustard to variations in fluence rate and red: far-red ratio. *Photochem. Photobiol.* 52, 131–142. doi: 10.1111/j.1751-1097.1990.tb01766.x

Smith, R. W., and Fleck, C. (2019). "Basic phytochrome B calculations," in *Phytochromes: Methods and Protocols*, ed. A. Hiltbrunner (New York, NY: Humana), 121–133. doi: 10.1007/978-1-4939-9612-4_9

Snowden, C. M., Cope, K. R., and Bugbee, B. (2016). Sensitivity of seven diverse species to blue and green light: integrations with photon flux. *PLoS One* 11:e0163121. doi: 10.1371/journal.pone.0163121

Somers, D. E., and Quail, P. H. (1995). Temporal and spatial expression patterns of PHYA and PHYB genes in Arabidopsis. *Plant J.* 7, 413–427. doi: 10.1046/j.1365-313X.1995.7030413.x

Tanaka, S. I., Nakamura, S., Mochizuki, N., and Nagatani, A. (2002). Phytochrome in cotyledons regulates the expression of genes in the hypocotyl through auxin-dependent and-independent pathways. *Plant Cell Physiol.* 43, 1171–1181. doi: 10.1093/pcp/pcf133

USU Crop Physiology Laboratory (2020). "Utah monocot/dicot solution," in *Nutrients. Paper 2.* Available online at: https://digitalcommons.usu.edu/cgi/viewcontent.cgi?article=1001&context=cpl_nutrients (accessed December 10, 2020).

Vogelmann, T. C. (1994). "Light within the plant," in *Photomorphogenesis in Plants*, eds R. E. Kendrick and G. H. M. Kronenberg (Netherlands: Springer), 491–535. doi: 10.1007/978-94-011-1884-2_18

Whitelam, G. C., Johnson, E., Peng, J., Carol, P., Anderson, M. L., Cowl, J. S., et al. (1993). Phytochrome a null mutants of Arabidopsis display a wild-type phenotype in white light. *Plant Cell* 5, 757–768. doi: 10.1105/tpc.5.7.757

Zhen, S., and Bugbee, B. (2020). Far-red photons have equivalent efficiency to traditional photosynthetic photons: Implications for redefining photosynthetically active radiation. *Plant Cell Environ.* 43, 1259–1272. doi: 10.1111/pce.13730

Zhen, S., and van Iersel, M. W. (2017). Far-red light is needed for efficient photochemistry and photosynthesis. *J. Plant Physiol.* 209, 115–122. doi: 10.1016/j.jplph.2016.12.004

Zhen, S. Y., Haidekker, M., and van Iersel, M. W. (2018). Far-red light enhances photochemical eficiency in a wavelength-dependent manner. *Physiol. Plant* 167, 21–33. doi: 10.1111/ppl.12834

Conflict of Interest: The authors declare that the research was conducted in the absence of any commercial or financial relationships that could be construed as a potential conflict of interest.

Copyright © 2021 Kusuma and Bugbee. This is an open-access article distributed under the terms of the Creative Commons Attribution License (CC BY). The use, distribution or reproduction in other forums is permitted, provided the original author(s) and the copyright owner(s) are credited and that the original publication in this journal is cited, in accordance with accepted academic practice. No use, distribution or reproduction is permitted which does not comply with these terms.

frontiers in Plant Science

ORIGINAL RESEARCH
published: 27 July 2021
doi: 10.3389/fpls.2021.620642

LED Intercanopy Lighting in Blackberry During Spring Improves Yield as a Result of Increased Number of Fruiting Laterals and Has a Positive Carryover Effect on Autumn Yield

*Anabel Rivas, Kang Liu and Ep Heuvelink**

Horticulture and Product Physiology, Wageningen University and Research, Wageningen, Netherlands

High market price and low availability of local winter and spring production has stimulated production of blackberries in glasshouses at northern latitudes. For this production, light is the main limiting factor. We investigated the potential of intercanopy lighting (ICL) using light emitting diodes (LEDs) to improve blackberry fruit yield in a crop with a spring and an autumn production cycle. During the spring production cycle three light treatments were applied: only natural light (no ICL), 93 or 185 μmol m^{-2} s^{-1} ICL In summer the lateral shoots were cut back and 93 μmol m^{-2} s^{-1} ICL was applied to all plants after cutting back, investigating a possible carryover effect of supplemental light in spring on autumn production. Fresh fruit yield in spring increased by 79 and 122% with 93 and 185 μmol m^{-2} s^{-1} ICL, respectively, compared to no ICL. This represents 3.6 and 2.8% increase in harvestable product for every additional 1% of light. A yield component analysis and leaf photosynthesis measurements were conducted. Maximum photosynthetic capacity (A_{max}) for leaves at 185 μmol m^{-2} s^{-1} ICL was about 50% higher, and LAI was 41% higher compared to no ICL. ICL increased the number of fruiting laterals per cane, and this explained 75% of the increase in yield. ICL at 185 μmol m^{-2} s^{-1} resulted in a higher yield compared to no ICL, primarily as a result of higher total dry matter production. Furthermore, a higher fraction of dry matter partitioned to the fruits (0.59 compared to 0.52) contributed to yield increase, whereas fruit dry matter content and fruit quality (sugar and acid content) was not affected by ICL. Averaged over the three light treatments autumn yield was 47% lower than spring yield. Autumn yield was 10% higher for plants at ICL 93 μmol m^{-2} s^{-1} in spring and 36% higher for plants at 185 μmol m^{-2} s^{-1} in spring compared to no ICL in spring. This increased autumn yield was caused by more fruiting laterals (less necrotic buds). It is concluded that management practices in spring can have a carryover effect on the autumn production. This is the first scientific paper on the potential for applying LED ICL in blackberries. Further research should focus on optimal intensity of ICL, positioning of supplementary lighting and economic feasibility.

Keywords: supplemental light, intercanopy lighting, blackberries, light emitting diode, bud break, fruiting laterals, fruit quality, yield component analysis

OPEN ACCESS

Edited by:
Sissel Torre, Norwegian University of Life Sciences, Norway

Reviewed by:
Brian Farneti, Fondazione Edmund Mach, Italy
Juan Luis Valenzuela, University of Almería, Spain

***Correspondence:**
Ep Heuvelink
ep.heuvelink@wur.nl

Specialty section:
This article was submitted to Crop and Product Physiology, a section of the journal Frontiers in Plant Science

Received: *23 October 2020*
Accepted: *22 April 2021*
Published: *27 July 2021*

Citation:
Rivas A, Liu K and Heuvelink E (2021) LED Intercanopy Lighting in Blackberry During Spring Improves Yield as a Result of Increased Number of Fruiting Laterals and Has a Positive Carryover Effect on Autumn Yield. Front. Plant Sci. 12:620642. doi: 10.3389/fpls.2021.620642

INTRODUCTION

Given the relatively small size of the commercial industry, little work has been done to optimize growth conditions for blackberry (*Rubus* spp.) in glasshouse environments. High market price and low availability of local winter and spring production (Centre for the Promotion of Imports from Developing Countries, 2016) has stimulated production of blackberries in glasshouses at northern latitudes. As reported for other winter-produced crops in northern latitudes, light is a significant environmental factor limiting growth and yield (Marcelis et al., 2006). Consequently, supplemental lighting with High-Pressure Sodium (HPS) lamps during winter has become quite widespread in order to overcome this challenge (Hemming, 2011). Supplemental lighting has been shown to increase photosynthetic rates (Trouwborst et al., 2010) as well as budbreak, for example in roses (Zieslin and Tsujita, 1990). Light-Emitting Diodes (LEDs) make a more energy efficient supplementary lighting possible compared to HPS (Singh et al., 2015). Besides that, LEDs allow for the optimization of light spectra (Massa et al., 2008) and for placing supplementary light in a crop canopy instead of only above the canopy. Higher yields have been reported in cucumber (Hovi et al., 2004) and sweet pepper (Hovi-Pekkanen et al., 2006) when part of the supplementary light is provided as intercanopy lighting (ICL), compared to toplighting only, with the same total supplementary light intensity. These higher yields are mainly due to improved vertical light distribution, which results in increased actual and maximum photosynthesis rates in the lower canopy leaves (Tewolde et al., 2016; Paponov et al., 2020).

Within a canopy receiving only toplighting the exponential decrease in irradiance from the top to the bottom is coupled with a decrease in the red (R): far-red (FR) ratio because unlike red-light (630 nm), the transmission of far-red light (730 nm) through the canopy is quite high (Holmes and Smith, 1977). As has been extensively reported, low red:far-red ratios can cause significant phytochrome-mediated morphological responses (Franklin and Whitelam, 2005) including higher internode elongation, larger leaf expansion, reduced leaf thickness, and reduced branching (Dale and Blom, 2004; Leduc et al., 2014) or reduced budbreak in roses (Mor and Halevy, 1984; Wubs et al., 2014).

Typical glasshouse blackberry production systems make use of dormant, biennial-fruiting cultivars. Unlike tomato or cucumber where the apical meristem is always on top, a blackberry cane has approximately 20–25 potentially active meristems distributed vertically along the cane. After budbreak, subsequent internode elongation and expansion of leaves on the fruiting laterals occurs horizontally, toward the center of the path between rows until a previously formed terminal flower is expressed (Sønsteby and Heide, 2008). In raspberry (*Rubus* spp.), a closely related crop, it has been observed that a lower red:far-red ratio results in higher internode elongation, and therefore longer fruiting laterals in the lower part of the canopy (Sønsteby et al., 2013). In raspberry the uppermost laterals on a shoot tend to produce the fewest inflorescences. Inflorescence complexity in the buds increases along the cane from the top to the base of the main cane, due to a higher number of buds along the inflorescence axis in the lower bud positions (Heide and Sønsteby, 2011). The yield of a blackberry cane is a function of the number of buds along the main cane that produce laterals, as well as the productivity of each of these fruiting laterals. This varies with the percentage of buds within the lateral that express flowers, the quantity of flowers expressed per bud position, and fruit size (Sønsteby et al., 2009). In raspberry, it has been suggested that this yield potential is often not realized due to insufficient light (Fernandez and Pritts, 1994). Therefore, the application of supplemental light in the lower sections of the canopy could not only improve photosynthesis of the lower leaves, but also the morphological development of the meristems and the potential productivity of the fruiting laterals.

In cultivation under high tunnels or rain shelters, it is generally only possible to produce one summer blackberry crop. In greenhouse cultivation, however, the climate can be controlled which creates possibilities for not only increased fruit yield but also two cropping cycles in the same year. It is possible to obtain a second crop cycle (harvest in autumn) by cutting back the fruiting laterals in summer after the spring harvest has stopped (Pitsioudis et al., 2009).

To date, no work has been done on the modification of light quality and light quantity in a blackberry canopy through the use of LED ICL. ICL offers an opportunity to improve the production of blackberry in greenhouses during low-light conditions. Therefore, the objective of this study was to determine the potential of LED ICL for improved blackberry yields, particularly in the lower part of the canopy where production is low. Additionally, this study should improve our understanding of the possible effect higher spring yields as a result of ICL has on autumn yields from the same plants.

Morphological development, growth and yield of blackberry plants under natural light was compared with plants under a low or high intensity of supplemental LED ICL in spring in a greenhouse experiment. After spring harvest, the fruiting laterals were cut back and autumn cycle on the same plants started, with all plants receiving the same amount of ICL. We tested two hypotheses: (1) Blackberry yield per cane in the spring crop will increase under ICL, primarily resulting from a higher number of fruits per lateral, and (2) Applying ICL in spring will improve spring yield at the expense of autumn yield.

MATERIALS AND METHODS

Facilities and Plant Material

On 11 November, 2016, blackberry long cane plants [commercially-grown Driscoll's variety, interspecific hybrid *Rubus* spp.; nursery located in Abingdon, United Kingdom (51°N, 1°W)] were delivered to Breda, Netherlands. Pots (7 L filled with 100% coir) containing five canes with a minimum cane diameter of 5 mm were selected and placed in cold storage at 2°C. On 11 January 2017, these pots were delivered to Wageningen, Netherlands (52°N, 5.5°E), and placed the following day into two adjacent Venlo-type glasshouse compartments (12 m × 12 m). The canes were pruned to a length of 2.0 m.

In each compartment seven, 9.5 m long plant rows were grown spaced 1.9 m apart, oriented North-South. The distance between pots was 0.38 m. Three adjacent rows were taken as a block. Each block was divided into three plots (three light treatments). Light treatments were allocated according to a latin square and layout was such that buffer rows were kept between the blocks. Each 2.5 m plot contained six pots with the two outer ones as borders on each end. All rows had four buffer pots on each end of the row.

The plants were grown in the glasshouse for almost 1 year. The first (spring) crop cycle took place from 12 January to 7 July, and after cutting back the fruiting laterals a second (autumn) crop cycle took place from 14 July to 22 December.

Spring Crop Cycle

Growing Conditions

Minimum realized temperature during the diel cycle increased gradually from 7°C in February to 12°C in June and July, maximum temperature increased from 17 to 30°C. Liquid CO_2 was used to enrich the greenhouse air to 600–800 ppm when vents were closed. During ventilation, greenhouse air was kept at ambient CO_2 level.

Solar radiation was recorded every 5 min. based on a Kipp solarimeter placed outside the glasshouse. Three quantum sensors (Li-190R, Li-Cor Inc., Lincoln, NE, United States) were placed inside each glasshouse compartment, 3.50 m above floor level, near the top of the glasshouse, to measure incoming photosynthetically active radiation (PAR). These sensors were connected to a data logger (Li-1400, Li-Cor Inc., Lincoln, NE, United States). Fraction PAR in solar radiation was assumed to be 0.5 (Jacovides et al., 2004). Greenhouse transmissivity was calculated as the ratio between measured PAR inside the greenhouse and calculated PAR outside.

The fruiting laterals were trellised according to commercial standards. At the onset of flowering, a small hive of bumblebees was introduced in the greenhouse compartments. Two weeks later, the bumblebees were removed and replaced by honey bees. A three stage (vegetative growth, flowering and fruiting) standard blackberry nutrient solution was applied according to commercial standards.

LED Intercanopy Lighting Treatments

Three light treatments were applied: 0, 93, or 185 μmol m^{-2} s^{-1} ICL. ICL was applied with two (93 μmol m^{-2} s^{-1}) or four (185 μmol m^{-2} s^{-1}) interlighting LED modules, each 2.5 m long and providing 95% red and 5% blue light (Philips, Greenpower Production Interlighting Module, 107W, 220 μmol s^{-1} PPF, Eindhoven, Netherlands). The total light output of the LED modules has been measured by Philips own certified lab according to IES LM-79-08; CIE S 025/E:2015; prEN13032-4:2013.2 standards. Light intensity at plant level was calculated based on this lamp output and the number of modules per m^2 ground area. The ICL modules were placed parallel to the row, in the middle of the walkway, 0.95 m from the center trellis. They centered at 1.34 m height relative to the floor and were each spaced 0.20 m apart (**Figure 1**).

Intercanopy lighting started on 10 February (13 h supplemental light, lamps turned on 1 h before sunrise). From 6 April onward lamps were on only during the natural photoperiod. In order to prevent light pollution between treatments across the blocks, the side of the LED modules facing the buffer rows was covered with aluminum foil. Rectangles of 0.40 by 0.90 m white plastic were centered on the ends of the LED modules and hung on the ends of every plot perpendicular to the row orientation, to prevent light pollution between treatments within a block. These were removed on 22 March once the fruiting laterals were elongated enough such that this light pollution could no longer occur.

Destructive Crop Measurements

A total of seven destructive harvests were made over the course of the experiment approximately every 3 weeks from the start of the experiment. The first two destructive harvests were made on two canes randomly selected from the buffer rows (before start of the ICL treatments). The following destructive harvests were made on two canes randomly selected from pots that were not next to each other within the four plant plot, alternating between selected pots across destructive harvest times. Two canes were collected from each treatment in each block (n = 6) in all harvests except the last one (11 July) when samples were only collected from one compartment (n = 3). When ICL started, cane density was 13.1 canes m^{-1}. From the start of fruit harvest until the end of the first crop cycle 3 canes per pot were kept which resulted in 7.9 canes m^{-1}.

Bud positions on each cane were numbered from 1 upward, starting at the base of the cane. At each bud position, the fruiting lateral length was measured and the number of receptacles (fruit already harvested), ripe fruits, green fruits, open flowers, closed flower buds, aborted flower buds, and expanded and unexpanded (>1 cm in length) leaves were counted. A lateral was considered elongated when the length from the base to the apex was more than 3 cm. Leaves, fruiting laterals and fruit were grouped in sets of five bud positions: 1–5, 6–10, 11–15, 16–20, and 21+. Measurements including leaf area and dry weight were made in these bud position groups.

All vegetative plant material was dried for 16 h at 105°C in a ventilated oven. Fruit samples were dried at 50°C for 48 h and then at 105°C for 16 h. Primocane shoots (vegetative shoots produced from the crown for production in the following year) were removed, dried, and weighed four times during the first crop cycle.

Fresh Fruit Harvest

Fresh fruit was harvested twice a week from 16 May until 4 July. Only fully ripe, black fruit was selected for harvest. Malformed fruit, defined as fruit with more than 50% of the drupelets not fully formed, unevenly ripened fruit and overripe fruit/fruit fallen on the floor were all categorized. Then, all fruit was weighed by category. 10 fully ripe black fruits were randomly selected from the fruit harvested from each plot at every harvest and their fresh weight was determined. These fruits were dried and fruit dry matter content was calculated. This dry matter content was multiplied by the total fresh weight harvested to estimate the total dry weight of the harvested fruit.

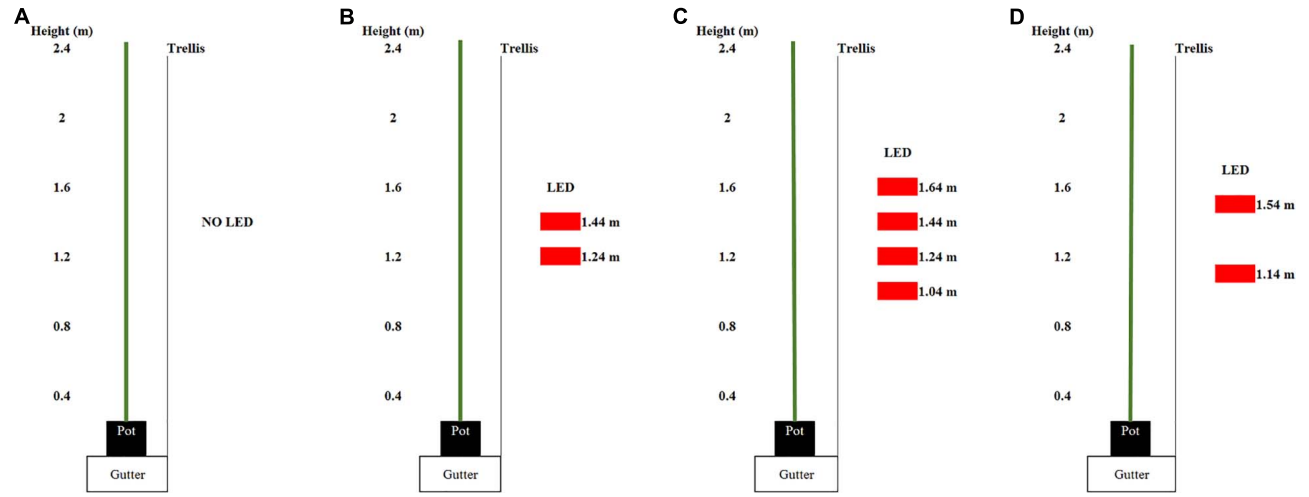

FIGURE 1 | Arrangement of the light emitting diode (LED) modules (displayed as red rectangles) in the spring crop cycle for **(A)** 0, **(B)** 93, and **(C)** 185 intercanopy lighting (ICL) and in the autum crop cycle **(D)**. The numbers beside the LED modules show the distance from the LED module to the ground.

Fruit Chemical Analysis

Three ripe fruits were collected from each plot from the mid-section of the canopy between 1.04 and 1.64 m on three different dates. Fresh berries were frozen in liquid nitrogen and stored at −20°C. The berries were freeze dried until stable weight was achieved and then powdered, and then dry weight was taken. For extraction of organic acids and carbohydrates, 5 ml of 75% ethanol was added to 12 and 18 mg of powder. Samples were vortexed, put in a water bath (80°C, 20 min) and then vortexed again. Samples were then centrifuged (4°C, 8,790 rpm) and 1 ml of supernatant was pipetted to another tube where ethanol was evaporated out at 55°C. 1 ml deionized water was added, samples were vortexed then put into an ultrasonic bath (10 min). Afterward they were vortexed again and then placed into a centrifuge (10 min). Carbohydrate samples were diluted with deionized water at a ratio of 50:1 and organic acid samples at a ratio of 5:1. Carbohydrate samples were analyzed with HPLC (Thermo Scientific Dionex ICS-5000). Organic acids samples were loaded into a different HPLC (Dionex DX-600).

Leaf Photosynthesis

Photosynthesis light-response curves were determined during the week of 6 March which was during vegetative lateral growth, and during the week of 9 May, which was at the onset of fruit harvest. Measurements were conducted on two representative leaves per plot, only for 0 and 185 μmol m^{-2} s^{-1} ICL treatments, and in five randomly selected blocks ($n = 5$).

Measurements were conducted using a Li-6400 portable photosynthesis system (LiCor Inc., Lincoln, NE, United States) equipped with a leaf chamber fluorometer (Li-Cor Part No. 6400-40, area 2 cm^2). During measurements, CO_2 concentration in the leaf chamber was 400 ppm, the airflow at 400 μmol s^{-1}, block temperature at 22°C and RH between 60 and 70%. The percentage of red light and blue light in the chamber was set at 90%/10%. Average achieved leaf temperature across all light steps was higher in the measurements collected in May (26.7 ± 0.47°C) compared to March (21.8 ± 0.24°C) due to issues in the regulation of the block temperature.

Leaves were first adapted to 2,000 μmol m^{-2} s^{-1} for approximately 15 min until net photosynthetic rate (A_n) and stomatal conductance (g_s) were stable. Then data was logged every 5 s, each light step from 2,000 μmol m^{-2} s^{-1} down to 1,500, 1,000, 800, 600, 400, 200, 150, 100, 50, 30, and finally 0 μmol m^{-2} s^{-1} was held for a minimum of 30 s or until A_n and g_s were stable (Kaiser et al., 2017).

Measured A_n values were averaged over the last 30 s to give one value per light step per leaf. The data for A_n response to absorbed irradiance (assuming 0.85 absorbance of incident light) was then fitted using Equation 1 (Ögren and Evans, 1993).

$$A_n = \frac{\varphi * I + A_{max} - [(\varphi * I + A_{max})^2 - 4 * \theta * \varphi * I * A_{max}]^{0.5}}{2*\theta}$$

Where φ is the maximal quantum yield, I is the absorbed irradiance, A_n is the leaf photosynthetic rate (μmol CO_2 m^{-2} s^{-1}), A_{max} is the light-saturated leaf photosynthetic rate and θ is the convexity.

Autumn Crop Cycle

Growing Conditions

On 20 and 21 July, all fruiting laterals from the first crop were cut back to one node below the last fruiting node. On this date, the cane density was 7.9 canes m^{-1} in one experimental compartment and 5.3 canes m^{-1} in the other compartment. This difference occurred from the week of 11 July onward, since a final destructive harvest concluding the spring cycle was taken from one of the compartments only ($n = 3$). On 24 July a destructive harvest was conducted in the other compartment ($n = 3$) such that the cane density during autumn production cycle was

5.3 canes m^{-1} in both compartments. Average greenhouse air temperature gradually decreased from 20°C in July and August to 15°C in November and December. Liquid CO_2 was used to enrich the greenhouse air to 600–800 ppm when vents were closed. During ventilation, greenhouse air was kept at ambient CO_2 level.

Light Emitting Diode Interlighting Treatments

After the spring cropping cycle, LED modules were rearranged such that all plots had two modules and received 93 μmol m^{-2} s^{-1}. In this way supplementary LED light could also be used in the autumn cycle and a possible carry-over effect of spring lighting on autumn production could be studied without the need for more LED modules compared to spring. Modules were placed at a height of 1.14 and 1.54 m (**Figure 1**). Supplemental lighting (6 a.m. till 8 p.m.; 14 h) started on 28 July.

Fresh Fruit Harvest and Destructive Crop Measurements

Fresh fruit was harvested two times per week starting on 3 October until 12 December using the same protocol as for the spring crop. Vegetative laterals that emerged after the July lateral prune were removed once a week. Laterals were considered vegetative if longer than 0.40 m and only having leaves with five leaflets. The laterals were classified by their point of origin within the vertical canopy: 0.0–1.0 m from the floor, 1.0–1.8 m and above 1.8 m. All material was dried and weighed according to the spring protocol.

Two destructive harvests were conducted. The first one was on 24 July, only in the compartment with 7.9 canes m^{-1}. Two canes were randomly selected from two pots in each plot (n = 3). The second destructive harvest took place at the end of the experiment on 15 Dec. Two canes were selected from each plot in each compartment (n = 6).

At each destructive harvest, buds along the cane were numbered as before and data were collected in groups of 10 buds (1–10, 11–20, and 21+). Fruit laterals were categorized as emerging from a primary bud or secondary bud. Secondary buds, axillary buds and scale leaf on each lateral were counted. Additionally, the number of necrotic buds along a fruiting lateral was counted. Buds were considered necrotic when more than 50% of their area was brown. Leaf area, fruiting lateral length, leaf dry weight, fruiting lateral dry weight and cane dry weight of each bud position group previously mentioned were evaluated. On the last destructive harvest date, the number of scars from vegetative laterals as well as the number of unharvested fruits was also counted and weighed. Vegetative and fruit tissues were then oven dried as for the spring cropping cycle.

Data Analysis

Measures of technical replicates were averaged first and then entered into SPSS (Version 23, IBM Corp, Armonk, NY, United States) as one value for each experimental unit. Analysis of Variance (ANOVA) was conducted to test (P = 0.05) for effects of treatment and bud position (when applicable) using row position (n = 3), position across greenhouse (n = 3) and compartment (n = 2) as blocking factors. An error was made during spring fruit harvest in the peak production period, resulting in a missing value for one block, hence final fruit yield analysis was based on five instead of six repetitions. Normality and homogeneity of variance of the residuals was tested using the Shapiro-Wilk test and Levene's test, respectively. Mean separation was conducted using Fisher's protected LSD-test at P = 0.05. Data that violated the assumptions of normality were transformed using a square root or natural logarithm function. Data that did not fit assumptions of normality after transformation were analyzed using a Kruskal-Wallis test followed by a Mann-Whitney test for mean separation (P = 0.05).

RESULTS

Spring Crop Cycle

Total light sum incident on the crop was 22 or 45% higher when 93 or 185 μmol m^{-2} s^{-1} ICL was applied, compared to no ICL (**Table 1**). In February, with an average daily solar light sum of 5.8 mol m^{-2}, supplemental light represented 43 or 60% of the total incoming light. In June, the average daily solar light sum was much higher at 30.2 mol m^{-2}, therefore supplemental LED light represented only 15 and 27% of the total incoming light for 93 and 185 μmol m^{-2} s^{-1} ICL, respectively.

Fruit harvest started mid May for all three treatments. The cumulatively harvested fresh fruit yield per cane was 79 and 122% higher for ICL 93 and 185 μmol m^{-2} s^{-1}, respectively, compared to no ICL (**Table 2**) as a result of more fruits harvested per cane (**Table 2**). Individual fruit weight was only slightly higher (5%) at 185 μmol m^{-2} s^{-1}. Fruit dry matter content was not significantly affected by ICL (**Table 2**).

The number of fruits still on the plant at the end of the spring cropping cycle was higher for both levels of ICL compared to no ICL (**Table 3**). Vegetative biomass increased with increasing ICL intensity although not statistically significant (**Table 3**). ICL resulted in a larger fraction of biomass allocated to the fruit (0.59–0.60) compared to no ICL (0.52). For bud positions 11–15, biomass allocation to the fruit was 0.67 for 93 μmol m^{-2} s^{-1} ICL and 0.62 for 185 μmol m^{-2} s^{-1} ICL compared to 0.43 without ICL.

The proportion of elongated laterals was much lower (0.49) on the canes grown without ICL compared to those with ICL

TABLE 1 | Natural and supplemental total light sum when no intercanopy lighting (ICL) was applied, or with 93 or 185 μmol m^{-2} s^{-1} ICL, during spring cultivation of blackberries.

	ICL (μmol m^{-2} s^{-1})		
	0	**93**	**185**
Natural light sum (mol m^{-2})	3,342	3,342	3,342
Supplemental light sum (mol m^{-2})	0	755	1501
Total light sum (mol m^{-2})	3,342	4,097	4,843
Light sum increase (%)	–	22.3	44.9

TABLE 2 | Blackberry fresh fruit harvest for 0, 93, or 185 μmol m^{-2} s^{-1} ICL.

Fruit yield parameter (per cane)	ICL (μmol m^{-2} s^{-1})		
	0	93	185
Marketable fresh fruit weight (g)	636 a[3]	1139 b	1416 c
Non-marketable fresh fruit weight (g)	19.2 a	50.5 b	49.7 b
Number of fruits[1]	61.5 a	111 b	131 c
Fruit weight (g $berry^{-1}$)	10.1 a	10.1 a	10.7 b
Fruit dry matter content (%)[2]	12.0 a	11.9 a	12.1 a

Fresh fruit was harvested between 16 May and 04 July (Spring production cycle).
[1]Square root transformed data used in ANOVA.
[2]Log-transformed data used in ANOVA.
[3]Different letters within a row indicate significant differences according to Fisher's protected LSD-test (P = 0.05); n = 5.

(0.74 for 93 μmol m^{-2} s^{-1} and 0.80 for 185 μmol m^{-2} s^{-1}) (**Figure 2A**). ICL of 93 μmol m^{-2} s^{-1} showed a nearly maximum proportion of elongated laterals in bud positions 11–15, which did not change when 185 μmol m^{-2} s^{-1} ICL was applied (**Figure 2B**). In bud positions 6–10, 93 μmol m^{-2} s^{-1} ICL increased the proportion of elongated laterals by 76%, while 185 μmol m^{-2} s^{-1} ICL resulted in a 113% increase compared to no ICL. ICL treatments did not significantly influence total fruit number per fruiting lateral (**Supplementary Table 1**). The correlation between fruit fresh yield per cane and number of fruiting laterals per cane was 0.867 (**Figure 3**), which means that 75% of the variation in yield per cane was explained by the number of fruiting laterals per cane.

TABLE 3 | Blackberry crop parameters for 0, 93, or 185 μmol m^{-2} s^{-1} ICL.

Crop parameter (per cane)	ICL (μmol m^{-2} s^{-1})		
	0	93	185
Total fruit number[1,2]	115 a[4]	185 b	169 b
Number of unharvested (unripe) fruits	45 a	42 a	28 a
Dry weight of unharvested fruit (g)	27.1 a	37.4 a	24.1 a
Increase in cane dry weight (g)	5.07 a	3.69 a	8.89 a
Leaf area (m^2)	1.32 a	1.69 ab	1.86 b
Leaf dry weight (g)	58.5 a	72.8 ab	91.0 b
Specific leaf area (cm^2 g^{-1} dry weight)	230 ab	236 b	206 a
Fruiting lateral dry weight (g)	43.1 a	43.4 a	49.0 a
Total vegetative dry weight (g)	102 a	116 a	140 a
Proportion of biomass allocation to fruits (at destructive harvest)[3]	0.52 a	0.60 b	0.59 b

The final destructive analysis of the plant occurred during the week of 11 July.
[1]Square root transformed data used in ANOVA.
[2]Includes total number of receptacles (fruit already harvested) and unharvested fruit remaining on plant.
[3]Estimated by multiplying number of receptacles, fruit and flower by average dry matter content and fruit fresh weight.
[4]Different letters within rows indicate significant difference according to Fisher's protected LSD-test (P = 0.05); n = 3.

TABLE 4 | Photosynthesis light-response curve (Eq. 1) parameters for blackberry leaves grown at 0 or 185 μmol m^{-2} s^{-1} LED ICL: quantum yield (φ; μmol μmol^{-1}), convexity (θ), and maximum assimilation rate (A_{max}; μmol CO_2 m^{-2} s^{-1}).

Month	Photosynthetic parameter	Intercanopy lighting (μmol m^{-2} s^{-1})	
		0	185
March			
	φ	0.07 a[1]	0.06 b
	θ	0.54 a	0.63 a
	A_{max}	10.5 a	16.5 b
May			
	φ	0.06 a	0.06 a
	θ	0.67 a	0.75 a
	A_{max}	11.6 a	16.4 b

[1]Different letters within rows indicate significant difference according to Fisher's protected LSD-test (P = 0.05); n = 5.

In March, the quantum yield, or initial slope of the photosynthesis light-response curve (**Figure 4**) was higher in leaves of no ICL compared to leaves exposed to 185 μmol m^{-2} s^{-1} ICL (**Table 4**). This difference between treatments had disappeared in May. In March, A_{max} for 185 μmol m^{-2} s^{-1} ICL was a 58% higher compared to no ICL. This difference was somewhat lower in May (42%) caused by a higher A_{max} for no ICL.

Considering fruit fresh yield as the product of total dry matter production and fraction of dry matter partitioned to the fruits divided by the fruit dry matter content revealed (**Figure 5**) that 185 μmol m^{-2} s^{-1} ICL resulted in a higher yield compared to no ICL, primarily as a result of higher total dry matter production. Besides more light, a higher LAI and A_{max} contributed to this higher dry matter. Furthermore, a higher fraction of dry matter partitioned to the fruits contributed to yield increase, whereas fruit dry matter content was not influenced by ICL.

Intercanopy lighting did not influence glucose, fructose, sucrose, malate, citrate, and isocitrate concentrations in the fruit (**Table 5**).

Autumn Crop Cycle

Despite receiving identical amounts of light during the autumn crop cycle, yield of plants that received 93 or 185 μmol m^{-2} s^{-1} ICL in spring were 11 and 36% higher compared to no ICL in spring, respectively. Only for 185 μmol m^{-2} s^{-1} ICL this increase in fresh and dry fruit yield was statistically significant (**Table 6**). Just like in spring, the higher fruit yield resulted from a larger number of fruit harvested, not from heavier fruit (**Table 6**). The total number of fruit remaining on the plant when harvest stopped was not significantly affected by spring ICL intensities. Total fruit number per cane was significantly higher for 185 μmol m^{-2} s^{-1} ICL applied in spring, compared to no ICL in spring (**Table 6**). Although not statistically significant, 93 μmol m^{-2} s^{-1} ICL during spring, resulted in 27% higher total fruit number. Number of harvested ripe fruit was about 56% of the total fruit number and the fruit

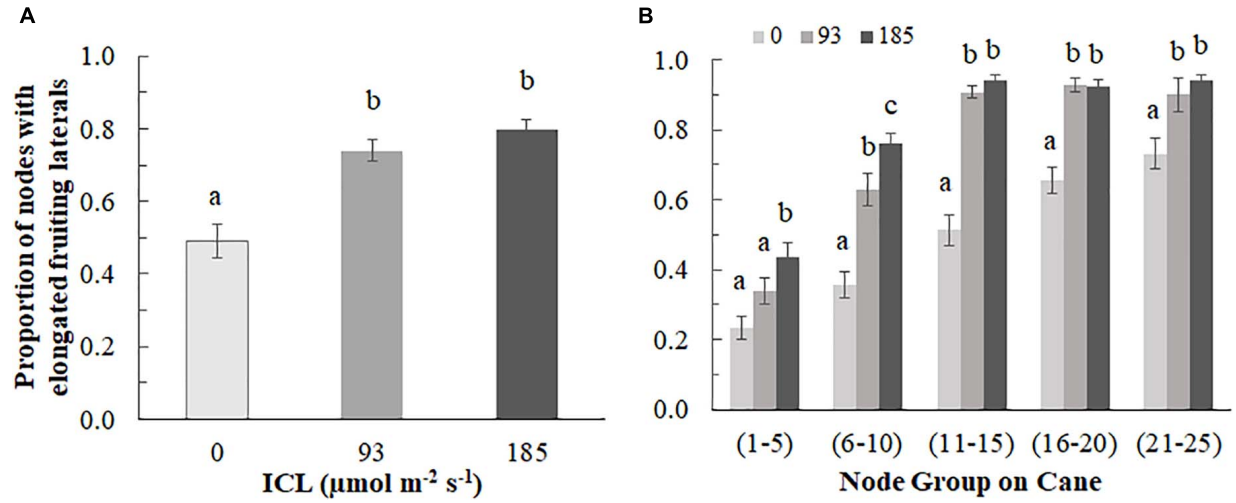

FIGURE 2 | Proportion of buds with elongated fruiting laterals (>3 cm) per blackberry cane for 0, 93, or 185 µmol m^{-2} s^{-1} ICL **(A)** on the entire cane and **(B)** by bud position group (counting from the base of the cane). Data is an average of observations from destructive harvests on 14 March, 4 April, 24 April, and 11 July. **(A)** Different letters indicate significant differences according to Fisher's protected LSD-test (P = 0.05); **(B)** Different letters within a bud position group, indicate significant differences (Mann-Whitney test, P = 0.05). Error bars indicate SEM (n = 6).

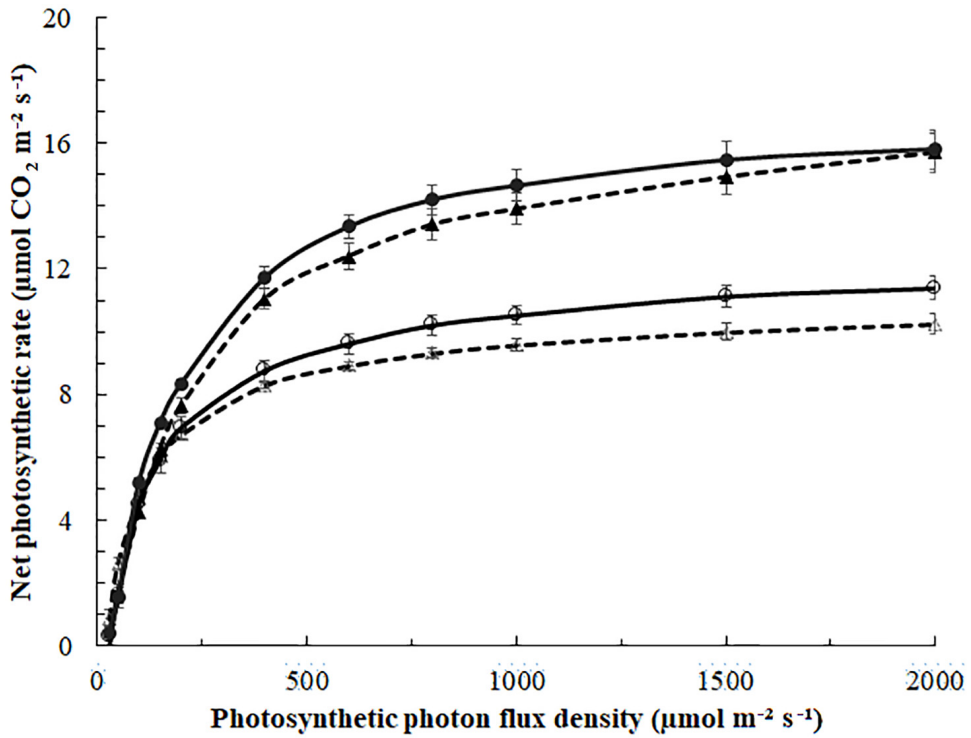

FIGURE 3 | Photosynthesis light-response curves of blackberry leaves exposed to 0 (Δ,○) or 185 (▲,●) µmol m^{-2} s^{-1} ICL approximately 29 days (March, Δ,▲, - - -) or 89 days (May,○,●—) after starting the ICL treatment. Leaf temperature was 22°C in March and 27°C in May. Curves represent fitted non-rectangular hyperbola (Eq. 1); parameters in **Table 4**. Error bars indicate SEM (n = 5).

number remaining on the plant accounted for about 30%. Total fruit number was about 3 times higher for bud positions 11 to 20 compared to lower or higher bud position groups (**Supplementary Table 2**). Averaged over the 3 ICL treatments autumn yield was 47% lower than spring yield. No ICL during the spring cycle resulted in the highest amount of necrotic

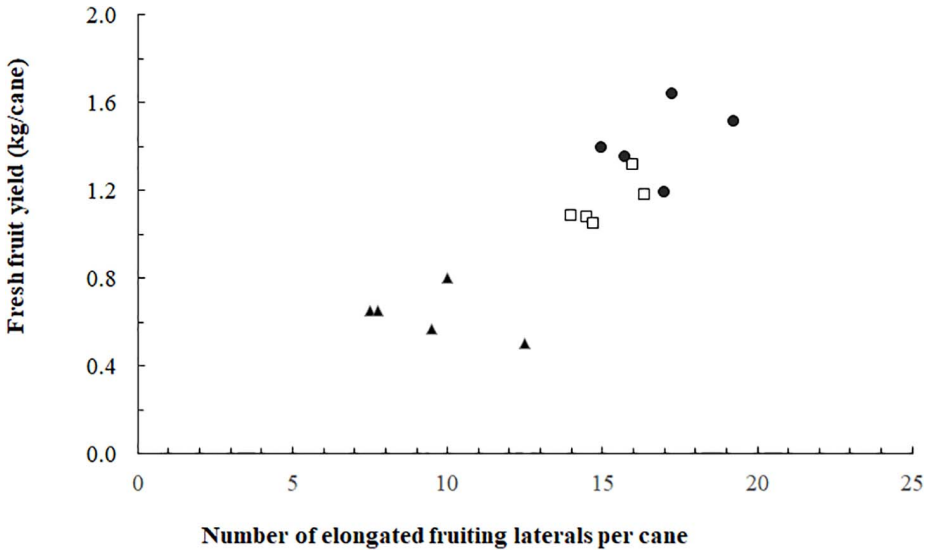

FIGURE 4 | Blackberry fresh fruit yield per cane as a function of the number of fruiting laterals per cane (spring crop cycle). Data for 0 (▲), 93 (□), and 185 (●) mol m^{-2} s^{-1} ICL (n = 15; five replicates for each of the three ICL treatments).

TABLE 5 | Sugar and organic acids content of ripe blackberry fruits grown at 0, 93, or 185 μmol m^{-2} s^{-1} ICL.

Sugar/acid (g/kg fresh)	ICL (μmol m^{-2} s^{-1})		
	0	93	185
Glucose	38.5 a[1]	39.6 a	38.4 a
Fructose	37.4 a	38.5 a	37.4 a
Sucrose	7.0 a	6.5 a	6.9 a
Malate	1.5 a	1.6 a	1.7 a
Citrate	0.10 a	0.10 a	0.10 a
Isocitrate	8.3 a	7.7 a	7.2 a

[1]*Different letters within rows indicate significant difference according to Fisher's protected LSD-test (P = 0.05); n = 6.*

buds per cane at the start of the autumn production cycle, whereas the total lateral shoot length did not significantly differ (**Table 7**).

DISCUSSION

Light Emitting Diode Intercanopy Lighting Increased Number of Fruiting Laterals and Therefore Yield

Supplementary light has been shown to increase yield in several crops like raspberry (Carew et al., 2003; Sønsteby and Heide, 2008), tomato (Lu et al., 2012), and cucumber (Hao and Papadopoulos, 1999). Intercanopy lighting at 93 or 185 μmol m^{-2} s^{-1} increased blackberry fresh fruit yield by 79 and 122%, respectively, compared to no ICL (**Table 2**). This represents 3.6 and 2.8% increase in harvestable product for every additional 1% of light (**Table 1**). This increase in yield is much larger than the often-cited rule of thumb of 1% yield increase resulting from 1% more light (Marcelis et al., 2006). This effect might be somewhat overestimated, as the number of unripe fruit, removed when cutting back for the autumn production cycle, was much higher without ICL (**Table 3**). At 185 μmol m^{-2} s^{-1} ICL 17% of the fruit was left unharvested, whereas without ICL this was 39%. These unripe fruits would have been harvested ripe when spring cycle was continued for a few more weeks. Taking this into account, based on fruit numbers, for 185 μmol m^{-2} s^{-1} ICL yield would have increased by exactly 1% for every additional 1% of light. However, a delay in cutting back would have negatively affected autumn production. Fruit sugar and carbohydrate contents were not significantly affected by ICL (**Table 5**). Similarly, in tomato increase in yield was reported with LED supplemental lighting while sugar (Lu et al., 2012) and soluble solid (Paponov et al., 2020) content remained unchanged. It is commercially of great importance that such a large yield increase was obtained without negative impact on some key flavor components.

We hypothesized that the number of fruit per lateral would increase when ICL was applied, however, there appeared to be no significant treatment effect on this yield component (**Supplementary Table 1**). Instead, we observed that the yield component most affected by ICL was the number of elongated fruiting laterals. Approximately 49% of the laterals elongated when no ICL was applied, whereas this was 74% for 93 μmol m^{-2} s^{-1} ICL and slightly higher for 185 μmol m^{-2} s^{-1} ICL (**Figure 2A**). Yield increases in roses in response to supplementary lighting applied in winter have also been attributed to increased bud break (Khosh-Khui and George, 1977). ICL with LEDs (*0% red and 20% blue) increased the red:far-red ratio at the middle and low positions in a tomato canopy (Paponov et al., 2020), which is known to stimulate bud

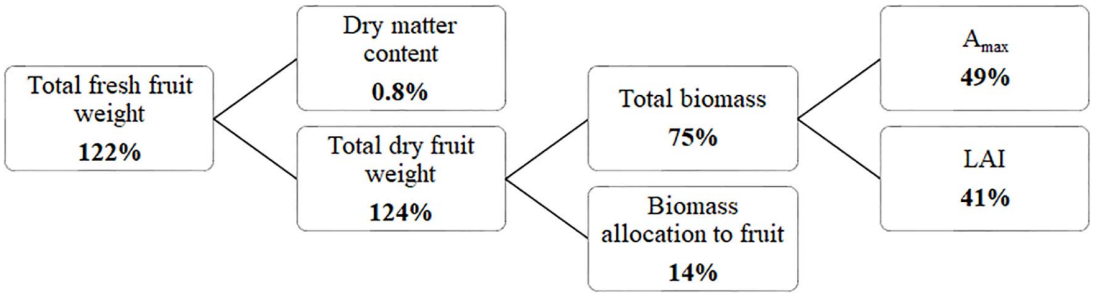

FIGURE 5 | Yield component analysis for a blackberry crop (spring crop cycle). Percentages indicate how much higher the component was for 185 μmol m^{-2} s^{-1} ICL compared to no ICL. Yield (kg fresh fruit mass m^{-2}) = Total dry mass (kg plant dry mass m^{-2}) × Fraction to fruits (fruit dry mass/total dry mass)/fruit dry matter content (fruit dry mass/fruit fresh mass).

TABLE 6 | Blackberry yield per cane during the autumn production cycle (harvest from 3 October till 12 December as affected by spring production cycle ICL treatments.

	ICL intensity (μmol m^{-2} s^{-1})		
	0	**93**	**185**
Marketable			
Fruit fresh weight (g)	488 a[1]	540 a	664 b
Harvested fruit number	57.9 a	70.0 b	84.6 c
Fruit dry weight (g)	55.1 a	62.1 a	76.1 b
Non-marketable			
Fruit fresh weight (g)	48.9 a	73.5 b	102.7 c
Remaining fruit number[2]	29.1 a	38.5 a	41.7 a

[1]*Different letters in a row indicate significant differences according to Fisher's protected LSD-test (P = 0.05).*
[2]*The remaining fruit harvest includes unripe fruit and was conducted on Dec 14th.*

break (Wubs et al., 2014). Our experiment does not allow to discriminate between the effect of light intensity and light quality on bud break. However, Wubs et al. (2014) concluded that local light intensity, not red:far-red ratio, was the most important factor influencing bud break in rose.

The proportion of elongated laterals in biennial-producing canes of raspberries tends to be higher in the top of the cane due to paradormancy imposed on the basal buds by the apical buds (White et al., 1999). In this experiment, a similar response was observed. Consequently, from bud position 11 and higher, 93 μmol m^{-2} s^{-1} ICL seemed to provide enough light to achieve maximum number of elongated fruiting laterals (**Figure 2B**) as 185 μmol m^{-2} s^{-1} ICL did not further increase this number. For the basal buds (position 1–10), the fruiting lateral elongation showed a positive correlation with increasing light intensity. In rose, the role of local light on the bud (Girault et al., 2008; Roman et al., 2016), has been shown to function mainly by influencing the ability of the developing shoots to draw assimilates (Mor and Halevy, 1980). The unsaturated response to ICL intensities for the basal buds (position 1–10) suggests further increases in lateral elongation rates could have been achieved by supplying higher light intensities directly on the lower part of the canes.

Biomass Partitioning and Leaf Photosynthesis

Biomass partitioning to the fruits was higher when ICL was applied (**Table 3**), which is in accordance with various works reported for other crops (Marcelis, 1993). The largest positive effects of ICL were found in bud positions 11–15, the positions receiving the highest supplemental light intensity and red:far-red ratio (data not shown). Biomass partitioning to the fruit is highly correlated with the number of fruits (Marcelis, 1996) and we observed the greatest increases in fruit number under ICL in the lower part of the canopy. The low SLA at 185 μmol m^{-2} s^{-1} ICL reflects thicker leaves (**Table 3**) and is a well-known acclimation response to higher light intensity (Evans and Poorter, 2001).

TABLE 7 | Total number of necrotic buds and total lateral length (destructive measurement at start of autumn cycle, 24–28 July). No significant interaction between bud position and spring ICL intensity was found.

	ICL (μmol m^{-2} s^{-1})			Bud position[3]		
Parameter (per cane)	**0**	**93**	**185**	**1–10**	**11–20**	**21+**
Number of necrotic buds [1]	13.3 b[2]	10.0 a	9.2 a	11.4 a	17.8 b	3.3 c
Total lateral length (cm)	325 a	390 a	398 a	126 a	192 b	54 c

[1]*Buds with internal brown colour larger than 50% of their area were considered necrotic.*
[2]*Means followed by a different letter in a row comparing the 3 ICL intensities, or comparing the 3 bud positions differ significantly according to Fisher's protected LSD-test (P = 0.05), n = 3.*
[3]*Bud position counted from the base of the cane.*

Under low light conditions, quantum yield and convexity of the photosynthesis light-response curve are the most important parameters for assessing the productivity of a leaf. In March, leaves not exposed to ICL showed a higher quantum yield compared to 185 μmol m^{-2} s^{-1} ICL (**Table 4**), which suggests higher efficiency under low light conditions (Boardman, 1977). In May, this difference had disappeared. In both March and May, leaves exposed to 185 μmol m^{-2} s^{-1} ICL showed a higher A_{max}, 58 and 42%, respectively, when compared to no ICL. ICL resulting in increased leaf photosynthetic capacity for lower leaves in the canopy was also shown by Dueck et al. (2012) for tomato and Pettersen et al. (2010) for cucumber.

Positive Effect of ICL on Yield in Spring Carries Over to Autumn Production Cycle

We hypothesized that an increased spring production as a result of spring ICL would come at the expense of autumn production. However, results showed the opposite, ICL in spring increased spring production (**Table 2**) as well as autumn production (**Table 6**). The number of secondary laterals from scale buds increased with increased supplementary light intensity in spring (**Table 4**). This increase is most likely caused by the lower number of necrotic buds. A negative relationship between light intensity and bud necrosis was also found in grapevines. A period of 15 days of shading of individual buds or entire shoots at photosynthetic photon flux density (PPFD) less than 1–2% of full sunlight was sufficient to significantly raise bud necrosis above that of non-shaded control vines (Perez and Kliewer, 1990).

The much lower yield in the autumn cycle compared to the spring cycle probably results from the lower light levels during the fruit production period in autumn.

This it the first scientific report on the potential for applying LED ICL in greenhouse-grown blackberries. Further research should focus on optimal intensity of ICL and the positioning of supplementary lighting (position of ICL modules in the crop, but also ratio between toplighting and ICL). Furthermore, a yield increase by 79% in spring production and a positive carryover effect of 11% yield increase in autumn as a result of 93 μmol m^{-2} s^{-1} ICL is very promising and certainly warrants investigation in the economic feasibility of ICL in blackberries.

CONCLUSION

- Applying 93 or 185 μmol m^{-2} s^{-1} ICL in greenhouse-grown blackberry during spring increased spring fresh fruit yields by 79 and 122%, respectively.
- Higher yield mainly resulted from higher total dry matter production and to a lesser extend from a higher partitioning to the fruits.
- A larger number of elongated laterals per cane under LED ICL explained 75% of this yield increase.
- Fruit sugar or acid content was not influenced by LED ICL.
- Autumn yield was 11% higher for 93 μmol m^{-2} s^{-1} and 36% higher for 185 μmol m^{-2} s^{-1} spring ICL, despite the fact that in autumn no difference in LED light treatments was implied (same light level).
- This increased autumn yield was caused by more fruiting laterals (less necrotic buds).

DATA AVAILABILITY STATEMENT

The raw data supporting the conclusions of this article will be made available by the authors, without undue reservation.

AUTHOR CONTRIBUTIONS

AR and EH designed and initiated the experiment. AR conducted the measurements and analysis for the spring cropping cycle and wrote a first draft of the manuscript. KL conducted the measurements and analysis for the autumn cropping cycle. EH supervised the measurements and data analysis and finalized the manuscript. The manuscript has been read and approved by all authors.

FUNDING

We gratefully acknowledge the financial support by Driscoll's Strawberry Associates, Watsonville, CA, United States.

ACKNOWLEDGMENTS

We thank Jelle Geurts for conducting the fruit quality analysis as well as the personnel of Unifarm, Wageningen University for excellent crop cultivation. Finally, we would also like to thank the late Fanny Pitsoudis of Driscoll's for his stimulating interest in our work and for providing crop cultivation advice.

SUPPLEMENTARY MATERIAL

The Supplementary Material for this article can be found online at: https://www.frontiersin.org/articles/10.3389/fpls.2021.620642/full#supplementary-material

REFERENCES

Boardman, N. K. (1977). Comparative photosynthesis of sun and shade plants. *Annu. Rev. Plant Physiol.* 28, 355–377. doi: 10.1146/annurev.pp.28.060177.002035

Carew, J. G., Mahmood, K., Darby, J., Hadley, P., and Battey, N. H. (2003). The effect of temperature, photosynthetic photon flux density, and photoperiod on the vegetative growth and flowering of 'Autumn Bliss' raspberry. *J. Am. Soc. Hortic. Sci.* 128, 291–296. doi: 10.21273/jashs.128.3.0291

Centre for the Promotion of Imports from Developing Countries (2016). *Exporting Fresh Berries to Europe*. The Hague: Centre for the Promotion of Imports from Developing Countries.

Dale, A., and Blom, T. J. (2004). Far-red light alters primocane morphology of red raspberry. *HortScience* 39, 973–974. doi: 10.21273/HORTSCI.39.5.973

Dueck, T. A., Janse, J., Eveleens, B. A., Kempkes, F. L. K., and Marcelis, L. F. M. (2012). Growth of tomatoes under hybrid LED and HPS lighting. *Acta Hortic.* 952, 335–342. doi: 10.17660/actahortic.2012.952.42

Evans, J. R., and Poorter, H. (2001). Photosynthetic acclimation of plants to growth irradiance: the relative importance of specific leaf area and nitrogen partitioning in maximizing carbon gain. *Plant Cell Environ.* 24, 755–767. doi: 10.1046/j.1365-3040.2001.00724.x

Fernandez, G. E., and Pritts, M. P. (1994). Growth, carbon acquisition, and source-sink relationships in 'Titan' red raspberry. *J. Am. Soc. Hortic. Sci.* 119, 1163–1168. doi: 10.21273/jashs.119.6.1163

Franklin, K. A., and Whitelam, G. C. (2005). Phytochromes and shade-avoidance responses in plants. *Ann. Bot.* 96, 169–175. doi: 10.1093/aob/mci165

Girault, T., Bergougnoux, V., Combes, D., Viemont, J. D., and Leduc, N. (2008). Light controls shoot meristem organogenic activity and leaf primordia growth during bud burst in *Rosa* sp. *Plant Cell Environ.* 31, 1534–1544. doi: 10.1111/j.1365-3040.2008.01856.x

Hao, X., and Papadopoulos, A. P. (1999). Effects of supplemental lighting and cover materials on growth, photosynthesis, biomass partitioning, early yield and quality of greenhouse cucumber. *Sci. Hortic.* 80, 1–18. doi: 10.1016/s0304-4238(98)00217-9

Heide, O. M., and Sønsteby, A. (2011). Physiology of flowering and dormancy regulation in annual- and biennial-fruiting red raspberry (*Rubus idaeus* L.) - a review. *J. Hortic. Sci. Biotechnol.* 86, 433–442. doi: 10.1080/14620316.2011.11512785

Hemming, S. (2011). "Use of natural and artificial light in horticulture -interaction of plant and technology," in *Proceedings of the VI International Symposium on Light in Horticulture*, eds E. Goto and S. Hikosaka (Tsukuba: Acta Hort.), 15–19. doi: 10.1016/b978-0-12-813973-8.00003-8

Holmes, M. G., and Smith, H. (1977). The function of phytochrome in the natural environment—II. The influence of vegetation canopies on the spectral energy distribution of natural daylight. *Photochem. Photobiol.* 25, 539–545. doi: 10.1111/j.1751-1097.1977.tb09125.x

Hovi, T., Näkkilä, J., and Tahvonen, R. (2004). Interlighting improves production of year-round cucumber. *Sci. Hortic.* 102, 283–294. doi: 10.1016/j.scienta.2004.04.003

Hovi-Pekkanen, T., Näkkilä, J., and Tahvonen, R. (2006*). Increasing productivity of sweet pepper with interlighting. *Acta Hortic.* 711, 165–170. doi: 10.17660/actahortic.2006.711.19

Jacovides, C. P., Timvios, F. S., Papaioannou, G., Asimakopoulos, D. N., and Theofilou, C. M. (2004). Ratio of PAR to broadband solar radiation measured in Cyprus. *Agric. For. Meteorol.* 121, 135–140. doi: 10.1016/j.agrformet.2003.10.001

Kaiser, E., Kromdijk, J., Harbinson, J., Heuvelink, E., and Marcelis, L. F. M. (2017). Photosynthetic induction and its diffusional, carboxylation and electron transport processes as affected by CO_2 partial pressure, temperature, air humidity and blue irradiance. *Ann. Bot.* 119, 191–205. doi: 10.1093/aob/mcw226

Khosh-Khui, M., and George, R. A. T. (1977). Responses of glasshouse roses to light conditions. *Sci. Hortic.* 6, 223–235. doi: 10.1016/0304-4238(77)90066-8

Leduc, N., Roman, H., Barbier, F., Péron, T., Huché-Thélier, L., Lothier, J., et al. (2014). Light signaling in bud outgrowth and branching in plants. *Plants* 3, 223–250. doi: 10.3390/plants3020223

Lu, N., Maruo, T., Johkan, M., Hohjo, M., Tsukagoshi, S., Ito, Y., et al. (2012). Effects of supplemental lighting with Light-Emitting Diodes (LEDs) on tomato yield and quality of single-truss tomato plants grown at high planting density. *Environ. Control Biol.* 50, 63–74. doi: 10.2525/ecb.50.63

Marcelis, L. F. M. (1993). Fruit growth and biomass allocation to the fruits in cucumber. 2. effect of irradiance. *Sci. Hortic.* 54, 123–130. doi: 10.1016/0304-4238(93)90060-4

Marcelis, L. F. M. (1996). Sink strength as a determinant of dry matter partitioning in the whole plant. *J. Exp. Bot.* 47, 1281–1291. doi: 10.1093/jxb/47.special_issue.1281

Marcelis, L. F. M., Broekhuijsen, A. G. M., Nijs, E. M. F. M., Raaphorst, M. G. M., and Meinen, E. (2006). Quantification of the growth response to light quantity of greenhouse grown crops. *Acta Hortic.* 711, 97–104. doi: 10.17660/actahortic.2006.711.9

Massa, G. D., Kim, H.-H., Wheeler, R. M., and Mitchell, C. A. (2008). Plant productivity in response to LED lighting. *HortScience* 43, 1951–1956. doi: 10.21273/hortsci.43.7.1951

Mor, Y., and Halevy, A. H. (1980). Promotion of sink activity of developing rose shoots by light. *Plant Physiol.* 66, 990–995. doi: 10.1104/pp.66.5.990

Mor, Y., and Halevy, A. H. (1984). Dual effect of light on flowering and sprouting of rose shoots. *Physiol. Plant.* 61, 119–124.

Ögren, E., and Evans, J. R. (1993). Photosynthetic light-response curves. *Planta* 189, 182–190.

Paponov, M., Kechasov, D., Lacek, J., Verheul, M. J., and Paponov, I. A. (2020). Supplemental light-emitting diode inter-lighting increases tomato fruit growth through enhanced photosynthetic light use efficiency and modulated root activity. *Front. Plant Sci.* 10:1656. doi: 10.3389/fpls.2019.01656

Perez, J., and Kliewer, W. M. (1990). Effect of shading on bud necrosis and bud fruitfulness of Thompson seedless grapevines. *Am. J. Enol. Vitic.* 41, 168–175.

Pettersen, R. I., Torre, S., and Gislerød, H. R. (2010). Effects of intracanopy lighting on photosynthetic characteristics in cucumber. *Sci. Hortic.* 125, 77–81.

Pitsioudis, F., Odeurs, W., and Meesters, P. (2009). Early and late production of raspberries, blackberries and red currants. *Acta Hortic.* 838, 33–37. doi: 10.17660/ActaHortic.2009.838.3

Roman, H., Girault, T., Barbier, F., Péron, T., Brouard, N., Pìnèík, A., et al. (2016). Cytokinins are initial targets of light in the control of bud outgrowth. *Plant Physiol.* 172, 489–509.

Singh, D., Basu, C., Meinhardt-Wollweber, M., and Roth, B. (2015). LEDs for energy efficient greenhouse lighting. *Renewable Sustainable Energy Rev.* 49, 139–147.

Sønsteby, A., and Heide, O. M. (2008). Environmental control of growth and flowering of *Rubus idaeus* L. cv. glen ample. *Sci. Hortic.* 117, 249–256.

Sønsteby, A., Myrheim, U., Heiberg, N., and Heide, O. M. (2009). Production of high yielding red raspberry long canes in a Northern climate. *Sci. Hortic.* 121, 289–297.

Sønsteby, A., Stavang, J. A., and Heide, O. M. (2013). Production of high-yielding raspberry long canes: the way to 3 kg of fruit per cane. *J. Hortic. Sci. Biotechnol.* 88, 591–599.

Tewolde, F. T., Lu, N., Shiina, K., Maruo, T., Takagaki, M., Kozai, T., et al. (2016). Nighttime supplemental LED inter-lighting improves growth and yield of single-truss tomatoes by enhancing photosynthesis in both winter and summer. *Front. Plant Sci.* 7:448. doi: 10.3389/fpls.2016.00448

Trouwborst, G., Oosterkamp, J., Hogewoning, S. W., Harbinson, J., and van Ieperen, W. (2010). The responses of light interception, photosynthesis and fruit yield of cucumber to LED-lighting within the canopy. *Physiol. Plant.* 138, 289–300.

White, J. M., Wainwright, H., and Ireland, C. R. (1999). Endodormancy and paradormancy in the raspberry cultivar 'Glen Clova'. *Acta Hortic.* 505, 199–205.

Wubs, A. M., Heuvelink, E., Marcelis, L. F. M., Buck-Sorlin, G. H., and Vos, J. (2014). Axillary budbreak in a cut rose crop as influenced by light ntensity and red:far-red ratio at bud level. *J. Amer. Soc. Hort. Sci.* 139, 131–138.

Zieslin, N., and Tsujita, M. J. (1990). *Response of Miniature Roses to Supplementary Illumination. 1. Light Intensity*. Amsterdam: Elsevier Science Publishers B.V, 113–121.

Conflict of Interest: The authors declare that the research was conducted in the absence of any commercial or financial relationships that could be construed as a potential conflict of interest.

Publisher's Note: All claims expressed in this article are solely those of the authors and do not necessarily represent those of their affiliated organizations, or those of the publisher, the editors and the reviewers. Any product that may be evaluated in this article, or claim that may be made by its manufacturer, is not guaranteed or endorsed by the publisher.

Copyright © 2021 Rivas, Liu and Heuvelink. This is an open-access article distributed under the terms of the Creative Commons Attribution License (CC BY). The use, distribution or reproduction in other forums is permitted, provided the original author(s) and the copyright owner(s) are credited and that the original publication in this journal is cited, in accordance with accepted academic practice. No use, distribution or reproduction is permitted which does not comply with these terms.

Advantages of publishing in Frontiers

OPEN ACCESS
Articles are free to read for greatest visibility and readership

FAST PUBLICATION
Around 90 days from submission to decision

HIGH QUALITY PEER-REVIEW
Rigorous, collaborative, and constructive peer-review

TRANSPARENT PEER-REVIEW
Editors and reviewers acknowledged by name on published articles

Frontiers
Avenue du Tribunal-Fédéral 34
1005 Lausanne | Switzerland

Visit us: www.frontiersin.org
Contact us: frontiersin.org/about/contact

REPRODUCIBILITY OF RESEARCH
Support open data and methods to enhance research reproducibility

DIGITAL PUBLISHING
Articles designed for optimal readership across devices

FOLLOW US
@frontiersin

IMPACT METRICS
Advanced article metrics track visibility across digital media

EXTENSIVE PROMOTION
Marketing and promotion of impactful research

LOOP RESEARCH NETWORK
Our network increases your article's readership